NATIONAL TECHNICAL UNIVERSITY OF ATHENS
SCHOOL OF MECHANICAL ENGINEERING
MECHANICAL DESIGN AND CONTROL SYSTEMS SECTION
LABORATORY OF DYNAMICS AND STRUCTURES

DEVELOPMENT OF METHODS FOR TOPOLOGY AND SHAPE OPTIMIZATION OF MECHANICAL STRUCTURES

by

Demetrios T. Venetsanos
Dipl. Mech. Eng. NTUA

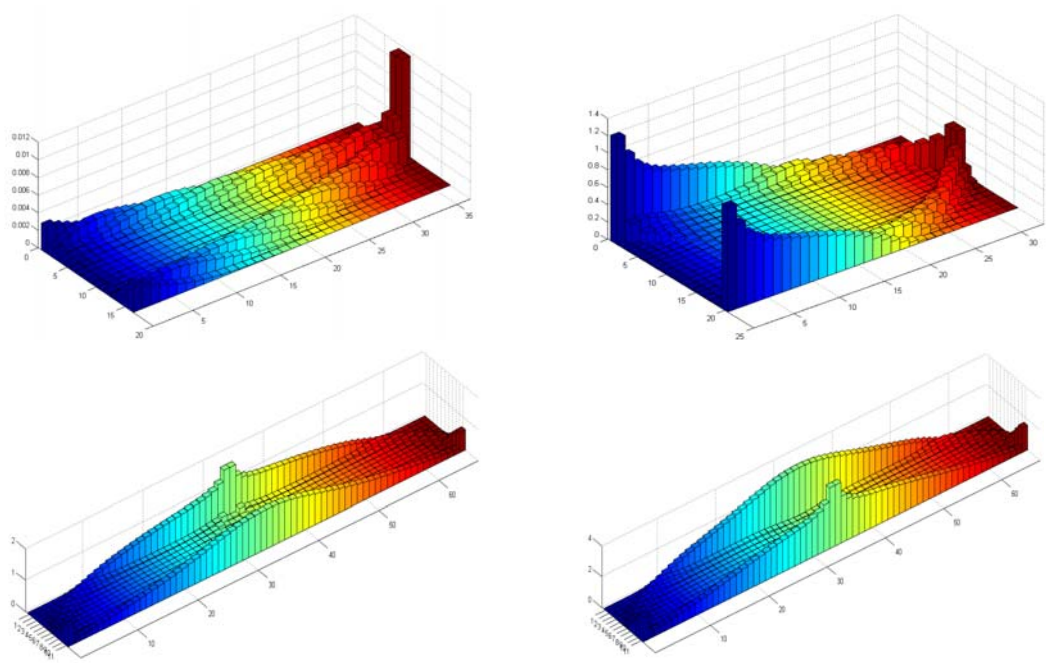

Submitted in total fulfillment of the requirements for the degree of
Doctor of Philosophy in Mechanical Engineering

Athens, 2010

This page has been left intentionally blank

This page has been left intentionally blank

PhD Examination Committee

I certify that I have read this dissertation and that in my opinion it is fully adequate, in scope and quality, as a dissertation for the degree of Doctor of Philosophy.

Christopher G. Provatidis
Professor
(Principal Advisor)
School of Mechanical Engineering
National Technical University of Athens

I certify that I have read this dissertation and that in my opinion it is fully adequate, in scope and quality, as a dissertation for the degree of Doctor of Philosophy.

Manolis Papadrakakis
Professor
School of Civil Engineering
National Technical University of Athens

I certify that I have read this dissertation and that in my opinion it is fully adequate, in scope and quality, as a dissertation for the degree of Doctor of Philosophy.

Vlassios Koumousis
Professor
School of Civil Engineering
National Technical University of Athens

I certify that I have read this dissertation and that in my opinion it is fully adequate, in scope and quality, as a dissertation for the degree of Doctor of Philosophy.

Kyriakos Giannakoglou
Professor
School of Mechanical Engineering
National Technical University of Athens

I certify that I have read this dissertation and that in my opinion it is fully adequate, in scope and quality, as a dissertation for the degree of Doctor of Philosophy.

Theodore Costopoulos
Associate Professor
School of Mechanical Engineering
National Technical University of Athens

I certify that I have read this dissertation and that in my opinion it is fully adequate, in scope and quality, as a dissertation for the degree of Doctor of Philosophy.

Ioannis Antoniadis
Associate Professor
School of Mechanical Engineering
National Technical University of Athens

I certify that I have read this dissertation and that in my opinion it is fully adequate, in scope and quality, as a dissertation for the degree of Doctor of Philosophy.

Stephanos Diplaris
Assistant Professor
School of Mechanical Engineering
National Technical University of Athens

This page has been left intentionally blank

This page has been left intentionally blank

Αφιερώνεται
σε εκείνους που αναπαύθηκαν νωρίς
και
σε εκείνους που διάγουν
με ηθικό ακμαιότατο, αντοχή ατελείωτη και μεγαλείο ψυχικό …

Ευχαριστίες

Κάθε ταξιδιώτης, όταν πλησιάζει το τέλος ενός μεγάλου και περιπετειώδους ταξιδιού, πραγματοποιεί έναν απολογισμό. Στο πλαίσιο αυτού του απολογισμού, θα ήταν σημαντικότατη παράλειψη η μη-αναφορά προσώπων που συνέβαλαν, ο καθένας με τον δικό του τρόπο, στην υποστήριξη του ταξιδιώτη-γράφοντος κατά τη διάρκεια της εκπόνησης της παρούσας.

Πρώτα και πάνω απ' όλα, ιδιαίτερη ευγνωμοσύνη οφείλω στην οικογένειά μου, στους γονείς μου Τιμολέοντα και Ναυσικά, καθώς και στην αδελφή μου Αθηνά. Οι λόγοι προφανείς και η όποια απόπειρα αιτιολόγησης αυτού απλά θα μείωνε την ανεκτίμητη προσφορά τους. Επίσης, οφείλω να ευχαριστήσω τα μέλη της Τριμελούς Συμβουλευτικής μου Επιτροπής, Καθηγητή ΕΜΠ κο Χριστόφορο Προβατίδη, Αν. Καθηγητή ΕΜΠ κο Παναγιώτη Μακρή και Καθηγητή ΕΜΠ Ανδρέα Κανάραχο. Κατά πρώτον, οφείλω να ευχαριστήσω τον επιβλέποντά μου, Καθηγητή ΕΜΠ κο Χριστόφορο Προβατίδη, η συνεργασία με τον οποίο υπήρξε καταλυτική σε εκπαιδευτικό, σε ερευνητικό αλλά και σε επαγγελματικό επίπεδο. Ασχέτως των όποιων μεταξύ μας διαφωνιών, κάτι που, άλλωστε, προβλέπεται και επιβάλλεται σε τέτοιου είδους συνεργασίες, δεν είναι δυνατόν να μην αναγνωρίσω την πάντοτε καλόψυχη και άκρως θετική επίδρασή του στην όλη πορεία μου. Η επιμονή του τόσο για μία πρώτη προσέγγιση των όποιων εξεταζόμενων φαινομένων, μέσα από την ενδελεχή μελέτη απλοποιημένων και ελεγχόμενων υπολογιστικών μοντέλων, όσο και για τη διατύπωση θεωρήσεων, με τρόπο πλήρη, τεκμηριωμένο και πλαισιωμένο με πληθώρα αριθμητικών αποτελεσμάτων, αποτελεί για μένα ένα σπουδαίο και χρήσιμο μάθημα. Παρόμοιας αξίας είναι για μένα και όλες οι ευκαιρίες που συνεχώς μου δίνει ο κος Προβατίδης, τόσο σε εκπαιδευτικό όσο και σε ερευνητικό επίπεδο, καθ' όλη τη διάρκεια της ενδεκαετούς παρουσίας μου στην ερευνητική του ομάδα, διότι μέσω αυτών μου δίδεται η δυνατότητα να ασχοληθώ με μία ποικιλία θεμάτων, διαφορετικής φύσεως και πολυπλοκότητας, κάτι που σαφώς συμβάλλει σημαντικά στην προσαύξηση της γνώσης, στην απόκτηση πολύτιμης εμπειρίας και στη σφυρηλάτηση νοοτροπίας, τρόπου σκέψης και τρόπου εργασίας. Το πραγματικό ενδιαφέρον και η υποστήριξη του επιβλέποντός μου προς το πρόσωπό μου έχει αποδειχθεί επανειλημμένως. Από βάθους ψυχής οφείλω να ευχαριστήσω και τον Αν. Καθηγητή ΕΜΠ κο Παναγιώτη Μακρή, δίπλα στον οποίο συνειδητοποίησα τι εστί ακαδημαϊκός Παιδαγωγός (με κεφαλαίο Π), τι εστί Άνθρωπος (με κεφαλαίο Α) και τι εστί Μηχανικός (με κεφαλαίο Μ). Μακάρι με κάποιον τρόπο, κάποτε να μπορέσω να ανταποδώσω το καλό που εισέπραξα από αυτόν τον εκπληκτικό και υποδειγματικό Δάσκαλο και Άνθρωπο. Ένα μεγάλο ευχαριστώ οφείλω και στον Καθηγητή ΕΜΠ κο Ανδρέα Κανάραχο, ο οποίος, τις όποιες φορές συνομιλήσαμε, ήταν προθυμότατος να ακούσει, να υποδείξει, να συμβουλεύσει και να βοηθήσει. Ιδιαίτερη αναφορά οφείλω στον Καθηγητή ΤΕΙ Πειραιά κο Σάββα Βασιλειάδη. Η γνωριμία και συνεργασία μαζί του υπήρξε σταθμός, τόσο σε ανθρώπινο επίπεδο όσο και σε επίπεδο παραγωγής έργου. Απλά, εξαιρετικός. Τυχεροί εκείνοι οι φοιτητές που τον είχαν και εκείνοι οι φοιτητές που θα τον έχουν Καθηγητή τους. Ένα μεγάλο ευχαριστώ οφείλω στον Καθηγητή ΕΜΠ κο Βασίλειο Παπάζογλου και στον Αν. Καθηγητή ΕΜΠ κο Νικόλαο Τσούβαλη, δίπλα στους οποίους μου δόθηκε η ευκαιρία όχι μόνον να μάθω πολλά, τόσο σε θεωρητικό όσο και σε πρακτικό επίπεδο, αλλά και να συμμετάσχω σε έργα μοναδικής σημασίας και παγκοσμίου εμβέλειας, όπως είναι το πρόγραμμα ΝΕΣΤΩΡ. Θα πρέπει να ευχαριστήσω και τον Καθηγητή ΕΜΠ κο Κωνσταντίνο Σπέντζα, ο οποίος με την αυστηρή, αλλά πάντοτε καλοπροαίρετη, κριτική του έθετε ψηλά τον πήχυ των απαιτήσεων, ενώ σε συγκεκριμένη χρονική στιγμή, με μία αξιοθαύμαστη υπέρβαση, με υποστήριξε και έδωσε άμεσα λύση σε καίριο επαγγελματικό ζήτημα. Τέτοιες ενέργειες δεν είναι δυνατόν να λησμονούνται ή να μην μνημονεύονται. Στο ίδιο

μήκος κύματος, θα πρέπει να αναφερθώ στους Καθηγητές ΕΜΠ κ.κ. Σωκράτη Τσαγγάρη, Κωνσταντίνο Κυριακόπουλο και Δημήτριο Μανωλάκο, όπως επίσης και στους Επίκουρους Καθηγητές Μάριο Αναγνωστάκη και Ευάγγελο Χίνη, οι οποίοι, σε διάφορες χρονικές στιγμές παρείχαν πολυτιμότατες συμβουλές και υποστήριξη, χωρίς τις οποίες συγκεκριμένοι στόχοι δεν θα είχαν υλοποιηθεί. Ιδιαίτερη μνεία οφείλω στον Αν. Καθηγητή κο Θεόδωρο Κωστόπουλο, ο οποίος πάντοτε διέθετε χρόνο και διάθεση για συζήτηση και πάντοτε προέτρεπε, με τον χαρακτηριστικό δυναμικό και μοναδικό του τρόπο, για την επίτευξη του καλύτερου δυνατού αποτελέσματος. Ομοίως, οφείλω να ευχαριστήσω τον Καθηγητή ΕΜΠ κο Δημήτριο Παντελή και τον Αν. Καθηγητή ΕΜΠ κο Κυριάκο Γιαννάκογλου διότι, στις κατά καιρούς συζητήσεις μας, πάντοτε και με καλή διάθεση διετύπωναν εύστοχες παρατηρήσεις και συμβουλές προς το συμφέρον του γράφοντος. Επίσης, θα πρέπει να αναφερθώ στον Επίκουρο Καθηγητή κο Στέφανο Διπλάρη, ο οποίος έχει αποτελέσει για τον γράφοντα παράδειγμα ήθους, ευφυούς νου και μαχόμενου Μηχανικού, καθώς και στον Καθηγητή ΕΜΠ κο Ευάγγελο Παπαδόπουλο, ο οποίος, με τον εξαιρετικά δομημένο και συστηματικό τρόπο εργασίας του, σηματοδοτεί το δρόμο προς την υλοποίηση υψηλών στόχων και οραμάτων. Ένας ακόμη άνθρωπος στον οποίο οφείλω ένα μεγάλο ευχαριστώ είναι ο Αν. Καθηγητής ΕΜΠ κος Ιωάννης Αντωνιάδης, ο οποίος, με τον δικό του τρόπο, με έχει υποστηρίξει και βοηθήσει σε διάφορα θέματα. Ομοίως, θα πρέπει να ευχαριστήσω τους Καθηγητές ΤΕΙ Πειραιά, κ.κ. Αθανάσιο Πέππα και Αντώνιο Πριμέντα, για τις ευκαιρίες και την εμπιστοσύνη που μου έδειξαν, τόσο σε εκπαιδευτικά όσο και σε ερευνητικά θέματα.

Εκτός των Καθηγητών και δασκάλων μου, δεν είναι δυνατόν να μην αναφερθώ στην κα Αδαμαντία Άννη και στην κα Αναστασία Κοτσιρέα, αμφότερες ανεκτίμητης αξίας στελέχη του Τομέα Μηχανολογικών Κατασκευών και Αυτομάτου Ελέγχου (Τομέας ΜΚΑΕ) της Σχολής Μηχανολόγων Μηχανικών ΕΜΠ. Ουκ ολίγες φορές με συμβούλευσαν σε διοικητικά θέματα και ουκ ολίγες φορές ανταλλάξαμε απόψεις επί παντός επιστητού. Οι κ.κ. Μιχάλης Δροσάκης, Δρ ΕΜΠ Λεωνίδας Μενδρινός, Διονύσιος Ασβεστάς, Αθανάσιος Τριάντης και η Δρ ΕΜΠ κα Βίκυ Λούλη, επίσης στελέχη του Τομέα ΜΚΑΕ, είναι άνθρωποι στους οποίους θα πρέπει να αναφερθώ τόσο για την ευγένειά τους όσο και για την προθυμία τους να εξυπηρετήσουν σε όποιο τεχνικό ή διοικητικό πρόβλημα ανέκυπτε κατά διαστήματα. Επίσης, θα πρέπει να αναφερθώ στον Δρ ΕΜΠ κο Νικόλαο Παντελέλη για τις εποικοδομητικές συζητήσεις μας, όπως και στον Δρ ΕΜΠ κο Δημήτριο Κουλοχέρη, ομοίως για τις αμέτρητες συζητήσεις μας, για την αμέριστη πρακτική του συμπαράσταση σε ποικίλα θέματα καθώς και για τη δυνατότητα που μου έδωσε να ασχοληθώ με θέματα εφηρμοσμένης υπολογιστικής μηχανικής. Τέλος, θα πρέπει να αναφερθώ στις κυρίες της Γραμματείας της Σχολής Μηχανολόγων Μηχανικών ΕΜΠ, κ.κ. Ειρήνη Μουντζουρίδη, Καίτη Φούσκα και Ειρήνη Βαρδακώστα, οι οποίες πάντοτε με ευγένεια, προθυμία και αποτελεσματικότητα επέλυαν όποιο διαδικαστικό θέμα προέκυπτε.

Εκτός διδασκόντων και στελεχών της Σχολής, νοιώθω την ανάγκη να αναφερθώ στους συνεργάτες και συναδέλφους, προπτυχιακούς και μεταπτυχιακούς, από τους οποίους έχω εισπράξει πάρα πολλά και σε πολλά επίπεδα. Κατά πρώτον, θα πρέπει να αναφερθώ στα παιδιά του Εργαστηρίου, τον ανεπανάληπτο Βασίλη 'Billy' Γεωργιόπουλο, τον ικανότατο Ευάγγελο Θεοδώρου, το διαμάντι του Εργαστηρίου Αργυρώ 'Arkal' Καλλιβρετάκη, τον εξαίρετο Στέλιο Ισιδώρου, την Κλειώ Βόσου και τον Γιάννη Κουκούλη. Επίσης, θα πρέπει να αναφερθώ σε όλες και σε όλους εκείνους με τους οποίους είχα την τύχη να συνεργαστώ: τον Γιώργο Παραδείση, τη Τζένη Μαρώση, τον Λάμπρο Τσιγγινό, τον Άκη Κουφή, τον Θέμη Μπαλωμένο, τον Αθανάσιο Νιαούρη, τον Δημήτρη Ρελλάκη, την ασυναγώνιστη Λένα Αναστασιάδου, τον Παναγιώτη Καλογιάννη, τον Δημήτρη Γεωργούλα, τον Θοδωρή Αλυσανδράτο, τον Δημήτρη Μητράκο, τον

Μάνθο Χιονίδη, τον Διονύσιο Αποστόλου, τον Γεώργιο Βαονάκη, τον Σταύρο Καραγιάννη, τον Μάνο Τζανακάκη, την Βάσω Καμπύλη, τον Κώστα Αργυρό, τον Τάσο Παπαγεωργίου, τον Νίκο Κεσίμογλου, τον Παναγιώτη Μάρκο, τον Μελέτη Λινάρδο, τον Σαράντη Χαμπιλό, την Νατάσα Βασιλείου, τον Όμηρο Έξαρχο, την Έφη Κυριαζή, τη Σοφία Μωυσιάδου, τον Γιάννη Νικητάκη, τον Γιάννη Λογοθέτη, τον Σωτήρη Σκαρμέα, την Ευφροσύνη-Αικατερίνη Μαγουλά, την Λίνα Καβάγια, την Πένυ Κούλη, τον Κλήμη Ιωάννου, τον Ευάγγελο Κασελούρη, τον Αλέξανδρο Καπόγιαννη και τον Στράτο Σπαθάρη. Η συνεργασία και συνύπαρξη με όλους αυτούς τους εξαίρετους χαρακτήρες και μοναδικούς ανθρώπους υπήρξε μία ανεκτίμητη και μη-ανταλλάξιμη εμπειρία. Χίλια καλά πράγματα θα μπορούσαν να ειπωθούν για κάθε έναν και κάθε μία από τους προαναφερομένους, οι οποίοι είτε είναι πλέον κάτοχοι ενός μεταπτυχιακού ή και δύο μεταπτυχιακών τίτλων, ή έχουν ξεκινήσει ή κοντεύουν να ολοκληρώσουν ή έχουν ολοκληρώσει το δικό τους περιπετειώδες ταξίδι στον κόσμο της έρευνας ή σταδιοδρομούν ως εξαίρετοι νέοι Μηχανικοί. Σε αυτό το σημείο, θα πρέπει να αναφερθώ με ιδιαίτερη θέρμη στην Ευφροσύνη-Αικατερίνη, στην Λίνα και ειδικά στον Σωτήρη, στον Όμηρο και στην οικογένειά του, για την μοναδική υποστήριξή τους σε δεδομένη χρονική στιγμή, καθώς και στη Νατάσα, η παρουσία της οποίας αποτέλεσε αρωγό, έως και έμπνευση, στο τελευταίο στάδιο εκπόνησης της παρούσης. Ιδιαίτερη αναφορά οφείλω στον Διευθυντή-Αν. Καθηγητή της Β' Ορθοπαιδικής Κλινικής Ιατρικής Σχολής του Πανεπιστημίου Αθηνών κο Νικόλαο Ευσταθόπουλο και στον Ορθοπαιδικό Χειρουργό Δρ Πανεπιστημίου Αθηνών κο Φραγκίσκο Ξυπνητό για την πολλά υποσχόμενη συνεργασία που έχουμε αναπτύξει σε θέματα αιχμής στην περιοχή της ορθοπαιδικής χειρουργικής. Ιδιαίτερη ευγνωμοσύνη και ευχαριστίες οφείλω και στην Υποψήφια Διδάκτορα κα Αναστασία Πετράκη, Κοινωνιολόγο MSc, ΜΕ, για την αμέριστη υποστήριξη και συνεχή συμπαράστασή της προς το πρόσωπό μου τα τελευταία χρόνια.

Τέλος, θα ήθελα να αναφερθώ στον αποθανόντα Δρ ΕΜΠ Νικόλαο Ζαφειρόπουλο, με τον οποίο περάσαμε αμέτρητες στιγμές στο Εργαστήριο συζητώντας επί θεωρητικών θεμάτων, αναπτύσσοντας κάποιον υπολογιστικό κώδικα, αναφερόμενοι στις στρατιωτικές μας θητείες και ανταλλάσοντας απόψεις επί διαφόρων θεμάτων. Ο Νίκος, μαζί με τον κο Βασιλειάδη, ήταν οι άνθρωποι που με παρακίνησαν πρώτοι για αυτό το μεγάλο και περιπετειώδες ταξίδι που ονομάζεται Διδακτορική Διατριβή, παρακίνηση η οποία δεν είναι δυνατόν να περάσει στη λήθη.

Το παρόν ταξίδι τελείωσε – πέρας αποστολής. Καιρός να ξεκινήσει το επόμενο ταξίδι…

Δημήτριος Τ. Βενετσάνος

Διπλ. Μηχ/λογος Μηχ/κος ΕΜΠ

Ιούλιος 2009

Εισαγωγή

Το αντικείμενο της παρούσας Διδακτορικής Διατριβής, όπως άλλωστε δηλώνει και ο τίτλος της, είναι η μελέτη και ανάπτυξη μεθοδολογιών βελτιστοποίησης τοπολογίας και σχήματος μηχανολογικών κατασκευών. Για την καλύτερη περιγραφή τόσο του περιεχόμενου όσο και του αντικειμενικού σκοπού της παρούσης, κρίνεται σκόπιμη μία σύντομη ετυμολογική ερμηνεία των όρων του τίτλου αυτής. Ειδικότερα, ο όρος 'μεθοδολογία' δηλώνει την αναφορά (λόγος) σε 'μέθοδο', δηλαδή σε δρόμο (οδός) αναζήτησης και επιδίωξης της γνώσης. Ο όρος 'βέλτιστος' αποτελεί τον υπερθετικό βαθμό του επιθέτου 'αγαθός', δηλαδή 'άξιος'. Ο όρος 'κατασκευή' έχει ως δεύτερο συνθετικό τη λέξη 'σκευή' που σημαίνει ενδυμασία, στολή. Ο επιθετικός προσδιορισμός 'μηχανολογική' χαρακτηρίζει την κατασκευή και δηλώνει ότι αυτή σχετίζεται με την μετατροπή ενέργειας από μία μορφή σε μία άλλη. Τέλος, οι όροι 'τοπολογία' και 'σχήμα' αφορούν στην (εξωτερική) μορφή που μπορεί να λάβει μία εφεύρεση/επινόηση που σχετίζεται με την μετατροπή ενέργειας (μηχανή). Συνεπώς, σε ελεύθερη απόδοση, στην παρούσα Διδακτορική Διατριβή γίνεται λόγος για αναζήτηση τρόπων, μέσω των οποίων επιδιώκεται η εύρεση της πλέον κατάλληλης μορφής την οποία μπορεί να λάβει μία μηχανή. Ισοδύναμα, αναζητείται ο καλύτερος τρόπος διαστασιολόγησης και συνδεσμολογίας ενός συνόλου δομικών στοιχείων, έτσι ώστε να καθίσταται ασφαλής η, για συγκεκριμένο σκοπό, χρήση του.

Το κριτήριο για την επιλογή της πλέον κατάλληλης μορφής, ανάμεσα από ένα, θεωρητικώς άπειρο, πλήθος δυνατών σχεδιάσεων, πρέπει να είναι μία ποσότητα άκρως αντιπροσωπευτική και χαρακτηριστική για κάθε σχεδίαση. Το συνολικό κατασκευαστικό κόστος μπορεί και ενδείκνυται να χρησιμοποιείται ως τέτοια ποσότητα, δεδομένου ότι σε αυτό συμπεριλαμβάνονται τόσο ο βαθμός δυσκολίας υλοποίησης της εκάστοτε σχεδίασης όσο και ο χρόνος που απαιτείται για την ολοκλήρωση της κατασκευής. Ωστόσο, ο υπολογισμός του συνολικού κατασκευαστικού κόστους αποτελεί μία εξαιρετικά σύνθετη διαδικασία, το τελικό αποτέλεσμα της οποίας δεν είναι σταθερό αλλά, αντιθέτως, μεταβάλλεται ανάλογα με τις εκάστοτε τιμές που έχουν διάφορες οικονομικές παράμετροι, όπως το κόστος μεταφοράς και τα επιτόκια. Για αυτόν το λόγο και σε πρακτικές εφαρμογές Μηχανικού, αντί του συνολικού κατασκευαστικού κόστους, προτιμάται ο υπολογισμός της ποσότητας του υλικού (είτε ως βάρος είτε ως όγκος) που πρέπει να χρησιμοποιηθεί για την υλοποίηση μίας σχεδίασης. Αν και πρόκειται για ένα αντιπροσωπευτικό μέγεθος, τονίζεται όλως ιδιαιτέρως ότι η επίτευξη της ελαχιστοποίησης του βάρους (ή του όγκου) του υλικού δεν συνεπάγεται πάντοτε και ελαχιστοποίηση του συνολικού κόστους. Αυτό είναι ιδιαίτερα αληθές σε περιπτώσεις στις οποίες πρέπει να χρησιμοποιηθούν δομικά στοιχεία τυποποιημένων (διακριτών) διαστάσεων, όπως συμβαίνει στους συγκολλητούς φορείς γερανογεφυρών και στις δεξαμενές αποθήκευσης πετρελαιοειδών. Είναι προφανές ότι η ελάχιστη ποσότητα της ύλης που πρέπει να χρησιμοποιηθεί σε μία κατασκευή εξαρτάται από τους περιορισμούς που επιβάλλονται στην συμπεριφορά αυτής υπό την εφαρμογή συγκεκριμένων εξωτερικών αιτίων. Τέτοιοι περιορισμοί είναι μέγιστες τιμές τασικού και παραμορφωσιακού πεδίου, μέγιστες τιμές βελών κάμψης, ελάχιστες τιμές κρισίμων φορτίων λυγισμού, ελάχιστες τιμές συχνοτήτων κ.α.

Η περιοχή της βελτιστοποίησης μηχανολογικών κατασκευών έχει τεράστια πρακτική αξία σε πολλούς τομείς. Μερικοί εκ των σημαντικότερων τομέων είναι η αυτοκινητοβιομηχανία, η αεροπορική και η διαστημική βιομηχανία, η ναυπηγική βιομηχανία και γενικά ο χώρος των μεταλλικών και των ελαφρών κατασκευών. Εκτός της πρακτικής αξίας της, η βελτιστοποίηση μηχανολογικών κατασκευών παρέχει εξαιρετικές προκλήσεις σε επίπεδο τόσο Θεωρητικής όσο και Υπολογιστικής Μηχανικής. Ως εκ τούτου, δεν είναι απορίας άξιον το γεγονός ότι έχει αποτελέσει πεδίο ενδελεχούς έρευνας και συστηματικής μελέτης κυρίως τα τελευταία 60 χρόνια, δηλαδή από

την εποχή γένεσης της Υπολογιστικής Μηχανικής. Είναι πρόδηλο ότι μέσα σε αυτές τις έξι δεκαετίες, χιλιάδες Μηχανικοί και, γενικότερα, Ερευνητές, είτε μέσα από το Ακαδημαϊκό περιβάλλον είτε μέσα από κάποιον δημόσιο ή ιδιωτικό φορέα/βιομηχανία, έχουν συμβάλλει στο συγκεκριμένο ερευνητικό πεδίο με το προσωπικό τους έργο, το οποίο, συνολικά, έχει αποτυπωθεί σε χιλιάδες βιβλία και εκατομμύρια δημοσιεύσεων σε έγκριτα επιστημονικά περιοδικά. Μέσα σε αυτό το πλαίσιο, το εύλογο ερώτημα που ανακύπτει είναι τι θα μπορούσε να προσφέρει μία ακόμα Διδακτορική Διατριβή σε ένα πεδίο που έχει διερευνηθεί τόσο πολύ, από τόσο πολλούς και για τόσο μακρύ χρονικό διάστημα. Το ερώτημα αυτό καθίσταται ακόμα πιο οξύ, εάν σε αυτό προστεθεί τόσο η γενικότερη αίσθηση της επιστημονικής κοινότητας ότι, λίγο έως πολύ, ο,τιδήποτε υπήρχε να ειπωθεί στη βελτιστοποίηση έχει ήδη ειπωθεί όσο και η άποψη ότι η γνώση σχετικά με τη βελτιστοποίηση κατασκευών έχει χαθεί μέσα στα χρόνια, δηλαδή ότι οι νεώτεροι απλά ανακαλύπτουν εκ νέου θεωρίες και απόψεις που κάποτε είχαν, έστω και σε πρωτόλεια μορφή, διατυπωθεί.

Η απάντηση στο ερώτημα 'προς τι ετούτη η Διατριβή' είναι εξαιρετικά απλή και ταυτόσημη με την απάντηση στο ίδιο ερώτημα που θα μπορούσε να είχε τεθεί 10 ή και 20 χρόνια νωρίτερα. Η εσφαλμένη αίσθηση σχετικά με τον κορεσμό και την εξάντληση ενός επιστημονικού πεδίου απλά διαψεύδεται, όχι καθημερινά, αλλά σε τακτά χρονικά διαστήματα, είτε με εντελώς νέες ανακαλύψεις είτε με νέες παραλλαγές πάνω σε ήδη υπάρχουσες θεωρίες. Αν με τις πρώτες επιτυγχάνεται '*ένα τεράστιο άλμα για την ανθρωπότητα*', με τις δεύτερες επιτυγχάνεται '*ένα μικρό βήμα για τον άνθρωπο*', το οποίο κάποια στιγμή σίγουρα θα οδηγήσει σε ένα μεγαλύτερο βήμα και γιατί όχι σε ένα τεράστιο άλμα. Άλλωστε μία από τις βασικές αρχές του Μηχανικού είναι '*ένα βήμα κάθε φορά*' ('*one step at a time*'). Μάλιστα, από φιλοσοφική άποψη, η έμπνευση, ακρογωνιαίος λίθος για την πραγματοποίηση αλμάτων, θα έλθει σε κάποια στιγμή κατά την οποία, μέσα από την συστηματική ποσοτική και ποιοτική εργασία, ιδέες θα έχουν ωριμάσει. Όπως άλλωστε έχει ειπωθεί, '*η έμπνευση είναι μία πολύ περίεργη κυρία, η οποία δεν θα σε προειδοποιήσει, όταν κάποτε αποφασίσει να σε επισκεφθεί, γι' αυτό κι εσύ θα πρέπει να είσαι στο γραφείο σου*'. Εκτός αυτού, πάντοτε υπάρχει το περιθώριο περαιτέρω έρευνας πάνω σε θέματα τα οποία έχουν ήδη προσεγγιστεί ίσως με έναν πιο χονδροειδή τρόπο, οπότε προσεγγίσεις που ενδεχομένως και να έχουν παρουσιασθεί κάποτε στο παρελθόν είναι δυνατόν να διατυπωθούν εκ νέου σε ένα πιο πλήρες και στιβαρό πλαίσιο. Κάτι τέτοιο προφανώς δεν ακυρώνει την πρωτογενή διατύπωση, χωρίς την οποία δεν θα υπήρχε το υλικό για την νεώτερη προσέγγιση, αλλά ούτε μειώνει τη νεώτερη προσέγγιση, χωρίς την οποία η αρχική διατύπωση θα παρέμενε σημαντικά μικρότερη σε εμβέλεια και ισχύ. Τέλος, δεν πρέπει να λησμονείται ότι ο σκοπός μίας Διδακτορικής Διατριβής δεν είναι άλλος από την πραγματοποίηση μίας συστηματικής, αυτοδύναμης και εμπεριστατωμένης έρευνας σε ένα θεματικό πεδίο, η οποία καταλήγει σε μία συγκεκριμένη συνεισφορά και σαφώς δεν αποσκοπεί στην ανακάλυψη του αεικίνητου.

Μέσα στο προαναφερθέν ρεαλιστικό πλαίσιο, η παρούσα εργασία αποτελεί μέρος του έργου του γράφοντος από το 2000 στο Εργαστήριο Δυναμικής και Κατασκευών του Εθνικού Μετσοβίου Πολυτεχνείου υπό την διαρκή επίβλεψη και άοκνη καθοδήγηση του Καθηγητή Χρ. Γ. Προβατίδη. Ο κεντρικός θεματικός πυρήνας της αφορά στην βελτιστοποίηση της τοπολογίας και του σχήματος μηχανολογικών κατασκευών συνεχούς μέσου. Ακολουθήθηκαν δύο προσεγγίσεις των εν λόγω κατασκευών. Στην πρώτη χρησιμοποιήθηκαν σκελετικές κατασκευές (δηλαδή το συνεχές μέσο αντικαταστάθηκε από μία σκελετική, άρα διακριτή, κατασκευή) και στη δεύτερη το συνεχές μέσο αντιμετωπίσθηκε ως τέτοιο.

Η βελτιστοποίηση των σκελετικών κατασκευών στηρίχθηκε στη δημιουργία ενός πλέγματος ραβδόμορφων στοιχείων, με το οποίο υποκαταστάθηκε το συνεχές μέσο. Οι διατομές των στοιχείων

αυτών υποβλήθηκαν σε μία διαδικασία επαναδιαστασιολόγησης σύμφωνα με τρόπους που προέκυψαν μέσα από ενεργειακές θεωρήσεις. Ακρογωνιαίος λίθος στην όλη προσέγγιση αποτέλεσε η έννοια της πυκνότητας της ενέργειας παραμόρφωσης καθώς και της πυκνότητας της δυνατής συμπληρωματικής ενέργειας παραμόρφωσης. Η μεταβολή της τοπολογίας επετεύχθη μέσα από συστηματική αλλαγή του λόγου πλευρών (aspect ratio) του προαναφερθέντος πλέγματος. Η συνδυασμένη αξιοποίηση της επαναδιαστασιολόγησης και της αλλαγής της τοπολογίας, είτε μέσα σε ένα σχήμα σειριακής εκτέλεσης διαδικασιών είτε μέσα στο πλαίσιο μίας ιεραρχικής βελτιστοποίησης, παρείχε την καλύτερη δυνατή λύση. Προς αυτήν την κατεύθυνση, αναπτύχθηκε και ένας αλγόριθμος '*ομαδοποίησης και διαγραφής*', έτσι ώστε να μειωθεί και το πλήθος των δομικών στοιχείων της βέλτιστης σχεδίασης αλλά και η ανομοιογένεια μεταξύ των στοιχείων αυτών, ως προς το εμβαδόν των διατομών τους, συμβάλλοντας με τον τρόπο αυτό στην ελαχιστοποίηση όχι μόνον του βάρους αλλά και του κόστους της κατασκευής. Οι ενεργειακές θεωρήσεις που αναπτύχθηκαν, στηρίχθηκαν στην εφαρμογή της Μεθόδου των πολλαπλασιαστών Lagrange σε κατάλληλη διατύπωση του αντιστοίχου προβλήματος βελτιστοποίησης. Με τον τρόπο αυτό προέκυψαν ενεργειακές προτάσεις που ισχύουν στην βέλτιστη σχεδίαση. Διευκρινίζεται ότι σκελετικές κατασκευές εξετάσθηκαν και στις δύο και στις τρεις διαστάσεις.

Η βελτιστοποίηση κατασκευών συνεχούς μέσου, θεωρώντας τες ως τέτοιες, διακρίθηκε σε δύο στάδια. Κατά το πρώτο στάδιο εξετάσθηκε το πρόβλημα βελτιστοποίησης στις δύο διαστάσεις (ψευδο-τρισδιάστατη κατάσταση), ενώ κατά το δεύτερο στάδιο αντιμετωπίστηκε το αντίστοιχο πρόβλημα στις τρεις διαστάσεις. Και σε αυτά τα προβλήματα βελτιστοποίησης, αναπτύχθηκαν ενεργειακές θεωρήσεις βάσει της Μεθόδου των πολλαπλασιαστών Lagrange, καταλήγοντας σε ενεργειακές προτάσεις που ισχύουν στην βέλτιστη σχεδίαση. Η κεντρική ιδέα σε αυτές τις περιπτώσεις ήταν η ενεργειακή αξιολόγηση (βαθμολόγηση) της συμμετοχής υλικού στην παραλαβή των εξωτερικώς ασκουμένων φορτίων, είτε σε επίπεδο πεπερασμένου στοιχείου είτε σε επίπεδο κόμβου πλέγματος, και η αντίστοιχη προσθήκη ή αφαίρεση υλικού υπό την μορφή κατάλληλης μεταβολής του πάχους της κατασκευής, είτε σε επίπεδο πεπερασμένου στοιχείου είτε σε επίπεδο κόμβου πλέγματος. Η μεταβολή πάχους υπαγορευόταν από τις προαναφερθείσες ενεργειακές προτάσεις.

Συνοψίζοντας, στην παρούσα Διδακτορική Διατριβή:

- συγκεντρώθηκαν οι βασικότερες προσεγγίσεις στο πεδίο της βελτιστοποίησης μηχανολογικών κατασκευών, με έμφαση στην βελτιστοποίηση της τοπολογίας και του σχήματος αυτών,
- εξετάσθηκε πλήθος χαρακτηριστικών βιβλιογραφικών παραδειγμάτων προς βαθύτερη κατανόηση των εν λόγω θεωριών και αποκάλυψη σημείων που έχρηζαν βελτίωσης,
- εισήχθησαν νέοι δείκτες απόδοσης προς πληρέστερη αξιολόγηση των εκάστοτε μεθοδολογιών βελτιστοποίησης,
- διατυπώθηκαν, επί συγκεκριμένων θεωριών, παραλλαγές οι οποίες εμφάνισαν βελτιωμένη απόδοση συγκριτικά με τις αρχικές προσεγγίσεις,
- αναπτύχθηκαν νέα αριθμητικά σχήματα βελτιστοποίησης,
- συντάχθηκαν κώδικες σε FOTRAN, σε MatLab και σε APDL (ενσωματωμένη γλώσσα προγραμματισμού στο εμπορικό λογισμικό Ansys) και τέλος

Ωστόσο, η μεγαλύτερη συνεισφορά της παρούσης Διδακτορικής Διατριβής έγκειται στην επιτυχή αντιμετώπιση δύο κατηγοριών προβλημάτων βελτιστοποίησης.

Πιο συγκεκριμένα, στη διεθνή βιβλιογραφία, ήδη από τις αρχές της δεκαετίας του ’70, είναι γνωστή η επίλυση του ειδικού προβλήματος της ελαχιστοποίησης βάρους μίας κατασκευής υπό την επιβολή ενός περιορισμού κομβικής μετατόπισης, αλλά υπό την αυστηρή προϋπόθεση ότι ο υπό περιορισμό κόμβος, ή ακριβέστερα ο υπό περιορισμό βαθμός ελευθερίας, είναι εκ των προτέρων γνωστός (single displacement constraint problem). Στην παρούσα Διδακτορική Διατριβή επελύθη η γενίκευση του εν λόγω προβλήματος, κατά την οποία θεωρείται μεν ότι στη βέλτιστη σχεδίαση είναι ενεργός ένας περιορισμός μετατόπισης αλλά χωρίς να είναι εκ των προτέρων γνωστό σε ποιο βαθμό ελευθερίας αυτός ο περιορισμός τελικά επιβάλλεται. Η επίλυση επετεύχθη μέσα από τη διατύπωση μίας πρωτότυπης, ενεργειακής φύσεως μεθοδολογίας, η οποία στηρίζεται στη μέθοδο πολλαπλασιαστών Lagrange, αλλά, σε αντίθεση με τις υπάρχουσες διεθνώς δημοσιευμένες θεωρήσεις, τελικώς παρακάμπτεται ο υπολογισμός τέτοιου τύπου πολλαπλασιαστών.

Κατ’ επέκταση του ανωτέρω προβλήματος, διατυπώθηκε η θεωρητική λύση του αντιστοίχου προβλήματος της επιβολής περιορισμού τάσης, κατά το οποίο θεωρείται μεν ότι στη βέλτιστη σχεδίαση είναι ενεργός ένας περιορισμός τάσης, αλλά χωρίς να είναι εκ των προτέρων γνωστό το δομικό μέλος στο οποίο ο εν λόγω περιορισμός τελικά επιβάλλεται. Και πάλι, η επίλυση στηρίχθηκε στη μέθοδο πολλαπλασιαστών Lagrange, χωρίς τελικά να απαιτείται ο υπολογισμός τέτοιων πολλαπλασιαστών. Σε αντίθεση με τις διεθνώς δημοσιευμένες θεωρήσεις, η συγκεκριμένη προσέγγιση προκύπτει μέσα από ένα αυστηρά μαθηματικό πλαίσιο και περιγράφει την ενεργειακή κατάσταση της βέλτιστης σχεδίασης, χωρίς παραδοχές σχετιζόμενες με την υπερστατικότητα της κατασκευής. Γι’ αυτόν το λόγο υπερτερεί της εξαιρετικώς διαδεδομένης και γνωστής τεχνικής stress-ratio, βάσει της οποίας προκύπτει μία σχεδίαση πλήρους εντάσεως (Fully Stressed Design), δηλαδή μία σχεδίαση στην οποία επιδιώκεται όλα τα δομικά της μέλη να εμφανίσουν τάση ίση με την μέγιστη επιτρεπόμενη, κάτι που μαθηματικά αποδεικνύεται ότι δεν αντιστοιχεί σε ελάχιστο βάρος, παρά μόνον υπό αυστηρές και συγκεκριμένες προϋποθέσεις.

Αναφορικά με την διάρθρωση της παρούσας, στο 1^{ο} Κεφάλαιο διατυπώνεται το γενικευμένο πρόβλημα της ελαχιστοποίησης του βάρους κατασκευών και παρουσιάζονται οι βασικότερες ‘Σχολές’ βελτιστοποίησης τοπολογίας και σχήματος μηχανολογικών κατασκευών. Ειδικότερα, γίνεται αναφορά στην εφαρμογή γενικών αιτιοκρατικών μαθηματικών μεθοδολογιών βελτιστοποίησης, οι πιο αντιπροσωπευτικές από τις οποίες παρατίθενται με τρόπο συνοπτικό και προσανατολισμένο προς το πρόβλημα της βελτιστοποίησης κατασκευών. Στο ίδιο μήκος κύματος κινείται και η παρουσίαση των πλέον αντιπροσωπευτικών στοχαστικών μεθοδολογιών βελτιστοποίησης. Ακολουθεί η διατύπωση μεθοδολογιών που στηρίζονται στα επονομαζόμενα Βέλτιστα Κριτήρια, δηλαδή σε προτάσεις που περιγράφουν την ενεργειακή ή άλλη κατάσταση που επικρατεί στην βέλτιστη σχεδίαση, ενώ στη συνέχεια αναφέρονται οι μεθοδολογίες COC και DCOC που αναπτύχθηκαν υπό την καθοδήγηση και εποπτεία του G.I.N. Rozvany, του άξιου μαθητή και συνεχιστή του έργου του W. Prager. Στο ίδιο κεφάλαιο παρατίθενται συνοπτικά η προσέγγιση του τεχνητού υλικού (artificial material) του N. Olhoff, αναπτύσσεται η θεωρία ομογενοποίησης (Homogenization theory) που εισήγαγε ο N. Kikuchi, καταγράφεται η προσέγγιση του M.P. Bendsøe (μοντέλο SIMP), αναφέρεται η μέθοδος των Μετακινουμένων Ασυμπτώτων (Method of Moving Asymptotes) του C. Svanberg και, τέλος, περιγράφεται η μέθοδος των φυσαλίδων (Bubble method) του H. Eschenauer. Ιδιαίτερη αναφορά γίνεται στην μέθοδο Evolutionary Structural Optimization (ESO) των Steven και Xie. Στο ίδιο κεφάλαιο γίνεται μνεία στη χρήση των Νευρωνικών Δικτύων, των μη-πλεγματικών μεθόδων και στην τεχνική Design Of Experiment (DOE).

Στο 2^{ο} Κεφάλαιο παρατίθεται μία ενδελεχής ενασχόληση με τις κυριότερες άμεσες μεθοδολογίες βελτιστοποίησης (αιτιοκρατικές και στοχαστικές), οι οποίες και αξιολογήθηκαν μέσα από μία εκτενή σειρά βιβλιογραφικών παραδειγμάτων (μαθηματικές συναρτήσεις και δικτυώματα).

Επίσης, παρουσιάζεται μία πρωτότυπη υβριδική μέθοδος κατά την οποία μία αιτιοκρατική διαδικασία (μέθοδος Powell) συνδυάστηκε κατάλληλα με μία στοχαστική διαδικασία (μέθοδος Προσομοιούμενης Ανόπτησης) προς επίλυση προβλημάτων βελτιστοποίησης μετά περιορισμών.

Στο 3^{ο} Κεφάλαιο πραγματοποιείται μία ενεργειακής θεώρησης προσέγγιση του προβλήματος βελτιστοποίησης κατασκευών που αφορά στην μερική ή ολική αφαίρεση υλικού από ένα συνεχές μέσο, με σκοπό την ελαχιστοποίηση του βάρους. Στο ίδιο κεφάλαιο, διατυπώνεται και σχολιάζεται το πρόβλημα ελαχιστοποίησης του βάρους μίας κατασκευής υπό έναν περιορισμό ανάπαλσης καθώς και το πρόβλημα ελαχιστοποίησης του βάρους μίας κατασκευής, όταν αυτή βρίσκεται σε πλήρη ένταση (Fully Stress Design – FSD).

Στο 4^{ο} Κεφάλαιο εξετάζεται το πρόβλημα της βελτιστοποίησης μίας κατασκευής, όταν χρησιμοποιείται η σχεδίαση πλήρους εντάσεως. Αρχικά, αντιμετωπίζονται σκελετικές κατασκευές που αντικαθιστούν το συνεχές μέσο, ενώ στη συνέχεια αντιμετωπίζεται το συνεχές μέσο ως τέτοιο. Ειδικότερα, διατυπώνονται δύο προσεγγίσεις: η πρώτη αφορά σε επανασχεδίαση σε επίπεδο πάχους πεπερασμένων στοιχείων και η δεύτερη αφορά σε επανασχεδίαση σε επίπεδο ανεξάρτητης μετακίνησης κόμβων του πλέγματος, ακόμα και εάν αυτοί ανήκουν στο ίδιο πεπερασμένο στοιχείο. Στη συνέχεια εξετάζεται η εφαρμογή της μεθόδου FSD και ESO στην περίπτωση πλακών, ενώ, τέλος, εξετάζεται το πρόβλημα της ελαχιστοποίησης του βάρους 3Δ κατασκευών συνεχούς μέσου με ολική αφαίρεση πεπερασμένων στοιχείων, σύμφωνα με μία βιβλιογραφική μέθοδο, που χρησιμοποιήθηκε ως αναφορά, και σύμφωνα με μία προτεινόμενη παραλλαγή αυτής, η οποία προέκυψε ότι οδηγεί σε ανώτερες σχεδιάσεις και με λιγότερες επαναλήψεις. Τέλος, διατυπώνεται η θεωρητική λύση της γενικευμένης θεώρησης του προβλήματος της βελτιστοποίησης μίας κατασκευής, όταν επιβάλλεται ένας περιορισμός τάσης.

Στο 5^{ο} Κεφάλαιο εξετάζεται η γενικευμένη θεώρηση του προβλήματος της βελτιστοποίησης μίας κατασκευής, όταν επιβάλλεται ένας περιορισμός μετατόπισης. Διατυπώνεται μία πρωτότυπη μεθοδολογία βάσει της οποίας είναι δυνατή η αντιμετώπιση τόσο ισοστατικών όσο και υπερστατικών σκελετικών κατασκευών, οι οποίες χρησιμοποιούνται για τη μοντελοποίηση συνεχών μέσων, σύμφωνα με την κλασσική θεώρηση του προβλήματος βέλτιστης κατανομής υλικού.

Στο 6^{ο} Κεφάλαιο εξετάζεται η επέκταση της θεώρησης που παρουσιάστηκε στο 5^{ο} Κεφάλαιο, σε προβλήματα 2Δ συνεχών μέσων, τα οποία αντιμετωπίζονται ως τέτοια. Και πάλι, εξετάζονται δύο προσεγγίσεις. Σύμφωνα με την πρώτη προσέγγιση, η επανασχεδίαση του συνεχούς μέσου επιτυγχάνεται σε επίπεδο πάχους πεπερασμένων στοιχείων, ενώ σύμφωνα με την δεύτερη προσέγγιση, η επανασχεδίαση επιτυγχάνεται μέσω της ανεξάρτητης μετακίνησης κόμβων του πλέγματος, ακόμα και εάν αυτοί ανήκουν στο ίδιο πεπερασμένο στοιχείο. Επίσης, εξετάζεται η επανασχεδίαση σύμφωνα με την μέθοδο ESO (ολική αφαίρεση πεπερασμένων στοιχείων) και σύμφωνα με μία προτεινόμενη παραλλαγή της μεθόδου, η οποία προέκυψε ότι οδηγεί σε ανώτερες σχεδιάσεις, ενώ απαιτεί και λιγότερες επαναλήψεις.

Στο 7^{ο} Κεφάλαιο εξετάζεται το πρόβλημα της ελαχιστοποίησης του κόστους μίας μηχανολογικής κατασκευής, μέσα από την επιδίωξη της ελαχιστοποίησης του βάρους της κατασκευής και την ταυτόχρονη επιδίωξη της μεγιστοποίησης της κοινοτυπίας της ίδιας κατασκευής. Για τον σκοπό αυτό, παρουσιάζεται μία πρωτότυπη διαδικασία ομαδοποίησης και διαγραφής δομικών στοιχείων σε σκελετικές κατασκευές. Επίσης, εξετάζεται η ελαχιστοποίηση του κόστους κατασκευής δεξαμενών αποθήκευσης πετρελαιοειδών ως παράδειγμα ελαχιστοποίηση του κόστους μίας πραγματικής κατασκευής από ελάσματα, λαμβάνοντας υπόψη το κόστος των μέσων σύνδεσης (συγκόλληση) αλλά και την αναξιοποίητη ποσότητα της πρώτης ύλης (φύρα). Το εν λόγω παράδειγμα αποτελεί αντιπροσωπευτική περίπτωση κατά την οποία η διαδικασία βελτιστοποίησης

πρέπει να διαμορφωθεί κατάλληλα, έτσι ώστε να ανταποκρίνεται στις απαιτήσεις της εκάστοτε συγκεκριμένης εφαρμογής.

Στο 8^{ο} Κεφάλαιο διατυπώνεται μία πρωτότυπη ευριστική μέθοδος συνδυαστικού τύπου, κατάλληλη για την ελαχιστοποίηση του βάρους μίας κατασκευής αποτελούμενης από τυποποιημένες διατομές εμπορίου. Ως εφαρμογές, εξετάζονται τυπικές περιπτώσεις από τον χώρο των γερανογεφυρών, ενώ παρατίθεται και μία εφαρμογή μεγάλης κλίμακας (ελαχιστοποίηση βάρους υποστέγου αεροσκαφών).

Στο 9^{ο} Κεφάλαιο καταγράφονται επιγραμματικά τα συμπεράσματα τα οποία προκύπτουν από την παρούσα Διδακτορική Διατριβή, ενώ διατυπώνονται και σκέψεις για περαιτέρω έρευνα.

Τέλος, στο Παράρτημα Ι παρατίθεται μία σειρά παραδειγμάτων βελτιστοποίησης πραγματικών κατασκευών είτε μελετώντας παραμετρικά τα βασικά σχεδιαστικά χαρακτηριστικά της κατασκευής (ανάλυση ευαισθησίας), είτε αξιοποιώντας τις δυνατότητες βελτιστοποίησης που είναι ενσωματωμένες σε εμπορικό λογισμικό ανάλυσης κατασκευών με τη Μέθοδο των Πεπερασμένων Στοιχείων (ΜΠΣ).

Μέρος της παρούσης Διδακτορικής Διατριβής έχει καταγραφεί σε δύο δημοσιεύσεις σε έγκριτα επιστημονικά περιοδικά και σε 25 εργασίες σε διεθνή επιστημονικά συνέδρια.

To those who passed away early
and
to those who live in
high moral, endless stamina and mental greatness …

This page has been left intentionally blank

Acknowledgements

A PhD Thesis is a lot of things, among them an adventurous journey in the design space of science, and not only. With the current work, the author's aforementioned adventurous journey ends. At this point it would be improper, even an insolence, not to mention certain persons without the presence of which certain goals would not have been achieved. First of all, I am more than grateful to my parents, Timoleon and Nafsika, and to my sister, Athina. The reason for this is more than obvious and any attempt to justify it would just degrade their priceless contribution. Furthermore, I would like to express my gratitude to my supervisor Prof. Christopher Provatidis, as well as my acknowledgements to the members of my Advisory Committee, Prof. A. Kanarachos and Assoc. Prof P. Makris. Finally, I would like to acknowledge everyone that I had the chance and the honor to collaborate with during this journey. Their presence will ineffaceably remain in my memory.

This journey is over – end of mission. It's high time another journey began….

Demetrios T. Venetsanos

July 2009

This page has been left intentionally blank

Preface

The present PhD thesis concerns the optimization of engineering structures and more particularly the weight minimization of a structure when various and different constraints are imposed. This subject is most important and popular in the Engineering community, with a wide range of research, application and history. Based on the existing literature, the structural optimization methodologies may be categorized in three large groups: those concerning size optimization, those concerning topology optimization and those concerning shape optimization. The first group includes those methodologies that seek the cross-section of the structural members for the total weight to be minimized and for no constraint to be violated. The second group includes those procedures which result in the formation of holes inside the design domain by appropriately moving inner nodes; in this way, redundant material is removed and the structural weight is minimized while no constraint is violated. The third group includes those methods according to which the border nodes are appropriately moved so that again the structural weight is minimized and all of the constraints are fulfilled. In the most general case, the aforementioned optimization problems are not uncoupled. This is the reason why the interest has been focused on methodologies that simultaneously deal with all three problems. From this viewpoint, the term 'layout optimization' refers to that optimization procedure that seeks for the best distribution/configuration/layout of the available material so that the objective target is achieved, while at the same time the imposed constraints are not violated. According to G.I.N. Rozvany, a distinguishing person in the field of Computational Mechanics, there are two possible approaches for the layout optimization problem, the former being termed as the 'classical layout optimization' and the latter being termed as 'advanced layout optimization'. In the current Thesis, the aforementioned consideration was adopted, and served as a basis on which known optimization techniques were investigated, their limits were defined and new suggestions for improving their performance were proposed. In addition, new novel approaches were introduced and evaluated through a comparison with already existing ones.

The main contribution of the present thesis boils down to the formulation of a novel, energy-oriented, weight minimization procedure, which was used to successfully solve the generalized problem of minimizing the structural weight under a displacement constraint. Extending this approach, the problem of minimizing the structural weight under a stress constraint was also solved.

In brief, in the present Thesis:

- the state-of-the-art procedures for optimizing engineering structures were gathered, with emphasis being put on those procedures applicable to the shape and topology optimization of structures,
- characteristic literature examples were investigated for understanding better the applied procedures and disclosing weak points that needed to be improved,
- new performance indices were introduced, suitable for evaluating the examined optimization procedures,
- variations of approaches found in the literature were introduced, the variations providing an improved performance with respect to the initially stated procedures,
- new numerical schemes for structural optimization were developed,

- codes in FOTRAN, MatLab and APDL (the programming language found in Ansys, which is a commercial software for structural analysis) were developed and finally
- the entire research work was supported with three journal papers and 27 papers in world congresses and international conferences.

However, as mentioned earlier, the main contribution of the present Thesis was the successful handling of two types of optimization problems.

More particularly, in the literature, from the early 70s, the solution to the single constraint optimization problem was known. However, this type of problem strictly assumed that, at the optimum, not only was one displacement constraint active but also the corresponding degree of freedom was a priori known. In the present Thesis, the generalization of this problem was solved meaning that the aforementioned a priori knowledge was removed. The solution was achieved using an energy-oriented procedure based on the Lagrange multipliers method, but, opposing to the existing published approaches, the estimation of such a multiplier is avoided.

Extending the aforementioned proposed approach, the theoretical solution to the problem of imposing a single stress constraint was also solved. In this case, again only one constraint, a stress constraint this time, is active at the optimum but it is not known a priori the structural member corresponding to the active constraint. Once again, even though the solution was based on the Lagrange multipliers method, such a multiplier was not necessary to be estimated, while no assumptions concerning the indeterminacy of the structure was made. Due to this reason, the proposed approach outmatches the most popular and widely known Stress-Ratio (SR) technique because the latter tends to make all structural members take on the maximum allowable stress (Fully Stressed Design), which has been mathematically proved to be an optimal design only if certain conditions of determinacy hold.

Regarding the structure of the present Thesis, in Chapter 1 the generalized problem of minimizing the structural weight is stated and some of the modern optimization methodologies attacking this problem are briefly referred. More particularly, general deterministic mathematical programming methods are presented. Similarly, the most representative stochastic optimization methods are discussed. In the sequel, the so-called Optimality Criteria are mentioned; these are statements that describe some sort of energy state at the optimum. In the same Chapter, the homogenization method by Kikuchi, the SIMP method by Bendsøe, the Method of Moving Asymptotes by Svanberg, the Bubble method by Eschenauer as well as the Evolutionary Structural Optimization (ESO) method by Xie and Steven are presented.

In Chapter 2, some of the most well-known and widely-used optimization methods, both deterministic and stochastic are thoroughly evaluated through an extensive series of literature benchmarking problems (mathematical functions and trusses). Furthermore, a novel hybrid optimization method combining a deterministic search direction, using Powell's method, and a stochastic determination of the step size, using Simulated Annealing, is introduced. According to the presented evaluation, this method outperforms the competition but has a higher computational cost.

In Chapter 3, the structural optimization problem is approached from an energy viewpoint that concerns the, partial or total, removal of excessive material from a continuum aiming at its weight reduction but without violating any of the imposed constraints. In the same chapter the compliance

constraint optimization problem is discussed, as well as the problem of minimizing the structural weight for a Fully Stressed Design (FSD).

In Chapter 4, the optimization of a structure utilizing FSD is examined. In the beginning, skeletal structures, substituting the continuum, are examined, while in the sequel the continuum is examined as such. More particularly, two approaches are presented, the former being the redesign of the continuum using finite elements of constant thickness and the latter using for the redesign finite elements of element-wise variable thickness, thus permitting the uncoupled movement of the nodes, even if these nodes belong to the same element. In the sequel, the application of the (FSD) and the (ESO) methods in plates is examined. Furthermore, for the minimum weight of a 3D continuum through the total removal of finite elements, a removal scheme using the von Mises stress was applied and compared to a proposed variation, which the cases studied show that outperforms the originally stated approach because it results in better designs and in a lower number of iterations. Finally, a theoretical solution to the, as coined in the present Thesis, extended single stress constrained problem is introduced.

In Chapter 5, the, as coined in the present Thesis, extended single displacement constrained problem is solved for skeletal structures. The solution is based on a novel redesign procedure and the validity of the proposed method is thoroughly examined through 48 examined cases. The applicability of this procedure extends to both determinate and indeterminate structures.

In Chapter 6, the applicability to 2D continua of the procedure introduced in Chapter 5 is examined, when the 2D continua are dealt as such. Once again, two approaches are examined the former being the implementation of constant element-wise thickness and the latter being the implementation of variable element-wise thickness. On top of that, a variation of the (ESO) method is introduced. According to this variation, the criterion for selecting the redundant material (finite elements) to be removed is normalized with respect to the active part of the structure. This variation is shown to result in better designs and with a lower computational cost.

In Chapter 7, the problem of minimizing the cost of an engineering structure is examined through minimizing the structural weight and increasing the commonality of the remaining structural members. To this end, a novel procedure for skeletal structures is introduced implementing two operators, one for grouping structural members with similar cross section (commonality) and one for eliminating redundant structural members. On top of that, the real-life problem of minimizing the cost of oil tanks is examined. In this case, for the cost minimization, the cost for welding, as well as the quantity of the remaining unexploited material (scrap), is taken into consideration.

In Chapter 8, a novel heuristic combinatorial optimization method is introduced, suitable for minimizing the weight of structures assembled from standard beams or standard plates. As real-life applications, crane girders and crane runway beams, as well as a hangar, are examined.

In Chapter 9, the conclusions of the present Thesis and ideas for further research are briefly presented.

Last, in Appendix I, the optimization of a series of real-life engineering structures is examined either through the implementation of a sensitivity analysis with respect to the basic geometric characteristics of the structures or through the use of optimizers embedded in commercially available software suitable for structural analysis with the Finite Element Method (FEM). For the needs of this section, optimizers found in Ansys were used.

This page has been left intentionally blank

TABLE OF CONTENTS

LIST OF FIGURES

LIST OF TABLES

This page has been left intentionally blank

CHAPTER 1

The generalized optimization problem of minimum structural weight

---

In this chapter, the generalized optimization problem of minimum structural weight is stated and some of the most well-known and important structural optimization methodologies are presented within an adequately extensive literature review.

1.1. Introduction

The term 'optimization' has always been one of the most popular terms, due to the fact that it reflects the desire of achieving a certain goal using the least possible sources. Therefore, this term has a classical and decisive importance, emerging in all expressions of life, from the creation of the universe itself and the everyday struggle for survival to the most unique human achievements.

Looking back to the very birth of the universe and according to the most modern cosmogonic theory, at first, matter started to scatter after the Big Bang and then, slowly but progressively, the formation of the celestial bodies took place. However, these bodies are nothing else than matter restrained in stable structures, which are structures characterized by a low energy level. Therefore, the celestial bodies have been created through a sort of optimization procedure where the objective was the minimization of the energy level of the body. There is a great many number of examples in optimization found in the immediate environment of the human. The trunk of almost all trees has a larger cross-section near its root and becomes smaller towards the tree apex, thus both facilitating the development of a more effective nutrition network and allowing for carrying more safely strong wind loads. The fish and other creatures living in the water have hydrodynamic shapes, so that their motion in the water is characterized by low energy losses due to water friction; that is, with these shapes, the aforementioned creatures have been optimally adapted to their physical environment. Furthermore, the light bone structure of the birds, in combination with flexible flow-control surfaces (wings), forms a flying machine with improved characteristics. The list of such examples is very long, since the evolutionary procedure that takes place in nature is nothing else than preserving and updating those characteristics that endure a higher probability for survival, as the Darwinian approach dictates. In other words, it is about characteristics derived from some sort of optimization procedure aiming at maximizing the probability of survival. Of course, in all of these cases, the final result is not necessarily the best possible (optimum); however, it is significantly improved compared to the initial state and, in many cases, this is adequately enough.

Apart from observing the way that nature implements the concept of optimization, man himself embodied this concept in his everyday life from the early moments of his existence. In order first to ensure his survival and then to improve his standard of living, man was forced to find ways of using the resources available in his surrounding environment. His first and main priority was to develop techniques both for finding food and for protecting himself from whatever he considered as a threat. Towards this direction, man started using pointed objects, such as pointed stones and branches. Based on his imagination and ingenuity, he started developing techniques in order to make his weapons more lethal; that is, to cause the maximum possible damage with the least possible effort. The same elements of imagination and ingenuity were also used in more amicable designs, such as the invention of the wheel (optimum shape for rolling), the use of clothes depending on the season (optimum use of natural fibres for protection against the cold during the winter and the heat during the summer), the construction of houses (optimum protection against the elements of nature) and the construction of ships (optimum means for sea transportations).

Apart from seeking the best possible solutions for problems related to his survival, man started embedding the optimization concept in other aspects of life as well, such as athletics, art, military and religion. Numerous distinctive examples may be found in the ancient Greek civilization. In more details, during athletic competitions, an athlete had to perfect (optimize) his technique in order to achieve the best performance and win. The ancient Greek theatres are famous for their excellent acoustic; that is, they have been built in such a way (optimum way) so that the same crystal clear and loud sound is distributed all over the theatre. During the symposia, the delicacies were served in such an order and the day-beds were of such

shapes so that the guests could be highly pleased (optimization in delight). The battleships had a ram bow not only for minimizing the hydrodynamic resistance (optimizing the cruise) but also for ramming enemy ships (optimizing the military performance of the ship). The columns found in the ancient Greek temples have a circumferential uniform distribution of ribs; these ribs provide an optimum aestheticism when light is shed over them, as is apposite to places of worship, and an optimum structural reinforcement of the columns with respect to their strength against bending loads, as in earthquakes. In addition, Ancient Greek architects designed marble beams (coffer slabs, ceiling beams) using different techniques (stiffening/hollowing), in order to meet the relevant requirements, namely structural integrity and lightness. For instance, in order to facilitate the transportation of heavy marbles in the mountainous region of Apollo Epicurios at Bassae, instead of stiffening the porch beams, the architect decided to hollow them out reducing the weight by 50%, while it can be shown that these U-shaped beams were hollowed out to such a degree that the maximum bending stress remains lower than that of the initial block.

Similar examples of applied optimization may be found in all civilizations and at all times. The common characteristic in these cases is that the optimal result is mainly sought though a trial-and-error procedure. However, during the last two centuries, the development of mathematics made possible the statement of both optimization problems and optimization solution procedures in a formal and systematic manner. Especially in the field of Mechanics, a titanic effort for developing, exploring and exploiting effective optimization procedures has been taking place during the past sixty years, that is, since the birth of Computational Mechanics. The most impressive achievements resulting from these efforts have been recorded as monumental moments of conquering the deep seas, the sky and the outer space. These achievements have been derived while seeking the distribution of the least material quantity required for building a structure which can carry with safety the externally applied loads while violating none of the imposed constraints related to the response of the structure. That is, these achievements result from trying to solve the generalized optimization problem of minimizing the structural weight.

1.2. Statement of the generalized problem of minimizing the structural weight

In the generalized problem of minimizing the structural weight, a design vector $\mathbf{X}$ is sought such that a scalar quantity $f(\mathbf{X})$ is minimized under the restriction that no imposed constraints, both equality $h_j(\mathbf{X}) = 0$ and inequality $g_j(\mathbf{X}) \le 0$, are violated. The mathematical statement of this problem is the following:

$$\min f(\mathbf{X}), \mathbf{X} = [x_i],\ x_{i,lower} \le x_i \le x_{i,upper} \tag{1.1}$$

such that:

$$\begin{aligned} &h_j(\mathbf{X}) = 0, \quad j = 1, 2, ..., m \\ &g_j(\mathbf{X}) \le 0, \quad j = m+1, m+2, ..., p \end{aligned} \tag{1.2}$$

where:

$$\mathbf{X} = \begin{bmatrix} x_1 & x_2 & \dots & x_n \end{bmatrix}^T \tag{1.3}$$

The quantity f is called the objective function, the vector $\mathbf{X}$ contains all the independent design variable of the problem, while the elements x_i of $\mathbf{X}$ are called design variables. Each one of the design variables has its own domain. For mechanical structures, the domain of the design variables must be adequately wide. Having in mind that mechanical structures have a physical substance and are not abstract theoretical concepts, both the lower bounds $x_{i,lower}$ and the upper bounds $x_{i,upper}$ must obtain logical values with physical meaning. The number n of the design variables denotes the dimension of the solution space R^n of the corresponding optimization problem. In case where the maximization of the objective function is sought, then the following statement is used:

$$\max f(\mathbf{X}) = \min(-f(\mathbf{X})) \tag{1.4}$$

The number n of the design variables depends on neither the number m of the equality constraints nor the number p of the inequality constraints. In case were $m = p = 0$, then the optimization problem is characterized as 'unconstrained', while in the opposite case, that is when $m \neq 0$ and/or $p \neq 0$, then the optimization problem is characterized as 'constrained'.

With respect to the constraints, a constraint is called linear, when it is expressed as a linear combination of the design variables, and non-linear in any other case. Furthermore, an objective function is characterized as linear, when it is expressed as a linear combination of the design variables, and non-linear otherwise. In the special case where the objective function and all of the constraints (both equality and inequality) are linear, the optimization problem is characterized as linear. In any other case, it is characterized as non-linear.

With respect to the existence of a minimum, generally speaking, the range of a function f defined in the solution space R^n may have none, one or many local minima. In the first case, the function is constant thus independent from the design vector:

$$f(\mathbf{X}) = ct, \quad \forall \mathbf{X} \in R^n \tag{1.5}$$

In the second case, there is a design vector $\mathbf{X}_{opti}$ for which it holds:

$$f(\mathbf{X}_{opti}) < f(\mathbf{X}), \quad \forall \mathbf{X} \in R^n, \ \mathbf{X} \neq \mathbf{X}_{opti} \tag{1.6}$$

In the third case, there are many design vectors $\mathbf{X}_{local\_opti,k}$, $k = 1,2,..,l$ for which it holds:

$$f(\mathbf{X}_{local\_opti,k}) < f(\mathbf{X}_{local\_opti,k} \pm \varepsilon) \tag{1.7}$$

where ε is a small positive quantity. Among the design vectors $\mathbf{X}_{local\_opti,k}$, it is possible that there exists a design vector $\mathbf{X}_{local\_opti,g}$ such that:

$$f(\mathbf{X}_{local\_opti,g}) < \min\left\{ f(\mathbf{X}_{local\_opti,k}), k = 1,2,..,g-1,g+1,..,l \right\} \tag{1.8}$$

In this case, the vector $\mathbf{X}_{local\_opti,g}$ corresponds to the global minimum value (minimum between the minimum values of the function). At this point, it is clarified that a function f may have the same minimum value for different design vectors (solution multiplicity).

The optimization problem, as stated in Eqs.(1.1-1.3), is general and applicable in any case that the minimum structural weight is sought. As mentioned in the Introduction, based on the existing literature, the methodologies attacking this problem may be categorized in three large groups: those concerning size optimization, those concerning topology optimization and those concerning shape optimization. The first group includes those methodologies that seek the cross-section of the structural members for the total weight to be minimized and for no constraint to be violated. The second group includes those procedures which result in the formation of holes inside the design domain by appropriately moving inner nodes; in this way, redundant material is removed and the structural weight is minimized while no constraint is violated. The third group includes those methods according to which the border nodes are appropriately moved so that again the structural weight is minimized and all of the constraints are fulfilled. In the most general case, the aforementioned optimization problems are not uncoupled. This is the reason why the interest has been focused on methodologies that simultaneously deal with all three problems; these are the so-called layout optimization methods.

Without loss of generality, the optimization of a structure, or, more correctly, the optimization of the design of a structure, constitutes a systematic procedure of determining that design, among many feasible ones, that satisfies in the best possible way one or more objectives, while at the same time fulfils well-defined constraints referring to the design variables and the behavior of the structure under optimization. In most cases, the optimization of a structure is sought using an iterative procedure, the route of which as well as its ending are strongly affected by many factors, such as the size of the design domain, the form of the objective function, the imposed constraints and the accuracy used for terminating the iterative optimization procedure. Even though the scientific community is systematically and intensively active in the field of optimization, especially during the past decades, no procedure has been stated so far that can be proved to solve the generalized optimization problem successfully. This means that tracing the global optimum for the generalized optimization problem still remains the Holy Grail for the scientific community.

1.3. Short historical review

Optimization, as mentioned in Section 1.1, is dated since the creation of the world. However, the first optimization problems stated in the formal and strict language of mathematics are dated some centuries B.C. More specifically, Euclid (300B.C.) dealt with various optimization problems, such as finding the shortest distance between a given point and a given line, finding the shortest and the longest line that can be drawn from a given point to the circumference of a given point and finding the largest parallelogram that can be drawn for a parallelogram of given perimeter. In addition, Heron of Alexandria (100B.C.) dealt with the problem of finding the shortest distance that a light beam travels between two given points in space (Russo, 2004).

Several centuries later, Fermat (1657) stated the general principle that light requires the minimum time when it travels between two points (Veselago, 2002), while Cauchy (1847) presented for the first time a mathematically-based optimization procedure (Method of Steepest Descent), in which first derivatives of the objective function were implemented (Cauchy, 1847). Due to the development of the numerical analysis, the mathematical theory of optimization was introduced and the so-called Mathematical Programming Optimization Methods were formed. The beginning of the modern era of optimization was denoted by the

pioneering papers by Courant (1943) on the penalty functions (Courant, 1943), Dantzig (1951) on linear programming (Dantzig, 1951), Karush (1939) and Kuhn & Tucker (1951) on the necessary and sufficient conditions for optimality in constrained problems (Karush, 1939; Kuhn and Tucker, 1951). During the 60's numerous mathematical methods for solving non-linear optimization problems were published. Rosenbrock (1960) presented the Method or Orthogonal Directions (Rosenbrock, 1960), Rosen (1960) suggested the Gradient Projection Method (Rosen, 1960), Zoutendijk (1960) introduced the Method of Feasible Directions (Zoutendijk, 1960), Hooke και Jeeves (1961) developed a pattern search method (Hooke and Jeeves, 1961), Davidon, Fletcher and Powell (1963) introduced the Variable Metric Method (Fletcher and Powell, 1963), Powell (1964) suggested the Conjugate Direction Method (Powell, 1964), Fletcher and Reeves (1964) presented the Method of Conjugate Gradients (Fletcher and Reeves, 1964), Nelder and Mead (1965) suggested a variation of the Simplex Method (Nelder and Mead, 1965), Box (1965) published the homonymous method (Box, 1965), while Fiacco and McCormick (1966) formed the so-called Sequential Unconstrained Minimization Technique (SUMT) (Fiacco and McCormick, 1966).

From the previous brief report of only but a few of the hundreds papers published during the 60s on optimization, it becomes clear that, during that period of time, optimization methods and their variations were being presented at very high rates. However, the vast majority of those methods and variations were deterministic, meaning that no matter how many times the procedure is initiated from the same design vector $\mathbf{X}_{ini}$, always the same final design vector $\mathbf{X}_{fin}$ is derived, which is not ensured that describes the global optimum design (it often corresponds to a local optimum design). Since the methodologies of this type are based on the generalized optimization problem, it is possible to be used in any type of optimization problem, independently of the inherent nature of the problem, as long as the statement described in Eqs.(1.1, 1.2) is followed. Due to the general character of the aforementioned optimization procedures, initially it was believed that these procedures could be used for solving structural optimization problems as well. At the same time, significant steps forward were achieved in developing new computational systems which appeared more and more frequently with more and more computational power. Eventually, a strong belief started to be formed according to which it was just a matter of time until such optimization methods could be used for solving efficiently structural optimization problems. However, the initial enthusiasm did not last for very long. In practice, it was proven that the aforementioned methodologies presented two major drawbacks, the former being that these procedures could easily get trapped into local minima and the latter being that the computational cost increased significantly, even becoming prohibitive, as the number of the design variables increased. These two issues became the apple of discord between the members of the scientific community, who soon enough were separated in two groups: those in favor of the Mathematical Optimization Methods (MOPs) and those in favor of methods based more on an engineering viewpoint.

Those advocating the (MOPs) were claiming that the necessary element for stating any kind of optimization method was the formulation of a sound mathematical background; therefore, according to their opinion, the right way of conducting research was by investing time and effort in extending already existing methods, in investigating in a more thorough way already stated methods or even in developing entirely new procedures but without any trade-offs concerning the existence of the aforementioned mathematical background. Within this framework, a step forward was the formulation of the sequential programming techniques, such as Sequential Linear Programming (SLP) and the most powerful Sequential Quadratic Programming (SQP) (Venkatamaran, 2002). However, the revolutionary new element was the introduction of randomness during the optimization procedures, which increased the probability of not getting trapped at local minima. Among the most important

delegates of this trend, one must refer the Evolutionary Strategies (Rechenberg, 1989), the Genetic Algorithms (Goldberg, 1989) and the Simulated Annealing (Kirkpatrick, 1984).

On the other hand, those advocating the use of an engineering viewpoint, supported the development of methodologies that had a less strict mathematical background but allowed for the engineer's intuition and judgment to be a part of the optimization procedure. In the same category, one can find methodologies whose validity can be proved in a strict mathematical way but only for some specific cases, while their generalization is accepted as an adequate approximation. Within this frame, the famous Optimality Criteria (OC) methods were developed; that is methods which describe explicitly or implicitly some kind of energy state at the optimum. The (OC) statements were also combined with elements of numerical analysis, such as the gradient of a vector function and the binomial expansion, resulting in powerful optimization procedures. However, these procedures were suitable only for structural optimization problems exactly because they were formulated using inherent characteristics of the problem to be solved (strain energy or some other similar expression). The golden age of the (OC) methods, as proved from the huge numbers of published papers at that time, was the 70s. Indicatively, it is mentioned that it was reported (Sargent, 1980) in 1979 papers on (OC) methods were being published at the rate of about 200 per month in more than 30 journals, not counting conference proceedings and special collections (a conference in 1979 added 450 papers to the list). The spearhead of the (OC) approaches was the fact that they were able to handle very large numbers of design variables since they used the same simplified redesign formula for all of the design variables.

Between the two aforementioned groups, the most significant difference concerns the perception with respect to the description of the objective target. From the Engineer's viewpoint, the objective target is the formulation of a design which is adequately optimized under the strict assumption that all of the imposed constraints are either not violated or violated in such a way that the structural behavior is negligibly affected. In other words, from the Engineer's viewpoint, the objective target is to find a feasible design that satisfactorily compromises the demand for high-level safety with the demand for a low cost. On the contrary, the mathematical perception requires a completely theoretical approach, without taking into consideration the physical interpretation of the involved quantities. Consequently, it rejects solutions which are either non- strictly proved to be optimal or non-optimal but of high practical value. As always in such cases, the optimum compromise lies somewhere in the middle, meaning that neither the theoretical-mathematical background nor the Engineer's intuition and judgment may be neglected. As a matter of fact, it is the combination of those that results to the best possible designs, as far as structural optimization is concerned.

From the short history review mentioned in this section, it becomes obvious that numerous methodologies and even more papers have been published on the layout optimization of structures. In the literature, one can find very enlightening review papers referring to hundreds of papers, while there are many textbooks that one may consult in order to find detailed information on a specific optimization method. Therefore, it is not the intention of the writer to refer to information that can be retrieved from the literature and for this reason a short description and an extended bibliography is reported for the most significant categories of optimization problems and/or procedure.

1.4. Representative optimization methods

A first categorization of the existing optimization methods is with respect to the explicit or the implicit way of searching for the optimum. From this viewpoint, there are methods that seek to explicitly minimize the structural weight, while, on the other hand, there are methods that aim at fulfilling a certain criterion that describes the structural energy state at the optimum. In addition, the explicit optimization methods may be further subdivided into two

categories, the former including the deterministic and the latter including the stochastic optimization methods.

In the category of the explicit deterministic optimization methods, one may find the method by Hooke & Jeeves, the Simplex method, the Complex method (Box), the Powell's method, the Steepest Descent Method, the Conjugate Gradient Method, the Conjugate Direction Method, the Sequential Linear Programming (SLP) and the Sequential Quadratic Programming (SQP).

In the category of the explicit stochastic optimization methods, the most characteristic representatives of which are the Evolution Strategies (ES) with all of their variations, the Genetic Algorithms (GA), again with a vast number of variations, the Simulated Annealing (SA), the Tabu Search Method, the Swarm Particles Technique and the Harmony method. For each one of the aforementioned methods, a short description follows.

Evolution strategy (ES) is an optimization technique based on ideas of adaptation and evolution. It was created in the early 1960s and developed further along the 1970s and later by Rechenberg, Schwefel and his co-workers, and belongs to the more general class of evolutionary computation or artificial evolution. Evolution strategies use natural problem-dependent representations, and primarily mutation and selection as search operators. As common with evolutionary algorithms, the operators are applied in a loop. An iteration of the loop is called a generation. The sequence of generations is continued until a termination criterion is met. As far as real-valued search spaces are concerned, mutation is normally performed by adding a normally distributed random value to each vector component. The step size or mutation strength (i.e. the standard deviation of the normal distribution) is often governed by self-adaptation (see evolution window). Individual step sizes for each coordinate or correlations between coordinates are either governed by self-adaptation or by covariance matrix adaptation (CMA-ES). The (environmental) selection in evolution strategies is deterministic and only based on the fitness rankings, not on the actual fitness values. The simplest (ES) operates on a population of size two: the current point (parent) and the result of its mutation. Only if the mutant's fitness is at least as good as the parent one, it becomes the parent of the next generation. Otherwise the mutant is disregarded. This is a (1+1)-ES. More generally, λ mutants can be generated and compete with the parent, called (1+λ)-ES. In a (1,λ)-ES the best mutant becomes the parent of the next generation while the current parent is always disregarded (Beyer, 2001; Beyer and Schwefel, 2002; Rechenberg, 1971; Schwefel, 1995; Schwefel, 2002).

A Genetic Algorithm (GA) is a search technique used in computing to find exact or approximate solutions to optimization and search problems. Genetic algorithms are categorized as global search heuristics and are a particular class of Evolutionary Algorithms (EA) that use techniques inspired by evolutionary biology such as inheritance, mutation, selection, and crossover. Genetic Algorithms are implemented in a computer simulation according to which a population of abstract representations (so-termed 'chromosomes') of candidate solutions (so-termed 'individuals') to an optimization problem evolves toward better solutions. The most common type of representation is to use the binary of the Gray code, that is strings of 0s and 1s, but other encodings are also possible. The evolution usually starts from a population of randomly generated individuals and takes place in generations. In each generation, the fitness, that is the value of the augmented objective function, of every individual in the population is evaluated, multiple individuals are stochastically selected from the current population (based on their fitness), and modified (recombined and possibly randomly mutated) to form a new population. The new population is then used in the next iteration of the algorithm. With respect to the termination criteria of a typical GA, it is possible to use either a maximum number of generations or a satisfactory fitness level for the population. However, if the algorithm has terminated because the maximum number of

generations has been reached, it is not necessary for a satisfactory solution to have been found. A typical genetic algorithm requires a genetic representation of the solution domain and a fitness function to evaluate the solution domain. A standard representation of the solution is as an array of bits, while arrays of other types and structures can be used in essentially the same way. The main characteristic that makes these genetic representations convenient to handle is that their parts are easily aligned due to their fixed size, which facilitates simple crossover operations. However, it is possible to use variable length representations as well but in this case crossover implementation is more complex. The fitness function is defined over the genetic representation and measures the quality of the represented solution. The fitness function is always problem dependent. A representation of a solution might be an array of bits, where each bit represents a different object, and the value of the bit (0 or 1) represents whether or not the object is in the knapsack. In some problems, it is hard or even impossible to define the fitness expression; in these cases, interactive genetic algorithms are used. Once the genetic representation and the fitness function are defined, GA proceeds to initialize a population of solutions randomly, then improve it through repetitive application of mutation, crossover, inversion and selection operators (Goldberg, 1989; Goldberg, 2002; Fogel, 2006; Holland, 1975; Koza, 1992; Michalewicz, 1999).

Simulated annealing (SA) is a related global optimization technique that traverses the search space by testing random mutations on an individual solution. A mutation that increases fitness is always accepted while a mutation that lowers fitness is accepted probabilistically based on the difference in fitness and a decreasing temperature parameter (Metropolis criterion). In (SA) terminology, the lowest energy, instead of the maximum fitness, is sought. (SA) can also be used within a standard GA algorithm by starting with a relatively high rate of mutation and decreasing it over time along a given schedule (Kirkpatrick et al, 1983; Cerny, 1985; Metropolis et al, 1953). Tabu search (TS) is similar to simulated annealing in that both traverse the solution space by testing mutations of an individual solution. While simulated annealing generates only one mutated solution, (TS) generates many mutated solutions and moves to the solution with the lowest energy of those generated. In order to prevent cycling and encourage greater movement through the solution space, a Tabu list is maintained of partial or complete solutions. It is forbidden to move to a solution that contains elements of the Tabu list, which is updated as the solution traverses the solution space. (TS) is a metaheuristic algorithm that can be used for solving combinatorial optimization problems (Glover and Laguna, 1997; Glover, 1989; Glover, 1990; Cvijovic et al, 1995).

Harmony search (HS) is a metaheuristic algorithm (also known as soft computing algorithm or evolutionary algorithm) mimicking the improvisation process of musicians. In the process, each musician, that is each decision variable, plays, that is generates, a note, that is a value, for finding a best harmony, that is the global optimum, all together. The (HS) algorithm has a novel stochastic derivative (for discrete variable) based on musician's experience, rather than gradient (for continuous variable) in differential calculus. The (HS) method is a recent numerical optimization technique that imitates the musical performance process which takes place when a musician searches for a better state of harmony. Jazz improvisation seeks to find musically pleasing harmony similar to the optimum design process which seeks to find the optimum solution (Saka and Kameshki, 1998; Erdal and Saka, 2006; Geem et al, 2001; Geem et al, 2002; Saka, 2003).

The Particle Swarm Optimization (PSO) is a direct search, stochastic, population-based computer algorithm, modeled on swarm intelligence. Swarm intelligence is based on social-psychological principles and not only does it provide insights into social behavior but also contributes to engineering applications. Social influence and social learning enable a person to maintain cognitive consistency. It is a fact that people solve problems by talking with other people about them. As they interact their beliefs, attitudes, and behaviors, they change. The

changes could typically be depicted as the individuals moving toward one another in a socio-cognitive space. The (PSO) resembles this kind of social behavior. More particularly, first the optimization problem must be clearly described and then an objective function for measuring the efficiency of a proposed solution is defined. In addition, a communication structure is also created, assigning neighbors for each individual to interact with. Then a population of individuals, also known as particles or candidate solutions, is defined as random guesses at the problem solutions is initialized. In the sequel, an iterative process aiming at improving these particles is initiated. The objective function is estimated for every candidate solution. The individual's best solution is called the particle best or the local best. Each particle makes this information available to their neighbors. They are also able to see where their neighbors have had success. Movements through the search space are guided by these successes, with the population usually converging, by the end of a trial, on a problem solution better than that of non-swarm approach using the same methods (Kennedy and Eberhart, 1995; Eberhart and Kennedy, 1995; Eberhart and Shi, 1998; Shi and Eberhart, 1998a; Shi and Eberhart, 1998b; Eberhart and Shi, 2001).

The ant colony optimization (ACO) is a probabilistic technique for solving optimization problems which can be reduced to finding good paths through graphs. (ACO) may be considered as a metaheuristic optimization procedure, the basic idea which is found in the way ants behave when seeking for food. In more details, ants initially wander randomly in search of food and when they succeed in doing so they return to their colony while laying down pheromone trails. If other ants detect such trails, it is highly probable to stop travelling at random and to start following the trails towards the food. Once they also find the food, they also return to their colony thus reinforcing the initial path with pheromone trails. However, the pheromone trails tend to evaporate thus trails corresponding to longer paths disappear faster than trails corresponding to shorter paths. In this way, shorter paths present higher pheromone densities and over time the ants are attracted to these densities thus preferring the shorter paths than the longer ones (Dorigo, 1992; Deneubourg et al, 1990; Di Caro and Dorigo, 1998; Dorigo and Blum, 2005; Dorigo and Gambardella, 1997; Dorigo et al, 1996; Dorigo and Stützle, 2004; Gutjahr, 2000; Stützle and Hoos, 2000; Serra and Venini, 2006).

In the category of the implicit optimization methods, one may find the so-termed Optimality Criteria and the seminal works by Michell, Venkayya, Gelatly, Khot, Berke, Allwood and Patnaik. In the same wavelength, the so-called COC and DCOC methods, developed by Rozvany and his team, remain on the top of the OC procedures. Since the most recent of these works have been published more than twenty years ago, these procedures cannot be regarded as state-of-the-art, thus related literature references are recorded (Michell, 1904; Venkayya, 1971; Allwood and Chung, 1984; Patnaik et al, 1993; Zhou and Rozvany, 1992/93; Rozvany and Zhou, 1989/90; Rozvany and Zhou, 1990).

Apart from all the aforementioned procedures, special reference must be made to methodologies that now are considered to be state-of-the-art. From this perspective, the homogenization method, the SIMP method, the Method of Moving Asymptotes (MMA), the bubble method as well as the ESO method must be referred.

In general, it is possible, from structural elements based on boundary variations, to get final designs that are topologically equivalent to the initial choice of design. For this purpose, stable computational schemes often require some kind of remeshing of the finite element approximation of the analysis problem. On the contrary, the so-called homogenization method refers to optimal shape design where no such drawbacks are present. This method is related to modern production techniques and consists of computing the optimal distribution in space of an anisotropic material that is constructed by introducing an infimum of periodically distributed small holes in a given homogeneous, isotropic material, with the requirement that

the resulting structure can carry the given loads as well as satisfy other design requirements (Bendsøe and Kikuchi, 1988).

Another approach of the shape optimization problem is to consider it as determining the optimal spatial material distribution for given loads and boundary conditions (SIMP method). In this way, every point in space is a material point or a void and the optimization problem is a discrete variable one. From this viewpoint, it is possible to describe various ways of removing this discrete nature of the problem by introducing a density function that is a continuous design variable. Domains of high density then define the shape of the mechanical element. For intermediate densities, material parameters given by an artificial material law can be used. Alternatively, the density can arise naturally through the introduction of periodically distributed, microscopic voids, so that effective material parameters for intermediate density values can be computed through homogenization. (Bendsøe, 1989).

The 'Method of Moving Asymptotes' (MMA) developed by Svanberg is an iterative process, in each step of which a strictly convex approximation subproblem is generated and solved. The generation of these subproblems is controlled by the so-called 'moving asymptotes', which may stabilize and speed up the convergence of the general process. This method is able to handle all kinds of constraints, the only limitation being that the derivatives of the constraint functions can be calculated, either numerically or analytically (Svanberg, 1987).

The so-called 'Bubble Method' developed by Eschenauer is based on the iterative positioning of new holes (termed as 'bubbles') into the present structure of the component. This concept is therefore called the 'bubble method'. The iterative positioning of new bubbles is carried out by means of different methods, among others by solving a variational problem. The insertion of a new bubble leads to a change of the class of topology. For these different classes of topology, hierarchically structured shape optimizations that determine the optimal shape of the current bubble, as well as the other variable boundaries, are carried out (Eschenauer, 1994).

The ESO method proposed by Xie and Steven has been developed to simplify the traditional structural optimization procedures. Its main idea is to find a Optimum Uniform Design (OUD), meaning to find that thickness for which the imposed constraints become active and then systematically remove material from the least efficient regions. Two variations of this extremely but working simple concept is the so-called Additive ESO (ESO) and the co-called Bidirectional ESO (BESO). The former enables the initiation of the optimization procedure from an under-dimensioned structure and then starts adding material onto the most efficient regions. The latter allows for both addition and removal of material from the structure.

Another very interesting category of optimization methods refers to integer programming techniques, which are suitable for solving the minimum structural weight problem when standard structural members, such as beams and plates, are to be used. In this category, one may find the branch-and-bound method and the cutting plane method of Gomory (Neumaier 1990, Hansen 1992, Ratschek and Rokne 1995, Kearfott 1996, Horst and Tuy 1996, Pintér 1996).

Apart from dealing with only one target, it is possible to seek for the best compromise between two or even more targets, which, on top of that, may be contradictory. A typical example is the desire to have a top speed vehicle with low-fuel consumption. The Pareto technique and the formation of the Pareto front still remains one of the most popular tools for dealing with such problems. In the same category of multi-objective problems, one may find the so-called MultiDisciplinary Optimization (MDO) problems, for which various disciplines are taken into consideration in the same optimization problem statement. Last but not least, the Design of Experiments (DOE), the use of Artificial Neural Networks (ANN), as well as

the implementation of meshless methods must be referred. Finally, an illustrative literature review is presented at the end of this chapter.

1.5. Recapitulation

From the aforementioned short literature review, it is more than obvious that a lot of researchers have done a lot on the area of structural optimization. The published works cover a very wide range of structural optimization problems, both in terms of optimization problem type (size, shape, topology, layout) and in terms of the disciplines involved (static or dynamic elasticity, thermal, acoustics, fluids etc). It is possible to distinguish several seminal works that serve not only as breakthrough points but also as an inspiration for the others. It is also possible to endlessly debate about the most promising concepts and methods that should be followed in the quest of the Engineer's Holy Grail, which is nothing less than the global optimum design. The bottom line is that the generalized structural optimization problem has not yet been solved thus the challenge for dealing with it either in its full statement or in some partial sub-problem statement remains a fascinating aim.

References

Allwood, R.J. and Chung, Y.S., (1984), Minimum-weight design of trusses by an optimality criteria method. *Int. J. Numer. Meth. Eng.* **20**, pp. 697–713

Bendsøe, M.P., (1989), Optimal shape design as a material distribution problem. Struct. Optimiz. **1**, pp.193–202

Bendsøe, M.P.; Kikuchi, N. (1988): Generating optimal topologies in structural design using a homogenization method.Comput. Meth. Appl. Mech. Engrg. 71, 197–224

Berke, L., (1970), An efficient approach to the minimum weight design of deflection limited structures', *AFFDL-TM-70-4*.

Berke, L., and Mallet, R. M., (1967), Automated large deflection and stability analysis of three-dimensional bar structures', Int. Sym. on Stru. Tech. for Large Radio and Radar Telescope Systems held at MIT, Cambridge, Mass.

Beyer, H.G., (2001), The Theory of Evolution Strategies: Springer-Verlag.

Beyer, H.G., Schwefel, H.P., (2002), Evolution Strategies: A Comprehensive Introduction. Journal Natural Computing, 1(1), pp.3-52.

Box, M.J., (1965), A New Method of Constrained Optimization and a Comparison with Other Methods, Computer J, Vol.8, pp.42-52.

Cauchy, A., (1847), Methode generale pour la resolution des systemes d'equations simultanes, Compt. Rend., Vol.25, pp.536-538.

Cerny, V., (1985), A thermodynamical approach to the travelling salesman problem: an efficient simulation algorithm. Journal of Optimization Theory and Applications, 45:41-51.

Courant, R., (1943)"Variational methods for the solution of problems of equilibrium and vibrations", *BullAmerMathSoc.*,Vol.49,pp.1–23.

Cvijovic, D.; Klinowski, J., (1995), Taboo search - an approach to the multiple minima problem". Science, 267, 664-666.

Dantzig, G. B., (1951), Maximization of a linear function of variables subject to linear inequalities,, *Activity Analysis of Production and Allocation, Koopman (Ed.)*, Cowles Commission Monograph, 13, John Wiley and Sons, New York.

Deneubourg, J.-L., Aron, S., Goss, S., Pasteels, J.M, (1990) The self-organizing exploratory pattern of the Argentine ant, Journal of Insect Behavior, 3:159–168.

Di Caro, G. and Dorigo, M., (1998), AntNet: Distributed stigmergetic control for communications networks. Journal of Artificial Intelligence Research, 9:317–365.

Dorigo, M. (1992), Optimization, Learning and Natural Algorithms (in Italian). PhD thesis, Dipartimento di Elettronica, Politecnico di Milano, Milan, Italy.

Dorigo, M., Maniezzo, V., Colorni, A., (1996), Ant System: Optimization by a colony of cooperating agents. IEEE Transactions on Systems, Man, and Cybernetics – Part B, 26(1):29–41.

Dorigo, M., Gambardella, L. M., (1997), Ant Colony System: A cooperative learning approach to the traveling salesman problem. IEEE Transactions on Evolutionary Computation, 1(1):53–66.

Dorigo, M., Stützle, T., (2004), Ant Colony Optimization. MIT Press, Cambridge, MA.

Dorigo, M. and Blum, C., (2005), Ant colony optimization theory: A survey. Theoretical Computer Science, 344(2–3):243–278.

Eberhart, R. C. and Kennedy, J., (1995), A new optimizer using particle swarm theory. Proceedings of the sixth international symposium on micro machine and human science pp. 39-43. IEEE service center, Piscataway, NJ, Nagoya, Japan.

Eberhart, R. C. and Shi, Y., (1998), Comparison between genetic algorithms and particle swarm optimization. Evolutionary programming vii: proc. 7th ann. conf. on evolutionary conf., Springer-Verlag, Berlin, San Diego, CA.

Eberhart, R. C. and Shi, Y., (2001), Particle swarm optimization: developments, applications and resources. Proc. congress on evolutionary computation 2001 IEEE service center, Piscataway, NJ., Seoul, Korea.

Erdal, F., Saka MP, (2006), Optimum design of grillage systems using harmony search algorithm. In: Proceedings of 8th international conference on computational structures technology

Eschenauer, H.A. (1994), 'Bubble method for topology and shape optimization of structures', Struct Optim. vol.8(1), pp.142-151.

Fiacco, A.V., McCormick, G.P. (1966), "Extension of SUMT for nonlinear programming: equality constraints and extrapolation", Management Science, Vol. 12, pp.816-828.

Fletcher, R., Powell, M.J.D. (1963), "A rapidly convergent descent method for minimization", Computer J., Vol.6(2), pp.163-168.

Fletcher, R., Reeves, C.M (1964), "Function Minimization by Conjugate Gradients", Computer J., Vol.7, pp.149-154.

Fogel, David B (2006), Evolutionary Computation: Toward a New Philosophy of Machine Intelligence, IEEE Press, Piscataway, NJ. Third Edition

Geem, Z.W., Kim , J.-H. and Loganathan, G.V., (2001), A new heuristic optimization algorithm: harmony search. Simulation **76(**2), pp. 60–68

Geem, Z.W., Kim, J.-H. and Loganathan, G.V., (2002), Harmony search optimization: Application to pipe network design. Int. J. Modell. Simulat. **22**(2),pp. 125–133.

Gellatly, R.A. and Berke, L., "Optimum structural design", *AFFDL_TR-70-165*, 1971.

Glover, F. "Tabu Search — Part I", ORSA Journal on Computing 1989 1: 3, 190-206.

Glover, F. "Tabu Search — Part II", ORSA Journal on Computing 1990 2: 1, 4-32.

Glover, F. and M. Laguna. (1997). Tabu Search. Kluwer, Norwell, MA.

Goldberg, David E (1989), Genetic Algorithms in Search, Optimization and Machine Learning, Kluwer Academic Publishers, Boston, MA.

Goldberg, David E (2002), The Design of Innovation: Lessons from and for Competent Genetic Algorithms, Addison-Wesley, Reading, MA.

Gutjahr, W. J. (2000), A Graph-based Ant System and its convergence. Future Generation Computer Systems, 16(8):873–888

Hansen, E.R., (1992), Global Optimization Using Interval Analysis. New York: Dekker.

Hinton, E., Sienz, J., Fully stressed topological design of structures using an evolutionary procedure, Eng. Comput. 12 (1995) 229-244.

Holland, John H (1975), Adaptation in Natural and Artificial Systems, University of Michigan Press, Ann Arbor

Hooke, R., Jeeves, T.A. (1961), "Direct Search Solution of Numerical and Statistical Problems", J of the ACM, Vol.8, pp.212-229.

Horst, R., Tuy, H., (1996), Global Optimization: Deterministic Approaches, 3rd ed. Berlin: Springer-Verlag.

Huang, N.C. and Sheu, C.Y., "Optimal design of an elastic column of thin-walled cross section", *J. Appl. Mech.* **25**, 285 (1968).

Kanarachos, A., Makris, P. and Koch, M. (1985), Localization of multi-constrained optima and avoidance of local optima in structural optimization problems, Comp Meth App Mech Engin, Vol. 51, Issues 1-3, Pages 79-106.

Karush, W. (1939), *Minima of Functions of Several Variables with Inequalities as Side Conditions*, MS Thesis, Dept. of Mathematics, University of Chicago, Chicago, IL.

Kearfott, R.B., (1996), Rigorous Global Search: Continuous Problems. Dordrecht, Netherlands: Kluwer.

Keller, J.B., "The shape of the strongest column", *Arch. Ration. Mech. Analysis* , **5**, 275 (1960).

Kennedy, J. and Eberhart, R. C. Particle swarm optimization. Proc. IEEE int'l conf. on neural networks Vol. IV, pp. 1942-1948. IEEE service center, Piscataway, NJ, 1995.

Khot, N.S., Venkayya, V.B., Johnson, C.D. and Tischler, V.A., "Optimization of fiber reinforced composite structures", *Int. J. Solids Struct.* **9**, 1225 (1973)

Kirkpatrick, S. (1984), "Optimization by simulated annealing: quantitative studies", J Statist Phys, Vol. 34, pp. 975-986.

Kirkpatrick, S.; Gelatt, C. D., Vecchi, M. P. (1983). "Optimization by Simulated Annealing". Science. New Series 220 (4598): 671-680.

Kiusalaas, J., "Optimal design of structures with buckling constraints", *Int. J. Solids Struct.* **9**, 863 (1973).

Koza, John (1992), Genetic Programming: On the Programming of Computers by Means of Natural Selection,

Kuhn, H.W., Tucker A.W. (1951) "Non-linear Programming", in J.Neyman (Ed.), Proceedings of the Second Berkeley Symposium on Mathematical Statistics and Probability, University of California Press, Berkeley, CA , pp.481-493.

Lagaros, N.D. and Papadrakakis, M., Improving the condition of the Jacobian in neural network training Advances in Engineering Software, (2003).

Lagaros, N.D., Papadrakakis, M., and Kokossalakis, G., (2002), Structural optimization using evolutionary algorithms, Computers & Structures, 80, 571-589.

Manickarajah, D., Y.M. Xie, G.P. Steven, (1995), Simple method for the optimization of columns, frames and plates against buckling, in: S. Kitipornchai, G.J. Hancock, M.A. Bradford (Eds.), Structural Stability and Design, A.A. Balkema Publishers, Rotterman, Brookfield, pp. 80-175.

Metropolis, N., Rosenbluth, A.W., Rosenbluth, M.N., Teller, A.H., and Teller, E., (1953) "Equations of State Calculations by Fast Computing Machines". Journal of Chemical Physics, 21(6):1087-1092.

Michalewicz, Zbigniew (1999), Genetic Algorithms + Data Structures = Evolution Programs, Springer-Verlag.

Michell, A.G.M. 1904: The limits of economy of material in framestructures.*Phil. Mag.* **8**, 589–597

Nelder, J.A., Mead, R. (1965), "A Simplex Method for Function Minimization", Computer Journal, Vol.7, pp. 308-313.

Neumaier, A., (1990), Interval Methods for Systems of Equations. Cambridge, England: Cambridge University Press.

Nha Chu, D., Xie, Y. M., Hira, A., Steven, G.P., (1997), On various aspects of evolutionary structural optimization for problems with stiffness constraints, Finite Elements in Analysis and Design, v.24 n.4, p.197-212.

Nha Chu, D., Y.M. Xie, G.P. Steven, (1998), An evolutionary structural optimization method for sizing problems with discrete design variables, Comput. Struct. 68, 419-431.

Papadrakakis, M., Tsompanakis, J. and Lagaros, N., (1999), Structural shape optimisation using evolution strategies, Eng. Optimization, 31, 515-540.

Papadrakakis, M., Lagaros, N.D., Tsompanakis, Y. and Plevris, V., (2001), Large scale structural optimization: Computational methods and optimization algorithms, Archives of Computational Methods in Engineering, State of the art Reviews, 8 (3), 239-301.

Papadrakakis, M., Lagaros, N.D., Plevris, V., (2002), Multi-objective optimization of skeletal structures under static and seismic loading conditions, engineering Optimization Journal,34, 645-669.

Papadrakakis, M., Lagaros, N.D., (2002), Reliability-based structural optimization using neural networks and Monte Carlo simulation, Computer Methods in Applied Mechanics and Engineering , 191(32), 3491-3507.

Papadrakakis, M., Lagaros, N.D., (2004), Soft computing methodologies for structural optimization, J. Applied Soft Computing, V3, 283-300.

Patnaik, S.N., Berke, L. and Guptill, J.D., (1993), Merits and limitations of optimality criteria method for structural optimization. *NASA TP-3373*.

Pintér, J.D., (1996), Global Optimization in Action. Dordrecht, Netherlands: Kluwer.

Powell, M.J.D. (1964), "An efficient Method for finding the minimum of a function of several variables without calculating derivatives", Computer Journal, Vol.7 (4), pp.303-307.

Querin, O.M., G.P. Steven, Y.M. Xie, (1998), Evolutionary structural optimization (ESO) using bi-directional algorithm, Eng. Comput. 15, 1031-1048.

Querin, O. M. , G. P. Steven, Y. M. Xie, (2000), Evolutionary structural optimisation using an additive algorithm, Finite Elements in Analysis and Design, v.34 n.3-4, p.291-308.

Ratschek, H., Rokne, J.G., (1995), "Interval Methods." In Handbook of Global Optimization: Nonconvex Optimization and Its Applications (Ed. R. Horst and P. M. Pardalos). Dordrecht, Netherlands: Kluwer, pp.751-828.

Rechenberg, I. (1971), Evolutionsstrategie - Optimierung technischer Systeme nach Prinzipien der biologischen Evolution (PhD thesis).

Rechenberg, I., (1989), Evolution strategy—nature's way of optimization, in Optimization: Methods and Applications, Possibilities and Limitations, Bergmann, H.W. (ed.), DLR lecture notes in engineering, Springer, Berlin, 47:106–128.

Rosen, J. (1960), "The Gradient Projection Method for Nonlinear Programming, I. Linear Constraints", *Journal of the Society for Industrial and Applied Mathematics*, Vol.8, pp.181–217.

Rosenbrock, H.H. (1960), "An Automatic Method for finding the Greatest or Least Value of a Function", Comp J, Vol.3, pp.175-184.

Rozvany, GIN, Zhou M et al. (1989/90) Continuum type optimality criteria methods for large finite element systems with a displacement constraint. Parts I and II. Struct. Optim. 1:47–72; 2:77–104

Russo, L. (2004), *The forgotten revolution: How science was born in 300BC and why it had to be reborn.* Springer, Berlin.

Saka, M.P. and Kameshki, E., (1998), Optimum design of multi-storey sway steel frames to BS5950 using genetic algorithm. In: B.H.V. Topping, Editor, Advances in engineering computational technology, Civil-Comp Press, pp. 135–141.

Saka, M.P., (2003), Optimum design of skeletal structures: A review. In: B.H.V. Topping, Editor, Progress in civil and structural engineering computing, Saxe-Coburg Publications, pp. 237–284.

Sargent, R. W. H., (1980),"A Review of Optimization Methods for Nonlinear Problems" in Computer Applications to Chemical Engineering, Ed. R.G. Squires and G. V. Reklaitis, ACS Symposium Series No. 124, American Chemical Society, Washington, D.C.

Schwefel, H.P., (1995), Evolution and Optimum Seeking: New York: Wiley & Sons.

Schwefel, H.P., (2002), Evolution Strategies: A Comprehensive Introduction. Journal Natural Computing, 1(1):3-52.

Serra, M., Venini, P., (2006), On some applications of ant colony optimization metaheuristic to plane truss optimization, Struct Multidisc Optim, vol.32, pp.499–506.

Shi, Y. and Eberhart, R. C., (1998), A modified particle swarm optimizer. Proceedings of the IEEE International Conference on Evolutionary Computation pp. 69-73. IEEE Press, Piscataway, NJ.

Shi, Y. and Eberhart, R. C., (1998), Parameter selection in particle swarm optimization. Evolutionary Programming VII: Proc. EP 98 pp. 591-600. Springer-Verlag, New York.

Stützle, T., Hoos, H.H., (2000), MAX–MIN Ant System. Future Generation Computer Systems, 16(8):889–914.

Svanberg, K. (1987), 'The method of moving asymptotes a new method for structural optimization', International Journal for Numerical Methods in Engineering, 24:359–373.

Tadjbakhsh, I. and Keller, J.B., (1962) Strongest columns and isoperimetric inequalities for eigenvalues, *J. Appl. Mech.* **29**, 159.

Tanskanen, P., (2002), The evolutionary structural optimization method: theoretical aspects, Comput. Methods Appl. Mech. Eng. 191, 5485-5498.

Taylor, J.E. and Liu, C.Y., (1968), Optimal design of columns, *AIAA J.*, **6**, 1497.

Venkatamaran, P. (2002), *Applied Optimiization with Matlab Programming*, Wiley.

Venkayya, V.B., (1971), Design of optimum structures, *Int. J. Comp. Struct.* **1**, 265.

Venkayya, V.B., Khot, N.S. and Reddy, V.S., (1968), Energy distribution in an optimum structural design, *AFFDL-TR-68-156*.

Venkayya, V.B., Khot, N.S., Tischler, V.A. and Taylor, R.F., (1971), Design of optimum structures for dynamic loads', *3rd Air Force Conference on Matrix Methods in Structural Mechanics*.

Venkayya, V.B., Khot, N.S., (1975), Design of optimum structures for impulse type loading', *AIAA J.* **13**, 989.

Veselago, V.G. (2002), "Formulating Fermat's principle for light traveling in negative refraction materials", *PHYS-USP*, Vol. 45(10), pp. 1097-1099.

Xie, Y. M., Steven, G.P., (1993), A simple evolutionary procedure for structural optimization, Comput. Struct. 49 885-896.

Xie, Y. M., Steven, G.P., (1994), Optimal design of multiple load case structures using an evolutionary procedure, Eng. Comput. 11,295-302.

Xie, Y.M., Steven, G.P., (1997), Evolutionary Structural Optimization, Springer, London,.

Yang, X.Y., Xie, Y.M., Liu, J.S., Parks, G.T., Clarkson, P.J., (2003), Perimeter control in the bi-directional evolutionary optimization method, Struct. Multidiscip. Optim. 24, 430-440.

Zhou M., Rozvany G.I.N., (1992/93), DCOC: an optimality criterion method for large systems. Part I: Theory, Part II: algorithm. Structural and Multidisciplinary Optimization, 5, 12-25; 6, 250-262.

Zoutendijk, G. (1960), *Methods of Feasible Directions*, Elsevier.

This page has been left intentionally blank

CHAPTER 2

DIRECT SEARCH IN OPTIMIZATION AND INTRODUCTION OF A NEW HYBRID OPTIMIZATION METHOD

Abstract

In this chapter, some of the most popular direct search methods in optimization are investigated for their performance to be evaluated, while a new hybrid optimization procedure is introduced. More particularly, the deterministic methods of Box, Hooke & Jeeves, Nelder & Mead, the Sequential Quadratic Programming technique, the stochastic methods of Genetic Algorithms (GAs) and Simulated Annealing (SA), as well as a stochastic method implementing Artificial Neural Networks (EASY) are applied for the solution of various mathematical benchmark problems as well as of typical size structural optimization problems found in the literature. From this investigation it was found that for optimization problems with a small number of design variables, the (SA) procedure outperformed the other methods, while for optimization problems with a larger number of design variables it is preferable to choose a deterministic optimization procedure. Based on this fact, a new hybrid optimization procedure is introduced, the main features of which are the determination of the search direction using Powell's method (deterministic procedure), the search of the optimal design along a search direction using (SA) (stochastic procedure) and the initiation of a local search using (SA) when convergence seems to have been achieved. The evaluation of the proposed method took place using twelve mathematical benchmark functions. The conclusion of this investigation was that the proposed hybrid scheme presented an exceptional behavior with respect to the location of the global minimum but at a high computational cost, which denoted the necessity for exploring other types of optimization schemes, such as indirect search procedures.

Keywords

Direct search methods, benchmark problems, hybrid optimization, deterministic direction exploration, stochastic search.

2.1. Introduction

Optimization is the process of maximizing or minimizing the value of a desired objective function while satisfying the prevailing constraints. For this purpose, it is possible to use numerous techniques, the so-called optimization methods, which may be categorized in two large groups, the former being the direct search methods and the latter being the indirect search methods. For the methods of the former group, the aim is to explicitly minimize (or maximize) the value of a given objective function. For the methods of the latter group, the aim is to construct an optimality condition which is then tried to be reached, thus the quantity to be minimized (or maximized) is implicitly improved. In the literature, a great many number of methods of both groups may be found, some of which are more popular mainly due to some inherent characteristic that allows for a very good performance under certain conditions. Therefore, the vexed question is whether the existing optimization techniques may be considered adequately efficient for the solution of structural layout optimization problems. Furthermore, another interesting question to be answered is whether the combination of existing optimization techniques may provide an even better behavior with respect to locating the global minimum (or optimum), on the basis that the combination of the advantages of various methods may annihilate the disadvantaged, which each method separately suffers from. The aim of this chapter is to provide insight into these questions. Towards this direction, the following four-step procedure was carried out:

Step 1: Retrieve from the literature some of the most popular optimization methods and evaluate them.

Step 2: Apply the same methods to structural optimization problems.

Step 3: Investigate the Genetic Algorithms (GA), which formulate a separate concept in optimization.

Step 4: Based on the obtained experience, introduce a new optimization method and apply a thorough evaluation.

In the next sections of the present chapter, the aforementioned steps are presented in more details. For each step, the implemented methods, the examined optimization problems, the used performance indices and the corresponding conclusions are recorded.

2.2. Theoretical analysis

The direct search methods explore the design space and seek the optimum through the explicit evaluation of the quantity to be minimized or maximized. The exploration may be performed either in a deterministic or in a stochastic way. In the former way, the same optimum design vector yields no matter how many times the optimization procedure is initiated from the same, but randomly selected, initial design vector. In the latter way, it is possible, but not necessary, to get different optimum design vectors even though the procedure is initiated from the same initial design vector.

The deterministic optimization procedures may use either objective function values only (zero order or non-gradient methods), or gradients (first order methods) or even Hessian information (second order methods). The basic difference between gradient and non-gradient methods is the nature of the pattern search. In the former methods, the implementation of gradient and/or Hessian information demands the calculation of derivatives, which has a significant computational cost, may cause numerical instabilities and may result in locating local rather than global minima. On the other hand, the stochastic techniques are derivative-free, at least at their basic version, but need to perform a thorough exploration and exploitation of the feasible region, which in turn results to a cumulated high computational cost. Obviously, each technique has its own advantages and disadvantages, while a logical addition to the existing deterministic and stochastic optimization methods would be the

introduction of deterministic elements as operators in a stochastic procedure and vice versa. In order to obtain a first-hand experience with respect to the performance of characteristic optimization methods, two sets of benchmark problems were formed.

The first set of benchmark problems concerned mathematical functions (**B**enchmark **M**athematical **F**unctions - BMF), retrieved from the literature, with one variable (BMF1), two variables (BMF2), three variables (BMF3), four variables (BMF4) and eight variables (BMF5), respectively; that is a total of five cases for which the global optimum is known. For the trace of the optimum, six most popular methods, also retrieved from the literature, were applied. In more details, the Simulated Annealing (SA), which is a stochastic procedure, the Downhill Simplex (variation of Nelder & Mead), the Box (complex) method, and the Hooke & Jeeves method, all three being of deterministic nature, were used. More information concerning these procedures may be found in Chapter 1. For the implementation of the Sequential Quadratic Programming (SQP), the corresponding routine found in FORTRAN/IMSL was used. On top of that, a stochastic method implementing Artificial Neural Networks (ANN) and meta-models, developed at the Laboratory of Thermal Turbomachines (National Technical University of Athens) and named ***E***volutionary ***A***lgorithm ***SY***stem v.1.3.4 (EASY) was also used. For the quantification of their efficiency, four evaluation indices were used while, in total, 2500 (2.5K) analyses were carried out. The investigation of the first set of benchmark problems is presented in the section '*Investigation of the mathematical functions*'.

The second set of benchmark problems concerned the weight minimization of typical trusses, under a variety of constraints, both in type and in number. In more details, the same optimization algorithms, as of the first set of benchmark problems, were used (EASY excluded), while four very well-known problems (**S**keletal **S**tructural **B**enchmarks - SSB)) were selected, namely the 3-bar problem, two variations of the 10-bar problem and the 25-bar problem. The results were ranked according to the required number of iterations and to the ability of locating the global optimum. In this way, a clear impression regarding the performance of the aforementioned algorithms in size optimization of trusses was obtained. Again, the evaluation indices used for the first set of benchmark problems were applied, while, in total, 2000 (2K) analyses were carried out. The investigation of the first set of benchmark problems is presented in the section '*Investigation of skeletal structures*'.

Apart from the aforementioned sets of benchmark problems, a further investigation was carried out with respect to the GAs. It is true that (GAs) consist a special class of optimization methods because they are based on the Darwinian approach concerning the evolution of species, an evolution that is of some billion years of age. The main characteristic of GAs is that not only do they implement a stochastic optimization procedure but also they handle a *set* of design vectors, and not only one design vector at a time. For the investigation of the GAs, the corresponding tool found in MatLab was extensively tested, using four mathematical functions, two from the first set of MBFs and two other (the so-called Powell and Suzuki functions). In total, eleven GA controlling parameters were examined. For the evaluation of the GA efficiency, two new performance indices were introduced (normalized sensitivity and cumulative probability), while, in total, 1.120.000 (1.12M) analyses were carried out. The investigation of the GAs is presented in the section '*Investigation of Genetic Algorithms*'.

The experience obtained from the aforementioned investigations was quite revealing. One of the main observations was that the stochastic methods for direct search outperform the deterministic ones, when the number of the design variables is small. On the contrary, as the dimension of the design space increases so does the relative efficiency of the deterministic procedures with respect to the stochastic ones. Therefore, within an optimization scheme, a good idea would be to handle, with a stochastic (deterministic) approach, procedures that embed a small (large) number of design variables. Towards this direction, the proposed

hybrid procedure was formulated. In more details, a typical deterministic optimization scheme consists of two operators, the former regarding the estimation of the direction that must be followed (search direction) and the latter regarding how far the aforementioned direction should be followed (step size). The search direction is described by a vector whose dimension is, obviously, equal to the dimension of the design space. As a result, the higher this dimension is the more design variables are involved, thus a deterministic scheme seems more appropriate for solving the problem of the search direction. In the present study, the Powell's method was selected for this task. The reasoning behind this selection was straightforward: Powell's method is simple to program and very powerful due to the so-called 'left-shifting' of the pattern search that Powell introduced. On the other hand, the step size is a scalar quantity, thus its estimation along a search direction may be expressed as a 1-D optimization problem; in turn, a stochastic procedure seems more suitable for this estimation. In the present study, the (SA) algorithm was selected for this task. Again, the reasoning behind this selection was straightforward: the (SA) approach significantly outperformed the other methods for the examined 1-D mathematical benchmark function. Apart from the aforementioned operators, another operator was introduced as an effort to provide the optimization procedure with the ability to escape from potentially local minima. This phase is nothing else than a local search, using the (SA) approach, within a sphere around the current optimum design vector. The iterative application of the aforementioned operators consists the proposed optimization procedure. For its evaluation, another set of mathematical benchmark functions was formulated. In more details, the aforementioned benchmark mathematical functions (BMF1), (BMF2), (BMF4) and (BMF5) were examined, while two more variations for each function were introduced and examined (in total, twelve cases). In addition, three performance indices were recorded while a comparison with the (SA), the Powell method, the Hooke & Jeeves method and the Nelder & Mead method was carried out. In total, 7200 (7.2K) analyses were carried out. The investigation of the first set of benchmark problems is presented in the section '*The proposed hybrid optimization procedure*'.

One important aspect concerning the performance of an optimization procedure is the way the constraints are handled. This task can be carried out in various ways, such as the use of penalty functions (exterior, interior or combination of them), where the initial constrained optimization problem is turned into a sequence of unconstrained optimization problems. The same optimization algorithm, when combined with different penalty functions, may provide different outputs (converged value and number of required iterations). Therefore, in order to evaluate the optimization algorithm itself, it is necessary to eliminate any beneficial contribution originating from the chosen penalty method. In the investigation presented in this chapter, if a constraint was violated, then the objective function was given a very large value (hard kill penalization scheme). This choice pushed the optimization algorithms to their limits because this kind of penalization is definitely hard, as its name implies, since no distinction between design vectors causing small or large violations was made.

Another very important aspect in evaluating an optimization algorithm is related to its sensitivity to various parameters, such as the initial design vector. If different optimization methods are initiated from the same design vector, then it is highly possible to get different optimum values. Therefore, in order to get a representative picture of the behavior of an optimization method it is required to perform a parametric investigation; that is to run the method many times using different initial values for the governing parameter. In the investigation presented in this chapter, each one of the benchmark functions was analyzed by each one of the tested methods 100 times using different initial design vectors. Especially for the (SA), the parametric investigation was performed with respect to the initial temperature, which is a governing parameter; on the contrary, the initial design vector does not play any role because, according to the concept of (SA), all the tested design vectors are randomly

formed (there is no dependency between two successive design vectors). Furthermore, (EASY) was excluded from this parametric investigation because (EASY) asks only for the domain of the design variables and not for an initial design vector as well (results from EASY are discussed separately).

2.3. Investigation of mathematical functions

The first set of benchmark problems, concerning mathematical functions retrieved from the literature, is briefly presented in the next paragraph. In the sequel, the evaluation indices used, as well as the analysis carried out, a brief discussion and the conclusions drawn are stated.

2.3.1. Definition of the Benchmark Mathematical Functions (BMF)

2.3.1.1. Benchmark Mathematical Function - 1 (BMF-1)

The one-variable benchmark function used was (let it be BMF1):

$$f(x) = \sin x + \sin\left(\frac{10x}{3}\right) \tag{2.1}$$

where $x \in [2.7,\ 7.5]$. The graph of (Eq.2.1) is shown in Fig.2.1a. For the aforementioned domain, the global minimum is located at $x = 5.145$ with $f_{\min} = -1.8996$, while two more local minima also exist.

2.3.1.2. Benchmark Mathematical Function - 2 (BMF-2)

The two-variable benchmark function used (let it be BMF2) was the Rastrigin function for the 2-D space:

$$f(x_1, x_2) = x_1^2 + x_2^2 - \cos(18x_1) - \cos(18x_2) \tag{2.2}$$

where $x_1, x_2 \in [-1,\ 1]$. For the specific domain, (Eq.2.2) has 50 local minima and 1 global minimum located at $(x_1, x_2) = (0, 0)$ with $f_{\min} = -2.0$. The iso-curve graph of (Eq.2.2) is illustrated in Fig.2.1b.

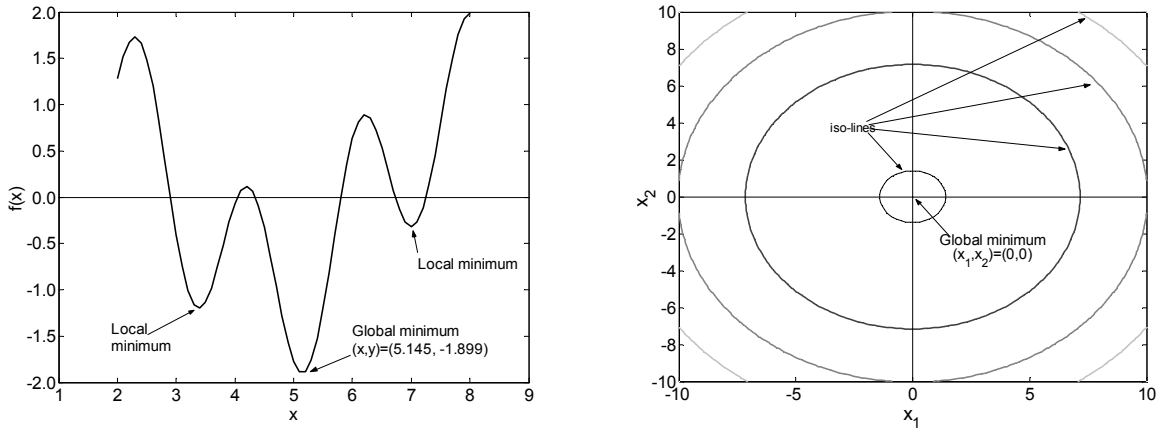

(a) (b)

Figure 2.1: Range of the benchmark functions with (a) one variable and (b) two variables

2.3.1.3. Benchmark Mathematical Function - 3 (BMF-3)

The three–variable benchmark function used (let it be BMF3) was the constrained Rosenbrock function:

$$f\left(x_1, x_2, x_3\right) = -x_1 x_2 x_3 \tag{2.3}$$

where $x_1, x_2, x_3 \in \left[0,\ 42\right]$, while the following additional constraint was also imposed:

$$0 \le x_1 + 2x_2 + 2x_3 \le 72 \tag{2.4}$$

The global minimum of (Eq.2.3) is located at $\left(x_1, x_2, x_3\right) = \left(24,12,12\right)$ with $f_{\min} = -3456$.

2.3.1.4. Benchmark Mathematical Function - 4 (BMF-4)

The four-variable benchmark function used (let it be BMF4) was:

$$f\left(x_1, x_2, x_3, x_4\right) = \frac{1}{2}\sum_{j=1}^{4}\left(x_j^4 - 16x_j^2 + 5x_j\right) \tag{2.5}$$

where $x_1, x_2, x_3, x_4 \in \left[-4.0,\ 0\right]$. The global minimum of (Eq.2.5) is $f_{\min} = -156$.

2.3.1.5. Benchmark Mathematical Function - 4 (BMF-4)

The eight-variable benchmark function used (let it be BMF5) was the Rastrigin function:

$$f\left(\vec{x}\right) = 80 + \sum_{m=1}^{8}\left(x_m^2 - 10\cos(2\pi x_m)\right) \tag{2.6}$$

where $x_m \in \left[0,0,...,0\right]$, $m = 1,...,8$. The global minimum of (Eq.2.6) is $f_{\min} = 0$.

2.3.2. Evaluation Indices

In order to evaluate the performance of the tested optimization algorithms, four evaluation indices were used. Three of them are well-known indices, while a new index is introduced for quantifying the probability of tracing the global optimum.

2.3.2.1. *Probability of getting the global minimum and near global minimum values.*

Each Mathematical Benchmark Function was analyzed $N = 100$ times. The tested algorithm did converge (successive runs) N_s times but $N_f = N - N_s$ times failed to converge within the prescribed limits (maximum number of function evaluations, maximum number of iterations etc) or the converged solution failed when checked after the completion of the optimization procedure for constraint violations. Among the N_s results, there was a minimum $F_{s,\min}$ and a maximum $F_{s,\max}$ value. The range $\left[F_{s,\min}, F_{s,\min}\right]$ was divided in 5 intervals of the form $\left[F_{s,\min,j}, F_{s,\min,j}\right]$ where $F_{s,\max,j} = F_{s,\min} + \left(j-1\right)\cdot\left(F_{s,\max} - F_{s,\min}\right)/5$ and $j = 1,..,6$. Obviously, for $j = 1$ it holds $F_{s,\min,1} = F_{s,\min}$. The probability of getting a value F within the interval $\left[F_{s,\min}, F_{s,\max,j}\right]$ was defined as:

$$\Pr\left(F\right) = \left(N_F / N\right) \tag{2.7a}$$

or equivalently as:

$$\Pr\left(F \le F_{s,\max,j}\right) = \left(1/N\right)\sum N_{F \le F_{s,\max,j}} \tag{2.7b}$$

(Eqs.2.7) represent the cumulative probability and the corresponding histograms, for each one of the examples and for all the tested methods (EASY excluded), were plotted. It is emphasized that (Eq.2.7) must be evaluated in combination with the width of $\left[F_{s,\min}, F_{s,\max}\right]$ (see Section 2.3.2.3, below). Evidently, the performance of an algorithm is better when the probability of getting results within the first interval is high and the range $\left[F_{s,\min}, F_{s,\max}\right]$ is short. Furthermore, the plots of cumulative probability implicitly inform on the number of successive runs, which is another performance index. The total cumulative probability is equal to $\Pr\left(F \le F_{s,\max}\right) = \left(N_s/N\right)$, thus multiplication of $\Pr\left(F \le F_{s,\max}\right)$ by N, which is equal to 100, gives N_s.

2.3.2.2. *Average and standard deviation of the required evaluations of the objective function.*

Another performance index of an algorithm is the total number of objective function evaluations required until convergence is achieved. Alternatively, the total number of iterations or the CPU time may be used.

2.3.2.3. *Range of the objective function minima.*

As mentioned in 1 above, for each benchmark function and for each algorithm, among the N_s results (optima), there was a minimum $F_{s,\min}$ and a maximum $F_{s,\max}$ value. It is evident that the shorter the range $\left[F_{s,\min}, F_{s,\max}\right]$ is, the better the optimization algorithm is because the deviation from the global optimum is small.

2.3.2.4. *Convergence history.*

In order to demonstrate the behavior of each one of the tested optimization algorithms, the convergence history of the analyses that resulted in the global optimum was recorded and plotted.

2.3.3. Numerical Results

The results of the current work are illustrated in the Figures 2.2-2.6. In total, four indices were used for the evaluation of the tested methods:

2.3.3.1. *Results for (MBF1)*

The results of the investigation concerning the one-variable benchmark function are illustrated in Fig.2.2. Especially for this function, it is possible to locate in an analytical way the minima within the examined domain. As Fig.2.1a illustrates, there are three minima; $F_{\min,global} = -1.8996$ (global minimum) and two local minima $F_{\min,loc,1} = -1.1999$ and $F_{\min,loc,1} = -0.317$. The results obtained for this case showed that all algorithms converged to one of these minima, thus there was no need to create a cumulative probability diagram; instead, the probability of converging to each one of the aforementioned values was estimated. In more details, Fig.2.3a shows this probability, defined as $\left(N_{\min,k}/N_s\right)$ where $k = 1,2,3$ respectively for the aforementioned minimum values. It is noted that no failures

were observed (all methods gave $N_s = 100$). Evidently, (SA) outperformed the other optimization methods in terms of locating the global optimum. However, it required a significantly larger number of objective function evaluations (Fig2b). Finally, the convergence history diagrams showed that the selected penalty scheme did push the tested optimization algorithms to their limits (peaks along the convergence history curve).

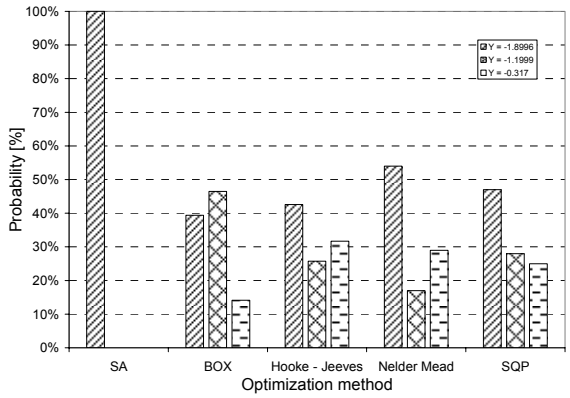

(a) probability of getting the global minimum value

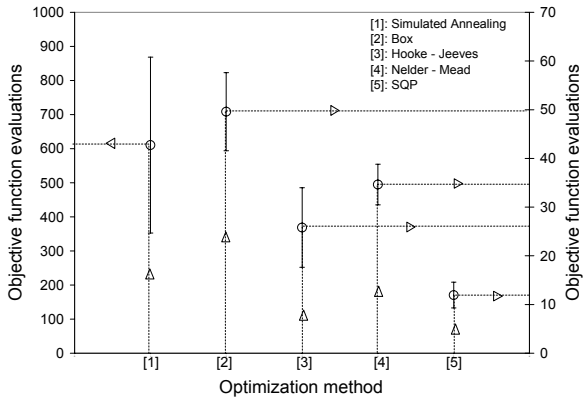

(b) average and standard deviation of the required objective function evaluations

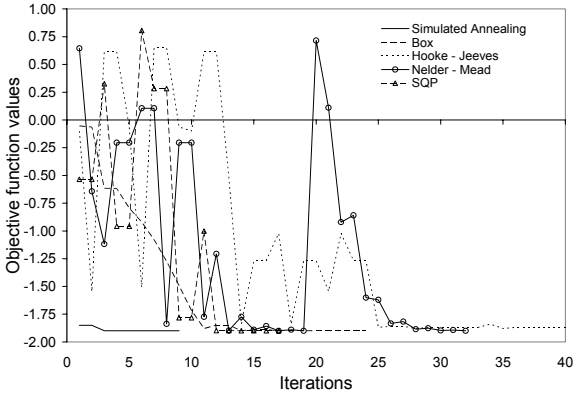

(c) convergence history

Figure 2.2: Results for the one-variable benchmark function

2.3.3.2. *Results for (MBF2)*

The results of the investigation concerning the two-variable benchmark function are illustrated in Fig.2.3. As Fig.2.3a shows, only (SA) managed to converge to an acceptable value in all 100 runs. Furthermore, as Fig.2.3c shows, the deviation from the global minimum is least for (SA). Therefore, it is evident that (SA) outperformed the other methods in terms of locating the global minimum. However, it required a significantly larger number of objective function evaluations (Fig3b). On the contrary, SQP required the least number of function evaluations but performed worse since it got trapped to a local minimum (Fig.2.3a) and had a wider range of results(Fig3c).

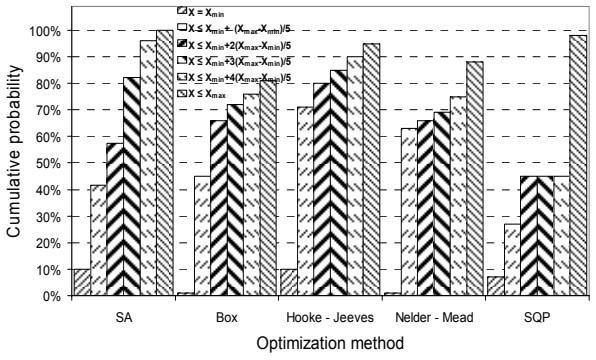

(a) cumulative probability distribution

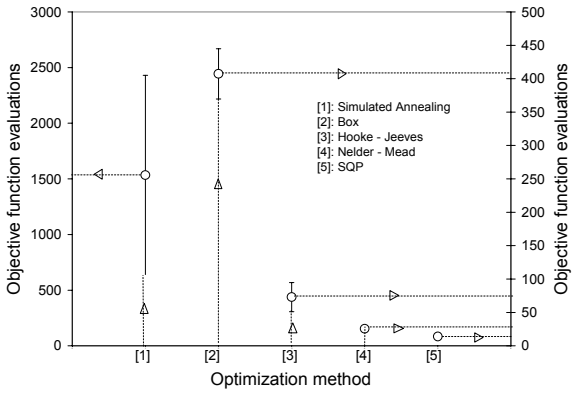

(b) average and standard deviation of the required objective function evaluations

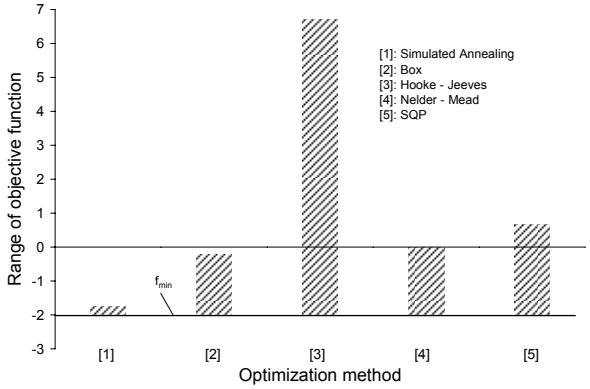

(c) range of objective function

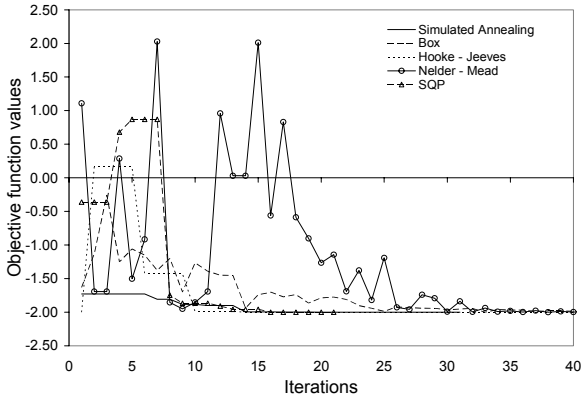

(d) convergence history

Figure 2.3: Results for the two-variable benchmark function

The convergence history diagrams (Fig.2.3d) show that peaks do appear due to the hard penalty scheme selected.

2.3.3.3. *Results for (MBF3)*

The results of the investigation concerning the three-variable benchmark function are illustrated in Fig.2.4. This time SQP outperformed the other methods because it required the least number of function evaluations (Fig.2.4b), converged only to the global optimum (Fig.2.4c) and appeared negligible failures (Fig.2.4b).

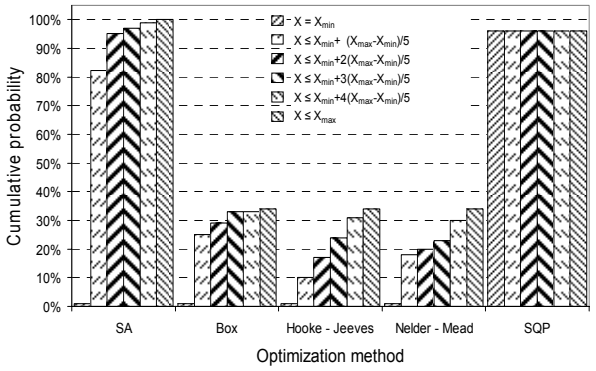

(a) cumulative probability distribution

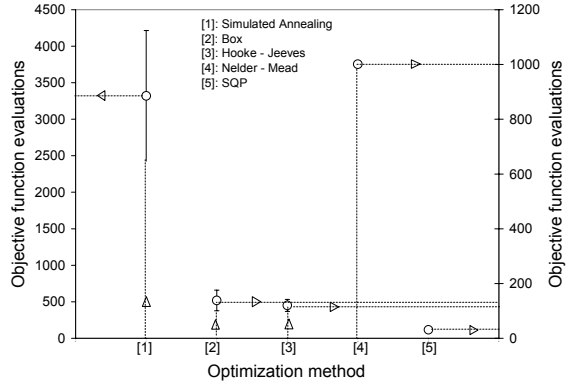

(b) average and standard deviation of the required objective function evaluations

Figure 2.4: Results for the three-variable benchmark function

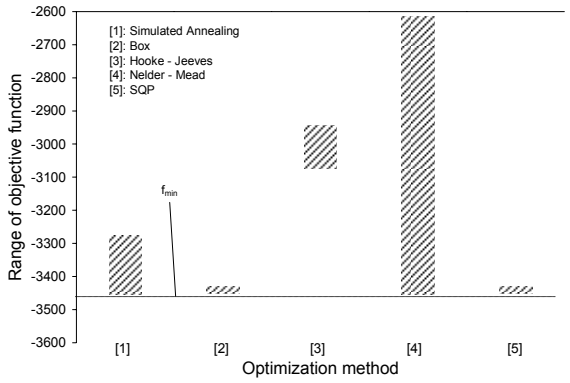

(c) range of objective function

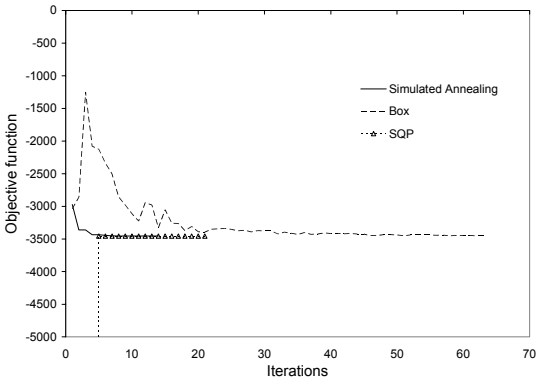

(d) convergence history

Figure 2.5: *(continued)***:** Results for the three-variable benchmark function

On the contrary, Hooke-Jeeves and Nelder-Mead algorithms presented a very poor performance (high number of failures, wide range of minima while Hooke-Jeeves converged to values away from the global minimum). However, it is strongly emphasized that this poor behavior was due to the domain of the initial design vectors. When this domain was narrowed, the performance became significantly better. The same was valid for Box as well. It is also noted that Fig.2.4d does not include convergence histories for Hooke-Jeeves and Nelder-Mead due to presentation reasons (they presented very strong peaks and valleys).

2.3.3.4. *Results for (MBF4)*

The results of the investigation concerning the four-variable benchmark function are illustrated in Fig.2.5.

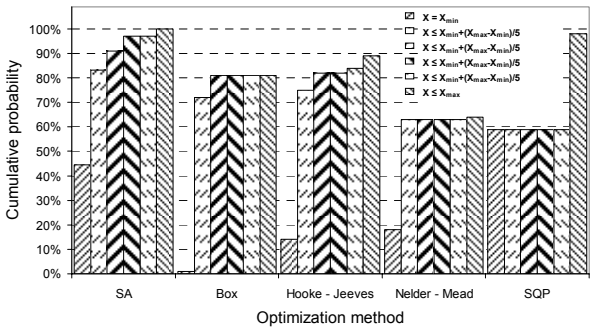

(a) cumulative probability distribution

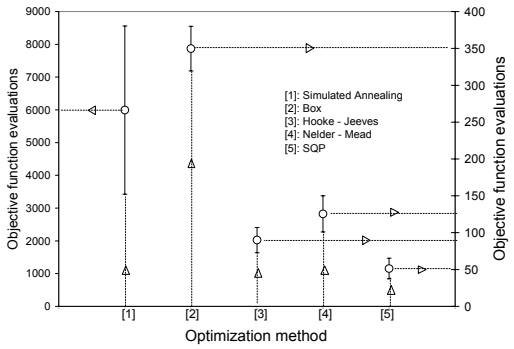

(b) average and standard deviation of the required objective function evaluations

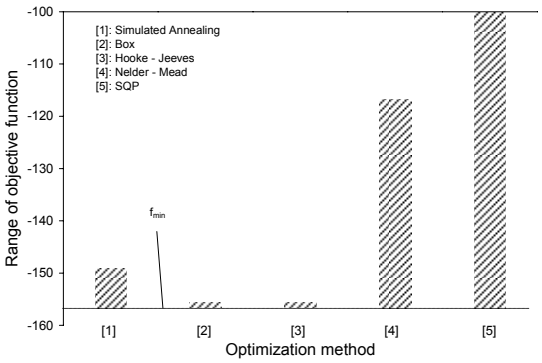

(c) range of objective function

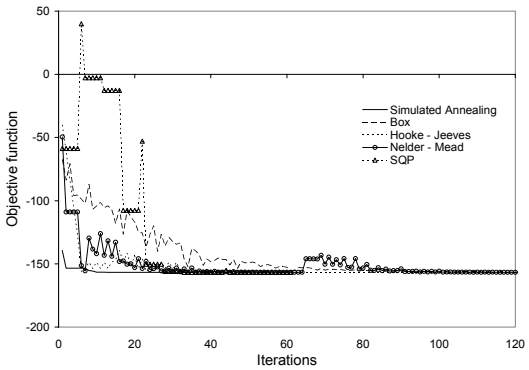

(d) convergence history

Figure 2.6: Results for the four-variable benchmark function

This time (SA) outperformed the other methods in terms of locating the global minimum because it presented the best cumulative probability distribution with no failures (Fig.2.5a) and the resulting range of the objective value functions was quite narrow (Fig.2.5c). However, as in the previous cases, it required a significantly larger number of objective function evaluations (Fig.2.5b). On the contrary, SQP presented the worst behavior, because it got trapped in a local minimum (Fig.2.5a), while Box and Hooke-Jeeves presented a quite good behavior. The convergence history diagram (Fig.2.5d) shows that this time all algorithms did not encounter problems with the imposed penalty scheme.

2.3.3.5. *Results for (MBF5)*

The results of the investigation concerning the eight-variable benchmark function are illustrated in Fig.2.6.

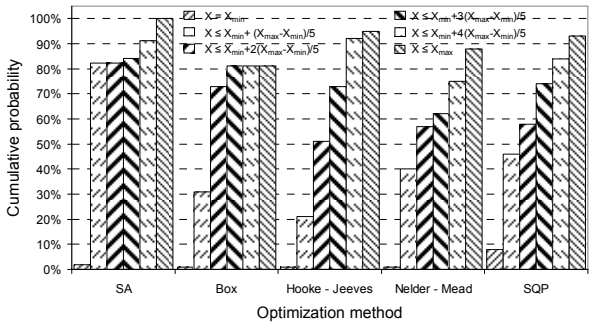

(a) cumulative probability distribution

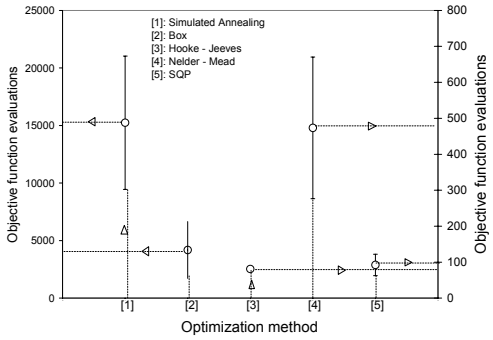

(b) average and standard deviation of the required objective function evaluations

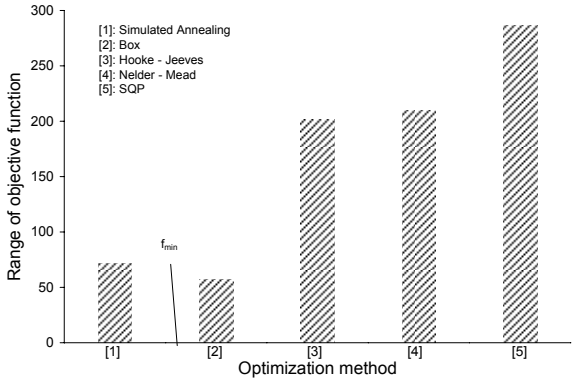

(c) range of objective function

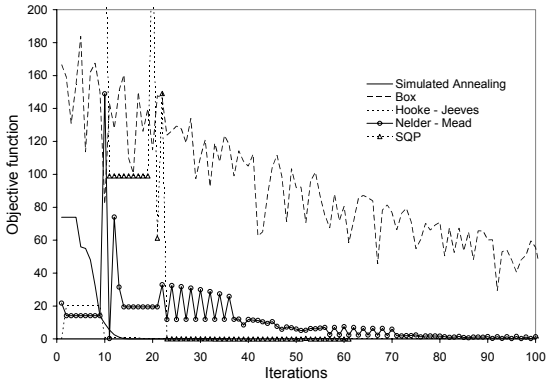

(d) convergence history

Figure 2.7: Results for the eight-variable benchmark function

Again (SA) outperformed the other methods in terms of locating the global minimum because it presented the best cumulative probability distribution with no failures (Fig.2.6a) and the resulting range of the objective value functions was quite narrow (Fig.2.6c). However, as in all previous cases, it required a significantly larger number of objective function evaluations (Fig.2.6b). From the same figures, it is evident that Box also presented a very good behavior. The convergence history diagram (Fig.2.6d) shows a quite smooth convergence (weak peaks and valleys). It is also noted that for presentation reason the maximum value along the horizontal axis is 100.

2.3.3.6. *Results from (EASY)*

As mentioned before, EASY is a GA-based optimization software that may also implement Artificial Neural Networks (ANN). The benchmark functions used in the current work were

optimized with EASY (with and without the activation of ANN). The results (Table 1) showed that in all cases the global minimum was located.

Table 2.1: Results from EASY

	MBF1	MBF2	MBF3	MBF4	MBF5
Optimum (without ANN)	-1.8996	-2.0000	-3456	-156.665	0.0000
Iterations (without ANN)	980	1050	2048	1015	5553
Optimum (with ANN)	-1.8996	-2.0000	-3456	-156.665	0.0000
Iterations (with ANN)	980	785	1011	1750	1481

2.3.4. Conclusions

The investigation presented concerning the application of popular deterministic and stochastic optimization methods in tracing the global minimum of Mathematical Benchmark Functions showed that, for the examined functions, none of the tested optimization algorithms outperformed the others. However, especially for the MBF1, it was found that the (SA) algorithm did outperform the competitive optimizers, thus strongly suggesting that (SA) should be the preference for such type of problems.

2.4. Investigation of skeletal structures

The second set of benchmark problems, concerning the weight minimization of skeletal structures retrieved from the literature, is briefly presented in the next paragraph. As in the Section 'Investigation of Benchmark Mathematical Functions', the evaluation indices used, as well as the analysis carried out, a brief discussion and the conclusions drawn are stated.

2.4.1. Description

The cases studied were three plane trusses, namely the 3-bar truss and two variations of the 10-bar truss, and a space truss, namely the 25-bar truss. All the Finite Element Analyses performed were based on an in-house code.

2.4.2. Skeletal Structure Benchmarks (SSB1)

2.4.2.1. (SSB1): 3-bar plane truss

The minimum weight of the 3-bar plane truss illustrated in Fig.2.1a is sought. The topology of the structure is fixed and only the cross-sectional areas of the bars may change. The structure is subjected to two load cases (see Fig.2.1). The allowable stress is equal to $\sigma_o = 20ksi$ both in tension and in compression. This limitation is imposed to all bars. The displacement constraints are $u_o = \pm 0.20in$ and $v_o = \pm 0.05in$ respectively for the horizontal and the vertical direction respectively. Obviously these constraints refer to the only free node of the structure The modulus of elasticity is considered to be $E = 30{,}000ksi$, while the material density is $\rho_o = 0.1lb/in^3$. It is noted that there is no lower bound for the cross-sectional areas, which are the design variables of the optimization problem.

2.4.2.2. (SSB2, SSB3): 10-bar plane truss (variation A – variation B)

The minimum weight of the 10-bar plane truss illustrated in Fig.2.1b is sought. Again, the topology of the structure is fixed and only the cross-sectional areas of the bars may change. The allowable stress is equal to $\sigma_o = 25{,}000psi$ both in tension and in compression, while this limitation is imposed to all bars. The displacement constraints for all the free nodes of the structure are $u_o = v_o = \pm 0.20in$; that is the same displacement limitation is imposed for both the

horizontal and the vertical direction. The modulus of elasticity is considered to be $E = 10^7 psi$, while the material density is $\rho_o = 0.1 lb/in^3$. The lower bound for the design variables (cross-sectional areas) is $A_{\min} = 0.1 in^2$. In the present work, two variations concerning the loads that the structure is subjected to are studied.

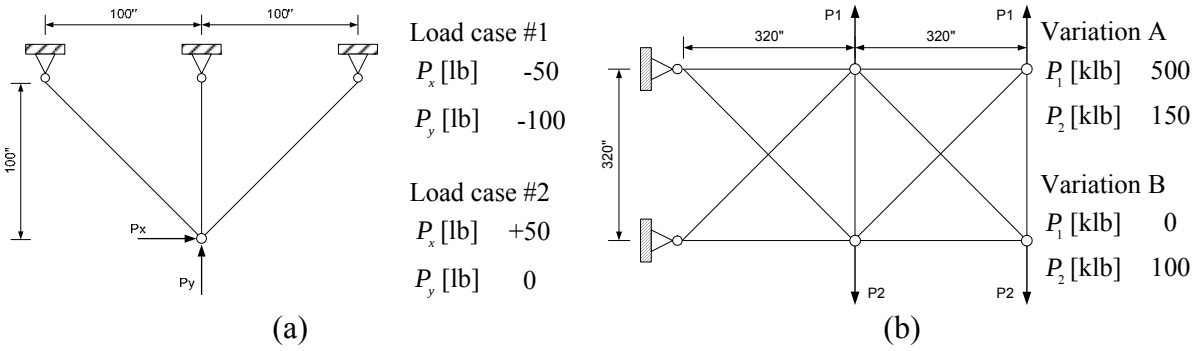

Figure 2.8: Problem definition for (a) the 3-bar truss and (b) the 10-bar truss

2.4.2.3. (SSB4): 25-bar space truss (power transmission tower)

The minimum weight of the 25-bar space truss illustrated in Fig.2.2 is sought. This structure represents a tower used for carrying transmission lines. Once again, the topology of the structure is fixed and only the cross-sectional areas of the bars may change. The allowable stress is equal to $\sigma_o = 40,000 psi$ in tension. The allowable compressive stresses are shown in Fig.2.2. The displacement constraints are $u_o = v_o = \pm 0.35 in$, that is the same displacement limitation is imposed for both the horizontal and the vertical direction, only for the top most nodes 1 and 2 (see Fig.2.2). The modulus of elasticity is considered to be $E = 10^7 psi$, while the material density is $\rho_o = 0.1 lb/in^3$. The lower bound for the design variables (cross-sectional areas) is $A_{\min} = 0.1 in^2$. It is noted that the bars of this structure are grouped, as shown in Fig.2.2.

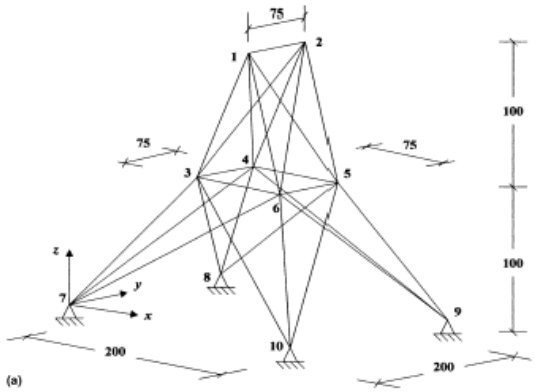

Group	Bars
1	1
2	2, 3, 4, 5
3	6, 7, 8, 9
4	10, 11
5	12, 13
6	14, 15, 16, 17
7	18, 19, 20, 21
8	22, 23, 24, 25

		Applied force [lb]		
Case	Node	F_x	F_y	F_z
1	1	1000	10000	-5000
	2	0	10000	-5000
	3	500	0	0
	6	500	0	0
2	1	0	20000	-5000
	2	0	-20000	-5000

Figure 2.9: Problem definition for the 25-bar truss

2.4.3. Results

For the cases studied, the upper bound for the design variable (cross-sectional area) was selected to be equal to $X_u = 100 in^2$. The main reason for this choice was based on the fact that from a Fully Stressed Design (FSD) analysis it was possible to get a good impression concerning the order of the cross-sectional areas corresponding to the optimum design (the selected value $X_u = 100 in^2$ was adequately large). Not imposing an upper limit, or equivalently letting the upper limit be infinite, would force the optimization methods to

explore and exploit a very large domain, thus increasing the computation cost in a meaningless way, since from the FSD analysis it was already estimated that no cross-sectional area would exceed the aforementioned bound.

With respect to the results of the current work, these are illustrated in Figures 2.3-2.6. The evaluation of the tested optimization algorithms was based on four indices presented below.

2.4.3.1. Results for (SSB1)

The results of the investigation concerning the 3-bar problem are illustrated in Fig.2.3. Especially for this case, it is possible to estimate the global minimum, which is $W_{\min,global} = 100.0lb$, in an analytical way [8]. The results obtained for this case showed that (SQP) outperformed the other methods because it required the smaller number of objective function calls (Fig.2.3b), it presented the only two failures (Fig.2.3a) and it converged to the optimum result in all successful analyses (Fig.2.3c). On the contrary, Box presented the worst behavior with the lowest percentage of successful analyses (Fig.2.3a) and the largest range of optimum values (Fig.2.3c). However, at this point it must be strongly emphasized that Box is based on the formation of the so-called 'complex'; if the initial design vector forms an unacceptable 'complex', then no analysis is performed and this is the main reason for Box's low percentage of successful analyses. Furthermore, (SA) performed very well in locating the global optimum (Figs.3a, 3c) but, in comparison to the other methods, it required a significantly larger number of objective function evaluations NFE, while it presented the largest standard deviation for NFE as well (Fig.2.3b). Finally, the convergence history diagrams (Fig.2.3d) showed that the selected penalty scheme did push the tested optimization algorithms to their limits (peaks along the convergence history curve).

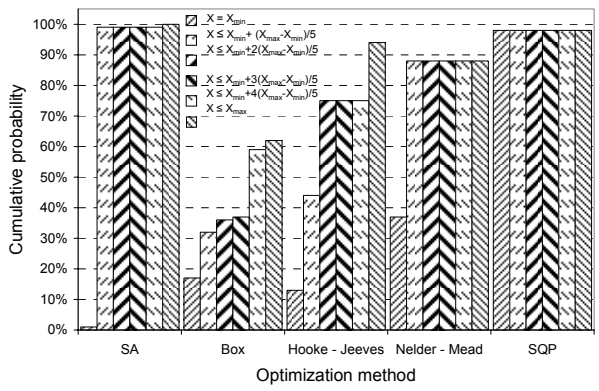

(a) cumulative probability distribution

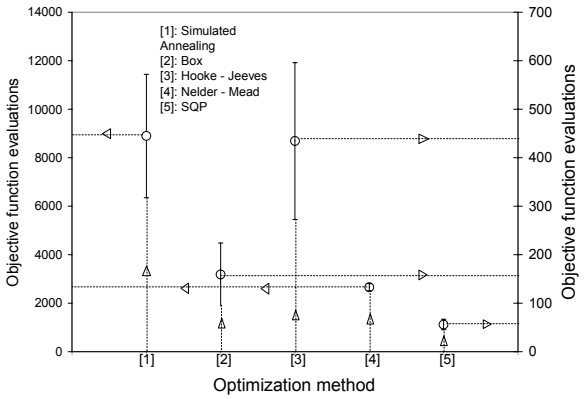

(b) average and standard deviation of the required objective function evaluations

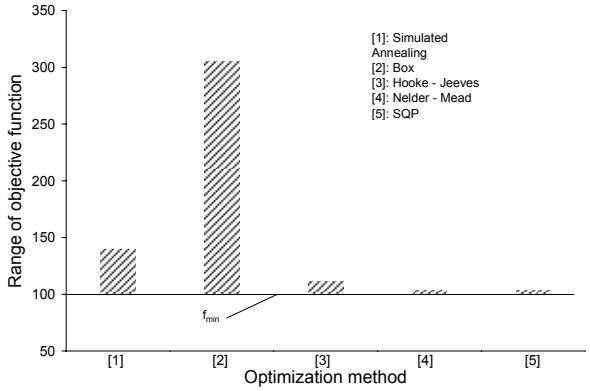

(c) range of objective function

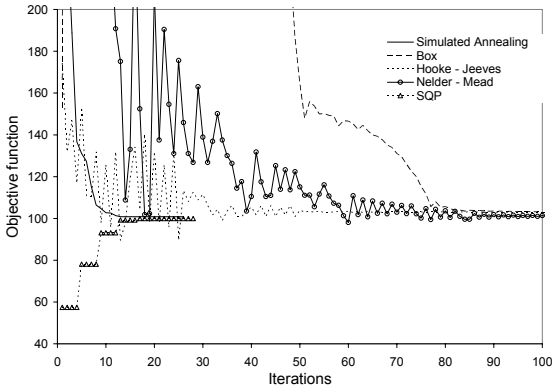

(d) convergence history

Figure 2.10: Results for the three-bar problem

2.4.3.2. Results for (SSB2)

The results of the investigation concerning the first variation of the 10-bar problem are illustrated in Fig.2.4. Again, the obtained results showed that (SQP) outperformed the other methods, because it required the smaller number of objective function calls (Fig.2.4b), it presented now failures (Fig.2.4a) and it converged to the optimum result in all successful analyses (Fig.2.4c). As in the previous case study, Box presented the worst behavior with a very low percentage of successful analyses (Fig.2.4a) and the largest range of optimum values (Fig.2.4c). (HJ) and (NM) also presented a poor behavior. Especially (NM) had the second wider range of optimum values (Fig.2.4c). Furthermore, (SA) performed quite well in locating the global optimum (Figs.4a, 4c) but, in comparison to the other methods, it required a significantly larger number of objective function evaluations *NFE* , while it presented the largest standard deviation for *NFE* as well (Fig.2.4b). It is worth mentioning that these differences between (SA) and the other methods were as high as of order 1 and this is the reason why a logarithmic scale was selected for the x-axis of Fig.2.4d. Finally, the convergence history diagrams (Fig.2.4d) showed that the selected penalty scheme was indeed hard because the convergence history curves, although smooth enough, were quite long.

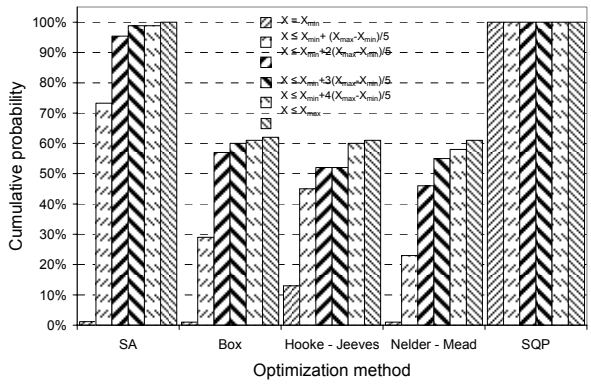

(a) cumulative probability distribution

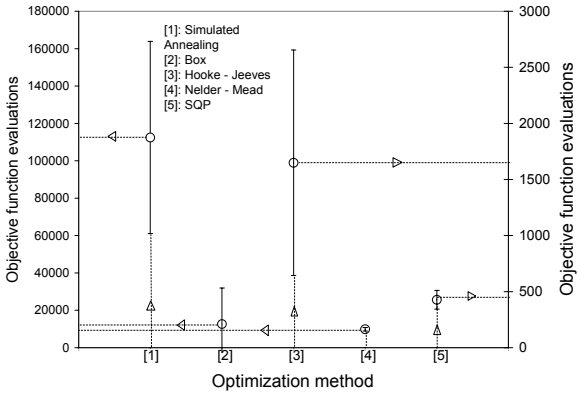

(b) average and standard deviation of the required objective function evaluations

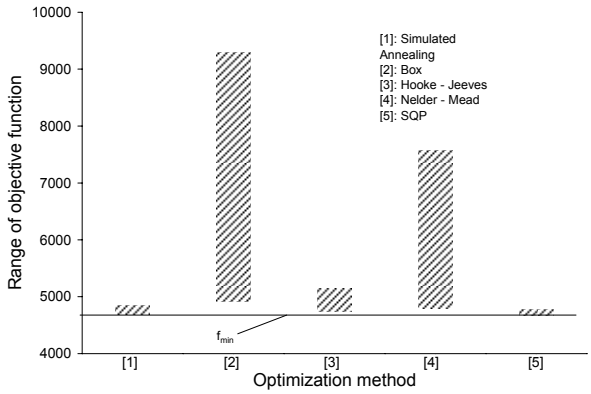

(c) range of objective function

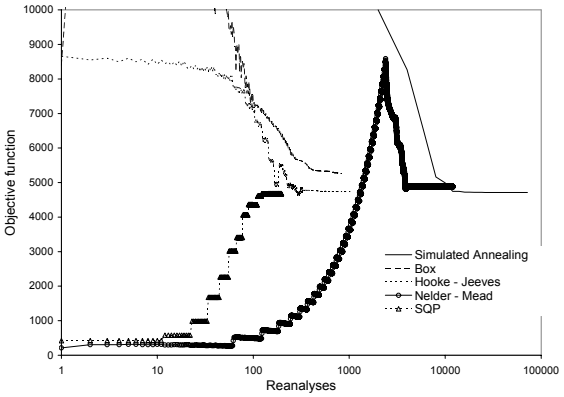

(d) convergence history

Figure 2.11: Results for the ten-bar problem (variation A)

2.4.3.3. Results for (SSB3)

The results of the investigation concerning the second variation of the 10-bar problem are illustrated in Fig.2.5. Once again, the obtained results showed that (SQP) outperformed the other methods because it required the smaller number of objective function calls (Fig.2.5b), it presented now failures (Fig.2.5a) and it converged to the optimum result in all successful

analyses (Fig.2.5c). As in the previous cases, Box's behavior was poor with a very low percentage of successful analyses (Fig.2.5a) and the largest range of optimum values (Fig.2.5c), while it never converged to the global optimum (distance between the bottom of the corresponding column and the line depicting $f_{\min}$ in Fig.2.5c).

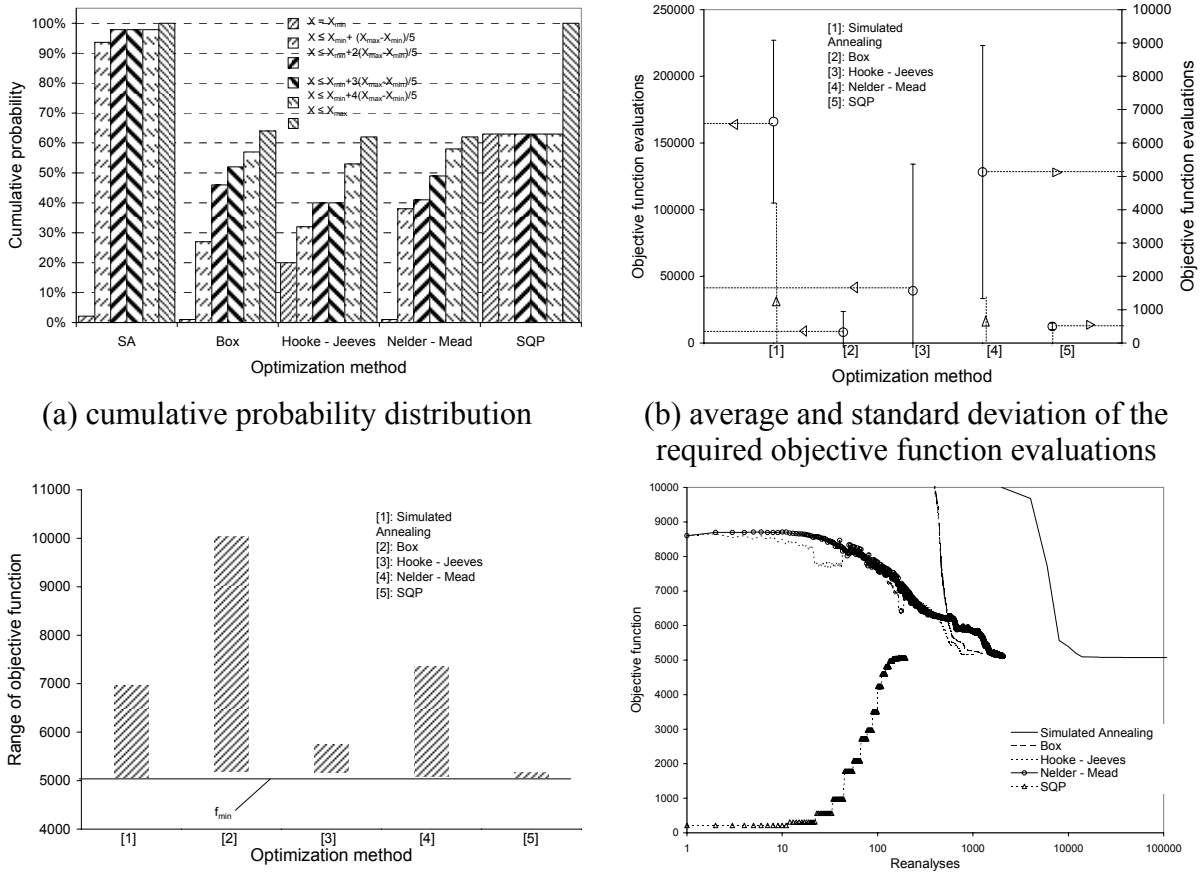

(a) cumulative probability distribution

(b) average and standard deviation of the required objective function evaluations

(c) range of objective function

(d) convergence history

Figure 2.12: Results for the ten-bar problem (variation B)

(HJ) and (NM) also presented a poor behavior. In more details, (HJ) was characterized by a short range of optimum values (Fig.2.5c) but, like Box, it never converged to the global optimum. On the contrary, (NM) appeared a shorter range of optimum values (Fig.2.5c) and it did converge to global optimum (Fig.2.5a) but only a very few times (poor performance). Furthermore, (SA) did not perform as well as in the previous cases since its range of optimum values was quite wide (Fig.2.5c). Once again, in comparison to the other methods, (SA) required a significantly larger number of objective function evaluations *NFE* and presented the largest standard deviation for *NFE* as well (Fig.2.5b). Finally, the convergence history diagrams (Fig.2.5d) showed that the selected penalty scheme was indeed hard because the convergence history curves, although smooth enough, were quite long. It is also noted that, like in the previous case, a logarithmic scale was selected for the x-axis of Fig.2.5d.

2.4.3.4. Results for (SSB4)

The results of the investigation concerning the 25-bar problem are illustrated in Fig.2.6. This time the performance picture of the optimization algorithms was not so clear.

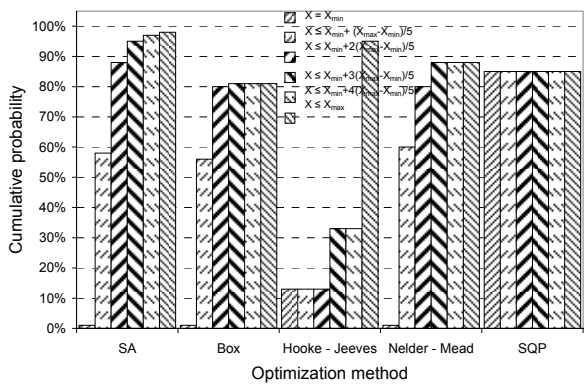

(a) cumulative probability distribution

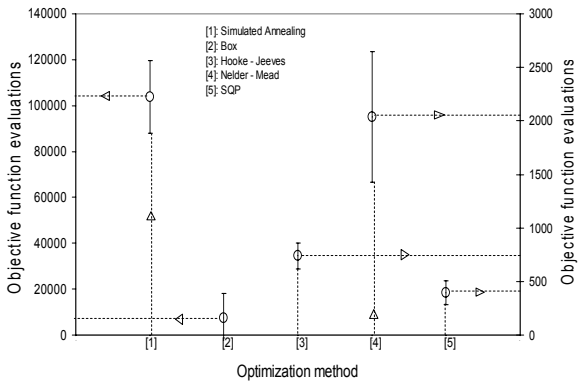

(b) average and standard deviation of the required objective function evaluations

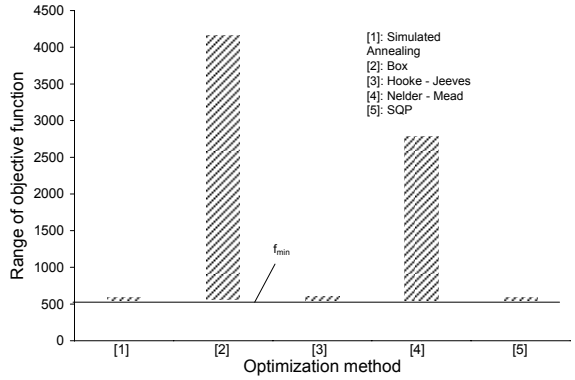

(c) range of objective function

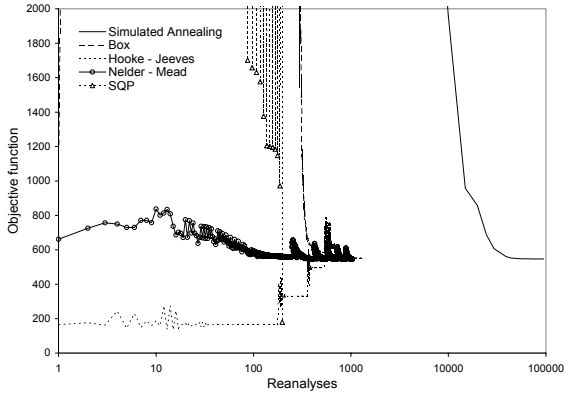

(d) convergence history

Figure 2.13: Results for the 25-bar problem

In more details, (SQP) again required the smallest number of objective function calls (Fig.2.6b) and it converged to the optimum result in all successful analyses (Fig.2.6c) but it presented the second largest number of failures (Fig.2.6a). (SA) had the lowest number of failures (Fig.2.6a) and a negligible width of range of optimum values (Fig.2.6c) but appeared a worse cumulative distribution profile than SQP (Fig.2.6a) and required a significantly amount of re-analyses (Fig.2.6b). Box's behavior was very poor because it resulted in an extremely wide range of optimum values (Fig.2.6c); (NM) presented a similar behavior (Fig.2.6c). On the other hand, (HJ) behaved very well in terms of required re-analyses (Fig.2.6b) and in terms of converging to the global optimum (Fig.2.6c) but its cumulative distribution profile was worse than that of (SA) or (SQP) (Fig.2.6a). Finally, the convergence history diagrams (Fig.2.5d) showed that the selected penalty scheme was quite hard because the convergence history curves did appear several peaks and were quite long. It is also noted that, like in the previous case, a logarithmic scale was selected for the x-axis of Fig.2.5d.

2.4.4. Other penalty schemes

Apart from the investigation presented above and due to the poor performance of Box, (HJ) and (NM), a further investigation was performed on these three optimization algorithms using other penalty schemes, namely the classical scheme for exterior penalizing and the inverse barrier and the inverse log barrier interior penalty functions. The result was that their behavior was dramatically improved as they almost always converged to the global minimum; the only drawback was the necessity for many iterations.

2.4.5. Conclusions

The current work presented the application of some of the most popular optimization algorithms, namely Simulated Annealing (SA), Box, Hooke & Jeeves (HJ), Downhill Simplex (Nelder-Mead) and a Sequential Quadratic Programming (SQP) approach, in four cases of size optimization of trusses, namely the 3-bar problem, two variations of the 10-bar problem and the 25-bar problem which is a space truss. Each algorithm was applied to each case 100 times initiating from a different design vector; especially for the Simulated Annealing the optimization procedure was initiating from a different temperature instead. The results obtained from the 2000 runs were evaluated according to four performance indices, namely the probability of getting the global minimum and near global minimum values (cumulative distribution profiles), the average and standard deviation of the required evaluations of the objective function, the range of the objective function minima and the convergence history. The output of the current investigation was that the SQP approach, in almost all cases, outperformed the other methods, because it required the least number of objective function evaluations, it presented a very high percentage of successive runs and the range of the optimum values was insignificantly wide. The (SA) presented a very good ability in locating the global optimum but proved to be very demanding in terms of computational cost. Box, (HJ) and (NM), when using a hard penalty scheme, generally presented a poor performance, while when the classical exterior or interior penalty methods were applied, their performance was impressively improved.

2.5. Investigation of Genetic Algorithms

2.5.1. Description

Genetic Algorithms (GAs) have a history extending in several decades. Cannon, one of the earliest progenitors of that history noted that evolution was a learning process and made a direct comparison to individual learning (Cannon, 1932). Turing stated that there is an obvious connection between machine learning and evolution (Turing, 1950). Barricelli worked on John von Neumann's high-speed computer at the Institute for Advanced Study in Princeton in the area of artificial life, in which numbers were placed in a grid and moved based on local interaction rules. His original research was published in Italian, but was republished in 1957 in English, while two additional publications extended his work (Barricelli, 1962a; 1962b). As noted in Fogel, Barricelli perhaps published the earliest record of any work in evolutionary computation (Fogel, 2006). In the late 1950s and early 1960s, evolutionary biologists were trying to model aspects of natural evolution on computers. By that time, it was not clear that this strategy could be applied to artificial problems. By 1962, researchers such as Box (Box, 1957), Friedberg (Friedberg, 1958; 1959), Bledsoe (Bledsoe, 1962a; 1962b) and Bremermann (Bremermann, 1962) had all independently developed evolution-inspired algorithms for function optimization and machine learning. In the late 1960s, Conrad offered a seminal contribution to artificial life (Conrad, 1969), the journal version of which was published by Conrad and Pattee (Conrad and Pattee, 1970). A population of cell-like individual organisms was subjected to a strict material conservation law that induced competition for survival. The organisms were capable of mutual cooperation as well as executing biological strategies that included genetic recombination and modification. No fitness criteria were introduced explicitly as part of the program. Instead, the simulation was viewed as an ecosystem in which genetic, individual, and population interactions would occur and behavior patterns would emerge. However, the work of the aforementioned researchers attracted little follow-up due to both the shortcomings that the methodologies presented suffered from and the lack of available powerful computer platforms at that time. A fundamental contribution is due to Rechenberg, who introduced the evolution

strategy technique, which was more similar to hill-climbing methods than to genetic algorithms (Rechenberg, 1965). In this technique, there was no population or crossover; one parent was mutated to produce one offspring, and the better of the two was kept and became the parent for the next round of mutation. In later versions, the idea of a population was introduced. Another very important development was due to Fogel, Owens and Walsh, who introduced the evolutionary programming technique (Fogel, Owens and Walsh, 1966). In this method, simple finite-state machines resembled candidate solutions to the investigated problems. Similarly to Rechenberg's evolution strategy, the algorithm worked by randomly mutating one of these simulated machines and keeping the better of the two. However, what was still lacking in both these methodologies was recognition of the importance of crossover. Holland was the first to explicitly propose crossover and other recombination operators. Although he had published other papers as well (Holland, 1973), his seminal work in the field of genetic algorithms came in 1975 (Holland, 1975). In this book, research and papers both by Holland and by his colleagues at the University of Michigan, perhaps for the first time, systematically and rigorously presented the concept of adaptive digital systems using mutation, selection and crossover, thus simulating processes of biological evolution as a problem-solving strategy. The book also attempted to put genetic algorithms on a firm theoretical footing by introducing the notion of schemata (Haupt and Haupt, 1998). That same year, De Jong's important dissertation established the potential of GAs by showing that they could perform well on a wide variety of test functions, including noisy, discontinuous, and multimodal search landscapes (De Jong, 1975). Another pioneer in GA optimization was Goldberg, with a landmark text published in 1989 (Goldberg, 1989), who believes that 'Three billion years of evolution can't be wrong. It's the most powerful algorithm there is'. These foundational works were the cornerstone for the explosive development that followed in the next years (Michalewicz, 1996). By the early to mid-1980s, genetic algorithms were being applied to a broad range of subjects, such as biology, computer science, engineering, operations research, image processing, pattern recognition, physical sciences and social sciences to name but a few (Goldberg, 1989). Some examples of successful engineering applications in various industries is the use of GA by J. Deere to optimize plant production scheduling, the implementation of GA by Texas Instruments for circuit design to minimize computer chip sizes, the use of GA by General Electric for gas turbine design to increase fuel efficiency, which led to the development of the Boeing 777 engine, the use of GA by the US West to design fiber-optic cable networks, cutting design times from two months to two days, and saving US West $1 million to $10 million on each network design, and many more (Begley, 1995).

Therefore, it is more than obvious that the performance of a GA is of major importance and controlled by various parameters. The aim of investigating GAs was to evaluate the influence that these parameters have on their performance, or equivalently to investigate the sensitivity of the GA performance with respect to the controlling parameters. The set of benchmark problems used for this investigation, also retrieved from the literature, is briefly presented in the next paragraph. In the sequel, the evaluation indices used, as well as the analysis carried out, a brief discussion and the conclusions drawn are stated.

2.5.2. GA controlling parameters

For the completeness of the text, a brief presentation of a typical GA is required. However, since there are many text books describing GAs very thoroughly (Holland, 1975; Goldberg, 1989; Michalewicz, 1996), emphasis has been put only on presenting the parameters, along with their main options, that control the GA performance. Therefore, the parameters investigated in the present work are presented in the following paragraphs.

The parameter *Generations* determines the maximum number of iterations that the GA will perform and serves as a stopping criterion. It is emphasized that this quantity should not be confused with the *Stall Generation* parameter mentioned later.

The parameter *Population Size* determines the number of individuals existing in each generation. It is clarified that the population size remains unchanged during the optimization process.

The parameter *Population creation* determines the method that the creation of the initial population is based on. For the present work, the initial population was created randomly by implementing a uniform distribution.

The parameter *Fitness Scaling* converts raw fitness scores obtained using the objective (fitness) function to values in a range that is suitable for the selection function. A specific function, called scaling function, specifies the way the scaling is to be performed. The scaling functions investigated were:

- The *Rank* function, which removes the effect of the spread of the raw scores by scaling the raw scores according to the rank of each individual and not according to the score itself. The rank of an individual is defined as its position in the sorted scores (the fittest individual has rank 1, the next fittest has rank 2, etc).
- The *Proportional* function, which makes the expectation proportional to the raw fitness score. It is noted that the performance of this function may be poor depending on the disparity of the raw scores.
- The *Top* function, which scales the individuals with the highest fitness values equally, thus each one of these individuals has an equal probability of reproducing.
- The *Shift linear* function, which scales the raw scores so that the expectation of the fittest individual is equal to a user-defined constant multiplied by the average score.

The parameter *Selection* defines the parents for the next generation taking into consideration their scaled values. The following functions were investigated:

- The *Stochastic uniform* function, which, as the name suggests, assigns parents stochastically. In more details, a line is constructed of segments each length of which is proportional to the expectation of each parent and then a movement along this line is performed in steps of equal size (one step for each parent). At each step the aforementioned movement ends in a segment and the corresponding parent is chosen. It is noted that the first step is a uniform random number less than the step size.
- The *Remainder* function, which attributes each individual with a scaled value having an integer part and a fractional part. For the parent selection, the integer part is combined with the result of a roulette selection performed on the remaining fractional part.
- The *Uniform* function, which, based on the expectations and the number of parents, uses a uniform distribution for the random selection of the parents (undirected search). Although the uniform selection is not a very useful search strategy, it is used for evaluation purposes.
- The *Roulette* function, which simulates a roulette wheel. More particularly, a wheel is divided in as many sectors as the potential parents are and each sector has an area proportional to the expectation of the corresponding potential parent. In the sequel, a random number is used to select one of the sectors with a probability equal to its area, thus the corresponding parent is selected.
- The *Tournament* function, which picks an individual to be a parent as the fittest out of a group of individuals which are randomly selected and evaluated. The size of the group is defined by the user.

The parameter *Crossover* defines the way two individuals (parents) are to be combined so that a new individual (offspring or child) is created for the next generation. The crossover options investigated were:

- The *Scattered* crossover with which a new individual is created in a two-step procedure, the first step being the random creation of a binary vector and the second step being the use of information from the first or the second parent depending whether the aforementioned vector has an entry '1' or '0', respectively.
- The *Single point* crossover with which a new individual is created in a two-step procedure. The first step is the random selection of an integer number N_{sc} between 1 and the total number of the design variables. The second step is the concatenation of information retrieved from the first parent and for the first N_{sc} entries with information retrieved from the second parent and for the rest entries, respectively.
- The *Two point* crossover, which, as the term suggests, is a single point crossover performed twice. In more detail, two integer number $N_{tp,1}$ and $N_{tp,2}$ between 1 and the total number of the design variables are selected. A new individual is created as follows: for the first $N_{tp,1}$ entries information is retrieved from the first parent, for the next $\left(N_{tp,2}-N_{tp,1}\right)$ entries information is retrieved from the second parent, while for the rest entries information is retrieved from the first parent again.
- The *Intermediate* crossover with which children are created by a weighted average of their parents. The controlling quantity (*Ratio*) in this case is a random positive real number less or at most equal to one.
- The *Heuristic* crossover uses the fitness values of the two parents to determine the direction of the search. The offspring are created according to the following equations: $\text{Offspring\_1=Best parent} + r\left(\text{Best parent - Worst parent}\right)$, $\text{Offspring\_2=Best parent}$ where r is a random number between 0 and 1.

The parameter *Mutation* is a genetic operator that alters one or more design variables (genes in the GA terminology) from its initial state. In this way entirely new design vectors can be formed and the GA may be able to arrive at a better solution than was previously possible. Mutation is an important part of the genetic search as it helps the prevention from stagnating at local optima. Mutation occurs during evolution according to a user-definable mutation probability, which should be set fairly low (as low as 0.01). If this value is high, then the search will turn into a primitive random search. The mutation options investigated were:

- The *Uniform* mutation which is a two-step process. In the first step, the design variables to be mutated are defined. In the second step, each one of these variables is replaced by a uniform random value selected between the user-specified upper and lower bounds corresponding to each variable.
- The *Gaussian* mutation which adds a random number, taken from a Gaussian distribution centered on zero, to each design variable that will be mutated. This procedure is controlled with two parameters, the first being the *Scale* and the second being the *Shrink*. The former parameter determines the variance at the first generation, while the latter parameter controls how variance shrinks as generations go by.

The parameter *Migration Direction* is combined with the ability of evolving several subpopulations at the same time. In more details, individuals are said to migrate if they move from one subpopulation to another. The migration aims at replacing the worst individuals of a subpopulation with the best individuals from another subpopulation. Migration can be either unidirectional (*Forward*), where the n-th subpopulation migrates into the $\left(n+1\right)$-th subpopulation, or bidirectional (*Both*), where the n-th subpopulation migrates not only into the $\left(n+1\right)$-th subpopulation but also into the $\left(n-1\right)$-th subpopulation.

The parameter *Stall Generation* terminates the algorithm if for a user-defined number of generations the value of the objective function presents negligible improvement.

2.5.3. Examples

From a theoretical point of view, all the aforementioned parameters have a significant influence on the performance of a typical GA. However, such a theoretical and vague evaluation should be quantified. Towards this direction, the present work investigated the parameters mentioned in Section 2. More particularly, eight parameters were studied using four well-known benchmark mathematical functions retrieved from the literature. The benchmark functions implemented are presented in the following Tables. In more details, the definition of the functions is presented in Table 1.

Table 2.2: Names, expression and domain of the examined benchmark functions

Function	Mathematical expression	Domain
3-variable (Rosenbrock)	$f(x_1, x_2, x_3) = -x_1 x_2 x_3$	$x_1, x_2, x_3 \in [0, 42]$
4-variable	$f(x_1, x_2, x_3, x_4) = 0.5\sum_{j=1}^{4}\left(x_j^4 - 16x_j^2 + 5x_j\right)$	$x_1, x_2, x_3, x_4 \in [-4.0,\ 0]$
Powell	$f(\vec{x}) = (x_1 + 10x_2)^2 + 5(x_3 - x_4)^2 + (x_2 - 2x_3)^4 + 10(x_1 - x_4)^4$	$x_j \in \square$, $j = 1,..,4$
Suzuki	$f(\vec{x}) = x_1^2 + x_2^2 + 2x_3^2 + x_4^2 - 5x_1 - 21x_3 + 7x_4 - 5x_2$	$x_j \in \square$, $j = 1,..,4$

The imposed constraints, as well as the optimal solutions, are presented in Table 2. It is noted that for the 4-variable function, no constraints are imposed.

Table 2.3: Constraints, optimal design vector and optimal objective function value

Constraints	Optimal design vector	Minimum value
$0 \le x_1 + 2x_2 + 2x_3 \le 72$	$(x_1, x_2, x_3) = (24, 12, 12)$	$f_{\min} = -3456$
No constraints imposed	$(x_1, x_2, x_3, x_4) = (-3, -3, -3, -3)$	$f_{\min} = -156$
$g_j(\vec{x}) = x_{j+2} - 2 \ge 0,\ \ j = 1,2\ x_j,\ j = 1,..,4$	$\vec{x} = (1.275, 0.6348, 2, 2)$	$f_{\min} = 189.1$
$g_1(\vec{x}) = -2x_1^2 - x_2^2 - x_3^2 - 2x_1 + x_2 + x_4 + 5 \ge 0$ $g_2(\vec{x}) = -x_1^2 - x_2^2 - x_3^2 - x_4^2 - x_1 + x_2 - x_3 + x_4 + 8 \ge 0$ $g_3(\vec{x}) = -x_1^2 - 2x_2^2 - x_3^2 - 2x_4^2 + x_1 + x_4 + 10 \ge 0$	$\vec{x} = (0, 1, 2, -1)$	$f_{\min} = -44$

Due to the stochastic character of the GA method and in order to get reliable and representative results, for each benchmark function and for each one of the examined parameters, 100 analyses were performed initiating from randomly generated but feasible design vectors and each group of 100 results was distinguished in 'successful' and 'failed' runs, depending on whether the runs were terminated normally or not, respectively. In the sequel, the mean value of the 'successful' runs, normalized with respect to the corresponding optimum retrieved from the literature, as well as the corresponding standard deviation were estimated. In addition, a cumulative probability-based index was also estimated. For the aforementioned index, the interested reader may find details in [25].

The work plan of the present research was as follows:

Step #1: for each examined option, perform 100 analyses, get the results derived and keep the analyses that were terminated normally (successful runs)
Step #2: for the successful runs, normalize the optimal values of the objective functions with respect to the minimum values referred in the literature for each examined function
Step #3: using the values from Step #2, for each examined case, estimate the cumulative probability index of 1st class, the normalized mean value and the normalized standard deviation
Step #4: create a bar chart where the middle of each bar corresponds to the normalized mean value, while, above and below this point, a length equal to the corresponding normalized standard deviation is added
Step #5: create a bar chart for the cumulative probability index showing only the first class
Step #6: for each option investigated, choose the best performance based on the plots; from the plots of Step #4, reject all the options with poor performance and keep only options with similarly good performance; for these options, use the plots from Step #5 to estimate the best option.

It is clarified that when a parameter was investigated, the other controlling parameters were kept unchanged and equal to a default value. Finally, normalized mean values less than unity are due to the optimal values' sign.

2.5.4. Numerical results

2.5.4.1. The Crossover parameter

Seven functions were investigated, namely the scattered, the single point, the two-point, two variations of the intermediate ($ratio = 0.5$ and $ratio = 1.0$) and two variations of the heuristic ($ratio = 1.2$ and $ratio = 2.0$). The normalized sensitivities and the cumulative probability of 1st class derived are illustrated in Fig.2.1, respectively. In Fig.2.1a, the absence of bars for the 4-variable function is due to the fact that the normalized values were equal to 0.999 and the corresponding bars are of zero height (degenerated bars) thus not visible. From Fig.2.1a, it yields that the heuristic crossover with $ratio = 1.2$ outperformed the other schemes. However, the heuristic crossover with $ratio = 2.0$ did not perform well at all. Therefore, the conclusion is that it was the combination of the heuristic type of the crossover with an appropriate value for $ratio$ that performed so well. Furthermore, again from Fig.2.1a, the crossover functions presented the poorest performance for the Powell function, while, in the majority, the normalized range of the results is within a zone of 1% around the optimal value. Fig.2.1b with Fig.2.1a also suggest that the heuristic crossover with $ratio = 1.2$ performed best.

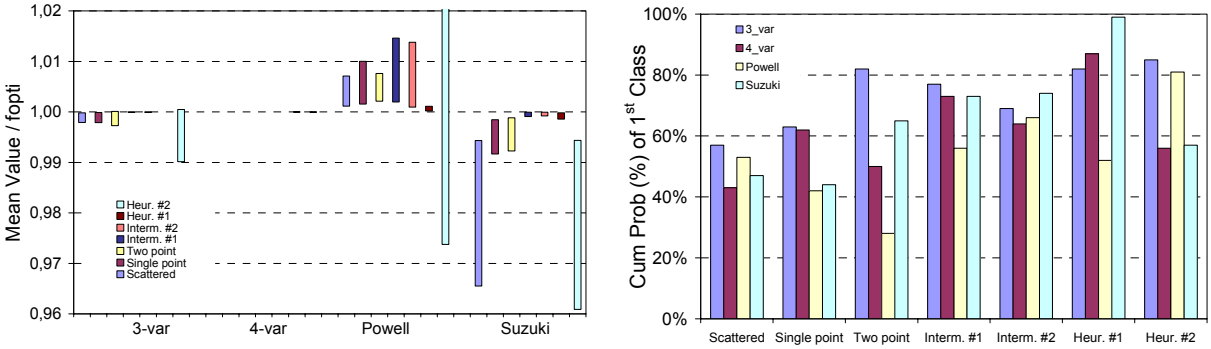

Figure 2.14: (a) normalized sensitivity and (b) cumulative probability of 1st class for the crossover functions

2.5.4.2. The Fitness scaling parameter

For the *Fitness scaling* parameter, four functions were investigated, namely the rank, the proportional, the top and the shift linear. The normalized sensitivities and the cumulative probability of 1st class derived are illustrated in Fig.2.2, respectively. Again, an absence of bars is observed in Fig.2.2a for the 4-variable function due to the fact that the normalized values were equal to 0.999 and the corresponding bars are of zero height (degenerated bars) thus not visible. From Fig.2.2a, it yields that the rank function outperformed the other schemes. The same conclusion is derived from Fig.2.2b as well, since the top function must be excluded due to its very poor performance when applied to the Powell function (Fig.2.2a).

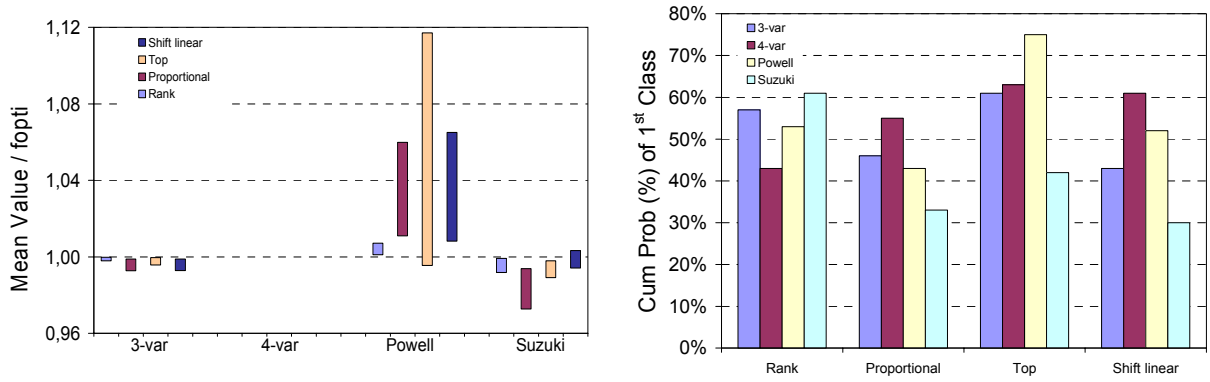

Figure 2.15: (a) normalized sensitivity and (b) cumulative probability of 1st class for the fitness scaling functions

2.5.4.3. The Generations parameter

Five options were investigated, namely with 200, 400, 600, 800 and 1000 maximum iterations, respectively. There seems to appear some kind of malfunction for the 600 generations, thus the corresponding results are not considered reliable From Fig.2.3a, it results that for the 3-variable function, there was no improvement in the optimal objective function value as the number of generations increased. This observation was considered to be problem-oriented, thus not taken into consideration. For the 4-variable function, apart from the value of 600 generations, all the analyses converged to very near optimum values thus no bars are visible for evaluation. For the Powell and for the Suzuki functions, it is obvious that increasing the number of generations means improving the derived optimal values.

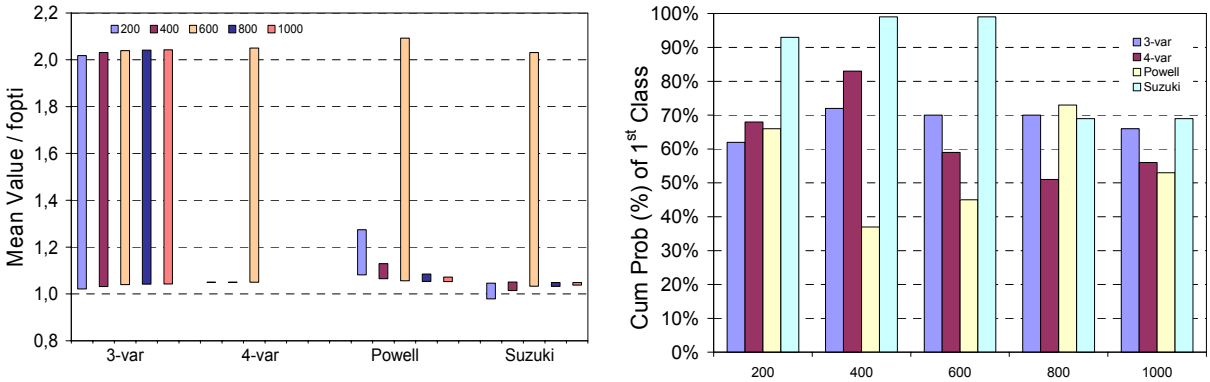

Figure 2.16: (a) normalized sensitivity and (b) cumulative probability of 1st class for the number of generations

2.5.4.4. The Migration parameter

Two options were investigated, namely the 'Forward' and 'Both' migration direction. For the 3-variable function, from Fig.2.4a it seems that both migration directions perform equally well, while from Fig.2.4b it yields that the 'Forward' option is better. For the 4-variable function, from Fig.2.4a it yields that all the results are negligible away from the optimum value while from Fig.2.4b it yields thus the 'Both' options is strongly better. From the reaming two functions, it is obvious that the 'Both' option has a better performance, a remark also in agreement with Fig.2.4b.

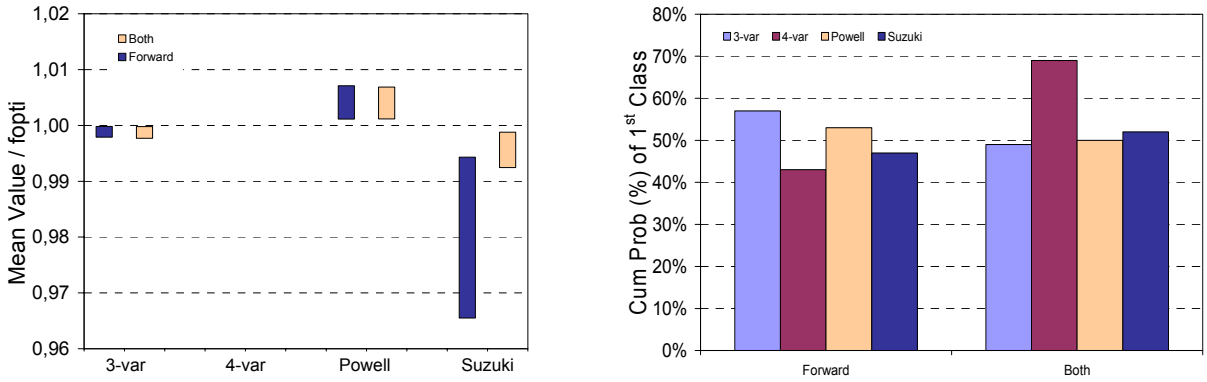

Figure 2.17: (a) normalized sensitivity and (b) cumulative probability of 1st class for the direction of migration

2.5.4.5. The Mutation parameter

Four options were investigated, namely 'Gaussian #1', 'Gaussian #2', 'Uniform #1' and 'Uniform #2'. For the first option, the controlling parameter 'scale' and 'shrink' were set equal to 0.5 and 0.75, respectively. For the second option, these parameters were set equal to 1 and 1, respectively. For the third and forth option, the controlling parameter 'rate' was set equal to 0.01 and 0.10, respectively. From Fig.2.5a, the 'Gaussian #1' option performs best, although no information can be retrieved from the 4-variable function for the reason already mentioned in the previous paragraphs. Due to its poor performance with the Powell and the Suzuki functions, the 'Uniform' scheme is rejected. From Fig.2.5b, it is shown that 'Gaussian #2' outperforms 'Gaussian #1' only once (for the 3-variable function). Therefore, it is derived that 'Gaussian #1' should be the preferred option.

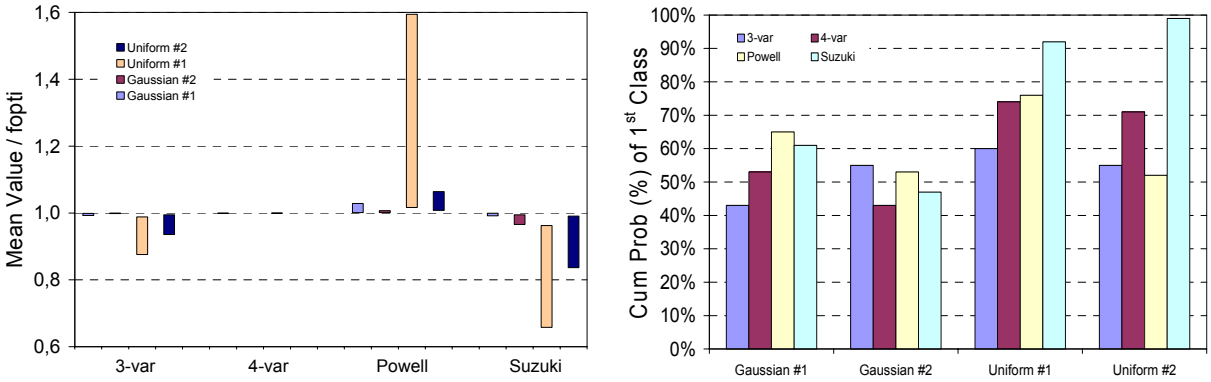

Figure 2.18: (a) normalized sensitivity and (b) cumulative probability of 1st class for the mutation operators

2.5.4.6. The Population size parameter

Five options were investigated, with populations of 20, 40, 60, 80 and 100 individuals, respectively. As Fig.2.6a shows, increasing the population size resulted in improving the optimal objective function value.

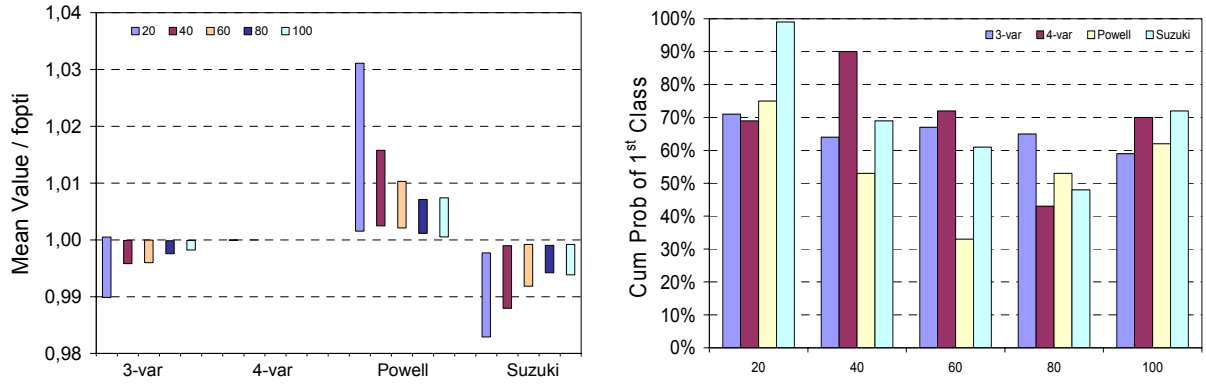

Figure 2.19: (a) normalized sensitivity and (b) cumulative probability of 1st class for the population size

2.5.4.7. The Selection parameter

Five functions were investigated, namely the stochastic uniform, the remainder, the uniform, the roulette and the tournament. From Fig.2.7a, it is obvious that the 'Uniform' and the 'Tournament' functions performed worst for the Powell function, while the other functions performed in a quite similar way. From Fig.2.7b, it yields that, excluding the 3-variable function, the 'Roulette' function outperforms the others.

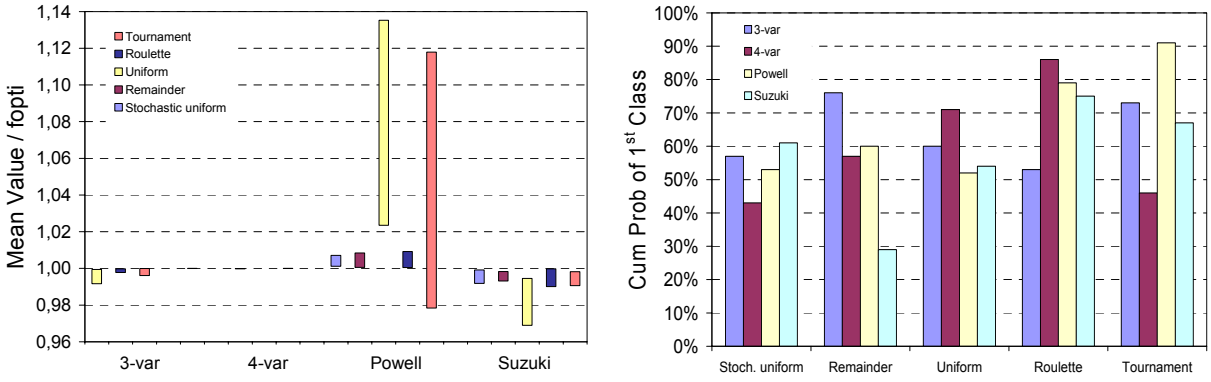

Figure 2.20: (a) normalized sensitivity and (b) cumulative probability of 1st class for the selection function

2.5.4.8. The Stall generations parameter

Ten options were investigated, with stall generations equal to 50, 100, 200, 250, 300, 400, 450, 500, 550, 600 and 700, respectively. From Fig.2.8a, it is clear that the higher the stall generation value is, the better the performance becomes. Practically, this means to let the GA explore and exploit the feasible domain the longer possible. In Fig.2.8b, only indicative cases are illustrated.

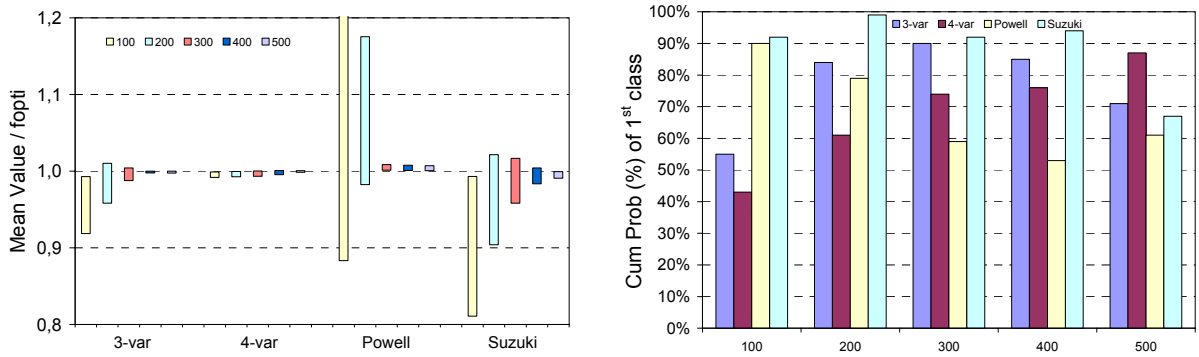

Figure 2.21: (a) normalized sensitivity and (b) cumulative probability of 1st class for the stall generations

2.5.5. Conclusions

The present work aimed at ranking the influence of each one of the investigated parameters in locating the global minimum. For this purpose, an extensive parametric investigation of eight parameters was carried out. The first and most important conclusion is that in all cases, it was possible to get optimum or very near optimum values by appropriately selecting ('trimming') the controlling parameters. Among the options examined, it was possible to distinguish some that outperformed the others. More particularly, for the crossover, the heuristic function with ratio equal to 1.2 was the best. For the fitness scaling, the rank function is a very good choice. For the decision over the number of generations, it should be kept in mind that increasing the number of generations means improving the derived optimal values. For the migration direction, 'Both' seems to be a good selection. For the mutation, a Gaussian scheme with the parameters 'scale' and 'shrink' set equal to 0.5 and 0.75 is suggested. With respect to the population size, it should be taken into consideration that increasing the population size results in improving the optimal objective function value. For the selection, the roulette function seems to outperform the others. Finally, the higher the stall generation value is, the better the performance becomes. Last, but far from least, it is clarified that the aforementioned suggestions aim at providing a guide rather than a bulletproof set of rules-of-thumb for performing optimization with a typical GA. More general suggestions may be derived only if the presented investigation is repeated for a very large number of functions.

2.6. The proposed hybrid optimization procedure

Based on the experience obtained from the aforementioned investigations, a new hybrid optimization scheme was formulated and is presented in this Section. For its evaluation, an extended set of Mathematical Benchmark Functions, also briefly presented in this Section, was used. In the sequel, the implemented evaluation indices, as well as the analysis carried out, a brief discussion and the conclusions drawn are also stated.

2.6.1. On hybrid optimization procedures

Hybrid search techniques are widely used for structural optimization. An approach for hybrid optimization is to embed local search into the framework of evolutionary algorithms or the combinations of various techniques.

Mahfoud and Goldberg presented the Parallel Recombinative Simulated Annealing. After initialization of a population and choice of a system temperature T, parents are selected. The

offsprings are produced by recombination and mutation, followed by a comparison between parents and their offsprings. Subsequently, the parents are replaced by the winners and T is reduced. This process is repeated for the complete population in every iteration (Mahfoud and Goldberg, 1994). Renders and Flasse examined the trade-off between accuracy, reliability and computing time in global optimization. In more details, first they examined the compromises provided by traditional methods (Quasi-Newton and Nelder-Mead's simplex methods) and then they referred to new hybrid methods, which combine principles from genetic algorithms and "hill-climbing" methods in order to find a better compromise to the trade-off. These hybrid methods are inspired by biology and involve two interwoven levels of optimization, namely evolution (genetic algorithms) and individual learning (Quasi-Newton), which cooperate in a global process of optimization. Renders and Flasse proposed a hybrid method that combines the reliability properties of the genetic algorithms with the accuracy of Quasi-Newton method, while requiring a computation time only slightly higher than the latter (Renders and Flasse, 1996). Botello et al. combined the search-operators selection, crossover, mutation of genetic algorithms with the acceptance operator of the Simulated Annealing and calls this the General Stochastic Search Algorithm. The unmodified individuals of a population (before variation by recombination and mutation) are compared with the varied ones. The acceptance operator selects solutions to be carried over to the next generation (Botello et al, 1999). Galinier and Hao presented a Hybrid Evolutionary Algorithm which embeds local search into the framework of population-based Evolutionary Algorithms, leading to Hybrid Evolutionary Algorithms. The basic idea consists of using the crossover-operator (Greedy Partition Crossover) to create new and potentially interesting configurations, which are then improved by the local search operator (Tabu Search) (Galinier and Hao, 1999). Burke and Smith incorporated a local search operator into a genetic algorithm. The resulting algorithm from this hybrid approach has been termed a Memetic Algorithm. The paper investigates the use of a memetic algorithm in solving a thermal generator maintenance scheduling problem. The main purpose is to discover whether a memetic approach can be advanced (Burke and Smith, 2000). Magoulas et al. introduced a new hybrid evolutionary approach for improving the performance of neural network classifiers in slowly varying environments. They investigated a combination of Differential Evolution Strategy and Stochastic Gradient Descent. The use of a Differential Evolution Strategy is based on the concept of evolution of a number of individuals from generation to generation, while the on-line gradient descent refers to the concept of adaptation to the environment by learning (Magoulas et al., 2001). Schmidt and Thierauf examined the combination with the Threshold Accepting Algorithm (TA), which computes the functional in every cycle of the iteration and is essential for the increased performance. The Differential Evolution (DE) helps to avoid local optima. By application of penalty functions even inadmissible solutions are allowed, whereby the approximation of the global optimum is possible either from the admissible direction as well as from the inadmissible direction. Admissible results are stored and treated similar to the elite individual in the Genetic Algorithms (Schmidt and Thierauf, 2005).

Within the frame defined by the aforementioned methods, a new hybrid method is proposed according to which the search direction is sough using Powell's method, while the distance to be followed along this direction is sought using Simulated Annealing (SA). It is strongly emphasized that the selection of these two search procedures was based on two facts. The first fact is that, while being a very simple variation of the univariate optimization procedure, Powell's method consists a tremendous improvement (Venkatamaran, 2002). The second fact is that (SA) seems to outperform the other optimizers as far as 1D optimization problems are concerned, and the distance to be followed along a search direction is exactly such an optimization problem.

2.6.2. Theoretical basis

The basic components of the proposed procedure, namely the univariate optimization, the so-called 'left-shifting' of the search direction and the Simulated Annealing (SA), are discussed briefly in the following paragraphs.

The univariate optimization is nothing else but solving, for each design variable and in a cyclic manner, the 1-D optimization problem:

$$\min f\left(\underset{\sim}{x}_i + \alpha \underset{\sim}{d}_j\right),\ \underset{\sim}{x}_{low} \le \underset{\sim}{x}_i \le \underset{\sim}{x}_{up} \tag{2.8}$$

where $\underset{\sim}{x}_i$ is the design vector of the $i-$th iteration, the scalar quantity α is the step size for the vector direction $\underset{\sim}{d}_j$ and $\underset{\sim}{d}_j$ is the $j-$th univariate search direction with $j = 1,...,N_{\text{var}}$, while N_{var} is the number of the design variables. It is possible to store these search directions in a vector **SD** of dimension $N_{\text{var}} \times N_{\text{var}}$. The lower and upper bounds of the design vector $\underset{\sim}{x}_i$ are denoted as $\underset{\sim}{x}_{low}$ and $\underset{\sim}{x}_{up}$, respectively. The 1-D optimization problem may be solved using various techniques (Golden Section, Fibonacci, polynomial-based methods, etc.). One complete cycle consists of solving problem (2.8) for $j = 1,...,N_{\text{var}}$.

Let $\underset{\sim}{x}_{i,before}$ and $\underset{\sim}{x}_{i,after}$ be the design vectors before and after the application of a complete cycle. The pattern search direction is defined as:

$$\underset{\sim}{d}_{ps} = \underset{\sim}{x}_{i,after} - \underset{\sim}{x}_{i,before} \tag{2.9}$$

Therefore, it is possible to state another 1-D optimization problem of the following form:

$$\min f\left(\underset{\sim}{x}_{i,after} + \alpha_{ps} \underset{\sim}{d}_{ps}\right),\ \underset{\sim}{x}_{low} \le \underset{\sim}{x}_i \le \underset{\sim}{x}_{up} \tag{2.10}$$

It is possible to store the pattern search direction in the vector **SD** as the $\left(N_{\text{var}}+1\right)$-th entry. The so-called 'left shifting' of the search directions is using the $j+1$ search direction of the i iteration as the j search direction of the $i+1$ iteration. The $j+1$ search direction of the $i+1$ iteration is created from Eq.2.(2).

If a deterministic 1-D optimizer is used for solving the problem in Eq.(2.10), then tracing the global minimum is guaranteed if the function to be optimized is unimodal, that is the function has only one minimum, within the feasible domain of a. If unimodality is not present then a poor performance of the deterministic optimizer may occur, depending on the value $a_{ps,ini}$ (initial value of a in problem (2.10)). The reason for this is the fact that the deterministic procedures tend to bracket a minimum, thus if bracketing is miss driven then another but the global minimum is traced. Better results may be obtained when sweeping the domain of a in small steps, which, of course, is computationally expensive. On the contrary, a stochastic 1-D optimizer is less prone to get trapped in local minima because it has the inherent ability of making random changes in the step size. In this way, the probability of 'getting out' of local minima is higher, thus the element of randomness needs to be present in an optimization procedure. In addition, as shown in the previous sections of this chapter, the lower the number of the design variables gets the more effective the stochastic optimizers become. Therefore, problem (2.10), which involves one variable only, is the best possible case for a stochastic optimizer to be applied.

Based on these thoughts, it is obvious that solving problem (2.8) using a deterministic optimizer and solving problem (2.10) using a stochastic optimizer is a good theoretical compromise because not only is randomness introduced but also the computational cost remains low and the ability of getting out of local minima is maximized. On top of that, if solving problem (2.10) provides no improvement, then a *local* stochastic search, around the design vector found last, is performed as a means of continuing the search in case the aforementioned vector corresponded to a local minimum. The proposed procedure is as follows:

Step 1: Create randomly a $N_{\text{var}} \times 1$ design vector $\underset{\sim}{X}_o$

Step 2: Create a $\left(N_{\text{var}}+1\right) \times N_{\text{var}}$ vector of univariate search directions **SD**. For the first iteration only, the first N_{var} entries are the unit vectors corresponding to each one for the coordinate axes, while the $\left(N_{\text{var}}+1\right)$-th entry corresponds to the pattern search direction to be created in step 4.

Step 3: Perform a univariate deterministic optimization to find a new optimal and feasible design vector $\underset{\sim}{X}_1$.

Step 4: Define a pattern search direction as $\underset{\sim}{d}_{ps} = \underset{\sim}{X}_1 - \underset{\sim}{X}_o$.

Step 5: For the objective function $f\left(\underset{\sim}{X}_1 + \alpha \underset{\sim}{d}_{ps}\right)$, search stochastically along the pattern search direction (1D-optimization w.r.t. the step size a) to find a new optimal and feasible design vector $\underset{\sim}{X}_2$.

Step 6: Check for convergence

IF $\left|\underset{\sim}{X}_2 - \underset{\sim}{X}_1\right| \le tol$, where tol is a given tolerance, *THEN*

stochastically search a region around $\underset{\sim}{X}_2$ to find a new optimal and feasible design vector $\underset{\sim}{X}_3$

IF $\left|\underset{\sim}{X}_3 - \underset{\sim}{X}_2\right| \le tol$ *THEN*

Stop

ELSE

update **SD** with the pattern direction $\left(\underset{\sim}{X}_3 - \underset{\sim}{X}_2\right)$, set $\underset{\sim}{X}_o = \underset{\sim}{X}_3$ and return to Step 3

ELSE

set $\underset{\sim}{X}_o = \underset{\sim}{X}_2$, 'left-shift' the search directions and return to Step 3.

The physical interpretation of Step 5 is the uniform scaling of a design vector until no further improvement is noted, where α is the scaling parameter. There are two ways the domain of α may be handled, either as an unconstrained domain or as a constrained domain. In the former case, *first* any value may be attributed to α and *then* it is checked whether both the objective function decreases and the corresponding design vector is feasible. In the latter case, based on the search direction and the feasible domain of the design variables, *first* the feasible domain of α is estimated and *then* the optimization procedure takes place within this domain. The feasible domain of α may be estimated using a search scheme, such as the bisection method, while in the present work, the upper and lower values of α are estimated explicitly, as shown, with a symbolic vector notation, in Eqs.(2.11):

$$a_{upper} = \min\left\{\left(\underset{\sim}{X}_l - \underset{\sim}{X}_S\right) / \underset{\sim}{d}_{ps}\right\} \tag{2.11a}$$

$$a_{lower} = \min\left\{\left(\underset{\sim}{X}_u - \underset{\sim}{X}_S\right) / \underset{\sim}{d}_{ps}\right\} \tag{2.11b}$$

As $\underset{\sim}{X}_l$ and $\underset{\sim}{X}_u$, the vectors for the minimum and the maximum values of the design variables are noted, respectively, while $\underset{\sim}{d}_{ps}$ represents the pattern search direction. In this way, the feasible domain of α is bracketed thus any 1-D deterministic optimizer may be applied. In the present paper, the Golden section technique and the Simulated Annealing (SA) were chosen as the deterministic and the stochastic optimizer, respectively. Alternatively, instead of the SA, a Genetic Algorithm, Tabu Search or even a powerful second-order method, such as the Sequential Quadratic Programming (SQP) technique, may be applied as well.

2.6.3. Numerical analysis

For the purposes of the present paper, four popular benchmark functions were selected, implementing one, two, four and eight variables, respectively. For each one of these functions, the domain, the optimal design vector and the global minimum are known. In order to investigate the performance of the proposed procedures, for each benchmark function, certain variations were introduced, as presented in the following paragraphs.

2.6.3.1. (MBF1) with variations

For this benchmark function (Eq.2.12a), the domain is $[2.7, 7.5]$ while there are three minima, the global minimum being $f_{opti} = -1.886$ at $x = 5.145$. The other two variations examined are presented in Eqs.(2.12b, 2.12c).

$$f(x) = \sin(x) + \sin\left(10\frac{x}{3}\right) \tag{2.12a}$$

$$f(x) = \sin(x) + \sin\left(20\frac{x}{3}\right) \tag{2.12b}$$

$$f(x) = \sin(x) + 2\sin\left(10\frac{x}{3}\right) \tag{2.12c}$$

The function plots (Fig.2.1) show that, for the introduced variations, the difficulty in tracing the minimum is higher due to an increased number of local minima (Fig.2.1(b) or due to more steep valleys (increased gradients) that make trapping at local minima easier (fig.2.1(c)).

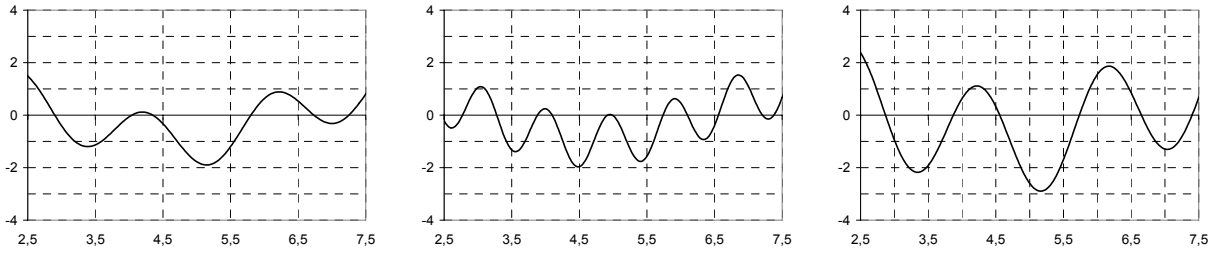

(a) **(b)** increased number of optima **(c)** strong peaks and valleys

Figure 2.22: Plots for the examined one-variable function (a) basic expression, (b) and (c) variations introduced

2.6.3.2. (MBF2) with variations

For this benchmark function (Eq.2.6a), the domain is $\underset{\sim}{x} \in [-1,1]$ and the global minimum is $f_{opti} = -2.000$ at $\underset{\sim}{x} = \underset{\sim}{0}$. The variations examined are presented in Eqs.(2.13b, 2.13c).

$$f\left(\underset{\sim}{x}\right) = \sum_{j=1}^{2}\left(x_j^2 - \cos\left(18x_j\right)\right) \tag{2.13a}$$

$$f\left(\underset{\sim}{x}\right) = \sum_{j=1}^{2}\left(x_j^2 - \cos\left(25x_j\right)\right) \tag{2.13b}$$

$$f\left(\underset{\sim}{x}\right) = \sum_{j=1}^{2}\left(x_j^2 - 3\cos\left(18x_j\right)\right) \tag{2.13c}$$

Generally speaking, it is possible to create a plot for a two-variable function. However, the mathematical expression of the examined function suggests that only the plot of one addendum is required for a good impression of the function to be obtained, since there are no terms in both x_1 and x_2 (Eqs.2.13). Therefore, it is sufficient to plot an addend in x_1 or in x_2 only, as shown in Fig.2.2.

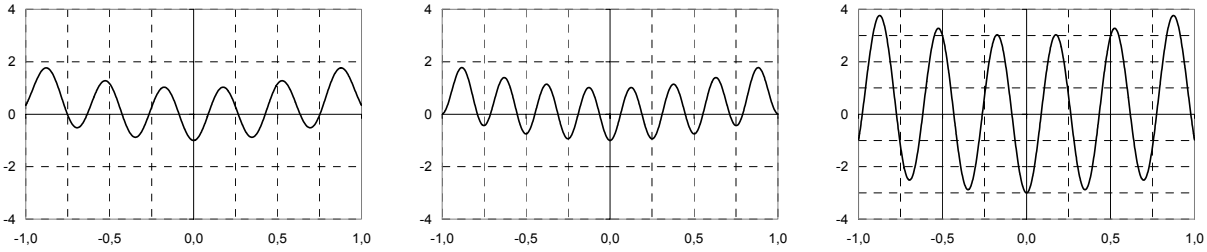

(a) **(b)** increased number of optima **(c)** strong peaks and valleys

Figure 2.23: Plots for the examined two-variable function (a) basic expression, (b) and (c) variations introduced

Again, an increase in the number of minima is clear in Fig.2.2b, while Fig.2.2c illustrates a function with strong peaks and valleys, thus the difficulty in tracing the minimum is increased as well.

2.6.3.3. (MBF3) with variations

For this benchmark function (Eq.2.14a), the domain is $\underset{\sim}{x} \in [-4,0]$, and the global minimum is $f_{opti} = -156.66$ at $x_i = 2.9035,\ i = 1,..,4$. The variations examined are presented in Eqs.(2.14b, 2.14c).

$$f\left(\underset{\sim}{x}\right) = 0.5\sum_{j=1}^{4}\left(x_j^4 - 16x_j^2 + 5x_j\right) \tag{2.14a}$$

$$f\left(\underset{\sim}{x}\right) = 0.5\sum_{j=1}^{4}\left(x_j^4 - 16x_j^2 + 5x_j - 15\cos\left(5x_j\right)\right) \tag{2.14b}$$

$$f\left(\underset{\sim}{x}\right) = 0.5\sum_{j=1}^{4}\left(x_j^4 - 16x_j^2 + 5x_j - 25\cos\left(5x_j\right)\right) \tag{2.14c}$$

As in the previous case, the function has no terms in two or more different design variables, thus a good impression of the function can be obtained from the plot of only one addendum in an arbitrarily selected design variable, as shown in Fig.2.3.

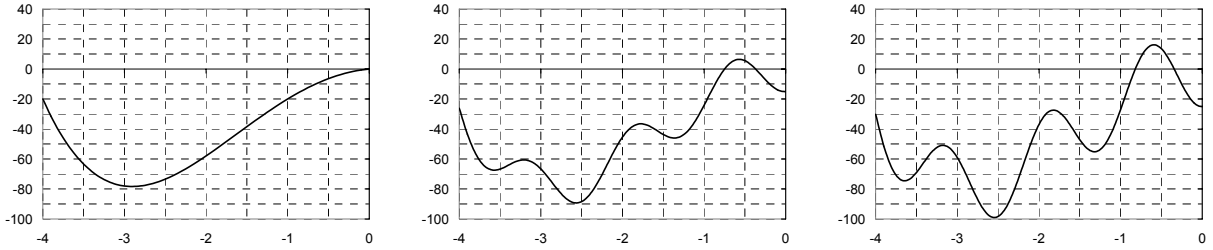

(a) **(b)** increased number of optima **(c)** strong peaks and valleys

Figure 2.24: Plot for the examined four-variable function (a) from literature, (b) and (c) the variations introduced

2.6.3.4. (MBF4) with variations

For this function (Eq.2.15a), the domain is $\underset{\sim}{x} \in [-5.12, 5.12]$ and the global minimum is $f_{opti} = 0$ at $\underset{\sim}{x} = \underset{\sim}{0}$. The variations examined are presented in Eqs.(2.15b, 2.15c).

$$f(\underset{\sim}{x}) = 80 + \sum_{j=1}^{4}\left(x_j^2 - 10\cos(2\pi x_j)\right) \tag{2.15a}$$

$$f(\underset{\sim}{x}) = 80 + \sum_{j=1}^{4}\left(x_j^2 - 10\cos(4\pi x_j)\right) \tag{2.15b}$$

$$f(\underset{\sim}{x}) = 80 + \sum_{j=1}^{4}\left(x_j^2 - 30\cos(2\pi x_j)\right) \tag{2.15c}$$

Once again, the plot of only one addendum in an arbitrarily selected design variable may provide a representative impression of the function, as shown in Fig.2.24.

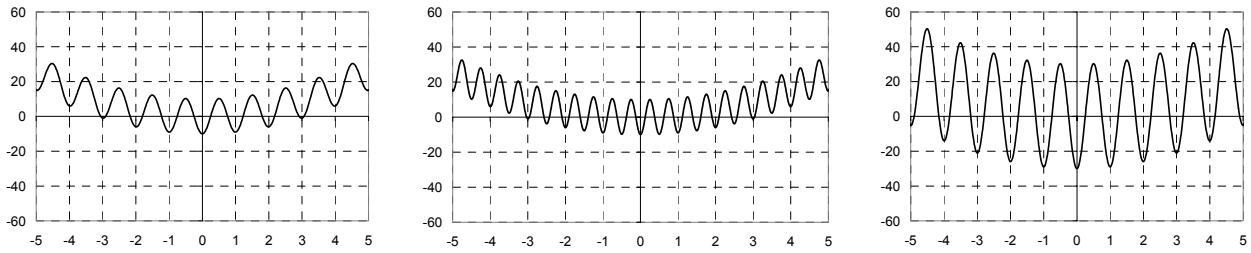

(a) **(b)** increased number of optima **(c)** strong peaks and valleys

Figure 2.25: Plot for the examined two-variable function (a) from literature, (b) and (c) variations introduced

2.6.4. Numerical results

In order to evaluate the performance of the proposed hybrid procedure (Hybrid), $N_{\max} = 100$ analyses were performed for each one of the examined functions. For an analysis k, the initial design vector $\underset{\sim}{x}_{ini,k}$ was estimated as:

$$\underset{\sim}{x}_{ini,k} = \underset{\sim}{x}_{\min} + (k-1)\left(\underset{\sim}{x}_{\max} - \underset{\sim}{x}_{\min}\right) / \left(N_{\max} - 1\right),\ k = 1,2,...,100 \tag{2.16}$$

where $\underset{\sim}{x}_{\min}$ and $\underset{\sim}{x}_{\max}$ are vectors containing the lower and the upper bounds of the design variables, respectively. For reasons of comparison, the same work was repeated using other optimization procedures, namely the Powell method, the Nelder-Mead simplex method (N-M), the Hooke and Jeeves pattern search method (H-J) and the Simulated Annealing (SA), which are indeed comparable since they all are zero-order methods thus belong to the same class of optimization procedures. Again, for each method and for each function, 100 optimization analyses were performed, thus the present work was based on the results retrieved from 7200 runs. An analysis was characterized as successful if it resulted in a vector $\underset{\sim}{X}_{converg}$ in the neighborhood of the global minimum $\underset{\sim}{X}_{opt}$:

$$\left|\underset{\sim}{X}_{converg} - \underset{\sim}{X}_{opt}\right| \le tol \tag{2.17}$$

It was of interest to estimate the percentage of successful runs thus the following evaluation index was defined:

$$EI_1 = \left(N_{success} / N_{total}\right) \tag{2.18}$$

Obviously, $EI_1 = 1$ is the maximum value that this index may take and corresponds to the best possible performance. The values for the evaluation index EI_1 for the various objective functions and optimization methods were appropriately illustrated in bar charts. Furthermore, it was of interest to estimate the number of iterations required until convergence was achieved. To this end, for each set of 100 analyses, the mean value and the corresponding standard deviation concerning the recorded iterations were estimated and illustrated appropriately in diagrams, where a logarithmic scale was used for the vertical axis.

2.6.4.1. Results for (MBF1) with variations

For the one-variable functions, the Powell method outperformed the others since it was rated with $EI_1 = 1$ (Fig.2.4a) and required the least number of iterations for such a performance (Fig.2.4b). The Hybrid method was rated the same with the Powell method and the SA, but it required more iterations than the SA.

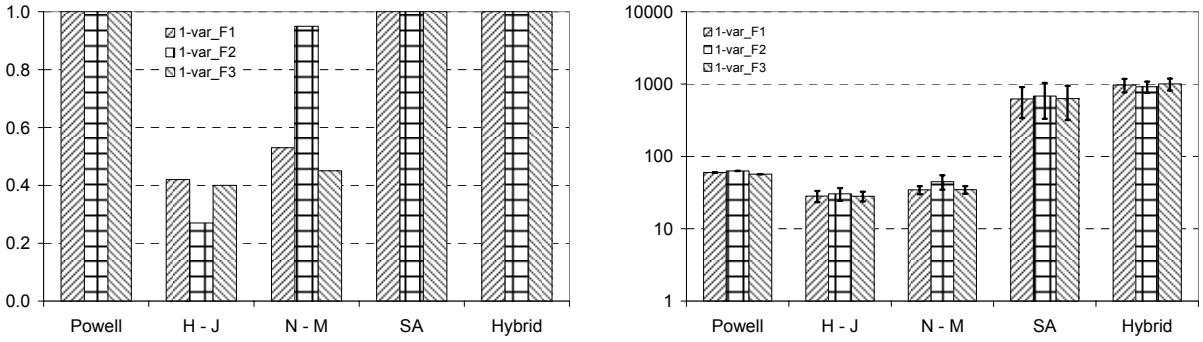

(a) evaluation index (b) iterations required

Figure 2.26: Performance of the optimization procedures for the one-variable functions

2.6.4.2. Results for (MBF2) with variations

For the two-variable functions, the Hybrid method outperformed the others since it was rated with $EI_1 = 1$ and required slightly more iterations than the second best method which was the SA with $EI_1 < 0.4$. All the others methods were trapped in local minima and presented a very poor performance (Fig.2.5a).

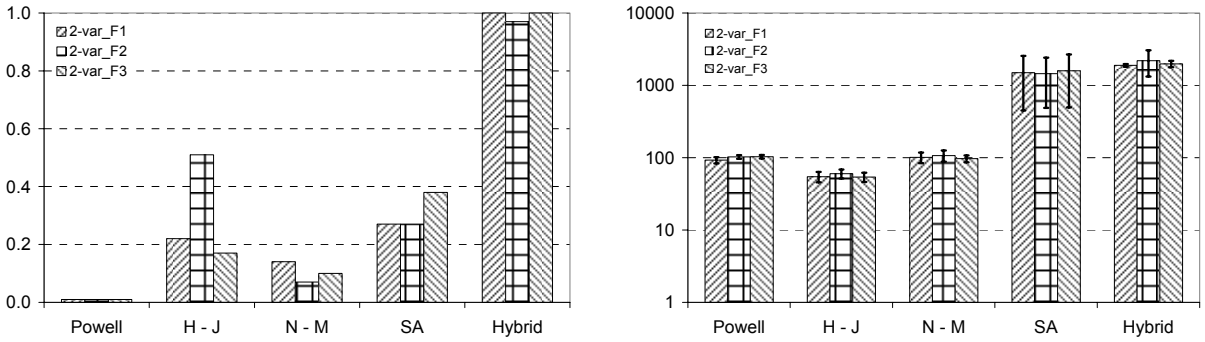

(a) evaluation index (b) iterations required

Figure 2.27: Performance of the optimization procedures for the two-variable functions

2.6.4.3. Results for (MBF3) with variations

For the four-variable functions, the picture is quite the same with that for the one-variable functions. The Powell method performed best because it was rated with $EI_1 = 1$ (Fig.2.6a) and required the least number of iterations (Fig.2.6b). The Hybrid scheme performed equally excellently as the SA did but required more iterations. The other two methods, that is H-J and N-M, performed very well for the basic formulation of the objective function but had serious trouble with locating the global minimum for the second and the third proposed variations of the objective function.

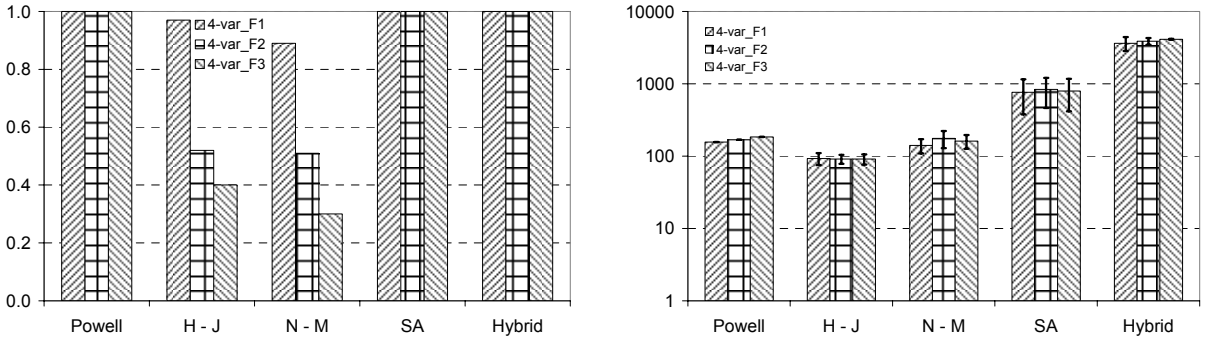

(a) evaluation index (b) iterations required

Figure 2.28: Performance of the optimization procedures for the four-variable functions

2.6.4.4. Results for (MBF4) with variations

For the eight-variable functions, only the SA and the proposed Hybrid scheme managed to have a very near-excellent performance for all of the objective functions (Fig.2.7a), with the Hybrid scheme having a slight advantage in terms of the evaluation index EI_1 and a disadvantage in terms of iterations required until convergence was achieved (Fig.2.7b). The Powell method managed to locate the global minimum excellently only for one of the

examined objective functions, while in the other two cases it failed totally. The H-J method did not perform well, while the N-M technique performed most inadequately.

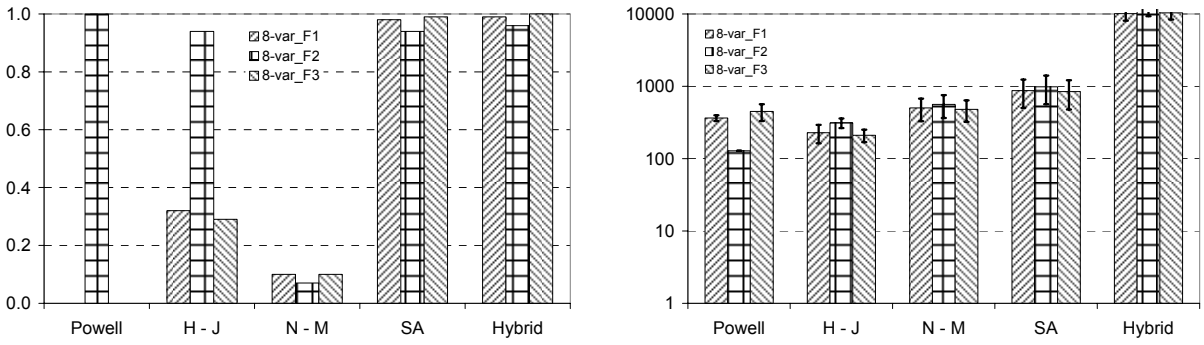

(a) evaluation index (b) iterations required

Figure 2.29: Performance of the optimization procedures for the eight-variable functions

2.6.5. Discussion

A new hybrid scheme for dealing with the minimization of unconstrained mathematical functions was proposed. The basic idea was to introduce some element of randomness in a powerful *deterministic* technique, when no further improvement from the deterministic steps is achieved. More particularly, a deterministic procedure will stop either when the global optimum has been found or when a local optimum is erroneously recognized as a global optimum. If the latter case occurs, then the introduction of some randomness increases the probability of 'getting out' of the local minimum, although not annihilating the chance of failing to do so. For the needs of the present study, Powell's variation for the univariate optimization technique was selected as the deterministic procedure, while the element of randomness was introduced using the Simulated Annealing (SA) technique in two ways. First, a (SA) *line* search was activated along the last formed pattern search direction, when a complete deterministic iteration provided no improvement. Second, a (SA) *local* search in a hyper-sphere surrounding the location of no improvement was initiated, when no improvement from the SA line search was achieved. The radius of this hyper-sphere was a user-defined parameter and severely affected the efficiency of the entire procedure. If again no improvement was achieved, then the search was terminated and the location of no improvement was recognized as the global optimum. The proposed scheme was expected to combine the superior performance of a pure SA and the lower number of iterations characterizing Powell's method. It was shown that in all of the examined cases, the global optimum was indeed located; however, the iterations required were more than those corresponding to a pure SA. The reason for this was the fact that convergence was checked at the end of a *complete* iteration, *all* of the deterministic and the stochastic steps being included. However, the number of function calls for such iterations may become very large since the same (SA) optimizer, with the same adjustments, may be called twice within the same step. This implies that a further improvement, concerning the total number of function calls, may be achieved if convergence is checked within a complete iteration and the adjustments for the (SA) are different for the line search and the local search.

A point worth noting is the sensitivity with respect to the domain of the examined functions. It was observed that either a slight or a significant change in the upper bound or the lower bound or both, severely affected the values of the evaluation index EI_1 for the examined *deterministic* procedures. This is the reason why the performance in some cases, especially of the Powell method, was so poor. In addition, it was observed that, in some cases,

when the domain of an *even* function was changed from symmetric to asymmetric then the performance was better. On the contrary, the proposed hybrid scheme and the (SA) presented a very robust behavior, insensitive to changes in domain bounds.

2.6.6. Conclusions

The proposed hybrid scheme falls in the class of the non-zero optimization methods. It was tested in four triplets of objective functions, each triplet consisting of one function retrieved from the literature and two more variations introduced for the need of the present study. One variation concerned the introduction of more local minima only, while the other variation concerned the introduction of stronger peaks and valleys only. In this way, the difficulty in locating the global minimum was significantly increased. In all of the twelve examined objective functions, the proposed hybrid scheme presented an excellent or very near-excellent performance. Furthermore, the proposed scheme was compared to four other well-known optimization methods of the same class, namely the Powell variation for the univariate optimization, the Nelder-Mead simplex method (N-M), the Hooke and Jeeves pattern search method (H-J) and the Simulated Annealing (SA) technique. It was found out that none of the aforementioned methods outperformed the proposed hybrid scheme in terms of locating the minimum, while the cost for this was an increased number of iterations required until convergence was achieved. The promising performance of the proposed hybrid scheme, when applied to unconstrained mathematical functions, encourages for extending the examination to optimization problems not only of constrained mathematical functions but also of constrained structural layouts. However, it is anticipated to get a significantly high computational cost which denotes the necessity for examining other types of optimization schemes, such as indirect search procedures.

2.7 Recapitulation

Based on the analysis presented in the previous sections, it yields that:

- The direct search stochastic optimization methods perform better as the number of the design variables decreases.
- The direct search deterministic optimization methods perform better than the direct search stochastic optimization methods as the number of the design variables increases.
- The penalty scheme implemented in an optimization procedure seriously affects its performance.
- For 1D optimization problems, the Simulated Annealing (SA) optimization method seems to outperform the other optimization procedures.
- It is possible to combine a deterministic search scheme with a stochastic search scheme in order to create a hybrid optimization procedure. For instance, it is possible to use a deterministic procedure for estimating a search direction and a stochastic procedure for estimating the step size or vice versa. Such combinations are numerous and involve some innovation since all they actually do is combining already known optimization procedures, or variations of them, in a different order. Nevertheless, they do contribute in the exploration of the potential that such optimization methods have.
- The proposed hybrid optimization method outperforms the competition in terms of tracing the global optimum but its computational cost is very high.
- The increased computational cost of direct search methods suggest that other types of optimization procedures, such as the indirect methods, be investigated.

The direct search methods, either deterministic or stochastic, do not take into consideration intrinsic characteristics of the problem at hand. Therefore, a structural optimization problem,

at the eyes of a direct search optimization method, is the same as any other optimization problem, such as describing a diet of minimum calories or minimizing the idle time in typical queue problems. However, especially for the structures, there is one quantity that does have physical interpretation and its distribution over the structure is uniquely associated with the structural design, the material, the support and the loading. This quantity is the strain energy, while other energy derivatives, such as the virtual strain energy and the corresponding densities, may be used as well. A direct search method, used for the weight minimization of a structure, does not take into consideration this information. Generally speaking, it is best when all of the available information is exploited. For this to be applied in structural optimization problems, it is necessary that the optimization method includes energy formulations. Consequently, and since the direct search methods do not present an exceptionally good performance in solving mathematical optimization problems, it yields that another optimization scheme, embedding energy concepts, should be formulated.

References

Barricelli, N.A. (1962a), "Numerical testing of evolution theories: I. Theoretical introduction and basic tests", Acta Biotheoretica, Vol. 16:1-2, pp.69-98.

Barricelli, N.A. (1962b), "Numerical testing of evolution theories: II. Preliminary tests of performance symbiogenesis and terrestrial life", Acta Biotheoretica, Vol. 16:1-2, pp.69-98.

Begley, S. (1995), "Software au Naturel", Newsweek, May 8.

Belegundu, A.D., Chandrupatla, T.R. (1999), Optimization concepts and applications in engineering, Prentice Hall.

Bendsøe, M.P., Sigmund O. (2003), Topology Optimization, Theory, Methods and Applications, Springer-Verlag, Berlin.

Bledsoe, W.W. (1962), An Analysis of Genetic Populations, Technical Report, Panoramic Research Inc., Palo Alto, California.

Bledsoe, W.W. (1962), The Evolutionary Method in Hill Climbing: Convergence Rates, Technical Report, Panoramic Research, Inc., Palo Alto, California.

Botello S, Marraquin J.L, Onãte E, Van Horebeek J (1999), "Solving structural optimization problems with genetic algorithms and simulated annealing", Int J Numer Methods Eng, Vol.45, pp.1069–1084.

Box, G.E.P. (1957), "Evolutionary operation: A method for increasing industrial productivity", Appl. Statistics, vol. VI (2), pp.81-101.

Box, M.J. (1965), "A New Method of Constrained Optimization and a Comparison with Other Methods", Computer J, Vol.8, pp.42-52.

Bremermann, H.J. (1962), "Optimization through Evolution and Recombination", In Self-Organizing Systems, eds. M. T. Yovits, Jacobi, and Goldstein. Washington, D. C.: Spartan, pp.93-106.

Burke E.K., Smith A.J. (2000), "Hybrid evolutionary techniques for the maintenance scheduling problem", IEEE Trans Power Syst , Vol.15(1), pp.122–128.

Cannon, W.D. (1932), The Wisdom of the Body, W.W. Norton, New York.

Cauchy, A. (1847), "Methode generale pour la resolution des systemes d'equations simultanes", Compt. Rend., Vol.25, pp.536-538.

Conrad, M. (1969), Computer experiments on the evolution of coadaptation in a primitive ecosystem, Ph.D. Diss., Biophysics Program, Stanford, CA.

Conrad, M., Pattee, H.H. (1970), "Evolution experiments with an artificial ecosystem", J. Theoret. Biol., Vol. 28, pp.393-409.

Courant, R. (1943)"Variational methods for the solution of problems of equilibrium and vibrations", BullAmerMathSoc.,Vol.49,pp.1–23.

Dantzig, G. B., (1951)) "Maximization of a linear function of variables subject to linear inequalities", Activity Analysis of Production and Allocation, Koopman (Ed.), Cowles Commission Monograph, 13, John Wiley and Sons, New York.

De Jong, K. (1975), An analysis of the behaviour of a class of genetic adaptive systems, PhD thesis, University of Michigan.

Fiacco, A.V., McCormick, G.P. (1966), "Extension of SUMT for nonlinear programming: equality constraints and extrapolation", Management Science, Vol. 12, pp.816-828.

Fletcher, R., Powell, M.J.D. (1963), "A rapidly convergent descent method for minimization", Computer J., Vol.6(2), pp.163-168.

Fletcher, R., Reeves, C.M (1964), "Function Minimization by Conjugate Gradients", Computer J., Vol.7, pp.149-154.

Fogel, D.B. (2006), Evolutionary Computation: Toward a New Philosophy of Machine Intelligence, 3rd ed., IEEE Press, New York.

Fogel, L. J., Owens, A.J., Walsh, M.J. (1966). Artificial Intelligence through Simulated Evolution. John Wiley & Sons, New York.

Friedberg, R.M. (1958), "A Learning Machine: Part I"," IBM J. Research and Development, Vol. 2, pp.2-13.

Friedberg, R.M., Dunham B., North,J.H. (1959),"A Learning Machine: Part II", IBM J. Research and Development, Vol. 3, pp.183-191.

Galinier P, Hao J.K. (1999), "Hybrid evolutionary algorithms for graph coloring", J Comb Optim, Vol. 3(4), pp.379–397.

Giotis A., Giannakoglou K. (2004), Evolutionary Algorithm SYstem version 1.3.4, manual, Laboratory of Thermal Turbomachines, National Technical University of Athens.

Goldberg, D. (1989), Genetic Algorithms in Search, Optimization, and Machine Learning. Addison-Wesley.

Haftka, R.T., Gurdal, Z., Kamat, M. (1990), Elements of Structural Optimization, Kluwer.

Haupt, R., Haupt S.E. (1998), Practical Genetic Algorithms, John Wiley & Sons, New York.

Holland, J.H. (1973), "Genetic Algorithms and the Optimal Allocation of Trials", SIAM J. Comput. Vol.2(2), pp.88-105.

Holland, J.H. (1975), Adaptation in natural artificial systems, University of Michigan Press, Ann Arbor, MI.

Hooke, R., Jeeves, T.A. (1961), "Direct Search Solution of Numerical and Statistical Problems", J of the ACM, Vol.8, pp.212-229.

Karush, W. (1939), Minima of Functions of Several Variables with Inequalities as Side Conditions, MS Thesis, Dept. of Mathematics, University of Chicago, Chicago, IL.

Kirkpatrick, S. (1984), "Optimization by simulated annealing: quantitative studies", J Statist Phys, Vol. 34, pp. 975-986.

Kirsch, U. (1993), Structural Optimization, Springer-Verlag.

Kuhn, H.W., Tucker A.W. (1951) "Non-linear Programming", in J.Neyman (Ed.), Proceedings of the Second Berkeley Symposium on Mathematical Statistics and Probability, University of California Press, Berkeley, CA , pp.481-493.

Magoulas G.D., Plagianakos V.P., Vrahatis M.N. (2001), "Hybrid methods using evolutionary algorithms for on-line training", In: Proceedings of the INNS-IEEE International Joint Conference on Neural Networks, Washington DC; 14–19 July 2001, USA.

Mahfoud W.S., Goldberg D.E. (1994), "Parallel recombinative simulated annealing: a genetic algorithm", IlliGAL Report No. 93006, Department of Computer Science, University of Illinois.

Makris, P., Provatidis, C. (2002), "Weight minimisation of displacement-constrained truss structures using a strain energy criterion", Computer Methods Appl. Mech. Engrg., Vol. 191, pp. 2159-2177.

Michalewicz, Z. (1996), Genetic Algorithms + Data Structures = Evolution Programs, 3rd ed., Springer Verlag, Berlin.

Morris, A.J. (1982), Foundations of Structural Optimization: A Unified Approach, John Wiley & Sons.

Nagendra, S. (1997), Catalogue of test problems for Optimization Algorithms verification, GE Research & Development Center.

Nelder, J.A., Mead, R. (1965), "A Simplex Method for Function Minimization", Computer Journal, Vol.7, pp. 308-313.

Pham, D.T., Karaboga D. (2000), Intelligent Optimisation Techniques: Genetic Algorithms, Tabu Search, Similated Annealing and Neural Netwroks, Springer-Verlag.

Powell, M.J.D. (1964), "An efficient Method for finding the minimum of a function of several variables without calculating derivatives", Computer Journal, Vol.7 (4), pp.303-307.

Rechenberg, I. (1965), Cybernetic solution path of an experimental problem. Royal Aircraft Establishment, Farnborough, page Library Translation 1122.

Renders, J.M., Flasse, S.P. (1996), "Hybrid methods using genetic algorithms for global optimization", IEEE Transactions on Systems, Man, and Cybernetics, Part B.

Rosen, J. (1960), "The Gradient Projection Method for Nonlinear Programming, I. Linear Constraints", *Journal of the Society for Industrial and Applied Mathematics*, Vol.8, pp.181–217.

Rosenbrock, H.H. (1960), "An Automatic Method for finding the Greatest or Least Value of a Function", Comp J, Vol.3, pp.175-184.

Rozvany, G.I.N. (2001), "Aims, scope, methods, history and unified terminology of computer-aided topology optimization in structural mechanics", Struct. Multidisc Optim, Vol. 21, pp. 90-108.

Russo, L. (2004), *The forgotten revolution: How science was born in 300BC and why it had to be reborn.* Springer, Berlin.

Schmidt, H., Thierauf G. (2005), "A combined heuristic optimization technique", Advances in Engineering Software, Vol.36, pp. 11–19.

Suzuki, K., Kikuchi, N. (1991), "A Homogenization Method for Shape and Topology Optimization", Computer Methods Appl. Mech. Engrg., Vol. 93, pp. 291-318.

Turing, A.M. (1950), "Computing machinery and intelligence", Mind, Vol. 59, pp.433-460.

Venkatamaran, P. (2002), *Applied Optimization with Matlab Programming*, Wiley.

Veselago, V.G. (2002), "Formulating Fermat's principle for light traveling in negative refraction materials", *PHYS-USP*, Vol. 45(10), pp. 1097-1099.

Xie, Y.M., Steven, G.P. (1997), *Evolutionary Structural Optimization*, Springer-Verlag.

Zoutendijk, G. (1960), Methods of Feasible Directions, Elsevier.

Contributed papers

[1] Provatidis, C.G., Vossou C.G., **Venetsanos D.T.**, "Verification of popular deterministic and stochastic optimization methods using benchmark mathematical functions", In: D.Tsahalis (ed.), CD Proc. 1st International Conference "From Specific Computing to Computational Engineering", 8-10 September, 2004, Athens, Greece.

[2] Provatidis C.G., **Venetsanos D.T.**, Vossou C.G., "A comparative study on deterministic and stochastic optimization algorithms applied to truss design", In: D.Tsahalis (ed.), CD Proc. 1st International Conference "From Specific Computing to Computational Engineering", 8-10 September, 2004, Athens, Greece.

[3] Provatidis C.G., **Venetsanos D.T.**, Markos P.A., "Investigation Of Hybrid Optimization Schemes With A Deterministic Search Direction And A Stochastic Step Size", 2nd International Conference "From Scientific Computing to Computational Engineering", 5-8 July, 2006, Athens, Greece.

[4] Papageorgiou A.A., **Venetsanos D.T.**, Provatidis C.G., "Investigating The Influence Of Typical Genetic Algorithm Parameters On The Optimization Of Benchmark Mathematical Functions", 2nd International Conference "From Scientific Computing to Computational Engineering", 5-8 July, 2006, Athens, Greece.

CHAPTER 3

THEORETICAL ASPECTS IN LAYOUT STRUCTURAL OPTIMIZATION

Abstract

In this chapter, theoretical aspects concerning the layout structural optimization problem are presented. In more details, various modes of material removal are theoretically examined, such as the removal of a single element at a time or the thickness reduction of elements. Since the aforementioned material removal is based on an energy approach, it can be used for any kind of constraints. In this chapter, the compliance constraint problem that has attracted the interest of the researchers, as well as the Fully Stressed Design that addresses to stress constrained structures, is discussed.

Keywords

Layout optimization, compliance constraint, Fully Stressed Design.

3.1. Introduction

After the seminal work by Michell (Michell, 1904), the optimal design of structures have been considered as a material distribution problem, or equivalently as a layout optimization problem. This layout optimization is sought in various ways, all of which aim either at removing material that is characterized as redundant or at redistributing the available material more efficiently. For this material elimination or redistribution, it is possible to implement pure mathematically-oriented techniques Svanberg, 1987; 1995; Stolpe and Svanberg, 2001; Bruyneel et al, 2002). However, in this way, it is not possible to take advantage of the energy stored in a deformed body, which is a valuable inherent characteristic of structural optimization problems. Alternatively, it is possible to formulate energy-based techniques. In this chapter, such an approach is presented from a critical viewpoint. More particularly, the total material elimination, in the form of element removal, as well as the partial material elimination, in the form of thickness reduction, is examined. Furthermore, the single compliance constraint problem is discussed, and the very well-known concept of a fully-stressed design is also presented.

The partial or complete material elimination may be sought using the so-called Evolutionary Structural Optimization (ESO) method (Xie and Steven, 1993; 1996; 1997; Xie et al, 2005; Steven et al, 2000). According to this approach, it is possible to define sensitivity or performance indices, as a means to detecting material candidate for removal (Nha Chu et al, 1996; 1997). Based on the value of these indices, the available material is ranked and that part with the smaller sensitivity is removed, either partially or completely (Querin et al, 2000a; 2000b; Yang et al, 1999; 2005). The concept of the ESO method is very simple, straightforward, and with a wide range of applications (Rong et al, 2000; Das et al, 2005; Ren et al, 2005; Zuo et al, 2005; Wei, 2005). However, for the time being, it is based more on the logical thought of removing redundant material in order to reduce the total structural weight and lacks a sound mathematical proof (Zhou and Rozvany, 2001; Edwards et al, 2007), even though such approaches have been published (Tanskanen, 2002). In the present Chapter, the theoretical approach of an ESO-type element elimination is first presented and then discussed. This presentation makes the current text self-contained, while it also serves as a means to denote, in a clear and well-defined manner, the differences between this approach, found in the literature, and that proposed in Section 3.3.

The compliance constraint problem is another type of optimization problem for which a great many number of papers have been published (Bendsøe and Kikuchi, 1988; Bendsøe, 1989; Haber et al, 1996; Kita and Tanie, 1999; Fujii and Kikuchi, 2000; Bendsøe and Sigmund, 2003; Burns and Tortorelli, 2003; Allaire et al, 2004; Burns, 2005). This problem may be found in the literature in two formulations, the former being seeking for the minimization of the compliance under a given material quantity (Bendsøe and Sigmund, 2003; Sigmund, 2001a; 2001b; 2001c), let it be Problem CCA, and the latter being seeking for the minimization of the structural weight under a given compliance, let it be Problem CCB (Xie and Steven, 1993). However, it is true that none of the standards used for steel structures, or for any other kind of structure, imposes a constraint regarding the compliance. Therefore, the question at hand is why deal with this type of problem. The answer to this question is quite simple: it can be proved that the compliance constraint optimization problem is convex thus a local solution to this problem is a global solution at the same time (Svanberg, 1994). On top of that, the compliance constraint is the simplest type of constraint that may be imposed, while other types of constraints are more difficult to handle (Duysinx and Sigmund, 1988; Duysinx and Bendsøe, 1998; Bendsøe and Sigmund, 2003). This is particularly true with the stress constraints. Furthermore, minimum compliance means maximum stiffness, and in this way it is possible to obtain a good impression of how to distribute available material in order to get maximum stiffness. By now, the compliance topology design problem is a well-

studied class of problems, in particular if the underlying mechanical model represents a truss structure. Several convex formulations of minimum compliance problems exist. This class of problems can be reformulated as linear semi-definite programs (Ben-Tal and Nemirovski, 1995; 1997; 2000), second order cone programs (Ben-Tal and Nemirovski, 1994), or non-smooth problems (Achtziger et al., 1992; Ben-Tal and Bendsøe, 1993).

For the compliance constraint problem, a new optimization procedure is proposed. The differences between this procedure and the ones existing in the literature are obvious. Since it addresses the aforementioned Problem CCA, it differs from all the methods that address Problem CCB. In addition, it differs from ESO-type approaches, because the proposed approach is based on the Lagrange multipliers method, which is a pure mathematical approach. Furthermore, while the ESO-type approaches required that the material elimination cause a small change in the stiffness of the remaining structure, there is no need to make such assumptions for the proposed procedure. These differences are more than clear and well-defined if one compares the two approaches, as presented in Sections 3.2.1 and 3.3.1.

Last, the Fully-Stressed Design (FSD) is briefly presented (Gallagher, 1973; Morris, 1982; Haftka et al, 1990). This presentation aims at stating the basis of the analysis and the proposed procedures, which are stated in the following Chapter. Furthermore, this presentation also serves as a means to denote the differences between this approach and the one introduced in Section 4.6. Even though there are counterexamples, which prove that FSD cannot be used for optimum design (Rozvany, 2001), the implementation of FSD is a good choice for a large number of engineering applications (Berke and Khot, 1987).

3.2. Optimization of a 2D continuum using material removal

3.2.1. Theoretical approach

Let a 2D deformable body, discretized into a number of finite elements and loaded by a set of external forces. Independent from the selected reference coordinate system, the work of the external forces is stored in the deformable body as strain energy; that is:

$$W^{\text{int}} = W^{ext} = \left(\frac{1}{2}\right)\{u\}^T [K]\{u\} \tag{3.1}$$

where $\{u\}$ is the nodal displacement vector and $[K]$ is the stiffness matrix of the discretized deformable body. From the force balance on the deformable body, it holds:

$$\{F\}^{ext} = [K]\{u\} \tag{3.2}$$

If it is required to remove material from the aforementioned body, then the stiffness matrix of the body decreases by $[\Delta K]$, while the nodal displacements are increased by $\{\delta u\}$. That is:

$$\{F\}^{ext} = [K]\{u\} = [K - \Delta K]\{u + \delta u\} \tag{3.3}$$

From basic manipulations, it yields:

$$[K]\{u\} = [K]\{u\} + [K]\{\delta u\} - [\Delta K]\{u\} - [\Delta K]\{\delta u\} \tag{3.4}$$

Due to the material removal, the nodal displacement field changes, thus the work of the external forces become equal to:

$$W^{ext,new} = \left(\frac{1}{2}\right)\left(\{u+\delta u\}^T \{F\}^{ext}\right) \tag{3.5}$$

or, equivalently, equal to:

$$W^{ext,new} = \left(\frac{1}{2}\right)\left(\{u\}^T \{F\}^{ext} + \{\delta u\}^T \{F\}^{ext}\right) \tag{3.6}$$

Therefore, the change of the work of the external forces becomes equal to:

$$\Delta W^{ext} = \left(\frac{1}{2}\right)\{\delta u\}^T \{F\}^{ext} \tag{3.7}$$

or, equivalently, equal to:

$$\Delta W^{ext} = \left(\frac{1}{2}\right)\{\delta u\}^T [K]\{u\} \tag{3.8}$$

Form Eq.(3.4), after simplifications, it yields:

$$[K]\{\delta u\} = [\Delta K]\{u\} + [\Delta K]\{\delta u\} \tag{3.9}$$

Taking into consideration the properties of the transpose matrix, it yields:

$$\{\delta u\}^T [K] = \{\delta u\}^T [K]^T = \left([K]\{\delta u\}\right)^T \tag{3.10}$$

The combination of Eqs(3.9, 3.10) yields:

$$\begin{aligned} &\left([K]\{\delta u\}\right)^T = \left([\Delta K]\{u\} + [\Delta K]\{\delta u\}\right)^T = \left([\Delta K]\{u\}\right)^T + \left([\Delta K]\{\delta u\}\right)^T \\ &= \{u\}^T [\Delta K]^T + \{\delta u\}^T [\Delta K]^T \end{aligned} \tag{3.11}$$

Introducing Eq.(3.10) and Eq.(3.11) into Eq.(3.8), the external work may be written as:

$$\Delta W^{ext} = \left(\frac{1}{2}\right)\left(\{u\}^T [\Delta K]^T + \{\delta u\}^T [\Delta K]^T\right)\{u\} \tag{3.12}$$

Due to symmetry of the stiffness matrix, it yields:

$$[\Delta K]^T = [\Delta K] \tag{3.13}$$

The combination of Eqs.(3.12, 3.13) yields:

$$\Delta W^{ext} = \left(\frac{1}{2}\right)\left(\{u\}^T [\Delta K] + \{\delta u\}^T [\Delta K]\right)\{u\} \tag{3.14}$$

or, equivalently, it holds:

$$\Delta W^{ext} = \left(\frac{1}{2}\right)\{u\}^T [\Delta K]\{u\} + \left(\frac{1}{2}\right)\{\delta u\}^T [\Delta K]\{u\} \tag{3.15}$$

In Eq.(3.15), two terms, of energy origin, appear:

$$\Delta W_1^{ext} = \left(\frac{1}{2}\right)\{u\}^T [\Delta K]\{u\} \text{ and } \Delta W_2^{ext} = \left(\frac{1}{2}\right)\{\delta u\}^T [\Delta K]\{u\} \tag{3.16}$$

In each one of these terms, the quantity $\{\Delta F\} = [\Delta K]\{u\}$ is found; that is, a change in the stiffness matrix times the initial nodal displacement vector. Furthermore, the displacement of the application point of the force change $\{\Delta F\}$ also appears as $\{u\}$ in term ΔW_1 and as $\{\delta u\}$ in term ΔW_2, respectively. The physical interpretation of these terms is as follows:

$\left(\frac{1}{2}\right)\{\delta u\}^T [\Delta K]\{u\}$: work is done because the application point of the force $\{\Delta F\}$ is displaced by $\{\delta u\}$

$\left(\frac{1}{2}\right)\{u\}^T [\Delta K]\{u\}$: work is done because the application point of the force $\{\Delta F\}$ is displaced by $\{u\}$

In the special case where the changes are small, the term $\{\delta u\}^T [\Delta K]$ may be considered as negligible, thus it yields:

$$\Delta W^{ext} \approx \left(\frac{1}{2}\right)\{u\}^T [\Delta K]\{u\} \tag{3.17}$$

According to the Finite Element Method (FEM), the examined deformable body is substituted by a mesh of finite elements. Generally speaking, material removal means the removal of one or more finite elements from the mesh. This is achieved either by considering that the corresponding place in the mesh is empty (no material exists – void) or by attributing to the specific finite element a very small value of a characteristic quantity, such as the modulus of elasticity or the density; that is, the reality is simulated by a numerical intervention. The validity of Eqs.(3.15, 3.17), as shown from the aforementioned line of arguments, is not related to the number of the finite elements. Consequently, these equations are still valid whether one or more finite elements are eliminated.

In the case where only one finite element is eliminated, let it be the j-element, the quantity $[\Delta K]$ expresses the stiffness matrix change of the deformable body, which is numerically equal to the stiffness matrix of the eliminated element:

$$[\Delta K] = [K_j] \tag{3.18}$$

The quantity $\{u\}$ is the nodal displacement vector, which is multiplied, in Eqs.(3.15, 3.17) by the change in the stiffness matrix $[\Delta K]$. Therefore, it is possible to be substituted by the quantity $\{u_j\}$; that is:

$$[\Delta K]\{u\} = [K_j]\{u_j\} \tag{3.19}$$

The last equation is interpreted as follows: the matrix $[\Delta K]$ has dimensions $N_{DOF} \times N_{DOF}$, where N_{DOF} represents the degrees of freedom of the examined body, while its non-zero entries are those corresponding to the degrees of freedom of the j-element. The vector $\{u\}$ contains the nodal displacements corresponding to the degrees of freedom N_{DOF}. However, since the vector $\{u\}$ is multiplied by $[\Delta K]$, all the products that correspond to degrees of freedom different than those of j-element will be zero. Therefore, the result of the multiplications $[\Delta K]\{u\}$ and $[K_j]\{u_j\}$ will be the same and it will hold:

$$\Delta W^{ext} = \left(\frac{1}{2}\right)\{u_j\}^T [\Delta K_j]\{u_j\} + \left(\frac{1}{2}\right)\{\delta u_j\}^T [\Delta K_j]\{u_j\} \tag{3.20}$$

Under the assumption that the products between quantities representing changes may be considered as negligible, it holds:

$$\Delta W^{ext} \approx \left(\frac{1}{2}\right)\{u_j\}^T [\Delta K_j]\{u_j\} \tag{3.21}$$

The last equation suggests that, under the aforementioned assumption and due to the elimination of one finite element, the change of the work done by the external forces is equal to the strain energy that had been stored in the eliminated element.
From the above analysis, it yields that in a 2D deformable body it is possible to find elements that have very small (negligible) energy contribution to the total energy state of the body, thus their elimination is strongly suggested in a weight minimization problem. After this element elimination, the remaining elements (active elements) are upgraded from an energy viewpoint, thus their energy contribution must be re-evaluated. In other words, the element elimination must both take place progressively and be embodied in a more general iterative procedure. Two criteria, among the various ones to be used for estimating the number of elements to be eliminated, are the following:

Criterion #1: Remove those elements for which $\Delta W^{ext} \le \alpha W^{ext}$, where $\alpha \in (0,1)$; that is, the elements to be eliminated may cause a change in the work done at most equal to a proportion α of the work done by the external forces. The value of the parameter α is defined by the user.

Criterion #2: Remove those elements for which $\Delta W^{ext} \le W_{thresh}$, where W_{thresh} is a user-defined threshold.

It is possible to embed the aforementioned energy-based criteria in an optimization procedure for weight minimization, and more specifically in topology and shape optimization procedures. Imposing an upper threshold for the energy state of the examined body ensures the elimination of a different number of elements in each iteration. That is, during an optimization procedure, as the element elimination advances and the elimination of one element causes a higher change in the energy state of the deformable body, the number of the elements to be eliminated between two successive iterations decreases until no more elements may be eliminated. At that point, there are two options, the former concerning the interruption of the optimization procedure and the latter concerning the increase of the aforementioned upper threshold thus enabling the continuation of the procedure. Obviously, these steps may be repeated as many times as the user wishers thus ensuring an interactive communication between the user and the software used for the optimization. In addition, instead of the criteria previously presented, it is possible to introduce combined criteria as well. As far as the element elimination process is concerned, this may be achieved in many ways, four of which are presented in the next Sections.

3.2.2. Uniform thickness scaling

The Criterion #1 (see Section 3.1.1) may be used in order to reduce uniformly the thickness of the elements being candidate for elimination, and is described by the inequality:

$$\Delta W^{ext} \le \alpha W^{ext}, \alpha \in (0,1) \tag{3.22}$$

From the combination of Eqs.(3.1, 3.17, 3.22), it yields:

$$\left(\frac{1}{2}\right)\left(\{u\}^T[\Delta K]\{u\}\right) \le \alpha\left(\frac{1}{2}\right)\{u\}^T[K]\{u\} \tag{3.23}$$

or, equivalently, it yields:

$$\left(\frac{1}{2}\right)\left(\{u\}^T[\Delta K]\{u\}\right) \le \left(\frac{1}{2}\right)\{u\}^T[\alpha K]\{u\} \tag{3.24}$$

From the last inequality, it is obvious that it holds:

$$[\Delta K] \le \alpha[K] \tag{3.25}$$

The interpretation of the last inequality is straight-forward: it is possible to increase the strain energy state of a structure by uniformly reducing the stiffness of part of the structure. For skeletal structures and for continua, one way to achieve this is by uniformly decreasing the size (cross-section or thickness) of the corresponding structural members.

3.2.3. Total elimination of one finite element only

The corresponding energy change is estimated using Eq.(3.20), according to which, in general, each element is characterized by a different amount of strain energy. Elements that comply with Criterion #1 are candidates for elimination. Among them, the one characterized by the lower amount of strain energy is the one that, once eliminated, causes the least possible change in the energy state of the structure. In this way, the optimum shape is sculptured following the path of the minimum rate of energy change. Alternatively, it is possible to select

for elimination one element that is near the threshold imposed by the user. In this way, the elimination procedure is accelerated because all the elements with lower strain energy than the eliminated one will be, from an energy viewpoint, downgraded faster.

3.2.4. Simultaneous total elimination of more than one finite elements

With respect to the total elimination of more than one finite elements at one step, there are several choices, such as:

- Deterministic elimination. The remaining elements are sorted in an ascending order of strain energy and in the sequel the first n elements of the sorted list are selected such that $\sum_{j=1}^{n} W_j^{ext} \le \Delta W$, where ΔW is an upper energy-state threshold defined by the user.
- Stochastic elimination. The remaining elements are first sorted in an ascending order of strain energy and then m elements are randomly selected such that $\sum_{j=1}^{m} W_j^{ext} \le \Delta W$, where ΔW is an upper energy-state threshold defined by the user.

3.2.5. Simultaneous partial elimination of more than one finite elements

It is possible to achieve a partial material elimination either in the form of thickness variation or in the form of area changing, as in the fixed-grid method. This means that special care should be given in the estimation of the quantity $[\Delta K]$.

3.2.6. Conclusions

From the aforementioned line of arguments, it is clear that the material elimination may take place in various forms and is independent from the optimization problem to be solved. That is, the same procedure may be used for shape, topology and layout optimization problems. Furthermore, it is strongly emphasized that the material elimination, as described in the preceding Sections, is independent from the imposed constraints. This means that it is possible to use the same procedure for optimizing with respect to different constraints. Moreover, it is of essence to allow for the re-use of eliminated material; that is to implement a 'die and birth' scheme in the optimization procedure. Finally, and of most significance, due to the definition of the strain energy and of the virtual strain energy, statements similar to the ones presented in the previous sections may be stated for the virtual strain energy as well.

3.3. Optimization of a 2D continuum under a single compliance constraint

3.3.1. Theoretical approach

In this Section, the problem of optimizing a 2D continuum under a single compliance constraint is investigated; that is, the optimum layout is sought such that the minimum weight is acquired under the constraint that the work done by the externally applied forces must not exceed a maximum value. The mathematical statement of this problem is as follows:

$$\min W = \sum A_i t_i \rho_i \tag{3.26}$$

$$\text{where } t_i \ge t_{\min} \text{ and } \left(\frac{1}{2}\right)\{u\}^T \{F\} \le C_{\max} \tag{3.27}$$

From Eq.(3.27) it is evident that a constraint is imposed on the minimum element thickness as well as on the compliance. The former constraint is used for numerical instabilities to be

avoided (complete element elimination from the mesh may result in the formation of an ill-conditioned stiffness matrix, which cannot be inverted). The constraint with respect to the work done by the external forces may be written as:

$$g(t) \le 0 \text{ where } g(t) = \frac{\left(\frac{1}{2}\right)\{u\}^T \{F\}}{C_{\max}} - 1 \tag{3.28}$$

According to the method of Lagrange multipliers, the Lagrangian is equal to:

$$L(\mathbf{t}, \lambda) = \sum A_i t_i \rho_i + \lambda_1 g_1(t) \tag{3.29}$$

Letting $\mathbf{t}$ be the design vector concerning the thickness of the finite elements, which the 2D continuum is discretized into, Eq.(3.4) may be written as:

$$L(\mathbf{t}, \lambda) = \sum A_i t_i \rho_i + \lambda_1 \left(\frac{\left(\frac{1}{2}\right)\{u\}^T \{F\}}{C_{\max}} - 1 \right) \tag{3.30}$$

According to the Karush-Kuhn-Tucker conditions, the vector $\mathbf{t}$ corresponds to the minimum weight design when it holds:

$$\nabla_t L(\mathbf{t}, \lambda) = 0 \text{ and } \nabla_\lambda L(\mathbf{t}, \lambda) = 0 \tag{3.31}$$

The combination of Eqs.(3.30, 3.31), after basic manipulations, yields:

$$\frac{\partial\left(L(\mathbf{t}, \lambda)\right)}{\partial t_i} = 0 \Rightarrow \frac{\partial}{\partial t_i} \left(\sum A_i t_i \rho_i + \lambda_1 \left(\frac{\left(\frac{1}{2}\right)\{u\}^T \{F\}}{C_{\max}} - 1 \right) \right) = 0 \tag{3.32}$$

With respect to Eq.(3.32), the partial derivative of the first term in the parenthesis is equal to:

$$\frac{\partial}{\partial t_i} \left(\sum A_i t_i \rho_i \right) = A_i \rho_i \tag{3.33}$$

Again, with respect to Eq.(3.32), the partial derivative of the second term in the parenthesis is equal to:

$$\frac{\partial}{\partial t_i} \left(\lambda_1 \left(\frac{\left(\frac{1}{2}\right)\{u\}^T \{F\}}{C_{\max}} - 1 \right) \right) = \left(\frac{\lambda_1}{C_{\max}} \right) \frac{\partial}{\partial t_i} \left(\left(\frac{1}{2}\right)\{u\}^T \{F\} \right) \tag{3.34}$$

In Eq.(3.34), the ratio $\left(\frac{\lambda_1}{C_{\max}}\right)$ is constant, while the derivative $\frac{\partial}{\partial t_i}\left(\left(\frac{1}{2}\right)\{u\}^T\{F\}\right)$ must be estimated. Towards this direction and after simplifications, it yields:

$$\frac{\partial}{\partial t_i}\left(\left(\frac{1}{2}\right)\{u\}^T\{F\}\right)=\left(\frac{1}{2}\right)\frac{\partial\left(\{u\}^T\right)}{\partial t_i}\{F\}+\left(\frac{1}{2}\right)\{u\}^T\frac{\partial\left(\{F\}\right)}{\partial t_i} \tag{3.35}$$

The force vector is considered to be independent from the thickness of the 2D continuum:

$$\frac{\partial\left(\{F\}\right)}{\partial t_i}=0 \tag{3.36}$$

This means that the second term in Eq.(3.35) becomes equal to zero:

$$\left(\frac{1}{2}\right)\{u\}^T\frac{\partial\left(\{F\}\right)}{\partial t_i}=0 \tag{3.37}$$

The combination of Eqs.(3.35, 3.37) yields:

$$\frac{\partial}{\partial t_i}\left(\left(\frac{1}{2}\right)\{u\}^T\{F\}\right)=\left(\frac{1}{2}\right)\frac{\partial\left(\{u\}^T\right)}{\partial t_i}\{F\} \tag{3.38}$$

The vector of the externally applied forces $\{F\}$ is initially defined, thus initially known. Consequently, the partial derivative $\left(\partial\left(\{u\}^T\right)/\partial t_i\right)$ is the unknown to be estimated. From the Finite Element Method, it is known that:

$$\{F\}=[K]\{u\} \tag{3.39}$$

The derivative of Eq.(3.39) with respect to the thickness t_i is equal to:

$$\frac{\partial\{F\}}{\partial t_i}=\frac{\partial}{\partial t_i}\left([K]\{u\}\right)=\frac{\partial\left([K]\right)}{\partial t_i}\{u\}+[K]\frac{\partial\left(\{u\}\right)}{\partial t_i} \tag{3.40}$$

The combination of Eqs.(3.36, 3.41) yields:

$$\frac{\partial\left([K]\right)}{\partial t_i}\{u\}+[K]\frac{\partial\left(\{u\}\right)}{\partial t_i}=0 \tag{3.41}$$

Solving the last equation with respect to $\frac{\partial\left(\{u\}\right)}{\partial t_i}$ gives:

$$\frac{\partial(\{u\})}{\partial t_i} = -[K]^{-1} \frac{\partial([K])}{\partial t_i}\{u\} \tag{3.42}$$

The stiffness matrix $[K]$ is symmetric thus has the following properties:

$$[K] = [K]^T \text{ and } [K]^{-1} = \left([K]^{-1}\right)^T \tag{3.43}$$

From the combination of the last two equations, the partial derivative $\left(\partial\left(\{u\}^T\right)/\partial t_i\right)$ becomes equal to:

$$\begin{aligned} \frac{\partial\left(\{u\}^T\right)}{\partial t_i} &= -\left([K]^{-1}\frac{\partial([K])}{\partial t_i}\{u\}\right)^T = -\left(\left(\frac{\partial([K])}{\partial t_i}\{u\}\right)^T \left([K]^{-1}\right)^T\right) \\ &= -\left(\{u\}^T\left(\frac{\partial([K])}{\partial t_i}\right)^T \left([K]^{-1}\right)^T\right) = -\left(\{u\}^T\left(\frac{\partial([K])}{\partial t_i}\right)[K]^{-1}\right) \end{aligned} \tag{3.44}$$

The combination of Eqs.(3.38, 3.44) yields:

$$\frac{\partial}{\partial t_i}\left(\left(\frac{1}{2}\right)\{u\}^T\{F\}\right) = \left(\frac{1}{2}\right)\left(-\left(\{u\}^T\left(\frac{\partial([K])}{\partial t_i}\right)[K]^{-1}\right)\right)\{F\} \tag{3.45}$$

From Eq.(3.39) and solving with respect to $\{u\}$, it yields:

$$\{u\} = [K]^{-1}\{F\} \tag{3.46}$$

The combination of Eqs.(3.45, 3.46), after basic manipulations, yields:

$$\frac{\partial}{\partial t_i}\left(\left(\frac{1}{2}\right)\{u\}^T\{F\}\right) = -\left(\frac{1}{2}\right)\{u\}^T\left(\frac{\partial([K])}{\partial t_i}\right)\{u\} \tag{3.47}$$

After manipulations, Eq.(3.37) obtains the following form:

$$A_i\rho_i + \left(\frac{\lambda_1}{C_{\max}}\right)\frac{\partial}{\partial t_i}\left(\left(\frac{1}{2}\right)\{u\}^T\{F\}\right) = 0 \tag{3.48}$$

Introducing Eq.(3.48) in Eq.(3.47), it yields:

$$A_i\rho_i - \left(\frac{1}{2}\right)\left(\frac{\lambda_1}{C_{\max}}\right)\{u\}^T\left(\frac{\partial([K])}{\partial t_i}\right)\{u\} = 0 \tag{3.49}$$

Re-ordering the terms in the last equation, it yields:

$$1 = \lambda_1 \left(\frac{1}{2}\right)\left(\frac{1}{C_{\max}}\right)\left(\frac{1}{A_i \rho_i}\right)\{u\}^T \left(\frac{\partial([K])}{\partial t_i}\right)\{u\} \tag{3.50}$$

Multiplication and division of the right-hand-side of Eq.(3.50) by t_i gives:

$$1 = \lambda_1 \left(\frac{1}{2}\right)\left(\frac{1}{C_{\max}}\right)\left(\frac{1}{A_i t_i \rho_i}\right)\{u\}^T \left(\frac{t_i \partial([K])}{\partial t_i}\right)\{u\} \tag{3.51}$$

It can be proved (see Appendix 3.A) that the following is true:

$$\{u\}^T \left(\frac{t_i \partial([K])}{\partial t_i}\right)\{u\} = \{u_i\}^T \left(\frac{t_i \partial([K_i])}{\partial t_i}\right)\{u_i\} \tag{3.52}$$

The stiffness matrix of the finite elements for plane elasticity is equal to:

$$K_i = \int_A t_i \mathbf{B}^T \mathbf{E} \mathbf{B} dA \tag{3.53}$$

where t_i is the thickness of the finite element, $\mathbf{E}$ is the elasticity matrix and $\mathbf{B}$ the strain-displacement matrix. Derivation with respect to the thickness t_i yields:

$$\frac{\partial}{\partial t_i}(K_i) = \int_A \mathbf{B}^T \mathbf{E} \mathbf{B} dA \tag{3.54}$$

Multiplication of both sides of Eq.(3.54) by t_i results in the following expression:

$$t_i \frac{\partial}{\partial t_i}(K_i) = t_i \int_A \mathbf{B}^T \mathbf{E} \mathbf{B} dA = \int_A t_i \mathbf{B}^T \mathbf{E} \mathbf{B} dA = K_i \tag{3.55}$$

The combination of Eqs.(3.51, 3.55) yields:

$$1 = \lambda_1 \left(\frac{1}{2}\right)\left(\frac{1}{C_{\max}}\right)\left(\frac{1}{A_i t_i \rho_i}\right)\{u_i\}^T [K]_i \{u_i\} \tag{3.56}$$

Eq.(3.56) may be written as:

$$1 = \lambda_1 \left(\frac{1}{2}\right)\left(\frac{1}{C_{\max}}\right)\left(\frac{1}{\rho_i}\right)\left(\frac{\{u\}_i^T [K]_i \{u\}_i}{A_i t_i}\right) \tag{3.57}$$

Since $\lambda_1 = const$ and $C_{\max} = const$, Eq.(3.57) suggests that:

$$\left(\frac{1}{\rho_i}\right)\left(\frac{\{u\}_i^T [K]_i \{u\}_i}{A_i t_i}\right) = const \tag{3.58}$$

Eq.(3.58) is the mathematical expression of an Optimality Criterion, according to which:

When the minimum weight of a 2D continuum is sought under the single compliance constraint then, at the optimum, the strain energy density, normalized to the material density, is constant.

Generally speaking, it is possible to estimate the thickness distribution t_i through an iterative procedure during which the element thicknesses are re-estimated according to some re-design formula. A typical application of the Lagrange multipliers method suggests that first Eq.(3.57) be solved with respect to the Lagrange multiplier and then this multiplier be introduced into the equation that describes the corresponding constraint. However, for the specific case of the compliance constrained optimization problem, the constraint is expressed with respect to the design *vector* (3.28) and not with respect to a design *variable* (3.57), thus the elimination of the Lagrange multiplier is not a straight-forward procedure. As an alternative, the iterative procedure of the following Section is proposed.

3.3.2. Proposed procedure

Eq.(3.57) describes an energy state of the structure at the optimum. However, it does not describe a way to reach that state, thus various procedures may be formulated. Towards this direction and considering that the same material is used though the entire continuum, it is possible to introduce the following index:

$$a_i = \left(\frac{1}{\rho_i C_{\max}}\right)\left(\frac{\{u\}_i^T [K]_i \{u\}_i}{A_i t_i}\right) \tag{3.59}$$

The physical interpretation of this index is that the strain energy density, normalized with respect to the maximum allowable compliance, must be constant over the entire structure. Taking into consideration the constraint for minimum thickness, as described in Eq.(3.27), it yields that the strain energy density must be constant over the *active* part of the structure, active denoting all elements with non-critical thickness. Consequently, the corresponding mean value $\overline{a}$ from all of the active elements is equal to:

$$\overline{a} = \left(\frac{\sum_{i=1}^{N_{active}} a_i}{N_{active}}\right) \tag{3.60}$$

Therefore, at the optimum and for the active part of the structure, it holds:

$$\left(\frac{\alpha_i}{\overline{\alpha}}\right) \to 1 \tag{3.61}$$

Dividing Eqs.(3.59, 3.60) by parts and taking into consideration Eq.(3.61), it holds:

$$\left(\frac{\sum_{i=1}^{N_{active}} a_i}{N_{active}} \right) = \left(\frac{1}{\rho_i \, C_{\max}} \right) \left(\frac{\{u\}_i^T [K]_i \{u\}_i}{A_i t_{i,new}} \right) \tag{3.62}$$

where $t_{i,new}$ is the re-designed thickness of the $i-$element. Solving Eq.(3.62) with respect to $t_{i,new}$ a relation to be applied iteratively is reached:

$$t_{i,new} = \left(\frac{N_{active}}{\sum_{i=1}^{N_{active}} a_i} \right) \left(\frac{1}{\rho_i \, C_{\max}} \right) \left(\frac{\{u\}_i^T [K]_i \{u\}_i}{A_i} \right) \tag{3.63}$$

A more convenient form of Eq.(3.63) for programming is:

$$t_{i,k+1} = \left(\frac{N_{active}}{\sum_{i=1}^{N_{active}} a_{i,k}} \right) \left(\frac{1}{\rho_i \, C_{\max}} \right) \left(\frac{\{u\}_{i,k}^T [K]_{i,k} \{u\}_{i,k}}{A_i} \right) \tag{3.64}$$

where k denoted iteration number. Based on the preceded analysis, the following optimization procedure is proposed:

Step 1: Select randomly a uniform thickness distribution t_i.

Step 2: Estimate the indices α_i, using Eq.(3.59).

Step 3: Estimate the mean value $\overline{\alpha_i}$, using Eq.(3.60).

Step 4: Re-design the element thickness distribution t_i using Eq.(3.64).

Step 5: Check for convergence; possible convergence criteria are:

Criterion #1: the maximum change in element thickness between two successive iterations is less than a predefined tolerance: $\max \left| t_i^k - t_i^{k+1} \right| \le tol_1$

Criterion #2: the Coefficient of Variation (%CV) for the distribution of the α_i indices is less than a predefined tolerance: $\%CV\left(\overline{a_i}\right) \le tol_2$

Step 6: If convergence has not been achieved and a predefined maximum number of iterations has not been exceeded, then go back to Step 2.

3.3.3. Conclusions

The preceded analysis refers to a thorough theoretical investigation of the single compliance constraint problem. At this point it is strongly emphasized that the aforementioned approach differs from those found in the literature, where the minimum compliance constraint problem suggests that the minimum compliance is sought under the assumption of a given material volume. Therefore, the present analysis is worth mentioning from the viewpoint that it actually deals with a problem that has not been yet attacked, or, at least, has not been extensively investigated. It is also emphasized that compliance design and stress design are equivalent if the stress criterion is consistent with the elastic energy measure.

Considering the von Mises criterion, which is not consistent with the energy criterion, results in different stress and compliance topology designs, the exception being the case where the Poisson's ratio is equal to 0.5 (Bendsøe and Sigmund, 2003). Consequently, the compliance constraint problem may be considered as mainly of academic interest, thus no further elaboration with it takes place in the present investigation.

3.4. Fully Stressed Design

The Fully Stressed Design (FSD) is well-known to be one of the simplest and most popular procedures for reaching an optimized design under stress constraints. For a truss, the statement of the corresponding problem is as follows:

$$\text{minimize } W = \sum_{k=1}^{NEL} \left(\rho_k \, A_k \, L_k \right) \tag{3.65}$$

$$\text{such that } g_i = \left(\frac{\sigma_i}{\sigma_{allow}} - 1 \right) \leq 0 \text{ and } A_{\min} \leq A_i \tag{3.66}$$

where A is the cross-sectional area, L is the length of a bar, ρ is the material density, σ is the member stress, while the indices i and $allow$ denote the $i-$bar and the allowable value, respectively. Assuming that the number of constraints is equal to the number of elements, bars in case of a truss, the aforementioned statement suggests that all members take the limit stress value σ_{allow}. Considering that the axial stress of a bar is defined as:

$$\sigma_i = \left(\frac{F_i}{A_i} \right) \tag{3.66}$$

where F is the member force, it yields that, according to the method of Lagrange multipliers, the Lagrangian function $\mathfrak{L}$ corresponding to the aforementioned problem, if the constraint for the minimum cross-sectional area is dropped, may be stated as:

$$\mathfrak{L} = \sum_{i=1}^{NEL} \left(\rho_i \, A_i \, L_i \right) + \sum_{i=1}^{NEL} \lambda_i \left(\frac{F_i}{A_i \, \sigma_{allow}} - 1 \right) \tag{3.67}$$

Differentiating Eq.(3.67) with respect to the cross-sectional value A_i, which is the design variable, and setting it equal to zero, as the Lagrange multipliers method suggests, yields:

$$\rho_i \, L_i - \lambda_i \frac{F_i}{A_i^2 \, \sigma_{allow}} + \frac{1}{A_i \sigma_{allow}} \sum_{p=1}^{NEL} \left(\lambda_p \frac{\partial F_p}{\partial A_i} \right) = 0 \tag{3.68}$$

In the last equation, the term $\left(\partial F_p / \partial A_i \right)$ represents the gradient of the member force in a bar. If the truss under examination is determinate then the member forces are independent from the cross-sectional areas and this term becomes equal to zero; consequently, the third term in Eq.(3.68) vanishes. Even though this is not the general case, if it is assumed that this specific term vanishes, then Eq.(3.68) turns into the following form:

$$\rho_i L_i - \lambda_i \frac{F_i}{A_i^2 \sigma_{allow}} = 0 \tag{3.69}$$

Solving Eq.(3.69) with respect to the cross-sectional value A_i yields:

$$A_i = \sqrt{\lambda_i} \sqrt{\left(\frac{F_i}{\sigma_{allow} \rho_i L_i} \right)} \tag{3.70}$$

Furthermore, if it is assumed that all of the stress constraints g_i are active (Fully Stressed Design - FSD) then it holds:

$$\sigma_{allow} = \left(\frac{F_i}{A_i} \right) \tag{3.71}$$

Introducing Eq.(3.71) into Eq.(3.70) yields:

$$\sqrt{\lambda_i} = \sqrt{\left(\frac{F_i \rho_i L_i}{\sigma_{allow}} \right)} \tag{3.72}$$

Introducing Eq.(3.72) into Eq.(3.70) yields:

$$A_i = \left(\frac{F_i}{\sigma_{allow}} \right) \tag{3.73}$$

The last equation is the famous stress-ratio redesign formula. From its derivation, it is obvious that only for a determinate truss does this approach result in the global minimum structural weight. For indeterminate trusses, Eq.(3.73) is only an approximation. As a matter of fact, the more the third term in Eq.(3.68) tends to zero the closer the derived optimum design is to the global optimum. Therefore, the (FSD) has the advantage of being very simple to apply and the disadvantage of being an approximation to the optimum design for the majority of the real-life problems. However, for good practical engineering purposes, it is interesting to examine its applicability and efficiency in skeletal structures and continua, which is the subject of the next Chapter.

3.5. Recapitulation

The layout optimization of a structure may be achieved by removing redundant material, either completely or partially. The criterion for determining which part of the structure to remove depends on the imposed constraint. One of the most common types of such problems is related to the compliance of the structure. In the literature, the corresponding problem has been solved when a volume constraint is also imposed. In the present chapter, a more general case was theoretically investigated, where the volume constraint is not present. However, since no standard for structures refers to a compliance constraint, no further effort was put on exploring this issue. On the other hand, the stress-ratio technique is an optimization procedure that tends to Fully Stressed Designs which, for the majority of real-life structures, results in near-optimum solutions and thus is acceptable and interesting to explore.

References

Achtziger W, Bendsøe M, Ben-Tal A, Zowe J (1992) Equivalent displacement based formulations for maximum strength truss topology design. Impact Comput Sci Eng 4:315–345

Allaire, G, Jouve F, Maillot H (2004) Topology optimization for minimum stress design with the homogenization method. Struct Multidisc Optim 28:87–98

Bendsøe, MP (1989) Optimal shape design as a material distribution problem. Struct Optim 1(4):193–202

Bendsøe, MP, Kikuchi N (1988) Generating optimal topologies in structure design using a homogenization method. Comput Methods Appl Mech Eng 71:197–224

Bendsøe, MP, Sigmund O (2003) Topology optimization: theory, methods and applications. Springer, Berlin.

Ben-Tal A, Bendsøe M (1993) A new method for optimal truss topology design. SIAM J Optim 3(2):322–358

Ben-Tal A, Nemirovski A (1994) Potential reduction polynomial time method for truss topology design. SIAM J Optim 4(3):596–612

Ben-Tal A, Nemirovski A (1995) Optimal design of engineering structures. OPTIMA Mathematical Programming Society Newsletter No. 47

Ben-Tal A, Nemirovski A (1997) Robust truss topology design via semidefinite programming. SIAM J Optim 7(4):991–1016

Ben-Tal A, Nemirovski A (2000) Handbook of semidefinite programming, chap Structural Design. Kluwer, pp 443–467

Berke L, Khot N.S., (1987), "Structural optimization using optimality criteria", in: Computer Aided Optimal Design: Structural and Mechanical Systems, edited by C.A. Mota Soares, NATO, ASI series, F27B.

Bruyneel, M, Duysinx P, Fleury C (2002) A family of MMA approximations for structural optimization. Struct Multidisc Optim 24:263–276

Burns, TE, Tortorelli DA (2003) An element removal and reintroduction strategy for the topology optimization of structures and compliant mechanisms. Int J Numer Methods Eng 57:1413–1430

Burns, TE (2005) A reevalution of the SIMP method with filtering and an alternative formulation for solid-void topology optimization. Struct Multidisc Optim 30(6):428–436

Das, R., Jones R., Xie Y. M., Design of structures for optimal static strength using ESO, Engineering Failure Analysis, Volume 12, Issue 1, February 2005, Pages 61-80

Duysinx, P, Sigmund O (1988) New developments in handling stress constraints in optimal material distribution. In: 7th AIAA/USAF/NASA/ISSMO symposium on multidisciplinary design optimization, American Institute of Aeronautics and Astronautics, Saint Louis, MI, USA, pp 1501–1509, September

Duysinx, P, Bendsøe M (1998) Topology optimization of continuum structures with local stress constraints. Int J Numer Methods Eng 43:1453–1478

Edwards, CS, Kim HA, Budd CJ (2007) An evaluative study on ESO and SIMP for optimizing a cantilever tie-beam. Struct Multidisc Optim (in press)

Fujii, D, Kikuchi N (2000) Improvement of numerical instabilities in topology optimization using the SLP method. Struct Multidisc Optim 19:113–121

Gallagher RH. Fully Stressed Design, In: R. H. Gallagher & O. C. Zienkiewicz (eds.), Optimum Structural Design: Theory and Applications. John Wiley & Sons:1973.

Haber, RB, Jog CS, Bendsøe MP (1996) A new approach to variable-topology shape design using a constraint on perimeter. Struct Optim 11:1–12

Haftka R T, Gurdal Z and Kamat M. Elements of Structural Optimization. Kluwer: 1990.

Kita E, Tanie H (1999) Topology and shape optimization of continuum structures using GA and BEM. Struct Multidisc Optim 17(2–3):130–139

Michell AGM (1904) The limit of economy of material in frame structures. Philos Mag 8:589-597

Morris, A.J. (1982), Foundations of Structural Optimization: A Unified Approach, John Wiley & Sons.

Nha Chu, D, Xie YM, Hira A, Steven GP (1996) Evolutionary structural optimization for problems with stiffness constraints. Finite Elem Anal Des 21:239–251

Nha Chu, D, Xie Y. M., Hira A., Steven G.P., (1997) On various aspects of evolutionary structural optimization for problems with stiffness constraints, Finite Elements in Analysis and Design, Volume 24, Issue 4, pp.197-212

Querin O. M., Steven G. P., Xie Y. M., (2000a), Evolutionary structural optimisation using an additive algorithm, Finite Elements in Analysis and Design, Volume 34, Issues 3-4, pp. 291-308

Querin O. M., Young V., Steven G. P., Xie Y. M., (2000b) Computational efficiency and validation of bi-directional evolutionary structural optimisation, Computer Methods in Applied Mechanics and Engineering, Volume 189, Issue 2, pp. 559-573

Ren G., Smith J.V., Tang J.W., Xie Y.M., Underground excavation shape optimization using an evolutionary procedure, Computers and Geotechnics, Volume 32, Issue 2, March 2005, Pages 122-132

Rong JH, Xie YM, Yang XY, Liang QQ, (2000), Topology optimization of structures under dynamic response constraints, Journal of Sound and Vibration, Volume 234, Issue 2, pp.177-189

Rozvany GIN. Stress ratio and compliance based methods in topology optimization – a critical review. Struct. Multidisc. Optim., 2001, 21:109-119.

Sigmund O (2001a) Design of multiphysics actuators using topology optimization—part I: one-material structures. Comput Methods Appl Mech Eng 190:6577–6604

Sigmund O (2001b) Design of multiphysics actuators using topology optimization—part II: two-material structures. Comput Methods Appl Mech Eng 190:6605–6627

Sigmund O (2001c) A 99 line topology optimization code written in Matlab. Struct Multidisc Optim 21:120–127

Steven G, Querin O, Xie M, (2000), Evolutionary structural optimisation (ESO) for combined topology and size optimisation of discrete structures, Computer Methods in Applied Mechanics and Engineering, Volume 188, Issue 4, IVth World Congress on Computational Mechanics. (II). Optimum, pp. 743-754

Stolpe M, Svanberg K (2001) An alternative interpolation scheme for minimum compliance topology optimization. Struct Multidisc Optim 22:116–124

Svanberg K (1987) The method of moving asymptotes—a new method for structural optimization. Int J Numer Methods Eng 24:359–373

Svanberg K, (1994) On the convexity and concavity of compliances. Struct Optim 7(1–2):42–46

Svanberg K (1995) A globally convergent version of MMA without linesearch. Proceedings of the First World Congress of Structural and Multidisciplinary Optimization (Goslar, Germany), pp 9–16

Tanskanen P (2002) The evolutionary structural optimization method: theoretical aspects. Comput Methods Appl Mech Eng 191:5485–5498

Wei Li, Qing Li, Grant P. Steven, Y.M. Xie, (2005), An evolutionary shape optimization for elastic contact problems subject to multiple load cases, Computer Methods in Applied Mechanics and Engineering, Volume 194, Issues 30-33, Structural and Design Optimization, pp. 3394-3415

Xie Y.M., Felicetti P., Tang J.W., Burry M.C. (2005), Form finding for complex structures using evolutionary structural optimization method, Design Studies, Volume 26, Issue 1, Pages 55-72

Xie YM, Steven GP (1993) A simple evolutionary procedure for structural optimization. Comput Struct 49:885–896

Xie, YM, Steven, G.P., (1996) Evolutionary structural optimization for dynamic problems, Computers & Structures, Volume 58, Issue 6, pp.1067-1073

Xie YM, Steven GP (1997) Evolutionary structural optimization. Springer, Berlin

Yang XY, Xie YM, Steven GP, Querin OM (1999) Bidirectional evolutionary method for stiffness optimization. AIAA J 37(11):1483–1488.

Yang XY, Xie YM, Steven G.P., (2005) Evolutionary methods for topology optimisation of continuous structures with design dependent loads, Computers & Structures, Volume 83, Issues 12-13pp.956-963.

Zhou M, Rozvany GIN (2001) On the validity of ESO type methods in topology optimization. Struct Multidisc Optim 21:80–83

Zuo KT, Chen LP, Zhang YQ, Yang JZ (2005) Manufacturing-and machining-based topology optimization. Int J Adv Manuf Technol 27(5–6):531–536

APPENDIX 3.A: Work done by the externally applied forces

It can be proved that the following equation is true:

$$\{u\}^T \left(\frac{t_i \partial \left([K] \right)}{\partial t_i} \right) \{u\} = \{u_i\}^T \left(\frac{t_i \partial \left([K_i] \right)}{\partial t_i} \right) \{u_i\} \tag{3.A1}$$

It is obvious that both the left-hand-side and the right-hand-side of Eq.(3.A1) are scalar quantities. In order to prove that these scalars are equal, let a 2D continuum discretized using a mesh of NN nodes and NEL finite elements of plane elasticity and of constant thickness. Let $[K_i]$ be the stiffness matrix of the $i-$element, whose thickness is t_i. For reasons of completeness, it is referred that it holds:

$$[K_i] = \int_A t_i \mathbf{B}^T \mathbf{E} \mathbf{B} dA \tag{3.A2}$$

where $\mathbf{E}$ is the elasticity matrix and $\mathbf{B}$ is the strain-displacement matrix. The partial derivative of $[K_i]$ with respect to the element thickness t_i, yields:

$$\frac{\partial}{\partial t_i} \left([K_i] \right) = \int_A \mathbf{B}^T \mathbf{E} \mathbf{B} dA \tag{3.A3}$$

Multiplying Eq.(3.A3) by t_i, then, from Eq.(3.A2), it yields:

$$t_i \frac{\partial}{\partial t_i} \left(K_i \right) = t_i \int_A \mathbf{B}^T \mathbf{E} \mathbf{B} dA = \int_A t_i \mathbf{B}^T \mathbf{E} \mathbf{B} dA = K_i \tag{3.A4}$$

In other words, the product of the thickness t_i time the partial derivative of $[K_i]$ with respect to the thickness t_i is equal to the matrix $[K_i]$ itself. Therefore, the right-hand-side of Eq.(3.A1) becomes:

$$\{u_i\}^T \left(\frac{t_i \partial \left([K_i] \right)}{\partial t_i} \right) \{u_i\} = \{u_i\}^T [K_i] \{u_i\} \tag{3.A5}$$

On the right-hand-side of Eq.(3.A5), it is recognized that:

$$[K_i] \{u_i\} = \{F_i\} \tag{3.A6}$$

From Eqs.(3.A1, 3.A5 and 3. A6), the following conclusion may be drawn:

Conclusion #1: *The right-hand-side of Eq.(3.A1) is numerically equal to the work done by the external forces applied at the nodes of the $i-$element.*

With respect to plane elasticity, each node of the mesh to be used has two translational degrees of freedom, thus in total $2NN \times 2NN$ degrees of freedom are involved. This means

that the dimension of the stiffness matrix $[K]$ of the examined structure is equal to $2NN \times 2NN$. The thickness t_i of the $i-$element appears at those entries in $[K]$ that correspond to the degrees of freedom of matrix $[K_i]$. Therefore, the partial derivative of matrix $[K]$ with respect to the thickness t_i will be equal to a $2NN \times 2NN$ matrix, whose entries are all zero but those corresponding to the degrees of freedom of matrix $[K_i]$. These non-zero entries come from the derivation of $[K_i]$ with respect to t_i (see Eq.(3.A3)). Multiplying the $2NN \times 2NN$ matrix $\frac{\partial([K])}{\partial t_i}$ by the scalar quantity t_i results in the matrix $\frac{t_i \partial([K])}{\partial t_i}$, for which the following statements hold:

- The dimension of the matrix is $2NN \times 2NN$ and the non-zero entries are the entries of $[K_i]$, appropriately placed at the corresponding matrix locations.
- The matrix is numerically equal to the stiffness matrix of the entire structure if the latter one has been updated using only the elements of matrix $[K_i]$ of the $i-$element.
- The matrix is equal to $[K_i]$, when the latter matrix has been augmented with zero entries such that its dimension becomes equal to the dimension of the stiffness matrix of the entire structure under consideration.
- From a qualitative viewpoint, the matrix expresses the stiffness of the $i-$element only.

The vector $\{u\}$ contains all the nodal displacements of the structure under consideration and its dimension is $2NN \times 1$. When the vector $\{u\}$ is multiplied from the left-hand-side by $\left(\frac{t_i \partial([K])}{\partial t_i}\right)$, which expresses the stiffness of the $i-$element, then the derived product describes the external forces applied at the $i-$element. A further multiplication of the left-hand-side by $\{u\}^T$ gives the work done by those forces. Therefore, the following conclusion is drawn:

Conclusion #2: *The left-hand-side of Eq.(3.A1) is numerically equal to the work done by the external forces applied at the nodes of the $i-$element.*

From Conclusion #1 and Conclusion #2, it yields that Eq.(3.A1) is true, because both sides of the equation describe the same scalar quantity (work done by the external forces applied at the nodes of the $i-$*element*).

APPENDIX 3.B: Non-equivalence between displacement constraint and compliance constraint

Imposing a constraint on the maximum value of the work done by the externally applied loads (compliance constraint, let it be constraint A) is not always equivalent to imposing a constraint on the maximum value of the nodal displacement (let it be constraint B) because in constraint A the only nodes that participate are those carrying an external load; however, it is not necessary for these nodes to present the maximum displacement. As a typical example of such a case, let a horizontal simply supported beam loaded with a vertical force. In this case, it is clear that the work done by the externally applied loads is equal to:

$$\{u\}^T \{F\} = u_i F_i \tag{3.B1}$$

while the constraint on this work may be written as:

$$\{u\}^T \{F\} \le C_{\max} \tag{3.B2}$$

where $C_{\max}$ is an upper bound. The combination of Eqs.(3.B1, 3.B2), it yields:

$$u_i F_i \le C_{\max} \Rightarrow u_i \le \left(\frac{C_{\max}}{F_i} \right) \tag{3.B3}$$

thus the maximum displacement of the loaded node is equal to:

$$u_{i,\max} = \left(\frac{C_{\max}}{F_i} \right) \tag{3.B4}$$

From Engineering Handbooks (e.g. Stahl im Hochbau, s.1110), it can be found that for a horizontal simply supported beam under a vertical load F_i, the maximum deflection occurs at the load application point if and only if that point is at the mid-span of the beam, for which case it holds:

$$y_{\max} = u_{i,\max} \tag{3.B5}$$

However, in every other case, the maximum deflection occurs at a location different than that of the applied load and it holds:

$$y_{\max} > u_{i,\max} \tag{3.B6}$$

From Eq.(3.B6), it is clear that imposing constraint A results in a different situation than imposing constraint B, because, according to constraint A, a larger beam deflection is allowed. Therefore, the displacement constrained optimization problem and the compliance constrained optimization problem are two different problems being only conditionally coincident.

This page has been left intentionally blank

CHAPTER 4

LAYOUT OPTIMIZATION UNDER STRESS CONSTRAINTS

Abstract

In this chapter, the layout optimization problem under stress constraints is discussed. First, the application of the well-known Fully Stressed Design (FSD) in 2D skeletal structures is investigated. In the sequel, the same technique is examined for the optimization of 2D continua, for the optimization of 2D plates and for the optimization of 3D continua. Last, the single stress constrained problem is solved using the Lagrange multipliers method.

Keywords

layout optimization, stress constraint, skeletal structure, 2D continuum, 2D plate, single stress constraint problem.

4.1. Introduction

The stress constraint problem is one of the most important problems in structural optimization because it addresses to a real-life constraint of major significance for the structural safety. For this reason, one would expect this problem to have been thoroughly and exhaustively investigated. However, this is not the case because the stress-constraint problem presents a singularity (Bendsøe and Sigmund, 2003), thus makes it a difficult problem to deal with, while other types of problems, such as the compliance constraint problem or the single displacement constraint problem are easier to handle. Consequently, there is still room for further research not only in the area of re-formulating known techniques for solving the aforementioned problem but also in the area of solving variations of the initial problem statement that have not attracted much attention of the research community. Within this frame, the present chapter discusses the stress constraint problem.

In more details, first the capabilities of the Fully Stressed Design (FSD) in layout optimization of 2D structures are examined. For this purpose, two approaches were investigated, the former being the substitution of a 2D continuum with a skeletal structure and the latter being the consideration of the 2D continuum as such. In both approaches, the redesign was based on changing either the cross-section of the skeletal structural members or the thickness of the continuum. To this end, four examples retrieved from the literature were examined.

In the sequel, the concept of using finite elements of variable thickness for the stress constrained layout optimization of 2D continua is explored. For the thickness interpolation within each element an isoparametric consideration is used, meaning that the same shape functions used for the interpolation of the nodal displacements are also used for interpolating the element thickness. In this way, the nodes of the generated mesh serve as control points for the thickness distribution thus as control points for the optimum layout of the structure. For reasons of verification, four characteristic literature examples are optimized once using elements of constant thickness and once using elements of variable thickness.

Next, the optimization of 2D plates is investigated. To this end, various typical test cases are optimized once using the stress-ratio technique, with which the (FSD) is achieved, and once using the Evolutionary Structural Optimization (ESO) approach. In this way, the concept of varying the element thickness is compared to the concept of completely removing elements, thus material, characterized as corresponding to redundant material.

Last, the optimization of 3D continua is investigated. To this end, the continuum is discretized into finite elements of 3D elasticity, each one of which is examined with respect to its contribution to carrying the externally applied loads. The aforementioned contribution is quantified first in terms of the element von Mises equivalent stress and then in terms of the element strain energy density normalized with respect to the mean value of the strain energy density of the active part of the structure.

In addition a variation of the stress constraint problem is analytically presented on a theoretical basis. According to this variation, no matter how many stress constraints are imposed, only one such constraint is active at the optimum, without knowing a priori the structural member with the critical stress. This problem statement is here termed as ‘extended single stress constraint problem’ and is dealt with the Lagrange multipliers method. The result of this analysis is the formulation of a new optimality criterion, free of any assumptions concerning the determinacy of the optimized structure. Based on this criterion, a new redesign formula is also developed. The main difference between the Fully Stressed Design and the proposed approach is the fact that the former tends to make *all* structural members obtain the critical stress value while the latter seeks for such a design where *one* structural member takes on the critical stress value, without necessarily preventing the other structural members from obtaining the imposed upper stress bound.

4.2. Stress constrained skeletal structures

This section is a preliminary study that investigates the capabilities of the Fully Stressed Design (FSD) in shape and topology optimization of two-dimensional structures under stress constraints only. Furthermore, the efficiency of modeling a continuum as a skeletal structure is also examined. The structures studied were the short cantilever, the cantilever, the MBB and the L-shaped beam. These structures were modeled in two ways: as an assembly of quadrilateral bilinear elements of variable thickness (continuum) and as an assembly of truss elements (discrete body – skeletal structures). For each case study, seven different aspect ratios were used and three different mesh densities were chosen. The stress-ratio redesign formula was based on the von Mises equivalent stress and the axial stress, for the bilinear and the truss elements respectively. The purpose of modeling a continuum with truss elements is the fact that, in this simple way, anisotropy may be introduced into the structure, without using composite materials or other more complicated theories (ASE, ISEP, ISECP). The validity of this idea was examined by comparing the optimum designs obtained for the continuum and the skeletal structures, while the performance of the (FSD) was examined through a comparison with the Sequential Quadratic Programming (SQP), which is a powerful mathematical programming optimization method.

4.2.1. In general

Shape and topology optimization has always been an issue of major importance for engineering designers. For simple cases only, such as a cantilever beam, it is possible to derive optimized shapes in an analytical way. Nevertheless, for the majority of the engineering structures, the use of recursive algorithms involving Finite Element Analysis (FEA) is inevitable in order to get an optimized design. The main difficulties in developing efficient algorithms of that kind are the large number of design variables, the equal or even larger number of constraints and the non-linear nature of the problems. On top of that, in most cases, each FEA requires the solution of a large system of equations, which is of a high computational cost. Engineering ingenuity and experience has resulted in the development of several structural optimization methods.

The Fully Stressed Design (FSD) is an optimality criterion very well known since the late 50's (Schmidt, 1958). Its popularity was mainly due to the fact that it results in a very simple recursive formula that converges fast in comparison with other techniques. Gallagher (Gallagher, 1973), Morris (Morris, 1982), Haftka (Haftka et al, 1990), Patnaik (Patnaik et al, 1995), Rozvany (Rozvany, 2001a, Rozvany et al, 1995), Kirsch (Kirsch, 1989) and others have analyzed the efficiency of this method. These works revealed the major drawback of the method: only under certain circumstances does it provide the optimum design (minimum weight) for stress constrained problems. A common practice followed extensively was to use FSD as a first optimization step and then use the FSD result as a starting point for a powerful deterministic optimization algorithm (Schmidt, 1958).

An interesting step forward was made when the Lagrange multipliers technique in combination with duality entered the area of optimization. Generally speaking, it was possible to encounter not only stress but displacement and other constraints (i.e. buckling loads) as well. The difficulty of dealing with such problems was focused on determining the Lagrange multipliers, a task that was not so easy to handle because the Lagrange multipliers should be calculated from solving non-linear systems of equations (Morris, 1982). Nevertheless, for specific cases of constraints, the Lagrange multipliers method led to very elegant propositions, called Optimality Criteria (OC) concerning the conditions that hold for an optimum design (Morris, 1982). Once again, what was good from an engineering point of view, was insufficient from a mathematical point of view: generally speaking, while the

Lagrange multiplier method could provide an improved design, it could not be proved that this design was optimum.

An even more interesting step was made when purely Mathematical Programming (MP) techniques were developed, meaning that the minimum weight of a structure under any kind of constraints was sought without taking into consideration the mechanical nature of the problem; instead, derivative information was implemented. A plethora of such techniques were developed, like the Steepest Descent Method, Sequential Linear Programming, Sequential Quadratic Programming etc (Vanderplaats, 1984). The major drawback of these MP techniques was the fact that a systematic search of the feasible region required very high, frequently prohibitively high, computational cost, while the possibility of converging to a local minimum was high as well.

Alternatively to the MP methods, probabilistic techniques, like the Genetic Algorithms (GAs), Simulated Annealing (SA) and Tabu search, were developed (Pham and Karaboga, 2000). These methods are of zero order, meaning that they require no derivative information therefore it is less possible to converge to a local minimum. Nevertheless, "less possible" does not necessarily mean "impossible" to converge to local minima, thus it is required to solve the same problem many times beginning from different initial vectors in order to ensure optimality. On top of that, these methods are inefficient when the number of design variables is large, exactly due to the probabilistic nature of exploring and exploiting the feasible region.
In the recent years, a great many structural optimization methods have appeared, such as swarm particles, methods of natural growth and meshless techniques. A major breakthrough was achieved by Suzuki and Kikuchi (Suzuki and Kikuchi, 1991) who introduced material anisotropy (homogenization method), while a monumental contribution is attributed to Bendsøe and his SIMP method (Bendsøe, 1995, Duysinx and Bendsøe, 1998). On the other hand, optimality criteria still appear in new forms. Makris and Provatidis (Makris and Provatidis, 2002), using a virtual energy-based approach, proposed the combination of a Fully Utilized Method (FUD) with Fully Stressed Design (FSD). Furthermore, Qing et al. (Qing et al, 2000), in their Evolutionary Structural Optimization (ESO) method, introduced an updated use of the good-old stress-ratio technique.

Taking into consideration all the techniques mentioned above, it is evident that each one of them has certain advantages and certain disadvantages. A question that rises is whether it would be a good idea to combine certain features of different methods in order to get a better result. To this direction, the performance of the stress-ratio technique (FSD) is investigated, which engineering experience has shown to be a very simple and fast redesign technique, in combination with structural anisotropy; that is with the feature that scientists deal with lately (state-of-the-art). As a first step, the stress constrained shape and topology optimization problem of 2D continuum structures is examined using the FSD method (first group of results). Then the same structures are modeled as assemblies of discrete bodies (bars – skeletal structures), a substitution that introduces anisotropic behavior to the structure, and the minimum weight is sought again with the same method and the same stress constraints (second group of results). In the sequel, the two groups of results are compared in order to evaluate the efficiency of the aforementioned substitution. As a final step and in order to evaluate the performance of the FSD, the entire study is repeated using the powerful method of Sequential Quadratic Programming (SQP) as embedded in MatLab.

4.2.2. Theoretical background

The main idea is based on the fact that the stiffness matrices of the basic structural units that are used to assemble a structure depend on the dimensions of these units. To be more specific, a continuum can be considered as an assembly of Basic Continuum Units (BCUs). Introduction of material anisotropy changes the stiffness of a body along different directions

thus forces the body to behave differently along different directions. In Finite Element Analysis (FEA) and for 2D cases, a BCU can be modeled as a Bilinear Element (BE). The stiffness matrix of this element (Appendix 4A) suggests that a change in its dimensions changes its stiffness and as a consequence the stiffness of the BCU and the entire structure changes as well. Therefore, instead of introducing material anisotropy, a structural anisotropic behavior can be caused by changing the dimensions of the Basic Continuum Unit (BCU). It is strongly emphasized that the quantitative relationship between material anisotropy and anisotropic behavior due to changes in geometric dimensions is not examined in the present work.

The same idea is valid for the discrete bodies as well. In more details (Fig. 4.1), the Basic Continuum Unit can be replaced by a 6-bar assembly (Basic Discrete Unit – BDU). Again, an anisotropic behavior can be caused either by introducing material anisotropy or by changing the dimensions of the BDU (Appendix 4A). In this case, a change in dimensions causes a change in the orientation of the diagonal elements of the BDU, which affects severely the stiffness of the unit. It is strongly emphasized that the replacement of a BCU by a BDU is qualitative and not quantitative, meaning that the stiffness matrices of the two units are not equal.

(a) (b)

Figure 4.1: Basic units for modeling (a) continuum (Basic Continuum Unit - BCU) and (b) discrete structures (Basic Discrete Unit - BDU)

4.2.3. Analysis

Four typical cases were examined; that is the short cantilever, the cantilever, the MBB and the L-shape beam (Fig. 4.2). For each case, two kinds of models were used: one with bilinear elements (continuum) and one with truss elements (skeletal structure – discrete body). Therefore, eight different models were developed at first. The basic mesh unit for the bilinear models was an $(2a \times 2b)$ orthogonal, while the basic mesh unit for the skeletal structures was formed by introducing the diagonals in this geometrical shape. Each complete mesh was an assembly of an integer number of basic units. For each one of the aforementioned eight models, a parametric investigation with respect to the aspect ratio $\lambda = (a/b)$ and the mesh density was conducted. In more details, for each model, seven different aspect ratio values were chosen, $\lambda \in \{1/4, 1/3, 1/2, 1, 2, 3, 4\}$, while for each one of them three different mesh sizes were used ($7 \times 3 = 21$ runs). For the skeletal structures, the different aspect ratio values were used in order to examine the relationship between the optimum design and the variation in the structural stiffness due to the orientation of the trusses, while the different mesh sizes were used in order to ensure that the results were mesh-independent. For the bilinear models, both the different aspect ratio values and the different mesh sizes were used in order to examine mesh-independency. In total, $21 \times 8 = 168$ different models were examined. Each one of these models was analyzed twice: first by using the stress-ratio technique and then by using the SQP method. For the latter method, a variety of initial vectors was used, such as the output of the FSD or randomly formed vectors. It is clarified that for the skeletal structures the axial stresses were used in the recursive formula of the stress-ratio technique, while for the bilinear models the von Mises equivalent stress was used instead. It is also noted that the Matlab

Optimization Toolbox was selected for the implementation of the SQP method, while all analyses were run with an in-house code.

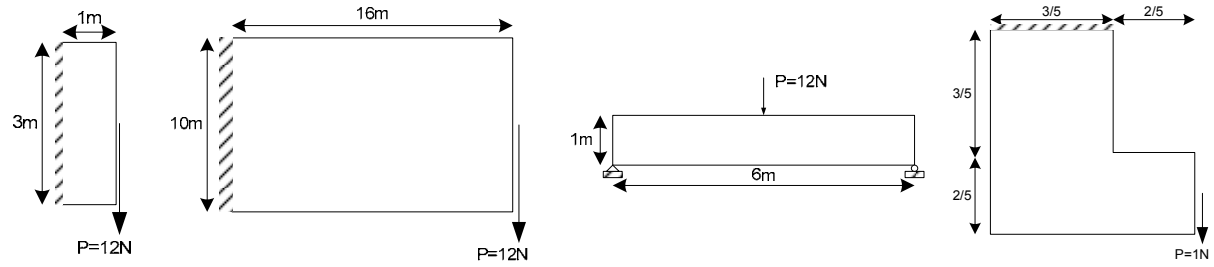

(a) (b) (c) (d)

Figure 4.2: Geometry and loading of the examined cases (a) deep cantilever, (b) short cantilever, (c) MBB beam and (d) L-shaped beam

In all cases, the material density was considered to be unity, thus each volume was equal to the corresponding weight. The Poisson ratio was selected to be $v = 0.3$, the modulus of elasticity was $E = 1MPa$ and the initial thickness (cross sections in the case of bar elements) equal to one. The maximum allowable stress was set to $\sigma_{\max} = 30MPa$. It is clarified that for the skeletal structures the maximum stress refers to the axial stresses, while for the bilinear models the maximum stress refers to the von Mises equivalent stress. The final volumes ($168 \times 2 = 336$ values) were recorded and the best results are presented in Tables 4.1 and 4.2.

Table 4.1: Best results for continuum structures

	Deep cantilever	Short cantilever	MBB beam	L-shaped beam
Aspect ratio [Hor : Ver]	1:1	1:2	1:1	1:2
Initial volume [m^3]	3.0	160.0	6.0	0.64
Final volume FSD [m^3]	0.7863	19.24	1.3814	0.2096
Final volume SQP [m^3]	0.7863	19.24	1.3814	0.2096
V_{final}/Vo [%]	26.21%	12.02%	23.02%	32.75%

Table 4.2: Best results for skeletal structures

	Short cantilever	Cantilever	MBB beam	L-shaped beam
Aspect ratio [Hor : Ver]	1:1	1:2	1:1	1:2
Initial volume [m^3]	3.0	160.0	6.0	0.64
Final volume FSD [m^3]	0.800	22.010	1.500	0.223
Final volume SQP [m^3]	0.800	22.010	1.500	0.223
V_{final}/V_o [%]	26.67%	13.75%	25.00%	34.84%

The material distributions for the final designs (continuum and skeletal structures) as well as results from literature are presented in Figure 4.3.

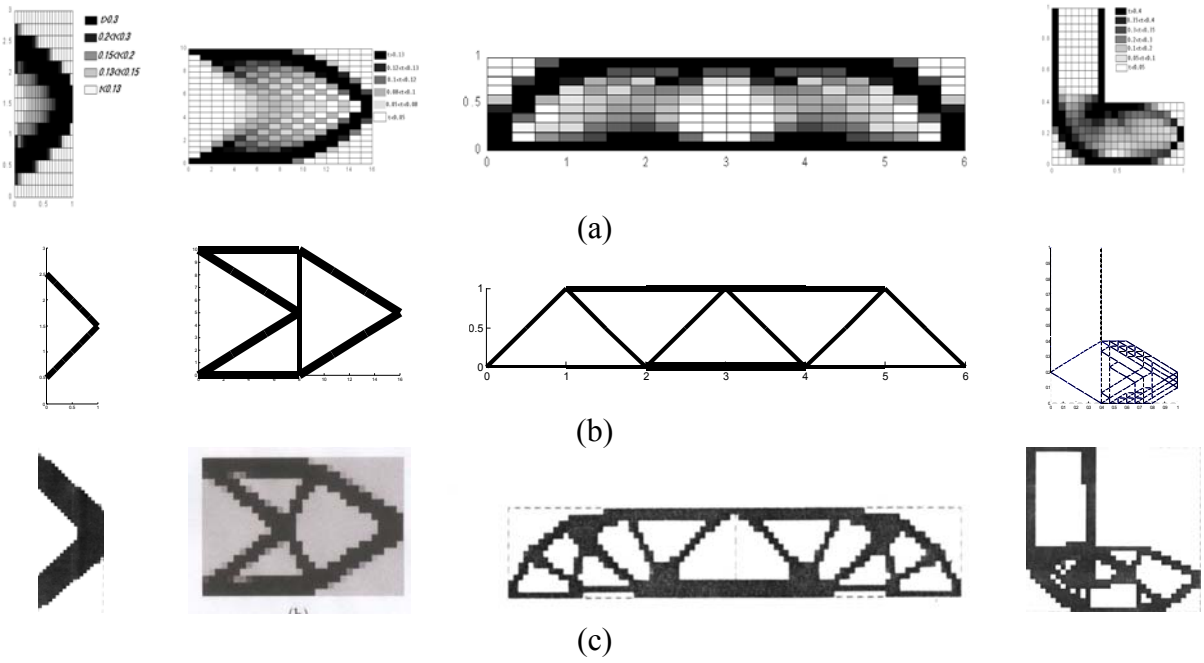

Figure 4.3: Fully Stressed Designs for (a) continuum, (b) discrete structures, (c) after (Duysinx and Bendsøe, 1998)

It is noted that the used skeletal structures have straight members only. This is a disadvantage in comparison with the continuum structures, which permit the appearance of 'curved' material distribution thus resulting in smaller volume (weight), as Table 4.3 shows.

Table 4.3: Volume reductions for optimum designs.

	Deep cantilever	Short cantilever	MBB beam	L-shaped beam
$1-(V_{final}/V_o)$ [%] (Skeletal)	73.33%	86.25%	75.00%	65.16%
$1-(V_{final}/V_o)$ [%] (Bilinear)	73.79%	87.98%	76.98%	67.25%
(Skeletal-Bilinear)	-0.46%	-1.73%	-1.98%	-2.09%

It is evident that the % difference in weight between the skeletal and the continuum structures is negligible in the case of the short cantilever, while the maximum difference is 2.09% (L-shaped beam). As far as the relationship between the aspect ratio and the optimum volume is concerned, Figure 4.4 provides the relevant information.

For the skeletal structures and for the first three cases, the volume of the structure is a convex function of the aspect ratio. This is not the case for the L-shape beam but still the function is monotonous and has a minimum. While four cases were studied, the minimum volume appeared for two distinct aspect ratio values (1 and ½). In addition, a small deviation from the value of the aspect ratio that corresponds to the minimum volume (weight) results in a severe change in the volume (weight) of the structure.

For the continuum structures the behavior is entirely different. In more details, for the first two cases, the volume of the structure appears to be independent of the aspect ratio. Furthermore, for the MBB and the L-shape beam, the curve seems to have a "flat" part for aspect ratios greater than 1 but it diverges for low aspect ratio values. Therefore, the change in the dimensions of the elements causes a change in their stiffness but this does not changes dramatically the volume (weight) of the structure. The reason for this is explained in Appendix 4A.

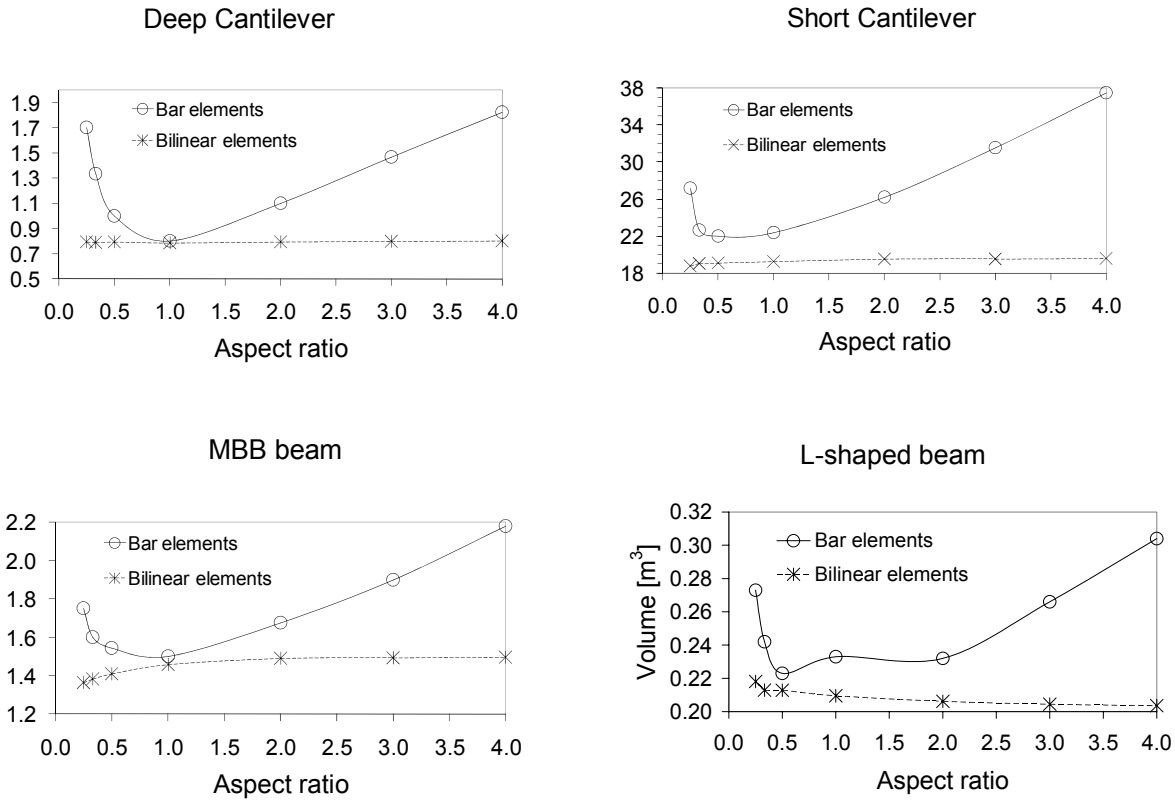

Figure 4.4: Change in optimum volume with respect to the aspect ratio

As it was previously mentioned, apart from the comparison between the skeletal structures and the continuum, the current work also encountered a comparison between FSD and SQP. The results of this comparison for the skeletal structures are presented in Table 4.4. Similar results are valid for the continuum as well.

Table 4.4: Comparison between FSD and SQP results (skeletal structures).

	FSD		**SQP**		
Case study	Optimum volume	Elapsed time t_1	Optimum volume	Elapsed time t_2	t_1 / t_2
#1	0.8004	0.99	0.8003	58.500	59
#2	21.3633	2.25	21.3613	120.010	53
#3	1.5000	2.86	1.5002	225.420	78
#4	0.2235	4.22	0.2235	1235.100	292

It is obvious that, for the cases studied, there is no difference between the optimum values obtained by FSD and SQP. On the contrary, there is a significant difference in the time

required for the optimum value to be obtained. It is clarified that both FSD and SQP were programmed in Matlab and all runs took place on the same computer (P4, 2MHz, 512MB RAM), thus the elapsed times are comparable.

4.2.4. Conclusions

The goals of the present study were first to investigate the capabilities of the Fully Stressed Design (FSD) in shape and topology optimization of two-dimensional structures under stress constraints only and second to examine the efficiency of modeling a continuum as a skeletal structure. For this purpose, four typical examples were examined. The results of the study were the following:

- The implementation of the stress-ratio technique for optimizing either a 2D continuum or a 2D skeletal structure was extremely easy and time-saving.
- The final shapes and topologies obtained by the FSD were similar to those obtained by using more sophisticated optimization techniques (Fig. 4.3).
- For the cases examined, the optimal results from the FSD and the SQP were identical. On the contrary, the solution time required for the former method was significantly lower.
- For the cases examined, the optimal volume (weight) for the continuum was slightly lighter than that for the skeletal structure. The reason for this was the fact that in skeletal structures only straight members appear, thus it is possible to have material only along straight lines, whose directions are predefined by the mesh. On the contrary, in a continuum it is possible to have material distribution in a checkerboard pattern, which is a more versatile material allocation.
- A change in the geometrical dimensions of a quadrilateral bilinear element in such a way that the aspect ratio remains the same, results in no change in the corresponding stiffness matrix. As a consequence, the stiffness of a structure assembled by such elements remains unchanged as well.
- A change in the geometrical dimensions of a 6-bar assembly, independently of whether the aspect ratio changes or not, causes a change in the corresponding stiffness matrix. As a result, the stiffness of a structure of such assemblies changes as well.
- The orientation of the trusses is of major importance both in the optimum layout and in the optimum volume (weight). Depending on this orientation, the FSD method may result in non-optimum designs. Nevertheless, in this way the optimum volume (weight) is bracketed by an upper bound, which is a very useful piece of information for structural optimization designers.
- The optimum volume, using either bilinear elements or truss elements, is almost the same. Nevertheless, the cost of constructing an assembly of trusses with various section areas is lower than the cost of producing a continuum of variable thickness. Therefore, the idea of substituting the continuum by discrete elements is of practical value.

In accordance to the aforementioned conclusions, the combination of discrete elements and the FSD method is a good investment in searching for the optimum layout of a continuum under stress constraints and is of practical value.

4.3. Stress constrained 2D continua and variable thickness elements

The fully stressed design of a structure is usually sought by changing the structural thickness according to the very well-known stress-ratio technique. In this approach, it is usual to implement an assembly of finite elements, each one of which has its own thickness that changes during the optimization procedure but remains constant throughout the element surface. For this reason, a severe thickness discontinuity among the elements appears thus resulting in shapes of low manufacturability. Alternatively, it is possible to develop finite

elements of variable thickness throughout their surface. Towards this direction, one choice is to use the same shape functions for both the thickness and the nodal displacement interpolation. In this way, it is possible to ensure thickness continuation among the elements, thus to get a smoother surface. Compared to the constant thickness elements, the final shape is smoother but the final weight is expected to be higher, since additional material is used in order to achieve the aforementioned smoothness. In this chapter, the influence of coupling the traditional stress-ratio technique with finite elements of variable thickness is investigated. Four typical cases of 2D continuum structures are examined, namely the deep cantilever, the short cantilever, the MBB beam and a Michell type structure. The quantified results revealed that, when elements of variable thickness are used, not only is the manufacturability significantly enforced but also the structural weight decreases as well.

4.3.1. In general

During the last decades, structural optimization has been one of the greatest challenges among the engineering community. In the beginning of the optimization era, the aim was to optimize either the size or the shape or the topology of a structure. In the recent years, a new concept, termed layout optimization, was introduced aiming at the simultaneous optimization of all three aforementioned characteristics (Rozvany, 2001). Towards this direction, a lot of research effort has been invested and the outcome was the development of a variety of different approaches. These approaches can be categorized in two large groups. The first group contains all those methods that introduce movable control points on the structural surface and try to find the optimum result by changing the co-ordinates of the control points. It is noted that during the optimization procedure, the material characteristics do not change. In this group, one can find not only deterministic approaches, such as the Sequential Quadratic Approach (SQP) (Belegundu and Chandrupatla, 1999) and the bubble method by Eschenauer et al. (Eschenauer et al, 1994), but also stochastic procedures (Giannakoglou et al, 2002). A common characteristic in these approaches is that at each iterative step a new mesh must be created because the domain of the optimization problem (area or volume of the structure under optimization) changes. The second group contains all those methods that use the same mesh throughout the optimization procedure and try to locate the optimum geometry by properly changing a *material* characteristic, such as the Young's modulus or the density. The ultimate goal is to reach such material distribution where either material exists or not (0-1 patterns). In this category, one can find the COC approach by Rozvany (Rozvany, 1997), which is based on the optimality criteria concept, the method of Mljeniek (Mlejnek and Schirrmacher, 1993), where the value of the Young's modulus depends on the material density, the SIMP method by Bendsøe (Bendsøe and Sigmund, 2003), where the material density is properly penalized, the homogenization method by Suzuki and Kikuchi (Suzuki and Kikuchi, 1991), where material of different ranks are used, the Evolutionary Structural Optimization (ESO) method by Xie and Steven (Xie et al, 1997), where underutilized material is gradually removed, and the method by Makris and Provatidis (Makris and Provatidis, 2002), who proposed a virtual strain energy density optimization approach. In all these methods, the thickness of the used finite elements is considered to be constant. Alternatively, it is possible to use finite elements of variable thickness (Felippa, 2001), thus it is of interest to investigate the implementation of the aforementioned elements with well known optimization techniques.

Towards this direction, the present paper examined the coupling of the stress-ratio technique, which is the simplest optimization scheme for single stress constrained problems, with elements whose variable thickness is described by the same shape functions used for the nodal displacement interpolation. More particularly, constant strain triangular (CST) finite elements were used. The main idea behind the examined concept is very simple. The

proposed scheme of thickness interpolation ensures thickness continuity along the structural surface, while at the same time the mesh nodes can be used as surface control points. Moving such control points according to a simple and efficient technique, such as the stress-ratio technique, it is possible to avoid severe thickness discontinuities, thus enforcing the manufacturability of the structure, and getting quickly the optimum layout.

4.3.2. Theoretical approach

The proposed approach is based on two theoretical aspects, the former being the stress-ratio redesign equation and the latter being the formation of the stiffness matrix of a variable thickness finite element. In this chapter, two types of such elements have been implemented, namely the constant strain triangular finite element (CST) and the 4-node quadrilateral element of plane elasticity. This selection is justified in the corresponding paragraphs. However, it is noted that the concept of interpolating the thickness within an element is applicable to any type of finite element, either of the Lagrange or of the Serendipity family. In the next sections, the aforementioned stress-ratio redesign equation is presented, while the investigation of typical literature examples, for each one of the aforementioned finite elements, follows.

4.3.3. The stress-ratio redesign equation

According to the Lagrange multipliers method (Morris, 1982), for the case of a truss under stress constraints g_i only, the Lagrangian that describes the optimization problem of minimum weight is:

$$\mathfrak{L}\left(x,\lambda\right) = W + \sum_{i=1}^{NEL} \lambda_i g_i \tag{4.1}$$

where W is the weight of the entire structure, x_i is the cross-sectional area of the i-th bar, λ_i is the Lagrange multiplier for the stress constraint of the i-th bar, g_i is the imposed stress constraint for the i-th bar. Basic manipulations of Eq.(4.1), under the assumption that the member forces do not depend on the member sizes, results in Eq.(4.2), which is well-known as the 'stress-ratio formula' (also see Section 3.3.1):

$${}^{k}x_i = {}^{k-1}x_i \left(\frac{\sigma_i}{\sigma_{\max,i}} \right) \tag{4.2}$$

where k denotes the iteration. For a determinate structure, the minimum weight is reached in one step. For an indeterminate structure, Eq.(4.2) can be used only as an acceptable approximation to a near-minimum design. However, experience has shown that for the majority of the engineering problems, Eq.(4.2) provides acceptably adequate results (Berke and Khot, 1987). Therefore, for stress constrained structures, the stress-ratio redesign formula is a good choice for seeking the layout of minimum weight

Generalizing Eq.(4.2), x_i may represent element thickness for 2D continua (Morris, 1982). For the needs of the present paper, a further generalization was adopted, according to which the quantity x_i in Eq.(4.2) represented *nodal* thickness. At this point, it is strongly emphasized that a minimum thickness value must be imposed; a negative thickness has no physical meaning, while a zero thickness may cause severe numerical instabilities during the optimization procedure.

4.3.4. Implementation of a CST finite element of variable thickness

A Constant Strain Triangle (CST) is a three-noded triangular finite element that has three nodes at the vertices of the triangle (Fig.4.1a). Its name is due to the fact that the strains are constant over the element. The displacement interpolation within the CST element is linear in x and y:

$$\mathbf{u}(x,y) = \mathbf{N}^e \mathbf{a}^e = \bar{\mathbf{N}} C^{-1} \mathbf{a}^e \tag{4.3}$$

More particularly, $\mathbf{N}^e$ refers to the interpolation scheme C describes the nodal coordinates of the element e and $\mathbf{a}^e$ denotes the corresponding nodal displacements. From the theory of the Finite Element Method (FEM), it is well known that for a (CST) of area A, the stiffness matrix equals to:

$$\mathbf{K}^e = \mathbf{B}^T \ \mathbf{E}\ \mathbf{B} \int_A t\, dA \tag{4.4}$$

where $\mathbf{E}$ is the 3×3 stress-strain matrix of elastic moduli ($\mathbf{E}_1$ for plane stress and $\mathbf{E}_2$ for plane strain) and $\mathbf{B}$ is the 3×6 strain-displacement matrix. For a constant thickness CST element, Eq.(4.4) becomes

$$\mathbf{K}^e = t\, A\, \mathbf{B}^T \ \mathbf{E}\ \mathbf{B} \tag{4.5}$$

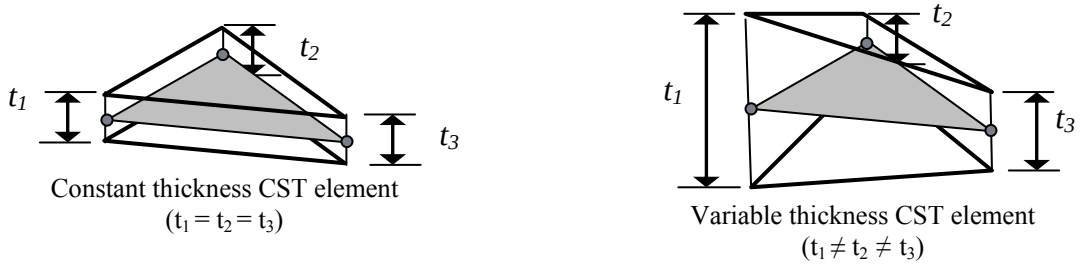

(a) (b)

Figure 4.5: CST element with (a) constant and (b) variable thickness

For a variable thickness CST element (Fig.4.1b), it is evident that only the quantity inside the integral of Eq.(4.1) changes and requires a re-estimation. If the thickness is interpolated with the shape functions used for the interpolation of the displacements, then, after some basic integrations, the stiffness matrix becomes equal to:

$$\mathbf{K}^e = \left(\frac{t_1 + t_2 + t_3}{3} \right) A\, \mathbf{B}^T \ \mathbf{E}\ \mathbf{B} \tag{4.6}$$

where $t_i, i = 1,2,3$ is the nodal thickness. It is clarified that all the matrices involved in the aforementioned equations are omitted because they are very easily retrieved from textbooks concerning the Finite Element Method (FEM).

At this point, it is noted that the implementation of the CST element has the important advantage that three nodes always define a plane, thus an assembly of such elements do define a C^0 surface, which will be a polygonal.

4.3.4.1. Procedure of Evaluation

In order to evaluate the implementation of a CST finite element of variable thickness in searching for the optimum layout of stress constrained 2D continuum, five evaluation indices, two plots concerning the history of the iterative optimization procedure, as well as three plots and three 3-D graphs concerning the final optimization stage (optimal layout) were introduced. In more details, the evaluation indices used are presented in Table 4.1 For reasons of comparison, the proposed optimization procedure was applied first using finite elements of constant thickness (let it be 'Approach #1') and then using finite elements of variable thickness (let it be 'Approach #2').

Table 4.5: Evaluation indices

Name	Definition	Aim
EI_1	$\frac{W_{opti}-W_{oud}}{W_{oud}}\times 100$	for each approach, to compare the weight of the final layout to the weight of the initial layout in order to estimate the (%) weight reduction
EI_2	$\frac{Nodes_{active}}{NN}$	for each approach, to estimate the surface coverage by comparing the number of nodes with thickness larger than the minimum ('active' nodes) to the total number of mesh nodes
EI_3	$CV(\sigma_{vonMises})$	for each approach, to find out how much 'fully stressed' the final layout is (estimate the Coefficient of Variation of the vonMises stress for the 'active' nodes of the final layout)
EI_4	$\frac{A_{surfer}-A_{oud}}{A_{oud}}\times 100$	for each approach, to compare the area of the surface interpolating the mesh nodes of the final layout to the area of the initial layout
EI_5	$\frac{W_{surfer}-W_{oud}}{W_{oud}}\times 100$	for each approach, to compare the weight of the volume, limited by the surface interpolating the mesh nodes of the final layout and the mid plane of the structure, to the weight of the initial layout

It is clarified that, for a stress constrained structure, the so-called Optimum Uniform Design (OUD) is defined as the initial layout of constant thickness which is then uniformly scaled so that the stress constraint becomes active. Such designs are used as a reference for weight comparisons. The plots and the graphs introduced for the evaluation of the proposed approach are presented in Table 4.2.

Table 4.6: Graphical means of evaluation

Plot	Aim
Plot_a	to evaluate the convergence of each approach with respect to the maximum von Mises stress appearing in every iterative step (intermediate layouts)
Plot_b	to evaluate the convergence of each approach with respect to the weight of every intermediate layout
Plot_c	to evaluate how much more or less 'fully stressed' the layout of Approach #2 is with respect to the layout of Approach #1
Plot_d	to evaluate how much lighter or heavier the layout of Approach #2 is with respect to the layout of Approach #1
Graph_a	to visualize the optimal layout
Graph_b	for each approach, to interpolate the mesh nodes of the final layout and estimate the material volume (weight) required for manufacturing the layout

At this point, it must be noted that Plot_c and Plot_d were created in two steps, the former being the use of the equations presented in Table 4.3 and the latter being the sorting of the results. From the first step, it is ensured that the thickness of a node from Approach #1 will be compared to the thickness of the *same* node from Approach #2, while from the second step a better visualization is achieved. In addition, Graph_a presents the final layout without any intervention (smoothening or other), while Graph_b is created using the commercial software SURFER by Golden Software and implementing the Krigging method of interpolation. A good visualization of Graph_a and Graph_b require an adequately large size of the graphs. For reasons of space economy, only the Graph_b for the Approach #1 is presented.

Table 4.7: Equations used for the creation of Plot_3 and Plot_4 (reference: Approach #1)

Plot	Equation
Plot_3	$(\%)\Delta\left(\sigma_{vonMises}\right)=\dfrac{\left(\sigma_{vonMises}\right)_{t\neq const}-\left(\sigma_{vonMises}\right)_{t=const}}{\left(\sigma_{vonMises}\right)_{t=const}}\times 100$
Plot_4	$(\%)\Delta\left(thickness_{nodal}\right)=\dfrac{\left(thickness_{nodal}\right)_{t\neq const}-\left(thickness_{nodal}\right)_{t=const}}{\left(thickness_{nodal}\right)_{t=const}}\times 100$

4.3.4.2. Proposed optimization procedure

The proposed optimization procedure may be divided into two phases:

Phase A: History of the optimization procedure (initial design: Optimum Uniform Design)
Step A1: Estimate the (OUD) and record weight, thickness distribution and stress distribution
Step A2: From (OUD), initiate optimization procedure for adequate number of iterations
Step A3: For each iteration, update Plot_a (see Table 4.2)
Step A4: For each iteration, update Plot_b (see Table 4.2)
Step A5: From Plot_a, locate iteration with zero (or minimum) stress violation
Phase B: Determination of the optimum layout (for the iteration taken from Step A5)
Step B1: Perform a uniform thickness scaling so that no stress violation occurs
Step B2: From Step A1 and Step B1, create Plot_c (see Tables 4.2, 4.3)
Step B3: From Step A1 and Step B1, create Plot_d (see Tables 4.2, 4.3)
Step B4: From Step A1 and Step B1, calculate EI_1 (see Table 4.1)
Step B5: Record number of 'active' nodes and calculate EI_2 (see Table 4.1)
Step B6: For the active nodes only, calculate the mean value, the standard deviation and the CV for the von Mises stress (EI_3 - see Table 4.1)
Step B7: Create Graph_a and Graph_b (see Table 4.2)
Step B8: From Step B5, record area and calculate EI_4 (see Table 4.1)
Step B9: From Step B5, record volume and calculate EI_5 (see Table 4.1)

4.3.4.3. Investigated test cases

The investigated test cases and their data are shown in Fig.4.2 and Table 4.4, respectively.

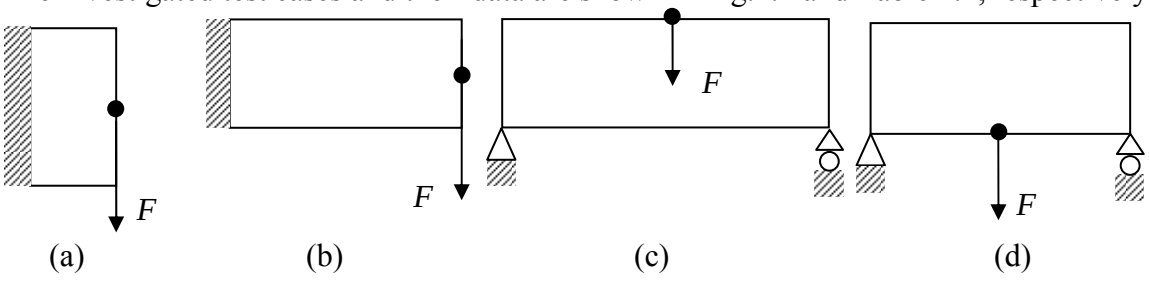

Figure 4.6: The examined examples (a) deep cantilever, (b) short cantilever, (c) MBB beam, (d) Michell-type structure

Table 4.8: Data for the examined examples

Example	L_x $[m]$	L_y $[m]$	E $[Pa]$	v	*dens*	F $[N]$	Application point of F	σ_{allow} $[Pa]$	*NN*	*NEL*
Deep cantilever	3	1	1	0.3	1	12	Right side – middle	30	641	1200
Short cantilever	16	10	1	0.3	1	12	Right side-middle	20	1333	2560
MBB beam	6	1	1	0.3	1	2	Top side-middle	20	1271	2400
Michell structure	10	5	100e06	0.3	1	1000	Bottom side – middle	35000	1661	3200

In Table 4.4, L_x denotes the horizontal dimension (width), L_y denotes the vertical dimension (height), E denotes the modulus of elasticity, v denotes Poisson's ratio, *dens* denotes the material density, F denotes the applied load, σ_{allow} denotes the allowable stress, *NN* denotes the Number of Nodes and *NEL* stands for the Number of Elements.

4.3.4.4. Results

The Evaluation Indices for the examined applications are shown in Table 4.5 while all the plots are shown in Figs.4.3 and 4.4.

Table 4.9: Evaluation Indices for the examined applications

		Volume (FSD Design)	Uniform scaling factor	EI_1	EI_2	mean Svonmises	EI_3	EI_4	EI_5
Deep cantilever	t=const	0.8017	1.0071	-93.504	88.768	28.10	17.372	1.955	68.893
	t<>const	0.8431	1.0017	-93.132	78.783	26.78	21.513	1.693	10.419
	% difference	5.17%	-0.54%	-0.40%	-11.25%	-4.69%	23.84%	-13.40%	-84.88%
Short cantilever	t=const	28.4073	1.0086	-85.098	97.900	19.56	8.323	1.117	84.964
	t<>const	30.4316	1.0020	-83.931	94.149	18.93	11.944	1.037	1.670
	% difference	7.13%	-0.65%	-1.37%	-3.83%	-3.19%	43.50%	-7.15%	-98.03%
MBB beam	t=const	1.3481	1.0154	-81.644	99.685	19.48	3.631	3.268	93.716
	t<>const	1.5380	1.0002	-78.735	96.223	18.62	8.651	1.883	6.294
	% difference	14.09%	-1.50%	-3.56%	-3.47%	-4.39%	138.23%	-42.37%	-93.28%
Michel structure	t=const	0.4259	1.0054	-93.609	96.869	34.58	2.388	16.688	76.727
	t<>const	0.4652	1.0045	-93.018	92.655	33.09	7.481	16.674	1.957
	% difference	9.24%	-0.09%	-0.63%	-4.35%	-4.33%	213.28%	-0.08%	-97.45%

In more details, Fig.4.3 shows the optimum material distribution (optimum structural layout) for each examined example (see Table 4.2). Due to symmetry, only half of the structural thickness is shown (top half). For each example and for each pair of graphs ('a', 'b'), the same axis scaling has been used so that a visual comparison between the corresponding material distributions can be made. The graphs denoted as 'c' have different scaling because they were created with different software, thus they can be compared to graphs 'a' and 'b' only qualitatively. It is noted that for the details to be better visualized, the maximum value for the x-axis and the y-axis (data aspect ratio) is not the same only for the graphs (a) and (b) concerning the MBB beam and the Michell-type structure, respectively.

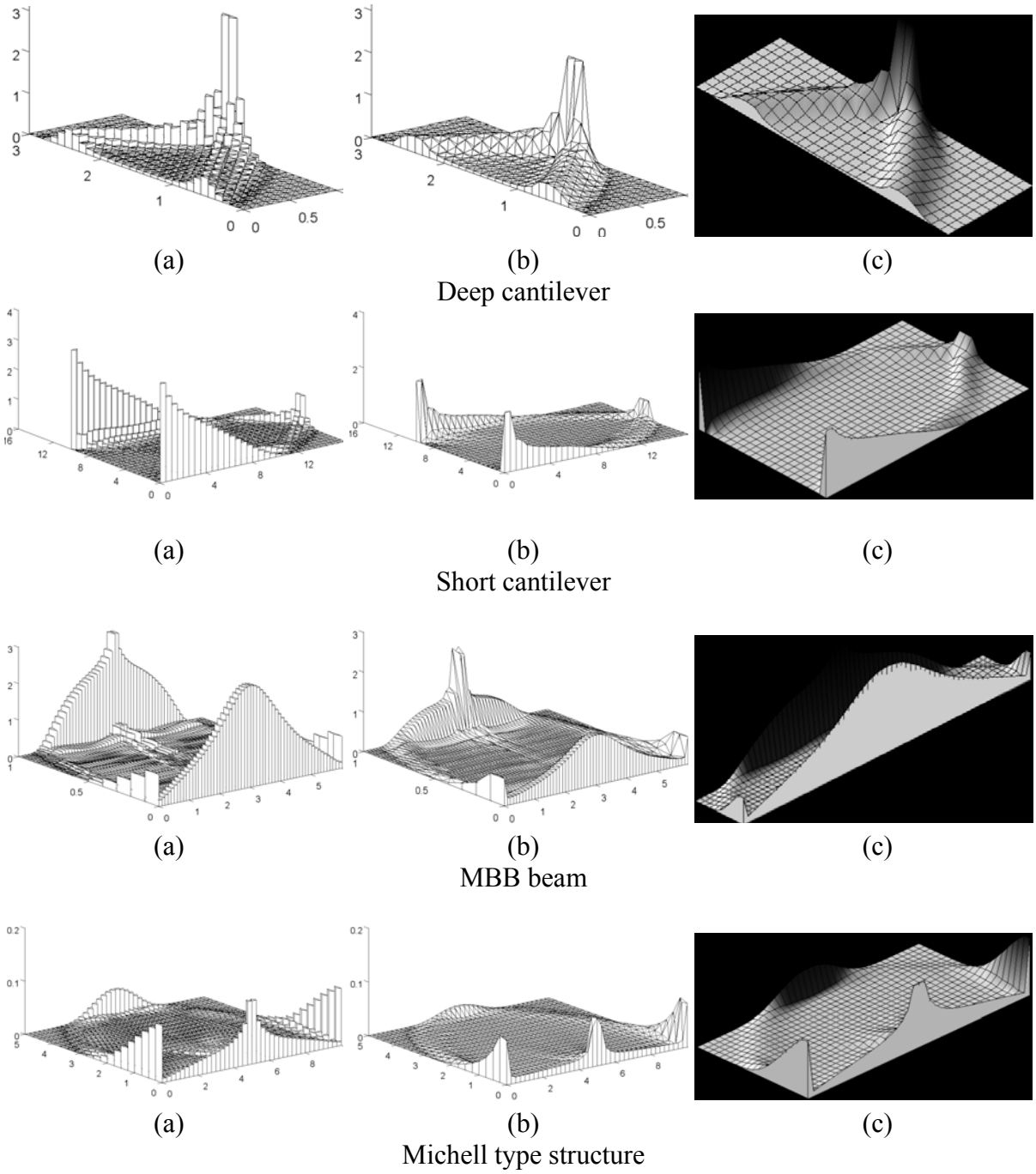

(a) (b) (c)
Deep cantilever

(a) (b) (c)
Short cantilever

(a) (b) (c)
MBB beam

(a) (b) (c)
Michell type structure

Figure 4.7: Optimum structural layouts

The plots in Fig.4.4 concern the history of the iterative optimization procedure as well as the performance of the final optimum layout (for more details for each plot type, see Table 4.2). It is noted that all plots of type Plot_3 have the same scaling along the y-axis, so that a visual comparison may be performed easily. The same holds for all plots of type Plot_4. Obviously, it was not possible to do the same with the x-axis of the aforementioned plots because the number of nodes and elements is different for each examined example. Each plot has a small label, either at the top left corner or the bottom right corner, denoting the example it corresponds to.

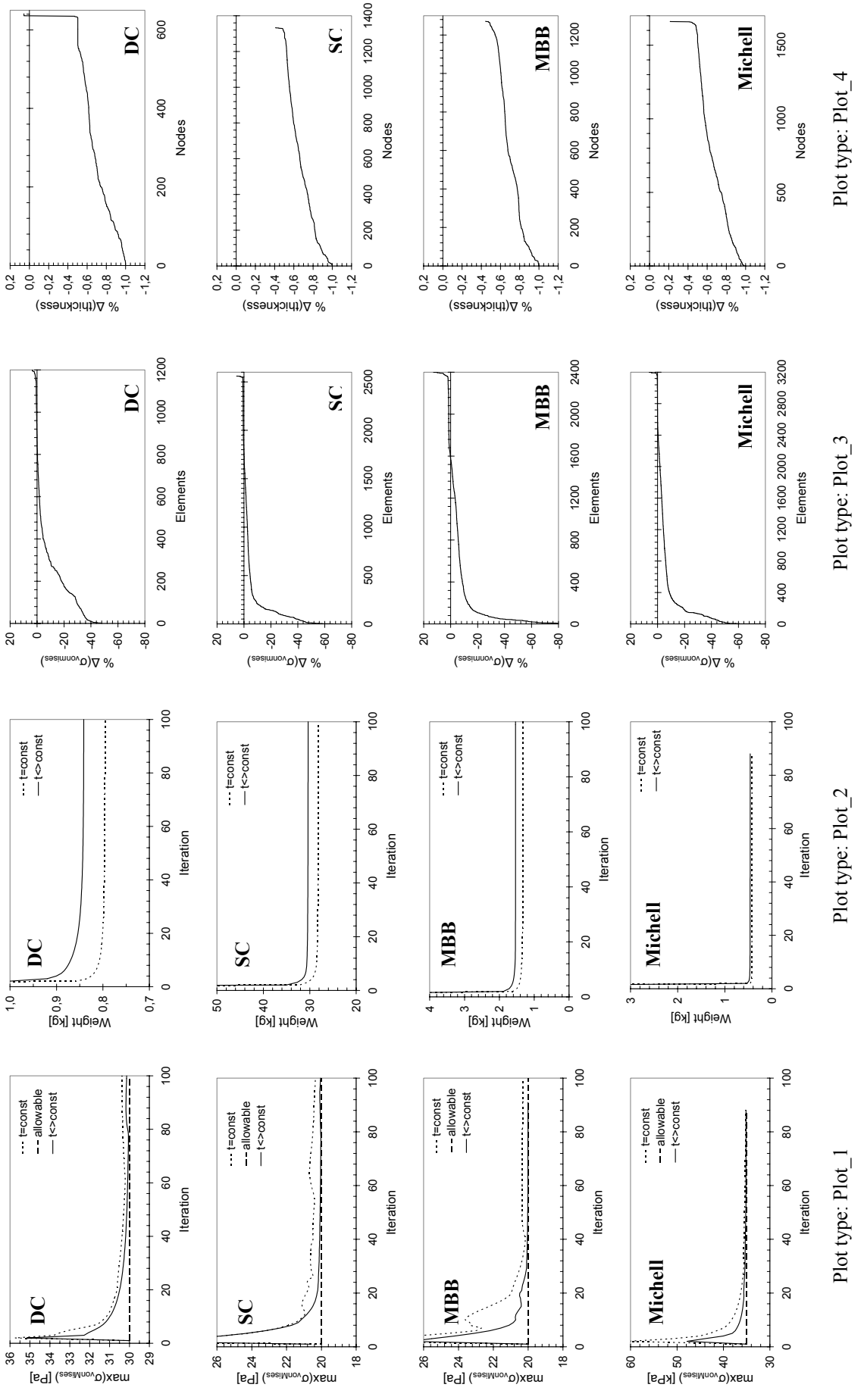

Figure 4.8: Plots

4.3.4.5. Discussion

The finite element selected in the present paper was the Constant Strain Triangle (CST). It is well known that the displacement interpolation within the CST element is linear in *x* and *y*, thus its behavior is inferior when compared to other finite elements, such as the 4-node plane element. Furthermore, a coarse mesh may affect significantly the results. In order to deal with this reality, it was decided to build a fine and fully symmetric mesh. This was achieved by dividing first the structural domain in a large number of rectangles (unitary aspect ratio) and then each rectangle into four equal triangles, which had a common node at the centre of the rectangle.

With respect to the stress-ratio technique, it is a good practice to let the optimization procedure run for some iterations in order to get a near optimum result. In the present paper, it was considered that 100 iterations were adequately enough. As the Plot_1's and the Plot_2's suggest, convergence is practically achieved after a few iterations, accompanied by a small stress violation, which is easy to overcome with a uniform thickness scaling. As the 'Uniform Scaling factor' in Table 4.5 suggests, the cancellation of the appearing stress violation causes negligible increase of the structural weight.

Another point worth mentioning concerns the estimation of the *nodal* stresses in a (CST) mesh. Such a nodal stress may be considered as equal, either to the average value of or to the maximum value, among the stresses of all elements connected to the specific node. In the present paper, the latter approach was selected. The same principle holds for estimating the nodal thickness in a CST mesh.

The study of Table 4.5 reveals that the layout obtained with Appoach #2 (variable thickness elements) is more promising than the layout obtained with Appoach #1 (constant thickness elements). This conclusion is derived from the fact that, for the former layout and for all the examined examples, the Evaluation Indices EI_1, EI_2, EI_4 and EI_5 were lower. Furthermore, the lower value of both the mean von Mises stress and the EI_3, in combination with the Plot_3 and the Plot_4 suggest that there is still a margin for further improvement because the layout is less fully-stressed than that obtained with Approach #1. Furthermore, simple visual inspection of Fig.3 reveals that the Approach #2 results inherently and without any further interpolation in significantly smoother layouts thus enforces the manufacturability of the optimal layout.

4.3.4.6. Conclusions

In the present section, the use of the well known stress-ratio technique in combination with CST finite elements of variable thickness for the determination of the fully-stressed optimal layout of 2D continua was investigated. The element thickness description was based on the shape functions used for the nodal displacement interpolation. The proposed procedure was tested in four typical stress constrained examples retrieved from the literature, namely the deep cantilever, the short cantilever, the MBB beam and a Michell type structure. For the evaluation of the proposed approach, five performance indices, two plots concerning the history of the iterative optimization procedure, as well as two plots and three 3D graphs concerning the optimum material distribution were introduced. It was shown that, in all cases, the use of the variable element thickness concept resulted in layouts with improved characteristics, such as less weight and smoother material distribution, thus enforced manufacturability. In conclusion, the current investigation showed that the proposed approach contributes towards the location of the optimal structural layout and the encouraging results suggested that further investigation be carried out with other types of finite elements and thickness interpolation schemes. Within this frame, the 4-node quadrilateral isoparametric finite element is examined in the next section.

4.3.5. Implementation of a 4-node quadrilateral finite element of variable thickness

The 4-node quadrilateral element is the simplest member of the quadrilateral family. The corresponding shape functions vary linearly on quadrilateral coordinate lines $\xi = const$ and $\eta = const$, but are not linear polynomials. More particularly, the displacement interpolation within the element is given by:

$$\begin{aligned} \mathbf{u}(x,y) &= \mathbf{N}^e \mathbf{a}^e = \bar{\mathbf{N}} C^{-1} \mathbf{a}^e \\ N_i^e &= 0.25(1-\xi\xi_i)(1-\eta\eta_i) \end{aligned} \tag{4.7}$$

where $\mathbf{N}^e$ refers to the interpolation scheme, $\mathbf{C}$ describes the nodal coordinates of the element e and $\mathbf{a}^e$ denotes the corresponding nodal displacements. From the theory of the Finite Element Method (FEM), it is well known that the stiffness matrix $\mathbf{K}^e$ of the element e is given by the general equation:

$$\mathbf{K}^e = \int_A t\, \mathbf{B}^T\, \mathbf{E}\, \mathbf{B}\, dA \tag{4.8}$$

where $\mathbf{E}$ is the 3×3 stress-strain matrix of elastic moduli (let it be $\mathbf{E}_1$ for plane stress and $\mathbf{E}_2$ for plane strain) and $\mathbf{B}$ is the 3×8 strain-displacement matrix. In order to estimate $\mathbf{K}^e$, the standard practice has been to use Gauss integration because such rules use a minimal number of sample points to achieve a desired level of accuracy. For plane elasticity problems, the two dimensional Gauss rules must be applied, according to which first the integrand must be reduced to a canonical form and then the following approximate formula must be applied:

$$\int_{-1}^{+1}\int_{-1}^{+1} F(\xi,\eta)\, d\xi d\eta \approx \sum_{i=1}^{p_1}\sum_{j=1}^{p_2} w_i w_j F(\xi_i,\eta_j) \tag{4.9}$$

In Eq.(4.9), p_1 and p_2 are the number of Gauss points in the ξ and η directions, respectively. Usually the same number $p = p_1 = p_2$ is chosen if the shape functions are taken to be the same in the ξ and η directions. The combination of Eqs.(4.8, 4.9) yields that it is possible to estimate $\mathbf{K}^e$ as long as the differential dA is expressed in terms of the differentials $d\xi$ and $d\eta$. This reduction is achieved using the following relation:

$$dA = \det \mathbf{J}\, d\xi\, d\eta \tag{4.10}$$

where $\mathbf{J}$ is the Jacobian matrix that connects the differentials of $\{x,y\}$ to those of $\{\xi,\eta\}$.

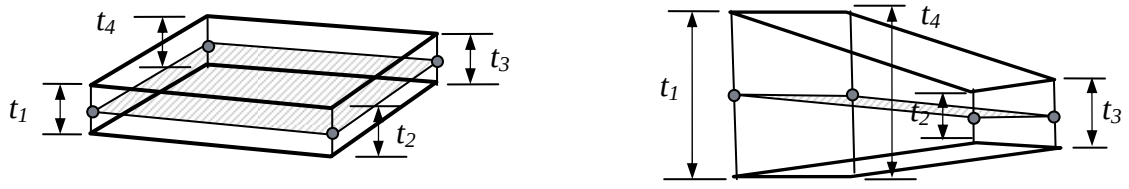

($t_1 = t_2 = t_3 = t_4$) (a)

($t_1 \neq t_2 \neq t_3 \neq t_4$) (b)

Figure 4.9: 4-node quadrilateral element with (a) constant and (b) variable thickness

For a 4-node quadrilateral element with constant element-wise thickness (Fig.4.5a), it holds:

$$\mathbf{K}^e = t \int_A \mathbf{B}^T \, \mathbf{E} \, \mathbf{B} \, dA \tag{4.11}$$

For a 4-node quadrilateral element with variable element-wise thickness (Fig.4.5b), under the assumption of isoparametric thickness interpolation, it holds:

$$t = \sum_{i=1}^{4} \left(N_i \, t_i \right) \tag{4.12}$$

where t_i is the thickness at the $i-th$ corner node of the element and N_i is the corresponding shape function. The combination of Eqs.(4.11, 4.12) yields:

$$\mathbf{K}^e = \int_A \sum_{i=1}^{4} \left(N_i t_i \right) \mathbf{B}^T \, \mathrm{E} \, \mathrm{B} \, dA \tag{4.13}$$

Introducing the Gauss rule stated in Eq.(4.9) into Eq.(4.13) yields:

$$\mathbf{K}^e = \int_{-1}^{1} \int_{-1}^{-1} \sum_{i=1}^{4} \left(N_i t_i \right) \mathbf{B}^T \, \mathrm{E} \, \mathrm{B} \, \det J \, d\xi \, d\eta \tag{4.14}$$

The matrices $\mathbf{E}$ and $\mathbf{B}$ can very easily be retrieved from text books on (FEM).

4.3.5.1. Procedure of Evaluation

The performance of the 4-node quadrilateral isoparamteric element of plane elasticity was evaluated through the introduction of three Evaluation Indices (EI) defined as follows:

- Evaluation Index EI_1, informing about the normalized relation between the weight of the optimum layout *before* the application of the global smoothing procedure and the weight of the (OUD) and defined as:

$$EI_1 = \left(\frac{W_{opti}}{W_{OUD}} \right) \tag{4.15}$$

- Evaluation Index EI_2, informing about the stress state of the structure *before* the application of the global smoothing procedure and defined as the average of the equivalent von Mises stress of the active structural part:

$$EI_2 = \overline{\left(\sigma_{vonMises,active} \right)} \tag{4.16}$$

- Evaluation Index EI_3, informing about how fully stressed the final layout *itself* is and defined as the Coefficient of Variation $\left(CV \right)$ of the equivalent von Mises stress of the active structural part:

$$EI_3 = CV \left(\sigma_{vonMises,active} \right) \tag{4.17}$$

Moreover, the convergence history, in terms of structural weight, was also recorded and presented as a plot. Obviously, similar indices may be defined for the state after the application of the global smoothing procedure.

4.3.5.2. Proposed optimization procedure

In the current section, an optimization procedure that uses elements of variable element-wise thickness, let it be Approach #3, is proposed. For reasons of comparison, another optimization procedure, let it be Approach #4), using elements of constant element-wise thickness, was also developed. In both cases, the Optimum Uniform Design (OUD) was used as the optimum design of reference. For the completeness of the text, it is reminded that the (OUD) is the design obtained when the thickness distribution over the discretized domain is uniform and has the minimum possible value that does not cause any constraint violation.

4.3.5.2.1. Proposed optimization procedure for 4-node variable thickness elements

The proposed optimization procedure is as follows:

Step 1: Estimate the (OUD) and record weight, thickness and stress distribution to be used as references

Step 2: Carry out a Finite Element Analysis (FEA) and for each element estimate the equivalent von Mises stress at the Gauss points

Step 3: Update the thickness distribution of the structure at the Gauss points with the stress-ratio technique

Step 4: Interpolate the thickness at the Gauss points and update the nodal thickness

Step 5: Carry out a (FEA) with the nodal thicknesses from Step 4

Step 6: Apply a uniform scaling so that no stress violations occur

Step 7: Check for convergence; if convergence has not been achieved and the maximum number of iterations has not been exceeded, then go back to Step 2.

Step 8: Apply a global smoothing procedure (e.g. Kriging technique).

Step 9: Apply a uniform scaling to the smoothed layout so that no stress violations occur.

Step 10: Evaluate the Performance Indices.

The nodal thickness distribution may be derived from the thickness distribution at the Gauss points using a mixed scheme of global *interpolation* for the *internal* nodes and global *extrapolation* for the *boundary* nodes. The interpolation schemes used in the present paper are presented in Section 4.3.5.2.3.

4.3.5.2.2. Proposed optimization procedure for 4-node constant thickness elements

The corresponding optimization procedure for constant-thickness elements is as follows:

Step 1: Estimate the (OUD) and record weight, thickness and stress distribution to be used as references

Step 2: Carry out a Finite Element Analysis (FEA) and for each element estimate the equivalent von Mises stress at the Gauss points

Step 3: For each element, interpolate the equivalent von Mises stress at the Gauss points and estimate a stress value for the element at its centroid

Step 4: Update the element thickness using the stress-ratio technique

Step 5: Carry out a (FEA) with the element thicknesses from Step 4

Step 6: Apply a uniform scaling so that no stress violations occur

Step 7: Check for convergence; if convergence has not been achieved and the maximum number of iterations has not been exceeded then go back to Step 2.

Step 8: Apply a global smoothing procedure (e.g. Kriging technique).

Step 9: Apply a uniform scaling to the smoothed layout so that no stress violations occur.

Step 10: Evaluate the Performance Indices.

The stress estimation at an element centroid in Step 3 may be based on a global interpolation scheme. The interpolation schemes used in the present paper are presented in Section 4.3.5.2.2.

4.3.5.2.3. Estimation of the nodal stress values

The main idea of the proposed procedure was first to evaluate the stresses at the gauss points and then to estimate the nodal stresses through an interpolation scheme over the stresses at the gauss points. In total, three Stress Interpolation Schemes (#1, #2, #3) were used. For the variable-thickness elements and according to the first scheme, the stress at a node was estimated as the maximum of the values corresponding to the stresses at the gauss points surrounding the specific node. For a 2×2 integration rule and a mesh of 4-node quadrilateral elements, it is obvious that a node *inside* the mesh (design space) was surrounded by four gauss points, a node along the border of the mesh was surrounded by 2 gauss points, while for a *corner node* of the mesh the stress was equal to the stress of the nearest gauss point. According to the second and the third scheme, the average value and the minimum value of the stresses at the aforementioned gauss points were to be estimated, respectively. For the constant-thickness elements, the gauss points belonging to each one of these elements were located and the three aforementioned ways of handling the stress values (estimation of the maximum, the average or the minimum value) was applied and a stress at the centroid of each element was estimated.

4.3.5.3. Verification of the implemented finite elements

The verification of the implemented finite element was carried out through a comparison with the element SHELL63 of the Finite Element Analysis (FEA) software Ansys (ver.10). For the verification, a rectangular 2D cantilever first under in-plane bending and then under unsymmetrical tension (compression) was examined for various mesh densities with unit aspect ratio. A coincidence in stresses at the gauss points between the in-house code and Ansys was achieved (keyoptions for SHEL63: extra displacement shape functions excluded, membrane element stiffness only).

At this point, it is clarified that all the investigation mentioned above regarding the variable-thickness elements could had been carried out in Ansys or in another commercial software for structural analysis. However, such a choice has certain drawbacks. First, the user does not have complete control of the integration schemes implemented for the estimation of the stiffness matrix. For instance, it is not possible to select the type of the Gauss rule to be applied. Second, and most important, the access to the results data, in the form of raw data, is not that user-friendly. Instead, if an in-house code is developed in MatLab, or in an equivalent environment, then these disadvantages do not appear and the user has a much better control of what he/she is doing and how he/she can obtain the desired numerical information in the desired format.

Finally, it is noted that in order to verify that the optimized layouts, after the smoothing procedure was applied, did not violate any of the imposed constraints, one last (FEA) was carried out and then a uniform scaling was applied. In this way, a slightly oversized design was uniformly shrunk and a slightly undersized design was uniformly enlarged. The uniform change of the layout is not a necessary optimality condition but for good practical engineering purposes is totally acceptable.

4.3.5.4. Investigated test cases

The investigated test cases are exactly the same with those examined in Section 4.3.4.3. In addition, it is clarified that all of the examined domains were discretized with rectangular elements of unit aspect ratio so that the effects from the element shape would be minimized.

4.3.5.5. Results

The Evaluation Indices (EIs) for the examined applications are shown in Table 4.6 while selected plots concerning the optimal layouts and the corresponding convergence histories are shown in Fig.4.6.

In Table 4.6, the symbols $t = const$ and $t \neq const$ correspond to constant and variable thickness elements, respectively. The % difference is defined as the % relative difference with respect to the results obtained with the use of constant thickness elements.

Table 4.10: Evaluation Indices for the examined applications

		Stress interpolation scheme #1			Stress interpolation scheme #2			Stress interpolation scheme #3		
		EI_1	EI_2	EI_3	EI_1	EI_2	EI_3	EI_1	EI_2	EI_3
Deep cantilever	t=const	0,2568	0,9912	1,2926	0,2458	0,9900	0,9188	0,2330	0,9917	1,1984
	t≠const	0,2554	0,9898	0,9501	0,2445	0,9885	1,2616	0,2317	0,9865	1,6532
	% difference	-0,56%	-0,13%	-26,50%	-0,51%	-0,15%	37,31%	-0,58%	-0,53%	37,95%
Short cantilever	t=const	0,2399	0,9962	0,1920	0,2252	0,9985	0,6435	0,2155	0,9997	0,2988
	t≠const	0,2351	0,9860	0,5176	0,2218	0,9954	0,4290	0,2141	0,9936	0,4840
	% difference	-1,97%	-1,03%	169,68%	-1,52%	-0,31%	-33,33%	-0,64%	-0,60%	61,96%
MBB beam	t=const	0,1967	0,9997	0,1499	0,1806	0,9995	0,3194	0,1660	0,9990	0,1901
	t≠const	0,1876	0,9816	0,2775	0,1734	0,9799	0,2910	0,1609	0,9755	0,3654
	% difference	-4,63%	-1,81%	85,05%	-4,00%	-1,96%	-8,89%	-3,05%	-2,34%	92,20%
Michell structure (bridge)	t=const	0,2855	0,9930	0,2537	0,2633	0,9887	0,5086	0,2432	0,9838	1,0144
	t≠const	0,2760	0,9552	0,3348	0,2571	0,9523	0,4399	0,2400	0,9461	0,3514
	% difference	-3,32%	-3,80%	31,97%	-2,35%	-3,68%	-13,52%	-1,32%	-3,83%	-65,36%

From Table 4.6, it yields that, in all cases, the proposed procedure, implementing variable thickness elements, results in a structural weight reduction (EI_1) ranging from 0.56% to 4.63% with respect to the use of constant thickness elements. Furthermore, the corresponding optimal layouts are from 0.13% to 3.83% less fully stressed (EI_2), while the stress distributions over the active part are significantly different (EI_3).

For each one of the examined examples, there are six possible solutions resulting from the combination of the two optimization procedures used (Approach #3 and Approach #4) and the three different stress interpolation schemes implemented. Therefore, for each example, six layouts and six convergence histories with respect to the structural weight were obtained. In the current section, for reasons of laconism, only two representative layouts are presented per example (one for each optimization procedure and for the 'maximum' stress interpolation scheme). More particularly, representative optimal layouts derived with variable thickness elements are shown in the first column of Fig.4.6, while corresponding layouts derived with constant thickness elements are shown in the second column of the same figure. The plots of the convergence histories per example are illustrated in the third column of Fig.4.6. It is clarified that, due to symmetry along the mid-plane of the structures, only half of the structural thickness distributions are shown (from the mid-plane and towards the upper surface). Furthermore, for reasons of visual inspection, the material distributions corresponding to the variable and to the constant thickness elements were plotted as colored unfilled meshes (Fig.4.6, 1st column) and as filled columns (Fig.4.6, 2nd column), respectively. In addition, for each one of the convergence history plots, the illustrated weights were normalized with respect to the minimum value among the six optimal weights obtained for each example.

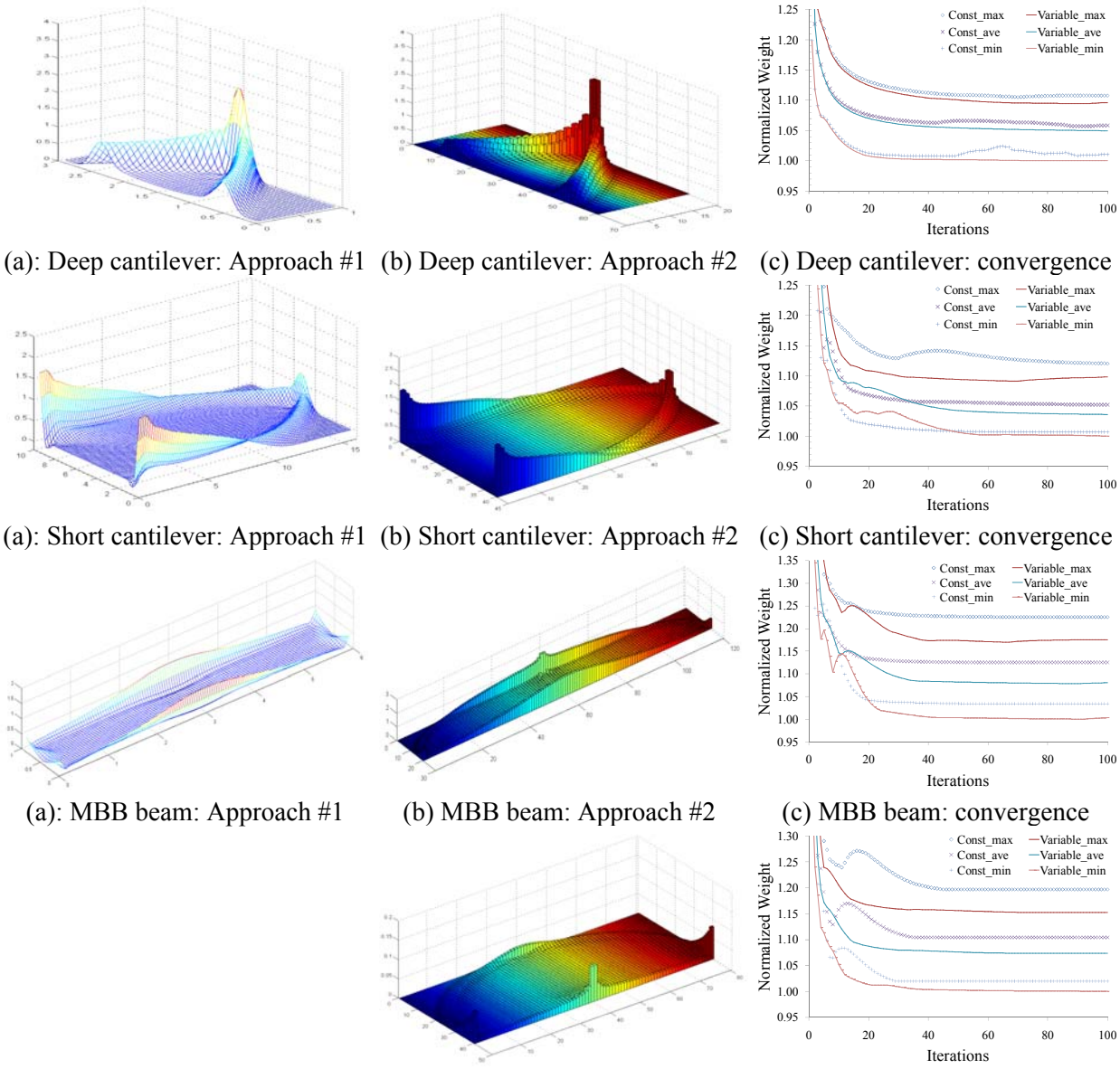

(a): Deep cantilever: Approach #1 (b) Deep cantilever: Approach #2 (c) Deep cantilever: convergence

(a): Short cantilever: Approach #1 (b) Short cantilever: Approach #2 (c) Short cantilever: convergence

(a): MBB beam: Approach #1 (b) MBB beam: Approach #2 (c) MBB beam: convergence

(a) Michell bridge: Approach #1 (b) Michell bridge: Approach #2 (c) Michell bridge: convergence

Figure 4.10: Optimal layouts and convergence histories for the investigated examples

The appropriate comparison between the plots in the first two columns of Fig.4.6 revealed several interesting details, among which the most interesting one was the fact that *non-skeletal* layouts were obtained. On the contrary, there was a pattern that always appeared, according to which the optimal layout could be divided into three regions. The first region concerned a thicker material distribution, easily located with visual inspection, forming a kind of boundary. The second region concerned the part of the domain *inside* the aforementioned boundary; this region had an almost constant thickness but *not equal* to the lower thickness bound. The third region concerned the part of the domain *outside* the aforementioned boundary; the thickness of this region was equal to the lower thickness bound. This means that, in all cases, a redundant part of the domain (third region) was clearly formed; this part can be removed without causing any problems to the structural stability. Furthermore, the aforementioned *inner* region provides a very good way for carrying the shear and it is due to this reason that reinforcing ribs are not required thus not formed. Another significant

observation concerns the continuity of the thickness distributions. When variable thickness elements were used, the thickness distributions were continuous thus significantly smoother (of higher degree of manufacturability) layouts were obtained.

With respect to the convergence, the corresponding history plots (Fig.4.6, 3rd column) revealed that, in almost all cases, the use of variable thickness elements resulted in a faster and smoother convergence (continuous lines in the plots) when compared to the converging behavior of constant thickness elements (denoted with markers only in the plots). Finally, among the applied stress interpolation schemes applied (Section 4.3.5.2.3), it was the consideration of the minimum stress value between the appropriately selected gauss points that gave the best results.

4.3.5.6. Discussion

It is well-known that the optimal layouts are usually dependent on the density of the domain discretization. The reason for this has a pure numerical analysis origin. In more details, load concentrations appear at the load application points. As a mesh becomes finer, the area, thus the stiffness, of the corresponding finite elements becomes lower and one simple way to equalize this reduction is to increase the element thickness. Therefore, as the number of elements increases so does the maximum structural thickness at the points where the external load is applied. Depending on the optimization procedure, the aforementioned sensitivity varies. In order to investigate its effect on the proposed procedure, a parametric investigation was carried out where the examined examples were optimized using different mesh densities (the case of the Deep cantilever is presented in Fig.4.7.

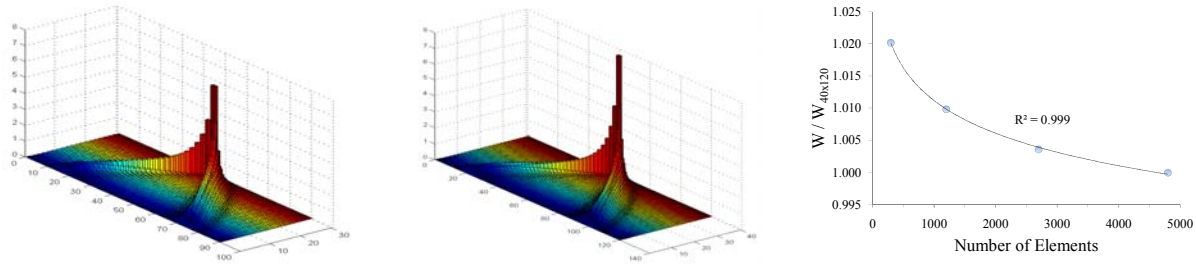

(a) (b) (c)

Figure 4.11: Optimized layout for the deep cantilever: (a) mesh 30x90, (b) mesh 40x120 and (c) normalized weight vs Number of Elements

More particularly, Fig.4.7a and Fig.4.7b illustrate the optimal layouts when a 30×90 and a 40×120 mesh is used, respectively. The corresponding result for a 20×60 mesh is illustrated in Fig.4.6a. From visual inspection of the aforementioned plots, it is obvious that the maximum element thickness significantly varies for these meshes. However, such a strong sensitivity does not appear with respect to the structural weight. In more details, it is possible first to normalize all structural weights with respect to the weight corresponding to the finest mesh used and then to plot the normalized values with respect to the number of elements. For the case of the deep cantilever and for the Approach #4, such a plot is illustrated in Fig.4.7c, according to which the difference between a very coarse mesh (10×30) and a mesh of fourfold density (40×120) is only 2%. Therefore, for an adequately fine mesh density, the proposed procedure for constant-thickness elements provides acceptable insensitivity in terms of structural weight. Similar results, not presented here for reasons of space limitations, were obtained for the other three examined examples and for both of the proposed approaches (Section 4.3.4.3).

As already mentioned, one well-intentioned question would be why develop in-house codes and use commercial software (Ansys) for verification purposes only and not use that software for optimizing the design space at hand. The answer to this question lies in the fact that Ansys allows the attribution of thickness to a theoretically unlimited number of nodes but provides the user with no control neither on the integration rule applied nor on the method used for the thickness interpolation within an element. Thus, instead of developing models in Ansys that could be used only for part of the investigation, the strategic decision of investing time and effort in developing versatile in-house codes with no such restrictions was made.

Another issue worth mentioning is the fact that four points do not necessarily lie on the same plane thus it is highly possible for variable-thickness elements to present element-wise warping distortions. In order to avoid such a situation, it is advisable to use an adequately large number of elements. Another go-around thought would be to degenerate the 4-node elements into 3-node ones since three nodes always define a plane. However, this is not advisable, because it is well-known that such a selection leads to significantly less accurate results.

With respect to the convergence of the proposed optimization procedures, it was decided to let the procedures be carried out for an adequate number of iterations so that the procedure robustness could be evaluated (early convergence may hide a later diverging behavior). As Fig.4.6(3rd column) shows, convergence was practically achieved after a few iterations and no diverging or oscillating behavior in later stages was observed.

The study of Table 4.6 revealed that the layouts obtained with Appoach #3 are more promising since they are of lower structural weight and less fully stressed, suggesting that there is still a margin for further improvement. Moreover, simple visual inspection of Fig.4.6 reveals that the Approach #1 results, inherently and without any further interpolation, in significantly smoother layouts thus enforces the manufacturability of the optimal layout.

4.3.5.7. Conclusions

The current investigation, based on the examination of 24 models in total, showed that the proposed optimization scheme regarding the redesign of the nodal thickness, thus regarding finite elements of variable thickness, contributes towards the determination of the optimal structural layout, providing encouraging enough results. Therefore, a further investigation of other thickness interpolation schemes seems to be a good investment.

4.4. Layout optimization of a stress-constrained plate

The layout optimization of continuum structures has been, and still is, one of the most challenging structural optimization problems, which a stress-constrained plate under out-of-plane loading belongs to. In such problems, it is of interest to investigate the influence that certain parameters, such as the initial geometry, the imposed boundary conditions and the externally applied loading have on the optimal layout. Towards this direction, four characteristic examples, retrieved from the literature, were investigated. The first example concerned a square plate, loaded with a single vertical nodal force at its middle and supported in two different ways (simple support and clamp). The second example concerned a cantilever plate under equal and unequal nodal loading at its free corners. The third example concerned a cantilever plate under uniform and triangular load distribution at its free end, while the forth example referred to a cantilever plate with opposite-directed equal and unequal nodal loads at its free corners. All of the examined examples were investigated for a variety of aspect ratios, while they were optimized using two conceptually similar optimizing methods, namely the Fully Stressed Design (FSD) and the Evolutionary Structural Optimization (ESO). The aforementioned investigation contributes in determining the directions that the optimal strain energy distribution followed in each case.

4.4.1. In general

Plates form the building blocks of larger structures and they can be used as reinforcements on other constructions as well, thus contributing to the reduction of the structural weight. It is obvious that the engineering value of the optimal layout of plates is of utmost importance and due to this reason the layout optimization problem of a plate under transverse loading has been treated extensively in the literature. A typical formulation of the aforementioned problem is to seek for the optimal thickness distribution of a given plan-form of the plate for which the plate volume attains a minimum, provided that the supports and the load limit are prescribed. Another very popular version of the same optimization problem is, for a given volume reduction, to solve for the maximum stiffness, or equivalently for the minimum compliance. A great many number of papers in the literature handle this problem.

Hopkins and Prager considered a simply supported circular plate and obtained the solution for the Tresca material (Hopkins and Prager, 1955), while Freiberger and Tekinalp obtained the solution for the Mises material and also derived the condition of analytical extremum, according to which the mean rate of energy dissipation per unit area of the middle surface is constant (Freiberger and Tekinalp, 1956). Drucker and Shield discussed general criteria of optimum design of plates (Drucker and Shield, 1957), while Mróz investigated the optimal design of solid annular plates, where it was shown that the criterion introduced by Freiberger and Tekinalp corresponds to a local minimum only for states represented by corners of the Tresca hexagon (Mróz, 1961). Megarefs dealt with the problem of optimizing axisymmetric plates (Megarefs, 1966), while Sheu and Prager handled the problem of optimizing annular sandwich plates assuming piecewise constant thickness (Sheu and Prager, 1969). Huang dealt with the problem of optimal design of an elastic circular plate under uniform pressure for maximum stiffness (Huang, 1968) and Mróz investigated the optimal design of plates and shells (Mróz, 1973). Olhoff studied the optimal design of vibrating rectangular plates (Olhoff, 1970) while Armand and Lodier derived an optimality criterion for the design of bending elements (simply supported and clamped elastic plates for concentrated and distributed loading conditions under a single displacement constraint - Armand and Lodier, 1978). Prasad and Haftka have described a general resizing procedure applicable to structures modeled by plate (bending) finite elements, based on the implementation of triangular and quadrilateral elements and combining the Sequence of Unconstrained Minimization Technique (SUMT) with an extended interior cubic penalty function (Prasad and Haftka, 1979). Cheng and Olhoff (Cheng and Olhoff, 1981) considered the problem of maximizing the integral stiffness of solid elastic plates described by thin plate theory. Their work was based on a tensorial formulation of the problem; they derived the governing equations by variational analysis and they developed an efficient and quite general numerical algorithm for locating stationary solutions for rectangular and axisymmetric annular plates with various boundary conditions. By the early 80's, it was well-understood that the optimum reinforcement of plates may include infinitely fine arrangements of ribs (Cheng and Olhoff, 1981). This gave a strong motivation for the implementation of microscopically anisotropic plates using homogenization or other 'smear-out' techniques. Bendsøe have investigated the optimum plate topology based on Kirchhoff's theory (Bendsøe, 1986), while Bendsøe and Kikuchi (Bendsøe and Kikuchi, 1988), Soto and Diáz (Soto and Diáz, 1993) and Lipton and Diáz have used the Mindlin-Reissner plate theory in combination with the homogenization theory (Lipton and Diáz, 1997). Tenek and Hagiwara worked on the shape and topology optimization of isotropic, single-layered orthotropic and multilayered anisotropic plates (Tenek and Hagiwara, 1993). Lipton studied multiple load problems and random load problems (Lipton, 1994), while Olhoff compared the plate model and a 3D model (Olhoff, 2000). For the stress constrained problem, Morris suggested the use of the stress-ratio redesign formula of the Fully Stressed Design (FSD) for optimizing structures under stress

constraints (Morris, 1982), while Xie and Steven (Xie and Steven, 1997) have introduced the Evolutionary Structural Optimization (ESO) method according to which inefficient material is gradually removed.

The optimal layout of a plate is not determined only by the optimization procedure followed. Therefore, it is of major interest to investigate the influence that certain parameters, such as the initial geometry, the imposed boundary conditions and the externally applied loading have on the optimal layout of plates under stress constraints, which are of primary importance in real-life engineering applications. Towards this direction, the optimal layouts of four characteristic examples are investigated thoroughly in this section. As optimizers, the (FSD) and the (ESO) techniques were used. The aforementioned investigation contributes in determining the directions that the optimal strain energy distribution follows in each case.

4.4.2. Theoretical background

A plate is defined as a three-dimensional body endowed with special geometric features, prominent among them being its thinness, that is one of the plate dimensions, called its thickness, is much smaller than the other two, and its flatness, that is the midsurface of the plate, which is the locus of the points that halve the thickness 'fibers' or 'filaments', is a plane. There are three types of plates, one of them being the bending plates. For such a plate, the virtual work of the internal forces, the stress resultants and the external forces can be expressed as:

$$\delta W = \delta W_{\text{int}} + \delta W_{ext} = 0 \tag{4.18}$$

where

$$-\delta W_{\text{int}} = \int_A \left(m_x \delta k_x + 2 m_{xy} \delta k_{xy} + m_y \delta k_y + q_x \delta \gamma_x + q_y \delta \gamma_y \right) dA \tag{4.19}$$

and

$$\delta W_{ext} = \int_A p\, \delta w\, dA + \left(\text{boundary terms}\right) \tag{4.20}$$

The internal work written in matrix notation and separated into bending and shear terms is:

$$-\delta W_{\text{int}} = \int_A \delta \left(\mathbf{L}\boldsymbol{\varphi} \right)^T \mathbf{D}_b \mathbf{L}\boldsymbol{\varphi} dA + \int_A \delta \left(\nabla w + \boldsymbol{\varphi} \right)^T \mathbf{D}_S \left(\nabla w + \boldsymbol{\varphi} \right) dA \tag{4.21}$$

where the unknowns are the displacement field $w(x, y)$ as well as the rotation vector $\boldsymbol{\varphi} = \begin{bmatrix} \varphi_x & \varphi_y \end{bmatrix}^T$. According to the Kirchhoff constraint for thin plates (negligible shear energy):

$$\boldsymbol{\gamma} = \nabla w + \boldsymbol{\varphi} = \mathbf{0} \tag{4.22}$$

the above equation reduces to

$$-\delta W_{\text{int}} = \int_A \delta \left(\mathbf{L} \nabla w \right)^T \mathbf{D}_b \mathbf{L} \nabla w dA \tag{4.23}$$

In Eq.4.23, only the displacement field is unknown. According to the trivial finite element technique for discretization using a set of discrete values and shape functions, it holds:

$$w = \mathbf{N}_w \mathbf{v} \text{ and } \boldsymbol{\varphi} = \mathbf{N}_\varphi \mathbf{v} \tag{4.24}$$

where $\mathbf{v}$ is the vector of nodal displacement and rotation values, while $\mathbf{N}_w$ and $\mathbf{N}_\varphi$ are the matrices of shape functions, arranged for the interpolation of the approximated displacement and rotations respectively. According to the Kirchhoff theory for thin plates, only the bending term remains in the virtual work expression:

$$-\delta W_{\text{int}} = \int_A \delta \mathbf{v}^T \left(\mathbf{L}\tilde{\mathbf{N}}_\varphi\right)^T \mathbf{D}_b \mathbf{L}\tilde{\mathbf{N}}_\varphi \mathbf{v} dA \tag{4.25}$$

where

$$\boldsymbol{\varphi} = \tilde{\mathbf{N}}_\varphi \mathbf{v} = -\nabla w = -\nabla \tilde{\mathbf{N}}_w \mathbf{v} \tag{4.26}$$

The stiffness matrix is then equal to:

$$\mathbf{k} = \mathbf{k}_b = \int_A \mathbf{B}_b^T \mathbf{D}_b \mathbf{B}_b dA \tag{4.27}$$

where

$$\mathbf{B}_b = \mathbf{L}\tilde{\mathbf{N}}_\varphi \tag{4.28}$$

In this way, the incompatible rectangular 12-degrees of freedom plate element, used in the present work, is formed. According to the thin plate theory, the plate bending rigidity is cubic with respect to the thickness:

$$\mathbf{D}_b = K \begin{bmatrix} 1 & \nu & 0 \\ \nu & 1 & 0 \\ 0 & 0 & 0.5(1-\nu) \end{bmatrix} \tag{4.29}$$

where

$$K = \frac{Et^3}{12\left(1-\nu^2\right)} \tag{4.30}$$

In the present paper, two optimization procedures were implemented, the former being the Fully Stressed Design (FSD) and the latter being the Evolutionary Structural Optimization (ESO) technique. These two methods aim at the same target; that is to end up with a layout of uniform stress field equal to the maximum allowable value.

The redesign equation of the (FSD) is derived from the Lagrange multipliers method (Morris, 1982), according to which the Lagrangian for a structure of weight W, under stress constraints g_i only and modeled with plate elements, is:

$$\mathcal{L}(\mathbf{t},\lambda) = W + \sum_{i=1}^{NEL} \lambda_i \, g_i \tag{4.31}$$

where $\mathbf{t}$ is the thickness vector of the plate elements. If the minimum weight W is sought, then the gradient of the Lagrangian (Eq.4.31) must be set equal to zero. After basic manipulation, and considering a fully stressed state for the elements with non-critical volume, the well-known stress-ratio recursive formula yields:

$$^{k}t_i = {}^{k-1}t_i \left(\frac{\sigma_i}{\sigma_{\max,i}} \right)^{(1/n)} \tag{4.32}$$

where n is a relaxation exponent for smoother convergence. In the present paper, it was considered $n = 2$. The redesign of the structure to be optimized with the (ESO) technique is based on the gradual removal of inefficient material. More particularly, at each iteration (ESO) removes a small fraction of the elements with the lowest von Misses stress. The elements to be removed satisfy the following inequality (Xie and Steven, 1999):

$$\sigma_{vonMises,e} \le RR \le \sigma_{vonMises,\max} \tag{4.33}$$

where $\sigma_{vonMises,e}$ is the Von Mises stress of an element, $\sigma_{vonMises,\max}$ is the maximum von Mises stress occurring in the structure at that iteration and RR is the Rejection Ratio that controls the element removal process and is controlled by:

$$RR = a_o + a_1 \times SS + a_2 \times SS + a_3 \times SS + \ldots \tag{4.34}$$

The integer SS is called the Steady State number that is incremented each time the application of Eq.(4.33) results in no element removals. The choice of when to cease removing elements depends on the designer's judgment concerning the evaluation of the optimality of the evolving design. In the present paper, it was taken $SS = 10$.

4.4.3. Investigated test cases

In total, four different cases were studied, namely:

Case #1: Analysis of a square plate (Fig.4.8, Fig.4.9), examined both as simply supported and as clamped. Due to symmetry, only one quarter of the plate was necessary to be modeled, introducing the appropriate boundary conditions of symmetry.

Case #2: Analysis of a cantilever plate under two corner loads (Fig.4.10, Fig.4.11), once the loads being equal and once having a ratio $(1/2)$ (unequal loads).

Case #3: Analysis of a cantilever plate under load distribution (Fig.4.12, Fig.4.13), once the distribution being uniform and once being triangular.

Case #4: Analysis of a cantilever plate under two opposite-directed nodal loads (Fig.4.14, Fig.4.15), once the loads being equal and once having a ratio $(1/2)$ (unequal loads).

In all cases, the Young's modulus was considered equal to $E = 70GPa$, the Poisson's ratio was taken equal to $v = 0.3$, while the density was considered to be $\rho = 2707kg/m^3$. The quantities F and q are of unit magnitude. For all the cases but the first, three ratios $(a/b) \in \{1,2,3\}$ were examined, each one of which represented a different aspect ratio of the plate.

4.4.4. Results

4.4.4.1. Case #1

The type of the boundary conditions applied on the entire perimeter of the plate determines the orientation of the well-formed grid or, equivalently, it determines the optimum path through which the applied load is transferred to the supports. Fig.4.8 shows the initial and other characteristic stages of the optimization procedure.

For a fully supported square plate, the optimal layout obtained using the FSD approach was a strongly grid-like structure (Fig.4.8a). It is well-known (Tenek and Hagiwara, 1993) that, for the specific case, material remains along the paths between the centre of the plate (application point of load) and the corner nodes, which are the most constrained boundary nodes. Furthermore, an elastic hinge, almost in the middle of the grid-like members of the optimal layout, appeared. The resulted layout (Fig.4.8a), although in accordance with the literature, presented an interesting detail: near the corners, the remaining material bifurcates, following directions normal to the plate sides, and never reaches the corner nodes.

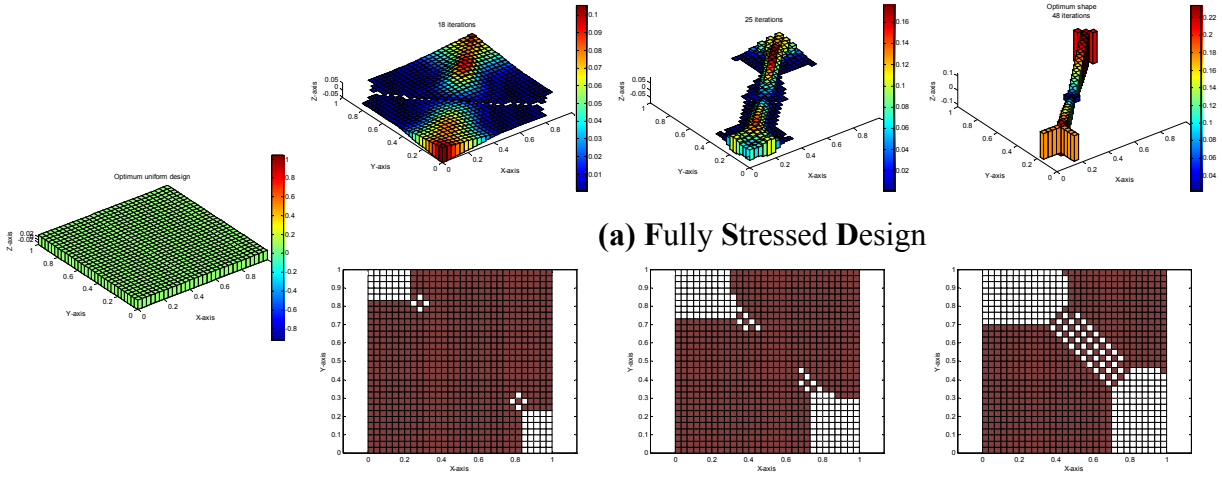

(a) Fully **S**tressed **D**esign

(b) Evolutionary **S**tructural **O**ptimization

(i) Problem definition (initial stage) (ii) Post-initial stage (iii) Intermediate stage (iv) Final stage

Figure 4.12: Optimal layout of a simply supported square plate

The optimal layout using the ESO procedure (Fig.4.8b) also tends to present the aforementioned elastic hinge (checkerboard area near the plate centre). Obviously, the fact that the thickness of the plate remains the same results in a different shape.

For a clamped square plate, where all the boundary nodes are equally constrained, the optimal layout obtained using the FSD approach was again a strongly grid-like structure (Fig.4.9a). According to the literature (Tenek and Hagiwara, 1993), material remains along the paths between the centre of the plate (application point of load) and the mid-sides of the plates, which are the shortest paths connecting the centre of the plate with the most constrained nodes. Furthermore, as in the previous case, an elastic hinge appeared. As shown in Fig.4.9a, again the resulted layout, although in accordance with the literature, presented an interesting detail: the remaining material is distributed along a curved rather than on a straight path. The optimal layout using the ESO procedure (Fig. 4.9b) also tends to present the aforementioned elastic hinge (checkerboard area near the plate centre), while it results in a layout where the number of the remaining elements is higher than it was with FSD optimizer (higher coefficient of coverage).

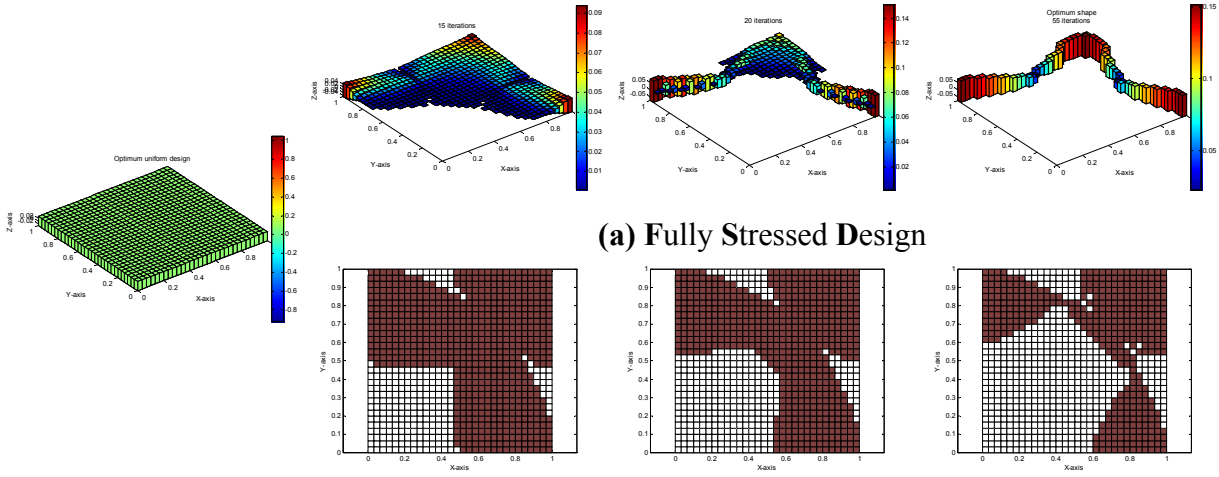

Figure 4.13: Optimal layout of a clamped square plate

For both types of boundary conditions, the optimal layout is a specific set of grid-like members servicing as reinforcements (stiffeners).

4.4.4.2. Case #2

In this case, the applied loads result in a pure bending of the plate. Fig.4.10 illustrates the problem domain as well as the optimal layouts, for three characteristic aspect ratios of the plate, obtained with the FSD (Fig.4.10a) and the ESO approach (Fig.4.10b). In both approaches, the optimal layout obtained is strongly determined by the distance between the applied nodal forces (plate width a - Fig.4.10a). For the FSD approach, it yields that if the plate is adequately wide (Fig. 4.10iia), then the optimal solution is a set of two parallel cantilevers being completely independent of each other. If the applied corner-loads are equal then the formed cantilevers are similar, otherwise the thickness distribution of the cantilever corresponding to the lower load is lower as well

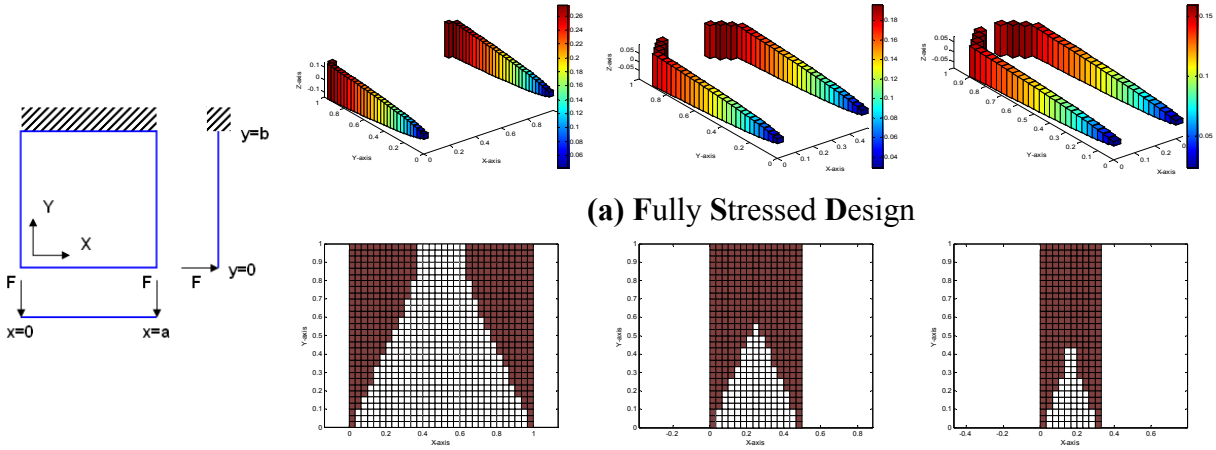

(a) Fully Stressed Design

(b) Evolutionary Structural Optimization

(i) Problem definition (ii) $(a/b)=(1/1)$ (iii) $(a/b)=(1/2)$ (iv) $(a/b)=(1/3)$

Figure 4.14: Optimal layout of a cantilever plate under two equal and same-directed corner loads

However, as the width of the plate becomes smaller, the aforementioned cantilevers are again well-formed but they tend to join each other. If the applied nodal forces are equal, then this tendency appears near the cantilever bases (Fig.4.10ii and Fig.4.10iii), otherwise it appears at some point along the cantilever corresponding to the higher nodal force while the part of the other cantilever between the joint and its base is eliminated (Fig.4.11ii and Fig.4.11iii). In all cases, the optimum layout is a fork-like structure.

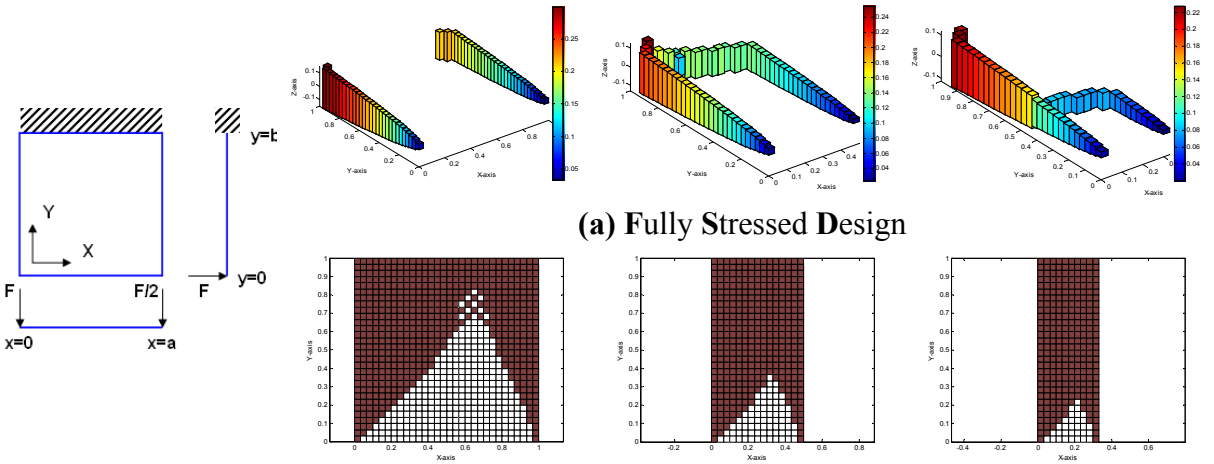

(a) Fully Stressed Design

(b) Evolutionary Structural Optimization

(i) Problem definition (ii) $(a/b)=(1/1)$ (iii) $(a/b)=(1/2)$ (iv) $(a/b)=(1/3)$

Figure 4.15: Optimal layout of a cantilever plate under two unequal corner loads

For the (ESO) approach and for an adequately wide plate, two independent cantilevers are also formed. Since they are of constant thickness and length, it is obvious that their width will be varying (Fig.4.10iib, Fig.4.11iib). As the plate width decreases, the aforementioned cantilevers are joined near their basis with the joint extending towards the free edge (Fig.4.10iiib, Fig.4.10ivb) and the remaining material tending to occupy the entire domain.

Ultimately, the optimal layout will be a continuum. If the applied loads are unequal (Fig.4.11), then the derived optimal layouts are asymmetric (Fig.4.11b) while the other comments mentioned above are still valid.

4.4.4.3. Case #3

In this case, a cantilever rectangle plate carries a load distributed along the free edge. Two different cases of load distribution were applied, the former being a uniform and the latter being a triangular distribution. It was observed that if all element thicknesses were left free to change, then a checkerboard-like free edge occurred, no two successive elements being eliminated however. In order to avoid such a pattern, which needs further investigation, it was decided to keep the elements at the free edge frozen, meaning that their thickness remained unchanged during the optimization procedure. Fig.4.13 illustrates the problem domain and the optimal layouts, for three characteristic aspect ratios of the plate, obtained with the FSD (Fig.4.12a) and the ESO approach (Fig.4.12b).

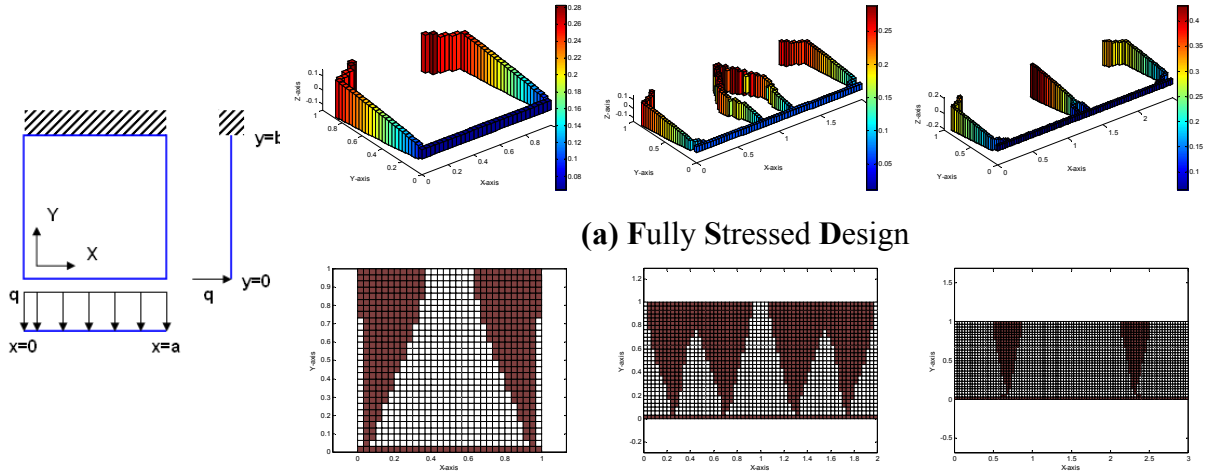

(a) Fully **S**tressed **D**esign

(b) Evolutionary **S**tructural **O**ptimization

(i) Problem definition (ii) $(a/b)=(1/1)$ (iii) $(a/b)=(2/1)$ (iii) $(a/b)=(3/1)$

Figure 4.16: Optimal layout of a cantilever plate under uniform load distribution

For the uniform distribution, the FSD approach resulted in a horseshoe-like structure. If the width of the initial plate is adequately small, then a simple horseshoe with two similar cantilevers at the ends of the plate is formed (Fig.4.13iia). As the plate becomes wider, the presence of reinforcing cantilevers is required. Experimentation with various aspect ratio values revealed that the reinforcing cantilevers may be introduced in a two fold manner; either as a bifurcated cantilever (Fig.4.13iiia) or as a single cantilever (Fig.4.13iva). Another point of interest is that, depending on the aspect ratio of the plate, it is possible to have thicker reinforcing cantilevers and thinner initial cantilevers or vice versa. The ESO approach resulted in the formation of reinforcing cantilevers, symmetric with respect to the mid-axis of the plate and varying in number and shape, as shown in Fig.4.13b.

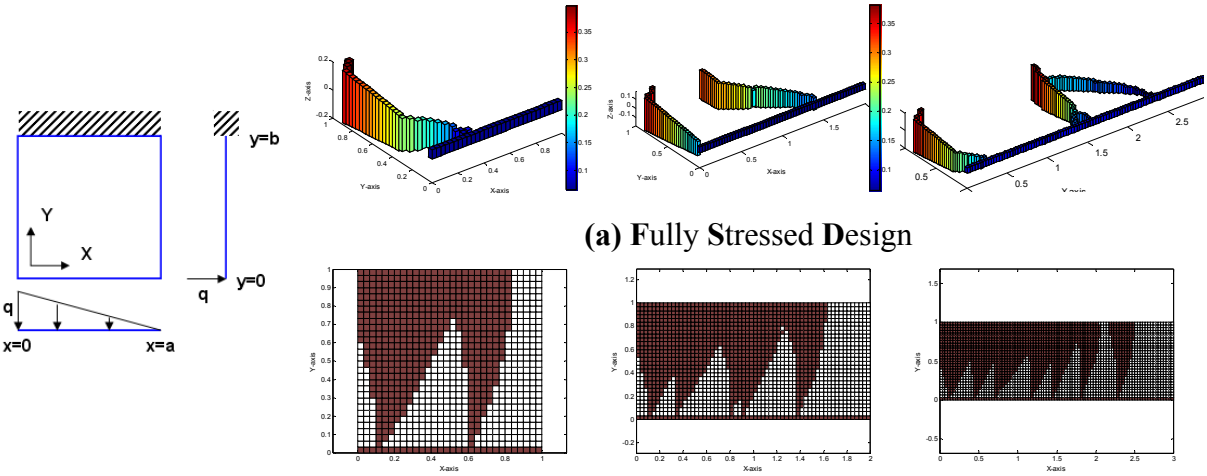

(a) Fully **S**tressed **D**esign

(b) Evolutionary **S**tructural **O**ptimization

(i) Problem definition (ii) $(a/b)=(1/1)$ (iii) $(a/b)=(2/1)$ (iii) $(a/b)=(3/1)$

Figure 4.17: Optimal layout of a cantilever plate under triangular load distribution

For a triangular load distribution, due to the fact that the load has a zero value at $x=a$, the aforementioned horseshoe optimal layout degenerates. For a square plate, the FSD approach resulted into an L-shape beam (Fig.4.13iia), while the ESO approach resulted in an asymmetric layout (Fig.4.13iib). If the plate is adequately wide, then cantilever-like reinforcements appear. It is noted that these reinforcements are of a curved shape and that the closer they are to the position $x=a$ the thinner they become.

4.4.4.4. Case #4

In this case, if the applied loads are equal, then they produce an out-of-plane (torsional) moment only, otherwise they produce an additional asymmetric bending of the plate.

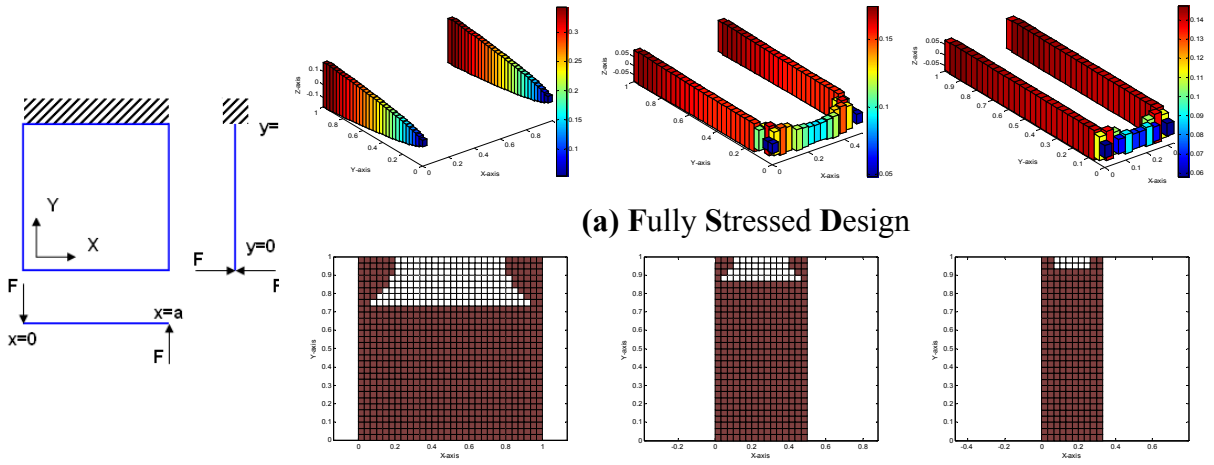

(a) Fully **S**tressed **D**esign

(b) Evolutionary **S**tructural **O**ptimization

(i) Problem definition (ii) $(a/b)=(1/1)$ (iii) $(a/b)=(1/2)$ (iv) $(a/b)=(1/3)$

Figure 4.18: Optimal layout of a cantilever plate under two opposite-directed equal nodal loads

Again, the distance between the applied nodal forces (plate width) determines the optimum layout (Fig.4.14). For the FSD approach, if the plate is adequately wide, then, as expected, the optimum solution is a couple of parallel cantilevers being completely independent of each other (Fig.4.14iia). Furthermore, if the applied loads are equal, then the formed cantilevers are equal as well, otherwise a horseshoe structure is formed. More precisely, two cantilevers of constant thickness are formed while a third beam of varying thickness joins their free ends.

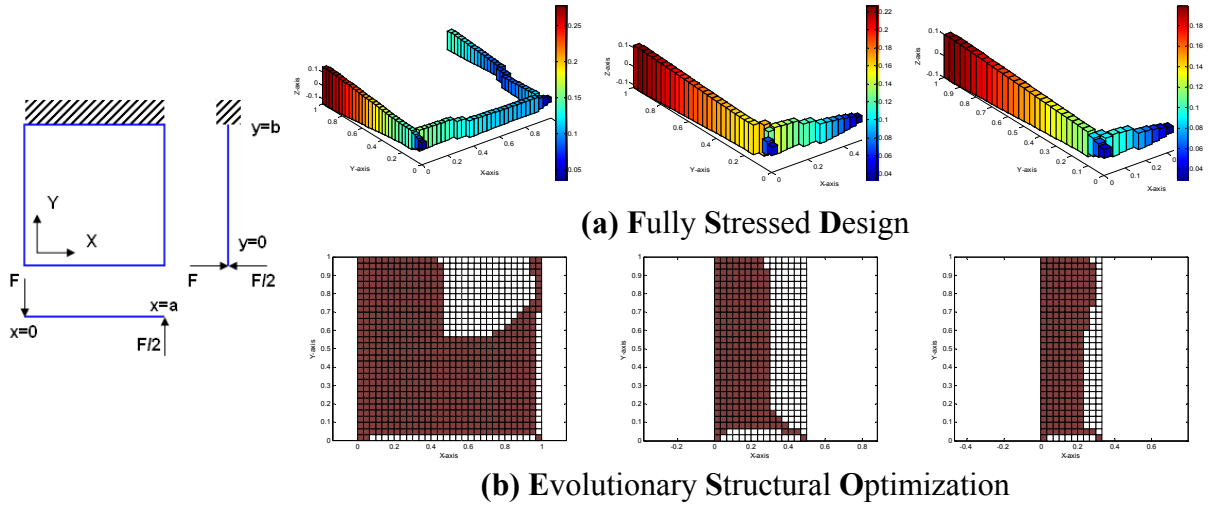

Figure 4.19: Optimal layout of a cantilever plate under two opposite-directed unequal nodal loads

However, if the applied loads are unequal, then the cantilever corresponding to the lower load is eliminated and the resulting structure is an L-shape beam (Fig.4.15a), both members of which are of varying thickness along their length. On the contrary, the optimal layout following the ESO approach tends to a continuum (Fig.4.14b, Fig.4.15b).

4.4.5. Conclusions

The parameters that define the optimal layout of plates obtained using the FSD and the ESO techniques were investigated in the current section. The investigation revealed that, although the two techniques are conceptually similar, they result in strongly different paths along which material is optimally distributed (directions of higher optimal strain energy distribution).

4.5. Layout optimization of 3D continuum under stress constraints

The weight minimization of 3D continuum structures under stress constraints is one of the most popular problems in structural optimization. Its popularity is due to the fact that for real-life applications, stress constraints are of most vital importance while simplified 2D approximations of the 3D-reality are not always representative. In the quest of the minimum weight, various techniques have been proposed, the Evolutionary Structural Optimization (ESO) being among the state-of-the-art structural optimization techniques. According to its developers, the variation of ESO that addresses the stress constraint problem has the ability to provide an optimized structure by removing elements of low von Mises equivalent stress. Furthermore, the introduction of a normalized expression for the energy density of the entire

structure during the optimization procedure is beneficial. The current section investigates the coupling of the aforementioned version of ESO with the aforementioned normalization concept for the optimization of 3D-continua, where the values of the normalized strain energy density were derived from the non-vanishing elements (active elements) only. The specific coupling is tested in four typical examples of 3D continua, namely the deep cantilever, the long cantilever, the MBB beam and a block under compression.

4.5.1. In general

The methods used for topology optimization of continuum structures may be categorized roughly in two large categories, the former including the so-called Material or Micro-approaches and the latter including the so-called Geometrical or Macro-approaches. According to the Material approaches, the aim is to find the structural topology that results in the optimum value of a given objective function provided that only a prescribed amount of structural material is used. The material density of each element is defined as a design variable whose domain is [0, 1], where 0 corresponds to void and 1 corresponds to solid material. The result of the optimization procedure is a set of solid materials and voids describing both the outer and the inner boundaries of the optimized structure. Further treatment of the jagged boundaries results in smooth shapes that can be manufactured. According to the Geometrical approaches, constitutive laws for usual solid, isotropic materials are implemented, while during the optimization procedure the finite element mesh must follow the changes of the design boundaries of the structure. Furthermore, the changes in the topology of the continuum under optimization are based on growing or degenerating material or by inserting holes. The present paper falls in the category of Geometrical approaches thus a brief reference is made to them.

Rossow and Taylor introduced the variable thickness sheet model for topology prediction, where the admissible domain for topology optimization is divided into a large number of smaller sub-areas, the thicknesses of which are defined as design variables and are then optimized subject to minimum compliance (Rossow and Taylor, 1973). Atrek and Kodali developed the shape-method which is similar to the method of Rossow and Taylor, the difference being the implementation of the technique for removing those sub-areas of the structure for which the thicknesses ends up being equal to the prescribed lower limit value (Atrek and Kodali, 1989). Mattheck, based on the aforementioned idea, stated the CAO (Computer Aided Optimization)/SKO (Soft Kill Option) Method, where the Young's Modulus is the controlling parameter and understressed elements are removed, thus resulting in a fully stressed design (Mattheck, 1992). Xie and Steven developed the Evolutionary Structural Optimization (ESO) method according to which inefficient material from an initial oversized design is gradually removed (Xie and Steven, 1993). Two variations of ESO are the Additive ESO (AESO) by Querin *et al*, where material is added to an initial undersize design (Querin *et al*, 2000), and the Bidirectional ESO (BESO) by Querin *et al*, where material may be removed from one location of the structure and then added to another location of the same structure (Querin *et al*, 1998). Liu *et al* at the Engineering Design Centre of the University of Cambridge developed a novel topology optimization method, called Metamorphic Development (MD), for both trusses and continuum structures and also for combined truss/continuum structures (Liu *et al*, 2000). Eschenauer *et al* introduced the bubble method which uses an iterative positioning and hierarchically structured shape optimization of new holes (bubbles). This method considers the boundaries of the structure to be variable thus shape optimization is carried out not only for the new bubbles but for the other variable structural boundaries as well (Eschenauer *et al*, 1994). Following this idea, Garreau *et al* proposed a similar yet modified approach, by using so-called topological gradients, which provides information on the possible advantage of the occurrence of a small hole in the body

(Garreau et al, 1999). Cea and Malanowski developed a topological optimization algorithm based on a fixed point method using the topological gradient (Cea and Malanowski, 1970). Sokolowski and Zochowski gave some mathematical justifications to the topological gradient in the case of free boundary conditions on the hole and generalized it to various cost functions (Sokolowski and Zochowski, 1997). Makris and Provatidis introduced a virtual strain energy density method for structural optimization (Makris and Provatidis, 2002), while Provatidis and Venetsanos investigated the influence of normalizing the virtual strain energy density on the shape optimization of 2D continua (Provatidis and Venetsanos, 2005).

The current section deals with a further investigation of the latter two aforementioned works in 3D continua. In more details, for stress constrained 3D continuum structures, it is proposed to gradually remove inefficient material until the stress constraints are marginally met. The material efficiency is quantified through ranking the elements with respect to their normalized strain energy density; the elements at the end of the ranked and sorted list are the most inefficient. The proposed procedure is coded in APDL, the script language of the commercial Finite Element Analysis software ANSYS, and tested in four typical cases, namely the Deep cantilever, the Short cantilever, the MBB beam and the Block under compression. Finally, the proposed method is compared to removing elements based on the von Mises stress only (Basic Removal Scheme).

4.5.2. Theoretical background

The weight minimization problem of a stressed constrained 3D continuum discretized in solid finite elements of the same density can be stated in terms of volume as follows:

$$minimize\ V = \sum_{j=1}^{NEL,act} V_j \tag{4.35}$$

$$subject\ to\ \frac{\max|\sigma_i|}{\sigma_{allow}} - 1 \le 0 \tag{4.36}$$

where V_j is the volume of the $j-th$ remaining finite element of the final design, σ_j is the von Mises equivalent stress of the $j-th$ remaining finite element of the final design, σ_{allow} is the allowable von Mises equivalent stress (stress constraint) and NEL,act is the total number of the remaining (active) finite elements of the final design.

It is clarified that, as Eq.4.36 suggests, the stress limit for both compression and tension has been considered to be the same. In order to find the optimum (final) design, three basic factors must be determined, the first being the material removal criterion (redesign scheme), the second being the convergence criterion and the third being the termination criterion of the iterative optimization procedure.

4.5.2.1. The material removal criterion

The redesign scheme is based on the gradual elimination of underutilized elements from the discretized design domain. The determination of the material utilization could be based on the strain energy of each element. However, if the elements are of different size, then the strain energy is not the best evaluation index for the material utilization. Instead, the more representative strain energy density u_j of each element must be used:

$$u_j = \int \boldsymbol{\sigma}^T d\boldsymbol{\varepsilon} \tag{4.37}$$

For the first iteration, where all the elements are considered, the mean strain energy density of the structure is:

$$\overline{u}_j = \left(\frac{1}{NEL} \right) \sum_{j=1}^{NEL} u_j \tag{4.38}$$

Diving Eq.4.37 by Eq.4.38, the *normalized* strain energy density for each element yields:

$$n_j = \left(u_j / \overline{u}_j \right) \tag{4.39}$$

The normalization takes place with respect to the mean strain energy density of the structure. In this way, it is possible to quantify the contribution of each element to the behavior of the entire structure. Evidently, elements with low contribution may be removed (passive elements) thus the structural weight decreases. As far as the number of elements eliminated each time is concerned, first the available finite elements are ranked with respect to their normalized strain energy density value and then either a constant *number* or a constant *percentage* of the elements is removed (Material Removal Step). Therefore, for the $k-th$ iteration and for the subscript j in Eqts.(4.37, 4.38, 4.39), it holds:

$$1 \le j \le NEL_{act,k-1} \tag{4.40}$$

At this point, it is strongly emphasized that in the following paragraphs the material removal is actual, meaning that the total number of elements decreases from one iteration to the next one. This approach is closer to the reality than other techniques where a very low value is attributed to some characteristic property of the passive elements as an attempt to make their contribution to the global stiffness matrix negligible.

4.5.2.2. The convergence criterion

For the convergence of the numerical procedure, it is possible to use either one of the following criteria:

$$\left(V_{k-1} - V_k \right) < tol \text{ or } \left(MRS_k \right) < MRS_{\min} \tag{4.41}$$

where V represents the remaining volume, MRS stands for the Material Removal Step, while k denotes the current iteration. The first inequality suggests that the iterative procedure be stopped when the change in volume between two consecutive iterations is less than a pre-selected tolerance, while the second inequality suggests that convergence is considered to have been achieved when the Material Removal Step gets a smaller value than a pre-selected minimum one. More details concerning the MRS are presented in the next paragraph.

4.5.2.3. The termination criterion

With respect to the termination criterion, it is only required to check whether the prescribed limit for the stress is exceeded:

$$\left(\max \left| \sigma_i \right| / \sigma_{allow} \right) > 1 \tag{4.42}$$

When this happens then the optimization procedure terminates and the design corresponding to the last-but-one iteration is assumed to be the optimized topology. However, this assumption is not completely true since there is still room for further improvement. In more details, if the design corresponding to the k-iteration violates the imposed stress constraint but the design corresponding to the $(k-1)$-iteration does not then the latter design is the best that can be obtained with the *initially defined* Material Removal Step. If this ratio changes, and more particularly if it is reduced with respect to the initial one, then, for the transition from the k-iteration to the next one, it is possible to obtain another feasible design with less weight. The optimization procedure may be continued, until a new stress violation occurs. At that point, it will be possible either to use a new reduced removal ratio or to stop. The aforementioned reducing technique may be applied up to a point where the removal ratio gets a value less than a pre-defined tolerance, as Eq.7 suggests. In the present paper, a constant removal ratio was used throughout the investigations. This selection was based on a practicing engineering point of view, according to which reducing gradually the removal ratio is an additional means to refine an already optimized design, while getting an optimized design is of primary importance. Finally, as in all iterative procedures, a pre-defined maximum number of iterations was also introduced as a termination criterion:

$$N_k > N_{\max} \tag{4.43}$$

where N_k represents the current number of iteration and $N_{\max}$ is the maximum allowable number of iterations

4.5.3. The proposed procedure

The proposed procedure consists of the following steps:

Step 1: Discretize the 3D-domain and define an initial value for the Material Removal Step (MRS)
Step 2: Estimate the Strain Energy Density (SED) of each element
Step 3: Estimate the Normalized Strain Energy Density (NSED) of the each element
Step 4: Remove (MRS) elements with the lowest values of NSED
Step 5: Estimate the (NSED) of the remaining elements (active elements)
Step 6: Check for convergence; if convergence is achieved then stop
Step 7: Check for stress violation; if stress violation occurs, then reduce the Material Removal Step (MRS)
Step 8: Return to Step 4

For the domain discretization, a good choice is to use 8-nodal brick while using the enhanced 20-nodal brick elements is a selection mainly aiming at handling the checkerboard problem that near optimum designs present. More details on this issue are referred in 'Discussion' (Section 4.5.6).

4.5.4. Investigated test cases

The evaluation of the proposed procedure was based on the examination of the four examples shown in Fig.4.16 and was distinguished in two phases. In Phase #1, the effect of the main controlling parameter of the proposed procedure, which is the Material Removal Step, was quantified and illustrated in charts showing both the remained material volume (primary y-axis) and the number of iterations required until convergence was achieved (secondary y-axis). In Phase #2, the comparison between the proposed procedure and

removing elements based on the von Mises stress only (Basic Removal Scheme) was appropriately quantified and illustrated in charts. At this point, it is clarified that three out of the four examined examples, namely the deep cantilever, the short cantilever and the MBB beam, are described in details in Section 4.3.4.3. However, since a 3D mesh is used in the current investigation and for the completeness of the text, all of the investigated test cases are shown in Fig.4.16 and quantified in Table 4.7.

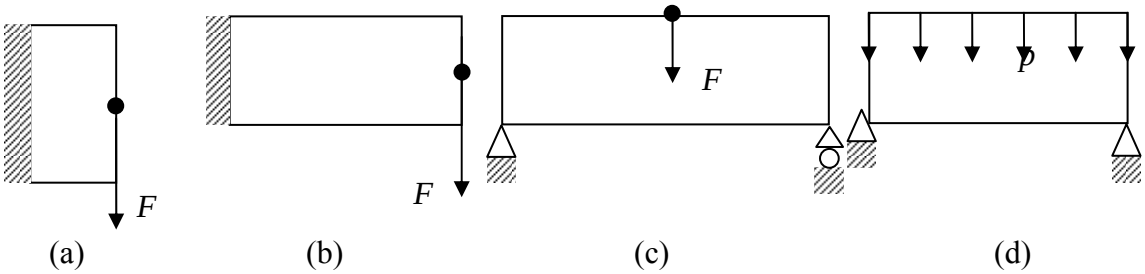

Figure 4.20: The examined examples (a) deep cantilever, (b) short cantilever, (c) MBB beam and (d) block under compression

All the necessary data for the corresponding problem descriptions are found in Table 4.7, where L_x denotes the horizontal dimension (width), L_y is the vertical dimension (height), E is the Modulus of elasticity, v is the Poisson's ratio, $dens$ is the material density, F is the applied load, σ_{allow} is the allowable stress, NN is the Number of Nodes and NEL is the Number of Elements of the developed models.

Table 4.11: Data for the examined examples

Examined example	L_x $[m]$	L_y $[m]$	E $[Pa]$	v	$dens$	Load F	Application point of F	σ_{allow} $[Pa]$	NN	NEL
Deep cantilever	3	1	1	0.3	1	12N	Right side middle	30	10571	9000
Long cantilever	16	10	1	0.3	1	12N	Right side middle	20	2079	1300
MBB beam	6	1	1	0.3	1	2N	Top side middle	20	4092	3000
Block under compression	1	0.4	1	0.3	1	0.1 N/mm^2	Top side distributed	16	3960	3200

The initial thickness of the structure is another parameter that affects the optimum design. For this effect to be revealed, three out of the four examined examples were analyzed for two different thickness values. More particularly, a thickness of $3mm$ and $4mm$ was used for the Deep cantilever, a thickness of $1mm$ and $2mm$ was used for the Long cantilever and a thickness of $3mm$ and $4mm$ was used for the MBB beam, respectively. It is clarified that, for the aforementioned selected problems, the thickness, that is the dimension vertical to the plane of the paper, may change without altering the other two dimensions. For the forth example, this is not the case since the plane where the pressure is applied to is rectangular, thus only one geometry was analyzed.

4.5.5. Results

The results for the first Phase of the evaluation are illustrated in Fig.4.17. The horizontal axis represents the values of MRS that were used, the left vertical axis represents the normalized value of the remained material at the optimum over the material at the initial state and the right axis represents the number of iterations required until convergence was achieved. It is reminded that there are two series of charts for the two different thickness values implemented, the Block under compression being the exception to this implementation.

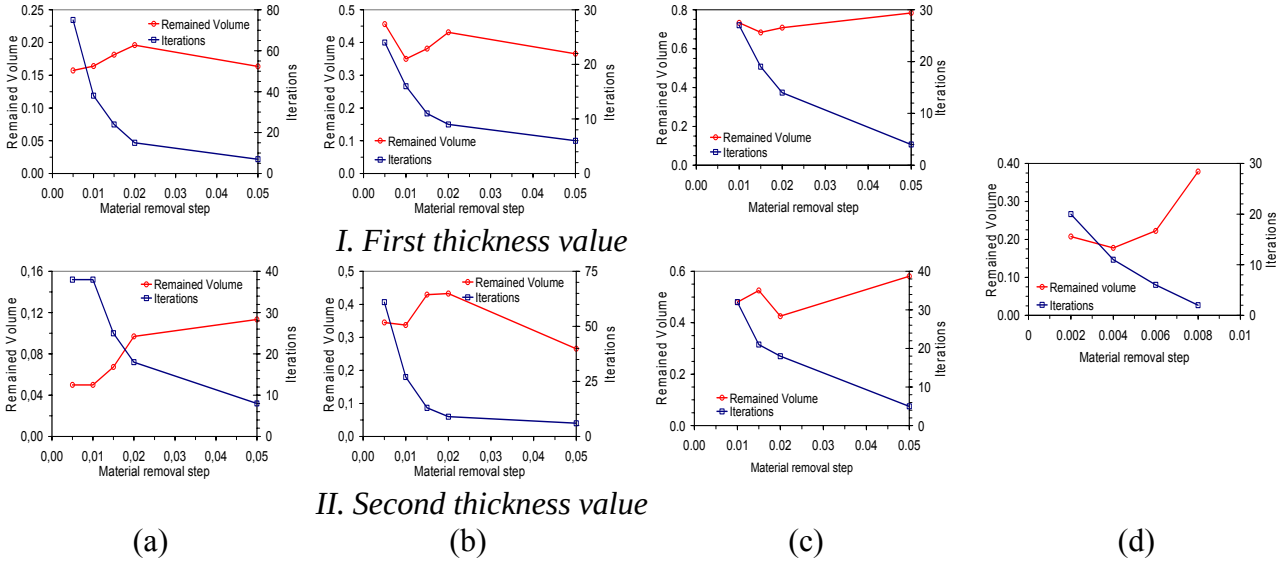

Figure 4.21: Performance of the proposed procedure for (a) the deep cantilever, (b) the short cantilever & (c) the MBB beam for two different thicknesses and (d) the Block under compression for one thickness

In all cases, the larger the Material Removal Step was, the smaller the number of iterations required until convergence became. This behavior was logical to appear because small MRS causes small changes to the structure thus more steps are required, until a large structural change occurs. Evidently, the maximum MRS value corresponded to the minimum number of iterations and vice versa. Furthermore, for the Block under compression and for the examined domain of MRS, the curve MRS vs Iterations was quite linear. However, in all of the other cases, a strong non-linear behavior appeared. On top of that, it was not possible to establish a pattern concerning the change of the normalized Remained Volume with respect to the Material Removal Step. In more details, there were cases, such as the Block under compression and the MBB beam for thickness of $3mm$, where a unimodal behavior was present, while there were cases, such as the Long cantilever, where a non-unimodal behavior was present. This strongly suggests that the presence of unimodality is case-dependent. The explanation for this lies in the fact that *different MRS* values result in *different layouts*, as Fig.4.18 illustrates.

In more details, the optimal material layouts in Fig.4.18 are not similar in the sense that one layout does not result from the other by simply reducing the thickness of the material distribution paths. They are completely different layouts suggesting that the Material Removal Step (MRS) value affects both the number of iterations required until convergence is achieved and the optimization route. Therefore, it is not surprising to find a lighter structural layout for a MRS value other than the smallest between the ones implemented. Another significant remark that results from Fig.4.18 is the fact the smaller the MRS value used the stronger the checkerboard problem is. A comment on this is referred in the section 'Discussion'.

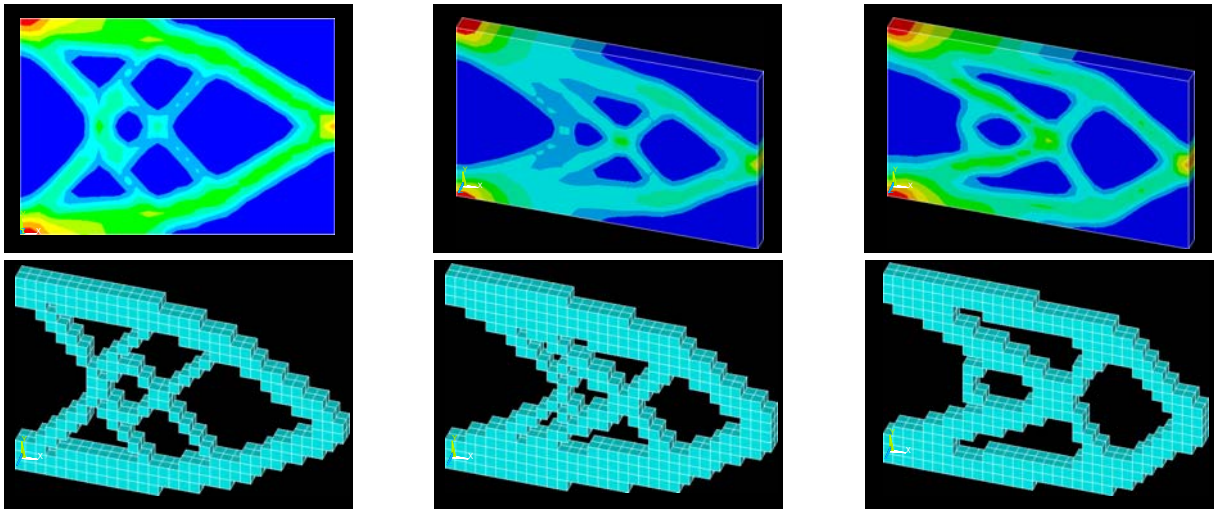

MRR = 0.005 MRR = 0.01 MRR = 0.015

Figure 4.22: Optimal designs for the Long Cantilever
(Top row: von Mises stress distribution, Bottom row: Remained material)

The results for the second Phase, that is the comparison between the proposed procedure and removing elements using only a von Mises-based ranking (Basic Removal Scheme - BRS), are illustrated in Fig.4.19. The comparison was based on three Performance Indices (PI's), the first being the remained volume normalized with respect to the initial volume, the second being the maximum appearing von Mises stress normalized to the allowable one and the third being the number of iterations required until convergence was achieved:

$$PI_1 = \left(\frac{NEL_{act}}{NEL_{ini}} \right) \qquad PI_2 = \left(\frac{\sigma_{vonMises,\max}}{\sigma_{vonMises,allow}} \right) \qquad PI_3 = N_{iter} \tag{4.44}$$

It is noted that the first index (PI_1) may be expressed in many ways, such as in terms of volumes as well as in terms of number of elements. In the present work, it was expressed as the ratio of the active elements (elements of the optimal design) over the number of elements of the initial design.

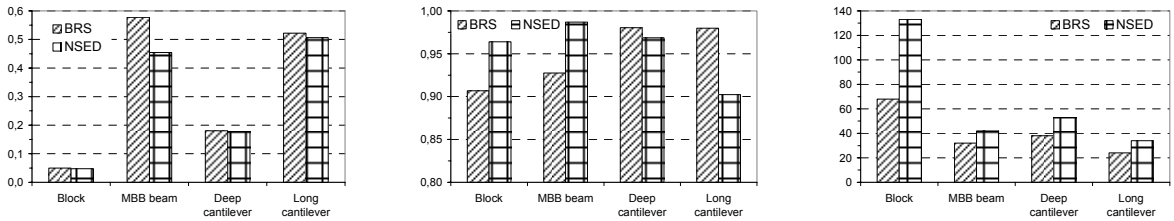

(a) (b) (c)

Figure 4.23: Comparison between the proposed procedure and the Basic Removal Scheme in terms of (a) the normalized remained volume, (b) the normalized maximum stress and (c) the number of iterations

The first PI, which is illustrated in Fig.4.19a, represents an absolute performance valuator. It is evident that, in all of the examined cases, the proposed procedure resulted in a lighter optimal structural layout, the difference being stronger for the MBB beam.

The second PI, which is illustrated in Fig.4.19b, represents the degree of material utilization. The higher the degree is the less redundant material exists in the layout. Obviously, the material is not fully utilized for the obtained optimal layouts; otherwise a unity normalized value would have been obtained. More particularly, both the examined procedures resulted in a larger than 90% material utilization, with the proposed procedure giving a 95% material utilization in three cases thus outperforming the Basic Removal Scheme. For the Long cantilever, the material utilization obtained with the proposed material is lower than that obtained with BRS. However, if this remark is evaluated in combination with Fig.4a, then it results that this optimal design is of least material utilization but, at the same time, is of least weight as well. This implies that a further *feasible* material removal is theoretically possible but a mesh of different element size is required.

The third PI, which is illustrated in Fig.4.19c, informs on how fast the optimal design may be obtained. It is evident that, in all cases, the proposed procedure required more iterations until convergence was achieved. This behavior was due to the inherent characteristic that the material removal takes place in a slower rate. In more details, for the proposed procedure, the criterion for removing material combines the rank, the elements have when sorted according to their normalized strain energy density, with an underutilized material threshold, dictated by the Material Removal Step. This combination determines the number of elements to be removed. However, if an element ranking according to the von Mises equivalent stress takes place, then, for the same underutilized material threshold, a different number of elements may, though not necessarily, be removed. In addition, the aforementioned number will be lower. This can be easily justified from the fact that two elements differing 1% in their von Mises stress differ 2% in their strain energy values; that is, their relative distance has doubled. In this way, the optimization route is strongly affected and leads to a different layout. The most characteristic example is that of the Block under compression. After the first iteration, the proposed procedure suggests that only 7% of the elements be removed while the Basic Removal Scheme suggests that 40% of the elements should be removed, instead. This tremendous difference definitely affects the further route of the optimization procedure, as very vividly illustrated in Fig.4.20b. More particularly, Figs.4.20-4.22 illustrate the initial, the mid and the final state of the four examples studied in the present paper.

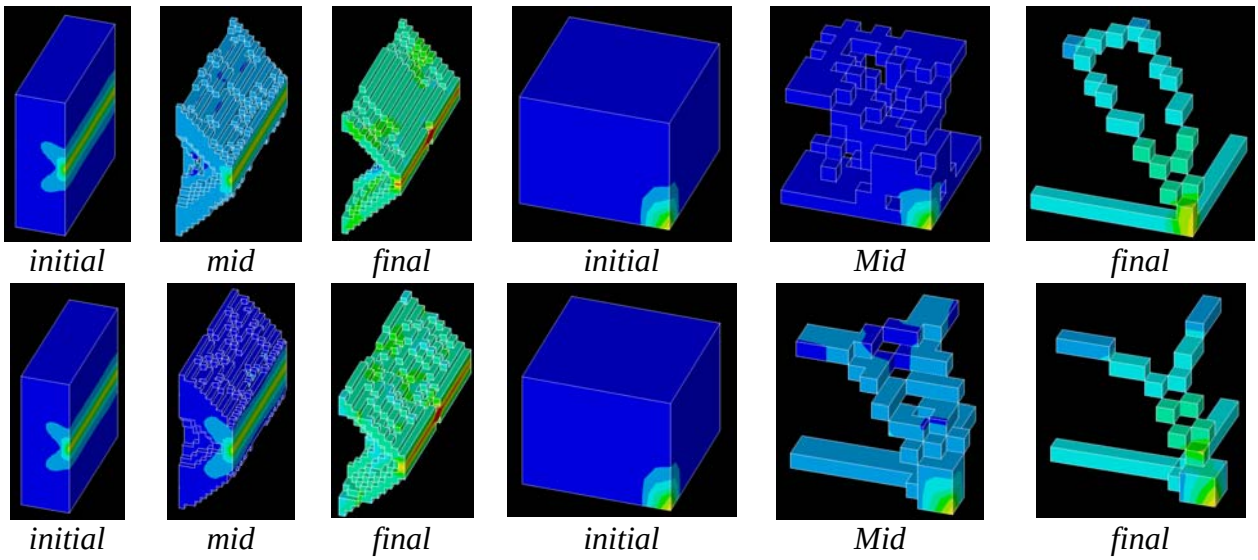

Figure 4.24: Optimized designs for (a) the Deep cantilever and (b) the Block under pressure (Top row: Proposed procedure, Bottom row: Basic Removal Scheme)

It is evident that Fig.4.20 refers to the Deep cantilever and to the Block under compression. For the latter and due to double symmetry, only one-forth of the full model is shown. The comparison between the final outputs reveals that the proposed procedure and the Basic Removal Scheme provide different optimal solutions. The difference is stronger between the final skeletal structures corresponding to the Block under compression.

Furthermore, Fig.4.21 refers to the Long cantilever. It is obvious that the proposed procedure results in a skeletal-like structure with larger void areas, which is of importance in practicing engineering applications.

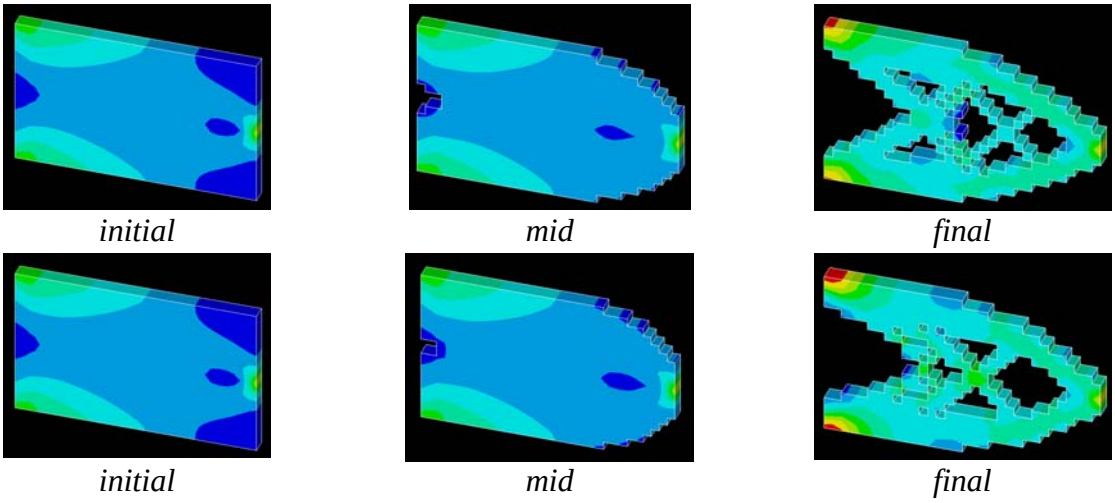

Figure 4.25: Optimized Long cantilever (Top row: Proposed procedure, Bottom row: Basic Removal Scheme)

Finally, Fig.4.22 refers to the MMB beam, for which, due to symmetry, only half the model is shown.

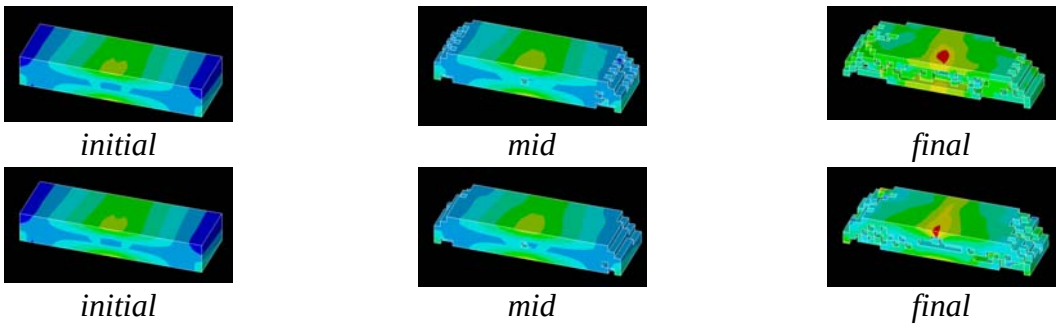

Figure 4.26: Optimized MBB beam (Top row: Proposed procedure, Bottom row: Basic Removal Scheme)

4.5.6. Discussion

The main idea of all weight minimization techniques is to eliminate underutilized elements. However, a question arises concerning the way the aforementioned underutilization may be quantified. The present paper suggests that the normalized strain energy density (NSED) of the elements of a fixed grid be used, the normalization being carried out for the active elements only. This approach has three advantages, the first being that a fixed grid may be applied, the second being that the underutilized elements are completely removed from the stiffness matrix of the structure and the third being that the NSED distribution makes

elements more distinct. More particularly, it is self-evident that the use of a fixed grid, that is of a grid that does not require re-meshing during the optimization procedure, is very convenient. Furthermore, in most optimization techniques, the element elimination is numerically simulated by attributing a very low value to some elemental characteristic. In this way, the problem is well-posed and the stiffness matrix has a non-zero determinant. However, in the present paper those elements recognized as passive are completely excluded from the formation of the stiffness matrix, whose rank thus becomes lower. In turn, this means that the finite element analysis is carried out in less time and due to this acceleration in the solution time during the optimization procedure it is possible to use thinner initial meshes thus increasing the reliability of the results. Finally, rating the elements with respect to their NSED value provides a tool that forbids the massive material elimination. As mentioned in Section 4.5.5, the use of the NSED for rating the elements makes them more distinct in the sense that, in a sorted list, the difference between two successive values is larger than if the rating was based on another quantity, such as the von Mises stress. Therefore, if a threshold is imposed such that all elements below it be removed, then fewer elements will be eliminated, exactly because they are distributed in a wider manner. Another issue worth commenting is that the removal of underutilized material results in skeletal-like structures characterized by strong checkerboard patterns, which are unfavorable since they suggest that a mechanism is present. There have been many techniques proposed as a solution to this problem, such as the suggestion by Diaz and Sigmund of a p-enhancement implementation (Diaz and Sigmund, 1995). Since the main goal of the present paper was to investigate the potentiality of using the strain energy density for structural optimization, the checkerboard problem was not examined.

4.5.7. Conclusions

In the current section, the weight minimization of 3D stress constrained continuum structures was investigated. According to the proposed procedure, underutilized material is gradually removed from the structure. For every iteration of the optimization procedure the elements are sorted with respect to their normalized strain energy density (NSED) and those elements with a NSED value lower than a threshold are eliminated. The normalization is based on the active elements, only while the threshold is initially defined and increases during the optimization procedure, which is stopped when the maximum appearing von Mises stress in the structure exceeds a pre-defined limit. Therefore, the last-but-one design corresponds to the optimal layout. The proposed procedure was tested on four well-known case studies retrieved from the literature and compared to removing elements using as a criterion the elemental von Mises stress. It was shown that the proposed procedure resulted in the lightest optimal designs in all cases. Furthermore, it was shown that the use of the NSED criterion affected the optimization route thus resulting in significantly different layouts of most importance for practicing engineering purposes. Therefore, it was shown that when the normalized strain energy density of the active elements is used as a criterion for removing inefficient material then significant improvements can be achieved both in terms of weight and layout.

4.6. A new OC for extended single stress constrained skeletal structures

4.6.1. Theoretical background

According to the description of the *extended* single stress constrained optimization problem of a 2D ground structure (truss), no matter how many stress constraints are imposed, only one is active at the optimum thus one structural member takes on a pre-determined maximum value. However, it is not known a priori which member is related to the aforementioned stress constraint. In this case, the optimization problem is stated as follows:

$$\text{minimize } W = \sum_{k=1}^{NEL} \left(\rho_k \, A_k \, L_k \right) \tag{4.45}$$

$$\text{such that } \left| \sigma \right| \le \sigma_{allow} \text{ and } A_{\min} \le A \tag{4.46}$$

where A is the cross-sectional area, L is the length, ρ is the material density, σ is the member stress, while the indices k and $allow$ denote the $k-$bar and the allowable value, respectively. The total number of bars (elements) in the structure is declared as NEL, while the absolute sign denotes that the same limiting stress value is used for both tension and compression. Furthermore, the cross-sectional area is also constrained with a lower bound so that the formation of a positive definite stiffness matrix is ensured. According to the method of Lagrange multipliers, the Lagrangian function $\mathfrak{L}$ corresponding to the aforementioned problem, if the constraint for the minimum cross-sectional area is dropped, may be stated as:

$$\mathfrak{L} = \sum_{i=1}^{NEL} \left(\rho_i \, A_i \, L_i \right) + \lambda_1 \left(\left| \sigma \right| - \sigma_{allow} \right) \tag{4.47}$$

where λ_1 is the Lagrange multiplier for the stress constraint. From Mechanics, it is known that a member stress, based on the concept of virtual work, may be expressed as:

$$\sigma_j = \sum_{i=1}^{NEL} \left(\frac{F_i^P F_i^Q}{A_i E_i} L_i \frac{E_j}{L_j} \right) \tag{4.48}$$

where, in addition to the symbols previously used, j denotes the structural member under consideration, on which two opposing unit loads are applied to each end and in the direction of the member. Furthermore, E stands for the modulus of elasticity, F^P is the member force due to the application of the actual loads, F^Q denotes the member force due to the application of the two opposing unit loads, while the index i is used to denote each one of the NEL structural elements. Introducing Eq.(4.47) in Eq.(4.48) yields:

$$\mathfrak{L} = \sum_{i=1}^{NEL} \left(\rho_i \, A_i \, L_i \right) + \lambda_1 \left(\left| \sum_{i=1}^{NEL} \left(\frac{F_i^P F_i^Q}{A_i E_i} L_i \frac{E_j}{L_j} \right) \right| - \sigma_{allow} \right) \tag{4.49}$$

The partial derivative of Eq.(4.49) with respect to the cross-sectional areas A_i equals to:

$$\nabla \mathfrak{L}_{A_i} = \rho_i \, L_i - \lambda_1 \left| \left(\frac{F_i^P F_i^Q}{A_i^2 E_i} L_i \frac{E_j}{L_j} \right) \right| + \lambda_1 \sum_l \left(\left(\left(\frac{\partial F_l^P}{\partial A_i} \right) F_l^Q + \left(\frac{\partial F_l^Q}{\partial A_i} \right) F_l \right) \left(\frac{L_l}{A_l E_l} \frac{E_j}{L_j} \right) \right) \tag{4.50}$$

However, the terms in the summation are identically zero because for determinate structures, the member forces are independent from the cross-sectional, while for indeterminate structures, Berke has shown that the derivative terms form a self-equilibrating internal load system (Berke and Khot, 1987). Consequently, Eq.(4.50) becomes:

$$\nabla \mathcal{L}_{A_i} = \rho_i L_i - \lambda_1 \left| \left(\frac{F_i^P F_i^Q}{A_i^2 E_i} L_i \frac{E_j}{L_j} \right) \right| \tag{4.51}$$

According to the method of Lagrange multipliers, it must hold:

$$\nabla \mathcal{L}_{A_i} = 0 \tag{4.52}$$

The combination of Eqs.(4.51, 4.52), after basic manipulations, yields:

$$1 = \lambda_1 \left| \left(\frac{F_i^P F_i^Q}{A_i A_i} \frac{1}{E_i} \frac{E_j}{L_j} \right) \right| \left(\frac{1}{\rho_i} \right) \tag{4.53}$$

The coefficient λ_1, being a single quantity, is constant, thus:

$$\lambda_1 = const \tag{4.54}$$

Under the assumption that all bars are made of the same material, it holds:

$$\rho_i = const \tag{4.55}$$

The combination of the last three equations, after basic manipulations, yields:

$$\underbrace{\left| \left(\frac{F_i^P F_i^Q}{A_i A_i} \frac{1}{E_i} \right) \right|}_{w_i} \underbrace{\left(\frac{E_j}{L_j} \right)}_{v_j} = const \tag{4.56}$$

The first term on the left-hand-side of Eq.(4.56) represents the virtual strain energy density w_i of the i-bar of the examined truss, while the second term, let it be v_j, expresses the modulus of elasticity of the $j-$bar, that is the bar under consideration, normalized with respect to its length. Therefore, according to Eq.(4.56), for the design that corresponds to minimum weight under the extended consideration of the single stress constraint, it is the product of w_i times v_j that is constant over the *active* part of the optimized structure. This means that the length of the structural member does play a significant role in determining the energy state at which the optimum design may be achieved. However, even though Eq.(4.56) describes the energy state at the optimum, it does not define a way to reach that state, thus allows for new procedures to be developed. Within this frame, a new redesign procedure is stated which is of a closed-form character for determinate trusses and of a recursive-form character for indeterminate trusses.

4.6.2. Proposed redesign procedure

Let a set of NEL bars with randomly selected cross-sectional areas be used as the initial design vector. A Finite Element Analysis (FEA) with the real loads provides both the member forces F_i^P and the displacement field, from which the structural member with the maximum

axial stress, let it be $N_{\sigma_{max}}$, may be located. Another (FEA) with a pair of virtual unit loads applied at the ends of $N_{\sigma_{max}}$ provides the member forces F_i^Q. With these member forces at hand, it is possible to detect the non-zero-force members $\left|F_i^P F_i^Q\right| > tol$, the tolerance tol being a small positive number, say 1E-06. For each one of these bars, it is possible to define the following quantity:

$$\mathfrak{w}_i = w_i v_j \tag{4.57}$$

The corresponding mean value $\overline{\mathfrak{w}}$ of all the $\mathfrak{w}_i$ values is equal to:

$$\overline{\mathfrak{w}} = \left(\frac{\sum_{i=1}^{N_{active}} \mathfrak{w}_i}{N_{active}} \right) \tag{4.58}$$

Substituting $\mathfrak{w}_i$ in Eq.(4.57) with the mean value $\overline{\mathfrak{w}}$ from Eq.(4.58) yields:

$$\overline{\mathfrak{w}} = \left(\frac{F_{i,new}^P F_{i,new}^Q}{A_{i,new} A_{i,new}} \frac{1}{E_i} \right) \left(\frac{E_j}{L_j} \right) \tag{4.59}$$

where $A_{i,new}$ is the re-designed cross-sectional area of the $i-$bar. Dividing Eq.(4.57) by Eq.(4.59) yields:

$$\frac{\mathfrak{w}_i}{\overline{\mathfrak{w}}} = \frac{\left(\frac{F_i^P F_i^Q}{A_i A_i} \frac{1}{E_i} \right) \left(\frac{E_j}{L_j} \right)}{\left(\frac{F_{i,new}^P F_{i,new}^Q}{A_{i,new} A_{i,new}} \frac{1}{E_i} \right) \left(\frac{E_j}{L_j} \right)} \tag{4.60}$$

However, for a statically determinate truss, the member forces F_i^P and F_i^Q are independent from the cross-sectional values:

$$\left(\frac{\partial F_i^P}{\partial A_i} \right) = \left(\frac{\partial F_i^Q}{\partial A_i} \right) = 0 \tag{4.61}$$

Consequently, Eq.(4.61) may be written, after basic manipulations, as:

$$\frac{\mathfrak{w}_i}{\overline{\mathfrak{w}}} = \left(\frac{A_{i,new}^2}{A_i^2} \right) \tag{4.62}$$

Solving the last equation with respect to the re-designed cross-sectional area of the $k-$bar yields:

$$A_{i,new} = A_i \sqrt{\left(\frac{\mathfrak{w}_i}{\overline{\mathfrak{w}}} \right)} \tag{4.63}$$

Although Eq.(4.63) was derived for a determinate truss, it may also be applied in cases of indeterminate trusses where the sensitivity of the axial forces to cross-sectional changes is low; that is, for cases where equilibrium governs rather than compatibility or for designs that are very near-optimum. For other indeterminate trusses, Eq.(4.63) must be used iteratively until convergence to a solution is achieved. In order to ensure that the redesigned cross-sections do not violate the imposed stress constraint, a scaling of the cross-sections is required.

4.6.3. Uniform scaling of the design vector

For a statically determinate structure, the *value* of the quantity $\mathfrak{w}_i$ depends on the virtual member force F_i^Q, the cross-sectional area A_i and the lengths L_i and L_j. Therefore, for a structure of constant topology, where the bar lengths are well defined and remain unchanged, and assuming that all bars are made of the same material, thus E_i and E_j are also well defined and constant, it holds:

$$\left(\frac{F_i^P F_i^Q}{A_i E_i} \right) L_i \left(\frac{E_j}{L_j} \right) = f\left(F_i^Q, A_i \right) \tag{4.64}$$

If the structural member, which the opposing virtual unit loads are applied to, is known, then the virtual member forces F_i^Q are also known and well defined and Eq.(4.64) reduces to the following form:

$$\left(\frac{F_i^P F_i^Q}{A_i E_i} \right) L_i \left(\frac{E_j}{L_j} \right) = f\left(A_i \right) \tag{4.65}$$

where the cross-sectional area A_i is the only unknown. Therefore, each addend in Eq.(4.48), which is numerically equal to the contribution of each bar to the stress of the $j-$bar, may be scaled simply by changing the cross-sectional area A_i. Furthermore, the combination of the aforementioned equations suggests that if the same scaling is applied to all of the cross-sectional areas A_i (uniform scaling) then the stress of the $j-$bar is also scaled by the same amount; that is:

$$\sigma_{scaled} = a_\sigma \ \sigma_{before\_scaling} \tag{4.66}$$

The constant a_σ denotes a scaling coefficient with respect to the maximum axial stress appearing in the examined structure. The subscripts of the other two terms adequately describe their physical interpretation. If the maximum allowable stress σ_{allow} is selected as σ_{scaled}, then the scaling coefficient a_σ equals to the ratio of the allowable to the appearing axial stress (for convenience, the subscript *before_scaling* is dropped):

$$a_\sigma = \left(\frac{\sigma_{allow}}{\sigma} \right) \tag{4.67}$$

The combination of Eqs.(4.48, 4.66) yields:

$$\sigma_{allow} = a_\sigma \left(\sum_{i=1}^{NEL} \left(\frac{F_i^P F_i^Q}{A_i E_i} L_i \frac{E_j}{L_j} \right) \right) \tag{4.68}$$

Since the scaling coefficient is constant, Eq.(4.68) may be written as:

$$\sigma_{allow} = \sum_{i=1}^{NEL} \left(\frac{F_i^P F_i^Q}{\left(\frac{A_i}{a_\sigma} \right) E_i} L_i \frac{E_j}{L_j} \right) \tag{4.69}$$

The comparison of Eq.(4.69) with Eq.(4.48) provides the following re-design formula:

$$A_{i,new} = \left(\frac{A_{i,old}}{a_\sigma} \right) \tag{4.70}$$

where the indices *new* and *old* denote the new and the old value of the cross-sectional area of the $i-$bar, respectively. Therefore, it is possible to uniformly scale the redesigned cross-sections in Eq.(4.63) of all active bars simply dividing by the scaling coefficient a_σ. The aforementioned analysis is based on the fact that a pair of opposite virtual unit loads is applied to the examined structural member, which was termed as the $j-$bar. It is essential that this bar is appropriately selected. The easiest thing to do is select this bar randomly. However, in an optimization procedure the initial design vector may decisively affect the optimization route thus local optima may be found. In order to maximize the probability of locating the global optimum, it is suggested that the optimization procedure be initiated from a design for which each structural member has unit stiffness. More details on this selection are presented in Section 5.2.4.

4.6.4. Discussion

Based on the above analysis, a theoretical solution to the problem of the extended single stress constrained optimization problem of a 2D ground structure (truss) has been stated. In this statement, there are certain issues that require investigation, such as the selection of the initial design vector and the way the structural members may be characterized as 'active' or 'passive'. These issues are extensively examined in the next Chapter, where the problem of the extended single displacement constraint problem is analyzed. The extended single stress constraint problem and the extended single displacement constraint problem may be dealt in the same way from a point on, this point being the formulation of the redesign equation. Therefore, for the extended single stress constraint problem, it is suggested that the iterative optimization procedure presented in the next Chapter be used as well, provided that the appropriate modifications are made (e.g. instead of a virtual unit load, a pair of opposing virtual unit loads is applied).

4.7. Recapitulation

In the present chapter, the stress constraint problem was investigated. More particularly, the capabilities of the Fully Stressed Design (FSD) in layout optimization were examined first of 2D skeletal structures and then on 2D continua. In both approaches, the redesign was based on changing either the cross-section of the skeletal structural members or the thickness of the continuum. In the sequel, the concept of using finite elements of variable thickness for the stress constrained layout optimization of 2D continua was explored. To this end, the element thickness was interpolated within each element in an isoparametric way. Next, the optimization of 2D plates was investigated, where the (FSD) was examined along with the application of the Evolutionary Structural Optimization (ESO) approach. Last, the optimization of 3D continua was investigated, where material elimination was achieved through the element contribution to carrying the externally applied loads. Finally, a variation of the stress constraint problem, here termed as the extended single stress constraint problem, was analyzed. The result of this analysis was the formulation of a new optimality criterion which is free of any assumptions concerning the determinacy of the optimized structure and seeks for a design where *one* structural member takes on the critical stress value, without necessarily preventing the other structural members from obtaining the imposed upper stress bound. In this way, the aforementioned OC is significantly different in concept from the (FSD) approach.

References

Armand, J.L., Lodier, B. (1978), "Optimal design of bending elements", Int. J. Num. Meth. Engng., Vol. 13, pp.373-384.

Atrek, E., Kodali, R. (1989), :Optimum design of continuum structures, with SHAPE:, In: Prasad B.: *CAD/CAM Robotics and Factories of the Future*, Vol. 2, pp.11–15, Proc of 3rd Int. Conf CARS and FOF-'88, Berlin, Springer.

Belegundu, A.D., Chandrupatla, T.R. (1999), *Optimization concepts and applications in engineering*, Prentice Hall.

Bendsøe, M.P. (1986), Generalized plate models and optimal design, in J.L.Ericksen, D. Kinderlehrer, R.V. Kohn & J.L. Lions (eds), *Homogenization and Effective Moduli of Materials and Media*, Springer-Verlag, Berlin;New York, pp.1-26.

Bendsøe, M.P., Kikuchi, N. (1988), "Generating optimal topologies in structural design using a homogenization method", Comp. Meth. App. Mechs. Engng, Vol. 71(2), pp.197-224.

Bendsøe, M.P., Sigmund O. (2003), *Topology Optimization, Theory, Methods and Applications*, Springer-Verlag.

Bendsøe, M.P. Optimization of Structural Topology, Shape, and Material. Berlin: Springer-Verlag, 1995.

Berke L, Khot N.S., (1987), "Structural optimization using optimality criteria", in: Computer Aided Optimal Design: Structural and Mechanical Systems, edited by C.A. Mota Soares, NATO, ASI series, F27B.

Cea, J., Malanowski, K. (1970), "An example of a max-min problem in partial differential equations", SIAM J. Control, Vol. 8, pp.305–316.

Cheng, K.T., Olhoff, N. (1981), "An investigation concerning optimal design of solids elastic plates", Int. J. Solids Structures, Vol.17, pp.305-323.

Diaz, A., Sigmund, 0. (1995), "Checkerboard Patterns in Layout Optimization", Struct Optim, Vol.10, pp.40-45.

Drucker, D.C., Shield, R.T. (1957), "Bounds on minimum-weight design", Q. appl. Math., Vol.5, pp.269-281.

Duysinx P and Bendsøe M P. Topology optimization of continuum structures with local stress constraints. Int. J. Numer. Meth. Engng., 1998, 43:1456-1478.

Eschenauer, H.A., Kobelev, H.A., Schumacher A., (1994), "Bubble method for topology and shape optimization of structures", Struct Optimization, vol. 8, pp.142-51.

Eschenauer, H.A., Kobelev, V.V., Schumacher, A. (1994), "Bubble method for topology and shape optimization of structures", Struct. Multidisc. Optim., Vol. 8, pp.42–51.

Felippa, C.A. (2001), *Introduction to Finite Element Methods*, University of Colorado, Boulder.

Freiberger, W., Tekinalp, B. (1956), "Minimum-weight design of circular plates", J. Mech. Phys. Solids, Vol.4, pp.294-299.

Gallagher RH. Fully Stressed Design, In: R. H. Gallagher & O. C. Zienkiewicz (eds.), Optimum Structural Design: Theory and Applications. John Wiley & Sons:1973.

Garreau, S., Masmoudi, M., Guillaume, P. (1999), "The topological sensitivity for linear isotropic elasticity", *ECCM'99*, Germany.

Giannakoglou, K., Tsahalis, D., Periaux, J., Papailiou, K. and Fogarty, T. C., (2002), "Evolutionary Methods for Design, Optimisation and Control", CIMNE, Barcelona.

Haftka R T, Gurdal Z and Kamat M. Elements of Structural Optimization. Kluwer: 1990.

Hassani B and Hinton E. A review of homogenization and topology optimization III-topology optimization using optimality criteria. Comp. Struct., 1998, 69:739-756.

Hopkins, H.G, Prager, W. (1955), "Limits of economy of materials in plates", J. appl. Mech., Vol.22, pp.372-374.

Huang, N.C. (1968), "Optimal design of elastic structures for maximum stiffness", Int. J. Solids Structures, Vol.4, pp.689-700.

Kirsch U. Optimal Topologies of Structures. Appl Mech Rev, 1989, 42: 238.

Lipton, R. (1994), "Optimal design and relaxation for reinforced plates subject to random transverse loads", J. Prob. Engng. Mech., Vol. 9, pp.167-177.

Lipton, R., Diáz, A.R. (1997), "Reinforced Mindlin plates with extremal stiffness", Int. J. Solids Structures, Vol. 24(28), 3691-3704.

Liu, J.S., Parks, G.T., Clarkson, P.J. (2000), "Metamorphic development: A new topology optimization method for continuum structures", Struct. Multidisc. Optim., Vol. 20, pp.288–300.

Makris, P., Provatidis, C. (2002), "Weight minimisation of displacement-constrained truss structures using a strain energy criterion", Computer Methods Appl. Mech. Engrg., vol. 191, pp. 2159-2177.

Mattheck, C. (1992), *Design in Nature*, Freiburg.

Megarefs, G.J. (1966), "Method of minimal design of axisymmetric plates", J. Engng Mech. Div. Am. Soc. Civ. Engrs, Vol.92, No. EM6, pp.79-99.

Mlejnek, H.P., Schirrmacher R., (1993), "An engineer's approach to optimal material distribution and shape finding", Computer Methods Appl. Mech. Engrg., vol. 106, pp. 1-26.

Morris, A.J. (1982), Foundations of Structural Optimization: A Unified Approach, John Wiley & Sons.

Mróz, Z. (1961), "On a problem of minimum-weight design", Q. appl. Math., Vol.19, pp.127-135.

Mróz, Z. (1973), "Multi-parameter optimal design of plates and shells", J. Struct. Mech, Vol.1, pp.371-392.

Olhoff, N. (1970), "Optimal design of vibrating plates", Int. J. Solids Structures, Vol.6, pp.139-156.

Olhoff, N. (2000), Comparative study of optimizing the topology of plate-like structures via plate theory and 3-D elasticity, in G.I.N. Rozvany & N. Olhoff (eds), *Topology Optimization of Structures and Composite Continua*, Kluwer Academic Publishers, Dordrecht, pp.37-48.

Patnaik SN, Guptill JD and Berke L. Merits and limitations of optimality criteria method for structural optimization, Int. J. Numer. Meth. Engng, 1995, 38: 3087-3120.

Pham D T and Karaboga D. Intelligent Optimisation Techniques: Genetic Algorithms, Tabu Search, Similated Annealing and Neural Netwroks. Springer: 2000.

Prasad, B., Haftka, R.T. (1979), "Optimal structural design with plate finite elements", J. Struct. Div., Vol. 105, pp. 2367-2382.

Provatidis. C.G., Venetsanos, D.T. (2005), "The Influence Of Normalizing The Virtual Strain Energy Density On The Shape Optimization Of 2D Continua", 1st IC-EpsMsO, Athens, 6-9 July, 2005.

Qing L and Steven G P and Xie Y M. Evolutionary structural optimization for stress minimization problems by discrete thickness design. Comp. Struct., 2000, 78(6): 769-780.

Querin, O.M, Steven, G.P., Xie, Y.M. (1998), "Evolutionary structural optimization – ESO: Using a bidirectional algorithm", J. Eng. Comput. Vol. 15, pp., 1031–1048.

Querin, O.M, Steven, G.P., Xie, Y.M. (2000), "Evolutionary structural optimisation using an additive algorithm", Finite Elements in Analysis and Design, Vol.34, pp.291-308.

Rossow, H.P., Taylor, J.E. (1973), "A finite element method for the optimal design of variable thickness sheets", AIAA J, Vol.11, pp.1566–1569.

Rozvany GIN, Bendsoe M P and Kirsch U. Layout Optimization of Structures. Appl Mech Rev, 1995, 48: 41-119.

Rozvany GIN. Aims, scope, methods, history and unified terminology of computer-aided topology optimization in structural mechanics. Struct. Multidisc Optim., 2001, 21:90-108.

Rozvany GIN. Stress ratio and compliance based methods in topology optimization – a critical review. Struct. Multidisc. Optim., 2001, 21:109-119.

Rozvany, G.I.N., (1997), *Topology optimization in structural mechanics*, CISM, Springer-Verlag.

Rozvany, G.I.N, (2001), "Aims, scope, methods, history and unified terminology of computer-aided topology optimization in structural mechanics", Struct. Multidisc Optim., vol. 21, pp. 90-108.

Schmidt L A. Fully Stressed Design of elastic redundant trusses under alternative loading systems. Australian Journal of Applied Science, 1958, (9):337-348.

Sheu, C.Y., Prager, W. (1969), "Optimal plastic design of circular and annular sandwich plates with piecewise constant cross section", J. Mech., Phys. Solids., Vol.17, pp.11-16.

Sokolowski, J., Zochowski, A. (1997), *On topological derivative in shape optimization*, RR No 3170, INRIA Lorraine, Nancy, France.

Soto, C.A., Diáz, A.R. (1993), "On modeling of ribbed plates for shape optimization", Struct. Opt., Vol. 6, pp.175-188.

Suzuki, K., Kikuchi, N., (1991), "A Homogenization Method for Shape and Topology Optimization", Computer Methods Appl. Mech. Engrg., vol. 93, pp. 291-318.

Tenek, L.H., Hagiwara, I. (1993), "Optimization of material distribution within isotropic and anisotropic plates using homogenization", Comp. Meth. App. Mechs. Engng, Vol. 109(1-2), pp.155-167.

Vanderplaats G N. Numerical Optimization Techniques for Engineering Design. McGraw-Hill: 1984.

Xie, Y.M., Steven, G.P. (1997), *Evolutionary Structural Optimization*, Springer-Verlag.

Xie,Y.M., Steven, G.P. (1993), "A simple evolutionary procedure for structural optimization", Comp Struct,Vol.49, pp.885–896.

Contributed papers

[1] Provatidis, C.G. and **Venetsanos, D.T.**, "Performance of the FSD in shape and topology optimization of two-dimensional structures using continuous and truss-like models", In: C. Cinquini, M. Rovati, P. Venini and R. Nascimbene (eds.), Proceedings Fifth World Congress of Structural and Multidisciplinary Optimization, May 19-23, 2003, Lido di Jesolo, Italy, pp. 385-386, Schönenfeld & Ziegler (ISBN 88-88412-18-2).

[2] **Venetsanos D.T.** and Provatidis C.G., "Fully stressed 2D continua formed by applying the stress-ratio technique to finite elements of variable thickness", *1st IC-EpsMsO, 6-9 July 2005, Athens, Greece*.

[3] Provatidis C.G., **Venetsanos D.T.**, Kesimoglou N.C., "Layout Optimization Of A Stress-Constrained Plate Under Out-Of-Plane Loading", *2nd International Conference "From Scientific Computing to Computational Engineering", Athens, 5-8 July, 2006.*

[4] Provatidis C.G., **Venetsanos D.T.**, Champilos S.D. "Weight Minimization Of 3D Continuum Structures Under Stress Constraints", *2nd International Conference "From Scientific Computing to Computational Engineering", Athens, 5-8 July, 2006.*

[5] **Venetsanos D.**, Magoula E. and Provatidis C. "Layout Optimization of Stressed Constrained 2D Continua Using Finite Elements of Variable Thickness", *6th International Congress on Computational Mechanics (GRACM), Thessaloniki, 19-21 June 2008.*

Appendix 4A: Stiffness matrices for the Basic Continuum Unit (BCU) and the Basic Discrete Unit (BDU)

The stiffness matrix for the quadrilateral bilinear element (Basic Continuum Unit - BCU) is given by:

$$K_{2D}=\begin{bmatrix} 2s_1+2s_4 & & & & & & & \\ s_3+s_6 & 2s_2+2s_5 & & & & & & \\ -2s_1+s_4 & -s_3+s_6 & 2s_1+2s_4 & & (sym.) & & & \\ s_3-s_6 & s_2-2s_5 & -s_3-s_6 & 2s_2+2s_5 & & & & \\ -s_1-s_4 & -s_3-s_6 & s_1-2s_4 & -s_3+s_6 & 2s_1+2s_4 & & & \\ -s_3-s_6 & -s_2-s_5 & s_3-s_6 & -2s_2+s_5 & s_3+s_6 & 2s_2+2s_5 & & \\ s_1-2s_4 & s_3-s_6 & -s_1-s_4 & s_3+s_6 & -2s_1+s_4 & -s_3+s_6 & 2s_1+2s_4 & \\ -s_3+s_6 & -2s_2+s_5 & s_3+s_6 & -s_2-s_5 & s_3-s_6 & s_2-2s_5 & -s_3-s_6 & 2s_2+2s_5 \end{bmatrix} \quad (4.A1)$$

where

$$s_1=\frac{tb}{6a}D_{11} \quad s_2=\frac{ta}{6b}D_{22} \quad s_3=\frac{t}{4}D_{12} \quad s_4=\frac{ta}{6b}D_{33} \quad s_5=\frac{tb}{6a}D_{33} \quad s_6=\frac{t}{4}D_{33} \quad (4.A2)$$

and

$$D=\frac{E}{1-\nu^2}\begin{bmatrix} 1 & \nu & 0 \\ \nu & 1 & 0 \\ 0 & 0 & \kappa \end{bmatrix} \qquad \kappa=\frac{1-\nu}{2} \quad (4.A3)$$

It is obvious that the elements of K_{2D} are linear combinations of (s_1,s_4), or (s_2,s_5), or (s_3,s_6). The elements of the last pair are independent of the dimensions (a,b) of the BCU, thus the corresponding elements of K_{2D} do not change with respect to the aspect ratio $\lambda=(a/b)$. Concerning the elements of the pair (s_1,s_4), and the elements of the pair (s_2,s_5), it holds that:

$$(s_1,s_4)=\left(\frac{t}{6}\frac{E}{(1-\nu^2)}\right)\left(\frac{1}{\lambda},\lambda\frac{1-\nu}{2}\right) \qquad (s_2,s_5)=\left(\frac{t}{6}\frac{E}{(1-\nu^2)}\right)\left(\lambda,\frac{1}{\lambda}\frac{1-\nu}{2}\right) \quad (4.A4)$$

The appearing combinations in K_{2D} are:

$$\begin{Bmatrix} 2(s_1+s_4) \\ -2s_1+s_4 \\ -(s_1+s_4) \\ (s_1-2s_4) \end{Bmatrix}=\left(\frac{t}{6}\cdot\frac{E}{(1-\nu^2)}\right)\cdot\begin{Bmatrix} 2\left(\frac{1}{\lambda}+\lambda\cdot C\right) \\ -2\frac{1}{\lambda}+\lambda\cdot C \\ -\left(\frac{1}{\lambda}+\lambda\cdot C\right) \\ \frac{1}{\lambda}-2\cdot\lambda\cdot C \end{Bmatrix} \qquad \begin{Bmatrix} 2(s_2+s_5) \\ -2s_2+s_5 \\ -(s_2+s_5) \\ (s_2-2s_5) \end{Bmatrix}=\left(\frac{t}{6}\cdot\frac{E}{(1-\nu^2)}\right)\cdot\begin{Bmatrix} 2\left(\lambda+\frac{1}{\lambda}\cdot C\right) \\ -2\lambda+\frac{1}{\lambda}\cdot C \\ -\left(\lambda+\frac{1}{\lambda}\cdot C\right) \\ \lambda-2\cdot\frac{1}{\lambda}\cdot C \end{Bmatrix} \quad (4.A5)$$

where

$$C = \left(\frac{1-\nu}{2} \right) \tag{4.A6}$$

It is evident that the terms of the last two groups depend only on the aspect ratio (the quantity C is constant). The stiffness matrix for the 6-bar assembly (Basic Discrete Unit - BDU) is given by:

$$K_{TRUSS} = \begin{bmatrix} \frac{EA_1}{2a} + \frac{EA_5}{l}c^2 & & & & & & & \\ \frac{EA_5}{l}cs & \frac{EA_4}{2b} + \frac{EA_5}{l}s^2 & & & & & & \\ \frac{-EA_1}{2a} & 0 & \frac{EA_1}{2a} + \frac{EA_6}{l}c^2 & & & (sym.) & & \\ 0 & 0 & -\frac{EA_6}{l}cs & \frac{EA_2}{2b} + \frac{EA_6}{l}s^2 & & & & \\ -\frac{EA_5}{l}c^2 & -\frac{EA_5}{l}cs & 0 & 0 & \frac{EA_3}{2a} + \frac{EA_5}{l}c^2 & & & \\ -\frac{EA_5}{l}cs & -\frac{EA_5}{l}c^2 & 0 & \frac{-EA_2}{2b} & \frac{EA_5}{l}cs & \frac{EA_2}{2b} + \frac{EA_5}{l}c^2 & & \\ 0 & 0 & -\frac{EA_6}{l}c^2 & \frac{EA_6}{l}cs & -\frac{EA_3}{2a} & 0 & \frac{EA_3}{2a} + \frac{EA_6}{l}c^2 & \\ 0 & \frac{EA_4}{2b} & \frac{EA_6}{l}cs & -\frac{EA_6}{l}s^2 & 0 & 0 & -\frac{EA_6}{l}cs & \frac{EA_4}{2b} + \frac{EA_6}{l}s^2 \end{bmatrix} \tag{4.A7}$$

where

$$|c| = \left(\frac{2b}{l} \right) \qquad |s| = \left(\frac{2a}{l} \right) \qquad l = \sqrt{(2a)^2 + (2b)^2} \tag{4.A8}$$

Consequently, some of the terms of this matrix depend on the aspect ratio $\lambda = (a/b)$, while some others also depend on individual values of the variables a and/or b. As a consequence, if the geometrical dimensions of the BDU change, then the stiffness matrix K_{TRUSS} will change as well, even if the aspect ratio remains the same. Furthermore, K_{TRUSS} includes zero terms, while K_{2D} does not. On top of that, all terms in K_{2D} are linear functions of the element thickness (only one variable), while the non-zero terms in K_{TRUSS} depend on the cross section areas of the bars that form the 6-bar assembly (six variables). The three aforementioned differences, with emphasis on the last one, justify the great difference between the dependence of the (BCU) and the (BDU) on the aspect ratio.

Appendix 4B: Stiffness matrix for a variable thickness element of plane elasticity

4B.1 In general

Let a finite element of plane elasticity, for which the thickness is not element-wise constant. Furthermore, assume that the element thickness is interpolated using the thickness at the nodes of the element, while the interpolation functions are the same with those used for interpolating the displacement field; that is, an isoparametric interpolation is considered. For such a finite element, the stiffness matrix is formed if the thickness is properly expressed in a mathematical way. Towards this direction, from the theory of the Finite Element Method, it is known that the following holds:

$$\left[k\right]_e = \int_{-1}^{+1}\int_{-1}^{+1} t_e \left[B\right]^T \left[D\right]\left[B\right] \det\left[J\right] d\xi\, d\eta \tag{4.B1}$$

where t_e is the thickness of the e-element, $\left[B\right]$ yields from the strain-displacement matrix, $\left[D\right]$ is the elasticity matrix and $\left[J\right]$ is the Jacobian. If this quantity is interpolated in an isoparametric way, then it holds:

$$t_e = N_1 t_1 + N_2 t_2 + N_3 t_3 + N_4 t_4 \tag{4.B2}$$

where N_i and t_i are the shape function and the thickness of the $i-$node. It is possible to write Eq.(4B.2) in a matrix form as follows:

$$t_e = \left[N\right]\left\{t\right\} \tag{4.B3}$$

where the matrix $\left[N\right]$ is of dimension 4×1 and the matrix $\left\{t\right\}$ is of dimension 1×4. The combination of Eqs.(4B.1, 4B.3) yields:

$$\left[k\right]_e = \int_{-1}^{+1}\int_{-1}^{+1} \left[N\right]\left\{t\right\} \left[B\right]^T \left[D\right]\left[B\right] \det\left[J\right] d\xi\, d\eta \tag{4.B4}$$

According to the Gauss integration method, the value of the following integral:

$$I = \int_{-1}^{+1}\int_{-1}^{+1} f\left(\xi,\eta\right) d\xi\, d\eta \tag{4.B5}$$

is approximated through the following expression:

$$I \approx \sum_{l=1}^{n}\sum_{m=1}^{n}\left(w_l\, w_m\, f\left(\xi_l,\eta_m\right)\right) \tag{4.B6}$$

where n is the number of the Gauss points that will be used, the indices l,m denote the current Gauss point, while the quantities w_l and w_m represent the weights that correspond to the Gauss point $\left(\xi_l,\eta_m\right)$. Combining Eq.(4B.5) with Eq.(4B.6) yields:

$$\left[k\right]_e = \sum_{l=1}^{n}\sum_{m=1}^{n}\left(w_l\, w_m\, f_i\left(\xi_l,\eta_m\right)\right) \tag{4.B7}$$

where the function within the sum is equal to:

$$f\left(\xi_l,\eta_m\right)=\left(\left[N\right]\{t\}\left[B\right]^T\left[D\right]\left[B\right]\det\left[J\right]\right)_{lm} \tag{4.B8}$$

Therefore, the stiffness matrix $\left[k\right]_e$ may be estimated according to the following procedure:

Step 1: select the number of Gauss points to be used and for each Gauss point define the coordinates $\left(\xi_l,\eta_m\right)$ and the weights w_l, w_m

Step 2: estimate the value N_i of the shape functions at each Gauss point $\left(\xi_l,\eta_m\right)$

Step 3: estimate the matrices $\left[B\right]$ and $\left[J\right]$ at each Gauss point $\left(\xi_l,\eta_m\right)$

Step 4: estimate the quantity $f_i\left(\xi_l,\eta_m\right)$ according to Eq.(4B.8)

Step 5: estimate the stiffness matrix $\left[k\right]_e$ according to Eq.(4B.7)

4B.2 Application: 4-node quadrilateral finite element of plane elasticity

Let a 4-node quadrilateral finite element of plane elasticity. The displacements $\left(u,v\right)$ of any point of this element are equal to:

$$\begin{aligned} u &= N_1u_1+N_2u_2+N_3u_3+N_4u_4 \\ v &= N_1v_1+N_2v_2+N_3v_3+N_4v_4 \end{aligned} \tag{4.B9}$$

For this specific finite element, the shape functions N_i, expressed in the physical coordinate system, are equal to:

$$\begin{aligned} N_1 &= 0.25\left(1-\xi\right)\left(1-\eta\right) \\ N_2 &= 0.25\left(1+\xi\right)\left(1-\eta\right) \\ N_3 &= 0.25\left(1+\xi\right)\left(1+\eta\right) \\ N_4 &= 0.25\left(1-\xi\right)\left(1+\eta\right) \end{aligned} \tag{4.B10}$$

The strain vector is equal to:

$$\{\varepsilon\}=\left\{\frac{\partial u}{\partial x}\quad\frac{\partial v}{\partial y}\quad\frac{\partial u}{\partial y}+\frac{\partial v}{\partial x}\right\}^T \tag{4.B11}$$

For the estimation of the partial derivatives of the displacements u and v in the Cartesian coordinate system, the aforementioned displacements are considered as:

$$\left.\begin{aligned} &u=u\left(x,y\right),v=v\left(x,y\right), \\ &x=x\left(\xi,\eta\right),y=y\left(\xi,\eta\right) \end{aligned}\right\}\Rightarrow\left\{\begin{aligned} &u=u\left(x\left(\xi,\eta\right),y\left(\xi,\eta\right)\right) \\ &v=v\left(x\left(\xi,\eta\right),y\left(\xi,\eta\right)\right) \end{aligned}\right\} \tag{4.B12}$$

Applying the chain rule, it yields:

$$\left\{\begin{array}{l}\dfrac{\partial u}{\partial \xi}=\dfrac{\partial u}{\partial x}\dfrac{\partial x}{\partial \xi}+\dfrac{\partial u}{\partial y}\dfrac{\partial y}{\partial \xi}\\ \dfrac{\partial u}{\partial \eta}=\dfrac{\partial u}{\partial x}\dfrac{\partial x}{\partial \eta}+\dfrac{\partial u}{\partial y}\dfrac{\partial y}{\partial \eta}\end{array}\right\},\qquad \left\{\begin{array}{l}\dfrac{\partial v}{\partial \xi}=\dfrac{\partial v}{\partial x}\dfrac{\partial x}{\partial \xi}+\dfrac{\partial v}{\partial y}\dfrac{\partial y}{\partial \xi}\\ \dfrac{\partial v}{\partial \eta}=\dfrac{\partial v}{\partial x}\dfrac{\partial x}{\partial \eta}+\dfrac{\partial v}{\partial y}\dfrac{\partial y}{\partial \eta}\end{array}\right\} \tag{4.B13}$$

or, equivalently:

$$\left\{\begin{array}{l}\dfrac{\partial u}{\partial \xi}\\ \dfrac{\partial u}{\partial \eta}\end{array}\right\}=\underbrace{\left[\begin{array}{ll}\dfrac{\partial x}{\partial \xi} & \dfrac{\partial y}{\partial \xi}\\ \dfrac{\partial x}{\partial \eta} & \dfrac{\partial y}{\partial \eta}\end{array}\right]}_{J}\left\{\begin{array}{l}\dfrac{\partial u}{\partial x}\\ \dfrac{\partial u}{\partial y}\end{array}\right\},\qquad \left\{\begin{array}{l}\dfrac{\partial v}{\partial \xi}\\ \dfrac{\partial v}{\partial \eta}\end{array}\right\}=\underbrace{\left[\begin{array}{ll}\dfrac{\partial x}{\partial \xi} & \dfrac{\partial y}{\partial \xi}\\ \dfrac{\partial x}{\partial \eta} & \dfrac{\partial y}{\partial \eta}\end{array}\right]}_{J}\left\{\begin{array}{l}\dfrac{\partial v}{\partial x}\\ \dfrac{\partial v}{\partial y}\end{array}\right\} \tag{4.B14}$$

For the formation of the 2×2 matrix that appears in Eq.(4B.14) (Jacobian matrix J), it is required to estimate the derivatives of the Cartesian coordinates (x,y) with respect to the physical coordinates (ξ,η). The Cartesian coordinates (x,y) of any point of a finite element of plane elasticity are described as follows:

$$\begin{aligned}x&=N_1x_1+N_2x_2+N_3x_3+N_4x_4\\ y&=N_1y_1+N_2y_2+N_3y_3+N_4y_4\end{aligned} \tag{4.B15}$$

The derivative of Eq.(4B.15) with respect to ξ and η is equal to:

$$\begin{aligned}\frac{\partial x}{\partial \xi}&=\frac{\partial N_1}{\partial \xi}x_1+\frac{\partial N_2}{\partial \xi}x_2+\frac{\partial N_3}{\partial \xi}x_3+\frac{\partial N_4}{\partial \xi}x_4\\ \frac{\partial y}{\partial \xi}&=\frac{\partial N_1}{\partial \xi}y_1+\frac{\partial N_2}{\partial \xi}y_2+\frac{\partial N_3}{\partial \xi}y_3+\frac{\partial N_4}{\partial \xi}y_4\\ \frac{\partial x}{\partial \eta}&=\frac{\partial N_1}{\partial \eta}x_1+\frac{\partial N_2}{\partial \eta}x_2+\frac{\partial N_3}{\partial \eta}x_3+\frac{\partial N_4}{\partial \eta}x_4\\ \frac{\partial y}{\partial \eta}&=\frac{\partial N_1}{\partial \eta}y_1+\frac{\partial N_2}{\partial \eta}y_2+\frac{\partial N_3}{\partial \eta}y_3+\frac{\partial N_4}{\partial \eta}y_4\end{aligned} \tag{4.B16}$$

In matrix notation, it holds:

$$\begin{aligned}\frac{\partial x}{\partial \xi}&=\left[\frac{\partial N_1}{\partial \xi}\quad\frac{\partial N_2}{\partial \xi}\quad\frac{\partial N_3}{\partial \xi}\quad\frac{\partial N_4}{\partial \xi}\right]\left[x_1\quad x_2\quad x_3\quad x_4\right]^T\\ \frac{\partial y}{\partial \xi}&=\left[\frac{\partial N_1}{\partial \xi}\quad\frac{\partial N_2}{\partial \xi}\quad\frac{\partial N_3}{\partial \xi}\quad\frac{\partial N_4}{\partial \xi}\right]\left[y_1\quad y_2\quad y_3\quad y_4\right]^T\\ \frac{\partial x}{\partial \eta}&=\left[\frac{\partial N_1}{\partial \eta}\quad\frac{\partial N_2}{\partial \eta}\quad\frac{\partial N_3}{\partial \eta}\quad\frac{\partial N_4}{\partial \eta}\right]\left[x_1\quad x_2\quad x_3\quad x_4\right]^T\\ \frac{\partial y}{\partial \eta}&=\left[\frac{\partial N_1}{\partial \eta}\quad\frac{\partial N_2}{\partial \eta}\quad\frac{\partial N_3}{\partial \eta}\quad\frac{\partial N_4}{\partial \eta}\right]\left[y_1\quad y_2\quad y_3\quad y_4\right]^T\end{aligned} \tag{4.B17}$$

The partial derivatives of the shape functions N_i can be derived from Eq.(4B.10) and are equal to:

$$\left\{\begin{array}{l}\dfrac{\partial N_1}{\partial \xi}=-0.25(1-\eta)\\ \dfrac{\partial N_2}{\partial \xi}=+0.25(1-\eta)\\ \dfrac{\partial N_3}{\partial \xi}=+0.25(1+\eta)\\ \dfrac{\partial N_4}{\partial \xi}=-0.25(1+\eta)\end{array}\right\},\qquad \left\{\begin{array}{l}\dfrac{\partial N_1}{\partial \eta}=-0.25(1-\xi)\\ \dfrac{\partial N_2}{\partial \eta}=-0.25(1+\xi)\\ \dfrac{\partial N_3}{\partial \eta}=+0.25(1+\xi)\\ \dfrac{\partial N_4}{\partial \eta}=+0.25(1-\xi)\end{array}\right\} \tag{4.B18}$$

According to Eq.(4B.14), it holds:

$$\left\{\begin{array}{l}\dfrac{\partial u}{\partial x}\\ \dfrac{\partial u}{\partial y}\end{array}\right\}=J^{-1}\left\{\begin{array}{l}\dfrac{\partial u}{\partial \xi}\\ \dfrac{\partial u}{\partial \eta}\end{array}\right\},\qquad \left\{\begin{array}{l}\dfrac{\partial v}{\partial x}\\ \dfrac{\partial v}{\partial y}\end{array}\right\}=J^{-1}\left\{\begin{array}{l}\dfrac{\partial v}{\partial \xi}\\ \dfrac{\partial v}{\partial \eta}\end{array}\right\} \tag{4.B19}$$

Therefore, all the necessary information for the estimation of the strain vector is now available.

CHAPTER 5

LAYOUT OPTIMIZATION OF SKELETAL STRUCTURES UNDER AN EXTENDED SINGLE DISPLACEMENT CONSTRAINT

Abstract

In this chapter, the problem of minimizing the weight of skeletal structures under a single displacement constraint is revisited. The contribution to this most popular and most investigated structural optimization problem is the development of an optimization procedure implementing three new features. The first feature is the formulation of a new and efficient Optimality Criterion-type redesign scheme where no Lagrange multipliers are required to be estimated. The second feature is the introduction of a new categorization of the structural elements according to which the elements, in opposition to the preponderant common practice, are characterized in a more detailed manner as force-active or force-passive and as area-active/area-passive. In this chapter, it is shown that it is for the force-passive or area-active elements that search methods are trapped at local minima. The third feature is the application of a typical line-search optimization method on the structural elements diagnosed as force-passive/area-active so that their contribution to the structural weight is minimized and a better design is obtained. The validity of the proposed optimization procedure was successfully tested for determinate and indeterminate skeletal structures using a series of literature examples and newly introduced benchmarking examples with their variations, all of which were also optimized, for evaluating reasons, using the Sequential Quadratic Programming (SQP) routine found in Matlab.

Keywords

layout optimization, virtual strain energy density, single displacement constraint, grid-like structure.

5.1. Introduction

The layout optimization of continua has always been a great challenge to the engineering community because the nature of the problem provides a plethora of most interesting theoretical aspects needing exploration and explanation while at the same time the problem itself is strongly related to everyday practicing engineering case studies. According to Rozvany (Rozvany 1995), the so-called *classical approach* to the layout optimization of continua is first to replace the continuum with a skeletal structure (structural universe or ground structure) and then to optimize the skeletal structure. However, even with this simplification, the generalized layout optimization of a skeletal structure remains quite difficult to deal with, thus its decomposition into a series of simpler sub-problems, in order to get a better insight, is advisable. Within this framework, the present chapter deals with the sub-problem of the weight minimization of determinate and indeterminate skeletal (pin-joined) structures under a single displacement constraint. Generally speaking, the solution to this type of structural optimization problem may be sought through a direct technique (such as a Mathematical Programming (MP) method or a stochastic optimization method), or an indirect technique (such as an Optimality Criteria (OC) method).

With respect to the (MP) methods, Schmit was the first to introduce the idea of coupling the Finite Element Method (FEM) with (MP) techniques to solve nonlinear inequality constrained problems concerning the design of elastic structures under a multiplicity of loading conditions (Schmit 1960). Since then, a great many number of mathematical methods have been developed (Belegundu and Chandrupatla 1999), all of which, however, suffer from the same disadvantage of very limited optimization capability with respect to the number of variables and the number of active constraints, respectively (Rozvany 1992). Among these techniques, the Sequential Quadratic Programming (SQP) has proven to be most powerful for detecting the global optimum and due to this characteristic the optimal designs obtained with it can be used as reference for comparisons in terms of minimum weight (Provatidis et al 2004). With respect to the stochastic approaches (Goldberg 1989; Michalewicz 1999), it is true that they provide a better exploration and exploitation, while they have the ability not to get trapped so easily at local minima. However, their performance reduces rapidly as the size of the design space increases thus limits their applicability into optimization problems with a small number of design variables.

On the other hand, the OC methods are capable of handling efficiently a large number of design variables and they do lead to the optimum design provided the problem at hand does not include constraints on sizes and multiple loading conditions (Venkayya 1971). The origin of the OC methods can be found in Michell's work who investigated the minimum weight of a planar truss that transmits a given load to a given rigid foundation with the requirement that the axial stresses in the bars of the truss stay within an allowable range (Michell 1904). According to Michell, at the optimum, the axial strain has a constant absolute value, say k, in directions of non-zero axial forces, while in the directions of zero axial forces the absolute value of the strain must be at most equal to k (Michell 1904). Half a century later Foulkes introduced another optimality condition according to which for a segment-wise prismatic frames the average absolute curvature for each segment must be the same (Foulkes 1954). Five years later, Heyman extended Foulkes' optimality criterion to include plastic beams having a rectangular cross-section that could freely vary, while the depth was given but the width was variable (Heyman 1950). A general optimality criterion for the optimal plastic design of structures with freely varying cross-sectional dimensions was proposed by Shield and Prager (Shield and Prager 1970). This criterion was considerably extended by Rozvany who stated that in the optimal strain-stress relation, the adjoint strains must be kinematically admissible and are given by the gradient of a specific cost function, in which the stress vector must be statically admissible (Rozvany 1992). Prager also used extensively the concept of

structural universe (ground structure) for substituting a continuum with a skeletal structure (Rozvany 1992). In the 70's, major contributions in OC methods took place. In the early 70's, Venkayya stated that the optimum structure is the one in which the average strain energy density is the same in all its elements (Venkayya 1971). At the same time, Berke (Berke 1990) attacked the single displacement constraint problem proving the validity of the separability concept and using it for the derivation of an optimality criterion based on which he formed various recursive redesign equations. Furthermore, Khot (Khot 1981), based on the Lagrange multipliers method, proved that the optimum design of a single displacement constrained truss has a uniform virtual strain energy density distribution over its active part. Gellatly and Berke proposed an optimality criteria approach for indeterminate trusses constrained both in stress and displacement, also valid for displacement-constrained statically determinate trusses (Gellatly and Berke 1973).

In the last two decades, significant works on the subject have been carried out. Patnaik et al. dealt with displacement constrained problems and introduced a design update expressed in an exponential, a linearized, a reciprocal and a melange form (Patnaik et al 1995). In these forms, the estimation of the corresponding Lagrange multiplier was mandatory and for this purpose a linear, an exponential, an unrestricted and a diagonalized inverse approach were developed (Patnaik et al 1995). Rozvany and Zhou formulated the fundamental relations of optimal elastic design using a Continuum-based Optimality Criteria (COC) approach for freely varying cross-sections and one deflection constraint (Rozvany and Zhou 1991; Rozvany and Zhou 1991b). Bendsoe dealt with topology optimization of trusses in the form of grid-like continua. More specifically, he investigated various formulations of truss topology design, while he considered primarily the minimization of compliance (maximization of stiffness) for a given total mass of the structure (Bendsoe and Sigmund 2001). Xie and Steven, the developers of the Evolutionary Structural Optimization (ESO) method, handled the single displacement constraint optimization problem of 2D continuum domains but from the viewpoint of plane elasticity only and not from the viewpoint of the ground structure approach. They have also developed an ESO variation suitable for optimizing truss weight but only when stress constraints are imposed (Xie and Steven 1997). Makris and Provatidis proposed an iterative procedure where the optimality criterion demanding a uniform virtual strain energy density distribution over the entire structure was introduced into their redesign formula as a normalized penalization factor (Makris and Provatidis 2002). Extending this work, Makris et al. introduced the concept of a dummy stress bound in order to deal with problems where only displacement limitations are imposed (Makris et al 2006).

From the aforementioned literature review, it is evident that the single displacement constraint problem is one of the most popular and most investigated structural optimization problems. However, there are still some issues open for discussion which actually motivated the research presented in the current work. Stated briefly, the present chapter describes a new optimization procedure introducing three new features. The first feature is a new redesign equation which, although derived rigorously from the Lagrange multipliers method, has the advantage of not requiring the estimation of any Lagrange multiplier. The second feature is the characterization of the structural members in a more detailed manner both as force-active or force-passive and as area-active or area-passive (and not only as active or passive, according to the preponderant practice). The third feature is the application of a typical line-search optimization to the elements diagnosed as force-passive/area-active, so that their contribution to the structural weight be minimized and a better design be obtained. The proposed optimization procedure was successfully applied for the optimization of both determinate and indeterminate skeletal structures. In total, 48 cases were successfully analyzed: from the literature, two variations for the 3-bar truss, two variations for the 5-bar,

two variations for the 56-bar truss and two variations for the MBB beam were retrieved, while newly introduced benchmarking examples were optimized as well (five variations of the MBB beam with three different mesh densities each and six variations of the 9-bar truss under four load cases each). In order to have a more representative evaluation, all of the investigated examples, apart from those for which an analytical solution was available, were also optimized using the Sequential Quadratic Programming (SQP) routine found in Matlab (routine fmincon). The results of the present research suggest that the aforementioned features do play a significant role in the structural layout optimization process and, when embedded in an optimization procedure, they form a simple and efficient optimization tool.

5.2. Theoretical approach

5.2.1. The Optimality Criterion statement

According to the description of the single displacement constrained optimization problem of a 2D ground structure (truss), one nodal displacement is considered. The generalization of this concept is to consider that, no matter how many displacement constraints are imposed, only one is active at the optimum, without knowing a priori the *degree of freedom* related to the aforementioned nodal displacement. The statement of this problem, which is the one studied in the present chapter, follows:

$$\text{minimize } W = \sum_{k=1}^{NEL} \left(\rho_k \, A_k \, L_k \right) \tag{5.1a}$$

$$\text{such that } |u| \le u_{allow} \text{ and } A_{\min} \le A \tag{5.1b}$$

where A is the cross-sectional area, L is the length, ρ is the material density, u is the nodal displacement, while the indices k and *allow* denote the $k-$bar and the allowable value, respectively. The total number of bars (elements) in the structure is declared as NEL. The imposed constraint on the displacement (1b) suggests that the nodal displacement may not be greater than u_{allow} either in the x or the y direction. Furthermore, a constraint with respect to the minimum cross-sectional area is imposed so that the formation of a positive definite stiffness matrix is ensured. According to the method of Lagrange multipliers, the Lagrangian function corresponding to the aforementioned problem, if the constraint for the minimum cross-sectional area is dropped, may be stated as:

$$\mathfrak{L} = \sum_{i=1}^{NEL} \left(\rho_i \, A_i \, L_i \right) + \lambda_1 \left(|u| - u_{allow} \right) \tag{5.2}$$

where λ_1 is the Lagrange multiplier for the displacement constraint. From Mechanics, it is well-known that a nodal displacement, based on the concept of virtual work, may be expressed as:

$$u = \sum_{i=1}^{NEL} \left(\frac{F_i^P F_i^Q}{A_i E_i} L_i \right) \tag{5.3}$$

where, in addition to the symbols previously used, E denotes the modulus of elasticity, F_i^P is the member force due to the application of the actual loads, F_i^Q denotes the member force due

to an appropriately applied unit virtual load, while i denotes the structural member under consideration. Introducing Eq.(5.3) in Eq.(5.2) yields:

$$\mathfrak{L} = \sum_{i=1}^{NEL} (\rho_i A_i L_i) + \lambda_1 \left(\left| \sum_{i=1}^{NEL} \left(\frac{F_i^P F_i^Q}{A_i E_i} L_i \right) \right| - u_{allow} \right) \tag{5.4}$$

The partial derivative of Eq.(5.4) with respect to the cross-sectional areas A_i equals to:

$$\nabla \mathfrak{L}_{A_i} = \rho_i L_i - \lambda_1 \left| \left(\frac{F_i^P F_i^Q}{A_i^2 E_i} L_i \right) \right| + \lambda_1 \sum_l \left(\left(\left(\frac{\partial F_l^P}{\partial A_i^2} \right) F_l^Q + \left(\frac{\partial F_l^Q}{\partial A_i^2} \right) F_l \right) \left(\frac{L_l}{A_l E_l} \right) \right) \tag{5.5a}$$

However, the terms in the summation are identically zero. For determinate structures, the member forces do not depend on the cross-sectional areas thus the partial derivatives are equal to zero. For indeterminate structures, Berke has shown that the derivative terms form a self-equilibrating internal load system. The virtual work of this system, represented by the summation, is zero, by the principle of virtual displacements. Therefore, Eq.(5.5a) becomes:

$$\nabla \mathfrak{L}_{A_i} = \rho_i L_i - \lambda_1 \left| \left(\frac{F_i^P F_i^Q}{A_i^2 E_i} L_i \right) \right| \tag{5.5b}$$

According to the method of Lagrange multipliers, it must hold:

$$\nabla \mathfrak{L}_{A_i} = 0 \tag{5.6}$$

The combination of Eqs.(5.5b, 5.6), after basic manipulations, yields:

$$1 = \lambda_1 \left| \left(\frac{F_i^P F_i^Q}{A_i A_i} \frac{1}{E_i} \right) \right| \left(\frac{1}{\rho_i} \right) \tag{5.7}$$

The coefficient λ_1, being a single quantity, is constant:

$$\lambda_1 = const \tag{5.8}$$

Under the assumption that all bars are made of the same material, it holds:

$$\rho_i = const \tag{5.9}$$

The combination of Eqs(5.7, 5.8, 5.9) yields:

$$\left| \left(\frac{F_i^P F_i^Q}{A_i A_i} \frac{1}{E_i} \right) \right| = const \tag{5.10}$$

The left-hand-side of Eq.(5.10) represents the virtual strain energy density of the i-bar of the examined truss. According to the last equation, for the design that corresponds to minimum

weight under a single displacement constraint, the absolute value of the virtual strain energy density is the same over the *active* part of the optimized structure. This is an optimality criterion well-known since the early 70's and provides a description of the optimal structure from an energy-state point of view. However, this criterion *does not* provide a method for reaching this energy state, thus allowing new procedures to be stated. Towards this direction, the present chapter proposes a redesign procedure which is of a closed-form character for determinate trusses and of a recursive-form character for indeterminate trusses.

5.2.2. Proposed redesign based on the Optimality Criterion statement

Let a set of NEL bars with randomly selected cross-sectional areas be used as the initial design vector. A Finite Element Analysis (FEA) with the real loads provides both the member forces F_i and the displacement field, from which the node with the maximum displacement, let it be $N_{u_{max}}$, may be located. Another (FEA) with a virtual unit load applied to $N_{u_{max}}$ provides the member forces F_i^Q. With these member forces at hand, it is possible to detect the non-zero-force members $\left|F_i^P F_i^Q\right| > tol$, the tolerance tol being a small positive number, say 1E-06. Each one of the these bars has its own virtual strain energy density w_i:

$$w_i = \left(\frac{F_i^P F_i^Q}{A_i A_i} \frac{1}{E_i} \right) \tag{5.11}$$

The corresponding mean value $\overline{w}$ of all the w_i values is equal to:

$$\overline{w} = \left(\frac{\sum_{i=1}^{N_{active}} w_i}{N_{active}} \right) \tag{5.12}$$

Substituting w_i on the r.h.s. of Eq.(5.11) with the mean value $\overline{w}$ yields:

$$\overline{w} = \left(\frac{F_{i,new}^P F_{i,new}^Q}{A_{i,new} A_{i,new}} \frac{1}{E_i} \right) \tag{5.13}$$

where $A_{i,new}$ is the re-designed cross-sectional area of the $i-$bar. Dividing Eq.(5.11) by (Eq.5.13) yields:

$$\frac{w_i}{\overline{w}} = \frac{\left(\frac{F_i^P F_i^Q}{A_i A_i} \frac{1}{E_i} \right)}{\left(\frac{F_{i,new}^P F_{i,new}^Q}{A_{i,new} A_{i,new}} \frac{1}{E_i} \right)} \tag{5.14}$$

However, for a statically determinate truss, the member forces F_i^P and F_i^Q are affected only by the structural topology (they are independent from the cross-sectional values).

$$\left(\frac{\partial F_i^P}{\partial A_i}\right) = \left(\frac{\partial F_i^Q}{\partial A_i}\right) = 0 \tag{5.15}$$

Consequently, Eq.(5.14) may be written after basic manipulations as:

$$\frac{w_i}{\bar{w}} = \left(\frac{A_{i,new}^2}{A_i^2}\right) \tag{5.16}$$

Solving the last equation with respect to the re-designed cross-sectional area of the $i-$bar yields:

$$A_{i,new} = A_i \sqrt{\left(\frac{w_i}{\bar{w}}\right)} \tag{5.17}$$

The proposed redesign formula (Eq.(5.17)) expresses a '*virtual-strain-energy-density-ratio technique*' similar to the famous '*stress-ratio technique*' used for stress-constrained problems. Although it was derived for a determinate truss, it may also be applied in cases of indeterminate trusses where the sensitivity of the axial forces to cross-sectional changes is low; that is, for cases where equilibrium governs rather than compatibility or for designs that are very near-optimum. For other indeterminate trusses, Eq.(5.17) must be used iteratively until convergence to a solution is achieved. Even though the design vector $\mathbf{A_{new}}$ with the design variables $A_{i,new}$ formed with Eq.(5.17) fulfills the demand for uniform distribution of virtual strain energy density over the active structural elements, it is not ensured that the imposed constraint concerning the maximum allowable displacement is fulfilled as well. For this purpose, a uniform scaling of the design vector $\mathbf{A_{new}}$ is required.

5.2.3. Uniform scaling of the design vector

For a statically determinate structure, the *value* of the virtual strain energy of the active $i-$bar depends on both the virtual member force F_i^Q and the cross-sectional area A_i. Therefore, for a structure of constant topology, where the bar lengths L_i are well defined and remain unchanged, and assuming that all bars are made of the same material, thus E_i is also well defined and constant, it holds:

$$\frac{F_i^P F_i^Q}{A_i E_i} L_i = f\left(F_i^Q, A_i\right) \tag{5.18}$$

If the application point of the virtual unit load is known, then the virtual member forces F_i^Q are also known and well defined and Eq.(5.18) reduces to the following form:

$$\frac{F_i^P F_i^Q}{A_i E_i} L_i = f\left(A_i\right) \tag{5.19}$$

where the cross-sectional area A_i is the only unknown. Therefore, the virtual strain energy of each bar, which is numerically equal to the contribution of each bar to the displacement of the application point of the virtual load, can be scaled simply by changing the cross-sectional area A_i. Furthermore, the combination of Eqs(5.3, 5.19) suggests that if the same scaling is applied to all of the cross-sectional areas A_i (uniform scaling) then the displacement of the application point of the virtual load is also scaled by the same amount; that is:

$$u_{scaled} = a\, u_{before\_scaling} \tag{5.20}$$

The constant a denotes a scaling coefficient while the subscripts adequately describe the meaning of the other two terms. If the maximum allowable value for nodal displacement u_{allow} is selected as u_{scaled}, then the scaling coefficient a equals to the ratio of the allowable to the appearing nodal displacement u (for convenience, the subscript *before_scaling* is dropped):

$$a = \left(\frac{u_{allow}}{u} \right) \tag{5.21}$$

The combination of Eqs.(5.3, 5.20) yields:

$$u_{allow} = a \left(\sum_{i=1}^{NEL} \left(\frac{F_i^P F_i^Q}{A_i E_i} L_i \right) \right) \tag{5.22}$$

Since the scaling coefficient is constant, Eq.(5.22) may be written as:

$$u_{allow} = \sum_{i=1}^{NEL} \left(\frac{F_i^P F_i^Q}{\left(\frac{A_i}{a} \right) E_i} L_i \right) \tag{5.23}$$

The comparison of Eq.(5.23) with Eq.(5.3) provides the following re-design formula:

$$A_{i,new} = \left(\frac{A_{i,old}}{a} \right) \tag{5.24}$$

where the indices *new* and *old* denote the new and the old value of the cross-sectional area of the $i-$bar, respectively. Therefore, for the uniform scaling to be applied, the re-designed cross-sections with Eq.(5.17) of all active bars must be divided by the scaling coefficient a. However, there is still one issue left: the selection of the degree of freedom that the virtual load must be applied to. A first thought would be to randomly select a design vector, find the degree of freedom corresponding to the maximum displacement and apply a virtual load to it. This is not a safe selection because, generally speaking, different initial design vectors provide different displacement fields thus different locations of maximum nodal displacements. In this way, local minima can be found, which may be adequate for practicing engineering problems; however, the global minimum can be located only by chance. Nevertheless, for the global optimum design to be obtained without violating the imposed

displacement constraint, it is imperative the degree of freedom, that the virtual load must be applied to, be appropriately selected. This subject is analyzed in the next section.

5.2.4. Design of Unit Stiffness (Unit Stiffness Design)

For a statically determinate truss, it is possible to estimate the member forces using the method of joints, according to which the value of each member force is related only to the externally applied loads and the spatial orientation of the members. On the other hand, the same goal may be achieved using the Finite Element Method (FEM), according to which the following equation must be solved:

$$\{F\} = [K]\{U\} \tag{5.25}$$

where $\{F\}$ is the externally applied force vector, $[K]$ is the global stiffness matrix of the structure and $\{U\}$ is the nodal displacement vector. The $[K]$ matrix is the assembly of the element stiffness matrices $[K]_j$, where:

$$[K]_j = \left(\frac{AE}{L}\right)_j \begin{bmatrix} c^2 & cs & -c^2 & -cs \\ cs & s^2 & -cs & s^2 \\ -c^2 & -cs & c^2 & cs \\ -cs & -s^2 & cs & s^2 \end{bmatrix}_j \tag{5.26}$$

The symbols s and c, respectively, stand for the sine and the cosine of the orientation angle of each $j-$element (spatial orientation of the $j-$member). For the two aforementioned approaches (method of joints and FEM) to coincide, it is necessary that only the impact of the orientation angles be present in the latter approach. This means that the stiffness constants $(AE/L)_j$ must become equal to one, or, equivalently, that each cross-sectional area must be equal to:

$$A_j = \left(\frac{L}{E}\right)_j \tag{5.27}$$

Let the design with cross-sections as defined in Eq.(5.27) be the 'Unit Stiffness Design' or USD. As shown in Section 5, the numerical results implied that, for the determinate trusses, initiating the proposed optimization procedure from the USD made the global optimum more likely to be found, while if a random initial design vector was used then local minima could be located instead. Consequently and for the needs of the present investigation, the USD was preferred to be the initial design vector for all of the examined cases.

5.2.5. Detecting active and passive elements

The optimality criterion stated in Eq.(5.10) is based on two assumptions, the former being that only one nodal displacement constraint is active at the optimum and the latter being that all structural members can affect the displacement field of the structure (active elements). However, it is not possible to ensure in advance the validity of these assumptions thus appropriate procedures must be developed if one or both of them are violated.

The redesign procedure described in Sections 5.2.2 and 5.2.3 is initiated from a design vector, let it be $\mathbf{A_{ini}}$. According to Section 5.2.2, if only the force products are considered, then all terms with $\left|F_i^P F_i^Q\right| \le tol$ (force-type criterion), with tol being an adequately small value, have negligible contribution to Eq.(5.3), thus the corresponding $i-$bars may be characterized as passive and since this characterization is based on a force-type criterion the term *force-passive* elements is justified. Equivalently, all $i-$bars with $\left|F_i^P F_i^Q\right| > tol$ are *force-active* elements. On the other hand, if only the cross-sections are considered, then members with a cross-sectional area A_i less than an adequately small value $A_{\min}$ (area-type criterion) have negligible contribution to the global stiffness matrix thus the corresponding $i-$bars may be characterized as passive and since this characterization is based on an area -type criterion the term *area-passive* elements is justified. Equivalently, all $i-$bars with $A_i > A_{\min}$ are *area-active* elements. Using the aforementioned criteria, if both the force products and the cross-sections are considered, a member may be:

- force-active and area-active: such members participate in the redesign procedure described in sections 5.2.2 and 5.2.3
- force-active and area-passive: such members participate in the redesign procedure, from which they obtain a cross-sectional area A_d smaller than $A_{\min}$; however, due to the imposed lower bound $A_{\min}$, it then becomes $A_d = A_{\min}$, which is acceptable since a larger than the necessary cross-section is attributed to the structural member
- force-passive and area-active: this interesting case is discussed in the next paragraph
- force-passive and area-passive: such members do not participate in the redesign procedure and the minimum cross-sectional area $A_{\min}$ is attributed to them

The force-passive/area-active members $\mathbf{A}_{pass-act}$ have the following characteristics:

C1) For the current iteration step, they cannot participate in the redesign procedure of Sections 5.2.2 and 5.2.3 (the numerator in Eq.(5.17) tends to zero), so they keep their cross-sectional value from the previous iteration step.

C2) They have a cross-sectional area larger than the minimum value $A_{\min}$, therefore if $A_{\min}$ is attributed to them the imposed displacement constraint will be violated. However, without loss of generality, it is possible to further reduce their cross-sectional value by using a line search scheme, such as the binary search (the reduction procedure may be continued as long as the imposed displacement constraint is not violated). Consequently, an optimization sub-problem is formulated.

According to (C2) above, the new optimization problem formulated is as follows:

$$\text{Minimize } \mathbf{A}_{pass-act} \tag{5.28a}$$

$$\text{with } \mathbf{A}_{pass-act} > A_{\min} \tag{5.28b}$$

$$\text{such that } \max|u| = U_{allow} \tag{5.28c}$$

If N_{pass_act} is the number of force-passive/area-active elements, then the solution space of the aforementioned optimization problem described in Eqs.(5.28a-5.28c) is the $R^{N_{pass\_act}}$ set. Generally speaking, a line search is described as $\vec{X}_{i+1} = \vec{X}_i + a\,\vec{d}$, where $\vec{X}$ denotes the design vector, $\vec{d}$ represents the search direction, a stands for the scalar step size and i is the current iteration. If $N_{pass\_act} = 1$ then the solution space is the $R-$set, the entire line search problem is scalar and a simple search along the line of the real positive numbers is adequate

to provide the optimum solution. However, if $N_{pass\_act} > 1$ then the optimum solution lies in a vector space and there are two choices:

1) Implement a Mathematical Programming (MP) method for solving the problem described in Eqs.(5.28a-5.28c). In this case, the initial optimization problem is divided into two parts, the first being solved with the proposed procedure and the second being handled by one of the many MP methods available in the literature. The advantages of this hybrid optimization scheme is that a final solution is indeed provided, while the computational time is generally less than that required when using the selected MP method for solving the entire problem (for the entire problem, the number of the design variables is NEL while for the problem in Eq.(5.28) there are only $N_{pass\_act} << NEL$ unknowns).
2) Perform a line search with *constant* search direction, that is a sort of uniform scaling applied to the force-passive/area-active elements, for solving the problem described in Eqs.(5.28a-5.28c). This approach is a compromise between using the design vector derived from the proposed procedure and using a MP method for solving the problem in Eqs.(5.28a-5.28c).

Based on the line of thoughts expressed in (1) and (2) above, it is a good choice to append to the proposed procedure an extra step of low computational cost in order to get an improved but only near optimum design if it is detected that the weight minimization problem at hand is non-singular displacement constrained. The use of a constant search direction is explained more analytically in the next Section.

5.2.6. Line search with a constant search direction

In a typical line search, noted as $\vec{X}_{i+1} = \vec{X}_i + a\,\vec{d}$, the scalar step size a and the search direction $\vec{d}$ are continuously updated until convergence is achieved. If the search direction $\vec{d}$ is kept constant, then the $R-$set becomes the solution space (1D optimization problem), which is nothing else but a uniform scaling of the corresponding design variables $\vec{X}$. For the problem at hand, the ultimate goal is to find such a step size a that reduces the vector $\mathbf{A}_{pass-act}$ without violating the imposed displacement constraint. To this end, any line search techniques can be used. In the present section the binary search was selected and the following procedure is proposed:

Step 1: Set the lower bound as $A_{pass-act,LowerBound,j} = A_{\min}$, where j counts all the force-passive/area-active elements

Step 2: Set the initial design vector as $\mathbf{A}_{pass-act}$

Step 3: while convergence is not achieved and the maximum number of iterations has not been exceeded

Step 3a: set $\mathbf{A}_{new,pass-act} = 0.5\left(\mathbf{A}_{pass-act,LowerBound} + \mathbf{A}_{pass-act}\right)$

Step 3b: calculate the 1-norm condition number of the global stiffness matrix $cond\left(\mathbf{K}_{glob}\right)$

Step 3c: If $cond\left(\mathbf{K}_{glob}\right) \in [LB,UB]$ then

carry out a Finite Element Analysis (FEA)

if $\max|u| > U_{allow}$ then $\mathbf{A}_{pass-act,LowerBound} = \mathbf{A}_{new,pass-act}$

else $\mathbf{A}_{pass-act} = \mathbf{A}_{new,pass-act}$

Step 3d: increase the iteration counter

Convergence is considered to have been achieved if $\left|\mathbf{A}_{new,pass-act} - \mathbf{A}_{pass-act}\right| \le tol\_1$, where tol_1 is a small positive number, say $1E-06$. The lower and upper bounds for the 1-norm

condition number of the global stiffness matrix are a small and a large quantity, respectively, say $LB = 1e-3$ and $UB = 1e20$. The limitation of the condition number of the global stiffness matrix ensures that the inverse of this matrix can be obtained thus a Finite Element Analysis, required for checking the maximum nodal displacement, can be carried out. Otherwise, an ill-conditioned matrix is formed and the entire procedure stalls. As in all iterative schemes, a counter is used to stop the procedure if a maximum number of iterations is exceeded.

5.2.7. Special case of a single load

There is a special case when a single load is applied to the structure and, at the optimum, the maximum displacement appears at the load application point and along the direction of the applied load. In more details, if there is only one external point load P, then, from Castigliano's second theorem (Appendix 5.A), it holds:

$$u = \sum_{i=1}^{NEL} \left(\frac{c_i b_i L_i}{A_i E_i} P \right) \tag{5.29}$$

where c_i represents the weighted contribution of the real load P to the axial force carried by the $i-$bar and b_i expresses the weighted contribution of the virtual unit load to the virtual axial force carried by the $i-$bar. If a virtual unit load is applied to the application point of load P, then, due to linearity, it holds:

$$b_i = \left(\frac{c_i}{P} \right) \tag{5.30}$$

The combination of the last two equations yields:

$$u = \sum_{i=1}^{NEL} \left(\frac{c_i^2 L_i}{A_i E_i} \right) \tag{5.31}$$

Eq.(5.31) suggests that each $i-$bar with $c_i \neq 0$ contributes increasingly to the displacement of the load application point. On the contrary, all bars with $c_i = 0$ have a zero contribution. Obviously, this is a very convenient situation because one does not have to worry about members with $c_i b_i < 0$ simply because there are no such members. Therefore, cases with a single load, where the maximum displacement at the optimum appears at the load application point, consist a special (convenient) class of problems that can 'hide' possible inefficiencies of an optimization procedure under evaluation since the thorn of members with $c_i b_i < 0$ is eliminated. Consequently, a 'fair-play' evaluation of a new optimization procedure should also include examples not falling in the aforementioned class of problems.

5.2.8. Sensitivity analysis

For a given topology and loading and under the assumption that all members are made of the same material, it holds (for the symbols used in Eq.(5.31)):

$$c_{il} = const \quad L_i = const \quad E_i = const \quad P_l = const \tag{5.32}$$

The quantities b_i depend on the application point of the virtual load, or, equivalently, on the position of the node for which the displacement is sought. Without loss of generality, it holds:

$$u = f\left(b_i, A_i\right) \tag{5.33}$$

From Eq.(5.17) it is obvious that the nodal displacement u is a continuous function in cross-sectional areas and a discontinuous (discrete) function on the application points of the virtual load, since these points are discrete and depend on the topology of the truss. Therefore, for the location of an extremum in nodal displacement with respect to the continuous variables A_i, it must hold:

$$\frac{\partial u}{\partial A_i} = 0 \tag{5.34}$$

or, equivalently, after basic manipulations of Eq.(5.29):

$$\frac{\partial u}{\partial A_i} = -\left(\frac{b_i L_i}{A_i^2 E_i}\right)\sum_{l=1}^{m} c_{il} P_l = 0 \tag{5.35}$$

It is obvious that Eq.(5.34) is true for any value of A_i if $b_i = 0$ or $\sum_{l=1}^{m} c_{il} P_l = 0$; that is when the contribution of the virtual load to the $i-$bar is zero or when the member force of the $i-$bar is zero.

5.3. Numerical approach

5.3.1. The proposed procedure

The proposed procedure, that minimizes the weight of a 2D skeletal structure under a single displacement constraint, is as follows:

Step 1: Estimate the Unit Stiffness Initial Design (U.S.I.D.) for the structure under examination.

Step 2: Carry out a Finite Element Analysis (FEA) using the real loads.

Step 3: Based on the results of Step 2, find the maximum nodal displacement $u_{\max,u}$ and trace the elements with $|F_i| > tol$ (temporarily active elements).

Step 4: Perform a uniform scaling of the temporarily active elements with a scaling coefficient $\left(U_{allow} / u_{\max,u}\right)$ and attribute the minimum cross-sectional value $A_{\min}$ to the other elements.

Step 5: Apply Steps 6-14 iteratively until converge is achieved or the maximum iteration number is exceeded.

Step 6: Carry out a (FEA) using a virtual unit load applied to the degree of freedom corresponding to the displacement $u_{\max,u}$.

Step 7: Categorize the structural elements using the force-criterion and the area-criterion (Section 5.2.5) into force-active/area-active, force-active/area-passive, force-passive/area-active and force-passive/area-passive.

Step 8: For the force-active/area-active elements, apply the redesign procedure described in Section 5.2.2; that is:

Step 8a: For each such element, calculate the virtual strain energy density w_i using Eq.(5.11).

Step 8b: For all such elements, estimate the mean value $\overline{w}$ using Eq.(5.12).

Step 8c: For each such element, redesign the cross-sectional areas using Eq.(5.17).

Step 8d: Carry out a FEA and estimate the maximum nodal displacement.

Step 8e: Perform a Uniform Scaling using Eqs.(5.21, 5.24)

Step 9: For the force-passive/area-active elements, apply the redesign procedure described in Section 5.2.3; that is:

Step 9a: For all such elements, test whether the lower bound $A_{\min}$ for the design variables may be attributed; if not proceed with Step 9b

Step 9b: Using a binary search in combination with a FEA, find the shrinking factor that may be applied to the force-passive/area-active elements without causing any displacement violations

Step 10: For the force-active/area-passive and the force-passive/area-passive elements, attribute the lower bound for the design variables

Step 11: If a new cross-sectional area $A_{i,new}$ derived from Steps 9-10 is less than $A_{\min}$ then set $A_{i,new} = A_{\min}$

Step 14: Return to Step 6 unless convergence with respect to both the structural weight and the maximum change in any design variable has been achieved (see next Section 5.3.2); if the maximum number of iterations has been exceeded, terminate the procedure with a corresponding message

Step 15: Present results in a report form

5.3.2. Convergence criteria

Following Rozvany, for the convergence of the proposed optimization procedure two criteria were introduced. According to the first criterion, convergence is considered to have been achieved if the change in the total structural weight is less than a predefined tolerance tol_{C1}:

$$\frac{\left|W_{new} - W_{old}\right|}{W_{old}} \le tol_{C1} \tag{5.36}$$

According to the second criterion, convergence is considered to have been achieved if the maximum change in any of the design variables is less than a predefined tolerance tol_{C2}:

$$\max\left\{\frac{\left|A_{i,new} - A_{i,old}\right|}{A_{i,old}}\right\} \le tol_{C2} \tag{5.37}$$

Generally speaking, if a relatively high tolerance value is chosen then the iterative procedure is terminated quite soon thus not allowing for any convergence difficulties to be revealed. In order to avoid such a situation, in the present chapter it was set $tol_1 = tol_2 = 1E-15$, unless differently stated. This is a very low tolerance value which guarantees that a normal termination of the optimization procedure corresponds to a true convergence.

5.3.3. Evaluation of results

In order to evaluate the proposed procedure, an extended set of examples was investigated, each one of which was handled as follows:

Step E1: Data retrieval from the literature. If an optimum design vector was available, its validity was tested by carrying out a FE analysis and by checking whether any displacement violations occurred.

Step E2: Solution of the optimization problem using the Matlab SQP optimization routine (fmincon), initiating the procedure from 100 different and random design vectors and for each successful run recording the number of iterations, the number of objective function evaluations (thus equal number of FE analyses), the minimum structural weight and the optimum design vector. However, this step was skipped for those case studies where an exact analytical solution was available.

Step E3: Solution of the optimization problem using the proposed optimization procedure, initiating the procedure from a design vector corresponding the Unit Stiffness Design and recording the number of iterations, the number of FE analyses, the minimum structural weight and the optimum design vector. Furthermore, the convergence history with respect to the convergence criteria described in Section5.3.2 was recorded and plotted in a semi-log diagram.

Step E4: Solution of the optimization problem using the proposed optimization procedure, initiating the procedure from 100 different and random design vectors (*not* corresponding to the Unit Stiffness Design) and recording the number of iterations, the number of FE analyses, the minimum structural weight and the optimum design vector.

At this point, it is clarified that the set of 100 runs mentioned in Step E2 aimed at increasing the probability of locating the global optimum design, while the set of 100 runs mentioned in Step E4 aimed at investigating the influence of the initial design vector on tracing the optimum.

5.4. Examples

For the evaluation of the proposed optimization procedure, various examples, both from the literature and newly introduced in the present chapter, were investigated. The examples were divided into two large groups. In the first group, four different *indeterminate* trusses, some of them with variations, were optimized, namely the 3-bar truss (three variations), the 5-bar truss, the 56-bar truss (two variations) and a typical ground structure for the MBB beam (two different mesh densities); that is a subtotal of eight cases. In the second group, three different *determinate* trusses, some of them with variations, were optimized, namely the 5-bar truss, the MBB beam (five variations with three mesh densities each) and the 9-bar truss (six variations under four different load cases each); that is a subtotal of 40 cases.

At this point, it is clarified that the five determinate aforementioned variations for the MMB beam are the well-known Pratt, Howe, Warren, Baltimore and K-truss designs (Beer and Johnston, 1988). In accordance to the ‘fair-play’ suggestion of Section 5.2.7, the 9-bar truss was created based on the well-known 10-bar truss.

Taking into consideration all of the topological and loading variations, a grand total of 48 cases was investigated, while all the results were properly arranged in Tables and Figures.

5.4.1. Indeterminate truss topologies

5.4.1.1. Case study: 3-bar truss (case Bar3_A)

This example was retrieved from (Morris, 1982). The truss consists of three bars having the topology shown in Fig.5.1a. It is assumed that all bars are made of the same material having Young's modulus equal to $E = 1e7\,psi$ and weight density equal to $\rho = 0.1lb/in^3$. Only node 4 is externally loaded with a vertical load component P_y and a horizontal load component P_x equal to $10000lbs$ each, while the nodal displacement must not be greater than $0.005in$, along either the horizontal or the vertical direction. The lower bound for the cross-sectional area was set equal to $A_{\min} = 0.1in^2$.

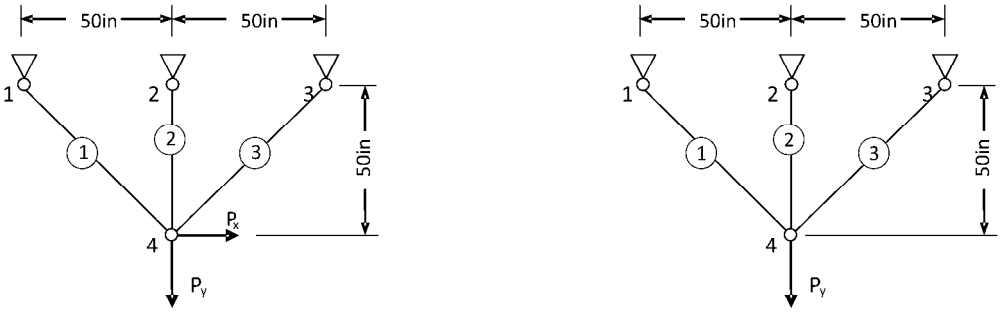

Figure 5.1: Topology for the case of (a) Bar3_A and (b) Bar3_B

5.4.1.2. Case study: 3-bar truss (case Bar3_B)

Another 3-bar indeterminate truss is found in (Rozvany and Zhou, 1991). The truss consists of three bars having the topology shown in Fig.5.1a. It is assumed that all bars are made of the same material having Young's modulus equal to E and weight density equal to ρ. Node 4 is externally loaded only with a vertical load component P_y, while the vertical nodal displacement is constrained. For this problem, a non-dimensional approach is adopted (Rozvany and Zhou, 1991), according to which each design variable is denoted as:

$$\tilde{z}_i = \left(\frac{z_i \, E \, U_{allow}}{P_y \, L_y} \right) \tag{5.38}$$

while the non-dimensional notation for the minimum weight is:

$$\tilde{\Phi}_s = \left(\frac{\tilde{\Phi}_s \, E \, U_{allow}}{P_y \, L_y^2} \right) \tag{5.39}$$

In Eqs.(5.38, 5.39), additionally to the symbols used earlier in the text, U_{allow} is the imposed displacement constraint and L_y is the length of the middle bar. There are two variations for this problem, the former letting the design variables unconstrained and the latter imposing to them a lower non-dimensional bound equal to $\tilde{z}_a = 0.06$. For both variations, apart from the numerical approximation of the optimal design, there exists an exact analytical estimation as well.

5.4.1.3. Case study: 5-bar truss (case Bar5_A)

This problem is found in (Patnaik et al, 1995, Patnaik et al, 1998) in many variations. According to one of the indeterminate variations, the topology is the one shown in Fig.5.2a, only node 4 is externally loaded with a vertical load component $P_y = 100kips$, while the vertical displacement along the $y-$direction must be at most equal to $2.0in$. Since it is not referred in (Patnaik et al, 1995, Patnaik et al, 1998) whether a lower bound for the cross-sectional areas exists, a challenging very low bound was set ($A_{\min} = 1e-12in^2$). It is also noted that a Young's modulus equal to $E = 10000ksi$ and a weight density equal to $\rho = 0.1lb/in^3$ were attributed to all bars.

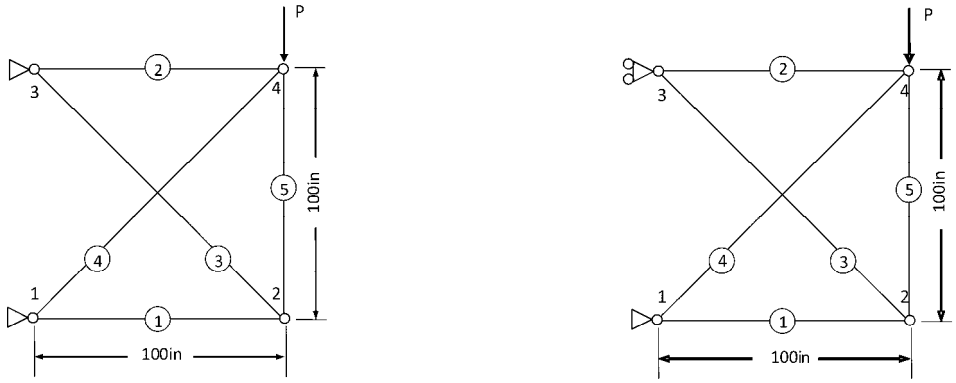

(a) (b)

Figure 5.2: Topology of the 5-bar truss: (a) indeterminate and (b) determinate variation

5.4.1.4. Case study: 56-bar truss (case Bar56)

The parametric formulation of this optimization problem, along with its analytical solution, is found in (Rozvany and Zhou, 1991).

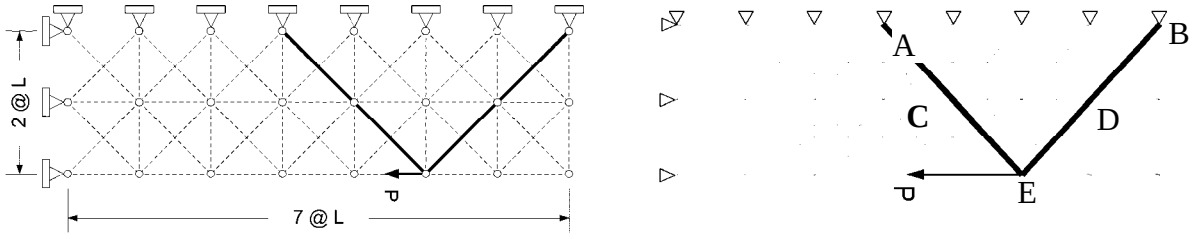

(a) (b)

Figure 5.3: (a) 56-bar truss (thick lines: remaining members, dashed lines: vanishing members) and (b) variation using a structural universe with 276 bars (thick lines: remaining members, thin lines: vanishing members)

The main objective is to minimize the weight of a 56-bar structure such that a transverse load is transmitted to the given rigid foundation without violating the imposed displacement constraint. The initial topology of the truss and the exact optimal layout are presented in Fig.5.3a. A variation of this problem found in (Rozvany, 1992) concerns the implementation of a structural universe with 114 members, which results from the same grid of (3×8) nodes as the one shown in Fig.5.3a. Instead of optimizing this case, as more challenging, the structural universe with 276 bars shown in Fig.5.3b was selected. This variation is presented in Section 5.1.4.

5.4.1.5. Case study: The MBB beam

The formulation of the weight minimization of the MBB beam can be found in (Nha Chu et al, 1997) and is illustrated in Fig.5.4a. The length L and the height H of the simply supported beam are $2400mm$ and $400mm$, respectively. The beam is assumed to be made of a material with a Young's modulus $E = 200GPa$ while the externally applied point load is $20kN$ acting at the middle of the top edge. The maximum allowable displacement is $9.4mm$.

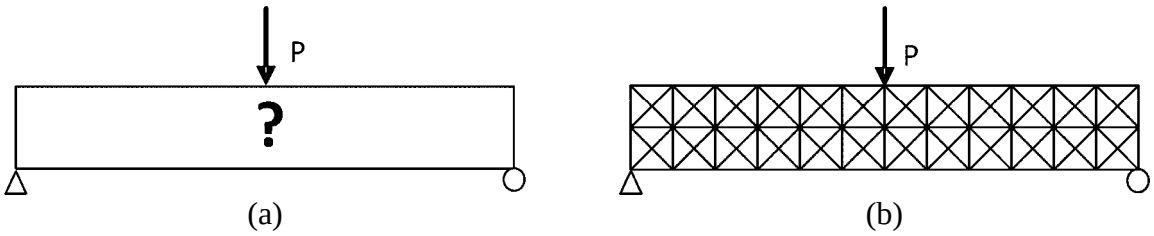

Figure 5.4: (a) Design domain and (b) typical indeterminate design for the MBB beam

An indeterminate ground structure for the domain of Fig.5.4a is shown in Fig.5.4b, where the ratio of the length of any vertical element over the length of any horizontal element is equal to one. The selection of this aspect ratio was based on (Provatidis and Venetsanos, 2003), according to which the discretization of the MBB domain, with ground structures of unit aspect ratio, leads to layouts of minimum weight.

5.4.2. Determinate truss topologies

5.4.2.1. Case study: 5-bar truss

The determinate variation of this problem is found in (Patnaik et al, 1995), according to which only node 4 is externally loaded with a vertical load component $P_y = 100kips$, while the vertical displacement along the $y-$direction must be at most equal to $2.0in$. As far as the support is concerned, it is referred in (Patnaik et al, 1995) that node 3 obtains a roller restraining the horizontal displacement and node 2 is loaded with $P_y = 100kips$. However, such a configuration results in optimal designs significantly different than those described in (Patnaik et al, 1995) (the application of the Matlab routine fmincon converges to a minimum weight equal to approximately $80lb$ while according to (Patnaik et al, 1995), the optimum weight is approximately $45lb$). Nevertheless, if the load is applied to node 4 and not to node 2 then weights similar to those found in (Patnaik et al, 1995) are obtained. Therefore, the second variation of the 5-bar truss examined in the present section is the one illustrated in Fig.5.2b. Since it is not referred in (Patnaik et al, 1995) whether a lower bound for the cross-sectional areas exists, a challenging very low bound was set ($A_{\min} = 1e-12in^2$). It is also noted that, for both variations, the same material properties (Young's modulus equal to $E = 10000ksi$ and weight density equal to $\rho = 0.1lb/in^3$) were attributed to all bars.

5.4.2.2. Case study: The MBB beam

In this case, the examined design domain was discretized using five typical determinate designs, namely the Baltimore, the Howe, the K-truss, the Pratt and the Warren design (Beer and Johnston, 1988), as shown in Fig.5.5b-5.5f.

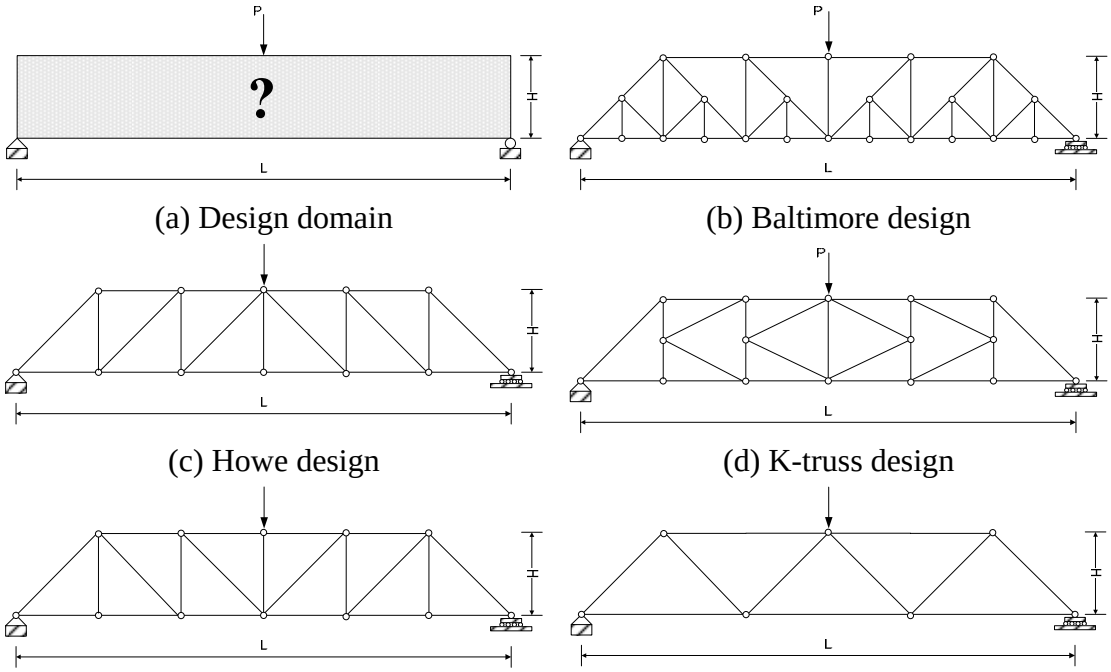

Figure 5.5: Design domain and typical determinate truss designs for the MBB beam

For each design, three different mesh densities, thus different number of elements and number of nodes, were used (Table 5.1). Apart from the discretization, all the other data concerning the problem formulation is the same with that of Section 4.1.5.

Table 5.1: Data for the determinate designs of the MBB beam

Variation		DESIGN				
		Baltimore	Howe	K-truss	Pratt	Warren
#1	*Elements*	*29*	*13*	*17*	*13*	*11*
	Nodes	16	8	10	8	7
#2	*Elements*	*45*	*21*	*29*	*21*	*19*
	Nodes	24	12	16	12	11
#3	*Elements*	*61*	*29*	*41*	*29*	*27*
	Nodes	32	16	22	16	15

5.4.2.3. Variations of the 9-bar determinate truss

The 9-bar determinate truss is derived from the 10-bar truss (Fig.5.8a), where one hinge is replaced by a roller and one bar is removed (Fig.5.8b). This structure may be considered as a ground structure of a 2D cantilever domain.

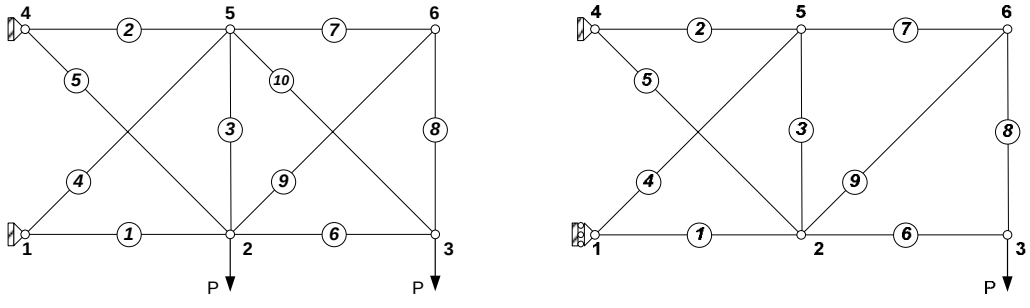

Figure 5.6: (a) Original description and (b) a determinate variation of the 10-bar truss

Ten bars taken in sets of nine give ten different trusses, as described in Table 5.2, where the original topology of the 10-bar truss (Fig.5.8a) has been used as a reference for numbering the bars. Four out of the ten aforementioned topologies are not rigid thus they give either an ill-conditioned (Table 5.2, designs 9f and 9g) or a singular stiffness matrix (Table 5.2, designs 9i and 9j). Consequently, these designs were not examined.

Table 5.2: Possible topologies of the 9-bar truss (reference: Fig.5.8a)

Design	Remaining elements x_i, $i=1,2,\ldots,9$								
9a	1	2	3	4	5	6	7	8	9
9b	1	2	3	4	5	6	7	8	10
9c	1	2	3	4	5	6	7	9	10
9d	1	2	3	4	5	6	8	9	10
9e	1	2	3	4	5	7	8	9	10
9f	1	2	3	4	6	7	8	9	10
9g	1	2	3	5	6	7	8	9	10
9h	1	2	4	5	6	7	8	9	10
9i	1	3	4	5	6	7	8	9	10
9j	2	3	4	5	6	7	8	9	10

In the present section, the four load cases described in Table 5.3 were examined.

Table 5.3: Loads in kips used for the 9-bar determinate truss

Force component	Load cases			
	#1	#2	#3	#4
F2,y	-100	-100	0	-150
F3,y	-100	0	-100	-150
F5,y	0	0	0	50
F6,y	0	0	0	50

5.5. Results

5.5.1. Indeterminate trusses

5.5.1.1. Case study: 3-bar truss (case Bar3_A)

The convergence history of the proposed optimization procedure is shown in Fig.5.9. The cost function (structural weight) is normalized with respect to the maximum cost function value and the convergence history of this normalized quantity is illustrated in Fig.5.9a.

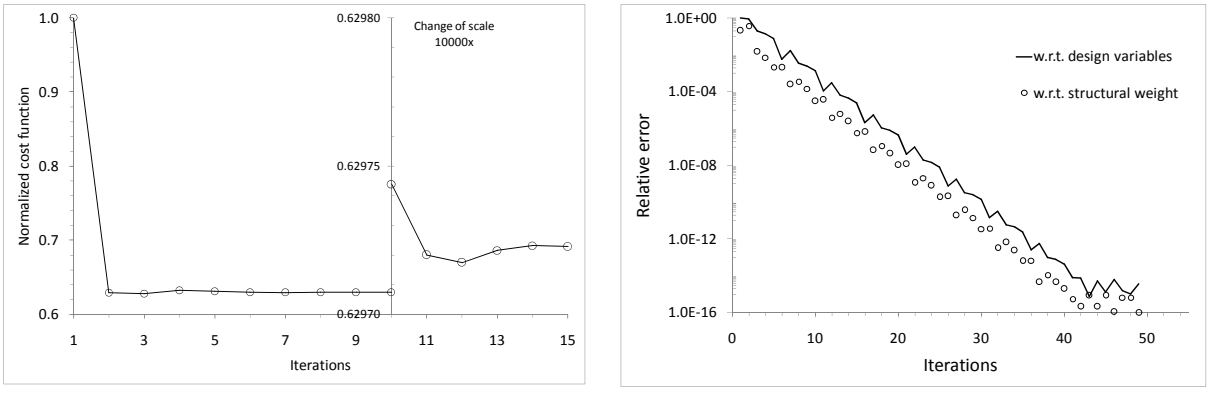

(a) (b)

Figure 5.7: Convergence history for the case Bar3_A with respect to (a) the normalized cost function ($tol = 1E-6$) and (b) the relative errors ($tol = 1E-16$)

From this figure, as the part of the plot after the change of scale suggests, after 10 iterations, an accuracy of the normalized cost function of four significant digits is achieved. For a termination tolerance on the function value equal to $1E-6$, 15 iterations are required for the optimum design to be found. Furthermore, the convergence history of the criteria mentioned in Section 5.2 are shown in Fig.9b, for $tol_1 = tol_2 = 1E-16$ as defined in Eqs.(5.36, 5.37). From this figure, it is clear that within the first ten iterations, the proposed procedure achieves a relative error of 0.01% between two successive optimal designs. Furthermore, for the next iterations, the relative error drops almost in the same rate, as the slope in the corresponding semi-log plot suggests, while a total of less than 50 iterations were required for a relative error of $1E-16\%$, with respect to the structural weight, to be achieved.

In (Morris, 1982) and from the tables presenting results per iteration for the specific problem, it can be found that, among various recursive equations for the cross-sectional redesign and the Lagrange multiplier estimation, the best converging performance requires five iterations but corresponds to an accuracy of $1E-1$ with respect to the structural weight. For such an accuracy, the proposed optimization procedure converges after three iterations only and provides the optimal design presented in Table 5.4 and in the column 'Convergence accuracy similar to Reference'. This design is 0.1533% heavier than the one referred in (Schmit, 1960) and it causes a per cent relative constraint violation of less than $2.2E-3$, while the design in (Morris, 1982) causes a per cent relative constraint violation of $2.6E-2$ (that is of one order higher).

Data corresponding to optimal designs are presented in Table 5.4. More particularly, in this Table, the values for the cross-sectional areas and for the minimum structural weight, shown in the column 'Reference' were retrieved from (Morris, 1982) with the appearing number of significant digits. The nodal displacements shown in italics were obtained from a FE analysis using the cross-sectional areas from the specific reference. For these areas, the imposed displacement constraint is violated by 0.026%, which is considered as negligible. Furthermore, with these areas the minimum structural weight is $113.6498 lbs$, which, when truncated upwards gives $113.7 lbs$; that is, the value in (Morris, 1982). Consequently, this literature reference is reliable and can be used as a basis for comparison. The column 'SQP' corresponds to the optimal solution found with the SQP routine embedded in Matlab (routine fmincon). The next four columns correspond to results obtained using the proposed optimization procedure and for various situations, as the column titles describe.

Table 5.4: Optimum design for the 3-bar truss (case: Bar3_A)

	Reference	SQP	Present paper			
			Unit Stiffness Design (accuracy:1E-15)	Random Initial Design (accuracy:1E-15)	Convergence accuracy similar to 'Reference'	Convergence accuracy similar to 'SQP'
x_1 [in^2]	15.07	1.50739210E+01	1.50739218E+01	1.80509258E+01	1.52563007E+01	1.50739148E+01
x_2 [in^2]	0.1	1.00000000E-01	1.00000000E-01	3.41640786E+00	1.00000000E-01	1.00000000E-01
x_3 [in^2]	0.9318	9.31786600E-01	9.31786205E-01	3.90879015E+00	7.77238782E-01	9.31793251E-01
U_{4x} [in]	*5.0013E-03*	5.00000014E-03	5.00000001E-03	5.00000000E-03	5.00010978E-03	4.99999999E-03
U_{4y} [in]	*-4.3423E-03*	-4.34112802E-03	-4.34112766E-03	-2.23606798E-03	-4.23037756E-03	-4.34113197E-03
min W [lbs]	113.7	113.67744382	113.67744668	172.36067977	113.87424499	113.67744718

With respect to the SQP procedure and in order to get a representative behavior, the fmincon routine was initiated from 100 random and different initial design vectors. Using a termination tolerance on the function value equal to $1E-6$ and a termination tolerance on the constraint violation equal to $1E-6$, the fmincon routine converged in all cases to the same

design (column 'SQP' in Table 4). Depending on the initial design vector, it required from 8 to 18 iterations (45 to 95 evaluations of the objective function thus equal number of FE analyses) until convergence was achieved. For a relative error, as defined in Eq.(5.36) and Eq.(5.37), equal to $1E-6$, the proposed procedure converged after 15 iterations (32 FE analyses) to a design agreeing with the SQP best design in 8 significant digits (Table 5.4**,** column 'Convergence accuracy similar to SQP').

With respect to the selection of the initial design vector, the comparison between the columns 'Unit Stiffness Design' (USD) and 'Random Initial Design' (RID) in Table 5.4 suggests that a vector corresponding to the former design should be used; otherwise, most probably a local minimum will be reached. To check the validity of this statement, the proposed procedure was initiated from 100 random and different design vectors, none of which corresponded to the (USD). In all cases, the procedure converged, after a different number of iterations, to the same design vector (the one presented in Table 4 in the column 'Random Initial Design'). Furthermore, if one estimates the virtual strain energy density (VSED) distribution for the USD-optimum design and the RID-optimum design, respectively, it will yield that in both cases a *uniform* distribution over the active structural part has been achieved (for the USD case, the mean value of (VSED) is $4.67e-6$ and the corresponding % Coefficient of Variation is $9.94e\text{-}4$, while for the RID case it is $3.63e-6$ and $4.35e-4$, respectively). However, there is a difference concerning the active structural part. For the RID-optimum design, all of the structural elements have a non-minimum cross-sectional area, in opposition to the USD-optimum design where the cross-sectional area of one structural element is equal to the imposed lower bound. This difference is due to the fact that if an external load vector is applied to a USD structure then the structural response is entirely governed by the *topology* of the structure (insensitivity to the element size). It is in such a case that the element participation in the structural response should be determined as active or passive. Otherwise, the route of the optimization procedure may deviate, being affected significantly by the structural sensitivity to the element size, and may lead to suboptimal solutions.

5.5.1.2. Case study: 3-bar truss (case Bar3_B)

The results obtained using the proposed optimization procedure are presented in Table 5.5. It is clarified that for both cases (without and with lower bounds), it was set $tol_1 = tol_2 = 1E-12$ as defined in Eqs.(5.36, 5.37), while for the former case it was also set $\tilde{z}_{i,\min} = 2.0E-15$.

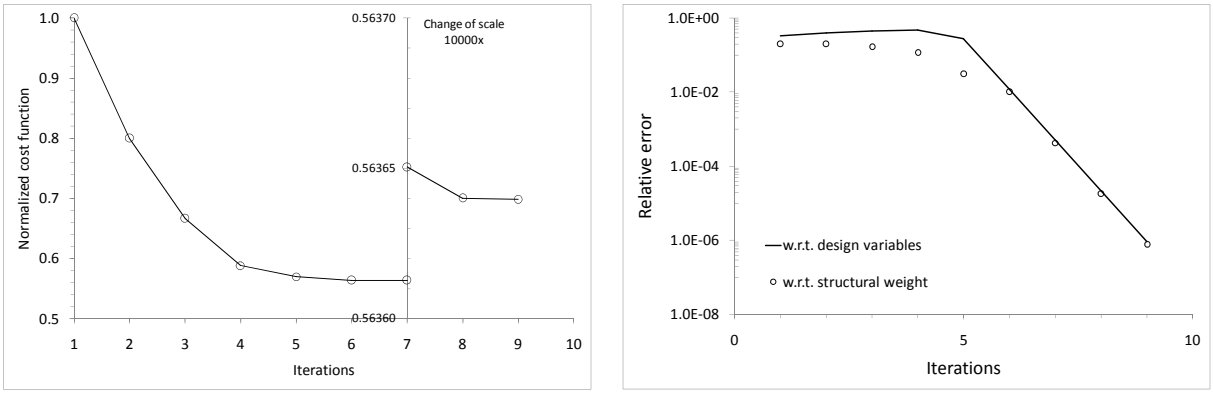

(a) (b)

Figure 5.8: Convergence history for the case Bar3_B (with lower bounds) with respect to (a) the normalized cost function and (b) the relative errors

Furthermore, for the aforementioned tolerance adjustments, the proposed optimization procedure required 14 and 30 iterations for the cases with and without lower bounds, respectively, until convergence was achieved. However, for $tol_1 = tol_2 = 1E-6$, which is still a very strict tolerance, it required 9 and 20 iterations, respectively. In (Rozvany amd Zhou, 1991), it is not explicitly stated how many iterations were required for convergence; a relative plot shows tendency to convergence after 6 and 9 iterations, respectively. Concerning the convergence history, it is obvious that a smooth convergence is achieved for the case when lower bounds are imposed on the design variables (Fig.5.10), both with respect to the normalized cost function and the relative errors (as in the previous example, the cost function is normalized with respect to the maximum cost function value obtained during the optimization procedure). In more details, from Fig.5.10a, seven iterations are enough for an accuracy of the normalized cost function of four significant digits to be achieved, as the part of the plot after the change of scale suggests. Furthermore, from Fig.5.10b, it is clear that the relative errors follow approximately the same descending path.

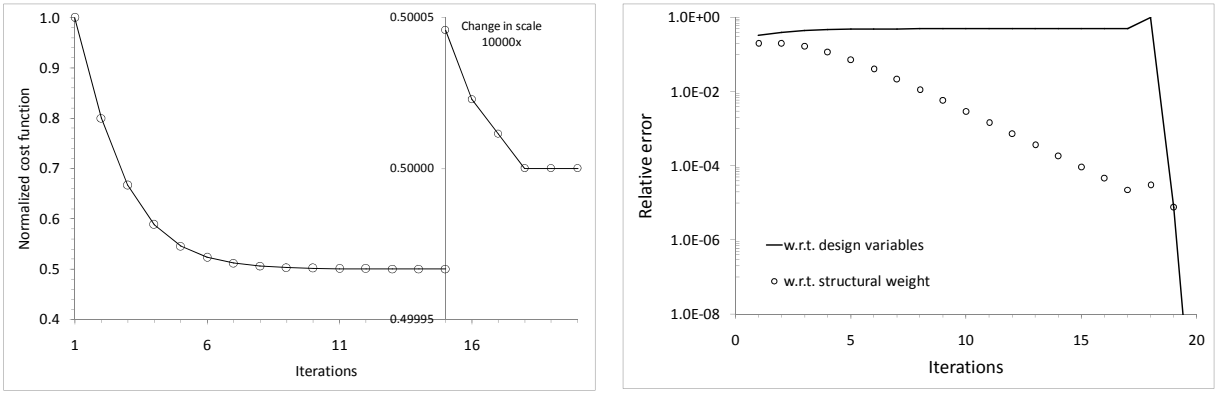

(a) (b)

Figure 5.9: Convergence history for the case Bar3_B (without lower bounds) with respect to (a) the normalized cost function and (b) the relative errors

With respect to the case where the design variables are left unconstrained, the normalized cost function (Fig.5.11a) presents a smooth convergence, while an accuracy of four significant digits is achieved after 15 iterations. Furthermore, the relative error with respect to the structural weight presents an approximately constant rate as the semi-log plot in Fig.5.11b suggests. On the contrary, the relative error of the maximum changes in the design variables (Fig.5.11b) does not vary significantly during the largest part of the optimization procedure but it suddenly drops to the converging tolerance value. The same behavior, thus not shown, is recorded for $tol_1 = tol_2 = 1E-12$. Results for the specific case are presented in Table 5.5.

Table 5.5: Optimum design for the 3-bar truss (case: Bar3_B with two variations)

Normalized variables	Reference		Present paper			
	No lower bound	With lower bound	Unit Stiffness Design (no lower bound)	Random Initial Design (no lower bound)	Unit Stiffness Design (with lower bound)	Random Initial Design (with lower bound)
z_1	0.00	0.06	1.00000000E-13	1.00000000E-13	6.00000000E-02	1.32936075E+00
z_2	1.00	1.00	1.00000000E+00	1.00000000E+00	9.57573593E-01	6.00000000E-02
z_3	0.00	0.06	1.00000000E-13	1.00000000E-13	6.00000000E-02	1.32936076E+00
U_{4x}	0.00	0.00	0.00000000E+00	0.00000000E+00	0.00000000E+00	4.38556657E-09
U_{4y}	-1.00	-1.00	-1.00000000E+00	-1.00000000E+00	-9.999999999998E-01	-9.999999953548E-01
min W	1.0000000	1.1272792	1.0000000000003	1.0000000000003	1.127279221	3.820000019

As easily seen, for the case with no lower bounds, the proposed optimization procedure does find the global minimum when the initial design vector corresponds to the USD (agreement with the exact solution of 13 significant digits). Furthermore, experimentation with 100 random and different initial design vectors did not result in any other but the global optimum solution. For the case where a lower bound for the design variables exists, the global minimum was also found in an agreement of 8 significant digits, when the proposed optimization procedure was initiated from a design vector corresponding to the USD. However, experimentation with random initial vectors revealed that it is possible to get trapped to a significantly suboptimal design, more than 3 times heavier than the optimal one (last column in Table 5.5). It is noted that, for the specific case study, the SQP approach was not applied since an exact analytical optimal solution was available in the literature.

5.5.1.3. Case study: 5-bar truss indeterminate variation Bar5_var1)

With respect to the evaluation of the literature data, the optimum design referred in (Patnaik et al, 1995) was used for a FE analysis, which showed that the displacement constraint is violated by 0.439%. This is considered to be a rather non-negligible violation thus the corresponding design vector may be accepted with reservation as an optimum one. With respect to the application of the Matlab routine, 100 analyses initiating from different design vectors converged to the same optimum design vector (the one described in Table 5.6, column 'SQP'), requiring from 10 to 20 iterations (83 to 202 evaluations of the objective function thus equal number of FE analyses). For the optimization with the Matlab routine, the termination tolerance on the function value was set equal to $1E-6$ and the termination tolerance on the constraint violation was set equal to $1E-6$. Based on these results, it is considered that the aforementioned optimum found with SQP is the global one.

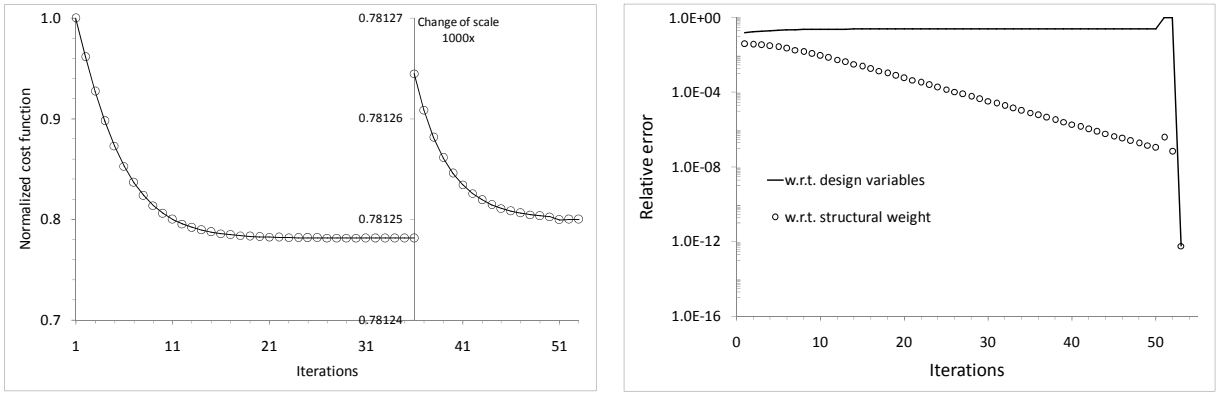

(a) (b)

Figure 5.10: Convergence history for the 5-bar indeterminate truss with respect to (a) the normalized cost function and (b) the relative errors

With respect to the application of the proposed optimization procedure, initiating from the vector corresponding to the Unit Stiffness Design a convergence was achieved after 53 iterations. It is noted that for this case, the tolerances defined in Eqs.(5.36, 5.37) were set equal to $tol_1 = tol_2 = 1E-12$, while different tolerance values affect significantly the convergence behavior (e.g. for $tol_1 = tol_2 = 1E-6$, 32 iterations (64 FE analyses) are required). The convergence history for $tol_1 = tol_2 = 1E-12$ is illustrated in Fig.5.12, from which it is seen that the convergence with respect to either the normalized cost function or the relative error of the structural weight is smooth. On the contrary, convergence with respect to the maximum change in the design variables is achieved in an abrupt way. The optimum

design vector obtained with the proposed procedure (Table 5.6, column 'USD') results in a structural weight which differs from the one obtained with the Matlab routine (Table 6, column 'SQP') in the tenth decimal digit. Finally, extended experimentation on initiating the proposed optimization procedure from a random design vector (100 runs) did not give other than the aforementioned optimum design (last column in Table 5.6).

Table 5.6: Optimum design for the 5-bar indeterminate truss

	Reference	SQP	Present paper	
			Unit Stiffness Design (accuracy:1E-12)	Random Initial Design (accuracy:1E-12)
x_1 [in^2]	0.001	9.999999995186E-13	1.000000000000E-12	1.000000000000E-12
x_2 [in^2]	1.475	1.500000008427E+00	1.499999999999E+00	1.499999999999E+00
x_3 [in^2]	0.001	9.999999990372E-13	1.000000000000E-12	1.000000000000E-12
x_4 [in^2]	2.124	2.121320337564E+00	2.121320343559E+00	2.121320343559E+00
x_5 [in^2]	0.001	9.999999998731E-13	1.000000000000E-12	1.000000000000E-12
U_{4x} [in]	*0.677684*	6.666666629209E-01	6.666666666667E-01	6.666666666667E-01
U_{4y} [in]	*-2.008781*	-2.000000000022E+00	-2.000000000000E+00	-2.000000000000E+00
min W [lbs]	44.817	44.9999999995132	45.0000000000155	45.0000000000155

5.5.1.4. Case study: 56--bar truss (case Bar56)

Using the same nondimensionalization as in Bar3_B and letting the design variables unconstrained (theoretically assuming $\tilde{z}_i \to 0$ and practically setting $\tilde{z}_{i,\min} = 1E-12$), the exact optimal structural weight is $\tilde{\Phi}_s = 16$ (Rozvany and Zhou, 1991). According to (Rozvany and Zhou, 1991), the iterative COC optimization method yielded after 126 iterations a weight of $\tilde{\Phi}_s = 16.000000000048$, which agrees with the exact optimal solution in twelve significant digits. The exact optimal layout is a clear four-member structure (Fig.5.3b). Furthermore, in the COC optimal design all non-optimal members take on the prescribed minimum cross-section, apart from two members which take a value very close but not equal to the prescribed lower bound. However, according to (Rozvany and Zhou, 1991), since the ratio of the cross-sectional area of these members over the imposed lower bound does not depend on the value of the prescribed lower bound, it is indicated that these members also vanish as $\tilde{z}_i \to 0$. For the specific problem, the Matlab routine had a hard time locating the global optimum. More particularly, persisting numerical instabilities led to adopting the less strict lower bound of $\tilde{z}_{i,\min} = 1E-8$, while the termination tolerance on the function value and the constraint violation were kept equal to $1E-6$. Even with these adjustments, frequently enough an ill-conditioned matrix was formed forcing the termination of the optimization procedure. Consequently, the set of 100 runs was not applied in this case. Instead, several analyses took place, out of the successful ones the best design vector, presented in Table 5.7 (column 'SQP') in non-dimensional notation was derived after 85 iterations and 5542 evaluations of the objective function (thus equal number of FE analyses). The corresponding nondimensional optimal weight agrees with the exact analytical one in six significant digits. However, it is strongly emphasized that apart from the group of these four non-vanishing members and the group of the members clearly taking on the minimum cross-sectional area, there was another group whose members had a near-vanishing cross-section. In other words, the SQP did not result in a clear four-member optimum structure.

Attacking the 56-bar problem with the proposed optimization procedure and using as initial design vector the one corresponding to the Unit Stiffness Design, an optimal layout was derived after 61 iterations. As Fig.5.13a indicates, the convergence history of the proposed

optimization procedure with respect to the cost function $\tilde{\Phi}_s$ is very smooth and gets stabilized approximately after half the number of iterations required for normal termination of the procedure. Furthermore, the convergence history with respect to the relative error of the cost function (Fig.5.13b) presents a general decreasing trajectory, even though discontinuities do appear. In order to trace the cause of these discontinuities, the proposed optimization procedure was closely monitored. It was found out that the iterations for which valleys occurred corresponded to iterations for which Step 9a (Section 5.1; treatment of force-passive/area-active elements) was activated. That is, when force-passive/area-active elements turned into force-passive/area-passive elements thus changing the number of the 'fully passive' elements.

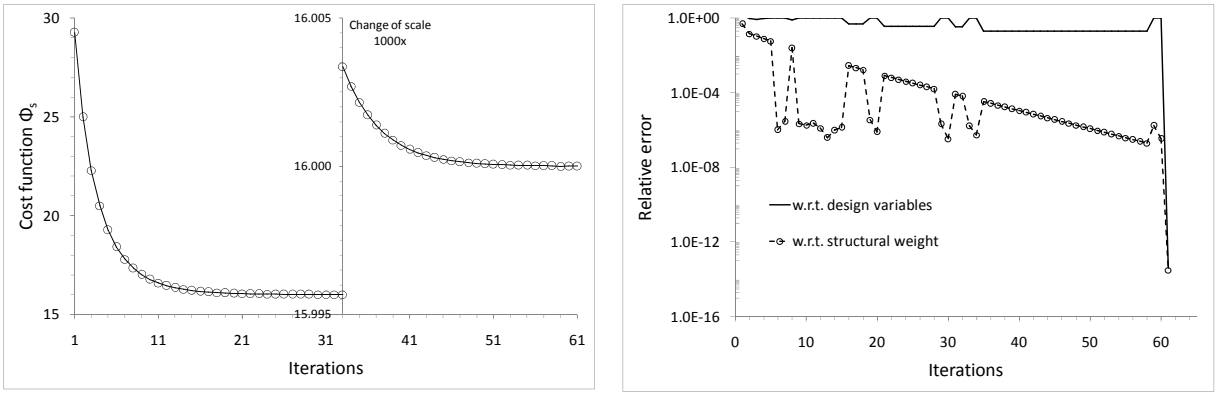

(a) (b)

Figure 5.11: Convergence history of the proposed optimization procedure for the 56-bar truss with respect to (a) the cost function and (b) the relative error

With respect to the convergence history of the maximum change in the design variables (Fig.5.13b), it is evident that it does not follow a clear decreasing tendency but suddenly drops to the converging tolerance. With respect to the optimum layout, all but four members from the initial design were vanished having a nondimensional cross-section equal to $\tilde{z}_{i,\min} = 1E-12$. That is, a clear four-member layout was formed without the presence of any members being in ambiguity (Fig.5.3a). The non-vanishing members are presented in Table 5.7 (column 'Unit Stiffness Design') and have the same cross-sectional area with an agreement of twelve significant digits.

Table 5.7: Optimum design for the 56-bar indeterminate truss

Nondimensional quantities	Reference	SQP	Present paper	
			Unit Stiffness Design (accuracy:1E-12)	Random Initial Design (accuracy:1E-12)
z_1		2.83642084582115E+00	2.82842712474591E+00	2.82842712474591E+00
z_2		2.82931425525085E+00	2.82842712474601E+00	2.82842712474601E+00
z_3		2.82403815657757E+00	2.82842712474600E+00	2.82842712474600E+00
z_4		2.82397042932332E+00	2.82842712474596E+00	2.82842712474596E+00
min Φ_s	16.0000	16.0000684808730	16.0000000000049	16.0000000000049

The nondimensional minimum weight agrees with the exact analytical one in thirteen significant digits. Extended experimentations applying the proposed optimization procedure with random initial design vectors did not converge into another optimal layout (Table 5.7, column 'Random Initial Design').

As mentioned in Section 5.1.4, there is one variation of the same problem with 114 members, for which it is reported that the COC program gave an optimal total cost of $\tilde{\Phi}_s = 16.00000000016$ after 231 iterations (Rozvany, 1992). Instead of optimizing this topology, a more challenging one was selected; that of connecting each node with all the other nodes (structural universe with 276 members, Fig.5.3b). The challenge in this situation lies in the fact that not only more members but also overlapping members are involved. Using the proposed optimization procedure, having set the tolerance for detecting both zero-force members and weight convergence equal to $1E-13$ and the minimum nondimensional cross-section equal to $\tilde{z}_{i,\min} = 1E-14$, a minimum structural weight of $\tilde{\Phi}_s = 16.0000000000076$ was achieved after 220 iteration (agreement with the analytical solution of thirteen digits). The convergence histories of the proposed optimization procedure with respect to the cost function $\tilde{\Phi}_s$ and the relative errors are shown in Fig.5.14a and in Fig.5.14b, respectively.

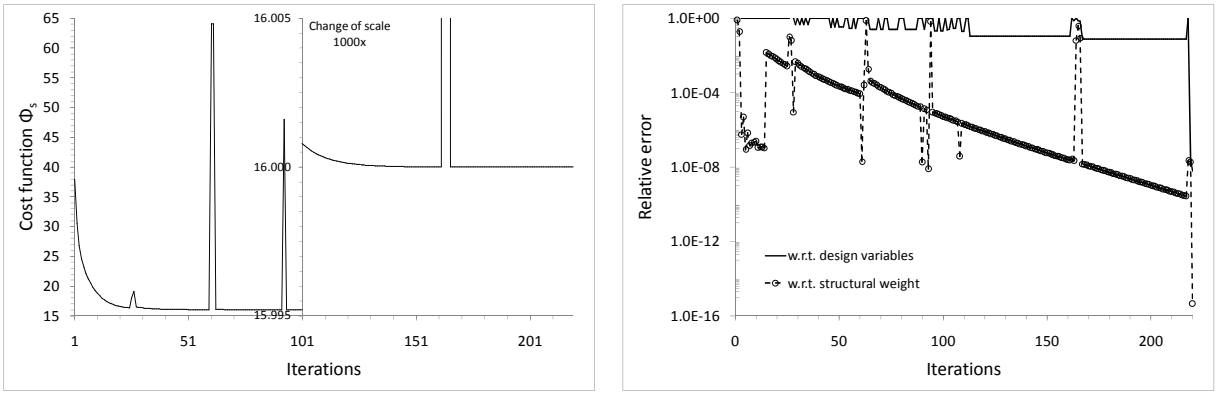

(a) (b)

Figure 5.12: Convergence history with respect to (a) the cost function and (b) the relative errors for a structural universe with 276 members

It is clear that the smooth convergence in Fig.5.14a is disrupted by four peaks (for better visualization, the markers are dropped from the plot). Again, from monitoring the proposed procedure, it was found out that the peaks in Fig.5.14a and the peaks in Fig.5.14b appear at the same iterations and correspond to the activation of the line-search procedure (Section 5.1, Step9b). That is when the new design has force-passive/area-active elements that cannot take the minimum cross-sectional value. Furthermore, valleys also appear in Fig.5.14b, the explanation being the same as for Fig.5.13b. A more detailed analysis on this issue is presented in the following Section ('Discussion'), where the role of Step 9 is fully commented.

With respect to the optimal layout, the non-minimum non-dimensional cross-sections are shown in Table 5.8.

Table 5.8: Optimum design for the 56-bar indeterminate truss

Nondimensional quantities	Member	Unit Stiffness Design (accuracy:1E-13)		
		Cross-sectional area	Overlapping	Overlapped cross-sectional area
z_1	(AC)	5.8504246394E-01	(AC) + (AE)	2.8284271247E+00
z_2	(AE)	2.2433846608E+00	(CE) + (AE)	2.8284271247E+00
z_3	(CE)	5.8504246394E-01		
z_4	(BD)	7.7174302143E-01	(BD) + (DE)	2.8284271247E+00
z_5	(DE)	2.0566841033E+00	(BE) + (DE)	2.8284271247E+00
z_6	(BE)	7.7174302143E-01		

It is noted that, apart from the members mentioned in Table 5.8, all the other members had taken the imposed minimum cross-section (there were no members with non-minimum cross-section for which it could be deducted that they actually were vanishing members, as in (Rozvany, 1992). Furthermore, the six non-vanishing members are the members (AC), (CE), (AE) (the last member overlaps the previous ones), and their symmetric ones (BD), (DE), (BE), as illustrated in Fig.5.3b. The symmetry can be checked as shown in Table 8 (last column). It is also noted that the cross-sectional areas of the over-lapping members are those obtained with the proposed optimization procedure for the 56-bar topology (consistency of optimal designs).

5.5.1.5. Case study: The MBB beam

The skeletal version of this example was investigated for three different mesh densities, namely 12×2 ($NEL_1 = 110$ elements), 24×4 ($NEL_2 = 412$ elements) and 48×8 ($NEL_1 = 1592$ elements); that is, in all cases a unit aspect ratio was selected. Furthermore, the tolerances defined in Eqs.(5.36, 5.37) were set equal to $tol_1 = tol_2 = 1E-12$, while the minimum cross-sectional area was also set equal to $A_{\min} = 1E-12$. For the aforementioned mesh densities, the proposed procedure initiating from the (USD) converged after 126, 218 and 845 iterations, respectively (for the latter case, something less than 1700 FE analyses) to the same minimum volume of 382978.723404mm^3. For the 12×2 mesh density, the Matlab SQP routine, with the termination tolerance both on the function value and the constraint violation being equal to $1E-6$ (that is, less strict tolerances of six orders), required 44 iterations and 5104 objective function evaluations, thus equal number of FE analyses, converging to the minimum volume of $382978.7239120032\text{mm}^3$ (agreement in 9 significant digits with the minimum weight derived from the application of the proposed optimization procedure). Therefore, the optimization using the SQP routine, for the first mesh density, required three times more FE analyses than the proposed procedure required for the third mesh density, for which it is $(NEL_3/NEL_1) > 14$. Obviously, a further comparison with the SQP for higher mesh densities is meaningless.

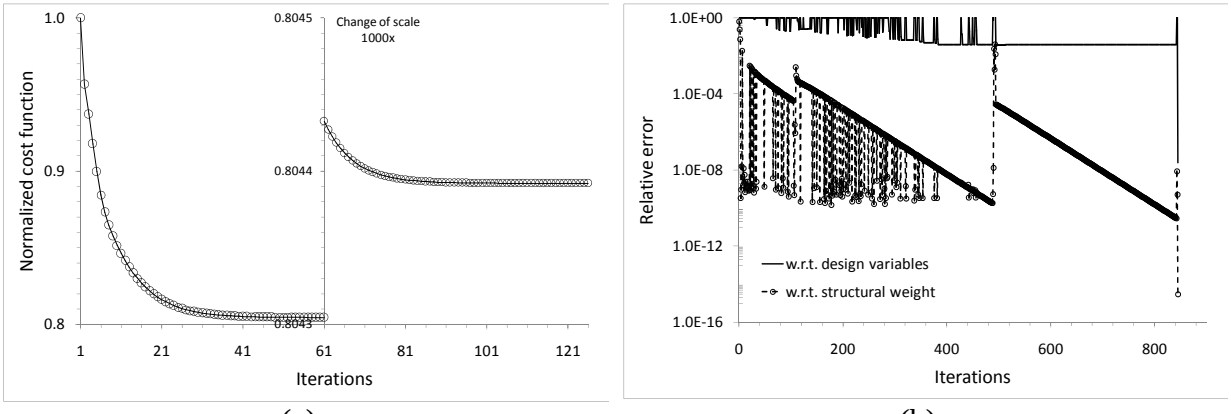

(a) (b)

Figure 5.13: Convergence history with respect to (a) the cost function (mesh: 12×2) and (b) the relative errors (mesh: 48×8) for the MBB beam

As far as the convergence history of the proposed procedure is concerned, the normalized cost function converges smoothly to the optimum. This behavior is illustrated in Fig.5.15a for

a 12×2 mesh but the same holds for the other meshes as well (not shown). The convergence history of the relative errors in Fig.5.15b corresponds to a 48×8 mesh. However, similar histories appear for the other meshes as well (not shown). From Fig.5.15b, it is clear that for the relative error with respect to the structural weight, there is a clear decreasing mode even though discontinuities do appear. This situation is exactly the same with the one appearing in previous plots (Fig.5.13b and Fig.5.14b) and has the same reasoning. However, the convergence with respect to the maximum change in the design variables does not follow this decrease (a sudden drop to the converging tolerance value is recorded).

The optimal layouts obtained with the proposed optimization procedure for the examined mesh densities are shown in Fig.5.16, where the light gray lines represent vanishing members and the continuous lines represent remaining members. The different line thicknesses correspond to different cross-sectional area groups. From Fig.5.16, it is obvious that there is a consistency between the optimal designs obtained with the proposed optimization procedure and for various meshes because not only was the same minimum structural weight found, as mentioned in the beginning of this subsection, but also the same layout was obtained.

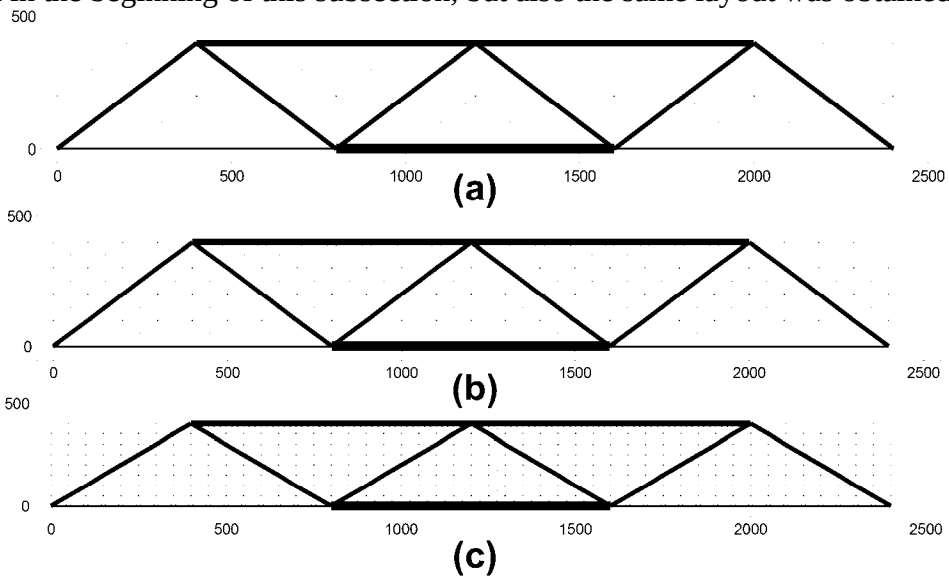

Figure 5.14: Optimal MBB layouts obtained with the proposed optimization procedure for a grid of (a) 12×2, (b) 24×4 and (c) 48×8 divisions

In all three cases, the proposed optimization procedure resulted in a layout where only five different groups of cross-sectional areas were present, one of which containing the vanishing members. This categorization is illustrated in Fig.5.17, where the cross-sectional areas have been normalized with respect to the maximum appearing cross-sectional value (y-axis), while the x-axis represents the structural member index.

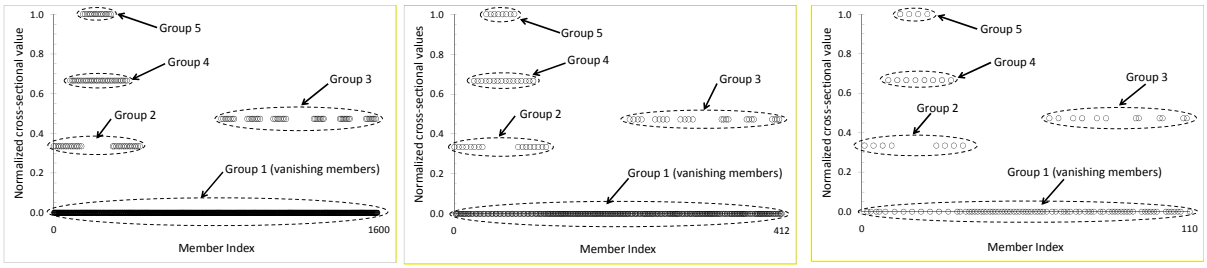

Figure 5.15: Grouping of non-vanishing members for the MBB beam using a grid of (a) 48×8, (b) 24×4 and (c) 12×2 divisions

Therefore, apart from the weight minimization, the commonality between the non-vanishing members seems to have been maximized as well.

5.5.2. Determinate trusses

5.5.2.1. Case study: 5-bar truss (variation Bar5_var2)

With respect to the evaluation of the literature data, only the optimum weight was referred in (Patnaik et al, 1995), therefore no optimum design vector was available for testing. With respect to the application of the Matlab SQP routine, 100 analyses initiating from different design vectors converged to the same optimum design vector (the one described in Table 5.9, column 'SQP'), requiring from 11 to 38 iterations (86 to 401 evaluations of the objective function thus equal number of FE analyses). For the optimization with the Matlab routine, the termination tolerance on the function value and the constraint violation, as well as the lower bound for the design variables were set equal to $1E-6$ (numerical instabilities were experienced if the lower bound lb was set as $lb<1E-6$). Based on these facts, it was considered that the design vector obtained with the Matlab SQP routine was the global optimum one. With respect to the application of the proposed optimization procedure, the global optimum was found after one iteration provided that the vector corresponding to the Unit Stiffness Design was used as the initial design vector (see corresponding column in Table 5.9). For a randomly chosen initial design vector, extended experimentation showed that the global optimum was reached after two iterations (see corresponding column of Table 5.9). It is noted that in all the analyses with the proposed optimization procedure, the tolerances defined in Eqs.(5.36, 5.37) were set equal to $tol_1 = tol_2 = 1E-12$. The fact that only one iteration was required with the proposed optimization procedure, when initiated from a design vector corresponding to the USD, is totally expected, because this procedure implements a redesign equation which if of 'closed-form' for determinate trusses.

Table 5.9: Optimum design for the 5-bar determinate truss

	Reference	SQP	Present paper	
			Unit Stiffness Design (accuracy:1E-12)	Random Initial Design (accuracy:1E-12)
x_1 [in^2]		1.000000000000E-12	1.000000000000E-12	1.000000000000E-12
x_2 [in^2]		9.715414157277E-01	1.500000000000E+00	1.500000000000E+00
x_3 [in^2]		9.999999999948E-13	1.000000000000E-12	1.000000000000E-12
x_4 [in^2]		2.913778091812E+00	2.121320343560E+00	2.121320343560E+00
x_5 [in^2]		2.867287369717E-07	1.000000000000E-12	1.000000000000E-12
max(abs(U_y)) [in]		2.000000000000E+00	2.000000000000E+00	2.000000000000E+00
min W [lbs]	45.051	45.0000000227642	45.0000000000341	45.0000000000341

Furthermore, the minimum weight obtained with the proposed procedure agrees with the one obtained with the Matlab SQP routine in 9 significant digits. Finally, it is noted that the SQP approach converged to a design where members 2, 4 *and* 5 are present, even though member 5 tends to take a vanishing cross-section, while the proposed approach converged to a clear two-member design

5.5.2.2. Case study: The MBB beam

The performance with respect to the number of iterations is described in Table 5.10, while the normalized minimum weight with respect to the SQP results are presented in Table 5.11. From Table 5.10, it is obvious that the proposed procedure converges in either two or three

iterations when the (R.I.D.) is selected and in two iterations if the (U.S.I.D.) is used. Consequently, the estimation of the corresponding standard deviations and the Coefficients of Variation is meaningless, and so is the creation of convergence history diagrams.

Table 5.10: Performance with respect to the number of iterations

Variation		DESIGN															
		Baltimore			Howe			K-truss			Pratt			Warren			
		S.Q.P.	R.I.D.	U.S.I.D	S.Q.P.	R.I.D.	U.S.I.D	S.Q.P.	R.I.D.	U.S.I.D	S.Q.P.	R.I.D.	U.S.I.D	S.Q.P.	R.I.D.	U.S.I.D
#1	*mean value*	82	*2 or 3*	2	88	*2 or 3*	2	113	*2 or 3*	2	85	*2 or 3*	2	82	*2 or 3*	2
	st deviation	10	-	-	13	-	-	26	-	-	12	-	-	10	-	-
	(%) CV	11.9	-	-	15.2	-	-	23.0	-	-	14.6	-	-	11.9	-	-
#2	*mean value*	139	*2 or 3*	2	144	*2 or 3*	2	210	*2 or 3*	2	150	*2 or 3*	2	139	*2 or 3*	2
	st deviation	30	-	-	32	-	-	20	-	-	30	-	-	30	-	-
	(%) CV	21.5	-	-	21.9	-	-	9.6	-	-	20.1	-	-	21.5	-	-
#3	*mean value*	202	*2 or 3*	2	210	*2 or 3*	2	253	*2 or 3*	2	206	*2 or 3*	2	202	*2 or 3*	2
	st deviation	21	-	-	17	-	-	17	-	-	20	-	-	21	-	-
	(%) CV	10.3	-	-	8.2	-	-	6.8	-	-	9.7	-	-	10.3	-	-

S.Q.P.: Sequential Quadratic Programming
R.I.D.: Random Initial Design
U.S.I.D.: Unit Stiffness Initial Design

Furthermore, it is evident that the required computational cost for the SQP is significantly higher (Table 5.10, column 'SQP'). In addition, Table 5.11 shows that if the (U.S.I.D.) is selected then the same minima with the SQP approach are located in all cases; however, this does happen when the (R.I.D.) is used (see columns for K-truss, Pratt and Warren designs in Table 5.11). For example, for the first (R.I.D.) variation of the Warren design, the final weight is almost 28% higher than the optimum one. This result proves that using a random initial design vector is not a safe selection, the theoretical explanation being analyzed in Section 5.6.

Table 5.11: Normalized minimum weight with respect to the SQP results

Variation		DESIGN				
		Baltimore	Howe	K-truss	Pratt	Warren
#1	R.I.D.	1.000	1.000	1.000	1.000	1.277
	U.S.I.D.	1.000	1.000	1.000	1.000	1.000
#2	R.I.D.	1.000	1.000	1.130	1.087	1.000
	U.S.I.D.	1.000	1.000	1.000	1.000	1.000
#3	R.I.D.	1.000	1.000	1.050	1.057	1.000
	U.S.I.D.	1.000	1.000	1.000	1.000	1.000

R.I.D.: Random Initial Design
U.S.I.D.: Unit Stiffness Initial Design

In order to compare the optimum design vectors obtained with the proposed procedure with those obtained with the SQP, the plots in Figs.5.18-5.22 present, in a sorted form, the normalized values of the components of the optimum design vector obtained with the proposed method over those obtained with the Matlab routine (fmincon). The red horizontal line in these figures denotes coincidence between the two compared methods. From these plots, it is obvious that the proposed approach and the SQP approach result to quite similar optimum design vectors, the difference between them ranging from negligible (e.g. Warren design, variation #1) up to 5% (Howe Design, variation #3).

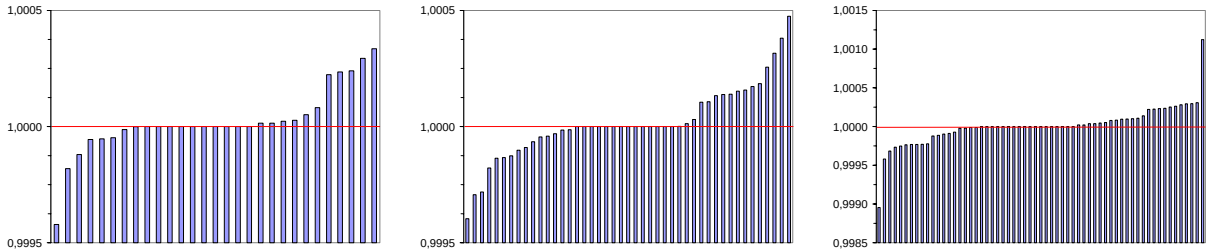

(#1) (#2) (#3)

Figure 5.16: MBB – Baltimore design

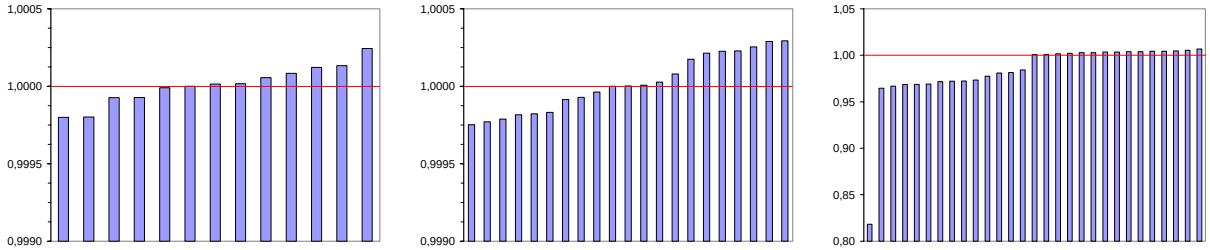

(#1) (#2) (#3)

Figure 5.17: MBB – Howe design

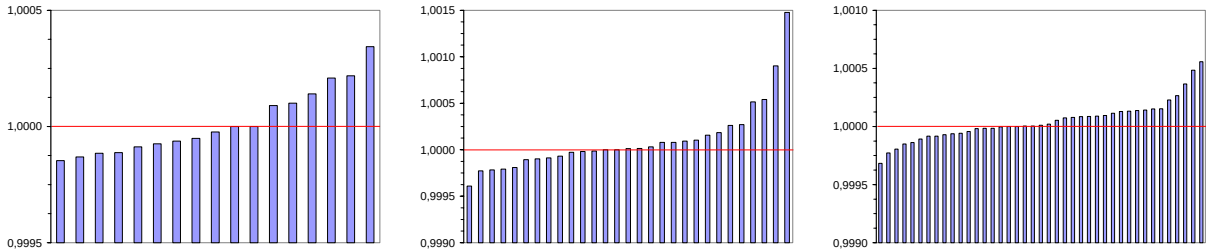

(#1) (#2) (#3)

Figure 5.18: MBB – K-truss design

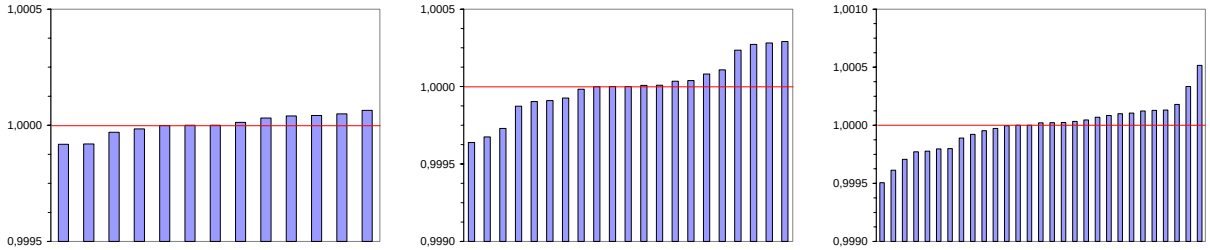

(#1) (#2) (#3)

Figure 5.19: MBB – Pratt design

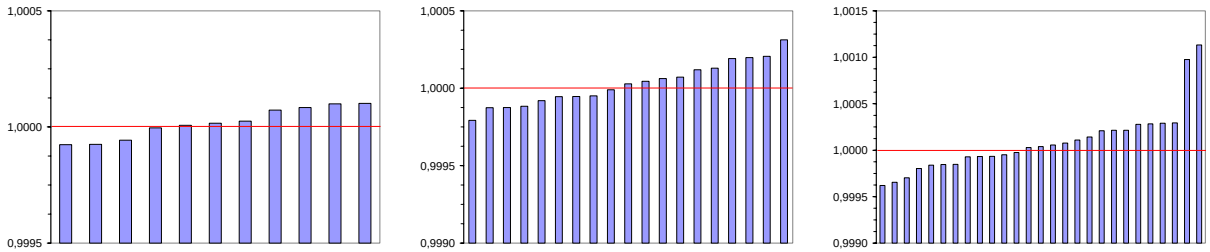

(#1) (#2) (#3)

Figure 5.20: MBB – Warren design

In order to find out which design among the examined ones was the best, the corresponding minimum structural weights were normalized with respect to the minimum of these values. The result of this normalization is shown in Table 5.12, according to which the first variation of the Warren design was, by far, the best. The second best design was the second variation of the K-truss with a minimum structural weight being higher by 6.9%. Another interesting remark derived from this Table is that for all but the K-truss variations, the minimum structural weight increases as the number of elements and nodes of the design increases.

Table 5.12: Normalized minimum weights for the MBB determinate truss

Design	Variation #1	Variation #2	Variation #3
Baltimore	1.218	1.294	1.492
Howe	1.211	1.285	1.481
K_truss	1.139	1.069	1.104
Pratt	1.212	1.287	1.482
Warren	1.000	1.110	1.328

Finally, the interested reader, who wishes to verify the optimum design vectors obtained with the proposed procedure, may find connectivity data and the corresponding cross-sectional values in Appendix 5B.

5.5.2.3. Case study: 9-bar truss

As mentioned in Section 5.2.3, six 9-bar truss topologies under four load cases were examined. In more details, these topologies were optimized first with the fmincon routine (MatLab) and then with the proposed procedure. Indicatively, the obtained results, with the SQP and with the proposed procedure (the tolerances defined in Eqs.(5.36, 5.37) were set equal to $tol_1 = tol_2 = 1E-6$), in terms of minimum structural weight and final design vector, for the first variation of the examined topologies, are presented in Table 5.13. It is clear that the two approaches provide results that appear an agreement of at least five significant digits in terms of design variables.

Table 5.13: Results for the first variation of the 9-bar truss

	Design 9a Load Case 1		Design 9a Load Case 2		Design 9a Load Case 3		Design 9a Load Case 4	
	SQP	Present paper	SQP	Present paper	SQP	Present paper	SQP	Present paper
W_{opti}	8867.234400	8867.234400	1287.228600	1287.228600	6488.691200	6488.691200	9470.672909	9470.672900
x_1	21.045831	21.045835	0.100000	0.100000	18.000021	18.000000	21.750839	21.750841
x_2	51.551611	51.551556	11.236751	11.236753	36.000001	36.000000	53.278522	53.278462
x_3	29.763207	29.763305	7.945585	7.945584	18.000028	18.000000	34.391054	34.391099
x_4	42.091664	42.091670	11.236754	11.236753	25.455901	25.455844	43.501691	43.501682
x_5	0.100000	0.100000	0.100000	0.100000	0.100000	0.100000	0.100000	0.100000
x_6	0.100000	0.100000	0.100000	0.100000	0.100000	0.100000	0.100000	0.100000
x_7	21.045865	21.045835	0.100000	0.100000	17.999898	18.000000	21.750772	21.750841
x_8	21.045884	21.045835	0.100000	0.100000	18.000017	18.000000	26.639117	26.639231
x_9	29.763288	29.763305	0.100000	0.100000	25.455811	25.455844	30.760447	30.760334

Working in a similar manner, it is possible to form the tables corresponding to the other variations of the 9-bar truss (these Tables are presented in Appendix 5C). Indicatively, Table 14 presents the results for all the variations of the 9-bar truss and for the third load case (truncation at the third decimal digit for the design variables). At this point, it is noted that the symbolic names used to describe the aforementioned variations are presented in Table 5.2.

Table 5.14: Results for all variations of the 9-bar truss and for the third load case

	9a		9b		9c		9d		9e		9h	
	SQP	Present paper	SQP	Present paper	SQP	Present paper	SQP	Present paper	SQP	Present paper	SQP	Present paper
Weight	6488,70	6488,70	4163,10	4163,10	4164,6	4164,6	4164,6	4164,6	6490,2	6490,2	4164,6	4164,6
x1	18,000	18,000	14,400	14,400	14,400	14,400	14,400	14,400	18,000	18,000	14,400	14,400
x2	36,000	36,000	28,800	28,800	28,800	28,800	28,800	28,800	36,000	36,000	28,800	28,800
x3	18,000	18,000	0,100	0,100	0,100	0,100	0,100	0,100	18,000	18,000	20,365	20,365
x4	25,456	25,456	20,365	20,365	20,365	20,365	20,365	20,365	25,456	25,456	0,100	0,100
x5	0,100	0,100	0,100	0,100	0,100	0,100	0,100	0,100	0,100	0,100	14,400	14,400
x6	0,100	0,100	14,400	14,400	14,400	14,400	14,400	14,400	18,000	18,000	0,100	0,100
x7	18,000	18,000	0,100	0,100	0,100	0,100	0,100	0,100	18,000	18,000	0,100	0,100
x8	18,000	18,000	0,100	0,100	0,100	0,100	0,100	0,100	25,456	25,456	0,100	0,100
x9	25,456	25,456	20,365	20,365	20,365	20,365	20,365	20,365	0,100	0,100	20,365	20,365

From Table 5.14, it is clear that the SQP and the proposed optimization procedure result in the same optimal designs. However, the computational cost of the SQP is significantly higher. More details on the performance of the SQP are presented separately in Table 5.15, where the mean value, the standard deviation and the coefficient of variation (CV) have been calculated as measures of the computational effort required until convergence was achieved. As Table 5.15 shows, the SQP approach, on average, requires more than 34 iterations but mainly more than 476 evaluations of the objective function thus equal number of FEAs. On the contrary, the proposed procedure required only three FEAs.

Table 5.15: Performance of the SQP approach

Design	Iterations				Objective function evaluations		
	Average	Standard Deviation	CV (%)		Average	Standard Deviation	CV (%)
9a	39	8	21.70		517	116	22.40
9b	35	6	18.14		476	110	23.11
9c	35	6	16.38		483	99	20.49
9d	35	7	18.68		476	112	23.60
9e	39	8	20.91		522	114	21.83
9h	35	6	17.56		476	107	22.48

Finally, it is strongly emphasized that the results in Table 5.14 came from using as initial design vector the one corresponding to the USD. However, a few times trapping at local minima was recorded if random initials vectors were implemented.

5.6. Discussion

The problem of minimizing the structural weight under a single displacement constraint has been extensively analyzed since the early 70's, as numerous references on the subject suggest. Therefore, a very logical question would be why revisit this, so much and for so long being investigated, problem. The answer to this question, which was the motivation of the present chapter, will become clear within the next paragraph.

With respect to the investigated subject, among numerous references, one may distinguish three milestone contributions, namely by Berke (Berke, 1990), Khot (Khot, 1981) and Rozvany (Rozvany, 1992), all of which are rigorously and very rigidly stated. In these approaches there are three common characteristics. The first characteristic is the fact that even though the optimum is described in terms of a virtual strain energy density state, the path towards this state is not uniquely defined. This means that paths other than the already known in the literature (Berke, 1990, Khot, 1981 and Rozvany, 1992) may be followed. The second characteristic is the fact that, within the redesign procedure, a Lagrange multiplier is involved. This multiplier must be either numerically estimated (Berke, 1990 and Rozvany, 1992) or embedded in the redesign equation (Khot, 1981). The former approach requires the development of a recursive equation which is typical for numerical methods but also increases the computational cost not to mention convergence difficulties. The latter approach results in a cumbersome redesign equation. Therefore, it would be ideal if the Lagrange multiplier did not participate explicitly in the redesign procedure. The third characteristic has to do with the selection of the passive members, which are defined as members either obtaining a design value less than the imposed lower bound or having a force product $F_i^P F_i^Q < tol, 0 \le tol$ (the components of the force product were presented in Section 5.2) (Berke, 1990, Khot, 1981 and Rozvany, 1992). This means that the cases where the negative force product was near zero and far away from it were handled similarly. However, a force product $F_i^P F_i^Q$ significantly different than zero denotes that the corresponding $i-$member participates vividly in carrying

both the externally applied load and the unit virtual load, while a force product $F_i^P F_i^Q$ near zero denotes exactly the opposite. Therefore, a question is posed with respect to the influence of separating the two cases over an optimization procedure. Having the aforementioned thoughts in mind, the present investigation, based on the Lagrange multipliers method, revisited the OC approach of the single displacement constraint problem and ended up with an optimization procedure that embeds three new features:

- a new and simple redesign formula, requiring the estimation of no Lagrange multipliers,
- a new and more detailed categorization of the structural elements and
- a new and different handling of the structural elements with $\left|F_i^P F_i^Q\right| < tol,\ 0 \le tol$.

The recursive formula for the cross-sectional redesign was derived entirely from a sound mathematical approach with no elements of intuition or numerical-analysis origin being embedded. This formula strongly resembles the stress-ratio technique used in fully stressed designs and can be considered as a virtual-strain-energy-density-ratio technique used in single displacement constrained designs. The investigated examples showed that, for determinate trusses, if the optimization problem at hand is truly single displacement constrained then the proposed procedure reaches the optimum design in two iterations. This is not surprising because the core of the procedure (redesign formula) is actually of closed-form, provided that the assumptions mentioned in Section 5.5 are valid. The fact that two iterations were required lies in the very small tolerances used in the convergence criteria. However, if the problem is actually a multiple displacement constrained one, then the proposed procedure may provide the global optimum as well, as the results in 5.4.2 suggest, without being claimed that the proposed procedure, as presented here, is completely suitable for such problems.

Furthermore, the Lagrange multiplier λ_1 appearing in Eq.(5.8) is not equal to the scalar coefficient a used for the uniform scaling in Eq.(5.20). The multiplier λ_1 is used for ensuring the existence of a uniform virtual strain energy density distribution over the active part of the structure, while the coefficient a is used for matching a maximum value for nodal displacement.

One of the most interesting points in the proposed procedure is the criterion for characterizing an element as active or passive. In the literature (Berke, 1990, Khot, 1981 and Rozvany, 1992), the inequality $F_i^P F_i^Q < tol$, tol being zero or a small positive number, serves as such a criterion, where F_i^P and F_i^Q are the member forces due to the real load and the virtual unit load, respectively. However, in the present chapter the inequality $\left|F_i^P F_i^Q\right| < tol$ was used instead, tol being a small positive number. As shown in Section 5.3, this leads to a different than the usual member categorization, within which the force-passive/area-active elements are introduced. These elements have the following characteristic: although the corresponding member forces satisfy the inequality $F_i^P F_i^Q < tol$, these members cannot take the lower bound imposed for the design variables; if they do so then a constraint violation occurs. At first, this sounds as a paradox but it is not, as Eq.(5.3) reveals. In more details, according to Eq.(5.3), each term within the sum represents a contribution to the nodal displacement. If this term is negligible then so is the corresponding contribution. However, for an $i-$member with $\left|F_i^P F_i^Q\right| < tol$, it is possible to set $A_i = A_{\min}$ and get a *non-negligible* contribution:

$$\left(\frac{\left| F_i^P F_i^Q \right|}{A_i E_i} L_i \right) >> 0 \tag{5.40}$$

Consequently, it is obligatory to set $A_i > A_{\min}$, which means that another than the minimum cross-sectional value must be attributed thus the member has to be area-active. Members presenting the aforementioned behavior are termed in the present chapter as force-passive/area-active. Their presence in a determinate structure, where the member forces do not depend on the cross-sectional values, denote structural members that cannot be removed and, for them to provide a negligible contribution to the nodal displacement, they must take on a larger than the minimum cross-sectional area. Their presence in an indeterminate structure, where the member forces do depend on the cross-sectional values, denote structural members that can be removed but for this to happen a different virtual strain energy density distribution than the current must be obtained. In both cases, the cross-sectional areas that these members must take on may be found from the solution of an optimization problem, as mentioned in Section 5.5. The line-search procedure proposed in the present chapter is a substitute to implementing an MP method for solving the aforementioned optimization problem. If the solution from this substitute differs from the ideal one then peaks, as those in Fig.5.14a, appear. The reason for this is quite simple. Since the contribution of the force-passive/area-active members does not vanish, as it should, the contribution of the other members, which is either positive due to the presence of the absolute sign in Eq.5.40 or zero, must be decreased for no displacement constraint violations to appear. As a result, the contribution of the other members is decreased 'artificially' through the redesign procedure by having the corresponding cross-sectional areas increased. In this 'artificial' state, the virtual strain energy density is redistributed. After this redistribution and since the structure is indeterminate, the member forces are re-estimated due to which the force-passive/area-active elements of the previous step change their status, become 'fully' passive elements and are 'removed' from the structure by taking on the lower bound imposed for the design variables. In this way, after one or two iterations, the virtual strain energy density balance within the structure is re-obtained and the optimization procedure continues normally. Furthermore, the stronger the presence of this 'artificial' state is the higher the peaks, as those in Fig.5.14a, are. From a theoretical point of view, the proposed approach uses the absolute sign in the force product $\left| F_i^P F_i^Q \right|$ and allows all of the structural members to be counted in Eq.(5.3); that is to include the influence of all members in the redesign procedure. This is an approach opposite to that by (Khot, 1981) who used the signed force products to detect passive elements (those with a negative force product), gather them in a separate set and exclude their influence from the redesign procedure.

On the issue of the member characterization, it is further clarified that both the force product $F_i^P F_i^Q$ and the cross-sections must be implemented. Using only the force product $F_i^P F_i^Q$ as a criterion is not a bulletproof choice because it is possible to get a non-negligible contribution from a member with small $F_i^P F_i^Q$ value if its cross-sectional area is small. Exactly in order to handle such cases, the present chapter suggests the use of a criterion, where a member is characterized twice, once with respect to its $F_i^P F_i^Q$ value and once with respect to its cross-sectional area. Depending on the result of this "double" characterization, a member may belong to one of the four groups described in Section 2.5 and is handled accordingly, as also described in the same Section. Furthermore, it is strongly emphasized that the proposed categorization of the structural members aims only at *selecting* those members that will participate, *at each iteration*, in the redesign procedure. Those members that are not

selected remain unchanged *only* for that iteration (they are neither eliminated from the structure nor kept frozen for the rest of the optimization procedure).

Continuing the train of thoughts of the previous paragraph, in the general case where for some $i-$element it holds $c_i b_i < 0$ (see Eq.29), or, equivalently, its force product $F_i^P F_i^Q$ is negative, it is possible to get a displacement decrease if the cross-section of this $i-$element obtains a smaller cross-section than the current one. However, this case has been foreseen in the proposed procedure. In more details, once the vector $\mathbf{A}_{pass-act}$ with the force-passive/area-active elements has been formed, a line search is initiated seeking for a structural weight reduction by further reducing the cross-sections of the aforementioned vector (it is of no interest to examine what happens when the cross-sections are increased because in this way the structural weight is increased, which is opposite to the aim of minimizing the structural weight). For this line search (optimization sub-problem) and for the corresponding design space, the upper bound is $\mathbf{A}_{pass-act}$ and the lower bound is $\mathbf{A}_{pass-act,LowerBound} = \mathbf{A}_{\min}$. If reducing $\mathbf{A}_{pass-act}$ results in increasing the displacement, then the limiting case would be for the new 'optimized' vector $\mathbf{A}_{new,pass-act}$ to be equal to the vector $\mathbf{A}_{pass-act}$ (the new vector coincides with the upper bound). If reducing $\mathbf{A}_{pass-act}$ results in decreasing the displacement, then the limiting case would be for the new 'optimized' vector $\mathbf{A}_{new,pass-act}$ to be equal to the vector $\mathbf{A}_{\min}$ (the new vector coincides with the lower bound). Therefore, the proposed procedure can efficiently handle the case where a potential reduction of the cross-sections of the vector $\mathbf{A}_{pass-act}$ may cause either a displacement increase or a displacement decrease.

Another important issue concerns the selection of the initial design vector. From the obtained results, it was shown than the use of random initial values for the cross-sectional areas could lead to local minima. An explanation for such a behavior follows. It is well-known that the stiffness of a truss is nothing else but a combination of the stiffness of its structural members. According to Eq.(5.26), which is repeated here for convenience:

$$[K]_j = \underbrace{\left(\frac{AE}{L}\right)}_{c_j}{}_j \underbrace{\begin{bmatrix} c^2 & cs & -c^2 & -cs \\ cs & s^2 & -cs & s^2 \\ -c^2 & -cs & c^2 & cs \\ -cs & -s^2 & cs & s^2 \end{bmatrix}}_{m_j}{}_j \tag{5.41}$$

the stiffness $[K]_j$ of the $j-$member is defined by two terms, the coefficient c_j and the matrix m_j shown in Eq.(5.41). For a given topology and a given material, the coefficient c_j depends entirely on the cross-sectional area A. On the other hand, the matrix m_j depends entirely on the orientation of the $j-$member. Therefore, the elements within the matrix (matrix entries) vary, because of the orientation, thus of the topology, while the coefficient outside the matrix operates as a uniform scaling factor to the matrix entries. From this perspective, the stiffness $[K]_j$ may be considered as a 'vector' whose direction is dictated by the matrix m_j and whose value is denoted by the coefficient c_j. Expanding this approach, the set of the stiffness of all structural members form the basis $\left\{[K]_1, [K]_2, ..., [K]_j, ..., [K]_{NEL}\right\}$

that spans the space which the stiffness of the entire structure belongs to. A symbolic representation of this approach is:

$$[K]_{Total} = c_1 m_1 + c_2 m_2 + ... + c_j m_j + ... + c_{NEL} m_{NEL} \tag{5.41}$$

Therefore, the stiffness matrix of the entire structure is a linear combination of the linear independent 'vectors' m_j that form the aforementioned basis, the linear coefficients being the quantities c_j. Setting $c_j = 1$ results in

$$[K]_{Total,UnitStiffness} = m_1 + m_2 + ... + m_j + ... + m_{NEL} \tag{5.42}$$

The Finite Element Analysis of a structure using the stiffness matrix of Eq.(5.42) provides the response of the structure under the influence of the topology only. However, the Finite Element Analysis of the same structure using the stiffness matrix of Eq.(5.41) provides the response of the structure under a *weighted* influence of the topology, the weights being the coefficients c_j which represent the size of the structure. In other words, in the latter approach, a mixed influence from size and topology appears. The line between the effect of these two approaches on an optimization scheme is quite indistinguishable but exists. As shown from the examined examples (e.g. 3-bar truss, 5-bar truss) initiating the optimization procedure using the mixed influence can be 'misleading' in the sense that another than the global optimum is traced. On the contrary, when a Unit Stiffness Design (USD) was selected to be the initial design vector, the global optimum was more likely to be traced.

With respect to the USD and the RID approaches, among the examined examples, the Bar3-A test case was quite interesting because all of the 100 RID runs converged to local optima. The basic difference between the results coming from using USD and RID has to do with the categorization of the structural members that takes place during the optimization procedure. In more details, as presented in Section 2.4, the present chapter suggests that the structural members be categorized in four groups. From iteration history data that can be obtained for the Bar3-A example, it yields that initiating the procedure with the USD, the line search routine is activated for the first iteration only, while, from that point on and until convergence is achieved, two structural members (the inclined ones) are detected as force-active/area-active and one structural member (the one in the middle) is detected as force-active/area-passive element. On the other hand, initiating the procedure with the RID yields that the line search routine is never activated, while, at all iterations, three structural members are detected as force-active/area-active, until convergence is achieved. As a result, with the former approach a clear two-member layout is formed from the very beginning of the optimization procedure, while with the latter approach a three-member layout is formed, being characterized by a lower Virtual Strain Energy Density, in comparison with the layout yielding using USD. The explanation of this behavior is related to the topological symmetry of the specific structure. More particularly, using the USD approach initiates the optimization procedure from a design where the symmetrical structural members (the inclined bars in particular) have the same stiffness; that is a 'symmetry' in stiffness. However, using the RID approach, the aforementioned stiffness symmetry is never achieved because the random generator that creates the initial design vector does not provide two or more identical numbers; thus, with the RID approach, it is certain that the initial cross-section of the inclined bars will not be the same, thus their stiffness will be different as well.

At this point, the concept of USD is based more on the thoughts presented in Section 2.4 and on the obtained numerical results presented in Section 5, rather on a pure mathematical

proof. The concept of USD raises some very interesting questions among which the most crucial one is: why does it work? At this moment, the author is in position to contribute the statement of this concept, his thoughts as presented in Section 2.4 and in 'Discussion', and the numerical results from 48 case studies that support the use of this statement. However, the author knows very well that '*even though there is no adequate number of results to support the applicability of a concept, it takes only one result to vitiate it'*. From this viewpoint, it seems that the examination of the USD concept could be a subject for further research.

At this point, it must be noted that there are examples used as benchmarks for optimization under a single displacement constraint, presenting one particular characteristic: the load application point corresponds to the node with the maximum displacement. However, this characteristic is a necessary and sufficient condition for the design variables either to be active or to take a minimum allowable value (there are no passive elements with other than the minimum cross-section), as proven through Castigliano's second theorem (Appendix 5I). These optimization problems form a separate class of problems and can be solved using the first two steps of the proposed procedure. However, they must not be used as the only evaluators of a newly introduced optimization method because they do not test the capabilities of the method for members with $F_i^P F_i^Q < 0$. For this reason, the 9-bar truss was introduced.

Another worth-mentioning point is the fact that, in all of the test cases, the proposed optimization procedure converged to a final design. For the examined indeterminate trusses, this is shown from the convergence history diagrams in Section 5.1. For the determinate trusses, this is shown in Table 10 (Section 5.2). Therefore, setting an adequately large, but finite, allowable number of iterations as the case may be, the termination criterion with respect to the maximum number of iterations (Section 3.1, Step 14) was never utilized.

In brief, the advantages of the proposed optimization procedure are the following:

- The recursive redesign equation is extremely simply
- No Lagrange multipliers must be estimated implicitly or explicitly
- It is the topology of the structure and not its size that determines the initial design vector, which is of crucial importance for tracing the path to the global optimum
- The derived design vectors always belong to the feasible region, thus the optimization procedure may be terminated any time providing a design vector that does not violate the imposed displacement constraint
- There is no step size parameter introduced in the recursive equation, thus a stable behavior is reported

Last, but certainly not least, it is reminded that '*layout optimization problems under a single displacement constraint, although not suitable for describing practical applications, are very useful in exploring basic algorithms'* (Rozvany and Zhou, 1991).

5.7. Conclusions

In the current chapter, a new Optimality Criteria-type optimization procedure for single displacement constraint problems was proposed and tested in over 46 cases. The conclusions drawn from this investigation are the following:

- For the examples retrieved from the literature but having no analytical solution, the proposed procedure resulted in the referenced optimum weights after an approximately equal number of iterations such as the referenced ones.
- For the examples retrieved from the literature having analytical solutions, the proposed procedure resulted in the referenced optimum weights with an agreement of at least twelve significant digits after less iterations than the referenced ones.

- For the examples newly introduced in the present chapter, the proposed procedure resulted in the same optimum weights (slightly different optimum design vectors) as those obtained when implementing the SQP routine found in Matlab (fmincon).
- In all cases, initiating the proposed procedure from a design vector corresponding to a Unit Stiffness Design structure resulted in the, considered to be, global optimum. However, in some cases, initiation from a random design vector resulted in significant sub-optimal solutions.
- The proposed categorization of the members as in Section 5.3 is more detailed than those referred in the literature and highlights the presence of the newly introduced force-passive/area-active elements which play a significant role in the optimization procedure.
- In general, the convergence history with respect to the structural weight is very smooth. Peaks appear only when force-passive/area-active elements change their status and become 'fully' passive elements.
- In general, the convergence history with respect to the relative error of the structural weight is smooth and decreasing. As previously, peaks appear only when force-passive/area-active elements change their status and become 'fully' passive elements, while valleys appear when the force-passive/area-active elements are allowed to take on the imposed lower bound for the design variables.
- The convergence history, with respect to the relative error of the maximum change in the design variables structural weight, is either smooth and decreasing or quite steady and drops suddenly to the converging tolerance value.
- The extension of the proposed procedure for optimizing 3D skeletal structures is trivial.

Overall, the results of the present research suggest that the proposed optimization procedure form a simple and efficient optimization tool.

References

Beer FP, Johnston ER Jr (1988) Vector mechanics for engineers: Statics, 5thed., McGraw-Hill.

Belegundu AD, Chandrupatla TR (1999) Optimization concepts and applications in engineering, Prentice Hall.

Bendsøe M. P., Sigmund O., (2001), Topology optimization. Theory, methods and applications, Springer Verlag, Berlin

Berke L Structural optimization of large structural systems by optimality criteria methods NASA TM-105423

Foulkes, J., The Minimum-Weight Design of Structural Frames, Proceedings of the Royal Society of London. Series A, Mathematical and Physical Sciences, Volume 223, Issue 1155, pp. 482-494

Gellatly RA, Berke L (1973) Optimality-criterion-based algorithms. In: Gallagher RH, Zienkiewicz OC (eds) Optimum structural design. Wiley, Chichester, pp 33–49

Goldberg DE (1989) Genetic Algorithms in Search, Optimization and Machine Learning, Kluwer Academic Publishers, Boston, MA.

Heyman, J. 1950: On the absolute minimum weight design of framed structures. Q. J. Mech. Appl. Math. 12, 314–324

Khot NS (1981) Algorithms based on optimality criteria to design minimum weight strucutures. Engineering Optimization, 5:73-90.

Makris P, Provatidis C, (2002), Weight minimisation of displacement-constrained truss structures using a strain energy criterion. Comput Methods Appl Mech Eng 191:2159–2177

Michalewicz Z (1999) Genetic Algorithms+Data Structures=Evolution Programs, Springer.

Michell, A.G.M., (1904) The Limits of Economy of Material in Frame-Structures", Phil. Mag., 8: 589 -- 597.

Morris AJ (1982) Foundations of structural optimization: a unified approach. Wiley.

Nha Chu D, Xie YM, Hira A, Steven GP (1997) On various aspects of evolutionary structural optimization for problems with stiffness constraints. Finite Elements in Analysis and Design; 24: 197-212.

Makris, P.A., Provatidis, C.G., Venetsanos, D.T., (2006) Structural Optimisation of thin-walled tubular trusses using a virtual strain energy density approach, Thin-Walled Structures, Vol.44, pp.235-246

Patnaik SN, Gendy AS, Berke L, Hopkins DA (1998) Modified fully utilized design (MFUD) method for stress and displacement constraints. Int J Numer Methods Eng 41:1171-1194

Patnaik SN, Guptill JD, Berke L (1995) Merits and limitations of optimality criteria method for structural optimization. Int J Numer Methods Eng 38:3087–3120

Provatidis CG, Venetsanos DT, Vossou CG (2004) A comparative study on deterministic and stochastic optimization algorithms applied to truss design. In: Proceedings of 1st International Conference "From Scientific Computing to Computational Engineering", Athens, Greece, 8-10 September.

Provatidis CG, Venetsanos DT, (2003), Performance of the FSD in shape and topology optimization of two-dimensional structures using continuous and truss-like models, In: C. Cinquini, M. Rovati, P. Venini and R. Nascimbene (eds.), Proceedings Fifth World Congress of Structural and Multidisciplinary Optimization, May 19-23, 2003, Lido di Jesolo, Italy, pp. 385-386, Schönenfeld & Ziegler.

Shield R.T., W. Prager, (1970), Optimal structural design for given deflection, J. Appl. Math. Phys, 21, 513-523

Rozvany GIN (1992) Shape and layout optimization of structural systems and optimality criteria methods. Springer Verlag.

Rozvany GIN (1995) What is meaningful in topology design? An engineer's viewpoint. In: Herskovits J (ed), Advances in Structural Optimization, Kluwer, pp 149-188.

Rozvany GIN, Zhou M (1991), The COC algorithm, Part I: cross section optimization or sizing, Comput. Methods Appl. Mech. Eng. 89, 281-308

Rozvany GIN, Zhou M. (1991), The COC algorithm, Part II: topological, geometrical and generalized shape optimization. Comput. Methods Appl. Mech. Eng. 89, 309-336

Schmit LA. (1960), Structural Design by Systematic Synthesis. In: Proceedings of 2nd Conference on Electronic Computation, ASCE, New York, 105-132.

Venkayya VB (1971), Design of optimum structures, Computer and Structures, 1:265-309

Xie, Y.M, Steven, G.P (1997), Evolutionary Structural Optimization, Springer-Verlag, Berlin

Contributed papers

[1] **Venetsanos DT.**, Provatidis CG (2010), "On the layout optimization of 2D skeletal structures under a single displacement constraint", Struct Multidisc Optim, vol.42, pp.125–155.

APPENDIX 5.A: Nodal displacements using Castigliano's second theorem

Based on the mathematical expression of Castigliano's second theorem, it holds that:

$$u = \sum_{k=1}^{NEL} \left(\left(\frac{F_k L_k}{A_k E_k} \right) \frac{\partial F}{\partial F_k^*} \right) \Bigg|_{F_k^*=0} \tag{5.A1}$$

The symbols are the same to those used in the main text, the only difference (generalization) being that as F_k^* any virtual load is denoted, not necessarily one of unit magnitude. It is clarified that in Eq.(5A.1) and for the implemented partial derivative to be estimated, first the analytical expression for the member forces, developed due to the application of both the real loads and the virtual load, must be formed and then the terms corresponding to the virtual load must be eliminated. For the case of a statically determinate truss under the application of the real loads P_l, $l = 1,2,...,m$, the terms in Eq.(5A.1) may be written as follows:

$$F_k = c_{k1} P_1 + c_{k2} P_2 + ... + c_{km} P_m + b_k F_a^* \tag{5.A2}$$

$$\left(\frac{\partial F_k}{\partial F_a^*} \right) = b_k \tag{5.A3}$$

$$\left(\frac{F_k L_k}{A_k E_k} \right) \left(\frac{\partial F_k}{\partial F_a^*} \right) = d_{11} P_1 + d_{12} P_2 + ... + d_{1m} P_m + e_k F_a^* \tag{5.A4}$$

In more details, the analysis of the structure using the method of joints results in describing each member force F_k as a linear combination of the applied real loads and of the virtual applied load as well. The quantity c_{il} is a coefficient depending only on the truss topology and the application point of the real loads P_l, while, qualitatively, it expresses the weighted contribution of the real load P_l to the axial force carried by the $i-$bar. Therefore, for a given truss topology and load set, the coefficients c_{il} are constants. Respectively, the quantity b_k depends on the truss topology and the application point of the virtual load F_k^*, while qualitatively it expresses the weighted contribution of the virtual load to the virtual axial force carried by the $i-$bar. In Eq.(5A.4), a more compact description has been used where:

$$d_{kl} = \left(\frac{c_{kl} b_k L_k}{A_k E_k} \right) \quad \text{and} \quad e_k = \left(\frac{b_k L_k}{A_k E_k} \right) \tag{5.A5}$$

The combination of Eqs.(5A.1-5A.5) yields:

$$u = \sum_{k=1}^{NEL} \left(\sum_{l=1}^{m} \left(\left(\frac{c_{kl} b_k L_k}{A_k E_k} \right) P_l \right) + \left(\frac{b_k L_k}{A_k E_k} \right) F_k^* \right) \Bigg|_{F_k^*=0} \tag{5.A6}$$

which, after some basic manipulations, gives:

$$u_j = \sum_{k=1}^{NEL} \left(b_{k,j} \left(\frac{L_k}{A_k E_k} \right) \sum_{l=1}^{m} \left(c_{kl} P_l \right) \right) \tag{5.A7}$$

where the subscript j indicates the degree of freedom under consideration. Eq.(5.A7) describes the displacement u of any node in terms of topology, size and stiffness under the application of any given load. For the case where only one external load is applied ($l = 1$), the nodal displacement u_j becomes:

$$u_j = \sum_{k=1}^{NEL} \left(\left(\frac{b_{k,j} c_k L_k}{A_k E_k} P \right) \right) \tag{5.A8}$$

APPENDIX 5.B: Data for the optimal designs of the MBB beam

In this chapter, five determinate designs (Baltimore, Howe, Pratt, K-truss and Warren) for the MBB beam, each one for three different mesh densities, were examined. In this Appendix, the connectivity data and the corresponding cross-sectional areas are presented. It is noted that not all of the structural members are numbered but only an adequate numbering is illustrated.

	Area [mm^2]	Bars
Variation #1	1.00000E-06	11,12,13,15,16,17,20,21,26,27
	5.26596E-05	1,2,3,4,5,6,7,8
	6.32889E-05	18,19,22,23,24,25,28,29
	7.02128E-05	14
	1.05319E-04	9,10

	Area [mm^2]	Bars
Variation #2	1.00000E-06	17,18,19,20,21,22,23 27,30,31,34,39,42,43
	3.61702E-05	1,2,3,4,9,10,11,12,24,26
	5.11524E-05	28,29,32,33,35,36 37,38,40,41,44,45
	7.23404E-05	5,6,7,8,13,16,25,
	1.08511E-04	14,15

	Area [mm^2]	Bars
Variation #3	1.00000E-06	17,18,19,21,23,25,27,29,30 30,31,33,34,36,38,41,43,45,46
	2.91223E-05	1,2,3,4,13,14,15,16
	3.88298E-05	20,22,26,28
	4.85372E-05	32,35,37,39,40,42,44,47 48,49,50,51,52,53,54,55
	5.82447E-05	5,6,11,12,56,61
	7.76596E-05	24
	8.73670E-05	7,8,9,10,57,60
	1.16489E-04	58,59

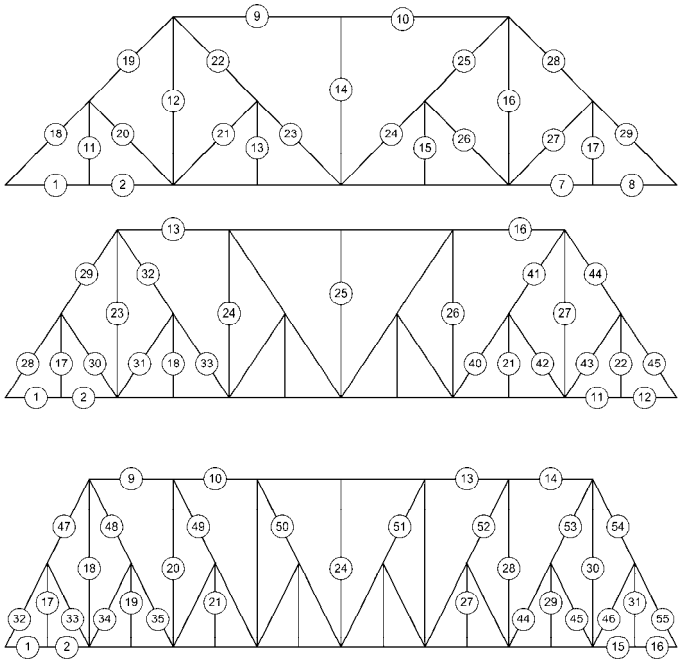

(a) (b)

Figure 5.B1: Optimum Baltimore design (a) cross-sectional areas and (b) connectivity

	Area [mm^2]	Bars
Variation #1	1.00000E-06	10
	3.51064E-05	8.12
	5.26596E-05	1,4,5,6
	6.32889E-05	7,9,11,13
	1.05319E-04	2,3

	Area [mm^2]	Bars
Variation #2	1.00000E-06	16
	3.61702E-05	1,6,7,10,12,14,18,20
	5.11524E-05	11,13,15,17,19,21
	7.23404E-05	2,5,8,9
	1.08511E-04	3,4

	Area [mm^2]	Bars
Variation #3	1.00000E-06	22
	2.91223E-05	1,8,9,14
	3.88298E-05	16,18,20,24,26,28
	4.85372E-05	15,17,19,21,23,25,27,29
	5.82447E-05	2,7,10,13
	8.73670E-05	3,6,11,12
	1.16489E-04	4,5

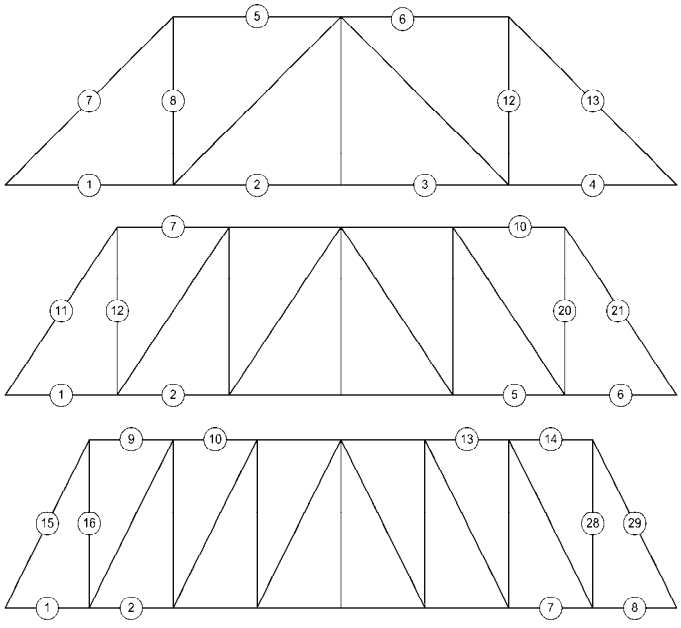

(a) (b)

Figure 5.B2: Optimum Howe design (a) cross-sectional areas and (b) connectivity

	Area [mm^2]	Bars
Variation #1	1.00000E-06	7,10
	3.40426E-05	8,9,11
	5.10638E-05	1,2,3,4,5,6
	5.38260E-05	13,14,15,16
	6.13711E-05	12,17

	Area [mm^2]	Bars
Variation #2	1.00000E-06	11,18
	1.64894E-05	13,14,16,17
	3.29787E-05	1,2,5,6,7,10,12,15,19
	3.68713E-05	20,21,22,23,24,25,26,27
	4.66390E-05	28,29
	6.59574E-05	3,4,8,9

	Area [mm^2]	Bars
Variation #3	1.00000E-06	15,26
	1.67553E-05	17,18,19,20,22,23,24,25
	2.51330E-05	1,2,7,8,9,14
	3.02061E-05	28,29,30,31,32,33 34,35,36,37,38,39
	3.35106E-05	16,21,27
	4.18883E-05	40,41
	5.02660E-05	3,6,10,13
	7.53989E-05	4,5,11,12

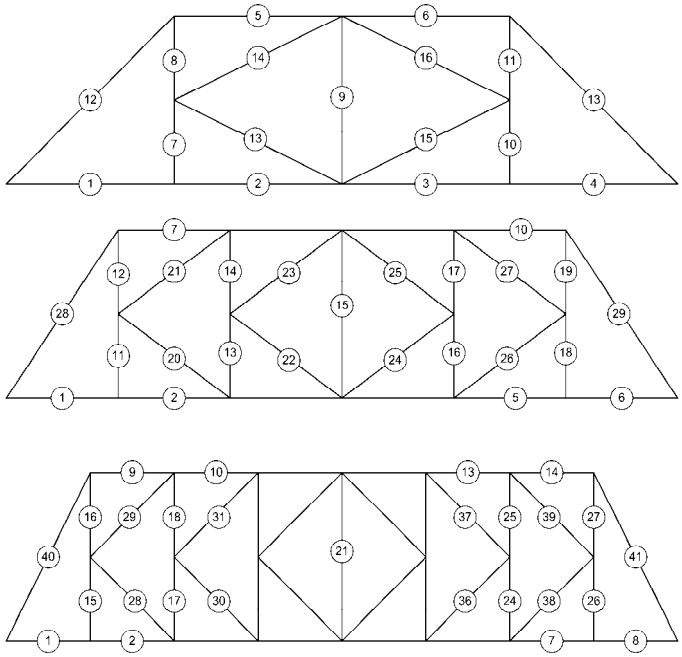

(a) (b)

Figure 5.B3: Optimum K-truss design (a) cross-sectional areas and (b) connectivity

	Area [mm^2]	Bars
Variation #1	1.00000E-06	8,12
	5.26596E-05	1,2,3,4
	6.32889E-05	7,9,11,13
	7.02128E-05	10
	1.05319E-04	5,6

	Area [mm^2]	Bars
Variation #2	1.00000E-06	12,20
	3.61702E-05	1,2,5,6,14,18
	5.11524E-05	11,13,15,17,21
	7.23404E-05	3,4,7,10,16
	1.08511E-04	8,9

	Area [mm^2]	Bars
Variation #3	1.00000E-06	16,28
	2.91223E-05	1,2,7,8
	3.88298E-05	18,20,24,26
	4.85372E-05	15,17,19,21,23,25,27,29
	5.82447E-05	3,6,9,14
	7.76596E-05	22
	8.73670E-05	4,5,10,13
	1.16489E-04	11,12

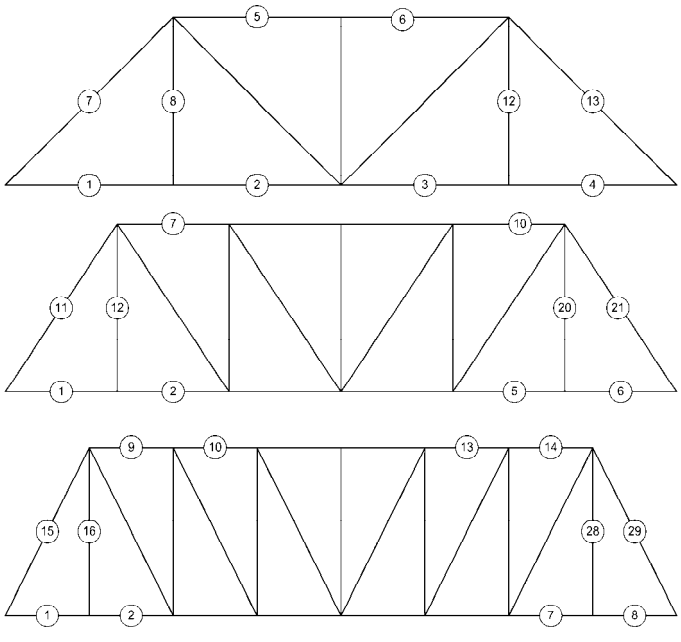

(a) (b)

Figure 5.B4: Optimum Pratt design (a) cross-sectional areas and (b) connectivity

	Area [mm^2]	Bars
Variation #1	3.19149E-05	1,3
	4.51345E-05	6,7,8,9,10,11
	6.38298E-05	4,5
	9.57447E-05	2

	Area [mm^2]	Bars
Variation #2	2.01702E-05	1,5
	3.92038E-05	10,11,12,13,14,15,16,17,18,19
	4.03404E-05	6,9
	6.05106E-05	2,4
	8.06809E-05	7,8
	1.00851E-04	3

	Area [mm^2]	Bars
Variation #3	1.57620E-05	1,7
	3.15244E-05	13,8
	4.00131E-05	14,15,16,17,18,19,20 21,22,23,24,25,26,27
	4.72865E-05	2,6
	6.30478E-05	9,12
	7.88100E-05	3.5
	9.45722E-05	10,11
	1.10334E-04	4

(a)

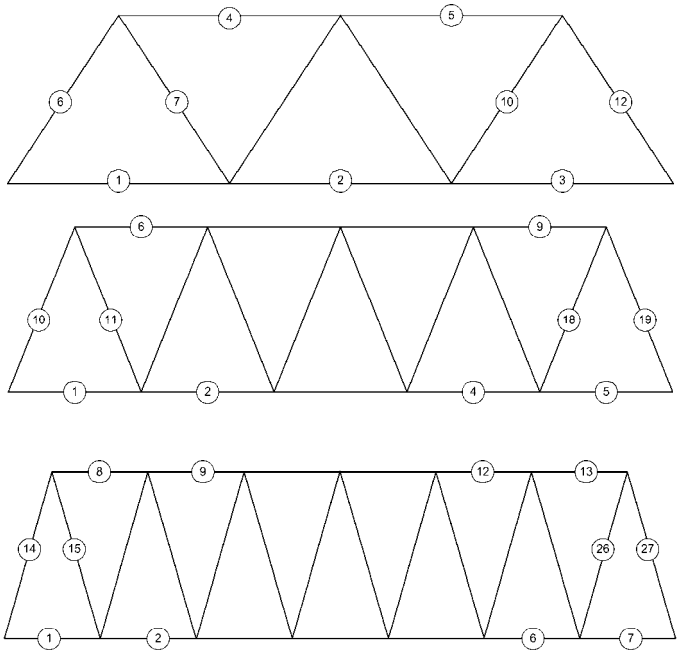

(b)

Figure 5.B5: Optimum Warren design (a) cross-sectional areas and (b) connectivity

APPENDIX 5.C: Results for the variations of the 9-bar truss

In this Appendix, the results from the application of the proposed optimization procedure to six different topologies of the 9-bar truss, each under four loading conditions, are presented. For each design and for each load case, the minimum structural weight, the optimum design vector and the nodal displacements of the unrestrained degrees of freedom are recorded.

Table 5.C1: Optimization results for the first Load Case

	Design 9a	Design 9b	Design 9c	Design 9d	Design 9e	Design 9h
W_{opti}	8867.234	5708.034	5790.766	5709.559	8868.726	11135.735
x_1	21.046	16.641	16.964	16.579	21.046	12.106
x_2	51.552	40.906	41.716	41.034	51.552	45.882
x_3	29.763	3.198	5.374	3.183	29.763	47.170
x_4	42.092	33.721	33.965	33.745	42.092	0.100
x_5	0.100	0.100	0.113	0.100	0.100	33.357
x_6	0.100	16.623	16.124	16.637	21.046	20.266
x_7	21.046	0.100	0.100	0.100	21.046	23.597
x_8	21.046	0.100	0.100	0.100	29.763	28.671
x_9	29.763	23.447	22.799	23.376	0.100	47.179
$U_{2,x}$	-0.171	-0.216	-0.212	-0.217	-0.171	-0.297
$U_{2,y}$	-0.935	-1.996	-1.529	-1.998	-0.935	-2.000
$U_{3,x}$	-0.171	-0.433	-0.436	-0.434	-1.097	-0.513
$U_{3,y}$	-2.000	-2.000	-2.000	-2.000	-2.000	-1.847
$U_{4,y}$	-0.764	-1.779	-1.316	-1.781	-0.764	-1.703
$U_{5,x}$	0.209	0.264	0.259	0.263	0.209	0.235
$U_{5,y}$	-0.693	-0.868	-0.859	-0.867	-0.693	-0.667
$U_{6,x}$	0.381	0.264	0.259	-0.216	0.381	0.058
$U_{6,y}$	-1.829	-2.000	-2.000	-2.000	-1.829	-2.000

Table 5.C2: Optimization results for the second Load Case

	Design 9a	Design 9b	Design 9c	Design 9d	Design 9e	Design 9h
W_{opti}	1287.229	1061.383	1288.720	1062.874	1288.720	6488.691
x_1	0.100	0.100	0.100	0.100	0.100	0.100
x_2	11.237	7.201	11.237	7.200	11.237	18.000
x_3	7.946	7.200	7.946	7.200	7.946	25.456
x_4	11.237	10.182	11.237	10.182	11.237	0.100
x_5	0.100	0.100	0.100	0.100	0.100	18.000
x_6	0.100	0.100	0.100	0.100	0.100	18.000
x_7	0.100	0.100	0.100	0.100	0.100	18.000
x_8	0.100	0.100	0.100	0.100	0.100	25.456
x_9	0.100	0.100	0.100	0.100	0.100	25.456
$U_{2,x}$	0.000	0.000	0.000	0.000	0.000	0.000
$U_{2,y}$	-1.680	-2.000	-1.680	-2.000	-1.680	-2.000
$U_{3,x}$	0.000	0.000	0.000	0.000	-0.453	-0.200
$U_{3,y}$	-2.000	-2.000	-1.547	-2.000	-2.000	-1.400
$U_{4,y}$	-1.680	-2.000	-1.680	-2.000	-1.680	-2.000
$U_{5,x}$	0.320	0.500	0.320	0.500	0.320	0.200
$U_{5,y}$	-1.227	-1.500	-1.227	-1.500	-1.227	-0.600
$U_{6,x}$	0.320	0.500	0.320	0.000	0.320	0.000
$U_{6,y}$	-2.000	-2.000	-2.000	-2.000	-2.000	-1.600

Table 5.C3: Optimization results for the third Load Case

	Design 9a	Design 9b	Design 9c	Design 9d	Design 9e	Design 9h
W_{opti}	6488.691	4163.091	4164.582	4164.582	6490.182	4164.582
x_1	18.000	14.400	14.400	14.400	18.000	14.400
x_2	36.000	28.800	28.800	28.800	36.000	28.800
x_3	18.000	0.100	0.100	0.100	18.000	20.365
x_4	25.456	20.365	20.365	20.365	25.456	0.100
x_5	0.100	0.100	0.100	0.100	0.100	14.400
x_6	0.100	14.400	14.400	14.400	18.000	0.100
x_7	18.000	0.100	0.100	0.100	18.000	0.100
x_8	18.000	0.100	0.100	0.100	25.456	0.100
x_9	25.456	20.365	20.365	20.365	0.100	20.365
$U_{2,x}$	-0.200	-0.250	-0.250	-0.250	-0.200	-0.250
$U_{2,y}$	-0.800	-0.750	-0.750	-0.750	-0.800	-1.500
$U_{3,x}$	-0.200	-0.500	-0.500	-0.500	-1.200	-0.500
$U_{3,y}$	-2.000	-2.000	-2.000	-2.000	-2.000	-2.000
$U_{4,y}$	-0.600	-0.500	-0.500	-0.500	-0.600	-1.250
$U_{5,x}$	0.200	0.250	0.250	0.250	0.200	0.250
$U_{5,y}$	-0.600	-0.750	-0.750	-0.750	-0.600	-0.750
$U_{6,x}$	0.400	0.250	0.250	1.000	0.400	0.250
$U_{6,y}$	-1.800	-2.000	-1.250	-2.000	-1.800	-2.000

Table 5.C4: Optimization results for the forth Load Case

	Design 9a	Design 9b	Design 9c	Design 9d	Design 9e	Design 9h
W_{opti}	9470.673	5823.972	6677.074	5804.790	9472.164	13081.144
x_1	21.751	16.575	17.546	16.786	21.750	10.514
x_2	53.278	40.994	44.071	40.996	53.279	47.914
x_3	34.391	4.776	3.060	4.853	34.391	51.167
x_4	43.502	33.753	36.222	33.911	43.502	0.100
x_5	0.100	0.101	0.101	0.102	0.100	40.419
x_6	0.100	16.629	21.893	16.452	21.751	28.475
x_7	21.751	1.292	1.279	1.021	26.640	25.573
x_8	26.639	0.470	1.777	0.102	30.760	40.387
x_9	30.760	23.451	30.932	23.257	0.100	57.171
$U_{2,x}$	-0.166	-0.217	-0.206	-0.215	-0.166	-0.342
$U_{2,y}$	-0.933	-1.998	-1.986	-1.984	-0.933	-2.000
$U_{3,x}$	-0.166	-0.434	-0.453	-0.434	-1.126	-0.565
$U_{3,y}$	-2.000	-2.000	-2.000	-2.000	-2.000	-1.859
$U_{4,y}$	-0.767	-1.781	-1.781	-1.769	-0.767	-1.658
$U_{5,x}$	0.203	0.264	0.245	0.264	0.203	0.225
$U_{5,y}$	-0.671	-0.867	-0.808	-0.864	-0.671	-0.623
$U_{6,x}$	0.368	0.264	-1.247	-1.974	0.368	0.036
$U_{6,y}$	-1.797	1.883	1.972	-0.225	-1.797	-2.000

At this point, it is noted that from Table 5.C2 it is evident that optimum solutions can be obtained with the proposed procedure for multiple displacement constraint problems as well. However, it is not claimed that the procedure, in its present form, is suitable for such problems as well. The optimal layouts, numerically described in the aforementioned Tables, are illustrated in Fig.5.C1. The vanishing members are denoted as broken lines while the remaining elements are shown as continuous thick lines. The nodes that present the maximum

displacements are denoted with a hatched circle while the externally applied loads are shown as arrowed lines.

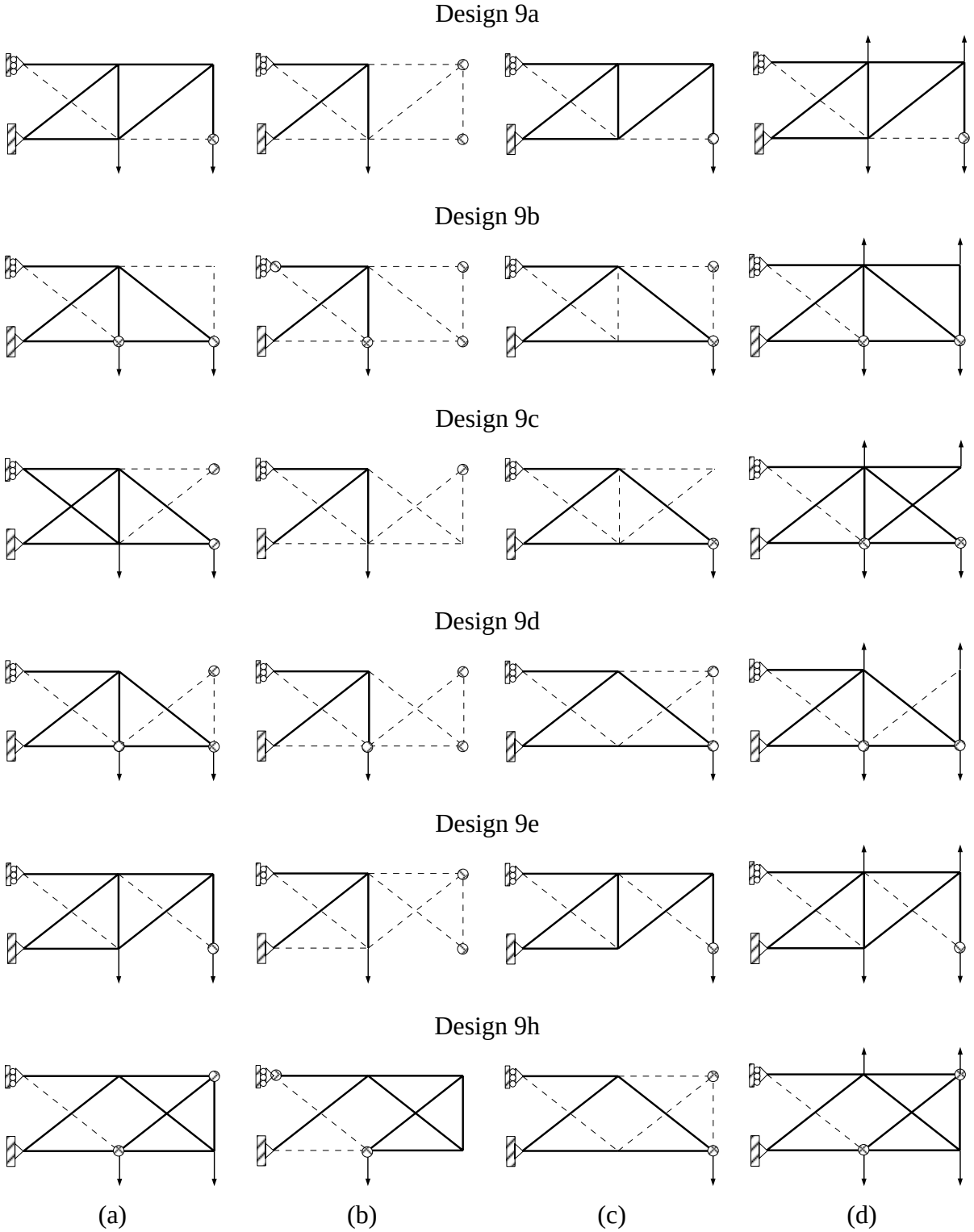

Figure 5.C1: Optimal layouts for the 9-bar variations and for (a) Load Case #1, (b) Load Case #2, (c) Load Case #3 and (a) Load Case #1.

From Fig.5.C1 it is clear that the proposed 9-bar variations include cases where, at the optimum, the maximum nodal displacements do not always correspond to load application points in accordance to the 'fair-play' mentioned in Section 5.2.7.

This page has been left intentionally blank

CHAPTER 6

LAYOUT OPTIMIZATION OF 2D CONTINUA UNDER AN EXTENDED SINGLE DISPLACEMENT CONSTRAINT

Abstract

In this chapter, the layout optimization of 2D continua under an extended single displacement constraint is discussed, the concept of the 'extended' displacement constraint being introduced in Chapter 5. More particularly, the layout optimization is sought following two conceptually different approaches. According to the first approach, the thickness of the 2D continuum is kept constant, while material that has been detected as redundant is completely removed from it. To this end, a new efficient variation of an already existing methodology is proposed. According to the second approach, the thickness of the 2D continuum is isoparametrically interpolated, the nodes being the interpolation points. Furthermore, a variation of the methodology introduced in Chapter 5 is developed. Both approaches are examined through four typical literature benchmarking problems in structural optimization and the encouraging results suggest that these approaches be a useful and efficient tool in 2D layout optimization.

Keywords

Layout optimization, 2D continuum, single displacement constraint, material removal, thickness redesign.

6.1. Introduction

The layout optimization of 2D continua under a single displacement constraint has always been a very attractive optimization problem and consists an ideal field for investigations because it attains two basic characteristics. First, 2D continua are the simplest continuum structures, thus convenient for testing new approaches, and second, 2D continua may be considered as quasi-3D bodies, thus every theory developed for them is potentially valid for 3D bodies as well. For their layout optimization, removal of redundant material is required. Towards this direction, there are two questions that must be answered, the former being how a material is characterized as redundant and the second being how it is possible to remove excessive material from a 2D continuum. These two questions are not decoupled, meaning that the determination of the criterion for material removal is related to the manner on which material will be removed. In the present chapter, two basic approaches are examined, both concerning not only the single displacement constraint but also its extended definition, as presented in Chapter 5.

The first approach concerns the total material removal from a constant thickness 2D continuum. The criterion for selecting the material to be removed is based on a simple consideration: useful (excessive) material has a high (low) energy contribution to the structure. Therefore, it is possible to iteratively detect the material with the lower aforementioned contribution and then attribute to it a very low modulus of elasticity. In this way, the excessive material is artificially removed from the stiffness matrix of the structure in the sense that its presence from that point on has a negligible effect on the structural behavior. The concept just described is already known in the literature as the Evolutionary Structural Optimization (ESO) method. Even though there has been a strong dispute concerning both the correctness of the name and the efficiency of this approach, publications on this method has shown a good performance in a wide range of applications. In the present chapter, a variation of this method is proposed, according to which both the computational cost and the final structural weight decrease, as the examined literature benchmarking problems show.

The second approach concerns the extension in 2D continua of the novel consideration presented in Chapter 5. In more details, this extension considers that the thickness of a 2D continuum is varying, the control points being the nodes of the structure. The nodal thickness changes according to a redesign rule similar to the one proposed in Chapter 5. As a result, areas with excessive material become thinner while areas with utilized material become thicker. This approach is also evaluated through a series of literature benchmarking problems, while the final design presents a layout significantly different from the ones in the literature.

6.2. Total removal of material from a constant thickness sheet

One of the most popular problems in structural optimization is the single displacement constraint problem. Its popularity is due to the fact that the problem is convex, thus it attains a global minimum. Towards the trace of the optimum, various techniques have been proposed, the Evolutionary Structural Optimization (ESO) being one of them. According to its developers, the variation of ESO that addresses the single displacement constraint problem has the ability to provide an optimized structure by removing elements of low virtual strain energy density. Furthermore, it has been shown that the introduction of the *normalized* virtual strain energy density of the entire structure during the optimization procedure is beneficial. The current work investigates the coupling of the aforementioned version of ESO with the aforementioned normalization concept for the optimization of 2D-continua. On top of that, the values of the normalized virtual strain energy density are derived from the non-vanishing elements (active elements) only. The specific coupling is tested in four typical examples of 2D continua, namely the deep cantilever, the short cantilever, the MBB beam and a Michell

type structure. The quantified results reveal the improvement that can be achieved when the normalized virtual strain energy density of the active elements is used as a criterion for removing inefficient material.

6.2.1. In general

Structural optimization has long been one of the most interesting challenges among the engineering community not only as a theoretical problem but mainly as an issue of major practical importance. During the last fifty years, numerous techniques have been proposed and tested. However, the estimation of the global optimum in the general optimization problem has not yet been solved.

Among the published optimization techniques, one can find various deterministic or stochastic procedures. The deterministic procedures perform a systematic search of the feasible region, possibly using derivative information (i.e. Steepest Descent Method, Sequential Linear Programming (SLP), Sequential Quadratic Programming (SQP), etc). The stochastic procedures perform a thorough exploration and exploitation of the feasible region (i.e. Genetic Algorithms (GA), Simulated Annealing (SA), Tabu search, etc) ((Belegundu and Chandrupatla, 1999); Pham and Karaboga, 2000). Their common element and main advantage is that they are derivative-free ('zero-order' techniques), meaning that they use no derivative (gradient or Hessian) information. In addition to these techniques, other approaches have also appeared, such as the Lagrange multipliers approach and the SIMP method by Bendsøe (Bendsøe and Sigmund, 2003). Another category of optimization techniques include the well-known optimality criteria, which appeared first in the late 50's (Haftka et al, 1990; Morris, 1982; Rozvany, 2001). The Evolutionary Structural Optimization (ESO) by Steven et al. is a novel zero-order technique (Xie and Steven, 1997; Chu Nha et al, 1996). Its origin is based on the simple principle that underutilized material should be gradually removed. In addition, new formulations of OC still appear, as by Makris and Provatidis who proposed a virtual strain energy density optimization approach (Makris and Provatidis, 2002). Apart from the individual development of techniques, it is possible to combine the advantageous characteristics of different methods. Towards this direction, in the present section the combination of the ESO method with the method of Makris and Provatidis is investigated and updated. The investigation is based on an in-house Finite Element Analysis (FEA) code and includes four well-known typical literature examples.

6.2.2. Theoretical background

In a shape optimization problem, the domain of the design model is the design variable and the goal is to find its optimum shape (Haftka et al, 1990). The simplest type of such problems is designing for minimum compliance, or, equivalently, for maximum stiffness, under simple resource constraints. These constraints are imposed as a somewhat arbitrarily chosen material volume fraction (Rozvany, 2001). A realistic optimization approach for this kind of problems is to use the structural weight as the objective function and the displacements as the constraints (Xie et al, 1997). Therefore, the simplest formulation for the weight minimization of 2D-continuum structures implements only one displacement constraint (single displacement constraint problem) and can be stated as follows:

$$minimize\ W = \sum_{j=1}^{NEL} w_j(t) \tag{6.1}$$

$$subject\ to\ \frac{\max|u_i|}{u_{allow}} - 1 \le 0 \tag{6.2}$$

This approach suggests that the 2D-continuum design space be discretized in NEL finite elements, each one of which has a thickness t. The weight of the $j-th$ finite element is denoted as $w_j(t)$, the total weight of the structure is W, the maximum nodal displacement of the examined structure is $\max|u_i|$, while the prescribed displacement limit is u_{allow}. In order to find the optimum design, three basic factors must be determined; that is the material removal criterion (redesign scheme), the termination criterion of the recursive optimization procedure and the optimality criterion based on which the optimum shape is determined.

6.2.2.1. The material removal criterion

According to the Evolutionary Structural Optimization (ESO) method, the redesign is based on the gradual elimination of underutilized elements from the discretized design domain (Xie et al, 1997). The determination of the material utilization is based on the absolute value of the element virtual strain energy u_i derived from the application of a virtual unit load at the most critical degree of freedom:

$$u_i = \{U_{q,i}\}[K_{elem,i}]\{U_{p,i}\} \tag{6.3}$$

where

u_i: the virtual strain energy of the $i-th$ element

$\{U_{q,i}\}$: the nodal displacement vector of the $i-th$ element due to the virtual unit load

$[K_{elem,i}]$: the stiffness matrix of the $i-th$ element

$\{U_{p,i}\}$: the nodal displacement vector of the $i-th$ element due to the real load

More specifically, all elements are ranked according to their virtual strain energy and a predefined percentage of elements with the lowest values is eliminated. The developers of ESO also make two important remarks, the first being that if the continuum structure is discretized using finite elements of different size then the virtual strain energy *density* must be used instead, and the second being that the averaged *nodal* strain energy densities of neighboring elements can be used as a means of dealing with the so-called checkerboard problem.

6.2.2.2. The termination criterion

With respect to the termination criterion, the developers of ESO had proposed to check whether the prescribed limit for the displacement was exceeded:

$$\frac{\max|u_i|}{u_{allow}} > 1 \tag{6.4}$$

If this was the case, then the design corresponding to the last-but-one iteration was used as the optimized topology. In the sequel, a uniform scaling was applied on the thickness of this topology so that the displacement constraint (Eq.6.2) was satisfied as an equality (active constraint).

6.2.2.3. The optimal shape criterion

In a later version of ESO, another criterion for selecting the optimal shape was introduced; that of the so-called Performance Index (PI). The PI is a means to compare a current design with the initial one, which is used as a design of reference:

$$PI = \frac{u_{o,\max}}{u_{cur,\max}} \frac{W_o}{W_{cur}} \tag{6.5}$$

where

$u_{o,\max}$: the absolute value of the most critical displacement in the initial design

$u_{cur,\max}$: the absolute value of the most critical displacement in the current design

W_o : the structural weight of the initial design

W_i : the structural weight of the current design

When a value of PI less than unity is reached, then from that point on the efficiency of any new design is less than that of the initial design, thus the optimization procedure can be terminated. On the contrary, the maximum PI denotes the best material distribution that can be achieved (optimal shape) with respect to the initial design. Obviously, the maximum PI value is not known *a priori*. This means that the maximum PI value cannot be located unless the optimization procedure is completed. Therefore, another termination criterion can be defined:

$$PI < 1 \tag{6.6}$$

6.2.3. The proposed optimization procedure

One of the main advantages of the ESO procedure described in Section 6.2.2 is the fact that it does not require a mesh re-generation at each iteration step. On the contrary, the material removal is approximated by setting the Young's modulus of the removed elements equal to unity, thus the initial mesh can be used. At the same time, this is a drawback, because both removed and remaining elements contribute to the formation of the global stiffness matrix. In turn, the estimation of the element virtual strain energy is an approximation and not the outcome of an accurate calculation. In order to minimize the effect that the removed elements have on the evolutionary procedure, the present chapter suggests the introduction of the *normalized virtual strain energy density* as the material removal criterion, the normalization being with respect to the remaining (active) elements only:

$$n_j = \frac{u_{VSED,j}}{\left(\frac{1}{NAE}\right)\sum_{j=1}^{NAE} u_{VSED,j}} \tag{6.7}$$

where

n_j : the normalized virtual strain energy density of the $j-th$ active element

$u_{VSED,j}$: the virtual strain energy density of the $j-th$ active element

NAE : the total Number of the Active Elements

This alteration is based on a previous paper by the first author of the present work, where it was shown that the integration of the *normalized* virtual strain energy density into the structural optimization procedure of trusses was beneficial (Makris and Provatidis, 2002). In that paper, the normalization was with respect to all elements, while in this chapter the normalization is with respect to the active elements only. It is evident that the effect of the active elements is stronger in Eq.(6.7) than in Eq.(6.3).

Taking all the above into consideration, the proposed version of the ESO method for 2D-continua can be divided in two phases, described as follows:

Phase #1:

Step 1: Discretize the design domain using a fine mesh of finite elements

Step 2: Analyze the structure for the applied loads

Step 3: If the termination criterion (Eq.6.4) is violated, then STOP

Step 4: Estimate the Performance Index (PI) for the current design (Eq.6.5)

Step 5: Apply the virtual unit load theorem for the most critical degree of freedom (dof)

Step 6: Estimate the normalized virtual strain energy density n_j of all active elements using Eq.(6.7)

Step 7: Rank the active elements in an ascending order based on their n_j values

Step 8: Eliminate a predefined small proportion of the material with the lower n_j (underutilized material)

Step 9: Go to Step 3

Phase #2:

Step 10: From the Phase #1 results, locate the design with the highest PI value (optimal shape)

Step 11: On the design of the previous step, apply a uniform scaling on the element thickness so that the corresponding weight is minimized

6.2.4. Evaluation indices

In order to evaluate the proposed procedure, the iterations required until the termination of the optimization procedure, as well as four more indices, termed as PI_1, PI_2, PI_3 and PI_4 respectively, were used. All these quantities are discussed briefly in the following paragraphs.

6.2.4.1. Number of iterations

It is self-evident that the evaluation of an iterative procedure performance is based on the number of iterations required until convergence is achieved. This criterion is also applied for the proposed ESO iterative scheme.

6.2.4.2. The weight of the structure with respect to the initial design

One of the primal objectives is to minimize the structural weight. In order to determine the material reduction of a design, it is required to use another design as a reference. As such, it is possible to use the initial design. It is obvious that the larger the reduction is, the better the design is. In mathematical terms:

$$PI\_1 = \left(\frac{W_{cur} - W_{ini}}{W_{ini}} \right) \tag{6.8}$$

where

W_{cur} : the weight of the current design and

W_{ini} : the weight of the initial design (design of reference)

6.2.4.3. The weight of the structure with respect to the optimized uniform design

The initial design may be scaled uniformly with respect to the element thickness so that the displacement constraint becomes active. The so formed design is called optimized uniform

design (OUD). Therefore, it is possible to use the (OUD) as reference for weight comparisons. In this case, the corresponding index is defined as:

$$PI\_2 = \left(\frac{W_{cur} - W_{OUD}}{W_{OUD}} \right) \tag{6.9}$$

where

W_{cur} : the weight of the current design and

W_{OUD} : the weight of the optimized uniform design (design of reference)

6.2.4.4. The total area of the topology

For practical engineering purposes, the knowledge of the area that the optimal topology covers is important because it determines the practical value of the structure. The MBB beam is a very good example. As it is known, this beam carries the floor in the fuselage of the Airbus passenger carrier. Apart from stress and displacement constraints, it is of major importance to ensure the presence of adequate openings so that all the systems running under the floor can be installed; otherwise, although a minimum weight may be achieved, the practical value may be minimized as well. A simple index that can be used for ranking the topologies with respect to their surface coverage is defined as:

$$PI\_3 = \left(\frac{A_{N_{ActElem}}}{A_{NEL}} \right) \tag{6.10}$$

where

$A_{N,ActElem}$: the total area of the non-vanishing elements

A_{NEL} : the total area of the initial topology

If the continuum structure is discretized using finite elements of the same size, then the aforementioned index can be further simplified as:

$$PI\_3 = \left(\frac{N_{ActElem}}{NEL} \right) \tag{6.11}$$

where

$N_{ActElem}$: the number of the non-vanishing elements

NEL : the total number of elements

6.2.4.5. The performance index (PI)

The optimal shape criterion defined through the ESO Performance Index (PI) (Eq.6.5) is another quantity that can be used in order to evaluate a design:

$$PI\_4 = PI \tag{6.12}$$

6.2.5. Investigated test cases

The proposed procedure was tested in four typical examples retrieved from the literature, namely the deep cantilever, the short cantilever, the MBB beam and a Michell type structure (Fig.6.1).

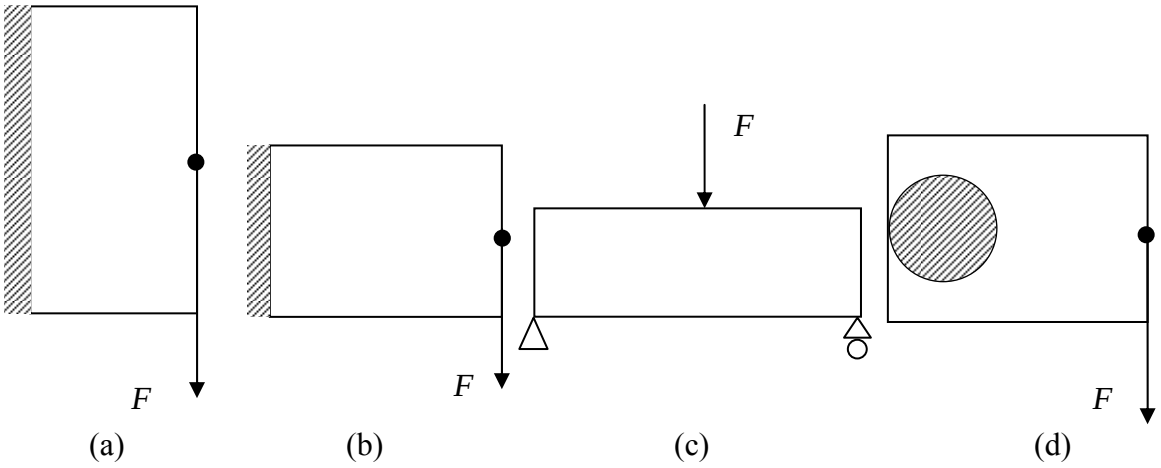

Figure 6.1: The domain of the examined examples (a) deep cantilever, (b) short cantilever, (c) MBB beam and (d) Michell-type structure

6.2.5.1. Test case#1: Deep cantilever

The deep cantilever is illustrated in Fig.6.1a. The dimensions $L_x \times L_y$ *(Length x Height)* of the design domain (rectangular shape) are $L_x = 200mm$ and $L_y = 450mm$ while the initial uniform thickness of the beam is $t = 1mm$. The entire left side of the structure is fixed and the centre of the right side is the point of application of a concentrated load $F = 200N$. Only one constraint is imposed and it concerns the maximum allowable displacement $(1mm)$ both along the horizontal and the vertical direction. The Young's modulus is considered to be $E = 200GPa$, the material density is set equal to unity, while the Poisson's ratio is assumed to be $v = 0.3$. The design domain was divided into 36×16 four node rectangular finite elements. For each iteration, the Element Elimination Ratio (EER) used was constant and equal to 2%, while it was applied only to the non-vanishing elements.

6.2.5.2. Test case #2: Short cantilever

The short cantilever is illustrated in Fig.6.1b. The dimensions $L_x \times L_y$ of the design domain (rectangular shape) are $L_x = 160mm$ and $L_y = 100mm$ while the initial uniform thickness of the beam is $t = 1mm$. Once again, the entire left side of the structure is fixed and the centre of the right side is the point of application of a concentrated load $F = 3kN$. Only one constraint is imposed and it concerns the maximum allowable displacement $(1mm)$ both along the horizontal and the vertical direction. It is noted that there are two other variations of the same problem with $u_{allow} = 0.50mm$ and $u_{allow} = 0.75mm$. The Young's modulus is considered to be $E = 207GPa$, the material density is set equal to unity, while the Poisson's ratio is assumed to be $v = 0.3$. The design domain was divided into 32×20 four node rectangular finite elements. For each iteration, the Element Elimination Ratio (EER) used was constant and equal to 1%, while it was applied only to the non-vanishing elements.

6.2.5.3. Test case #3: MBB beam

The MBB beam is a simply supported beam illustrated in Fig.6.1c. The dimensions $L_x \times L_y$ of the rectangular design domain are $L_x = 2400mm$ and $L_y = 400mm$, while the initial uniform thickness of the beam is $t = 1mm$. A concentrated load $F = 20kN$ is applied at the middle of the top side of the beam. There is only one imposed constraint concerning the deflection of the beam which is required to be less than $9.4mm$. For this case, the Young's

modulus is considered to be $E = 200GPa$, the material density is set equal to unity, while the Poisson's ratio is assumed to be $v = 0.3$. The design domain was divided into 66×11 four node rectangular finite elements. Once again, for each iteration, the Element Elimination Ratio (EER) used was constant and equal to 1%, while it was applied only to the non-vanishing elements. It is noted that due to symmetry of the beam, only the right or left half can be used.

6.2.5.4. Test case #4: Michell structure

The examined Michell type structure is illustrated in Fig.6.1d. The design domain is the section of a rectangular region $L_x \times L_y$ with a circle. The dimensions of the rectangle are $L_x = 550mm$ and $L_y = 400mm$, while the radius of the circle is $r = 100mm$. The circle is tangent to the middle of the left side of the domain and is fixed along its entire perimeter. The initial uniform thickness of the structure is $t = 1mm$. A point load $F = 50kN$ acts at the middle of the right side of the rectangular region. The imposed single displacement constraint concerns the deflection of the loaded point which must not move vertically more than $9mm$. It is noted that there are two other variations of the same problem with $u_{allow} = 5mm$ and $u_{allow} = 7mm$. A Young's modulus of $E = 205GPa$, a unitary material density and a Poisson's ratio $v = 0.3$ are also assumed. The design domain is divided into 33×24 four node rectangular finite elements. For each iteration, the Element Elimination Ratio (EER) used was constant and equal to 0.5%, while it was applied only to the non-vanishing elements. Again, due to symmetry, only the top half can be used.

6.2.6. Results

The results of the examined examples are presented in the following Table (Table 6.1).

Table 6.1: Results

Example	Scenario	ERR (%)	Iterations	PI_1	PI_2	PI_3	PI_4
Deep cantilever	A	2	73	-99.80	-44.23	19.44	1.793
	B	2	52	-99.80	-44.14	19.79	1.790
			-28.77%	***0.00%***	***-0.22%***	***1.79%***	***-0.17%***
Short cantilever	A	1	52	-72.70	-16.37	56.88	1.196
	B	1	42	-73.16	-17.79	55.00	1.216
			-19.23%	***0.63%***	***8.64%***	***-3.30%***	***1.71%***
MBB beam	A	1	82	-99.98	-35.50	39.67	1.550
	B	1	68	-99.98	-35.99	39.95	1.562
			-17.07%	***0.00%***	***1.39%***	***0.70%***	***0.77%***
Michell structure	A	0.5	171	-77.28	-28.40	37.88	1.397
	B	0.5	78	-76.84	-27.02	56.06	1.370
			-54.39%	***-0.57%***	***-4.85%***	***48.00%***	***-1.89%***

The terms 'Scenario A' and 'Scenario B' correspond to the typical ESO procedure and the proposed ESO variation, respectively. The columns 'Iterations', PI_1, PI_2, PI_3 and PI_4 correspond to the evaluation indices. For each example in the Table, there are three rows, the first two containing the results of the performed investigation and the third row

representing the comparison between the two scenarios, 'Scenario A' being the reference. In mathematical terms, each third-row value is defined as:

$$Value = \left(\frac{Value_{Scenario\_B} - Value_{Scenario\_A}}{Value_{Scenario\_A}} \right) \tag{6.13}$$

At this point, it is strongly emphasized that, depending on the combination of the Element Elimination Ratio (EER) value and the mesh fineness, it is possible to get results in favor of the first or the second scenario. Towards this direction and for the needs of the current work, it was decided to present such combinations of ERR and mesh fineness that would pinpoint this characteristic. From Table 6.1 it is evident that, in all cases, the proposed procedure results in a significant reduction of the required number of iterations (from 17% to 54%), while the superiority with respect to the other evaluation indices depends on the evaluation index selected and the example examined, or, more accurately, on the selected combination of the ERR and the mesh.

For each example, the optimal shape is illustrated in Fig.(6.2).

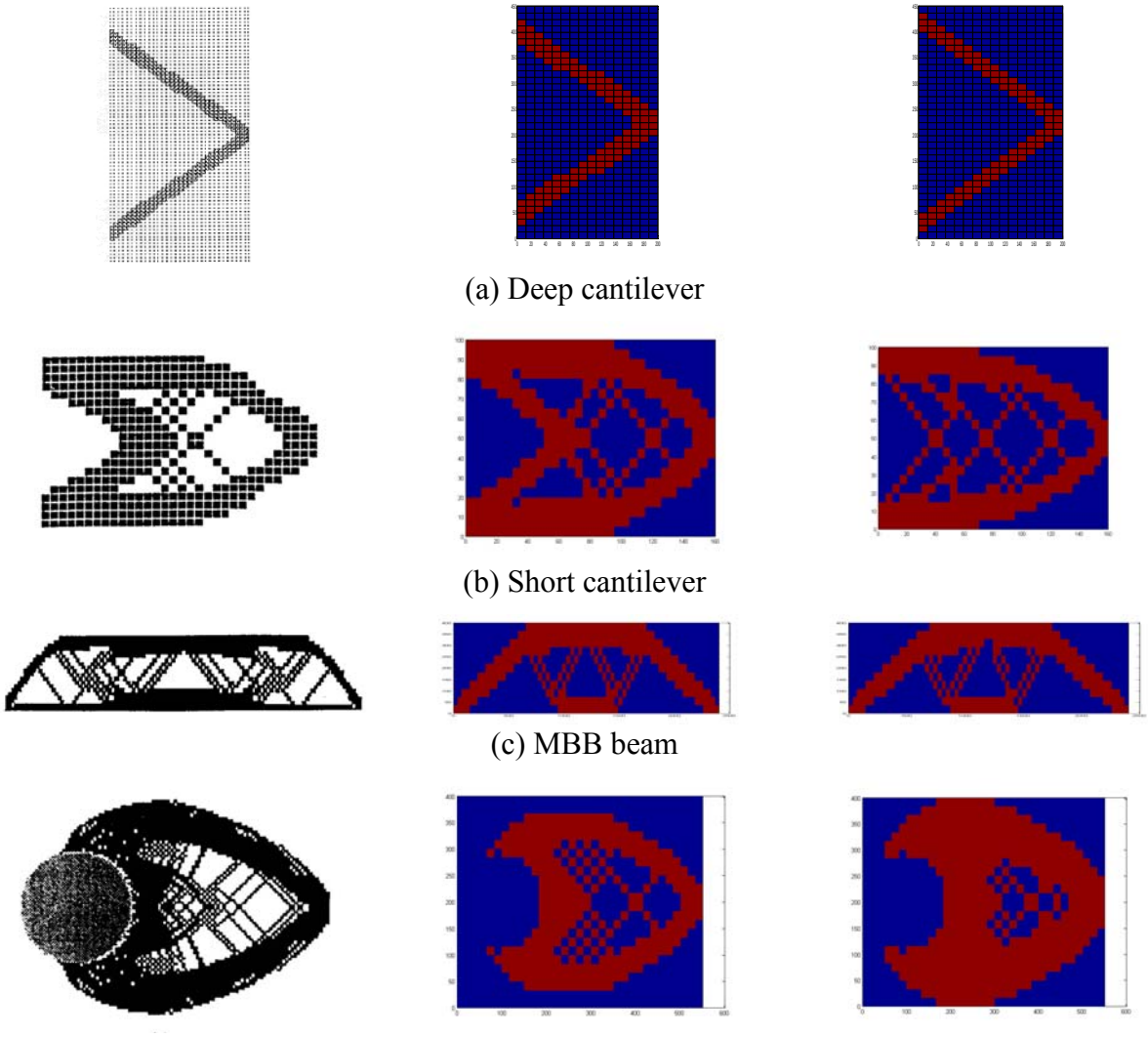

(a) Deep cantilever

(b) Short cantilever

(c) MBB beam

(d) Michell type structure

Literature | Scenario A – ERR: 0.5% | Scenario B – ERR: 0.5%

Figure 6.2: Optimal shapes

There is a variety of results. For example, the optimal shape for the deep cantilever is almost the same, independed from the scenario, while for the short cantilever, depending on the scenario, the optimal shape is completely different.

6.2.7. Conclusions

The present investigation concerned the use of the normalized virtual strain energy density, the normalization being with respect to the remaining (active) elements, as a criterion for material removal in the well-known Evolutionary Structural Optimization (ESO) method. The main idea behind this approach was that the remaining (active) elements must have a stronger influence on the optimization procedure than the removed elements. The investigation included four typical examples, namely the deep cantilever, the short cantilever, the MBB beam and a Michell type structure, and the evaluation of the results was based on five indices ('Iterations', PI_1, PI_2, PI_3 and PI_4). It was shown that, in all cases, the optimum shape was reached in significantly less iterations when the proposed criterion was implemented. On top of that, it was also shown that a design better than that obtained by the application of the typical ESO procedure could be located. Therefore, the conclusion of the current investigation was that, apart from the Element Elimination Ratio (EER) and the mesh fineness, the proposed material removal criterion is of major importance in the quest of the optimal shape and must be considered as an optimization parameter.

6.3. Variable thickness sheet under an extended single displacement constraint

In the present section, the problem of seeking the optimum layout of a 2D continuum structure is sought under the assumption that an extended single active displacement constraint is imposed and elements of variable element-wise thickness are combined with the Finite Element Method (FEM). The specific optimization problem is of high importance because it is related to the serviceability limit state constraints imposed to a structure in real-life engineering problems. The use of variable element-wise thickness elements aimed at deriving a continuous thickness distribution at the optimum, in contrast to the highly discontinuous distributions obtained, when elements of constant thickness are used. The element type introduced was a 4-node quadrilateral element with isoparametric thickness interpolation. The weight-minimization constraint-fulfilling redesign rule was the imposition of a uniform virtual strain energy density distribution over the active part of the structure under examination. For the evaluation of the proposed approach, four cases retrieved from the literature were examined, namely the deep cantilever, the short cantilever, the MBB beam and a Michell type structure (bridge), while appropriate performance indices were introduced. It was found out that getting superior layouts, when using elements with variable thickness, was possible thus suggesting that a further investigation should be carried out.

6.3.1. In general

The layout optimization problem of single displacement constrained 2D continua may be sought either with a direct technique, such as a Mathematical Programming (MP) technique, or with an indirect method, such as an Optimality Criteria (OC) method. Schmit (1960) introduced the idea of coupling Finite Element Analysis (FEA) with mathematical programming techniques to solve nonlinear inequality constrained problems concerning the design of elastic structures under a multiplicity of loading conditions (Schmit, 1960). Since then, a great many number of mathematical methods have been developed, all of which, however, suffer from the same disadvantage of very limited optimization capability with respect to the number of variables and number of active constraints, respectively (Rozvany,

1992). On the other hand, the origin of the OC methods can be found in Michell's work (1904) who investigated the minimum weight of a planar truss that transmits a given load to a given rigid foundation with the requirement that the axial stresses in the bars of the truss stay within an allowable range (Ostola-Starzewski, 2001). According to Michell, at the optimum, the axial strain has a constant absolute value, say k, in directions of non-zero axial forces while in the directions of zero axial forces the absolute value of the strain must be at most equal to k (Michell, 1904). Half a century later Foulkes (1954) introduced another optimality condition. More specifically, he examined the problem of assigning economical sections to frames that obtain their strength from a bending action, while he used both the theory of plastic collapse in order to determine the strength of a design and a virtual work approach in order to derive the equations governing the problem. He concluded that for a segment-wise prismatic frames the average absolute curvature for each segment must be the same (Foulkes, 1954). Five years later, Heyman (1959) extended Foulkes' optimality criterion to include plastic beams having a rectangular cross-section that could freely vary, while the depth was given but the width was variable (Heyman, 1950). A general optimality criterion for the optimal plastic design of structures with freely varying cross-sectional dimensions was proposed by (Shield and Prager, 1970). This criterion was considerable extended by Rozvany (1976) who stated that in the optimal strain-stress relation, the adjoint strains must be kinematically admissible and are given by the gradient of a specific cost function, in which the stress vector must be statically admissible (Rozvany, 1992). Prager also introduced the concept of structural universe (ground structure) for substituting a continuum with a skeletal structure (Rozvany, 1992). In the early 70's, Venkayya showed that for the optimum design is the one in which the strain energy of each element bears a constant ratio to its energy capacity (Venkayya, 1971). At the same time, Gellatly and Berke proposed an optimality criteria approach for dealing with indeterminate trusses constrained both in stress and displacement (Gellatly and Berke, 1973). For the displacement constrained part of the problem, based on the method of Lagrange multipliers, they developed a recursive redesign formula utilizing both the aforementioned optimality condition and the imposed displacement constraint (for multiple displacement constraints, the recursive formula was used for each one of the displacement constraints and the largest resulting cross-sectional area was picked for the next iteration). The criterion for selecting the active elements was the signum of the product of the member stress due to the actual loads times the member stress due to the appropriately applied virtual load. The derivation of the optimality criterion for uniform virtual strain energy density distribution over the active part of a truss under single displacement constraint is very well presented in Morris (Morris, 1982), where the contribution of the passive and the active elements is discussed in detail. Patnaik et al. also dealt with displacement constrained problems and introduced a design update expressed in an exponential, a linearized, a reciprocal and a melange form (Patnaik et al, 1995). In these forms, the estimation of the corresponding Lagrange multiplier was mandatory and for this purpose a linear, an exponential, an unrestricted and a diagonalized inverse approach were developed (Rozvany, 1989; Rozvany, 1997). Rozvany and Zou have formulated the fundamental relations of optimal elastic design using a Continuous-based Optimality Criteria (COC) approach for freely varying cross-sections and one deflection constraint (Rozvany and Zhou, 1991). Xie and Steven, the developers of the Evolutionary Structural Optimization (ESO) method, have handled the single displacement constraint optimization problem of 2D continuum (Xie and Steven, 1997; Querin et al, 2000). Within the frame of Optimality Criteria, Makris and Provatidis (2002) proposed an iterative procedure were the optimality criterion demanding a uniform virtual strain energy density distribution over the active part of the structure was introduced into their redesign formula as a normalized penalization factor (Makris and Provatidis, 2002). Extending this work, Makris et al. introduced the concept of a dummy

stress bound in order to deal with problems in which only displacement limitations are imposed (Makris et al, 2006). However, in all of the aforementioned papers, finite elements of *constant* geometrical characteristics were used, either in the form of a constant cross-section or in the form of a constant thickness. Therefore, it would be interesting to investigate the performance of finite element of *variable* geometrical characteristics.

Towards this direction, the present chapter examined the performance of 4-node quadrilateral elements of element-wise variable thickness when used in the layout optimization of single displacement 2D continua. For the thickness interpolation within each element, the shape functions used for the nodal displacement interpolation (isoparametric thickness interpolation) were applied. For the optimization itself, a novel iterative procedure was tested according to which first the Virtual Strain Energy Density (VSED) was estimated for each element, then VSED was estimated for each node of the discretized domain and finally the nodal thickness was appropriately updated so that, ultimately, a uniform virtual strain energy density distribution over the active part of the structural domain was achieved. The nodal estimation of VSED from element VSED values was based on three simple interpolation schemes of local character, while a global interpolation scheme may be applied as well. For the purposes of the present investigation, first the calculation of the stiffness matrix for a 4-node quadrilateral element with variable isoparametric thickness was developed and then four typical literature cases of 2D continua under a single displacement constraint were examined, namely the deep cantilever, the short cantilever, the MBB beam and a Michell type structure (bridge). For the quantification of the obtained results, three Evaluation Indices (EIs) were introduced, while the convergence histories for each case were also recorded. The evaluation of the aforementioned indices provided useful insight concerning the use of quasi-3D analyses with variable thickness elements as a computationally economic but qualitatively and quantitatively trustworthy alternative to a full-scale 3D elasticity approach.

6.3.2. Theoretical background

The proposed approach is based on two theoretical aspects, the former being the Optimality Criterion for the single displacement constraint problem and the latter being the formation of the stiffness matrix for a 4-node quadrilateral finite element of variable thickness, whose thickness is interpolated by the shape functions used for the nodal displacement interpolation (isoparametric thickness interpolation). For reasons of completion, these aspects are briefly presented in the following paragraphs.

6.3.3. The Optimality Criterion for the single displacement constraint problem

The expression of the Optimality Criterion redesign technique suitable for 2D continua under a single displacement constraint may be formulated if first the corresponding formula for trusses is derived and then the derived formula is appropriately updated for use for a 2D continuum.

According to the statement of the single displacement constrained optimization problem of a 2D ground structure (truss), a pre-determined value is imposed as the maximum allowable nodal displacement that may appear in the truss; however, the degree of freedom related to the aforementioned nodal displacement is not known *a priori*. The problem statement is as follows:

$$\begin{aligned} &\min \quad W = \sum_{k=1}^{NEL} \left(\rho_k \, A_k \, L_k \right) \\ &\text{such that } \left| u \right| \le u_{allow} \; and \; A_{\min} \le A_k \end{aligned} \tag{6.14}$$

where A is the cross-sectional area, L is the length, ρ is the material density, u is the nodal displacement, while the indices k and $allow$ denote the $k-$bar and the allowable value, respectively. The total number of bars (elements) in the structure is declared as NEL. The imposed constraint on the displacement suggests that the nodal displacement not be greater than u_{allow} in both x and y directions. Furthermore, the constraint with respect to the minimum cross-sectional area is imposed so that the formation of a positive definite stiffness matrix is ensured. Using the method of Lagrange multipliers, as presented in Section 5.2.1, an Optimality Criterion is formulated, according to which, at the optimum, the virtual strain energy density (VSED) is uniformly distributed over the *active* part of the optimized structure. Generalizing the aforementioned analysis for 2D continua (Venetsanos et al, 2008), at the optimum, the same condition for the VSED holds, while, instead of using the cross-sectional area A_k, the structural thickness is introduced as a design variable. At this point, it is clarified that, for severe numerical instabilities to be avoided during the optimization procedure due to zero thickness values, a lower positive bound on thickness was imposed.

The aforementioned OC has two imperfections, the former being that it neither suggests a way to reach the optimum nor ensures that the imposed constraint will be active. Therefore, it is possible to develop a plethora of redesign formulas aiming at achieving a uniform VSED distribution. Extending the analysis of Section 5.2.1, in the present chapter, the nodal thickness redesign is based on the following formula:

$$t_{i,new} = t_i \left(\frac{w_i}{\overline{w}} \right) \tag{6.15}$$

Furthermore, a uniform scaling applied to the design variables at each iteration ensured that the imposed displacement restriction was satisfied as an equality constraint.

6.3.4. Stiffness matrix of a 4-node quadrilateral finite element with variable thickness

The stiffness matrix of the 4-node quadrilateral element with isoparametric thickness interpolation is described analytically in Appendix 4B, according to which it holds:

$$\mathbf{K}^e = \int_{-1}^{+1}\int_{-1}^{+1} \sum_{i=1}^{4} \left(N_i t_i \right) \mathbf{B}^T \, \mathrm{E} \, \mathrm{B} \, \det J \, d\xi \, d\eta \tag{6.16}$$

where t_i is the thickness at the $i-th$ corner node of the $e-$element, N_i is the corresponding shape function, $\mathbf{B}$ is the 3×8 strain-displacement matrix, $\mathbf{E}$ is the 3×3 stress-strain matrix of elastic moduli (different for plane stress and plane strain poblems) and $\mathbf{J}$ is the Jacobian matrix that connects the differentials of the global variables $\{x, y\}$ to the local ones $\{\xi, \eta\}$. The 4-node quadrilateral element with constant and variable element-wise thickness is illustrated in Fig.6.3.

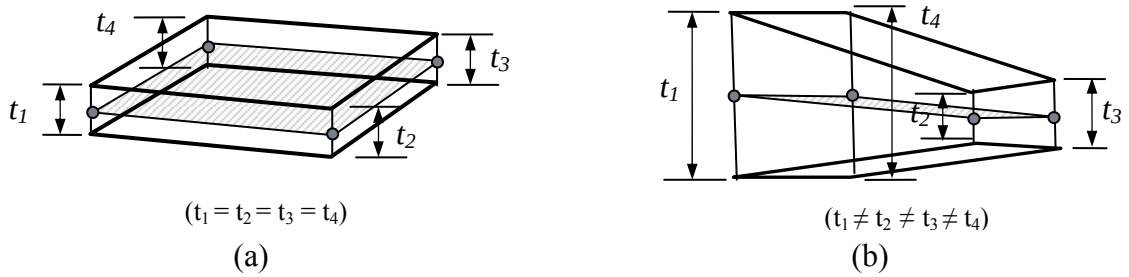

($t_1 = t_2 = t_3 = t_4$) ($t_1 \neq t_2 \neq t_3 \neq t_4$)

(a) (b)

Figure 6.3: 4-node quadrilateral element with (a) constant and (b) variable thickness

6.3.5. The proposed optimization procedure

The present chapter proposes an optimization procedure that uses elements of variable element-wise thickness (Approach #1). For reasons of comparison, another optimization procedure, using elements of constant element-wise thickness, was also developed (Approach #2). In both cases, the so-called Optimum Uniform Design (OUD), that is the design obtained when the thickness distribution over the discretized domain is uniform and has the minimum possible value that does not cause any constraint violation, was used as reference.

6.3.5.1. Optimization procedure with elements of variable element-wise thickness (Approach #1)

The proposed optimization procedure is as follows:

Step 1: Estimate the (OUD) and record weight, thickness and virtual strain energy density to be used as references
Step 2: Apply the virtual unit load theorem to the most critical degree of freedom (dof)
Step 3: Estimate the normalized virtual strain energy density for each *active* element
Step 4: Estimate the normalized virtual strain energy density for each node of the *active* elements (active nodes)
Step 5: Update the thicknesses of the *active* nodes with the proposed redesign formula
Step 6: Apply a uniform thickness scaling so that no displacement violations occur
Step 7: Check for convergence; if convergence has not been achieved and the maximum number of iterations has not been exceeded, then go back to Step 2.
Step 8: Apply a global smoothing procedure to the nodal thickness distribution (e.g. Kriging technique).
Step 9: Apply a uniform scaling to the smoothed layout of Step 7 so that no displacement violations occur
Step 10: Evaluate the Performance Indices.

The nodal estimation of the VSED was derived from the element VSED values with the application of an interpolation scheme. The interpolation schemes used in the present chapter are presented in Section 6.3.6.

6.3.5.2. Optimization procedure with elements of constant element-wise thickness (Approach #2)

The corresponding optimization procedure for constant-thickness elements is as follows:

Step 1: Estimate the (OUD) and record weight, thickness and virtual strain energy density to be used as references
Step 2: Apply the virtual unit load theorem to the most critical degree of freedom (dof)
Step 3: Estimate the normalized virtual strain energy density for each *active* element
Step 4: Update the thicknesses of the *active* element with the proposed redesign formula
Step 5: Apply a uniform thickness scaling so that no displacement violations occur
Step 6: Check for convergence; if convergence has not been achieved and the maximum number of iterations has not been exceeded, then go back to Step 2.
Step 7: Apply a global smoothing procedure to the element thickness distribution (e.g. Kriging technique).
Step 8: Apply a uniform scaling to the smoothed layout of Step 7 so that no displacement violations occur
Step 9: Evaluate the Performance Indices.

It is clarified that the nodal estimation of the VSED was derived from the element VSED values with the application of one of the interpolation schemes described in Section 6.3.6.

6.3.6. Estimation of the nodal values for the virtual strain energy density

The main idea of the proposed procedure was first to evaluate the virtual strain energy density for each element and then to estimate the corresponding nodal values through an interpolation scheme. In total, three VSED Interpolation Schemes (#1, #2, #3) were used. For the variable-thickness elements and according to the first scheme, the VSED at a node was estimated as the maximum of the VSED values corresponding to the element surrounding the specific node. According to the second and the third scheme, the nodal VSED values were estimated from the average and the minimum VSED values, respectively, of the elements surrounding the specific node. For a structured mesh with 4-node rectangular elements, it is obvious that for a node *inside* the mesh (design space) four elements contributed to the aforementioned nodal VSED estimation, while for a node along the border of the mesh and for a *corner node*, two and one elements contributed, respectively. For the constant-thickness elements, only one VSED value corresponded to each element.

6.3.7. Evaluation of the proposed optimization procedure

The evaluation of the proposed approach was divided into two parts, the former being the verification of the in-house 4-node quadrilateral element with isoparametric thickness and the latter being the evaluation of the performance of the proposed procedures in terms of structural weight, virtual strain energy density distribution and convergence behavior.

6.3.7.1. Verification of the introduced finite element

The verification of the introduced finite element was carried out through a comparison with the element SHELL63 of the Finite Element Analysis (FEA) software Ansys (ver.10). For the verification, a rectangular 2D cantilever first under in-plane bending and then under unsymmetrical tension (compression) was examined for various mesh densities with unit aspect ratio. A coincidence in nodal displacements between the in-house code and Ansys was achieved (keyoptions for SHEL63: extra displacement shape functions excluded, membrane element stiffness only).

6.3.7.2. Definition of the Evaluation Indices

The evaluation of the performance of the proposed procedures was achieved through the introduction of three Evaluation Indices (EI) defined as follows:

- Evaluation Index EI_1, informing about the normalized relation between the weight of the optimum layout *before* the application of the global smoothing procedure and the weight of the (OUD) and defined as:

$$EI_1 = \left(\frac{W_{opti}}{W_{OUD}} \right) \tag{6.17}$$

- Evaluation Index EI_2, informing about the virtual strain energy density distribution of the structure *before* the application of the global smoothing procedure and defined as the Coefficient of Variation (CV) of the VSED values corresponding to the active nodes:

$$EI_2 = CV\left(VSED_{active\_nodes}\right) \tag{6.18}$$

- Evaluation Index EI_3, informing about the size of the active structural part and defined as (for the variable and the constant thickness elements, respectively, where NN stands for Number of Nodes and NEL for Number of Elements):

$$EI_3 = \left\{ \left(\frac{NN_{active}}{NN} \right), \left(\frac{NEL_{active}}{NEL} \right) \right\} \tag{6.19}$$

Moreover, the convergence history, in terms of structural weight, was also recorded and presented as a plot. Obviously, similar indices may be defined for the state after the application of the global smoothing procedure. At this point, it is clarified that the active part of a structure is defined as the one with size larger than the minimum imposed one. Therefore, for an active node and an active element, the corresponding thickness is higher than the imposed lower bound.

6.3.7.3. Verification of the optimized smoothed layouts

In order to verify that the optimized layouts, after the smoothing procedure was applied, did not violate any of the imposed constraints, one last (FEA) was carried out and then a uniform scaling was applied. In this way, a slightly oversized design was uniformly shrunk and a slightly undersized design was uniformly enlarged. The uniform change of the layout is not a necessary optimality condition but for good practical engineering purposes is totally acceptable.

6.3.8. Investigated test cases

A schematic illustration of the examined 2D continua is presented in Fig.6.4.

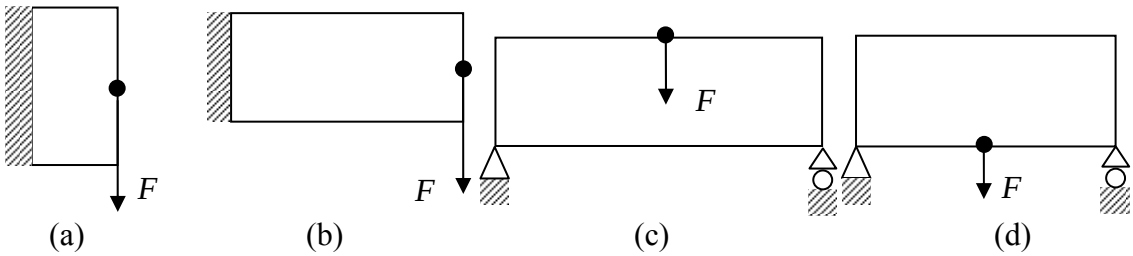

Figure 6.4: The investigated structures (a) deep cantilever, (b) short cantilever, (c) MBB beam and (d) Michell bridge

6.3.8.1. Test case #1: Deep cantilever

The data for this test case may be found in Section 6.2.5.1.

6.3.8.2. Test case #2: Short cantilever

The data for this test case may be found in Section 6.2.5.2.

6.3.8.3. Test case #3: MBB beam

The data for this test case may be found in Section 6.2.5.3.

6.3.8.4. Test case #4: Michell structure

The examined Michell type structure is illustrated in Fig.6.4d. The dimensions of the rectangular design domain are $L_x = 2400mm$ (width) and $L_y = 400mm$ (height), while the initial uniform thickness of the beam is $t = 1mm$. A concentrated load $F = 50kN$ is applied at the middle of the top side of the beam. There is only one imposed constraint concerning the deflection of the beam which is required to be less than $9.4mm$. For this case, the modulus of elasticity is considered to be $E = 200GPa$, the material density is set equal to unity, while the

Poisson's ratio is assumed to be $v = 0.3$. The design domain was divided into 66×11 4-node rectangular finite elements.

6.3.9. Results

The Evaluation Indices (EIs) for the examined applications are shown in Table 2 while selected plots concerning the optimal layouts and the corresponding convergence histories are shown in Fig.6.5.

6.3.9.1. Evaluation Indices

In Table 6.2, the symbols $t = const$ and $t \neq const$ correspond to constant and variable thickness elements, respectively. The % difference is defined as the % relative difference with respect to the results obtained with the use of constant thickness elements. At this point it is clarified that the % difference was not calculated for the evaluation index EI_2, while a qualitative interpretation was preferred instead. The reason for this choice is related to the physical interpretation of the Coefficient of Variation (CV). In more details, a small (CV) for the EI_2 index denotes a very strong uniform VSED distribution, which was the case for both the constant and the variable thickness elements, as Table 2 suggests. However, a visual inspection reveals that the (CV) values for the two types of elements were *significantly* different in all cases. Since it is meaningless to quantify how much *significantly* different the corresponding values were, it was selected to proceed with the qualitative evaluation of the EI_2 values.

Table 6.2: Evaluation Indices for the examined applications

		VSED interpolation scheme #1			VSED interpolation scheme #2			VSED interpolation scheme #3		
		EI_1	EI_2	EI_3	EI_1	EI_2	EI_3	EI_1	EI_2	EI_3
Deep cantilever	t=const	0,5061	0,6420	0,9340	0,5061	0,6420	0,9340	0,5061	0,6420	0,9340
	t≠const	0,5180	1,1399	0,9094	0,5025	3,1369	0,9030	0,5044	0,3627	0,9634
	% difference	2,34%		-2,64%	-0,72%		-3,32%	-0,34%		3,15%
Short cantilever	t=const	0,6220	1,5188	0,9906	0,6220	1,5188	0,9906	0,6220	1,5188	0,9906
	t≠const	0,6356	2,9201	0,9740	0,6112	2,5655	0,9870	0,6116	0,0179	1,0000
	% difference	2,20%		-1,68%	-1,73%		-0,36%	-1,67%		0,95%
MBB beam	t=const	0,5343	0,0078	1,0000	0,5343	0,0078	1,0000	0,5343	0,0078	1,0000
	t≠const	0,5603	2,1304	0,9876	0,5094	1,9019	0,9988	0,5099	0,0025	1,0000
	% difference	4,86%		-1,24%	-4,66%		-0,12%	-4,56%		0,00%
Michell structure (bridge)	t=const	0,5343	0,0078	1,0000	0,5343	0,0078	1,0000	0,5343	0,0078	1,0000
	t≠const	0,5603	2,2111	0,9888	0,5093	1,9877	1,0000	0,5098	0,0017	1,0000
	% difference	4,87%		-1,12%	-4,68%		0,00%	-4,58%		0,00%

From Table 6.2, it yields that for the second and the third interpolation schemes, the proposed procedure with the variable thickness elements, resulted in a structural weight reduction (EI_1) ranging from 0.34% to 4.68% with respect to the use of constant thickness elements. Furthermore, the first two interpolation schemes resulted in a reduction of the size of the active structural part (EI_3) up to 3.32%, while the third interpolation scheme resulted in an increase of the active structural part.

6.3.9.2. Optimal layouts

For each one of the examined examples, there were four possible solutions resulting from the three different VSED interpolation schemes for Approach #1 and one such scheme for Approach #2. Therefore, for each example, four layouts and four convergence histories with

respect to the structural weight were obtained. Due to space limitations, only two representative layouts are presented per example (the 'average' VSED interpolation scheme and the one for the constant thickness elements). More particularly, the optimal layouts derived with variable thickness elements and the 'average' VSED interpolation scheme are shown in the first column of Fig.6.5, while the optimal layouts derived with constant thickness elements are shown in the second column of the same figure. The plots of the convergence histories per example are illustrated in the third column of Fig.6.5

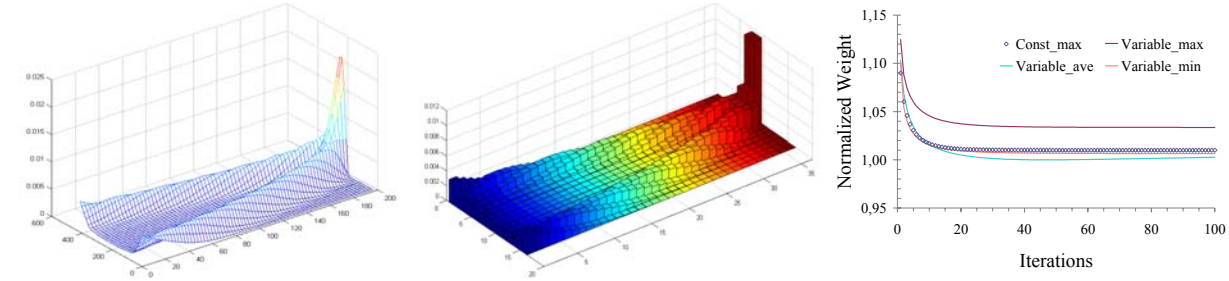

(a): Deep cantilever: Approach #1 (b) Deep cantilever: Approach #2 (c) Deep cantilever: convergence

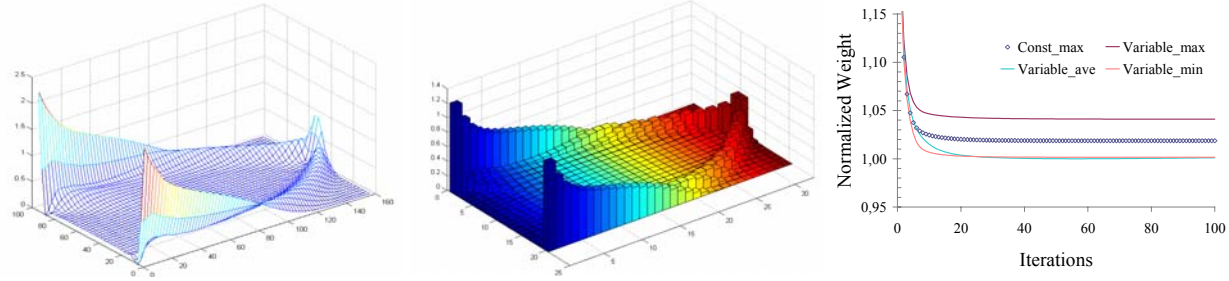

(a): Short cantilever: Approach #1 (b) Short cantilever: Approach #2 (c) Short cantilever: convergence

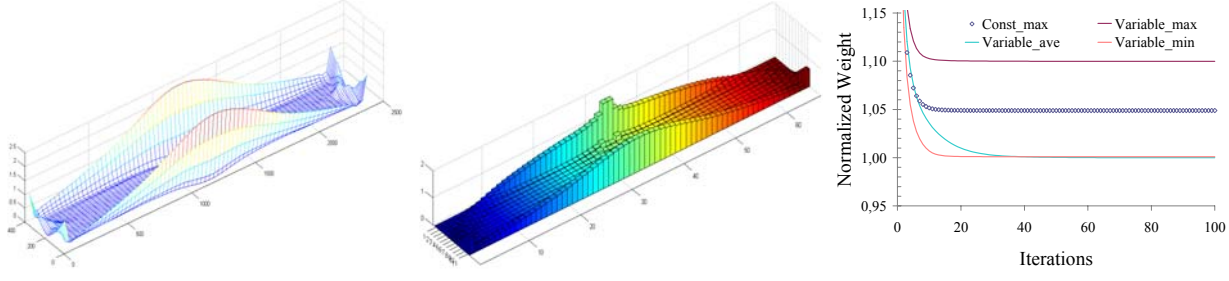

(a): MBB beam: Approach #1 (b) MBB beam: Approach #2 (c) MBB beam: convergence

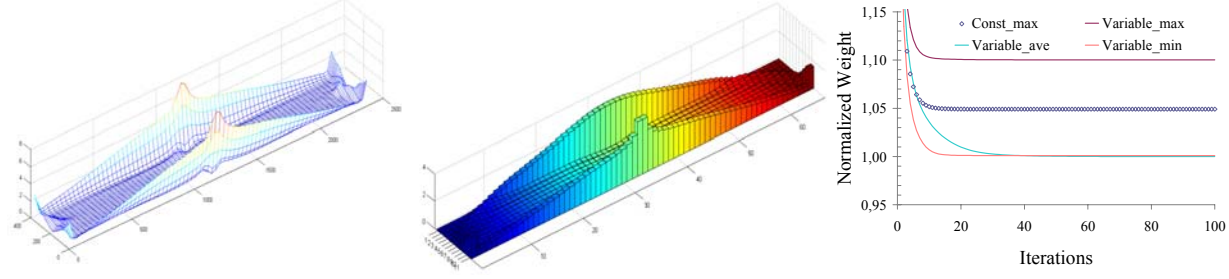

(a) Michell bridge: Approach #1 (b) Michell bridge: Approach #2 (c) Michell bridge: convergence

Figure 6.5: Optimal layouts and convergence histories for the investigated examples

It is clarified that, due to symmetry along the mid-plane of the structures, only half of the structural thickness distributions are shown (from the mid-plane and towards the upper surface). Furthermore, for reasons of visual inspection, the material distributions corresponding to the variable and to the constant thickness elements were plotted as colored

unfilled meshes (Fig.6.5, 1st column) and as filled columns (Fig.6.5, 2nd column), respectively. In addition, for each one of the convergence history plots, the illustrated weights were normalized with respect to the minimum value among the four optimal weights obtained for each example.

The appropriate comparison between the plots in the first two columns of Fig.6.5 revealed several interesting details, among which the most interesting one was the fact that *non-skeletal* layouts were obtained. On the contrary, there was a pattern that always appeared, according to which the optimal layout could be divided clearly into three regions. The first region concerned a thicker material distribution, easily located with visual inspection, forming a kind of boundary. The second region concerned the part of the domain *inside* the aforementioned boundary; this region had a varying thickness close to the lower thickness bound. The third region concerned the part of the domain *outside* the aforementioned boundary; the thickness of this region was equal to the lower thickness bound, denoting the existence of a part of the domain which is redundant and can be removed without causing any problems to the structural stability. The clear absence of reinforcing ribs is due to the existence of the aforementioned *inner* region which provides a very good way for carrying the shear. On top of that, the use of variable thickness elements results in much smoother thickness distributions. This means that the result of the proposed optimization procedure is characterized by a high degree of manufacturability, while a further global smoothing procedure actually serves for a better smear-off of the distributed material.

From the convergence history plots (Fig.6.5, 3rd column) it is clear that in all cases a very smooth and fast convergence is achieved. Furthermore, if the second or the third VSED interpolation schemes are used, then the structural weight of the optimal layout is lower when compared to the corresponding one obtained using constant thickness elements (denoted with markers only in the plots). In addition, the slower convergence is achieved with the 'average' VSED interpolation scheme. Finally, in order to ensure that an early convergence did not hide a later diverging behavior, the iterative procedure was forced to be carried out 100 times. As Fig.3(3rd column) shows, convergence was practically achieved after a few iterations and no diverging behavior in later stages appeared.

6.3.10. Discussion

The topic presented in this section concerned a newly introduced procedure, which is suitable for minimizing the weight of 2D continua under an extended single displacement constraint only. For its study in-house codes were developed for both constant and variable thickness elements, 16 models were analyzed, while the approach introduced in the previous chapter was the basis of the current investigation. At this point it is clarified that the development of in-house codes was more a strategic decision, as explained in Section 4.3.5.6.

Furthermore, in order to avoid element-wise warping distortions due to the fact that four points do not necessarily lie on the same plane, the use of an adequate large number of elements is required. The go-around way of degenerating the 4-node elements into 3-node ones (three nodes always define a plane), is not advisable, because such a degeneration results in significantly less accurate results.

The use of elements with element-wise variable thickness seems to be a very good compromise between 2D and full 3D analyses, since the computational cost is sufficiently low and the ability to get continuous thickness distributions is ensured. Furthermore, since the optimization procedure is based on nodal thickness redesign, it is obvious that all of the nodes serve as control points that can move vertically to the mid-surface of the structure. In this way, the thickness envelope is highly parameterized, thus enabling the formation of a fine thickness distribution. Further steps towards this direction are the implementation of various schemes of, local or global, thickness interpolation and the implementation of CAD features,

such as the NURBS and the related mathematical functions that permit shifting and cavity creation, the ultimate goal being the development of a variable thickness super-element.

6.3.11. Conclusions

The current investigation showed that the novel approach introduced in Chapter 5 for skeletal structures is possible to be adjusted for solving the layout optimization of 2D continua under the extended single displacement constraint. The central idea in this adjustment is to implement elements of variable thickness in combination with certain interpolation schemes, concerning the appearance of a uniform virtual strain energy distribution at the optimum. The encouraging results suggested that further investigation be carried out with other types of thickness description and thickness interpolation schemes.

6.4. Recapitulation

In this chapter, the layout optimization of 2D continua under an extended single displacement constraint was discussed, the concept of the 'extended' displacement constraint being introduced in Chapter 5. The current chapter contributes in three ways, the first being the redesign of the structure using nodal-based, and not element-based, information, the second being the introduction of a variation of an already existing material-removing methodology and the third being the extension to 2D continua of the new procedure, which was proposed in Chapter 5. More particularly,

More particularly, the use of nodal-based information for the redesign of a 2D continuum is nothing else than controlling its thickness using a nodal-wise thickness distribution within each finite element, which are used for the discretization of the continuum. To this end, the current chapter proposes the implementation of an isoparametric interpolation scheme. That is, to implement the same interpolation functions for the interpolation of geometry, thickness and displacements, the nodes being the interpolation points.

In addition, the introduced variation of an already existing material-removing methodology concerned the criterion based on which material is detected as redundant. In opposition to the existing literature, for this detection it is proposed to use the normalized virtual strain energy density, the normalization taking place with respect to the active part of the structure. To this end, the examined examples showed that the aforementioned variation is more efficient than the initial version of the existing methodology.

Last, the concept of interpolating nodal-based information was combined with the redesign methodology, which was introduced in Chapter 5, and extends its application in 2D continua. The encouraging results from this investigation suggest that the aforementioned approaches be useful and efficient tools for 2D layout optimization problems when an extended singe displacement constraint is imposed.

References

Belegundu, A.D., Chandrupatla, T.R. (1999), *Optimization concepts and applications in engineering*, Prentice Hall.

Bendsøe, M.P., Sigmund O. (2003), *Topology Optimization, Theory, Methods and Applications*, Springer-Verlag, Berlin.

Chu Nha, D., Xie, Y.M., Hira, A., Steven, G.P. (1996), "Evolutionary structural optimization for problems with stiffness constraints", Finite Elements in Analysis and Design, Vol. 21, pp.239-251.

Foulkes, J. (1954), "The Minimum-Weight Design of Structural Frames", *Proceedings of the Royal Society of London*, A 223 (1155), pp. 482-494.

Gellatly, R.A., Berke, L. (1973), "Optimality-criterion-based algorithms", In: Gallagher RH, Zienkiewicz OC (eds) *Optimum structural design*, Wiley, Chichester, pp 33–49.

Haftka, R.T., Gurdal, Z., Kamat, M. (1990), *Elements of Structural Optimization*, Kluwer.

Heyman, J. (1950), "On the absolute minimum weight design of framed structures", *Q. J. Mech. Appl. Math*., Vol.12, pp. 314–324.

Makris, P., Provatidis, C. (2002), "Weight minimisation of displacement-constrained truss structures using a strain energy criterion", Computer Methods Appl. Mech. Engrg., Vol. 191, pp. 2159-2177.

Michell, A.G.M. (1904), "The Limits of Economy of Material in Frame-Structures", *Phil. Mag.*, Vol. 8, pp. 589-597.

Morris, A.J. (1982), *Foundations of Structural Optimization: A Unified Approach*, John Wiley & Sons.

Ostola-Starzewski, M. (2001), "Michell trusses in the presence of microscale material randomness: limitation of optimality", *Proceedings of the Royal Society of London*, A 457, pp. 1787-1797.

Patnaik, S.N., Guptill, J.D., Berke, L. (1995), "Merits and limitations of optimality criteria method for structural optimization", *Int J Numer Methods Eng,* Vol.38, pp.3087–3120.

Pham, D.T., Karaboga D. (2000), *Intelligent Optimisation Techniques: Genetic Algorithms, Tabu Search, Simulated Annealing and Neural Netwroks*, Springer-Verlag.

Querin, O.M., Steven, G.P., Xie, Y.M., (2000), "Evolutionary structural optimisation using an additive algorithm", *Fin Elem Anal Design*, Vol. 34, Issues 3-4, pp.291-308.

Rozvany, G.I.N. (2001), "Aims, scope, methods, history and unified terminology of computer-aided topology optimization in structural mechanics", Struct. Multidisc Optim, Vol. 21, pp. 90-108.

Rozvany, G.I.N., (1989), *Structural design via optimality criteria*, Kluwer, Dordrecht.

Rozvany, G.I.N., (1992), *Shape and Layout optimization of structural systems and optimality criteria methods*, Springer-Verlag, Wien-NewYork.

Rozvany, G.I.N., (1997), *Topology optimization in structural mechanics*, CISM, Springer-Verlag.

Rozvany, G.I.N.; Zhou, M. (1991), "The COC algorithm, Part I: cross section optimization or sizing", *Comput. Methods Appl. Mech. Eng*., Vol.89, pp.281-308.

Schmit, L. A., (1960), "Structural Design by Systematic Synthesis", *Proceedings of the 2nd Conference on Electronic Computation, American Society of Civil Engineers*, New York, pp. 105-132.

Shield, R.T., Prager, W. (1970), "Optimal structural design for given deflection", *J. Appl. Math. Phys*, Vol. 21, pp. 513-523.

Venetsanos, D.T. Magoula, E.A.T. and Provatidis, C.G. (2008), "Layout optimization of stressed constrained 2D continua using finite elements of variable thickness", *6th GRACM International Congress on Computational Mechanics,* Thessaloniki, 19-21 June 2008.

Venkayya, V.B. (1971), "Design of optimum structures", *Computer & Structures*, Vol. 1, pp. 265-309.

Xie, Y.M., Steven, G.P. (1997), *Evolutionary Structural Optimization*, Springer-Verlag.

Contributed papers

[1] Provatidis C. G. and **Venetsanos, D. T.**, "The influence of normalizing the virtual strain energy density on the shape optimization of 2D continua", 1st IC-EpsMsO, 6-9 July 2005, Athens, Greece.

[2] **Venetsanos D.** and Provatidis C., "Layout Optimization of Single Displacement Constrained 2D Continua Using Finite Elements of Variable Thickness", 6th International Congress on Computational Mechanics (GRACM), Thessaloniki, 19-21 June 2008.

[3] **Venetsanos, D.T.**, Provatidis, C.G., Minimum weight designs for single displacement constrained 2D continua using variable element-wise thickness, 8th World Congress on Structural and Multidisciplinary Optimization (WCSMO8), LNEC (National Laboratory for Civil Engineering), Lisboa, Portugal, June 1- 5, 2009.

CHAPTER 7

ON THE MINIMIZATION OF THE STRUCTURAL COST

Abstract

In this chapter, the minimization of the structural cost is investigated. It is well known that, in real-life engineering problems, minimum weight does not necessarily mean minimum cost, thus it is of practical value to simultaneously achieve both structural optimization and cost minimization of a structure. However, it is not possible to establish a generalized procedure applicable in all cases, because for the cost minimization to be achieved special design characteristics of each case must be exploited. Within this concept, the present chapter presents two optimization procedures, one suitable for skeletal structures under stress constraints only and one suitable for welded steel tanks for oil-storage. For the former case, a post-optimization procedure is formulated, according to which the optimized structural members of equal or near-equal cross-sections are appropriately grouped and finally all optimized structural members of the imposed critical minimum or near minimum cross-section are eliminated. Both grouping and elimination procedures are based on a statistical approach. The proposed procedure was applied to four test cases, namely the short and long cantilever, the MBB beam and the L-shaped beam. The conclusion was that the proposed procedure provided the means for both layout optimization and structural cost minimization. The extension of the proposed procedure to 3D skeletal structures, as well as to other types of constraints, is trivial. For the latter case, a design optimization procedure is formulated, according to which the minimum structural cost is sought in terms of volume of material used, scrap material and cost for welding. The proposed procedure was applied in a series of designs, thus resulting in nomograms that can be used for selecting explicitly decisive design dimensions for minimum structural cost. From the aforementioned investigation it becomes obvious that, instead of pass-par-tous methods, the development of case-oriented optimization procedures may be most beneficial.

Keywords

layout optimization, skeletal structures, welded tank, oil-storage, cost minimization.

7.1. Introduction

It is well known that, in real-life engineering problems, minimum weight does not necessarily mean minimum cost, the reason for this being that the estimation of the structural cost takes into account various parameters, not explicitly apparent, three of which, perhaps the most important ones, being the lack of commonality, the cost of the welding and the quantity of the remaining material (scrap).

The term 'commonality' describes how similar or different the profiles of a structure are. For instance, a truss consists of a number of bar elements, each one of which, theoretically speaking, may have a different profile. However, while this may be good from the viewpoint of the total structural weight, it is not good from the viewpoint of the total structural cost, because it is almost always cheaper to buy larger amounts of the same profile than to purchase smaller amounts of different profiles. Therefore, it is of interest to increase the commonality of a structure, so that fewer different profiles can be ordered.

The cost of the welding is another parameter that may significantly affect the design of a structure. For instance, in order to minimize the weight of a closed cross-section, as is the case of a box girder, it is possible to come out with a design with longitudinal reinforcements. However, these reinforcements must be welded to the cross-section, thus the structural cost increases due to the welding, which is expensive. Instead, it would be possible to increase the thickness of the cross-section plates such that no longitudinal reinforcement is required. In the latter case, while the structural weight is higher, the structural cost may be lower, because there is a break-even-point where the increase of the structural cost due to purchasing plates is less than the increase of the structural cost due to welding. As a result, it is possible to adopt a whole new design trend which, although heavier than the one proposed by weight minimization procedures, is preferable in terms of structural cost.

Another parameter that determines the structural cost is the scrap material; that is the material that remains after the construction is completed. Having zero scrap is the ideal case and for this to occur the optimization procedure to be applied must be case-oriented; in this way, the design characteristics and particularities of the structure under examination can be exploited as much as possible. According to the ideal case of 'zero-scrap design', the structure consists of an integer number of commercially available structural members, such as sheet plates or beams.

In the remaining of this chapter, the concept of commonality will be investigated through the examination of skeletal structures. Such structures may be used as substitutes to continuum structures, as well. On top of that, an optimization procedure embedding the cost of welding and the concept of scrap material is also presented through the case of welded tanks for oil-storage.

7.2. Cost minimization through increasing commonality

7.2.1. In general

The motivation of cost optimization is to exploit the available limited resources in a manner that maximizes utility (Kirsch, 1993). Therefore, the objective of an optimal design is to achieve the best feasible result with respect to a pre-selected measure of effectiveness. In other words, the optimal design must have certain characteristics that distinguishes it among and makes it superior to other designs. There are many difficulties in getting a structural design of minimum cost, such as the handling of a large number of design variables, the imposition of multiple constraints and the non-linear nature of the problem. In all cases, the application of the Finite Element Method (FEM) of the studied structure is required. As Bruce Irons, one of the pioneers of finite element methods, said: '*If there is an opportunity for improving the design, then somebody, somewhere is attempting to do so using Finite*

Elements' (Xie and Steven, 1997). Concerning the optimization algorithms one can apply, there are numerous.

For the solution of the cost minimization problem, it is possible to apply various optimization techniques. For instance, it would be possible to use a deterministic procedure that takes into consideration no derivative information, or the first derivative or both the first and the second derivatives (Belegundu and Chandrupatla, 1999). However, the computational cost for such a systematic search is high, even prohibitively high depending on the size of the problem, while the possibility of converging to a local minimum is high as well. Alternatively it is possible to use stochastic techniques such as the Genetic Algorithms (GAs), Simulated Annealing (SA), Swarm Particles, Natural Growth and Tabu search (Pham and Karaboga, 2000). Many of these techniques, as their name suggests, attempt to mimic some kind of natural procedure. The common element in all stochastic methods is that they are derivative-free ('zero-order' techniques), meaning that they use no derivative (gradient or Hessian) information. This is advantageous, because the calculation of the derivatives has a significant computational cost, may cause numerical instabilities and, most probably, will converge to a local rather than to a global minimum. Instead, the stochastic techniques perform a thorough exploration and exploitation of the feasible region, which is achieved by testing a large number of design vectors. However, this results in a cumulated high computational cost.

Another option in minimizing the structural cost is to use the Lagrange multipliers method (Morris, 1982). According to this method, the imposed equality or inequality constraints are introduced into the objective function, which is the quantity to be minimized, in a weighted manner. The weighted coefficients used are known as Lagrange multipliers and are calculated by solving a non-linear system of equations, which is not always an easy task to accomplish. Furthermore, since the final solution of a non-linear system definitely depends on the initial point of the solution procedure, the Lagrange multipliers method results in a design, which is improved compared to the initial design but cannot be algorithmically proved to be the optimal design. However, for particular cases of constraints, the specific method leads to very elegant statements, called Optimality Criteria (OC), concerning the conditions that hold at the optimum (Morris, 1982). Among the (OC) methods, the Fully Stressed Design (FSD) is perhaps the most popular one. Its popularity is mainly due to the fact that it uses a very simple stress-ratio recursive formula that converges fast in comparison to other techniques. Gallagher, Morris, Haftka et al., Patnaik et al., Rozvany, Kirsch and others have analyzed the efficiency of this method (Gallagher, 1973, Morris, 1982, Haftka et al, 1990, Patnaik et al, 1995, Rozvany, 2001, Kirsch, 1989).

These works revealed the major drawback of the method: only under certain circumstances does it provide the optimum design (minimum weight) for stress-constrained problems. A common practice followed extensively was to use FSD as a first optimization step and then use the FSD result as a starting point for a powerful deterministic optimization algorithm (Schmit, 1995). In recent years, a great many optimization algorithms have been developed for the solution of the layout optimization problem, thus, implicitly attacking the cost minimization problem. Suzuki and Kikuchi achieved a major breakthrough by introducing material anisotropy (homogenization method) (Suzuki and Kikuchi, 1991), while a monumental contribution is attributed to Bendsøe and his SIMP method (Rozvany, 2001b, Bendsøe, 1995). Nevertheless, optimality criteria still appear in new forms. Makris and Provatidis proposed a virtual strain energy density optimization approach (Makris and Provatidis, 2002), while Qing et al. proposed an iterative use of the stress-ratio technique in their Evolutionary Structural Optimization (ESO) method(Qing et al, 2000). It is evident that each one of the aforementioned techniques has certain advantages and certain disadvantages. In all cases, the goal is to achieve a design with minimum weight. However, minimum weight does not necessarily mean minimum cost. Therefore, not only minimum weight but also

minimum cost must be sought. The latter task may be achieved if the optimized structure is characterized by a high commonality between its members and at the same time critical members are eliminated. Towards this direction and for 2D continuum structures under stress constraints only, the present investigation is based on a previous work on layout optimization (Provatidis and Venetsanos, 2003), extending it into the area of post-optimization processing.

More particularly, the cost minimization of skeletal structures may be achieved in two ways, the former being the high commonality between the members of the optimized design and the latter being the elimination of members with critical cross-section. Therefore, it is possible to introduce a post-optimization processing, in which grouping and elimination of structural members may take place. For the optimization phase, it is possible to use any optimizer; in the current chapter the function 'fmincon' found in the Optimization Toolbox in MatLab was implemented. The two post-optimization procedures introduced are a simple statistical-based routine for grouping members with equal or near-equal cross-sections and the second being a routine for eliminating critical or near-critical members. In total, four typical test cases were studied and the results showed that the proposed procedure does provide the means for both weight and structural cost minimization. In the present chapter, 2D skeletal structures and stress constraints were selected. However, any type of skeletal structures, both in 2D and in 3D, with any type of constraints may be selected as well, because the proposed procedure for increasing commonality is a *post-optimization* procedure, thus requiring no further structural analysis.

7.2.2. Theoretical approach

The proposed procedure consists of four steps. The first two steps, that is the formulation of the skeletal structure as well as its layout optimization, have been adequately analyzed in previous chapters. For the completeness of the text, the optimization problem will be stated. The last two steps, that is grouping and elimination, consist the novel features of the current work, thus they will be analyzed extensively. Grouping is closely related to the principle of commonality introduced by Papalambros (Papalambros, 1995, Fellini et al, 2003), which states that the fewer components a structure has and the more similar these components are between them, the lower the cost becomes. Elimination is closely related to the fact that members with critical cross-sections should actually be removed, because they increase the structural weight without any beneficial contribution to the structural stiffness. Therefore, the overall optimization problem can be divided into three sub-problems, namely the layout optimization, the grouping of structural elements and the elimination of critical structural elements. It is possible to deal with these sub-problems in the aforementioned order (layout optimization, grouping, elimination) either iteratively or sequentially. According to the former scheme, a recursive procedure is established, such that every recursion consists of performing one iteration step for each sub-problem. According to the latter scheme, each sub-problem is dealt with only if the previous one is completed. For the purposes of the present chapter the sequential scheme was selected mainly for reasons of simplicity, since the iterative scheme requires 'hard kill' and 'rebirth' of structural members to be allowed, a task that is neither simple nor easy to accomplish. With respect to its interpretation, grouping is a twofold concept related both to cross-sectional grouping and to member grouping. Concerning the cross-sectional grouping, suppose that a structure has N structural elements. In the most general case, in the optimized structure N cross-sections will appear, N_c of which will be critical and $N_{nc} = N - N_c$ will be non-critical. Although not necessary, it is possible that these N_{nc} cross-sections can be divided into N_g groups, where elements of each group will have almost the same cross-section. In such a case and from a constructional point of view, it would be desirable to attribute to all members of a group the same cross-section, such as the

mean value of the cross-sections of the elements belonging to the corresponding group, thus ending up with N_g different profiles and not with $N > N_g$. From a purely theoretical point of view, this is not a good choice, because even a small modification in any cross-section of an optimized structure results in a violation, thus into an infeasible design. Nevertheless, from a real-life engineering approach, this is a very good idea, because, if the grouping is performed in an appropriate way, then not only will the constructional cost be significantly lower, but also the increase in the total structural weight and the occurred violations will be negligible for practical engineering purposes. Therefore, it is shelf-evident that the cross-sectional grouping is desirable for and beneficial to real-life optimized applications, as long as such a grouping is possible. At this point, it is strongly emphasized that cross-sectional grouping must not be dealt as an end in itself. On the contrary, it is on the engineer's judgment to decide whether the initially optimized design allows for such a grouping or not. Concerning the member grouping, let it be that the members of a structure have already been grouped with respect to their cross-sections, according to the aforementioned procedure, and some of them happen to be collinear as well. In this case, it is possible to 'merge' them, meaning to substitute two or more collinear elements of the same cross-section with one element that has the same cross-section and length equal to the total length of the members to be substituted. From a purely theoretical point of view, this choice may result in an ill-posed stiffness matrix, because merging practically means removal of nodes from the mesh, thus other members attached to nodes that must be removed may become inadequately supported. However, from a real life engineering approach, member grouping is a very good idea, because, every time two structural members are substituted by one of equal length, the total number of fastenings over the construction is reduced by one. In turn, this means lower manufacturing cost, lower assembling cost and lower maintenance cost. On top of that, since the fastening areas are areas of potential corrosion, the minimization of their number results in the minimization of the corresponding danger against potential corrosion as well.

7.2.3. The problem statement

A 2D skeletal structure, which may also be considered as a bar-type skeletal equivalent of a continuum structure under in-plane loading, is nothing else but an assembly of bars whose weight W equals to:

$$W = \sum_{i=1}^{n} x_i \rho_i l_i \tag{7.1}$$

The axial stress of the i-th bar equals to:

$$\sigma_i = \left(\frac{^{\text{int}}F_i}{x_i} \right) \tag{7.2}$$

and the stress constraint concerning the i-th bar is expressed as follows:

$$g_i = \left(\frac{\sigma_i}{\sigma_{\max,i}} - 1 \right) \leq 0 \tag{7.3}$$

If the minimum weight W is sought, then the SQP statement of the problem, with respect to the cross-sectional areas is:

$$\min\ W\left(\Delta\underset{\sim}{x}\right) = W\left(\underset{\sim}{x}\right) + \nabla W\left(\underset{\sim}{x}\right)\Delta\underset{\sim}{x} + \left(\frac{1}{2}\right)\Delta\underset{\sim}{x}^T\nabla^2 W\left(\underset{\sim}{x}\right)\Delta\underset{\sim}{x} \tag{7.4}$$

$$\text{subject to } g_i\left(\underset{\sim}{x}\right) + \nabla g_i\left(\underset{\sim}{x}\right)^T \Delta\underset{\sim}{x} \le 0, \quad i = 1,2,...,N \tag{7.5}$$

If the bars are considered to be of circular cross section, then the structural weight, instead of a linear form with respect to the cross-section, is expressed in a quadratic form with respect to the cross-sectional radius R_i:

$$W = \sum_{i=1}^{n} \pi R_i^2 \rho_i l_i \tag{7.6}$$

The axial stress of the *i*-th bar then becomes equal to:

$$\sigma_i = \left(\frac{^{\text{int}}F_i}{\pi R_i^2}\right) \tag{7.7}$$

With respect to the cross-sectional radius R_i, the SQP statement of the problem is:

$$\min\ W\left(\Delta\underset{\sim}{R}\right) = W\left(\underset{\sim}{R}\right) + \nabla W\left(\underset{\sim}{R}\right)\Delta\underset{\sim}{R} + \left(\frac{1}{2}\right)\Delta\underset{\sim}{R}^T\nabla^2 W\left(\underset{\sim}{R}\right)\Delta\underset{\sim}{R} \tag{7.8}$$

$$\text{subject to } g_i\left(\underset{\sim}{R}\right) + \nabla g_i\left(\underset{\sim}{R}\right)^T \Delta\underset{\sim}{R} \le 0, \quad i = 1,2,...,N \tag{7.9}$$

The latter statement is preferred, because the objective function is a quadratic expression of the design variables, thus the Hessian $\nabla^2 W\left(\underset{\sim}{R}\right)$ is a well-defined diagonal matrix.

7.2.4. The grouping procedure

Cross-sectional grouping (Fig.7.1) concerns structural elements of equal or near-equal cross-sections. In this case, it is possible to attribute the same cross-section to all of these members, which, in turn, form one group, thus the final number of discrete cross sections used for achieving the optimal layout is decreased. Member grouping (Fig.7.2), on the other hand, concerns skeletal structural members which not only have equal cross-sections but also are collinear and placed one after another forming a line of length L. In this case, such members are replaced by only one member of the same cross-section and of length L. In this way, the number of structural members within each group is decreased as well.

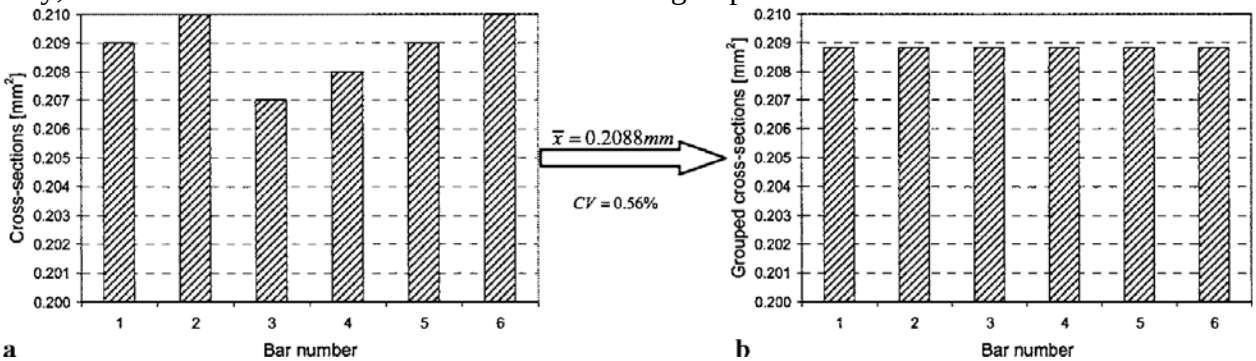

Figure 7.1: Cross-sectional area grouping

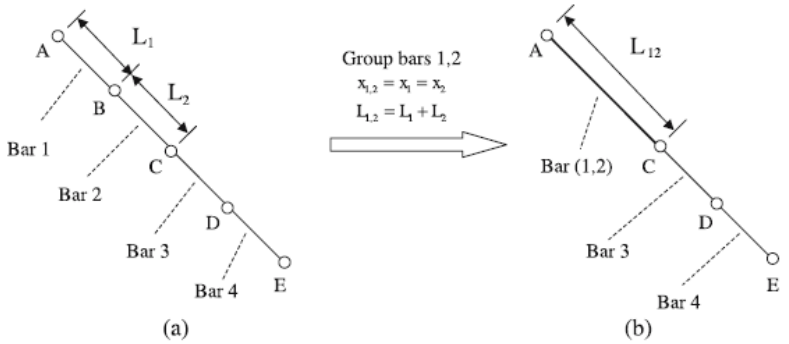

Figure 7.2: Member grouping.

7.2.5. Cross-sectional area grouping

The proposed post-optimization cross-sectional grouping procedure is based on the simple statistical rule that a group of values *xi* may be replaced by their mean value $\overline{x}$ if the corresponding standard deviation s, or equivalently the corresponding coefficient of variation CV, is adequately small. In more details, the grouping procedure is as follows:

Step 1: sort in a descending order all the optimized cross-sectional values $x_i, i = 1,2,...,N$

Step 2**:** set group number (gn) and current element (ce) equal to 1 $(gn = ce = 1)$

Step 3: attribute value x_1 to group $gn = 1$

Step 4: set current element ce equal to 2

Step 5: attribute value x_{ce} to group gn

Step 6: for group gn, calculate the mean value $\overline{x}_{gn}$ and the standard deviation s_{gn} (or the coefficient of variation CV_{gn})

Step 7: if $s_{gn} \le tol$ (or $CV_{gn} \le tol$) then increase ce by 1 and go to Step 5

Step 8: if $s_{gn} > tol$ (or $CV_{gn} > tol$) then
remove ce from group gn
increase group number gn by 1
attribute ce to (the new group) gn
increase current element ce by 1

Step 9: if $ce < N$ then go to Step 5 else stop

It is noted that tol refers to a user-defined tolerance (small positive number). It is evident that significantly different values for tol may result to significantly different outputs. The aforementioned procedure is a systematic statistical allocation of element values into groups. The next step is to eliminate unnecessary groups; that is to minimize gn.

7.2.6. The elimination process

From a statistical viewpoint, group elimination has the meaning of group merging, a procedure that obeys to certain statistical rules (Petruccelli, 1999). From an engineering perspective, group elimination has the meaning of removing all members with minimum or near minimum cross-sectional areas, because such members do not actually contribute to the strength of the structure (their elimination during the optimization process is avoided due to reasons of numerical stability). It is possible to achieve this task in a two step procedure; that

is, based on a cross-sectional area distribution histogram, to decide which groups are unnecessary and, based on the mesh used, to check whether this elimination endangers the stability of the structure. In the present work, the engineering oriented elimination process was applied after the completion of the layout optimization.

7.2.7. Possible additional manipulation

In engineering terms, the elimination process is nothing else but removing material from the structure, thus the quantity of the remaining material is decreased. In turn, this means that the weight of the remaining material decreases as well, while the developed stresses increase, slightly violating the imposed stress constraints. For practical engineering purposes, this situation is acceptable and if the resulting structure is indeterminate, no further process is possible. However, if the resulting structure is determinate, then an additional application of the SQP procedure to the resulting structure will eliminate any stress violations. Furthermore, if the resulting structure is under-determinate, then the addition of structural members by the designer is required in order to get a determinate structure and an additional SQP analysis will again result in the satisfaction of all the imposed stress constraints.

7.2.8. Numerical examples

In the present work, four examples, namely the short cantilever, the long cantilever, the MMB (Messerschmitt-Bölkow-Blohm) beam and the L-shaped beam, were studied in the following way:

Phase 1: Optimization of the structure using SQP (see Sect. 8.2.3)
Phase 2: Grouping of the structural members (see Sect. 8.2.4)
Phase 3: Elimination of unnecessary groups (see Sect. 8.2.5)
Phase 4: If applicable, post-grouping process (see Sect. 8.2.6)

The volume and the maximum axial stress after Phase 1, after Phase 3 and after Phase 4 were recorded and compared. The entire work was repeated using an SQP optimizer for non-linear constrained problems found in Matlab ver.6. As a last step and for reasons of cross-checking, the final layouts were analyzed using ALGOR v.12, which is a commercial Finite Element Analysis (FEA) software.

Table 7.1: Comparison in terms of structural simplicity (cross-sectional area groups and number of bars)

	Short cantilever			Long cantilever			MBB beam			L-shape beam		
Bars	[P1]	[P4]	[%]	[P1]	[P4]	[%]	[P1]	[P4]	[%]	[P1]	[P4]	[%]
$x_i = x_{\min}$	408	0	−100	322	0	−100	279	0	−100	722	1	−99
$x_i \approx x_{\min}$	36	0	−100	58	0	−100	69	0	−100	43	0	−100
$x_i \neq x_{\min}$ $x_i \not\approx x_{\min}$	12	2	−84	40	8	−80	64	11	−83	60	7	−88
Total	456	2	−99	420	8	−98	412	11	−97	825	8	−99
Groups	20	1	−95	33	3	−91	41	4	−90	48	6	−87

In the following sections, the results for each case-study are presented. Each example is accompanied by two figures. The first figure has four plots. Plot (a) illustrates the 2D continuum structure (dimensions in meters), plot (b) shows the mesh of its skeletal equivalent, plot (c) illustrates the result of Phase 1 and plot (d) illustrates the result of Phase 4. The second figure hosts a plot that presents the cross-sectional area distribution for the examined

structure after the completion of Phase 1, and a table with statistical data concerning cross-sectional area grouping. A comparison between Phases 1, 3 and 4, in terms of structural volume and of maximum developed axial stress is presented in Table 7.1, while a comparison between these phases in terms of cross-sectional area groups and of structural members involved is shown in Table 7.2.

Table 7.2: Comparison in terms of structural volume

	Short cantilever	Long cantilever	MBB beam	L-shape beam
Volume [P1]	0.807	21.392	1.505	22.750
Volume [P4]	0.800	21.360	1.503	22.342
δVolume (%)	−0.81	−0.15	−0.13	−1.79

7.2.8.1. The sort cantilever

The short-cantilever beam as a 2D skeletal structure is illustrated in Fig. 8.3a. The entire left side $(x=0)$ is fixed and a negative vertical load $F=12N$ is externally applied at $(x,y)=(1,1.5)$. The maximum allowable axial stress is $\sigma_{\max}=30Pa$, while the modulus of elasticity is $E=1Pa$. For the short cantilever it is known that the optimal layout of its skeletal equivalent is achieved when a mesh with aspect ratio $\lambda=1$ is used (Provatidis and Venetsanos, 2003). Based on this information, the mesh illustrated in Fig. 8.3b was generated consisting of 456 bars.

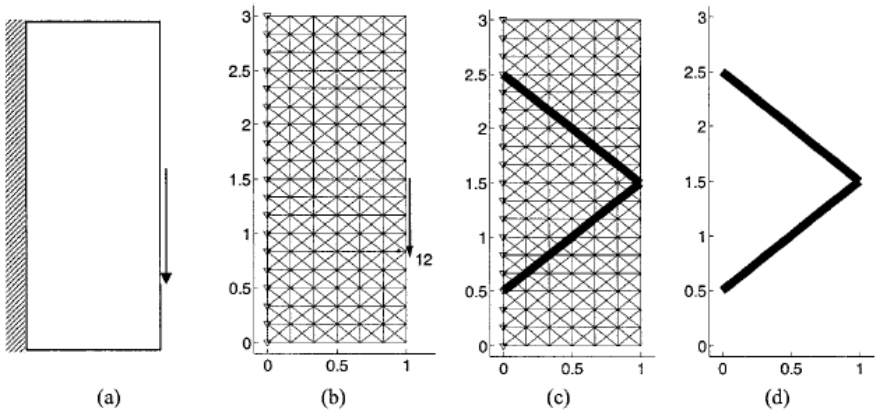

Figure 7.3: The short cantilever beam

The result of Phase 1 is illustrated in Fig.7.3c and the final layout of Phase 4 is shown in Fig.7.3d. The cross-sectional area distribution after Phase 1 is shown in Fig.7.4a, while statistical details concerning the outcome of Phase 4 is presented in Fig.7.4b.

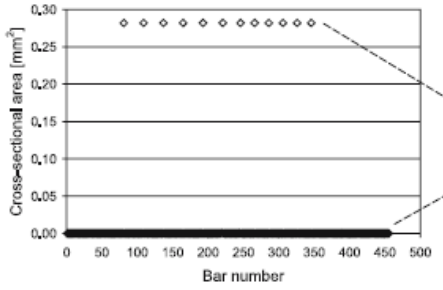

	Mean Value $\overline{x}$ [mm²]	Standard Deviation s [mm²]	Coefficient of Variation CV%
Group 1	0.281	0.0001	0.047%
Bars (1)	*ELIMINATED*		

(1): with minimum or near minimum cross-section

(a) (b)

Figure 7.4: Statistical data for the short cantilever beam

7.2.8.2. The long cantilever

The long-cantilever beam is illustrated in Fig.7.5a. The entire left side $(x=0)$ is fixed and a negative vertical load $F=12N$ is externally applied at $(x,y)=(16,5)$. The maximum allowable axial stress is $\sigma_{\max}=30Pa$, while the modulus of elasticity is $E=1Pa$. For the long cantilever it is known that the optimal layout of its skeletal equivalent is achieved when a mesh with aspect ratio $\lambda=(5/8)$ is used (Provatidis and Venetsanos, 2003). Based on this information, the mesh illustrated in Fig.7.5b was generated consisting of 420 bars. The result of Phase 1 is illustrated in Fig.7.5c and the final layout of Phase 4 is shown in Fig.7.5d. The cross-sectional area distribution after Phase 1 is shown in Fig.7.6a, while statistical details concerning the outcome of Phase 4 is presented in Fig.7.6b.

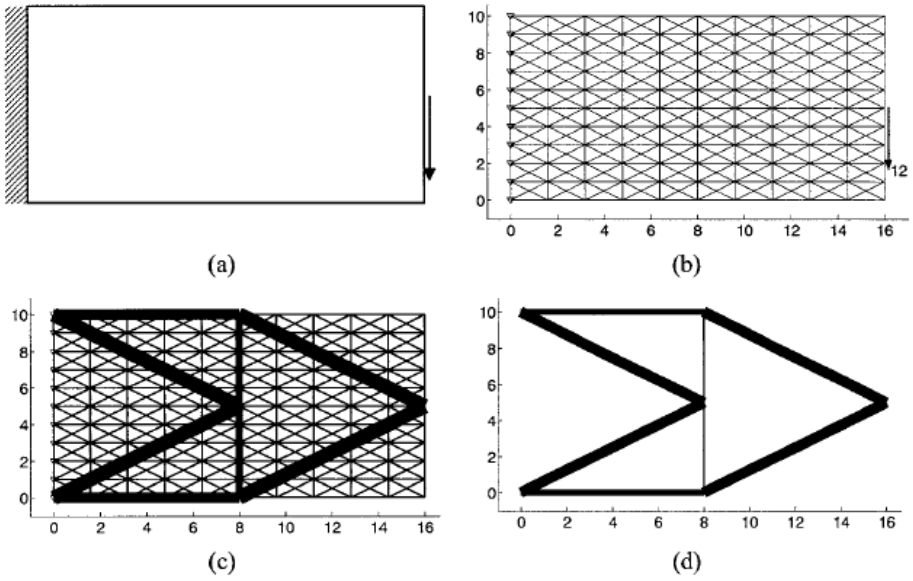

Figure 7.5: The long cantilever beam

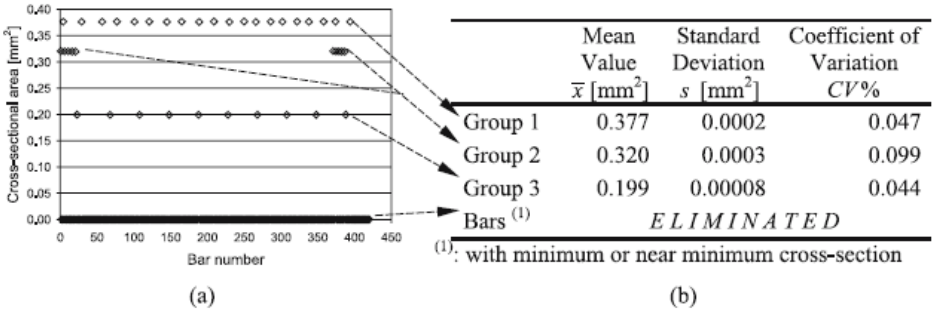

	Mean Value $\overline{x}$ [mm²]	Standard Deviation s [mm²]	Coefficient of Variation CV%
Group 1	0.377	0.0002	0.047
Group 2	0.320	0.0003	0.099
Group 3	0.199	0.00008	0.044
Bars (1)	*ELIMINATED*		

(1): with minimum or near minimum cross-section

Figure 7.6: Statistical data for the long cantilever beam

7.2.8.3. The MBB beam

The MBB beam is illustrated in Fig.7.7a. The lower left edge $(x,y)=(0,0)$ is fixed while the vertical displacement of the lower right edge $(x,y)=(6,0)$ is restrained. A negative vertical load $F=2N$ is externally applied at $(x,y)=(3,1)$. The maximum allowable axial stress is $\sigma_{\max}=20Pa$, while the modulus of elasticity is $E=1Pa$. For the MBB beam, it is

known that the optimal layout of its skeletal equivalent is achieved when a mesh with aspect ratio $\lambda = 1$ is used (Provatidis and Venetsanos, 2003). Based on this information, the mesh illustrated in Fig.7.7a was generated consisting of 412 bars.

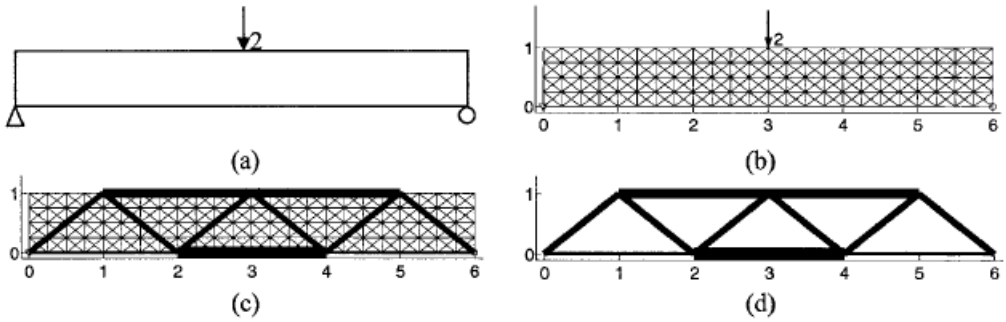

Figure 7.7: The MBB beam

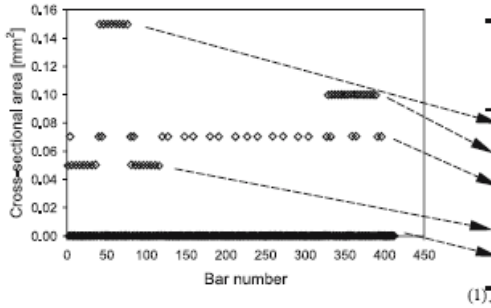

	Mean Value $\bar{x}$ [mm²]	Standard Deviation s [mm²]	Coefficient of Variation CV%
Group 1	0.149	0.00015	0.100
Group 2	0.099	0.00029	0.299
Group 3	0.070	0.00014	0.206
Group 4	0.049	0.00033	0.659
Bars (1)	*ELIMINATED*		

(1): with minimum or near minimum cross-section

(b)

Figure 7.8: Statistical data for the MBB beam

The result of Phase 1 is illustrated in Fig.7.7c and the final layout of Phase 4 is shown in Fig.7.7d. The cross-sectional area distribution after Phase 1 is shown in Fig.7.8a, while statistical details concerning the outcome of Phase 4 is presented in Fig.7.8b.

7.2.8.4. The L-shaped beam

The L-shaped beam is illustrated in Fig.7.10a. The upper edge $(y = 0)$ is fixed, while a negative vertical load $F = 1N$ is externally applied at $(x, y) = (1, 0.2)$. The maximum allowable axial stress is $\sigma_{\max} = 30Pa$ and the modulus of elasticity is $E = 1Pa$. For the L-shaped beam, it is known that, if a uniform aspect ratio λ is used throughout the mesh, the optimal layout of its skeletal equivalent is achieved when a mesh with $\lambda = (1/2)$ is used (Provatidis and Venetsanos, 2003). However, if $\lambda = const$ then the optimization procedure results in a highly dispersed cross-sectional area distribution (Fig.7.9b), thus makes grouping inefficient. Therefore, it was inevitable to use a non-uniform aspect ratio (Fig.7.10b). For $\lambda_1 = 1$, $\lambda_2 = (1/2)$ and $\lambda_3 = (1/3)$, a mesh consisting of 825 bars was generated. The result of Phase 1 is illustrated in Fig.7.10c and the final layout of Phase 4 is shown in Fig.7.10d (*continuous lines*). The cross-sectional area distribution after Phase 1 is shown in Fig.7.11a, while statistical details concerning the outcome of Phase 4 is presented in Fig.7.11b. At this point it must be emphasized that the layout of Phase 4 is under-determinate. Therefore, the designer must introduce an additional member in order to turn the structure into a determinate form. For this purpose, a bar between nodes *A* and *C* (*dashed line*) was added.

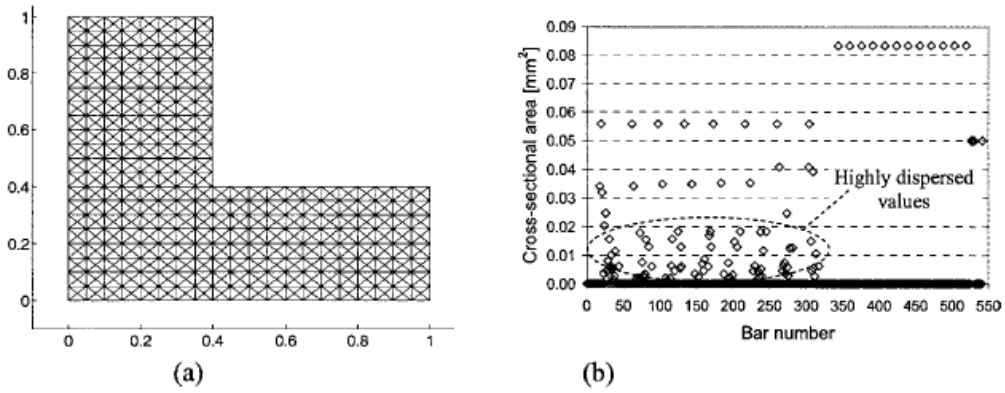

Figure 7.9: The L-shape beam with aspect ratio of mesh $\lambda = ct$

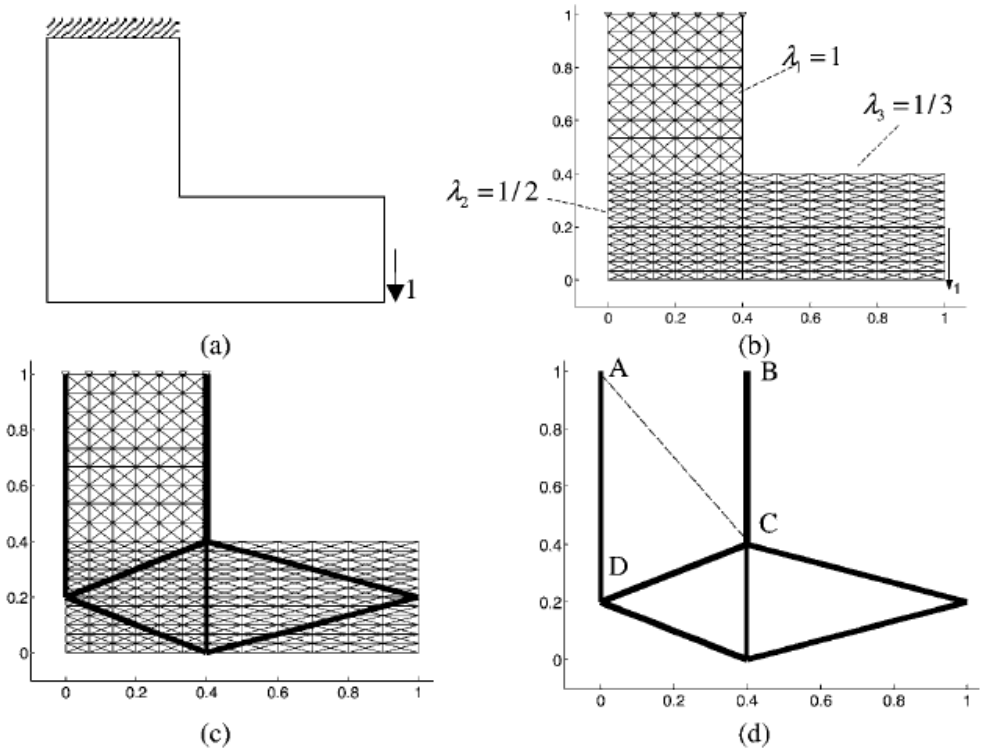

Figure 7.10: The L-shape beam with aspect ratio of mesh $\lambda \neq ct$

7.2.9. Evaluation

The present work suggests the application of a four-phase procedure. In order to evaluate its efficiency, it is necessary to compare the results derived from the proposed procedure to those obtained by the application of an optimization routine such as SQP. Towards this direction, Table 1 and Table 2 were formed. The output of Phase 1 is denoted as [P1], while the output of Phase 4 is denoted as [P4]. Table 1 presents a comparison between states [P1] and [P4] in terms of structural members involved and of cross-sectional area groups formed; that is in terms of structural simplicity. In more details, a triplet of columns corresponds to each one of the four investigated examples. Columns headed as [P1] and [P4] show data concerning state [P1] and [P4] respectively. Columns headed as [%] present a comparison between states [P1] and [P4] in a percentage notation and with respect to state [P1]. Row $x_i = x_{\min}$ refers to those bars whose cross-sectional area x_i is equal to the minimum imposed value $x_{\min}$. Row $x_i \approx x_{\min}$ refers to those bars whose cross-sectional area x_i is very close to

the minimum imposed value x_{min}. Row $x_i \neq x_{min}$ and $x_i \not\approx x_{min}$ refers to those bars whose cross-sectional area x_i is neither equal nor very close to the minimum imposed value x_{min}. Row headed as 'Total' refers to the total number of the structural members involved, while row headed as 'Groups' refers to the number of the appearing different cross-sectional areas. It is clarified that for simplicity reasons, the % differences are rounded to the nearest integer.

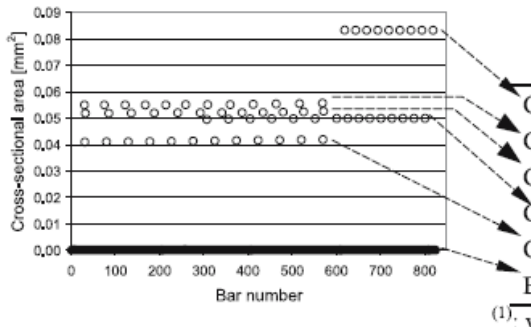

(a)

	Mean Value $\bar{x}$ [mm²]	Standard Deviation s [mm²]	Coefficient of Variation CV%
Group 1	0.083	0.00002	0.023
Group 2	0.055	0.00022	0.401
Group 3	0.052	0.00024	0.455
Group 4	0.049	0.00013	0.272
Group 5	0.041	0.00032	0.768
Bars (1)	*ELIMINATED*		

(1): with minimum or near minimum cross-section

(b)

Figure 7.11: Statistical data for the L-shape beam with aspect ratio of mesh $\lambda \neq ct$

From Table 5.1, it is obvious that the design of state [P4] is superior to that of stage [P1]. In more details, for the short cantilever, the former design required 2 structural elements of the same cross-sectional area (one group), while the latter design required 456 structural elements and 20 different profiles (groups). Therefore, the application of the proposed procedure resulted in 99% reduction of the number of the required structural members and in a 95% reduction of the number of the required cross-section profiles. Taking into consideration all the studied cases, it emerged that a reduction of 97% to 99% in the number of the required structural members was achieved, while a reduction of 87% to 95% in the number of the required cross-section profiles was possible. It is self-evident that such a reduction is of high importance in practical engineering purposes. Table 2 presents a comparison between states [P1] and [P4] in terms of the structural volume. Rows headed as *Volume* [1] and as *Volume* [4] refer to the structural volume in state [P1] and [P4] respectively. Their difference with respect to state [P1] is shown in the last row of Table 2 and in percentage notation. From Table 2, it is obvious that, compared to the design of stage [P1], the design of state [P4] is of less volume, thus weight. In more details, the volume reduction is between 0.13% and 1.79%. Definitely, this reduction is not as impressive as the previous one. However, the combination of both reductions is of importance.

7.2.10. Discussion

Layout optimization of 2D continuum structures has long been among the engineers' priorities due to its practical value, while cost minimization is a lasting engineering desire for all structures. One way of obtaining the optimal layout of a 2D continuum structure is by optimizing its skeletal equivalent (2D skeletal structure), which is formed when an appropriate assembly of bars substitutes the continuum. For this specific case, structural cost minimization may be achieved by introducing *cross-section* grouping, meaning that only a small number of *discrete* cross-sectional values can be used for the optimal layout. In addition, a further cost minimization is possible by introducing member grouping, meaning that a group of structural members, which have the same cross-sectional area and happen to be placed one after another forming a line of length *L*, is replaced by only one member of the same cross-section and of length *L*. The two aforementioned types of grouping aim at

increasing the commonality among the members of a structure. However, for reasons of numerical stability, a minimum cross-section value must be imposed when the optimum layout is sought; otherwise, the stiffness matrix may become ill-posed during the optimization stage. In turn, this means that the optimized structure has members with minimum or near minimum cross-sectional area. In other words, members that should be eliminated are present, which in turn increases the total volume, and consequently, the weight of the structure. It is evident that a further improvement is possible by implementing an appropriate elimination procedure. Therefore, the simultaneous layout optimization and cost minimization of a structure may be achieved if an optimization procedure, a cross-section grouping routine, a member grouping routine, and a group elimination procedure are appropriately combined together. Towards this direction and for the case of 2D skeletal structures under stress constraints only, the present work investigated the capabilities of applying a four-stage procedure, namely the substitution of the structure by a skeletal equivalent, the layout optimization, the grouping stage and finally the elimination stage. With respect to the first stage of the proposed procedure, the formation of the skeletal equivalent of a 2D continuum must be analyzed. A skeletal structure may have various forms, one of which is the well-known ground structure. The advantage of a ground structure is that the orientation of the appearing members has a very wide domain. The disadvantage of this approach is that it is highly possible to get overlapping effects, meaning that members with the same orientation but of different length and cross-section happen to appear one on top of the other in the optimized structure. This is a difficult situation to deal with during the grouping process, because, in this case, the best approach would be the introduction of a member of variable cross-section, which, however, increases the cost significantly. Therefore, for keeping the cost as low as possible, it was preferred to introduce complexes of six bars as in (Provatidis and Venetsanos, 2003). The second stage of the proposed procedure was the layout optimization of the structure. Obviously, this is a classical structural optimization problem, thus any optimizer may be used. This subject was partially investigated in (Provatidis and Venetsanos, 2003), where it was shown that the, well-known and very simple to apply, stress-ratio recursive formula, emerging from the Fully Stressed Design (FSD) technique, and the powerful Sequential Quadratic Programming (SQP) method, suitable for solving non-linear constrained optimization problems, provided the same optimized layouts. At this point, it is noted that the Fully Stressed Design of a structure is one of the oldest approaches concerning structural optimization. It is very well known that only under certain circumstances does it provide the minimum weight. Generally speaking, this is not the case. However, experience obtained during the last decades from the study of a great many practicing engineering problems, clearly suggests that FSD be used for engineering purposes (Berke and Khot, 1987). Therefore, although FSD is not today the state-of-the-art, it can provide very good near optimum results, which is more than adequate for the practicing engineer who needs to find a practical solution and not to invest time in hunting chimeras like a bulletproof, drawback free and solid mathematically-based black box procedure. The third and the forth phases are extensively analyzed in Sects. 2.3 and 2.4. In total, four examples (short cantilever, long cantilever, MBB beam, L-shape beam) were studied. In all cases, the developed stresses were estimated using an in-house code for Finite Element Analysis (FEA), which did not allow for elements to be 'killed' and/or 'reborn'. Instead, all vanishing members could obtain a minimum cross-sectional area value of $x_{\min} = 0.0001$, thus ensuring that neither any numerical stability problems (ill-positioned stiffness matrix) would occur nor the structural volume would be aggravated. Concerning the performed statistical analysis, built-in routines found in Matlab were implemented.

In all cases, the output of the first phase was a structure with a large number of bars with minimum or near minimum cross-sectional area, while the non-vanishing members (bars

with minimum or near-minimum cross-sectional areas) appeared a distribution highly recommending grouping. For the first three examples, the outcome from the final phase was a determinate fully-stressed structure of lower weight, when compared to that obtained after the application of the optimization procedure only. For the last example, the results showed that the aforementioned outcome was achievable only if the aspect ratio of the mesh was properly selected; otherwise, the resulting cross-sectional area distribution was wide enough to instigate grouping.

The dependency of the final skeletal layout on the initially chosen truss structure is worth commenting. The present chapter uses the concept of the ground structure as an initial design; a concept widely accepted, since it is referred in a great many number of papers and textbooks concerning structural optimization. In most examples, a ground structure consists of all possible connections or of only connections to the neighboring points (Bendsøe, 1995). One of its inherent characteristics is the strong dependence of the topology of the optimal solution on the suitable choice of the ground structure. Apart from that, there is a strong influence of the ground structure geometry on the optimal topology (Bendsøe, 1995). Due to the aforementioned influences, depending on the initial ground structure, it is possible to get different optimal designs, among which, one or more will be better than the others in terms of weight or structural simplicity or both. The most common type of ground structure topology is a grid of nodes, which are placed equidistantly from each other but not necessarily equidistantly along the x and y directions. Therefore, it is apparent that a simple parametric investigation is required with respect to the nodal aspect ratio, defined as the ratio of the equidistance along the x-direction over the equidistance along the y-direction. Towards this direction, the present chapter was based on the results of (Provatidis and Venetsanos, 2003), which investigated the aforementioned influences. Without loss of generality, such a parametric investigation is not that time consuming, while it can be considered as an optimization problem itself. Therefore, the inherent dependency of the final skeletal layout on the ground structure may be considered as a drawback. It is as much a drawback as is the mesh dependency of the power laws of SIMP models on the stress constrained minimum weight problem, which was shown clearly in (Duysinx and Bendsøe, 1998). In other words, even the use of state-of-the-art topology optimization techniques, such as the SIMP method, does not avoid mesh dependency. Last, but not least, the following statement, concerning mesh dependency, is referred: '*It is questionable enough to force the solution away from the exact optimal topology by arbitrary constraints, and even worse to prevent these topologies from improving their resolution at finer mesh levels*' (Rozvany et al, 2005). Another point that requires commenting concerns the fact that not in all cases is the final skeletal layout statically determinate and hence builds a mechanism. It is well known that truss topology compliance optimization under a single condition leads to statically determinate solutions, but the resultant structures are more than not mechanisms, which are stable under the applied load (Bendsøe, 1995). With respect to the present chapter, this is the case for the L-shape beam, thus the obtained layout falls within this statement and is not a drawback of the proposed procedure. Furthermore, designing the structure for multiple load cases, either in the weighted average formulation or in min-max formulations, is a way to avoid the aforementioned feature, though at the expense of much more complicated topologies (Bendsøe, 1995). As an alternative, the proposed procedure allows for the use of engineering experience and judgment by letting the designer introduce a structural element, thus gaining a lot both in time and in structural simplicity. The fact that the interaction with the user is allowed up to a point, such as selecting the aspect ratio of the mesh or adding members, is actually an advantage that in the hands of an experienced engineer can prove to be a valuable asset but in the hands of a novice user seems to be a drawback.

An alternative way of dealing with the simultaneous weight and cost minimization is by considering the problem as a multi-objective optimization problem, where not only the weight but also the number of group members and the size of each group have to be minimized as well. Obviously, this is a more complex optimization problem and its solution is definitely of a significant higher computational cost. On the contrary, the proposed procedure is much simpler due to the fact that neither the number of group members nor the size of each group is dealt as a design variable. Finally, reliability analysis is another issue that can be combined with the proposed procedure. As it was mentioned in Sect. 2, the proposed procedure has a practical engineering orientation. Therefore, it would be interesting to investigate the sensitivity of the behavior of the final design in slight changes either of the optimized and grouped structural members, or of the externally applied forces. The latter is equivalent to optimizing the structure for more than one load cases.

The main and strong advantage of the proposed procedure is that it depends neither on the optimization scheme to be applied nor to the dimension of the design space. In this way, it is possible to apply the same procedure to optimization problems of 3D skeletal structures, as well as to optimization problems of other types of constraints.

7.2.11. Conclusions

The goal of the present work was to investigate the efficiency of the proposed procedure for the simultaneous layout optimization and cost minimization of 2D continuum structures. For the needs of the investigation, stress constraints were imposed. The structures were substituted by equivalent skeletal assemblies, the layout optimization was achieved through the use of a very powerful optimizer (SQP), while the cost minimization was sought through a statistical procedure that aimed at increasing the commonality between the structural members. In total, four typical examples (short cantilever, long cantilever, MBB and L-shape beam) were examined. The results of the present work were the following: The implementation of the SQP method for the layout optimization of the 2D skeletal structures was straightforward but time consuming. Furthermore, the additional statistical process (grouping), of the optimized cross-sectional areas, resulted in near optimum designs of minimal cost. The aforementioned statistical process was implemented after the completion of the optimization procedure, thus it did not affect the required for the optimization CPU time. Therefore, the total CPU time depended mainly on the selected optimization procedure. The orientation of the diagonal truss elements is of major importance in obtaining the optimal layout, thus in obtaining the optimal grouping as well. Depending on this orientation (mesh topology), non-optimum designs may be obtained. However, a good engineering judgment concerning the mesh analysis may lead to a near optimum design, as is clearly shown in the case of the L-shaped beam. For the examined examples, the grouping procedure resulted in a reduction of 97% to 99% in the number of the required structural members and in a reduction of 87% to 95% in the number of the required cross-section profiles. In addition, the volume reduction was between 0.13% and 1.79% .

Based on the aforementioned conclusions, as well as on the fact that the proposed procedure is independent from both the optimization procedure and the imposed constraints, it yields that the proposed procedure is a good investment in searching for the minimum cost of skeletal structures and is of major practical value.

7.3. Cost minimization considering welding cost and scrap material

7.3.1. In general

As mentioned in the first section of this chapter, cost minimization may be achieved, when the cost of welding and the cost of scrap material are taken into consideration. However, there

is no generalized procedure embedding the two aforementioned costs, thus only case-oriented procedures are possible to be stated. Towards this direction, welded steel tanks for oil storage were selected as a case-study. Welded steel tanks are one of the most common types of structures used for oil storage. They are assembled from courses; each one of them has its own height and thickness and may be formed from two or more parts welded together. As structures, their manufacturing must be in accordance with certain specifications, such as the API standards, and their cost must be minimized. For the cost minimization, it is essential to take into consideration the number of the courses used, the volume of each course, the parts that each course is divided into, the length of the welding between the assembled parts and the assembled courses, as well as the wastage of the purchased material. Furthermore, the sketch plates and the bottom plates must be dealt with a similar concept. Towards this direction, the present work was focused on embedding the API standards with in-house developed optimization procedures in an integrated environment, where all of the aforementioned factors were considered. On top of that, other types of constraints were also implemented, such as the maximum size of a part that can be transported on a truck along the national roads of the Hellenic Republic and the standard dimensions of the steel plates sold in the Hellenic market. The contribution of the present work is the formation of diagrams that can be used for selecting explicitly decisive dimensions for the optimum oil tank design.

7.3.2. Problem statement

The most common type of tank for storing oil and oil products is a vertically oriented steel cylinder at atmospheric or at low pressure. The diameter of a cylindrical tank ranges from 3m up to about 100m, while the height may reach up to 25m. The main parts, a cylindrical tank consists of, are the bottom, the cylindrical wall or shell and the roof. The steel-plated bottom is flat or with a very small slope and sits on an properly prepared foundation. The shell is made up of a series of rectangular plates welded together, restrains the hydrostatic pressure by hoop tension forces and is largely unstiffened. The roof is usually fixed to the top of the shell and may be self supporting or partially supported through membrane action. In general, the roof plate is supported on radial beams or trusses and is of conical or domed shape. The standards applied most widely for the design of oil storage tanks are the British Standard BS 2654 (1984) and the American Petroleum Institute Standard API 650 (1988), while actions on tanks are also covered by the Eurocode (prEN 1991-4). Apart from the welded type, bolted 'smoothwall' tanks are an alternative for capacities ranging up to 2 million cubic feet of storage, while standards for bolted tanks also exist (API 12B, 1995).

The numerous papers found in the literature about oil-tanks mainly deal with special issues. More particularly, Perelmuter *et. al* investigated a cylindrical oil tank in which a part of its wall had been repaired by placing reinforcing patches on and around the area of defect. Due to this intervention, a mismatch in thickness appeared which was studied first with a linear analysis and then with an approach allowing for geometrical non-linearity (Perelmuter et al, 2003). Dawson and Gibson studied the behavior of compliant-cored cylindrical tank shells with linear-elastic buckling theory coupled with basic plasticity theory. They showed that thin-walled cylindrical structures having walls reinforced by a core, such as a honeycomb or a foam-like cellular core, provide an increased buckling resistance in comparison with a hollow cylinder of the same weight. Furthermore, they examined the feasibility of implementing compliant cores in thin-walled engineering structures, where the weight to load bearing ratio is a critical element of design (Dawson and Gibson, 2006). Hagihara and Miyazaki investigated, with the finite element method, the dynamic bifurcation buckling load appearing in cylindrical tanks with conical roof shells during accident conditions simulated by a step pressure loading, a ramp pressure loading and a pulse pressure loading and they concluded that the minimum bifurcation buckling pressure is a linear function of radius-to-thickness

ratio of the shell in a linear fashion on a logarithmic scale (Hagihara and Miyazaki, 2003). Yoshida investigated the so-called 'frangible roof joint' introduced in API Standard 650 and, through an elastic and elastic-plastic axisymmetric shell finite element analysis involving large deformation in the pre-buckling state, he concluded that the aforementioned standard does not evaluate the frangible roof joint conservatively in small diameter tanks (Yoshida, 2001). Furthermore, optimization in combination with oil storage tanks may be found in works handling the scheduling problem of refinery processes (Song et al, 2002). Surprisingly enough, in contradiction to the numerous published theoretical works, the market of commercial software for oil tank design is extremely limited. To the best knowledge of the authors of the present chapter, only one software solution is available (Tank version 2.5, ©1994-2003, COADE, USA). However, this solution does not include aspects of structural optimization concerning the oil tank itself, an area that the present chapter contributes to. In more details, the cost minimization of oil storage tanks was analyzed and solved with optimization procedures especially developed for this goal. In this way, the present work resulted in the formation of diagrams in accordance with the API Standard 650 that can be used for selecting explicitly decisive dimensions for an optimal oil tank design.

7.3.3. Definition of parameters

The most important parameters to consider, when specifying storage tanks, are their capacity and dimensions. The capacity of the tank is the internal volume available for the storage of materials, while the most commonly used orientation of an oil storage tank is vertical (Fig.7.12).

Figure 7.12: Typical oil storage tanks of different radius to height ratios

As mentioned in the introduction, a tank has three main components, namely the roof, the shell and a steel-plated bottom placed on a properly prepared foundation. The roof and the foundation are mainly responsibility of a civil engineer, while the shell and the plated bottom are mainly responsibility of a mechanical engineer. For this reason, only the latter are examined in the present chapter. Therefore, from the mechanical engineering viewpoint, the design optimization of a storage tank is decomposed into three optimization sub-problems, namely the optimization of the shell, the optimization of the annular bottom plates (sketch plates) and the optimization of the bottom plates. In turn, each sub-problem may be further decomposed into a layout and a size optimization problem, concerning the thickness of the plates. These aspects are covered in the following sections.

7.3.4. Optimization of the shell-wall

7.3.4.1. *Layout optimization*

For practical reasons, it is necessary to build up the shell of a tank using a number of plates having rectangular shape. After special treatment, each plate obtains a cylindrical curvature and several such plates butt welded together form a ring (or course). The shell is formed, when rings are put and welded one on top of the other. For the shell of oil storage tanks, it is mandatory to use plates of certified quality in terms of both material properties and

geometrical accuracy. From the optimization viewpoint, the best shell design is the one which requires an integer number of plates for its building because in this case all of the purchased material is used, or, equivalently, the material waste is zero. As a first approach, the optimization of the shell may be stated as:

$$\begin{gathered} \text{Minimize } \left(V - V_{specif}\right) \\ \text{with } V = f\left(N_{circ,j}, L_{circ,j}, N_{vert,j}, W_{vert,j}\right),\ j = 1,2,3,... \\ \text{under } D_{specif,low} \le D \le D_{specif,high},\ H_{specif,low} \le H \le H_{specif,high}, \\ \left(H/D\right)_{specif,low} \le \left(H/D\right) \le \left(H/D\right)_{specif,high} \end{gathered} \tag{7.10}$$

where

V is the volume of the optimized tank,

V_{specif} is the volume defined by the technical specification imposed by the tank purchaser,

$L_{circ,j}$ is the plate length of the plates along the circumferential direction,

$N_{circ,j}$ is the number of plates of length $L_{circ,j}$ along the circumferential direction,

$W_{vert,j}$ is the plate width of the plates along the vertical direction of the tank,

$N_{vert,j}$ is the number of plates of width $W_{vert,j}$ along the vertical direction of the tank,

D is the diameter of the tank,

D_{specif} is the constraint on the tank diameter (technical specification imposed by the tank purchaser),

H is the height of the tank and

H_{specif} is the constraint on the tank height (technical specification imposed by the tank purchaser).

The constraint concerning the ratio of the tank height over the tank diameter is also required; otherwise extreme designs of no engineering value will occur. It is noted that, for each imposed constraint, both a lower and an upper limit exist, as the corresponding subscripted indices inform. Furthermore, the subscript *j* denotes that it is possible to use certified plates of different rectangular shapes. In the Hellenic market, there is availability of certified plates of dimensions $2m \times 6m$ and $2.5m \times 6m$, respectively. Therefore, the optimization problem may be stated as (only the objective function is restated since the constraints are the same as previously (Eq.1)):

$$\begin{gathered} \text{Minimize } \left(V - V_{specif}\right) \\ \text{with } V = f\left(N_{circ}, L_{circ} = 6, N_{vert,1}, W_{vert,1} = 2, N_{vert,2}, W_{vert,2} = 2.5\right) \end{gathered} \tag{7.11}$$

Apart from the volume, which is the predominant specification in an oil-tank design, there are other issues that do matter and may play an important role in the final design. In more details, the cost for the necessary welding as well as the time required for the sand-blasting and painting of the shell are parameters that must be taken into consideration, because the building of an oil-tank is a practicing engineering problem thus all practical parameters must be recorded and evaluated. Therefore, the optimization problem in a more detailed statement becomes a complicated multi-objective problem (again, only the objective function is restated):

$$\text{Minimize } \left(V - V_{specif}\right),\ A_{shell},\ L_{weld,circ},\ L_{weld,vert}$$
$$\text{with } V = f\left(N_{circ}, L_{circ} = 6, N_{vert,1}, W_{vert,1} = 2, N_{vert,2}, W_{vert,2} = 2.5\right) \tag{7.12}$$

where A_{shell} denotes the area of the shell, $L_{weld,circ}$ represents the welding length along the circumferential direction and $L_{weld,vert}$ represents the welding length along the vertical direction. It is clarified that the aforementioned lengths of welding are accounted for separately, because it is possible to apply a different technique for each welding direction, thus the cost per meter becomes different as well. With respect to the optimization problem itself, it is obvious that it falls into the area of combinatorial optimization, since the design variables are discrete. The main characteristic and, at the same time, drawback, of this approach is that, the optimized volume may be far away from the specified volume V_{specif}. In this way, the *best numerical solution* to the problem may have *minimal practical value* and for this reason may be rejected. Another approach of the same philosophy is to let the volume be optimized around an acceptable area of interest:

$$\text{Minimize } \left(V - \left(V_{specif} \pm \Delta V\right)\right),\ A_{shell},\ L_{weld,circ},\ L_{weld,vert}$$
$$\text{with } V = f\left(N_{circ}, L_{circ} = 6, N_{vert,1}, W_{vert,1} = 2, N_{vert,2}, W_{vert,2} = 2.5\right) \tag{7.13}$$

where ΔV stands for an acceptable deviation from the initial volume specification. Obviously, this is an element that may be proposed by the engineer but must definitely be approved by the tank purchaser.

7.3.4.2. Size Optimization

The shell carries its weight, the weight of all components attached to it and the weight of the roof which it supports. Additionally, a load uniformly distributed over the horizontal projected area of the roof is also applied, simulating the nominal snow load and any other loads applied to the roof, such as the loads from maintenance equipment. These loads result in an axial stress. Furthermore, wind loading on the tank contributes tensile axial stress on one side of the tank and compressive stress on the other. The maximum wind speed taken into consideration in the calculations depends on the land where the tank is to be built on. In addition, the stored oil, up to the full capacity of the tank, applies an easily calculated hydrostatic pressure to the shell (Young, 1989). In particular, this pressure is carried by simple hoop tension, thus no circumferential stiffening is needed, while the circumferential tension in the shell varies linearly, in a vertical direction, with the fluid level. Finally, depending on the seismic activity of the area where the tank is to be built, resistance to seismic loads must also be accounted for. All of the aforementioned loads must be included for sizing the shell of a tank. The regulations, such as the API Standard 650, impose equations for the estimation of the shell thickness through an iterative procedure. Therefore, the optimization problem with respect to the thickness distribution of the shell along the vertical direction may be stated as follows:

$$\text{Minimize } V_{shell} = \sum_{j=1}^{N_c} V_{shell,j} \text{ with } V_{shell,j} = f\left(H, D, t_1, S_d, S_t, E, G, CA\right)$$
$$\text{under } \tau_{shell,j} \le \tau_{shell,allow} \tag{7.14}$$

where

D is the diameter of the tank,
H is the height of the tank,
t_1 is the thickness of the first course,
S_d is the allowable stress for the design condition,
S_t is the allowable stress for the hydrostatic test condition,
E is the joint efficiency,
G is the specific gravity of the oil product to be stored,
CA is the corrosion allowance, specified by the tank purchaser and
τ denotes the stress.

The subscripts j and $allow$ denote the course number and the allowable stress, respectively, while N_c denotes the total number of courses of the tank.

7.3.5. Optimization of the sketch plates

7.3.5.1. Layout of the shell-wall

The annular bottom plates (sketch plates) are equally cut and welded in such a way that they form a ring around the steel-plated bottom of the tank. The assembly of the sketch plates form a ring, thus each sketch plate, being cut from commercially available rectangular-shaped plates, will have the form of an arc. Obviously, cutting sketch plates from rectangular plates results in a material waste. From the layout optimization viewpoint, the best sketch plate design is the one characterized by the least material waste. In other words, the problem at hand it to optimize the fitting of the sketch plates on the area of the commercially available plates used for this purpose. Since no requirement for sketch plate certification is imposed, any commercially available steel plate may be used. The availability of the Hellenic market is illustrated in Table 5.3, where the length is not referred since, practically speaking, any length is orderable.

Table 7.3: Data for the commercially available sheet plates used for cutting the sketch plates

Width [mm]	Available thicknesses [mm]																					
	3	4	5	6	7	8	9	10	11	12	14	15	16	18	20	22	25	30	35	40	45	50
1000	✓	✓	✓	✓	✓	✓	✓	✓	✓	✓	✓	✓	✓	✓	✓	✓	✓	✓	✓	✓	✓	✓
1250	✓	✓	✓	✓	✓	✓	✓	✓	✓	✓	✓	✓	✓	✓	✓	✓	✓	✓	✓	✓	✓	✓
1500	✓	✓	✓	✓	✓	✓	✓	✓	✓	✓	✓	✓	✓	✓	✓	✓	✓	✓	✓	✓	✓	✓
1800		✓	✓	✓	✓	✓	✓	✓	✓	✓	✓	✓	✓	✓	✓	✓	✓	✓	✓	✓	✓	✓
2000		✓	✓	✓	✓	✓	✓	✓	✓	✓	✓	✓	✓	✓	✓	✓	✓	✓	✓	✓	✓	✓
2300		✓	✓	✓	✓	✓	✓	✓	✓	✓	✓	✓	✓	✓	✓	✓	✓	✓	✓	✓	✓	✓
2500		✓	✓	✓	✓	✓	✓	✓	✓	✓	✓	✓	✓	✓	✓	✓	✓	✓	✓	✓	✓	✓

Taking into consideration all of the above, the layout optimization of the sketch plates becomes a problem of fitting the sketch plates in an area of pre-defined width. A characteristic example is illustrated in Fig.7.13, where an annular ring of four parts is considered and different configurations result in different material exploitation, although the width of the plate being cut into sketch plates was the same in all cases. In more details, Fig.7.13a shows a typical fitting where the rectangles prescribing the sketch plates are placed one on top of the other (horizontal orientation); for this fitting let the required area be A_1. This fitting gives two kinds of material waste. The first concerns the area marked with the dashed line, which is unexploited for the specific design but, due to its shape, may be kept in stock for future use, thus becoming potentially exploitable.

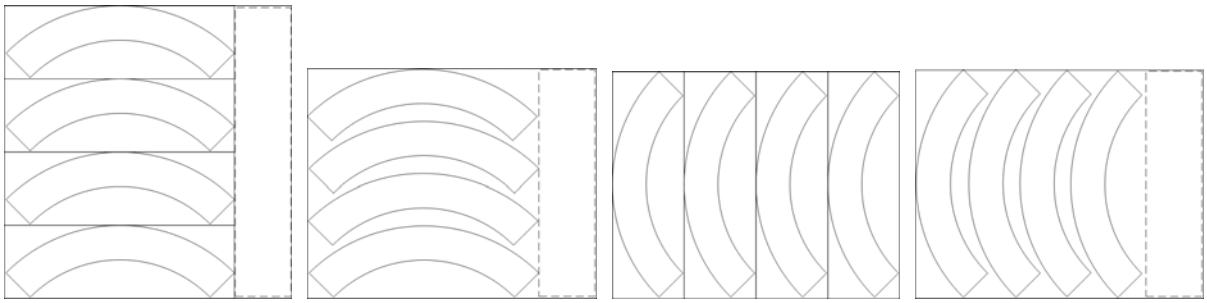

(a) (b) (c) (d)

Figure 7.13: Different fitting of the sketch plates results in different material exploitation

The second concerns the areas resulting from the subtraction of the sketch plates from the corresponding prescribing plates; these areas are considered as non- exploitable material (scrap). A more compact configuration is shown in Fig.7.13b; for this fitting let the required area be A_2. Since $A_2 < A_1$, the second configuration is superior but requires suitable equipment for such cuttings to be performed, thus, from a manufacturing viewpoint, it is more demanding. Two other configurations of required area A_2 are shown in Figs.5.13c,5.13d, where the orientation of the fitted plates has changed (vertical orientation). Of course, depending on the radii of the sketch plates, it is possible to combine horizontal with vertical fittings for even better results. Therefore, the layout optimization problem of the sketch plates may be stated as follows:

$$\begin{aligned} &\text{Minimize } A_{\text{unexploitable}} \text{ or } A_{scrap} \\ &\text{under } N \in \mathbb{N}^* \end{aligned} \tag{7.15}$$

where N is the total number of the sketch plates. It is clarified that after the optimization of the shell, the diameter of the tank, thus the inner and outer radius of the sketch plates, is well defined and the variable N becomes the only unknown.

7.3.5.2. Size optimization

According to the API Standard 650, the minimum thickness of the sketch plates is explicitly related to the tank diameter, which is estimated, when the optimization of the shell is performed (API 650/Section 3.5.3) Therefore, there is no need for solving an optimization problem.

7.3.6. Optimization of the bottom plates

7.3.6.1. Layout optimization of the shell-wall

The bottom of an oil storage tank must be steel-plated with plates of certified quality in terms of both material properties and geometrical accuracy. As already mentioned, such certified plates of dimensions $2m \times 6m$ and $2.5m \times 6m$ are available in the Hellenic market. Therefore, once again the problem at hand is a fitting problem, where rectangular plates must be fitted in a circle such that the non-exploitable material is minimized, as Fig.7.14 shows. More particularly, due to symmetry, only one-half of the layout is illustrated.

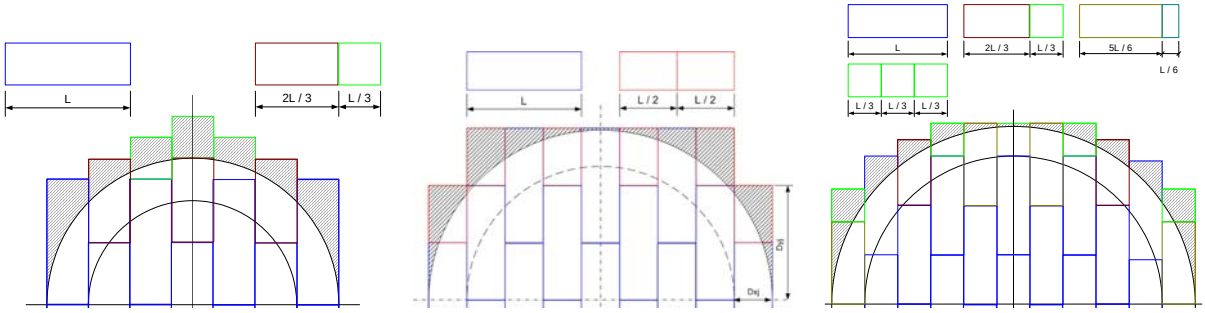

(a) $10m < D < 14m$ (b) $14m < D < 18m$ (c) $18m < D < 22m$

Figure 7.14: Bottom plates for various tank diameters

The main idea is to use an *odd* number of plates distributed along the horizontal direction and to fit the steel plates along the transverse direction such that either an entire plate or a well-defined fraction of it is used. In Fig.7.14, the case of a tank of diameter D between $D_{\min}$ and $D_{\max}$, as noted in the caption, is illustrated. The inner circle corresponds to $D_{\min}$ and the outer circle corresponds to $D_{\max}$. The subdivisions of the steel plate required for the distributions presented in Fig.7.16 are denoted with a different color (blue border for the entire plate, red border for one-half of a plate, green border for one-third of a plate, brown border for two-thirds of a plate and oil-green for five-sixths of a plate and another color for one-sixth of a plate). The shaded areas represent the material to be removed. Once again, material corresponding to rectangular areas is potentially exploitable while the other material left is non-exploitable material (scrap). In order to estimate the material S to be removed, it is sufficient to subtract the area of the outer circle of radius R from the total area of the columns $\left(\Delta x_j, \Delta y_j\right)$:

$$S = \sum_{j=1}^{N_j} S_j = \sum_{j=1}^{N_j} \left(\Delta x_j \, \Delta y_j - \int_{x_{j-1}}^{x_j} \sqrt{\left(R^2 - x^2\right)} \, dx \right) \tag{7.16}$$

Therefore, the layout optimization problem of the bottom plates may be stated as follows:

$$\text{Minimize } S \text{ with } S_j = f\left(L \le 6, W \in \{2.0, 2.5\}\right) \tag{7.17}$$

where L and W correspond to the length and the width of the steel plates used to cover the bottom of the tank.

7.3.6.2. Size Optimization

The thickness of the bottom plates is also specified (API 650 / Section 3.4.1) thus no optimization problem needs to be solved.

7.3.7. Calculations

The calculations required for the solutions of the aforementioned optimization problems are most extensive. Indicatively, the procedure for estimating the scrap from cutting the sketch plates (horizontal orientation, Fig.7.13a) is referred.

Step 0: Use the tank diameter D and the tank height H resulted from the optimization of the shell

Step 1: Determine the quantities d_1 and d_2 from standards (for API650: $d_1 = 2"$, $d_2 = 24"$)

Step 2: Estimate the thickness t_{c_1} of the first course

Step 3: Estimate the inner radius of the sketch plate $R_{in} = 0.5D - d_1$

Step 4: Estimate the outer radius of the sketch plate $R_{out} = 0.5D + t_{c_1} + d_2$

Step 5: For various $N \geq 2$, $N \in \mathbb{N}$

Step 6: Estimate the polar angle θ corresponding to the each sketch plate

Step 7: Estimate the width of the plate that the sketch plate will be cut from $W_j = 2R_{out} \sin(0.5\theta)$

Step 8: Find the standardized width W_{st} just greater than W (see Table 1)

Step 9: If $W_{st} > 2300mm$ then N is rejected; set $N = N + 1$ and return to Step 5

Step 10: Estimate the length of the plate that the sketch plate will be cut from $L_j = R_{out} - R_{in}$

Step 11: Estimate area of the prescribing rectangle $A_{pp,j} = W_j L_j$

Step 12: Estimate area of the sketch plate $A_{sp,j} = \theta_j \left(R_{out}^2 - R_{in}^2 \right)$

Step 13: Estimate the scrap area per sketch plate $A_{scrap,j} = A_{pp,j} - A_{sp,j}$

Step 14: Estimate the total scrap area $A_{scrap,sp} = \sum_{j=1}^{j=N_{sp}} A_{scrap,j}$

Step 15: Estimate the total length $h_{tot} = N\,h$

Step 16: Estimate the length for welding #1 (sketch plates one welded next to the other), $L_{w,1} = N\left(R_{out} - R_{in}\right)$

Step 17: Estimate length for welding #2 (sketch plates welded to the bottom plates), $L_{w,2} = \pi D_{in}$

Step 18: Record N, ΔE_{tot}, $L_{w,1}$, $L_{w,2}$, h_{tot}

The subscripts pp and sp stand for 'prescribing plate' and 'sketch plate', respectively.

7.3.8. Results

The optimization problems stated in the previous sections are all mixed-integer multi-objective optimization problems. It is possible either to embed all of them in a large optimization statement or to deal with each sub-problem separately. In the present chapter, the latter approach was selected, because it provides a better insight. For the solution of the sub-problems the brunch-and-bound technique was implemented. It is noted that if the solution of a *particular* problem was sought, then a Paretto front should be estimated. However, since the ultimate goal was to investigate the effect that various parameters had on the optimal solution, the estimation of the Paretto front was deactivated from the in-house code developed for the purposes of the present work. The overall results of the aforementioned investigation are presented in the next figures.

In more details, Fig.7.15 shows the tank diameters of the optimal designs versus the imposed constraint concerning the ratio of the tank diameter over the tank height (D/H). It is obvious that there is a plethora of optimal designs, depending on the diameter and the volume of the tank. For the charts in Fig.7.15a, only plates of dimensions 2x6 were used, for the charts in Fig.7.15b, only plates of dimensions 2.5x6 were used, while for the charts in Fig.7.15c combinations of both types of plates were used. In these diagrams, each point

represents an optimal design. Therefore, from Fig.7.15, it is possible to determine the diameter of the tank.

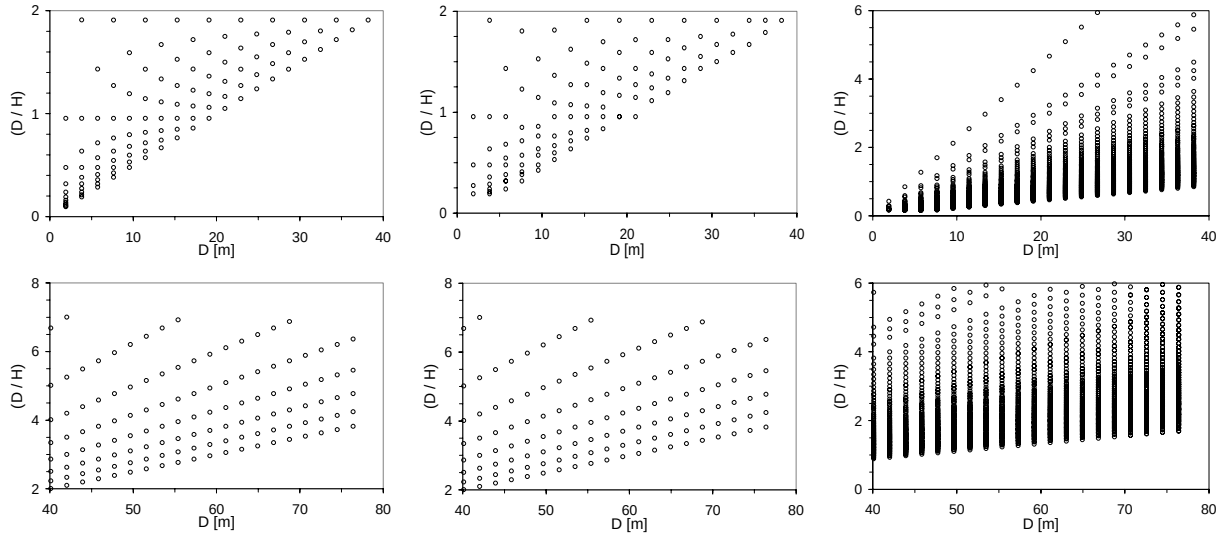

(a) (b) (b)

Figure 7.15: Tank diameters for optimal shell designs using certified plates from the Hellenic market: (a) plates 2m × 6m only, (b) plates 2.5m × 6m only and (c) plates 2m × 6m / 2.5m × 6m.

In Fig.7.16, the tank volume versus the ratio (D/H) is illustrated for various cases of plates. Knowing the value (D/H) from the previous figure, it is possible to determine the volume of the tank.

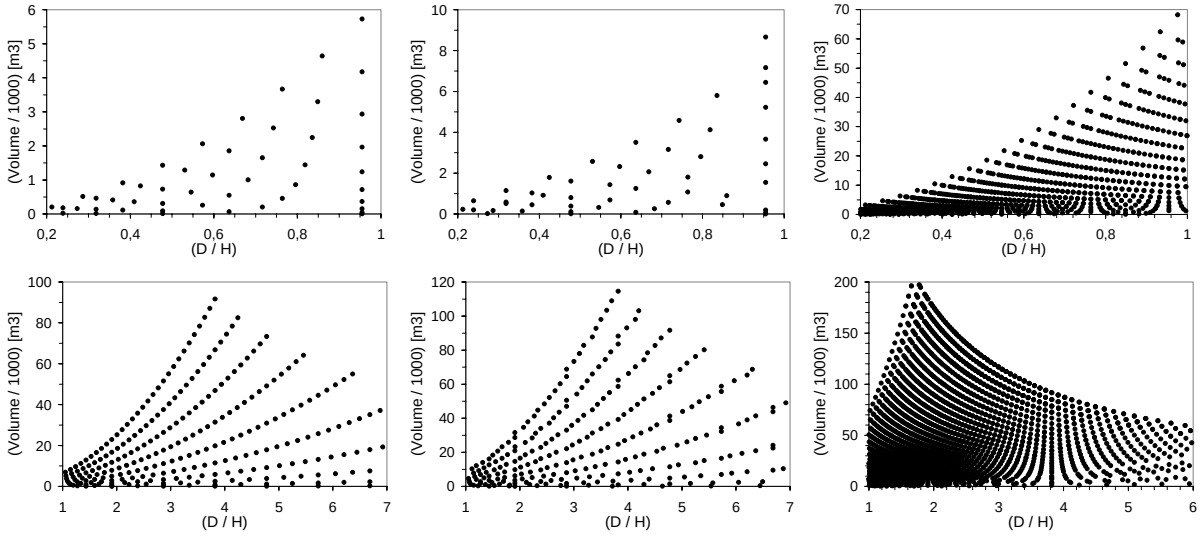

(a) (b) (c)

Figure 7.16: Tank volumes of optimal shell designs using certified plates from the Hellenic market: (a) plates 2m × 6m only, (b) plates 2.5m × 6m only and (c) plates 2m × 6m / 2.5m × 6m.

In Fig.7.17, the shell area versus the ratio (D/H) is illustrated, thus it is possible to estimate the area of the tank that will be sandblasted and painted. This is very useful to know basically for reasons of scheduling.

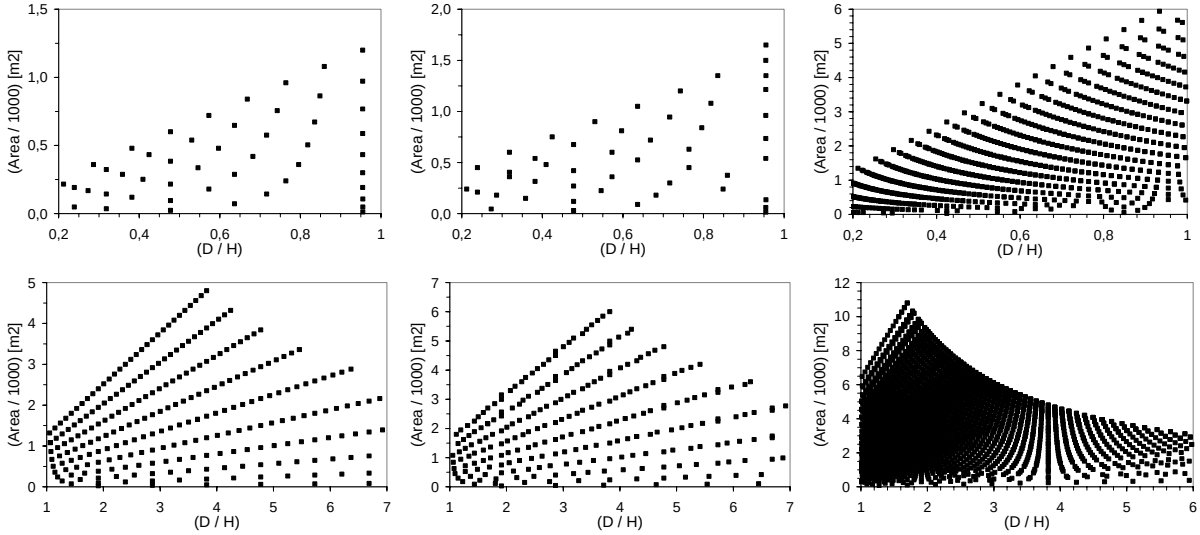

(a) Plates 2mx6m only (b) Plates 2.5mx6m only (c) Plates 2mx6m / 2.5mx6m

Figure 7.17: Areas of optimal shell designs using certified plates from the Hellenic market

Finally, the total length of the welding required for the tank to be built is illustrated in Fig.7.18. This information is very crucial not only in terms of cost, which is significantly high for the work itself, but also in terms of time.

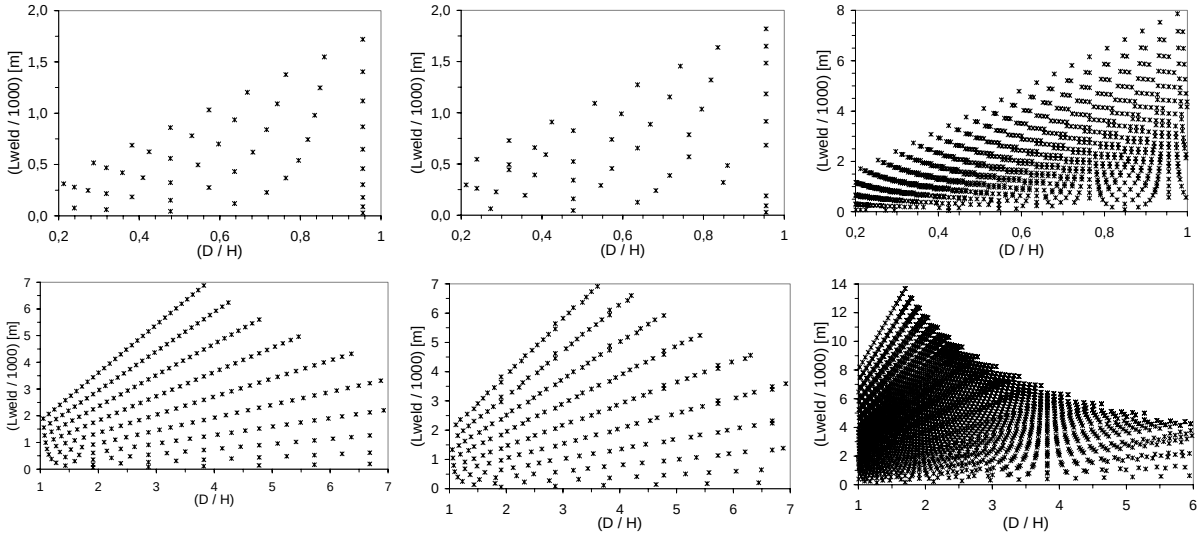

(a) (b) (c)

Figure 7.18: Welding length of optimal shell designs using certified plates from the Hellenic market: (a) plates $2\text{m} \times 6\text{m}$ only, (b) plates $2.5\text{m} \times 6\text{m}$ only and (c) plates $2\text{m} \times 6\text{m}$ / $2.5\text{m} \times 6\text{m}$.

7.3.9. Conclusion

The present work dealt with the problem of minimizing the cost of a structure taking into consideration both the cost of the welding and the cost of the scrap material. As an example, the case of an oil storage tank was investigated. In more details, the problem was decomposed into the design of the tank bottom, the annular bottom plates and the shell. The ultimate goal was to result in designs of both minimal weight and minimal scrap. The illustrated results provide an explicit way to select an optimal design. However, the current analysis suggests

that the most economically efficient solution be choosing one among the designs obtained in the present investigation. In other words, standardization in optimal oil storage tank design is strongly proposed.

7.4. Recapitulation

In this chapter, the minimization of the structural cost was investigated. Since the structural cost is a very complicated quantity to estimate, the investigation was focused on two subjects, the first being the commonality of the structural members within the structure and the second being the effect of the welding cost and the scrap material cost. For the needs of this investigation, two newly introduced optimization procedures, which consist the contribution of the current chapter, were developed and successfully tested. The former concerned the grouping of similar members and the elimination of critical members; this procedure is applicable to any skeletal structure and it was successfully tested in four literature problems. The latter concerned the solution of a complex optimization problem, involving design control for minimum scrap and minimum welding; it was successfully applied in welded tanks for oil-storage. The main outcome of the aforementioned investigation is that it is not possible to establish a generalized procedure for minimum structural cost applicable in all cases, because for the cost minimization to be achieved special design characteristics of each case must be exploited. However, it is possible to introduce optimization procedures, like the proposed ones, suitable for certain subclasses of the generalized optimization problem.

References

API 12B, (1995), *Specification for Bolted Tanks for Storage of Production Liquids*, 14th Edition, API.

API 650 (1988), *Welded Steel Tanks for Oil Storage*, 8th Edition, API.

Belegundu AD, Chandrupatla TR (1999) Optimization concepts and applications in engineering. Prentice Hall.

Bendsøe MP (1995) Optimization of Structural Topology, Shape, and Material. Berlin: Springer-Verlag.

Berke L, Khot NS (1987) Structural optimization using optimality criteria, in: Computer Aided Optimal Design: Structural and Mechanical Systems, edited by C.A. Mota Soares, NATO, ASI series, F27B.

BS 2654 (1984), *Specification for manufacture of vertical steel welded storage tanks with butt-welded shells for the petroleum industry*, British Standards Institution, London.

Dawson M.A., Gibson, L.J., (2006), "Optimization of cylindrical shells with compliant cores", Int J Solids Structs, in press.

Duysinx P, Bendsøe MP (1998) Topology optimization of continuum structures with local stress constraints. Int J Num Meth Eng, 43, 1453-1478.

Fellini R, Kokkolaras M, Papalambros P (2003) Efficient Product Portfolio Reduction. Proceedings of the 5th World Congress on Structural and Multidisciplinary Optimization, Lido di Jesolo-Venice, Italy, May 19-23.

Gallagher RH (1973) Fully Stressed Design, In: R. H. Gallagher & O. C. Zienkiewicz (eds.), Optimum Structural Design: Theory and Applications. John Wiley & Sons.

Haftka RT, Gurdal Z, Kamat M (1990) Elements of Structural Optimization. Kluwer.

Hagihara, S., Miyazaki, N. (2003), "Bifurcation Buckling Analysis of Conical Roof Shell Subjected to Dynamic Internal Pressure by the Finite Element Method", J Pressure Vessel Technology, Vol. 125, pp. 78-84.

Kirsch U (1989) Optimal Topologies of Structures. Appl Mech Rev, 42, 238.

Kirsch U (1993) Structural Optimization. Springer-Verlag.

Makris P, Provatidis C (2002) Weight minimisation of displacement-constrained truss structures using a strain energy criterion, Computer Methods Appl. Mech. Engrg., 191, 2159-2177.

Morris AJ (1982) Foundations of Structural Optimization: A Unified Approach. John Wiley & Sons.

Papalambros P (1995) Optimal Design of Mechanical Components and Systems. ASME Journal of Mechanical Design, Special 50th Anniversary Design Issue (B. Ravani, ed.), 117, 55-62.

Patnaik SN, Guptill JD, Berke L (1995) Merits and limitations of optimality criteria method for structural optimization. Int. J. Numer. Meth. Engng, 38, 3087-3120.

Perelmuter, A.V., Fialko, S.Y., Karpilovsky, V.S., Kryksunov, E.Z., "Analysis of the Stressed State of Cylindrical Tanks with Defects of Geometrical Shape", Computer Methods in Mechanics, June 3-6, 2003, Gliwice, Poland.

Petruccelli JD (1999) Applied statistics for engineers and scientists. Prentice Hall.

Pham DT, Karaboga D (2000) Intelligent Optimisation Techniques: Genetic Algorithms, Tabu Search, Simulated Annealing and Neural Networks. Springer.

prEN 1991-4: *Eurocode 1 – Actions on structures, Part 4: Actions of silos and tanks*.

Provatidis CG, Venetsanos DT (2003) Performance of the FSD in Shape and Topology Optimization of Two-Dimensional Structures Using Continuous and Truss-like Models. Proc. of the 5th World Congress on Structural and Multidisciplinary Optimization, Lido di Jesolo-Venice, Italy, May 19-23.

Qing L, Steven GP, Xie YM (2000) Evolutionary structural optimization for stress minimization problems by discrete thickness design. Comp. Struct., 78(6), 769-780.

Rozvany GIN (2001) Aims, scope, methods, history and unified terminology of computer-aided topology optimization in structural mechanics. Struct. Multidisc Optim., 2, 90-108.

Rozvany GIN (2001b) Stress ratio and compliance based methods in topology optimization – a critical review. Struct. Multidisc. Optim., 21, 109-119.

Rozvany GIN, Pomezanski V, Gaspar Z (2005) Some Pivotal Issues in Structural Topology Optimization. Proc. of the 6th World Congress on Structural and Multidisciplinary Optimization, Rio De Janeiro, Brazil, May 30-June3.

Schmit LA (1995) Fully Stressed Design of elastic redundant trusses under alternative loading systems. Australian Journal of Applied Science, 9, 337-348.

Song, J., Park, H., Lee D.Y., Park S. (2002), "Scheduling of Actual Size Refinery Processes Considering Environmental Impacts with Multiobjective Optimization", Ind. Eng. Chem. Res., Vol. 41, pp. 4794-4806.

Suzuki K, Kikuchi N (1991) A Homogenization Method for Shape and Topology Optimization. Computer Methods Appl. Mech. Engrg., 93, 291-318.

Tank version 2.5, ©1994-2003, COADE/Engineering Physics Software, Inc., Houston, Texas, USA.

Xie YM, Steven GP (1997) Evolutionary Structural Optimization. Springer-Verlag.

Yoshida, S. (2001), "Buckling of aboveground oil storage tanks under internal pressure", Steel and Composite Structures, Vol.1.

Young, W. C. (1989), *Roark's Formulas for Stress and Strain*, McGraw Hill.

Contributed papers

[1] **Venetsanos, D.T.**, Mitrakos, D. and Provatidis, C.G., "Layout optimization of 2D skeletal structures using the fully stressed design", 1st International Conference on Information Technology and Quality, 5-6 June 2004, Athens, Greece.

[2] Provatidis, C.G. and **Venetsanos, D.T.**, Cost minimization of 2D continuum structures under stress constraints by increasing commonality in their skeletal equivalents, Forschung im Ingenieurwesen vol.70 (3), pp. 159-169, 2006.

[3] Provatidis, C.G., **Venetsanos, D.T.,** Linardos, M.D., "Cost Minimization Of Welded Steel Tanks For Oil Storage According To API Standards", 2nd International Conference "From Scientific Computing to Computational Engineering", Athens, 5-8 July, 2006.

CHAPTER 8

PERFORMANCE-BASED LAYOUT OPTIMIZATION OF DISCRETE STRUCTURES

Abstract

In this chapter, the performance-based layout optimization of large structures is investigated. In real-life, many engineering structures are assemblies of commercially available structural members, such as beams and plates. For these structures, optimization means to seek for such a layout that may be constructed using the aforementioned members, while, at the same time, certain standards concerning their performance are met. Practically, this means to search among the commercially available members and find that combination for which a large group of imposed constraints is fulfilled. The problem just described is of a combinatorial nature and for its solution it is possible to use either a full-factorial approach or a partial-factorial approach, which is of a lower computational cost. Within this concept, two new heuristic partial-factorial optimization procedures are proposed in the present chapter, while their applicability is examined through the optimization of discrete structures, such as crane bridges, crane runway beams and a hangar, taking into consideration the EuroCode standards. On top of that, a performance comparison with a commercial software for structural analysis also takes place.

Keywords

Combinatorial optimization, partial-factorial, Eurocode standards, layout optimization.

8.1. Introduction

Combinatorial optimization problems are characterized by their well-structured problem definition as well as by their huge number of solution spaces in practical application areas. In structural optimization problems, a combinatorial approach is rather related to the fact that structures are often assemblies of commercially available plates and beams, thus the corresponding minimum weight problem is of a discrete nature. Theoretically speaking, the optimum structural design in such a case may be located if all of the possible combinations are explored and the one with the lowest structural weight, without violating any of the imposed constraints, is chosen. However, this is not a recommended approach due to the exponential growth of the computational cost as the number of the design variables, or the number of their discrete values, is increased. On top of that there are cases where a mixed-integer problem occurs, as is the case of welded crane girders or welded crane runway beams. This type of problem is even more difficult to solve, because some design variables take on discrete, thus finite number of, values, while some other design variables take on continuous, thus infinite number of, values. Consequently, in practice, heuristics are commonly used even thought it is not possible to prove that they result in the global optimal solution.

In the present chapter three types of combinatorial optimization problems are discussed, the first two having to do with the selection between standard rolled beam profiles and the third being the selection between standard plates for the formation of welded cross-sections, both in order to minimize the weight of a given structure. The main difference between the aforementioned problems is that in the first two cases the problem at hand is purely discrete, while in the third case it is of a mixed-integer type. In order to deal with them, three new heuristic optimization procedures are proposed in the present chapter, all supported extensively with characteristic examples of optimizing real-life full-scaled structures.

8.2. Discrete Optimization of structures with one design variable

8.2.1. In general

The specific type of problem is met in real-life, when the structure of interest is nothing else but one beam, e.g. single or double girder crane bridges and crane runway beams. Such problems are not that difficult to solve. A simple procedure would be to breakdown the initial list with the candidate profiles into a number of sublists, each one containing profiles of the same type, such as HEA, HEB, HEM etc., solve the weight minimization problem separately for each sublist and finally keep the best solution among the best solutions derived for each sublist. As far as the solution of the optimization problem for each sublist is concerned, it is possible to use simple line search procedures, such as the binary search method, the bisection method, the dichotomous search and the interval halving method. The key points in this type of optimization problem are first to use a *sorted* list of the available standard profiles and second to carry out the search using the *list index* of each profile.

More particularly, suppose that a rolled beam profile must be selected such that the structural weight is minimized and a set of constraints is fulfilled. The first and most important thing to do is separate the available beams in categories, as mentioned in the previous paragraph. Then for each category, a sorted list is formulated such that the profiles are listed in an ascending order with respect to their weight per unit length. Doing so, locating the beam profile that suits best the examined case is nothing else than a simple search within a 1D list. The heuristic proposed optimization procedure for such cases, implementing the binary search method, is described in more details in the next paragraph, while the application of this procedure in large-scale structures is discussed in Section 8.2.3.

8.2.2. Proposed optimization procedure

Let LL be the length of a profile beam list to be searched, x_l be the index corresponding to the first profile of the list, x_u be the index corresponding to the last profile of the list and x_m be the index corresponding to profile at the middle of the list. If a structural analysis with the profile for x_u is carried out and even one of the imposed constraints is violated, then the entire profile list is rejected. In the opposite case, a structural analysis with the profile for x_l is carried out and if none of the imposed constraints is violated, then the profile for x_l is considered to be the best solution for the specific profile list; otherwise, a binary search is initiated. The index x_m is estimated as $x_m = \text{int}\{0.5(x_l + x_u)\}$ and a structural analysis carried out for the profile corresponding to the index x_m. If even one constraint violation occurs, then the specific profile is rejected, the index x_l is set equal to x_m and a new iteration begins. If all of the imposed constraints are fulfilled, then the specific profile is accepted as the current optimum solution, the index x_u is set equal to x_m and a new iteration begins. The iterative procedure ends, when the difference between the indices x_u and x_l becomes equal to one and the then current optimum design is the optimum design for the examined profile list. The same procedure is then applied to each one of the other available profile lists. In this way, a pool of 'best solutions' is formed. The 'best of the best' solution from this pool is considered to be the global optimum solution. Algorithmically speaking, the optimization procedure may be described as follows:

Step 1: Separate available beams in categories and for each category create a sorted list with respect to the beam weight per unit length
Step 2: For each list, apply the following procedure:
Step 2a: Estimate the length of the list LL
Step 2b: Select the profile that corresponds to the last index in the list and carry out a structural analysis
IF even one of the imposed constraints is violated THEN
Reject the list
ELSE
Accept the profile as the current optimum
Select the profile that corresponds to the first index
Carry out a structural analysis
IF even one of the imposed constraints is violated THEN
Reject the profile
Initiate a binary search
ELSE
Accept the profile as the optimum of the current list

This approach has also the advantage of versatility, meaning that instead of a binary search it is possible to initiate another 1D search procedure by simply changing only one subroutine. With respect to the structural analysis, it is possible either to use classical mechanics or the Finite Element Method (FEM). Again, this selection refers to only a specific subroutine thus the rest of the procedure remains untouched. In this way, it is possible to implement various search procedures with various types of structural analysis (e.g. linear static, non-linear static, etc), depending on the specifications of the problem at hand. For instance, suppose that a crane runway beam is to be optimized. If the Engineer selects beam profiles which are

characterized as Class-1 according to the Eurocode 3 standards, then a simple linear static analysis is adequate because EC3 states that such profiles do not suffer from buckling, thus no non-linear analysis needs to be carried out. However, this is not the case if the selected beam profiles are of Class-4, where buckling must be taken into consideration, thus a snap-through buckling check (non-linear analysis) is mandatory. The applicability of the proposed optimization procedure is examined through two examples, namely the selection of a rolled beam to be used as the main girder of a single girder crane and the selection of the structural members for a hangar.

8.2.3. Application: Optimum selection of rolled beams for single girder cranes

In a typical single-girder overhead traveling crane with one hoist block, the lifted weight causes the loading of the girder at the areas of contact between the lower flange of the girder and the wheels of the trolley, which the hoist is attached to. A typical approach to the stress analysis of the girder is to consider it as a simply supported beam and to use analytical expressions from basic mechanics. However, in this way two important assumptions are made, the first being that the value of the normal stresses due to bending along the transverse direction of the flanges is constant, thus no shear lag effects are considered, and the second being that the load is applied at the web and not at the flanges as is the real case. Therefore, another approach is required for the influence of the aforementioned assumptions to be taken into consideration within an optimization procedure. Towards this direction, in this section the modeling of the girder with plate elements is proposed. In more details, for a typical case of lifted load and hook path and taking the dead weight of the girder into account as well, six different girder lengths were examined. For each modeled girder, six different standard beam profiles from four categories (HEA-IPBL, HEB-IPB, INP, IPE) were used. For each case, the corresponding minimum weight problem was solved using the procedure desdcribed in Section 8.2.2. For each optimum design, the maximum deflection, the maximum normal stress due to bending, the maximum shear stress and the maximum von Mises stress are recorded. In addition, these results are illustrated in four plots respectively, because having such nomographs at hand makes the selection of the standard profile of minimum weight with respect to the constraints imposed by the regulations, such as EC3, very easy. Therefore, the suggested approach is of significant value for practical engineering purposes.

8.2.3.1. In general

An overhead traveling crane is a machine for lifting and moving loads that moves on wheels along overhead crane runway beams, also called a bridge crane, and incorporates one or more hoists mounted on crabs or underslung trolleys (EC-3 PrENV 1993-6). Single girder cranes can be a very cost effective purchase for capacities up to 10tons and 60ft. girder lengths (spans), when the reduced wheel loads are combined with very low headroom standard hoists (Weaver, 1979). The main advantages of single girder traveling cranes are the low dead weight, the more available headroom by using a low headroom monorail hoist, which is the most economical solution in buildings with a span over 90ft, and the lower production cost, thus lower price, than a double girder model. Bridge cranes are available in top and under running designs. The under running design offers two additional advantages, the first being the maximum utilization of the building's width and height due to the very small trolley approach dimensions and the second being the possibility of using the existing ceiling girder for securing the crane track (Salmon and Johnson, 1997). Therefore, it is evident, that the overhead traveling crane is of high practical value. In its simplest version, the crane includes one trolley and a doubly symmetrical rolled beam as a girder. The choice of the girder beam profile may be stated as an optimization problem, where the objective function is

the cost of the beam and the constraints are the stress, displacement and buckling restrictions imposed by technical structural rules, such as DIN or Eurocode3. The description of the cost is a quite complicated issue, since the quantities involved, such as rates, purchase cost and transportation cost, are not constant. For this reason, the structural weight is used as the objective function instead. It is emphasized that minimum weight does not mean minimum cost (Vinnakota, 2005); it is only an indication of the goodness of a feasible design. The minimum weight girder that can undertake the applied loads without violating any structural rules may be sought either analytically or numerically.

The analytical approach suggests that the relationships from the mechanics of the deformable body for a simply supported beam be used. For the estimation of certain quantities, such as the deflection, this approach is simple and straightforward. However, for the estimation of the resistance against yielding or buckling, this approach becomes more complicated and cumbersome the reason being that the application of the actual loads causes local effects that can be neither ignored nor easily calculated (Ambrose, 1997). As an alternative, it is possible to implement the numerical approach which suggests that the Finite Element Method (FEM) be used. The girder is appropriately modeled and the results from the model analysis can be used explicitly for the validation of the design, a time saving and easy to apply procedure. However, since for each candidate girder design a separate model development and analysis is required, the aforementioned procedure obtains a cumulative time consuming character. Therefore, it would be of great convenience if there was a handy and simple way to foretell the behavior of a girder design without having to perform any calculations at all.

Towards this direction, the present work suggests the creation of appropriate nomographs based on the FEM parametric investigation of various girder profiles. In more details, for a typical hoist/trolley assembly and a typical lifted load, an extensive parametric investigation was performed with respect to the girder span (six different values), the profile category (four different categories) and the profile size (four different sizes). The quantities recorded were the maximum deflection, the maximum shear stress, the maximum normal stress due to bending and the maximum equivalent von Mises stress. For each quantity, a nomograph was created, so that the value of the corresponding quantity could be determined by simply selecting the span, as well as the profile category and size. In this way, it was possible to compare each one of the aforementioned quantities to the allowable values. Having such nomographs at hand, the practicing engineer can seek the optimum girder design at minimum time cost.

8.2.3.2. Theoretical backgroung

A typical single-girder overhead traveling crane is shown in Fig.8.1a.

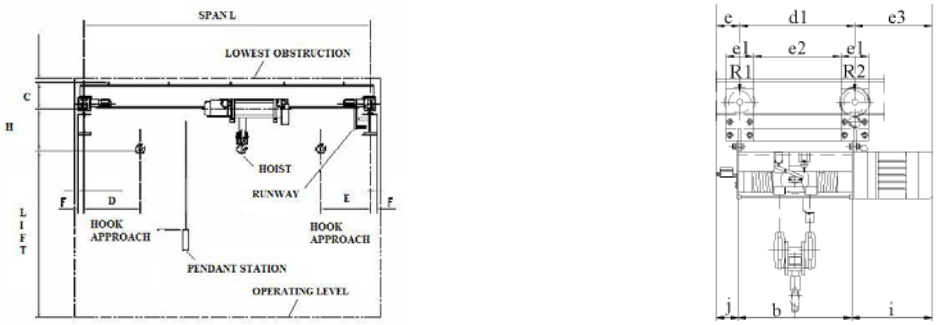

(a) (b)

Figure 8.1: Sketch of (a) a single-girder overhead traveling crane and (b) a hoist unit with its trolley

The main parts are the hoist, the trolley, the girder and the girder runway. For the selection of the girder beam profile, among other quantities such as the span and the lifted load, it is necessary to describe sufficiently the hoist and the trolley to be used. For the present paper, a commercially available hoist, with rope reeving 4/2, along with its trolley was selected (Fig.8.1b).

The hoists with rope reeving /2 have two characteristics, the former being that the lifted load is uniformly distributed among the trolley wheels and the latter being that there is no horizontal hook travel, thus the hook approach from the girder end is constant during the lifting procedure and so are the forces at the points of contact between the trolley wheels and the girder flange. In mathematical terms:

$$R_{11} = R_{12} = 0.5\left(0.5Q + aW\right) \tag{8.1}$$

$$R_{21} = R_{22} = 0.5\left(0.5Q + \left(1-a\right)W\right) \tag{8.2}$$

where

R_{11}, R_{12}: forces from the wheels of the axle #1 (Fig.8.1b)

R_{21}, R_{22}: forces from the two wheels of the axle #2 (Fig.8.1b)

Q: total lifted load

W: dead load

a: % of the dead load carried by the axle #1

From Eqs.(8.1, 8.2) it is obvious that the load distribution among the trolley wheels is constant as well. The characteristics of the hoist-trolley assembly selected for the needs of the present paper are shown in Table 8.1.

Table 8.1: Data for the selected hoist – trolley assembly

W	$575kg$		d_1	$498mm$
a	50%		e_3	$900mm$
Q	$3200kg$		e	$50mm$

With respect to the girder, it is possible either to select a standard rolled beam or to construct a welded one. In the current work, the former possibility was followed and the profiles examined were retrieved from catalogues available in the Hellenic market (Fig.8.2).

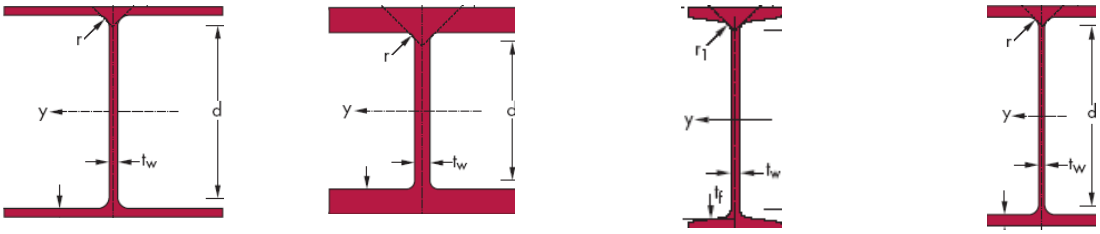

(a) (b) (c) (d)

Figure 8.2: The examined profiles (a) HEA-IPBL (wide flange bearing pile), (b) HEB-IPB (wide flange column), (c) INP and (d) IPE joist

For the single-girder overhead traveling crane examined, an underslung trolley was selected. As a consequence, each trolley wheel is in contact with the upper surface of the

bottom flange (Fig.8.3a) and exerts to it a concentrated load which is eccentric with respect to the center line of the web (Fig.8.3b). On top of that, each trolley cannot be mounted to any beam profile due to restrictions having to do with the geometry of the trolley and concern the flange thickness and width (Fig.8.3b).

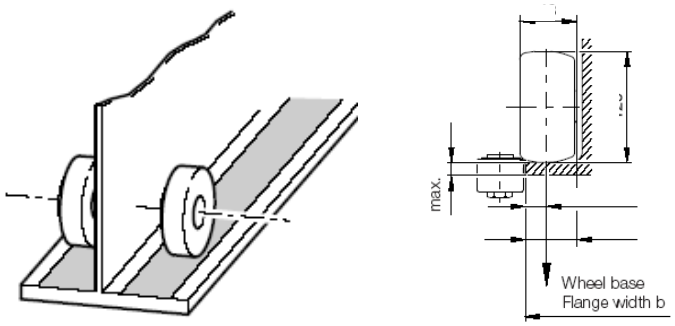

(a) (b)

Figure 8.3: The trolley wheels

A rolled beam profile may be considered as a feasible solution if and only if it can provide adequate resistance to the applied loading. The quantities that mainly define the aforementioned resistance are (a) the maximum deflection, (b) the maximum shear stress, (c) the maximum normal stress due to bending and (d) the maximum stress due to the combined action of these stresses (Stahl im Hochbau, 1967). In order to estimate (a)-(c), it is necessary to examine three different positions of the trolley (Fig.8.4):

Position #1: maximum deflection, where $x_1 = \frac{L}{2} - \frac{a}{2}$ (Fig.8.4a)

Position #2: maximum shear stress, where $x_2 = \min\left\{\frac{d_1}{2} + e_3, \frac{d_1}{2} + e\right\}$ (Fig 4.b)

Position #3: maximum bending moment, where $x_3 = \frac{L}{2} - \frac{a}{4}$ (Fig.8.4c)

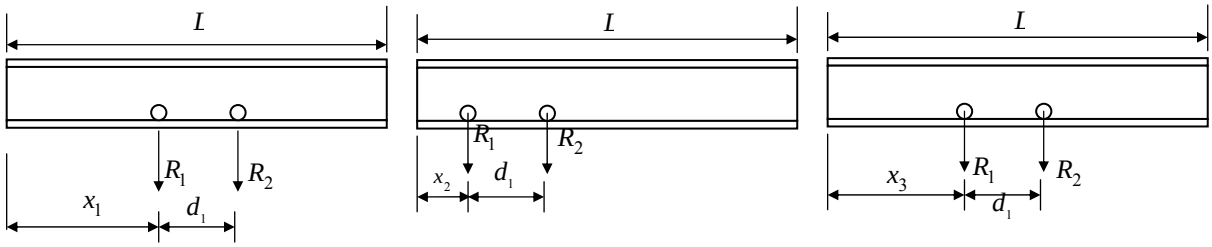

(a) **(b)** **(c)**

Figure 8.4: Trolley position for maximum (a) deflection, (b) shear and (c) bending

It is clarified that L is the girder span, while the dimensions d_1 (distance between trolley axles), e_3 and e are defined in Fig.8.1b and Table 8.1. It is also noted that the orientation of the hoist is related only to the end towards the maximum shear appears and not to the maximum value of the shear force. In more details, if the hoist is mounted to the trolley as in Fig.8.1b, then $e_3 < e$ which means that the hook can approach more the 'left' girder end than the 'right' girder end, thus the maximum shear appears towards the 'left' girder end. If the orientation of the hoist is reversed, then the maximum shear appears towards the 'right' girder

end. However, in both cases the maximum value is the same, because the minimum approach x_2 does not change.

8.2.3.3. Numerical approach

As mentioned in the Introduction, the numerical approach requires that the girder beam be modeled. For this task, the first and most simple choice is to use the beam element, where the loads are assumed to act along the center line of the web thus neither any effect from the application of local loads (Fig.8.3b) nor any shear lag effect (Cook, 1995), can be counted for (Fig.8.5a). A second choice for the aforementioned modeling is to use the brick element (Fig.8.5b). In this case, the numerical results are reliable under two important assumptions, the former being that the mesh has at least two elements along the thickness of both the web and the flanges and the latter being that the aspect ratio of the elements has an acceptable value. These two restrictions, in combination with the large girder span, result in a fine mesh consisting of a large number of elements, which in turn requires a time consuming analysis; this is not a good choice when a parametric investigation is to be performed. A third choice for the aforementioned modeling is to use the plate elements (Fig.8.5c). In this case, a very good compromise between the model accuracy and the time required for the repetitive model analysis is achieved. The present paper is based on an extensive parametric examination, thus a low computational cost is of importance.

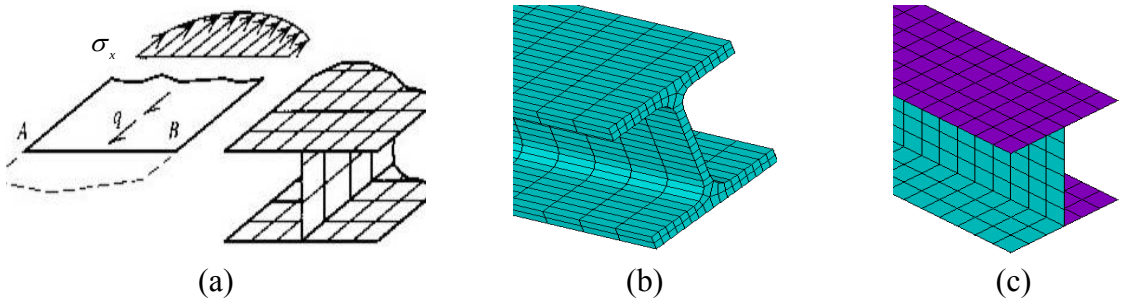

(a) (b) (c)

Figure 8.5: (a) Shear lag effect, (b) Brick model and (c) Plate model

8.2.3.4. Constraints

A structural design is accepted if and only if it satisfies a certain set of technical rules. Different Committees have stated different approaches for calculating the strength of a structure. As a result there is a plethora of regulations, such as DIN (Germany), BS (Great Britain), ASD - LRFD - AASHTO (USA), JIS (Japan), CAE (Canada) etc. During the past years, the Commission of the European Communities has worked on the establishment of harmonized technical design rules known as 'Structural Eurocodes' (EC-3 PrENV 1993-6). The common point in all technical rules is that the design value of member cross-section magnitudes (i.e. tensile force, compression force etc), as well as their combined action, must be at most equal to the corresponding resistance. The estimation of both the cross-section magnitudes and the corresponding resistances differs depending on the technical rules. Without loss of generality, it can be stated that the constraints are:

$$U_y \le \frac{L}{600} \qquad \sigma_{x,\max} \le \sigma_{x,allow} \qquad \tau_{\max} \le \tau_{allow} \qquad \sigma_{vonMises} \le \sigma_{vm,allow} \tag{8.3}$$

where U_y is the maximum deflection, while the subscripts 'x' and '$allow$' define the direction of the girder and the allowable values respectively. The allowable values can be

found either from tables, as is the case with the DIN rules, or analytically, as is the case with EC3, where the following elastic verification must be satisfied:

$$\left(\frac{\sigma_{x,Ed}}{f_y/\gamma_{M_o}}\right)^2+\left(\frac{\sigma_{z,Ed}}{f_y/\gamma_{M_o}}\right)^2-\left(\frac{\sigma_{x,Ed}}{f_y/\gamma_{M_o}}\right)\left(\frac{\sigma_{z,Ed}}{f_y/\gamma_{M_o}}\right)+3\left(\frac{\tau_{Ed}}{f_y/\gamma_{M_o}}\right)^2\le 1 \qquad (8.4)$$

where

$\sigma_{x,Ed}$: design value of the local longitudinal stress at the point of consideration

$\sigma_{z,Ed}$: design value of the local transverse stress at the point of consideration

τ_{Ed}: design value of the local shear stress at the point of consideration

f_y: yield stress for the selected material

γ_{M_o}: partial safety factor $\left(\gamma_{M_o}=1.1\right)$

In the general case, there are two more constraints that concern the buckling and the shear buckling of the profile due to the applied loads. However, the examined beam profiles belong to the Class 1 cross-sections, thus yield occurs before buckling, while they also provide adequate resistance against shear buckling (Falke, 1996).

8.2.3.5. Applied optimization procedure

The optimization procedure to apply is as follows:

Phase A: Acquire the required data

For each examined profile category (HEA-IPBL, HEB-IPB, INP, IPE)

For each examined girder span (from $5m$ to $30m$ with a step of $1m$)

Step 1: Model the girder with plate elements

Step 2: Solve the optimization problem using the procedure described in Section 8.2.2 and for the following load cases:

i) *Trolley at position #1 (see Figure 8.4a)*

ii) *Trolley at position #2 (see Figure 8.4b)*

iii) *Trolley at position #3 (see Figure 8.4c)*

Step 3: For the optimum design from Step 2, repeat Steps 2i, 2ii and 2iii and record maximum deflection, maximum shear stress, maximum bending stress and maximum von mises stress.

Phase B: Plot the data acquired from Phase #1

For each examined profile category

For all examined girder lengths

- Create Plot #1: maximum deflection vs girder span (Fig.8.6a)
- Create Plot #2: maximum shear stress vs girder span (Fig.8.6b)
- Create Plot #3: maximum bending stress vs girder span (Fig.8.6c)
- Create Plot #4: maximum von mises stress vs girder span (Fig.8.6d)

Especially for Plot#1, an additional line is drawn corresponding to the deflection constraint (Eq.8.3). Finally, it is emphasized that for every steel grade, another set of nomographs must be prepared. In addition, it is clarified that apart from the trolley wheel forces, the self-weight of the girder is also taken into account as a uniformly distributed load along the girder span.

8.2.3.6. Nomographs

The nomographs, created applying the procedure in Section 8.2.3.5, are shown in Fig.8.6.

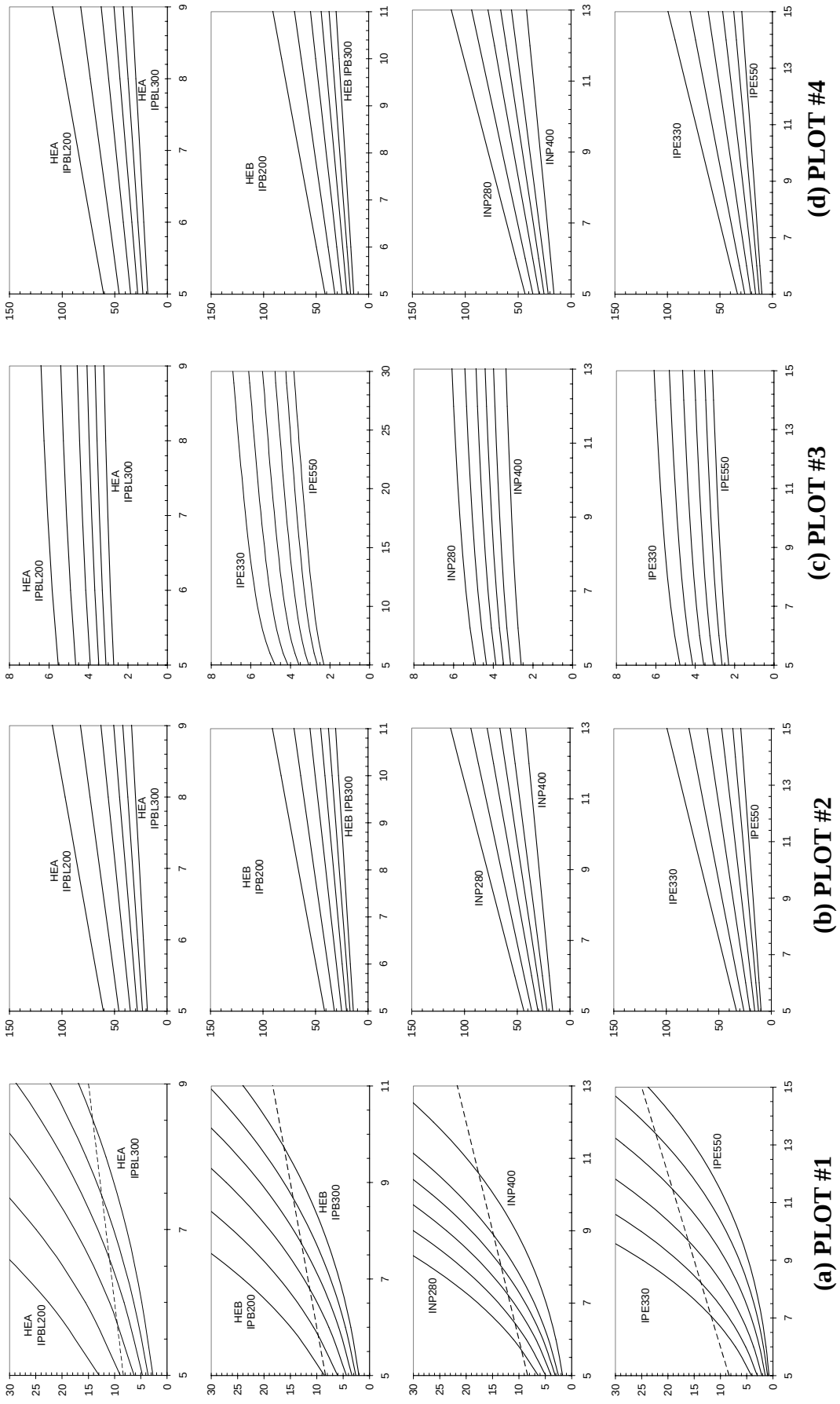

Figure 8.6: Nomographs

The profiles examined are shown in Table 8.2. The geometry of the profiles was retrieved from (Stahl im Hochbau, 1967).

Table 8.2: The examined profiles

Category	Size					
HEA-IPBL	200	220	240	260	280	300
HEB-IPB	200	220	240	260	280	300
INP	280	300	320	340	360	400
IPE	330	360	400	450	500	550

For each plot, the x-axis refers to the girder span while the y-axis axis refers to a response (maximum deflection, maximum shear stress, maximum bending stress or maximum equivalent von Mises stress for plots #1, #2, #3 and #4 respectively). Furthermore, each plot presents a family of six curves corresponding to the different sizes of a certain profile category (HEA-IPBL, HEB-IPB, INP, IPE). For reasons of illustration, a legend is added only to the first and the last curve of each family, while Table 8.2 can be used in order to correspond the other lines to profile sizes. In addition, each plot has a two-fold interpretation:

Interpretation (A): for a given profile category, find the response of a specific profile size

Step 1: From the x-axis and for the given girder span, draw a vertical line (VL)

Step 2: From the point of intersection between the (VL) and one of the aforementioned six curves, draw a horizontal line (HL) towards the y-axis

Step 3: Read the indication at the intersection point of the (HL) with the y-axis

Interpretation (B): for a given profile category, find the profile size whose response is conservatively closer to a given one

Step 1: From the x-axis and for the given girder span, draw a vertical line (VL)

Step 2: From the y-axis and for a given value of the quantity of interest, draw a horizontal line (HL)

Step 3: Trace the intersection point of the (VL) with the (HL)

Step 4: Select the closest curve that is below the intersection point; the profile size corresponding to this curve is the size sought

At this point it is clarified that, with respect to the nomographs (Fig.8.6), the scaling of the x-axis is based on the violation of the deflection constraint (Plot #1). In more details, the results obtained from the parametric investigation referred to spans up to $30m$. Obviously, it is of interest to present results for spans that violate no constraints. For the cases examined, it appeared that the deflection constraint was the predominant constraint. Therefore, it is meaningful to present results that correspond only to spans not violating the aforementioned constraint.

8.2.3.7. Use of nomographs

The nomographs of Section 8.2.2.6 are used as follows:

Step 1: Select a steel grade and a profile category and use the corresponding set of nomographs

Step 2: For a given span, use Plot#1 and Interpretation (B) (see Section 8.2.3.6) in order to find the profile size that gives a deflection closer to the maximum allowable one.

Step 3: For the profile size from Step#2, check for shear stress violation using plot #2 and Interpretation (A) (see Section 8.2.3.6). If a violation occurs, go to Step #2 and choose the next larger profile size; if not available, then stop (the current profile category is inadequate).

Step 4: For the profile size of Step#2, check for bending stress violation using plot #3 and Interpretation (A). If a violation occurs, go to Step #2 and choose the next larger profile size; if not available, then stop (the current profile category is inadequate).

Step 5: For the profile size of Step#2, check for violation due to combined action using plot #4 and Interpretation (A). If a violation occurs, go to Step #2 and choose the next larger profile size; if not available, then stop (the current profile category is inadequate).

Step 6: Since no violations occur, the profile at hand is the best choice for the examined profile category.

It is evident that the aforementioned procedure is very easy and quick to apply, while it requires only a very few repetitions for the optimum design to be located.

8.2.3.8. Discussion

It is possible to use commercial software, such as Statik2000 by DEMAG, Fastrak, F+L Statik etc., in order to select the optimum rolled beam girder for a single-girder traveling crane. If this approach is selected, then the practicing engineer must first purchase the software and then perform an entirely new study for each new project. Apart from a detailed study, which is definitely required, most of the times the practicing engineer needs to get very quickly a good approximation of the final design in order to take further decisions, mainly of logistic nature, concerning the specific project. For such cases, a common practice is to create charts which provide an easy and quick means for graphical estimation of the quantity of interest. Towards this direction, the present paper suggests an alternative handy and simple way to foretell the behavior of a girder design. In more details, given a typical hoist/trolley assembly, a typical lifted load and a specific steel grade (S235), a parametric FEM investigation was performed, the parameters being the girder span, the profile category and the profile size. The recorded results were appropriately plotted as nomographs ready to be used for the selection of the optimal girder beam profile. Such nomographs can be created for other combinations of hoist/trolley assemblies, lifted loads and steel grades. In this way, it is possible to perform an extensive parametric investigation only once and get an integrated series of plots that can be used any time and explicitly with no additional calculations required. Obviously, this is an approach of most importance for the practicing engineer who seeks the optimal girder design at minimum time cost.

In the present section, the FEM investigation was achieved using the ANSYS software. More particularly, the parametric investigation was coded using APDL, which is the built-in programming language of ANSYS. One of the difficulties met was to ensure that mesh nodes would exist at the points where the wheel loads are applied. There are various ways to deal with this requirement, one of which is first to create a uniform mesh and then to introduce hard points at the locations of the applied load. The models of the present work were based on this concept.

Furthermore, it is well known that all cranes are calculated for both static and dynamic loadings, while the nomographs presented in Section 8.2.2.6 were created for static loads only. Generally speaking, the technical rules, such as DIN15018 and EC1, consider the dynamic loading as static loadings appropriately amplified. Therefore, is possible to apply the procedure described in Section 5 using the appropriately amplified static loads. This was not done in the present work because the main goal was more to demonstrate the proposed approach rather than to result to bulletproof charts ready for professional use.

Another issue of high importance is the order of the applied Finite Element Analysis. If a first order approach is used, then buckling as well as other local effects must be examined separately. However, if a second order (non-linear) analysis is used, then there is no need for any further calculation. In the present work, a first order analysis was adequate, because the

selected rolled beams were of Class-1 and also provided adequate resistance against shear buckling.

Last but far from least, it is clarified that instead of the FEM approach, it would be possible to use analytical formulae provided by technical rules and textbooks of mechanics. However, in this case there are two important prerequisites, the first being the profound understanding and knowledge of the technical rules and the second being the careful planning of the calculations to be followed. If either prerequisite is not fulfilled, then the reliability of the corresponding nomographs is highly questionable.

8.2.3.9. Conclusions

The optimum selection of a rolled beam for a typical single-girder overhead traveling crane is a discrete optimization problem and as such, it requires the implementation of appropriate techniques. The proposed optimization procedure suggests a handy and simple way to achieve this goal. In more details, given a typical hoist/trolley assembly, a typical lifted load and a steel grade, it is possible to state the weight minimization optimization problem as a 1D optimization problem, where the design parameter is a standard profile within a predetermined sorted list. The structural analysis may be carried out using either classical mechanics or a numerical method, such as the Finite Element Method (FEM). In addition, solving this problem for various combinations of design parameters, such as the span of the girder, it is possible to create an integrated series of plots in a form of a handbook that can be used any time and explicitly in order to locate the optimum or a near-optimum design. Obviously, this is an approach of high applicability for practical engineering purposes, such as the quest of the optimal girder design at minimum time cost.

8.3. Discrete optimization of structures with many design variables

8.3.1. In general

The cases where the entire structure is a single beam are not that much. In a more general case, an engineering structure is an assembly of groups of structural members, each group containing different number of members but of the same cross-section. For such a structure, if the minimum weight is sought, then the procedure presented in Section 8.2.2 is not suitable because it can handle only one group of structural members. Therefore, a different approach is required. Towards this direction, the procedure in Section 8.2.2 is extended, so that an unlimited number of groups may be implemented. Obviously, the characterization ‘unlimited’ denotes that, from a theoretical viewpoint and for the procedure to be presented, there is no limitation with respect to the number of groups, even though, in practice, this number will always be limited to some tens due to the computational cost, which becomes prohibitively high. The aforementioned general optimization problem may be stated as trying to find the design vector $\mathbf{X}$ such that the scalar quantity $f(\mathbf{X})$ is minimized under the restriction that the imposed equality $h_j(\mathbf{X}) = 0$ and/or inequality constraints $g_j(\mathbf{X}) \le 0$ are not violated:

$$\min f(\mathbf{X}) \tag{8.5}$$

$$h_j(\mathbf{X}) = 0, \quad j = 1,2,...,m \tag{8.6}$$

$$g_j(\mathbf{X}) \le 0, \quad j = m+1, m+2,..., p \tag{8.7}$$

where

$$\mathbf{X} = \begin{bmatrix} x_1 & x_2 & ... & x_n \end{bmatrix}^T \tag{8.8}$$

In Eq.(8.8), x_i is the cross-section of a group of structural members, their domain being the set:

$$x_i \in \left[A_1 \quad A_2 \quad ... \quad A_n \right]^T \tag{8.9}$$

where the index i represent a group and $A_k, k = 1,...,n$ are commercially available profiles.

8.3.2. Proposed heuristic optimization procedure

Suppose that a structure has N profile groups and for each group there are M candidate profiles. A full-factorial approach would require N^M combinations, which may be a prohibitively high number of combinations. The proposed heuristic optimization procedure uses N groups and M candidate profiles but in such a way that it is not necessary to perform a full-factorial scheme. On the contrary, the design vector is progressively sliding towards what seems to be the global optimum design vector. The proposed procedure is as follows:

Step 1: The tables (lists) containing the standard profiles that consist the domain for each design variable are defined. The optimum weight is initially defined as a very large number. It is clarified that the profiles in the aforementioned tables must be sorted in ascending order.

Step 2: The user may either define the initial design vector or ask for a randomly created design vector.

Step 3: The step size (search width) regarding the tables in Step 1 is defined. The design vector in combination with the step size defines a sub-domain which will be exhaustively explored. In case this sub-domain is outside the design space, it is re-defined, so that it always lies inside the design space.

Step 4: For each design variable, a new value is retrieved from the corresponding table (see Step 1). In this way, a new design vector is formed.

Step 5: A structural analysis is carried out (it is possible to use either an in-house code or a commercial software as a solver).

Step 6: The analysis results from Step 5 are evaluated. If none of the imposed constraints is violated and the structural weight is less than the current optimum weight, then the current design vector is considered to be the new current optimum.

Step 7: If a new optimum design vector yields from Step 6, then this vector becomes the initial design vector for the next search cycle.

Step 8: If a new optimum design vector does not yield from Step 6, then the initial design vector for the next search cycle is the one of the previous search cycle shifted upwards according to a pre-defined step.

Step 9: The procedure is terminated when all the design variables reach their maximum cross-section, as defined in the tables of Step 1.

In the aforementioned iterative procedure, it is possible to embed four rules which significantly enhance the exploration performance. These rules are:

Rule #1: If a structural analysis, with cross-sections equal to their upper bound, fails, meaning that at least one of the imposed constraints is violated, then the available design space is infeasible, thus no optimization procedure initiates.

Rule #2: If a structural analysis, with cross-sections equal to their lower bound, does not fail, meaning that no imposed constraint is violated, then the corresponding design vector is considered to be the optimum one for the specific design space.

Rule #3: Any design vector having all of its design variables larger than the current optimum design vector results in a heavier structural weight thus no structural analysis using it takes place; anything different is just a waste of computational resources.

Rule #4: Assume that a design vector $\mathbf{X}$ is found to violate some constraints. This design vector is renamed as $\mathbf{X}_{viol}$ and any design vector having all of its design variables smaller than those of $\mathbf{X}_{viol}$ will also violate some constraints thus no structural analysis using it takes place. The $\mathbf{X}_{viol}$ design vector is updated each time another design vector is found, having all of its design variables larger than the current $\mathbf{X}_{viol}$.

The implementation of the aforementioned rules in an optimization code is a straightforward task.

8.3.3. Application: Optimal design of a steel hangar

Steel hangars are one of the most common types of aircraft maintenance facilities, assembled from structural members of different profiles. In the present section, a 4-pole steel hangar suitable for hosting two B747 aircrafts and carrying a $5t$ crane bridge is examined. More particularly, a typical hangar is designed taking into consideration the space occupied by two B737-700 and then it is optimized twice: once using a typical engineering-oriented trial-and-error design procedure (reference) and once using the in-house heuristic optimization procedure presented in Section 8.3.2. In both cases, the structural analysis was carried out in accordance to the Eurocode standards and using the commercial software SAP2000. The in-house optimizer was developed in MatLab and its main idea is to perform a search around a design vector by exhaustively searching the design space around each design variable and within a predefined width. The proposed iterative procedure is continued, until no further improvement on the structural weight can be achieved. The application of the aforementioned procedure to the aforementioned hangar, initiating from various random design vectors, resulted in a total weight reduction of 12.3%, with respect to the design used as a reference. This result is of most significance for steel structures, thus suggesting that the proposed procedure be a promising tool for practical engineering purposes.

8.3.3.1. In general

In modern days, air transportation is the safest and the less time consuming way of transportation; this is the reason why all airlines try to renew their fleets with more, new and modern airplanes. As a result, the demands for airplane maintenance facilities, such as hangars, continuously grow. Hangars are steel structures for which standards profiles are used, while they must comply with certain specifications regarding their safety and their serviceability. At the same time, it is desirable to keep their cost as low as possible. Consequently, the design of hangars consists a typical problem of structural optimization, where the total cost is the objective function, the commercially available standard profiles form the discrete design domain, while the national standards describe the constraints that must be imposed. In the most general case, the particular optimization problem is highly complicated, because, from a structural viewpoint, it refers to the shape, the topology and the dimensions of the structure, while, from a financial viewpoint, it refers to a situation where costs may severely change over the construction period. In a simpler form, the aforementioned problem may be formulated as a minimum weight design problem of a specific topology, which is determined using typical design rules for steel structures and for which commercially available standard profiles are used. The simplest way to deal with this

problem would be to apply a full combinatorial procedure. However, such a task is prohibitively time-consuming, thus other optimization methods must be used.

Schmit and Fleury, with respect to the aforementioned discrete optimization problem, suggested not to attack the discrete variable design optimization problem by employing discrete or integer variable algorithms to treat the problem directly in the primal variable space (Schmit and Fleury, 1980). Instead, they showed that approximation concepts and dual methods for continuous sizing type design variables can be extended to structural synthesis problems, involving a mix of discrete and continuous sizing type design variables. Hua suggested a simple procedure according to which the optimum design vector is sought near the limits of the feasible region (Hua, 1983). In more details, he suggested that in the case of discrete design variables, as in the case of continuous ones, at least one constraint be active at the optimum. He also considered that if a feasible design vector was detected, then any design vector with larger cross-sections would result in a heavier design, thus there was no reason to examine such design vectors. Furthermore, if a design vector violates a constraint, then any design vector with smaller cross-sections would also violate the same constraint, thus such design vectors should not be examined, either. With respect to the redesign procedure, Hua suggested to use a variation of the well-known stress-ratio technique (Fully Stressed Design) in the case of a stress constraint violation. For displacement violations, he suggested that an analogous technique should be used. As test cases, he solved two 2D trusses and on 3D truss. Grierson and Lee formulated a computer-based method for optimally sizing members of planar steel frameworks using commercially available standard sections (Grierson and Lee, 1984). For first-order behavior and static loads, they find a minimum-weight structure, while simultaneously ensuring stress and displacement performance conditions under applied service loads. They impose architectural conditions on section sizes to satisfy fabrication requirements related to member continuity and structure symmetry. They claimed that their, iterative in nature, design method was remarkably efficient, because the number of iterations was generally quite small and almost totally independent of the structural complexity. They optimized two steel frameworks that are typical of those encountered in professional practice. Bremicker et al developed a method that combined continuous and discrete variables in order to deal with the corresponding optimization problems (Bremicker et al, 1990). They stated that in practical structural optimization problems, it is often desirable to obtain solutions where all or some of the design variables take their values from a given set of discrete values. In more details, as structural optimization problems typically include large models that are expensive to compute, one of the major demands for optimization algorithms is that the number of structural evaluations (i.e. calculations of deformations and stresses) that are needed during the iterative optimization process is as small as possible. In their work, Bremicker et al developed an algorithm with respect to this requirement, while finding global solutions for the mixed-discrete problem. Their method was based on a combination of the well established branch and bound method with a sequential linearization procedure; branch and bound was applied within a sub-problem that was based on a linearization of the original problem. Wu and Chow presented the applications of steady-state genetic algorithms to discrete optimization of trusses (Wu and Chow, 1995). Their mathematical formulation was that of a constrained nonlinear optimization problem with discrete design variables. Discrete design variables were treated by a two-stage mapping process, which was constructed by the mapping relationships between unsigned decimal integers and discrete values. With small generation gap and careful modification, Wu and Chow suggested that steady-state genetic algorithms can significantly reduce the computational effort and promote the computational efficiency. The effectiveness, robustness and fast convergence of their approach was demonstrated through several examples, while the performance of four crossover operators was also examined. Erbatur et al also developed a computer-based systematic approach for

discrete optimal design of planar and space structures composed of one-dimensional elements (Erbatur et al, 2000). The main characteristic of their solution methodology was the use of a genetic algorithm (GA) as the optimizer, while applications and experience on steel frame and truss structures was also discussed. In order to show the efficiency of their approach, Erbatur et al also reported results from comparing their GA approach with other various discrete and continuous optimization algorithms for a class of representative structural design problems. They concluded that a GA often finds the region of the design domain containing the global optimum, but not the true optimum itself and in order to overcome this shortcoming they proposed a multilevel optimization approach. Guerlement et al presented a practical method for the discrete minimum weight design of steel structures based on a concept of removing redundant material by successively diminishing the size of the least stressed member (Guerlement et al, 2001). Assuming that the member sizes were available from the European Steel Profiles Catalogues, and the design constraints were given by the rules of the code EC3 for nonsway buildings, Guerlement et al examined two numerical examples, the former being the classical benchmark problem of a ten-bar truss made of circular hollow sections (24 element catalogue, buckling taken into account) and the latter being a portal frame made of HEB sections with broad parallel flanges (11 element catalogue). They concluded that, according to their method, a very good approach to the exact optimum solution was achieved after a reasonable computational time.

From the aforementioned papers, as well as from other published works (Tsompanakis and Papadrakakis, 2004; Hernández et al, 2005; Lagaros and Papadrakakis, 2007), it yields that there is still ground for other approaches with respect to the solution of discrete structural optimization problems. Within this frame, the present investigation concerns the application of a new heuristic optimization method to the weight minimization of a hangar capable of hosting two Boeing 737-700 aircrafts. According to the official website of the vendor, the specific airplane is $33.6m$ long, the wing span is $35.8m$ and the maximum height is $12.5m$. Based on this information, the hangar was decided to be $80m$ long, $44m$ wide and $16m$ tall (inside height), while the highest object to enter the hangar would be $9.55m$. The total floor plan was $80 \times 44 = 3520m^2$, while a $5t$ underslung crane bridge was also mounted to the hangar. Using the proposed procedure, the derived optimum design was approximately 12.3% lighter than that obtained using a commercially available software for steel structures.

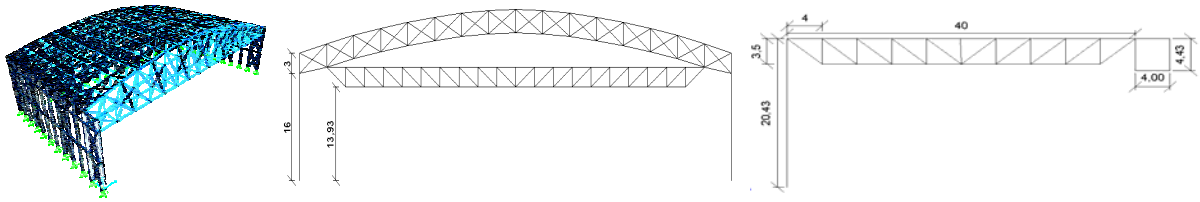

(a) (b) (c)

Figure 8.7: The optimized hangar (a) 3D iso-view of the entire structure, (b) typical section of the hangar and (c) view of the crane bridge.

8.3.3.2. Theoretical background

For the steel structure under examination, all the loads (self-weight, wind and snow) defined in EuroCode 1 were applied. On top of that, the effect of an earthquake was also taken into consideration by introducing a spectrum for the excitation force at the foundation of the hangar. With respect to the ultimate limit state as well as to the serviceability limit state, all of the corresponding constraints found in Eurocode 3 were applied.

8.3.3.3. MatLab/SAP2000 interface

The proposed heuristic optimization procedure was developed in MatLab, while the commercial software SAP2000 was used for the structural analysis. In order to achieve the collaboration between them, a specific procedure must be followed:

Step 1: The steel structure to be optimized is modeled in SAP2000. The structural topology, as well as the boundary conditions (supports and any number of load cases), are adequately defined.

Step 2: Useful results from the structural analysis are defined to be exported in a txt file. More particularly, using the option *Define →Named Sets→Tables*, the following tables were selected to be automatically stored after a structural analysis:

a. Material List 1 - By Obj Type: from this table, the structural weight is retrieved).
b. Steel Sum - EUROCODE 3-1993: from this table, the results regarding the limit state constraints imposed according to the Eurocode 3 are retrieved)
c. Program Control: from this table, the standards, according to which the structure is checked, are referred (EC3 is only one option, not the only one the software provides)
d. Material List 2 - By Sect Prop: from this table, it is possible to find out the cross-sections that were used for the analysis.

Using the option *Analyze→Set Analysis Option*, it is possible to define the name of the file where the results will be written into as well as the file type (Access or Excel).

Step 3: Once the model is ready, from the option *File → Export → Sap2000.s2k Text file* and choosing to export the so-called MODEL DEFINITION (that is, all the data that SAP2000 needs as input for developing the model), a file name *.s2k is created as defined (name and path).

Step 4: It is possible to open the file from Step 3 and manipulate it as a simple text file. This file is opened and divided in three parts, let them be Part1.txt, Part2.txt and Part3.txt (this step takes place only once for each examined structure).

a. Part1 contains the first segment of the *.s2k file, up to the title TABLE: "FRAME SECTION ASSIGNMENTS"
b. Part2 is the file segment that defines the cross-section attributed to each member. It contains the TABLE: "FRAME SECTION ASSIGNMENTS", without the title which is the last line of Part1. Part2 is a temporary file to be manipulated later.
c. Part3 contains the rest of the *.s2k file; that is, from TABLE: "FRAME OUTPUT STATION ASSIGNMENTS" to the end of the file.

In the sequel, the Part2 file segment is processed such that each the desired cross-section is attributed to each structural member. Exactly due to the way the Part2 file is created, it is possible to change the attributed cross-sections any time during the optimization procedure.

8.3.3.4. Data for the hangar

The steel structure that was optimized using the proposed heuristic procedure is the hangar described in Section 8.3.3.1. In total, the structural members were categorized in 19 groups. However, there were some members highly impossible not to fail for smaller cross-sections than the ones initially attributed to them (e.g. the poles of the hangar), thus the number of groups was reduced to 16. For each one of these groups, the corresponding design space is described in Table 8.1.

Table 8.3: Design space for the hangar

Group1	**Group5**	**Group9**	**Group13**
HEA200	HEA360	TUBO-D193.7X4.5	HEM180
HEB200	HEA400	TUBO-D219.1X5	HEM200
	HEA450	TUBO-D244.5X5.4	HEM220
Group2	**Group6**	**Group10**	**Group14**
TUBO-D323.9X5.9	TUBO-D193.7X4.5	HEA120	TUBO-D139.7X4
TUBO-D323.9X5.9	TUBO-D219.1X5	HEB140	TUBO-D152.4X4
	TUBO-D244.5X5.4	HEA160	TUBO-D168.3X4
Group3	**Group7**	**Group11**	**Group15**
TUBO-D298.5X5.9	HEA180	HEA240	HEA140
TUBO-D323.9X5.9	HEA200	HEA260	HEA160
	HEB220	HEB280	HEA180
Group4	**Group8**	**Group12**	**Group16**
HEB800	HEA140	TUBO-D193.7X4.5	HEB200
HEB1000	HEA160	TUBO-D219.1X5	HEB220
	HEA180	TUBO-D244.5X5.4	HEB240

The hangar was optimized twice, first using the optimization capability of SAP2000 and then using the proposed heuristic procedure. The derived optimum design vectors, as well as the corresponding total structural weight, are presented in Table 8.4.

Table 8.4: Optimum designs for the hangar

Structural members	Optimum design vector using the commercial s/w	Optimum design vector using the proposed method
Group #1	HEB220	HEA200
Group #2	TUBO-D323,9X5,9	TUBO-D323,9X5,9
Group #3	TUBO-D355,6X6,3	TUBO-D298,5X5,9
Group #4	HEB800	HEB800
Group #5	HEB400	HEA400
Group #6	TUBO-D219,1X5	TUBO-D219,1X5
Group #7	HEB220	HEA180
Group #8	HEB200	HEA160
Group #9	TUBO-D244,5x5,4	TUBO-D193,7X4,5
Group #10	HEA160	HEB140
Group #11	HEB280	HEA240
Group #12	TUBO-D273x5,6	TUBO-D219,1X5
Group #13	HEM200	HEM180
Group #14	TUBO-D168,3x4	TUBO-D152,4X4
Group #15	HEA180	HEA140
Group #16	HEB240	HEB220
Total Structural Weight [t]	62.7	55

It is obvious that the proposed procedure resulted in a design 12.3% lighter than that obtained with the commercial software. Especially for the serviceability limit state, it holds:

- Along the x-axis, the maximum displacements are $(L = 19m)$:

$$u_{x,\min} = |-51.046mm| < L/300 = 63mm \text{ and } u_{x,\max} = 56.105 < L/300 = 63mm \quad (8.10)$$

- Along the y-axis, the maximum displacements are $(L = 80m)$:

$$u_{y,\min} = |-143.851mm| < L/300 = 267mm \text{ and } u_{y,\min} = 81.621 < L/300 = 267mm \quad (8.11)$$

- Along the z-axis, the maximum displacement is $(L = 44m)$:

$$u_{z,\max} = 211.325 < L/200 = 220mm \quad (8.12)$$

From the above checks, it yields that the optimum design vector derived with the proposed heuristic optimization procedure results in no violation with respect to the structural displacements. In comparison with the displacements that correspond to the optimum vector derived with the commercial software, it yields that only the vertical displacement is significantly different, as shown in Table 8.5.

Table 8.5: Comparison between optimum designs w.r.t. the structural displacements

		Displacement [mm]	
		Optimum design using the commercial s/w	Optimum design using the proposed method
Horizontal	along the x-axis	57	56,105
		-51	-51,046
	along the y-axis	143	143,851
		-81	-81,621
Vertical	along the z-axis	145	211,325

8.3.3.5. Data for the crane bridge

As mentioned before, there was a crane bridge mounted to the hangar. Due to the limited height inside the hangar, an underslung crane bridge was chosen with limited lifting capacity, since the heaviest part to be lifted is the, relatively light, aircraft engine. For the examined case, the span was $70m$ and the bridge was a triangular-shaped truss of $3m$ height. It carried two upper flanges $2m$ apart from each other and $3m$ apart from the lower flange. It was assumed that the crane bridge could slide on the lower flanges of the corresponding runway beams.

The vertical loads on the runway beams come from the lifted weight, the self-weight of the crane bridge and the self-weight of the trolley. For the needs of the present work, a $5t$ lifting capacity was considered, while the self-weight of the crane bridge was $15.2t$, approximately. From the analysis, it yielded that the reactions at the crane bridge supports and for the worst case scenario were $87kN$ and $53kN$.

The horizontal forces on the runway beam are due to the crane bridge acceleration/deceleration during its operation. According to the Eurocode standards, it is assumed that the vertical loads and the horizontal loads are applied simultaneously. For the needs of the present study, it was considered that the horizontal forces were 15% of the vertical loads; that is, the horizontal forces were $10kN$, approximately.

The design space for the crane bridge is presented in Table 8.6, where the profiles derived with the proposed optimization procedure are noted in boldface.

Table 8.6: Design space for the mounted crane bridge

Group 1	Group 2	Group 3	Group 4	Group 5
2L150X100X14/25/	2L150X100X14/25/	L90X8	L65X6	L65X6
2L150X100X14/30/	***2L150X100X14/30/***	L90X10	***L65X7***	***L65X7***
2L150X100X14/40/	2L150X100X14/40/	***L90X12***	L70X10	L70X10

It is noted that, for the crane bridge, the optimum design vector derived using the commercial software and the proposed procedure was the same. This means that a weight reduction of the crane bridge may be possible if the topology or the shape, and not the size, of the crane bridge is changed.

8.3.3.6. Computational cost breakdown

In order to evaluate the proposed optimization procedure, it is imperative that the computational cost is analyzed. Towards this direction, the CPU time breakdown shown in Fig.8.8 is discussed.

R1: open files
R2: read data from SAP file
R3: new design vector (NDV)
R4: store (NDV)
R5: open auxiliary files
R6: create new SAP file
R7: call SAP
R8: check constraints
R9: delete old SAP file, check for new optimal design vector

(a)

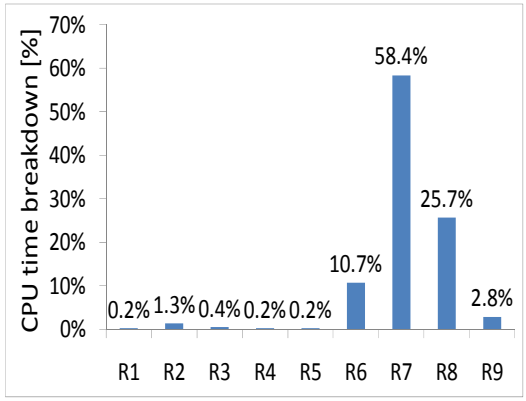

(b)

Figure 8.8: CPU time breakdown (a) operations and (b) percentage with respect to the total CPU time

The main operations performed during the execution of the proposed procedure are recorded in Fig.8.8a. From the chart in Fig.8.8b it yields that four operations, out of a total of nine, do consume a significant part of the CPU time. The most time-consuming task (58.4%) is to call the commercial software from the command line and perform a structural analysis. A significant part of this task is literally a waste because the commercial software must initiate and terminate each time a new design vector must be analyzed. The CPU time would be severely reduced if it were possible to keep the commercial software running and just carry out the analysis whenever it is needed. However, this is not possible, when a command line call is used.

Two other tasks that are time-consuming are related to the creation, manipulation and deletion of the txt files that serve for the communication between the in-house code developed in MatLab and the commercial software. The use of txt files is not the best choice, when it is possible to use database files. However, this selection was based on the concept of 'making things happen', while the use of db files may be a future enhancement.

Finally, it is noted that, for the examined hangar and for the selected design space, the total number of combinations was 8.503.056, while the proposed heuristic optimization procedure located the optimum design vector approximately after examining 0.01% of these combinations.

8.3.3.7. Discussion

The present paper dealt with the weight minimization of a hangar. For the structural analysis the commercially available software SAP2000 was used. This software embeds an optimization capability according to which, based on the initial structural analysis, smaller profiles are suggested to the user. However, this approach is of limited practical value in large-scale structures, because one of the basic design parameters (the structural weight) is not taken into consideration. On the contrary, the proposed heuristic optimization procedure, which uses SAP2000 as an external solver only, did not suffer from such a shortcoming. Using the proposed procedure, the optimum structure was 12.3% lighter than that obtained using SAP2000 and its optimization capability. For such structures, the aforementioned weight decrease is of most importance. The basic conclusions drawn from the present investigation were the following:

- The application of the proposed optimization procedure, which is of a partial-factorial character, provided very satisfying results and with an acceptable computational cost.
- For the weight minimization of a structure, it is required to handle certain structural members with a specific manner. More particularly, in steel structures, where the number of structural members with standard profiles is large, structural member grouping may benefit commonality but may severely affect the total weight. This may occur, when a few members of the group are loaded significantly more than the other members of the same group, thus their adequate dimensioning results in significant over-dimensioning of the other members of the same group. In the present paper, this problem was handled by tracing such members and imposing an individual redesign of their cross-section.
- It is possible to reduce the computational cost of a combinatorial procedure, when logical rules are used. More particularly, if a feasible design vector is detected, then any design vector with larger cross-sections results in a heavier design. Furthermore, if a design vector violates a constraint, then any design vector with smaller cross-sections also violates the same constraint. These two rules significantly reduce the total number of design vectors that a combinatorial procedure may examine.
- Using a commercial software as solver, even if the call takes place from the command line, is time consuming, because every time the objective function must be evaluated the commercial software initiates, analyses and terminates; this cycle is unavoidable.

In addition, based on the obtained experience, the following are proposed:

- For large-scale structures containing sub-structures (in the present paper, the crane bridge was a sub-structure), it may be beneficial to solve a small-scaled topology and shape optimization problem for the substructure.
- Use data base structures instead of simple txt files. In this way, the time required for accessing and manipulating the data files will be reduced.
- Apply a soft-kill penalization scheme instead of a hard-kill one (the latter was used in the present work).
- Apply a varying step size, while sweeping the design space for achieving a better exploration.
- Apply the proposed procedure as an operator in a stochastic optimization method such that the combinatorial exploration may take place about a stochastically located design vector.

8.3.3.8. Conclusions

A new heuristic discrete optimization procedure regarding real-life large-scale engineering structures was presented. The main idea of this procedure was to carry out a limited full-combinatorial exploration about a design vector. In this way, the feasible design vector progressively slides towards the optimum. As a case study, a hangar with an underslung crane bridge was examined. For reasons of comparison, a commercially available software for analysis of steel structures was used. It yielded that the proposed procedure resulted in a design approximately 12% lighter than that obtained with the optimization capability embedded in the aforementioned software, while the analyses required were approximately 0.01% of the total number of all combinations formed for the selected design space. Similar encouraging results were also derived from two other case studies (1-storey 2D frame and a 6-storey 2D frame), which were not presented here. In conclusion, the proposed procedure may be a promising tool for optimizing real-life large-scale engineering structures.

8.4. Mixed-type optimization of structures with many design variables

8.4.1. In general

Assume a structure which is an assembly of commercially available plates, e.g. the box girder of a gantry crane. The commercially available plates have specific dimensions. Even though cutting and welding allows for forming an area of any dimensions, the thicknesses of the plates are standard. If the minimum weight of a box girder is sought, then there are design variables of discrete nature (e.g. thickness of webs and flanges) and design variables of continuous nature (e.g. width of flanges and height of webs). The latter ones are related to the dimensions that the plates are cut into. Such a problem that implements design variables of different nature is termed as a 'mixed-type' problem. However, for a plated structure the dimensions of the plates are rounded with respect to a specific tolerance, both for manufacturing and cost reasons. From this perspective, the design variables of continuous nature may be considered as quasi-discrete variables, meaning that they take on discrete values, which, however, are numbered in hundreds. Consequently, the 'mixed-type' problem may be considered as a discete one. In turn, the heuristic procedure presented in Section 8.3.2 may be used, after the modifications presented in the next paragraphs.

8.4.2. Proposed optimization procedure

Suppose that a structure has N design variables, out of which N_D are of discrete nature and N_{qD} are of quasi-discrete nature. For the former set of variables, each variable may take on $M_i, i = 1,...,D$ discrete values and for the latter set of variables, each variable may take on $M_j, i = 1,...,qD$ discrete values, where $M_j \subset M_i$. A full-factorial approach requires a prohibitively high number of combinations that should be examined, thus this approach is rejected. Instead, a partial-factorial approach is proposed, where the user is allowed to intervene during the optimization process so that the optimization route may be altered depending on the intermediate results. In this way, the design vector is progressively sliding towards what seems to be the global optimum design vector. The proposed procedure is as follows:

Step 1: Form the lists that contain the domain values for each design variable. These lists are sorted in an ascending order.

Step 2: Define an initial design vector or ask for a random initial design vector.

Step 3: For each design variable, define the upper bound, the lower bound and the step size of the subregion to be explored. The exploration will be exhaustive and embeds logical rules (see Section 8.3.2) that exclude design vectors that definitely violate some constraint.

Step 4: Initiate an exploration cycle. If there are feasible design vectors, then keep the one corresponding to the lower weight. Otherwise, the user must change the bounds or/and the step size of the design space and Step 4 must be carried out again, until a successful cycle is carried out.

Step 5: Based on the design vector obtained after a successful execution of Step 4, an exhaustive exploration of the region, around the design variables and within a predefined width, is carried out.

Step 6: Repeat Step 5 until no further imporovent on the structural weight is recorded.

At this point, it is noted that after an exploration cycle, the user is allowed to change or freeze bounds and step sizes. In this way, it is possible to embed experience and personal judgment in the optimization procedure. Even though it cannot be proved that the final outcome is the global optimum design vector, the user has the ability to initiate the optimization procedure from different design vectors, thus obtaining a good feeling about how optimimum the final design is. As a matter of fact, this is a typical way of judging things: form a personal opinion after having obtained a vast number of numerical results using a versatile optimization procedure. Furthermore, the logical rules stated in Section 8.3.2 are applicable in the aforementioned algorithm as well. These rules accelerate the entire procedure, because they do not allow for the structural analysis, when it is detected that the current design vector will definitely violate some constraint.

8.4.3. Application: Optimal design of a double girder crane box cross-section

Double girder bridge cranes are the most favorable design solution for capacities over 10tons and/or spans of $60\,ft$, since they can be utilized at any capacity where extremely high hook lift or high speeds and heavy service are required. As steel structures, the bridge cranes must be optimized, so that they both meet the principals described in technical standards, such as the Structural Eurocodes, and be cost efficient. Towards this direction, a typical welded box cross section of a double girder crane, with respect to the principals imposed by the EC1 and EC3 standards, was extensively investigated in the present work. In more details, the sensitivities of the optimal girder beam weight per unit length with respect to the design variables were recorded, while a thorough parametric investigation with respect to the crane bridge span, the lifting weight and the wheel base of the trolley was also conducted. The recorded results were appropriately illustrated in plots that reveal the dependency of the optimal design on the girder cross-sectional properties and serve as nomographs for making the selection of the optimal profile a trivial task. Therefore, the present work is of significance both for research and for practicing engineering purposes.

8.4.3.1. In general

An overhead traveling crane, also called a bridge crane, is a machine that moves on wheels along overhead crane runway beams, used for lifting and moving loads and incorporates one or more hoists mounted on crabs or underslung trolleys (EC-3 PrENV 1993-6). Single girder cranes can be a very cost effective purchase for capacities up to $10t$ and $60\,ft$ girder lengths (spans), when the reduced wheel loads are combined with very low headroom standard hoists. However, for larger capacities a double box girder crane is recommended (Weaver, 1979). The main advantages of double girder traveling cranes are two, the former being the increased

stiffness, when compared to single girder cranes and the latter being that they are the most economical solution in cases with a span over $90t$. Bridge cranes are available in top and under running designs. The under running design offers two additional advantages, the first being the maximum utilization of the building's width and height due to the very small trolley approach dimensions and the second being the possibility of using the existing ceiling girder for securing the crane track (Salmon and Johnson, 1997). Evidently, the overhead traveling crane is of high practical value. In its simplest version, a double box girder crane includes one trolley and two box beams, which serve as girders and are symmetric with each other. The choice of the box beam profile may be stated as an optimization problem, where the objective function is the cost of the beam and the constraints are the stress, displacement and buckling restrictions imposed by technical structural rules, such as DIN or Eurocode3. Since the description of the cost involves many non-constant quantities, such as rates, purchase cost and transportation cost, the structural weight is used as the objective function instead. It is strongly emphasized that minimum weight does not mean minimum cost (Vinnakota, 2005). On the contrary, it is only an indication of how good a feasible design is. The girder of minimum weight that can carry the applied loads without violating any structural rules may be sought either numerically or analytically.

According to the numerical approach, first a model of the girder under investigation is developed and then this model is analyzed with the Finite Element Method (FEM). The results of the analysis can be used explicitly for the validation of the design, which is a time saving and easily applied procedure. The main advantage of this approach is that a most accurate description of the developed stress and the strain field is obtained, assuming that a mesh of good quality has been used. In this way, it is possible to get easily results concerning the more complicated and cumbersome estimation of the resistance against yielding or buckling due to local effects caused by the application of the actual loads (Ambrose, 1997). The main disadvantage of the same approach is that a Finite Element Analysis (FEA) must be included inside the optimization loop. This means that not only is it necessary to use a code for FEA but also the computational cost increases. On the other hand, the analytical approach suggests that the theory from the mechanics of the deformable body for a simply supported beam be used. The main advantage of this approach is that calculations are performed in a simple and straight forward manner. The main disadvantage of this approach is that it does not provide a detailed description of the developed stress and strain field, as a FEA does. However, for both practicing and research engineering purposes, the analytical approach is more than adequate. On top of that, analytical approaches have been significantly enhanced with elements of uncertainty concerning the applied loads and elements of reliability analysis involving statistical models for crane loads (Köppe, 1981; Pasternak et al, 1996). Furthermore, the results of the various analyses confirmed that the local stresses produced by the passage of concentrated wheel loads, as it occurs when a trolley is moving along a crane girder, were sufficient to cause fatigue cracks (Demo, 1976). From all the above, it becomes apparent that the estimation of the sensitivities of representative quantities, like the optimal structural weight and other normalized values of cross-sectional properties, with respect to independent design variables, such as the geometrical dimensions of a cross-section, is most useful in stating reliable and cost effective design trends concerning the box girder cranes. Towards this direction, the present investigation contributes with a thorough examination concerning the welded closed cross-section beams used in double girder overhead travelling cranes. For this purpose, first an in-house code was developed in MatLab© and in accordance with the Eurocodes (EC1 & EC3) (Stahl im Hochbau, 1967; Falke, 1996; prEN 1993-1-1; prEN 1991-3; prENV 1993-6) and then this code was appropriately linked to another in-house code implementing the optimization procedure described in Section 8.4.2. For a variety of controlling parameters (girder span, hoisting capacity and trolley wheel base), the

optimization problem of minimizing the structural weight was solved; the minimum weights found, as well as the design vectors corresponding to those weights, were recorded. Based on these results, appropriately defined normalized indices were introduced, illustrated and evaluated, thus providing insight for both research and practicing engineering purposes.

8.4.3.2. Theoretical background

It is a fact that the dead load of the girder in combination with the lifting capacity of the crane and the other live loads such as rain, snow, wind, earthquakes, lateral loads due to pressure of soil and water, as well as due to temperature effects, determine the design of the structural elements involved in a box girder. One of the most decisive parameters in the evaluation of a design is its behavior against fatigue. Generally speaking, designers consider first the ultimate limit states of strength and stability that are likely to occur and then check for the fatigue and serviceability limit states. For the ultimate limit states, it is possible to allow a limited yielding over portions of the cross section depending on the class of the cross-section so that the resistance of the cross-section is increased but not in expense of its weight. The fatigue limit state is considered at the specified load level, which represents the load that is most likely to be applied repeatedly. The fatigue resistance depends very much on particular details, e.g. the type of weld in a welded cross-section. However, the details can be modified, relocated or even avoided such that fatigue does not control. Serviceability criteria such as deflections are also satisfied at the specified load level.

(a) (b) (c) (d)

Figure 8.9: Typical cases of double girder cranes: (a) gantry, (b) overhead box, (c) underslung and (d) tri girder.

The loads involved in checking the adequacy of a design have many characteristics that lead to important considerations some of which are the following:

(i) An impact factor must be applied to vertical wheel loads, so that the dynamic effects, as the trolley moves, and other effects, such as snatching of the load from the floor and from braking of the hoist mechanism, are taken into consideration.

(ii) For double girder cranes, the improbability of some loads (nominal or accidental) acting simultaneously but for a short duration, is considered.

(iii) For multiple double girder cranes in one aisle or double girder cranes in several aisles, the load combinations examined are restricted to those that appear to have a reasonable probability to occur.

A double girder crane, as a structure, must not violate certain specifications concerning its ability to carry the nominal load with safety. Except for special designs, the crane girders are symmetric, as assumed in the present paper. The actions on the crane girder were estimated according to EC1, while all of the verifications were in accordance with EC-3. At this point, it is reminded that the Eurocodes (ECs) are standards which, when applied, provide designs with adequate resistance against the ultimate limit state, the serviceability limit state and fatigue. For this goal to be achieved, an extended group of inequalities is stated and adequacy against the aforementioned limit states is guaranteed if none of these inequalities is violated,

that is, if the design values of particular effects of actions are less than the design capacity for those effects of actions. For example, the design value of an internal force or moment must be less than the corresponding design resistance. The exact number of the verifications to be examined, as well as the selection of which of them are appropriate to be examined in each case, depends on the structure under investigation. In this section, it is assumed that the girder has a welded closed cross-section, thus the appropriate set of verifications must be formed.

8.4.3.3. Ultimate Limit State requirements

According to EC3, the adequacy of a design is examined in terms of both Ultimate and Serviceability Limit States, while fatigue must also be examined. Towards this direction, the box girder is designed, so that it can provide adequate resistance to the applied loads and results in such deformations that cannot cancel the utility of the crane. In the following paragraphs, the corresponding verifications are very briefly presented.

8.4.3.3.1. Axial force

The design value of an axial force N_{ed} at each cross section of the box girder shall satisfy the following inequality:

$$\frac{N_{Ed}}{A_{eff}\ f_y / \gamma_{M_o}} \le 1.0 \tag{8.13}$$

where A_{eff} is the effective cross section area, which is calculated under uniform compression, f_y is the yield strength of the material and γ_{M0} is a partial safety factor.

8.4.3.3.2. Bending moment

The design value of the bending moment M_{ed} at each cross section of the girder shall satisfy the inequality:

$$\frac{M_{Ed}}{W_{eff}\ f_y / \gamma_{M1}} \le 1.0 \tag{8.14}$$

where W_{eff} is the effective elastic section modulus corresponding to the maximum elastic stress and γ_{M1} is a partial safety factor.

8.4.3.3.3. Transverse force

The design value of a transverse force F_{Ed} at each cross section of the girder shall satisfy the inequality:

$$\frac{F_{Ed}}{f_y\, L_{eff}\, t_w / \gamma_{M_1}} \le 1.0 \tag{8.15}$$

where t_w is the web thickness, L_{eff} is the effective length for resistance against transverse forces, given by:

$$L_{eff} = \chi_f\, l_y \tag{8.16}$$

with l_y being the effective loaded length and χ_f being the reduction factor due to local buckling.

8.4.3.3.4. Shear

The design value of a shear force V_{Ed} at each cross section of the girder shall satisfy the following inequality:

$$\frac{V_{Ed}}{\chi_V \, d \, t_w f_y / \sqrt{3} \gamma_{M_1}} \leq 1.0 \tag{8.17}$$

where t_w is the web thickness, d is the web height and χ_V is a factor for shear resistance.

8.4.3.3.5. Biaxial bending and axial force

Normal stresses from compression and biaxial bending shall satisfy the following inequality:

$$\frac{N_{Ed}}{f_y \, A_{eff} / \gamma_{M_o}} + \frac{M_{y,Ed} + N_{Ed} \, e_{y,N}}{f_y \, W_{eff,y} / \gamma_{M_o}} + \frac{M_{z,Ed} + N_{Ed} \, e_{z,N}}{f_y \, W_{eff,z} / \gamma_{M_o}} \leq 1.0 \tag{8.18}$$

where $e_{y,N}$ and $e_{z,N}$ are the shifts in the position of the neutral axis with respect to the neutral $y-y$ and the $z-z$ axes of the gross section, respectively, due to the effective part of the cross-section, while γ_{M_b} is the introduced partial factor of safety.

8.4.3.3.6. Bending moment and shear force

Where the design shear force V_{Ed} exceeds 50% of $V_{pl,Rd}$, the design resistance of the cross section against the combined action of bending moment and shear force should be calculated using a reduced yield strength $(1-\rho) f_y$:

$$\frac{M_{Ed}}{W_{eff} \, (1-\rho) f_y / \gamma_{M_1}} \leq 1.0 \tag{8.19}$$

where $\rho = \left(2V_{Ed} / V_{pl,Rd} - 1\right)^2$ and $V_{pl,Rd}$ is the design plastic shear resistance, given by:

$$V_{pl,Rd} = \frac{A_V f_y}{\sqrt{3} \gamma_{M_o}} \tag{8.20}$$

In Eq.8.8, A_V is the shear area, the estimation of which depends on whether the load force is parallel either to the depth (Eq.8.9a) or to the width of the cross-section (Eq.8.9b):

$$A_V = \frac{Ah}{b+h} \qquad\qquad A_V = \frac{Ab}{b+h} \tag{8.21}$$

8.4.3.3.7. Bending moment and shear and axial force

Where the design shear force V_{Ed} exceeds 50% of $V_{pl,Rd}$, the design resistance of the cross section against combined action of bending moment and shear force should be calculated using a reduced yield strength $(1-\rho) f_y$:

$$n_1 + \left(1 - \frac{M_{f,Rd}}{M_{pl,Rd}}\right)(2n_3 - 1)^2 \leq 1.0 \tag{8.22}$$

where n_1 is the result of the verification against biaxial bending and axial force, n_3 is the result of the verification against shear, $M_{f,Rd}$ is the design plastic moment of a section consisting only of the effective flanges and $M_{pl,Rd}$ is the plastic resistance of the cross section.

8.4.3.3.8. Bending moment and transverse and axial force

Where the design shear force V_{Ed} exceeds 50% of $V_{pl,Rd}$, the design resistance of the cross section against the combined action of bending moment and shear force should be verified with the following inequality:

$$n_2 + 0.8 n_1 \leq 1.4 \tag{8.23}$$

using a reduced yield strength and the result of the verification against transverse (normalized index n_2)

8.4.3.3.9. Buckling resistance of members (uniform member in compression)

A compression member shall be verified against buckling using the following inequality:

$$\frac{N_{Ed}}{\chi A_{eff} f_y / \gamma_{M_1}} \leq 1.0 \tag{8.24}$$

where χ is the reduction factor from the corresponding buckling curve. At this stage, two points must be clarified, the former being that the verifications presented in the previous paragraphs concern the ultimate limit state of plated structural elements (prEN 1993-1-5) and the latter being that no longitudinal stiffeners are present, as the latest design trend suggests so that the total structural cost is minimized.

8.4.3.4. Serviceability Limit State requirements

8.4.3.4.1. Vertical deflection

The design value of a vertical deflection w_z shall satisfy the following inequality:

$$w_z \leq \min\left\{0.25, \frac{L}{600}\right\} \tag{8.25}$$

where L is the span of the double girder bridge crane

8.4.3.4.2. Horizontal deflection

The design value of a horizontal w_y shall satisfy the following inequality:

$$w_y \leq \min\left\{0.25, \frac{L}{600}\right\} \tag{8.26}$$

8.4.3.4.3. Oscillation of the bottom flange

The bottom flange of the cross section shall satisfy the following inequality:

$$\frac{L}{i} < 250 \tag{8.27}$$

where i is the radius of gyration with respect to the vertical axis. In this calculation, the moment of inertia about the vertical axis, as well as the area of the examined cross-section, is involved.

8.4.3.5. Fillet weld Limit State requirements

8.4.3.5.1. Resultant stress

The resultant design resistance of the fillet weld, σ_{Ed} shall satisfy the following inequality:

$$\sigma_{Ed} < \frac{f_u}{\sqrt{3}\beta_w \gamma_{M_w}} \tag{8.28}$$

where σ_{Ed} is given by

$$\sigma_{Ed} = [(\sigma_w + \sigma_{w,Ed})^2 + 3\left(\tau_1^2 + \tau_2^2\right)]^{1/2} \tag{8.29}$$

where σ_w is the normal stress due to the force applied to the wheel (perpendicular to the throat section of the weld), $\sigma_{w,Ed}$ is the normal stress due to bending of the top flange (perpendicular to the throat section of the weld), τ_1 is the shear stress due to bending (perpendicular to the axis of the weld), τ_2 is the shear stress due to the force applied to the the wheel (parallel to the axis of the weld), γ_{M_w} is the weld factor $\left(\gamma_{M_w} = 1.25\right)$ f_u is the nominal ultimate tensile strength of the material and β_w with $0.8 \leq \beta_w \leq 1.0$, is the appropriate correlation factor defined by the steel grade.

8.4.3.5.2. *Fatigue due to normal stress*

The fatigue check due to normal stress shall satisfy the following inequality:

$$\gamma_{F_f} \Delta\sigma_{E_2} < \frac{\Delta\sigma_c}{\gamma_{M_f}} \tag{8.30}$$

where $\Delta\sigma_{E_2}$ is the range of the normal stress values given by $\Delta\sigma_{E_2} = \sigma_w + \sigma_{w,Ed}$, $\Delta\sigma_c$ is the resistance against fatigue defined by the detail category of the weld used for the double girder

bridge crane, γ_{Ff} is the partial factor for equivalent constant amplitude stress ranges and γ_{Mf} is the partial factor for fatigue strength.

8.4.3.5.3. *Fatigue due to shear stress*

The fatigue check due to shear stress shall satisfy the following inequality:

$$\gamma_{Ff}\,\Delta\tau_{E_2} \le \frac{\Delta\tau_c}{\gamma_{M_f}} \tag{8.31}$$

where $\Delta\tau_{E_2}$ is the range of the shear stress given by $\Delta\tau_{E_2} = \tau_1 + 2\tau_2$ and $\Delta\tau_c$ is the resistance against fatigue given by the detail category of the weld used for the double girder bridge crane.

8.4.3.5.4. Fatigue due to interaction between direct and shear stress

The verification against fatigue due to the interaction between direct and shear stress shall satisfy the following inequality:

$$\left[\frac{\gamma_{F_f}\Delta\sigma_{E_2}}{\Delta\sigma_c / \gamma_{M_f}}\right]^3 + \left[\frac{\gamma_{F_f}\Delta\tau_{E_2}}{\Delta\tau_c / \gamma_{M_f}}\right]^5 \le 1 \tag{8.32}$$

Where σ_w is the direct stress due to the force applied to the wheel (perpendicular to the throat section of the weld), $\sigma_{w,Ed}$ is the direct stress due to bending of the top flange (perpendicular to the throat section of the weld), τ_1 is the shear stress due to bending (parallel to the axis of the weld), τ_2 is the shear stress due to the force applied to the wheel (perpendicular to the axis of the weld).

8.4.3.6. Numerical approach

The problem of minimizing the weight of a crane girder belongs to the category of constrained optimization, the constraints being all the verifications stated earlier. Furthermore, the welded cross-sections are manufactured by cutting and welding together commercially available metal plates which have standard thicknesses. As far as the other dimensions (width and height) of these plates are concerned, the standard design procedure is to round off their values to the nearest higher integer, the dimensions being expressed in [mm]. Consequently, the actual optimization problem at hand is not a continuous but a discrete one and a combinatorial approach would be the best choice. However, using the continuous variable approach may lead to results that could cause major changes concerning the decision for the final design due to the fact that negligible violation of one or more constraints, which definitely do not endanger the structural integrity, may lead to a design with major savings in terms of scrap material. Within this frame, the investigation in the present paper was carried out using the MatLab routine *fmincon*, which is a very powerful build-in optimizer for solving non-linear constrained problems. More particularly, 75 different cases were analyzed and the minimum weight, along with the corresponding design vector, was recorded. The aforementioned cases were created from combining three design parameters as shown in Table 8.7.

Table 8.7: Parametric variables and their values

Index	Variable	Value	Units
1	***C***rane ***B***ridge ***S***pan	$CBS \in \{10,15,20,25,30\}$	[m]
2	***T***otal ***H***oisting ***M***ass	$THM \in \{10,15,20,25,30\}$	[tn]
3	***T***rolley ***W***heel ***B***ase	$TWB \in \{1000,1250,1500\}$	[mm]

It is obvious that increasing the number of the independent variables as well as the values attributed to each one of them results in a significant increase of the combinations to be examined. However, the 75 cases studied consist a good sample, according to the central limit theorem of statistics.

8.4.3.7. Evaluation Indices and Plots

In order to evaluate the results of the investigation, three groups of normalized indices were introduced and illustrated in plots. The first group consisted of the following indices (Fig.8.2a):

$$\left(t_1/t_2\right)_i \quad \left(t_2/t_3\right)_i \quad \left(t_2/b\right)_i \quad \left(b/h_w\right)_i \quad \left(t_4/h_w\right)_i \quad \left(t_3/h_w\right)_i \tag{8.33}$$

where b_1, t_1 are the width and thickness of the lower flange, b_2, t_2 are the width and thickness of the upper flange, h_w, t_3, t_4 are the height of the webs, the thickness of the left web and the thickness of the right web, respectively. The subscript $i \in [1,2,...,75]$ defines the index of the analysis that was carried out. The second group of indices consisted of the quantities:

$$\left(\frac{A_1}{A_4}\right)_i \quad \left(\frac{A_2}{A_4}\right)_i \quad \left(\frac{A_2}{A_3}\right)_i \quad \left(\frac{A_2}{A_{tot}}\right)_i \quad \left(\frac{A_3}{A_{tot}}\right)_i \quad \left(\frac{A_4}{A_{tot}}\right)_i \tag{8.34}$$

where A represents areas and the subscripts $1,2,3,4,tot$ stand for the lower flange, the upper flange, the left web, the right web and the gross section, respectively, all quantities referring to a box cross-section. The subscript i is used as in Eq.(8.21). The indices in Eq.(8.21) reveal the relationship between of the structural elements involved in the box cross-section in terms of dimensions while the indices in Eq.(8.22) reveal their relationship in terms of areas. The third group of evaluation normalized indices consisted of the ratios:

$$\begin{array}{ccc} \left(\dfrac{\left(I_{yy,uf}/I_{yy,w}\right)_i}{\left(I_{yy,uf}/I_{yy,w}\right)_{\max}}\right) & \left(\dfrac{\left(I_{yy,lf}/I_{yy,w}\right)_i}{\left(I_{yy,lf}/I_{yy,w}\right)_{\max}}\right) & \left(\dfrac{\left(I_{yy,uf}/I_{yy,lf}\right)_i}{\left(I_{yy,uf}/I_{yy,lf}\right)_{\max}}\right) \\ \left(\dfrac{\left(I_{yy,uf}/I_{yy,tot}\right)_i}{\left(I_{yy,uf}/I_{yy,tot}\right)_{\max}}\right) & \left(\dfrac{\left(I_{yy,lf}/I_{yy,tot}\right)_i}{\left(I_{yy,lf}/I_{yy,tot}\right)_{\max}}\right) & \left(\dfrac{\left(I_{yy,w}/I_{yy,tot}\right)_i}{\left(I_{yy,w}/I_{yy,tot}\right)_{\max}}\right) \end{array} \tag{8.35}$$

where I represents moment of inertia, the subscripts uf, lf, w represent the upper flange, the lower flange and the webs, while the subscript y stands the horizontal axis, respectively. In this case, a second normalization took place so that an even more representative impression could be obtained.

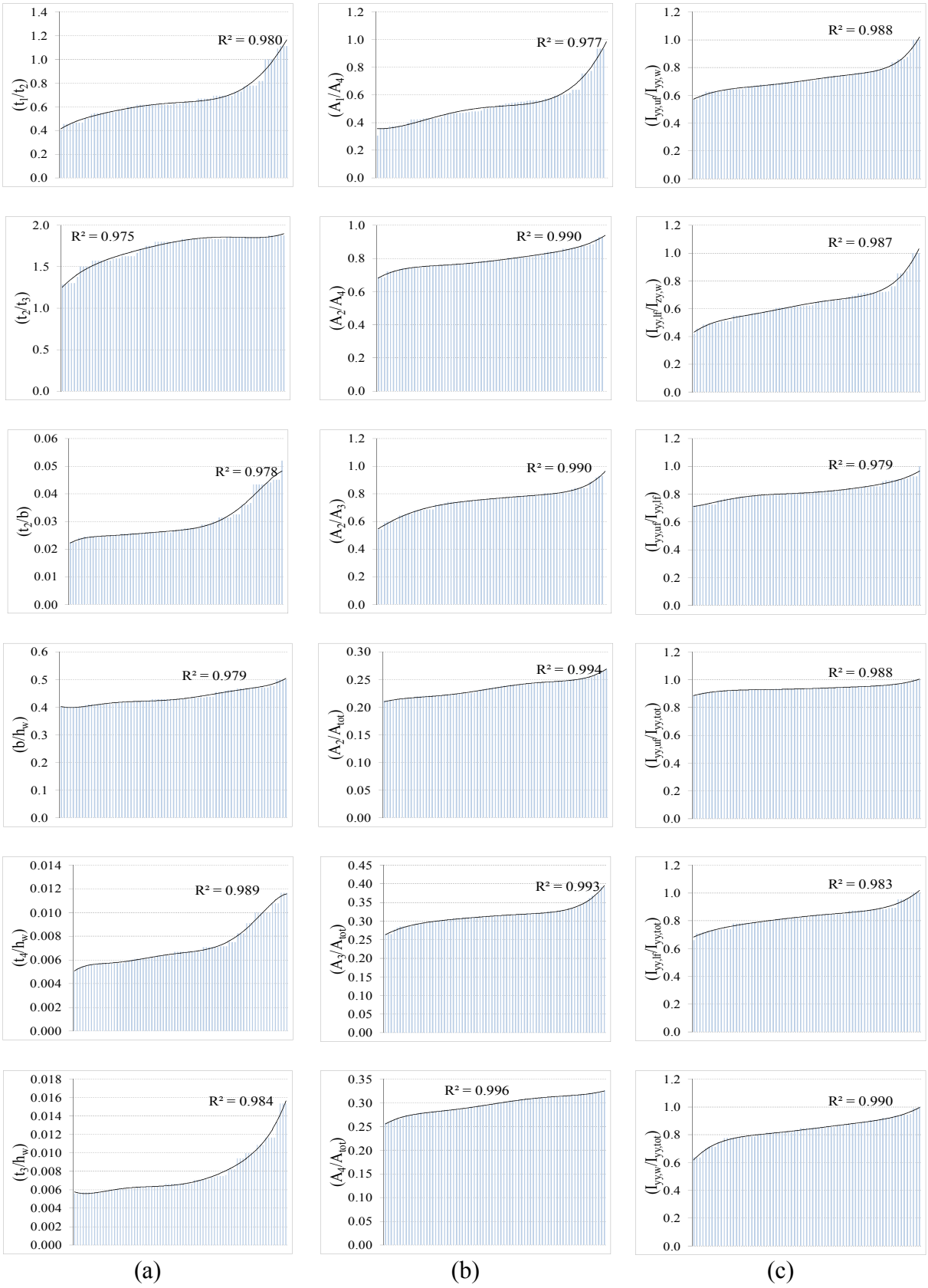

Figure 8.10: Illustrations of the evaluation indices for (a) the geometric dimensions, (b) the areas and (c) the moments of inertia of the examined cross-sections

8.4.3.8. Results

The designs mentioned in the previous section were analyzed with an in-house code developed especially for this research area and the results are illustrated in Fig.8.8. In more details, the ordinate represents the normalized index shown along the y-axis of each plot, while the values of this index corresponding to optimal designs are presented along the x-axis and in an increasing sorted order. On these plots, a polynomial regression was performed aiming at revealing any relationship (sensitivity) among the examined variables. As Fig.8.8 shows, all distributions were characterized by a very high correlation factor, clearly declaring that the introduced normalized quantities obey to low up to medium degree polynomial expressions. The main conclusions derived from the performed investigation were that among designs with increasing minimum weight:

- the aspect ratio $\left(t_3/h_w\right)$ increases in a highly nonlinear and concave manner (Fig.8.8a),
- the normalized index $\left(A_4/A_{tot}\right)$ presents a very slow increase in an almost constant rate, while the normalized index $\left(A_1/A_4\right)$ increases very fast (Fig.8.8b),
- the contribution of the webs to the moment of inertia about the horizontal axis is stronger than the contribution of the flanges (Fig.8.8c),
- the contribution of the upper flange to the moment of inertia about the horizontal axis is very high (Fig.8.8c).

8.4.3.9. Conclusions

The requirements for the design of crane girders are such that deterioration will not impair their durability and performance. For this purpose, the optimal design of a welded closed cross section, used in the design of a typical single-trolley overhead traveling double girder crane and with respect to the constraints described in EC1 and EC3 standards, was extensively investigated. The sensitivities of the optimal beam weight per unit length with respect to appropriately introduced normalized indices were recorded, while a thorough investigation with respect to the bridge span, the lifting weight and the trolley wheel base was also conducted. The recorded results were illustrated in plots, which reveal the dependency of the optimal design on the beam dimensions and its cross-sectional properties. The overall conclusion of the present paper was that the proposed optimization procedure (see Section 8.4.2) is of high value and may be used for the creation of handy nomographs.

8.4.4. Application: Optimal design of a runway beam

The design of crane runway beams must be such that deterioration will not impair their durability and performance. For this purpose, the design must meet certain standards, such as the Structural Eurocodes, which comprise a group of standards for engineering structures. At the same time, the design must be optimized, so that no material waste takes place. Towards this direction, the optimal design of a typical welded open cross section crane runway beam, for single-girder overhead traveling cranes and with respect to the principals imposed by the EC1 and EC3 standards, was extensively investigated in the present work. In more details, the sensitivities of the optimal beam weight per unit length with respect to the design variables were recorded, while a thorough parametric investigation with respect to the crane bridge span, the runaway beam span, the lifting weight and the wheel base of the end carriage was also conducted. The recorded results were appropriately illustrated in plots. Not only do these plots reveal the dependency of the optimal design on the beam cross-sectional properties but also serve as nomographs, thus making the selection of the optimal profile a trivial task. The present work is of significance both for research and for practicing engineering purposes.

8.4.4.1. In general

Overhead travelling cranes are used in industrial applications for moving loads without causing disruption to activities on the ground. They can be described as machines for lifting and moving loads, consisting of a crane bridge which travels on wheels along overhead crane runway beams, a crab which travels across the bridge and a hoist for lifting the loads (EC-3 PrENV 1993-6). Top running (overhead) double girder cranes have up to 150-ton in capacity and up to 150in on the span while utilizing a Box Girder in lieu of a standard I-Beam minimizes the wheel loads (Weaver, 1979). The overhead travelling cranes rest on a crane support structure, which must comply with specific design requirements, so that the applying loads are carried with safety during the operational life time of the structure (Salmon and Johnson, 1997). At the same time, it is most desirable to minimize the total cost of the support structure. Therefore, the selection of the beam profile may be stated as an optimization problem where the cost of the beam would be the objective function and the stress, displacement and buckling restrictions would be the constraints. The estimation of the cost of the crane runway beam is a very complicated problem, because it depends on various parameters such as beam manufacture, transportation and type of material. Therefore, the weight of the structure could be considered as an objective function, the minimization of it being the ultimate goal. It is important to know that a minimum weight structural design is not always the design of minimum cost (Vinnakota, 2005). For instance, a welded runway beam may be of less weight, when compared to a rolled beam; however, the former requires welding processes, which cost both in time and in money. Consequently, the minimum weight is only an indication of a feasible design. Furthermore, the estimation of the resistance against yielding or buckling becomes more complicated and cumbersome, the reason being that the application of the actual loads causes local effects that can be neither ignored nor easily calculated (Ambrose, 1997). On top of that, there is an uncertainty concerning the applied loads and studies have been reported in reliability analysis involving statistical models for crane loads, such as those by Köppe and Pasternak et al. (Köppe, 1981; Pasternak et al, 1996). In addition, various problems have been encountered in practice with crane support structures, mainly due to excessive deflections. In a typical case, an overhead crane moves loads by travelling along the crane runway beams, thus imposing on the support structure a cyclic loading that may lead to fatigue, which is the most common type of failure in practice. The results of the various analyses confirmed that the local stresses produced by the passage of concentrated wheel loads were sufficient to cause fatigue cracks (Demo, 1976). From all the above, it is evident that for both research and practicing engineering reasons, it is of interest to reveal the sensitivities of representative quantities, such as the minimum structural weight and normalized values of cross-sectional properties, with respect to independent design variables, such as the geometrical dimensions of a cross-section. Information of this kind is most useful in determining reliable and most cost effective trends concerning the design of crane runways. Towards this direction, the present paper contributes with a thorough investigation concerning the welded open cross-section runway beam of a single overhead travelling crane. More particularly, a full in-house code was developed in MatLab© and in accordance with the Eurocodes (EC1 & EC3) (prEN 1993-1-1; prEN 1991-3; EC-3 PrENV 1993-6); in the sequel, this code was appropriately linked to another in-house code implementing the optimization procedure presented in Section 8.4.2. For a variety of controlling parameters (runway beam spans, crane bridges loads, end-carriage base wheel and crane bridge spans), the optimization problem of minimizing the structural weight was solved and the minimum beam weights, as well as the design vectors corresponding to minimum weights, were recorded. Based on these results, appropriately defined normalized indices were introduced, illustrated and evaluated. Consequently, the present investigation is of significance not only from a research viewpoint but also for practicing engineering purposes.

8.4.4.2. Theoretical background

It is a fact that crane loads dominate the design of many structural elements in crane-supporting structures. These loads are considered to be separate loads from the other live loads due to use and occupancy and environmental effects such as rain, snow, wind, earthquakes, lateral loads due to pressure of soil and water, and temperature effects, because they are independent from them. Of all considerations, fatigue is the most important for structures supporting cranes. Designers generally design first for the ultimate limit states of strength and stability that are likely to control and then check for the fatigue and serviceability limit states. For the ultimate limit states, the factored resistance may allow yielding over portions of the cross section depending on the class of the cross-section. The fatigue limit state is considered at the specified load level-the load that is likely to be applied repeatedly. The fatigue resistance very much depends on particular details, e.g. the type of weld in a welded cross-section. However, the details can be modified, relocated or even avoided so that fatigue does not control. Serviceability criteria are also satisfied for the specified load.

(a) (b) (c) (d)

Figure 8.11: Typical cases of overhead travelling crane supporting structures: (a) gantries, (b) support, (c) knee and (d) typical crane runway cross-section

Crane loads have many unique characteristics that lead to the following considerations:

(i) An impact factor must be applied to vertical wheel loads, so that the dynamic effects, as the crane moves, and other effects, such as snatching of the load from the floor and from braking of the hoist mechanism, are taken into consideration.

(ii) For single cranes, the improbability of some loads acting simultaneously but for a short duration is considered.

(iii) For multiple cranes in one aisle or cranes in several aisles, the load combinations examined are restricted to those that appear to have a reasonable probability to occur.

(iv) For effects, such as acceleration and braking forces of the trolley and lifted load, skewing of the travelling crane, rail misalignment and not-vertical picking up of the load, to be taken into consideration, lateral forces acting on the crane rail are introduced.

(v) Acceleration and braking of the crane bridge, as well as not picking the load up vertically, result in longitudinal forces that must be accounted for.

(vi) Although general rules are applicable to all cranes, special consideration is appropriate and mandatory for various specialized classes of cranes such as magnet cranes, clamshell bucket cranes and cranes with rigid masts.

Apart from the above, there are various issues that the designer must decide upon, such as the selection of the rail, the type of mounting the rail to the crane runway beam and the design of the end stops. For the latter, it is clarified that, although cut-off PLC systems are available for decelerating a crane bridge, when it reaches a runway end stop, these end stops are designed for providing adequate resistance to accidental impact at full crane bridge speed.

Finally, it must be clarified that a crane runway beam may be considered either as a simply supported beam or as a continuous beam. In the present paper, an investigation based on the

former consideration is presented. Based on all the above, it is evident that a crane runway beam, as a steel structure, must comply with certain design specifications. In the present paper, the crane actions on the runway beam were estimated according to EC1 and verifications were applied according to EC-3. More particularly, various limit states are considered, when a structure is designed, such as the ultimate limit state, the serviceability limit state and fatigue. In general, a structure fulfills the design requirements described by the Eurocodes, when the design values of particular effects of actions are less than the design capacity for those effects of actions. Furthermore, the design value of an internal force or moment must be less than the corresponding design resistance. Therefore, each structural design must fulfill a set of verifications that describe various action effects and resistances. The number of the aforementioned verifications, as well as the determination of which of them will be examined, depends on the structure under investigation.

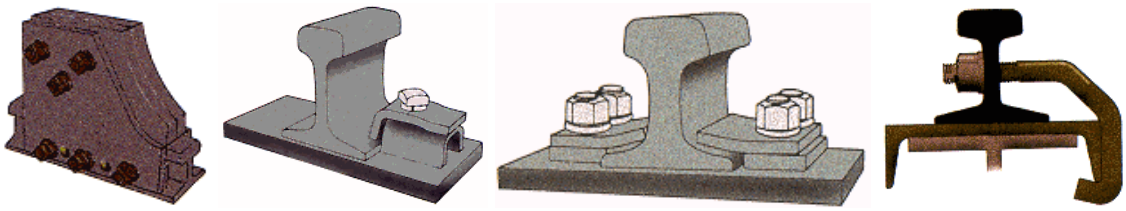

(a) (b) (c) (d)

Figure 8.12: Accessory components for a typical crane runway beam: (a) crane end stop, (b) single hole clamp and holder, (c) double clamp and (d) hook bolts.

In the present chapter, a welded crane runway beam was examined, thus a specific set of verifications was formed.

8.4.4.3. Design Specifications

For the Ultimate Limit State, the Serviceability Limit State and the fatigue, the design specifications are those described in Sections 8.4.2.3-8.4.2.5.

8.4.4.4. Numerical approach

The problem of finding the minimum weight of a welded crane runway beam belongs to the category of constrained optimization, the constraints being all the verifications stated earlier. On top of that, all the commercially available metal plates, which, when appropriately cut and welded together, form the runway beam, have standard integer values of thickness. As far as the other dimensions (width and height) of these plates are concerned, the standard design procedure is to round off their values to the nearest higher integer, the dimensions being expressed in [mm]. Consequently, the actual optimization problem at hand is of a discrete combinatorial nature. However, solving the same problem as a continuous variable problem results in a continuous solution, which, when compared to the optimal discrete one, provides the designer with information that may prove to be of crucial importance. Such cases occur, when a negligible violation of the active constraints results in having zero scrap material, which is the best possible scenario for a manufacturer. Within this frame, the investigation in the present investigation was carried out using the proposed optimization procedure (see Section 8.4.2). In total, 300 different cases were analyzed and the minimum weight, along with the corresponding design vector, was recorded. These cases were created from combining four design parameters as shown in Table 8.8.

Table 8.8: Parametric variables and their values

Index	Variable	Value	Units
1	***C***rane ***R***unway ***B***eam ***S***pan	$CRBS \in \{6,8,10,12\}$	[m]
2	***C***rane ***B***ridge ***S***pan	$CBS \in \{10,12,14,16,18\}$	[m]
3	***T***otal ***H***oisting ***M***ass	$THM \in \{3,5,6.3,10,12\}$	[tn]
4	***E***nd-carriage ***W***heel ***B***ase	$EWB \in \{1500,2000,2500\}$	[mm]

Increasing the number of the independent variables, as well as the values attributed to each one of them, results in a significant increase of the combinations to be examined. According to the central limit theorem of statistics, the 300 cases studied is a good sample.

8.4.4.5. Evaluation Indices and Plots

In order to evaluate the results of the investigation, three groups of normalized indices were introduced and illustrated in plots. The first group consisted of the following indices:

$$\left(\frac{(b_1/h_w)_i}{(b_1/h_w)_{\max}}\right)\left(\frac{(b_2/h_w)_i}{(b_2/h_w)_{\max}}\right)\left(\frac{(b_1/t_1)_i}{(b_1/t_1)_{\max}}\right)\left(\frac{(b_2/t_2)_i}{(b_2/t_2)_{\max}}\right)\left(\frac{(t_2/t_1)_i}{(t_2/t_1)_{\max}}\right)\left(\frac{(t_w/t_1)_i}{(t_w/t_1)_{\max}}\right) \quad (8.36)$$

where b_1, t_1 are the width and thickness of the lower flange, b_2, t_2 are the width and thickness of the upper flange and h_w, t_w are the height and thickness of the web, respectively. These numerators of the aforementioned indices express the relationship between the geometrical dimensions of the plated elements used for manufacturing the welded open cross-section of the examined runway beams. The subscript $i \in [1,2,...,300]$ defines the index of the analysis that was carried out. The denominators of the indices in Eq.(8.36) represent the maximum value recorded concerning the corresponding numerator among the 300 optimizations. This second normalization was introduced so that an even more representative impression could be obtained. The second group of indices consisted of the quantities:

$$\left(\frac{A_2}{A_w}\right) \quad \left(\frac{A_1}{A_w}\right) \quad \left(\frac{A_2}{A_{tot}}\right) \quad \left(\frac{A_1}{A_{tot}}\right) \quad \left(\frac{A_w}{A_{tot}}\right) \quad (C_w) \qquad (8.37)$$

where A represents areas, subscripts $1,2,w,tot$ stand for the lower flange, the upper flange, the web and the gross section, respectively, while C_w is the warping constant. In this case, a second normalization did not take place, so that an explicit comparison between the quantities involved in the normalized indices could be performed. The third group of evaluation normalized indices consisted of the ratios:

$$\left(\frac{I_{zz,1}}{I_{zz,w}}\right) \quad \left(\frac{I_{zz,2}}{I_{zz,w}}\right) \quad \left(\frac{I_{yy,2}}{I_{yy,w}}\right) \quad \left(\frac{I_{yy,1}}{I_{yy,w}}\right) \quad \left(\frac{I_{yy,1}}{I_{yy,2}}\right) \quad \left(\frac{I_{zz}}{I_{yy}}\right) \qquad (8.38)$$

where I is the moment of inertia, y, z denote the horizontal and the vertical centroidal axis, while the subscripts $1,2,w$ stand for the lower flange, the upper flange and the web.

8.4.4.6. Results

The results from the analysis of the aforementioned designs are illustrated in Fig.8.13.

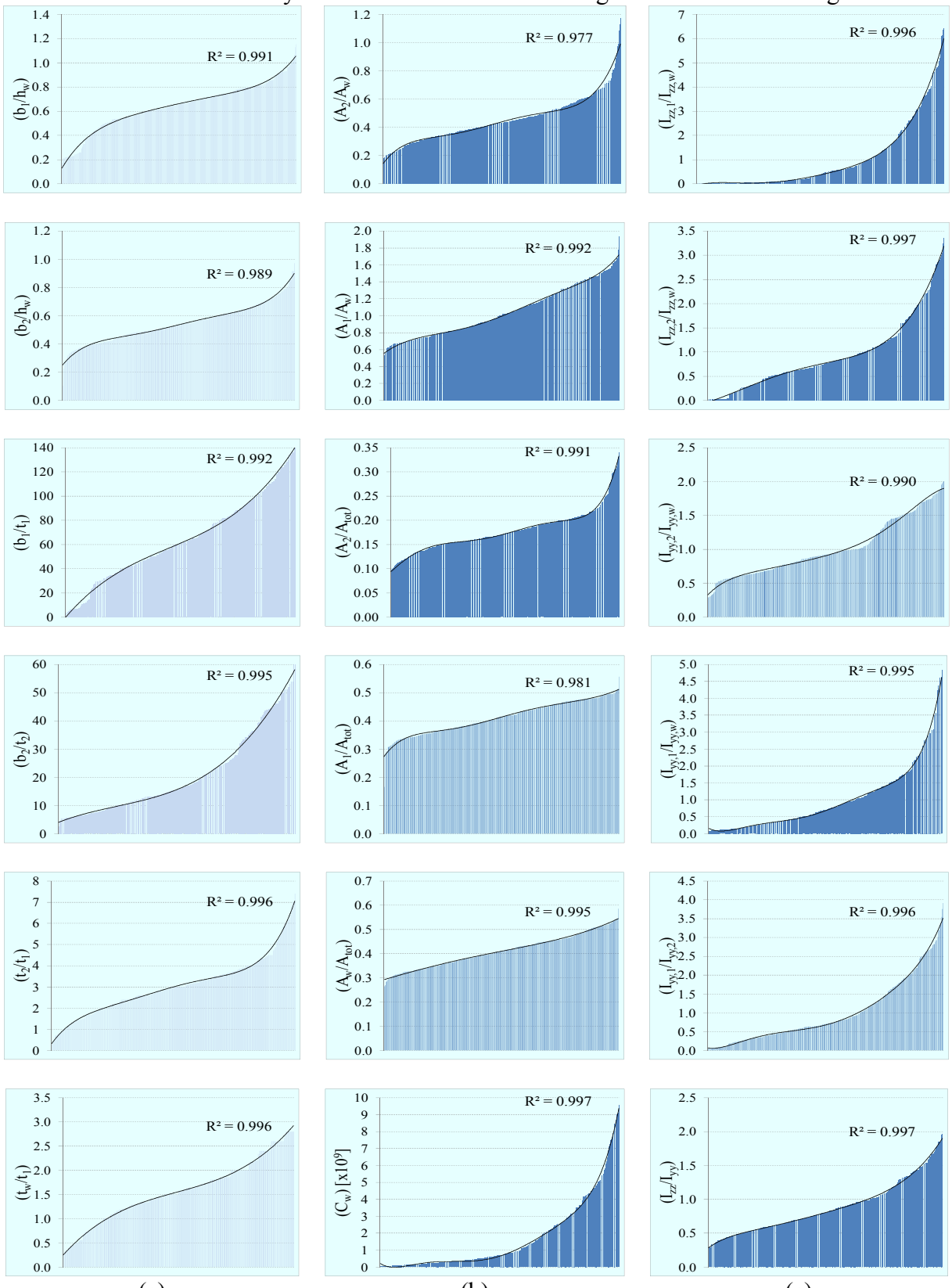

Figure 8.13: Illustrations of the evaluation indices for (a) the geometric dimensions, (b) the areas and the warping constant and (c) the moments of inertia of the examined cross-sections

In more details, the ordinate represents the normalized index shown along the y-axis of each plot, while the values of this index corresponding to optimal designs are presented along the x-axis and in an increasing sorted order. On these plots, a polynomial regression was performed aiming at revealing any relationship (sensitivity) among the examined variables. As Fig.8.13 shows, all distributions were characterized by a very high correlation factor, clearly declaring that the introduced normalized quantities obey to low up to medium degree polynomial expressions. The main conclusions derived from the performed investigation were that among designs with increasing minimum weight:

- the aspect ratio (b_1/t_1) increases in an approximately linear way, while the aspect ratio (b_2/t_2) is highly concave (non-linear) (Fig.8.13a),
- the area A_w increases in an almost constant rate, while the area A_2 increases in a non-linear way and always having the smallest portion of the gross cross-section (Fig.8.13b),
- the warping constant increases exponentially due to the need for resisting the warping effect caused by torsion in open cross-sections,
- the moment of inertia about the horizontal axis becomes significantly higher (much higher than 50%) than that about the vertical axis (Fig.8.13c). This is due to the fact that the vertical loading dominates over the transverse loading, which, from a point on, has a small contribution.

8.4.4.7. Conclusions

The requirements for the design of crane runway beams are such that deterioration will not impair their durability and performance. For this purpose, the optimal design of a welded open cross section of a typical crane runway beam, for single-girder overhead traveling cranes and with respect to the principals imposed by the EC1 and EC3 standards, was extensively investigated. The sensitivities of the optimal beam weight per unit length with respect to appropriately introduced normalized indices were recorded, while a thorough parametric investigation with respect to the crane bridge span, the runaway beam span, the lifting weight and the wheel base of the end carriage was also conducted. The recorded results were illustrated in plots. These plots reveal the dependency of the optimal design on the beam cross-sectional properties. Therefore, the present work is of significance both for research and practicing engineering purposes.

8.5. Recapitulation

In this chapter, the performance-based layout optimization of large structures was investigated. In total, three different cases were examined. The first case referred to structures which consist of one standard beam. The second case referred to structures which are assemblies of commercially available standard beams, while the third case referred to structures that are made of standard plates. For all three cases, the minimum weight problem may be stated in terms of a discrete optimization problem. For each case, a specific optimization procedure was proposed. More particularly, for the latter two cases, two new heuristic optimization procedures were introduced. These newly introduced procedures consist the main contribution of the current chapter. All of the proposed procedures were evaluated through the optimization of real-life structures, which consists another contribution of the present chapter. The encouranging results suggest that these procedures be an efficient tool that can be used for solving performance-based layout optimization problems.

References

Ambrose J (1997), Simplified design of steel structures, Wiley.

Bremicker, M., Papalambros, PY., Loh, H.T., (1990), "Solution of mixed-discrete structural optimization problems with a new sequential linearization algorithm", Computers & Structures, Vol. 37(4), pp.451-461.

Demo, D.A., (1976), "Analysis of Fatigue of Welded Crane Runway Girders", J. of Struct Div, Vol.102(5), pp. 919-933.

Draft prEN 1991-3, EUROCODE 1 - Actions on structures Part 3: Actions induced by cranes and machinery

EC-3 PrENV 1993-6 Crane Supporting Structures (N760e), CEN/TC250/SC3, 1998.

Erbatur, F., Hasançebi, O., Tütüncü, I., Kiliç, H., (2000), "Optimal design of planar and space structures with Genetic Algorithms", Computers & Structures, Vol. 75, pp. 209-224.

Falke J (1996), Ingenieurhochbau: Tragwerke aus Stahl nach Eurocode 3 (DIN V ENV 1993-1-1), DIN, Werner Verlag.

Grierson, D.E., Lee, W.H., (1984), "Optimal Synthesis of Steel Frameworks Using Standard Sections", Mechanics Based Design of Structures and Machines, Vol. 12(3), pp.335-370.

Guerlement, G., Targowski, R., Gutkowski, W., Zawidzka, J., Zawidzki, J., (2001), "Discrete minimum weight design of steel structures using EC3 code", Struct Multidisc Optim, Vol. 22, pp. 322–327.

Hernández, S, Fontán, A.N., Perezzán, J.C., Loscos, P., (2005), "Design optimization of steel portal frames", Advances in Engineering Software, Vol. 36, pp.626–633.

Hua, H. (1983), "Optimization for structures of discrete-size elements", Computers & Structures,Vol. 17(3), pp. 327-333.

Köppe, U. (1981), "Nutzlastkollektive von kranen", Hebezeuge und Fördermittel, vol. 21(2), pp.36–39.

Lagaros, N.D., Papadrakakis, M., (2007) "Robust seismic design optimization of steel structures", Struct Multidisc Optim, Vol. 33, pp.457–469.

Pasternak, H., Rozmarynowski, B., Wen, Y.-K. (1996), "Crane load modeling", Structural Safety, vol. 17, pp. 205–224.

prEN 1991-3, EUROCODE 1 - Actions on structures Part 3: Actions induced by cranes and machinery

prEN 1993-1-1, Eurocode 3: Design of steel structures - Part 1-1: General rules and rules for buildings

prEN 1993-1-5, 2004: Part 1-5: Plated structural elements, CEN.

prENV 1993-6, Crane Supporting Structures (N760e), CEN/TC250/SC3, 1998.

Salmon, CG, Johnson JE (1997), Steel structures: design and behavior (4th ed.), Prentice Hall.

Schmit, L., Fleury, C. (1980), "Discrete-continuous variable structural synthesis using dual methods", AIAA J, Vol. 18, pp. 1515–1524.

Stahl im Hochbau (1967), Verlag Stahleisen MBH.

Tsompanakis, Y., Papadrakakis, M., (2204), "Large-scale reliability-based structural optimization", Struct Multidisc Optim, Vol. 26, pp.429–440.

Vinnakota RS (2005), Steel structures: behavior and LRFD, McGraw-Hill.

Weaver, WM (1979), Crane handbook: Design data and engineering information used in the manufacture and application of overhead and gantry cranes (4th ed.), Whiting Corp.

Wu, S.J., Chow, P.T., (1995), "Steady-state genetic algorithms for discrete optimization of trusses", Computers & Structures, Vol. 56(6), pp.919-991.

Contributed papers

[1] Provatidis C.G., Tzanakakis E.D., and **Venetsanos D.T.**, "Optimum selection of doubly symmetric rolled beams for single-girder overhead travelling cranes using finite element plate models", 1st IC-EpsMsO, 6-9 July 2005, Athens, Greece.

[2] **Venetsanos D.T.**, Provatidis C.G., Magoula E-A.T., "Optimal design of a welded open cross-section crane runway beam in accordance with EC1 and EC3", 2nd International Conference on Experiments/Process/System Modelling/Simulation & Optimization Athens, 4-7 July, 2007.

[3] **Venetsanos D.T.**, Provatidis C.G., Skarmeas S.G., "Optimal Design Of A Box Cross Section Of A Double Girder Crane In Accordance With EC1 AND EC3", 2nd International Conference on Experiments/Process/System Modelling/Simulation & Optimization, Athens, 4-7 July, 2007.

[4] **Venetsanos D.**, Magoula E. and Provatidis C., "Performance-based optimization of the welded box of a single girder overhead travelling crane according to EC3 and EC1, 8th. World Congress on Computational Mechanics (WCCM8), 5th. European Congress on Computational Methods in Applied Sciences and Engineering (ECCOMAS 2008), June 30–July 4, 2008, Venice, Italy.

[5] **Venetsanos D.** and Provatidis C., "Performance-based optimization of a welded open cross section runway beam according to EC3 and EC1", 8th. World Congress on Computational Mechanics (WCCM8), 5th.

European Congress on Computational Methods in Applied Sciences and Engineering (ECCOMAS 2008), June 30–July 4, 2008, Venice, Italy.

[6] Kapogiannis A.K., **Venetsanos D.T.** and Provatidis C.G., Weight minimization of a steel hangar using a new heuristic optimization procedure and according to the Eurocode standards, 3rd International Conference "From Scientific Computing to Computational Engineering", Athens, 8-11 July, 2009.

CHAPTER 9

CONCLUSIONS AND FURTHER RESEARCH

Abstract

In this chapter, the recapitulation of the current Thesis is briefly presented, as well as the main innovative elements, which this Thesis contributes to.

Keywords
Layout optimization, Optimality Criteria, hybrid method, heuristic method.

9.1. Thesis recapitulation

In the current Thesis, a wide range of issues concerning the layout optimization of structures were examined.

With respect to the deterministic and the stochastic optimization methods, the investigation of the current Thesis yielded that:

- The direct search stochastic optimization methods perform better, as the number of the design variables decreases.
- The direct search deterministic optimization methods perform better than the direct search stochastic optimization methods, as the number of the design variables increases.
- The penalty scheme implemented in an optimization procedure seriously affects its performance.
- For 1D optimization problems, the Simulated Annealing (SA) optimization method seems to outperform the other optimization procedures.
- It is possible to combine a deterministic search scheme with a stochastic search scheme in order to create a hybrid optimization procedure. For instance, it is possible to use a deterministic procedure for estimating a search direction and a stochastic procedure for estimating the step size or vice versa. Such combinations are numerous and involve some innovation, since all they actually do is combining already known optimization procedures, or variations of them, in a different order. Nevertheless, they do contribute in the exploration of the potential that such optimization methods have.
- The increased computational cost of direct search methods suggest that other types of optimization procedures, such as the indirect methods, be investigated.

In addition, a novel hybrid optimization method was proposed, combining a deterministic search direction (Powell's method) with a stochastic step size search (SA). This hybrid optimization method outperformed the competition in terms of tracing the global optimum but its computational cost was very high. Due to this reason, in combination with the fact that the direct search methods, either deterministic or stochastic, do not take into consideration intrinsic characteristics of the problem at hand, it was decided to turn the investigation more towards the indirect search methods.

Doing so, the first thing to do is find a way to remove, either completely or partially, redundant material from a structure. The criterion for determining which part of the structure to remove depends on the imposed constraint. One of the most common types of such problems is related to the compliance of the structure. In the literature, the corresponding problem has been solved, when a volume constraint is also imposed. In the present Thesis, a more general case was theoretically investigated, where the volume constraint is not present. However, since no standard for structures refers to a compliance constraint, no further effort was put on exploring this issue. On the other hand, the stress-ratio technique is an optimization procedure that tends to Fully Stressed Designs which, for the majority of real-life structures, results in near-optimum solutions and, thus, is acceptable and interesting to explore.

Consequently, the stress constraint problem was investigated. More particularly, the capabilities of the Fully Stressed Design (FSD) in layout optimization were examined first of 2D skeletal structures and then on 2D continua. In both approaches, the redesign was based on changing either the cross-section of the skeletal structural members or the thickness of the continuum. In the sequel, the concept of using finite elements of variable thickness for the stress constrained layout optimization of 2D continua was explored. To this end, the element thickness was interpolated within each element in an isoparametric way. Next, the optimization of 2D plates was investigated, where the (FSD) was examined along with the application of the Evolutionary Structural Optimization (ESO) approach. Last, the

optimization of 3D continua was investigated, where material elimination was achieved through the element contribution to carrying the externally applied loads. Finally, a variation of the stress constraint problem, here termed as the extended single stress constraint problem, was analyzed. The result of this analysis was the formulation of a new optimality criterion, which is free of any assumptions concerning the determinacy of the optimized structure and seeks for a design where *one* structural member takes on the critical stress value, without necessarily preventing the other structural members from obtaining the imposed upper stress bound. In this way, the aforementioned OC is significantly different in concept from the (FSD) approach.

Furthermore, in the current Thesis, a new Optimality Criteria-type optimization procedure for single displacement constraint problems was proposed and tested in over 46 cases. The conclusions drawn from this investigation are the following:

- For the examples retrieved from the literature but having no analytical solution, the proposed procedure resulted in the referenced optimum weights after approximately equal number of iterations as the referenced ones.
- For the examples retrieved from the literature having analytical solutions, the proposed procedure resulted in the referenced optimum weights with an agreement of at least twelve significant digits after less iterations than the referenced ones.
- For the examples newly introduced in the present paper, the proposed procedure resulted in the same optimum weights (slightly different optimum design vectors) with those obtained when implementing the SQP routine found in Matlab (fmincon).
- In all cases, initiating the proposed procedure from a design vector corresponding to a Unit Stiffness Design structure resulted in the, considered to be, global optimum. However, in some cases, initiation from a random design vector resulted in significant sub-optimal solutions.
- The proposed categorization of the members as in Section 5.3 is more detailed than those referred in the literature and highlights the presence of the newly introduced force passive/area-active elements, which play a significant role in the optimization procedure.
- In general, the convergence history with respect to the structural weight is very smooth. Peaks appear only when force-passive/area-active elements change their status and become ‘fully’ passive elements
- In general, the convergence history with respect to the relative error of the structural weight is smooth and decreasing. As previously, peaks appear only when force passive/area-active elements change their status and become ‘fully’ passive elements, while valleys appear when the force-passive/area-active elements are allowed to take on the imposed lower bound for the design variables.
- The convergence history with respect to the relative error of the maximum change in the design variables structural weight is either smooth and decreasing or quite steady and drops suddenly to the converging tolerance value.
- The extension of the proposed procedure for optimizing 3D skeletal structures is trivial.

Overall, the results of the present research suggest that the proposed optimization procedure form a simple and efficient optimization tool.

In addition, the layout optimization of 2D continua under an extended single displacement constraint was discussed, where the concept of the ‘extended’ displacement constraint was introduced in Chapter 5. More particularly, the layout optimization was sought following two conceptually different approaches. According to the first approach, the thickness of the 2D continuum is kept constant, while material that has been detected as redundant is completely removed from it. To this end, a new efficient variation of an already existing methodology was proposed, examined and found to be more efficient than the initial version of the existing methodology. According to the second approach, the thickness of the 2D continuum is

isoparametrically interpolated, the nodes being the interpolation points. To this end, a variation of the methodology introduced in Chapter 5 was developed and found to provide encouraging results. Consequently, both of the proposed approaches are useful and efficient tools for 2D layout optimization problems, when an extended singe displacement constraint is imposed.

Furthermore, the minimization of the structural cost was investigated. Since the structural cost is a very complicated quantity to estimate, the investigation was focused on two subjects, the first being the commonality of the structural members within the structure and the second being the effect of the welding cost and the scrap material cost. For the needs of this investigation, two optimization procedures were developed and successfully tested. The former concerned the grouping of similar members and the elimination of critical members; this procedure is applicable to any skeletal structure and it was successfully tested in four literature problems. The latter concerned the solution of a complex optimization problem involving design control for minimum scrap and minimum welding; it was successfully applied in welded tanks for oil-storage. The main outcome of the aforementioned investigation is that it is not possible to establish a generalized procedure for minimum structural cost applicable in all cases, because for the cost minimization to be achieved special design characteristics of each case must be exploited. However, it is possible to introduce optimization procedures, like the proposed ones, suitable for certain subclasses of the generalized optimization problem

Finally, the performance-based layout optimization of large structures was investigated. In total, three different cases were examined. The first case referred to structures which consist of one standard beam. The second case referred to structures which are assemblies of commercially available standard beams, while the third case referred to structures that are made of standard plates. For all three cases, the minimum weight problem may be stated in terms of a discrete optimization problem. For each case, a specific optimization procedure was proposed. More particularly, for the latter two cases, two new heuristic optimization procedures were introduced. All of the proposed procedures were evaluated through the optimization of real-life structures and the encouraging results suggest that these procedures be an efficient tool that can be used for solving performance-based layout optimization problems.

Apart from all the above, a thorough investigation of an optimization method, retrieved from the literature, was carried out. More particularly, an extension of this method was applied to four tubular trusses and four medium/large scale trusses, the results indicating a good performance in terms of convergence, but not that good of a performance in terms of locating the global minimum. These results suggests that a further research on the concept of this method be carried out, such as implementing the categorization of the structural members as force active/passive and area active/passive, which was introduced in Chapter 5.

Last, an issue of high practical importance was examined, that of getting quickly a design, which may be improved with respect to an initial one, but is not necessarily the optimum. For such cases, it is recommended to use simple optimization tools, such as the sensitivity analysis, in the form of a parametric investigation with respect to the most important design variables, and simple optimization procedures of zero-order or of first-order. Towards this direction, four typical applications were examined, namely the design of a car suspension, the optimum single-sided and double-sided bolted reinforcement of a plate under uniaxial tension, the optimum design of a racking system and the layout optimization of a solar tracker. The first three applications were handled using a simple sensitivity analysis as described above, while the last example was dealt with using the Subproblem approximation method and a first order method, both found in Ansys, which is a commercial software for structural analysis.

With respect to ideas for further research, the immediately next step is to apply to 3D continua the newly introduced optimality criterion for the extended single displacement constraint problem. Next follows the implementation in various 2D and 3D structures of the newly introduced optimality criterion for the extended single stress constraint problem. In the sequel, coupling the aforementioned newly introduced optimality criteria would be appropiate. This coupling would aim at solving the optimization problem under an extended single displacement and/or an extended single stress constraint. Furthermore, the investigation of other constraints, such as frequency or thermal constraints, in the form of single constraint problems would be interesting. Obviously, the integration of displacement, stress, frequency and buckling constraints would be the ultimate goal. In addition, sculpturing the surface of a continuum using concepts borrowed from CAD would also provide useful insight concerning the optimum layout that may be achieved if the nodes are treated as control points of a well-defined surface and the thickness interpolation is achieved using different types of isoparametric interpolation schemes. Finally, another completely different route would be the implementation of such ideas, as the aforementioned ones, in different numerical methods, such as the boundary element method and the meshless method, or in different materials, such as the composites.

9.2. Thesis contribution

In brief, the main innovative elements, which this Thesis contributes to, are the following:

- Introduction of new normalized indices for evaluating the performance of an optimization method.
- Development of a new hybrid method for solving the optimization problem of minimizing the weight of skeletal structures under any number of displacement and/or stress constraints. The extension of this method to continua is straightforward.
- Statement of a new Optimality Criterion for solving the optimization problem of minimizing the structural weight of 2D continua under a single compliance constraint.
- Development of a new optimization method for solving the optimization problem of minimizing the structural weight of 2D continua under stress constraints, implementing the concept of element-wise variable thickness and the use of nodes as control points for sculpturing the structural surface.
- Investigation and comparison of applying the ESO and the FSD method in solving the optimization problem of minimizing the structural weight of 2D plates under stress constraints.
- Development of a new optimization procedure for solving the optimization problem of minimizing the weight of 3D continua under stress constraints.
- Statement of a new Optimality Criterion for solving the optimization problem of minimizing the weight of skeletal structures under an extended single stress constraint.
- Statement of a new redesign procedure for solving the optimization problem of minimizing the weight of skeletal structures under an extended single stress constraint.
- Statement of a new Optimality Criterion for solving the optimization problem of minimizing the weight of skeletal structures under an extended single displacement constraint.
- Development of a new optimization method for solving the optimization problem of minimizing the weight of skeletal structures under an extended single displacement constraint.
- Development of a variation of the ESO method for solving the optimization problem of minimizing the weight of 2D continua under a single displacement constraint.

- Development of a new optimization method for solving the optimization problem of minimizing the weight of 2D continua under an extended single displacement constraint, implementing the concept of element-wise variable thickness and the use of nodes as control points for sculpturing the structural surface.
- Development of a new optimization method for solving the optimization problem of minimizing the cost of skeletal structures, implementing a concept of grouping and elimination that aims at increasing the commonality of the active members of the structure.
- Development of a new optimization procedure for solving the optimization problem of minimizing the cost of oil storage tanks, using commercially available plates, taking into consideration the cost for the welds, and aiming at minimizing the scrap material.
- Development of an optimization procedure for solving the discrete optimization problem of minimizing the weight of structures, which may be considered as a single beam of standard profile, while the case of a single girder crane was solved.
- Development of a new heuristic optimization method for solving the optimization problem of minimizing the weight of discrete structures, consisting of standard beams.
- Development of a new 'mixed-type' heuristic optimization method for solving the problem of minimizing the weight of structures, consisting of standard plates, whose thickness is discrete but whose width and length may be considered as continuous variables.
- Solution of the weight minimization problem for a series of full-scale, real-life structures, using sensitivity analysis and commercially available optimizers.

APPENDIX I

STRUCTURAL OPTIMIZATION USING SENSITIVITY ANALYSIS AND COMMERCIALLY AVAILABLE OPTIMIZERS

Abstract

In this Appendix, four typical applications in structural optimization are presented, for which either a sensitivity analysis or a commercially available optimizer was used. More particularly, the design of a car suspension, the optimum single-sided and double-sided bolted reinforcement of a plate under uniaxial tension and the optimum design of a racking system are examined through a sensitivity analysis of the main geometric characteristics. In addition, the layout optimization of a solar tracker is examined using two optimizers found in Ansys, which is a commercial software for Finite Element Analysis of structures. These optimizers concern the Subproblem approximation method and a first order method. The results of the aforementioned cases denote that sometimes in structural optimization it is adequate to get an improved design, which may be achieved using simple means of optimization such as a typical sensitivity analysis or a zero-order or a first-order search of the design domain.

Keywords

Structural optimization, sensitivity analysis, sub-problem approximation, first order method.

I.1. Introduction

The global optimum solution of a structural optimization problem may be hard to be located and for this reason there are cases where improved designs with respect to an initial one are considered to be adequate. For such improved designs to be traced, it is possible to use either an optimizer embedded in some commercial software for structural analysis or a sensitivity analysis with respect to some characteristic geometric dimensions. Towards this direction, four typical applications are presented, namely the design of a car suspension, the optimum single-sided and double-sided bolted reinforcement of a plate under uniaxial tension, the optimum design of a racking system and the layout optimization of a solar tracker. The first two applications were handled using a simple sensitivity analysis in the form of a thorough parametric investigation of the main geometric characteristics of the examined structure, while the other two examples were dealt using the Subproblem approximation method and a first order method, both found in the Ansys software.

I.2. Case study: Car suspension design

I.2.1. Introduction

The suspensions for advanced automotive applications aiming at improving the ride comfort and handling properties of vehicles has been a topic of vigorous research during the past two or three decades (Zaremba et al., 1997). The majority of the research work has been focused on the estimation and optimization of suspension characteristics, such as damping. In most cases, quarter-car or half-car models are used, while various types of suspension mechanisms have been examined. Chen and Beale modeled the MacPherson suspension mechanism as a two-degrees-of-freedom spatial mechanism and simulated its dynamic response under two excitement forces (Chen and Beale, 2003). Thompson and Davis developed matrix expressions for the direct computation of RMS values for the optimal control forces, front and rear suspension strokes and dynamic tyre deflections in a half-car model on a random road of given roughness (Thompson and Davis, 2003). Quaglia and Sorli presented a dimensionless model and the design considerations of a pneumatic suspension with auxiliary reservoir (Quaglia and Sorli, 2001). Their dimensionless model made it possible to fully understand the effect of the parameters which define the suspension and to select the spring type correctly. Without this selection, the suspension generates transmissibility curves with excessive amplification in the vicinity of the resonance, even after optimum definition of auxiliary volume and resistance. Bolzern et al discussed the application to real data of an identification procedure based on an Extended Kalman Filter, for estimating the equivalent non-linear suspension tyre cornering forces of a road vehicle from a single standard manoeuvre, where both the steady-state and the dynamic handling characteristics can be evaluated (Bolzern et al., 1999). The Finite Element Method (FEM) has also been used in structural vibration analysis of vehicles. Kuti applied the finite element method in order to determinate more accurately both the local (structural vibrations) and global (overall motions) dynamic behaviour of vehicles using pre-determinate time variable external forces and kinematic excitations (Kuti, 2001). He presented results about the effects of the elastic deformation of the chassis on the overall motions of vehicles, using a simple truck finite element model of 1874 degrees of freedom. Dukkipati and Dong used a Finite Element (FE) model of a vehicle-track system in order to duplicate the experiments carried out by British Rail and CP Rail System (Dukkipati and Dong, 1999). Their theoretical results of the wheel/rail contact forces, rail-pad forces and strains in the rail showed very good correlation to the experimental data. Optimization methods have been extensively used in order to determine the elastic and damping characteristics of a vehicle suspension that optimize the ride properties of a car. Demič applied a modified version of the Nelder-Mead algorithm to a four-degree-of-freedom model (Demič, 1989) and a modified version of the Hooke-Jeeves algorithm to a seven-degree-of-freedom model (Demič, 1992), while Spentzas applied Box's method to a seven-degree-of-freedom model (Spentzas, 1993).

Within the frame of the aforementioned works, the present paper aimed at revealing the way geometric characteristics affect the stress field of a typical car suspension dome under typical loads. The interest was focused on the area of the strut mount of a front wheel. A front wheel was selected because almost in all cases the vehicle weight is distributed in such a way that the front axle, thus the domes of the front wheels, undertakes the larger part of the sprung mass. Towards this direction, an extensive parametric investigation was performed, where three dome shapes, three design parameters and two load cases were implemented. In more details a cylindrical, a spherical and a conical dome shape were studied while the design parameters were the dome height (six cases), the diameter of the strut mount hole (six cases) and the edge height of the strut mount hole (six cases). The two load cases concerned the application of vertical forces and tangential forces. In total, 108 models were examined, providing useful insight concerning the optimal shape of a car suspension dome.

I.2.2. Theoretical calculation of loads

In order to estimate the external loads applied at the area of interest, Pawlowski's approach was used for a first but on-the-safe-side approximation, as shown in the paragraphs that follow. The main idea of Pawlowski's theory is that any service load may be satisfactorily estimated through the multiplication of the corresponding

static load by a suitable coefficient (Pawlowski, 1969). The static loads can be analytically calculated, while the aforementioned coefficients have been derived from an extended series of experiments and measurements. According to Pawlowksi's approach, five loading cases must be examined, namely the steady state loading, the symmetric vertical loading, the asymmetric vertical loading, the longitudinal loading and the side loading.

I.2.2.1. Steady State Loading

In a steady state loading condition, the vehicle is moving forward, on a horizontal plane, in a constant velocity and without encountering any obstacles. In turn, all wheels are in contact with the road, the sprung mass of the vehicle is distributed between the front and the rear axle according to the designed distribution ratio, while the sprung mass suspended by each axle is equally divided to the two wheels of the corresponding axle. Therefore, the vertical load on a front wheel is given by:

$$P_{st,1i} = \left(\frac{1}{2}\right) maM_{sp}g, \quad i \in \{l, r\} \tag{I.1}$$

where $P_{st,1i}$ is the vertical load on a front wheel in N, m is the dimensionless dynamic coefficient (for the specific case: $m = 1$), a is the dimensionless weight distribution ratio between front and rear axle, M_{sp} is the sprung mass in kg, g is the acceleration of gravity in $m/\sec^2$ and $\{l, r\}$ is the index denoting the left and the right wheel, respectively.

I.2.2.2. Symmetric Vertical Loading

In a symmetric vertical loading condition, the vehicle is moving forward in a constant velocity and on a horizontal plane, where a uniform lateral obstacle exists. At some instant, both front wheels encounter simultaneously the aforementioned obstacle and afterwards the rear wheels do the same. When the wheels of an axle reach the obstacle, then the corresponding suspensions are further compressed, thus causing an alteration of the weight distribution of the vehicle between the front and the rear axle. In the extreme case, the wheels of the axle not encountering the obstacle will loose contact with the ground (horizontal plane), thus the sprung mass will be suspended completely by the two wheels that do encounter the obstacle. For such a case, the vertical load on a front wheel is given by:

$$P_{zs,1i} = \left(\frac{1}{2}\right) m_{zs}M_{sp}g, \quad i \in \{l, r\} \tag{I.2}$$

where $P_{zs,1i}$ is the vertical load on a front wheel in N and m_{zs} is the dimensionless dynamic coefficient (for typical passenger vehicles: $m_{zs} = 2.5$). The other symbols have already been explained in the previous section. From (Eq.I.2), it is obvious that the height of the obstacle does not play any role in the appearing loads. However, it is reminded that (Eq.I.2) describes an extreme case, where the wheels of one axle have lost contact with the ground. In most cases, designers select such suspension characteristics that prevent this situation to occur for common obstacles. Maximum heights for obstacles, which are categorized as common, with respect to the vehicle type are shown in Table II.1 (the minus sign denotes puddles).

Table I.1: Maximum heights for common obstacles

Obstacle height	Passenger vehicle	Bus	Truck	Special Vehicle
h_r [mm]	±200	±250	±300	± (>400)

I.2.2.3. Asymmetric Vertical Loading

In an asymmetric vertical loading condition, the vehicle is moving forward in a constant velocity and on a horizontal plane, where a lateral obstacle, less wide than the lateral distance between the wheels of an axle, exists. At some instant, only one of the front wheels encounters the obstacle (the other wheels are in contact with the ground). In this way, the suspension of the aforementioned wheel is further compressed, thus causing an alteration of the weight distribution of the vehicle between the two front wheels but not between the front and the rear axle. In the extreme case (worst case scenario), the front wheel not encountering the obstacle will loose contact with the ground (horizontal plane), thus the sprung mass of the front axle will be suspended completely by the front wheel that does encounter the obstacle, for which the corresponding vertical load is given by:

$$P_{zns,1} = m_{zns}aM_{sp}g \tag{I.3}$$

where $P_{zns,1}$ is the vertical load on the front wheel that encounters the obstacle in N and m_{zns} is the dimensionless dynamic coefficient (for typical passenger vehicles: $m_{zns} = 1.3$). The other symbols have already been explained in the previous section. Once again, it is noted that (Eq.I.3), does not include the height of the obstacle. This is due to the fact that (Eq.I.3) corresponds to an extreme case, that of one wheel loosing contact with the ground, which is preferred for on-the-safe-side estimations. However, it is noted that in most cases, designers try to avoid such situations by appropriately selecting the suspension characteristics. The maximum heights for obstacles categorized as 'common' have already been presented in Table II.1.

I.2.2.4. Longitudinal Loading

There are two cases longitudinal loads may appear, the former being the acceleration or deceleration of the vehicle (the deceleration due to crash excluded) and the latter being the striking of an obstacle, such as a curb. For the first case, it holds that:

$$P_x = \pm\left(\frac{1}{2}\right) m_x a M_{sp} g \tag{I.4a}$$

where P_x is the vehicle front wheel longitudinal load in N, a is the dimensionless weight distribution ratio between front and rear axle, m_x is the dimensionless dynamic coefficient (for typical passenger vehicles: $m_x \in [0.7,\ 1]$), while the sign $+, -$ denotes acceleration and deceleration, respectively. For the second case, it holds that:

$$\vartheta = \sin^{-1}\left(1 - \frac{h_r}{r_d}\right) \qquad\qquad P_x = m_z \frac{P_y}{\tan\vartheta} \tag{I.4b}$$

where P_x is the vehicle front wheel longitudinal load in N, m_z is the dimensionless dynamic coefficient (for typical passenger vehicles: $m_z = 2.5$), P_y is the vertical load on the wheel that encounters the obstacle (see 2.2 and 2.3) in N, h_r is the obstacle height in cm and r_d is the dynamic wheel radius in cm. It is evident, that the maximum longitudinal load is defined by the largest value between (Eq.I.4a) and (Eq.I.4b). For the height of the obstacle, Table II.1 should be used.

I.2.2.5. Side Loading

There are two cases side loads may appear, the former being during driving along a curved path and the latter being the side striking of an obstacle, such as a curb. For the first case, it holds that:

$$R_{x,1i} = m_{zs} a \left(\frac{r_t/2}{z_{sc}}\right) M_{sp} g \tag{I.5a}$$

where $P_{x,1i}$ is the vehicle front wheel side load in N, m_{zs} is the dimensionless dynamic coefficient (for typical passenger vehicles: $m_z = 2.5$), a is the dimensionless weight distribution ratio between front and rear axle, r_t is the distance between the wheels of the front axle, and $z_{sc}s$ is the vertical distance of the vehicle centre of mass from the ground. For the second case, it holds that:

$$R_{x,1i} = m_y a M_{sp} g \tag{I.5b}$$

where m_y is the dimensionless dynamic coefficient (for typical passenger vehicles: $m_y \in [0.7,\ 1]$). The other symbols have already been explained. It is evident, that the maximum side load is defined by the largest value between (Eq.I.5a) and (Eq.I.5b).

I.2.2.6. Combined Loading

From all the above equations, it results that the combined loading at the strut mount may be described by a force vector:

$$\mathbf{R} = \begin{bmatrix} R_x & R_y & R_z \end{bmatrix}^T \tag{I.6a}$$

and a moment vector

$$\mathbf{M} = \begin{vmatrix} \vec{i} & \vec{j} & \vec{k} \\ r_x & r_y & r_z \\ R_x & R_y & R_z \end{vmatrix} \tag{I.6b}$$

where r_x is the longitudinal distance between the strut mount and the wheel, r_y is the lateral distance between the strut mount and the wheel and r_z is the vertical distance between the strut mount and the wheel.

I.2.3. Numerical application

The equations derived in the previous sections were used in order to calculate the loads that a typical front wheel suspension dome experiences. As a reference, a 1970's passenger car suspension dome was used. The corresponding front wheel suspension dome was measured and a first model was build in order to estimate the stress and the displacement field. In the sequel, this study was extended to a parametric investigation, which aimed not only at revealing the way important geometric characteristics affect the stress and the displacement field but also at proposing an improved design without enlarging the volume that the specific structural component initially occupied. Therefore, the minimum and maximum parameter values were limited by the initial design, while the intermediate values came from a logical division of the corresponding domains.

I.2.3.1. Investigated parameters

In the present work, four parameters were investigated, namely the dome shape, the dome height, as well as the diameter and the edge height of the strut mount hole. The examined dome shapes are illustrated in Fig.I.1.

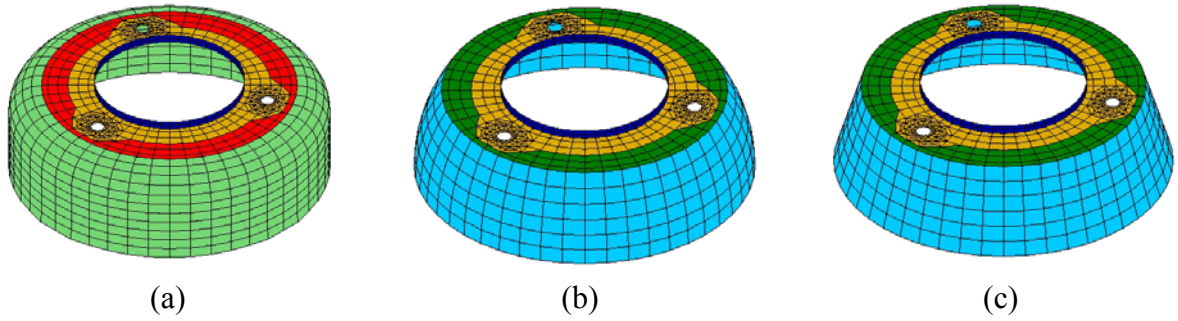

Figure I.1: Car suspension dome shapes: (a) cylindrical, (b) spherical and (c) conical

Geometrical details of a typical dome, as well as a typical coordinate system, are shown in Fig.I.2. As Fig.I.2 suggests, it may be assumed that the external loads are uniformly applied only to a part of the dome roof (Part5).

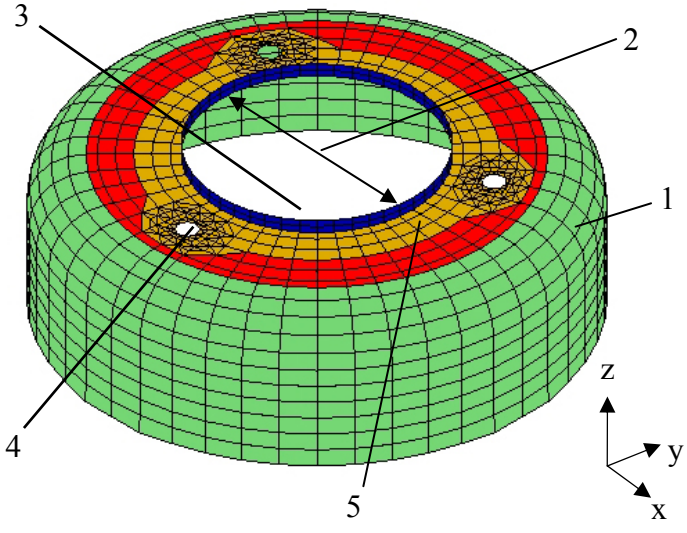

1: side dome wall
2: strut mount hole
3: edge of the strut mount hole
4: bolt holes for fastening purposes
5: part of the dome roof where all loads are applied to

Notes
- The side dome wall may have a cylindrical or a spherical or a conical shape.
- The number of the bolt holes, as well as their distribution, may differ.
- The height of the side dome wall, the height of the edge of the strut mount hole, as well as its diameter, may differ.

Figure I.2: Details of a typical car suspension dome

The values used for the other examined parameters (see Fig.I.3) were the following:

Dome height: $h \in \{21.5, 26.8, 32.1, 37.4, 42.7, 48\} mm$, thus $\{h_{\min}, h_{\max}\} = \{21.5, 48\}$

Strut mount hole diameter: $D \in \{70, 72, 74, 76, 78, 80\} mm$, thus $\{D_{\max}, D_{\min}\} = \{70, 80\}$

Strut mount hole edge height: $h_{hole} \in \{0, 2, 4, 6, 8, 10\} mm$, thus $\{h_{hole,\max}, h_{hole,\min}\} = \{0, 10\}$

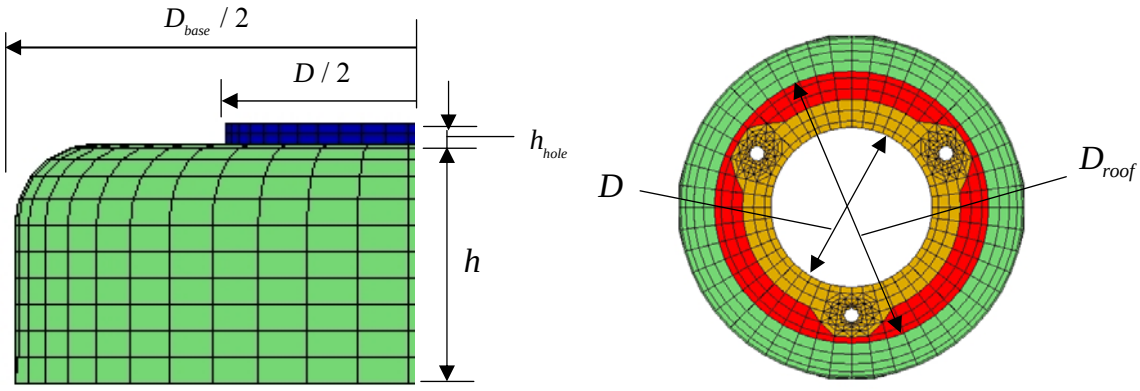

(a) side view (b) top view

Figure I.3: Definition of basic geometrical dimensions

Two other important dimensions for the model development were the diameter of the dome at its base $D_{base} = 158mm$ and the diameter of the plane part of the dome roof $D_{roof} = 126mm$ (Fig. I.3). However, it is clarified that these last dimensions were not used as parameters in the current investigation.

I.2.3.2. External loads

In the present work, the following values were used:

$$M_{sp} = 990kg \qquad a = 0.55 \qquad r_d = 300cm \qquad r = 1290mm \qquad Z_{sc} = 541mm \tag{I.7}$$

Typical distances (in mm) between the strut mount and the wheel were considered to be:

$$\mathbf{r} = \begin{bmatrix} 300 & 350 & 860 \end{bmatrix}^T \tag{I.8}$$

Substituting the above values in (Eq.I.1-Eq.I.6) and keeping the maximum loads for each direction, the force vector and the corresponding moment vector were formed, due to which a displacement field, thus a stress field, is developed. A complete analysis requires the application of each one of the aforementioned force and moment components. In the current work, the examination is limited to the force components only. Although there are three force components, it is adequate to examine only two of them, namely the z-component (vertical forces) and, due to the symmetry of the dome (Fig.I.2), either the x-component or the y-component. In the present investigation, the y-component was chosen.

I.2.3.3. Boundary conditions

The car suspension dome is usually attached to another structural component, which is mounted to the chassis. Without loss of generality, it is possible to examine the dome as a separate part considering that all degrees of freedom of its lower part (base) are restrained. In the current work, this approach, which significantly simplifies the model development, was selected.

I.2.4. Results

In the current study, a cylindrical, a spherical and a conical dome shape were investigated while the implemented parameters were three, namely the dome height (six cases), the diameter of the strut mount hole (six cases) and the edge height of strut mount hole (six cases). Furthermore, two load cases were applied (vertical forces and tangential forces, respectively). In total, 108 models were built and analyzed. The corresponding results were grouped with respect to the examined parameter, thus three groups of results were formed. Each group included eight plots divided in two subgroups of four plots each. The first subgroup

concerned a comparison of results between the dome shapes, while the second subgroup concerned a comparison of results within each dome shape. From the four plots of each subgroup, two concerned the maximum appearing von Mises stress (stress plots) and the other two concerned the maximum appearing displacement (displacement plots). In the current work, it is the relative changes and not the absolute values that were of interest, thus reduced quantities were used. It is noted that for the subgroup of results between the dome shapes, the cylindrical dome shape was selected as the reference.

I.2.4.1. Investigation with respect to the dome height

The results from the investigation with respect to the dome height are illustrated in Figs.I.4-I.5.

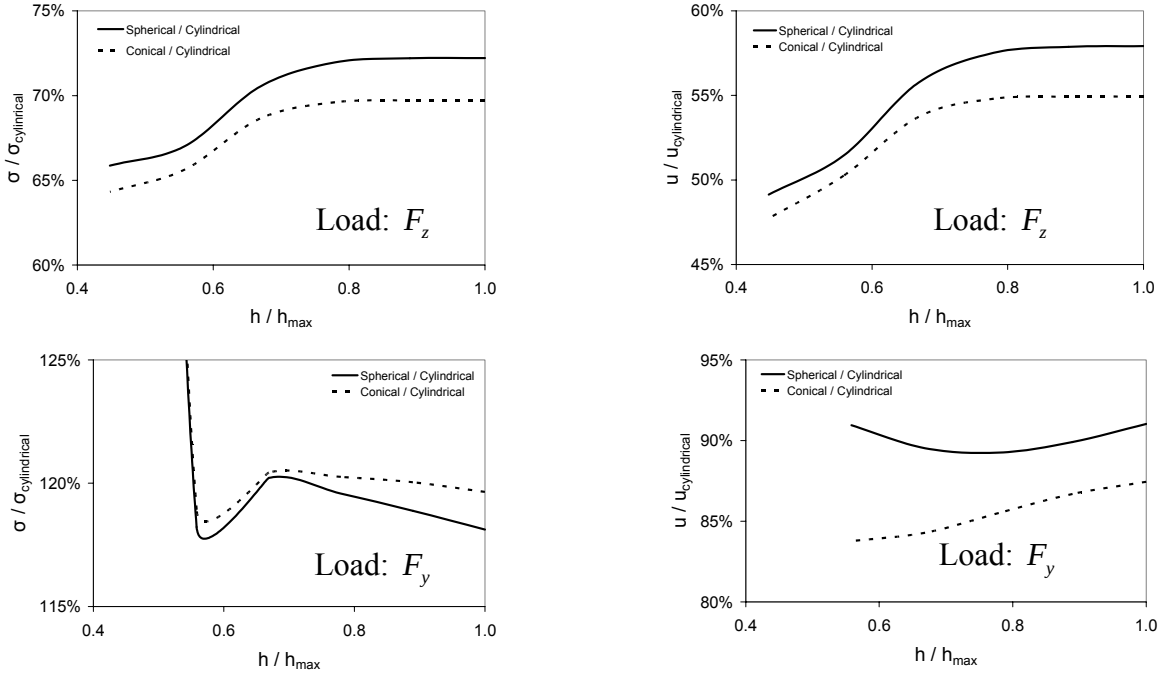

Figure I.4: Results "between" the dome shapes for (a) stress and (b) displacement

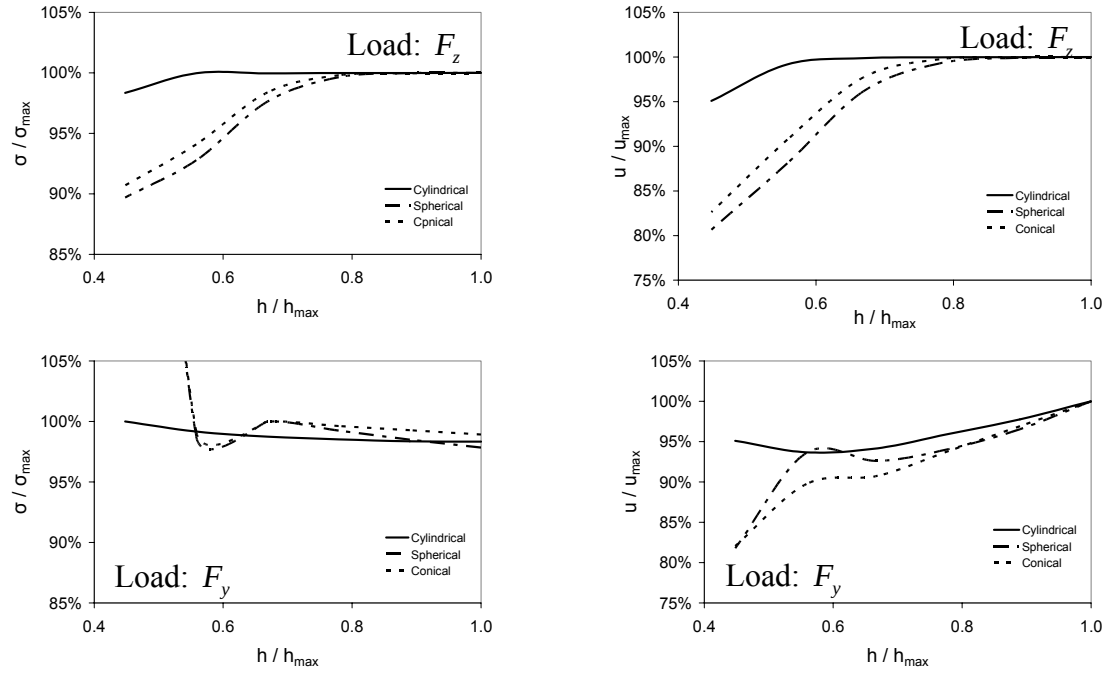

Figure I.5: Results "within" the dome shapes for (a) stress and (b) displacement

In all plots, the horizontal axis is h / h_{max}, where h denotes one of the examined dome heights and h_{max} denotes the maximum dome height used in the present work. For the stress and the displacement plots concerning the results between the dome shapes, the vertical axis is $\sigma / \sigma_{cylindrical}$ and $u / u_{cylindrical}$, respectively. For either the spherical or the conical dome of height h, the von Mises stress is denoted as σ, and the displacement is denoted as u. For the corresponding cylindrical dome, which was used as a reference, the von Mises stress and the displacement are denoted as $\sigma_{cylindrical}$ and $u_{cylindrical}$, respectively. For the stress and the displacement plots concerning the results within the dome shapes, the vertical axis is σ / σ_{max} and u / u_{max}, respectively. For a dome of height h, the corresponding von Mises stress and the displacement are denoted as σ and u, respectively. The maximum stress and displacement values are denoted as σ_{max} and u_{max}, respectively. At this point, it is strongly emphasized that the maximum appearing stress and displacement values do not necessarily corresponding to h_{max}. Observation of Figs.I.4-I.5 reveals that the dome height affects the displacement field more than the stress field and it is preferable to have a short dome either of spherical or of conical shape. However, the height must not be very short otherwise problems occur (Fig.I.4a, Load: F_y).

I.2.4.2. Investigation with respect to the diameter of the strut mount hole

The results from the investigation with respect to the dome height are illustrated in Figs.I.6-I.7.

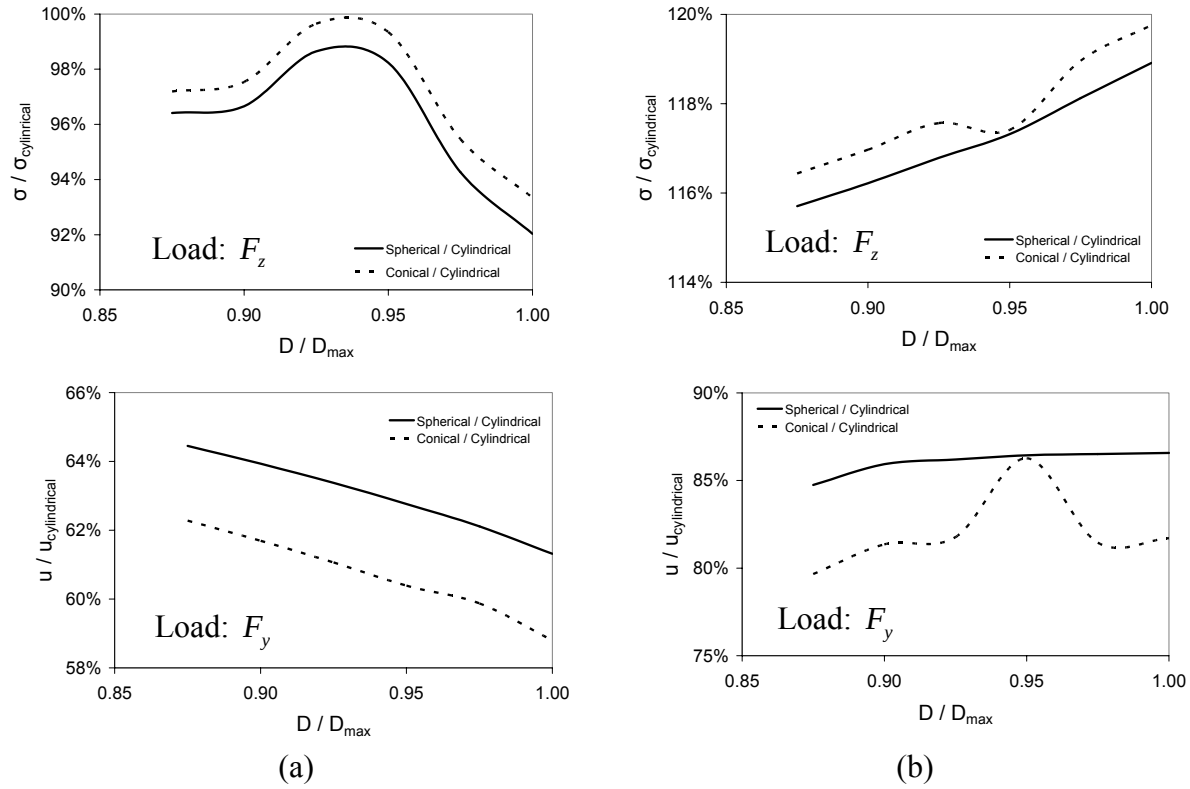

Figure I.6: Results "between" the dome shapes for (a) stress and (b) displacement

In all plots, the horizontal axis is D / D_{max}, where D denotes one of the examined diameters and D_{max} denotes the maximum strut mount hole diameter used in the present work. For the stress and the displacement, the symbols presented in the previous paragraph are used once again. From Fig.I.7, it is obvious that for vertical loads it is better to have a large strut mount hole while from tangential loads a small strut mount hole is preferable. However, it can be shown (Eqs.I.1-I.8) that the vertical loads predominate, thus a large strut mount hole is recommended. Furthermore, from a stress-point-of-view, the spherical shape is preferable (up to 8% reduction) while from a displacement-point-of-view it is better to have a conical shaped dome (up to 41% reduction). It is reminded that the cylindrical dome is used as a reference. Observation of Fig.I.7 reveals that, with respect to the diameter of the strut mount hole of a spherical dome where vertical loads are applied to, the stress and the displacement field may be reduced up to 10% and 30%, respectively. For tangential loads, the corresponding reduction is significantly smaller.

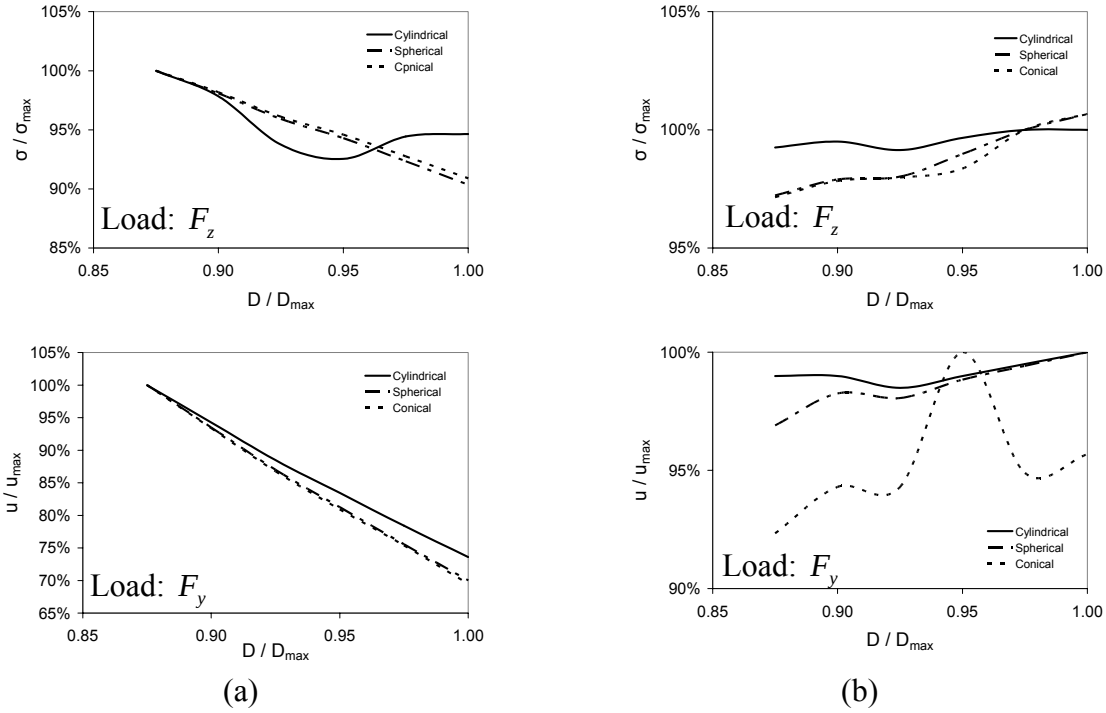

(a) (b)

Figure I.7: Results "within" the dome shapes for (a) stress and (b) displacement

At this point, it is worth mentioning that the conical shaped dome behaves very similar to the spherical shaped dome and both of them present a linear behaviour with respect to the strut mount hole diameter, if vertical loads are applied (Fig.I.7a-Load: F_z, I.7b-Load: F_z). Therefore, if one of these shapes is selected, it should bear a large strut mount hole. On the contrary, the cylindrical dome experienced the largest stress reduction for an intermediate hole diameter value (Fig.I.7a-Load: F_z).

I.2.4.3. Investigation with respect to the edge height of the strut mount hole

The investigation with respect to the edge height of the strut mount hole is illustrated in Figs.I.8-I.9.

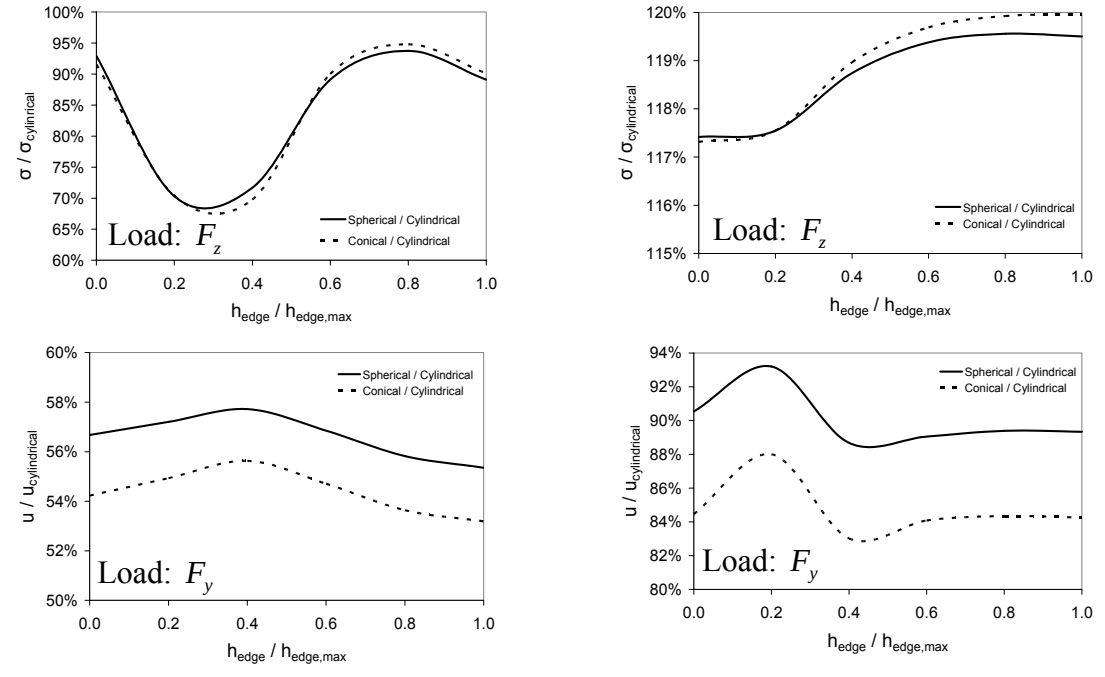

(a) (b)

Figure I.8: Results "between" the dome shapes for (a) stress and (b) displacement

In all plots, the horizontal axis is $h_{edge} / h_{edge,\max}$, where h_{edge} denotes one of the examined edge heights and $h_{edge,\max}$ denotes the maximum edge height of the strut mount hole used in the present work. For the stress and the displacement, the symbols presented in the previous paragraph are used once again. From Fig.I.8, it is obvious that for vertical loads it is better to have a tall strut mount hole edge while for tangential loads a short strut mount hole edge is preferable. As previously mentioned, it can be shown that the vertical loads predominate, therefore a tall strut mount hole edge is recommended. In addition, the conical dome shape is preferable from both a stress-point-of-view and a displacement-point-of-view (reduction of almost 33% and 46%, respectively). As previously, the cylindrical dome is used as a reference.

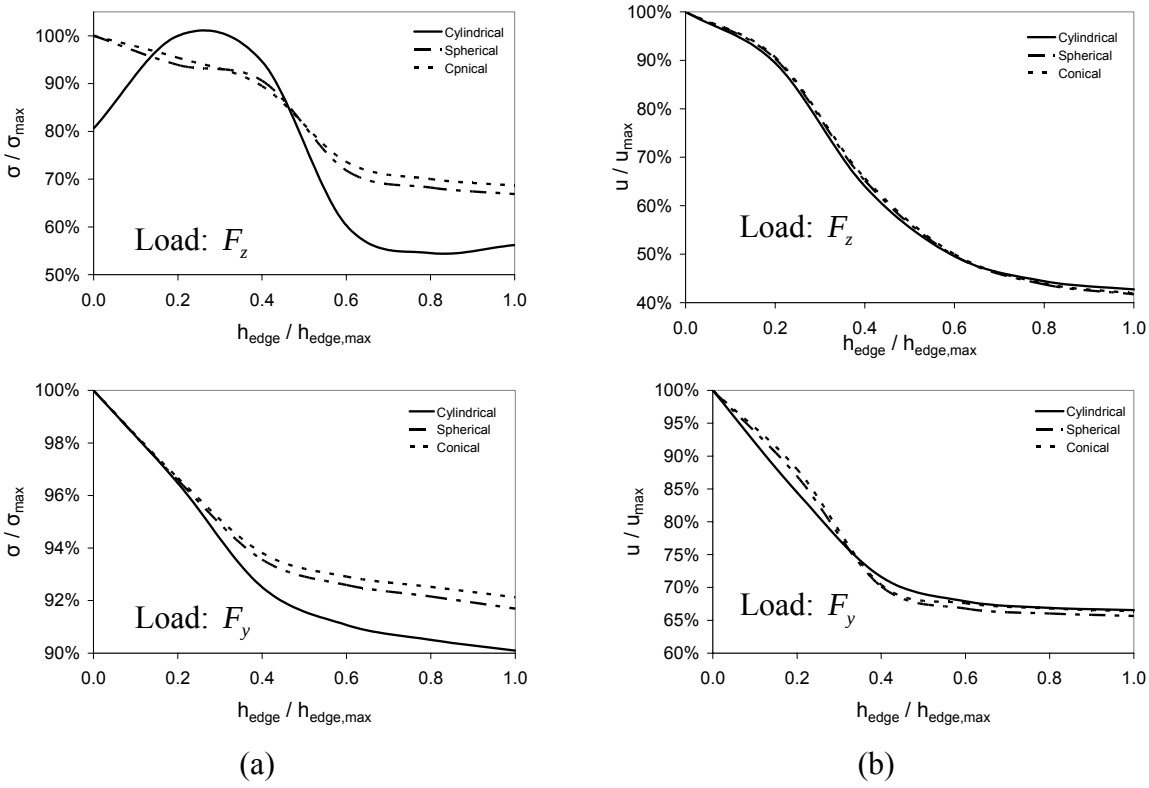

Figure I.9: Results "within" the dome shapes for (a) stress and (b) displacement

Observation of Fig.I.9 reveals that, with respect to the edge height of the strut mount hole of a cylindrical dome where vertical loads are applied to, the stress and the displacement field may be reduced up to 45% and almost 60%, respectively. For tangential loads, the corresponding reduction is quite smaller. At this point, it is worth mentioning that all three dome shapes behave very similar from a displacement-point-of-view (Fig.I.9b). However, their behaviour differs from a stress-point-of-view, where the cylindrical dome outperforms the others (Fig.I.9a). Furthermore, from Fig.I.9 it is evident the increase of the edge height is beneficial only up to a point; afterwards, both the stress and the displacement field remain almost unaltered.

I.2.4.4. Typical stress and displacement fields

A typical stress and displacement field developed due to the application of vertical and tangential forces respectively is shown in Fig.I.10.

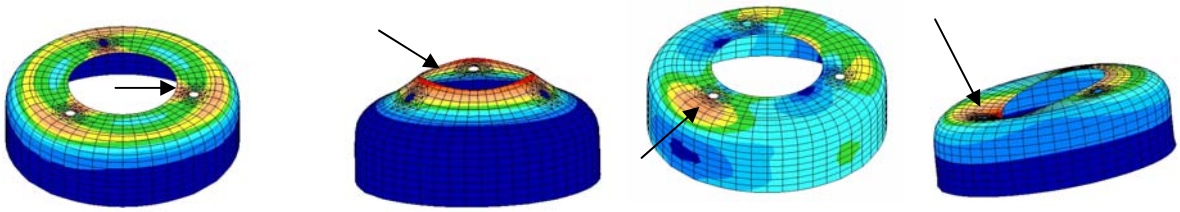

Figure I.10: Typical stress and displacement field for (a) vertical and (b) tangential loads

For reasons of visual clarity, the edge of the strut mount hole has been removed, while arrows point at some indicative areas of high stress and/or displacement values.It is obvious that in both load cases the areas where the largest stress and displacement values appear are the bolt holes and the edge of the strut mount hole. It is worth noting that the vertical part of the side wall suffers significantly less than the top part of the dome, thus it is possible to remove material from the side wall. This is in accordance to the remark that the dome height does not significantly affect the stress and the displacement field (see section II.2.4.1). Furthermore, Fig.I.10 shows that attention should be paid at the intersection between the top part of the dome and the side wall, because along that intersection and near the bolt holes, the stress field is strong. Finally, as Fig.I.10b illustrates, in the case of tangential loads neither the stress nor the displacement field is symmetric, thus the orientation of the bolt hole distribution with respect to the direction of the load is important

I.2.5. Conclusions

The present study aimed at revealing the way a sensitivity analysis in the form of a parametric investigation may be used for structural optimization purposes. The case studied referred on the strut mount of a front wheel. This selection was based on the fact that in almost all cases the vehicle weight is distributed in such a way that the front axle, thus the domes of the front wheels, undertakes the larger part of the sprung mass. An extensive parametric investigation took place, where three dome shapes (cylindrical, conical and spherical), six different dome heights, six different strut mount hole diameters, six different strut mount hole edge height and two load cases were implemented. In total, 108 cases were studied. The results were plotted in a reduced format thus providing a visual representation of the effect that each parameter had on the stress and the displacement field. From the plotted diagrams, it was revealed that the edge height of the strut mount hole mostly affected the developed stress and displacement fields, the diameter of the same hole had a weaker effect, while the dome height presented the smaller effect. Furthermore, it was found out that a tall strut mount hole edge, a large strut mount hole and a small dome height is a preferable combination. With respect to the dome shape, depending on the view point (stress or displacement), a different design is recommended. However, a cylindrical dome seemed to be a good compromise. Concluding, the present investigation provided useful insight concerning the optimal shape of a car suspension dome using a simple parametric study as a means for a sensitivity analysis.

I.3. Case study: Bolted reinforcement of a plate under uniaxial tension

I.3.1. Introduction

All structures during their service life may experience local failures due to various reasons, such as corrosion, unpredicted accidental action, overloading or poor maintenance. For the structure to be restored into its initial state, it is required to reinforce the area that presents the problem (area of interest), so that the maximum developed stress will be reduced (stress-relief of the area of interest). For plate structures, such as the box-girder of a gantry crane or of an overhead traveling crane, one typical way of achieving this goal is appropriately placing reinforcing plates, also called doublers, at the area of interest. More than frequently, the area of interest is under non-negligible stress due to dead loads thus for the aforementioned placing not all means of fastening may be used. The most common solution is the use of High Strength Friction Grip (HSFG) bolts. The dimensions of the doublers, the number of bolts to be used, their grade and their distribution over the fastening is a crucial issue to be dealt with. In all cases, the interest is focused on the stress relief that bolted doublers may provide, which may be estimated using theoretical but simplified approaches. As a result, a confirmation using a numerical approach, such as the Finite Element Method (FEM), is required.

Towards this direction, many works have been published. Bursi and Jaspart investigated bolted steel connections using FEM and evaluated the results introducing benchmark indices (Bursi and Jaspart, 1997). Hwang and Stallings, based on Finite Element Analysis (FEA), analyzed bolted flange connections (Hwang and Stallings, 1994). Furthermore, Stallings and Hwang investigated the way pretension may be introduced in bolted connections (Stallings and Hwang, 1992). Chung and Ip used FEA in order to investigate bolted connections between cold-formed steel strips and hot rolled steel plates under static shear loading (Chung and Ip, 2000). Sherbourne and Bahaari (Sherbourne and Bahaari, 1996) developed full 3-D models and studied the bolted connections introduced in unstiffened columns. Rothert et al. examined bolted connections in steel frames and for this purpose they developed a 3-D model and performed a non-linear contact analysis (Rothert et al, 1992). Citipitioglu et al. dealt with the problem of partially-restrained connections and to this end a refined 3D finite element model was developed so that slip could be included (Citipitioglu et al, 2002). Furthermore, Zerres compared the mechanical behavior of bolted joints as predicted by the FEM and as described by the European approach (PR EN 1591) (Zerres, 1998). Ju et al. used the 3-D elasto-plastic FEM to study the structural behavior of the butt-type steel bolted joint and compared their numerical results with AISC specification data (Ju et al, 2004). Olsen investigated, in a revised manner, typical bolted endplate connections (Olsen, 2002). Puthli and Fleischer performed a series of tests on 25 bolted connections and confirmed that the minimum bolt spacing and edge distance specified in Eurocode 3 can also be used for steel grade S460 (Puthli and Fleischer, 2001). Maggi et al. performed a series of parametric analyses on the behavior of bolted extended end plate connections using

Finite Element (FE) modeling tools and calibrated their results to experimental ones (Maggi et al, 2005). Kasai et al. conducted tests of full size beam-column subassemblies employing new types of bolted connections in order to evaluate the use of bolted connections for rigid moment frame connections in high seismic zones (Kasai et al, 1998). Furthermore, the symmetric reinforcement of plates under tension has also been investigated with a 3D nonlinear finite element contact analysis on a structural strip (Venetsanos et al, 2004).

Extending the latter work, the ideal case would be the 3D modeling of the entire bolted joint reinforcement using brick elements and its analysis implementing nonlinear contact theory. However, the computational cost for such a numerical approach is prohibitively high. Another alternative would be the development of 3D models using plate elements. This approach is indeed adequately accurate but suffers from the drawback that every time a new model must be built, analyzed and evaluated. Another alternative would be the development of a mechanical equivalent based on a parallel spring configuration. This is a theoretical approach very easy and quick to apply but of questionable reliability due to the introduced simplifications. In the present paper, a compromise between the two latter alternatives is proposed. In more details, it is proposed that the results of an extensive parametric numerical investigation be used for correcting the predictions of the simplified theoretical approach. The numerical investigation is carried out only once and the derived results not only inform about the sensitivity of the stress relief at the area of interest with respect to the controlling parameters but also can be illustrated in diagrams ready to be used for the design of the optimum bolted reinforcement.

Towards this direction and within the frame of this paper, a versatile environment was developed in ANSYS/APDL. The main characteristics of this environment were the use of plate elements for all of the structural components, the implementation of rigid links for the modeling of the bolts and the selection of a linear static solver. In addition, each model was highly parameterized. The dimensions of the doublers (length, width and thickness), the dimensions of the reinforced plate (length, width and thickness), the grade and size of the bolts, the bolt edge and end distances as well as the bolt spacing were the controlling parameters. Furthermore, two types of bolted reinforcement, a single-sided and a double-sided, were applicable. Using this environment it was possible to perform an extensive parametric investigation using combinations of all of the aforementioned parameters. The derived results, when normalized with respect to the corresponding values obtained using the theoretical approach mentioned in the previous paragraph, show how well the simple theoretical approach resembles the more accurate numerical approach. The appropriate illustration of these normalized values provides ready-to-use diagrams. It is strongly emphasized that, in the aforementioned environment, the bolt end and edge distances as well as the bolt spacing and the capacity of the bolted joint, were estimated according to Eurocode3, while only plates commercially available in the Hellenic market were used as doublers.

I.3.2. Theoretical aspects

In a High Strength Friction Grip (HSFG) bolted joint under in-plane loads, the fastened parts are strongly pressed against each other, due to the pretension, thus resulting in the appearance of high shear that resists to their separation.

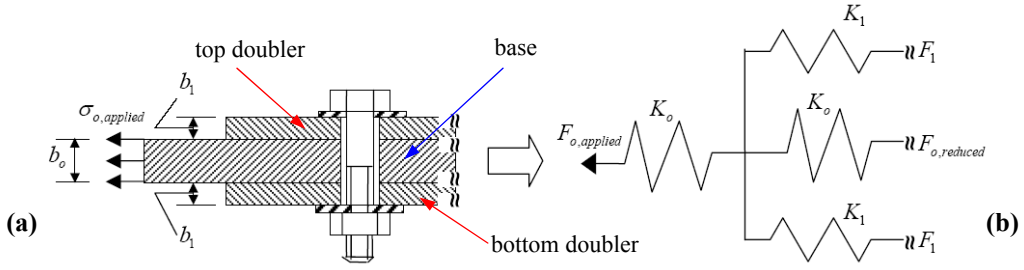

Figure I.11: A double-sided symmetric reinforcement (a) section and (b) equivalent spring model

Consequently, at a wider area around a bolt, the cross-section that carries the load is the sum of the cross-sections of the fastened parts, or, equivalently, not only one but all of the parts participate in carrying the load. This is very useful in cases where a plate needs to be reinforced. For a single-sided reinforcement only one doubler is placed on the reinforced plate, while for a double-sided reinforcement one doubler is placed on each side (top and bottom) of the reinforced plate (base), as illustrated in Fig.I.11a. Furthermore, a double-sided reinforcement is characterized as symmetric if the top and bottom doublers are the same; otherwise, it is called asymmetric. In practice, a double-sided reinforcement is preferred, because no eccentricity phenomena appear; this is desirable from an engineering perspective. Furthermore, if two doublers are to be manufactured then it is time-saving and cheaper to manufacture two similar than two different pieces. Therefore, a symmetric double-sided reinforcement is preferable. In such a case, it is possible to establish a simple mechanical equivalent of the fastened parts using linear springs, as illustrated in Fig.I.11b.This simplified theoretical approach is based on the

assumption that the doublers are of infinite width, thus no 3D effects are taken into account; only the axial stress components are considered, instead. After basic manipulations, the following equation may be derived:

$$\left(\frac{\sigma_{o,red,theor}}{\sigma_{o,app}} \right) = \left(\frac{b_o}{b_o + 2b_1} \right) \tag{I.9}$$

where $\sigma_{o,red,theor}$ is the reduced axial stress component on the base, $\sigma_{o,app}$ is the axial stress component on the base due to the initially applied load and b_o, b_1 are the thickness of the base and of the doublers, respectively. Therefore, it is possible to define a theoretical stress relief index as:

$$SR_{th} = \left(1 - \left(\frac{\sigma_{o,red,theor}}{\sigma_{o,app}} \right) \right) \times 100 \tag{I.10}$$

From a computational mechanics perspective, it is possible to model a symmetric double-sided reinforcement using plate elements for both the base and the doublers, while the bolts may be considered as rigid links. Obviously, the modeled base and doublers are so placed that the distance between the mid surface of the base and the mid surface of each doubler is equal to half the sum of the thickness of the base and the thickness of one doubler. In this way, a 3D model is developed thus, when analyzing it with the Finite Element Method (FEM), 3D effects may appear. The aforementioned modeling does not take into account the pretension of the bolts. The rigid links, which are used instead, ensure that the degrees of freedom of appropriately selected nodes on the base and on the doublers will be coupled. For this approach, it is possible to define a stress relief index as:

$$SR_{FEM} = \left(1 - \left(\frac{\sigma_{x,fin}}{\sigma_{x,app}} \right) \right) \times 100 \tag{I.11}$$

where $\sigma_{x,fin}$ is the axial stress component on the base and at the area of interest after the reinforcement and $\sigma_{x,ini}$ is the axial stress component on the base and at the area of interest before the reinforcement.

For the single-sided reinforcement, the simplified theoretical approach, neglecting eccentricity, yields:

$$\left(\frac{\sigma_{o,red,theor}}{\sigma_{o,app}} \right) = \left(\frac{b_o}{b_o + b_1} \right) \tag{I.12}$$

However, the FE approach is based on a 3D model consisting of the base and one doubler and allows for eccentricity effects to appear.

As Eqs.(II.9, II.10 and II.12) suggest, the evaluation of the approximating SR_{th} index is extremely easy and controlled only by the thicknesses b_1 and b_o. As Eq.(II.11) suggests, the estimation of the SR_{FEM} index is based on the results of a 3D Finite Element Analysis (FEA), thus not only is it more accurate but also its value is affected by the controlling parameters involved in the modeling. In general, the values of the two indices SR_{th} and SR_{FEM} are different. Therefore, it would be of interest, for various values of the controlling parameters, to quantify this difference and use it as a correcting factor applied to the theoretical index SR_{th}.

I.3.3. Modeling aspects

For the needs of the present paper, ANSYS, a very well-known commercial Finite Element Analysis (FEA) software, was used. For an extensive parametric investigation to be performed, a large number of models must be created and analyzed, thus writing a code for this iterative task is mandatory. To this end, a code was written in APDL, the scripting language of ANSYS. At a first glance, it seems that the model may be developed in three simple steps, the first being the creation of three areas (one for the base and two for the doublers), the second being their meshing with the mesh generator provided by the software and the third being the introduction of rigid links. Furthermore, assuming that the examined topology is of double symmetry, only one quarter of the topology was required to be modeled. Although the first two steps were extremely easy to apply, a significant

difficulty was met with the third step. In more details, in order to substitute a bolt with a rigid link, a node must exist on the base and on the doublers at the position where the bolt is supposed to be placed. If these nodes happen to exist on the mesh already created at step 2, then it is possible either to join them with very stiff beams or to couple their degrees of freedom (CERIG command in ANSYS). Otherwise, which is almost always the case, it is necessary to create such nodes. The difficulty met was to make these nodes part of an already existing mesh. Various efforts with 'fill between nodes', 'merge' nodes or first 'introduce key-points' and then 'create nodes on key-points' did not bring any result thus no kinematic connectivity between the base and the doublers could be established. As a solution, it was decided to code a mapped-mesh generator in APDL such that the nodes would be distributed according to the requirements of EC3 for the positioning of the bolt holes (Fig.I.12). In this way, it was ensured that the positioning of the nodes, both on the base and on the doublers, was completely controllable and the aforementioned kinematic connectivity achievable.

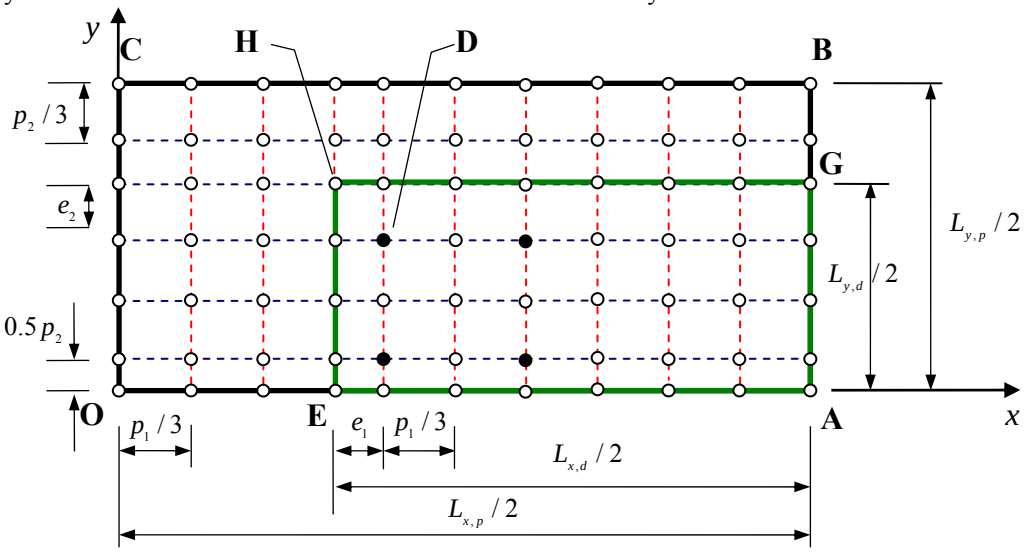

Figure I.12: Mapped mesh for the base

For the developed model, the dimensions of the base (length $L_{x,p}$ and width $L_{y,p}$) were related to those of the doublers (length $L_{x,d}$ and width $L_{y,d}$) as follows:

$$L_{x,p} = \alpha L_{x,d}, \quad a > 1 \qquad L_{y,p} = bL_{y,d}, \quad b > 1 \tag{I.13}$$

Other characteristic geometric dimensions were the end distance e_1, the edge distance e_2, the spacing in the direction of load transfer p_1 and the spacing measured perpendicular to the direction of load transfer p_2 (Fig.I.12). As mentioned before, it was assumed that the actual structure is doubly symmetric. In Fig.II.12, only one quarter of the structure is modeled, assuming that the lines OA and AB are lines of symmetry, on which appropriate boundary conditions of symmetry are imposed. Furthermore, the nodes along the line CB were assumed to have restrained the translations along the directions vertical to the specific line. The external load was a uniform reference tensional pressure of $100MPa$ applied along the line OC. The mesh generator required the dimensions of the doublers, the constants a, b and the bolt size as input, while it was possible to select either the most extended or the most condensed distribution of bolts (black circles in Fig.II.12) by applying the CERIG command appropriately. It is noted, that in all cases, there were uncoupled nodes between two consecutive bolts (white circles between the black circles in Fig.I.12) for the stress field to be developed in a more unrestricted, thus more representative way. It is also clarified that the SHELL63 element was used. The total number of elements was dependent on the initial selections (dimensions of the doublers, constants a, b, bolt diameter). It is noted that the doublers were created with an appropriate offset of the $EAGH$ meshed area.

I.3.4. Eurocode aspects

According to EC3, a HSFG bolted connection loaded in shear belongs to Category C and is slip-resistant at the ultimate limit state. Therefore, the constraints implemented are summarized as follows:

$$\left(F_{v,Sd}/F_{s,Rd}\right) \le 1 \qquad \left(F_{v,Sd}/F_{b,Rd}\right) \le 1 \qquad \left(F_{v,Sd}/N_{net,Rd}\right) \le 1 \tag{I.14}$$

where $F_{v,Sd}$ is the design ultimate shear load, $F_{s,Rd}$ is the design slip resistance, $F_{b,Rd}$ is the design bearing resistance and $N_{net,Rd}$ is the design plastic resistance of the net cross-section. Furthermore, according to EC3, the positioning of the bolt holes should be such as to prevent corrosion and local buckling, thus the minimum and maximum edge and end distances, as well as the spacing between the bolt holes, were determined according to the following constraints:

$$1.2d_0 \le e_1 \le \min\left\{12b_o, 150\text{ mm}\right\} \quad \text{and} \quad 1.5d_0 \le e_2 \le \min\left\{12b_o, 150\text{ mm}\right\} \tag{I.15}$$

$$2.2d_0 \le p_1 \le \min\left\{14b_o, 200\text{ mm}\right\} \quad \text{and} \quad 2.4d_0 \le p_2 \le \min\left\{14b_o, 200\text{ mm}\right\} \tag{I.16}$$

where d_o is the diameter of the bolt holes, while the other symbols have already been defined in Section 3. The design slip resistance of an individual HSFG bolt is given by:

$$F_{s,Rd} = k_s\ n\ \mu\ F_{p,cd} / \gamma_{Ms} \tag{I.17}$$

where k_s is a constant related to the clearance of the bolt holes (for standard nominal clearances, $k_s = 1$), n is the number of friction interfaces, μ is the coefficient of friction, $F_{p,cd}$ is the design preloading force and γ_{Ms} is the partial safety factor for the slip resistance. The bearing resistance of an individual bolt is:

$$F_{b,Rd} = k_1 a_b\ f_u d\ b_o / \gamma_{M2} \tag{I.18}$$

where $a_b = \min\left\{e_1 / 3d_0,\ p_1 / 3d_0 - 0.25,\ f_{ub} / f_u, 1\right\}$, $k_1 = 1$ for standard clearances, d is the bolt diameter, d_o is the bolt hole diameter and γ_{M2} is the partial safety factor for the resistance of bolted connections. A bolt subject to both shear and tensile force should conform with the following additional constraints:

$$\left(F_{t,Sd} / F_{t,Rd}\right) \le 1 \quad \text{and} \quad \left(F_{v,Sd} / F_{v,Rd}\right) + \left(F_{t,Sd} / \left(1.4F_{t,Rd}\right)\right) \le 1 \tag{I.19}$$

where $F_{t,Sd}$ is the tension resistance of a bolt. More details concerning the Eurocode3 may be found in the existing literature (e.g. Falke, 1996).

I.3.5. Numerical analysis

As mentioned in Introduction, the parameters of the developed environment were the doublers' dimensions (length, width and thickness), the dimensions of the reinforced plate (length, width and thickness), the grade and size of the bolts, the bolt edge and end distances as well as the bolt spacing. It is obvious that the exhaustive combination of all of these parameters gives a huge bulk of results impossible to fit in a few diagrams; thus only indicative cases will be presented. To this end, three typical HSFG bolts, namely $M16$, $M20$ and $M24$ of grade 10.9, were selected in combination with a $14mm$ thick base and doublers of dimensions $L_{x,d} \times 1250 \times 10$ mm (typical dimension in the Hellenic market), with three different values for the length of the doublers $L_{x,d} \in \left\{2000, 1600, 1200\right\}$ being investigated since quite rarely are commercially available plates used with their initial length. The most extreme bolt distributions are the ones were the bolts are positioned in the most condensed and in the most extended way; appropriate values for the parameters e_1, e_2, p_1 and p_2 were determined using Eqs.(7,8). Furthermore, it was considered that $b \in \left[1, 6\right]$ with a step of 0.5. In total, 423 analyses were carried out. The examination of the extreme bolt distributions provided a range covering all the other distributions in between. For the difference between the theoretical and the numerical index to be estimated, the following **N**ormalized **S**tress **R**elief **I**ndex ($NSRI$) was introduced:

$$NSRI = \frac{SR_{FEM}}{SR_{th}} \tag{I.20}$$

In order to examine the adequacy of the bolt connection, the maximum normalized F_{bolt} was defined as:

$$F_{bolt} = \max\left\{\left(F_{v,Sd} / F_{s,Rd}\right), \left(F_{v,Sd} / F_{b,Rd}\right)\right\} \quad \text{(I.21)}$$

The values for the design force components were retrieved from the FE analysis (loads for CERIG noads) and for the most loaded location (point D in Fig.I.12), while two values for the slip coefficient were used, namely $\mu = 0.4$ and $\mu = 0.5$.

I.3.6. Results

In this Section, results from the performed investigation are illustrated in Figs.(I.13-I.20). The stress relief is measured at point A (Fig.I.12); that is at the 50% of the doubler width. The influence on the $NSRI$ for a double-sided reinforcement is illustrated in Figs.(I.13, I.14). For the condensed bolt distribution (Fig.I.13), it is obvious that as the parameter b increases the $NSRI$ decreases approaching asymptotically a limiting value. Practically, for $b \geq 4$ the $NSRI$ is constant. Furthermore, the aforementioned limiting value decreases, as the length of the doublers increases. The type of the bolts has little effect on the $NSRI$. It is obvious that the lower the parameter b is and the shorter the doublers are, the higher the normalized stress relief is, thus the more the theoretical model approaches the numerical model.

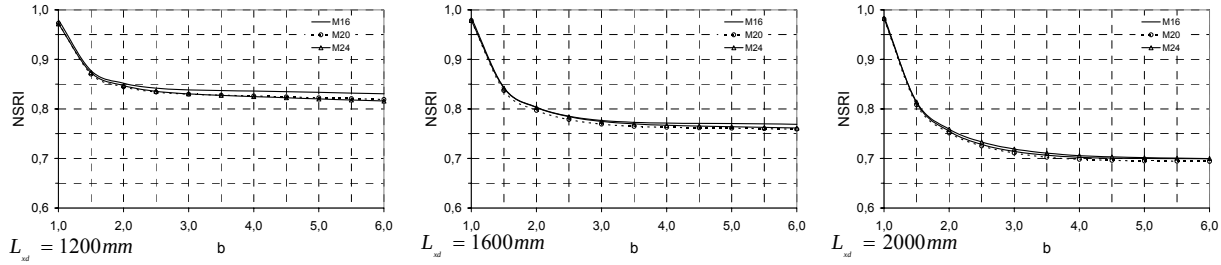

Figure I.13: Normalized stress relief for double-sided reinforcement (condensed bolt distribution)

For the expanded bolt distribution (Fig.I.14), the asymptotic behavior is also observed but is achieved for a definitely higher value of b. Again, this limiting value decreases as the length of the doublers increases, while this time the influence of the bolt size is absolutely negligible. It is strongly emphasized that in all cases the $NSRI$ is less than unity meaning that *the theoretical model predicts a higher stress relief than that estimated by the FE approach*. This is very important because a design based on the theoretical model and without being corrected using the reciprocal of the $NSRI$ is *not* on the safe side.

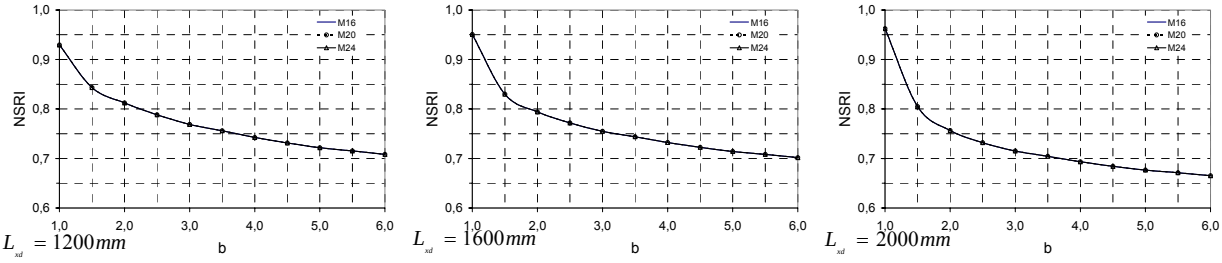

Figure I.14: Normalized stress relief for double-sided reinforcement (expanded bolt distribution)

The influence on the $NSRI$ for a single-sided reinforcement is illustrated in Figs.(I.15, I.16).

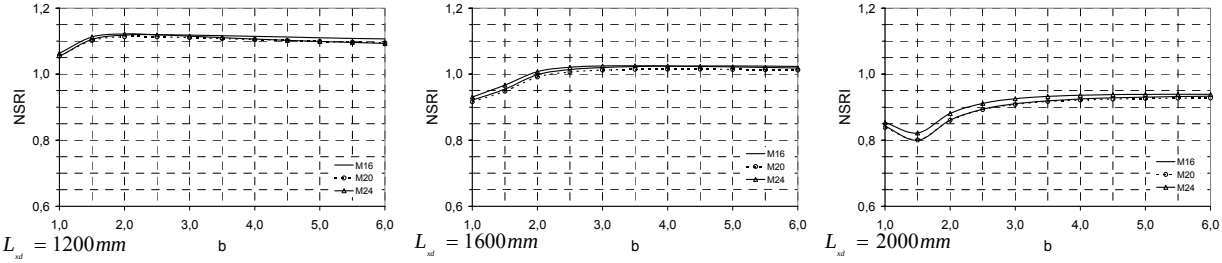

Figure I.15: Normalized stress relief for single-sided reinforcement (condensed bolt distribution)

In this case also, the asymptotic behavior of the *NSRI* with respect to the parameter *b* is present. However, the limiting value is reached quite early for the condensed bolt distribution, while for the expanded bolt distribution the *NSRI* becomes constant for a significantly higher value of *b*. Furthermore, the aforementioned limiting value decreases as the length of the doublers increases. In addition, the bolt type has little effect on the *NSRI*. Finally, it is observed that not always is the *NSRI* less than unity. This means, that for the cases where the *NSRI* is greater than unity, the theoretical approach may be used for a safe estimation of the stress relief. However, for the other cases, the reciprocal of the *NSRI* must be used as a correcting factor on the theoretical estimation.

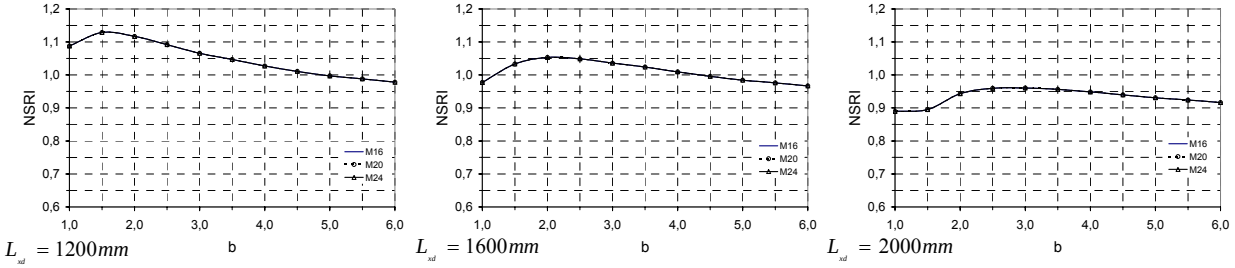

Figure I.16: Normalized stress relief for single-sided reinforcement (expanded bolt distribution)

The influence on the adequacy of the bolted joint for a double-sided reinforcement is illustrated in Figs.(I.17, I.18). It is obvious that in all cases, the bolt size not only is a significant controlling parameter but also affects the maximum normalized F_{bolt} in a clearly nonlinear manner.

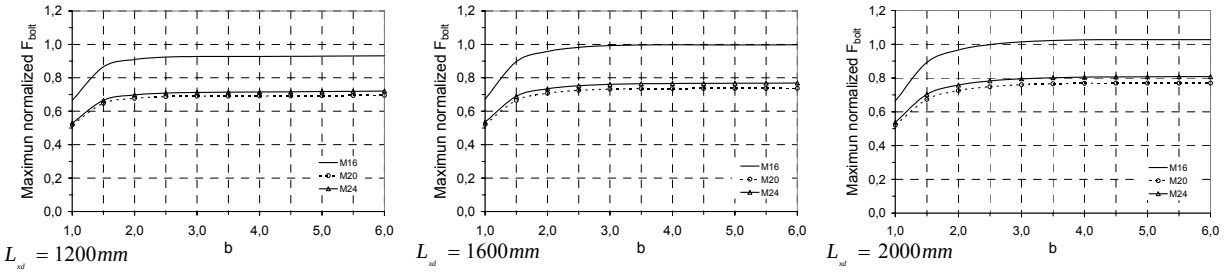

Figure I.17: Normalized bolt adequacy for double-sided reinforcement (condensed bolt distribution)

The parameter *b* has little (strong) influence on F_{bolt} for the condensed (expanded) bolt distribution. The length of the doubler also does not change the adequacy of the bolted joint. However, it is strongly emphasized that while for the condensed bolt distribution the maximum normalized F_{bolt} is at most slightly greater than unity, signifying the compliance with the EC-3 constraints, this is not the case for the expanded bolt distribution where heavy violations occur.

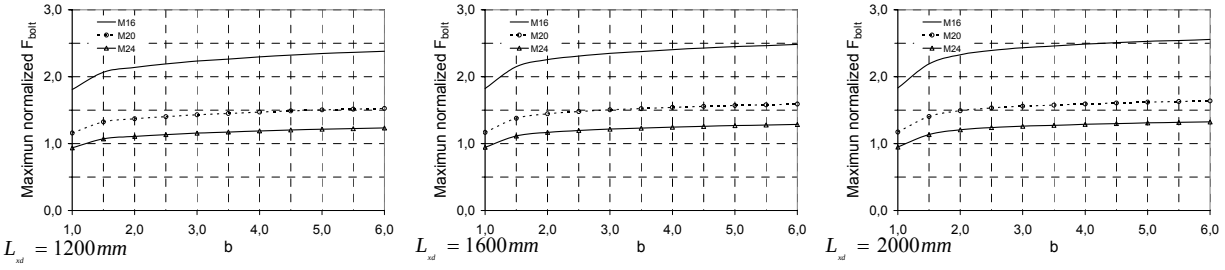

Figure I.18: Normalized bolt adequacy for double-sided reinforcement (expanded bolt distribution)

The adequacy of the bolted joint for a single-sided reinforcement is illustrated in Figs.(I.19, I.20). The remarks are more or less the same with those for Figs.(I.17, I.18). One point worth noting is that the imposed constraints are violated less when compared to those of the double-sided reinforcement. However, this is expected, because in a single-sided reinforcement less shear force will appear at the joint force since less force will be carried by the single doubler, which in turn results in a lower stress relief at the area of interest.

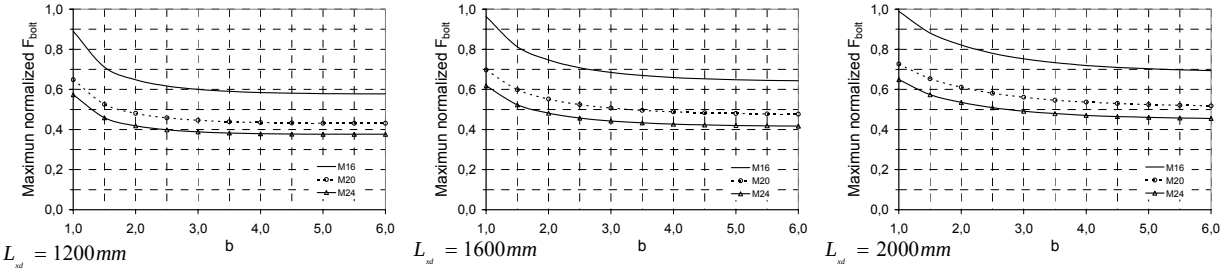

Figure I.19: Normalized bolt adequacy for single-sided reinforcement (condensed bolt distribution)

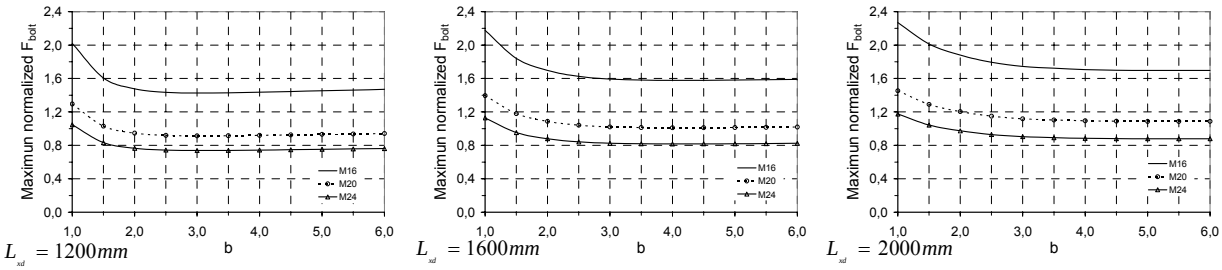

Figure I.20: Normalized bolt adequacy for single-sided reinforcement (expanded bolt distribution)

It is also noted that both for the single and the double sided reinforcement, the constraints stated in Eq.(11) were very far from being violated thus no diagrams were necessary to be created. At this point it is clarified that the $NSRI$ index, apart from indicating how far the theoretical approach is from the numerical approach, also informs about the sensitivity of the numerical approach with respect to the controlling parameters used in the present paper. This results from the fact that the theoretical approach is independent from the aforementioned parameters thus the SR_{FEM} index is proportional to the $NSRI$ index, the constant being the SR_{th} index. Therefore, the comments mentioned in this Section hold, from a qualitative viewpoint, for the numerical approach as well.

I.3.7. Conclusions

The present study is another typical characteristic example of using a sensitivity analysis in the form of a parametric investigation for structural optimization purposes. More particularly, the use of bolted doublers for the reinforcement of a longitudinally loaded plate was investigated. An extremely simple to apply theoretical approach and a more accurate numerical approach were investigated. The parameters examined were the bolt distribution, the bolt size, the length of the doublers, the ratio of the base width over the doublers' width (parameter b) and the single or double sided type of reinforcement. In addition, the constraints imposed by the EC-3 concerning the adequacy of a bolted joint were also taken into consideration. It was shown that the simplified theoretical approach may be used as far as correcting factors derived from the constructed diagrams shown in Section II.3.6 (Results) are introduced. This correction is weaker for the condensed bolt distribution when combined with a small doubler length and a small ratio of the base width over the doubler width. Furthermore, the stress relief at the area of interest, as the parameter b increases, tends asymptotically to a limiting finite value which decreases as the doubler length increases. Finally, the bolt size negligibly affected the stress relief, while small values for the parameter b and for the doublers' length are advantageous to the bolt adequacy, the bolt size affecting it nonlinearly. Concluding, the present investigation provided useful insight concerning the optimal single and double sided reinforcement of shape of a car suspension dome using a simple parametric study as a means for a sensitivity analysis.

I.4. Case study: Racking systems

I.4.1. Introduction

Racking systems are open shelving structures found in storage areas and made of anything from low-tech wood to high-tech metal and plastic. There are many types of racking, the most common of which are the boltless selective pallet rack, the standard configuration of selective pallet rack, the push-back racking, the gravity flow rack, the drive-in/drive-thru racking, the cantilever racking and the wire decking. The efficiency of the beam-end connectors is among the most important factors that determine the performance of a racking system. This efficiency, in combination with the column bases, provides stiffness for down-aisle stability. The

practical importance of racking systems was the motive for an extensive series of works. Hancock described a distortional mode of buckling for cold-formed lipped channel columns that have additional flanges attached to the flange stiffening lips, the so called 'rear flanges', which permit bolting of braces to the channel section so as to form upright frames of steel storage racks (Hancock, 1985). Godley investigated pallets racks using semi-continuous sway frames and concluded that the performance of base-plate connections depends significantly on the level of the axial load (Godley, 1991). In 1993, the Australian Standard for steel storage racking was issued by the Standards Australia Committee on Steel Storage Racking in response to several requests from the Australian racking industry, to improve uniformity of racking performance and enhance public safety (AS4084, 1993). This Standard aimed at setting out minimum requirements for adjustable static pallet racking made of cold-formed or hot-rolled steel. Leach and Davies compared the critical buckling predictions of Generalized Beam Theory (GBT) with the results obtained in two series of tests carried out on lipped and unlipped channels subject to a major axis bending moment and concluded that the GBT is a powerful and effective analysis tool for the solution of interactive buckling problems where both local and overall buckling can occur (Leach and Davies, 1996). Markazi et al. investigated boltless semi-rigid connections that are used in the storage rack industry and described a method which can be adopted to improve the torsional and also distortional strength of thin-walled cold-formed steel columns used in pallet racking systems (Markazi et al, 1997). Davies et al considered the problem of analytically designing the uprights which, in a typical pallet rack, are singly-symmetrical cold formed sections subject to axial load together with bending about both axes (Davies et al, 1997). They concluded that 'Generalized Beam Theory' (GBT) incorporating systematic imperfections can be modified to take account of perforations so that the lower bound results give a sufficiently accurate column design curve, which takes account of local, distortional and global buckling, thus making extensive testing unnecessary. In 1997, the Rack Manufacturers Institute (RMI), which is an independent incorporated trade association affiliated with the Material Handling Industry, issued a specification for the design, testing and utilization of industrial steel storage racks. The 1997 edition was expanded to include complete treatment of seismic design considerations more easily allowing its incorporation by reference into various code documents. Davies and Jiang handled the problem of distortional buckling and they concluded that 'Generalized Beam Theory' offers by far the best vehicle for a fundamental understanding of the subject of distortional buckling (Davies and Jiang, 1998). Baldassino and Bernuzzi presented results of a numerical study on the response of pallet racks commonly used in Europe (Baldassino and Bernuzzi, 2000). Bernuzzi and Castiglioni developed simplified rules for the design of steel storage pallet rack systems in seismic zones and more particularly they carried out an experimental analysis for investigating the behaviour of beam-to-column joints (Bernuzzi and Castiglioni, 2001). Kameshki and Saka developed a genetic-algorithm based optimum design method for nonlinear multistorey steel frames with semi-rigid connections, where the design algorithm resulted in a frame with the least weight by selecting appropriate sections from standard sets of steel sections (Kameshki and Saka, 2001). Papadrakakis et al examined large-scale structural optimization of skeletal structures, such as space frames and trusses, under static and/or seismic loading conditions using combinatorial optimization methods (Papadrakakis et al, 2002). Tian et al carried out a combined experimental and theoretical study on the racking strength and stiffness of cold-formed steel wall frames (Tian et al, 2004). Talikoti and Bajoria developed a method for improving the torsional and also distortional strength of thin-walled cold-formed steel columns used in pallet racking systems by adding simple spacers (Talikoti and Bajoria, 2005). Bajoria and Talikoti tested the flexibility of a connector using both the conventional cantilever method and a newly proposed double cantilever method, while a full scale frame test and a non-linear finite element analysis was also carried out (Bajoria and Talikoti, 2006).

Based on the aforementioned references, it is obvious that the behavior of a steel frame used for racking purposes is strongly dependent on the behavior of the structural elements involved. To this end, the sensitivity of such a frame with respect to characteristics of the posts, of the beams and of the bracing is of importance. Since the estimation of this sensitivity requires a very wide parametric investigation, for the needs of the present paper the interest was focused on the beams only, thus two common cross-sections of racking beams found in the Hellenic market were studied, with their length being a parameter, and the capacity of the corresponding steel frames was estimated. The imposed constraints were in accordance with the EuroCode3 and the parametric investigation carried out, combined with a simple line search technique, was illustrated in ready-to-use diagrams for the maximum capacity of a specific frame or for the length of a known-capacity frame to be estimated.

I.4.2. Theoretical approach

For the steel frame investigated, the constraints imposed were in accordance to EuroCode3 and are very briefly presented in the next paragraphs. More details about the symbols used and the quantities involved may be found in the literature (e.g. Falke, 1996). Furthermore, the actions were calculated in accordance to EuroCode1, while the seismic forces were introduced in a simple manner, as described in the 'Numerical Analysis' section.

I.4.2.1. Tension

At each cross-section of a member under axial tension, the ratio of the design value of the tensile force over the corresponding design tension resistance of the cross-section must be at most equal to unity:

$$\left(N_{Sd} / N_{t,Rd}\right) \leq 1 \tag{I.21}$$

Since no holes for fasteners are present, the design tension resistance is set equal to the design plastic resistance.

I.4.2.2. Compression

At each cross-section of a member under axial compression, the ratio of the design value of the compressive force over the corresponding design compression resistance of the cross-section must be at most equal to unity:

$$\left(N_{Sd} / N_{c,Rd}\right) \leq 1 \tag{I.22}$$

The design compression resistance is estimated differently for Class 1,2,3 and Class 4 cross-sections.

I.4.2.3. Bending (M_y or M_z)

At each cross-section of a member under bending, shear force being not present, the ratio of the design value of the bending moment over the corresponding design bending resistance of the cross-section must be at most equal to unity:

$$\left(M_{Sd} / M_{Rd}\right) \leq 1 \tag{I.23}$$

For uniaxial bending, the resistance is estimated according to the Class of the cross-section.

I.4.2.4. Shear (V_y or V_z)

At each cross-section of a member under shear, the ratio of the design value of the shear force over the corresponding design shear resistance of the cross-section must be at most equal to unity:

$$\left(V_{Sd} / V_{Rd}\right) \leq 1 \tag{I.24}$$

The design shear resistance is equal to the corresponding design plastic shear resistance.

I.4.2.5. Bending and shear (M_z,V_y or M_y,V_z)

The theoretical plastic resistance moment of a cross-section is reduced by the presence of shear. For small values of the shear force, this reduction is so small that it is counter-balanced by strain hardening and may be neglected. However, when the shear force exceeds half the plastic shear resistance, allowance is made for its effect on the plastic resistance moment. In the present paper, the beam profiles examined were of equal flanges, thus the bending about the major axis, if necessary, was appropriately estimated.

I.4.2.6. Biaxial bending and axial force

Depending on the Class of the cross-section, the following constraints with respect to the biaxial bending and the axial force must hold:

- For cross sections of Class-1 or 2:

$$\frac{N_{Sd}}{N_{pl,Rd}} + \frac{M_{y,Sd}}{M_{pl,y,Rd}} + \frac{M_{z,Sd}}{M_{pl,z,Rd}} \leq 1 \tag{I.25}$$

- For cross sections of Class-3:

$$\frac{N_{Sd}}{Af_{yd}} + \frac{M_{y,Sd}}{W_{el,y} f_{yd}} + \frac{M_{z,Sd}}{W_{el,z} f_{yd}} \leq 1 \tag{I.26}$$

- For cross sections of Class-4:

$$\frac{N_{Sd}}{A_{eff}\, f_{yd}} + \frac{M_{y,Sd} + N_{Sd} e_{Ny}}{W_{eff,y}\, f_{yd}} + \frac{M_{z,Sd} + N_{Sd} e_{Nz}}{W_{eff,z}\, f_{yd}} \leq 1 \tag{I.27}$$

It is noted that for the Class-3 and Class-4 cross-sections, it is assumed that no holes for fasteners exist.

I.4.2.7. Flexural buckling

For each compression member, the ratio of the design value of the compressive force over the design buckling resistance must be at most equal to unity:

$$\left(N_{Sd} / N_{b,Rd} \right) \leq 1 \tag{I.28}$$

The design buckling resistance of a compression member is equal to:

$$N_{b,Rd} = \chi \beta_A A f_y / \gamma_{M1} \tag{I.29}$$

where the reduction factor χ determined by the relevant buckling mode is of major importance since it takes into account imperfections that are always met in practice. The beam profiles examined in the present paper were of constant cross-section thus χ could be analytically determined, using values from a buckling curve appropriately selected based on the shape of the cross-section and whether the beam is assumed to be hot rolled or cold formed. It is reminded that lateral buckling and lateral-torsional buckling are not included, because their influence on closed cross-sections is weak. The interested reader may find more details in (Falke, 1996).

I.4.3. Numerical analysis

The behavior of the steel frame illustrated in Fig.I.21a was examined. The modeled frame consisted of four similar posts (or upright columns), six similar beams and a lateral bracing. Each post was of constant cross-section and of $3000\,\text{mm}$ height. The beams were positioned in such a way that the vertical and lateral distance between them was $1200\,\text{mm}$ and $600\,\text{mm}$, respectively. The longitudinal distance L_x between the posts was variable and six different values $L_x \in \{920, 1220, 1520, 1830, 2130, 2440\}$ were investigated. Two different beam profiles made of S235, found in the Hellenic market for racking beams, were examined (Fig.I.21b). The frame was fixed to the ground and the beam-to-post connections were considered to be fixed as well. For the analysis of the frame, the Finite Element Analysis (FEA) commercial software ANSYS was used. The posts and the beams were modeled with BEAM4 elements, while the bracing was modeled with LINK8 elements. It is noted that BEAM4 is a uniaxial element with tension, compression, torsion, and bending capabilities. This element has six degrees of freedom at each node, namely three translations in the nodal x, y, and z directions and three rotations about the nodal x, y, and z axes. Furthermore, LINK8 is a spar which may be used in a variety of engineering applications, such as to model trusses, sagging cables, links, springs, etc. The 3-D spar element is a uniaxial tension-compression element with three degrees of freedom at each node; the translations in the nodal x, y, and z directions. Each beam was divided in ten segments and the corresponding quantities (displacements, forces and moments) were estimated at each node. The frame carried a uniform load distribution q over the beams of each storey (vertical red arrows in Fig.I.21a). The maximum value of this load was sought so that no constraints according to EuroCode3 were violated. More particularly, constraints concerning compression, tension, bending, shear, shear and bending, biaxial bending and flexural buckling were imposed. Constraints concerning lateral-torsional buckling, as well as lateral buckling and bending due to compression were not imposed since closed cross-sections were used, for which the aforementioned constraints are not critical. In addition, the activation of the gravitational acceleration provided the means for the self-weight to be included as well. Furthermore, imperfections were also taken into consideration. For this purpose, horizontal forces (horizontal red arrows in Fig.I.21a) were estimated based on the number of the storeys, the number of the posts and the load distribution q. Two different cases were examined, namely with and without the contemporaneous presence of earthquake. In more details, the seismic coefficient is estimated according to the new Hellenic regulations for seismic design and with respect to significance of the structure, the ground, the foundation, the type of the structure, etc. For each storey, the corresponding equivalent horizontal seismic forces were applied as a static load, the permanent loads being taken into account. For the application of the earthquake, the combination $X + 0.3Y$ was used, which is the worst combination since the frame is laterally restrained along

the Y-direction (the coordinate system used is also illustrated in Fig.I.21a). For the application of the load distribution q, the coefficient for the permanent loading has not been introduced.

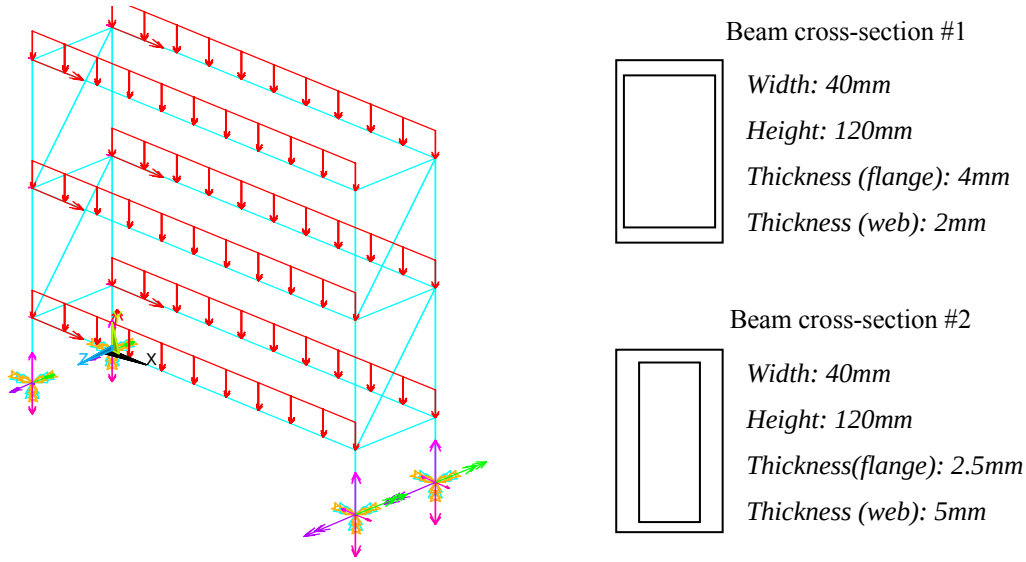

Figure I.21: Frame examined (a) developed model and (b) beam cross-sections used

Finally, it is clarified that for the needs of the performed investigation, it was required to analyze a large number of frames, thus a code in ANSYS/APDL, the script language of ANSYS, was developed, including the entire procedure of the parametric modeling, the analysis and the check against constraint violations.

I.4.4. Results

The maximum uniformly distributed load $q_{\max}$ that a beam, of the specific frame shown in Fig.I.22, can carry was estimated through the solution of a 1D constrained optimization problem, implementing a simple line search technique and a hard-kill penalization scheme for the violation of any imposed constraint.

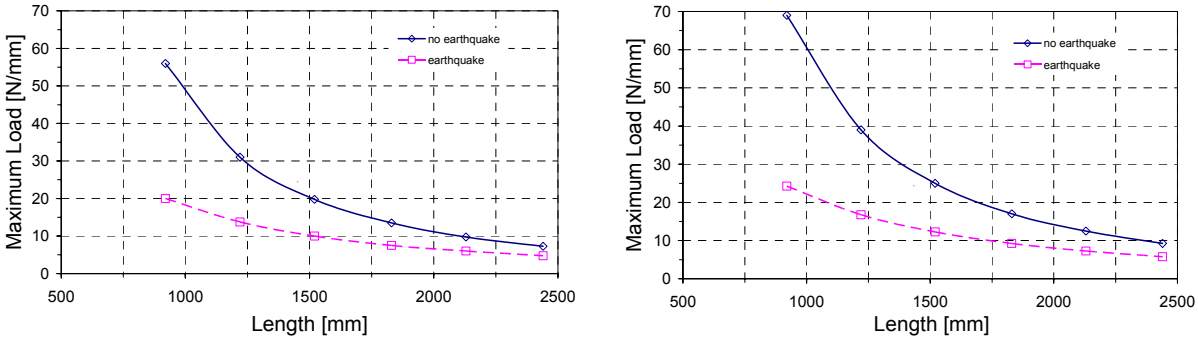

(a) Cross Section #1 (b) Cross-Section #2

Figure I.22: Maximum allowable load for (a) Beam Cross-Section #1 and (b) Beam Cross-Section #2

It is obvious that for different beam lengths and for different beam profiles, $q_{\max}$ is different. Fig.I.22a and Fig.I.22b illustrate the variation of $q_{\max}$ with respect to the beam length L_x (continuous line) for the first and the second beam profiles examined, respectively. It yields that as the length increases, $q_{\max}$ decreases tending asymptotically to a limiting and finite value, this decrease being very steep for short beams. For example, from Fig.I.22a, comparing two beams of lengths $1000\,\text{mm}$ and $2000\,\text{mm}$, respectively (increase of 100%), the corresponding values of $q_{\max}$ are $50\,\text{N/mm}$ and approximately $10\,\text{N/mm}$ (decrease of almost 80%). This means that, for short beams, the beam length is definitely of major importance in determining $q_{\max}$. Furthermore, $q_{\max}$ is larger in Fig.I.22b than in Fig.I.22a, meaning that the second beam profile with thicker

webs and thinner flanges generally provides larger resistance, thus the corresponding frame capacity is larger as well. In addition, Fig.I.22 illustrates the variation of $q_{\max}$ under the presence of earthquake (dashed line). It yields that taking earthquake resistance into account significantly decreases the maximum load that can be carried. This decrease is stronger for short beams, while as the beam length increases, $q_{\max}$ decreases asymptotically to a limiting and finite value. The diagrams in Fig.I.22a have a two-fold interpretation, the direct and the reverse. According to the direct interpretation, if the beam profile and beam length are known then it is possible to estimate the capacity of the beam, thus the capacity of the frame. According to the inverse interpretation, for a given capacity of the frame, thus for a given capacity of the beam, it is possible to estimate the maximum length a beam of a specific profile may have, with no constraints being violated. From this point of view, Fig.I.22a illustrates ready-to-use diagrams for practical engineering purposes. The maximum allowable load, that is the capacity of each beam, was based on using the absolute maximum values for the axial force, the shear force and the bending moments estimated at the nodes of the beams. For the structural-member adequacy, all of the nodes of each structural member were checked. For each check, the ratio of the design force S over the resistance R was estimated. The normalized quantity (S/R) should be less than or at most equal to unity, for no constraints according to EC3 to be violated.

Table I.2: Description of the constraints

Compression : C1	Buckling : C2	Tension : C3
Bending M_y : C4	Bending M_z : C5	Shear V_y : C6
Shear V_z : C7	Bending M_z and shear V_y : C8	Bending M_y and shear V_z : C9
Biaxial bending : C10	Flexular buckling : C11	

The EC3 constraints imposed in the present study are shown in Table II.2. The corresponding coded names are used in Figs.(I.23, I.24).

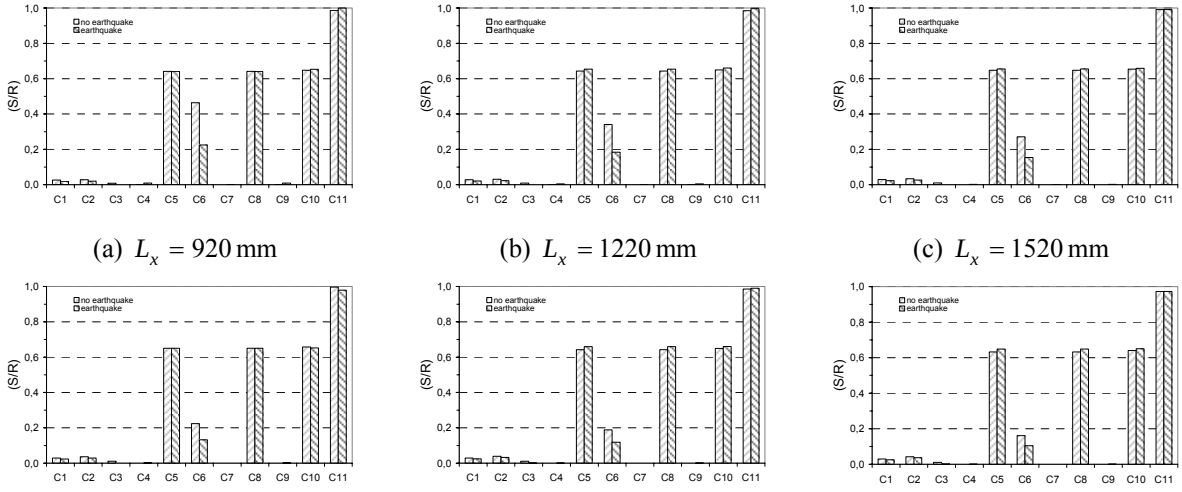

(a) $L_x = 920\,\text{mm}$ (b) $L_x = 1220\,\text{mm}$ (c) $L_x = 1520\,\text{mm}$

(d) $L_x = 1830\,\text{mm}$ (e) $L_x = 2130\,\text{mm}$ (f) $L_x = 2440\,\text{mm}$

Figure I.23: Adequacy of the frame for beam cross-section #1 and various beam lengths

These figures illustrate the aforementioned normalized ratios and describe vividly not only which constraints are dominating but also how much the constraints differ from each other. Having such information at hand makes improving the beam profile design and increasing the capacity of the frame possible. Fig.(I.23) illustrates the adequacy of the examined frame, for the first of the two beam profiles used, for various beam lengths, with and without the presence of earthquake.

It yields that, out of the eleven checks, four seem to be more 'active', namely the bending M_z, the bending M_z and shear V_y, the biaxial bending and the flexural buckling. However, the most dominating one was the constraint for the flexural buckling. When the value of the normalized ratio (S/R) was near unity, the corresponding values for the other three were approximately 0.7. Practically, this means that it is possible to

ignore all the constraints but the one for flexural buckling. As shown in Fig.(I.23), the effect of the earthquake on the normalized ratios is negligible for all the constraints but the shear V_y. However, it is strongly emphasized that this negligible effect concerns only the adequacy against failure of the structure and not its capacity, which is severely affected as illustrated in Fig.(I.22) and commented in the previous paragraph. Furthermore, the buckling resistance may be increased in various ways, such as appropriately increasing the area of the beam profile, decreasing the slenderness of the beam and changing the beam profile, so that it becomes a Class-1 to Class-3 cross-section. In addition, it yields that, for all the examined lengths, the constraints for tension, bending M_y, shear V_z, as well as bending M_y and shear V_z, have practically no effect on the resistance of the beam. The remarks for the plots of Fig.(I.23) also hold for the plots of Fig.(I.24), which were obtained for a closed beam profile with thicker webs and thinner flanges than the profile used for Fig.(I.23).

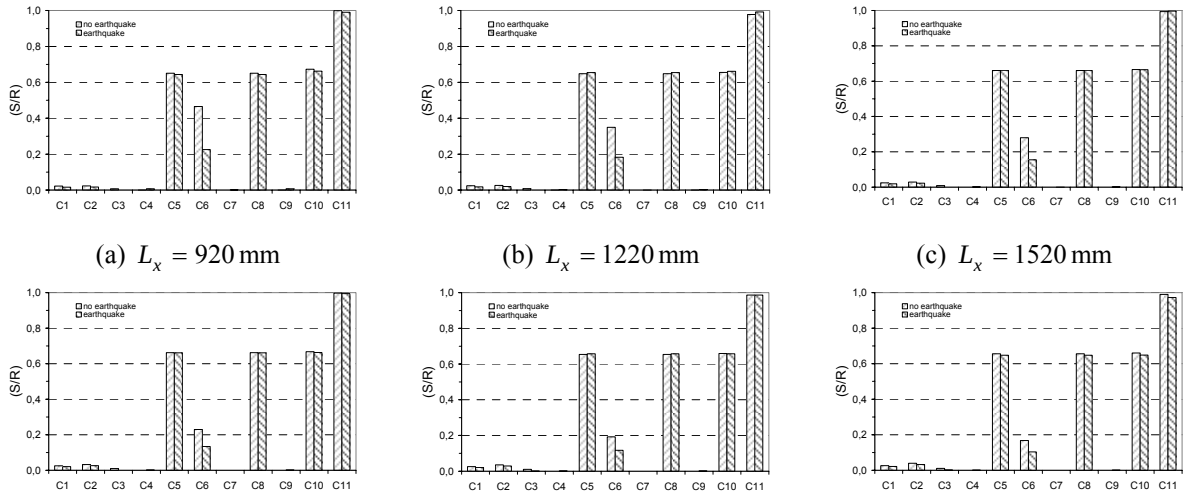

(a) $L_x = 920\,\text{mm}$ (b) $L_x = 1220\,\text{mm}$ (c) $L_x = 1520\,\text{mm}$

(d) $L_x = 1830\,\text{mm}$ (e) $L_x = 2130\,\text{mm}$ (f) $L_x = 2440\,\text{mm}$

Figure I.24: Adequacy of the frame for beam cross-section #2 and various beam lengths

It yields that for each examined beam length, the normalized values $\left(S / R\right)$ do not practically change.

I.4.5. Discussion

The complete study of a racking system is a very interesting and complicated issue, both from a structural and an economical point of view. The main goal is to maximize the capacity of the system, keeping the size of the structural elements involved as low as possible. To this end, the posts, the beams and the bracing must be thoroughly examined both individually and as an assembly. The parameters to be examined are mainly the profiles of the posts and the beams, as well as the dimensions of the racking system. The constraints that must be satisfied concern both ultimate limit and serviceability limit states, while the presence of earthquake must also be taken into account. Estimating the sensitivity of the racking system capacity with respect to all of the factors mentioned above requires an extensive parametric investigation, which may be divided in three parts, namely the investigation of the posts, of the beams and of the bracing. In the present paper, the beams are studied only.

The study of a racking beam should be such that its capacity is estimated for various determining characteristics, such as the beam profile, the beam length, the presence of earthquake and the beam-to-column connection. The beam profiles examined were two of the most common cross-sections found in the Hellenic market. Both of them were of closed type, doubly symmetric, they had the same width and height but differed in the flange and web thickness; the first had thicker flanges and the second had thicker webs, as shown in Fig.(I.21b). The beam lengths examined were also retrieved from the Hellenic market and concerned typical standard dimensions. The same holds for the lateral and the vertical distance between the beams. The presence of the earthquake was introduced in a simple but valid manner, often used in practicing engineering offices. Furthermore, it was assumed that the beam-to-column connection was fixed. This is a valid assumption since, in most practical cases, the beams have specially formed end-hooks which clasp in the posts and provide a rigid connection. Such a connection is desirable, because it ensures that the deflection of the beam (sagging) will be the least possible which in turn ensures that not only the bottom of the racked pieces will be in full contact with the beam but also the effective vertical space between two storeys is maintained. It is obvious that if a hinge was used instead, the sagging of the beam would severely reduce the serviceability of the racking system.

The entire investigation was coded in ANSYS/APDL. It is noted that this script language does not offer subroutines or functions, which other programming language have as a standard tool for obvious programming reasons. As an alternative, parts of the lengthy developed code, that in another programming language would have been written in subroutines or functions, were saved in different files, all of which were called from a main file. On the other hand, ANSYS software offers build-in optimizers which may be used for the optimum design of the entire racking system, which is the subject of an undergoing investigation by the authors.

The results of the parametric investigation were illustrated in diagrams which can be used in a two-fold manner, the former being the estimation of the capacity for a given beam and the latter being the estimation of the beam for a given capacity. For the former case, a vertical line is drawn for the respective value of the x-axis until the curves of Fig.(I.22) are met and then horizontal lines are drawn towards and up to the y-axis, the corresponding values being recorded. Each time, two values are recorded, with and without the presence of earthquake. For the latter case, the procedure is reversed, beginning from the y-axis and ending at the x-axis. Additionally, in both cases, information concerning the adequacy of the beams can be retrieved from Figs.(I.23, I.24).

I.4.6. Conclusions

The present study aimed at revealing the way a sensitivity analysis combined with a simple line search technique may be used for structural optimization purposes. More particularly, the beams in a steel frame used for racking purposes were examined through the investigation of 3D frames using the Finite Element Method. The actions were applied according to the EuroCode1, the constraints imposed were in accordance to the EuroCode3, while both the self-weight of the beams and their earthquake resistance were taken into account. It was found that for short beams, a small change in the beam length results in a severe change in the beam capacity. The same result occurs when earthquake is present. On the contrary, for lengthy beams these changes are less intense and asymptotically tend to become constant. Furthermore, it was found out that from the beams examined, the one with the thicker webs and thinner flanges had a higher load capacity. In addition, from the constraints imposed, flexural bending was the predominating one, the others being quite far from being violated. The results of the present study are illustrated in ready-to-use diagrams for either estimating the maximum capacity of the beams of a specific racking system or determining the beams for a racking system of known capacity. Therefore, the creative implementation of a typical sensitivity analysis in combination with a simple line search technique may be used for structural optimization practicing purposes.

I.5. Case study: Solar tracker

I.5.1. Introduction

A solar tracker is a device for orienting a day-lighting reflector, solar photovoltaic panel or concentrating solar reflector or lens toward the sun. The sun's position in the sky varies both with the seasons and time of day as the sun moves across the sky. Solar powered equipment works best when pointed at or near the sun, so a solar tracker can increase the effectiveness of such equipment over any fixed position, at the cost of additional system complexity. There are many types of solar trackers, of varying costs, sophistication, and performance. One well-known type of solar tracker is the two-axis mount, according to which one axis is a vertical pivot shaft, or horizontal ring mount, that allows the device to be swung to a compass point, while the second axis is a horizontal elevation pivot mounted upon the azimuth platform. By using combinations of the two axes, any location in the upward hemisphere may be pointed. The references with respect to the solar trackers may be categorized in three groups. The first group refers to publications regarding the photovoltaic cell technology, the second group refers to publications regarding the control systems that ensure the solar tracking, while the third group refers to steel structures used for supporting photovoltaic panels.

The present paper refers to the subject of the aforementioned third group. It is noted that the published works in this field are not as many as anticipated. The reason for this might be the fact that solar trackers are a relatively new technological product (in Greece, the first international exhibition was organized in November 2008) utilized for earning money, thus relative information is not widely spread. Another evidence for enforcing this opinion is the large number of patents issued for solar tracker drawings (e.g. US Patent nos: 3917942-1975, 4215410-1980, 6239353–2001, 200501330-2005, 4175391, 20040112373, 20070100557, 20080245402). Some of the most interesting publications on the subject are briefly presented in the following paragraphs. Helwa et al completed an experimental study, with four systems, the layout of which were a fixed system facing south, a vertical-axis tracker, a tilted-axis tracker and a two-axis tracker (Helwa et al, 2000). The purpose of the study was the comparison between the four systems and with respect to the collected solar energy. The measurements lasted one year and concerned the solar radiation input to the systems and the electric power output from them. The main conclusion was that the dual-axis solar tracker presented a higher capability of solar energy collection and electric power production.

Lorenzo et al dealt with the investigation of those parameters that define the formulation of the design of a single-axis solar tracker and they ended up with the best solar-tracker distribution for the photovoltaic park in

Tudela (Spain) (Lorenzo et al, 2002). For the optimization problem they solved, they considered that, approximately, the cost per unit of produced energy is a linear function of the ratio of the total investment over the yearly produced energy. They also considered that it is possible to apportion the total investment in two parts, the former being related to costs of land, such as purchase of land, fencing, wiring, infrastructure, etc), and the latter being related to solar tracker costs. In this study it is worth noting that, as the authors state, the optimum design of the park was based more on aesthetics rather than the optimum solution derived from their analysis, while the fact that the cost of dual-axes solar trackers continuously decreases, thus changes the parameters taken into account.

Abdallah carried out an experimental study in order to find out the differentiation in the current characteristics produced by static and rotating solar trackers. In this study, he used four solar trackers: one dual-axis tracker, one vertical axis tracker, one single-axis tracker oriented along the E-W direction and one single-axis tracker oriented along the N-S direction; he also used a heliostat. According to the results of this study, the characteristic properties of the current (nominal voltage, nominal amperage and nominal power) were much better for the rotating trackers than for the heliostat (Abdallah, 2004).

Luque-Heredia et al studied a dual-axis solar tracker using the Finite Element Method. In more details, they analyzed their designs using the commercial software Ansys ver.7, while they developed a certain concept regarding the design rules that should be followed (Luque-Heredia et al, 2007). According to their approach, the design of the steel structure of the solar tracker must be based on operational characteristics, such as the easy transportation to the location of installation and the simplicity in assembling the tracker. Once the design is determined, the dimensioning follows in such a way that the structural weight is minimized without violating any ultimate limit state or serviceability limit state constraints; for this purpose, the use of standard profiles is highly recommended. It is noted that Luque-Heredia et al consider the bending of the structure carrying the photovoltaic cells as of primary importance, because, due to this bending, the normal vector to the photovoltaic panel may decline from the direction of the solar beams thus reduce the efficiency of the solar device.

Mavromatakis and Franghiadakis suggested a new type of single–axis solar tracker, on which they adjusted a prototype mechanism which allows for the rotation of the photovoltaic panel about two axes (OBI, patent No. 1005380/2006). In this way, their tracker behaves as if it was a dual-axis tracker and at the same time it has a better performance on an annual basis (Mavromatakis and Franghiadakis, 2008). The latter conclusion was drawn from a study that Mavromatakis and Franghiadakis carried out comparing the efficiency of their tracker to that of two other trackers (one heliostat and one dual-axis tracker).

(a) (b) (c)

Figure I.25. Commercial solar trackers by (a) Poulek Solar, (b) ELBITYL and (c) Inspira.

Apart from interesting references on the subject (Geiger et al, 2002, Hay and Davies, 1978), various companies provide, through their websites, information with respect to specifications and designs. However, although almost all companies promote their products as of high efficiency, no comment is on the layout optimization of the trackers. Therefore, the challenge and the purpose of the present work were to investigate the layout optimization of solar trackers. Towards this direction, a fully-parameterized dual-axis solar tracker of a specific design concept (design type), having a total panel surface of 150m^2, was designed and optimized using the Finite Element Method and in accordance to the EuroCode 3 standard. For the structural analysis, the commercial software Ansys ver.10 was used, while the optimization was carried out based on the sub-problem approximation and the first-order method implemented in the aforementioned software. In total, the parametric design included 40 design parameters, as well as the corresponding geometric constraints ensuring the feasibility of the design. In this way, a high-level layout optimization was carried out. For each optimization step, a fully-scaled 3D plate model was developed, while for the analysis a large-displacement non-linear solver was used. The main contribution of the present work was the development of a procedure for getting the layout optimization of a solar tracker of a specific design type but of any total panel surface.

I.5.2. Theoretical approach

I.5.2.1. Parametric design of the solar tracker

The main aim of the present work was to optimize a parametric design of a typical dual-axis solar tracker. Towards this direction, first a typical design was selected and then the design variables serving as design parameters were defined. More particularly, the solar tracker consisted of:

- Two slew drives for the rotation about the horizontal and the vertical axis.
- Two vertical cylindrical members, the lower rigidly connected to the ground and the upper being able to rotate about the vertical axis.
- Four flanges.
- One RHS cross beam for supporting the entire upper part of the tracker.
- One CHS beam serving as the driving shaft of the tracker for the horizontal rotation.
- Two RHS beams forming a frame (frame beams) for supporting the panel with the photovoltaic cells.
- Plates for supporting the driving shaft on the cross beam.
- C-channels, where the photovoltaic cells are mounted on. These channels are placed in pairs, the only exception being the channels at the edge of the panel.
- Angles (in pairs) for mounting the C-channels on the aforementioned frame.
- Photovoltaic cells.

In total, 40 design variables were implemented, as shown in Table 1. In the same Table, 13 variables are shown in bold and italic font. These are the variables that affect more the structural weight and the ones finally used in the present investigation.

Table I.3: Parametric design variables

ID	Variable	ID	Variable
1	Number of photovoltaic cells (x-direction)	***21***	***Height of cross beam***
2	Number of photovoltaic cells (y-direction)	***22***	***Thickness of cross beam***
3	Length of photovoltaic cell	23	Length of driving shaft
4	Width of photovoltaic cell	***24***	***Radius of driving shaft***
5	Thickness of photovoltaic cell	***25***	***Thickness of driving shaft***
6	Maximum angle of horizontal rotation	26	Length of frame beam
7	Radius of lower cylindrical base	***27***	***Width of frame beam***
8	Height of lower cylindrical base	***28***	***Height of frame beam***
9	Thickness of lower cylindrical base	***29***	***Thickness of frame beam***
10	Radius of upper cylindrical body	30	Radius of support for driving shaft
11	Height of upper cylindrical body	31	Height of support for driving shaft
12	Thickness of upper cylindrical body	***32***	***Thickness of support for driving shaft***
13	Radius of lower flange	33	Length of C-channels
14	Thickness of lower flange	***34***	***Width of C-channels***
15	Flange radius for joint with slew drive	***35***	***Height of C-channels***
16	Flange thickness for joint with slew drive	36	Length of reinforcements for C-channels
17	Radius of upper flange	***37***	***Thickness of C-channels***
18	Thickness of upper flange	38	Length of angles for C-channel mounting
19	*Length of cross beam*	39	Width of angles for C-channel mounting
20	***Width of cross beam***	***40***	***Thickness of angles for C-channel mounting***

The dimensions, in meters, of each photovoltaic cell were $0.820 \times 1.650 \times 0.050$. The photovoltaic panel was chosen to carry 112 photovoltaic cells, corresponding to a total surface of $151 m^2$ and a total weight of $2023 kg$. In addition, the material used for the structure was plain structural steel (modulus of elasticity $210 GPa$, Poisson's ratio 0.3 and density equal to $7850 kg / m^3$).

I.5.2.2. Modeling

A full 3D surface model was created using the mean surfaces of the 3D solid parts consisting the solar tracker. Indicative modeled parts are shown in Fig.I.26.

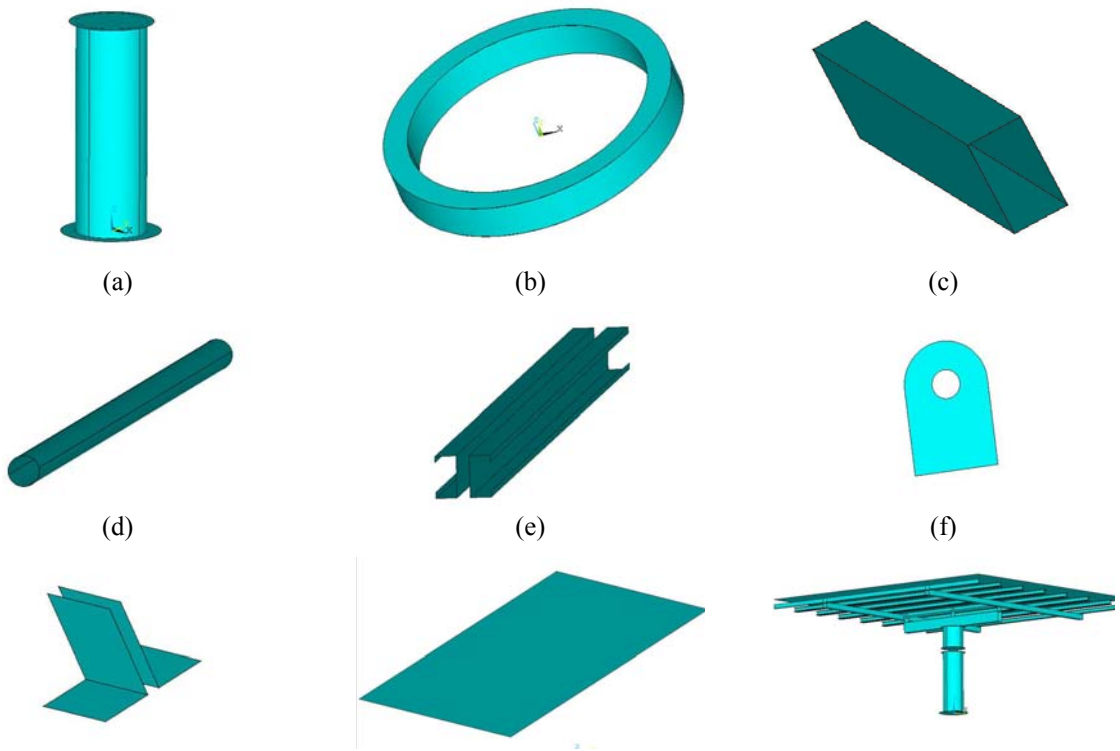

Figure I.26: Parts of the solar tracker model: (a) cylindrical base, (b) slew drive, (c) RHS cross beam, (d) CHS driving shaft, (e) pairs of C-channels, (f) driving-shaft supporting plates, (g) pairs for C-channel mounting, (h) photovoltaic panel and (i) assembly.

The ability of the parametric design is demonstrated in Fig.I.27, where two characteristically different designs are shown.

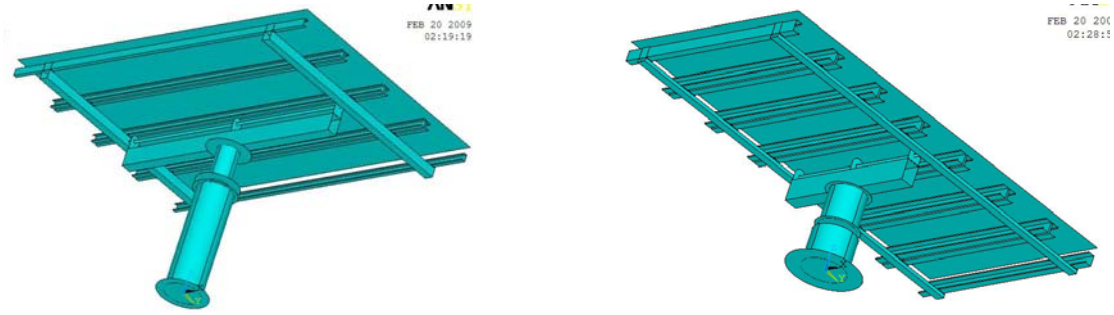

Figure I.27: Designs for a panel of $65m^2$ and for different number of photovoltaic cells (a) 4×12 and (b) 7×7 cell array.

Apart from the parametric design itself, it is of primary importance to ensure that a high-quality mesh may be created. For this purpose, creating a mapped mesh is a good choice. However, this may be achieved only if special care is taken with respect to the areas around member joints. More particularly, it is required to additionally divide the surfaces in such a way that always four-sided sub-areas are created, as illustrated Fig.I.28.

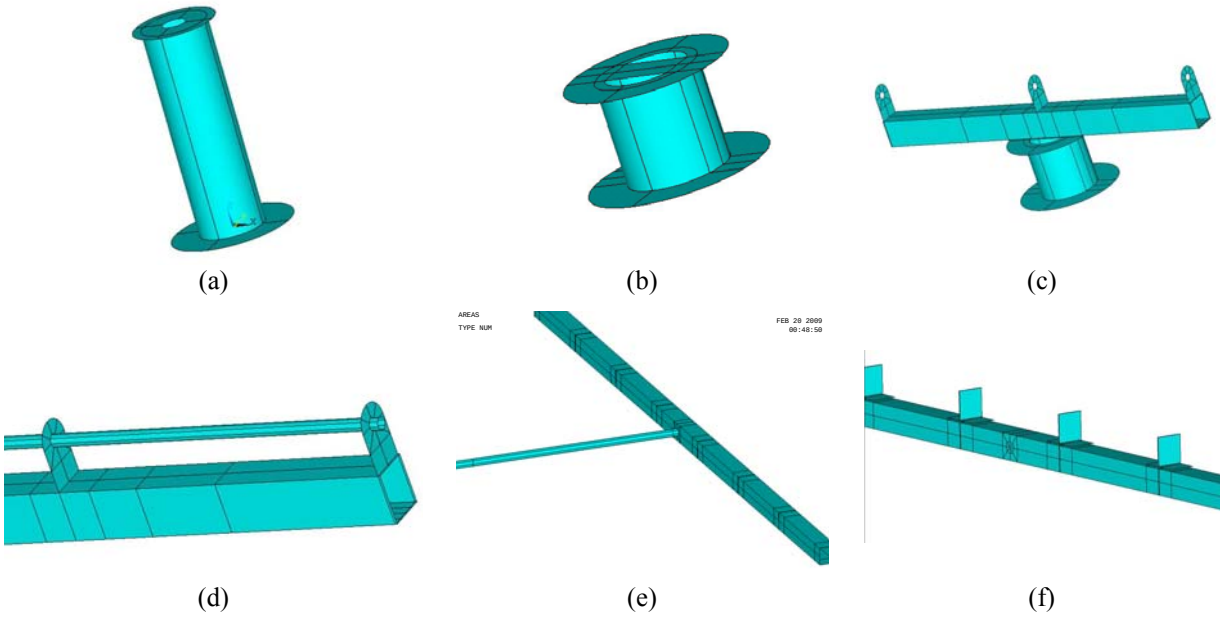

(a) (b) (c)

(d) (e) (f)

Figure I.28: Surface division necessary for creating a mapped mesh: (a) cylindrical base, (b) cylindrical body, (c) assembly of the cross beam, (d) detail of the driving shaft mounting, (e) driving shaft-RHS beam joint, and (f) beam with pairs for C-channel mounting plates.

I.5.2.3. Boundary conditions

It was assumed that the solar tracker was rigidly supported along the lower flange of its cylindrical base. In addition, a wind pressure of $1000Pa$ was assumed. This pressure corresponds either to a wind velocity of $30m$ / sec with a pressure coefficient 1.78 or to a wind velocity of $36m$ / sec with a pressure coefficient equal to 1.23. It is noted that the aforementioned wind velocities are specified for Greece according to EuroCode1. Furthermore, the self weight was taken into account. With respect to the collaborating surfaces, they were all assumed to be in an 'always-bonded' contact mode.

I.5.2.4. Constraints

For the ultimate limit state, it was assumed that the maximum von Mises stress should be at most equal to $140MPa$. For the serviceability limit state, it was assumed that the maximum deflection should be at most equal to $0.04m$. The stability of the structure was examined by carrying out a non-linear analysis; if no snap-through buckling was present along the compression zone of the structure then the structure was considered to be stable, as Eurocode 3 (Annex C) describes. The dynamic effects due to the wind loads were examined by carrying out an eigen-frequency and checking whether the fundamental frequency was higher than $1Hz$.

I.5.2.5. Selection of Slew-Drives

Two slew drives (IMO) were responsible for the rotational motion of the solar tracker. The size of the slew drives must be taken into consideration since certain geometric characteristics, such as the radius of the cylindrical base and the radius of the driving shaft. Therefore, the procedure for selecting a slew drives must be embedded in the optimization scheme. This procedure is as follows:

Step 1: Estimate the equivalent axial load F_{axD}:

$$F_{axD} = F_{ax}\ f_a \tag{I.30}$$

where F_{ax} is the axial load and f_a is a safety coefficient.

Step 2: Estimate the equivalent bending load M_{kD}:

$$M_{kD} = \left(M_k + 1.73F_{rad}\left(\frac{D_L}{1000}\right)\right) f_a \tag{I.31}$$

where F_{rad} is the radial load, M_k is the bending moment and D_L is the raceway diameter.

Step 3: Check for radial load (in case of violation, a special design is necessary):

$$F_{rad} \le \left(220\left(\frac{M_k}{1000} \right) + 0.5F_{ax} \right) \tag{I.32}$$

Step 4: Check with respect to the axial and bending load. For this purpose, appropriate diagrams of equivalent axial load and equivalent bending moments must be used (Fig.I.29). On this diagram, the point (F_{axD}, M_{kD}) estimated from the previous steps is marked. All curves lying above this point correspond to systems that can safely carry the applied loads, under the assumption that these loads are static. In case of dynamic loads, the system endurance must be also checked.

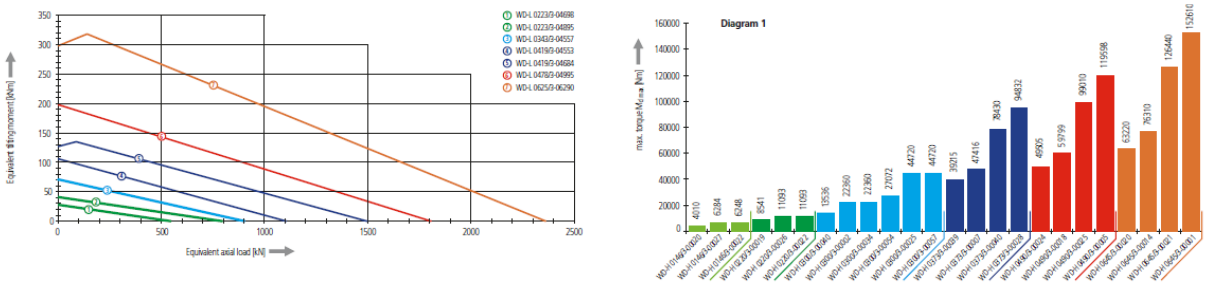

Figure I.29: Useful diagrams for selecting slew drive (Steps 4 and 5)

Step 5: Static reliability verification against operating torque. The operating torque must be in compliance with diagrams, such as the one shown in Fig.I.29. That is, all slew drives that can provide a maximum torque larger than the estimated one may be used.

Step 6: Estimate the maximum permissible duty per minute. First the following ratio is estimated:

$$f_{MD} = \left(\frac{M_{d,B}}{M_{d,\max}} \right) \tag{I.33}$$

where $M_{d,B}$ is the operating torque and $M_{d,\max}$ is the maximum operating torque of the system. In the sequel, diagrams, such as the one shown in Fig.I.30, are used so that the maximum permissible duty per minute $ED_{\max}$ (in %) is estimated. Obviously, for a slew drive it must hold $ED_B \le ED_{\max}$.

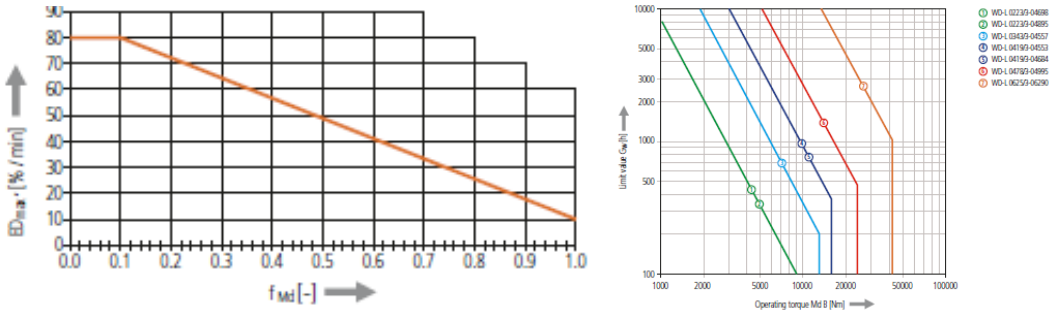

Figure I.30: Useful diagrams for selecting slew drive (Steps 6 and 7)

Step 7: Verify wear characteristics of worm gear. With respect to the operation time B_h and the specification ED_B, the following limit value is estimated:

$$G_{w,oper} = B_h \left(\frac{ED_B}{100} \right) \tag{I.34}$$

Based on the operational moment $M_{d,B}$ and diagrams such as the ones shown in Fig.I.30, the allowable value $G_{w,allow}$ is estimated. Obviously, a slew drive is adequate when $G_{w,allow} \ge G_{w,oper}$.

I.5.2.6. Optimization procedure

The optimization procedure applied in the present work was as follows:

Step 1: Definition of design parameters and selection of initial design vector
Step 2: Check geometric constraints; in case of violation, select another initial design vector
Step 3: Design of mean surfaces
Step 4: Boolean operations on surfaces (division and union) for a mapped mesh to be created
Step 5: Generate mapped mesh using shell elements
Step 6: Connect external surfaces of plates using contact elements
Step 7: Apply boundary conditions
Step 8: Analyze the structure
Step 9: Estimate the structural weight and quantify the mechanical behavior
Step 10: In case of convergence, or if the maximum number of iterations has been exceeded, then STOP
Step 11: Redesign the shell thicknesses and go to Step 8

For the redesign, first the subproblem approximation method was applied sequentially three times and then the first order method was implemented (both optimizers are embedded in Ansys). The sub-problem approximation method required 10 iterations (approximately 4 hours) to converge, while the first order method converged in two iterations only (approximately 12 hours).

I.5.3. Results

After the application of the procedure described in Section 2.6, an optimized design was derived, weighting $5965kg$ (the steel structure only). The imposed stress and displacement constraints were not violated, while the stability was examined through a non-linear analysis, characteristic results of which are shown in Fig.I.31.

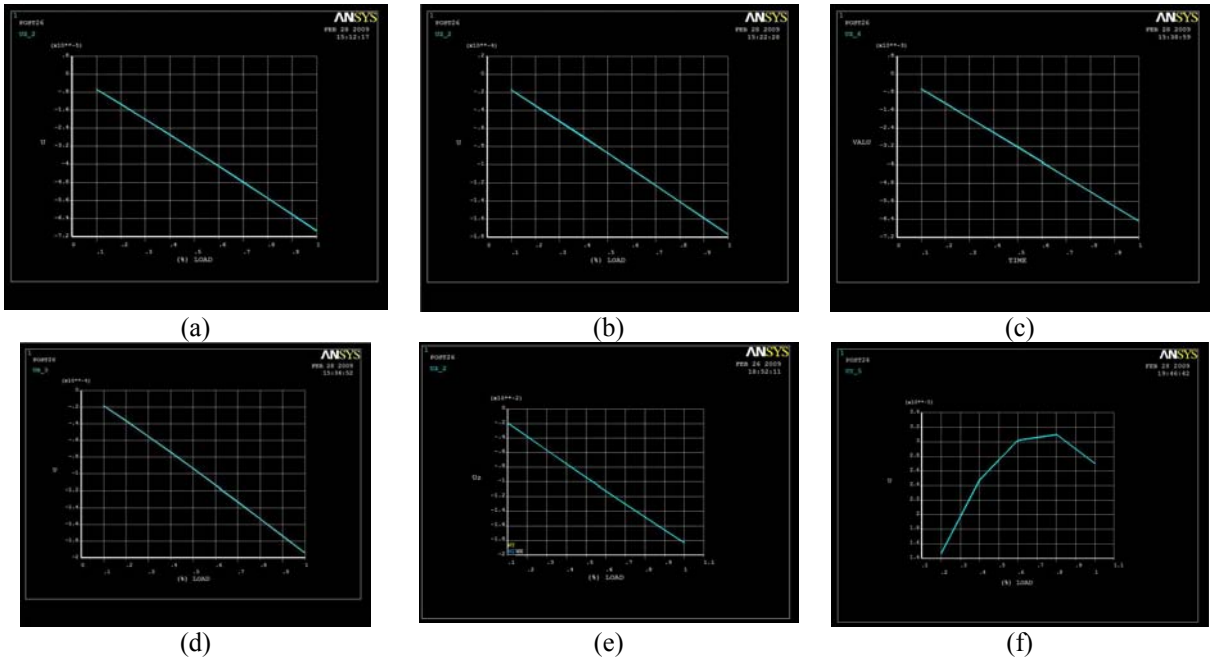

Figure I.31: Verification against stability for (a) the cylindrical base, (b) the cylindrical rotating body, (c) the frame beam, (d) the C-channels, (e) the cross-beam and (f) for wind pressure of $4.5kPa$.

From Fig.I.31, it is obvious that the optimized structure is stable, while instability problems occur for a wind pressure of approximately $0.8 \times 4.5 = 3.6kPa$ (Fig.I.31f). For the sensitivity of the structure with respect to dynamic effects, the eigenfrequencies were estimated using the PCG Lanczos method. The fundamental frequency was estimated to be approximately equal to $3.06Hz$, which is higher enough from the lower limit of $1Hz$. Therefore, the optimized structure may carry with safety the applied loads.

I.5.4. Discussion

Solar energy is everywhere and for free. Therefore, it is essential that, for environmental reasons, this reservoir be exploited. Towards this direction various types of solar trackers have been designed and manufactured. However, for the optimum solution to be found in terms of energy efficiency, and not only, the corresponding layout optimization problem must be solved. The present work contributes to this direction by proposing the creation of a fully parametric design, which in the sequel may be optimized using the Finite

Element Method and in accordance to the EuroCode standards. The derived optimum design is comparable to the commercially available ones, even though this was not the explicit aim of the investigation. From a constructional viewpoint, it is worth mentioning that the final design consists of standard profiles only, which facilitates the manufacturing and helps in keeping a low cost since no special structural treatments are required. Furthermore, since the design is fully parametric, the proposed procedure may be applied for the design of a solar tracker with any number of photovoltaic cells. Another important issue is that the verification procedure was based entirely on modern techniques (3D CAD design and computational mechanics), which means that not only no analytical calculations are needed to be carried out but also the entire procedure is easy to be programmed. As further improvements, it is possible to develop an automated procedure for verifying the joints (bolts and welds), while the ultimate goal would be the minimization of the cost of an entire solar park. Finally, an interesting problem to be solved is the way the photovoltaic cells may be kept free of dust and humidity for their efficiency to be kept as closer to the nominal efficiency as possible.

I.5.5. Conclusions

The present study aimed at revealing the way a zero-order and a first-order optimization method may be used for structural optimization purposes. More particularly, the present work dealt with the problem of the layout optimization of a dual-axis solar tracker. The proposed approach was based on the optimization of a fully parametric structural design, using the Finite Element Method and imposing the constraints dictated by the EuroCode standards. In total, 40 design parameters were handled while for good practical purposes it is possible first to define the design, thus fix a number of design parameters. As a result, the optimum layout of a solar tracker of any panel surface may be found.

I.6. Recapitulation

For good practical engineering purposes, there are times, when it is required to get quickly a design which is improved with respect to an initial one, but not necessarily the optimum. For such cases, it is recommended to use simple optimization tools, such as the sensitivity analysis, in the form of a parametric investigation with respect to the most important design variables, and simple optimization procedures of zero-order or of first-order. Towards this direction, four typical applications were examined, namely the design of a car suspension, the optimum single-sided and double-sided bolted reinforcement of a plate under uniaxial tension, the optimum design of a racking system and the layout optimization of a solar tracker. The first three applications were handled using a simple sensitivity analysis as described above, while the last example was dealt with using the Subproblem approximation method and a first order method, both found in Ansys, which is a commercial software for structural analysis.

References

Abdallah, S., The effect of using sun tracking systems on the voltage/current characteristics and power generation of flat plate photovoltaics, *Energy Conversion and Management* **45** (2004), pp. 1671–1679.

AS4084, 1993, Steel Storage Racking, Standards Australia.

Bajoria, K.M., Talikoti, R.S. (2006), "Determination of flexibility of beam-to-column connectors used in thin walled cold-formed steel pallet racking systems", Thin-Walled Structures, Vol.44, pp.372–380

Baldassino, N., Bernuzzi, C. (2000), "Analysis and behaviour of steel storage pallet Racks", Thin Wall Struct, Vol. 37(4), pp.277–304.

Bernuzzi, C., Castiglioni, C.A. (2001), "Experimental analysis on the cyclic behaviour of beam-to-column joints in steel storage pallet racks", Thin Wall Struct, Vol.39(10), pp.841–59.

Bolzern P, Cheli F., Falciola G., Resta F., "Estimation of the Non-Linear Suspension Tyre Cornering Forces from Experimental Road Test Data", Vehicle System Dynamics, Vol.31, No.1, 1999, pp.23-34.

Bursi, O.S., Jaspart, J.P. (1997), "Benchmarks for finite element modelling of bolted steel connections", J Constr Steel Res, Vol.43(1/3), pp.17–42.

Chen K., Beale D., "Base Dynamic Parameter Estimation of a MacPherson Suspension Mechanism", Vehicle System Dynamics, Vol.39, No.3, 2003, pp.227-244.

Chung, K.F., Ip, K.H. (2000), "Finite element modeling of bolted connections between cold-formed steel strips and hot rolled steel plates under static shear loading", Engng Struct, Vol.22(10), pp.1271–84.

Citipitioglu, A.M., Haj-Ali, R.H., White, D.W. (2002), "Refined 3D finite element modeling of partially-restrained connections including slip", J Constr Steel Res, Vol.58(5/8), pp.995–1013.

Davies, J.M., Leach, P., Tayloff, A. (1997), "The Design of Perforated Cold-Formed Steel Sections Subject to Axial Load and Bending",Thin-Walled Structures, Vol. 29, Nos. 1-4, pp. 141-157.

Davies, M., Jiang, C. (1998), "Design for Distorsional Buckling", Journal of Constructional Steel Research, Vol.46:1-3, pp.174-175.

Demič M., "Optimization of the characteristics of the elasto-damping elements of a passenger car by means of a modified Nelder-Mead method", Int. J. of Vehicle Design, Vol.10, No.2, 1989, pp.136-152.

Demič M., "Optimization of the characteristics of the elasto-damping elements of cars from the aspect of comfort and handling", Int. J. of Vehicle Design, Vol.13, No.1, 1992, pp.29-46.

Dukkipati R., Dong R, "Impact Loads due to Wheel Flats and Shells", Vehicle System Dynamics, Vol.31, No.1, 1999, pp.1-22.

ELVITYL, HELIOTROPIO, Active solar tracker system, patent pending with application Nr. 20070100557.

Falke, J. (1996), Ingenieurhochbau:Tragwerke aus Stahl nach Eurocode 3(DIN V ENV1993-1-1), Deutches Institut fuer Normung.

Geiger, M., Daibaté, L., Ménard, L. and Wald, L., A web service for controlling the quality of measurements of solar global radiation, *Solar Energy* **73** (6) (2002), pp. 475–480.

Godley, M.H.R. (1991), Storage Racking, Design of Cold Formed Steel, Rhodes ed. Elsevier Applied Science, London, UK.

Hancock, G.J. (1985), "Distortional Buckling of Steel Storage Rack Columns", J of Struct Engin, ASCE 111:12, 2770-2783.

Hay, J.E., Davies, J.A. In: Hay, J.E., Won, T.K. (Eds.), Calculation of the Solar Radiation Incident on an Inclined Surface. First Canadian Solar Radiation Data Workshop, Toronto, Ont., Canada, 1978.

Helwa, N.H., Bahgat, A.B.G., El Shafee, A.M.R. El Shenawy, E.T., Maximum collectable solar energy by different solar tracking systems, *Energy Sources* **22** (1) (2000), pp. 23–34.

Hwang, D.Y., Stallings, J.M. (1994), "Finite element analysis of bolted flange connections", Comput Struct, Vol.51(5), pp.521–33.

Ju, S.H., Fan, C.Y., Wu, G.H. (2004), "Three-dimensional finite elements of steel bolted connections", EnginStruct,Vol.26,pp.403–413.

Kameshki, E.S., Saka, M.P. (2001), „Optimum design of nonlinear steel frame semi-rigid connections using a genetic algorithm", Comput Struct, Vol.79, pp.1593-1604.

Kasai, K., Hodgson, I., Bieiman, D. (1998), "Rigid-bolted repair method for damaged moment connections", Engineering Struct, Vol.20, Nos 4-6, pp. 521-532.

Kuti I., "Simulation of Vehicle Motions on the Basis of the Finite Element Method", Vehicle System Dynamics, Vol.36, No.6, 2001, pp.445-469.

Leach, P., Davies, J. M. (1996), "An Experimental Verification of the Generalized Beam Theory Applied to Interactive Buckling Problems", Thin-Walled Structures, Vol. 25, No. 1, pp. 61-79.

Lorenzo, E., Pérez, M., Ezpeleta, A., Acedo, J., Design of tracking photovoltaic systems with a single vertical axis, *Progress in Photovoltaics: Research and Applications* **10** (2002), p. 533-543.

Luque-Heredia I et al. Spanish patent no. 200501330-2005

Luque-Heredia, I., Moreno, J.M., Magalhγes, P.H., Cervantes, R., Quumιrι, G., and Laurent, O., Inspira's CPV Sun Tracking, Concentrator Photovoltaics, ch.11, 2007

Maggi, Y.I., Gonçalves, R.M., Leon, R.T., Ribeiro, L.F.L. (2005), "Parametric analysis of steel bolted end plate connections using finite element modeling", J Constr Steel Res, Vol.61, pp. 689–708.

Markazi, F.D., Beale, R.G., Godley, M.H.R. (1997), "Experimental Analysis of Semi-Rigid Boltless Connectors", Thin-Walled Structures, Vol.28:1, pp.57-87.

Mavromatakis, F., Franghiadakis, Y., A highly efficient novel azimuthal heliotrope, *Solar Energy* **82** (2008), pp.336–342.

Olsen, P.C. (2002), "Bolted endplate connections revisited", J Constr Steel Res, Vol.58, pp.1265–1280.

Papadrakakis, M, Lagaros, N.D., Plevris V. (2002), "Multi-objective optimization of skeletal structures under static and seismic loading conditions", Eng. Opt., Vol. 34, pp. 645–669.

Passive Solar Tracker for a Solar Concentrator, US Patent Application 20040112373.

Pawlowski J., Vehicle Body Engineering, Business Books Ltd, London, 1969

Puthli, R., Fleischer, O. (2001), "Investigations on bolted connections for high strength steel members", J Constr Steel Res, Vol.57, pp.313–326.

Quaglia G., Sorli M., "Air Suspension Dimensionless Analysis and Design Procedure", Vehicle System Dynamics, Vol.35, No.6, 2001, pp.443-475.

Rothert, H., Gebbeken, N., Binder, B. (1992), "Non-linear three-dimensional finite element contact analysis of bolted connections in steel frames", Int J Numer Meth Engng, Vol.34(1), pp.303–18.

Self reorienting solar tracker, United States Patent 4175391.

Sherbourne, A.N., Bahaari, M.R. (1996), "Three-dimensional simulation of bolted connections to unstiffened columns - Part I: T-stub connections", J Constr Steel Res, Vol.40(3), pp.169–87.

Solar tracker, US Patent 6239353–2001

Solar tracker for thermal and photovoltaic panels with forced air system, applicable to buildings description, Patent No. 20080245402.

Solar tracker. United States Patent no. 4215410-1980.

Specification for the design, testing and utilization of industrial steel storage racks, Rack Manufacturers Institute, Material Handling Industry of America, 1997.

Spentzas C.,"Optimization of vehicle ride characteristics by means of Box's method", Int. J. of Vehicle Design, Vol.14, Nos.5/6, 1993, pp.539-551.

Stallings, J.M., Hwang, D.Y. (1992), "Modeling pretensions in bolted connections", Comput Struct, Vol.45(4), pp.801–3.

Sun tracking control apparatus, United States Patent no. 3917942-1975.

Talikoti, R. S., Bajoria, K. M. (2005), "New approach to improving distortional strength of intermediate length thin-walled open section columns", Electronic Journal of Structural Engineering, Vol.5, pp.69-79.

Thompson A., Davis B., "RMS Values of Force, Stroke and Tyre Deflection in a Half-Car Model with Preview Controlled Active Suspension", Vehicle System Dynamics, Vol.39, No.3, 2003, pp.245-253.

Tian, Y.S., Wang, J., Lu, T. J. (2004), "Racking strength and stiffness of cold-formed steel wall frames", Journal of Constructional Steel Research, Vol.60(7), pp.1069-1093.

Venetsanos, D.T., Alysandratos, T.E., Provatidis, C.G. (2004), "Investigation of symmetric reinforcement of metal plates under tension using the finite element analysis", *Proceedings of 1st Int. Scientific Conference on Information Technology and Quality*, Athens, GR.

Zaremba A., Hampo R., Hrovat D., "Optimal active suspension design using constrained optimization", Journal of Sound and Vibration, Vol.207, No.3, 1997, pp. 351-364.

Zerres, H., (1998), "Comparison between the analysis of the mechanical behaviour of bolted joints by the FEM and by the European approach (PR EN 1591)", ASME/JSME Joint Pressure Vessels Piping Conference, Vol.PVP 367, pp.69–73.

Contributed papers

[App.I.1] Provatidis, C., **Venetsanos**, D. and Spentzas, C., "Parametric investigation of car suspension design", Proceedings MVM XIII, International Scientific Meeting Motor Vehicle & Engines, 4-6 October 2004, Kragujevac, Serbia.

[App.I.2] **Venetsanos**, D.T., Alysandratos, Th. and Provatidis, C.G., "Investigation of symmetric reinforcement of metal plates under tension using the finite element analysis", 1st International Conference on Information Technology and Quality, 5-6 June 2004, Athens, Greece.

[App.I.3] Provatidis, C.G., **Venetsanos**, D.T., Kyriazi, E.A., "Optimum Design Of Single-Sided And Double-Sided Bolted Reinforcement Of A Plate Under Axial Loading According To Eurocode-3", 2nd International Conference "From Scientific Computing to Computational Engineering", Athens, 5-8 July, 2006.

[App.I.4] Provatidis, C.G., **Venetsanos**, D.T., Moissiadou, S.K., "Optimum Design Of Racking Systems According To The Eurocode Standards", 2nd International Conference "From Scientific Computing to Computational Engineering", Athens, 5-8 July, 2006.

[App.I.5] Spatharis, E.F., **Venetsanos**, D.T. and Provatidis, C.G., Layout optimization of a dual-axis solar tracker according to the Eurocode standards, 3rd International Conference "From Scientific Computing to Computational Engineering", Athens, 8-11 July, 2009.

APPENDIX II

LIST OF PUBLICATIONS

Abstract

This Appendix presents a list of publications by the author, concerning the current PhD. In total, 27 papers have been published, two of which in refereed international scientific journals and 25 in international scientific conference and world congress proceedings.

Publications in refereed international scientific journals

Chapter 5

[1] **Venetsanos D.T.**, Provatidis C.G. (2010), "On the layout optimization of 2D skeletal structures under a single displacement constraint", Struct Multidisc Optim, vol.42, pp.125–155.

Chapter 7

[2] Provatidis, C.G. and **Venetsanos, D.T.** (2006), "Cost minimization of 2D continuum structures under stress constraints by increasing commonality in their skeletal equivalents", Forsch Ingenieurwes, vol.70, pp.159–169.

Publications in international scientific conference and world congress proceedings

Chapter 2

[1] Provatidis, C.G., Vossou C.G., **Venetsanos D.T.**, "Verification of popular deterministic and stochastic optimization methods using benchmark mathematical functions", In: D.Tsahalis (ed.), CD Proc. *1st International Conference "From Specific Computing to Computational Engineering", 8-10 September, 2004, Athens, Greece.*

[2] Provatidis C.G., **Venetsanos D.T.**, Vossou C.G., "A comparative study on deterministic and stochastic optimization algorithms applied to truss design", In: D.Tsahalis (ed.), CD Proc. *1st International Conference "From Specific Computing to Computational Engineering", 8-10 September, 2004, Athens, Greece.*

[3] Provatidis C.G., **Venetsanos D.T.**, Markos P.A., "Investigation Of Hybrid Optimization Schemes With A Deterministic Search Direction And A Stochastic Step Size", *2nd International Conference "From Scientific Computing to Computational Engineering", 5-8 July, 2006, Athens, Greece.*

[4] Papageorgiou A.A., **Venetsanos D.T.**, Provatidis C.G., "Investigating The Influence Of Typical Genetic Algorithm Parameters On The Optimization Of Benchmark Mathematical Functions", *2nd International Conference "From Scientific Computing to Computational Engineering", 5-8 July, 2006, Athens, Greece.*

Chapter 4

[5] Provatidis, C.G. and **Venetsanos, D.T.**, "Performance of the FSD in shape and topology optimization of two-dimensional structures using continuous and truss-like models", In: C. Cinquini, M. Rovati, P. Venini and R. Nascimbene (eds.), Proceedings *Fifth World Congress of Structural and Multidisciplinary Optimization, May 19-23, 2003, Lido di Jesolo, Italy, pp. 385-386, Schönenfeld & Ziegler (ISBN 88-88412-18-2).*

[6] **Venetsanos D.T.** and Provatidis C.G., "Fully stressed 2D continua formed by applying the stress-ratio technique to finite elements of variable thickness", *1st IC-EpsMsO, 6-9 July 2005, Athens, Greece.*

[7] Provatidis C.G., **Venetsanos D.T.**, Kesimoglou N.C., "Layout Optimization Of A Stress-Constrained Plate Under Out-Of-Plane Loading", *2nd International Conference "From Scientific Computing to Computational Engineering", Athens, 5-8 July, 2006.*

[8] Provatidis C.G., **Venetsanos D.T.**, Champilos S.D. "Weight Minimization Of 3D Continuum Structures Under Stress Constraints", *2nd International Conference "From Scientific Computing to Computational Engineering", Athens, 5-8 July, 2006.*

[9] **Venetsanos D.**, Magoula E. and Provatidis C. "Layout Optimization of Stressed Constrained 2D Continua Using Finite Elements of Variable Thickness", *6th International Congress on Computational Mechanics (GRACM), Thessaloniki, 19-21 June 2008.*

Chapter 6

[10] Provatidis C. G. and **Venetsanos, D. T.**, "The influence of normalizing the virtual strain energy density on the shape optimization of 2D continua", *1st IC-EpsMsO, 6-9 July 2005, Athens, Greece.*

[11] **Venetsanos D.** and Provatidis C., "Layout Optimization of Single Displacement Constrained 2D Continua Using Finite Elements of Variable Thickness", *6th International Congress on Computational Mechanics (GRACM), Thessaloniki, 19-21 June 2008.*

[12] **Venetsanos, D.T.**, Provatidis, C.G., Minimum weight designs for single displacement constrained 2D continua using variable element-wise thickness, *8th World Congress on Structural and Multidisciplinary Optimization (WCSMO8), LNEC (National Laboratory for Civil Engineering), Lisboa, Portugal, June 1- 5, 2009.*

Chapter 7

[13] **Venetsanos, D.T.**, Mitrakos, D. and Provatidis, C.G., "Layout optimization of 2D skeletal structures using the fully stressed design", *1st International Conference on Information Technology and Quality, 5-6 June 2004, Athens, Greece.*

[14] Provatidis, C.G., **Venetsanos, D.T.,** Linardos, M.D., "Cost Minimization Of Welded Steel Tanks For Oil Storage According To API Standards", *2nd International Conference "From Scientific Computing to Computational Engineering", Athens, 5-8 July, 2006.*

Chapter 8

[15] Provatidis C.G., Tzanakakis E.D., and **Venetsanos D.T.**, "Optimum selection of doubly symmetric rolled beams for single-girder overhead travelling cranes using finite element plate models", *1st IC-EpsMsO, 6-9 July 2005, Athens, Greece.*

[16] **Venetsanos D.T.**, Provatidis C.G., Magoula E-A.T., "Optimal design of a welded open cross-section crane runway beam in accordance with EC1 and EC3", *2nd International Conference on Experiments/Process/System Modelling/Simulation & Optimization Athens, 4-7 July, 2007.*

[17] **Venetsanos D.T.**, Provatidis C.G., Skarmeas S.G., "Optimal Design Of A Box Cross Section Of A Double Girder Crane In Accordance With EC1 AND EC3", *2nd International Conference on Experiments/Process/System Modelling/Simulation & Optimization, Athens, 4-7 July, 2007.*

[18] **Venetsanos D.**, Magoula E. and Provatidis C., "Performance-based optimization of the welded box of a single girder overhead travelling crane according to EC3 and EC1, *8th. World Congress on Computational Mechanics (WCCM8), 5th. European Congress on Computational Methods in Applied Sciences and Engineering (ECCOMAS 2008), June 30–July 4, 2008, Venice, Italy.*

[19] **Venetsanos D.** and Provatidis C., "Performance-based optimization of a welded open cross section runway beam according to EC3 and EC1", *8th. World Congress on Computational Mechanics (WCCM8), 5th. European Congress on Computational Methods in Applied Sciences and Engineering (ECCOMAS 2008), June 30–July 4, 2008, Venice, Italy.*

[20] Kapogiannis A.K., **Venetsanos D.T.** and Provatidis C.G., Weight minimization of a steel hangar using a new heuristic optimization procedure and according to the Eurocode standards, *3rd International Conference "From Scientific Computing to Computational Engineering", Athens, 8-11 July, 2009.*

Appendix I

[21] Provatidis, C., **Venetsanos**, D. and Spentzas, C., "Parametric investigation of car suspension design", Proceedings MVM XIII, *International Scientific Meeting Motor Vehicle & Engines, 4-6 October 2004, Kragujevac, Serbia*.

[22] **Venetsanos**, D.T., Alysandratos, Th. and Provatidis, C.G., "Investigation of symmetric reinforcement of metal plates under tension using the finite element analysis", *1st International Conference on Information Technology and Quality, 5-6 June 2004, Athens, Greece.*

[23] Provatidis, C.G., **Venetsanos**, D.T., Kyriazi, E.A., "Optimum Design Of Single-Sided And Double-Sided Bolted Reinforcement Of A Plate Under Axial Loading According To Eurocode-3", *2nd International Conference "From Scientific Computing to Computational Engineering", Athens, 5-8 July, 2006.*

[24] Provatidis, C.G., **Venetsanos**, D.T., Moissiadou, S.K., "Optimum Design Of Racking Systems According To The Eurocode Standards", *2nd International Conference "From Scientific Computing to Computational Engineering", Athens, 5-8 July, 2006.*

[25] Spatharis, E.F., **Venetsanos**, D.T. and Provatidis, C.G., Layout optimization of a dual-axis solar tracker according to the Eurocode standards, *3rd International Conference "From Scientific Computing to Computational Engineering", Athens, 8-11 July, 2009.*

This page has been left intentionally blank

This page has been left intentionally blank

This page has been left intentionally blank

ΕΘΝΙΚΟ ΜΕΤΣΟΒΙΟ ΠΟΛΥΤΕΧΝΕΙΟ

ΣΧΟΛΗ ΜΗΧΑΝΟΛΟΓΩΝ ΜΗΧΑΝΙΚΩΝ

ΤΟΜΕΑΣ ΜΗΧΑΝΟΛΟΓΙΚΩΝ ΚΑΤΑΣΚΕΥΩΝ ΚΑΙ ΑΥΤΟΜΑΤΟΥ ΕΛΕΓΧΟΥ

ΕΡΓΑΣΤΗΡΙΟ ΔΥΝΑΜΙΚΗΣ ΚΑΙ ΚΑΤΑΣΚΕΥΩΝ

ΑΝΑΠΤΥΞΗ ΜΕΘΟΔΩΝ ΒΕΛΤΙΣΤΗΣ ΤΟΠΟΛΟΓΙΑΣ ΚΑΙ ΣΧΗΜΑΤΟΣ ΜΗΧΑΝΟΛΟΓΙΚΩΝ ΚΑΤΑΣΚΕΥΩΝ

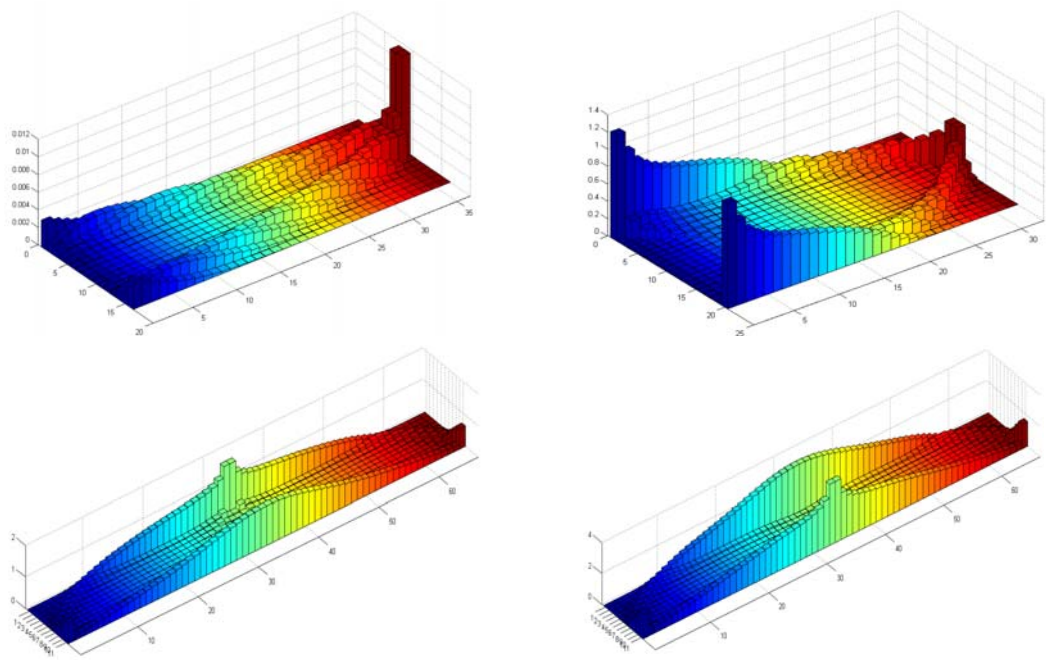

ΔΙΔΑΚΤΟΡΙΚΗ ΔΙΑΤΡΙΒΗ

Υπό

ΔΗΜΗΤΡΙΟΥ Τ. ΒΕΝΕΤΣΑΝΟΥ

ΔΙΠΛ. ΜΗΧ/ΤΟΥ ΜΗΧ/ΚΟΥ Ε.Μ.Π.

ΑΘΗΝΑ 2010

Αυτή η σελίδα είναι σκοπίμως κενή

Αυτή η σελίδα είναι σκοπίμως κενή

Π Ι Ν Α Κ Α Σ Π Ε Ρ Ι Ε Χ Ο Μ Ε Ν Ω Ν

ΚΕΦΑΛΑΙΟ 4 (ΠΕΡΙΛΗΨΗ): Βέλτιστη σχεδίαση υπό την επιβολή περιορισμών τάσης

Κ Α Τ Α Λ Ο Γ Ο Σ Σ Χ Η Μ Α Τ Ω Ν

Κ Α Τ Α Λ Ο Γ Ο Σ Π Ι Ν Α Κ Ω Ν

ΚΕΦΑΛΑΙΟ 1
(ΠΕΡΙΛΗΨΗ)

ΤΟ ΓΕΝΙΚΕΥΜΕΝΟ ΠΡΟΒΛΗΜΑ ΕΛΑΧΙΣΤΟΠΟΙΗΣΗΣ ΤΟΥ ΒΑΡΟΥΣ ΜΙΑΣ ΚΑΤΑΣΚΕΥΗΣ

Στην παρούσα περίληψη κεφαλαίου, διατυπώνεται το γενικευμένο πρόβλημα της ελαχιστοποίησης του βάρους μίας κατασκευής και παρουσιάζονται μερικές από τις πλέον γνωστές και σημαντικές μεθοδολογίες βελτιστοποίησης κατασκευών μέσα από μία επαρκώς εκτενή βιβλιογραφική ανασκόπηση.

1.1. Εισαγωγή

Ο όρος 'βελτιστοποίηση' ανέκαθεν αποτελούσε έναν από τους πλέον δημοφιλείς όρους, δεδομένου ότι αυτός αντανακλά τον πόθο για την επίτευξη ενός συγκεκριμένου στόχου καταναλώνοντας τους λιγότερους δυνατόν πόρους. Συνεπώς, αυτός ο όρος εμφανίζεται ως διαχρονικός και με βαρύνουσα σημασία σε πολλές εκφάνσεις της ζωής, από την απαρχή του σύμπαντος και τον καθημερινό αγώνα για επιβίωση μέχρι τα πλέον μοναδικά ανθρώπινα επιτεύγματα.

Ανατρέχοντας στο απώτατο παρελθόν της γένεσης του σύμπαντος και σύμφωνα με τις πιο μοντέρνες θεωρίες κοσμογονίας, μετά την μεγάλη έκρηξη (Big Bang), ύλη ΄διασκορπίστηκε στο σύμπαν και στη συνέχεια, αργά αλλά προοδευτικά, δημιουργήθηκαν τα ουράνια σώματα. Ωστόσο, αυτά τα σώματα δεν είναι τίποτε άλλο από ύλη, η οποία συγκρατείται με τη μορ΄φη σταθερών δομών, δηλαδή δομών χαμηλής ενεργειακής στάθμης. Συνεπώς, τα ουράνια σώματα έχουν προκύψει μέσα από ένα είδος διαδικασίας βελτιστοποίησης, η οποία αποσκοπούσε στην ελαχιστοποίηση της ενεργειακής στάθμης τους. Ένα ιδιαίτερα μεγάλο πλήθος παραδειγμάτων βελτιστοποίησης είναι δυνατόν να εντοπισθεί στο άμεσο περιβάλλον του ανθρώπου. Οι κορμοί των δέντρων είναι μεγαλύτερης διατομής κοντά στο έδαφος και μικρότερης κοντά στην κορυφή, διαμόρφωση η οποία διευκολύνει τόσο την ανάπτυξη ενός πιο αποδοτικού συστήματος μεταφοράς θρεπτικών συστατικών όσο και την ασφαλέστερη παραλαβή ισχυρών φορτίων ανέμου. Τα ψάρια και άλλα θαλάσσια όντα διαθέτουν υδροδυναμικά σχήματα, έτσι ώστε η υποθαλάσσια κίνησή τους να χαρακτηρίζεται από χαμηλές απώλειες λόγω τριβών, επιτυγχάνοντας, με αυτόν τον τρόπο, την βέλτιστη προσαρμογή στο φυσικό τους περιβάλλον. Επιπροσθέτως, η ελαφρά κατασκευή των πτηνών, σε συνδυασμό με τις εύκαμπτες επιφάνειες ελέγχου που διαθέτουν (φτερά), αποτελεί μία πτητική μηχανή με βελτιωμένα χαρακτηριστικά. Ο κατάλογος με παρόμοια παραδείγματα είναι πολύ μακρύς, δεδομένου ότι η εξελικτική διαδικασία, η οποία παρατηρείται στη φύση, δεν είναι τίποτε άλλο από τη διατήρηση και βελτίωση εκείνων των χαρακτηριστικών, τα οποία εξασφαλίζουν υψηλότερη πιθανότητα επιβίωσης, όπως άλλωστε ορίζει και η Δαρβίνεια θεωρία. Με άλλα λόγια, πρόκειται για μία διαδικασία βελτιστοποίησης, στην οποία επιδιώκεται η μεγιστοποίηση της πιθανότητας επιβίωσης. Προφανώς, σε όλες αυτές τις περιπτώσεις, το τελικό αποτέλεσμα δεν είναι απαραίτητα το απόλυτο (καθολικό) βέλτιστο, ωστόσο είναι σημαντικά βελτιωμένο συγκριτικά με το αρχικό αποτέλεσμα, κάτι που, σε πολλές περιπτώσεις, είναι επαρκές.

Εκτός από την φύση, η έννοια της βελτιστοποίησης ενσωματώθηκε στη ζωή του ανθρώπου από το πρώιμο ακόμα στάδιο της εμφανίσεώς του. Αρχικά προκειμένου να εξασφαλίσει την επιβίωσή του και στη συνέχεια προκειμένου να βελτιώσει το βιοτικό του επίπεδο, ο άνθρωπος ήταν υποχρεωμένος να αξιοποιήσει πόρους διαθέσιμους στο άμεσο περιβάλλον του. Το πρώτο και κύριο μέλημά του ήταν η χρήση εργαλείων και όπλων αφ' ενός μεν για την εξασφάλιση της τροφής τους και αφ' ετέρου δε για την προστασία του από ο,τιδήποτε θεωρούσε ως απειλή. Προς αυτήν την κατεύθυνση, ο άνθρωπος άρχισε να χρησιμοποιεί αιχμηρά αντικείμενα, όπως αιχμηρές πέτρες και κλαδιά. Αξιοποιώντας την εφευρετικότητα και τη φαντασία του, ο άνθρωπος άρχισε να αναπτύσσει τεχνικές προκειμένου να καταστήσει τα εν λόγω μέσα πιο αποτελεσματικά. Με άλλα λόγια, ο στόχος του ήταν η επίτευξη του καλύτερου δυνατού αποτελέσματος καταβάλλοντας τη μικρότερη δυνατή προσπάθεια.

Τα ίδια στοιχεία εφευρετικότητας και φαντασίας εμφανίζονται και σε κατασκευές πιο ειρηνικού χαρακτήρα, όπως είναι ο τροχός (βέλτιστο σχήμα για κύλιση), τα ρούχα (βέλτιστη αξιοποίηση των φυσικών ινών προκειμένου να εξασφαλισθεί προστασία έναντι του κρύου, το χειμώνα, και έναντι της ζέστης, το καλοκαίρι), οι κατοικίες (βέλτιστη προστασία έναντι των στοιχείων της φύσεως) και τα πλοία (βέλτιστος τρόπος μεταφοράς αγαθών δια θαλάσσης).

Ωστόσο, εκτός από την αναζήτηση βέλτιστων λύσεων σχετικά με θέματα επιβίωσης, ο άνθρωπος άρχισε να ενσωματώνει την έννοια της βελτιστοποίησης και σε άλλες δραστηριότητες της ζωής του, όπως ο αθλητισμός, η τέχνη, ο στρατός και η θρησκεία. Στον αρχαίο ελληνικό πολιτισμό, υπάρχει πλήθος τέτοιων παραδειγμάτων. Πιο συγκεκριμένα, κατά τη διάρκεια αθλητικών αγώνων, ένας αθλητής έπρεπε να βελτιστοποιήσει την τεχνική του προκειμένου να επιτύχει την καλύτερη επίδοση και να νικήσει. Τα αρχαία ελληνικά θέατρα είναι ξακουστά για την εξαιρετική τους ακουστική, δηλαδή για τη βέλτιστη διάδοση του ήχου στο χώρο του θεάτρου. Κατά τη διάρκεια των συμποσίων, οι γαστρονομικές λιχουδιές προσφέρονταν με τέτοια σειρά και τα ανάκλινδρα ήταν τέτοιου σχήματος, έτσι ώστε οι καλεσμένοι να έμεναν ιδιαίτερα ευχαριστημένοι (βελτιστοποίηση της απόλαυσης). Οι ναυτικοί στόλοι διέθεταν σκάφη με εμβολοφόρο πλώρη, όχι μόνον για την ελαχιστοποίηση της υδροδυναμικής αντίστασης (βελτιστοποίηση της πλεύσης) αλλά και για τον εμβολισμό εχθρικών σκαφών (βελτιστοποίηση της πολεμικής ικανότητας του σκάφους). Οι κολώνες στους αρχαίους Ελληνικούς ναούς φέρουν, ομοιόμορφη και περιμετρική, κατανομή ενισχύσεων. Αυτές οι ενισχύσεις, καθώς διαχέεται το φως, παρέχουν μία ιδιαίτερη καλαισθησία, όπως άλλωστε αρμόζει σε χώρους θρησκευτικής λατρείας, αλλά ταυτόχρονα εξασφαλίζουν τη βέλτιστη αντοχή τόσο έναντι καμπτικών φορτίων όσο και έναντι σεισμού. Επιπροσθέτως, ήταν γνωστό στους αρχαίους Έλληνες αρχιτέκτονες ότι σε μία κοίλη διατομή, συγκριτικά με μία συμπαγή διατομή, εξασφαλίζεται υψηλότερη αντοχή σε συνδυασμό με μικρότερο βάρος. Χαρακτηριστικό παράδειγμα αποτελεί ο ναός του Επικουρείου Απόλλωνος στις Βάσσες Μεσσηνίας. Εξ αιτίας της υποχρεωτικής μεταφοράς των μαρμάρινων δοκών στην εν λόγω ορεινή περιοχή, ο αρχιτέκτονας αποφάσισε να αφαιρέσει υλικό από ορισμένες δοκούς, προκειμένου να μειωθεί το βάρος τους. Όπως μπορεί να αποδειχθεί, ενώ το βάρος τους μειώθηκε κατά 50%, η μέγιστη, σε αυτές, αναπτυσσόμενη καμπτική τάση παραμένει μικρότερη από εκείνην που αναπτύσσεται εάν χρησιμοποιηθούν πλήρεις διατομές.

Παρόμοια παραδείγματα εντοπίζονται σε όλους τους πολιτισμούς και σε όλες τις εποχές. Το κοινό χαρακτηριστικό σε όλες αυτές τις περιπτώσεις είναι ότι το βέλτιστο αποτέλεσμα αναζητείται κυρίως μέσα από μία διαδικασία δοκιμής-σφάλματος. Ωστόσο, κατά τη διάρκεια των δύο τελευταίων αιώνων, η ανάπτυξη των μαθηματικών επέτρεψε τόσο τη διατύπωση προβλημάτων βελτιστοποίησης όσο και την ανάπτυξη συστηματικών μεθοδολογιών αναζήτησης της βέλτιστης λύσης. Ειδικότερα στο πεδίο της Μηχανικής, μία τιτάνια προσπάθεια ανάπτυξης, εξερεύνησης και αξιοποίησης αποτελεσματικών μεθόδων βελτιστοποίησης λαμβάνει χώρα τα τελευταία εξήντα χρόνια, δηλαδή από γεννήσεως της Υπολογιστικής Μηχανικής. Τα πλέον εντυπωσιακά επιτεύγματα, τα οποία προέκυψαν από αυτήν την προσπάθεια, έχουν καταγραφεί ως μνημειώδεις στιγμές κατάκτησης των ωκεανών, του ουρανού και του διαστήματος. Αυτά τα επιτεύγματα σημειώθηκαν κατά τη διάρκεια της αναζήτησης της μορφής μίας κατασκευής, στην οποία η κατανομή της ελάχιστης δυνατής ύλης είναι τέτοια ώστε τα εξωτερικώς επιβαλλόμενα φορτία να παραλαμβάνονται με ασφάλεια, ενώ ταυτόχρονα να ικανοποιούνται όλοι οι περιορισμοί σχετικά με την αντοχή, την ευστάθεια και τη λειτουργικότητα της κατασκευής. Με άλλα λόγια, αυτά τα επιτεύγματα σημειώθηκαν κατά την προσπάθεια επίλυσης του γενικευμένου προβλήματος της ελαχιστοποίησης του βάρους μίας κατασκευής.

1.2. Ορισμός του γενικευμένου προβλήματος ελαχιστοποίησης βάρους κατασκευών

Στη διατύπωση του γενικευμένου προβλήματος ελαχιστοποίησης του βάρους μίας κατασκευής, αναζητείται ένα διάνυσμα σχεδίασης $\mathbf{X}$ τέτοιο ώστε να ελαχιστοποιείται η βαθμωτή ποσότητα $f(\mathbf{X})$ υπό την προϋπόθεση ότι ικανοποιούνται τόσο οι ισοτικοί

περιορισμοί $h_j(\mathbf{X})=0$, όσο και οι ανισοτικοί περιορισμοί $g_j(\mathbf{X})\le 0$. Η μαθηματική διατύπωση αυτού του προβλήματος είναι:

$$\min f(\mathbf{X}), \mathbf{X}=[x_i], x_{i,lower}\le x_i\le x_{i,upper} \tag{1.1}$$

έτσι ώστε:

$$\begin{aligned} &h_j(\mathbf{X})=0, \quad j=1,2,...,m \\ &g_j(\mathbf{X})\le 0, \quad j=m+1,m+2,...,p \end{aligned} \tag{1.2}$$

όπου:

$$\mathbf{X}=\begin{bmatrix} x_1 & x_2 & ... & x_n \end{bmatrix}^T \tag{1.3}$$

Η ποσότητα f καλείται αντικειμενική συνάρτηση ή συνάρτηση κόστους, το διάνυσμα $\mathbf{X}$ περιλαμβάνει όλες τις ανεξάρτητες μεταβλητές σχεδίασης του προβλήματος, ενώ όλες οι συνιστώσες x_i του $\mathbf{X}$ καλούνται μεταβλητές σχεδίασης. Κάθε μία από τις μεταβλητές σχεδίασης διαθέτει το δικό της πεδίο ορισμού. Για τις μηχανολογικές κατασκευές, το εν λόγω πεδίο ορισμού πρέπει να είναι επαρκώς ευρύ. Δεδομένου ότι οι μηχανολογικές κατασκευές διαθέτουν φυσική υπόσταση, και δεν αποτελούν θεωρητικές ή αφηρημένες έννοιες, τόσο το κάτω όριο $x_{i,lower}$ όσο και το άνω όριο $x_{i,upper}$ του προαναφερθέντος πεδίου ορισμού πρέπει να χαρακτηρίζεται από λογικές τιμές με φυσική σημασία. Το πλήθος n των μεταβλητών σχεδίασης δηλοί και τη διάσταση του χώρου λύσης R^n του αντιστοίχου προβλήματος βελτιστοποίησης. Στην περίπτωσης μεγιστοποίησης της τιμής της αντικειμενικής συνάρτησης, τότε χρησιμοποιείται η ακόλουθη διατύπωση:

$$\max f(\mathbf{X})=\min\left(-f(\mathbf{X})\right) \tag{1.4}$$

Το πλήθος n των μεταβλητών σχεδίασης είναι ανεξάρτητο τόσο του πλήθους m των ισοτικών περιορισμών όσο και του πλήθους p των ισοτικών περιορισμών. Στην περίπτωση κατά την οποία $m=p=0$, τότε το πρόβλημα βελτιστοποίησης χαρακτηρίζεται ως '*άνευ περιορισμών*', ενώ στην αντίθετη περίπτωση, δηλαδή όταν $m\ne 0$ και/ή $p\ne 0$, τότε το πρόβλημα βελτιστοποίησης χαρακτηρίζεται ως '*μετά περιορισμών*'.

Σχετικά με τους περιορισμούς, ένας περιορισμός καλείται γραμμικός όταν εκφράζεται ως γραμμικός συνδυασμός των μεταβλητών σχεδίασης, ενώ καλείται μη-γραμμικός σε οποιαδήποτε άλλη περίπτωση. Επιπροσθέτως, η αντικειμενική συνάρτηση χαρακτηρίζεται ως γραμμική, όταν εκφράζεται ως γραμμικός συνδυασμός των μεταβλητών σχεδίασης, ενώ μη-γραμμική σε οποιαδήποτε άλλη περίπτωση. Στην ειδική περίπτωση κατά την οποία και η αντικειμενική συνάρτηση είναι γραμμική και όλοι οι περιορισμοί (γραμμικοί και μη-γραμμικοί) είναι γραμμικοί, το πρόβλημα βελτιστοποίησης καλείται γραμμικό, ενώ σε οποιαδήποτε άλλη περίπτωση καλείται μη-γραμμικό.

Με κριτήριο την ύπαρξη ελαχίστου, εν γένει, το πεδίο τιμών μίας συνάρτησης f στο χώρο λύσης R^n ενδεχομένως να έχει κανένα, ένα ή και πολλά τοπικά ελάχιστα. Στην πρώτη περίπτωση, η συνάρτηση είναι σταθερή, άρα ανεξάρτητη από το διάνυσμα σχεδίασης:

$$f(\mathbf{X})=ct, \quad \forall \mathbf{X}\in R^n \tag{1.5}$$

Στη δεύτερη περίπτωση, υπάρχει ένα διάνυσμα σχεδίασης $\mathbf{X}_{opti}$ για το οποίο ισχύει:

$$f\left(\mathbf{X}_{opti}\right) < f\left(\mathbf{X}\right),\ \ \forall \mathbf{X} \in R^n,\ \mathbf{X} \neq \mathbf{X}_{opti} \tag{1.6}$$

Στην τρίτη περίπτωση, υπάρχουν πολλά διανύσματα σχεδίασης $\mathbf{X}_{local\_opti,k}$, $k = 1,2,..,l$ για τα οποία ισχύει:

$$f\left(\mathbf{X}_{local\_opti,k}\right) < f\left(\mathbf{X}_{local\_opti,k} \pm \varepsilon\right) \tag{1.7}$$

όπου ε είναι μια μικρή θετική ποσότητα. Ανάμεσα στα διανύσματα σχεδίασης $\mathbf{X}_{local\_opti,k}$, είναι δυνατόν να υπάρχει ένα διάνυσμα σχεδίασης $\mathbf{X}_{local\_opti,g}$ τέτοιο ώστε:

$$f\left(\mathbf{X}_{local\_opti,g}\right) < \min\left\{f\left(\mathbf{X}_{local\_opti,k}\right), k = 1,2,..,g-1,g+1,..,l\right\} \tag{1.8}$$

Σε αυτήν την περίπτωση, το διάνυσμα $\mathbf{X}_{local\_opti,g}$ αντιστοιχεί στο καθολικό ελάχιστο (ελάχιστο μεταξύ ελαχίστων τιμών της συνάρτησης). Διευκρινίζεται ότι σε μία συνάρτηση f είναι δυνατόν να υπάρχουν περισσότερα από ένα διανύσματα σχεδίασης, τα οποία να αντιστοιχούν στην ελάχιστη τιμή (πολλαπλές λύσεις).

Το πρόβλημα βελτιστοποίησης, όπως αυτό διατυπώθηκε στις Εξ. (1.1-1.3), είναι γενικής ισχύος και εφαρμόσιμο σε κάθε περίπτωση αναζήτησης του ελαχίστου βάρους μίας κατασκευής. Όπως αναφέρθηκε στην Εισαγωγή, στην υπάρχουσα βιβλιογραφία αναφέρονται πολλές μεθοδολογίες βελτιστοποίησης, οι οποίες χωρίζονται σε τρεις ομάδες: σε μεθοδολογίες βελτιστοποίησης της διατομής (πάχους), σε μεθοδολογίες βελτιστοποίησης της τοπολογίας και σε μεθοδολογίες βελτιστοποίησης του σχήματος μίας κατασκευής. Η πρώτη ομάδα αφορά σε μεθοδολογίες αναζήτησης εκείνης της διατομής των δομικών στοιχείων έτσι ώστε το ολικό βάρος της κατασκευής να ελαχιστοποιείται και ταυτόχρονα να ικανοποιούνται όλοι οι περιορισμοί. Η δεύτερη ομάδα αφορά σε μεθοδολογίες δημιουργίας οπών εντός του πεδίου σχεδίασης με μετακίνηση εσωτερικών κόμβων, έτσι ώστε να απομακρυνθεί πλεονάζον υλικό και να ελαχιστοποιηθεί το βάρος της κατασκευής, χωρίς να παραβιασθεί κάποιος από τους επιβαλλομένους περιορισμούς. Η τρίτη ομάδα αφορά σε μεθοδολογίες σύμφωνα με τις οποίες συνοριακοί κόμβοι του πεδίου σχεδίασης μετακινούνται, προκειμένου να βρεθεί εκείνη η μορφή του πεδίου σχεδίασης η οποία αντιστοιχεί στο ελάχιστο βάρος και δεν προκαλεί παραβίαση κάποιου περιορισμού. Εν γένει, τα προαναφερθέντα προβλήματα βελτιστοποίησης, δηλαδή το πρόβλημα βελτιστοποίησης της διατομής, της τοπολογίας και του σχήματος, είναι συζευγμένα. Γι' αυτόν το λόγο, το ενδιαφέρον της επιστημονικής κοινότητας εστιάζεται σε μεθοδολογίες, οι οποίες αντιμετωπίζουν ταυτόχρονα και τα τρία αυτά προβλήματα. Με άλλα λόγια, το ενδιαφέρον είναι εστιασμένο σε μεθοδολογίες, οι οποίες ασχολούνται με την κατανομή της ύλης έτσι ώστε να επιλύονται ταυτόχρονα και τα τρία προαναφερθέντα προβλήματα.

Χωρίς βλάβη της γενικότητας, η βελτιστοποίηση μίας κατασκευής, ή, ακριβέστερα, η βελτιστοποίηση της σχεδίασης μίας κατασκευής, αποτελεί μία συστηματική διαδικασία αναζήτησης εκείνης της σχεδίασης, μεταξύ πολλών εφικτών σχεδιάσεων, η οποία ικανοποιεί, με τον καλύτερο δυνατό τρόπο, έναν ή και περισσότερους στόχους, ενώ ταυτόχρονα πληροί όλους τους, καλώς ορισμένους, περιορισμούς σχετικά τόσο με τις μεταβλητές σχεδίασης όσο και με την απόκριση της κατασκευής. Στις περισσότερες περιπτώσεις, η βελτιστοποίηση μίας

κατασκευής επιτυγχάνεται μέσω μίας επαναληπτικής διαδικασίας, η πορεία της οποίας, όπως άλλωστε και η κατάληξή της, επηρεάζεται από πολλούς παράγοντες, όπως είναι το μέγεθος του χώρου σχεδίασης, η μορφή της αντικειμενικής συνάρτησης, οι επιβαλλόμενοι περιορισμοί καθώς και η ακρίβεια με την οποία πρέπει να ικανοποιηθεί το κριτήριο τερματισμού της αναζήτησης. Αν και η επιστημονική κοινότητα έχει επιδείξει συστηματική και έντονη δραστηριότητα στο πεδίο της βελτιστοποίησης, ειδικά κατά τις τελευταίες δεκαετίες, μέχρι στιγμής δεν έχει διατυπωθεί κάποια διαδικασία, η οποία να *αποδεικνύεται* ότι επιλύει επιτυχώς το γενικευμένο πρόβλημα της βελτιστοποίησης. Αυτό σημαίνει ότι το καθολικό ελάχιστο για τη γενικευμένη διατύπωση του προβλήματος της βελτιστοποίησης παραμένει ως το Άγιο Δισκοπότηρο για την επιστημονική κοινότητα.

1.3. Σύντομη ιστορική αναδρομή

Η βελτιστοποίηση, όπως αναφέρθηκε στην Ενότητα 1.1, χρονολογείται από κτήσεως κόσμου. Ωστόσο, τα πρώτα προβλήματα βελτιστοποίησης, τα οποία διατυπώθηκαν στην αυστηρή γλώσσα των μαθηματικών χρονολογούνται από μερικούς αιώνες προ Χριστού. Πιο συγκεκριμένα, ο Ευκλείδης (300 π.Χ.) ασχολήθηκε με διάφορα προβλήματα βελτιστοποίησης, όπως η αναζήτηση της συντομότερης διαδρομής μεταξύ ενός σημείου και μίας δοθείσης γραμμής και η αναζήτηση του παραλληλογράμμου με το μεγαλύτερο εμβαδόν, όταν δίδεται η περίμετρος αυτού. Επίσης, ο Ήρων ο Αλεξανδρεύς (100 π.Χ.), ασχολήθηκε με το πρόβλημα της συντομότερης διαδρομής την οποία διανύει μία ακτίνα φωτός μεταξύ δύο σημείων στο χώρο (Russo, 2004).

Αρκετούς αιώνες αργότερα, ο Fermat (1657) διατύπωσε την γενική αρχή ότι το φως απαιτεί τον ελάχιστο χρόνο όταν ταξιδεύει μεταξύ δύο σημείων (Veselago, 2002), ενώ ο Cauchy (1847) παρουσίασε για πρώτη φορά μια, μαθηματικής φύσεως, διαδικασία βελτιστοποίησης (Μέθοδος Μεγίστης Κλίσεως), στην οποία χρησιμοποιήθηκαν οι πρώτες παράγωγοι της αντικειμενικής συνάρτησης (Cauchy, 1847). Η ανάπτυξη της αριθμητικής ανάλυσης οδήγησε στη διατύπωση της μαθηματικής θεωρίας της βελτιστοποίησης καθώς και στη διαμόρφωση μαθηματικών μεθόδων βελτιστοποίησης. Η απαρχή έγινε με τις πρωτοπόρες εργασίες του Courant επί των συναρτήσεων ποινής (Courant, 1943), του Dantzig επί του γραμμικού προγραμματισμού (Dantzig, 1951), των Karush και Kuhn & Tucker επί των αναγκαίων και ικανών συνθηκών σχετικά με την ύπαρξη ακροτάτου (Karush, 1939; Kuhn and Tucker, 1951).

Κατά τη δεκαετία του 60, δημοσιεύθηκε μεγάλο πλήθος μαθηματικών μεθόδων επίλυσης μη-γραμμικών προβλημάτων βελτιστοποίησης. Ειδικότερα, ο Rosenbrock παρουσίασε τη μέθοδο των ορθογωνίων διευθύνσεων (Method of Orthogonal Directions, Rosenbrock, 1960), ο Rosen πρότεινε τη μέθοδο προβολής κλίσης (Gradient Projection Method, Rosen, 1960), ο Zoutendijk εισήγαγε τη μέθοδο των δυνατών κατευθύνσεων (Method of Feasible Directions, Zoutendijk, 1960), οι Hooke και Jeeves ανέπτυξαν την ομώνυμη μέθοδο (Hooke and Jeeves, 1961), οι Davidon, Fletcher και Powell παρουσίασαν τη μέθοδο της μεταβλητής μετρικής (Variable Metric Method, Fletcher and Powell, 1963), ο Powell πρότεινε τη μέθοδο των συζυγών διευθύνσεων (Conjugate Direction Method, Powell, 1964), οι Fletcher και Reeves δημοσίευσαν τη μέθοδο των συζυγών κλίσεων (Method of Conjugate Gradients, Fletcher and Reeves, 1964), οι Nelder και Mead ανέπτυξαν μια παραλλαγή της μεθόδου Simplex (Nelder and Mead, 1965), ο Box πρότεινε την ομώνυμη μέθοδό του (Box, 1965), ενώ οι Fiacco και McCormick διαμόρφωσαν την αποκαλούμενη τεχνική της διαδοχικής βελτιστοποίησης άνευ περιορισμών (Sequential Unconstrained Minimization Technique (SUMT), Fiacco and McCormick, 1966).

Από την προηγηθείσα σύντομη ιστορική αναδρομή, στην οποία αναφέρθηκαν λίγες από τις εκατοντάδες των δημοσιευμένων εργασιών επί της βελτιστοποίησης, προκύπτει ότι, κατά τη δεκαετία του 60, δημοσιεύονταν με πολύ υψηλό ρυθμό τόσο μεθοδολογίες βελτιστοποίησης

όσο και παραλλαγές αυτών. Το μεγαλύτερο ποσοστό αυτών των μεθοδολογιών ήταν μαθηματικής φύσεως και αιτιοκρατικού χαρακτήρα, δηλαδή αφορούσαν σε διαδικασίες οι οποίες όσες φορές και εάν εκκινούσαν από ένα, αλλά το ίδιο, αρχικό διάνυσμα σχεδίασης $\mathbf{X}_{ini}$ πάντοτε κατέληγαν στο ίδιο τελικό διάνυσμα σχεδίασης $\mathbf{X}_{fin}$. Δεδομένου ότι οι μεθοδολογίες αυτού του τύπου αφορούν στο γενικευμένο πρόβλημα βελτιστοποίησης, είναι δυνατόν να χρησιμοποιηθούν για την επίλυση οποιουδήποτε προβλήματος βελτιστοποίησης, ανεξαρτήτως των ιδιαιτέρων χαρακτηριστικών της εκάστοτε εξεταζομένης περίπτωσης, αρκεί να χρησιμοποιείται η διατύπωση των Εξ.(1.1, 1.2). Εξ αιτίας της γενικότερης ισχύος των εν λόγω μεθοδολογιών, αρχικά είχε θεωρηθεί ότι αυτές θα ήταν δυνατόν να χρησιμοποιηθούν και για την επίλυση προβλημάτων βελτιστοποίησης κατασκευών. Παράλληλα, δε, σημειώνονταν σημαντικά βήματα στον τομέα των υπολογιστικών συστημάτων, τα οποία εμφανίζονταν ολοένα συχνότερα και ισχυρότερα. Λογικό επόμενο ήταν να αρχίσει να διαμορφώνεται η ισχυρή πεποίθηση ότι ήταν καθαρά θέμα χρόνου η χρήση των αιτιοκρατικών μεθόδων βελτιστοποίησης για την επίλυση προβλημάτων βελτιστοποίησης στις κατασκευές. Ωστόσο, ο αρχικός ενθουσιασμός δεν διήρκησε πολύ. Στην πράξη αποδείχθηκε ότι οι εν λόγω μεθοδολογίες υπέφεραν από δύο σημαντικά μειονεκτήματα: κατά πρώτον ήταν ευπαθείς στον εγκλωβισμό σε τοπικά ακρότατα και κατά δεύτερον το υπολογιστικό κόστος αυξανόταν πολύ, έως και απαγορευτικά πολύ, καθώς αύξανε το πλήθος των μεταβλητών σχεδίασης. Αυτά τα δύο θέματα αποτέλεσαν το μήλον της έριδος μεταξύ των μελών της επιστημονικής κοινότητας, η οποία, αρκετά σύντομα, διαιρέθηκε σε δύο στρατόπεδα: των υπερμάχων των αποκαλουμένων Μαθηματικών Μεθόδων Βελτιστοποίησης (ΜΜΒ) και των υποστηρικτών των μεθόδων εκείνων, οι οποίες διακρίνονταν για ένα πιο ‘μηχανολογικό προσανατολισμό’.

Όσοι υποστήριζαν τις (ΜΜΒ) ισχυρίζονταν ότι ο ακρογωνιαίος λίθος για τη διατύπωση οποιασδήποτε μεθόδου βελτιστοποίησης ήταν η διαμόρφωση ενός στιβαρού μαθηματικού υποβάθρου. Συνεπώς, σύμφωνα με την άποψή τους, ο ορθός τρόπος διεξαγωγής έρευνας επί θεμάτων βελτιστοποίησης ήταν η επένδυση χρόνου και προσπάθειας είτε στην ενδελεχή μελέτη και επέκταση ήδη διατυπωμένων θεωρήσεων είτε στην ανάπτυξη νέων θεωρήσεων, χωρίς, ωστόσο, κανέναν συμβιβασμό σχετικά με τη διαμόρφωση του προαναφερθέντος υποβάθρου. Σε αυτό το πλαίσιο, ένα σημαντικό βήμα προόδου σημειώθηκε με τη διατύπωση των διαδοχικών τεχνικών προγραμματισμού, όπως είναι ο Διαδοχικός Γραμμικός Προγραμματισμός (Sequential Linear Programming - SLP) και ο Διαδοχικός Τετραγωνικός Προγραμματισμός (Sequential Quadratic Programming - SQP) (Venkatamaran, 2002). Ωστόσο, το νέο και επαναστατικό στοιχείο στη διαδικασία βελτιστοποίησης ήταν η εισαγωγή της τυχαιότητας, η οποία αύξανε την πιθανότητα μη-εγκλωβισμού σε τοπικά ακρότατα. Ανάμεσα στους πλέον σημαντικούς αντιπροσώπους αυτής της τάσης, διακρίνονται οι Στρατηγικές Εξέλιξης (Rechenberg, 1989), οι Γενετικοί Αλγόριθμοι (Goldberg, 1989) και η Προσομοιούμενη Ανόπτηση (Kirkpatrick, 1984).

Στον αντίποδα, όσοι υποστήριζαν τη χρήση μιας πιο μηχανολογικής προσέγγισης, ήταν υπέρμαχοι της ανάπτυξης μεθοδολογιών, οι οποίες ενδεχομένως να στερούνταν το αυστηρό μαθηματικό υπόβαθρο, ωστόσο επέτρεπαν τη χρήση της κρίσης και της διαίσθησης του Μηχανικού. Σε αυτό το πλαίσιο, ανήκουν μεθοδολογίες, οι οποίες αποδεικνύεται, με αυστηρά μαθηματικό τρόπο, ότι ισχύουν μόνο υπό συγκεκριμένες περιπτώσεις, ενώ η γενίκευση τους είναι αποδεκτή μόνον ως μία επαρκής προσέγγιση. Σε αυτήν την κατηγορία ανήκουν τα φημισμένα Βέλτιστα Κριτήρια (Optimality Criteria - OC), δηλαδή προτάσεις οι οποίες περιγράφουν, άμεσα ή έμμεσα, κάποια ενεργειακής φύσεως κατάσταση, η οποία ισχύει για τη βέλτιστη σχεδίαση. Τα Βέλτιστα Κριτήρια συνδυάστηκαν με στοιχεία αριθμητικής αναλύσεως, όπως είναι η κλίση μίας διανυσματικής συνάρτησης και το διωνυμικό ανάπτυγμα, οδηγώντας στη διαμόρφωση ισχυρών μεθοδολογιών βελτιστοποίησης. Ωστόσο, αυτές οι μεθοδολογίες ήταν κατάλληλες μόνον για την επίλυση προβλημάτων

βελτιστοποίησης κατασκευών διότι ήταν διατυπωμένες βάσει εγγενών χαρακτηριστικών των προς επίλυση προβλημάτων, όπως είναι η ενέργεια παραμόρφωσης και παράγωγα αυτής. Η χρυσή εποχή των Βελτίστων Κριτηρίων, όπως αυτό υπαγορεύεται από το τεράστιο πλήθος των δημοσιεύσεων, ήταν η δεκαετία του 70. Ενδεικτικά, αναφέρεται ότι οι δημοσιεύσεις επί Βελτίστων Κριτηρίων το έτος 1979 ήταν περίπου 200 ανά μήνα σε περισσότερα από 30 επιστημονικά περιοδικά, χωρίς να περιλαμβάνονται ούτε πρακτικά συνεδρίων ούτε τεύχη-αφιερώματα (Sargent, 1980). Η αιχμή του δόρατος των Βελτίστων Κριτηρίων ήταν το γεγονός ότι χρησιμοποιούσαν τον ίδιο αναδρομικό τύπο για όλες τις μεταβλητές σχεδίασης, συνεπώς ήταν σε θέση να διαχειρισθούν αποτελεσματικά ένα πολύ μεγάλο πλήθος από αυτές.

Μεταξύ των προαναφερθέντων 'στρατοπέδων', η πλέον σημαντική διαφορά έγκειται στην αντίληψη σχετικά με την περιγραφή του αντικειμενικού σκοπού. Από την πλευρά του Μηχανικού, ο αντικειμενικός σκοπός είναι η διαμόρφωση μίας σχεδίασης, η οποία είναι επαρκώς βελτιωμένη (βελτιστοποιημένη) υπό την αυστηρή προϋπόθεση ότι οι επιβαλλόμενοι περιορισμοί είτε δεν παραβιάζονται είτε παραβιάζονται με τέτοιον τρόπο ώστε η συμπεριφορά της κατασκευής να επηρεάζεται αμελητέα. Με άλλα λόγια, σύμφωνα με την αντίληψη του Μηχανικού, ο αντικειμενικός σκοπός είναι η εύρεση μίας δυνατής σχεδίασης, η οποία συμβιβάζει με ικανοποιητικό τρόπο την απαίτηση για υψηλού επιπέδου ασφάλεια και την επιθυμία για μειωμένο κόστος. Αντιθέτως, η μαθηματική προσέγγιση αποτελεί μία άκρως θεωρητική προσέγγιση, χωρίς να συνυπολογίζει τη φυσική ερμηνεία των εμπλεκομένων ποσοτήτων. Ως εκ τούτου, απορρίπτει λύσεις οι οποίες είναι υψηλής πρακτικής αξίας αλλά είτε δεν αποδεικνύεται ότι αντιστοιχούν στο καθολικά βέλτιστο αποτέλεσμα είτε προκύπτει ότι αντιστοιχούν σε κάποιο τοπικό ακρότατο. Όπως συμβαίνει στις πλείστες των περιπτώσεων, η βέλτιστη προσέγγιση αντιστοιχεί σε έναν ενδιάμεσο συμβιβασμό. Στην προκειμένη περίπτωση, αυτός ο συμβιβασμός πρέπει να επιτευχθεί μεταξύ διαμόρφωσης μίας αυστηρής μαθηματικής προσέγγισης και αξιοποίησης της κρίσης και διαίσθησης του Μηχανικού. Στην πραγματικότητα, ο συνδυασμός αυτών των δύο στοιχείων οδηγεί στο βέλτιστο δυνατό αποτέλεσμα, όσον αφορά, τουλάχιστον, τη βελτιστοποίηση κατασκευών.

Από την προαναφερθείσα σύντομη ιστορική αναδρομή, προκύπτει ότι πλήθος μεθοδολογιών και ακόμα μεγαλύτερο πλήθος εργασιών, έχουν δημοσιευθεί στην περιοχή της βέλτιστης κατανομής υλικού στις κατασκευές. Στη διεθνή βιβλιογραφία υπάρχουν άρθρα ανασκόπησης, καθένα εκ των οποίων παραπέμπει σε εκατοντάδες άλλα άρθρα, ενώ υπάρχει και ένας πολύ μεγάλος αριθμός βιβλίων, στα οποία είναι δυνατόν να ανατρέξει κάποιος προκειμένου να βρει λεπτομερείς πληροφορίες επί ενός συγκεκριμένου θέματος στην περιοχή της βελτιστοποίησης. Συνεπώς, στην παρούσα Διδακτορική Διατριβή, δεν συντρέχει λόγος αναφοράς σε στοιχεία, τα οποία είναι δυνατόν να ανακτηθούν μέσα από μία βιβλιογραφική ανασκόπηση. Για λόγους πληρότητας, στην επόμενη ενότητα περιγράφονται συνοπτικά οι πλέον σημαντικές κατηγορίες προβλημάτων και μεθοδολογιών βελτιστοποίησης στις κατασκευές, ενώ για κάθε μία από τις εν λόγω κατηγορίες παρατίθεται μία λεπτομερής βιβλιογραφία.

1.4. Αντιπροσωπευτικές μέθοδοι βελτιστοποίησης κατασκευών

Μία πρώτη κατηγοριοποίηση των υπαρχόντων μεθόδων βελτιστοποίησης κατασκευών επιτυγχάνεται με κριτήριο τον άμεσο ή έμμεσο τρόπο αναζήτησης του βελτίστου. Ειδικότερα, υπάρχουν μέθοδοι στις οποίες το βάρος της κατασκευής αποτελεί την αντικειμενική συνάρτηση του προβλήματος βελτιστοποίησης (άμεση αναζήτηση), ενώ υπάρχουν και μέθοδοι στις οποίες η μείωση του βάρους μίας κατασκευής επιδιώκεται μέσω της ικανοποίησης ενός ενεργειακού κριτηρίου, ισχύοντος για την κατασκευή ελαχίστου βάρους (έμμεση αναζήτηση). Επιπροσθέτως, οι μέθοδοι άμεσης αναζήτησης είναι δυνατόν να διακριθούν περαιτέρω σε εκείνες αιτιοκρατικού χαρακτήρα και σε εκείνες στοχαστικού χαρακτήρα.

Στην υποκατηγορία των άμεσων και αιτιοκρατικών μεθόδων ανήκουν η μέθοδος των Hooke & Jeeves, η μέθοδος Simplex, η μέθοδος Complex (Box), η μέθοδος του Powell, η μέθοδος της Μεγίστης Κλίσεως, η μέθοδος των Συζυγών Κλίσεων, η μέθοδος των Συζυγών Διευθύνσεων, ο Διαδοχικός Γραμμικός Προγραμματισμός (SLP) και ο Διαδοχικός Τετραγωνικός Προγραμματισμός (SQP).

Στην υποκατηγορία των άμεσων και στοχαστικών μεθόδων, οι πλέον χαρακτηριστικοί αντιπρόσωποι είναι οι Στρατηγικές Εξέλιξης (ES) και οι παραλλαγές αυτών, οι Γενετικοί Αλγόριθμοι (GA) μαζί με όλες τις παραλλαγές αυτών, η Προσομοιούμενη Ανόπτηση (SA), η μέθοδος Tabu, η τεχνική Σμήνους Σωματιδίων (Swarm Particles Technique) και η μέθοδος της Αρμονίας (Harmony method). Ακολουθεί μια συνοπτική περιγραφή για κάθε μία από τις μεθόδους αυτές

Οι Στρατηγικές Εξέλιξης (Evolution Strategies - ES) αποτελούν μία τεχνική βελτιστοποίησης, η οποία στηρίζεται στην ιδέα της προσαρμοστικότητας και της εξέλιξης. Διατυπώθηκε στις αρχές της δεκαετίας του 60 και αναπτύχθηκε περαιτέρω στη δεκαετία του 70. Θεμελιωτές αυτής της προσέγγισης ήταν οι Rechenberg και Schwefel. Οι Στρατηγικές Εξέλιξης ανήκουν στην ευρύτερη τάξη της τεχνητής εξέλιξης, χρησιμοποιούν αντιστοιχίες από τον φυσικό κόσμο και διαθέτουν ως κύριους τελεστές τη μετάλλαξη και την επιλογή, τους οποίους χρησιμοποιούν επαναληπτικά μέχρι να ικανοποιηθεί κάποιο κριτήριο τερματισμού. Στην περίπτωση διανυσμάτων σχεδίασης με πραγματικούς αριθμούς, η μετάλλαξη συνήθως πραγματοποιείται προσθέτοντας έναν αριθμό από κανονική κατανομή σε κάθε μεταβλητή σχεδίασης. Η επιλογή στις Στρατηγικές Εξέλιξης είναι αιτιοκρατική και στηρίζεται στην κατάταξη των διανυσμάτων σχεδίασης βάσει της τιμής της αντικειμενικής συνάρτησης. Η πλέον απλή εκδοχή των Στρατηγικών Εξέλιξης περιλαμβάνει ένα πληθυσμό με δύο άτομα, έναν γονέα και το αποτέλεσμα της επιβολής σε αυτόν του τελεστή μετάλλαξης. Εάν το μεταλλαγμένο άτομο είναι τουλάχιστον εξίσου κατάλληλο με τον γονέα, τότε τον αντικαθιστά στην επόμενη επανάληψη (γενεά). Αυτός ο τύπος Στρατηγικής Εξέλιξης καλείται (1+1)-ES. Γενικεύοντας, λ μεταλλαγμένα άτομα είναι δυνατόν να δημιουργηθούν από ένα γονέα και να συγκριθούν μαζί του, διαμορφώνοντας τον αποκαλούμενο τύπο (1+λ)-ES. Σε αυτόν τον τύπο, το καλύτερο εκ των μεταλλαγμένων ατόμων ανάγεται σε γονέα στην επόμενη επανάληψη, ενώ ο εκάστοτε τρέχων γονέας εξαιρείται σε όλες τις επόμενες επαναλήψεις (Beyer, 2001; Beyer and Schwefel, 2002; Rechenberg, 1971; Schwefel, 1995; Schwefel, 2002).

Οι Γενετικοί Αλγόριθμοι (Genetic Algorithms - GA) κατατάσσονται ως ευριστικές μέθοδοι καθολικής αναζήτησης. Αποτελούν μία ειδική κλάση των Στρατηγικών Εξέλιξης και χρησιμοποιούν στοιχεία της Δαρβίνειας θεωρίας, όπως η κληρονομικότητα, η μετάλλαξη, η επιλογή και η διασταύρωση. Σε έναν τυπικό Γενετικό Αλγόριθμο, αρχικά δημιουργείται τυχαία ένας πληθυσμός από διανύσματα σχεδίασης (χρωμοσώματα), ο οποίος σταδιακά τροποποιείται, μέσω διαδικασιών εξέλιξης, κατευθυνόμενες προς διανύσματα σχεδίασης με καλύτερη τιμή αντικειμενικής συνάρτησης (καλύτερη συμπεριφορά). Για την κωδικοποίηση των διανυσμάτων σχεδίασης συνήθως χρησιμοποιείται είτε το δυαδικό σύστημα είτε ο κώδικας Gray, χωρίς, ωστόσο, να αποκλείεται κάποια άλλη κωδικοποίηση. Η διαδικασία της εξέλιξης εκκινεί από τον αρχικό πληθυσμό και λαμβάνει χώρα επαναληπτικά. Σε κάθε επανάληψη (γενεά), εκτιμάται η επίδοση κάθε μέλους του πληθυσμού, μέσω της τιμής της αντικειμενικής του συνάρτησης, ξεχωρίζονται τα μέλη με την καλύτερη επίδοση, τα οποία στη συνέχεια διασταυρώνονται και μεταλλάσσονται, δημιουργώντας έναν νέο πληθυσμό. Αυτός, με τη σειρά του, χρησιμοποιείται στην επόμενη επανάληψη και η όλη διαδικασία συνεχίζεται έως ότου ικανοποιηθεί κάποιο κριτήριο τερματισμού. Συνήθως, ως τέτοιο χρησιμοποιείται είτε ένα μέγιστο πλήθος επαναλήψεων είτε μία τιμή επίδοσης (τιμή αντικειμενικής συνάρτησης) για όλο τον πληθυσμό. Ωστόσο, εάν ο τερματισμός της επαναληπτικής διαδικασίας επέλθει λόγω εκτέλεσης του μεγίστου πλήθους επαναλήψεων,

τότε δεν είναι βέβαιο ότι ο πληθυσμός θα χαρακτηρίζεται από ικανοποιητικές επιδόσεις. Ένα ιδιαίτερο χαρακτηριστικό των Γενετικών Αλγορίθμων είναι το γεγονός ότι η κωδικοποίηση κάθε διανύσματος σχεδίασης ως μονοδιάστατο πίνακα διευκολύνει τη διαδικασία της διασταύρωσης (Goldberg, 1989; Goldberg, 2002; Fogel, 2006; Holland, 1975; Koza, 1992; Michalewicz, 1999).

Η Προσομοιούμενη Ανόπτηση (Simulated Annealing - SA) αποτελεί μία στοχαστική μεθοδολογία βελτιστοποίησης καθολικού χαρακτήρα, υπό την έννοια ότι σε κάθε επανάληψη δεν συμμετέχει μόνο κάποιο υποσύνολο του πεδίου σχεδίασης, το οποίο προοδευτικά συρρικνώνεται έως ότου τελικά καταλήξει σε ένα σημείο (βέλτιστο διάνυσμα σχεδίασης), αλλά είναι δυνατόν να χρησιμοποιείται ολόκληρο το πεδίο σχεδίασης. Το ιδιαίτερο χαρακτηριστικό αυτής της μεθοδολογίας είναι η αποδοχή όχι μόνον εκείνου του διανύσματος σχεδίασης, το οποίο είναι καλύτερο από το τρέχον βέλτιστο, αλλά και η στατιστική αποδοχή διανύσματος σχεδίασης με επίδοση χειρότερη από αυτήν του τρέχοντος βελτίστου διανύσματος. Για την στατιστική αποδοχή χρησιμοποιείται το κριτήριο του Metropolis. Η Προσομοιούμενη Ανόπτηση είναι δυνατόν να συνδυαστεί με έναν τυπικό Γενετικό Αλγόριθμο, στον οποίο, κατά τη διαδικασία της βελτιστοποίησης, το αρχικώς υψηλό ποσοστό μετάλλαξης προοδευτικά μειώνεται σύμφωνα με κάποιο σχήμα απόψυξης (Kirkpatrick et al, 1983; Cerny, 1985; Metropolis et al, 1953).

Η μέθοδος Tabu (Tabu Search - TS) είναι παρόμοια με την Προσομοιούμενη Ανόπτηση υπό την έννοια ότι και οι δύο διατρέχουν το πεδίο σχεδίασης και δοκιμάζουν αλλαγές επί μεμονωμένων λύσεων. Ωστόσο, ενώ η Προσομοιούμενη Ανόπτηση σε κάθε επανάληψη παράγει ένα νέο διάνυσμα σχεδίασης, η μέθοδος Tabu δημιουργεί πολλά νέα διανύσματα και αναζητεί, μεταξύ αυτών, εκείνο το διάνυσμα με τη χαμηλότερη ενέργεια. Προς ενίσχυση της διερεύνησης μεγαλύτερου μέρους του πεδίου σχεδίασης και προς αποφυγή επανεξέτασης ήδη εξετασθέντων και απορριφθέντων διανυσμάτων σχεδίασης, δημιουργείται μία λίστα με τα εν λόγω διανύσματα, η οποία ανανεώνεται διαρκώς σε κάθε επανάληψη. Απαγορεύεται, δε, να χρησιμοποιηθούν τα διανύσματα της λίστας αυτής. Η μέθοδος Tabu χαρακτηρίζεται ως ένας μετα-ευριστικός αλγόριθμος, κατάλληλος για την επίλυση προβλημάτων βελτιστοποίησης συνδυαστικού τύπου (Glover and Laguna, 1997; Glover, 1989; Glover, 1990; Cvijovic et al, 1995).

Η μέθοδος της Αρμονίας (Harmony Search - HS) αποτελεί μία μετα-ευριστική διαδικασία βελτιστοποίησης, η οποία μιμείται τη διαδικασία με την οποία αυτοσχεδιάζουν οι μουσικοί. Πιο συγκεκριμένα, δημιουργείται ένας πίνακας (*Harmony Memory - HM*) διάστασης $N \times M$, όπου N είναι το πλήθος των διανυσμάτων σχεδίασης (ανεξάρτητη μεταβλητή) και M το πλήθος των μεταβλητών σχεδίασης. Αρχικά, αποδίδονται τυχαίες τιμές σε όλες τις μεταβλητές σχεδίασης του εν λόγω πίνακα, υπολογίζεται η αντικειμενική συνάρτηση για κάθε διάνυσμα σχεδίασης και εντοπίζεται το διάνυσμα σχεδίασης με τη χειρότερη επίδοση (έστω $\mathbf{X}_{worst}$). Στη συνέχεια δημιουργείται ένα νέο διάνυσμα σχεδίασης. Για την απόδοση μίας νέας τιμής σε κάθε μεταβλητή σχεδίασης, λαμβάνονται υπόψη, με τρόπο πιθανοτικό, όχι μόνον όλες οι τιμές του προαναφερθέντος πίνακα για κάθε μεταβλητή σχεδίασης αλλά και το πεδίο ορισμού της κάθε μεταβλητής σχεδίασης. Κατόπιν, το νεοδημιουργηθέν διάνυσμα σχεδίασης υποβάλλεται σε μία διαδικασία διαμόρφωσης, στην οποία οι μεταβλητές σχεδίασης προσαυξάνονται κατά μια τυχαία ποσότητα. Τέλος, αξιολογείται η επίδοση του νέου διανύσματος σχεδίασης και εάν αυτή είναι καλύτερη από εκείνη του $\mathbf{X}_{worst}$, τότε το αντικαθιστά στον πίνακα (*HM)*, ενώ το $\mathbf{X}_{worst}$ εξαιρείται από όλες τις επόμενες αναζητήσεις. Η μέθοδος (HS) είναι κατάλληλη κυρίως για τον εντοπισμό περιοχών του πεδίου σχεδίασης υψηλών επιδόσεων (Saka and Kameshki, 1998; Erdal and Saka, 2006; Geem et al, 2001; Geem et al, 2002; Saka, 2003).

Η μέθοδος βελτιστοποίησης με Σμήνη Σωματιδίων (Particle Swarm Optimization - PSO) αποτελεί μία μέθοδο άμεσης αναζήτησης, διαχειρίζεται έναν πληθυσμό από διανύσματα σχεδίασης και είναι στοχαστικού χαρακτήρα. Η κεντρική ιδέα της μεθόδου στηρίζεται σε αρχές της κοινωνιολογίας και της ψυχολογίας, σχετικά με τον τρόπο συμπεριφοράς των μελών μίας ομάδας υπό την επίδραση διαφόρων και διαφορετικών ερεθισμάτων. Είναι γεγονός ότι ένας τρόπος, τον οποίο χρησιμοποιεί ο άνθρωπος για την επίλυση των προβλημάτων του, είναι η επικοινωνία με άλλους ανθρώπους και επί του συγκεκριμένου προβλήματος. Μέσω αυτής της επικοινωνίας, ο άνθρωπος αλληλεπιδρά και μεταβάλλεται. Μέσα από αυτήν την αλληλεπίδραση, επιτυγχάνεται μία προσέγγιση των ατόμων μεταξύ τους, η οποία οδηγεί στην τελική επικράτηση απόψεων και θέσεων, τις οποίες υιοθετούν τα αλληλεπιδρώντα άτομα, σχετικά με τη βέλτιστη αντιμετώπιση ενός προβλήματος. Η μέθοδος (PSO) προσομοιάζει αυτήν την κοινωνική συμπεριφορά. Κατά πρώτον, πρέπει να διατυπωθεί με πληρότητα το πρόβλημα βελτιστοποίησης και να ορισθεί με σαφήνεια η αντικειμενική συνάρτηση για την εκτίμηση της επίδοσης μία προτεινόμενης λύσης. Επίσης, πρέπει να δημιουργηθεί ένα πρωτόκολλο επικοινωνίας, έτσι ώστε να είναι δυνατή η επικοινωνία κάθε μέλους της ομάδος με τους γείτονές του. Στη συνέχεια δημιουργείται, με εντελώς τυχαίο τρόπο, ένας πληθυσμός από διανύσματα σχεδίασης, επονομαζόμενο και ως σμήνος σωματιδίων ή σμήνος μεμονωμένων ατόμων, ο οποίος βελτιώνεται συνεχώς μέσα από μια επαναληπτική διαδικασία. Σε αυτήν τη διαδικασία, εκτιμάται η επίδοση κάθε ατόμου και επιτρέπεται η ανταλλαγή πληροφορίας μεταξύ ατόμων και γειτόνων, σε επίπεδο τιμών μεταβλητών σχεδίασης και βάσει του προαναφερθέντος πρωτοκόλλου επικοινωνίας, έτσι ώστε το σμήνος προοδευτικά να κατευθύνεται προς καλύτερες επιδόσεις (Kennedy and Eberhart, 1995; Eberhart and Kennedy, 1995; Eberhart and Shi, 1998; Shi and Eberhart, 1998a; Shi and Eberhart, 1998b; Eberhart and Shi, 2001).

Η μέθοδος βελτιστοποίησης της Αποικίας Μυρμηγκιών (Ant Colony Optimization) είναι μία μετα-ευριστική τεχνική βελτιστοποίησης, στοχαστικής φύσεως, κατάλληλη για την επίλυση προβλημάτων, τα οποία ανάγονται στην εύρεση του καλύτερου δρόμου μέσω γράφων. Η κεντρική ιδέα της μεθόδου προέρχεται από τον τρόπο συμπεριφοράς των μυρμηγκιών, όταν αυτά αναζητούν την τροφή τους. Ειδικότερα, τα μυρμήγκια περιφέρονται με τυχαίο τρόπο προς αναζήτηση τροφής και όταν εντοπίσουν κάτι τότε αποκόπτουν ένα τμήμα της τροφής και το μεταφέρουν πίσω στην αποικία τους. Κατά την επιστροφή τους, αφήνουν πίσω τους ίχνη από τη χημική ουσία φερομόνη, προκειμένου να μεταβιβάσουν στα υπόλοιπα μέλη της αποικίας το γεγονός ότι έχει εντοπισθεί τροφή. Όταν άλλα περιπλανόμενα μυρμήγκια εντοπίσουν αυτά τα ίχνη, τότε κατευθύνονται προς την τροφή, αποκόπτουν και αυτά ένα τμήμα της και το μεταφέρουν πίσω στην αποικία τους. Κατά την επιστροφή τους, δε, αποθέτουν και αυτά με τη σειρά τους ίχνη φερομόνης, με αποτέλεσμα σχετικά σύντομα να σχηματισθεί ένα μονοπάτι με ισχυρά ίχνη φερομόνης. Ωστόσο, η φερομόνη έχει την τάση να εξατμίζεται, οπότε ίχνη σε μονοπάτια μεγαλύτερου μήκους εξαφανίζονται γρηγορότερα από τα αντίστοιχα ίχνη ενός μονοπατιού με μικρότερο μήκος. Με αυτόν τον τρόπο, προοδευτικά, ενισχύεται με ίχνη φερομόνης, και τελικά απομένει, η συντομότερη διαδρομή προς την τροφή (Dorigo, 1992; Deneubourg et al, 1990; Di Caro and Dorigo, 1998; Dorigo and Blum, 2005; Dorigo and Gambardella, 1997; Dorigo et al, 1996; Dorigo and Stützle, 2004; Gutjahr, 2000; Stützle and Hoos, 2000; Serra and Venini, 2006).

Στην κατηγορία των έμμεσων μεθοδολογιών βελτιστοποίησης ανήκουν τα λεγόμενα Βέλτιστα Κριτήρια καθώς και οι σημαντικότατες εργασίες των Michell, Venkayya, Gelatly, Khot, Berke, Allwood και Patnaik. Στο αυτό μήκος κύματος, οι μέθοδοι COC και DCOC, τις οποίες ανέπτυξε ο Rozvany και οι συνεργάτες του, παραμένουν μεταξύ των κορυφαίων μεθόδων της εν λόγω κατηγορίας. Δεδομένου ότι οι πλέον πρόσφατες από αυτές τις εργασίες χρονολογούνται πλέον των είκοσι ετών, δεν είναι δυνατόν να θεωρηθούν ως ανήκουσες στην τεχνολογική στάθμη της εποχής και για το λόγο αυτό παρατίθεται ενδεικτική βιβλιογραφία

(Michell, 1904; Venkayya, 1971; Allwood and Chung, 1984; Patnaik et al, 1993; Zhou and Rozvany, 1992/93; Rozvany and Zhou, 1989/90; Rozvany and Zhou, 1990).

Εκτός των προαναφερομένων μεθοδολογιών, ειδική μνεία αρμόζει σε σύγχρονες μεθόδους, οι οποίες θεωρούνται ως το σύγχρονο μέτωπο της επιστήμης. Από αυτήν την οπτική γωνία, αναφέρονται η Μέθοδος της Ομογενοποίησης (Homogenization Method), η μέθοδος SIMP (Solid Isotropic Material with Penalization), η Μέθοδος των Κινουμένων Ασυμπτώτων (Method of Moving Asymptotes), η Μέθοδος των Φυσαλίδων (Bubble Method) και η Μέθοδος ESO (Evolutionary Structural Optimization).

Σε ένα πρόβλημα βελτιστοποίησης σχήματος μίας κατασκευής, εν γένει είναι δυνατόν να μεταβάλλονται τα σύνορα, τόσο τα εξωτερικά όσο και τα εσωτερικά, του χώρου σχεδίασης μέχρι να εντοπισθεί το βέλτιστο σχήμα. Προς τούτο, συνήθως απαιτείται η πλεγματοποίηση του εκάστοτε νέου σχήματος. Αντιθέτως, με την μέθοδο της ομογενοποίησης κάτι τέτοιο δεν είναι αναγκαίο. Πιο συγκεκριμένα, σύμφωνα με την εν λόγω μέθοδο, ο χώρος σχεδίασης αρχικά πλεγματοποιείται και σε αυτόν αποδίδονται ιδιότητες ομογενούς και ισοτροπικού υλικού. Στη συνέχεια, και χρησιμοποιώντας πάντοτε το ίδιο πλέγμα, επιλύεται το πρόβλημα της αναζήτησης της βέλτιστης χωρικής περιοδικής κατανομής ενός πλήθους οπών μικροσκοπικών διαστάσεων, εξ αιτίας του οποίου το αρχικώς ισοτροπικό υλικό αποκτά ανισοτροπικές ιδιότητες. Προφανώς, στο ανωτέρω πρόβλημα βελτιστοποίησης επιβάλλεται η βασική προϋπόθεση ότι η τελική κατανομή δύναται να παραλάβει με ασφάλεια τα ονομαστικά φορτία και ικανοποιεί οποιονδήποτε άλλο σχεδιαστικό περιορισμό (Bendsøe and Kikuchi, 1988).

Μία ακόμα προσέγγιση σχετικά με το πρόβλημα βελτιστοποίησης σχήματος είναι η θεώρησή του ως πρόβλημα βέλτιστης κατανομής υλικού υπό δεδομένα φορτία και συνθήκες στήριξης (μέθοδος SIMP). Με αυτόν τον τρόπο, κάθε σημείο στο χώρο θεωρείται είτε ως πλήρες υλικού είτε ως κενό υλικού και το πρόβλημα βελτιστοποίησης ανάγεται σε πρόβλημα διακριτών μεταβλητών. Με βάση αυτή τη θεώρηση, είναι δυνατή η άρση της εν λόγω διακριτότητας μέσω της εισαγωγής μίας συνάρτησης πυκνότητας, η οποία είναι συνεχής στο χώρο σχεδίασης. Το σύνολο των θέσεων του χώρου σχεδίασης με υψηλή πυκνότητα οριοθετούν και το σχήμα της βέλτιστης κατανομής. Για ενδιάμεσες τιμές πυκνότητας είναι δυνατή η χρήση μίας συνάρτησης ποινής. Εναλλακτικά, είναι δυνατή η εισαγωγή, μικροσκοπικών διαστάσεων και περιοδικών, κενώ, έτσι ώστε οι φαινόμενες ιδιότητες του υλικού να υπολογίζονται μέσω διαδικασίας ομογενοποίησης (Bendsøe, 1989).

Η Μέθοδος των Κινουμένων Ασυμπτώτων (Method of Moving Asymptotes - MMA) αναπτύχθηκε από τον Svanberg και αφορά σε μία επαναληπτική διαδικασία, σε κάθε βήμα της οποίας δημιουργείται και επιλύεται ένα αυστηρώς κυρτό πρόβλημα προσέγγισης. Η δημιουργία αυτών των προσεγγίσεων ελέγχεται από τις αποκαλούμενες 'κινούμενες ασύμπτωτες', οι οποίες δύνανται να σταθεροποιήσουν και να επιταχύνουν την όλη διαδικασία. Αυτή η μέθοδος είναι ικανή να διαχειρίζεται όλα τα είδη των περιορισμών, με μοναδική προϋπόθεση τον υπολογισμό, είτε αριθμητικό είτε αναλυτικό, των παραγώγων των συναρτήσεων περιορισμού or analytically (Svanberg, 1987).

Η μέθοδος των φυσαλίδων (Bubble Method) αναπτύχθηκε από τον Eschenauer και στηρίζεται στην εισαγωγή οπών (φυσαλίδες) σε μία σχεδίαση. Η επαναληπτική εισαγωγή φυσαλίδων επιτυγχάνεται μέσω διαφόρων μεθόδων, μία εκ των οποίων είναι και η επίλυση ενός προβλήματος μεταβολών. Η εισαγωγή μίας φυσαλίδας έχει ως αποτέλεσμα να αλλάζει η τοπολογία της εξεταζόμενης κατασκευής. Για τις προκύπτουσες διαφορετικές τοπολογίες, εφαρμόζεται μία, ιεραρχικού τύπου, διαδικασία βελτιστοποίησης σχήματος, προκειμένου να εντοπισθεί το βέλτιστο σχήμα των φυσαλίδων (Eschenauer, 1994).

Η μέθοδος ESO, προταθείσα από τους Xie και Steven, αφορά σε μία εξαιρετικά απλή τεχνική βελτιστοποίησης, εν αντιθέσει με τις περισσότερες υπάρχουσες. Η κεντρική ιδέα είναι η εύρεση μίας βέλτιστης σχεδίασης ομοιόμορφου πάχους (Optimum Uniform Design -

OUD), για την οποία να ικανοποιείται ο εκάστοτε επιβαλλόμενος περιορισμός. Στη συνέχεια, από αυτήν τη σχεδίαση, απομακρύνεται πλεονάζον υλικό, το οποίο χαρακτηρίζεται από τη χαμηλότερη ενεργειακή συμμετοχή. Οι δύο βασικές παραλλαγές της μεθόδου είναι η Προσθετική ESO (Additive ESO - AESO) και η Αμφίδρομη ESO (Bidirectional ESO - BESO). Σύμφωνα με την πρώτη παραλλαγή, η διαδικασία εκκινεί από μία υποδιαστασιολογημένη σχεδίαση, στην οποία διαρκώς προστίθεται υλικό στις περιοχές με τη μεγαλύτερη ενεργειακή συμμετοχή, ενώ, σύμφωνα με τη δεύτερη παραλλαγή, επιτρέπεται τόσο η προσθήκη όσο και η αφαίρεση υλικού, ανάλογα, πάντοτε με ένα κριτήριο ενεργειακής συμμετοχής. Ωστόσο, σε όλες τις διατυπώσεις της, αυτή η προσέγγιση λαμβάνει χώρα με τρόπο διακριτό και όχι συνεχή (είτε η προσθήκη είτε η αφαίρεση υλικού γίνεται βάσει προκαθορισμένου βήματος).

Μία ακόμα πολύ ενδιαφέρουσα κατηγορία μεθόδων βελτιστοποίησης αφορά σε συνδυαστικού τύπου τεχνικές, οι οποίες είναι κατάλληλες όταν αναζητείται η ελαχιστοποίηση του βάρους μίας κατασκευής χρησιμοποιώντας μόνον τυποποιημένες διατομές. Σε αυτές τις περιπτώσεις, οι μεταβλητές σχεδίασης είναι τα εμπορικώς διαθέσιμα τυποποιημένα δομικά στοιχεία, ενώ η αναζήτηση λαμβάνει χώρα υποχρεωτικά μέσα από ένα πλήθος διακριτών μεταβλητών. Σε αυτήν την κατηγορία ανήκει η μέθοδος branch-and-bound καθώς και η μέθοδος Gomory (Neumaier 1990, Hansen 1992, Ratschek and Rokne 1995, Kearfott 1996, Horst and Tuy 1996, Pintér 1996).

Τέλος, εκτός της αντιμετώπισης ενός στόχου, είναι δυνατόν να αναζητείται ο βέλτιστος συμβιβασμός μεταξύ δύο ή περισσοτέρων στόχων, οι οποίοι, επιπροσθέτως, ενδεχομένως να είναι και αντικρουόμενοι. Ένα τυπικό παράδειγμα αποτελεί η επιθυμία σχεδίασης ενός αυτοκινήτου υψηλών επιδόσεων αλλά χαμηλής κατανάλωσης. Η τεχνική Pareto και ο σχηματισμός του λεγομένου μετώπου Pareto παραμένει μία από τους πλέον δημοφιλείς τρόπους επίλυσης προβλημάτων πολλαπλών στόχων. Στην ίδια κατηγορία ανήκουν και προβλήματα βελτιστοποίησης τα οποία συνδυάζουν δύο ή και περισσότερα γνωστικά αντικείμενα (MultiDisciplinary Optimization problems – MDO). Τελευταία, αλλά όχι έσχατα, αναφέρονται η τεχνική Design of Experiments (DOE), η χρήση νευρωνικών δικτύων (Artificial Neural Networks - ANN), καθώς και οι αποκαλούμενες μέθοδοι άνευ πλέγματος (meshless methods), ως μέσα χρήσιμα στις διαδικασίες βελτιστοποίησης.

Στο τέλος της παρούσης περίληψης κεφαλαίου παρατίθεται ενδεικτική βιβλιογραφία.

Βιβλιογραφία

Allwood, R.J. and Chung, Y.S., (1984), Minimum-weight design of trusses by an optimality criteria method. *Int. J. Numer. Meth. Eng.* **20**, pp. 697–713

Bendsøe, M.P., (1989), Optimal shape design as a material distribution problem. Struct. Optimiz. **1**, pp.193–202

Bendsøe, M.P.; Kikuchi, N. (1988): Generating optimal topologies in structural design using a homogenization method.Comput. Meth. Appl. Mech. Engrg. 71, 197–224

Berke, L., (1970), An efficient approach to the minimum weight design of deflection limited structures", *AFFDL-TM-70-4*.

Berke, L., and Mallet, R. M., (1967), Automated large deflection and stability analysis of three-dimensional bar structures", Int. Sym. on Stru. Tech. for Large Radio and Radar Telescope Systems held at MIT, Cambridge, Mass.

Beyer, H.G., (2001), The Theory of Evolution Strategies: Springer-Verlag.

Beyer, H.G., Schwefel, H.P., (2002), Evolution Strategies: A Comprehensive Introduction. Journal Natural Computing, 1(1), pp.3-52.

Box, M.J., (1965), A New Method of Constrained Optimization and a Comparison with Other Methods, Computer J, Vol.8, pp.42-52.

Cauchy, A., (1847), Methode generale pour la resolution des systemes d'equations simultanes, Compt. Rend., Vol.25, pp.536-538.

Cerny, V., (1985), A thermodynamical approach to the travelling salesman problem: an efficient simulation algorithm. Journal of Optimization Theory and Applications, 45:41-51.

Courant, R., (1943)"Variational methods for the solution of problems of equilibrium and vibrations", *BullAmerMathSoc.*,Vol.49,pp.1–23.

Cvijovic, D.; Klinowski, J., (1995), Taboo search - an approach to the multiple minima problem". Science, 267, 664-666.

Dantzig, G. B., (1951), Maximization of a linear function of variables subject to linear inequalities,, *Activity Analysis of Production and Allocation, Koopman (Ed.)*, Cowles Commission Monograph, 13, John Wiley and Sons, New York.

Deneubourg, J.-L., Aron, S., Goss, S., Pasteels, J.M, (1990) The self-organizing exploratory pattern of the Argentine ant, Journal of Insect Behavior, 3:159–168.

Di Caro, G. and Dorigo, M., (1998), AntNet: Distributed stigmergetic control for communications networks. Journal of Artificial Intelligence Research, 9:317–365.

Dorigo, M. (1992), Optimization, Learning and Natural Algorithms (in Italian). PhD thesis, Dipartimento di Elettronica, Politecnico di Milano, Milan, Italy.

Dorigo, M., Maniezzo, V., Colorni, A., (1996), Ant System: Optimization by a colony of cooperating agents. IEEE Transactions on Systems, Man, and Cybernetics – Part B, 26(1):29–41.

Dorigo, M., Gambardella, L. M., (1997), Ant Colony System: A cooperative learning approach to the traveling salesman problem. IEEE Transactions on Evolutionary Computation, 1(1):53–66.

Dorigo, M., Stützle, T., (2004), Ant Colony Optimization. MIT Press, Cambridge, MA.

Dorigo, M. and Blum, C., (2005), Ant colony optimization theory: A survey. Theoretical Computer Science, 344(2–3):243–278.

Eberhart, R. C. and Kennedy, J., (1995), A new optimizer using particle swarm theory. Proceedings of the sixth international symposium on micro machine and human science pp. 39-43. IEEE service center, Piscataway, NJ, Nagoya, Japan.

Eberhart, R. C. and Shi, Y., (1998), Comparison between genetic algorithms and particle swarm optimization. Evolutionary programming vii: proc. 7th ann. conf. on evolutionary conf., Springer-Verlag, Berlin, San Diego, CA.

Eberhart, R. C. and Shi, Y., (2001), Particle swarm optimization: developments, applications and resources. Proc. congress on evolutionary computation 2001 IEEE service center, Piscataway, NJ., Seoul, Korea.

Erdal, F., Saka MP, (2006), Optimum design of grillage systems using harmony search algorithm. In: Proceedings of 8th international conference on computational structures technology

Eschenauer, H.A. (1994), 'Bubble method for topology and shape optimization of structures', Struct Optim. vol.8(1), pp.142-151.

Fiacco, A.V., McCormick, G.P. (1966), "Extension of SUMT for nonlinear programming: equality constraints and extrapolation", Management Science, Vol. 12, pp.816-828.

Fletcher, R., Powell, M.J.D. (1963), "A rapidly convergent descent method for minimization", Computer J., Vol.6(2), pp.163-168.

Fletcher, R., Reeves, C.M (1964), "Function Minimization by Conjugate Gradients", Computer J., Vol.7, pp.149-154.

Fogel, David B (2006), Evolutionary Computation: Toward a New Philosophy of Machine Intelligence, IEEE Press, Piscataway, NJ. Third Edition

Geem, Z.W., Kim , J.-H. and Loganathan, G.V., (2001), A new heuristic optimization algorithm: harmony search. Simulation **76(**2), pp. 60–68

Geem, Z.W., Kim, J.-H. and Loganathan, G.V., (2002), Harmony search optimization: Application to pipe network design. Int. J. Modell. Simulat. **22**(2),pp. 125–133.

Gellatly, R.A. and Berke, L., "Optimum structural design", *AFFDL_TR-70-165*, 1971.

Glover, F. "Tabu Search — Part I", ORSA Journal on Computing 1989 1: 3, 190-206.

Glover, F. "Tabu Search — Part II", ORSA Journal on Computing 1990 2: 1, 4-32.

Glover, F. and M. Laguna. (1997). Tabu Search. Kluwer, Norwell, MA.

Goldberg, David E (1989), Genetic Algorithms in Search, Optimization and Machine Learning, Kluwer Academic Publishers, Boston, MA.

Goldberg, David E (2002), The Design of Innovation: Lessons from and for Competent Genetic Algorithms, Addison-Wesley, Reading, MA.

Gutjahr, W. J. (2000), A Graph-based Ant System and its convergence. Future Generation Computer Systems, 16(8):873–888

Hansen, E.R., (1992), Global Optimization Using Interval Analysis. New York: Dekker.

Hinton, E., Sienz, J., Fully stressed topological design of structures using an evolutionary procedure, Eng. Comput. 12 (1995) 229-244.

Holland, John H (1975), Adaptation in Natural and Artificial Systems, University of Michigan Press, Ann Arbor

Hooke, R., Jeeves, T.A. (1961), "Direct Search Solution of Numerical and Statistical Problems", J of the ACM, Vol.8, pp.212-229.

Horst, R., Tuy, H., (1996), Global Optimization: Deterministic Approaches, 3rd ed. Berlin: Springer-Verlag.
Huang, N.C. and Sheu, C.Y.," Optimal design of an elastic column of thin-walled cross section", *J. Appl. Mech.* **25**, 285 (1968).
Kanarachos, A., Makris, P. and Koch, M. (1985), Localization of multi-constrained optima and avoidance of local optima in structural optimization problems, Comp Meth App Mech Engin, Vol. 51, Issues 1-3, Pages 79-106.
Karush, W. (1939), *Minima of Functions of Several Variables with Inequalities as Side Conditions*, MS Thesis, Dept. of Mathematics, University of Chicago, Chicago, IL.
Kearfott, R.B., (1996), Rigorous Global Search: Continuous Problems. Dordrecht, Netherlands: Kluwer.
Keller, J.B.," The shape of the strongest column", *Arch. Ration. Mech. Analysis* , **5**, 275 (1960).
Kennedy, J. and Eberhart, R. C. Particle swarm optimization. Proc. IEEE int'l conf. on neural networks Vol. IV, pp. 1942-1948. IEEE service center, Piscataway, NJ, 1995.
Khot, N.S., Venkayya, V.B., Johnson, C.D. and Tischler, V.A.," Optimization of fiber reinforced composite structures", *Int. J. Solids Struct.* **9**, 1225 (1973)
Kirkpatrick, S. (1984), "Optimization by simulated annealing: quantitative studies", J Statist Phys, Vol. 34, pp. 975-986.
Kirkpatrick, S.; Gelatt, C. D., Vecchi, M. P. (1983). "Optimization by Simulated Annealing". Science. New Series 220 (4598): 671-680.
Kiusalaas, J.," Optimal design of structures with buckling constraints", *Int. J. Solids Struct.* **9**, 863 (1973).
Koza, John (1992), Genetic Programming: On the Programming of Computers by Means of Natural Selection,
Kuhn, H.W., Tucker A.W. (1951) "Non-linear Programming", in J.Neyman (Ed.), Proceedings of the Second Berkeley Symposium on Mathematical Statistics and Probability, University of California Press, Berkeley, CA , pp.481-493.
Lagaros, N.D. and Papadrakakis, M., Improving the condition of the Jacobian in neural network training Advances in Engineering Software, (2003).
Lagaros, N.D., Papadrakakis, M., and Kokossalakis, G., (2002), Structural optimization using evolutionary algorithms, Computers & Structures, 80, 571-589.
Manickarajah, D., Y.M. Xie, G.P. Steven, (1995), Simple method for the optimization of columns, frames and plates against buckling, in: S. Kitipornchai, G.J. Hancock, M.A. Bradford (Eds.), Structural Stability and Design, A.A. Balkema Publishers, Rotterman, Brookfield, pp. 80-175.
Metropolis, N., Rosenbluth, A.W., Rosenbluth, M.N., Teller, A.H., and Teller, E., (1953) "Equations of State Calculations by Fast Computing Machines". Journal of Chemical Physics, 21(6):1087-1092.
Michalewicz, Zbigniew (1999), Genetic Algorithms + Data Structures = Evolution Programs, Springer-Verlag.
Michell, A.G.M. 1904: The limits of economy of material in framestructures.*Phil. Mag.* **8**, 589–597
Nelder, J.A., Mead, R. (1965), "A Simplex Method for Function Minimization", Computer Journal, Vol.7, pp. 308-313.
Neumaier, A., (1990), Interval Methods for Systems of Equations. Cambridge, England: Cambridge University Press.
Nha Chu, D., Xie, Y. M., Hira, A., Steven, G.P., (1997), On various aspects of evolutionary structural optimization for problems with stiffness constraints, Finite Elements in Analysis and Design, v.24 n.4, p.197-212.
Nha Chu, D., Y.M. Xie, G.P. Steven, (1998), An evolutionary structural optimization method for sizing problems with discrete design variables, Comput. Struct. 68, 419-431.
Papadrakakis, M., Tsompanakis, J. and Lagaros, N., (1999), Structural shape optimisation using evolution strategies, Eng. Optimization, 31, 515-540.
Papadrakakis, M., Lagaros, N.D., Tsompanakis, Y. and Plevris, V., (2001), Large scale structural optimization: Computational methods and optimization algorithms, Archives of Computational Methods in Engineering, State of the art Reviews, 8 (3), 239-301.
Papadrakakis, M., Lagaros, N.D., Plevris, V., (2002), Multi-objective optimization of skeletal structures under static and seismic loading conditions, engineering Optimization Journal,34, 645-669.
Papadrakakis, M., Lagaros, N.D., (2002), Reliability-based structural optimization using neural networks and Monte Carlo simulation, Computer Methods in Applied Mechanics and Engineering , 191(32), 3491-3507.
Papadrakakis, M., Lagaros, N.D., (2004), Soft computing methodologies for structural optimization, J. Applied Soft Computing, V3, 283-300.
Patnaik, S.N., Berke, L. and Guptill, J.D., (1993), Merits and limitations of optimality criteria method for structural optimization. *NASA TP-3373*.
Pintér, J.D., (1996), Global Optimization in Action. Dordrecht, Netherlands: Kluwer.
Powell, M.J.D. (1964), "An efficient Method for finding the minimum of a function of several variables without calculating derivatives", Computer Journal, Vol.7 (4), pp.303-307.

Querin, O.M., G.P. Steven, Y.M. Xie, (1998), Evolutionary structural optimization (ESO) using bi-directional algorithm, Eng. Comput. 15, 1031-1048.

Querin, O. M. , G. P. Steven, Y. M. Xie, (2000), Evolutionary structural optimisation using an additive algorithm, Finite Elements in Analysis and Design, v.34 n.3-4, p.291-308.

Ratschek, H., Rokne, J.G., (1995), "Interval Methods." In Handbook of Global Optimization: Nonconvex Optimization and Its Applications (Ed. R. Horst and P. M. Pardalos). Dordrecht, Netherlands: Kluwer, pp.751-828.

Rechenberg, I. (1971), Evolutionsstrategie - Optimierung technischer Systeme nach Prinzipien der biologischen Evolution (PhD thesis).

Rechenberg, I., (1989), Evolution strategy—nature's way of optimization, in Optimization: Methods and Applications, Possibilities and Limitations, Bergmann, H.W. (ed.), DLR lecture notes in engineering, Springer, Berlin, 47:106–128.

Rosen, J. (1960), "The Gradient Projection Method for Nonlinear Programming, I. Linear Constraints", *Journal of the Society for Industrial and Applied Mathematics*, Vol.8, pp.181–217.

Rosenbrock, H.H. (1960), "An Automatic Method for finding the Greatest or Least Value of a Function", Comp J, Vol.3, pp.175-184.

Rozvany, GIN, Zhou M et al. (1989/90) Continuum type optimality criteria methods for large finite element systems with a displacement constraint. Parts I and II. Struct. Optim. 1:47–72; 2:77–104

Russo, L. (2004), *The forgotten revolution: How science was born in 300BC and why it had to be reborn.* Springer, Berlin.

Saka, M.P. and Kameshki, E., (1998), Optimum design of multi-storey sway steel frames to BS5950 using genetic algorithm. In: B.H.V. Topping, Editor, Advances in engineering computational technology, Civil-Comp Press, pp. 135–141.

Saka, M.P., (2003), Optimum design of skeletal structures: A review. In: B.H.V. Topping, Editor, Progress in civil and structural engineering computing, Saxe-Coburg Publications, pp. 237–284.

Sargent, R. W. H., (1980),"A Review of Optimization Methods for Nonlinear Problems" in Computer Applications to Chemical Engineering, Ed. R.G. Squires and G. V. Reklaitis, ACS Symposium Series No. 124, American Chemical Society, Washington, D.C.

Schwefel, H.P., (1995), Evolution and Optimum Seeking: New York: Wiley & Sons.

Schwefel, H.P., (2002), Evolution Strategies: A Comprehensive Introduction. Journal Natural Computing, 1(1):3-52.

Serra, M., Venini, P., (2006), On some applications of ant colony optimization metaheuristic to plane truss optimization, Struct Multidisc Optim, vol.32, pp.499–506.

Shi, Y. and Eberhart, R. C., (1998), A modified particle swarm optimizer. Proceedings of the IEEE International Conference on Evolutionary Computation pp. 69-73. IEEE Press, Piscataway, NJ.

Shi, Y. and Eberhart, R. C., (1998), Parameter selection in particle swarm optimization. Evolutionary Programming VII: Proc. EP 98 pp. 591-600. Springer-Verlag, New York.

Stützle, T., Hoos, H.H., (2000), MAX–MIN Ant System. Future Generation Computer Systems, 16(8):889–914.

Svanberg, K. (1987), 'The method of moving asymptotes a new method for structural optimization', International Journal for Numerical Methods in Engineering, 24:359–373.

Tadjbakhsh, I. and Keller, J.B., (1962) Strongest columns and isoperimetric inequalities for eigenvalues, *J. Appl. Mech.* **29**, 159.

Tanskanen, P., (2002), The evolutionary structural optimization method: theoretical aspects, Comput. Methods Appl. Mech. Eng. 191, 5485-5498.

Taylor, J.E. and Liu, C.Y., (1968), Optimal design of columns, *AIAA J.*, **6**, 1497.

Venkatamaran, P. (2002), *Applied Optimiization with Matlab Programming*, Wiley.

Venkayya, V.B., (1971), Design of optimum structures, *Int. J. Comp. Struct.* **1**, 265.

Venkayya, V.B., Khot, N.S. and Reddy, V.S., (1968), Energy distribution in an optimum structural design, *AFFDL-TR-68-156*.

Venkayya, V.B., Khot, N.S., Tischler, V.A. and Taylor, R.F., (1971), Design of optimum structures for dynamic loads", *3rd Air Force Conference on Matrix Methods in Structural Mechanics*.

Venkayya, V.B., Khot, N.S., (1975), Design of optimum structures for impulse type loading", *AIAA J.* **13**, 989.

Veselago, V.G. (2002), "Formulating Fermat's principle for light traveling in negative refraction materials", *PHYS-USP*, Vol. 45(10), pp. 1097-1099.

Xie, Y. M., Steven, G.P., (1993), A simple evolutionary procedure for structural optimization, Comput. Struct. 49 885-896.

Xie, Y. M., Steven, G.P., (1994), Optimal design of multiple load case structures using an evolutionary procedure, Eng. Comput. 11,295-302.

Xie, Y.M., Steven, G.P., (1997), Evolutionary Structural Optimization, Springer, London,.

Yang, X.Y., Xie, Y.M., Liu, J.S., Parks, G.T., Clarkson, P.J., (2003), Perimeter control in the bi-directional evolutionary optimization method, Struct. Multidiscip. Optim. 24, 430-440.

Zhou M., Rozvany G.I.N., (1992/93), DCOC: an optimality criterion method for large systems. Part I: Theory, Part II: algorithm. Structural and Multidisciplinary Optimization, 5, 12-25; 6, 250-262.

Zoutendijk, G. (1960), *Methods of Feasible Directions*, Elsevier.

Αυτή η σελίδα είναι σκοπίμως κενή

ΚΕΦΑΛΑΙΟ 2
(*ΠΕΡΙΛΗΨΗ*)

ΑΜΕΣΗ ΑΝΑΖΗΤΗΣΗ ΣΤΗ ΒΕΛΤΙΣΤΟΠΟΙΗΣΗ ΚΑΙ ΔΙΑΤΥΠΩΣΗ ΜΙΑΣ ΝΕΑΣ ΥΒΡΙΔΙΚΗΣ ΜΕΘΟΔΟΥ ΒΕΛΤΙΣΤΟΠΟΙΗΣΗΣ

Από την επιμέρους μελέτη διαφόρων βιβλιογραφικών μεθοδολογιών βελτιστοποίησης και στο πλαίσιο της παρούσης Διδακτορικής Διατριβής, προέκυψε ότι, για προβλήματα βελτιστοποίησης με μικρό αριθμό μεταβλητών σχεδίασης, η μέθοδος της Προσομοιούμενης Ανόπτησης (SA) εμφανίζει μία από τις καλύτερες επιδόσεις, ενώ για προβλήματα βελτιστοποίησης με μεγαλύτερο πλήθος μεταβλητών σχεδίασης είναι προτιμητέα η χρήση μίας αιτιοκρατικής διαδικασίας βελτιστοποίησης. Λαμβάνοντας αυτά τα ευρήματα υπόψη, προτείνεται μία νέα, υβριδικού χαρακτήρα, διαδικασία βελτιστοποίησης, τα βασικά χαρακτηριστικά της οποίας είναι η χρήση της αιτιοκρατικής μεθόδου Powell για την επιλογή της κατεύθυνσης αναζήτησης, η χρήση της στοχαστικής μεθόδου (SA) για την διερεύνηση κατά μήκος μίας κατεύθυνσης αναζήτησης και η εκκίνηση μίας, τοπικού χαρακτήρα, αναζήτησης με τη μέθοδο (SA), όταν διαγιγνώσκεται μη-περαιτέρω βελτίωση του διανύσματος σχεδίασης. Για την αξιολόγηση της προτεινομένης διαδικασίας χρησιμοποιήθηκαν δώδεκα μαθηματικές συναρτήσεις επίδοσης και προέκυψε ότι η προτεινόμενη διαδικασία εμφανίζει άριστα αποτελέσματα ως προς τον εντοπισμό του καθολικού ελαχίστου, αλλά με υψηλό υπολογιστικό κόστος. Ως εκ τούτου, αναδείχθηκε η ανάγκη για διερεύνηση και άλλων σχημάτων βελτιστοποίησης, όπως οι έμμεσες μέθοδοι αναζήτησης. Στην παρούσα περίληψη, παρουσιάζεται, εν συντομία, η πραγματοποιηθείσα βιβλιογραφική διερεύνηση, η προτεινόμενη διαδικασία βελτιστοποίησης, η αξιολόγησή της καθώς και τα προκύπτοντα συμπεράσματα.

2.1.Εισαγωγή

Ως βελτιστοποίηση ορίζεται η διαδικασία μεγιστοποίησης ή ελαχιστοποίησης της τιμής μίας αντικειμενικής συνάρτησης με ταυτόχρονη ικανοποίηση των επιβαλλομένων περιορισμών. Προς τούτο, είναι δυνατή η χρήση πληθώρας τεχνικών, των αποκαλουμένων 'μεθόδων βελτιστοποίησης', οι οποίες κατατάσσονται σε δύο μεγάλες ομάδες: τις μεθόδους άμεσης αναζήτησης και τις μεθόδους έμμεσης αναζήτησης. Σχετικά με τις μεθόδους της πρώτης ομάδας, ο αντικειμενικός σκοπός είναι η διατύπωση μίας αντικειμενικής συνάρτησης και η επιδίωξη ελαχιστοποίησης ή μεγιστοποίησης της τιμής της. Σχετικά με τις μεθόδους της δεύτερης ομάδας, ο αντικειμενικός σκοπός είναι η διατύπωση μίας συνθήκης ακροτάτου, η οποία αντιστοιχεί στη βέλτιστη κατάσταση, οπότε, επιδιώκοντας την ικανοποίηση της εν λόγω συνθήκης, ουσιαστικά επιτυγχάνεται και η ελαχιστοποίηση ή μεγιστοποίηση του μεγέθους ενδιαφέροντος. Στη βιβλιογραφία υπάρχει πλήθος μεθόδων και των δύο ομάδων, μερικές εκ των οποίων είναι πιο δημοφιλείς εξ αιτίας μίας πολύ καλής συμπεριφοράς, η οποία εμφανίζεται υπό συνθήκες και οφείλεται σε κάποιο ιδιαίτερο χαρακτηριστικού τους. Ένα επίμαχο ερώτημα είναι κατά πόσον οι υπάρχουσες μεθοδολογίες βελτιστοποίησης επαρκούν και για την αντιμετώπιση των προβλημάτων βελτιστοποίησης στις κατασκευές, ενώ ένα άλλο ενδιαφέρον ερώτημα είναι κατά πόσον ο συνδυασμός ήδη γνωστών μεθοδολογιών μπορεί να οδηγήσει στην ανάδειξη των επί μέρους πλεονεκτημάτων των μεθοδολογιών αυτών, με ταυτόχρονη συρρίκνωση των επί μέρους μειονεκτημάτων τους. Ο σκοπός του παρόντος κεφαλαίου είναι η απάντηση και η εμβάθυνση σε αυτά τα ερωτήματα. Προς αυτήν την κατεύθυνση, πραγματοποιήθηκε η ακόλουθη διαδικασία τεσσάρων βημάτων:

Βήμα 1: Εντοπισμός μερικών εκ των πλέον δημοφιλών βιβλιογραφικών μεθοδολογιών και αξιολόγηση αυτών μέσα από Μαθηματικές Συναρτήσεις Επίδοσης.

Βήμα 2: Χρήση των μεθόδων αυτών σε προβλήματα βελτιστοποίησης κατασκευών.

Βήμα 3: Ενδελεχής διερεύνηση των Γενετικών Αλγορίθμων (GA), οι οποίοι αποτελούν έναν διαφορετικό και ιδιαίτερο τρόπο προσέγγισης σε προβλήματα βελτιστοποίησης.

Βήμα 4: Βάσει της αποκτηθείσας γνώσης και εμπειρίας από τα ανωτέρω βήματα, διατύπωση μίας νέας διαδικασίας βελτιστοποίησης και αξιολόγηση αυτής.

Στις επόμενες ενότητες της παρούσης περίληψης κεφαλαίου, περιγράφονται εν συντομία τα Βήματα 1 έως και 3, ενώ το Βήμα 4 παρουσιάζεται πιο αναλυτικά.

2.2. Θεωρητική ανάλυση

Οι μέθοδοι άμεσης αναζήτησης εξερευνούν το χώρο σχεδίασης και αναζητούν το καθολικό ακρότατο μέσα από τον υπολογισμό της τιμής της αντικειμενικής συνάρτησης, η οποία είναι επιθυμητό να ελαχιστοποιηθεί ή να μεγιστοποιηθεί. Η αναζήτηση είναι δυνατόν να πραγματοποιηθεί είτε με αιτιοκρατικό είτε με στοχαστικό τρόπο. Με τον πρώτο τρόπο, εάν η διαδικασία βελτιστοποίησης ξεκινήσει N φορές από το ίδιο αρχικό διάνυσμα σχεδίασης $\underset{\sim}{X}_{ini}$, τότε και τις N φορές θα καταλήξει στο ίδιο τελικό διάνυσμα σχεδίασης $\underset{\sim}{X}_{fin}$, κάτι το οποίο, με τον δεύτερο τρόπο, είναι πιθανό αλλά όχι σίγουρο.

Οι αιτιοκρατικές μέθοδοι βελτιστοποίησης διακρίνονται σε μηδενικής, πρώτης και δευτέρας τάξεως, ανάλογα με τον τρόπο αξιοποίησης της αντικειμενικής συνάρτησης (αντίστοιχα, χρήση της αντικειμενικής συνάρτηση, της πρώτης παραγώγου και της δευτέρας παραγώγου αυτής). Η βασική διαφορά μεταξύ των προσεγγίσεων χωρίς και με πληροφορία από παραγώγους έγκειται στην ευστάθεια και στο υπολογιστικό κόστος. Για λόγους αριθμητικής φύσεως (λάθη αποκοπής και στρογγυλοποίησης), η χρήση παραγώγων είναι δυνατόν να προκαλέσει προβλήματα αριθμητικής ευστάθειας, ενώ το υπολογιστικό κόστος για τον υπολογισμό είτε του πίνακα Jacobian είτε (και κυρίως) του πίνακα Hessian, είναι υψηλό. Επίσης, ακριβώς λόγω της αξιοποίησης πληροφορίας σχετικά με το ρυθμό μεταβολής της τιμής της αντικειμενικής συνάρτησης, είναι δυνατόν να διαγνωσθεί ψευδώς ένα τοπικό

ακρότατο ως καθολικό (τάση εγκλωβισμού σε τοπικά ακρότατα). Από την άλλη πλευρά, οι στοχαστικές μέθοδοι, τουλάχιστον στις βασικές διατυπώσεις τους, είναι απαλλαγμένες από πληροφορίες σχετικά με παραγώγους, άρα είναι πιο εύκολα υλοποιήσιμες και εμφανίζουν μικρότερη τάση εγκλωβισμού σε τοπικά ακρότατα, ωστόσο απαιτούν λεπτομερέστερη διερεύνηση μεγαλύτερου τμήματος του πεδίου σχεδίασης, κάτι το οποίο καταλήγει σε υψηλό υπολογιστικό κόστος. Προφανώς, τόσο οι αιτιοκρατικές όσο και οι στοχαστικές μέθοδοι διακρίνονται για ορισμένα πλεονεκτήματα και υποφέρουν από κάποια μειονεκτήματα. Συνεπώς, μία λογική σκέψη θα ήταν να συνδυασθεί μία αιτιοκρατική με μία στοχαστική μέθοδο, για παράδειγμα εισάγοντας αιτιοκρατικούς τελεστές σε μία στοχαστική μέθοδο ή το αντίθετο, έτσι ώστε η παρουσία των πλεονεκτημάτων της μίας μεθόδου να αντισταθμίσει τα μειονεκτήματα της άλλης. Με αυτό το σκεπτικό, μελετήθηκε ένα πλήθος βιβλιογραφικών μεθόδων βελτιστοποίησης και επιδιώχθηκε η ανάδειξη της καλύτερης αιτιοκρατικής και της καλύτερης στοχαστικής μεθοδολογίας. Γι' αυτόν το σκοπό, χρησιμοποιήθηκαν δύο ομάδες προβλημάτων αξιολόγησης

Η πρώτη ομάδα προβλημάτων αξιολόγησης αφορούσε σε βιβλιογραφικές Μαθηματικές Συναρτήσεις Επίδοσης (**B**enchmark **M**athematical **F**unctions - BMF) με μία μεταβλητή (έστω συνάρτηση BMF-1), με δύο μεταβλητές (έστω BMF-2), με τρεις μεταβλητές (έστω BMF-3), με τέσσερεις μεταβλητές (έστω BMF-4) και με οκτώ μεταβλητές (έστω BMF-5). Συνολικά, χρησιμοποιήθηκαν πέντε Μαθηματικές Συναρτήσεις Επίδοσης, για τις οποίες είναι γνωστό το καθολικό ελάχιστο. Για τον εντοπισμό αυτού, χρησιμοποιήθηκαν συνολικά έξι δημοφιλείς μεθοδολογίες της βιβλιογραφίας: η στοχαστική μέθοδος της Προσομοιούμενης Ανόπτησης (Simulated Annealing - SA), οι αιτιοκρατικές μέθοδοι Downhill Simplex (παραλλαγή της μεθόδου Simplex διατυπωθείσα από τους Nelder και Mead), Box (ή μέθοδος Complex), Διαδοχικός Τετραγωνικός Προγραμματισμός (Sequantial Quadratic Programming - SQP), Hooke και Jeeves, καθώς και η μέθοδος EASY (***E***volutionary ***A***lgorithm ***SY***stem v.1.3.4). Η τελευταία μέθοδος, στοχαστικής φύσεως και αφορούσα στην ενσωμάτωση Νευρωνικών Δικτύων (Artificial Neural Networks - ANN) σε μετά-μοντέλα, έχει αναπτυχθεί από την ερευνητική ομάδα του Εργαστηρίου Θερμικών Στροβιλομηχανών της Σχολής Μηχανολόγων Μηχανικών του Εθνικού Μετσοβίου Πολυτεχνείου. Η ποσοτικοποίηση της συμπεριφοράς των εξεταζομένων μεθόδων βασίσθηκε στη χρήση τεσσάρων Δεικτών Επίδοσης και στα αποτελέσματα από 2500 διαφορετικές αναλύσεις.

Η δεύτερη ομάδα προβλημάτων αξιολόγησης αφορούσε στην ελαχιστοποίηση του βάρους τυπικών δικτυωμάτων υπό την επιβολή μίας ποικιλίας περιορισμών, τόσο ως προς το πλήθος τους όσο και ως προς τον τύπο τους. Ειδικότερα, χρησιμοποιήθηκαν οι διαδικασίες βελτιστοποίησης, οι οποίες είχαν χρησιμοποιηθεί και στην πρώτη ομάδα προβλημάτων αξιολόγησης, εξαιρουμένης της μεθόδου EASY. Επίσης, επιλέχθηκαν τέσσερα ευρέως γνωστά και χρησιμοποιούμενα βιβλιογραφικά παραδείγματα δικτυωμάτων (**S**keletal **S**tructural **B**enchmarks - SSB), ήτοι ένα δικτύωμα τριών ράβδων (έστω SSB-1), δύο παραλλαγές ενός δικτυώματος δέκα ράβδων (έστω SSB-2 και SSB-3) και ένα δικτύωμα 25 ράβδων (έστω SSB-4). Η ποσοτικοποίηση της συμπεριφοράς των εξεταζομένων μεθόδων βασίσθηκε στα αποτελέσματα από 2000 διαφορετικές αναλύσεις καθώς και στους τέσσερεις Δείκτες Επίδοσης της πρώτης ομάδας προβλημάτων αξιολόγησης.

Εκτός από τα προαναφερθέντα προβλήματα αξιολόγησης, πραγματοποιήθηκε μία περαιτέρω διερεύνηση σχετικά με τους Γενετικούς Αλγορίθμους (GA). Είναι αληθές ότι οι (GA) αποτελούν μία ξεχωριστή τάξη διαδικασιών βελτιστοποίησης διότι στηρίζονται στη Δαρβίνεια θεωρία της εξέλιξης, δηλαδή στηρίζονται σε ένα φυσικό φαινόμενο το οποίο λαμβάνει χώρα εδώ και δισεκατομμύρια χρόνια. Το βασικό χαρακτηριστικό των (GA) είναι η δυνατότητά τους να διαχειρίζονται ταυτόχρονα και να βελτιώνουν σε κάθε επανάληψη ένα *σύνολο* διανυσμάτων σχεδίασης και όχι ένα διάνυσμα σχεδίασης. Για τη διερεύνηση των (GA) χρησιμοποιήθηκε το αντίστοιχο περιβάλλον βελτιστοποίησης της MatLab (GADS

optimization toolbox) και εξετάστηκαν διεξοδικά τέσσερεις Μαθηματικές Συναρτήσεις Επίδοσης (δύο συναρτήσεις της πρώτης ομάδας αξιολόγησης, η λεγόμενη συνάρτηση Powell και η αποκαλούμενη συνάρτηση Suzuki). Συνολικά, εξετάσθηκε η επίδραση έντεκα παραμέτρων ελέγχου, ενώ για την ποσοτικοποίηση της συμπεριφοράς των (GA) χρησιμοποιήθηκαν τα αποτελέσματα από 1,120,000 διαφορετικές αναλύσεις.

Τα συμπεράσματα, τα οποία προέκυψαν μέσα από τη προαναφερθείσα διερεύνηση, ήταν αρκετά αποκαλυπτικά. Μία από τις βασικές παρατηρήσεις ήταν ότι οι στοχαστικές μέθοδοι άμεσης αναζήτησης υπερτερούσαν σημαντικά των αιτιοκρατικών, όταν το πλήθος των μεταβλητών σχεδίασης ήταν μικρό. Αντιθέτως, όσο αυξανόταν η διάσταση του χώρου σχεδίασης, τόσο καταλληλότερες καθίσταντο οι αιτιοκρατικές μέθοδοι βελτιστοποίησης. Συνεπώς, μία καλή ιδέα θα ήταν η χρήση στοχαστικής προσέγγισης για την επίλυση ενός προβλήματος με μικρό πλήθος μεταβλητών σχεδίασης και η χρήση αιτιοκρατικής προσέγγισης στην αντίθετη περίπτωση. Με γνώμονα αυτήν την παρατήρηση, διαμορφώθηκε η προτεινόμενη υβριδική διαδικασία βελτιστοποίησης. Ειδικότερα, μία τυπική αιτιοκρατική διαδικασία βελτιστοποίησης αποτελείται από δύο τελεστές: ο πρώτος καθορίζει την διεύθυνση κατά την οποία θα πραγματοποιηθεί η αναζήτηση και ο δεύτερος καθορίζει το βήμα της αναζήτησης. Η διεύθυνση αναζήτησης περιγράφεται από ένα διάνυσμα, η διάσταση του οποίου, προφανώς, ισούται με τη διάσταση του χώρου σχεδίασης. Ως εκ τούτου, όσο μεγαλύτερη είναι αυτή η διάσταση τόσο μεγαλύτερο είναι και το πλήθος των μεταβλητών σχεδίασης, άρα τόσο καταλληλότερη είναι η επιλογή ενός αιτιοκρατικού αλγορίθμου. Στην παρούσα μελέτη, επελέγη η μέθοδος Powell για τον προσδιορισμό της διεύθυνσης αναζήτησης. Η επιλογή αυτή στηρίχθηκε στο γεγονός ότι η μέθοδος Powell είναι απλή στον προγραμματισμό της αλλά διαθέτει την αποκαλούμενη ‘προς-τα-αριστερά ολίσθηση’ (left shifting) της διεύθυνσης αναζήτησης, εξ αιτίας της οποίας η εν λόγω μέθοδος εμφανίζει πολύ καλύτερη συμπεριφορά από άλλες όμοιές της. Από την άλλη πλευρά, το βήμα αναζήτησης αποτελεί ένα βαθμωτό μέγεθος, συνεπώς ο προσδιορισμός του είναι δυνατόν να εκφρασθεί ως ένα μονοδιάστατο πρόβλημα βελτιστοποίησης. Για τέτοιου είδους προβλήματα, είναι πιο δόκιμη η επιλογή μίας στοχαστικής μεθόδου βελτιστοποίησης. Στην παρούσα μελέτη, επελέγη η μέθοδος της Προσομοιούμενης Ανόπτησης (SA) διότι, από τη σχετική ανάλυση που πραγματοποιήθηκε, η εν λόγω μέθοδος εμφάνισε σημαντικώς υπέρτερη συμπεριφορά συγκριτικά με τις άλλες μεθόδους. Εκτός από τους δύο προαναφερθέντες τελεστές, στην προτεινόμενη διαδικασία βελτιστοποίησης εισήχθη ακόμα ένας τελεστής, η παρουσία του οποίου αποσκοπούσε στην αύξηση της πιθανότητας απεγκλωβισμού από τοπικά ακρότατα. Πρόκειται για έναν τελεστή τοπικής αναζήτησης, ο οποίος χρησιμοποιεί τη μέθοδο (SA) αλλά για αναζήτηση μόνον εντός μίας υπερ-σφαίρας γύρω από το τρέχον βέλτιστο διάνυσμα σχεδίασης. Η επαναληπτική εφαρμογή αυτών των τριών τελεστών αποτελεί, ουσιαστικά, την προτεινόμενη διαδικασία βελτιστοποίησης. Για την αξιολόγησή της, χρησιμοποιήθηκαν οι Μαθηματικές Συναρτήσεις Επίδοσης (BMF1), (BMF2), (BMF4) και (BMF5), ενώ για κάθε μία από αυτές τις συναρτήσεις διαμορφώθηκαν δύο επιπλέον παραλλαγές (συνολικά, δώδεκα μαθηματικές συναρτήσεις). Επίσης, χρησιμοποιήθηκαν τρεις Δείκτες Αξιολόγησης, ενώ πραγματοποιήθηκε και σύγκριση με τις μεθόδους (SA), Hooke και Jeeves, Nelder-Mead και Powell. Συνολικά πραγματοποιήθηκαν 7200 αναλύσεις.

Ένα σημαντικό σημείο στην αξιολόγηση μίας διαδικασίας βελτιστοποίησης αποτελεί ο χειρισμός των επιβαλλομένων περιορισμών, κάτι το οποίο είναι δυνατόν να επιτευχθεί με πολλούς τρόπους. Για παράδειγμα, είναι δυνατόν να χρησιμοποιηθούν συναρτήσεις ποινής, με τις οποίες το αρχικό πρόβλημα βελτιστοποίησης με περιορισμούς μετατρέπεται σε μία ακολουθία προβλημάτων χωρίς περιορισμούς. Ανάλογα, δε, με το σχήμα ποινικοποίησης είναι δυνατόν να ληφθούν διαφορετικά βέλτιστα διανύσματα σχεδίασης και μετά από διαφορετικό πλήθος επαναλήψεων. Συνεπώς, για την αντικειμενική αξιολόγηση της καθαυτής διαδικασίας βελτιστοποίησης, θα πρέπει η επίδραση του σχήματος ποινικοποίησης στην

τελικώς μετρηθείσα απόδοση να είναι αμελητέα. Ένας τρόπος για να επιτευχθεί αυτό είναι η απόδοση στην αντικειμενική συνάρτηση μίας πολύ μεγάλης τιμής, όταν παρατηρείται παραβίαση, ανεξαρτήτως του πλήθους των παραβιασθέντων περιορισμών και του ποσοστού παραβίασης (σχήμα ποινικοποίησης τύπου 'βίαιης θανάτωσης' - 'hard kill'). Πρόκειται για έναν πολύ αυστηρό τρόπο ποινικοποίησης, ο οποίος εξωθεί τη διαδικασία βελτιστοποίησης στα όριά της, δεδομένου ότι δεν υπάρχει διάκριση μεταξύ διανυσμάτων σχεδίασης τα οποία προκαλούν μικρή ή μεγάλη παραβίαση περιορισμών.

Βασικό παράγοντα αξιολόγησης μίας διαδικασίας βελτιστοποίησης αποτελεί και η ευαισθησία της σε διάφορες παραμέτρους. Προκειμένου να εξετασθεί αυτή η ευαισθησία, ενδείκνυται η πραγματοποίηση μίας σειράς αναλύσεων, στην οποία μεταβάλλεται μόνον η προς διερεύνηση παράμετρος. Σε αυτό το πλαίσιο, προκειμένου να εξετασθεί η ευαισθησία (εξάρτηση) μίας διαδικασίας βελτιστοποίησης από το αρχικό διάνυσμα σχεδίασης, είναι δυνατόν να επιλυθεί ένα πρόβλημα βελτιστοποίησης χρησιμοποιώντας πολλά και διαφορετικά σημεία εκκίνησης. Εν προκειμένω, για κάθε μία από τις διερευνηθείσες μεθοδολογίες και για κάθε ένα από τα εξετασθέντα παραδείγματα, χρησιμοποιήθηκαν 100 διαφορετικά αρχικά διανύσματα σχεδίασης.

2.3. Η προτεινόμενη υβριδική διαδικασία βελτιστοποίησης

Με βάση την αποκτηθείσα εμπειρία από τη διερεύνηση διαφόρων βιβλιογραφικών μεθόδων βελτιστοποίησης, διαμορφώθηκε μία νέα, υβριδικού χαρακτήρα, διαδικασία βελτιστοποίησης, ενώ για την αξιολόγησή της χρησιμοποιήθηκε ένα εκτεταμένο σύνολο Μαθηματικών Συναρτήσεων Επίδοσης. Στις ενότητες που ακολουθούν παρουσιάζεται αναλυτικά η προτεινόμενη διαδικασία, παρατίθεται η αξιολόγησή της και διατυπώνονται κριτικά σχόλια σχετικά με αυτήν.

2.3.1. Επί των υβριδικών διαδικασιών βελτιστοποίησης

Τα υβριδικά σχήματα αναζήτησης χρησιμοποιούνται εκτενώς στη βελτιστοποίηση κατασκευών. Μία προσέγγιση για υβριδικού τύπου βελτιστοποίηση είναι η ενσωμάτωση ενός αιτιοκρατικού τρόπου τοπικής αναζήτησης σε μία εξελικτική διαδικασία βελτιστοποίησης στοχαστικού χαρακτήρα.

Οι Mahfoud και Goldberg παρουσίασαν τη μέθοδο της Παράλληλης Επασυνδυαστικής Προσομοιούμενης Ανόπτησης (Parallel Recombinative Simulated Annealing). Ειδικότερα, σύμφωνα με αυτή τη μέθοδο, μετά τη διαμόρφωση του αρχικού πληθυσμού και την επιλογή μίας θερμοκρασιακής στάθμης Τ, επιλέγονται οι γονείς, από τους οποίους προκύπτουν οι απόγονοι με επανασυνδυασμό και μετάλλαξη. Στη συνέχεια, γονείς και απόγονοι συγκρίνονται ως προς την επίδοσή τους, γονείς αντικαθίστανται από απογόνους με καλύτερη επίδοση και η θερμοκρασιακή στάθμη μειώνεται. Η διαδικασία επαναλαμβάνεται μέχρι συγκλίσεως (Mahfoud και Goldberg, 1994). Οι Renders και Flasse ασχολήθηκαν με το θέμα της ακρίβειας, της αξιοπιστίας και υπολογιστικού χρόνου σε μία διαδικασία βελτιστοποίησης. Πιο συγκεκριμένα, πρώτα εξέτασαν παραδοσιακές μεθόδους βελτιστοποίησης, όπως είναι η μέθοδος Quasi-Newton και η μέθοδος Simplex των Nelder-Mead, και στη συνέχεια ασχολήθηκαν με νέες υβριδικές μεθόδους, συνδυάζουσες χαρακτηριστικά από γενετικούς αλγορίθμους και μεθόδους αναρρίχησης, προκειμένου να διαμορφώσουν μία διαδικασία στην οποία συνδυάζονται καλύτερα τα επιμέρους πλεονεκτήματα και μειονεκτημάτων των συμμετεχόντων μεθόδων. Τέτοιες υβριδικές μέθοδοι είναι εμπνευσμένες από τη βιολογία και εμπλέκουν δύο βασικά χαρακτηριστικά, την εξέλιξη, όπως αυτή εμφανίζεται στους Γενετικούς Αλγορίθμους, και την εκμάθηση, όπως αυτή είναι δυνατόν να επιτευχθεί με ένα σχήμα Quasi-Newton. Οι Renders και Flasse κατέληξαν στην πρόταση μίας υβριδικής μεθόδου, η οποία συνδυάζει την αξιοπιστία των Γενετικών Αλγορίθμων με την ακρίβεια της

μεθόδου Quasi-Newton, ενώ ταυτόχρονα το υπολογιστικό κόστος είναι ελαφρώς μεγαλύτερο από αυτόν που απαιτεί η χρήση μόνον της μεθόδου Quasi-Newton (Renders and Flasse, 1996). Οι Botello και συνεργάτες συνδύασαν τους τελεστές των Γενετικών Αλγορίθμων, σχετικά με την επιλογή, τη διασταύρωση και τη μετάλλαξη, με τον τελεστή αποδοχής της Προσομοιούμενης Ανόπτησης (κριτήριο Metropolis), διαμορφώνοντας τον αποκαλούμενο Αλγόριθμο Γενικής Στοχαστικής Αναζήτησης (General Stochastic Search Algorithm). Η μέθοδος εμφανίζει δύο βασικά σημεία. Το πρώτο σημείο είναι η σύγκριση των μελών ενός πληθυσμού πριν και μετά την επιβολή τελεστών συνδυασμού και μετάλλαξης. Το δεύτερο σημείο είναι η εφαρμογή του προαναφερθέντος τελεστού αποδοχής επί των γονέων και των απογόνων, προκειμένου να επιλεχθούν τα άτομα για την επόμενη επανάληψη (γενεά) (Botello et al, 1999). Οι Galinier και Hao παρουσίασαν έναν Υβριδικό Εξελικτικό Αλγόριθμο (Hybrid Evolutionary Algorithm), ο οποίος ενσωματώνει μία διαδικασία τοπικής αναζήτησης στο πλαίσιο ενός Εξελικτικού Αλγορίθμου. Η βασική ιδέα της μεθόδου τους είναι η δημιουργία νέων διανυσμάτων σχεδίαση μέσα από έναν τελεστή διασταύρωσης (Greedy Partition Crossover), τα οποία στη συνέχεια βελτιώνονται μέσω της χρήσης ενός τελεστή τοπικής αναζήτησης (Galinier and Hao, 1999). Οι Burke και Smith ενσωμάτωσαν έναν τελεστή τοπικής αναζήτησης σε έναν Γενετικό Αλγόριθμο, διαμορφώνοντας τον αποκαλούμενο Μιμητικό Αλγόριθμο (Memetic Algorithm), τον οποίο χρησιμοποίησαν για την επίλυση ενός προβλήματος διαμόρφωσης πλάνου συντήρησης θερμικών εγκαταστάσεων (Burke and Smith, 2000). Οι Magoulas και συνεργάτες εισήγαγαν μία νέα, υβριδική, εξελικτική διαδικασία προκειμένου να βελτιώσουν την απόδοση της χρήσης νευρωνικών δικτύων σε βραδέως μεταβαλλόμενα περιβάλλοντα. Ειδικότερα, εξέτασαν το συνδυασμό μίας Διαφορικής Στρατηγικής Εξέλιξης (Differential Evolution Strategy - DES) με μία Στοχαστική Καταρρίχηση (Stochastic Gradient Descent - SGD). Η Διαφορική Στρατηγική Εξέλιξης στηρίζεται στην ιδέα της εξέλιξης ενός πλήθους ατόμων από γενιά σε γενιά, ενώ η Στοχαστική Καταρρίχηση αφορά στην περιβαλλοντική προσαρμογή μέσω διαδικασίας εκμάθησης (Magoulas et al., 2001). Οι Schmidt και Thierauf εξέτασαν τον συνδυασμό της εν λόγω μεθόδου με τον λεγόμενο Αλγόριθμο Αποδοχής Κατωφλίου (Threshold Accepting Algorithm - TAA), ο οποίος υπολογίζει το αντίστοιχο συναρτησιακό σε κάθε επανάληψη, συμβάλλοντας σημαντικά στην προσπάθεια μείωσης του υπολογιστικού κόστους. Η μέθοδος της Διαφορικής Εξέλιξης (Differential Evolution - DE) βοηθά στην αποφυγή τοπικών ελαχίστων. Μέσω της χρήσης συναρτήσεων ποινής, επιτρέπεται η αξιοποίηση ακόμα και μη-αποδεκτών διανυσμάτων σχεδίασης, οπότε είναι δυνατή η προσέγγιση του καθολικού ελαχίστου όχι μόνον μέσα από δυνατές διευθύνσεις αλλά και μέσα από μη-δυνατές διευθύνσεις. Οι, δε, αποδεκτές λύσεις αποθηκεύονται και αξιοποιούνται, όπως ακριβώς συμβαίνει και με τα καλύτερα διανύσματα σχεδίασης (elite) σε έναν Γενετικό Αλγόριθμο (Schmidt and Thierauf, 2005).

Μέσα στο γενικότερο πλαίσιο, όπως αυτό περιγράφεται από τις προαναφερθείσες εργασίες, στην παρούσα Διδακτορική Διατριβή προτείνεται μία νέα, υβριδικού χαρακτήρα, διαδικασία βελτιστοποίησης, σύμφωνα με την οποία συνδυάζεται μία αιτιοκρατική και μία στοχαστική διαδικασία. Ειδικότερα, η επιλογή της διεύθυνσης αναζήτησης επιτυγχάνεται με την αιτιοκρατική μέθοδο Powell, ενώ η διερεύνηση κατά μήκος μίας διεύθυνσης αναζήτησης επιτυγχάνεται με τη στοχαστική μέθοδο της Προσομοιούμενης Ανόπτησης. Τονίζεται ιδιαιτέρως ότι αυτές οι δύο επιλογές δεν ήταν τυχαίες. Η μέθοδος Powell, αν και αποτελεί μία απλή παραλλαγή της διαδικασίας βελτιστοποίησης κατά διεύθυνση βάσης (univariate optimization), εμφανίζει εξαιρετικά καλύτερη συμπεριφορά (Venkatamaran, 2002). Επίσης, η μέθοδος της Προσομοιούμενης Ανόπτησης, όπως κατέδειξε η διερεύνηση, η οποία πραγματοποιήθηκε στο πλαίσιο της παρούσης Διδακτορικής Διατριβής, εμφανίζει την καλύτερη συμπεριφορά, συγκριτικά με όλες τις υπόλοιπες εξετασθείσες μεθόδους, στην

επίλυση μονοδιάστατων προβλημάτων. Υπενθυμίζεται, δε, ότι η διερεύνηση κατά μήκος μίας διεύθυνσης αναζήτησης είναι ακριβώς ένα τέτοιου είδους πρόβλημα.

2.3.2. Θεωρητικό υπόβαθρο

Τα βασικά συστατικά στοιχεία της προτεινομένης διαδικασίας, δηλαδή η διαδικασία βελτιστοποίησης κατά διεύθυνση βάσης (univariate optimization), η 'προς-τα-αριστερά-ολίσθηση' (left-shifting) της διεύθυνσης αναζήτησης καθώς και η Προσομοιούμενη Ανόπτηση, περιγράφονται συνοπτικά στις επόμενες παραγράφους.

Η διαδικασία βελτιστοποίησης κατά διεύθυνση βάσης (univariate optimization) δεν είναι τίποτε άλλο παρά η επίλυση, για κάθε μία μεταβλητή σχεδίασης και με τρόπο κυκλικό, του ακόλουθου 1-Δ προβλήματος βελτιστοίησης:

$$\min f\left(\underset{\sim}{x}_i + \alpha \underset{\sim}{d}_j\right),\ \underset{\sim}{x}_{low} \le \underset{\sim}{x}_i \le \underset{\sim}{x}_{up} \tag{2.1}$$

όπου $\underset{\sim}{x}_i$ είναι το διάνυσμα σχεδίασης στην $i-$επανάληψη, το βαθμωτό μέγεθος α είναι το βήμα αναζήτησης για τη διεύθυνση αναζήτησης $\underset{\sim}{d}_j$ και $\underset{\sim}{d}_j$ είναι η $j-$διεύθυνση βάσης, όπου $j = 1,...,N_{\text{var}}$ και N_{var} είναι το πλήθος των μεταβλητών σχεδίασης. Είναι δυνατή η αποθήκευση των διευθύνσεων αναζήτησης σε έναν πίνακα **SD** διάστασης $N_{\text{var}} \times N_{\text{var}}$. Τα άνω και κάτω όρια του διανύσματος σχεδίασης $\underset{\sim}{x}_i$ δηλώνονται ως $\underset{\sim}{x}_{low}$ και $\underset{\sim}{x}_{up}$, αντίστοιχα. Το 1-Δ πρόβλημα βελτιστοποίησης είναι δυνατόν να επιλυθεί με διάφορους τρόπους (Μέθοδος Χρυσής Τομής, Μέθοδος Fibonacci, Πολυωνυμικές μέθοδοι, κ.λ.π). Ένας πλήρης κύκλος (επανάληψη) αποτελείται από την επίλυση του προβλήματος (2.1) για $j = 1,...,N_{\text{var}}$.

Έστω $\underset{\sim}{x}_{i,before}$ και $\underset{\sim}{x}_{i,after}$ τα διανύσματα σχεδίασης πριν και μετά την εφαρμογή ενός πλήρους κύκλου. Είναι δυνατόν να ορισθεί η ακόλουθη διεύθυνση αναζήτησης (pattern search direction):

$$\underset{\sim}{d}_{ps} = \underset{\sim}{x}_{i,after} - \underset{\sim}{x}_{i,before} \tag{2.2}$$

Συνεπώς, είναι δυνατόν να διατυπωθεί ένα ακόμα 1-Δ πρόβλημα βελτιστοποίησης, της ακόλουθης μορφής:

$$\min f\left(\underset{\sim}{x}_{i,after} + \alpha_{ps}\underset{\sim}{d}_{ps}\right),\ \underset{\sim}{x}_{low} \le \underset{\sim}{x}_i \le \underset{\sim}{x}_{up} \tag{2.3}$$

Η προαναφερθείσα διεύθυνσης αναζήτησης (pattern search direction) είναι δυνατόν να αποθηκευθεί στον πίνακα **SD** ως η $\left(N_{\text{var}}+1\right)$ εγγραφή. Η αποκαλούμενη 'προς-τα-αριστερά-ολίσθηση' (left-shifting) των διευθύνσεων αναζήτησης επιτυγχάνεται χρησιμοποιώντας τη $j+1$ διεύθυνση αναζήτησης για την i επανάληψη και τη j διεύθυνση αναζήτησης για την $i+1$ επανάληψη. Η $j+1$ διεύθυνση αναζήτησης της $i+1$ επανάληψης δημιουργείται με τη βοήθεια της (Εξ.2.2).

Εάν χρησιμοποιηθεί μίας αιτιοκρατική διαδικασία βελτιστοποίησης για την επίλυση του προβλήματος (2.3), τότε ο εντοπισμός του καθολικού ελαχίστου είναι εγγυημένος, εάν και μόνον εάν υπάρχει ένα ελάχιστο στο εξεταζόμενο πεδίο ορισμού. Με άλλα λόγια, σε αυτήν την περίπτωση υπάρχει μόνον μία τιμή της παραμέτρου a, για την οποία το πρόβλημα (2.3) εμφανίζει καθολικό ελάχιστο. Ωστόσο, εάν στο εξεταζόμενο πεδίο ορισμού υπάρχουν πολλά τοπικά ελάχιστα, τότε η τελική έκβαση μίας αιτιοκρατικής αναζήτησης εξαρτάται από την

αρχική τιμή $a_{ps,ini}$ της εν λόγω παραμέτρου. Ο λόγος αυτής της συμπεριφοράς έγκειται στο γεγονός ότι η αιτιοκρατικότητα τείνει να εγκλωβίσει το ακρότατο μέσα σε ένα διάστημα, το οποίο διαρκώς συρρικνώνεται, έως ότου καταλήξει να είναι σημείο ή οιονεί σημείο. Συνεπώς, εάν αυτός ο εγκλωβισμός δεν καθοδηγηθεί σωστά, τότε εντοπίζεται κάποιο τοπικό ακρότατο και όχι το καθολικό ακρότατο. Καλύτερα αποτελέσματα προκύπτουν εάν το πεδίο ορισμού σαρωθεί με μικρά βήματα αναζήτησης, κάτι το οποίο είναι υπολογιστικά ακριβό, έως και απαγορευτικά ακριβό. Αντιθέτως, μία στοχαστική διαδικασία βελτιστοποίησης είναι λιγότερο επιρρεπής στον εγκλωβισμό σε τοπικό ακρότατο, διότι διαθέτει την εγγενή δυνατότητα της αλλαγής του βήματος αναζήτησης. Με αυτόν τον τρόπο, η πιθανότητα 'απεγκλωβισμού' από τοπικά ακρότατα είναι υψηλότερη. Επιπροσθέτως, όπως προέκυψε και από αντίστοιχη διερεύνηση στο πλαίσιο της παρούσας Διδακτορικής Διατριβής, όσο μικρότερο είναι το πλήθος των μεταβλητών σχεδίασης τόσο πιο αποδοτική είναι μία μέθοδος αναζήτησης στοχαστικού χαρακτήρα. Ιδανική, δε, περίπτωση αποτελεί το πρόβλημα (2.3), το οποίο εμπλέκει μόνον μία μεταβλητή σχεδίασης.

Με αφετηρία αυτές τις σκέψεις, είναι φανερό ότι η επίλυση του προβλήματος (2.1) με μία αιτιοκρατική διαδικασία και η επίλυση του προβλήματος (2.3) με μία στοχαστική διαδικασία αποτελεί έναν καλό θεωρητικό συμβιβασμό διότι εισάγεται η τυχαιότητα στη διαδικασία, το υπολογιστικό κόστος παραμένει σε χαμηλά επίπεδα, ενώ ενισχύεται και η ικανότητα απεγκλωβισμού. Η, δε, προταθείσα διαδικασία είναι η εξής:

Βήμα 1: Τυχαία δημιουργία ενός διανύσματος σχεδίασης $\underset{\sim}{X}_o$ διάστασης $N_{\text{var}} \times 1$

Βήμα 2: Δημιουργία ενός $\left(N_{\text{var}}+1\right) \times N_{\text{var}}$ πίνακα **SD** διανυσμάτων βάσης. Για την πρώτη επανάληψη, οι πρώτες N_{var} εγγραφές αποτελούν τα μοναδιαία διανύσματα της ορθοκανονικής βάσης που περιγράφει το χώρο σχεδίασης, ενώ η $\left(N_{\text{var}}+1\right)$ εγγραφή αντιστοιχεί στην αποκαλούμενη διεύθυνση 'pattern search', η οποία δημιουργείται στο Βήμα 4.

Βήμα 3: Διεξαγωγή μία μονοδιάστατης αιτιοκρατικής διαδικασίας βελτιστοποίησης προς εύρεση ενός νέου βέλτιστου και δυνατού διανύσματος σχεδίασης $\underset{\sim}{X}_1$.

Βήμα 4: Ορισμός της διεύθυνσης 'pattern search' ως $\underset{\sim}{d}_{ps} = \underset{\sim}{X}_1 - \underset{\sim}{X}_o$.

Βήμα 5: Για την αντικειμενική συνάρτηση $f\left(\underset{\sim}{X}_1 + \alpha \underset{\sim}{d}_{ps}\right)$, διεξαγωγή μίας στοχαστικής αναζήτησης κατά μήκος της διεύθυνσης $\underset{\sim}{d}_{ps}$ (μονοδιάστατο πρόβλημα βελτιστοποίησης ως προς το βήμα αναζήτησης a) προς εύρεση ενός νέου βέλτιστου και δυνατού διανύσματος σχεδίασης $\underset{\sim}{X}_2$.

Βήμα 6: Έλεγχος για σύγκλιση

Εάν $\left|\underset{\sim}{X}_2 - \underset{\sim}{X}_1\right| \le tol$, όπου tol μία μικρή, θετική ποσότητα, *Τότε*

διεξαγωγή μίας στοχαστικής αναζήτησης σε μία σφαίρα γύρω από το διάνυσμα $\underset{\sim}{X}_2$ προς εύρεση ενός νέου βέλτιστου και δυνατού διανύσματος σχεδίασης $\underset{\sim}{X}_3$

Εάν $\left|\underset{\sim}{X}_3 - \underset{\sim}{X}_2\right| \le tol$ *Τότε* Stop

Διαφορετικά

ενημέρωση του πίνακα **SD** με την διεύθυνση $\left(\underset{\sim}{X}_3 - \underset{\sim}{X}_2\right)$, ορισμός $\underset{\sim}{X}_o = \underset{\sim}{X}_3$ και επιστροφή στο Βήμα 3

Διαφορετικά

ορισμός $\underset{\sim}{X}_o = \underset{\sim}{X}_2$, 'προς-τα-αριστερά ολίσθηση' των διευθύνσεων αναζήτησης και επιστροφή στο Βήμα 3.

Η φυσική ερμηνεία του Βήματος 5 είναι η ομοιόμορφη διακλιμάκωση ενός διανύσματος σχεδίασης μέχρι να είναι αδύνατη οποιαδήποτε περαιτέρω βελτίωση. Η παράμετρος α αποτελεί τον παράγοντα της διακλιμάκωσης. Ένας τρόπος χειρισμού της παραμέτρου α είναι πρώτα να της αποδοθεί οποιαδήποτε τιμή και στη συνέχεια να ελεγχθεί κατά πόσο η τιμή της αντικειμενικής συνάρτησης μειώνεται και το προκύπτον διάνυσμα σχεδίασης είναι δυνατό. Ένας άλλος τρόπος χειρισμού αυτής της παραμέτρου είναι πρώτα να βρεθεί το αποδεκτό πεδίο ορισμού της, βάσει της διεύθυνσης αναζήτησης και του επιτρεπτού πεδίου ορισμού των μεταβλητών σχεδίασης, και στη συνέχεια να εφαρμοσθεί μία διαδικασία βελτιστοποίησης. Στην παρούσα, τα άνω και κάτω όρια της εν λόγω παραμέτρου καθορίζονται άμεσα, όπως φαίνεται στις κάτωθι Εξ.(2.4):

$$a_{upper} = \min\left\{\left(\underset{\sim}{X}_l - \underset{\sim}{X}_S\right) / \underset{\sim}{d}_{ps}\right\} \tag{2.4a}$$

$$a_{lower} = \min\left\{\left(\underset{\sim}{X}_u - \underset{\sim}{X}_S\right) / \underset{\sim}{d}_{ps}\right\} \tag{2.4b}$$

Διευκρινίζεται ότι στο διάνυσμα $\underset{\sim}{X}_l$ κάθε μεταβλητή σχεδίασης φέρει τις ελάχιστες τιμές της (κάτω όριο του πεδίου ορισμού της), ενώ στο διάνυσμα $\underset{\sim}{X}_u$ κάθε μεταβλητή σχεδίασης φέρει τις μέγιστες τιμές της (άνω όριο του πεδίου ορισμού της). Το , δε, διάνυσμα $\underset{\sim}{d}_{ps}$ περιγράφει την αποκαλούμενη διεύθυνση αναζήτησης 'pattern search'. Με τις Εξ.(2.4), το δυνατό πεδίο ορισμού της παραμέτρου α περιορίζεται εντός ενός διαστήματος πεπερασμένου εύρους.

Επίσης, διευκρινίζεται ότι η φυσική ερμηνεία του Βήματος 6 είναι ότι εάν η επίλυση του προβλήματος (2.3) δεν οδηγήσει σε βελτίωση του τρέχοντος διανύσματος σχεδίασης τότε ενεργοποιείται μία τοπικού χαρακτήρα αναζήτηση γύρω από το τελευταία σχηματισθέν διάνυσμα σχεδίασης, ως προσπάθεια διατήρησης της διαδικασίας αναζήτησης σε περίπτωση όπου το προαναφερθέν διάνυσμα αντιστοιχεί σε τοπικό ακρότατο.

2.3.3. Αριθμητική προσέγγιση

Για την αξιολόγηση της προτεινομένης μεθόδου, χρησιμοποιήθηκαν τέσσερεις Μαθηματικές Συναρτήσεις Επίδοσης, για κάθε μία εκ των οποίων είναι βιβλιογραφικά γνωστό το πεδίο ορισμού, το καθολικό ελάχιστο σε αυτό το πεδίο καθώς και το αντίστοιχο βέλτιστο διάνυσμα σχεδίασης. Προκειμένου να αυξηθεί η δυσκολία εντοπισμού του καθολικού ελαχίστου των εν λόγω συναρτήσεων, για κάθε μία από αυτές προτείνονται δύο παραλλαγές, όπως φαίνεται στις επόμενες παραγράφους.

2.3.3.1. Η συνάρτηση (MBF1) και παραλλαγές αυτής

Η μαθηματική έκφραση αυτής της συνάρτησης φαίνεται στην Εξ.(2.5a), το πεδίο ορισμού της είναι $[2.7, 7.5]$ και υπάρχουν τρία ελάχιστα, εκ των οποίων το καθολικό ελάχιστο βρίσκεται στη θέση $x = 5.145$ και αντιστοιχεί στην τιμή $f_{opti} = -1.886$. Οι άλλες δύο εξετασθείσες παραλλαγές περιγράφονται στις Εξ.(2.5b, 2.5c).

$$f(x) = \sin(x) + \sin\left(10\frac{x}{3}\right) \tag{2.5a}$$

$$f(x) = \sin(x) + \sin\left(20\frac{x}{3}\right) \tag{2.5b}$$

$$f(x) = \sin(x) + 2\sin\left(10\frac{x}{3}\right) \tag{2.5c}$$

Οι γραφικές παραστάσεις των εν λόγω συναρτήσεων φαίνονται στο Σχήμα 2.1, από το οποίο προκύπτει ότι οι παραλλαγές αυτές εισάγουν μεγαλύτερη δυσκολία στον εντοπισμό του ελαχίστου, είτε λόγω αυξημένου πλήθους τοπικών ακροτάτων (Σχήμα 2.1(b)) είτε λόγω μεγαλύτερης κλίσης πλησίον των ακροτάτων (Σχήμα 2.1(c)), καθιστώντας, με αυτόν τον τρόπο, πιο εύκολο τον εγκλωβισμό σε τοπικά ακρότατα.

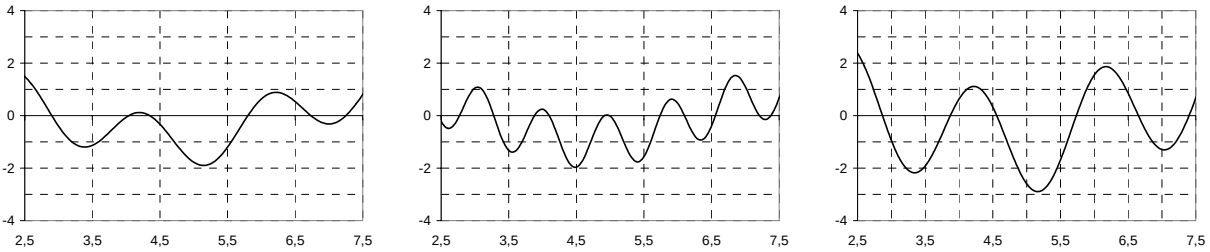

(a) **(b)** **(c)**

Σχήμα 2.1: Διαγράμματα για τη συνάρτηση MBF-1: (a) βασική διατύπωση, (b) αυξημένο πλήθος ακροτάτων και (c) μεγάλες κλίσεις πλησίον των ακροτάτων

2.3.3.2. Η συνάρτηση (MBF2) και παραλλαγές αυτής

Η μαθηματική έκφραση αυτής της συνάρτησης φαίνεται στην Εξ.(2.6a), το πεδίο ορισμού της είναι $\underset{\sim}{x} \in [-1,1]$, ενώ το καθολικό ελάχιστο βρίσκεται στη θέση $\underset{\sim}{x} = \underset{\sim}{0}$ και αντιστοιχεί στην τιμή $f_{opti} = -2.000$. Οι εξετασθείσες παραλλαγές περιγράφονται στις Εξ.(2.6b, 2.6c).

$$f\left(\underset{\sim}{x}\right) = \sum_{j=1}^{2}\left(x_j^2 - \cos\left(18x_j\right)\right) \tag{2.6a}$$

$$f\left(\underset{\sim}{x}\right) = \sum_{j=1}^{2}\left(x_j^2 - \cos\left(25x_j\right)\right) \tag{2.6b}$$

$$f\left(\underset{\sim}{x}\right) = \sum_{j=1}^{2}\left(x_j^2 - 3\cos\left(18x_j\right)\right) \tag{2.6c}$$

Εν γένει, είναι δυνατόν να κατασκευασθεί η γραφική παράσταση μίας συνάρτησης δύο μεταβλητών. Ωστόσο, η μαθηματική έκφραση των εξετασθέντων συναρτήσεων υποδεικνύει ότι η γραφική παράσταση ενός μόνον όρου του αθροίσματος επαρκεί για μία ικανοποιητική οπτικοποίηση των εν λόγω συναρτήσεων, δεδομένου ότι στις Εξ.(2.6) δεν υπάρχουν μη-γραμμικοί όροι περιέχοντες ταυτόχρονα τις μεταβλητές x_1 και x_2. Συνεπώς, είναι επαρκής η απεικόνιση ενός μόνον προσθετέου ως προς x_1 ή ως προς x_2, όπως φαίνεται στο Σχήμα 2.2.

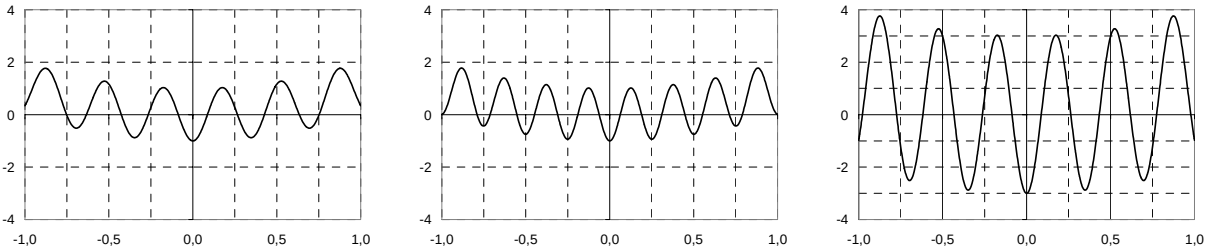

(a) **(b)** **(c)**

Σχήμα 2.2: Διαγράμματα για τη συνάρτηση MBF-2: (a) βασική διατύπωση, (b) αυξημένο πλήθος ακροτάτων και (c) μεγάλες κλίσεις πλησίον των ακροτάτων

Στο Σχήμα 2.2b είναι εμφανής η αύξηση του πλήθους των ακροτάτων, ενώ στο Σχήμα 2.2c είναι εμφανής η αύξηση της κλίσης της συνάρτησης πλησίον των ακροτάτων.

2.3.3.3. Η συνάρτηση (MBF4) και παραλλαγές αυτής

Η μαθηματική έκφραση αυτής της συνάρτησης φαίνεται στην Εξ.(2.7a), το πεδίο ορισμού της είναι $\underset{\sim}{x} \in [-4,0]$, ενώ το καθολικό ελάχιστο βρίσκεται στη θέση $x_i = 2.9035,\ i = 1,..,4$ με τιμή $f_{opti} = -156.66$. Οι εξετασθείσες παραλλαγές περιγράφονται στις Εξ.(2.7b, 2.7c).

$$f(\underset{\sim}{x}) = 0.5\sum_{j=1}^{4}\left(x_j^4 - 16x_j^2 + 5x_j\right) \tag{2.7a}$$

$$f(\underset{\sim}{x}) = 0.5\sum_{j=1}^{4}\left(x_j^4 - 16x_j^2 + 5x_j - 15\cos\left(5x_j\right)\right) \tag{2.7b}$$

$$f(\underset{\sim}{x}) = 0.5\sum_{j=1}^{4}\left(x_j^4 - 16x_j^2 + 5x_j - 25\cos\left(5x_j\right)\right) \tag{2.7c}$$

Στις Εξ.(2.7) δεν υπάρχουν μη-γραμμικοί όροι περιέχοντες ταυτόχρονα δύο διαφορετικές μεταβλητές, συνεπώς η γραφική παράσταση ενός μόνον όρου του αθροίσματος επαρκεί για μία ικανοποιητική οπτικοποίηση της εν λόγω συνάρτησης, όπως φαίνεται στο Σχήμα 2.3.

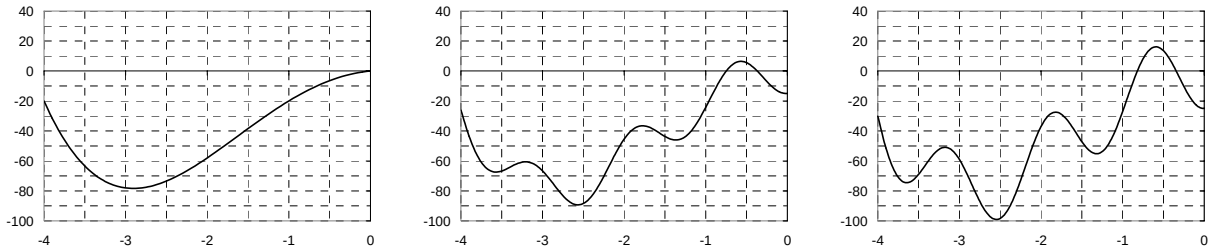

Σχήμα 2.3: Διαγράμματα για τη συνάρτηση MBF-4: (a) βασική διατύπωση, (b) αυξημένο πλήθος ακροτάτων και (c) μεγάλες κλίσεις πλησίον των ακροτάτων

Στο Σχήμα 2.3b είναι εμφανής η αύξηση του πλήθους των ακροτάτων, ενώ στο Σχήμα 2.3c είναι εμφανής η αύξηση της κλίσης της συνάρτησης πλησίον των ακροτάτων.

2.3.3.4. Η συνάρτηση (MBF5) και παραλλαγές αυτής

Η μαθηματική έκφραση αυτής της συνάρτησης φαίνεται στην Εξ.(2.8a), το πεδίο ορισμού της είναι $\underset{\sim}{x} \in [-5.12,5.12]$, ενώ το καθολικό ελάχιστο βρίσκεται στη θέση $\underset{\sim}{x} = \underset{\sim}{0}$ με τιμή $f_{opti} = 0$. Οι εξετασθείσες παραλλαγές περιγράφονται στις Εξ.(2.8b, 2.8c).

$$f(\underset{\sim}{x}) = 80 + \sum_{j=1}^{8}\left(x_j^2 - 10\cos\left(2\pi x_j\right)\right) \tag{2.8a}$$

$$f(\underset{\sim}{x}) = 80 + \sum_{j=1}^{8}\left(x_j^2 - 10\cos\left(4\pi x_j\right)\right) \tag{2.8b}$$

$$f(\underset{\sim}{x}) = 80 + \sum_{j=1}^{8}\left(x_j^2 - 30\cos\left(2\pi x_j\right)\right) \tag{2.8c}$$

Όπως προηγουμένως, η γραφική παράσταση ενός μόνον όρου του αθροίσματος επαρκεί για μία ικανοποιητική οπτικοποίηση της εν λόγω συνάρτησης, όπως φαίνεται στο Σχήμα 2.4.

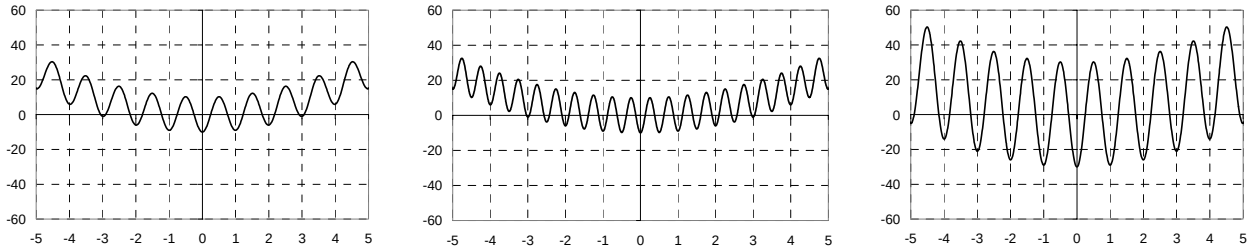

Σχήμα 2.4: Διαγράμματα για τη συνάρτηση MBF-5: (a) βασική διατύπωση, (b) αυξημένο πλήθος ακροτάτων και (c) μεγάλες κλίσεις πλησίον των ακροτάτων

2.4. Δείκτες Επίδοσης

Για την αξιολόγηση της προτεινομένης υβριδικής διαδικασίας βελτιστοποίησης (ονομαζόμενης ως 'Hybrid' εφεξής), πραγματοποιήθηκαν $N_{\max} = 100$ αναλύσεις για κάθε μία από τις εξεταζόμενες συναρτήσεις. Για την k-ιοστή ανάλυση, το αρχικό διάνυσμα σχεδίασης $\underset{\sim}{x}_{ini,k}$ οριζόταν ως φαίνεται στην Εξ.(2.9):

$$\underset{\sim}{x}_{ini,k} = \underset{\sim}{x}_{\min} + \left(k-1\right)\left(\underset{\sim}{x}_{\max} - \underset{\sim}{x}_{\min}\right) / \left(N_{\max} - 1\right),\ k = 1,2,...,100 \tag{2.9}$$

όπου $\underset{\sim}{x}_{\min}$ και $\underset{\sim}{x}_{\max}$ είναι τα διανύσματα σχεδίασης, τα οποία περιέχουν τα κάτω και άνω όρια των μεταβλητών σχεδίασης, αντίστοιχα. Για λόγους σύγκρισης, η ίδια διαδικασία των 100 αναλύσεων εφαρμόσθηκε και στις άλλες χρησιμοποιηθείσες διαδικασίες βελτιτοποίησης, ήτοι στη μέθοδο Powell, στη διατύπωση των Nelder-Mead (N-M) σχετικά με τη μέθοδο Simplex, στη μέθοδο των Hooke και Jeeves (H-J), καθώς και στη μέθοδο της Προσομοιούμενης Ανόπτησης (SA). Διευκρινίζεται ότι αυτές οι μέθοδοι είναι πράγματι συγκρίσιμες, διότι όλες ανήκουν στην ίδια κατηγορία (μέθοδοι μηδενικής τάξης). Δεδομένου, δε, ότι για κάθε μία μέθοδο και για κάθε μία Μαθηματική Συνάρτηση Επίδοσης, πραγματοποιήθηκαν 100 αναλύσεις βελτιστοποίησης, προκύπτει ότι η παρούσα διερεύνηση στηρίχθηκε σε αποτελέσματα από 7200 αναλύσεις. Μία ανάλυση χαρακτηριζόταν ως 'επιτυχής' εάν το διάνυσμα σχεδίασης $\underset{\sim}{X}_{converg}$, στο οποίο κατέληγε, ανήκε στην άμεση γειτονιά του καθολικά βελτίστου διανύσματος σχεδίασης $\underset{\sim}{X}_{opt}$:

$$\left|\underset{\sim}{X}_{converg} - \underset{\sim}{X}_{opt}\right| \le tol \tag{2.10}$$

Προκειμένου να ποσοτικοποιηθεί η συμπεριφορά των εξεταζομένων μεθοδολογιών, ορίσθηκε ο Δείκτης Επίδοσης EI_1, ο οποίος ερμηνεύεται ως 'ποσοστό επιτυχών αναλύσεων' και ορίζεται ως φαίνεται στην Εξ.(2.11):

$$EI_1 = \left(N_{success} / N_{total}\right) \tag{2.11}$$

Προφανώς, όταν $EI_1 = 1$ τότε όλες οι αναλύσεις είναι επιτυχείς. Με βάση τα προκύπτοντα αποτελέσματα, υπολογίσθηκαν οι δείκτες EI_1 και αποτυπώθηκαν σε ραβδογράμματα.

Επίσης, για την αξιολόγηση χρησιμοποιήθηκε η έννοια του μέσου όρου και της τυπικής απόκλισης του πλήθους των επαναλήψεων που απαιτήθηκαν μέχρι συγκλίσεως. Ειδικότερα, αυτά τα δύο μεγέθη υπολογίστηκαν για κάθε ομάδα των 100 αναλύσεων και αποτυπώθηκαν σε λογαριθμικά ραβδογράμματα.

2.4.1. Αριθμητικά αποτελέσματα

2.4.1.1. Αποτελέσματα για τη συνάρτηση (MBF-1) και τις παραλλαγές της

Για τη συνάρτηση MBF-1, η μέθοδος Powell αξιολογήθηκε με Δείκτη Επίδοσης $EI_1 = 1$ (Σχήμα 2.5a) και χρειάστηκε το μικρότερο πλήθος επαναλήψεων (Σχήμα 2.5b). Η προτεινόμενη μέθοδος εμφάνισε την ίδια ικανότητα εντοπισμού του καθολικού ακροτάτου με τη μέθοδο Powell και τη μέθοδο (SA) αλλά χρειάστηκε περισσότερες επαναλήψεις.

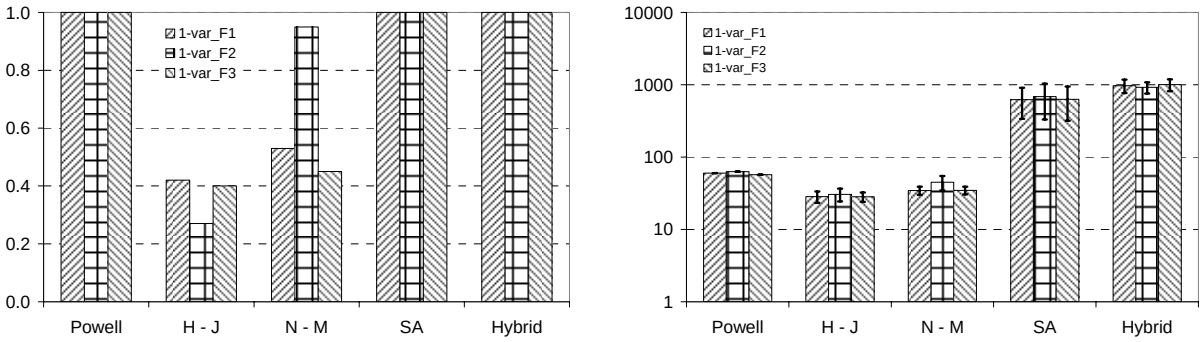

(a) (b)

Σχήμα 2.5: Αξιολόγηση της συνάρτησης MBF-1: (a) Δείκτης Επίδοσης και (b) πλήθος επαναλήψεων

2.4.1.2. Αποτελέσματα για τη συνάρτηση (MBF-2) και τις παραλλαγές της

Για τη συνάρτηση MBF-2, η προτεινόμενη, υβριδική μέθοδος μέθοδος ξεπέρασε τις υπόλοιπες διότι εμφάνισε τον απόλυτα καλύτερο Δείκτη Επίδοσης $EI_1 = 1$. Ωστόσο, χρειάστηκε λίγες επαναλήψεις περισσότερες από τη μέθοδο (SA), η οποία κατετάγη δεύτερη με Δείκτη Επίδοσης $EI_1 < 0.4$. Όλες οι υπόλοιπες μέθοδοι εγκλωβίζονταν σε τοπικά ακρότατα και εμφάνισαν πολύ χαμηλή απόδοση (Σχήμα2.6a).

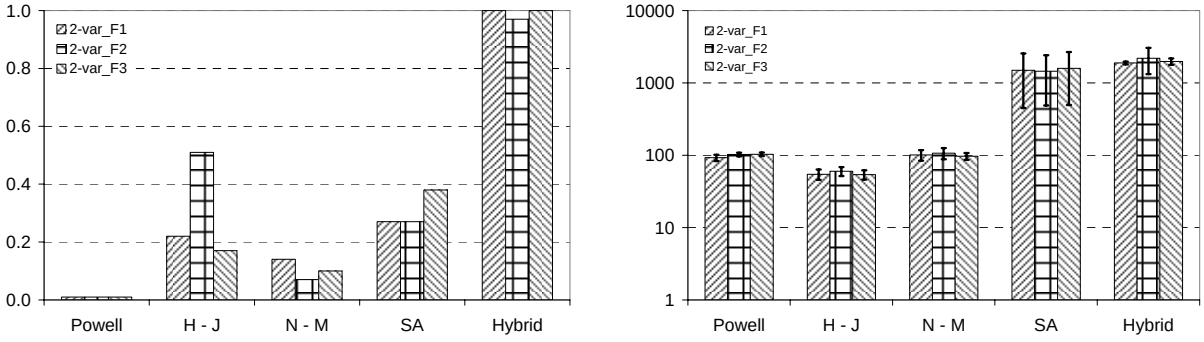

(a) (b)

Σχήμα 2.6: Αξιολόγηση της συνάρτησης BMF-2: (a) Δείκτης Επίδοσης και (b) πλήθος επαναλήψεων

2.4.1.3. Αποτελέσματα για τη συνάρτηση (MBF-4) και τις παραλλαγές της

Για τη συνάρτηση MBF-4, η εικόνα των αποτελεσμάτων είναι αρκετά παρεμφερής με εκείνην της συνάρτησης MBF-1. Πιο συγκεκριμένα, η μέθοδος Powell εμφάνισε την καλύτερη συμπεριφορά δεδομένου ότι είχε Δείκτη Επίδοσης $EI_1 = 1$ (Σχήμα 2.7a) και χρειάστηκε το μικρότερο πλήθος επαναλήψεων μέχρι συγκλίσεως (Σχήμα 2.6b). Το προτεινόμενο, υβριδικό σχήμα εμφάνισε την ίδια άριστη συμπεριφορά, ως προς τον εντοπισμό του καθολικού ελαχίστου, ωστόσο χρειάστηκε περισσότερες επαναλήψεις απ' αυτήν. Οι άλλες δύο μέθοδοι, δηλαδή η μέθοδος H-J και η μέθοδος N-M, είχαν πολύ καλή επίδοση για τη βασική διατύπωση των συναρτήσεων επίδοσης αλλά δυσκολεύθηκαν πολύ με τις παραλλαγές αυτών.

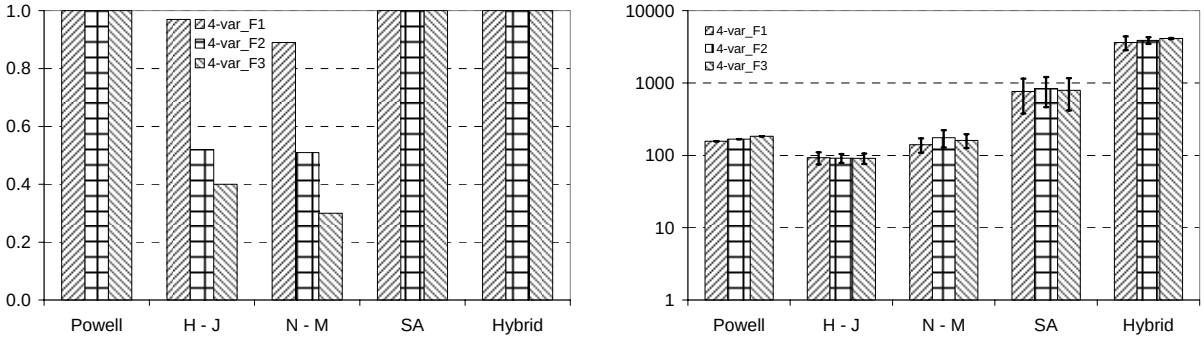

(a) (b)

Σχήμα 2.7: Αξιολόγηση της συνάρτησης BMF-4: (a) Δείκτης Επίδοσης και (b) πλήθος επαναλήψεων

2.4.1.4. Αποτελέσματα για τη συνάρτηση (MBF-5) και τις παραλλαγές της

Για τη συνάρτηση MBF-5, μόνον η μέθοδος (SA) και η προτεινόμενη, υβριδική διαδικασία κατάφεραν να έχουν έναν σχεδόν άριστο Δείκτη Επίδοσης για όλες τις εξετασθείσες περιπτώσεις (Σχήμα 2.8a), με την υβριδική μέθοδο να υπερτερεί ελαφρώς ως προς την τιμή του Δείκτη Επίδοσης EI_1 αλλά να υστερεί ως προς το απαιτούμενο πλήθος επαναλήψεων μέχρι συγκλίσεως (Σχήμα 2.8b). Η μέθοδος Powell επέδειξε άριστη συμπεριφορά αλλά μόνο για την πρώτη παραλλαγή της εξετασθείσας συνάρτησης επίδοσης, ενώ για τις άλλες δύο εκφράσεις απέτυχε πλήρως. Η μέθοδος H-J δεν επέδειξε καλή επίδοση, ενώ η μέθοδος N-M παρουσίασε τη χειρότερη συμπεριφορά.

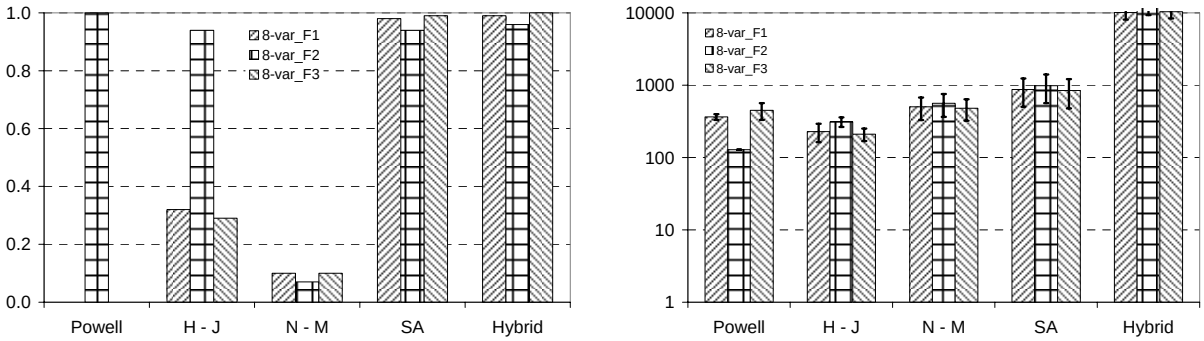

(a) (b)

Σχήμα 2.8: Αξιολόγηση της συνάρτησης BMF-5: (a) Δείκτης Επίδοσης και (b) πλήθος επαναλήψεων

2.4.2. Σχολιασμός

Μέσα από τις προηγούμενες ενότητες, παρουσιάσθηκε μία νέα, υβριδική μεθοδολογία κατάλληλη για την αντιμετώπιση προβλημάτων ελαχιστοποίησης μαθηματικών συναρτήσεων χωρίς περιορισμούς. Η βασική ιδέα ήταν η εισαγωγή του στοιχείου της τυχαιότητας σε μία ισχυρή αιτιοκρατική διαδικασία, όταν δεν είναι δυνατή η επίτευξη περαιτέρω βελτίωσης μέσα από την αιτιοκρατική αναζήτηση. Πιο συγκεκριμένα, μία αιτιοκρατική διαδικασία βελτιστοποίησης τερματίζεται είτε όταν έχει εντοπισθεί το καθολικό ακρότατο είτε όταν ένα τοπικό ακρότατο έχει ψευδώς αναγνωρισθεί ως καθολικό ακρότατο. Στη δεύτερη περίπτωση, ο κίνδυνος εγκλωβισμού σε τοπικό ακρότατο μειώνεται, χωρίς, ωστόσο, να απαλείφεται, όταν εισάγεται κάποια τυχαιότητα διότι με αυτόν τον τρόπο παρέχεται ένα μέσον για πιθανό απεγκλωβισμό. Για τις ανάγκες της παρούσας μελέτης, διαμορφώθηκε ένα υβριδικό σχήμα από μία αιτιοκρατική (μέθοδος Powell) και μία στοχαστική διαδικασία (μέθοδος Προσομοιούμενης Ανόπτησης - SA). Η μέθοδος Powell επιλέχθηκε λόγω της υψηλής της απόδοση σε συνδυασμό με την απλότητά της, ενώ η μέθοδος (SA) επιλέχθηκε λόγω της εξαιρετικής της απόδοσης σε 1-Δ προβλήματα βελτιστοποίησης. Στο προτεινόμενο υβρικό σχήμα, το στοιχείο της τυχαιότητας εμφανίζεται με δύο τρόπους. Κατά πρώτον, πραγματοποιείται αναζήτηση γραμμής με τη μέθοδο (SA) κατά τη διεύθυνση την οποία ορίζουν το πρώτο και το τελευταίο διάνυσμα σχεδίασης μίας επανάληψης (pattern search direction). Κατά δεύτερον, όταν διαπιστώνεται ότι το βέλτιστο διάνυσμα σχεδίασης δεν βελτιώνεται, εκκινείται μία διαδικασία τοπικής αναζήτησης με τη μέθοδο (SA), στην υπερ-σφαίρα γύρω από τη θέση του φαινομένου ως καθολικού ελαχίστου. Η διάμετρος αυτής της σφαίρας αποτελεί παράμετρο της διαδικασίας και διαπιστώθηκε ότι διαδραματίζει σημαντικό ρόλο στην τελική σύγκλιση. Εάν εκ νέου διαπιστώνεται ότι το βέλτιστο διάνυσμα σχεδίασης δεν βελτιώνεται, τότε η διαδικασία τερματίζεται.

Η προτεινόμενη διαδικασία βελτιστοποίησης αναμένεται να συνδυάζει την ανώτερη επίδοση της μεθόδου (SA), ως προς την επίλυση 1-Δ προβλημάτων βελτιστοποίησης, με το μικρό πλήθος επαναλήψεων, το οποίο απαιτεί η μέθοδος Powell. Προέκυψε ότι, σε όλα τα εξετασθέντα παραδείγματα, η προτεινόμενη διαδικασία όντως εντόπισε το καθολικό ακρότατο, απαιτώντας, ωστόσο, περισσότερες επαναλήψεις από τη μέθοδο (SA). Η αιτιολογία γι' αυτό είναι αρκετά απλή: η σύγκλιση εξετάζεται στο τέλος μίας *πλήρους* επανάληψης, δηλαδή όταν *όλα* τα αιτιοκρατικά και στοχαστικά βήματα έχουν ολοκληρωθεί. Ωστόσο, το αντίστοιχο πλήθος κλήσεων της αντικειμενικής συνάρτησης ενδεχομένως να καταστεί πολύ μεγάλο διότι η ίδια ρουτίνα (SA)-αναζήτησης, με της ίδιες ρυθμίσεις, είναι δυνατόν να κληθεί δύο φορές εντός της ίδιας επανάληψης. Αυτό σημαίνει ότι μία περαιτέρω βελτίωση, σχετικά με τη μείωση του πλήθους των κλήσεων της αντικειμενικής συνάρτησης, είναι εφικτή, εάν ο έλεγχος σύγκλισης υλοποιείται μεν εντός μίας πλήρους επανάληψης αλλά οι ρυθμίσεις της (SA)-αναζήτησης είναι διαφορετικές για την αναζήτηση γραμμής και για την αναζήτηση τοπικού χαρακτήρα στην προαναφερθείσα υπερ-σφάιρα.

Τέλος, ένα σημείο άξιο επισήμανσης αφορά στην ευαισθησία εντοπισμού του ελαχίστου ως προς τα όρια του πεδίου ορισμού. Όπως προέκυψε, ακόμα και μία μικρή μεταβολή σε αυτά τα όρια επηρέασε σημαντικά τον Δείκτη Επίδοσης EI_1 των αιτιοκρατικών μεθοδολογιών βελτιστοποίησης. Αυτός είναι και ο λόγος για τον οποίο ορισμένες μεθοδολογίες, ιδίως η μέθοδος Powell, εμφάνισαν χαμηλή απόδοση. Επιπροσθέτως, παρατηρήθηκε ότι, όταν το πεδίο ορισμού μίας *άρτιας* συνάρτησης μεταβαλλόταν από συμμετρικό σε μη-συμμετρικό, το καθολικό ελάχιστο εντοπιζόταν με μεγαλύτερη ευκολία. Στον αντίποδα, τόσο η μέθοδος της Προσομοιούμενης Ανόπτησης (SA) όσο και η προτεινόμενη διαδικασία βελτιστοποίησης, εμφάνισαν μία πολύ στιβαρή συμπεριφορά, μη-επηρεαζόμενη από μεταβολές στα όρια του πεδίου ορισμού.

2.5. Συμπεράσματα

Η προτεινόμενη υβρική διαδικασία βελτιστοποίησης ανήκει στην κατηγορία των μεθόδων μηδενικής τάξης. Για την αξιολόγησή της, χρησιμοποιήθηκαν, συνολικά, δώδεκα Μαθηματικές Συναρτήσεις Επίδοσης, χωρισμένες σε τέσσερεις τριάδες. Κάθε τριάδα περιείχε μια βιβλιογραφική Μαθηματική Συνάρτηση Επίδοσης και δύο παραλλαγές αυτής, οι οποίες διαμορφώθηκαν στο πλαίσιο της παρούσης Διδακτορικής Διατριβής με σκοπό την αύξηση της δυσκολίας εντοπισμού του καθολικού ελαχίστου. Ειδικότερα, η μία παραλλαγή εμφάνιζε μεγαλύτερο πλήθος τοπικών ελαχίστων ενώ η άλλη παραλλαγή εμφάνιζε μεγαλύτερες κλίσεις πλησίον των ακροτάτων. Τα αποτελέσματα, τα οποία προέκυψαν χρησιμοποιώντας την προτεινόμενη διαδικασία στις προαναφερθείσες συναρτήσεις, συγκρίθηκαν με τα αντίστοιχα αποτελέσματα, τα οποία ελήφθησαν χρησιμοποιώντας άλλες βιβλιογραφικές μεθοδολογίες μηδενικής τάξης. Ειδικότερα, πραγματοποιήθηκε σύγκριση με τη μέθοδο Powell, τη μέθοδο της Προσομοιούμενης Ανόπτησης, τη διατύπωση της μεθόδου Simplex κατά Nelder και Mead καθώς και τη μέθοδο των Hooke και Jeeves. Προέκυψε ότι η προτεινόμενη διαδικασία βελτιστοποίησης υπερτερούσε έναντι όλων των εν λόγω μεθοδολογιών ως προς τον εντοπισμό του καθολικού ελαχίστου, ωστόσο εμφάνισε υψηλό υπολογιστικό κόστος. Ως εκ τούτου, εξ ίσου υψηλό υπολογιστικό κόστος αναμένεται να εμφανισθεί και κατά την εφαρμογή της σε προβλήματα βελτιστοποίησης κατασκευών, κάτι το οποίο υποδεικνύει την ανάγκη για εξέταση μεθόδων, στις οποίες αξιοποιούνται εγγενή χαρακτηριστικά του προς επίλυση προβλήματος, κάτι το οποίο αναμένεται να συνοδευθεί από μείωση του υπολογιστικού κόστους.

Βιβλιογραφία

Barricelli, N.A. (1962a), "Numerical testing of evolution theories: I. Theoretical introduction and basic tests", Acta Biotheoretica, Vol. 16:1-2, pp.69-98.

Barricelli, N.A. (1962b), "Numerical testing of evolution theories: II. Preliminary tests of performance symbiogenesis and terrestrial life", Acta Biotheoretica, Vol. 16:1-2, pp.69-98.

Begley, S. (1995), "Software au Naturel", Newsweek, May 8.

Belegundu, A.D., Chandrupatla, T.R. (1999), Optimization concepts and applications in engineering, Prentice Hall.

Bendsøe, M.P., Sigmund O. (2003), Topology Optimization, Theory, Methods and Applications, Springer-Verlag, Berlin.

Bledsoe, W.W. (1962), An Analysis of Genetic Populations, Technical Report, Panoramic Research Inc., Palo Alto, California.

Bledsoe, W.W. (1962), The Evolutionary Method in Hill Climbing: Convergence Rates, Technical Report, Panoramic Research, Inc., Palo Alto, California.

Botello S, Marraquin J.L, Onãte E, Van Horebeek J (1999), "Solving structural optimization problems with genetic algorithms and simulated annealing", Int J Numer Methods Eng, Vol.45, pp.1069–1084.

Box, G.E.P. (1957), "Evolutionary operation: A method for increasing industrial productivity", Appl. Statistics, vol. VI (2), pp.81-101.

Box, M.J. (1965), "A New Method of Constrained Optimization and a Comparison with Other Methods", Computer J, Vol.8, pp.42-52.

Bremermann, H.J. (1962), "Optimization through Evolution and Recombination", In Self-Organizing Systems, eds. M. T. Yovits, Jacobi, and Goldstein. Washington, D. C.: Spartan, pp.93-106.

Burke E.K., Smith A.J. (2000), "Hybrid evolutionary techniques for the maintenance scheduling problem", IEEE Trans Power Syst , Vol.15(1), pp.122–128.

Cannon, W.D. (1932), The Wisdom of the Body, W.W. Norton, New York.

Cauchy, A. (1847), "Methode generale pour la resolution des systemes d'equations simultanes", Compt. Rend., Vol.25, pp.536-538.

Conrad, M. (1969), Computer experiments on the evolution of coadaptation in a primitive ecosystem, Ph.D. Diss., Biophysics Program, Stanford, CA.

Conrad, M., Pattee, H.H. (1970), "Evolution experiments with an artificial ecosystem", J. Theoret. Biol., Vol. 28, pp.393-409.

Courant, R. (1943)"Variational methods for the solution of problems of equilibrium and vibrations", BullAmerMathSoc.,Vol.49,pp.1–23.

Dantzig, G. B., (1951)) "Maximization of a linear function of variables subject to linear inequalities", Activity Analysis of Production and Allocation, Koopman (Ed.), Cowles Commission Monograph, 13, John Wiley and Sons, New York.

De Jong, K. (1975), An analysis of the behaviour of a class of genetic adaptive systems, PhD thesis, University of Michigan.

Fiacco, A.V., McCormick, G.P. (1966), "Extension of SUMT for nonlinear programming: equality constraints and extrapolation", Management Science, Vol. 12, pp.816-828.

Fletcher, R., Powell, M.J.D. (1963), "A rapidly convergent descent method for minimization", Computer J., Vol.6(2), pp.163-168.

Fletcher, R., Reeves, C.M (1964), "Function Minimization by Conjugate Gradients", Computer J., Vol.7, pp.149-154.

Fogel, D.B. (2006), Evolutionary Computation: Toward a New Philosophy of Machine Intelligence, 3rd ed., IEEE Press, New York.

Fogel, L. J., Owens, A.J., Walsh, M.J. (1966). Artificial Intelligence through Simulated Evolution. John Wiley & Sons, New York.

Friedberg, R.M. (1958), "A Learning Machine: Part I"," IBM J. Research and Development, Vol. 2, pp.2-13.

Friedberg, R.M., Dunham B., North,J.H. (1959),"A Learning Machine: Part II", IBM J. Research and Development, Vol. 3, pp.183-191.

Galinier P, Hao J.K. (1999), "Hybrid evolutionary algorithms for graph coloring", J Comb Optim, Vol. 3(4), pp.379–397.

Giotis A., Giannakoglou K. (2004), Evolutionary Algorithm SYstem version 1.3.4, manual, Laboratory of Thermal Turbomachines, National Technical University of Athens.

Goldberg, D. (1989), Genetic Algorithms in Search, Optimization, and Machine Learning. Addison-Wesley.

Haftka, R.T., Gurdal, Z., Kamat, M. (1990), Elements of Structural Optimization, Kluwer.

Haupt, R., Haupt S.E. (1998), Practical Genetic Algorithms, John Wiley & Sons, New York.

Holland, J.H. (1973), "Genetic Algorithms and the Optimal Allocation of Trials", SIAM J. Comput. Vol.2(2), pp.88-105.

Holland, J.H. (1975), Adaptation in natural artificial systems, University of Michigan Press, Ann Arbor, MI.

Hooke, R., Jeeves, T.A. (1961), "Direct Search Solution of Numerical and Statistical Problems", J of the ACM, Vol.8, pp.212-229.

Karush, W. (1939), Minima of Functions of Several Variables with Inequalities as Side Conditions, MS Thesis, Dept. of Mathematics, University of Chicago, Chicago, IL.

Kirkpatrick, S. (1984), "Optimization by simulated annealing: quantitative studies", J Statist Phys, Vol. 34, pp. 975-986.

Kirsch, U. (1993), Structural Optimization, Springer-Verlag.

Kuhn, H.W., Tucker A.W. (1951) "Non-linear Programming", in J.Neyman (Ed.), Proceedings of the Second Berkeley Symposium on Mathematical Statistics and Probability, University of California Press, Berkeley, CA , pp.481-493.

Magoulas G.D., Plagianakos V.P., Vrahatis M.N. (2001), "Hybrid methods using evolutionary algorithms for on-line training", In: Proceedings of the INNS-IEEE International Joint Conference on Neural Networks, Washington DC; 14–19 July 2001, USA.

Mahfoud W.S., Goldberg D.E. (1994), "Parallel recombinative simulated annealing: a genetic algorithm", IlliGAL Report No. 93006, Department of Computer Science, University of Illinois.

Makris, P., Provatidis, C. (2002), "Weight minimisation of displacement-constrained truss structures using a strain energy criterion", Computer Methods Appl. Mech. Engrg., Vol. 191, pp. 2159-2177.

Michalewicz, Z. (1996), Genetic Algorithms + Data Structures = Evolution Programs, 3rd ed., Springer Verlag, Berlin.

Morris, A.J. (1982), Foundations of Structural Optimization: A Unified Approach, John Wiley & Sons.

Nagendra, S. (1997), Catalogue of test problems for Optimization Algorithms verification, GE Research & Development Center.

Nelder, J.A., Mead, R. (1965), "A Simplex Method for Function Minimization", Computer Journal, Vol.7, pp. 308-313.

Pham, D.T., Karaboga D. (2000), Intelligent Optimisation Techniques: Genetic Algorithms, Tabu Search, Similated Annealing and Neural Netwroks, Springer-Verlag.

Powell, M.J.D. (1964), "An efficient Method for finding the minimum of a function of several variables without calculating derivatives", Computer Journal, Vol.7 (4), pp.303-307.

Rechenberg, I. (1965), Cybernetic solution path of an experimental problem. Royal Aircraft Establishment, Farnborough, page Library Translation 1122.

Renders, J.M., Flasse, S.P. (1996), "Hybrid methods using genetic algorithms for global optimization", IEEE Transactions on Systems, Man, and Cybernetics, Part B.

Rosen, J. (1960), "The Gradient Projection Method for Nonlinear Programming, I. Linear Constraints", *Journal of the Society for Industrial and Applied Mathematics*, Vol.8, pp.181–217.

Rosenbrock, H.H. (1960), "An Automatic Method for finding the Greatest or Least Value of a Function", Comp J, Vol.3, pp.175-184.

Rozvany, G.I.N. (2001), "Aims, scope, methods, history and unified terminology of computer-aided topology optimization in structural mechanics", Struct. Multidisc Optim, Vol. 21, pp. 90-108.

Russo, L. (2004), *The forgotten revolution: How science was born in 300BC and why it had to be reborn.* Springer, Berlin.

Schmidt, H., Thierauf G. (2005), "A combined heuristic optimization technique", Advances in Engineering Software, Vol.36, pp. 11–19.

Suzuki, K., Kikuchi, N. (1991), "A Homogenization Method for Shape and Topology Optimization", Computer Methods Appl. Mech. Engrg., Vol. 93, pp. 291-318.

Turing, A.M. (1950), "Computing machinery and intelligence", Mind, Vol. 59, pp.433-460.

Venkatamaran, P. (2002), *Applied Optimization with Matlab Programming*, Wiley.

Veselago, V.G. (2002), "Formulating Fermat's principle for light traveling in negative refraction materials", *PHYS-USP*, Vol. 45(10), pp. 1097-1099.

Xie, Y.M., Steven, G.P. (1997), *Evolutionary Structural Optimization*, Springer-Verlag.

Zoutendijk, G. (1960), *Methods of Feasible Directions*, Elsevier.

Εργασίες

[1] Provatidis, C.G., Vossou C.G., **Venetsanos D.T.**, "Verification of popular deterministic and stochastic optimization methods using benchmark mathematical functions", In: D.Tsahalis (ed.), CD Proc. 1st International Conference "From Specific Computing to Computational Engineering", 8-10 September, 2004, Athens, Greece.

[2] Provatidis C.G., **Venetsanos D.T.**, Vossou C.G., "A comparative study on deterministic and stochastic optimization algorithms applied to truss design", In: D.Tsahalis (ed.), CD Proc. 1st International Conference "From Specific Computing to Computational Engineering", 8-10 September, 2004, Athens, Greece.

[3] Provatidis C.G., **Venetsanos D.T.**, Markos P.A., "Investigation Of Hybrid Optimization Schemes With A Deterministic Search Direction And A Stochastic Step Size", 2nd International Conference "From Scientific Computing to Computational Engineering", 5-8 July, 2006, Athens, Greece.

[4] Papageorgiou A.A., **Venetsanos D.T.**, Provatidis C.G., "Investigating The Influence Of Typical Genetic Algorithm Parameters On The Optimization Of Benchmark Mathematical Functions", 2nd International Conference "From Scientific Computing to Computational Engineering", 5-8 July, 2006, Athens, Greece.

ΚΕΦΑΛΑΙΟ 3
(ΠΕΡΙΛΗΨΗ)

ΘΕΩΡΗΤΙΚΑ ΣΤΟΙΧΕΙΑ ΕΠΙ ΤΗΣ ΑΠΟΜΑΚΡΥΝΣΗΣ ΥΛΙΚΟΥ ΑΠΟ ΜΙΑ ΚΑΤΑΣΚΕΥΗ

Στην παρούσα περίληψη κεφαλαίου, παρατίθεται μία ενεργειακή προσέγγιση σχετικά με την απομάκρυνση υλικού από μία κατασκευή. Ειδικότερα, μετά από μία σύντομη βιβλιογραφική εισαγωγή, εξετάζονται διάφορα σχήματα απομάκρυνσης υλικού, διατυπώνεται ένα νέο Βέλτιστο Κριτήριο για την περίπτωση επιβολής ενός περιορισμού ανάπαλσης, διαμορφώνεται μια αντίστοιχη, νέα διαδικασία βελτιστοποίησης, ενώ καταδεικνύεται η διαφορά μεταξύ επιβολής περιορισμού ανάπαλσης και περιορισμού μετατόπισης.

3.1.Εισαγωγή

Μετά από την εργασία-ορόσημο του Michell (Michell, 1904), το πρόβλημα της βέλτιστης σχεδίασης μίας κατασκευής θεωρήθηκε πλέον ως πρόβλημα βέλτιστης κατανομής υλικού. Για την επίλυση του εν λόγω προβλήματος διατυπώθηκε πληθώρα μεθοδολογιών, οι οποίες είτε αναζητούσαν υλικό μικρής ενεργειακής συμμετοχής στην κατασκευή, προκειμένου να το απομακρύνουν, είτε επεδίωκαν την ανακατανομή του διαθεσίμου υλικού, προκειμένου να ενισχυθούν οι περισσότερο φορτιζόμενες περιοχές. Προς αυτήν την κατεύθυνση, έχουν διατυπωθεί αμιγώς μαθηματικές μεθοδολογίες (Svanberg, 1987; 1995; Stolpe και Svanberg, 2001; Bruyneel και συνεργάτες, 2002). Ωστόσο, τέτοιου είδους προσεγγίσεις δεν αξιοποιούν την έννοια της ενέργειας παραμόρφωσης, η οποία αποτελεί ένα εγγενές χαρακτηριστικό των κατασκευών, άρα και της βελτιστοποίησής τους. Μία τέτοια αξιοποίηση είναι δυνατόν να επιτευχθεί μέσω της διατύπωσης ενεργειακών προσεγγίσεων, κάτι που αποτελεί και το κύριο αντικείμενο της παρούσης περίληψης κεφαλαίου. Πιο συγκεκριμένα, εξετάζεται η ιδέα της ολικής και της μερικής απομάκρυνσης υλικού από μία κατασκευή, ενώ προσεγγίζεται το πρόβλημα βελτιστοποίησης κατασκευών υπό την επιβολή ενός περιορισμού ανάπαλσης.

Η μερική ή και η ολική αφαίρεση υλικού είναι δυνατόν να επιτευχθεί χρησιμοποιώντας τη μέθοδο Evolutionary Structural Optimization (ESO) (Xie και Steven, 1993; 1996; 1997; Xie και συνεργάτες, 2005; Steven και συνεργάτες, 2000). Η κεντρική ιδέα αυτής της μεθόδου είναι η διατύπωση δεικτών ευαισθησίας, ως μέσο εντοπισμού υλικού υποψηφίου προς απομάκρυνση (Nha Chu και συνεργάτες, 1996; 1997). Βάσει αυτών των δεικτών, το διαθέσιμο υλικό αξιολογείται και εκείνο με τους χαμηλότερους δείκτες απομακρύνεται, είτε μερικώς είτε ολικώς (Querin και συνεργάτες, 2000a; 2000b; Yang και συνεργάτες, 1999; 2005). Η μέθοδος ESO είναι πολύ απλή στην εφαρμογή της και καλύπτει ένα ευρύ φάσμα εφαρμογών (Rong και συνεργάτες, 2000; Das και συνεργάτες, 2005; Ren και συνεργάτες, 2005; Zuo και συνεργάτες, 2005; Wei, 2005). Ωστόσο, μέχρι στιγμής, στηρίζεται περισσότερο στη λογική σκέψη της απομάκρυνσης πλεονάζοντος υλικού προς μείωση του βάρους μίας κατασκευής παρά σε ένα στιβαρό μαθηματικό υπόβαθρο (Zhou και Rozvany, 2001; Edwards και συνεργάτες, 2007), αν και έχουν δημοσιευθεί προσπάθειες προς αυτήν την κατεύθυνση (Tanskanen, 2002). Στην παρούσα περίληψη κεφαλαίου, διατυπώνεται και σχολιάζεται η θεωρητική προσέγγιση της απομάκρυνσης υλικού βάσει σχημάτων τύπου ESO, προκειμένου να αναδειχθούν πτυχές αυτού του τρόπου μείωσης του βάρους μίας κατασκευής.

Το πρόβλημα της ελαχιστοποίησης του βάρους μίας κατασκευής υπό την επιβολή ενός περιορισμού ανάπαλσης αποτελεί μία ακόμα πολυσυζητημένη κατηγορία προβλημάτων βελτιστοποίησης (Bendsøe και Kikuchi, 1988; Bendsøe, 1989; Haber και συνεργάτες, 1996; Kita και Tanie, 1999; Fujii και Kikuchi, 2000; Bendsøe και Sigmund, 2003; Burns και Tortorelli, 2003; Allaire και συνεργάτες, 2004; Burns, 2005). Το εν λόγω πρόβλημα εμφανίζεται στη διεθνή βιβλιογραφία με δύο διατυπώσεις. Σύμφωνα με την πρώτη διατύπωση, αναζητείται η ελαχιστοποίηση της ανάπαλσης όταν δίδεται συγκεκριμένη ποσότητα διαθεσίμου υλικού (Bendsøe και Sigmund, 2003; Sigmund, 2001a; 2001b; 2001c), έστω πρόβλημα CCA (Complicance Constraint problem A), ενώ, σύμφωνα, με τη δεύτερη διατύπωση, αναζητείται η ελαχιστοποίηση του βάρους μίας κατασκευής όταν δίδεται συγκεκριμένη τιμή για την ανάπαλση (Xie και Steven, 1993), έστω πρόβλημα CCB (Complicance Constraint problem B). Ωστόσο, είναι αληθές ότι κανένα πρότυπο σχετικά με σιδηρές κατασκευές (Ευρωκώδικες, κανονισμοί DIN, κανονισμοί LRFD, κλπ) δεν περιλαμβάνει περιορισμό ως προς την ανάπαλση. Συνεπώς, είναι λογικό να αναρωτηθεί κανείς προς τι η ενασχόληση με αυτό το πρόβλημα. Η απάντηση σε αυτό το ερώτημα είναι σχετικά απλή: αποδεικνύεται ότι το πρόβλημα βελτιστοποίησης με περιορισμό ανάπαλσης είναι κυρτό πρόβλημα, οπότε ένα τοπικό ακρότατο αποτελεί ταυτόχρονα και ολικό ακρότατο (Svanberg, 1994). Επιπροσθέτως, το συγκεκριμένο πρόβλημα αποτελεί την απλούστερη δυνατή διατύπωση σχετικά με τη βελτιστοποίηση κατασκευών. Η διαχείριση άλλου είδους

περιορισμών είναι πολύ πιο δύσκολη (Duysinx και Sigmund, 1988; Duysinx και Bendsøe, 1998; Bendsøe και Sigmund, 2003), κάτι ιδιαιτέρως αληθές όταν πρόκειται για περιορισμούς τάσης. Ελαχιστοποίηση της ανάπαλσης, δε, σημαίνει μεγιστοποίηση της δυσκαμψίας, οπότε, υπό αυτήν την έννοια, είναι δυνατή η διαμόρφωση μίας καλής εκτίμησης σχετικά με τον τρόπο κατανομής του υλικού προκειμένου να εξασφαλισθεί η μέγιστη δυνατή δυσκαμψία. Το συγκεκριμένο πρόβλημα βελτιστοποίησης έχει μελετηθεί εκτενώς (Ben-Tal και Nemirovski, 1994; 1995; 1997; 2000; Achtziger και συνεργάτες, 1992; Ben-Tal και Bendsøe, 1993).

Στο πλαίσιο της παρούσας Διδακτορικής Διατριβής και σχετικά με το προαναφερθέν πρόβλημα CCA, προτείνεται μία νέα διαδικασία βελτιστοποίησης. Αυτή διαφοροποιείται από τις ήδη υπάρχουσες και αφορούσες στο πρόβλημα CCB. Επίσης, διαφοροποιείται από τις μεθόδους τύπου ESO αφορούσες στο πρόβλημα CCA διότι, σε αντίθεση με αυτές, διαθέτει ένα αμιγώς μαθηματικό υπόβαθρο, τη μέθοδο πολλαπλασιαστών Lagrange εν προκειμένω, εξ αιτίας του οποίου είναι δυνατή η αποβολή υλικού ανεξαρτήτως της επίδρασης που αυτό έχει στη δυσκαμψία της κατασκευής. Πρόκειται για μία σημαντική διαφοροποίηση, δεδομένου ότι οι μεθόδοι τύπου ESO προϋποθέτουν και απαιτούν την αποβολή υλικού μόνον εάν θα προκληθεί μικρή μεταβολή στη δυσκαμψία της κατασκευής.

3.2.Βελτιστοποίηση 2Δ συνεχούς μέσου με αποβολή υλικού

3.2.1. Θεωρητική προσέγγιση

Έστω ένα 2Δ παραμορφώσιμο σώμα, διακριτοποιημένο σε ένα πλήθος πεπερασμένων στοιχείων και φορτιζόμενο από ένα σύνολο εξωτερικών δυνάμεων. Ανεξαρτήτως συστήματος αναφοράς, το έργο που παράγουν οι εξωτερικές δυνάμεις αποθηκεύεται στο εν λόγω σώμα με τη μορφή ενέργειας παραμόρφωσης:

$$W^{\text{int}} = W^{ext} = \left(\frac{1}{2}\right)\{u\}^T [K]\{u\} \tag{3.1}$$

όπου $\{u\}$ είναι το διάνυσμα των κομβικών μετατοπίσεων και $[K]$ είναι το μητρώο δυσκαμψίας του σώματος. Από την ισορροπία δυνάμεων του σώματος, ισχύει:

$$\{F\}^{ext} = [K]\{u\} \tag{3.2}$$

Εάν πρέπει να αφαιρεθεί υλικό από το εν λόγω σώμα, τότε το μητρώο δυσκαμψίας του μειώνεται κατά $[\Delta K]$, ενώ οι κομβικές μετατοπίσεις αυξάνονται κατά $\{\delta u\}$:

$$\{F\}^{ext} = [K]\{u\} = [K - \Delta K]\{u + \delta u\} \tag{3.3}$$

Εκτελώντας πράξεις, προκύπτει:

$$[K]\{u\} = [K]\{u\} + [K]\{\delta u\} - [\Delta K]\{u\} - [\Delta K]\{\delta u\} \tag{3.4}$$

Εξ αιτίας της αποβολής υλικού, το πεδίο των κομβικών μετατοπίσεων μεταβάλλεται, άρα μεταβάλλεται και το έργο των εξωτερικά ασκουμένων δυνάμεων:

$$W^{ext,new} = \left(\frac{1}{2}\right)\left(\{u + \delta u\}^T \{F\}^{ext}\right) \tag{3.5}$$

Ισοδύναμα, ισχύει:

$$W^{ext,new} = \left(\frac{1}{2}\right)\left(\{u\}^T \{F\}^{ext} + \{\delta u\}^T \{F\}^{ext}\right) \tag{3.6}$$

Συνεπώς, η μεταβολή του έργου των εξωτερικών δυνάμεων καθίσταται ίση προς:

$$\Delta W^{ext} = \left(\frac{1}{2}\right)\{\delta u\}^T \{F\}^{ext} \tag{3.7}$$

Ισοδύναμα, ισχύει:

$$\Delta W^{ext} = \left(\frac{1}{2}\right)\{\delta u\}^T [K]\{u\} \tag{3.8}$$

Από την Εξ.(3.4), μετά από απλοποιήσεις, προκύπτει:

$$[K]\{\delta u\} = [\Delta K]\{u\} + [\Delta K]\{\delta u\} \tag{3.9}$$

Λαμβάνοντας υπόψη τις ιδιότητες ενός αναστρόφου πίνακα, ισχύει:

$$\{\delta u\}^T [K] = \{\delta u\}^T [K]^T = \left([K]\{\delta u\}\right)^T \tag{3.10}$$

Ο συνδυασμός των Εξ. (3.9, 3.10) δίδει:

$$\begin{aligned} \left([K]\{\delta u\}\right)^T &= \left([\Delta K]\{u\} + [\Delta K]\{\delta u\}\right)^T = \left([\Delta K]\{u\}\right)^T + \left([\Delta K]\{\delta u\}\right)^T \\ &= \{u\}^T [\Delta K]^T + \{\delta u\}^T [\Delta K]^T \end{aligned} \tag{3.11}$$

Εισάγοντας την Εξ.(3.10) και την Εξ.(3.11) στην Εξ.(3.8), το έργο των εξωτερικών δυνάμεων γράφεται ως:

$$\Delta W^{ext} = \left(\frac{1}{2}\right)\left(\{u\}^T [\Delta K]^T + \{\delta u\}^T [\Delta K]^T\right)\{u\} \tag{3.12}$$

Λόγω συμμετρίας του μητρώου δυσκαμψίας, προκύπτει:

$$[\Delta K]^T = [\Delta K] \tag{3.13}$$

Ο συνδυασμός των Εξ.(3.12, 3.13) δίδει:

$$\Delta W^{ext} = \left(\frac{1}{2}\right)\left(\{u\}^T [\Delta K] + \{\delta u\}^T [\Delta K]\right)\{u\} \tag{3.14}$$

Ισοδύναμα, είναι δυνατόν να γραφεί:

$$\Delta W^{ext} = \left(\frac{1}{2}\right)\{u\}^T [\Delta K]\{u\} + \left(\frac{1}{2}\right)\{\delta u\}^T [\Delta K]\{u\} \tag{3.15}$$

Στην Εξ.(3.15), εμφανίζονται δύο όροι ενεργειακής προέλευσης:

$$\Delta W_1^{ext} = \left(\frac{1}{2}\right)\{u\}^T [\Delta K]\{u\} \tag{3.16}$$

και

$$\Delta W_2^{ext} = \left(\frac{1}{2}\right)\{\delta u\}^T [\Delta K]\{u\} \tag{3.17}$$

Σε καθένα από τους παραπάνω όρους εμφανίζεται η ποσότητα $\{\Delta F\} = [\Delta K]\{u\}$, δηλαδή το γινόμενο της μεταβολής του μητρώου δυσκαμψίας επί το διάνυσμα των αρχικών κομβικών μετατοπίσεων. Επίσης, στον όρο ΔW_1, το φορτίο $\{\Delta F\}$ μετατοπίζει το σημείο εφαρμογής του κατά $\{u\}$, ενώ στον όρο ΔW_2 το μετατοπίζει κατά $\{\delta u\}$, αντίστοιχα. Η φυσική ερμηνεία των όρων αυτών έχει ως ακολούθως:

$\left(\frac{1}{2}\right)\{\delta u\}^T [\Delta K]\{u\}$: παράγεται έργο διότι το σημείο εφαρμογής της δύναμης $\{\Delta F\}$ μετατοπίζεται κατά $\{\delta u\}$

$\left(\frac{1}{2}\right)\{u\}^T [\Delta K]\{u\}$: παράγεται έργο διότι το σημείο εφαρμογής της δύναμης $\{\Delta F\}$ μετατοπίζεται κατά $\{u\}$

Στην ειδική περίπτωση, κατά την οποία οι μεταβολές είναι μικρές, ο όρος $\{\delta u\}^T [\Delta K]$ είναι δυνατόν να θεωρηθεί ως αμελητέος, οπότε προκύπτει:

$$\Delta W^{ext} \approx \left(\frac{1}{2}\right)\{u\}^T [\Delta K]\{u\} \tag{3.18}$$

Σύμφωνα με τη Μέθοδο των Πεπερασμένων Στοιχείων (ΜΠΣ), το εξεταζόμενο σώμα αντικαθίσταται από ένα πλέγμα πεπερασμένων στοιχείων. Εν γένει, αποβολή υλικού ή, ισοδύναμα, απομάκρυνση υλικού σημαίνει ότι ένα ή περισσότερα πεπερασμένα στοιχεία θα απομακρυνθούν από το πλέγμα. Αυτό επιτυγχάνεται με δύο τρόπους, είτε θεωρώντας ότι ο χώρος που καταλαμβάνει το στοιχείο μένει κενός (απουσία υλικού) είτε αποδίδοντας σε αυτόν το χώρο μία πολύ μικρή ενός χαρακτηριστικού μεγέθους, όπως είναι το μέτρο ελαστικότητας ή η πυκνότητα. Η ισχύς των Εξ.(3.15, 3.17), όπως προκύπτει από τα προαναφερθέντα, δεν εξαρτάται από το πλήθος των πεπερασμένων στοιχείων, συνεπώς αυτές είναι δυνατόν να χρησιμοποιηθούν είτε απομακρυνθεί ένα είτε απομακρυνθούν περισσότερα πεπερασμένα στοιχεία.

Η ποσότητα $\{u\}$ αποτελεί το διάνυσμα των κομβικών μετατοπίσεων, το οποίο πολλαπλασιάζεται, στις Εξ.(3.15, 3.17), επί τη μεταβολή του μητρώου δυσκαμψίας $[\Delta K]$. Συνεπώς, είναι δυνατόν να αντικατασταθεί με την ποσότητα $\{u_j\}$:

$$\left[\Delta K\right]\left\{u\right\} = \left[K_j\right]\left\{u_j\right\} \tag{3.19}$$

Η τελευταία εξίσωση μεταφράζεται ως εξής: το μητρώο $\left[\Delta K\right]$ έχει διαστάσεις $N_{DOF} \times N_{DOF}$, όπου N_{DOF} εκφράζει το πλήθος των βαθμών ελευθερίας του εξεταζομένου σώματος, και τα μη-μηδενικά στοιχεία του αντιστοιχούν στους βαθμούς ελευθερίας του j-στοιχείου. Το διάνυσμα $\left\{u\right\}$ περιέχει τις, αντιστοιχούσες στους N_{DOF} βαθμούς ελευθερίας, κομβικές μετατοπίσεις. Επειδή, δε, το διάνυσμα $\left\{u\right\}$ πολλαπλασιάζεται επί το μητρώο$\left[\Delta K\right]$, όλα τα γινόμενα, τα οποία αντιστοιχούν σε βαθμούς ελευθερίας διαφορετικούς από εκείνους του j-στοιχείου, θα είναι μηδενικά. Συνεπώς, το αποτέλεσμα των πολλαπλασιασμών $\left[\Delta K\right]\left\{u\right\}$ και $\left[K_j\right]\left\{u_j\right\}$ θα είναι το ίδιο και θα ισχύει:

$$\Delta W^{ext} = \left(\frac{1}{2}\right)\left\{u_j\right\}^T\left[\Delta K_j\right]\left\{u_j\right\} + \left(\frac{1}{2}\right)\left\{\delta u_j\right\}^T\left[\Delta K_j\right]\left\{u_j\right\} \tag{3.20}$$

Θεωρώντας ότι τα γινόμενα μεταξύ ποσοτήτων, οι οποίες εκφράζουν μεταβολές, είναι αμελητέα, ισχύει:

$$\Delta W^{ext} \approx \left(\frac{1}{2}\right)\left\{u_j\right\}^T\left[\Delta K_j\right]\left\{u_j\right\} \tag{3.21}$$

Η τελευταία εξίσωση υποδηλοί ότι, υπό την προαναφερθείσα θεώρηση και εξ αιτίας της αποβολής ενός πεπερασμένου στοιχείου, η μεταβολή του έργου των εξωτερικών δυνάμεων ισούται αριθμητικά με την, αποθηκευμένη σε αυτό το στοιχείο, ενέργεια παραμόρφωσης. Από την ανωτέρω ανάλυση προκύπτει ότι, σε ένα 2Δ παραμορφώσιμο σώμα, είναι δυνατή η εύρεση πεπερασμένων στοιχείων πολύ μικρής (αμελητέας) συμμετοχής στην συνολική ενεργειακή κατάσταση του σώματος, η αποβολή των οποίων ενδείκνυται προς μείωση του βάρους της κατασκευής. Μετά την εν λόγω αποβολή, τα εναπομείναντα πεπερασμένα στοιχεία (ενεργά στοιχεία) αναβαθμίζονται ενεργειακά και η ενεργειακή τους συνεισφορά πρέπει να εκτιμηθεί εκ νέου. Με άλλα λόγια, η αποβολή πεπερασμένων στοιχείων πρέπει να λαμβάνει χώρα προοδευτικά και να είναι ενσωματωμένη σε μία ευρύτερη επαναληπτική διαδικασία. Δύο κριτήρια, μεταξύ αρκετών, για την επιλογή των προς αποβολή στοιχείων είναι τα ακόλουθα:

Κριτήριο #1: Απομάκρυνση πεπερασμένων στοιχείων για τα οποία ισχύει $\Delta W^{ext} \le \alpha W^{ext}$, όπου $\alpha \in \left(0,1\right)$. Με άλλα λόγια, τα προς αποβολή στοιχεία είναι δυνατόν να προκαλέσουν μία μεταβολή στο έργο των εξωτερικών δυνάμεων το πολύ ίση με ένα κλάσμα α του έργου των εξωτερικών δυνάμεων (η τιμή της παραμέτρου α αποτελεί, ελεύθερη μεν αλλά λογική, επιλογή).

Κριτήριο #2: Απομάκρυνση πεπερασμένων στοιχείων για τα οποία ισχύει $\Delta W^{ext} \le W_{thresh}$, όπου W_{thresh} είναι μία ποσότητα ελεύθερα, αλλά λογικά, οριζόμενη και εκφράζει ποιοτικά ένα ενεργειακό κατώφλι.

3.2.2. Ομοιόμορφη διακλιμάκωση πάχους

Το Κριτήριο #1 (βλ. Ενότητα 3.2.1) δύναται να χρησιμοποιηθεί για την ομοιόμορφη μείωση του πάχους των, υποψηφίων προς αποβολή, στοιχείων και περιγράφεται από την κάτωθι ανισότητα:

$$\Delta W^{ext} \le \alpha W^{ext}, \alpha \in (0,1) \tag{3.22}$$

Ο συνδυασμός των Εξ. (3.1, 3.17, 3.22) δίδει:

$$\left(\frac{1}{2}\right)\left(\{u\}^T[\Delta K]\{u\}\right) \le \alpha\left(\frac{1}{2}\right)\{u\}^T[K]\{u\} \tag{3.23}$$

Ισοδύναμα, ισχύει:

$$\left(\frac{1}{2}\right)\left(\{u\}^T[\Delta K]\{u\}\right) \le \left(\frac{1}{2}\right)\{u\}^T[\alpha K]\{u\} \tag{3.24}$$

Από την τελευταία ανισότητα, είναι προφανές ότι ισχύει:

$$[\Delta K] \le \alpha [K] \tag{3.25}$$

Η φυσική σημασία της τελευταίας ανισότητας είναι άμεση: η ενέργεια παραμόρφωσης μίας κατασκευής είναι δυνατόν να αυξηθεί μέσω της ομοιόμορφης μείωσης της δυσκαμψίας μέρους της κατασκευής. Για σκελετικές κατασκευές και για συνεχή μέσα, αυτό επιτυγχάνεται με τη μείωση του μεγέθους (εμβαδόν διατομής ή πάχος) των αντιστοίχων δομικών στοιχείων.

3.2.3. Ολική αποβολή ενός πεπερασμένου στοιχείου

Η αντίστοιχη ενεργειακή μεταβολή εκτιμάται χρησιμοποιώντας την Εξ.(3.20), σύμφωνα με την οποία, εν γένει, κάθε στοιχείο χαρακτηρίζεται από μία διαφορετική στάθμη ενέργειας παραμόρφωσης. Στοιχεία, τα οποία εντοπίζονται βάσει του Κριτηρίου #1, είναι υποψήφια προς αποβολή. Μεταξύ αυτών, το στοιχείο με τη χαμηλότερη τιμή ενέργειας παραμόρφωσης είναι εκείνο το στοιχείο, η αποβολή του οποίου προκαλεί τη μικρότερη δυνατή μεταβολή στην ενεργειακή κατάσταση της κατασκευής. Με αυτόν τον τρόπο, σμιλεύεται το βέλτιστο σχήμα μέσα από ένα μονοπάτι ελάχιστου ρυθμού μεταβολής ενέργειας. Εναλλακτικά, είναι δυνατή η αποβολή ενός μόνον στοιχείου, το οποίο είναι κοντά στο οριζόμενο ενεργειακό κατώφλι. Με αυτόν τον τρόπο, η διαδικασία αποβολής υλικού επιταχύνεται διότι όλα τα στοιχεία, τα οποία είναι ενεργειακώς υποδεέστερα από το αποβληθέν στοιχείο, υποβαθμίζονται ενεργειακά με πιο γρήγορο ρυθμό.

3.2.4. Ολική αποβολή περισσοτέρων πεπερασμένων στοιχείων

Ως προς την ολική αποβολή, σε ένα βήμα, περισσοτέρων του ενός πεπερασμένων στοιχείων, υπάρχουν αρκετές επιλογές, όπως:

- Αιτιοκρατική αποβολή. Τα εναπομείναντα στοιχεία ταξινομούνται κατά αύξουσα σειρά με κριτήριο την ενέργεια παραμόρφωσης και στη συνέχεια αποβάλλονται τα πρώτα n στοιχεία της σειράς, για τα οποία ισχύει $\sum_{j=1}^{n} W_j^{ext} \le \Delta W$, όπου ΔW είναι ένα άνω ενεργειακό όριο, ελεύθερα, αλλά λογικά, οριζόμενο.

- Στοχαστική αποβολή. Τα εναπομείναντα στοιχεία ταξινομούνται κατά αύξουσα σειρά με κριτήριο την ενέργεια παραμόρφωσης και στη συνέχεια αποβάλλονται m στοιχεία, τα οποία επιλέγονται τυχαία αλλά ικανοποιούν τον περιορισμό $\sum_{j=1}^{m} W_j^{ext} \le \Delta W$, όπου ΔW είναι ένα άνω ενεργειακό όριο, ελεύθερα, αλλά λογικά, οριζόμενο.

3.2.5. Μερική αποβολή περισσοτέρων πεπερασμένων στοιχείων

Είναι δυνατή η μερική αποβολή υλικού είτε με τη μορφή μεταβολής του πάχους στοιχείων είτε με τη μορφή μεταβολής του εμβαδού στοιχείων, όπως συμβαίνει στις μεθόδους σταθερού πλέγματος (fixed-grid method). Αυτό σημαίνει ότι η ποσότητα $[\Delta K]$ χρήζει ιδιαίτερης προσοχής.

3.2.6. Συμπεράσματα

Από όλα τα προαναφερθέντα, προκύπτει ότι υπάρχουν διάφοροι τρόποι με τους οποίους είναι δυνατή η αποβολή υλικού. Επίσης, η ιδέα της αποβολής υλικού εφαρμόζεται σε προβλήματα ελαχιστοποίησης του βάρους μίας κατασκευής, ανεξάρτητα εάν πρόκειται για βελτιστοποίηση σχήματος, τοπολογίας ή κατανομής υλικού, και ανεξάρτητα από το είδος του επιβαλλομένου περιορισμού (περιορισμός ανάπαλσης, μετατόπισης, τάσης, κλπ). Επίσης, είναι θεμελιώδους σημασίας η δυνατότητα της επαναχρησιμοποίησης υλικού, το οποίο έχει αποβληθεί. Με άλλα λόγια, είναι σημαντική η ενσωμάτωση στη διαδικασία βελτιστοποίησης ενός σχήματος 'θανάτου και γένεσης' ('die and birth') του διαθεσίμου υλικού. Τέλος, βάσει του ορισμού της ενέργειας παραμόρφωσης και του ορισμού της συμπληρωματικής ενέργειας παραμόρφωσης, είναι δυνατή η διατύπωση ενεργειακών προτάσεων, παρεμφερών με αυτές που παρουσιάσθηκαν στις προηγούμενες ενότητες, αλλά εκπεφρασμένων ως προς τη συμπληρωματική ενέργεια παραμόρφωσης.

3.3.Βελτιστοποίηση 2Δ συνεχούς μέσου υπό περιορισμό ανάπαλσης

3.3.1. Θεωρητική προσέγγιση

Σε αυτήν την ενότητα, εξετάζεται το πρόβλημα της βελτιστοποίησης ενός 2Δ συνεχούς μέσου υπό την επιβολή ενός περιορισμού ανάπαλσης. Πιο συγκεκριμένα αναζητείται το ελάχιστο βάρος του εν λόγω σώματος υπό τον περιορισμό ότι το έργο των εξωτερικά ασκουμένων δυνάμεων δεν πρέπει να ξεπερνά μία μέγιστη τιμή. Η μαθηματική διατύπωση του αντίστοιχου προβλήματος είναι η ακόλουθη:

$$\min W = \sum A_i t_i \rho_i \tag{3.26}$$

$$\text{όπου } t_i \ge t_{\min} \text{ και } \left(\frac{1}{2}\right)\{u\}^T \{F\} \le C_{\max} \tag{3.27}$$

Από την Εξ.(3.27) προκύπτει ότι τίθεται ένας περιορισμός σχετικά με το ελάχιστο πάχος της κατασκευής και ένας περιορισμός σχετικά με την ανάπαλση. Ο πρώτος εκ των περιορισμών αυτών επιβάλλεται προς αποφυγή αριθμητικών ασταθειών, οι οποίες είναι δυνατόν να εμφανισθούν από τη μη-χρησιμοποίηση ενός πεπερασμένου στοιχείου σε ένα υπάρχον πλέγμα (υπάρχει κίνδυνος σχηματισμού κακώς ορισμένου μητρώου δυσκαμψίας, το οποίο δεν είναι δυνατόν να αντιστραφεί). Ο περιορισμός ανάπαλσης είναι δυνατόν να γραφεί ως εξής:

$$g(t) \le 0 \text{ όπου } g(t) = \frac{\left(\frac{1}{2}\right)\{u\}^T \{F\}}{C_{\max}} - 1 \tag{3.28}$$

Σύμφωνα με την μέθοδο πολλαπλασιαστών Lagrange, η συνάρτηση Lagrange ισούται με:

$$L(\mathbf{t}, \lambda) = \sum A_i t_i \rho_i + \lambda_1 g_1(t) \tag{3.29}$$

Ως **t** δηλώνεται το διάνυσμα σχεδίασης και περιέχει το πάχος των πεπερασμένων στοιχείων στα οποία έχει διακριτοποιηθεί το 2Δ συνεχές μέσο. Ο συνδυασμός των Εξ.(3.28, 3.29) δίδει:

$$L(\mathbf{t}, \lambda) = \sum A_i t_i \rho_i + \lambda_1 \left(\frac{\left(\frac{1}{2}\right)\{u\}^T \{F\}}{C_{\max}} - 1 \right) \tag{3.30}$$

Σύμφωνα με τις συνθήκες Karush-Kuhn-Tucker, όταν το διάνυσμα σχεδίασης, το διάνυσμα **t** εν προκειμένω, αντιστοιχεί στο ακρότατο της αντικειμενικής συνάρτησης, στην Εξ.(3.26) εν προκειμένω, τότε ισχύει:

$$\nabla_t L(\mathbf{t}, \lambda) = 0 \text{ και } \nabla_\lambda L(\mathbf{t}, \lambda) = 0 \tag{3.31}$$

Ο συνδυασμός των Εξ. (3.30, 3.31), μετά από εκτέλεση πράξεων, δίδει:

$$\frac{\partial\left(L(\mathbf{t}, \lambda)\right)}{\partial t_i} = 0 \Rightarrow \frac{\partial}{\partial t_i} \left(\sum A_i t_i \rho_i + \lambda_1 \left(\frac{\left(\frac{1}{2}\right)\{u\}^T \{F\}}{C_{\max}} - 1 \right) \right) = 0 \tag{3.32}$$

Στην Εξ. (3.32), η μερική παράγωγος του πρώτου όρου της παρένθεσης ισούται με:

$$\frac{\partial}{\partial t_i} \left(\sum A_i t_i \rho_i \right) = A_i \rho_i \tag{3.33}$$

Στην ίδια εξίσωση, η μερική παράγωγος του δεύτερου όρου της παρένθεσης ισούται με:

$$\frac{\partial}{\partial t_i} \left(\lambda_1 \left(\frac{\left(\frac{1}{2}\right)\{u\}^T \{F\}}{C_{\max}} - 1 \right) \right) = \left(\frac{\lambda_1}{C_{\max}} \right) \frac{\partial}{\partial t_i} \left(\left(\frac{1}{2}\right)\{u\}^T \{F\} \right) \tag{3.34}$$

Στην Εξ.(3.34) ο λόγος $\left(\frac{\lambda_1}{C_{\max}}\right)$ είναι σταθερός, ενώ η παράγωγος $\frac{\partial}{\partial t_i}\left(\left(\frac{1}{2}\right)\{u\}^T\{F\}\right)$ πρέπει να υπολογισθεί. Προς αυτήν την κατεύθυνση και μετά από μερικές απλοποιήσεις, προκύπτει:

$$\frac{\partial}{\partial t_i}\left(\left(\frac{1}{2}\right)\{u\}^T\{F\}\right)=\left(\frac{1}{2}\right)\frac{\partial\left(\{u\}^T\right)}{\partial t_i}\{F\}+\left(\frac{1}{2}\right)\{u\}^T\frac{\partial\left(\{F\}\right)}{\partial t_i} \tag{3.35}$$

Το διάνυσμα της δύναμης θεωρείται ότι είναι ανεξάρτητο του πάχους του 2Δ σώματος:

$$\frac{\partial\left(\{F\}\right)}{\partial t_i}=0 \tag{3.36}$$

Αυτό σημαίνει ότι ο δεύτερος όρος στο δεξί μέλος της Εξ. (3.35) μηδενίζεται:

$$\left(\frac{1}{2}\right)\{u\}^T\frac{\partial\left(\{F\}\right)}{\partial t_i}=0 \tag{3.37}$$

Ο συνδυασμός των Εξ.(3.35, 3.37) δίδει:

$$\frac{\partial}{\partial t_i}\left(\left(\frac{1}{2}\right)\{u\}^T\{F\}\right)=\left(\frac{1}{2}\right)\frac{\partial\left(\{u\}^T\right)}{\partial t_i}\{F\} \tag{3.38}$$

Το διάνυσμα $\{F\}$ των εξωτερικώς ασκουμένων δυνάμεων είναι αρχικά γνωστό. Συνεπώς, η μερική παράγωγος $\left(\partial\left(\{u\}^T\right)/\partial t_i\right)$ αποτελεί τον, προς υπολογισμό, άγνωστο. Από τη Μέθοδο των Πεπερασμένων Στοιχείων, είναι γνωστό ότι:

$$\{F\}=[K]\{u\} \tag{3.39}$$

Η παράγωγος της Εξ. (3.39) ως προς το πάχος t_i ισούται με:

$$\frac{\partial\{F\}}{\partial t_i}=\frac{\partial}{\partial t_i}\left([K]\{u\}\right)=\frac{\partial\left([K]\right)}{\partial t_i}\{u\}+[K]\frac{\partial\left(\{u\}\right)}{\partial t_i} \tag{3.40}$$

Ο συνδυασμός των Εξ. (3.36, 3.41) δίδει:

$$\frac{\partial\left([K]\right)}{\partial t_i}\{u\}+[K]\frac{\partial\left(\{u\}\right)}{\partial t_i}=0 \tag{3.41}$$

Επιλύοντας την τελευταία εξίσωση ως προς $\frac{\partial\left(\{u\}\right)}{\partial t_i}$, προκύπτει:

$$\frac{\partial(\{u\})}{\partial t_i} = -[K]^{-1}\frac{\partial([K])}{\partial t_i}\{u\} \tag{3.42}$$

Το μητρώο δυσκαμψίας $[K]$ είναι συμμετρικό, οπότε ισχύει:

$$[K] = [K]^T \text{ και } [K]^{-1} = \left([K]^{-1}\right)^T \tag{3.43}$$

Από τον συνδυασμό των δύο τελευταίων εξισώσεων, προκύπτει ότι η μερική παράγωγος $\left(\partial\left(\{u\}^T\right)/\partial t_i\right)$ ισούται με:

$$\begin{aligned}\frac{\partial\left(\{u\}^T\right)}{\partial t_i} &= -\left([K]^{-1}\frac{\partial([K])}{\partial t_i}\{u\}\right)^T = -\left(\left(\frac{\partial([K])}{\partial t_i}\{u\}\right)^T\left([K]^{-1}\right)^T\right)\\ &= -\left(\{u\}^T\left(\frac{\partial([K])}{\partial t_i}\right)^T\left([K]^{-1}\right)^T\right) = -\left(\{u\}^T\left(\frac{\partial([K])}{\partial t_i}\right)[K]^{-1}\right)\end{aligned} \tag{3.44}$$

Συνδυάζοντας τις Εξ. (3.38, 3.44) προκύπτει:

$$\frac{\partial}{\partial t_i}\left(\left(\frac{1}{2}\right)\{u\}^T\{F\}\right) = \left(\frac{1}{2}\right)\left(-\left(\{u\}^T\left(\frac{\partial([K])}{\partial t_i}\right)[K]^{-1}\right)\right)\{F\} \tag{3.45}$$

Από την Εξ. (3.39) και επιλύοντας ως προς $\{u\}$, προκύπτει:

$$\{u\} = [K]^{-1}\{F\} \tag{3.46}$$

Μετά από πράξεις, ο συνδυασμός των Εξ.(3.45, 3.46) δίδει:

$$\frac{\partial}{\partial t_i}\left(\left(\frac{1}{2}\right)\{u\}^T\{F\}\right) = -\left(\frac{1}{2}\right)\{u\}^T\left(\frac{\partial([K])}{\partial t_i}\right)\{u\} \tag{3.47}$$

Επίσης, μετά από πράξεις, η Εξ.(3.37) είναι δυνατόν να γραφεί και ως εξής:

$$A_i\rho_i + \left(\frac{\lambda_1}{C_{\max}}\right)\frac{\partial}{\partial t_i}\left(\left(\frac{1}{2}\right)\{u\}^T\{F\}\right) = 0 \tag{3.48}$$

Εισάγοντας την Εξ.(3.48) στην Εξ.(3.47), προκύπτει:

$$A_i\rho_i - \left(\frac{1}{2}\right)\left(\frac{\lambda_1}{C_{\max}}\right)\{u\}^T\left(\frac{\partial([K])}{\partial t_i}\right)\{u\} = 0 \tag{3.49}$$

Αναδιατάσσοντας τους όρους στην τελευταία εξίσωση, προκύπτει:

$$1 = \lambda_1 \left(\frac{1}{2}\right)\left(\frac{1}{C_{\max}}\right)\left(\frac{1}{A_i \rho_i}\right)\{u\}^T \left(\frac{\partial([K])}{\partial t_i}\right)\{u\} \tag{3.50}$$

Πολλαπλασιάζοντας και διαιρώντας το δεξί μέλος της Εξ. (3.50) με t_i, προκύπτει:

$$1 = \lambda_1 \left(\frac{1}{2}\right)\left(\frac{1}{C_{\max}}\right)\left(\frac{1}{A_i t_i \rho_i}\right)\{u\}^T \left(\frac{t_i \partial([K])}{\partial t_i}\right)\{u\} \tag{3.51}$$

Αποδεικνύεται (βλ. Παράρτημα 3.Α) ότι ισχύει η ακόλουθη ισότητα:

$$\{u\}^T \left(\frac{t_i \partial([K])}{\partial t_i}\right)\{u\} = \{u_i\}^T \left(\frac{t_i \partial([K_i])}{\partial t_i}\right)\{u_i\} \tag{3.52}$$

Στην επίπεδη ελαστικότητα, το μητρώο δυσκαμψίας ενός πεπερασμένου στοιχείου i είναι:

$$K_i = \int_A t_i \mathbf{B}^T \mathbf{E} \mathbf{B} dA \tag{3.53}$$

όπου t_i είναι το πάχος του πεπερασμένου στοιχείου, $\mathbf{E}$ είναι το μητρώο ελαστικότητας και $\mathbf{B}$ το μητρώο μετατοπίσεων-παραμορφώσεων. Παραγώγιση ως προς το πάχος t_i δίδει:

$$\frac{\partial}{\partial t_i}(K_i) = \int_A \mathbf{B}^T \mathbf{E} \mathbf{B} dA \tag{3.54}$$

Ο πολλαπλασιασμός και των δύο μελών της Εξ. (3.54) με t_i δίδει:

$$t_i \frac{\partial}{\partial t_i}(K_i) = t_i \int_A \mathbf{B}^T \mathbf{E} \mathbf{B} dA = \int_A t_i \mathbf{B}^T \mathbf{E} \mathbf{B} dA = K_i \tag{3.55}$$

Ο συνδυασμός των Εξ. (3.51, 3.55) δίδει:

$$1 = \lambda_1 \left(\frac{1}{2}\right)\left(\frac{1}{C_{\max}}\right)\left(\frac{1}{A_i t_i \rho_i}\right)\{u_i\}^T [K]_i \{u_i\} \tag{3.56}$$

Η Εξ. 3.56) γράφεται και ως εξής:

$$1 = \lambda_1 \left(\frac{1}{2}\right)\left(\frac{1}{C_{\max}}\right)\left(\frac{1}{\rho_i}\right)\left(\frac{\{u\}_i^T [K]_i \{u\}_i}{A_i t_i}\right) \tag{3.57}$$

Δεδομένου ότι $\lambda_1 = const$ και $C_{\max} = const$, από την Εξ. (3.57) προκύπτει ότι:

$$\left(\frac{1}{\rho_i}\right)\left(\frac{\{u\}_i^T [K]_i \{u\}_i}{A_i t_i}\right) = const \tag{3.58}$$

Η Εξ. (3.58) αποτελεί τη μαθηματική έκφραση ενός νέου Βελτίστου Κριτηρίου, σύμφωνα με το οποίο:

Όταν αναζητείται το ελάχιστο βάρος ενός 2Δ συνεχούς σώματος υπό την επιβολή ενός περιορισμού ανάπαλσης, τότε, στη βέλτιστη σχεδίαση, ο λόγος της πυκνότητας της ενέργειας παραμόρφωσης προς την πυκνότητα του υλικού είναι σταθερός.

Χωρίς βλάβη της γενικότητας, είναι δυνατός ο προσδιορισμός της κατανομής του πάχους t_i μέσα από μία επαναληπτική διαδικασία, κατά την οποία τα πάχη των στοιχείων προσδιορίζονται σύμφωνα με κάποια εξίσωση επανασχεδίασης. Μία τυπική εφαρμογή της μεθόδου των πολλαπλασιαστών Lagrange απαιτεί πρώτα την επίλυση της Εξ. (3.57) ως προς τον πολλαπλασιαστή Lagrange και στη συνέχεια την εισαγωγή αυτού του πολλαπλασιαστή στην εξίσωση που περιγράφει τον αντίστοιχο περιορισμό. Ωστόσο, για το εξεταζόμενο πρόβλημα βελτιστοποίησης, ο περιορισμός ανάπαλσης είναι εκπεφρασμένος ως προς το *διάνυσμα* σχεδίασης (Εξ.3.28) και όχι ως προς μία *μεταβλητή* σχεδίασης (Εξ.3.57). Αυτό σημαίνει ότι η απαλοιφή του εμπλεκομένου πολλαπλασιαστή Lagrange δεν αποτελεί μία τετριμμένη διαδικασία. Εναλλακτικά, είναι δυνατή η εφαρμογή της προτεινομένης διαδικασίας, η οποία παρουσιάζεται στην επόμενη Ενότητα.

3.3.2. Προτεινόμενη διαδικασία

Η Εξ.(3.57) περιγράφει την ενεργειακή κατάσταση της κατασκευής στη βέλτιστη σχεδίαση, χωρίς, ωστόσο, να περιγράφει με κάποιον τρόπο όδευσης προς αυτήν την κατάστασης. Συνεπώς είναι δυνατόν να διατυπωθούν διάφορες διαδικασίες. Προς αυτήν την κατεύθυνση, και θεωρώντας ότι χρησιμοποιείται το ίδιο υλικό σε όλη την κατασκευή, εισάγεται ο ακόλουθος Δείκτης:

$$a_i = \left(\frac{1}{\rho_i C_{\max}}\right)\left(\frac{\{u\}_i^T [K]_i \{u\}_i}{A_i t_i}\right) \tag{3.59}$$

Η φυσική σημασία αυτού του Δείκτη είναι ότι η πυκνότητα της ενέργειας παραμόρφωσης, κανονικοποιημένης ως προς τη μέγιστη επιτρεπόμενη τιμή της ανάπαλσης, πρέπει να είναι σταθερή σε όλη την έκταση της κατασκευής. Λαμβάνοντας υπόψη τον περιορισμό για ελάχιστο πάχος, όπως αυτός περιγράφεται στην Εξ.(3.27), προκύπτει ότι η πυκνότητα της ενέργειας παραμόρφωσης πρέπει να είναι σταθερή σε όλη την έκταση του *ενεργού μέρους* της κατασκευής, δηλαδή του μέρους της κατασκευής στο οποίο όλα τα μέλη έχουν μη-κρίσιμες τιμές πάχους. Ως εκ τούτου, η αντίστοιχη μέση τιμή $\overline{a}$ των ενεργών στοιχείων ισούται με:

$$\overline{a} = \left(\frac{\sum_{i=1}^{N_{active}} a_i}{N_{active}}\right) \tag{3.60}$$

Συνεπώς, στη βέλτιστη σχεδίαση και για το ενεργό τμήμα της κατασκευής, ισχύει:

$$\left(\frac{\alpha_i}{\overline{\alpha}}\right) \to 1 \tag{3.61}$$

Διαιρώντας τις Εξ. (3.59, 3.60) κατά μέλη και συνυπολογίζοντας την Εξ.(3.61), ισχύει:

$$\left(\frac{\sum_{i=1}^{N_{active}} a_i}{N_{active}}\right) = \left(\frac{1}{\rho_i\, C_{\max}}\right)\left(\frac{\{u\}_i^T [K]_i \{u\}_i}{A_i t_{i,new}}\right) \tag{3.62}$$

όπου $t_{i,new}$ είναι το επανασχεδιασθέν πάχος του $i-$στοιχείου. Επιλύοντας την Εξ.(3.62) ως προς το $t_{i,new}$ προκύπτει η ακόλουθη αναδρομική σχέση:

$$t_{i,new} = \left(\frac{N_{active}}{\sum_{i=1}^{N_{active}} a_i}\right)\left(\frac{1}{\rho_i\, C_{\max}}\right)\left(\frac{\{u\}_i^T [K]_i \{u\}_i}{A_i}\right) \tag{3.63}$$

Μία άλλη μορφή της Εξ.(3.63), πιο βολική για προγραμματισμό, είναι η εξής:

$$t_{i,k+1} = \left(\frac{N_{active}}{\sum_{i=1}^{N_{active}} a_{i,k}}\right)\left(\frac{1}{\rho_i\, C_{\max}}\right)\left(\frac{\{u\}_{i,k}^T [K]_{i,k} \{u\}_{i,k}}{A_i}\right) \tag{3.64}$$

όπου με k δηλώνεται ο αύξων αριθμός επανάληψης. Βάσει της ανωτέρω αναλύσεως, προτείνεται η ακόλουθη διαδικασία βελτιστοποίησης:

Βήμα 1: Τυχαία επιλογή ομοιόμορφης κατανομής πάχους t_i.

Βήμα 2: Εκτίμηση των Δεικτών α_i χρησιμοποιώντας την Εξ.(3.59).

Βήμα 3: Εκτίμηση της μέσης τιμής $\overline{\alpha_i}$ χρησιμοποιώντας την Eq.(3.60).

Βήμα 4: Επανασχεδίαση της κατατομής του πάχους t_i χρησιμοποιώντας την Εξ.(3.64).

Βήμα 5: Έλεγχος σύγκλισης, με πιθανά κριτήρια σύγκλισης τα εξής:

Κριτήριο #1: η μέγιστη μεταβολή του πάχους στοιχείου μεταξύ δύο διαδοχικών επαναλήψεων είναι μικρότερη από μία προκαθορισμένη ποσότητα, δηλαδή $\max\left|t_i^k - t_i^{k+1}\right| \le tol_1$

Κριτήριο #2: ο Συντελεστής Μεταβλητότητας (Coefficient of Variation - %CV) για την κατανομή των Δεικτών α_i είναι μικρότερος από μία προκαθορισμένη ποσότητα, δηλαδή $\%CV\left(\overline{a_i}\right) \le tol_2$

Βήμα 6: Εάν δεν έχει επιτευχθεί σύγκλιση και δεν έχει ξεπερασθεί το προκαθορισμένο μέγιστο πλήθος επαναλήψεων, τότε επιστροφή στο Βήμα 2.

3.3.3. Συμπεράσματα

Η προηγηθείσα ανάλυση αφορά σε μία ενδελεχή θεωρητική διερεύνηση του προβλήματος βελτιστοποίησης κατασκευών υπό την επιβολή ενός περιορισμού ανάπαλσης και κατέληξε στην παρουσίαση μίας νέας διαδικασίας βελτιστοποίησης. Σε αντίθεση με την υπάρχουσα βιβλιογραφία, στην προτεινόμενη διαδικασία δεν επιβάλλεται περιορισμός στην ποσότητα ύλης που πρόκειται να χρησιμοποιηθεί. Διευκρινίζεται ότι η σχεδίαση υπό περιορισμό ανάπαλσης και η σχεδίαση υπό περιορισμό τάσεων είναι ισοδύναμες μόνον υπό συνθήκες (Bendsøe and Sigmund, 2003). Επειδή, δε, κανένας κανονισμός δεν επιβάλλει περιορισμό ανάπαλσης ως περιορισμό αντοχής ή περιορισμό λειτουργικότητας, το πρόβλημα βελτιστοποίησης κατασκευών υπό την επιβολή περιορισμού ανάπαλσης έχει, κατά κύριο λόγο, ακαδημαϊκό ενδιαφέρον.

Βιβλιογραφία

Achtziger W, Bendsøe M, Ben-Tal A, Zowe J (1992) Equivalent displacement based formulations for maximum strength truss topology design. Impact Comput Sci Eng 4:315–345

Allaire, G, Jouve F, Maillot H (2004) Topology optimization for minimum stress design with the homogenization method. Struct Multidisc Optim 28:87–98

Bendsøe, MP (1989) Optimal shape design as a material distribution problem. Struct Optim 1(4):193–202

Bendsøe, MP, Kikuchi N (1988) Generating optimal topologies in structure design using a homogenization method. Comput Methods Appl Mech Eng 71:197–224

Bendsøe, MP, Sigmund O (2003) Topology optimization: theory, methods and applications. Springer, Berlin.

Ben-Tal A, Bendsøe M (1993) A new method for optimal truss topology design. SIAM J Optim 3(2):322–358

Ben-Tal A, Nemirovski A (1994) Potential reduction polynomial time method for truss topology design. SIAM J Optim 4(3):596–612

Ben-Tal A, Nemirovski A (1995) Optimal design of engineering structures. OPTIMA Mathematical Programming Society Newsletter No. 47

Ben-Tal A, Nemirovski A (1997) Robust truss topology design via semidefinite programming. SIAM J Optim 7(4):991–1016

Ben-Tal A, Nemirovski A (2000) Handbook of semidefinite programming, chap Structural Design. Kluwer, pp 443–467

Berke L, Khot N.S., (1987), "Structural optimization using optimality criteria", in: Computer Aided Optimal Design: Structural and Mechanical Systems, edited by C.A. Mota Soares, NATO, ASI series, F27B.

Bruyneel, M, Duysinx P, Fleury C (2002) A family of MMA approximations for structural optimization. Struct Multidisc Optim 24:263–276

Burns, TE, Tortorelli DA (2003) An element removal and reintroduction strategy for the topology optimization of structures and compliant mechanisms. Int J Numer Methods Eng 57:1413–1430

Burns, TE (2005) A reevalution of the SIMP method with filtering and an alternative formulation for solid-void topology optimization. Struct Multidisc Optim 30(6):428–436

Das, R., Jones R., Xie Y. M., Design of structures for optimal static strength using ESO, Engineering Failure Analysis, Volume 12, Issue 1, February 2005, Pages 61-80

Duysinx, P, Sigmund O (1988) New developments in handling stress constraints in optimal material distribution. In: 7th AIAA/USAF/NASA/ISSMO symposium on multidisciplinary design optimization, American Institute of Aeronautics and Astronautics, Saint Louis, MI, USA, pp 1501–1509, September

Duysinx, P, Bendsøe M (1998) Topology optimization of continuum structures with local stress constraints. Int J Numer Methods Eng 43:1453–1478

Edwards, CS, Kim HA, Budd CJ (2007) An evaluative study on ESO and SIMP for optimizing a cantilever tie-beam. Struct Multidisc Optim (in press)

Fujii, D, Kikuchi N (2000) Improvement of numerical instabilities in topology optimization using the SLP method. Struct Multidisc Optim 19:113–121

Gallagher RH. Fully Stressed Design, In: R. H. Gallagher & O. C. Zienkiewicz (eds.), Optimum Structural Design: Theory and Applications. John Wiley & Sons:1973.

Haber, RB, Jog CS, Bendsøe MP (1996) A new approach to variable-topology shape design using a constraint on perimeter. Struct Optim 11:1–12

Haftka R T, Gurdal Z and Kamat M. Elements of Structural Optimization. Kluwer: 1990.

Kita E, Tanie H (1999) Topology and shape optimization of continuum structures using GA and BEM. Struct Multidisc Optim 17(2–3):130–139

Michell AGM (1904) The limit of economy of material in frame structures. Philos Mag 8:589-597

Morris, A.J. (1982), Foundations of Structural Optimization: A Unified Approach, John Wiley & Sons.

Nha Chu, D, Xie YM, Hira A, Steven GP (1996) Evolutionary structural optimization for problems with stiffness constraints. Finite Elem Anal Des 21:239–251

Nha Chu, D, Xie Y. M., Hira A., Steven G.P., (1997) On various aspects of evolutionary structural optimization for problems with stiffness constraints, Finite Elements in Analysis and Design, Volume 24, Issue 4, pp.197-212

Querin O. M., Steven G. P., Xie Y. M., (2000a), Evolutionary structural optimisation using an additive algorithm, Finite Elements in Analysis and Design, Volume 34, Issues 3-4, pp. 291-308

Querin O. M., Young V., Steven G. P., Xie Y. M., (2000b) Computational efficiency and validation of bi-directional evolutionary structural optimisation, Computer Methods in Applied Mechanics and Engineering, Volume 189, Issue 2, pp. 559-573

Ren G., Smith J.V., Tang J.W., Xie Y.M., Underground excavation shape optimization using an evolutionary procedure, Computers and Geotechnics, Volume 32, Issue 2, March 2005, Pages 122-132

Rong JH, Xie YM, Yang XY, Liang QQ, (2000), Topology optimization of structures under dynamic response constraints, Journal of Sound and Vibration, Volume 234, Issue 2, pp.177-189

Rozvany GIN. Stress ratio and compliance based methods in topology optimization – a critical review. Struct. Multidisc. Optim., 2001, 21:109-119.

Sigmund O (2001a) Design of multiphysics actuators using topology optimization—part I: one-material structures. Comput Methods Appl Mech Eng 190:6577–6604

Sigmund O (2001b) Design of multiphysics actuators using topology optimization—part II: two-material structures. Comput Methods Appl Mech Eng 190:6605–6627

Sigmund O (2001c) A 99 line topology optimization code written in Matlab. Struct Multidisc Optim 21:120–127

Steven G, Querin O, Xie M, (2000), Evolutionary structural optimisation (ESO) for combined topology and size optimisation of discrete structures, Computer Methods in Applied Mechanics and Engineering, Volume 188, Issue 4, IVth World Congress on Computational Mechanics. (II). Optimum, pp. 743-754

Stolpe M, Svanberg K (2001) An alternative interpolation scheme for minimum compliance topology optimization. Struct Multidisc Optim 22:116–124

Svanberg K (1987) The method of moving asymptotes—a new method for structural optimization. Int J Numer Methods Eng 24:359–373

Svanberg K, (1994) On the convexity and concavity of compliances. Struct Optim 7(1–2):42–46

Svanberg K (1995) A globally convergent version of MMA without linesearch. Proceedings of the First World Congress of Structural and Multidisciplinary Optimization (Goslar, Germany), pp 9–16

Tanskanen P (2002) The evolutionary structural optimization method: theoretical aspects. Comput Methods Appl Mech Eng 191:5485–5498

Wei Li, Qing Li, Grant P. Steven, Y.M. Xie, (2005), An evolutionary shape optimization for elastic contact problems subject to multiple load cases, Computer Methods in Applied Mechanics and Engineering, Volume 194, Issues 30-33, Structural and Design Optimization, pp. 3394-3415

Xie Y.M., Felicetti P., Tang J.W., Burry M.C. (2005), Form finding for complex structures using evolutionary structural optimization method, Design Studies, Volume 26, Issue 1, Pages 55-72

Xie YM, Steven GP (1993) A simple evolutionary procedure for structural optimization. Comput Struct 49:885–896

Xie, YM, Steven, G.P., (1996) Evolutionary structural optimization for dynamic problems, Computers & Structures, Volume 58, Issue 6, pp.1067-1073

Xie YM, Steven GP (1997) Evolutionary structural optimization. Springer, Berlin

Yang XY, Xie YM, Steven GP, Querin OM (1999) Bidirectional evolutionary method for stiffness optimization. AIAA J 37(11):1483–1488.

Yang XY, Xie YM, Steven G.P., (2005) Evolutionary methods for topology optimisation of continuous structures with design dependent loads, Computers & Structures, Volume 83, Issues 12-13pp.956-963.

Zhou M, Rozvany GIN (2001) On the validity of ESO type methods in topology optimization. Struct Multidisc Optim 21:80–83

Zuo KT, Chen LP, Zhang YQ, Yang JZ (2005) Manufacturing-and machining-based topology optimization. Int J Adv Manuf Technol 27(5–6):531–536

ΠΑΡΑΡΤΗΜΑ 3.Α: Έργο εξωτερικών δυνάμεων

Είναι δυνατόν να αποδειχθεί ότι ισχύει η ακόλουθη ισότητα:

$$\{u\}^T \left(\frac{t_i \partial \left([K] \right)}{\partial t_i} \right) \{u\} = \{u_i\}^T \left(\frac{t_i \partial \left([K_i] \right)}{\partial t_i} \right) \{u_i\} \tag{3.A1}$$

Είναι προφανές ότι κάθε μέλος της ανωτέρω ισότητας εκφράζει ένα βαθμωτό μέγεθος. Προκειμένου να δειχθεί ότι αυτά τα βαθμωτά μεγέθη είναι μεταξύ τους ίσα, εξετάζεται ένα 2Δ συνεχές σώμα, διακριτοποιημένο με ένα πλέγμα από NN κόμβους και NEL πεπερασμένα στοιχεία επίπεδης ελαστικότητας και σταθερού πάχους. Έστω $[K_i]$ το μητρώο δυσκαμψίας του $i-$στοιχείου, του οποίου το πάχος είναι t_i. Για λόγους πληρότητας, αναφέρεται ότι ισχύει:

$$[K_i] = \int_A t_i \mathbf{B}^T \mathbf{E} \mathbf{B} dA \tag{3.A2}$$

όπου **E** είναι το μητρώο ελαστικότητας και **B** είναι το μητρώο παραμορφώσεων-μετατοπίσεων. Η μερική παράγωγος του μητρώου $[K_i]$ ως προς το πάχος t_i ισούται με:

$$\frac{\partial}{\partial t_i} \left([K_i] \right) = \int_A \mathbf{B}^T \mathbf{E} \mathbf{B} dA \tag{3.A3}$$

Πολλαπλασιάζοντας την Εξ.(3.A3) με t_i, τότε, από την Εξ. (3.A2), προκύπτει:

$$t_i \frac{\partial}{\partial t_i} \left(K_i \right) = t_i \int_A \mathbf{B}^T \mathbf{E} \mathbf{B} dA = \int_A t_i \mathbf{B}^T \mathbf{E} \mathbf{B} dA = K_i \tag{3.A4}$$

Με άλλα λόγια, το γινόμενο του πάχους t_i επί τη μερική παράγωγο του $[K_i]$ ως προς το πάχος t_i ισούται με το μητρώο $[K_i]$. Συνεπώς, το δεξί μέλος της Εξ. (3.A1) γράφεται:

$$\{u_i\}^T \left(\frac{t_i \partial \left([K_i] \right)}{\partial t_i} \right) \{u_i\} = \{u_i\}^T [K_i] \{u_i\} \tag{3.A5}$$

Στο δεξί μέλος της Εξ. (3.A5) αναγνωρίζεται ότι:

$$[K_i] \{u_i\} = \{F_i\} \tag{3.A6}$$

Από τις Εξ.(3.A1, 3.A5 και 3. A6), προκύπτει το ακόλουθο συμπέρασμα:

Συμπέρασμα #1: Το δεξί μέλος της Εξ. (3.A1) ισούται αριθμητικά με το έργο των εξωτερικών δυνάμεων, οι οποίες ασκούνται στους κόμβους του $i-$στοιχείου.

Στην επίπεδη ελαστικότητα, κάθε κόμβος του πλέγματος διαθέτει δύο μεταφορικούς βαθμούς ελευθερίας, συνεπώς, συνολικά, εμπλέκονται $2NN \times 2NN$ βαθμοί ελευθερίας. Αυτό σημαίνει

ότι η διάσταση του μητρώου δυσκαμψίας $[K]$ της εξεταζομένης κατασκευής είναι $2NN \times 2NN$. Το πάχος t_i του $i-$στοιχείου εμφανίζεται σε εκείνες τις θέσεις του μητρώου $[K]$, οι οποίες αντιστοιχούν στους βαθμούς ελευθερίας του μητρώου $[K_i]$. Συνεπώς, η μερική παράγωγος του μητρώου $[K]$ ως προς το πάχος t_i θα ισούται με έναν πίνακα διαστάσεων $2NN \times 2NN$, του οποίου όλα τα στοιχεία θα είναι μηδενικά πλην εκείνων, τα οποία αντιστοιχούν στους βαθμούς ελευθερίας του μητρώου $[K_i]$. Αυτά τα μη-μηδενικά στοιχεία προέρχονται από την παραγώγιση του μητρώου $[K_i]$ ως προς το πάχος t_i (βλ. Εξ.(3.A3)). Πολλαπλασιάζοντας τον πίνακα $\frac{\partial([K])}{\partial t_i}$ διαστάσεων $2NN \times 2NN$ επί το βαθμωτό μέγεθος t_i προκύπτει ο πίνακας $\frac{t_i \partial([K])}{\partial t_i}$, για τον οποίο ισχύουν τα ακόλουθα:

- Η διάσταση του πίνακα είναι $2NN \times 2NN$ και τα μη-μηδενικά στοιχεία του είναι τα στοιχεία του μητρώου $[K_i]$, τοποθετημένα κατάλληλα στις αντίστοιχες θέσεις.
- Ο πίνακας είναι αριθμητικά ίσος με το μητρώο δυσκαμψίας ολόκληρης της κατασκευής, εάν το εν λόγω μητρώο περιέχει πληροφορία μόνον από το μητρώο δυσκαμψίας $[K_i]$ του $i-$στοιχείου.
- Ο πίνακας ισούται με το μητρώο δυσκαμψίας $[K_i]$, όταν αυτό προσαυξάνεται με μηδενικά στοιχεία έτσι ώστε να αποκτήσει τις διαστάσεις του μητρώου δυσκαμψίας ολόκληρης της κατασκευής.
- Από ποιοτικής απόψεως, ο πίνακας εκφράζει τη δυσκαμψία μόνον του $i-$στοιχείου.

Το διάνυσμα $\{u\}$ περιέχει τις κομβικές μετατοπίσεις της εκάστοτε εξεταζομένης κατασκευής και η διάστασή του είναι $2NN \times 1$. Όταν το διάνυσμα $\{u\}$ πολλαπλασιάζεται από αριστερά επί $\left(\frac{t_i \partial([K])}{\partial t_i}\right)$, όρος ο οποίος εκφράζει τη δυσκαμψία του $i-$στοιχείου, τότε το προκύπτον γινόμενο εκφράζει τις εξωτερικές δυνάμεις, οι οποίες ασκούνται στο $i-$στοιχείο. Περαιτέρω εξ αριστερών πολλαπλασιασμός επί $\{u\}^T$ δίδει το έργο των δυνάμεων αυτών. Συνεπώς, προκύπτει το ακόλουθο συμπέρασμα:

Συμπέρασμα #2: Το αριστερό μέλος της Εξ. (3.A1) ισούται αριθμητικά με το έργο των εξωτερικών δυνάμεων, οι οποίες ασκούνται στους κόμβους του $i-$στοιχείου.

Από το Συμπέρασμα #1 και το Συμπέρασμα #2, προκύπτει ότι η Εξ. (3.A1) είναι αληθής, διότι τα δύο μέλη της είναι αριθμητικά ίσα μεταξύ τους και εκφράζουν το ίδιο βαθμωτό μέγεθος (έργο εξωτερικών δυνάμεων, ασκουμένων στους κόμβους του $i-$στοιχείου).

ΠΑΡΑΡΤΗΜΑ 3.Β: Μη-ισοδυναμία μεταξύ περιορισμού μετατόπισης και περιορισμού ανάπαλσης

Η επιβολή ενός περιορισμού ανάπαλσης δεν είναι πάντοτε ισοδύναμος με την επιβολή ενός περιορισμού μετατόπισης. Ο λόγος έγκειται στο γεγονός ότι στον περιορισμό ανάπαλσης συμμετέχουν μόνον οι, φέροντες εξωτερικό φορτίο, κόμβοι, οι οποίοι δεν είναι απαραίτητο να εμφανίζουν το μέγιστο βέλος κάμψης. Ως ένα τέτοιο τυπικό παράδειγμα, εξετάζεται μία οριζόντια αμφιέρειστη δοκός υπό την επιβολή ενός σημειακού κατακορύφου φορτίου. Σε αυτήν την περίπτωση, είναι σαφές ότι το έργο του εξωτερικού φορτίου ισούται με:

$$\{u\}^T \{F\} = u_i F_i \tag{3.B1}$$

ενώ ο περιορισμός ανάπαλσης είναι δυνατόν να γραφεί ως:

$$\{u\}^T \{F\} \le C_{\max} \tag{3.B2}$$

όπου $C_{\max}$ είναι ένα άνω όριο σχετικά με το έργο που παράγουν τα εξωτερικά φορτία. Ο συνδυασμός των Εξ.(3.B1, 3.B2) δίδει:

$$u_i F_i \le C_{\max} \Rightarrow u_i \le \left(\frac{C_{\max}}{F_i} \right) \tag{3.B3}$$

οπότε η μέγιστη μετατόπιση του φορτιζομένου κόμβου ισούται με:

$$u_{i,\max} = \left(\frac{C_{\max}}{F_i} \right) \tag{3.B4}$$

Από Εγχειρίδια Μηχανικής (π.χ. Stahl im Hochbau, s.1110), βρίσκεται ότι για μία οριζόντια αμφιέρειστη δοκό υπό την επιβολή ενός κατακορύφου φορτίου F_i, το μέγιστο βέλος κάμψης εμφανίζεται στο σημείο εφαρμογής της ασκουμένου φορτίου όταν και μόνον όταν το εν λόγω σημείο βρίσκεται στο μέσο του ανοίγματος της δοκού, οπότε και ισχύει:

$$y_{\max} = u_{i,\max} \tag{3.B5}$$

Ωστόσο, σε κάθε άλλη περίπτωση, το μέγιστο βέλος κάμψης εμφανίζεται σε μία θέση διαφορετική από εκείνην της επιβολής του φορτίου και ισχύει:

$$y_{\max} > u_{i,\max} \tag{3.B6}$$

Από την Εξ. (3.B6) προκύπτει ότι η επιβολή του περιορισμού ανάπαλσης οδηγεί σε διαφορετικά αποτελέσματα από εκείνα στα οποία καταλήγει η επιβολή του περιορισμού μετατόπισης, διότι ο περιορισμός ανάπαλσης επιτρέπει μεγαλύτερο βέλος κάμψης. Συνεπώς, το πρόβλημα ελαχιστοποίησης του βάρους μίας κατασκευής υπό την επιβολή περιορισμού μετατόπισης και το πρόβλημα ελαχιστοποίησης του βάρους μίας κατασκευής υπό την επιβολή περιορισμού ανάπαλσης είναι δύο διαφορετικά προβλήματα, τα οποία συμπίπτουν μόνον υπό συνθήκες.

Αυτή η σελίδα είναι σκοπίμως κενή

ΚΕΦΑΛΑΙΟ 4
(ΠΕΡΙΛΗΨΗ)

ΒΕΛΤΙΣΤΗ ΣΧΕΔΙΑΣΗ
ΥΠΟ ΤΗΝ ΕΠΙΒΟΛΗ ΠΕΡΙΟΡΙΣΜΩΝ ΤΑΣΗΣ

Σε αυτήν την περίληψη κεφαλαίου, εξετάσθηκε το πρόβλημα βελτιστοποίησης υπό την επιβολή περιορισμών τάσης. Πρώτα διερευνήθηκε η εφαρμογή της γνωστής μεθόδου Fully Stressed Design (FSD) σε 2Δ σκελετικές κατασκευές. Στη συνέχεια διερευνήθηκε η εφαρμογή της εν λόγω τεχνικής στη βελτιστοποίηση 2Δ κατασκευών συνεχούς μέσου, στη βελτιστοποίηση 2Δ πλακών καθώς και στη βελτιστοποίηση 3Δ κατασκευών συνεχούς μέσου. Για κάθε ένα από τα ανωτέρω προβλήματα, προτάθηκε μία νέα διαδικασία βελτιστοποίησης. Τέλος, επιλύθηκε θεωρητικά, με τη μέθοδο πολλαπλασιαστών Lagrange, το πρόβλημα της βελτιστοποίησης σκελετικών κατασκευών υπό την επιβολή ενός γενικευμένου περιορισμού τάσης.

4.1. Εισαγωγή

Το πρόβλημα βελτιστοποίησης κατασκευών υπό περιορισμό τάσεων είναι εξαιρετικά σημαντικό, διότι οι εν λόγω περιορισμοί αφορούν στην κατάσταση αστοχίας μίας κατασκευής. Συνεπώς, αιτιολογείται μια ενδελεχής μελέτη αυτού του προβλήματος.

Στο παρόν κεφάλαιο, διερευνήθηκε η δυνατότητα χρήσης της σχεδίασης πλήρους έντασης (Fully Stressed Design-FSD) στην αναζήτηση βελτίστων κατανομών υλικού σε 2Δ κατασκευές. Προς τούτο, εξετάστηκαν δύο προσεγγίσεις, θεωρώντας την κατασκευή ως συναρμολόγημα ακεραίου πολλαπλασίου πρώτα μίας βασικής μονάδος συνεχούς μέσου και έπειτα μίας βασικής μονάδος διακριτού μέσου. Και στις δύο προσεγγίσεις, η επανασχεδίαση στηρίχθηκε στη μεταβολή του πάχους, ή του εμβαδού αντίστοιχα, της εκάστοτε βασικής μονάδος. Στη συνέχεια, εξετάσθηκε η αναζήτηση της βέλτιστης σχεδίασης για διαφορετικές τοπολογίες. Από τη διεξαχθείσα διερεύνηση προέκυψε ένα νέο ιεραρχικό σχήμα βελτιστοποίησης δύο βημάτων: στο πρώτο βήμα ορίζεται μία τοπολογία και στο δεύτερο βήμα επιδιώκεται η διαστασιολόγησή της με τέτοιον τρόπο, ώστε να επιδιώκεται η πλήρης ένταση αυτής. Για την αξιολόγηση της προτεινομένης διαδικασίας, χρησιμοποιήθηκαν τέσσερα τυπικά βιβλιογραφικά παραδείγματα βελτιστοποίησης, τα οποία επελύθησαν την ισχυρή μαθηματική μεθοδολογία SQP (Sequential Quadratic Programming). Προέκυψε ότι η προτεινόμενη διαδικασία βελτιστοποίησης καταλήγει στα ίδια βέλτιστα βάρη αλλά απαιτεί πολύ λιγότερο υπολογιστικό χρόνο.

Στη συνέχεια, εξετάστηκε η ιδέα της χρήσης πεπερασμένων στοιχείων μεταβλητού πάχους στην επίλυση του προβλήματος της ελαχιστοποίησης του βάρους μίας κατασκευής υπό περιορισμό τάσεων. Για την ενδοστοιχειακή παρεμβολή του πάχους, χρησιμοποιήθηκαν οι συναρτήσεις παρεμβολής του στοιχείου (ισοπαραμετρική παρεμβολή πάχους). Με τον τρόπο αυτό, οι κόμβοι του πλέγματος μετατρέπονται σε σημεία ελέγχου, τα οποία δύνανται να μετακινηθούν κάθετα ως προς τη μεσοεπιφάνεια των στοιχείων, διαμορφώνοντας, με αυτόν τον τρόπο, μία συνεχή επιφάνεια. Για την αξιολόγηση της προτεινομένης διαδικασίας, εξετάσθηκαν τέσσερα τυπικά βιβλιογραφικά παραδείγματα. Συγκρίνοντας την προτεινόμενη διαδικασία με την αντίστοιχη, στην οποία χρησιμοποιούνται πεπερασμένα στοιχεία σταθερού πάχους, προέκυψε ότι η προτεινόμενη επανασχεδίαση του πάχους σε επίπεδο κόμβου, και όχι σε επίπεδο στοιχείου, είναι δυνατόν να καταλήξει σε ελαφρύτερες σχεδιάσεις.

Κατόπιν, μελετήθηκε το πρόβλημα της ελαχιστοποίησης του βάρους πλακών υπό τον περιορισμό τάσεων. Προς τούτο, διερευνήθηκαν οι διαφορές μεταξύ της μεταβολής της κατανομής του πάχους μίας πλάκας (προσέγγιση με τη μέθοδο FSD) και της ολικής αποβολής υλικού από έναν διακριτοποιημένο χώρο σχεδίασης (προσέγγιση με τη Evolutionary Structural Optimization - ESO). Σε αυτήν την περίπτωση, εξετάσθηκαν συνολικά οκτώ διαφορετικές περιπτώσεις (τέσσερα παραδείγματα με παραλλαγές). Προέκυψε ότι οι δύο προσεγγίσεις, αν και συλλογιστικά παρόμοιες ως προς την τελική μορφή του τασικού πεδίου, καταλήγουν σε σημαντικά διαφορετικές σχεδιάσεις.

Επίσης, διερευνήθηκε το πρόβλημα της ελαχιστοποίησης του βάρους μίας 3Δ κατασκευής υπό περιορισμό τάσεων. Ειδικότερα, διατυπώθηκε μία νέα διαδικασία βελτιστοποίησης, η επανασχεδίαση της οποίας στηρίζεται σε ένα νέο κριτήριο μέσης πυκνότητας ενέργειας παραμόρφωσης. Για την αξιολόγηση της προτεινομένης διαδικασίας, πραγματοποιήθηκε σύγκριση με μία βιβλιογραφική μεθοδολογία, η οποία στηρίζεται σε κριτήριο τασικού πεδίου κατά von Mises, και επί τεσσάρων τυπικών βιβλιογραφικών παραδειγμάτων. Προέκυψε ότι η προτεινόμενη διαδικασία βελτιστοποίησης κατέληξε σε ελαφρύτερες σχεδιάσεις.

Τέλος, εξετάστηκε το πρόβλημα της ελαχιστοποίησης του βάρους μίας σκελετικής κατασκευής υπό την επιβολή ενός γενικευμένου περιορισμού τάσης. Αναλυτικότερα, σε μία κατασκευή, ανεξαρτήτως του πλήθους των επιβαλλομένων περιορισμών τάσεων, θεωρείται ότι στη βέλτιστη σχεδίαση μόνον ένας περιορισμός είναι ενεργός, χωρίς, ωστόσο, να είναι εκ των προτέρων γνωστό σε ποιο στοιχείο της κατασκευής ενεργοποιείται αυτός ο περιορισμός.

Με βάση τη μέθοδο πολλαπλασιαστών Lagrange, διατυπώθηκε μια θεωρητική λύση, η οποία καταλήγει στη διαμόρφωση τόσο ενός νέου Βελτίστου Κριτηρίου όσο και μίας νέας αναδρομικής σχέσης επανασχεδίασης. Διευκρινίζεται ότι η εν λόγω προσέγγιση είναι διαφορετική από εκείνη της σχεδίασης Fully Stressed Design, διότι η πρώτη προσέγγιση επιβάλλει την ενεργοποίηση ενός περιορισμού τάσης, ενώ η δεύτερη επιδιώκει όλα τα δομικά στοιχεία να λάβουν τη μέγιστη επιτρεπόμενη τάση στη βέλτιστη σχεδίαση.

4.2. Σκελετικές κατασκευές υπό περιορισμό τάσης

4.2.1. Θεωρητικό υπόβαθρο

Μία κατασκευή αποτελεί το συναρμολόγημα πολλών επί μέρους δομικών μονάδων. Στην απλούστερη περίπτωση, μία κατασκευή προέρχεται από την επανάληψη μίας βασικής μονάδας. Στην περίπτωση ενός 2Δ σώματος συνεχούς μέσου, ένα τετραπλευρικό στοιχείο είναι δυνατόν να θεωρηθεί ως μία τέτοια βασική μονάδα, έστω Basic Continuum Unit (BCU). Εισάγοντας ανισοτροπία υλικού, η μονάδα (BCU) είναι δυνατόν να εμφανίσει διαφορετική συμπεριφορά κατά μήκος διαφορετικών διευθύνσεων. Ένας άλλος αριθμητικός τρόπος εισαγωγής ανισοτροπίας είναι η μεταβολή του λόγου πλευρών της μονάδος, η οποία επηρεάζει σαφώς το μητρώο δυσκαμψίας της μονάδος (βλ. Παράρτημα 4Α). Στην περίπτωση των διακριτών (σκελετικών) σωμάτων, ισχύουν αντίστοιχες προσεγγίσεις. Ειδικότερα, όπως φαίνεται στο Σχήμα 4.1, η δομική μονάδα Basic Continuum Unit είναι δυνατόν να αντικατασταθεί με ένα σχηματισμό 6 ράβδων (Basic Discrete Unit – BDU). Και σε αυτήν την περίπτωση, είναι δυνατή η εμφάνιση μίας ανισοτροπικής συμπεριφοράς μεταβάλλοντας τις διαστάσεις της μονάδας BDU (βλ. Παράρτημα 4Α). Σε αυτήν την περίπτωση, μία μεταβολή στις εξωτερικές διαστάσεις της μονάδας προκαλεί μεταβολή του προσανατολισμού των διαγωνίων στοιχείων της, κάτι το οποίο επηρεάζει σημαντικά τη δυσκαμψία της μονάδας. Η αντικατάσταση της μονάδος BCU από μία μονάδα BDU είναι ποιοτική και όχι ποσοτική, διότι το μητρώο δυσκαμψίας των δύο μονάδων είναι της αυτής διάστασης αλλά διαφορετικό.

(a) (b)

Σχήμα 4.1: Βασικές μονάδες μοντελοποίησης (a)συνεχές μέσο (Basic Continuum Unit - BCU) και (b) σκελετική κατασκευή (Basic Discrete Unit - BDU)

4.2.2. Αριθμητικά παραδείγματα

Εξετάστηκαν τέσσερα τυπικά βιβλιογραφικά παραδείγματα (Σχήμα 4.2): ο βαθύς πρόβολος, ο κοντός πρόβολος, η δοκός MBB και η δοκός σχήματος L (δοκός L). Για κάθε παράδειγμα, αναπτύχθηκαν δύο προσεγγίσεις, μία με διγραμμικά πεπερασμένα στοιχεία (προσέγγιση συνεχούς μέσου) και μία με στοιχεία ράβδου (προσέγγιση διακριτού μέσου), δηλαδή οκτώ διαφορετικά μοντέλα. Η μορφή της βασικής μονάδας πλέγματος του συνεχούς μέσου ήταν ένα ορθογωνικό χωρίο διαστάσεων $(2a \times 2b)$, ενώ η αντίστοιχη μονάδα για το διακριτό μέσο σχηματίστηκε τοποθετώντας στοιχεία ράβδου στην περίμετρο του εν λόγω χωρίου και εισάγοντας διαγώνια στοιχεία. Κάθε πλέγμα αποτελείτο από ακέραιο πλήθος βασικών δομικών μονάδων. Βασική παράμετρος σχεδίασης ήταν ο λόγος πλευρών $\lambda = (a/b)$ του εκάστοτε πλέγματος. Ως πεδίο ορισμού του λόγου λ ορίστηκε το σύνολο $\lambda \in \{1/4, 1/3, 1/2, 1, 2, 3, 4\}$. Για κάθε μία τιμή του λόγου λ, εξετάστηκαν τρεις διαφορετικές

πυκνότητες πλέγματος ($7 \times 3 = 21$ αναλύσεις). Για τις σκελετικές κατασκευές, η μελέτη των διαφορετικών τιμών του λόγου λ αποσκοπούσε στη εξέταση της επίδρασης, επί της βέλτιστης σχεδίασης, του προσανατολισμού των διαγωνίων ράβδων, ενώ τα πλέγματα διαφορετικής πυκνότητας εξυπηρετούσαν στην εξασφάλιση ανεξαρτησίας πλέγματος. Για τα διγραμμικά μοντέλα, τόσο οι διαφορετικές τιμές του λόγου λ όσο και οι διαφορετικές πυκνότητες πλέγματος εξυπηρετούσαν στην διερεύνηση της ανεξαρτησίας των αποτελεσμάτων από το πλέγμα. Συνολικά, εξετάστηκε ένας χώρος λύσεων με $21 \times 8 = 168$ σχεδιάσεις πρώτα χρησιμοποιώντας την τεχνική 'stress-ratio' και μετά χρησιμοποιώντας την Μέθοδο SQP (Sequential Quadratic Programming), όπως αυτή βρίσκεται στη MatLab.

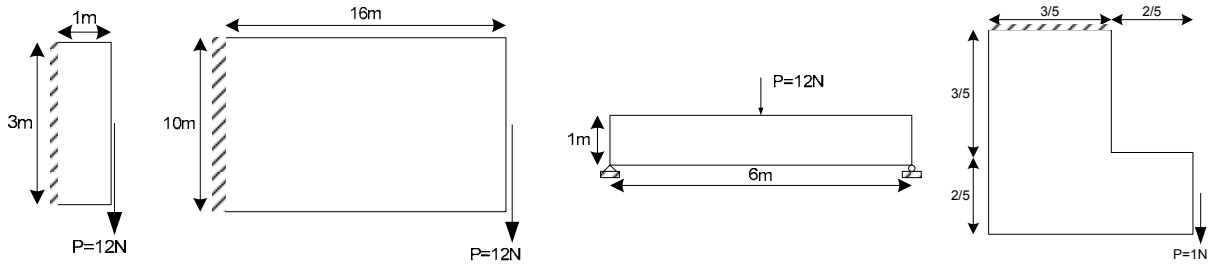

(a) (b) (c) (d)

Σχήμα 4.2: Γεωμετρία και φόρτιση εξετασθέντων παραδειγμάτων (a) βαθύς πρόβολος, (b) κοντός πρόβολος, (c) δοκός MBB και (d) δοκός L

Σε όλες τις περιπτώσεις, αποδίδεται μοναδιαία πυκνότητα, λόγος Poisson $\nu = 0.3$, μέτρο ελαστικότητας $E = 1MPa$ και μοναδιαίο αρχικό πάχος (στην περίπτωση των σκελετικών κατασκευών, μοναδιαίο αρχικό εμβαδόν διατομής). Η επιτρεπόμενη τάση ορίσθηκε ίση προς $\sigma_{\max} = 30MPa$ (von Mises τάση για τις προσεγγίσεις συνεχούς μέσου, αξονική τάση μελών για τις προσεγγίσεις σκελετικής κατασκευής). Στον Πίνακα 4.1 φαίνονται οι όγκοι των βελτίστων σχεδιάσεων για τις προσεγγίσεις του συνεχούς μέσου.

Πίνακας 4.1: Βέλτιστα αποτελέσματα (προσέγγιση συνεχούς μέσου)

	Βαθύς πρόβολος	Κοντός πρόβολος	Δοκός MBB	Δοκός L
Aspect ratio [Hor:Ver]	1:1	1:2	1:1	1:2
Initial volume [m^3]	3.0	160.0	6.0	0.64
Final volume FSD [m^3]	0.7863	19.24	1.3814	0.2096
Final volume SQP [m^3]	0.7863	19.24	1.3814	0.2096
V_{final}/V_o [%]	26.21%	12.02%	23.02%	32.75%

Στον Πίνακα 4.2 φαίνονται οι όγκοι των βελτίστων σχεδιάσεων για τη σκελετική προσέγγιση.

Πίνακας 4.2: Βέλτιστα αποτελέσματα (προσέγγιση σκελετικής κατασκευής)

	Βαθύς πρόβολος	Κοντός πρόβολος	Δοκός MBB	Δοκός L
Aspect ratio [Hor:Ver]	1:1	1:2	1:1	1:2
Initial volume [m^3]	3.0	160.0	6.0	0.64
Final volume FSD [m^3]	0.800	22.010	1.500	0.223
Final volume SQP [m^3]	0.800	22.010	1.500	0.223
V_{final}/V_o [%]	26.67%	13.75%	25.00%	34.84%

Οι βέλτιστες κατανομές υλικού, τόσο για την προσέγγιση συνεχούς μέσου όσο και για την προσέγγιση διακριτού μέσου, απεικονίζονται στο Σχήμα 4.3.

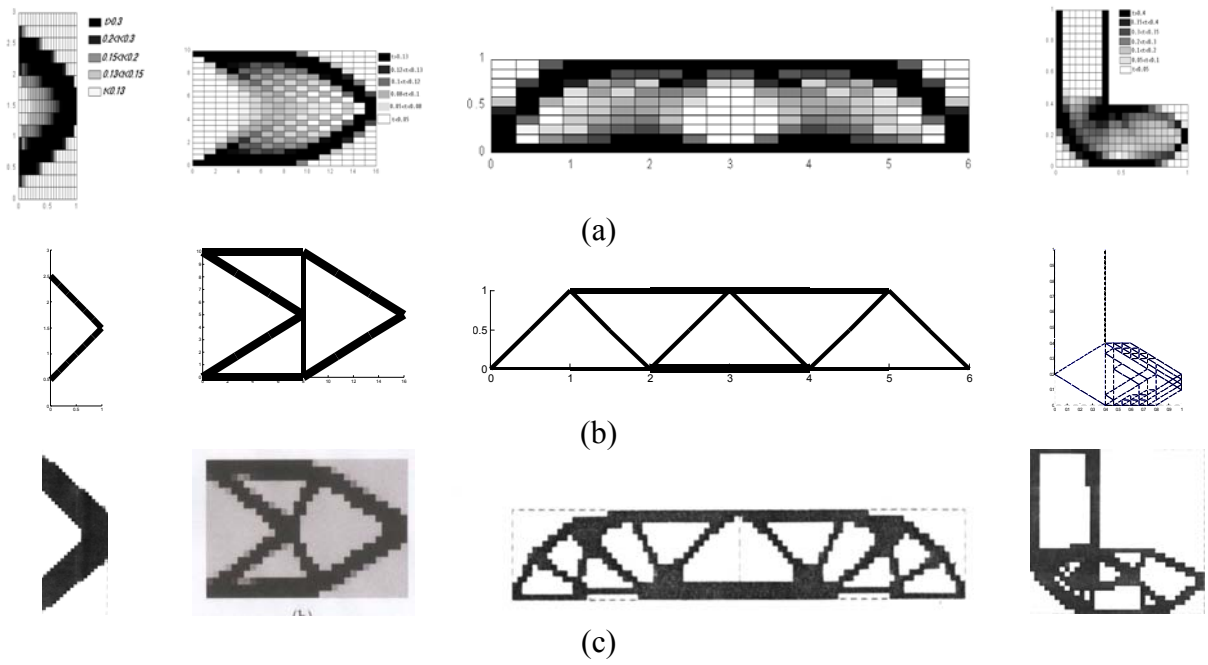

Βαθύς πρόβολος	Κοντός πρόβολος	Δοκός MBB	Δοκός L

Σχήμα 4.3:Σχεδιάσεις Πλήρους Έντασης (Fully Stressed Designs): (a) προσέγγιση συνεχούς μέσου, (b) προσέγγιση σκελετικής κατασκευής και (c) βιβλιογραφική αναφορά (Duysinx και Bendsøe, 1998)

4.2.3. Ιεραρχική διαδικασία βελτιστοποίησης

Με βάση τη διερεύνηση, η οποία παρουσιάστηκε στην προηγούμενη ενότητα, προκύπτει ότι είναι δυνατή η διατύπωση μίας νέας διαδικασίας, ιεραρχικής μορφής και δύο βημάτων. Στο πρώτο βήμα, επιλέγεται μία τοπολογία και στο δεύτερο βήμα αναζητείται η ελαχιστοποίηση του βάρους της. Η τοπολογία είναι δυνατόν να ορισθεί ως ο λόγος πλευρών του πλέγματος $\lambda = (a/b)$. Ισοδύναμα, η τοπολογία είναι δυνατόν να περιγραφεί και ως $\lambda = (1/b)$, όπου ο παρονομαστής b λαμβάνει οποιαδήποτε θετική τιμή. Συνεπώς, το πρόβλημα βελτιστοποίησης διατυπώνεται ως η αναζήτηση εκείνης της τιμής b, για την οποία η βελτιστοποίηση πλήρους έντασης καταλήγει στο ελάχιστο βάρος. Δεδομένου ότι η μεταβλητή b είναι μία παράμετρος, το αντίστοιχο πρόβλημα βελτιστοποίησης είναι μονοδιάστατο, συνεπώς, είναι δυνατόν για την επίλυσή του να χρησιμοποιηθεί οποιοδήποτε σχήμα αναζήτησης γραμμής. Η προτεινόμενη διαδικασία είναι η ακόλουθη:

Βήμα 1: Επιλογή αρχικής τοπολογίας με μεγάλη τιμή της παραμέτρου b
Βήμα 2: Για την τοπολογία του Βήματος 1, ελαχιστοποίηση βάρους με τη διαδικασία FSD
Βήμα 3: Απόδοση νέας τιμής για την παράμετρο b βάσει ενός (οποιουδήποτε) σχήματος αναζήτησης γραμμής.
Βήμα 4: Έλεγχος σύγκλισης. Εάν το βάρος μεταξύ δύο διαδοχικών τιμών της παραμέτρου b είναι μικρότερο από μία μικρή, προκαθορισμένη τιμή τότε η διαδικασία τερματίζεται.

Βήμα 5: Εάν έχει ξεπερασθεί το μέγιστο προβλεπόμενο πλήθος επαναλήψεων, τότε η διαδικασία διακόπτεται.

Βήμα 6: Επιστροφή στο Βήμα 2.

Η προτεινόμενη διαδικασία εφαρμόσθηκε στα παραδείγματα του Σχήματος 4.3 και τα αποτελέσματα παρουσιάζονται στον Πίνακα 4.3. Πιο συγκεκριμένα, η πρώτη γραμμή του Πίνακα 4.3 αφορά στη μείωση, η οποία σχετίζεται με την προσέγγιση διακριτού μέσου, ενώ η δεύτερη γραμμή του εν λόγω πίνακα αφορά στην προσέγγιση συνεχούς μέσου. Η σύγκριση μεταξύ των δύο προσεγγίσεων καταγράφεται στην τρίτη γραμμή του Πίνακα 4.3.

Πίνακας 4.3: Μειώσεις όγκου υλικού για τις βέλτιστες σχεδιάσεις.

	Βαθύς πρόβολος	Κοντός πρόβολος	Δοκός MBB	Δοκός L
1-(V_{final}/V_o) [%] (Skeletal)	73.33%	86.25%	75.00%	65.16%
1-(V_{final}/V_o) [%] (Bilinear)	73.79%	87.98%	76.98%	67.25%
(Skeletal-Bilinear)	-0.46%	-1.73%	-1.98%	-2.09%

Στο Σχήμα 4.4, αποτυπώνεται, σε μορφή διαγράμματος, η ποσότητα του υλικού στη βέλτιστη σχεδίαση συναρτήσει του λόγου πλευρών λ (βλ. Ενότητα 4.2.2). Χαρακτηριστική είναι η διαφορά μεταξύ της καμπύλης, η οποία αντιστοιχεί στην προσέγγιση του συνεχούς μέσου, και αυτής, η οποία αντιστοιχεί στην προσέγγιση του διακριτού μέσου.

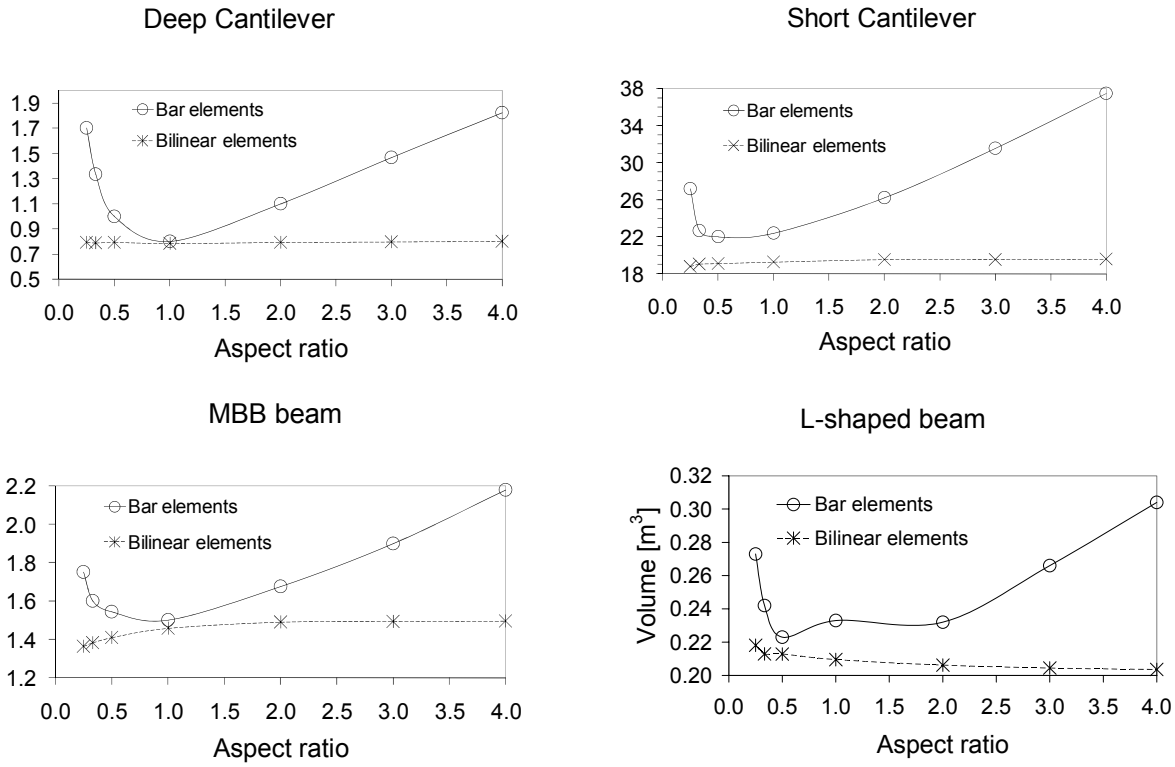

Σχήμα 4.4: Βέλτιστος όγκος υλικού συναρτήσει του λόγου πλευρών του πλέγματος

Στον Πίνακα 4.4 παρουσιάζονται τα βέλτιστα αποτελέσματα, τα οποία ελήφθησαν με την προτεινόμενη διαδικασία με τη μέθοδο SQP.

Πίνακας 4.4: Σύγκριση αποτελεσμάτων μεταξύ προτεινόμενης διαδικασίας και SQP (σκελετικές κατασκευές)

	Προτεινόμενη διαδικασία		**SQP**		
Παράδειγμα	Βέλτιστος όγκος	Χρόνος t_1	Βέλτιστος όγκος	Χρόνος t_2	t_1 / t_2
#1	0.8004	0.99	0.8003	58.500	59
#2	21.3633	2.25	21.3613	120.010	53
#3	1.5000	2.86	1.5002	225.420	78
#4	0.2235	4.22	0.2235	1235.100	292

4.2.4. Συμπεράσματα

Με βάση τα αποτελέσματα της προηγούμενης ενότητας σχετικά με τα εξετασθέντα παραδείγματα, προκύπτουν τα ακόλουθα συμπεράσματα:

- Οι βέλτιστες σχεδιάσεις, οι οποίες προέκυψαν από τις προσεγγίσεις FSD και SQP, ήταν ίδιες Αντιθέτως, το υπολογιστικό κόστος στην περίπτωση βελτιστοποίησης χρησιμοποιώντας την FSD ήταν σημαντικά μικρότερο.
- Ο βέλτιστος όγκος, ισοδύναμα το βέλτιστο βάρος, ήταν ελαφρώς μεγαλύτερο στην περίπτωση του συνεχούς μέσου.
- Ο προσανατολισμός των μελών μίας σκελετικής κατασκευής είναι πρωτευούσης σημασίας στη διαμόρφωση της βέλτιστης σχεδίασης, διότι, εξ αιτίας αυτού, είναι δυνατός ο εγκλωβισμός σε τοπικό ακρότατο.
- Δεδομένου ότι το βέλτιστο βάρος, το οποίο προκύπτει χρησιμοποιώντας σκελετική προσέγγιση ή προσέγγιση συνεχούς μέσου, δεν είναι σημαντικά διαφορετικό, το κριτήριο για την επιλογή της ανέγερσης μίας κατασκευής χρησιμοποιώντας είτε ραβδόμορφα στοιχεία είτε πλακοειδή στοιχεία, σχετίζεται με την ευκολία και το κόστος χρήσεως των εν λόγω στοιχείων.

Συμπερασματικά, για πρακτικές εφαρμογές μηχανικού, προκύπτει ότι η χρήση της μεθόδου FSD, είτε επί σκελετικής κατασκευής είτε επί κατασκευής συνεχούς μέσου, αποτελεί μία καλή επιλογή αναζήτησης του ελαχίστου βάρους.

4.3. Περιορισμός τάσης σε 2Δ συνεχή μέσα και πεπερασμένα στοιχεία μεταβλητού πάχους

4.3.1. Γενικά

Σε αυτήν την ενότητα εξετάζεται η σύζευξη της τεχνικής ‘stress-ratio’, η οποία αποτελεί το απλούστερο σχήμα βελτιστοποίησης κατασκευών υπό περιορισμό τάσεων, με πεπερασμένα στοιχεία, το πάχος των οποίων είναι δυνατόν να μεταβληθεί εντός του στοιχείου. Ειδικότερα, χρησιμοποιείται το 3-κομβικό τριγωνικό πεπερασμένο στοιχείο και για την παρεμβολή του πάχους χρησιμοποιούνται οι συναρτήσεις μορφής του στοιχείου. Η βασική ιδέα την εν λόγω προσέγγισης είναι η μετατροπή των κόμβων του πλέγματος σε σημεία ελέγχου της επιφανείας, η οποία καθορίζει την κατανομή του υλικού. Με τον τρόπο αυτό, είναι δυνατόν να ληφθούν συνεχείς, άρα εύκολα κατασκευάσιμες, επιφάνειες. Ταυτόχρονα, επιδιώκεται η μείωση του υπολογιστικού κόστους, διότι ο έλεγχος της κίνησης των κόμβων (κατακόρυφη κίνηση ως προς τη μεσοεπιφάνεια των στοιχείων) επιτυγχάνεται μέσα από μία απλή διαδικασία μηδενικής τάξεως.

4.3.2. Θεωρητική προσέγγιση

Η προτεινόμενη διαδικασία στηρίζεται σε δύο θεωρητικά στοιχεία. Το πρώτο στοιχείο είναι η βιβλιογραφική τεχνική επανασχεδίασης ‘stress-ratio’ και το δεύτερο στοιχείο είναι τα

πεπερασμένα στοιχεία μεταβλητού πάχους. Στο παρόν κεφάλαιο, χρησιμοποιούνται δύο τύποι τέτοιων στοιχείων επίπεδης ελαστικότητας: το 3-κομβικό τριγωνικό πεπερασμένο στοιχείο και το 4-κομβικό τετραπλευρικό πεπερασμένο στοιχείο. Η ιδέα της παρεμβολής του πάχους ενός στοιχείου εντός του στοιχείου είναι εφαρμόσιμη σε κάθε τύπο πεπερασμένου στοιχείου, είτε της οικογένειας Lagrange είτε της οικογένειας Serendipity. Στις επόμενες παραγράφους, ακολουθεί συνοπτική περιγραφή των προαναφερομένων θεωρητικών στοιχείων.

4.3.3. Η τεχνική επανασχεδίασης stress-ratio

Σύμφωνα με τη μέθοδο πολλαπλασιαστών Lagrange, η συνάρτηση Lagrange, στην περίπτωση αναζήτησης ελαχίστου βάρους ενός δικτυώματος υπό περιορισμούς τάσεων μόνον, έστω περιορισμοί g_i, είναι:

$$\mathcal{L}\left(x,\lambda\right) = W + \sum_{i=1}^{NEL} \lambda_i g_i \tag{4.1}$$

όπου W είναι το βάρος της κατασκευής, x_i είναι η διατομή της i-ράβδου, λ_i είναι ο πολλαπλασιαστής Lagrange για τον περιορισμό τάσης της i-ράβδου και g_i είναι ο επιβαλλόμενος περιορισμός στην i-ράβδο. Θεωρώντας ότι οι αξονικές δυνάμεις των μελών του δικτυώματος είναι ανεξάρτητες των διατομών, η Εξ.(4.1), μετά από πράξεις, δίδει την ακόλουθη αναδρομική σχέση (εξίσωση 'stress-ratio', βλ. Ενότητα 3.3.1):

$${}^{k}x_i = {}^{k-1}x_i \left(\frac{\sigma_i}{\sigma_{\max,i}} \right) \tag{4.2}$$

όπου k είναι ο αύξων αριθμός της επανάληψης. Για ένα ισοστατικό δικτύωμα, το ελάχιστο βάρος υπολογίζεται σε ένα βήμα. Για ένα υπερστατικό δικτύωμα, η Εξ.(4.2) είναι δυνατόν να χρησιμοποιηθεί μόνον ως μία προσέγγιση της βέλτιστης σχεδίασης. Ωστόσο, η αποκτηθείσα εμπειρία, η οποία είναι καταγεγραμμένη στη βιβλιογραφία, υποδεικνύει ότι η Εξ.(4.2) παρέχει καλά αποτελέσματα, για μία ποικιλία προβλημάτων βελτιστοποίησης κατασκευών.

Γενικεύοντας την ισχύ της Εξ.(4.2) σε προβλήματα 2Δ συνεχούς μέσου, η ποσότητα x_i είναι δυνατόν να αντιστοιχεί σε πάχος. Στην παρούσα, υιοθετείται μία περαιτέρω γενίκευση, σύμφωνα με την οποία η ποσότητα x_i της Εξ.(4.2) αντιστοιχεί σε *κομβική τιμή* μίας συνεχούς κατανομής πάχους. Διευκρινίζεται ότι είναι επιβεβλημένη η χρήση μίας ελάχιστης τιμής για την ποσότητα x_i, διότι μία αρνητική τιμή στερείται φυσικής σημασίας, ενώ μία μηδενική τιμή είναι δυνατόν να προκαλέσει σοβαρά προβλήματα αριθμητικής αστάθειας.

4.3.4. Ανάπτυξη τριγωνικού πεπερασμένου στοιχείου μεταβλητού πάχους

Σε ένα τριγωνικό πεπερασμένο στοιχείο, το πεδίο μετατοπίσεων παρεμβάλλεται ως εξής:

$$\mathbf{u}\left(x,y\right) = \mathbf{N}^e \mathbf{a}^e = \bar{\mathbf{N}} C^{-1} \mathbf{a}^e \tag{4.3}$$

όπου $\mathbf{N}^e$ είναι το μητρώο παρεμβολή, C είναι ο πίνακας των συντεταγμένων των κόμβων του στοιχείου e, $\mathbf{a}^e$ είναι το διάνυσμα των κομβικών μετατοπίσεων. Από τη θεωρία της Μεθόδου των Πεπερασμένων Στοιχείων (ΜΠΣ) είναι γνωστό ότι για ένα τριγωνικό στοιχείο εμβαδού A, το μητρώο δυσκαμψίας ισούται με:

$$\mathbf{K}^e = \mathbf{B}^T\ \mathbf{E}\ \mathbf{B} \int_A t\, dA \tag{4.4}$$

όπου $\mathbf{E}$ είναι ο 3×3 πίνακας ελαστικότητας και $\mathbf{B}$ είναι ο 3×6 πίνακας παραμορφώσεων – μετατοπίσεων. Εάν το πάχος του στοιχείου είναι σταθερό (Σχήμα 4.1b), τότε ισχύει:

$$\mathbf{K}^e = t\ A\ \mathbf{B}^T\ \mathbf{E}\ \mathbf{B} \tag{4.5}$$

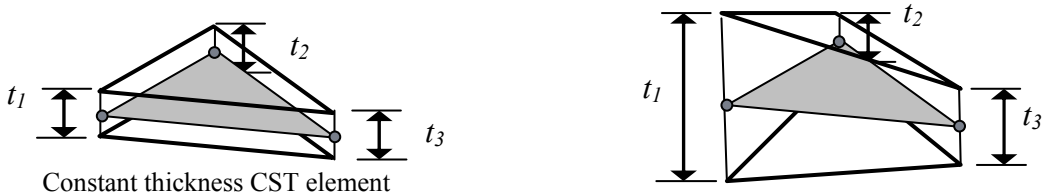

Constant thickness CST element
($t_1 = t_2 = t_3$)

(a)

Variable thickness CST element
($t_1 \neq t_2 \neq t_3$)

(b)

Σχήμα 4.5: Τριγωνικό πεπερασμένο στοιχείο με (a) σταθερό και (b) μεταβλητό πάχος

Έστω τριγωνικό πεπερασμένο στοιχείο μεταβλητού πάχους (Σχήμα 4.1b), στο οποίο το πάχος παρεμβάλλεται χρησιμοποιώντας τις συναρτήσεις μορφής του στοιχείου. Προκύπτει:

$$\mathbf{K}^e = \left(\frac{t_1 + t_2 + t_3}{3}\right) A\ \mathbf{B}^T\ \mathbf{E}\ \mathbf{B} \tag{4.6}$$

όπου $t_i, i = 1,2,3$ είναι οι κομβικές τιμές του πάχους.

4.3.4.1. Διαδικασία αξιολόγησης

Για την αξιολόγηση της προτεινομένης διαδικασίας, χρησιμοποιήθηκαν συνολικά πέντε Δείκτες Αξιολόγησης, δύο διαγράμματα σχετικά με την πορεία σύγκλισης, τρία διαγράμματα καθώς και τρία 3Δ σχήματα για την απεικόνιση της βέλτιστης κατανομής υλικού (βέλτιστη σχεδίαση). Οι Δείκτες Αξιολόγησης παρουσιάζονται στον Πίνακα 4.5.

Πίνακας 4.5: Δείκτες αξιολόγησης

Δείκτης	Ορισμός	Σκοπός
EI_1	$\frac{W_{opti} - W_{oud}}{W_{oud}} \times 100$	Για κάθε προσέγγιση, σύγκριση μεταξύ τελικού και αρχικού βάρους κατασκευής
EI_2	$\frac{Nodes_{active}}{NN}$	Για κάθε προσέγγιση, προσδιορισμός του βαθμού κάλυψης της επιφανείας, η οποία περιβάλλει τη βέλτιστη κατανομή
EI_3	$CV(\sigma_{vonMises})$	Για κάθε προσέγγιση, προσδιορισμός του βαθμού πλήρους εντάσεως της τελικής σχεδίασης
EI_4	$\frac{A_{surfer} - A_{oud}}{A_{oud}} \times 100$	Για κάθε προσέγγιση, σύγκριση του εμβαδού της επιφανείας, η οποία περιβάλλει τη βέλτιστη κατανομή, μεταξύ αρχικής και τελικής σχεδίασης
EI_5	$\frac{W_{surfer} - W_{oud}}{W_{oud}} \times 100$	Για κάθε προσέγγιση, σύγκριση του βάρους της τελικής σχεδίασης, μετά την επιβολή καθολικού σχήματος παρεμβολής της βέλτιστης κατανομής του πάχους, του βάρους της αρχικής σχεδίασης

Για λόγους σύγκρισης, η προτεινόμενη διαδικασία βελτιστοποίησης εφαρμόσθηκε μία φορά με πεπερασμένα στοιχεία σταθερού πάχους (έστω 'Προσέγγιση #1') και μία φορά με πεπερασμένα στοιχεία μεταβλητού πάχους (έστω 'Προσέγγιση #2').

Διευκρινίζεται ότι για μία κατασκευή υπό περιορισμό τάσης, η αποκαλούμενη Βέλτιστη Ισοπαχής Σχεδίαση (Optimum Uniform Design - OUD) ορίζεται ως η αρχική κατανομή σταθερού πάχους για την οποία ο επιβαλλόμενος περιορισμός ικανοποιείται ισοτικά. Αυτή η σχεδίαση χρησιμοποιείται εκτενώς για συγκρίσεις. Επίσης, διευκρινίζεται ότι την αξιολόγηση της προτεινομένης διαδικασίας βελτιστοποίησης, χρησιμοποιήθηκαν διαγράμματα, τα οποία παρουσιάζονται αναλυτικά στον Πίνακα 4.6 και στον Πίνακα 4.7.

Πίνακας 4.6: Γραφικά μέσα αξιολόγησης

Διάγραμμα	Σκοπός
Plot_a	Εκτίμηση σύγκλισης κάθε προσέγγισης ως προς τη μέγιστα εμφανιζόμενη τάση von Mises
Plot_b	Εκτίμηση σύγκλισης κάθε προσέγγισης ως προς το βάρος
Plot_c	Εκτίμηση βαθμού πλήρους εντάσεως μεταξύ των σχεδιάσεων από τις προσεγγίσεις #1 και #2
Plot_d	Απεικόνιση της διαφοράς βελτίστου βάρους μεταξύ των προσεγγίσεων #1 και #2
Graph_a	Απεικόνιση βέλτιστης σχεδίασης
Graph_b	Για κάθε προσέγγιση, παρεμβολή κομβικών τιμών πάχους τελικής κατανομής για την απόκτηση της σχεδίασης, η οποία θα κατασκευασθεί

Για τα διαγράμματα του Πίνακα 4.7, χρησιμοποιήθηκε ως αναφορά η Προσέγγιση #1.

Πίνακας 4.7: Διαγράμματα Plot_3 και Plot_4

Διάγραμμα	Προσδιορισμός τεταγμένης διαγράμματος
Plot_3	$(\%)\Delta\left(\sigma_{vonMises}\right)=\dfrac{\left(\sigma_{vonMises}\right)_{t\neq const}-\left(\sigma_{vonMises}\right)_{t=const}}{\left(\sigma_{vonMises}\right)_{t=const}}\times 100$
Plot_4	$(\%)\Delta\left(thickness_{nodal}\right)=\dfrac{\left(thickness_{nodal}\right)_{t\neq const}-\left(thickness_{nodal}\right)_{t=const}}{\left(thickness_{nodal}\right)_{t=const}}\times 100$

4.3.4.2. Προτεινόμενη διαδικασία βελτιστοποίησης

Η προτεινόμενη διαδικασία διακρίνεται σε δύο φάσεις. Στην πρώτη φάση, εφαρμόζεται μία επαναληπτική διαδικασία, η οποία εκκινείται από την, βιβλιογραφικά αποκαλούμενη, Βέλτιστη Ισοπαχή Σχεδίαση (Optimum Uniform Design - OUD). Πρόκειται για εκείνη την ισοπαχή κατανομή υλικού, για την οποία ικανοποιείται ισοτικά ο επιβαλλόμενος περιορισμός.

Φάση Α: Καταγραφή της πορείας βελτιστοποίησης (αρχική σχεδίαση: OUD)

Βήμα Α1: Προσδιορισμός της σχεδίασης (OUD) και καταγραφή βάρους, κατανομής πάχους και κατανομής τάσεων.

Βήμα Α2: Από τη σχεδίαση (OUD), εκκίνηση διαδικασίας βελτιστοποίησης για επαρκή πλήθος επαναλήψεων.

Βήμα Α3: Για κάθε επανάληψη, ενημέρωση του διαγράμματος Plot_a (βλ. Πίνακα 4.6).

Βήμα Α4: Για κάθε επανάληψη, ενημέρωση του διαγράμματος Plot_b (βλ. Πίνακα 4.6).

Βήμα Α5: Από το διάγραμμα Plot_a, προσδιορισμός της επανάληψης με μηδενική (ή ελάχιστη) παραβίαση τάσης.

Φάση Β: Προσδιορισμός της βέλτιστης σχεδίασης (για επανάληψη προσδιορισθείσα στο Βήμα Α5).

Βήμα Β1: Εφαρμογή ομοιόμορφης διακλιμάκωσης πάχους, προς αποφυγή παραβίασης τάσης.

Βήμα Β2: Από το Βήμα Α1 και το Βήμα Β1, διάγραμμα Plot_c (βλ. Πίνακα 4.6).

Βήμα Β3: Από το Βήμα Α1 και το Βήμα Β1, διάγραμμα Plot_d (βλ. Πίνακα 4.6).

Βήμα Β4: Από το Βήμα Α1 και το Βήμα Β1, Δείκτης EI_1 (βλ. Πίνακα 4.5).

Βήμα Β5: Καταγραφή πλήθους 'ενεργών' κόμβων και προσδιορισμός Δείκτη EI_2 (βλ. Πίνακα 4.5).

Βήμα Β6: Για τους ενεργούς κόμβους μόνο, προσδιορισμός της μέσης τιμής, της τυπικής απόκλισης και του συντελεστού μεταβλητότητας για την κατανομή των τάσεων von Mises (Δείκτης EI_3 - βλ. Πίνακα 4.1).

Βήμα Β7: Δημιουργία διαγραμμάτων Graph_a και Graph_b (βλ. Πίνακα 4.2).

Βήμα Β8: Από το Βήμα Β5, καταγραφή επιφανείας και προσδιορισμός Δείκτη EI_4 (βλ. Πίνακα 4.1).

Βήμα Β9: Από το Βήμα Β5, καταγραφή όγκου και προσδιορισμός Δείκτη EI_5 (βλ. Πίνακα 4.1).

4.3.4.3. Εξετασθέντα παραδείγματα

Τα εξετασθέντα παραδείγματα απεικονίζονται στο Σχήμα 4.2.

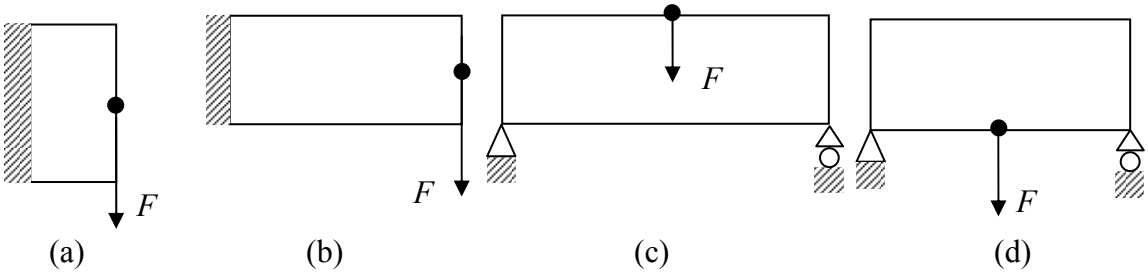

Σχήμα 4.6: Εξετασθέντα παραδείγματα (a) βαθύς πρόβολος, (b) κοντός πρόβολος, (c) δοκός MBB και (d) κατασκευή Michell

Δεδομένα για τα εξετασθέντα παραδείγματα καταγράφονται στον Πίνακα 4.4.

Πίνακας 4.8: Δεδομένα για τα εξετασθέντα παραδείγματα

Παράδειγμα	L_x $[m]$	L_y $[m]$	E $[Pa]$	v	*dens*	F $[N]$	Σημείο εφαρμογής F	σ_{allow} $[Pa]$	*NN*	*NEL*
Βαθύς πρόβολος	3	1	1	0.3	1	12	Δεξιά / μέσο	30	641	1200
Κοντός πρόβολος	16	10	1	0.3	1	12	Δεξιά / μέσο	20	1333	2560
Δοκός MBB	6	1	1	0.3	1	2	Άνω / μέσο	20	1271	2400
Κατασκευή Michell	10	5	100e06	0.3	1	1000	Κάτω / μέσο	35000	1661	3200

Στον Πίνακα 4.8, ως L_x συμβολίζεται το πλάτος (οριζόντια διάσταση), ως L_y σημειώνεται το ύψος (κατακόρυφη διάσταση), ως E δηλώνεται το μέτρο ελαστικότητας, ως ν δηλώνεται ο λόγος Poisson, ως *dens* δηλώνεται η πυκνότητα του υλικού, ως F συμβολίζεται το εφαρμοζόμενο φορτίο, ως σ_{allow} δηλώνεται η επιτρεπόμενη τάση, ως NN συμβολίζεται το πλήθος των κόμβων και ως NEL δηλώνεται το πλήθος των πεπερασμένων στοιχείων του πλέγματος.

4.3.4.4. Αποτελέσματα

Οι τιμές των Δεικτών Αξιολόγησης για τα εξετασθέντα παραδείγματα καταγράφονται αναλυτικά στον Πίνακα 4.9. Πιο συγκεκριμένα, για κάθε ένα από τα εξετασθέντα παραδείγματα παρατίθεται μία τριάδα γραμμών. Στην πρώτη γραμμή καταγράφονται διάφορα στοιχεία για τη βέλτιστη σχεδίαση, η οποία προκύπτει χρησιμοποιώντας 3-κομβικά τριγωνικά πεπερασμένα στοιχεία σταθερού πάχους,. Στη δεύτερη γραμμή καταγράφονται τα αντίστοιχα αποτελέσματα από τη χρήση των 3-κομβικών τριγωνικών πεπερασμένων στοιχείων μεταβλητού πάχους, ενώ στην τρίτη γραμμή καταγράφεται η διαφορά μεταξύ των δύο προσεγγίσεων, διατηρώντας ως αναφορά τη σχεδίαση με πεπερασμένα στοιχεία σταθερού πάχους.

Πίνακας 4.9: Δείκτες αξιολόγησης για τα εξετασθέντα παραδείγματα

		Volume (FSD Design)	Uniform scaling factor	EI_1	EI_2	mean Svonmises	EI_3	EI_4	EI_5
Deep cantilever	t=const	0.8017	1.0071	-93.504	88.768	28.10	17.372	1.955	68.893
	t<>const	0.8431	1.0017	-93.132	78.783	26.78	21.513	1.693	10.419
	% difference	5.17%	-0.54%	-0.40%	-11.25%	-4.69%	23.84%	-13.40%	-84.88%
Short cantilever	t=const	28.4073	1.0086	-85.098	97.900	19.56	8.323	1.117	84.964
	t<>const	30.4316	1.0020	-83.931	94.149	18.93	11.944	1.037	1.670
	% difference	7.13%	-0.65%	-1.37%	-3.83%	-3.19%	43.50%	-7.15%	-98.03%
MBB beam	t=const	1.3481	1.0154	-81.644	99.685	19.48	3.631	3.268	93.716
	t<>const	1.5380	1.0002	-78.735	96.223	18.62	8.651	1.883	6.294
	% difference	14.09%	-1.50%	-3.56%	-3.47%	-4.39%	138.23%	-42.37%	-93.28%
Michel structure	t=const	0.4259	1.0054	-93.609	96.869	34.58	2.388	16.688	76.727
	t<>const	0.4652	1.0045	-93.018	92.655	33.09	7.481	16.674	1.957
	% difference	9.24%	-0.09%	-0.63%	-4.35%	-4.33%	213.28%	-0.08%	-97.45%

Στο Σχήμα 4.7 απεικονίζονται οι βέλτιστες κατανομές για κάθε ένα από τα εξετασθέντα παραδείγματα. Ειδικότερα, για κάθε παράδειγμα, παρατίθεται μία τριάδα βελτίστων κατανομών. Η πρώτη βέλτιστη κατανομή προκύπτει από την εφαρμογή των 3-κομβικών τριγωνικών πεπερασμένων στοιχείων σταθερού πάχους, η δεύτερη κατανομή προκύπτει από τη χρήση των 3-κομβικών τριγωνικών πεπερασμένων στοιχείων μεταβλητού πάχους, ενώ η τρίτη βέλτιστη κατανομή προκύπτει από την επιβολή ενός καθολικού σχήματος εξομάλυνσης επί της δεύτερης, εκ των αναφερομένων, κατανομής.

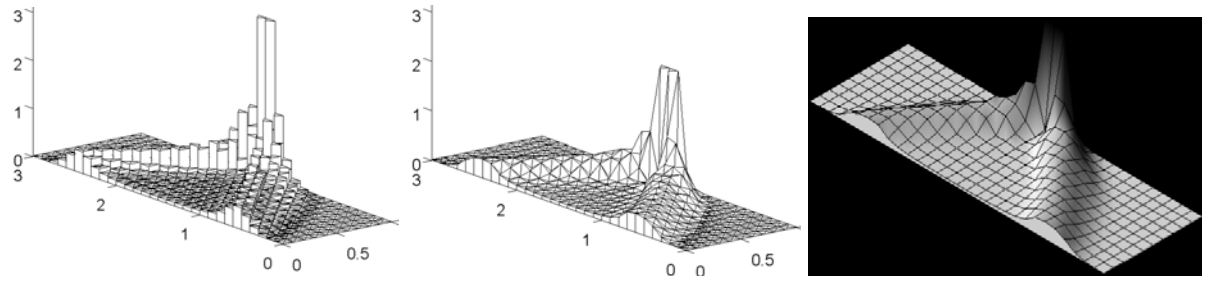

(a) (b) (c)

Βαθύς πρόβολος

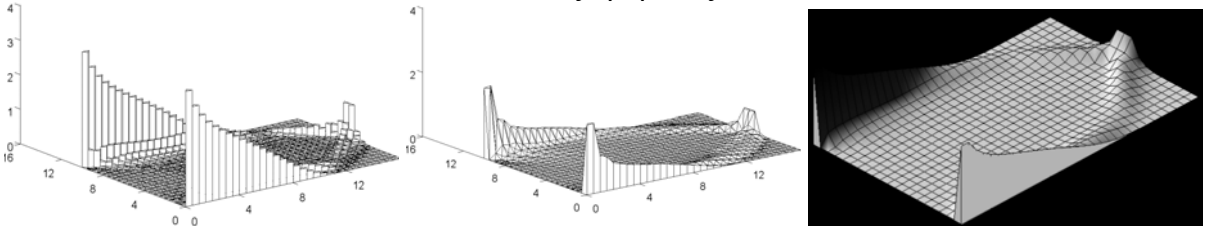

(a) (b) (c)

Κοντός πρόβολος

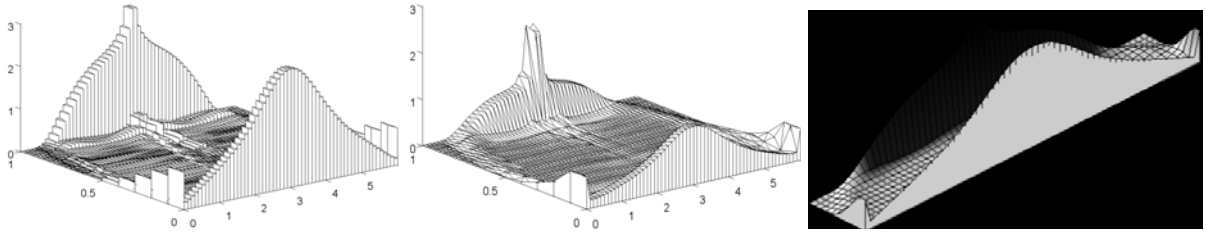

(a) (b) (c)

Δοκός MBB

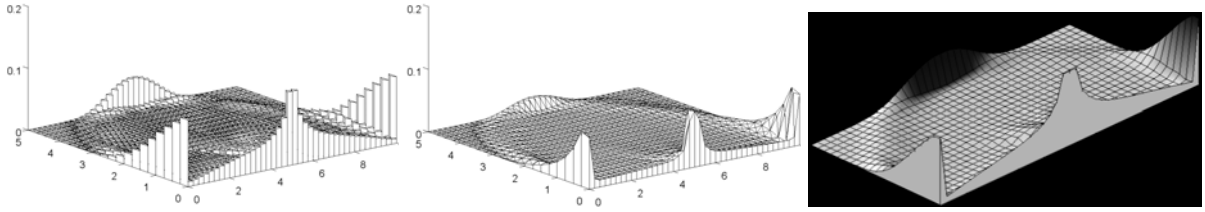

(a) (b) (c)

Κατασκευή Michell

Σχήμα 4.7: Βέλτιστες σχεδιάσεις

Στο Σχήμα 4.8 απεικονίζονται τα διαγράμματα, τα οποία περιγράφονται στον Πίνακα 4.6 και στον Πίνακα 4.7. Πιο συγκεκριμένα, για κάθε ένα από τα εξετασθέντα παραδείγματα, παρατίθεται μία τετράδα διαγραμμάτων, οπότε σχηματίζεται μία διάταξη με, συνολικά, 16 διαγράμματα. Τα διαγράμματα της πρώτης στήλης της εν λόγω διατάξεως απεικονίζουν την πορεία σύγκλισης, ως προς τη μέγιστη εμφανιζόμενη τιμή τάσης. Τα διαγράμματα της δεύτερης στήλης απεικονίζουν την πορεία σύγκλισης, ως προς το βάρος της κατασκευής. Τα διαγράμματα της τρίτης στήλης περιγράφουν πόσο κοντά στην κατάσταση πλήρους εντάσεως βρίσκεται η κατασκευή, ενώ τα διαγράμματα της τέταρτης στήλης δηλώνουν τη διαφορά μεταξύ των κομβικών τιμών της κατανομής του πάχους, όταν χρησιμοποιούνται πεπερασμένα στοιχεία σταθερού και μεταβλητού πάχους (αναφορά: στοιχεία σταθερού πάχους).

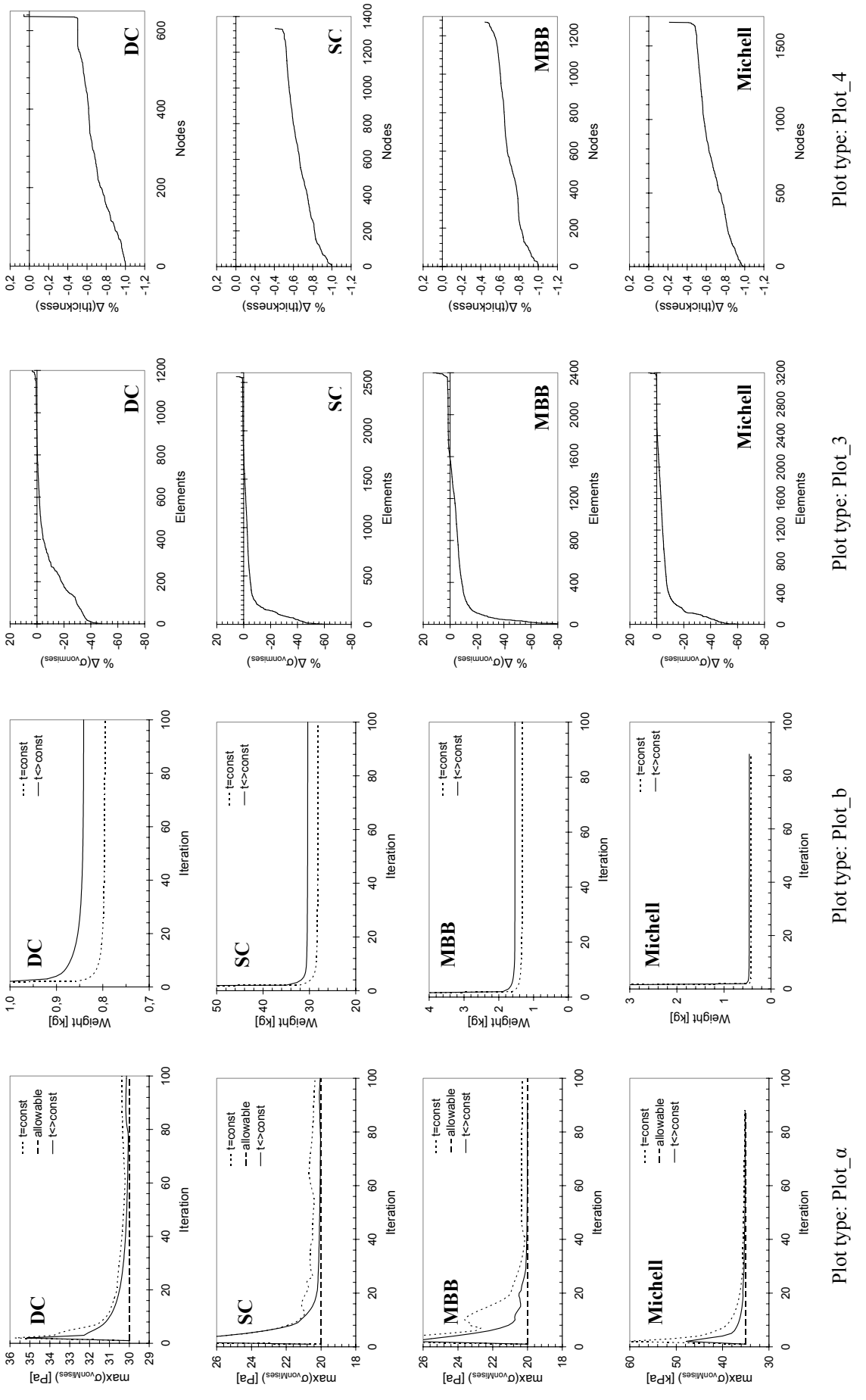

Σχήμα 4.8:. Διαγράμματα

4.3.4.5. Συμπεράσματα

Με βάση τα αποτελέσματα από τα εξετασθέντα παραδείγματα, τα οποία παρουσιάστηκαν στην προηγούμενη ενότητα, προκύπτει ότι, σε όλες τις περιπτώσεις, η προτεινόμενη διαδικασίας βελτιστοποίησης κατέληξε σε σχεδιάσεις μικροτέρου βάρους και πιο ομαλής κατανομής υλικού, κάτι που ενισχύει την ευκολία στην κατασκευή. Αυτό το συμπέρασμα ωθεί την έρευνα προς τη χρήση και άλλων τύπων πεπερασμένων στοιχείων με ανώτερα σχήματα παρεμβολής. Προς αυτήν την κατεύθυνση, εξετάστηκε και η περίπτωση του 4-κομβικού τετραπλευρικού στοιχείου, η οποία παρουσιάζεται στην επόμενη ενότητα.

4.3.5. Ανάπτυξη 4-κομβικού πεπερασμένου στοιχείου μεταβλητού πάχους

Το 4-κομβικό τετραπλευρικό πεπερασμένο στοιχείο επίπεδης ελαστικότητας είναι το απλούστερο μέλος της οικογενείας των τετραπλευρικών πεπερασμένων στοιχείων. Οι αντίστοιχες συναρτήσεις μορφής είναι:

$$\begin{aligned} &\mathbf{u}(x,y) = \mathbf{N}^e \mathbf{a}^e = \bar{\mathbf{N}} C^{-1} \mathbf{a}^e \\ &N_i^e = 0.25(1-\xi\xi_i)(1-\eta\eta_i) \end{aligned} \tag{4.7}$$

όπου $\mathbf{N}^e$ είναι ο πίνακας παρεμβολής, ως $\mathbf{C}$ περιγράφονται οι κομβικές συντεταγμένες του στοιχείου e και ως $\mathbf{a}^e$ δηλώνονται οι αντίστοιχες κομβικές συντεταγμένες. Από τη θεωρία της (ΜΠΣ), είναι γνωστό ότι το μητρώο δυσκαμψίας $\mathbf{K}^e$ του στοχείου e δίδεται από την εξίσωση:

$$\mathbf{K}^e = \int_A t\, \mathbf{B}^T\, \mathbf{E}\, \mathbf{B}\, dA \tag{4.8}$$

όπου $\mathbf{E}$ είναι ο 3×3 πίνακας ελαστικότητας και $\mathbf{B}$ είναι ο 3×8 πίνακας παραμορφώσεων-μετατοπίσεων. Για τον προσδιορισμό του μητρώου $\mathbf{K}^e$, η συνήθης πρακτική είναι η χρήση του κανόνα ολοκλήρωσης Gauss, ο οποίος, για 2Δ προβλήματα, περιγράφεται ως:

$$\int_{-1}^{+1}\int_{-1}^{+1} F(\xi,\eta)\, d\xi d\eta \approx \sum_{i=1}^{p_1}\sum_{j=1}^{p_2} w_i w_j F(\xi_i,\eta_j) \tag{4.9}$$

Στην Εξ.(4.9), p_1 και p_2 είναι το πλήθος των σημείων Gauss στις διευθύνσεις ξ και η, αντίστοιχα. Συνήθως χρησιμοποιείται το ίδιο πλήθος σημείων, δηλαδή $p = p_1 = p_2$, εάν χρησιμοποιούνται οι ίδιες συναρτήσεις μορφής ως προς τις δύο διευθύνσεις ξ και η. Από τον συνδυασμό των Εξ.(4.8, 4.9) προκύπτει ότι για τον προσδιορισμό του μητρώου $\mathbf{K}^e$ απαιτείται η έκφραση του διαφορικού dA σε όρους των διαφορικών $d\xi$ και $d\eta$. Αυτή η έκφραση (αναγωγή) είναι εφικτή μέσω της εξίσωσης:

$$dA = \det \mathbf{J}\, d\xi\, d\eta \tag{4.10}$$

όπου $\mathbf{J}$ είναι ο Ιακωβιανός πίνακας, ο οποίος συνδέει τα διαφορικά ως προς $\{x,y\}$ σε αυτά ως προς $\{\xi,\eta\}$.

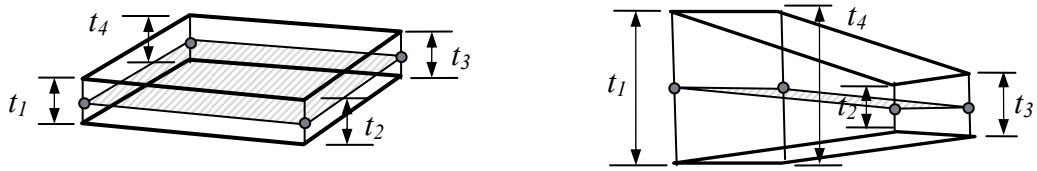

$(t_1 = t_2 = t_3 = t_4)$ $(t_1 \neq t_2 \neq t_3 \neq t_4)$

(a) (b)

Σχήμα 4.9: 4-κομβικό τετραπλευρικό πεπερασμένο στοιχείο με (a) σταθερό και (b) μεταβλητό πάχος

Για ένα 4-κομβικό τετραπλευρικό στοιχείο σταθερού πάχους (Σχήμα 4.9a), ισχύει:

$$\mathbf{K}^e = t\int_A \mathbf{B}^T\ \mathbf{E}\ \mathbf{B}\, dA \tag{4.11}$$

Για ένα 4-κομβικό τετραπλευρικό στοιχείο μεταβλητού πάχους (Σχήμα 4.9b), υπό την προϋπόθεση της ισοπαραμετρικής παρεμβολής του πάχους, ισχύει:

$$t = \sum_{i=1}^{4}\left(N_i\, t_i\right) \tag{4.12}$$

όπου t_i είναι το πάχος του $i-$γωνιακού κόμβου του στοιχείου και N_i είναι η αντίστοιχη συνάρτηση παρεμβολής. Ο συνδυασμός των Εξ.(4.11, 4.12) δίδει:

$$\mathbf{K}^e = \int_A \sum_{i=1}^{4}\left(N_i t_i\right)\mathbf{B}^T\,\mathrm{E}\,\mathrm{B}\, dA \tag{4.13}$$

Εισάγοντας τον κανόνα ολοκλήρωσης Gauss της Εξ.(4.9) στην Εξ.(4.13), προκύπτει:

$$\mathbf{K}^e = \int_{-1}^{1}\int_{-1}^{-1}\sum_{i=1}^{4}\left(N_i t_i\right)\mathbf{B}^T\,\mathrm{E}\,\mathrm{B}\,\det J\, d\xi\, d\eta \tag{4.14}$$

Σχετικά με τους πίνακες $\mathbf{E}$ και $\mathbf{B}$, αυτοί ανακτώνται εύκολα από τη βιβλιογραφία.

4.3.5.1. Διαδικασία αξιολόγησης

Για την αξιολόγηση της χρήσης του 4-κομβικού τετραπευρικού πλήρως ισοπαραμετρικού στοιχείου στη βελτιστοποίηση 2Δ χωρίων, ορίσθηκαν οι ακόλουθοι τρεις Δείκτες Αξιολόγησης (Evaluation Indices - EI):

- Δείκτης Αξιολόγησης EI_1: αφορά στην κανονικοποίηση του βελτίστου βάρους της κατασκευής, πριν την εφαρμογή διαδικασίας καθολικής εξομάλυνσης, ως προς το αρχικό βάρος της κατασκευής, δηλαδή το βάρος της σχεδίαση (OUD):

$$EI_1 = \left(\frac{W_{opti}}{W_{OUD}}\right) \tag{4.15}$$

- Δείκτης Αξιολόγησης EI_2: αφορά στην εντατική κατάσταση της κατασκευής, πριν την εφαρμογή διαδικασίας καθολικής εξομάλυνσης, και ισούται με τη μέση τιμή της τάσης von Mises του ενεργού τμήματος της κατασκευής:

$$EI_2 = \overline{\left(\sigma_{vonMises,active}\right)} \tag{4.16}$$

- Δείκτης Αξιολόγησης EI_3: αφορά στην ομοιομορφία της εντατικής κατάστασης της κατασκευής και ισούται με το συντελεστή μεταβλητότητας (Coefficient of Variation - CV) του τασικού κατά von Mises πεδίου, το οποίο αντιστοιχεί στο ενεργό τμήμα της κατασκευής:

$$EI_3 = CV\left(\sigma_{vonMises,active}\right) \tag{4.17}$$

Επιπροσθέτως, καταγράφεται η πορεία σύγκλισης, ως προς το βάρος της κατασκευής. Προφανώς, αντίστοιχοι δείκτες είναι δυνατόν να ορισθούν και για την κατάσταση μετά από την εφαρμογή διαδικασίας καθολικής εξομάλυνσης

4.3.5.2. Προτεινόμενη διαδικασία βελτιστοποίησης για 4-κομβικά στοιχεία μεταβλητού πάχους (Προσέγγιση #1)

Η προτεινόμενη διαδικασία είναι η ακόλουθη:

Βήμα 1: Προσδιορισμός της σχεδίασης (OUD) και καταγραφή βάρους, πάχους και συμπληρωματικής ενέργειας παραμόρφωσης (τιμές αναφοράς).

Βήμα 2: Ανάλυση της κατασκευής με τη (ΜΠΣ) και υπολογισμός της τάσης von Mises στα σημεία Gauss.

Βήμα 3: Επανασχεδίαση της κατανομής του πάχους της κατασκευής στα σημεία Gauss με την τεχνική stress-ratio.

Βήμα 4: Παρεμβολή των τιμών του πάχους στα σημεία Gauss και εκτίμηση του πάχους στον κόμβο, τον οποίο περιβάλουν τα σημεία Gauss.

Βήμα 5: Ανάλυση της κατασκευής χρησιμοποιώντας την κατανομή πάχους, η οποία προκύπτει από το Βήμα 4.

Βήμα 6: Εφαρμογή ομοιόμορφης διακλιμάκωσης πάχους ώστε να μην παραβιάζεται σε κανένα σημείο της κατασκευής ο επιβαλλόμενος περιορισμός τάσης.

Βήμα 7: Έλεγχος σύγκλισης. Εάν δεν έχει επιτευχθεί σύγκλιση ούτε έχει ξεπερασθεί το μέγιστο επιτρεπόμενο πλήθος επαναλήψεων, επιστροφή στο Βήμα 2.

Βήμα 8: Εφαρμογή μίας διαδικασίας εξομάλυνσης (π.χ. τεχνικής Kriging) των κομβικών τιμών της κατανομής του πάχους.

Βήμα 9: Εφαρμογή ομοιόμορφης διακλιμάκωσης στην εξομαλυμένη κατανομή υλικού (Βήμα 8), έτσι ώστε να μην παραβιάζεται κανένας περιορισμός τάσης.

Βήμα 10: Υπολογισμός των Δεικτών Αξιολόγησης.

Για εσωτερικούς κόμβους του πλέγματος, ο υπολογισμός της κομβικής τιμής του πάχους προκύπτει παρεμβάλλοντας κατάλληλα τις αντίστοιχες τιμές πάχους των σημείων Gauss, τα οποία περιβάλλουν τον εκάστοτε κόμβο. Για τους συνοριακούς κόμβους του πλέγματος, η κομβική τιμή του πάχους προκύπτει από προεκβολή των τιμών τιμές πάχους των σημείων Gauss, τα οποία βρίσκονται πλησιέστερα στον εκάστοτε συνοριακό κόμβο. Περισσότερες λεπτομέρειες επί του συγκεκριμένου θέματος παρατίθενται στην ενότητα 4.3.5.4.

4.3.5.3. Προτεινόμενη διαδικασία βελτιστοποίησης για 4-κομβικά στοιχεία σταθερού πάχους (Προσέγγιση #2)

Η διαδικασία είναι η ακόλουθη:

Βήμα 1: Προσδιορισμός της σχεδίασης (OUD) και καταγραφή βάρους, πάχους και συμπληρωματικής ενέργειας παραμόρφωσης (τιμές αναφοράς).

Βήμα 2: Ανάλυση της κατασκευής με τη (ΜΠΣ) και υπολογισμός της τάσης von Mises στα σημεία Gauss.

Βήμα 3: Για κάθε στοιχείο, παρεμβολή των τιμών της τάσης von Mises στα σημεία Gauss και υπολογισμός της τάσης στο κεντροειδές του στοιχείου.

Βήμα 4: Επανασχεδίαση της κατανομής του πάχους της κατασκευής στα σημεία Gauss με την τεχνική stress-ratio.

Βήμα 5: Ανάλυση της κατασκευής με τη (ΜΠΣ) και χρησιμοποιώντας την κατανομή του πάχους από το Βήμα 4.

Βήμα 6: Εφαρμογή ομοιόμορφης διακλιμάκωσης πάχους ώστε να μην παραβιάζεται σε κανένα σημείο της κατασκευής ο επιβαλλόμενος περιορισμός τάσης.

Βήμα 7: Έλεγχος σύγκλισης. Εάν δεν έχει επιτευχθεί σύγκλιση ούτε έχει ξεπερασθεί το μέγιστο επιτρεπόμενο πλήθος επαναλήψεων, επιστροφή στο Βήμα 2.

Βήμα 8: Εφαρμογή μίας διαδικασίας καθολικής εξομάλυνσης (π.χ. τεχνικής Kriging) της κατανομής πάχους των στοιχείων.

Βήμα 9: Εφαρμογή ομοιόμορφης διακλιμάκωσης στην εξομαλυμένη κατανομή υλικού (Βήμα 8), έτσι ώστε να μην παραβιάζεται κανένας περιορισμός μετατόπισης.

Βήμα 10: Υπολογισμός των Δεικτών Αξιολόγησης.

Στην παρούσα, ο προσδιορισμός της τάσης στο κεντροειδές ενός πεπερασμένου στοιχείου πραγματοποιήθηκε με τους τρόπους, οι οποίοι αναφέρονται στην επόμενη ενότητα.

4.3.5.4. Υπολογισμός κομβικών τιμών τάσης

Η κεντρική ιδέα της προτεινομένης διαδικασίας είναι πρώτα να υπολογισθούν οι τάσεις στα σημεία Gauss και στη συνέχεια να παρεμβληθούν οι εν λόγω τιμές στους κόμβους του πλέγματος. Συνολικά, προτείνονται τρία σχήματα παρεμβολής (έστω Σχήμα #1, Σχήμα #2 και Σχήμα #3). Για το Σχήμα #1, ως κομβική τιμή χρησιμοποιείται η μέγιστη εκ των τιμών τάσης των σημείων Gauss, τα οποία περιβάλλουν τον εκάστοτε κόμβο. Για το Σχήμα #2, ως κομβική τιμή χρησιμοποιείται ο μέσος όρων των τιμών τάσης των σημείων Gauss, τα οποία περιβάλλουν τον εκάστοτε κόμβο, ενώ για το Σχήμα #3, ως κομβική τιμή χρησιμοποιείται η μικρότερη των τιμών τάσης των σημείων Gauss. Στην παρούσα, επελέγη το 2×2 σχήμα ολοκλήρωσης κατά Gauss σε συνδυασμό με τετραπλευρικά στοιχεία. Σε αυτήν την περίπτωση, κάθε εσωτερικός κόμβος του πλέγματος περιβάλλεται από τέσσερα σημεία Gauss, κάθε κόμβος κατά μήκος του συνόρου από δύο σημεία Gauss, ενώ για κάθε γωνιακό κόμβο η τιμή τάσης τίθεται ίση προς εκείνην του πλησιέστερου σημείου Gauss. Στην περίπτωση πεπερασμένων στοιχείων σταθερού πάχους, με βάση τις τιμές στα σημεία Gauss, υπολογιζόταν, με βάση τα προαναφερθέντα τρία σχήματα παρεμβολής, η τιμή της τάσης στο κεντροειδές του στοιχείου.

4.3.5.5. Διακρίβωση του πεπερασμένου στοιχείου μεταβλητού πάχους

Για τη διακρίβωση του πεπερασμένου στοιχείου, το οποίο προγραμματίστηκε για τις ανάγκες της παρούσας μελέτης, χρησιμοποιήθηκε το στοιχείου SHELL63 του εμπορικού λογισμικού Ansys (ver.10). Ειδικότερα, εξετάσθηκε ένα 2Δ ορθογωνικό χωρίο σε απλή κάμψη και στη συνέχεια σε ασύμμετρο εφελκυσμό/θλίψη, για διάφορες πυκνότητες πλέγματος λόγου πλευρών 1:1. Το εν λόγω χωρίο αναλύθηκε πρώτα με κώδικα, ο οποίος

αναπτύχθηκε στο πλαίσιο της παρούσας Διδακτορικής Διατριβής, και στη συνέχεια με το εμπορικό λογισμικό Ansys (επιλογές για το στοιχείο SHEL63: extra displacement shape functions excluded, membrane element stiffness only). Από τη σύγκριση των λύσεων μεταξύ των δύο περιπτώσεων, προέκυψε σύμπτωση των τιμών των τάσεων στα σημεία Gauss.

4.3.5.6. Εξετασθέντα παραδείγματα

Τα εξετασθέντα παραδείγματα είναι εκείνα της ενότητας 4.3.4.3. Διευκρινίζεται, δε, ότι σε όλες τις περιπτώσεις χρησιμοποιήθηκε πλέγμα μοναδιαίου λόγου πλευρών, προκειμένου να ελαχιστοποιηθεί η επίδραση, του σχήματος των πεπερασμένων στοιχείων, στα αποτελέσματα.

4.3.5.7. Αποτελέσματα

Οι Δείκτες Αξιολόγησης (EIs) για τα εξετασθέντα παραδείγματα παρουσιάζονται στον Πίνακα 4.10. Διευκρινίζεται ότι στον Πίνακα 4.10, τα σύμβολα $t = const$ και $t \neq const$ δηλώνουν σταθερό και μεταβλητό πάχος στοιχείου, αντίστοιχα. Η % διαφορά εκφράζεται ως προς τα αποτελέσματα των πεπερασμένων στοιχείων σταθερού πάχους.

Πίνακας 4.10: Δείκτες Αξιολόγησης για τα εξετασθέντα παραδείγματα

		Stress interpolation scheme #1			Stress interpolation scheme #2			Stress interpolation scheme #3		
		EI_1	EI_2	EI_3	EI_1	EI_2	EI_3	EI_1	EI_2	EI_3
Deep cantilever	t=const	0,2568	0,9912	1,2926	0,2458	0,9900	0,9188	0,2330	0,9917	1,1984
	t≠const	0,2554	0,9898	0,9501	0,2445	0,9885	1,2616	0,2317	0,9865	1,6532
	% difference	-0,56%	-0,13%	-26,50%	-0,51%	-0,15%	37,31%	-0,58%	-0,53%	37,95%
Short cantilever	t=const	0,2399	0,9962	0,1920	0,2252	0,9985	0,6435	0,2155	0,9997	0,2988
	t≠const	0,2351	0,9860	0,5176	0,2218	0,9954	0,4290	0,2141	0,9936	0,4840
	% difference	-1,97%	-1,03%	169,68%	-1,52%	-0,31%	-33,33%	-0,64%	-0,60%	61,96%
MBB beam	t=const	0,1967	0,9997	0,1499	0,1806	0,9995	0,3194	0,1660	0,9990	0,1901
	t≠const	0,1876	0,9816	0,2775	0,1734	0,9799	0,2910	0,1609	0,9755	0,3654
	% difference	-4,63%	-1,81%	85,05%	-4,00%	-1,96%	-8,89%	-3,05%	-2,34%	92,20%
Michell structure (bridge)	t=const	0,2855	0,9930	0,2537	0,2633	0,9887	0,5086	0,2432	0,9838	1,0144
	t≠const	0,2760	0,9552	0,3348	0,2571	0,9523	0,4399	0,2400	0,9461	0,3514
	% difference	-3,32%	-3,80%	31,97%	-2,35%	-3,68%	-13,52%	-1,32%	-3,83%	-65,36%

Επιλεγμένες βέλτιστες σχεδιάσεις και πορείες σύγκλισης παρουσιάζονται στο Σχήμα 4.10. Το βασικό χαρακτηριστικό σε όλες τις βέλτιστες σχεδιάσεις είναι η ύπαρξη τριών ζωνών κατανομής πάχους. Πιο συγκεκριμένα, υπάρχει μία ζώνη ελαχίστου πάχους, η οποία αποτελείται από στοιχεία με κρίσιμη τιμή πάχους, άρα από στοιχεία, τα οποία είναι δυνατόν να απομακρυνθούν. Η δεύτερη ζώνη αποτελείται από στοιχεία μικρού μεν πάχους, αλλά όχι πλησίον της κρίσιμης τιμής. Παρατηρώντας, δε, την θέση στην οποία εμφανίζονται, πρόκειται για στοιχεία τα οποία συμβάλουν στην παραλαβή της διάτμησης λόγω κάμψης. Η τρίτη ζώνη αποτελείται από στοιχεία με πάχος σαφώς μεγαλύτερο από εκείνο των υπολοίπων στοιχείων. Πρόκειται για την πλέον ενεργή ζώνη της κατασκευής, η μορφή της οποίας υποδηλώνει και την πορεία που ακολουθεί το επιβαλλόμενο φορτίο προς τις θέσεις στήριξης. Ένα ακόμα σημείο άξιο λόγου είναι η υψηλή τιμή του πάχους, η οποία παρατηρείται στη θέση επιβολής του εξωτερικού φορτίου. Η εν λόγω τιμή είναι τόσο μεγαλύτερη όσο μικρότερο είναι το μέγεθος των πεπερασμένων στοιχείων του πλέγματος, κάτι αναμενόμενο από τη θεωρία της (ΜΠΣ). Ειδικότερα, θεωρώντας ότι το εξωτερικό φορτίο επιβάλλεται σημειακά, όσο μικρότερο είναι το μέγεθος του φορτιζομένου πεπερασμένου στοιχείου τόσο μεγαλύτερη είναι και η αναπτυσσόμενη τάση. Αυτός είναι ένας από τους λόγους για τους οποίους επιβάλλεται επιπρόσθετη μελέτη ανεξαρτησίας των αποτελεσμάτων από την λεπτότητα του χρησιμοποιηθέντος πλέγματος. Προς αντιμετώπιση του εν λόγω αριθμητικής φύσεως προβλήματος, υπάρχουν διάφορες τεχνικές, όπως η επιβολή του φορτίου σε ένα

πλήθος κόμβων, και όχι σημειακά σε έναν κόμβο, ή το αποκαλούμενο 'πάγωμα' του πάχους, δηλαδή η απόδοση μίας ικανοποιητικής τιμής πάχους σε μία ζώνη πλησίον της φορτιζόμενης θέσεως και η εξαίρεση της ζώνης αυτής από τη διαδικασία της βελτιστοποίησης.

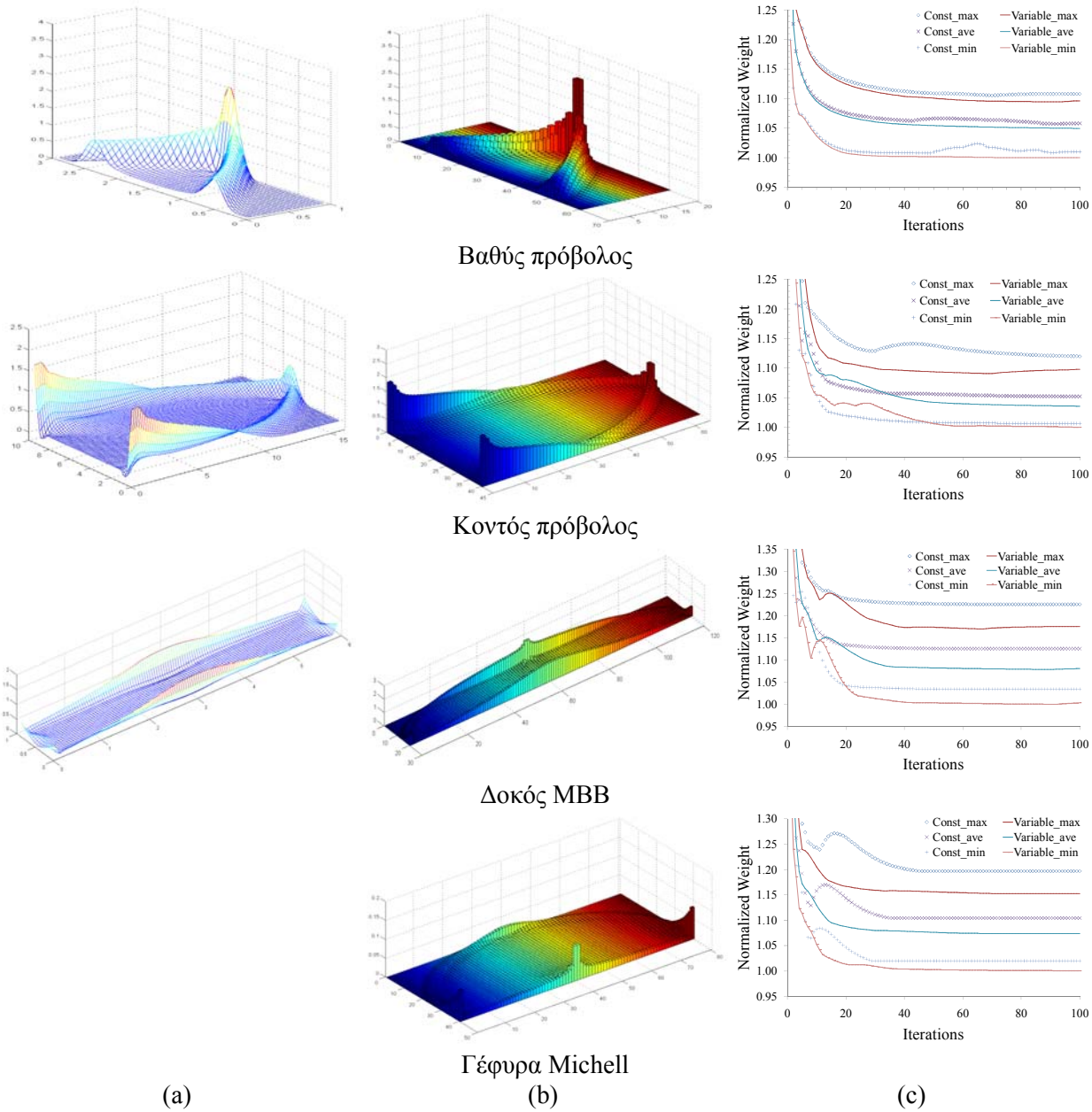

Σχήμα 4.10: Βέλτιστες κατανομές για τα εξετασθέντα παραδείγματα: (a) προσέγγιση #1, (b) προσέγγιση #2 και (c) πορεία σύγκλισης

Προκειμένου να διερευνηθεί η εξάρτηση της βέλτιστης κατανομής από τη διακριτοποίηση του χώρου σχεδίασης, πραγματοποιήθηκε μία παραμετρική ως προς την πυκνότητα του πλέγματος. Ενδεικτικά, απεικονίζονται οι βέλτιστες σχεδιάσεις για τον βαθύ πρόβολο και για δύο διαφορετικά πλέγματα (Σχήμα 4.11a, 4.11b). Επίσης, παρουσιάζεται και διάγραμμα σύγκλισης ως προς το κανονικοποιημένο βάρος της κατασκευής συναρτήσει του πλήθους των πεπερασμένων στοιχείων (Σχήμα 4.11c), από το οποίο φαίνεται ότι το βάρος τείνει ασυμπτωτικά προς μία τιμή.

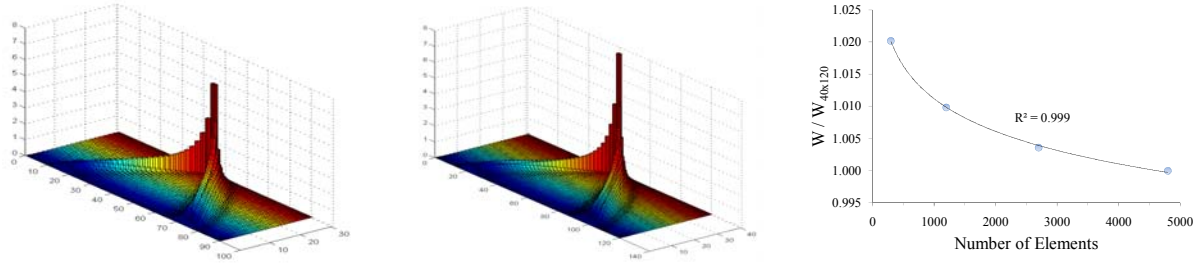

(a) (b) (c)

Σχήμα 4.11: Βέλτιστες σχεδιάσεις για τον βαθύ πρόβολο: (a) πλέγμα 30x90, (b) πλέγμα 40x120 και (c) κανονικοποιημένο βάρος συναρτήσει του πλήθους στοιχείων του πλέγματος

4.3.5.8. Συμπεράσματα

Με βάση τα αποτελέσματα από τα εξετασθέντα παραδείγματα, τα οποία παρουσιάστηκαν στην προηγούμενη ενότητα, προκύπτει ότι, σε όλες τις περιπτώσεις, η προτεινόμενη διαδικασίας βελτιστοποίησης με πεπερασμένα στοιχεία μεταβλητού πάχους κατέληξε σε σχεδιάσεις μικροτέρου βάρους και πιο ομαλής κατανομής υλικού

4.4. Βέλτιστη σχεδίαση πλάκας υπό περιορισμό τάσης

4.4.1. Γενικά

Η βέλτιστη σχεδίαση μίας πλάκας δεν εξαρτάται μόνον από τη εφαρμοζόμενη διαδικασία βελτιστοποίησης, αλλά και από άλλες παραμέτρους, όπως η αρχική γεωμετρία, οι συνθήκες στήριξης και η φόρτιση. Προς αυτήν την κατεύθυνση, στην παρούσα ενότητα διερευνήθηκαν ενδελεχώς τέσσερα χαρακτηριστικά παραδείγματα, κάποια από αυτά με παραλλαγές, προκειμένου να αναδειχθούν οι διαφορές μεταξύ των βελτίστων σχεδιάσεων, οι οποίες προκύπτουν όταν επιδιώκεται η μεταβολή του πάχους μίας κατανομής υλικού και όταν αποβάλλεται πλήρως υλικό από μία ισοπαχή κατανομή.

4.4.2. Θεωρητικό υπόβαθρο

Μία πλάκα ορίζεται ως ένα 3Δ σώμα, στο οποίο μία γεωμετρική διάσταση (πάχος) είναι σημαντικά μικρότερη από τις άλλες δύο γεωμετρικές διαστάσεις και η μεσοεπιφάνειά του είναι επίπεδη. Ένα είδος πλακός (πλάκες κάμψης - bending plates) είναι εκείνες για τις οποίες ισχύει:

$$\delta W = \delta W_{\text{int}} + \delta W_{ext} = 0 \tag{4.18}$$

όπου

$$-\delta W_{\text{int}} = \int_A \left(m_x \delta k_x + 2m_{xy} \delta k_{xy} + m_y \delta k_y + q_x \delta \gamma_x + q_y \delta \gamma_y \right) dA \tag{4.19}$$

και

$$\delta W_{ext} = \int_A p\ \delta w\ dA + \left(\text{boundary terms}\right) \tag{4.20}$$

Το έργο των εσωτερικών δυνάμεων σε μητρωική μορφή, γράφεται ως:

$$-\delta W_{\text{int}} = \int_A \delta\left(\mathbf{L}\boldsymbol{\varphi}\right)^T \mathbf{D}_b \mathbf{L}\boldsymbol{\varphi} dA + \int_A \delta\left(\nabla w + \boldsymbol{\varphi}\right)^T \mathbf{D}_S \left(\nabla w + \boldsymbol{\varphi}\right) dA \tag{4.21}$$

όπου οι άγνωστοι είναι το πεδίο των μετατοπίσεων $w(x,y)$ και το διάνυσμα των στροφών $\boldsymbol{\varphi} = \begin{bmatrix} \varphi_x & \varphi_y \end{bmatrix}^T$. Σύμφωνα με τη θεωρία Kirchhoff (θεωρία λεπτής πλακός), συνεισφορά της διάτμησης αμελείται, οπότε προκύπτει:

$$\boldsymbol{\gamma} = \nabla w + \boldsymbol{\varphi} = \mathbf{0} \tag{4.22}$$

Ο συνδυασμός των Εξ.(4.21, 4.22) δίδει:

$$-\delta W_{\text{int}} = \int_A \delta\left(\mathbf{L}\nabla w\right)^T \mathbf{D}_b \mathbf{L}\nabla w dA \tag{4.23}$$

Στην Εξ.(4.23), ο μόνος άγνωστος είναι το πεδίο των μετατοπίσεων. Σύμφωνα με τη (ΜΠΣ), ισχύει:

$$w = \mathbf{N}_w \mathbf{v} \quad \text{και} \quad \boldsymbol{\varphi} = \mathbf{N}_\varphi \mathbf{v} \tag{4.24}$$

όπου $\mathbf{v}$ είναι το διάνυσμα των κομβικών μετατοπίσεων και στροφών, ενώ $\mathbf{N}_w$ και $\mathbf{N}_\varphi$ είναι τα μητρώα των συναρτήσεων παρεμβολής. Σύμφωνα με τη θεωρία Kirchhoff για λεπτές πλάκες, λαμβάνονται υπόψη μόνον οι όροι κάμψης:

$$-\delta W_{\text{int}} = \int_A \delta \mathbf{v}^T \left(\mathbf{L}\tilde{\mathbf{N}}_\varphi\right)^T \mathbf{D}_b \mathbf{L}\tilde{\mathbf{N}}_\varphi \mathbf{v} dA \tag{4.25}$$

όπου

$$\boldsymbol{\varphi} = \tilde{\mathbf{N}}_\varphi \mathbf{v} = -\nabla w = -\nabla \tilde{\mathbf{N}}_w \mathbf{v} \tag{4.26}$$

Το μητρώο δυσκαμψίας ισούται με:

$$\mathbf{k} = \mathbf{k}_b = \int_A \mathbf{B}_b^T \mathbf{D}_b \mathbf{B}_b dA \tag{4.27}$$

όπου

$$\mathbf{B}_b = \mathbf{L}\tilde{\mathbf{N}}_\varphi \tag{4.28}$$

Με αυτόν τον τρόπο, σχηματίζεται το στοιχείο πλακός 12 βαθμών ελευθερίας, το οποίο χρησιμοποιήθηκε στην παρούσα. Σύμφωνα με τη θεωρία λεπτής πλακός, ισχύει:

$$\mathbf{D}_b = K \begin{bmatrix} 1 & \nu & 0 \\ \nu & 1 & 0 \\ 0 & 0 & 0.5(1-\nu) \end{bmatrix} \tag{4.29}$$

όπου

$$K = \frac{Et^3}{12\left(1-v^2\right)} \tag{4.30}$$

Στην παρούσα, χρησιμοποιήθηκαν δύο διαδικασίες βελτιστοποίησης: η διαδικασία Fully Stressed Design (FSD) και η διαδικασία Evolutionary Structural Optimization (ESO). Και οι δύο διαδικασίες αποσκοπούν στον ίδιο στόχο, δηλαδή στη διαμόρφωση ενός ομοιόμορφου τασικού πεδίου στην ενεργή περιοχή της κατασκευής, το οποίο να έχει τιμή πλησίον της μέγιστης επιτρεπόμενης.

Η αναδρομική σχέση επανασχεδίασης της διαδικασίας (FSD) προκύπτει από την εφαρμογή της μεθόδου των πολλαπλασιαστών Lagrange, σύμφωνα με την οποία η συνάρτηση Lagrange για την κατασκευή βάρους W, υπό την επιβολή μόνον περιορισμών τάσεων g_i και μοντελοποιούμενης με στοιχεία πλακός, είναι:

$$\mathcal{L}\left(\mathbf{t},\lambda\right) = W + \sum_{i=1}^{NEL} \lambda_i \, g_i \tag{4.31}$$

όπου $\mathbf{t}$ είναι το διάνυσμα με τα πάχη των στοιχείων πλακός. Εάν αναζητείται το ελάχιστο βάρος W, τότε η πρώτη παράγωγος της συνάρτησης Lagrange (Εξ.4.31) πρέπει να μηδενισθεί. Μετά από πράξεις, και θεωρώντας κατάσταση πλήρους εντάσεως για τα ενεργά στοιχεία της κατασκευής, προκύπτει η αναδρομική σχέση:

$${}^{k}t_i = {}^{k-1}t_i \left(\frac{\sigma_i}{\sigma_{\max,i}} \right)^{(1/n)} \tag{4.32}$$

όπου η ποσότητα n στον εκθέτη είναι ένας συντελεστής χαλάρωσης, προς επίτευξη πιο ομαλής σύγκλισης. Στην παρούσα, θεωρήθηκε ότι $n = 2$. Για την επανασχεδίαση της κατασκευής με τη μέθοδο (ESO), επιδιώκεται η προοδευτική αποβολή πλεονάζοντος υλικού, δηλαδή υλικού, στο οποίο οι αναπτυσσόμενες τάσεις είναι οι χαμηλότερες. Σύμφωνα με τη βιβλιογραφία, τα προς αποβολή στοιχεία ικανοποιούν την ανισότητα:

$$\sigma_{vonMises,e} \le RR \le \sigma_{vonMises,\max} \tag{4.33}$$

όπου $\sigma_{vonMises,e}$ είναι η τάση von Mises του e-στοιχείου, $\sigma_{vonMises,\max}$ είναι η μέγιστη τιμή τάσης von Mises, η οποία εμφανίζεται στην κατασκευής και στην τρέχουσα επανάληψη, ενώ ως RR συμβολίζεται ο ρυθμός αποβολής υλικού (Rejection Ratio):

$$RR = a_o + a_1 \times SS + a_2 \times SS + a_3 \times SS + \ldots \tag{4.34}$$

Ο ακέραιος αριθμός SS καλείται Αριθμός Σταθερής Κατάστασης (Steady State number), ο οποίος αυξάνεται κάθε φορά που το σχήμα αποβολής υλικού της Εξ.(4.33) δεν οδηγεί στην απομάκρυνση υλικού. Μία τυπική βιβλιογραφική τιμή είναι $SS = 10$.

4.4.3. Εξετασθέντα παραδείγματα

Συνολικά, εξετάσθηκαν τέσσερα παραδείγματα:

Παράδειγμα #1: Τετραγωνική πλάκα (Σχήματα 4.12, 4.13), περιμετρικά αρθρωμένη και περιμετρικά πακτωμένη. Λόγω συμμετρίας, εξετάζεται μόνο το ένα τέταρτο της πλάκας.

Παράδειγμα #2: Μονόπακτη πλάκα υπό την επίδραση δύο γωνιακών φορτίων της αυτής διεύθυνσης και φοράς (Σχήμα 4.14, Σχήμα 4.15). Εξετάζονται δύο περιπτώσεις: τα φορτία είναι ίσα μεταξύ τους και τα φορτία εμφανίζουν λόγο $(1/2)$ μεταξύ τους.

Παράδειγμα #3: Μονόπακτη πλάκα υπό την επίδραση κατανομής φορτίου επί της ακμής της ευρισκόμενης απέναντι από τη στήριξη (Σχήμα 4.16, Σχήμα 4.17). Εξετάζονται δύο περιπτώσεις: η κατανομή είναι σταθερή και η κατανομή είναι τριγωνική.

Παράδειγμα #4: Μονόπακτη πλάκα υπό την επίδραση δύο γωνιακών φορτίων της αυτής διεύθυνσης αλλά αντιθέτου φοράς (Σχήμα 4.18, Σχήμα 4.19). Εξετάζονται δύο περιπτώσεις: τα φορτία είναι ίσα μεταξύ τους και τα φορτία εμφανίζουν λόγο $(1/2)$ μεταξύ τους.

Σε όλες τις περιπτώσεις, χρησιμοποιήθηκε μέτρο ελαστικότητας $E = 70GPa$, λόγος Poisson $\nu = 0.3$ και πυκνότητα $\rho = 2707kg/m^3$. Όλες οι φορτίσεις, σημειακές και κατανεμημένες, θεωρήθηκαν ως μοναδιαίες. Επίσης, σε όλα τα παραδείγματα πλην του πρώτου, εξετάσθηκαν τρεις διαφορετικές γεωμετρίες με λόγο πλευρών $(a/b) \in \{1,2,3\}$.

4.4.4. Αποτελέσματα

Αποτελέσματα για το Παράδειγμα #1 και με την πλάκα περιμετρικά αρθρωμένη, απεικονίζονται στο Σχήμα 4.12.

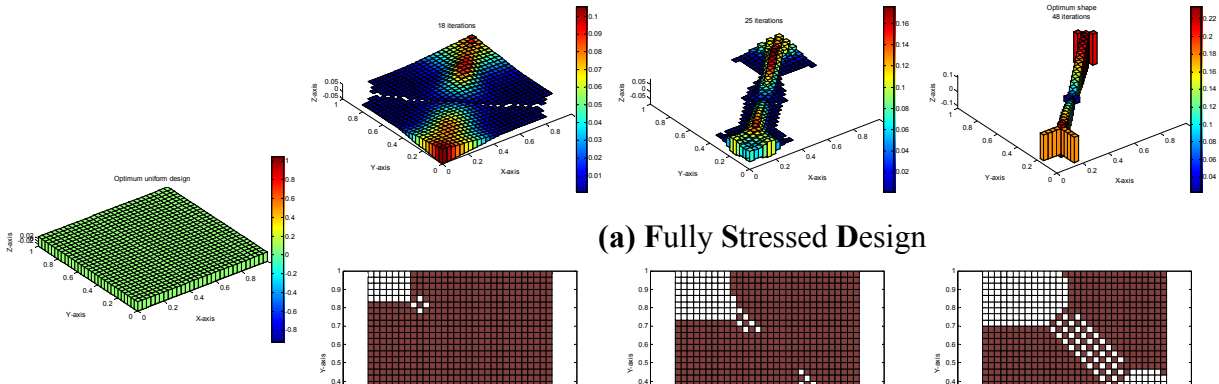

(a) Fully **S**tressed **D**esign

(b) Evolutionary **S**tructural **O**ptimization

(i) Ορισμός προβλήματος (αρχικό στάδιο) (ii) Post-initial stage (iii) Intermediate stage (iv) Final stage

Σχήμα 4.12: Βέλτιστη σχεδίαση περιμετρικά αρθρωμένης τετραγωνικής πλάκας

Αποτελέσματα για το Παράδειγμα #1 και με την πλάκα περιμετρικά πακτωμένη, απεικονίζονται στο Σχήμα 4.13.

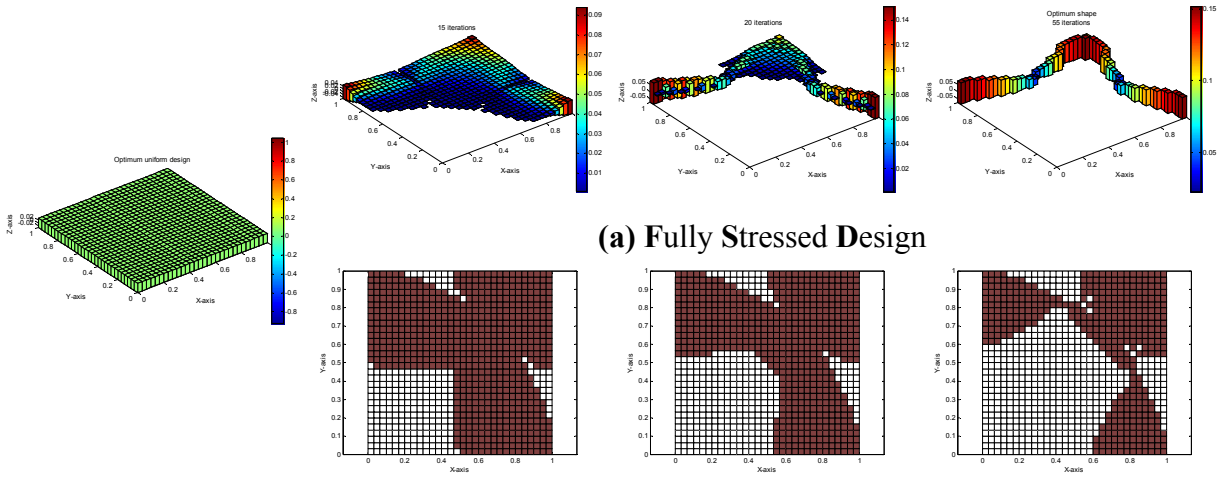

(a) Fully **S**tressed **D**esign

(b) Evolutionary **S**tructural **O**ptimization

(i) Ορισμός προβλήματος (αρχικό στάδιο) (ii) Post-initial stage (iii) Intermediate stage (iv) Final stage

Σχήμα 4.13: Βέλτιστη σχεδίαση περιμετρικά πακτωμένης τετραγωνικής πλάκας

Αποτελέσματα για το Παράδειγμα #2 και για ίσα φορτία, απεικονίζονται στο Σχήμα 4.14.

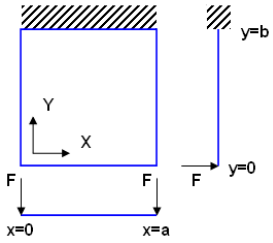

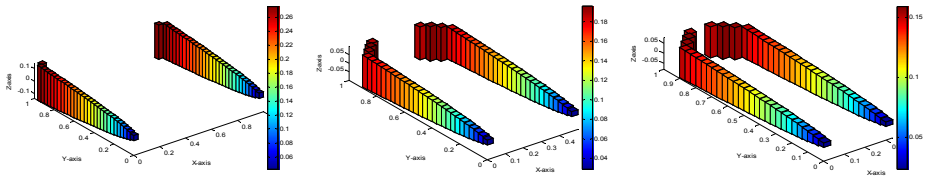

(a) Fully **S**tressed **D**esign

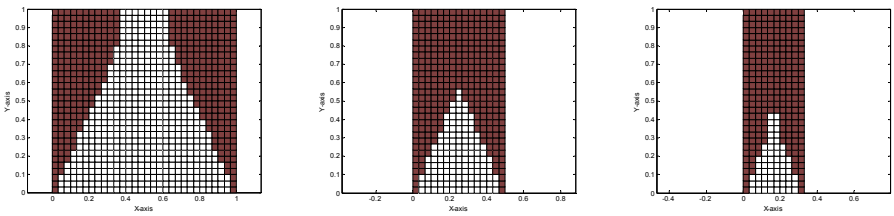

(b) Evolutionary **S**tructural **O**ptimization

(i) Ορισμός προβλήματος (ii) $(a/b)=(1/1)$ (iii) $(a/b)=(1/2)$ (iv) $(a/b)=(1/3)$

Σχήμα 4.14: Βέλτιστη σχεδίαση μονόπακτης πλάκας υπό την επιβολή δύο ίσων κομβικών φορτίων

Αποτελέσματα για το Παράδειγμα #2 και για άνισα φορτία, απεικονίζονται στο Σχήμα 4.15.

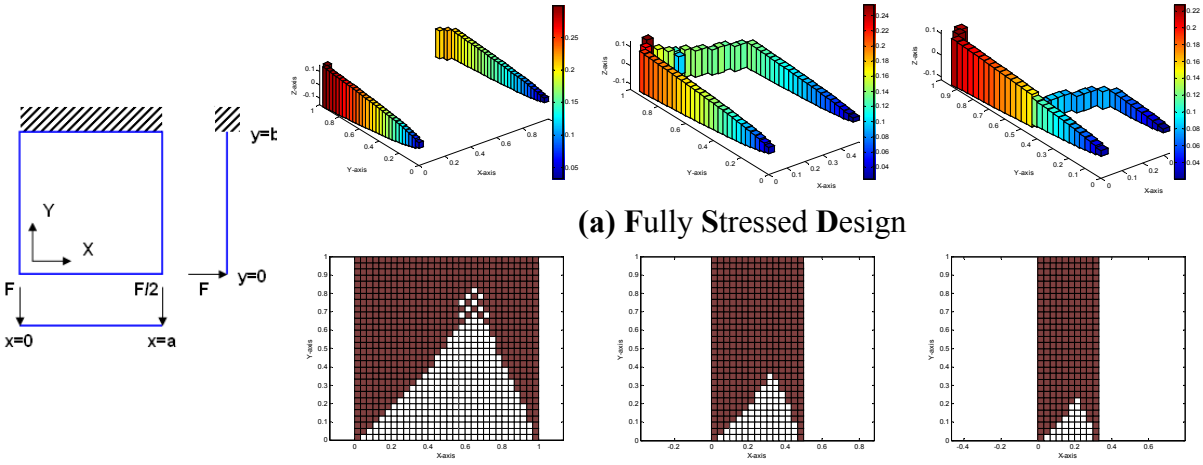

(a) Fully **S**tressed **D**esign

(b) Evolutionary **S**tructural **O**ptimization

(i) Ορισμός προβλήματος (ii) $(a/b)=(1/1)$ (iii) $(a/b)=(1/2)$ (iv) $(a/b)=(1/3)$

Σχήμα 4.15: Βέλτιστη κατανομή μονόπακτης πλάκας υπό την επιβολή δύο άνισων κομβικών φορτίων

Αποτελέσματα για το Παράδειγμα #3 και για σταθερή κατανομή φορτίου, απεικονίζονται στο Σχήμα 4.16.

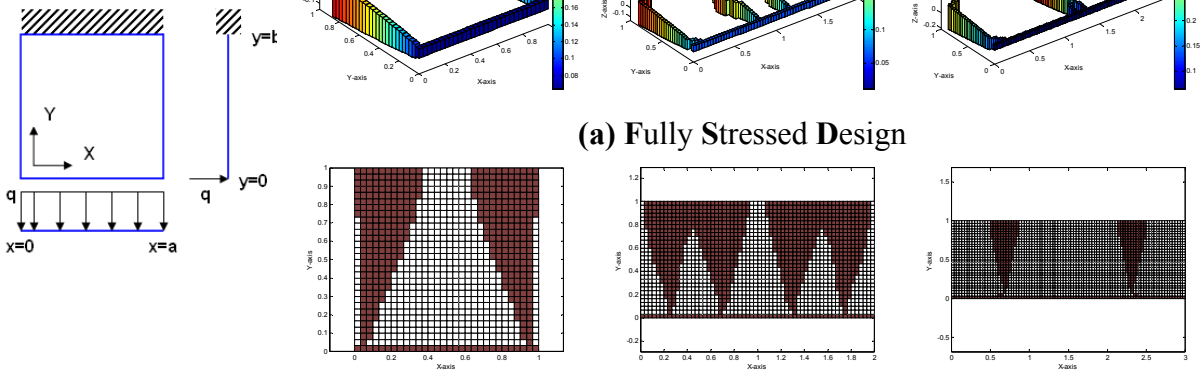

(a) Fully **S**tressed **D**esign

(b) Evolutionary **S**tructural **O**ptimization

(i) Ορισμός προβλήματος (ii) $(a/b)=(1/1)$ (iii) $(a/b)=(2/1)$ (iii) $(a/b)=(3/1)$

Σχήμα 4.16: Βέλτιστη κατανομή μονόπακτης πλάκας υπό την επιβολή ομοιόμορφης κατανομής φορτίου

Αποτελέσματα για το Παράδειγμα #3 και για τριγωνική κατανομή φορτίου, απεικονίζονται στο Σχήμα 4.17.

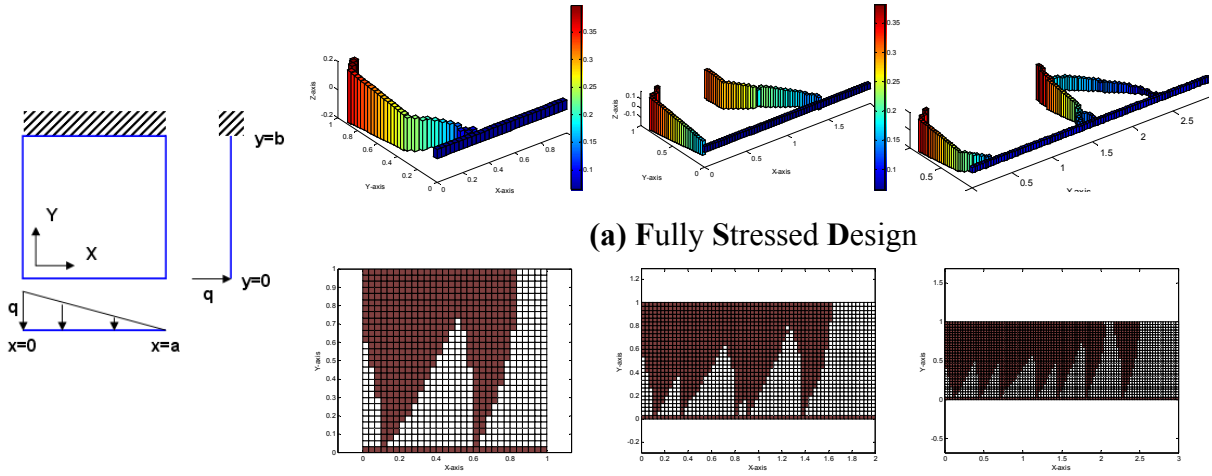

(a) Fully **S**tressed **D**esign

(b) Evolutionary **S**tructural **O**ptimization

(i) Ορισμός προβλήματος (ii) $(a/b)=(1/1)$ (iii) $(a/b)=(2/1)$ (iii) $(a/b)=(3/1)$

Σχήμα 4.17: Βέλτιστη κατανομή μονόπακτης πλάκας υπό την επιβολή τριγωνικής κατανομής φορτίου

Αποτελέσματα για το Παράδειγμα #4 και για ίσα φορτία, απεικονίζονται στο Σχήμα 4.18.

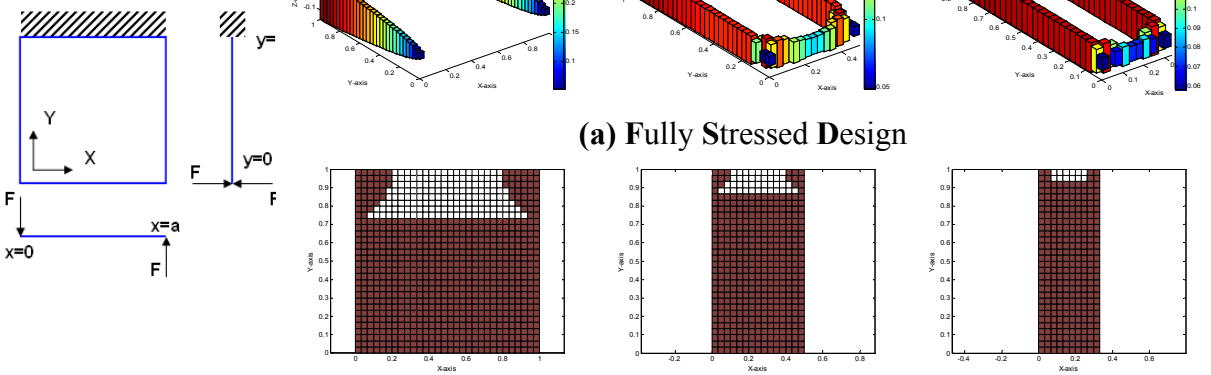

(a) Fully **S**tressed **D**esign

(b) Evolutionary **S**tructural **O**ptimization

(i) Ορισμός προβλήματος (ii) $(a/b)=(1/1)$ (iii) $(a/b)=(1/2)$ (iv) $(a/b)=(1/3)$

Σχήμα 4.18: Βέλτιστη κατανομή μονόπακτης πλάκας υπό την επιβολή δύο αντιθέτων και ίσων κομβικών φορτίων

Αποτελέσματα για το Παράδειγμα #4 και για άνισα φορτία, απεικονίζονται στο Σχήμα 4.19.

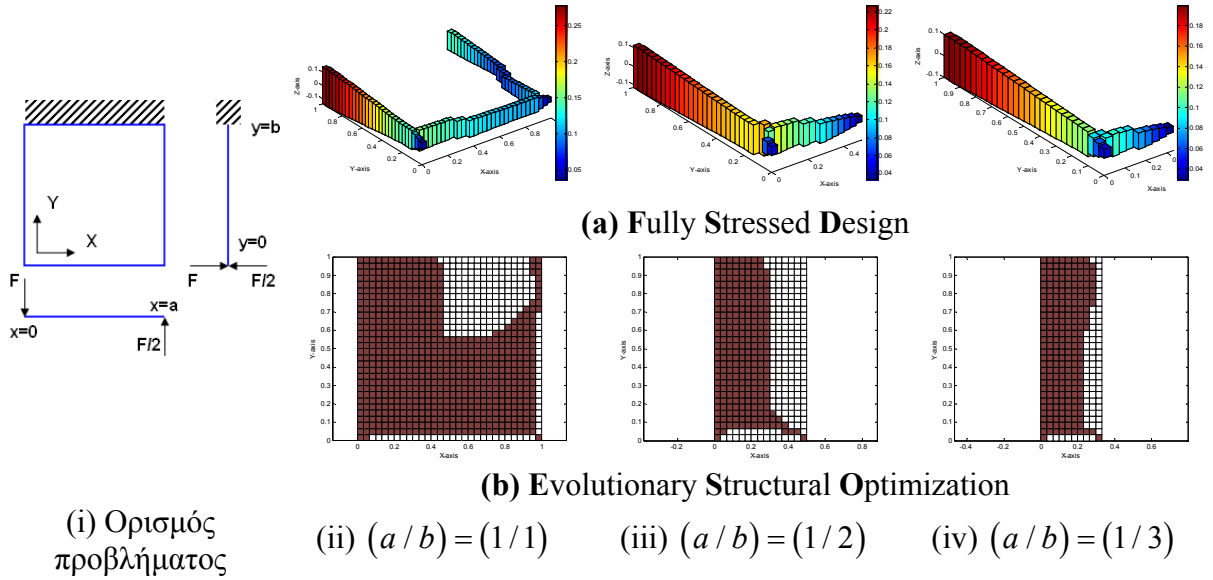

(a) Fully **S**tressed **D**esign

(b) Evolutionary **S**tructural **O**ptimization

(i) Ορισμός προβλήματος (ii) $(a/b)=(1/1)$ (iii) $(a/b)=(1/2)$ (iv) $(a/b)=(1/3)$

Σχήμα 4.19: Βέλτιστη κατανομή μονόπακτης πλάκας υπό την επιβολή δύο αντιθέτων και άνισων κομβικών φορτίων

Από το Σχήμα 4.12 έως και το Σχήμα 4.19, παρατίθεται, σε απλοποιημένο σκίτσο, η γεωμετρία, η στήριξη και η φόρτιση της πλάκας. Στα ίδια σχήματα, παρατίθεται μία τριάδα διαγραμμάτων με την ένδειξη (Fully Stressed Design), η οποία αντιστοιχεί στις βέλτιστες κατανομές υλικού, για διαφορετικό λόγο πλευρών της πλάκας και όταν επιτρέπεται η μεταβολή του πάχους των στοιχείων. Τέλος, στα ίδια σχήματα στην τριάδα παρατίθεται μία τριάδα διαγραμμάτων με την ένδειξη (Evolutionary Structural Optimization), η οποία αντιστοιχεί στις βέλτιστες κατανομές υλικού, για διαφορετικό λόγο πλευρών της πλάκας και όταν επιβάλλεται η κατανομή του υλικού να είναι διαρκώς ισοπαχής.

4.4.5. Συμπεράσματα

Μελετήθηκαν οι τεχνικές μεταβολής του πάχους μίας κατανομής υλικού και της πλήρους απομάκρυνσης υλικού από μία ισοπαχή κατανομή υλικού, οι οποίες είναι συλλογιστικά παραπλήσιες, δεδομένου ότι αμφότερες επιδιώκουν τη διαμόρφωση μίας σχεδίασης, στην οποία το εναπομείναν υλικό χαρακτηρίζεται από, περίπου, την ίδια τάση. Από τα αποτελέσματα, τα οποία παρουσιάστηκαν στην προηγούμενη ενότητα, καταδείχθηκε ότι οι εν λόγω τεχνικές, όταν εφαρμοσθούν σε προβλήματα εκτός-επιπέδου-κάμψης μίας πλάκας, καταλήγουν σε σημαντικά διαφορετικές βέλτιστες κατανομές υλικού.

4.5. Βέλτιστη σχεδίαση 3D συνεχούς μέσου υπό περιορισμό τάσεων

4.5.1. Γενικά

Η βέλτιστη σχεδίαση 3Δ κατασκευών συνεχούς μέσου υπό περιορισμό τάσης αποτελεί μία ιδιαίτερη κατηγορία προβλημάτων, δεδομένου ότι, λόγω της φύσεως του προβλήματος, είναι δυνατόν, κατά το πάχος, να δημιουργούνται ζώνες με υλικό και ζώνες κενές υλικού. Ισοδύναμα, προβλέπεται η δημιουργία εσωτερικών κοιλοτήτων, συνεπώς δεν ενδείκνυται η χρήση της προσέγγισης με την, κάθετα στη μεσοεπιφάνεια, μεταβολή του πάχους. Αντιθέτως, ενδείκνυται η ολική αφαίρεση υλικού από θέσεις, οι οποίες αντιστοιχούν σε πεπερασμένα στοιχεία του πλέγματος. Προς αυτήν την κατεύθυνση, αναπτύχθηκε μία νέα διαδικασία βελτιστοποίησης, σύμφωνα με την οποία η αποβολή υλικού στηρίζεται σε ένα ενεργειακό

κριτήριο, η μαθηματική έκφραση του οποίου εμπλέκει την κανονικοποιημένη μορφή της ενέργειας παραμόρφωσης του ενεργού τμήματος της κατασκευής. Για λόγους αξιολόγησης, πραγματοποιήθηκε σύγκριση με συναφή βιβλιογραφική μεθοδολογία, στην οποία η αποβολή υλικού στηρίζεται σε κριτήριο σχετιζόμενο με την τάση von Mises (έστω Basic Removal Scheme – BRS). Η σύγκριση συμπεριελάμβανε τέσσερα τυπικά βιβλιογραφικά παραδειγμάτων. Από τη, δε, σύγκριση προέκυψε η δυνατότητα διαμόρφωσης ανώτερων σχεδιάσεων με την προτεινόμενη διαδικασία βελτιστοποίησης.

4.5.2. Θεωρητικό υπόβαθρο

Το πρόβλημα της ελαχιστοποίησης του βάρους μίας 3Δ κατασκευής συνεχούς μέσου υπό την επιβολή περιορισμού τάσεων είναι δυνατόν να διατυπωθεί ως εξής:

$$mi\ V = \sum_{j=1}^{NEL,act} V_j \tag{4.35}$$

$$έτσι\ ώστε\ \frac{\max|\sigma_i|}{\sigma_{allow}} - 1 \le 0 \tag{4.36}$$

όπου V_j είναι ο όγκος του $j-$στοιχείου της τελικής σχεδίασης, σ_j είναι η τάση von Mises του στοιχείου αυτού, σ_{allow} είναι η επιτρεπόμενη τάση von Mises (περιορισμός τάσης) και NEL,act είναι το πλήθος των πεπερασμένων στοιχείων της τελικής σχεδίασης (ενεργά στοιχεία). Διευκρινίζεται ότι η Εξ.(4.36) περιγράφει την κατάσταση κατά την οποία θεωρείται ότι το επιτρεπόμενο όριο εφελκυσμού και θλίψης είναι, κατά απόλυτη τιμή, το ίδιο. Για την εύρεση της βέλτιστης σχεδίασης, απαιτείται ο καθορισμός τριών βασικών παραμέτρων: ο τρόπος απομάκρυνσης/αποβολής του υλικού (ή, ισοδύναμα, ο τρόπος επανασχεδίασης), το κριτήριο σύγκλισης και το κριτήριο τερματισμού της διαδικασίας βελτιστοποίησης. Τα θέματα αυτά αναπτύσσονται συνοπτικά στις επόμενες παραγράφους.

4.5.2.1. Κριτήριο αποβολής υλικού

Η επανασχεδίαση της κατασκευής στηρίζεται στη βαθμιαία αποβολή πλεονάζοντος υλικού, η οποία υλοποιείται μέσω της αποβολής ενός ή περισσοτέρων πεπερασμένων στοιχείων του πλέγματος. Ο χαρακτηρισμός ενός στοιχείου ως πλεονάζοντος είναι δυνατόν να στηριχθεί στην ενέργεια παραμόρφωσης του στοιχείου, η οποία αποθηκεύεται σε αυτό. Ωστόσο, εάν το πλέγμα αποτελείται από πεπερασμένα στοιχεία διαφορετικού μεγέθους, τότε η ενέργεια παραμόρφωσης δεν αποτελεί το καλύτερο κριτήριο χαρακτηρισμού. Αντιθέτως, είναι προτιμητέα η χρήση της εννοίας της *πυκνότητας* της ενέργειας παραμόρφωσης u_j κάθε στοιχείου:

$$u_j = \int \boldsymbol{\sigma}^T d\boldsymbol{\varepsilon} \tag{4.37}$$

Αρχικά, η μέση τιμή της πυκνότητας ενέργειας παραμόρφωσης της κατασκευής ισούται με:

$$\overline{u}_j = \left(\frac{1}{NEL}\right)\sum_{j=1}^{NEL} u_j \tag{4.38}$$

Διαιρώντας κατά μέλη την Εξ.(4.37) με την Εξ.(4.38), προκύπτει η κανονικοποιημένη πυκνότητα ενέργειας παραμόρφωσης (*Normalized* Strain Energy Density – NSED) για κάθε στοιχείο:

$$n_j = \left(u_j / \overline{u}_j \right) \tag{4.39}$$

Ο δείκτης n_j είναι δυνατόν να χρησιμοποιηθεί για την αξιολόγηση της ενεργειακής συμμετοχής κάθε στοιχείου του πλέγματος. Πεπερασμένα στοιχεία με χαμηλή τιμή n_j θεωρείται ότι αντιστοιχούν σε πλεονάζον υλικό, χαρακτηρίζονται ως παθητικά στοιχεία (passive elements) και θα πρέπει να απομακρυνθούν, συμβάλλοντας στη μείωση του βάρους της κατασκευής. Η, δε, απομάκρυνσή τους πραγματοποιείται σε δύο βήματα. Στο πρώτο βήμα, όλα τα εναπομείναντα (ενεργά) στοιχεία του πλέγματος ταξινομούνται με κριτήριο την τιμή του δείκτη n_j. Στο δεύτερο βήμα, απομακρύνεται είτε κάποιο προκαθορισμένο πλήθος στοιχείων είτε κάποιο προκαθορισμένο ποσοστό στοιχείων (Material Removal Step). Συνεπώς, στην $k-$επανάληψη, ο δείκτης j, ο οποίος εμφανίζεται στις Εξ.(4.37, 4.38, 4.39), λαμβάνει τιμές:

$$1 \le j \le NEL_{act,k-1} \tag{4.40}$$

Στο σημείο αυτό, τονίζεται ιδιαιτέρως ότι, στις επόμενες παραγράφους, η αποβολή του υλικού είναι φυσική, υπό την έννοια ότι τα αντίστοιχα πεπερασμένα στοιχεία του πλέγματος δεν λαμβάνονται υπόψη. Αντιθέτως, σε μία αριθμητική προσέγγιση, λαμβάνονται υπόψη όλα τα στοιχεία του πλέγματος και αποδίδεται μία τέτοια τιμή σε κάποια χαρακτηριστικά ιδιότητα του στοιχείου, έτσι ώστε η συνεισφορά του στο μητρώο δυσκαμψίας της κατασκευής να είναι αμελητέα.

4.5.2.2. Κριτήριο σύγκλισης

Για τη σύγκλιση της αριθμητικής διαδικασίας, είναι δυνατόν να χρησιμοποιηθεί ένα εκ των εξής κριτηρίων:

$$\left(V_{k-1} - V_k \right) < tol \quad \text{ή} \quad \left(MRS_k \right) < MRS_{\min} \tag{4.41}$$

όπου ως V συμβολίζεται ο όγκος του παρεμένοντος υλικού, ως MRS συμβολίζεται το Βήμα Αποβολής Υλικού (Material Removal Step - MRS), ενώ ως k δηλώνεται η τρέχουσα επανάληψη. Σύμφωνα με την πρώτη εκ των ανισοτήτων στην Εξ.(4.41), θεωρείται ότι έχει επιτευχθεί σύγκλιση όταν η μεταβολή του όγκου του εναπομείναντος υλικού στην κατασκευή και μεταξύ δύο διαδοχικών επαναλήψεων καταστεί μικρότερη από μια προκαθορισμένη τιμή. Σύμφωνα με τη δεύτερη εκ των εν λόγω ανισοτήτων θεωρείται ότι έχει επιτευχθεί σύγκλιση όταν η παράμετρος MRS (Material Removal Step) λάβει τιμή μικρότερη από μία προκαθορσιμένη.

4.5.2.3. Κριτήριο τερματισμού

Για τον τερματισμό της διαδικασίας, αρκεί να διαγνωσθεί ότι η εμφανιζόμενη μέγιστη τιμή του τασικού πεδίου von Mises είναι υψηλότερη της αντίστοιχης επιτρεπόμενης τιμής:

$$\left(\max \left| \sigma_i \right| / \sigma_{allow} \right) > 1 \tag{4.42}$$

Επίσης, όπως σε κάθε επαναληπτική διαδικασία, προβλέπεται ο τερματισμός της διαδικασίας εάν ξεπερασθεί κάποιο προκαθορισμένο μέγιστο πλήθος επαναλήψεων:

$$N_k > N_{\max} \tag{4.43}$$

όπου η ποσότητα N_k αντιστοιχεί στον αύξοντα αριθμό της τρέχουσας επανάληψης και $N_{\max}$ είναι το μέγιστο επιτρεπόμενο πλήθος επαναλήψεων.

4.5.3. Προτεινόμενη διαδικασία βελτιστοποίησης

Η προτεινόμενη διαδικασία βελτιστοποίησης είναι η ακόλουθη:

Βήμα 1: Δομημένη διακριτοποίηση του 3Δ χώρου σχεδίασης με πεπερασμένα στοιχεία και ορισμός αρχικής τιμής για το Βήμα Αποβολής Υλικού (Material Removal Step - MRS).
Βήμα 2: Υπολογισμός της πυκνότητας της ενέργειας παραμόρφωσης (Strain Energy Density - SED) κάθε πεπερασμένου στοιχείου.
Βήμα 3: Υπολογισμός της κανονικοποιημένης πυκνότητας της ενέργειας παραμόρφωσης (Normalized Strain Energy Density - NSED) για κάθε στοιχείο.
Βήμα 4: Απομάκρυνση (MRS) στοιχείων με τη μικρότερη τιμή NSED.
Βήμα 5: Υπολογισμός της τιμής (NSED) για τα εναπομείναντα στοιχεία (ενεργά στοιχεία).
Βήμα 6: Έλεγχος σύγκλισης και τερματισμός της διαδικασίας εάν έχει επιτευχθεί σύγκλιση.
Βήμα 7: Έλεγχος παραβιάσεων τάσεων. Εάν παρατηρείται παραβίαση τάσης, τότε μείωση του βήματος (MRS).
Βήμα 8: Επιστροφή στο Βήμα 4.

Για τη διακριτοποίηση του χώρου σχεδίασης, μία καλή επιλογή είναι η χρήση 8-κομβικών 6-εδρικών πεπερασμένων στοιχείων. Η χρήση 20-κομβικών 6-εδρικών στοιχείων κατά κύριο λόγο αποσκοπεί στην αντιμετώπιση του, αποκαλούμενου στη βιβλιογραφία, ‘προβλήματος σκακιέρας’ (checkerboard problem).

4.5.4. Εξετασθέντα παραδείγματα

Η αξιολόγηση της προτεινομένης διαδικασίας στηρίχθηκε σε τέσσερα βιβλιογραφικά παραδείγματα. Διευκρινίζεται ότι δεδομένα για τρία παραδείγματα (βαθύς πρόβολος, κοντός πρόβολος και δοκός MBB) παρατίθενται και σε άλλο σημείο της παρούσης. Ωστόσο, για την πληρότητα του κειμένου, στοιχεία για τα εν λόγω παραδείγματα παρατίθενται εκ νέου. Στο Σχήμα 4.20 απεικονίζεται σχηματικά η γεωμετρία, η στήριξη και η φόρτιση των εξετασθέντων παραδειγμάτων.

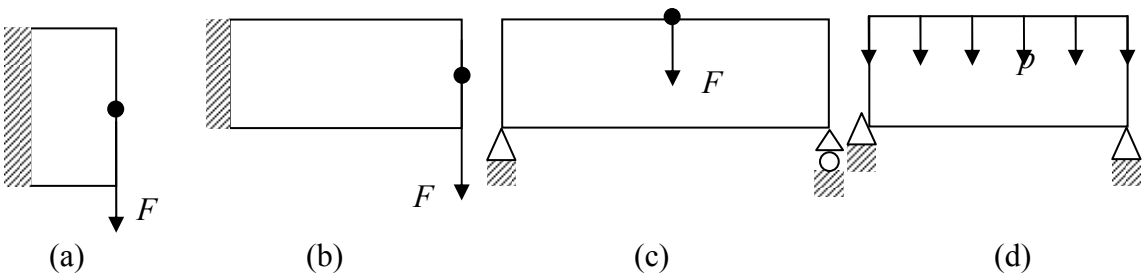

Σχήμα 4.20: Τα εξετασθέντα προβλήματα (a) βαθύς πρόβολος, (b) κοντός πρόβολος, (c) δοκός beam και (d) τάκος υπό θλίψη

Στον Πίνακα 4.10 καταγράφονται στοιχεία για τα εν λόγω παραδείγματα.

Πίνακας 4.11: Δεδομένα για τα εξετασθέντα προβλήματα

Πρόβλημα	L_x $[m]$	L_y $[m]$	E $[Pa]$	v	$dens$	Φορτίο F	Σημείο εφαρμογής του F	σ_{allow} $[Pa]$	NN	NEL
Βαθύς πρόβολος	3	1	1	0.3	1	12N	Δεξιά / Μέσο	30	10571	9000
Κοντός πρόβολος	16	10	1	0.3	1	12N	Δεξιά / Μέσο	20	2079	1300
Δοκός MBB	6	1	1	0.3	1	2N	Άνω / Μέσο	20	4092	3000
Τάκος υπό θλίψη	1	0.4	1	0.3	1	0.1 N/mm^2	Άνω / Κατανομή	16	3960	3200

Η αξιολόγηση της προτεινομένης διαδικασίας πραγματοποιήθηκε σε δύο φάσεις. Στην πρώτη φάση δημιουργήθηκαν διαγράμματα, στα οποία αποτυπώθηκε η επίδραση της παραμέτρου MRS (Material Removal Step) στη διαδικασία της βελτιστοποίησης. Πιο συγκεκριμένα, για κάθε παράδειγμα εκτός του τάκου υπό θλίψη, δημιουργήθηκε ένα διάγραμμα με άξονα τετμημένων τιμές της παραμέτρου MRS, πρωτεύοντα άξονα τεταγμένων τον παραμένοντα όγκο υλικού και δευτερεύοντα άξονα τεταγμένων το πλήθος των επαναλήψεων, οι οποίες απαιτήθηκαν κάθε φορά μέχρι επιτεύξεως συγκλίσεως. Στη δεύτερη φάση συγκρίθηκε η προτεινόμενη διαδικασία βελτιστοποίησης με την βιβλιογραφική μέθοδο ESO, σύμφωνα με την οποία η απομάκρυνση του υλικού στηρίζεται στο αναπτυσσόμενο πεδίο τάσεων von Mises (έστω Βασικό Σχήμα Αποβολής - Basic Removal Scheme - BRS). Η, δε, σύγκριση στηρίχθηκε στους εξής τρεις Δείκτες Αξιολόγησης (Performance Indices - PI's):

$$PI_1 = \left(\frac{NEL_{act}}{NEL_{ini}} \right) \qquad PI_2 = \left(\frac{\sigma_{vonMises,\max}}{\sigma_{vonMises,allow}} \right) \qquad PI_3 = N_{iter} \tag{4.44}$$

Ο δείκτης PI_1 εκφράζει, σε κανονικοποιημένη μορφή, τον όγκο του παραμένοντος υλικού. Ο δείκτης PI_2 εκφράζει τον λόγο της μέγιστης εμφανιζόμενης τάσης von Mises stress προς την επιτρεπόμενη τιμή και ο δείκτης PI_3 αντιστοιχεί στο πλήθος των επαναλήψεων, οι οποίες απαιτούνται μέχρι να επιτευχθεί η σύγκλιση.

4.5.5. Αποτελέσματα

Τα αποτελέσματα της πρώτης Φάσης απεικονίζονται στο Σχήμα 4.21. Σε τρία παραδείγματα εξετάσθηκαν δύο τιμές πάχους, ενώ σε ένα παράδειγμα (τάκος υπό θλίψη) εξετάστηκε μόνο μία περίπτωση, διότι από τον ορισμό του προβλήματος το πάχος ελάμβανε προκαθορισμένη τιμή. Συνεπώς, για τα τρία παραδείγματα με δύο τιμές πάχους παρατίθενται δύο τριάδες διαγραμμάτων, μία τριάδα για κάθε τιμή πάχους. Διευκρινίζεται ότι οι τιμές της τετμημένης των διαγραμμάτων (παράμετρος Material Removal Step - MRS) έχουν δοθεί αυθαίρετα και δεν προέρχονται από κάποιο σχήμα βελτιστοποίησης.

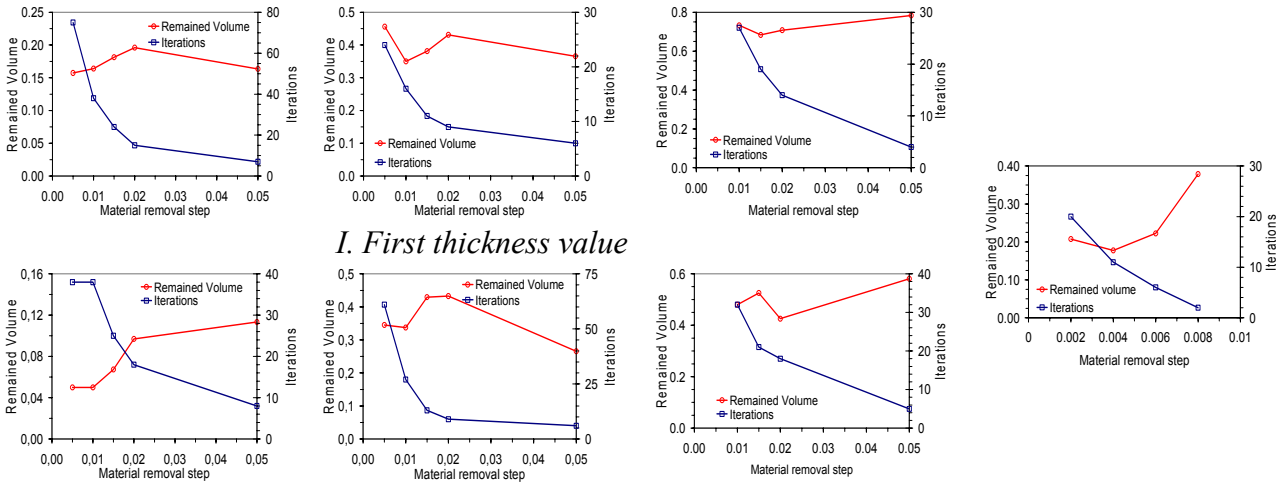

Σχήμα 4.21: Επίδοση της προτεινόμενης διαδικασίας: (a) βαθύς πρόβολος, (b) κοντός πρόβολος, (c) δοκός MBB και (d) τάκος υπό θλίψη.

Στο Σχήμα 4.22 παρουσιάζονται οι προκύπτουσες βέλτιστες σχεδιάσεις στην περίπτωση του κοντού προβόλου για διάφορες τιμές του ρυθμού αποβολής υλικού (Marerial Removal Ratio).

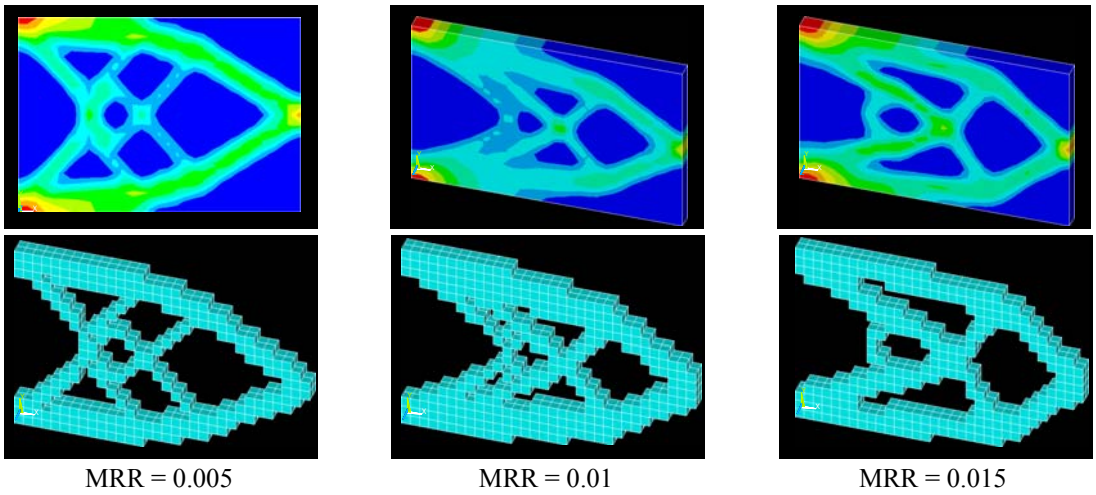

Σχήμα 4.22: Βελτιστοποιημένη σχεδίαση για τον κοντό πρόβολο (άνω σειρά: κατανομή τάσης von Mises, κάτω σειρά: παραμένον υλικό)

Στο Σχήμα 4.23 παρουσιάζονται συγκριτικά αποτελέσματα μεταξύ της προτεινομένης διαδικασίας βελτιστοποίησης και του Βασικού Σχήματος Αποβολής.

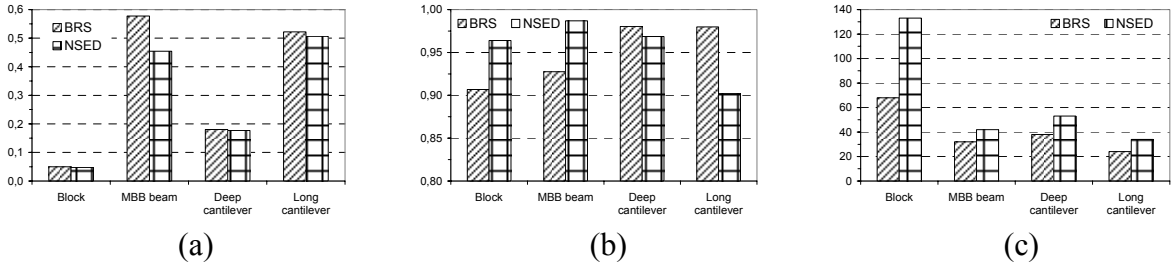

Σχήμα 4.19: Σύγκριση ανάμεσα στην προτεινόμενη διαδικασία και στο Βασικό Σχήμα Αποβολής: (a) δείκτης P1, (b) δείκτης P2 και (c) δείκτης P3.

Στο Σχήμα 4.23 παρουσιάζονται αποτελέσματα για τον βαθύ πρόβολο και τον τάκο υπό θλίψη. Πιο συγκεκριμένα, κάθε ένα από αυτά τα παραδείγματα βελτιστοποιήθηκε τόσο χρησιμοποιώντας το Βασικό Σχήμα Αποβολής (BRS, βλ. Ενότητα 4.5.4) όσο και την προτεινόμενη διαδικασία. Για κάθε ένα παράδειγμα και για κάθε μία διαδικασία βελτιστοποίησης, παρουσιάζεται μία τριάδα εικόνων. Στην πρώτη εικόνα (ένδειξη: Αρχική) παρουσιάζεται η αρχική σχεδίαση, στη δεύτερη εικόνα (έδειξη: Ενδιάμεση) παρουσιάζεται η μορφή της κατασκευής περίπου στο μέσο της διαδικασίας βελτιστοποίησης, ενώ στην τρίτη εικόνα απεικονίζεται η βέλτιστη σχεδίαση.

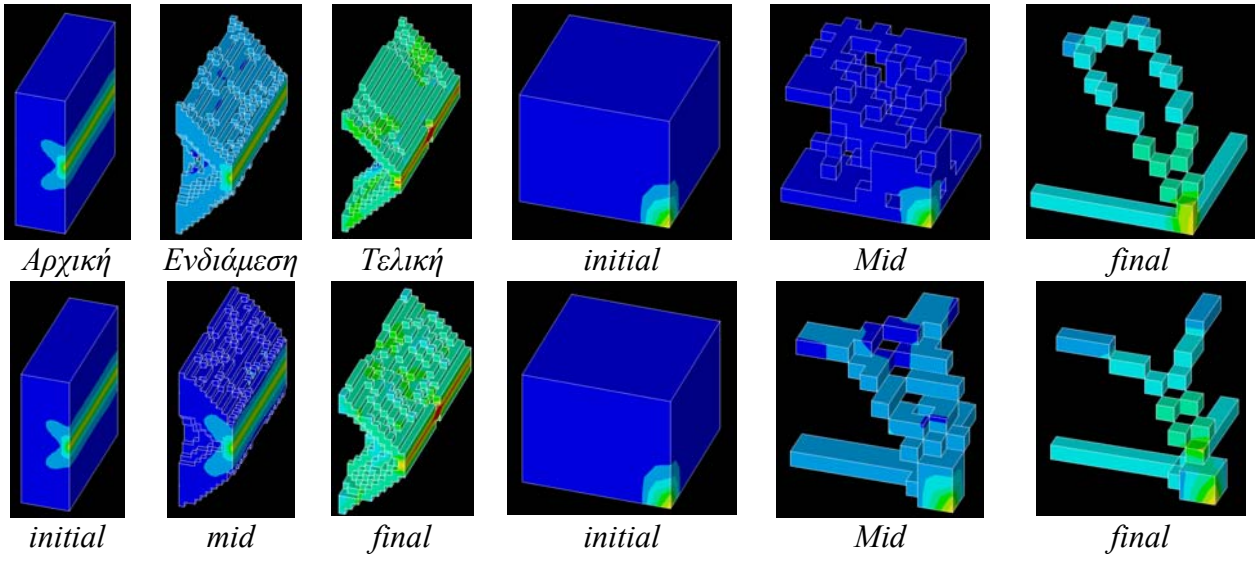

Σχήμα 4.23: Βελτιστοποιημένη σχεδίαση: (a) βαθύς πρόβολος και (b) τάκος υπό θλίψη (άνω σειρά: προτεινόμενη διαδικασία, κάτω σειρά: Βασικό Σχήμα Αποβολής - Basic Removal Scheme)

Κατ' αντιστοιχία του Σχήματος 4.22, στο Σχήμα 4.24 παρουσιάζονται τριάδες εικόνων για την περίπτωση του κοντού προβόλου.

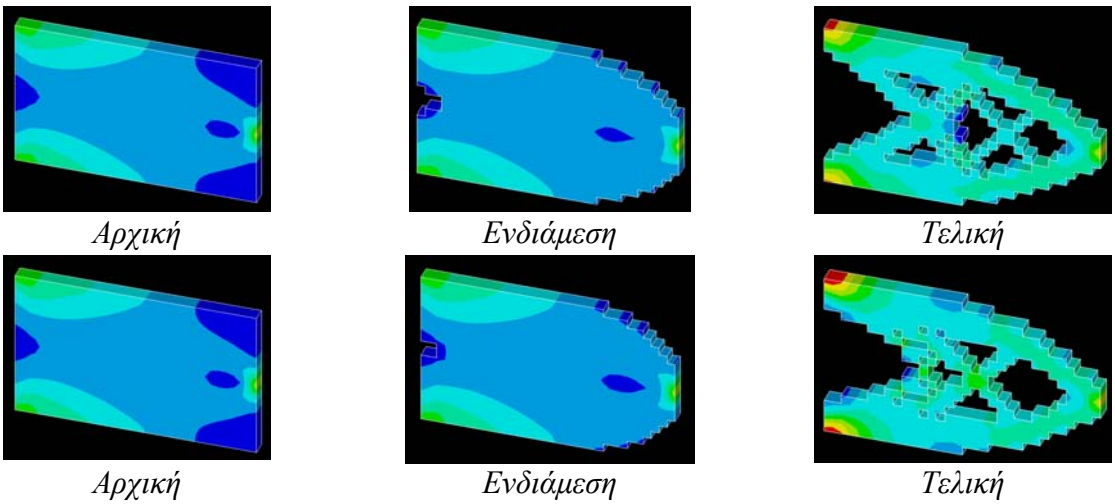

Σχήμα 4.24: Βελτιστοποιημένη σχεδίαση κοντού προβόλου (άνω σειρά: προτεινόμενη διαδικασία, κάτω σειρά: Βασικό Σχήμα Αποβολής - Basic Removal Scheme)

Κατ' αντιστοιχία του Σχήματος 4.22, στο Σχήμα 4.25 παρουσιάζονται τριάδες εικόνων για την περίπτωση της δοκού MBB.

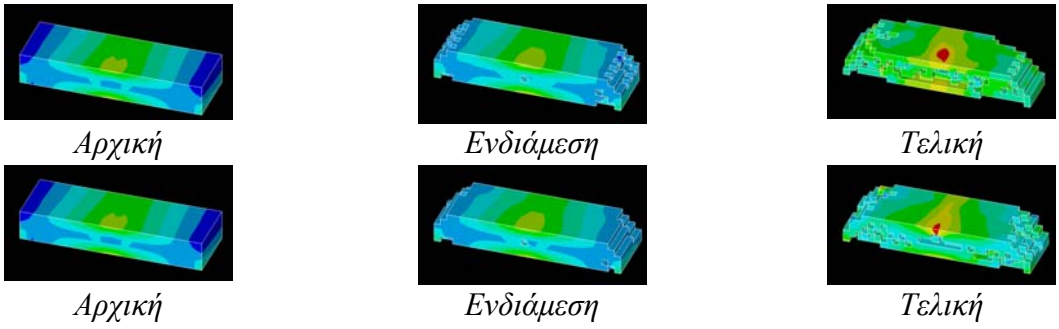

Σχήμα 4.25: Βελτιστοποιημένη σχεδίαση δοκού MBB (άνω σειρά: προτεινόμενη διαδικασία, κάτω σειρά: Βασικό Σχήμα Αποβολής - Basic Removal Scheme)

4.5.6. Συμπεράσματα

Από τα αποτελέσματα, τα οποία παρουσιάστηκαν στην προηγούμενη ενότητα, προέκυψε ότι, σε όλες τις περιπτώσεις, η προτεινόμενη διαδικασία βελτιστοποίησης κατέληξε σε ελαφρύτερες σχεδιάσεις. Επιπροσθέτως, διαπιστώθηκε ότι η χρήση του κριτηρίου αξιολόγησης του διαθέσιμου υλικού βάσει της κανονικοποιημένης πυκνότητας της ενέργειας παραμόρφωσης είναι δυνατόν να επηρεάσει την πορεία της βελτιστοποίησης, καταλήγοντας σε σχεδιάσεις ανώτερες, ως προς το βάρος και την κατανομή υλικού, από εκείνες οι οποίες έχουν καταγραφεί στη βιβλιογραφία και λαμβάνονται όταν χρησιμοποιείται η έννοια της ενέργειας παραμόρφωσης.

4.6. Ένα νέο Βέλτιστο Κριτήριο για την επιβολή περιορισμού τάσης σε σκελετικές κατασκευές

4.6.1. Θεωρητικό υπόβαθρό

Σύμφωνα με τον ορισμό του γενικευμένου προβλήματος βελτιστοποίησης μίας 2Δ σκελετικής κατασκευής υπό περιορισμό τάσεων, ανεξαρτήτως του πλήθους των επιβαλλομένων περιορισμών τάσεων, μόνον ένας τέτοιος περιορισμός είναι ενεργός στη βέλτιστη σχεδίαση. Αυτό σημαίνει ότι η μέγιστη επιτρεπόμενη τάση εμφανίζεται μόνο σε ένα δομικό στοιχείο, χωρίς, ωστόσο, να είναι γνωστό εκ των προτέρων ποιο είναι αυτό το στοιχείο. Η μαθηματική διατύπωση του εν λόγω προβλήματος είναι η εξής:

$$\text{minimize } W = \sum_{k=1}^{NEL} \left(\rho_k \, A_k \, L_k \right) \tag{4.45}$$

$$\text{such that } \left| \sigma \right| \le \sigma_{allow} \text{ and } A_{\min} \le A \tag{4.46}$$

όπου A είναι το εμβαδόν διατομής, L το μήκος στοιχείου, ρ η πυκνότητα υλικού, σ η αξονική τάση, ο δείκτης k αναφέρεται στην $k-$ράβδο, ενώ ο δείκτης $allow$ αφορά σε επιτρεπόμενη τιμή. Το ολικό πλήθος των στοιχείων, ράβδων εν προκειμένω, δηλώνεται ως NEL, ενώ η χρήση του απολύτου στην Εξ.(4.46) δηλώνει ότι η ίδια επιτρεπόμενη τιμή θα χρησιμοποιηθεί και για εφελκυστικές και για θλιπτικές τάσεις. Επιπροσθέτως, επιβάλλεται κατώτατο όριο σχετικά με το εμβαδόν της διατομής, έτσι ώστε να εξασφαλισθεί ο σχηματισμός ενός θετικά ορισμένου μητρώου δυσκαμψίας. Σύμφωνα με τη μέθοδο των

πολλαπλασιαστών Lagrange, για το προαναφερθέν πρόβλημα και μη λαμβάνοντας υπόψη τον περιορισμό στο εμβαδόν των διατομών, η αντίστοιχη συνάρτηση Lagrange, έστω $\mathfrak{L}$, είναι:

$$\mathfrak{L} = \sum_{i=1}^{NEL} \left(\rho_i \, A_i \, L_i \right) + \lambda_1 \left(\left| \sigma \right| - \sigma_{allow} \right) \tag{4.47}$$

όπου λ_1 είναι ο πολλαπλασιαστής Lagrange για τον περιορισμό τάσης. Από τη Μηχανική του Παραμορφωσίμου Σώματος και αξιοποιώντας την έννοια του μοναδιαίου φορτίου, η τάση ενός ραβδόμορφου στοιχείου ισούται με:

$$\sigma_j = \sum_{i=1}^{NEL} \left(\frac{F_i^P F_i^Q}{A_i E_i} L_i \frac{E_j}{L_j} \right) \tag{4.48}$$

όπου, επιπροσθέτως των προαναφερομένων συμβόλων, με τον δείκτη j σημειώνεται το υπό θεώρηση ραβδόμορφο στοιχείο, στα άκρα του οποίου επιβάλλονται δύο μοναδιαία φορτία αντιθέτου φοράς και κατά τη διεύθυνση του στοιχείου. Επίσης, με E συμβολίζεται το μέτρο ελαστικότητας, ως F^P περιγράφεται η αναπτυσσόμενη αξονική δύναμη εξ αιτίας της επιβολής των πραγματικών φορτίων, ως F^Q περιγράφεται η αναπτυσσόμενη αξονική δύναμη εξ αιτίας της επιβολής των μοναδιαίων φορτίων, ενώ με τον δείκτη i δηλώνεται κάθε ένα από τα NEL στοιχεία της σκελετικής κατασκευής. Εισάγοντας την Εξ.(4.47) στην Εξ. (4.48) προκύπτει:

$$\mathfrak{L} = \sum_{i=1}^{NEL} \left(\rho_i \, A_i \, L_i \right) + \lambda_1 \left(\left| \sum_{i=1}^{NEL} \left(\frac{F_i^P F_i^Q}{A_i E_i} L_i \frac{E_j}{L_j} \right) \right| - \sigma_{allow} \right) \tag{4.49}$$

Η μερική παράγωγος της Εξ.(4.49) ως προς το εμβαδόν διατομής A_i ισούται με:

$$\nabla \mathfrak{L}_{A_i} = \rho_i \, L_i - \lambda_1 \left| \left(\frac{F_i^P F_i^Q}{A_i^2 E_i} L_i \frac{E_j}{L_j} \right) \right| + \lambda_1 \sum_l \left(\left(\left(\frac{\partial F_l^P}{\partial A_i} \right) F_l^Q + \left(\frac{\partial F_l^Q}{\partial A_i} \right) F_l \right) \left(\frac{L_l}{A_l E_l} \frac{E_j}{L_j} \right) \right) \tag{4.50}$$

Ωστόσο, οι όροι εντός του αθροίσματος είναι, ταυτοτικά, ίσοι με μηδέν. Αυτό συμβαίνει διότι, σε ισοστατικά δικτυώματα, η αξονική δύναμη ενός μέλους είναι ανεξάρτητη της διατομής του, ενώ, σε υπερστατικά δικτυώματα, ο Berke έχει δείξει ότι αυτοί οι όροι σχηματίζουν ένα ισορροπούν σύστημα εσωτερικών δυνάμεων (Berke και Khot, 1987). Λαμβάνοντας υπόψη τα ανωτέρω, η Εξ.(4.50) γράφεται:

$$\nabla \mathfrak{L}_{A_i} = \rho_i \, L_i - \lambda_1 \left| \left(\frac{F_i^P F_i^Q}{A_i^2 E_i} L_i \frac{E_j}{L_j} \right) \right| \tag{4.51}$$

Σύμφωνα με τη μέθοδο των πολλαπλασιαστών Lagrange, ισχύει:

$$\nabla \mathfrak{L}_{A_i} = 0 \tag{4.52}$$

Ο συνδυασμός των Εξ.(4.51, 4.52), μετά από πράξεις, δίδει:

$$1 = \lambda_1 \left| \left(\frac{F_i^P F_i^Q}{A_i A_i} \frac{1}{E_i} \frac{E_j}{L_j} \right) \right| \left(\frac{1}{\rho_i} \right) \tag{4.53}$$

Ο συντελεστής λ_1, ως μεμονωμένη ποσότητα, έχει σταθερή τιμή:

$$\lambda_1 = const \tag{4.54}$$

Θεωρώντας ότι όλα το μέλη της υπό εξέταση σκελετικής κατασκευής είναι κατασκευασμένα από το ίδιο υλικό, ισχύει:

$$\rho_i = const \tag{4.55}$$

Ο συνδυασμός των τελευταίων τριών εξισώσεων, μετά από εκτέλεση πράξεων, δίδει:

$$\left| \underbrace{\left(\frac{F_i^P F_i^Q}{A_i A_i} \frac{1}{E_i} \right)}_{w_i} \right| \underbrace{\left(\frac{E_j}{L_j} \right)}_{v_j} = const \tag{4.56}$$

Ο πρώτος όρος στην αριστερή πλευρά της Εξ.(4.56) αντιστοιχεί στην πυκνότητα της συμπληρωματικής ενέργειας παραμόρφωσης w_i της i-ράβδου, ενώ ο δεύτερος όρος, έστω v_j, εκφράζει το λόγο του μέτρου ελαστικότητας της $j-$ράβδου προς το μήκος της. Συνεπώς, σύμφωνα με την Εξ.(4.56), για τη σχεδίαση ελαχίστου βάρους υπό την ενεργοποίηση ενός περιορισμού τάσης, το γινόμενο των όρων w_i και v_j είναι εκείνη η ποσότητα, η οποία παραμένει σταθερή. Αυτό σημαίνει ότι το μήκος των μελών συμμετέχει σημαντικά στον καθορισμό της, επικρατούσας στη βέλτιστη σχεδίαση, ενεργειακής κατάστασης. Αν και η Εξ.(4.56) αποτελεί τη μαθηματική περιγραφή της εν λόγω ενεργειακής κατάστασης, δεν υποδεικνύει κάποιον δρόμο προς την επίτευξη αυτής, οπότε υπάρχει περιθώριο ανάπτυξης νέων διαδικασιών, οι οποίες θα καταλήγουν στην ικανοποίηση της Εξ.(4.56). Σε αυτό το πλαίσιο, προτείνεται μία νέα διαδικασία, κλειστής μορφής για ισοστατικά δικτυώματα και αναδρομικής μορφής για υπερστατικά δικτυώματα, η οποία περιγράφεται λεπτομερέστερα στην επόμενη Ενότητα.

4.6.2. Προτεινόμενη διαδικασία

Έστω μία σκελετική κατασκευή από NEL ράβδους και έστω ένα αρχικό διάνυσμα σχεδίασης με τυχαία επιλεγμένες διατομές. Μία ανάλυση της κατασκευής με τη Μέθοδο των Πεπερασμένων Στοιχείων και χρησιμοποιώντας τα πραγματικά επιβαλλόμενα φορτία δίδει το πεδίο των κομβικών μετατοπίσεων καθώς και τα αξονικά φορτία F_i^P, βάσει των οποίων είναι δυνατόν να εντοπισθεί το μέλος, έστω $N_{\sigma_{max}}$, με την μεγαλύτερη αξονική τάση. Μία άλλη ανάλυση τέτοιου τύπου χρησιμοποιώντας ένα ζεύγος μοναδιαίων φορτίων, ασκουμένων στα άκρα του μέλους $N_{\sigma_{max}}$ δίδει τα αξονικά φορτία F_i^Q. Γνωρίζοντας τα προαναφερθέντα φορτία, είναι δυνατόν να εντοπισθούν τα μέλη με μη-μηδενικά γινόμενα φορτίων, δηλαδή τα μέλη για τα οποία ισχύει $\left| F_i^P F_i^Q \right| > tol$, όπου tol είναι μία μικρή, θετική ποσότητα (1E-06). Για κάθε μία από αυτές τις ράβδους, είναι δυνατόν να ορισθεί η ακόλουθη ποσότητα:

$$\mathbf{w}_i = w_i v_j \tag{4.57}$$

Η αντίστοιχη μέση τιμή $\bar{\mathbf{w}}$ όλων των τιμών $\mathbf{w}_i$ ισούται με:

$$\bar{\mathbf{w}} = \left(\frac{\sum_{i=1}^{N_{active}} \mathbf{w}_i}{N_{active}} \right) \tag{4.58}$$

Αντικαθιστώντας την ποσότητα $\mathbf{w}_i$ της Εξ.(4.57) με τη μέση τιμή $\bar{\mathbf{w}}$ από την Εξ.(4.58), προκύπτει:

$$\bar{\mathbf{w}} = \left(\frac{F_{i,new}^P F_{i,new}^Q}{A_{i,new} A_{i,new}} \frac{1}{E_i} \right) \left(\frac{E_j}{L_j} \right) \tag{4.59}$$

όπου $A_{i,new}$ είναι η νέα τιμή της διατομής της $i-$ράβδου. Διαιρώντας την Εξ.(4.57) με την Εξ.(4.59) προκύπτει:

$$\frac{\mathbf{w}_i}{\bar{\mathbf{w}}} = \frac{\left(\frac{F_i^P F_i^Q}{A_i A_i} \frac{1}{E_i} \right) \left(\frac{E_j}{L_j} \right)}{\left(\frac{F_{i,new}^P F_{i,new}^Q}{A_{i,new} A_{i,new}} \frac{1}{E_i} \right) \left(\frac{E_j}{L_j} \right)} \tag{4.60}$$

Ωστόσο, για ένα ισοστατικό δικτύωμα, οι αξονικές δυνάμεις F_i^P και F_i^Q είναι ανεξάρτητες από τα εμβαδά των διατομών:

$$\left(\frac{\partial F_i^P}{\partial A_i} \right) = \left(\frac{\partial F_i^Q}{\partial A_i} \right) = 0 \tag{4.61}$$

Συνεπώς, μετά από μερικές πράξεις, η Εξ. (4.61) είναι δυνατόν να γραφεί, ως:

$$\frac{\mathbf{w}_i}{\bar{\mathbf{w}}} = \left(\frac{A_{i,new}^2}{A_i^2} \right) \tag{4.62}$$

Επιλύοντας την τελευταία εξίσωση ως προς τη νέα διατομή της $i-$ράβδου, προκύπτει:

$$A_{i,new} = A_i \sqrt{\left(\frac{\mathbf{w}_i}{\bar{\mathbf{w}}} \right)} \tag{4.63}$$

Αν και η Εξ. (4.63) προέρχεται από την αντιμετώπιση ενός ισοστατικού δικτυώματος, είναι δυνατόν να εφαρμοσθεί και σε υπερστατικά δικτυώματα, στα οποία η ευαισθησία των

αξονικών φορτίων σε μεταβολές των εμβαδών των διατομών των ράβδων είναι μικρή. Αυτό συμβαίνει είτε όταν η ισορροπία των δυνάμεων έχει σημαντικά μεγαλύτερη επίδραση από τη συμβιβαστότητα των μετατοπίσεων είτε όταν η σχεδίαση βρίσκεται πλησίον της βέλτιστης. Για άλλες περιπτώσεις υπερστατικών δικτυωμάτων, η Εξ.(4.63) πρέπει να χρησιμοποιείται επαναληπτικά μέχρι συγκλίσεως. Προκειμένου, δε, να ελεγχθεί ότι οι επανασχεδιασθείσες διατομές δεν οδηγούν στην παραβίαση του επιβαλλομένου περιορισμού τάσης, απαιτείται μία ομοιόμορφη διακλιμάκωση των διατομών των ράβδων.

4.6.3. Ομοιόμορφη διακλιμάκωση του διανύσματος σχεδίασης

Για ένα ισοστατικό δικτύωμα, η τιμή της ποσότητας $\mathbf{w}_i$ εξαρτάται από τις δυνατές δυνάμεις F_i^Q, το εμβαδόν διατομής A_i, το μήκος L_i και το μήκος L_j. Συνεπώς, σε μία κατασκευή σταθερής τοπολογίας και υπό την προϋπόθεση ότι χρησιμοποιείται ένα υλικό, ισχύει:

$$\left(\frac{F_i^P F_i^Q}{A_i E_i}\right) L_i \left(\frac{E_j}{L_j}\right) = f\left(F_i^Q, A_i\right) \tag{4.64}$$

Θεωρώντας ότι το μέλος, στο οποίο ασκείται το ζεύγος των μοναδιαίων φορτίων είναι γνωστό, οι δυνάμεις F_i^Q είναι, επίσης, γνωστές, οπότε η Εξ.(4.64) λαμβάνει τη μορφή:

$$\left(\frac{F_i^P F_i^Q}{A_i E_i}\right) L_i \left(\frac{E_j}{L_j}\right) = f\left(A_i\right) \tag{4.65}$$

όπου η διατομή A_i αποτελεί τον μοναδικό άγνωστο. Συνεπώς, κάθε προσθετέος στην Εξ.(4.48), ο οποίος είναι αριθμητικά ίσος προς τη συνεισφορά της κάθε ράβδου στην τάση της $j-$ράβδου, είναι δυνατόν να υποστεί διακλιμάκωση μέσω της απλής μεταβολής της διατομής A_i. Επιπροσθέτως, από τον συνδυασμό των ανωτέρω εξισώσεων προκύπτει ότι εάν εφαρμοσθεί η ίδια διακλιμάκωση σε όλες τις διατομές A_i (ομοιόμορφη διακλιμάκωση), τότε η τάση στη $j-$ράβδο διακλιμακώνεται ισόποσα:

$$\sigma_{scaled} = a_\sigma \, \sigma_{before\_scaling} \tag{4.66}$$

Η σταθερά a_σ υποδηλώνει ένα συντελεστή διακλιμάκωσης, ως προς τη μέγιστη εμφανιζόμενη αξονική τάση. Εάν ως σ_{scaled} επιλεχθεί η μέγιστη επιτρεπόμενη τάση σ_{allow}, τότε ο συντελεστής a_σ καθίσταται ίσος προς το λόγο της επιτρεπόμενης προς την εμφανιζόμενη τάση (για απλότητα στη γραφή, ο δείκτης *before_scaling* παραλείπεται):

$$a_\sigma = \left(\frac{\sigma_{allow}}{\sigma}\right) \tag{4.67}$$

Ο συνδυασμός των Εξ. (4.48, 4.66) δίδει:

$$\sigma_{allow} = a_\sigma \left(\sum_{i=1}^{NEL} \left(\frac{F_i^P F_i^Q}{A_i E_i} L_i \frac{E_j}{L_j} \right) \right) \tag{4.68}$$

Δεδομένου ότι ο συντελεστής διακλιμάκωσης είναι σταθερός, η Εξ. (4.68) γράφεται ως:

$$\sigma_{allow} = \sum_{i=1}^{NEL} \left(\frac{F_i^P F_i^Q}{\left(\frac{A_i}{a_\sigma} \right) E_i} L_i \frac{E_j}{L_j} \right) \tag{4.69}$$

Η σύγκριση μεταξύ της Εξ.(4.69) και της Εξ.(4.48) δίδει την ακόλουθη εξίσωση επανασχεδίασης:

$$A_{i,new} = \left(\frac{A_{i,old}}{a_\sigma} \right) \tag{4.70}$$

όπου οι δείκτες *new* και *old* δηλώνουν τη νέα και την παλιά τιμή της διατομής της $i-$ράβδου, αντίστοιχα. Συνεπώς, είναι δυνατή η ομοιόμορφη διακλιμάκωση των, επανασχεδιασμένων με την Εξ.(4.63), διατομών διαιρώντας αυτές με τον συντελεστή διακλιμάκωσης a_σ.

Η ανωτέρω ανάλυση στηρίχθηκε στην εφαρμογή ενός ζεύγους μοναδιαίων φορτίων στην εκάστοτε υπό εξέταση ράβδο, η οποία ονομάσθηκε $j-$ράβδος. Η επιλογή αυτής της ράβδου είναι εξαιρετικής σημασίας. Σε μια διαδικασία βελτιστοποίησης, η κακή επιλογή της $j-$ράβδου είναι δυνατόν να οδηγήσει σε κάποιο τοπικό ακρότατο αρκετά μακριά από το καθολικό ακρότατο. Όπως περιγράφεται λεπτομερέστερα και στην Ενότητα 5.2.4, ειδικά η επιλογή της $j-$ράβδου στην πρώτη επανάληψη της διαδικασίας βελτιστοποίησης έχει ιδιαίτερη βαρύτητα. Ενδείκνυται, δε, η διαδικασία βελτιστοποίησης να εκκινείται από εκείνη τη σχεδίαση, στην οποία κάθε μέλος χαρακτηρίζεται από μοναδιαία δυσκαμψία. Περισσότερες λεπτομέρειες επ' αυτού αναφέρονται στο Κεφάλαιο 5.

4.6.4. Σχολιασμός

Με βάσει τα ανωτέρω, διατυπώθηκε μία θεωρητική λύση του προβλήματος της ελαχιστοποίησης βάρους μίας 2Δ σκελετικής κατασκευής υπό την επιβολή ενός γενικευμένου περιορισμού τάσης. Σε αυτήν τη διατύπωση, υπάρχουν διάφορα θέματα προς περαιτέρω διερεύνηση, όπως η επιλογή της αρχικής σχεδίασης και ο τρόπος χαρακτηρισμού ενός μέλους ως 'ενεργό' ή 'παθητικό'. Αυτά τα θέματα, εξετάζονται εκτενώς στο επόμενο κεφάλαιο.

Βιβλιογραφία

Armand, J.L., Lodier, B. (1978), "Optimal design of bending elements", Int. J. Num. Meth. Engng., Vol. 13, pp.373-384.

Atrek, E., Kodali, R. (1989), :Optimum design of continuum structures, with SHAPE:, In: Prasad B.: *CAD/CAM Robotics and Factories of the Future*, Vol. 2, pp.11–15, Proc of 3rd Int. Conf CARS and FOF-'88, Berlin, Springer.

Belegundu, A.D., Chandrupatla, T.R. (1999), *Optimization concepts and applications in engineering*, Prentice Hall.

Bendsøe, M.P. (1986), Generalized plate models and optimal design, in J.L.Ericksen, D. Kinderlehrer, R.V. Kohn & J.L. Lions (eds), *Homogenization and Effective Moduli of Materials and Media*, Springer-Verlag, Berlin;New York, pp.1-26.

Bendsøe, M.P., Kikuchi, N. (1988), "Generating optimal topologies in structural design using a homogenization method", Comp. Meth. App. Mechs. Engng, Vol. 71(2), pp.197-224.

Bendsøe, M.P., Sigmund O. (2003), *Topology Optimization, Theory, Methods and Applications*, Springer-Verlag.

Bendsøe, M.P. Optimization of Structural Topology, Shape, and Material. Berlin: Springer-Verlag, 1995.

Berke L, Khot N.S., (1987), "Structural optimization using optimality criteria", in: Computer Aided Optimal Design: Structural and Mechanical Systems, edited by C.A. Mota Soares, NATO, ASI series, F27B.

Cea, J., Malanowski, K. (1970), "An example of a max-min problem in partial differential equations", SIAM J. Control, Vol. 8, pp.305–316.

Cheng, K.T., Olhoff, N. (1981), "An investigation concerning optimal design of solids elastic plates", Int. J. Solids Structures, Vol.17, pp.305-323.

Diaz, A., Sigmund, 0. (1995), "Checkerboard Patterns in Layout Optimization", Struct Optim, Vol.10, pp.40-45.

Drucker, D.C., Shield, R.T. (1957), "Bounds on minimum-weight design", Q. appl. Math., Vol.5, pp.269-281.

Duysinx P and Bendsøe M P. Topology optimization of continuum structures with local stress constraints. Int. J. Numer. Meth. Engng., 1998, 43:1456-1478.

Eschenauer, H.A., Kobelev, H.A., Schumacher A., (1994), "Bubble method for topology and shape optimization of structures", Struct Optimization, vol. 8, pp.142-51.

Eschenauer, H.A., Kobelev, V.V., Schumacher, A. (1994), "Bubble method for topology and shape optimization of structures", Struct. Multidisc. Optim., Vol. 8, pp.42–51.

Felippa, C.A. (2001), *Introduction to Finite Element Methods*, University of Colorado, Boulder.

Freiberger, W., Tekinalp, B. (1956), "Minimum-weight design of circular plates", J. Mech. Phys. Solids, Vol.4, pp.294-299.

Gallagher RH. Fully Stressed Design, In: R. H. Gallagher & O. C. Zienkiewicz (eds.), Optimum Structural Design: Theory and Applications. John Wiley & Sons:1973.

Garreau, S., Masmoudi, M., Guillaume, P. (1999), "The topological sensitivity for linear isotropic elasticity", *ECCM'99*, Germany.

Giannakoglou, K., Tsahalis, D., Periaux, J., Papailiou, K. and Fogarty, T. C., (2002), "Evolutionary Methods for Design, Optimisation and Control", CIMNE, Barcelona.

Haftka R T, Gurdal Z and Kamat M. Elements of Structural Optimization. Kluwer: 1990.

Hassani B and Hinton E. A review of homogenization and topology optimization III-topology optimization using optimality criteria. Comp. Struct., 1998, 69:739-756.

Hopkins, H.G, Prager, W. (1955), "Limits of economy of materials in plates", J. appl. Mech., Vol.22, pp.372-374.

Huang, N.C. (1968), "Optimal design of elastic structures for maximum stiffness", Int. J. Solids Structures, Vol.4, pp.689-700.

Kirsch U. Optimal Topologies of Structures. Appl Mech Rev, 1989, 42: 238.

Lipton, R. (1994), "Optimal design and relaxation for reinforced plates subject to random transverse loads", J. Prob. Engng. Mech., Vol. 9, pp.167-177.

Lipton, R., Diáz, A.R. (1997), "Reinforced Mindlin plates with extremal stiffness", Int. J. Solids Structures, Vol. 24(28), 3691-3704.

Liu, J.S., Parks, G.T., Clarkson, P.J. (2000), "Metamorphic development: A new topology optimization method for continuum structures", Struct. Multidisc. Optim., Vol. 20, pp.288–300.

Makris, P., Provatidis, C. (2002), "Weight minimisation of displacement-constrained truss structures using a strain energy criterion", Computer Methods Appl. Mech. Engrg., vol. 191, pp. 2159-2177.

Mattheck, C. (1992), *Design in Nature*, Freiburg.

Megarefs, G.J. (1966), "Method of minimal design of axisymmetric plates", J. Engng Mech. Div. Am. Soc. Civ. Engrs, Vol.92, No. EM6, pp.79-99.

Mlejnek, H.P., Schirrmacher R., (1993), "An engineer's approach to optimal material distribution and shape finding", Computer Methods Appl. Mech. Engrg., vol. 106, pp. 1-26.

Morris, A.J. (1982), Foundations of Structural Optimization: A Unified Approach, John Wiley & Sons.

Mróz, Z. (1961), "On a problem of minimum-weight design", Q. appl. Math., Vol.19, pp.127-135.

Mróz, Z. (1973), "Multi-parameter optimal design of plates and shells", J. Struct. Mech, Vol.1, pp.371-392.

Olhoff, N. (1970), "Optimal design of vibrating plates", Int. J. Solids Structures, Vol.6, pp.139-156.

Olhoff, N. (2000), Comparative study of optimizing the topology of plate-like structures via plate theory and 3-D elasticity, in G.I.N. Rozvany & N. Olhoff (eds), *Topology Optimization of Structures and Composite Continua*, Kluwer Academic Publishers, Dordrecht, pp.37-48.

Patnaik SN, Guptill JD and Berke L. Merits and limitations of optimality criteria method for structural optimization, Int. J. Numer. Meth. Engng, 1995, 38: 3087-3120.

Pham D T and Karaboga D. Intelligent Optimisation Techniques: Genetic Algorithms, Tabu Search, Simuated Annealing and Neural Networks. Springer: 2000.

Prasad, B., Haftka, R.T. (1979), "Optimal structural design with plate finite elements", J. Struct. Div., Vol. 105, pp. 2367-2382.

Provatidis. C.G., Venetsanos, D.T. (2005), "The Influence Of Normalizing The Virtual Strain Energy Density On The Shape Optimization Of 2D Continua", 1st IC-EpsMsO, Athens, 6-9 July, 2005.

Qing L and Steven G P and Xie Y M. Evolutionary structural optimization for stress minimization problems by discrete thickness design. Comp. Struct., 2000, 78(6): 769-780.

Querin, O.M, Steven, G.P., Xie, Y.M. (1998), "Evolutionary structural optimization – ESO: Using a bidirectional algorithm", J. Eng. Comput. Vol. 15, pp., 1031–1048.

Querin, O.M, Steven, G.P., Xie, Y.M. (2000), "Evolutionary structural optimisation using an additive algorithm", Finite Elements in Analysis and Design, Vol.34, pp.291-308.

Rossow, H.P., Taylor, J.E. (1973), "A finite element method for the optimal design of variable thickness sheets", AIAA J, Vol.11, pp.1566–1569.

Rozvany GIN, Bendsoe M P and Kirsch U. Layout Optimization of Structures. Appl Mech Rev, 1995, 48: 41-119.

Rozvany GIN. Aims, scope, methods, history and unified terminology of computer-aided topology optimization in structural mechanics. Struct. Multidisc Optim., 2001, 21:90-108.

Rozvany GIN. Stress ratio and compliance based methods in topology optimization – a critical review. Struct. Multidisc. Optim., 2001, 21:109-119.

Rozvany, G.I.N., (1997), *Topology optimization in structural mechanics*, CISM, Springer-Verlag.

Rozvany, G.I.N, (2001), "Aims, scope, methods, history and unified terminology of computer-aided topology optimization in structural mechanics", Struct. Multidisc Optim., vol. 21, pp. 90-108.

Schmidt L A. Fully Stressed Design of elastic redundant trusses under alternative loading systems. Australian Journal of Applied Science, 1958, (9):337-348.

Sheu, C.Y., Prager, W. (1969), "Optimal plastic design of circular and annular sandwich plates with piecewise constant cross section", J. Mech., Phys. Solids., Vol.17, pp.11-16.

Sokolowski, J., Zochowski, A. (1997), *On topological derivative in shape optimization*, RR No 3170, INRIA Lorraine, Nancy, France.

Soto, C.A., Diáz, A.R. (1993), "On modeling of ribbed plates for shape optimization", Struct. Opt., Vol. 6, pp.175-188.

Suzuki, K., Kikuchi, N., (1991), "A Homogenization Method for Shape and Topology Optimization", Computer Methods Appl. Mech. Engrg., vol. 93, pp. 291-318.

Tenek, L.H., Hagiwara, I. (1993), "Optimization of material distribution within isotropic and anisotropic plates using homogenization", Comp. Meth. App. Mechs. Engng, Vol. 109(1-2), pp.155-167.

Vanderplaats G N. Numerical Optimization Techniques for Engineering Design. McGraw-Hill: 1984.

Xie, Y.M., Steven, G.P. (1997), *Evolutionary Structural Optimization*, Springer-Verlag.

Xie,Y.M., Steven, G.P. (1993), "A simple evolutionary procedure for structural optimization", Comp Struct,Vol.49, pp.885–896.

Εργασίες

[1] Provatidis, C.G. and **Venetsanos, D.T.**, "Performance of the FSD in shape and topology optimization of two-dimensional structures using continuous and truss-like models", In: C. Cinquini, M. Rovati, P. Venini and R. Nascimbene (eds.), Proceedings Fifth World Congress of Structural and Multidisciplinary Optimization, May 19-23, 2003, Lido di Jesolo, Italy, pp. 385-386, Schönenfeld & Ziegler (ISBN 88-88412-18-2).

[2] **Venetsanos D.T.** and Provatidis C.G., "Fully stressed 2D continua formed by applying the stress-ratio technique to finite elements of variable thickness", *1st IC-EpsMsO, 6-9 July 2005, Athens, Greece*.

[3] Provatidis C.G., **Venetsanos D.T.**, Kesimoglou N.C., "Layout Optimization Of A Stress-Constrained Plate Under Out-Of-Plane Loading", *2nd International Conference "From Scientific Computing to Computational Engineering", Athens, 5-8 July, 2006.*

[4] Provatidis C.G., **Venetsanos D.T.**, Champilos S.D. "Weight Minimization Of 3D Continuum Structures Under Stress Constraints", *2nd International Conference "From Scientific Computing to Computational Engineering", Athens, 5-8 July, 2006*.

[5] **Venetsanos D.**, Magoula E. and Provatidis C. "Layout Optimization of Stressed Constrained 2D Continua Using Finite Elements of Variable Thickness", *6th International Congress on Computational Mechanics (GRACM), Thessaloniki, 19-21 June 2008*.

ΠΑΡΑΡΤΗΜΑ 4Α: Μητρώο δυσκαμψίας για τη Βασική Συνεχή Μονάδα (Basic Continuum Unit - BCU) και τη Βασική Διακριτή Μονάδα (Basic Discrete Unit -BDU)

Το μητρώο δυσκαμψίας για το τετραπλευρικό ορθογωνικό στοιχείο επίπεδης ελαστικότητας (Basic Continuum Unit - BCU) είναι:

$$K_{2D}=\begin{bmatrix} 2s_1+2s_4 & & & & & & & \\ s_3+s_6 & 2s_2+2s_5 & & & & & & \\ -2s_1+s_4 & -s_3+s_6 & 2s_1+2s_4 & & (sym.) & & & \\ s_3-s_6 & s_2-2s_5 & -s_3-s_6 & 2s_2+2s_5 & & & & \\ -s_1-s_4 & -s_3-s_6 & s_1-2s_4 & -s_3+s_6 & 2s_1+2s_4 & & & \\ -s_3-s_6 & -s_2-s_5 & s_3-s_6 & -2s_2+s_5 & s_3+s_6 & 2s_2+2s_5 & & \\ s_1-2s_4 & s_3-s_6 & -s_1-s_4 & s_3+s_6 & -2s_1+s_4 & -s_3+s_6 & 2s_1+2s_4 & \\ -s_3+s_6 & -2s_2+s_5 & s_3+s_6 & -s_2-s_5 & s_3-s_6 & s_2-2s_5 & -s_3-s_6 & 2s_2+2s_5 \end{bmatrix} \quad (4.A1)$$

όπου

$$s_1=\frac{tb}{6a}D_{11} \quad s_2=\frac{ta}{6b}D_{22} \quad s_3=\frac{t}{4}D_{12} \quad s_4=\frac{ta}{6b}D_{33} \quad s_5=\frac{tb}{6a}D_{33} \quad s_6=\frac{t}{4}D_{33} \quad (4.A2)$$

και

$$D=\frac{E}{1-\nu^2}\begin{bmatrix} 1 & \nu & 0 \\ \nu & 1 & 0 \\ 0 & 0 & \kappa \end{bmatrix} \qquad \kappa=\frac{1-\nu}{2} \quad (4.A3)$$

Είναι προφανές ότι τα στοιχεία του μητρώου K_{2D} είναι γραμμικοί συνδυασμοί των ζευγών (s_1,s_4) ή (s_2,s_5) ή (s_3,s_6). Οι ποσότητες του τελευταίου ζεύγους είναι ανεξάρτητες από τις γεωμετρικές διαστάσεις (a,b) της Βασικής Συνεχούς Μονάδος (BCU), οπότε η τιμή των αντιστοίχων στοιχείων του μητρώου K_{2D} δεν μεταβάλλεται καθώς μεταβάλλεται ο λόγος πλευρών $\lambda=(a/b)$. Σχετικά με τα ζεύγη (s_1,s_4) και (s_2,s_5), ισχύει:

$$(s_1,s_4)=\left(\frac{t}{6}\frac{E}{(1-\nu^2)}\right)\left(\frac{1}{\lambda},\lambda\frac{1-\nu}{2}\right) \qquad (s_2,s_5)=\left(\frac{t}{6}\frac{E}{(1-\nu^2)}\right)\left(\lambda,\frac{1}{\lambda}\frac{1-\nu}{2}\right) \quad (4.A4)$$

Οι εμφανιζόμενοι συνδυασμοί, των όρων αυτών των ζευγών, στο μητρώο K_{2D} είναι:

$$\begin{Bmatrix} 2(s_1+s_4) \\ -2s_1+s_4 \\ -(s_1+s_4) \\ (s_1-2s_4) \end{Bmatrix}=\left(\frac{t}{6}\cdot\frac{E}{(1-\nu^2)}\right)\cdot\begin{Bmatrix} 2\left(\frac{1}{\lambda}+\lambda\cdot C\right) \\ -2\frac{1}{\lambda}+\lambda\cdot C \\ -\left(\frac{1}{\lambda}+\lambda\cdot C\right) \\ \frac{1}{\lambda}-2\cdot\lambda\cdot C \end{Bmatrix} \qquad \begin{Bmatrix} 2(s_2+s_5) \\ -2s_2+s_5 \\ -(s_2+s_5) \\ (s_2-2s_5) \end{Bmatrix}=\left(\frac{t}{6}\cdot\frac{E}{(1-\nu^2)}\right)\cdot\begin{Bmatrix} 2\left(\lambda+\frac{1}{\lambda}\cdot C\right) \\ -2\lambda+\frac{1}{\lambda}\cdot C \\ -\left(\lambda+\frac{1}{\lambda}\cdot C\right) \\ \lambda-2\cdot\frac{1}{\lambda}\cdot C \end{Bmatrix} \quad (4.A5)$$

όπου

$$C = \left(\frac{1-\nu}{2} \right) \tag{4.A6}$$

Είναι προφανές ότι οι όροι στην (4.A5) εξαρτώνται μόνο από τον λόγο πλευρών λ, δεδομένου ότι η ποσότητα C είναι σταθερή. Από την άλλη πλευρά, το μητρώο δυσκαμψίας του συναρμολογήματος των έξι ράβδων (Basic Discrete Unit - BDU) ισούται με:

$$K_{TRUSS} = \begin{bmatrix}
\frac{EA_1}{2a}+\frac{EA_5}{l}c^2 & & & & & & & \\
\frac{EA_5}{l}cs & \frac{EA_4}{2b}+\frac{EA_5}{l}s^2 & & & & & & \\
\frac{-EA_1}{2a} & 0 & \frac{EA_1}{2a}+\frac{EA_6}{l}c^2 & & (sym.) & & & \\
0 & 0 & -\frac{EA_6}{l}cs & \frac{EA_2}{2b}+\frac{EA_6}{l}s^2 & & & & \\
-\frac{EA_5}{l}c^2 & -\frac{EA_5}{l}cs & 0 & 0 & \frac{EA_3}{2a}+\frac{EA_5}{l}c^2 & & & \\
-\frac{EA_5}{l}cs & -\frac{EA_5}{l}c^2 & 0 & \frac{-EA_2}{2b} & \frac{EA_5}{l}cs & \frac{EA_2}{2b}+\frac{EA_5}{l}c^2 & & \\
0 & 0 & -\frac{EA_6}{l}c^2 & \frac{EA_6}{l}cs & -\frac{EA_3}{2a} & 0 & \frac{EA_3}{2a}+\frac{EA_6}{l}c^2 & \\
0 & \frac{EA_4}{2b} & \frac{EA_6}{l}cs & -\frac{EA_6}{l}s^2 & 0 & 0 & -\frac{EA_6}{l}cs & \frac{EA_4}{2b}+\frac{EA_6}{l}s^2
\end{bmatrix} \tag{4.A7}$$

όπου

$$|c| = \left(\frac{2b}{l} \right) \quad |s| = \left(\frac{2a}{l} \right) \quad l = \sqrt{(2a)^2 + (2b)^2} \tag{4.A8}$$

Καθίσταται φανερό ότι κάποιοι όροι του μητρώου εξαρτώνται από μεμονωμένες τιμές των μεταβλητών a και b. Αυτό σημαίνει ότι εάν μεταβληθούν οι γεωμετρικές διαστάσεις της Βασικής Διακριτής Μονάδος (BDU), τότε θα μεταβληθεί και το μητρώο δυσκαμψίας K_{TRUSS}, ακόμα και εάν ο λόγος πλευρών διατηρηθεί ο ίδιος. Επίσης, το μητρώο K_{TRUSS} περιέχει μηδενικά στοιχεία, σε αντίθεση με το μητρώο K_{2D}. Εάν, δε, θεωρηθεί μία σταθερή τοπολογία για τις Βασικές Μονάδες, τότε οι όροι του μητρώου K_{2D} συσχετίζονται με μία μόνο μεταβλητή (το πάχος της Μονάδος BCU), ενώ οι μη-μηδενικοί όροι του μητρώου K_{TRUSS} συσχετίζονται με έξι μεταβλητές (τις διατομές των ράβδων της Μονάδος BDU). Οι τρεις προαναφερθείσες διαφορές, με έμφαση στην τελευταία, δικαιολογούν τη διαφορά στη συμπεριφορά των εν λόγω Βασικών Μονάδων.

ΠΑΡΑΡΤΗΜΑ 4Β: Μητρώο δυσκαμψίας στοιχείου επίπεδης ελαστικότητας με μεταβλητό πάχος

4Β.1 Γενικά

Έστω πεπερασμένο στοιχείο επίπεδης ελαστικότητας και μεταβλητού ενδοστοιχειακού πάχους, παρεμβαλλομένου με τις συναρτήσεις μορφής του στοιχείου (ισοπαραμετρική παρεμβολή πάχους) και έστω ότι αναζητείται ο υπολογισμός του μητρώου δυσκαμψίας του. Από τη θεωρία της Μεθόδου των Πεπερασμένων Στοιχείων, είναι γνωστό ότι ισχύει:

$$\left[k\right]_e = \int_{-1}^{+1}\int_{-1}^{+1} t_e \left[B\right]^T \left[D\right]\left[B\right] \det\left[J\right] d\xi\, d\eta \tag{4.B1}$$

όπου t_e είναι το πάχος του e-στοιχείου, ο πίνακας $\left[B\right]$ προκύπτει από τις σχέσεις παραμορφώσεων-μετατοπίσεων, $\left[D\right]$ είναι το μητρώο ελαστικότητας και $\left[J\right]$ είναι ο Ιακωβιανός πίνακας. Έαν το πάχος παρεμβάλλεται ισοπαραμετρικά, τότε ισχύει:

$$t_e = N_1 t_1 + N_2 t_2 + N_3 t_3 + N_4 t_4 \tag{4.B2}$$

όπου N_i και t_i είναι οι συναρτήσεις μορφής και το πάχος του $i-$κόμβου, αντίστοιχα. Σε μητρωϊκή γραφή, ισχύει:

$$t_e = \left[N\right]\left\{t\right\} \tag{4.B3}$$

όπου ο πίνακας $\left[N\right]$ είναι διάστασης 4×1 και ο πίνακας $\left\{t\right\}$ είναι διάστασης 1×4. Ο συνδυασμός των Εξ. (4Β.1, 4Β.3) δίδει:

$$\left[k\right]_e = \int_{-1}^{+1}\int_{-1}^{+1} \left[N\right]\left\{t\right\} \left[B\right]^T \left[D\right]\left[B\right] \det\left[J\right] d\xi\, d\eta \tag{4.B4}$$

Σύμφωνα με τη μέθοδο ολοκλήρωσης κατά Gauss, η τιμή του 2Δ ολοκληρώματος

$$I = \int_{-1}^{+1}\int_{-1}^{+1} f\left(\xi,\eta\right) d\xi\, d\eta \tag{4.B5}$$

προσεγγίζεται ως:

$$I \approx \sum_{l=1}^{n}\sum_{m=1}^{n}\left(w_l\, w_m\, f\left(\xi_l,\eta_m\right)\right) \tag{4.B6}$$

όπου n είναι το πλήθος των σημείων Gauss, τα οποία πρόκειται να χρησιμοποιηθούν, οι δείκτες l,m δηλώνουν το τρέχον σημείο Gauss, ενώ οι ποσότητες w_l και w_m αντιπροσωπεύουν τα, αντιστοιχούντα στο σημείο Gauss $\left(\xi_l,\eta_m\right)$, βάρη. Ο συνδυασμός των Εξ. (4Β.5, 4Β.6) δίδει:

$$\left[k\right]_e = \sum_{l=1}^{n}\sum_{m=1}^{n}\left(w_l\, w_m\, f_i\left(\xi_l,\eta_m\right)\right) \tag{4.B7}$$

όπου η συνάρτηση εντός του αθροίσματος ισούται με:

$$f\left(\xi_l,\eta_m\right)=\left(\left[N\right]\{t\}\left[B\right]^T\left[D\right]\left[B\right]\det\left[J\right]\right)_{lm} \tag{4.B8}$$

Συνεπώς, το μητρώο δυσκαμψίας $\left[k\right]_e$ είναι δυνατόν να υπολογισθεί σύμφωνα με την ακόλουθη διαδικασία:

Βήμα 1: επιλογή του πλήθους των σημείων Gauss που πρόκειται να χρησιμοποιηθούν και για κάθε σημείο Gauss ορισμός των συντεταγμένων $\left(\xi_l,\eta_m\right)$ και των βαρών w_l, w_m

Βήμα 2: ορισμός της τιμής N_i των συναρτήσεων μορφής σε κάθε σημείο Gauss $\left(\xi_l,\eta_m\right)$

Βήμα 3: υπολογισμός των μητρώων $\left[B\right]$ και $\left[J\right]$ σε κάθε σημείο Gauss $\left(\xi_l,\eta_m\right)$

Βήμα 4: υπολογισμός της ποσότητας $f_i\left(\xi_l,\eta_m\right)$ σύμφωνα με την Εξ.(4B.8)

Βήμα 5: υπολογισμός του μητρώου δυσκαμψίας $\left[k\right]_e$ σύμφωνα με την Εξ.(4B.7)

4B.2 Εφαρμογή: τετρακομβικό τετραπλευρικό πεπερασμένο στοιχείο επίπεδης ελαστικότητας

Έστω ένα 4-κομβικό τετραπλευρικό πεπερασμένο στοιχείο επίπεδης ελαστικότητας. Η μετατόπιση $\left(u,v\right)$ ενός οποιουδήποτε σημείου του στοιχείου ισούται με:

$$\begin{aligned} u &= N_1u_1+N_2u_2+N_3u_3+N_4u_4 \\ v &= N_1v_1+N_2v_2+N_3v_3+N_4v_4 \end{aligned} \tag{4.B9}$$

Για το συγκεκριμένο πεπερασμένο στοιχείου, οι συναρτήσεις μορφής N_i, εκπεφρασμένες στο φυσικό σύστημα συντεταγμένων, γράφονται ως:

$$\begin{aligned} N_1 &= 0.25\left(1-\xi\right)\left(1-\eta\right) \\ N_2 &= 0.25\left(1+\xi\right)\left(1-\eta\right) \\ N_3 &= 0.25\left(1+\xi\right)\left(1+\eta\right) \\ N_4 &= 0.25\left(1-\xi\right)\left(1+\eta\right) \end{aligned} \tag{4.B10}$$

Το διάνυσμα των παραμορφώσεων ισούται με:

$$\{\varepsilon\}=\left\{\frac{\partial u}{\partial x}\quad\frac{\partial v}{\partial y}\quad\frac{\partial u}{\partial y}+\frac{\partial v}{\partial x}\right\}^T \tag{4.B11}$$

Για τον υπολογισμό των μερικών παραγώγων των μετατοπίσεων u και v στο Καρτεσιανό Σύστημα Συντεταγμένων, οι ανωτέρω μετατοπίσεις θεωρούνται ως:

$$\left.\begin{aligned} u=u\left(x,y\right),v=v\left(x,y\right), \\ x=x\left(\xi,\eta\right),y=y\left(\xi,\eta\right) \end{aligned}\right\}\Rightarrow\left\{\begin{aligned} u=u\left(x\left(\xi,\eta\right),y\left(\xi,\eta\right)\right) \\ v=v\left(x\left(\xi,\eta\right),y\left(\xi,\eta\right)\right) \end{aligned}\right\} \tag{4.B12}$$

Εφαρμόζοντας τον κανόνα της αλυσίδος, προκύπτει:

$$\left\{\begin{array}{l}\dfrac{\partial u}{\partial \xi}=\dfrac{\partial u}{\partial x}\dfrac{\partial x}{\partial \xi}+\dfrac{\partial u}{\partial y}\dfrac{\partial y}{\partial \xi}\\ \dfrac{\partial u}{\partial \eta}=\dfrac{\partial u}{\partial x}\dfrac{\partial x}{\partial \eta}+\dfrac{\partial u}{\partial y}\dfrac{\partial y}{\partial \eta}\end{array}\right\},\qquad \left\{\begin{array}{l}\dfrac{\partial v}{\partial \xi}=\dfrac{\partial v}{\partial x}\dfrac{\partial x}{\partial \xi}+\dfrac{\partial v}{\partial y}\dfrac{\partial y}{\partial \xi}\\ \dfrac{\partial v}{\partial \eta}=\dfrac{\partial v}{\partial x}\dfrac{\partial x}{\partial \eta}+\dfrac{\partial v}{\partial y}\dfrac{\partial y}{\partial \eta}\end{array}\right\} \tag{4.B13}$$

Ισοδύναμα, ισχύει:

$$\left\{\begin{array}{l}\dfrac{\partial u}{\partial \xi}\\ \dfrac{\partial u}{\partial \eta}\end{array}\right\}=\underbrace{\left[\begin{array}{ll}\dfrac{\partial x}{\partial \xi} & \dfrac{\partial y}{\partial \xi}\\ \dfrac{\partial x}{\partial \eta} & \dfrac{\partial y}{\partial \eta}\end{array}\right]}_{J}\left\{\begin{array}{l}\dfrac{\partial u}{\partial x}\\ \dfrac{\partial u}{\partial y}\end{array}\right\},\qquad \left\{\begin{array}{l}\dfrac{\partial v}{\partial \xi}\\ \dfrac{\partial v}{\partial \eta}\end{array}\right\}=\underbrace{\left[\begin{array}{ll}\dfrac{\partial x}{\partial \xi} & \dfrac{\partial y}{\partial \xi}\\ \dfrac{\partial x}{\partial \eta} & \dfrac{\partial y}{\partial \eta}\end{array}\right]}_{J}\left\{\begin{array}{l}\dfrac{\partial v}{\partial x}\\ \dfrac{\partial v}{\partial y}\end{array}\right\} \tag{4.B14}$$

Στην Εξ. (4Β.14) εμφανίζεται ο 2×2 Ιακωβιανός πίνακας J, ο οποίος συνδέει το Καρτεσιανό Σύστημα Συντεταγμένων (x,y) με το φυσικό σύστημα συντεταγμένων (ξ,η). Ειδικότερα, οι Καρτεσιανές Συντεταγμένες (x,y) οποιουδήποτε σημείου ενός πεπερασμένου στοιχείου επίπεδης ελαστικότητας είναι δυνατόν να περιγραφούν ως:

$$\begin{aligned}x&=N_1x_1+N_2x_2+N_3x_3+N_4x_4\\ y&=N_1y_1+N_2y_2+N_3y_3+N_4y_4\end{aligned} \tag{4.B15}$$

Η παράγωγος της Εξ. (4Β.15) ως προς ξ και η ισούται με:

$$\begin{aligned}\frac{\partial x}{\partial \xi}&=\frac{\partial N_1}{\partial \xi}x_1+\frac{\partial N_2}{\partial \xi}x_2+\frac{\partial N_3}{\partial \xi}x_3+\frac{\partial N_4}{\partial \xi}x_4\\ \frac{\partial y}{\partial \xi}&=\frac{\partial N_1}{\partial \xi}y_1+\frac{\partial N_2}{\partial \xi}y_2+\frac{\partial N_3}{\partial \xi}y_3+\frac{\partial N_4}{\partial \xi}y_4\\ \frac{\partial x}{\partial \eta}&=\frac{\partial N_1}{\partial \eta}x_1+\frac{\partial N_2}{\partial \eta}x_2+\frac{\partial N_3}{\partial \eta}x_3+\frac{\partial N_4}{\partial \eta}x_4\\ \frac{\partial y}{\partial \eta}&=\frac{\partial N_1}{\partial \eta}y_1+\frac{\partial N_2}{\partial \eta}y_2+\frac{\partial N_3}{\partial \eta}y_3+\frac{\partial N_4}{\partial \eta}y_4\end{aligned} \tag{4.B16}$$

Σε μητρωϊκή γραφή, ισχύει:

$$\begin{aligned}\frac{\partial x}{\partial \xi}&=\left[\frac{\partial N_1}{\partial \xi}\quad\frac{\partial N_2}{\partial \xi}\quad\frac{\partial N_3}{\partial \xi}\quad\frac{\partial N_4}{\partial \xi}\right]\left[x_1\quad x_2\quad x_3\quad x_4\right]^T\\ \frac{\partial y}{\partial \xi}&=\left[\frac{\partial N_1}{\partial \xi}\quad\frac{\partial N_2}{\partial \xi}\quad\frac{\partial N_3}{\partial \xi}\quad\frac{\partial N_4}{\partial \xi}\right]\left[y_1\quad y_2\quad y_3\quad y_4\right]^T\\ \frac{\partial x}{\partial \eta}&=\left[\frac{\partial N_1}{\partial \eta}\quad\frac{\partial N_2}{\partial \eta}\quad\frac{\partial N_3}{\partial \eta}\quad\frac{\partial N_4}{\partial \eta}\right]\left[x_1\quad x_2\quad x_3\quad x_4\right]^T\\ \frac{\partial y}{\partial \eta}&=\left[\frac{\partial N_1}{\partial \eta}\quad\frac{\partial N_2}{\partial \eta}\quad\frac{\partial N_3}{\partial \eta}\quad\frac{\partial N_4}{\partial \eta}\right]\left[y_1\quad y_2\quad y_3\quad y_4\right]^T\end{aligned} \tag{4.B17}$$

Οι μερικές παράγωγοι των συναρτήσεων μορφής N_i υπολογίζονται από την Εξ.(4Β.10) και είναι ίσες προς:

$$\left\{\begin{array}{l}\dfrac{\partial N_1}{\partial \xi}=-0.25(1-\eta)\\ \dfrac{\partial N_2}{\partial \xi}=+0.25(1-\eta)\\ \dfrac{\partial N_3}{\partial \xi}=+0.25(1+\eta)\\ \dfrac{\partial N_4}{\partial \xi}=-0.25(1+\eta)\end{array}\right\},\qquad \left\{\begin{array}{l}\dfrac{\partial N_1}{\partial \eta}=-0.25(1-\xi)\\ \dfrac{\partial N_2}{\partial \eta}=-0.25(1+\xi)\\ \dfrac{\partial N_3}{\partial \eta}=+0.25(1+\xi)\\ \dfrac{\partial N_4}{\partial \eta}=+0.25(1-\xi)\end{array}\right\} \tag{4.B18}$$

Σύμφωνα με την Εξ. (4Β.14), ισχύει:

$$\left\{\begin{array}{l}\dfrac{\partial u}{\partial x}\\ \dfrac{\partial u}{\partial y}\end{array}\right\}=J^{-1}\left\{\begin{array}{l}\dfrac{\partial u}{\partial \xi}\\ \dfrac{\partial u}{\partial \eta}\end{array}\right\},\qquad \left\{\begin{array}{l}\dfrac{\partial v}{\partial x}\\ \dfrac{\partial v}{\partial y}\end{array}\right\}=J^{-1}\left\{\begin{array}{l}\dfrac{\partial v}{\partial \xi}\\ \dfrac{\partial v}{\partial \eta}\end{array}\right\} \tag{4.B19}$$

Συνεπώς, είναι πλέον διαθέσιμες όλες οι απαραίτητες πληροφορίες για τον υπολογισμό του των παραμορφώσεων.

Αυτή η σελίδα είναι σκοπίμως κενή

ΚΕΦΑΛΑΙΟ 5
(ΠΕΡΙΛΗΨΗ)

ΒΕΛΤΙΣΤΟΠΟΙΗΣΗ
ΣΚΕΛΕΤΙΚΩΝ ΚΑΤΑΣΚΕΥΩΝ
ΥΠΟ ΤΗΝ ΕΠΙΒΟΛΗ
ΓΕΝΙΚΕΥΜΕΝΟΥ ΠΕΡΙΟΡΙΣΜΟΥ ΜΕΤΑΤΟΠΙΣΗΣ

Σε αυτήν την περίληψη κεφαλαίου, επανεξετάζεται το πρόβλημα της ελαχιστοποίησης του βάρους σκελετικών κατασκευών υπό την επιβολή ενός περιορισμού μετατόπισης. Η συνεισφορά της παρούσης σε αυτό το εξαιρετικά δημοφιλές και πολυμελετημένο πρόβλημα έγκειται στη διατύπωση μίας νέας μεθοδολογίας βελτιστοποίησης, η οποία εμφανίζει τέσσερα πρωτότυπα στοιχεία. Για την αξιολόγηση της μεθοδολογίας, εξετάσθηκαν συνολικά 48 περιπτώσεις. Ειδικότερα, μελετήθηκαν βιβλιογραφικά παραδείγματα (δύο παραλλαγές του δικτυώματος 3-bar, δύο παραλλαγές του δικτυώματος 5-bar, δύο παραλλαγές του δικτυώματος 56-bar και δύο παραλλαγές της δοκού MBB), ενώ διατυπώθηκαν και νέα παραδείγματα αξιολόγησης (πέντε παραλλαγές της δοκού MBB με τρεις διαφορετικές πυκνότητες πλέγματος και έξι παραλλαγές του δικτυώματος 9-bar, εκάστη για τέσσερα σενάρια φόρτισης). Προκειμένου να ισχυροποιηθεί η αξιολόγηση, όλα τα προαναφερθέντα παραδείγματα, εκτός εκείνων για τα οποία υπάρχει αναλυτική λύση στη βιβλιογραφία, επελύθησαν χρησιμοποιώντας την μέθοδο SQP (ρουτίνα fmincon στο λογισμικό MatLab), η οποία αποτελεί μία εξαιρετικά ισχυρή Μέθοδο Μαθηματικού Προγραμματισμού. Προέκυψε ότι, σε όλες τις περιπτώσεις, η προτεινόμενη μεθοδολογία βελτιστοποίησης συνέκλινε στις βέλτιστες λύσεις, οι οποίες είτε αναφέρονταν στη βιβλιογραφία είτε λαμβάνονταν από τη χρήση της μεθόδου SQP, και με υπολογιστικό κόστος το πολύ ίσο προς αυτό της βιβλιογραφίας και σημαντικά μικρότερο αυτού της SQP.

5.1. Εισαγωγή

Το πρόβλημα της ελαχιστοποίησης του βάρους μίας κατασκευής υπό την επιβολή ενός περιορισμού μετατόπισης αποτελεί ένα από τα πλέον δημοφιλή προβλήματα στην περιοχή της βελτιστοποίησης κατασκευών. Στο παρόν κεφάλαιο, παρουσιάζεται μία νέα μεθοδολογία βελτιστοποίησης σκελετικών κατασκευών. Πιο συγκεκριμένα, η εν λόγω μεθοδολογία εμφανίζει τέσσερα πρωτότυπα στοιχεία. Το πρώτο πρωτότυπο στοιχείο αφορά στην επίλυση του προβλήματος βελτιστοποίησης υπό την επιβολή ενός γενικευμένου περιορισμού μετατόπισης, σε αντίθεση με τις υπάρχουσες βιβλιογραφικές μεθοδολογίες, σύμφωνα με τις οποίες είναι εκ των προτέρων γνωστός ο βαθμός ελευθερίας στον οποίο επιβάλλεται ο περιορισμός μετατόπισης. Το δεύτερο πρωτότυπο στοιχείο αφορά στη διατύπωση μίας αναδρομικής σχέσεως, για την επανασχεδίαση της σκελετικής κατασκευής, η οποία, αν και προκύπτει με αυστηρά μαθηματικό τρόπο από τη μέθοδο πολλαπλασιαστών Lagrange, τελικά δεν εμπλέκει κανέναν τέτοιο συντελεστή, σε αντίθεση με την υπάρχουσα βιβλιογραφία. Το τρίτο πρωτότυπο στοιχείο αφορά στην κατηγοριοποίηση των μελών της κατασκευής χρησιμοποιώντας παράλληλα δύο κριτήρια, ένα κριτήριο δύναμης, διαφορετικό από εκείνο της υπάρχουσας βιβλιογραφίας, και ένα κριτήριο διατομής, με αποτέλεσμα τη διαμόρφωση τεσσάρων διαφορετικών κατηγοριών μελών, σε αντίθεση με την, επικρατούσα στη βιβλιογραφία, κατηγοριοποίηση. Η μελέτη της προτεινόμενης κατηγοριοποίησης απεκάλυψε την, καθοριστική δράση μίας συγκεκριμένης κατηγορίας. Το τέταρτο πρωτότυπο στοιχείο αφορά στη βελτιστοποίηση των μελών της κατασκευής, τα οποία διαπιστώνεται ότι ανήκουν στην προαναφερθείσα κατηγορία. Για λόγους αξιολόγησης, πραγματοποιήθηκε εκτενής μελέτη επί συνολικά 48 σκελετικών κατασκευών, από την οποία προέκυψε ότι η προτεινόμενη μεθοδολογία βελτιστοποίησης συνέκλινε πάντοτε στην καθολικά βέλτιστη σχεδίαση και με υπολογιστικό κόστος μικρότερο, ή το πολύ ίσο, με αυτό της βιβλιογραφίας.

5.2. Θεωρητική προσέγγιση

5.2.1. Η διατύπωση Βελτίστου Κριτήριου

Σύμφωνα με τη διατύπωση του προβλήματος βελτιστοποίησης 2Δ σκελετικών κατασκευών υπό την επιβολή ενός περιορισμού μετατόπισης, θεωρείται μόνον ένας περιορισμός μετατόπισης. Γενίκευση του εν λόγω προβλήματος αποτελεί η θεώρηση ότι, ασχέτως του πλήθους των επιβαλλομένων περιορισμών μετατόπισης, μόνον ένας τέτοιος περιορισμός είναι ενεργός στη βέλτιστη σχεδίαση και μάλιστα χωρίς να είναι εκ των προτέρων γνωστός ο βαθμός ελευθερίας, στον οποίο αντιστοιχεί ο ενεργός περιορισμός. Η μαθηματική διατύπωση του εν λόγω προβλήματος είναι:

$$\min W = \sum_{k=1}^{NEL} \left(\rho_k A_k L_k \right) \tag{5.1a}$$

$$\text{έτσι ώστε } |u| \le u_{allow} \text{ και } A_{\min} \le A \tag{5.1b}$$

όπου η ποσότητα A εκφράζει εμβαδόν διατομής δομικού μέλους, η ποσότητα L εκφράζει το μήκος δομικού μέλους, ρ είναι η πυκνότητα υλικού, η ποσότητα u δηλώνει κομβική μετατόπιση, ενώ οι δείκτες k και $allow$ δηλώνουν την k – ράβδο και την επιτρεπόμενη τιμή, αντίστοιχα. Το συνολικό πλήθος των ράβδων της σκελετικής κατασκευής δηλώνεται ως NEL. Ο επιβαλλόμενος περιορισμός μετατόπισης (1b) υποδηλοί ότι η κομβική μετατόπιση δεν επιτρέπεται να είναι μεγαλύτερη από u_{allow} είτε ως προς την x είτε ως προς την y διεύθυνση. Επιπροσθέτως, επιβάλλεται ένας περιορισμός σχετικά με την ελάχιστη τιμή, την οποία είναι δυνατόν να αποδοθεί στις διατομές των μελών, έτσι ώστε να εξασφαλίζεται ο

σχηματισμός ενός θετικά ορισμένου μητρώου δυσκαμψίας. Σύμφωνα με τη μέθοδο των πολλαπλασιαστών Lagrange, η συνάρτηση Lagrange του εν λόγω προβλήματος βελτιστοποίησης, εάν αμεληθεί ο περιορισμός επί των διατομών, διατυπώνεται ως εξής:

$$\mathfrak{L} = \sum_{i=1}^{NEL} \left(\rho_i \, A_i \, L_i \right) + \lambda_1 \left(|u| - u_{allow} \right) \tag{5.2}$$

όπου λ_1 είναι ο συντελεστής Lagrange για τον περιορισμό της μετατόπισης. Από τη Μηχανική είναι γνωστό ότι, βάσει της έννοιας του μοναδιαίου φορτίου, η κομβική μετατόπιση είναι δυνατόν να εκφρασθεί ως:

$$u = \sum_{i=1}^{NEL} \left(\frac{F_i^P F_i^Q}{A_i E_i} L_i \right) \tag{5.3}$$

όπου, επιπροσθέτως των προηγούμενων συμβόλων, ως E δηλώνεται το μέτρο ελαστικότητας, F_i^P είναι η αξονική δύναμη λόγω της επιβολής των πραγματικών φορτίων, ως F_i^Q δηλώνεται η αξονική δύναμη λόγω της κατάλληλης εφαρμογής μοναδιαίου φορτίου, ενώ ως i δηλώνεται το, υπό θεώρηση, δομικό μέλος. Ο συνδυασμός της Εξ.(5.3) με την Εξ.(5.2) δίδει:

$$\mathfrak{L} = \sum_{i=1}^{NEL} \left(\rho_i \, A_i \, L_i \right) + \lambda_1 \left(\left| \sum_{i=1}^{NEL} \left(\frac{F_i^P F_i^Q}{A_i E_i} L_i \right) \right| - u_{allow} \right) \tag{5.4}$$

Στην Εξ. (5.4), η μερική παράγωγος ως προς το εμβαδόν διατομής A_i ισούται με:

$$\nabla \mathfrak{L}_{A_i} = \rho_i \, L_i - \lambda_1 \left| \left(\frac{F_i^P F_i^Q}{A_i^2 E_i} L_i \right) \right| + \lambda_1 \sum_l \left(\left(\left(\frac{\partial F_l^P}{\partial A_i^2} \right) F_l^Q + \left(\frac{\partial F_l^Q}{\partial A_i^2} \right) F_l \right) \left(\frac{L_l}{A_l E_l} \right) \right) \tag{5.5a}$$

Ωστόσο, ο πρώτος, εντός του αθροίσματος της Εξ.(5.5α), όρος είναι ταυτοτικά μηδέν. Αυτό ισχύει διότι σε ισοστατικά δικτυώματα οι ραβδικές δυνάμεις είναι ανεξάρτητες των διατομών, ενώ σε υπερστατικά δικτυώματα ο Berke απέδειξε ότι ο συγκεκριμένος όρος είναι μηδενικός. Συνεπώς, η Εξ. (5.5a) γράφεται ως ακολούθως:

$$\nabla \mathfrak{L}_{A_i} = \rho_i \, L_i - \lambda_1 \left| \left(\frac{F_i^P F_i^Q}{A_i^2 E_i} L_i \right) \right| \tag{5.5b}$$

Σύμφωνα με τη μέθοδο των πολλαπλασιαστών Lagrange, πρέπει να ισχύει:

$$\nabla \mathfrak{L}_{A_i} = 0 \tag{5.6}$$

Ο συνδυασμός των Εξ.(5.5b, 5.6), μετά από πράξεις, δίδει:

$$1 = \lambda_1 \left| \left(\frac{F_i^P F_i^Q}{A_i A_i} \frac{1}{E_i} \right) \right| \left(\frac{1}{\rho_i} \right) \tag{5.7}$$

Ο συντελεστής λ_1 αποτελεί αυθύπαρκτη ποσότητα, οπότε διαθέτει σταθερή τιμή:

$$\lambda_1 = const \tag{5.8}$$

Υπό την παραδοχή ότι όλες οι ράβδοι κατασκευάζονται από το ίδιο υλικό, ισχύει:

$$\rho_i = const \tag{5.9}$$

Ο συνδυασμός των Εξ.(5.7, 5.8, 5.9) δίδει:

$$\left| \left(\frac{F_i^P F_i^Q}{A_i A_i} \frac{1}{E_i} \right) \right| = const \tag{5.10}$$

Το αριστερό μέλος Εξ.(5.10) αντιστοιχεί στην πυκνότητα της συμπληρωματικής ενέργειας παραμόρφωσης της i-ράβδου του εξεταζομένου δικτυώματος. Σύμφωνα με αυτήν την εξίσωση, η βέλτιστη σχεδίαση υπό την επιβολή ενός γενικευμένου περιορισμού μετατόπισης χαρακτηρίζεται, σε όλο το *ενεργό* τμήμα της κατασκευής, από σταθερή, κατά απόλυτη τιμή, πυκνότητα συμπληρωματικής ενέργειας παραμόρφωσης. Αυτή η διατύπωση αποτελεί γενίκευση ενός Βελτίστου Κριτηρίου ήδη γνωστού από τις αρχές της δεκαετίας του 70. Επιπροσθέτως, η διατύπωση μίας συνθήκης, η οποία περιγράφει μία ενεργειακή κατάσταση στο καθολικό ακρότατο, δεν προσδιορίζει την οδό, η οποία καταλήγει σε αυτήν την ενεργειακή κατάσταση. Συνεπώς, υπάρχει περιθώριο για διατύπωση νέων προσεγγίσεων και μάλιστα για τη γενικευμένη περίπτωση. Στην επόμενη ενότητα αναπτύσσεται ακριβώς αυτό το αντικείμενο. Ειδικότερα, παρουσιάζεται μία νέα μεθοδολογία βελτιστοποίησης, η οποία είναι κλειστής μορφής για ισοστατικά δικτυώματα και επαναληπτικής μορφής για υπερστατικά δικτυώματα.

5.2.2. Προτεινόμενη διαδικασία επανασχεδίασης

Έστω ένα σύνολο από NEL ράβδους, το εμβαδόν διατομής των οποίων επιλέγεται τυχαία. Μία ανάλυση με τη Μέθοδο των Πεπερασμένων Στοιχείων (ΜΠΣ) και χρησιμοποιώντας τα πραγματικά φορτία δίδει τόσο τις ραβδικές δυνάμεις F_i όσο και το πεδίο των μετατοπίσεων, από το οποίο εντοπίζεται ο κόμβος με τη μεγαλύτερη μετατόπιση, έστω κόμβος $N_{u_{\max}}$. Μία δεύτερη ανάλυση με τη (ΜΠΣ), επιβάλλοντας ένα μοναδιαίο φορτίο στον κόμβο $N_{u_{\max}}$ κατά την κατεύθυνση της μέγιστης μετατόπισης, θα δώσει τις ραβδικές δυνάμεις F_i^Q. Συνεπώς, καθίσταται πλέον δυνατός ο εντοπισμός των μελών για τα οποία ισχύει $\left| F_i^P F_i^Q \right| > tol$, όπου tol είναι μία μικρή θετική ποσότητα, έστω 1E-06. Τα εν λόγω μέλη χαρακτηρίζονται ως μη-μηδενικής δύναμης ή ,ισοδύναμα, ως ενεργά μέλη, και για κάθε ένα από αυτά η πυκνότητα συμπληρωματικής ενέργειας παραμόρφωσης w_i ισούται προς:

$$w_i = \left(\frac{F_i^P F_i^Q}{A_i A_i} \frac{1}{E_i} \right) \tag{5.11}$$

Η αντίστοιχη μέση τιμής $\overline{w}$ όλων των επί μέρους τιμών w_i είναι:

$$\overline{w} = \left(\frac{\sum_{i=1}^{N_{active}} w_i}{N_{active}} \right) \tag{5.12}$$

Σύμφωνα με το προαναφερθέν Βέλτιστο Κριτήριο, η μαθηματική έκφραση του οποίου δίδεται από την Εξ.(5.10), όλα τα ενεργά μέλη διαθέτουν την ίδια πυκνότητα συμπληρωματικής ενέργειας παραμόρφωσης, η οποία, κατ' επέκτασιν, θα ισούται προς τη μέση τιμή της πυκνότητας συμπληρωματικής ενέργειας παραμόρφωσης των ενεργών μελών. Ως εκ τούτου, το αριστερό μέλος της Εξ.(5.11) τίθεται ίσο προς $\overline{w}$, δηλαδή ισχύει:

$$\overline{w} = \left(\frac{F_{i,new}^{P} F_{i,new}^{Q}}{A_{i,new} A_{i,new}} \frac{1}{E_i} \right) \tag{5.13}$$

όπου $A_{i,new}$ είναι η επαναδιαστασιολογημένη διατομή της $i-$ράβδου. Διαιρώντας κατά μέλη την Εξ.(5.11) με την Εξ.(5.13), προκύπτει:

$$\frac{w_i}{\overline{w}} = \frac{\left(\frac{F_i^P F_i^Q}{A_i A_i} \frac{1}{E_i} \right)}{\left(\frac{F_{i,new}^P F_{i,new}^Q}{A_{i,new} A_{i,new}} \frac{1}{E_i} \right)} \tag{5.14}$$

Ωστόσο, σε ένα ισοστατικό δικτύωμα, οι ραβδικές δυνάμεις F_i^P και F_i^Q επηρεάζονται μόνον από την τοπολογία της κατασκευής και είναι ανεξάρτητες των διατομών, δηλαδή ισχύει:

$$\left(\frac{\partial F_i^P}{\partial A_i} \right) = \left(\frac{\partial F_i^Q}{\partial A_i} \right) = 0 \tag{5.15}$$

Συνεπώς, η Εξ.(5.14), μετά από πράξεις, γράφεται και ως εξής:

$$\frac{w_i}{\overline{w}} = \left(\frac{A_{i,new}^2}{A_i^2} \right) \tag{5.16}$$

Επιλύοντας την τελευταία εξίσωση, ως προς την επαναδιασιολογημένη διατομή της $i-$ράβδου, προκύπτει:

$$A_{i,new} = A_i \sqrt{\left(\frac{w_i}{\overline{w}} \right)} \tag{5.17}$$

Η Εξ.(5.17) προέκυψε για ισοστατικά δικτυώματα. Ωστόσο, είναι δυνατόν να χρησιμοποιηθεί και σε υπερστατικά δικτυώματα όταν η ευαισθησία των δυνάμεων των μελών του

δικτυώματος ως προς τις διατομές είναι χαμηλή, δηλαδή είτε όταν η ισορροπία των δυνάμεων υπερισχύει της συμβιβαστότητας των μετατοπίσεων είτε όταν πρόκειται για μία σχεδίαση πλησίον της βέλτιστης. Για άλλα υπερστατικά δικτυώματα, η Εξ.(5.17) πρέπει να χρησιμοποιείται επαναληπτική μέχρι συγκλίσεως. Ωστόσο, αν και το διάνυσμα σχεδίασης $\mathbf{A}_{\mathbf{new}}$, το οποίο προκύπτει από την Εξ.(5.17), πληροί την απαίτηση για ομοιόμορφη κατανομή της πυκνότητας της συμπληρωματικής ενέργειας παραμόρφωσης στο ενεργό τμήμα της κατασκευής, δεν διασφαλίζεται η απαίτηση για εμφάνιση κομβικής μετατόπισης το πολύ ίσης με μια μέγιστη επιτρεπόμενη. Προς τούτο, απαιτείται μία ομοιόμορφη διακλιμάκωση του διανύσματος σχεδίασης $\mathbf{A}_{\mathbf{new}}$, όπως περιγράφεται στην επόμενη ενότητα.

5.2.3. Ομοιόμορφη διακλιμάκωση του διανύσματος σχεδίασης

Σε ένα ισοστατικό δικτύωμα, η *τιμή* της πυκνότητας της συμπληρωματικής ενέργειας παραμόρφωσης της ενεργού $i-$ράβδου εξαρτάται και από την, αναπτυσσόμενη σε αυτήν, δύναμη F_i^Q λόγω μοναδιαίου φορτίου και από τη διατομή A_i της εν λόγω ράβδου. Συνεπώς, για μία κατασκευή σταθερής τοπολογίας, στην οποία τα μήκη L_i των ράβδων είναι σαφώς ορισμένα και αμετάβλητα, και υπό την προϋπόθεση ότι όλα τα μέλη είναι κατασκευασμένα από το ίδιο υλικό, άρα το μέτρο ελαστικότητας E_i για κάθε ράβδο είναι, ομοίως, σαφώς ορισμένο και αμετάβλητο, ισχύει:

$$\frac{F_i^P F_i^Q}{A_i E_i} L_i = f\left(F_i^Q, A_i\right) \tag{5.18}$$

Εάν το σημείο εφαρμογής του μοναδιαίου φορτίου είναι γνωστό, τότε οι αξονικές δυνάμεις F_i^Q λόγω μοναδιαίου φορτίου είναι, επίσης, γνωστές και καλώς ορισμένες, οπότε η Εξ.(5.18) λαμβάνει τη μορφή:

$$\frac{F_i^P F_i^Q}{A_i E_i} L_i = f\left(A_i\right) \tag{5.19}$$

Στην τελευταία εξίσωση, οι διατομές A_i αποτελούν τον μοναδικό άγνωστος. Συνεπώς, η συμπληρωματική ενέργεια παραμόρφωσης κάθε ράβδου, η οποία αριθμητικά ισούται με τη συνεισφορά κάθε ράβδου στη μετατόπιση του σημείου εφαρμογής του μοναδιαίου φορτίου, είναι δυνατόν να διακλιμακωθεί μεταβάλλοντας το εμβαδόν A_i. Επιπροσθέτως, ο συνδυασμός των Εξ.(5.3, 5.19) υποδηλοί ότι εάν εφαρμοσθεί η ίδια διακλιμάκωση σε όλες τις διατομές A_i (ομοιόμορφη διακλιμάκωση) τότε η μετατόπιση του σημείου εφαρμογής του μοναδιαίου φορτίου υφίσταται την ίδια διακλιμάκωση, δηλαδή ισχύει:

$$u_{scaled} = a\, u_{before\_scaling} \tag{5.20}$$

Η ποσότητα a δηλώνει τη σταθερά διακλιμάκωσης, ενώ οι δείκτες στις άλλες δύο ποσότητες της Εξ.(5.20) είναι επαρκώς περιγραφικοί. Εάν χρησιμοποιηθεί η ποσότητα u_{allow} στη θέση της ποσότητας u_{scaled}, τότε ο συντελεστής διακλιμάκωσης a τίθεται ίσος με το λόγο της επιτρεπόμενης προς την εμφανιζόμενη κομβική μετατόπιση u (για λόγους απλοποίησης της γραφής, ο δείκτης *before_scaling* παραλείπεται):

$$a = \left(\frac{u_{allow}}{u} \right) \tag{5.21}$$

Ο συνδυασμός των Εξ.(5.3, 5.20) δίδει:

$$u_{allow} = a \left(\sum_{i=1}^{NEL} \left(\frac{F_i^P F_i^Q}{A_i E_i} L_i \right) \right) \tag{5.22}$$

Δεδομένου ότι ο συντελεστής διακλιμάκωσης είναι σταθερός, η Εξ.(5.22) γράφεται και ως:

$$u_{allow} = \sum_{i=1}^{NEL} \left(\frac{F_i^P F_i^Q}{\left(\frac{A_i}{a} \right) E_i} L_i \right) \tag{5.23}$$

Από τη σύγκριση της Εξ. (5.23) με την Εξ. (5.3) προκύπτει η εξής αναδρομική σχέση:

$$A_{i,new} = \left(\frac{A_{i,old}}{a} \right) \tag{5.24}$$

όπου οι δείκτες *new* και *old* δηλώνουν τη νέα και την παλαιά τιμή της διατομής της $i-$ράβδου, αντίστοιχα. Συνεπώς, η εφαρμογή μίας ομοιόμορφης διακλιμάκωσης στα ενεργά μέλη της κατασκευής απαιτεί τη διαίρεση όλων των αντιστοίχων διατομών, οι οποίες προκύπτουν χρησιμοποιώντας την Εξ.(5.17), δια του συντελεστού a.

Ένα τελευταίο σημείο, το οποίο χρήζει διερεύνησης, αφορά στην επιλογή του βαθμού ελευθερίας, προκειμένου να επιβληθεί σε αυτόν το μοναδιαίο φορτίο. Μία πρώτη σκέψη θα ήταν η τυχαία δημιουργία ενός αρχικού διανύσματος σχεδίασης, η εύρεση του βαθμού ελευθερίας με τη μέγιστη μετατόπιση και η επιβολή σε αυτόν του μοναδιαίου φορτίου. Ωστόσο, αυτή η επιλογή δεν είναι η καλύτερη δυνατή διότι υπάρχει περίπτωση εσφαλμένης υπόδειξης του εν λόγω βαθμού ελευθερίας. Το συγκεκριμένο θέμα αναλύεται στην επόμενη ενότητα.

5.2.4. Σχεδίαση Μοναδιαίας Δυσκαμψίας (Unit Stiffness Design)

Σε ένα ισοστατικό δικτύωμα, ο υπολογισμός των αξονικών δυνάμεων των μελών του είναι δυνατόν να επιτευχθεί χρησιμοποιώντας τη Μέθοδο των Κόμβων, σύμφωνα με την οποία απαιτείται η γνώση των, εξωτερικώς επιβαλλομένων στην κατασκευή, φορτίων και του χωρικού προσανατολισμού της εκάστοτε ράβδου στο δικτύωμα. Με άλλα λόγια, η Μέθοδος των Κόμβων εμπλέκει εξωτερικά φορτία και προσανατολισμό μελών. Από την άλλη πλευρά, ο ίδιος υπολογισμός είναι δυνατόν να επιτευχθεί χρησιμοποιώντας τη Μέθοδο των Πεπερασμένων Στοιχείων (ΜΠΣ), σύμφωνα με την οποία επιλύεται η ακόλουθη εξίσωση:

$$\{F\} = [K]\{U\} \tag{5.25}$$

όπου $\{F\}$ είναι το διάνυσμα των, εξωτερικώς επιβαλλομένων στην κατασκευή, φορτίων, $[K]$ είναι το καθολικό μητρώο δυσκαμψίας της κατασκευής και $\{U\}$ είναι το διάνυσμα των

κομβικών μετατοπίσεων. Το μητρώο $[K]$ προκύπτει από την κατάλληλη σύνθεση των μητρώων δυσκαμψίας $[K]_j$ των μελών της κατασκευής, όπου:

$$[K]_j = \left(\frac{AE}{L}\right)_j \begin{bmatrix} c^2 & cs & -c^2 & -cs \\ cs & s^2 & -cs & s^2 \\ -c^2 & -cs & c^2 & cs \\ -cs & -s^2 & cs & s^2 \end{bmatrix}_j \tag{5.26}$$

Στο δεξί μέλος της Εξ.(5.26), εμφανίζεται το γινόμενο δύο όρων, εκ των οποίων ο πρώτος αφορά στη δυσκαμψία της $j-$ράβδου και ο δεύτερος αφορά στον χωρικό προσανατολισμό της εν λόγω ράβδου. Με άλλα λόγια, η Εξ.(5.25) εμπλέκει εξωτερικά φορτία, δυσκαμψία μελών και προσανατολισμό μελών. Δεδομένου ότι και οι δύο μέθοδοι εφαρμόζονται για την επίλυση του ίδιου προβλήματος, θα πρέπει να υπάρχει ποιοτική αντιστοιχία μεταξύ των εμπλεκομένων, σε κάθε μέθοδο, εννοιών. Βάσει της προηγηθείσας ανάλυσης, μία τέτοια αντιστοιχία επιτυγχάνεται εάν αναιρεθεί η επίδραση της παρουσίας της δυσκαμψίας μελών στην Εξ.(5.26). Προς τούτο, είναι απαραίτητη η απόδοση μοναδιαίας δυσκαμψίας σε κάθε μέλος της κατασκευής, οπότε, θεωρώντας ότι η τοπολογία της κατασκευής είναι γνωστή και αμετάβλητη, το εμβαδόν διατομής της $j-$ράβδου θα πρέπει να ισούται με:

$$A_j = \left(\frac{L}{E}\right)_j \tag{5.27}$$

Για λόγους ονοματοδοσίας, έστω ότι η σχεδίαση, η οποία προκύπτει χρησιμοποιώντας την Εξ.(5.27), καλείται 'Unit Stiffness Design' ή, εν συντομία, USD (αρκτικόλεξο των αγγλικών όρων 'Σχεδίαση Μοναδιαίας Δυσκαμψίας'). Όπως αναφέρεται στην επόμενη παράγραφο, από τα αριθμητικά αποτελέσματα της μελέτης ισοστατικών δικτυωμάτων, προέκυψε ότι εάν η διαδικασία βελτιστοποίησης εκκινηθεί από τη σχεδίαση USD τότε πάντοτε εντοπίζεται η καθολικά βέλτιστη λύση. Αντιθέτως, εάν χρησιμοποιηθεί ένα τυχαίο αρχικό διάνυσμα σχεδίασης, η διαδικασία βελτιστοποίησης είναι δυνατόν να εγκλωβισθεί σε τοπικό ακρότατο. Προεκβάλλοντας αυτήν την παρατήρηση, η χρήση αρχικού διανύσματος βάσει της σχεδίασης USD επεκτάθηκε και στη βελτιστοποίηση υπερστατικών κατασκευών.

5.2.5. Εντοπισμός ενεργών και παθητικών μελών

Το Βέλτιστο Κριτήριο, το οποίο περιγράφεται από την Εξ.(5.10), στηρίζεται σε δύο παραδοχές: κατά πρώτον ότι, στην καθολικά βέλτιστη σχεδίαση, μόνον ένας περιορισμός μετατόπισης είναι ενεργός και κατά δεύτερον ότι όλα τα μέλη της κατασκευής δύνανται να επηρεάζουν το πεδίο μετατοπίσεών της (ενεργά μέλη). Ωστόσο, δεν είναι δυνατή η, εκ των προτέρων, εξασφάλιση της ισχύος των εν λόγω παραδοχών, συνεπώς, προς αντιμετώπιση της περίπτωσης κατά την οποία είτε μία είτε και οι δύο από αυτές παραβιάζονται, θα πρέπει να αναπτυχθούν κατάλληλες αριθμητικές διαδικασίες.

Η διαδικασία επανασχεδίασης, όπως αυτή περιγράφεται στις ενότητες 5.2.2 και 5.2.3, εκκινείται από ένα διάνυσμα σχεδίασης, έστω $\mathbf{A}_{\mathbf{ini}}$. Σύμφωνα με την ενότητα 5.2.2, εάν ληφθούν υπόψη μόνο τα γινόμενα $F_i^P F_i^Q$, τότε όλοι οι όροι της μορφής $\left|F_i^P F_i^Q\right| \le tol$ (έστω κριτήριο βάσει δυνάμεων), όπου tol μία μικρή θετική ποσότητα, έχουν αμελητέα συμμετοχή στην Εξ.(5.3), συνεπώς οι αντίστοιχες $i-$ράβδοι δύνανται να χαρακτηρισθούν ως 'παθητικές'. Επειδή, δε, αυτός ο χαρακτηρισμός στηρίζεται σε κριτήριο βάσει δυνάμεων, οι

εν λόγω ράβδοι είναι δυνατόν να αποκληθούν ως 'παθητικά τη δυνάμει' στοιχεία. Κατ' αντιστοιχία, όλες οι ράβδοι για τις οποίες ισχύει $\left|F_i^P F_i^Q\right| > tol$ είναι δυνατόν να αποκληθούν ως 'ενεργά ως προς τη δύναμη' στοιχεία. Επιπροσθέτως, είναι δυνατόν να χρησιμοποιηθεί το εμβαδόν των διατομών ως κριτήριο χαρακτηρισμού των ράβδων (κριτήριο βάσει εμβαδού). Σε αυτήν την περίπτωση, όλες οι ράβδοι με εμβαδόν διατομής A_i μικρότερο από μία αρκούντως μικρή τιμή, έστω $A_{\min}$, έχουν μικρή συνεισφορά στη συνολική δυσκαμψία της κατασκευής. Σε αναλογία με τα προαναφερθέντα, αυτές οι ράβδοι είναι δυνατόν να χαρακτηρισθούν ως 'ενεργά ως προς τη διατομή' στοιχεία. Αντιθέτως, όλες οι ράβδοι με εμβαδόν διατομής $A_i > A_{\min}$ χαρακτηρίζονται, κατ' αντιστοιχία, ως 'παθητικά ως προς τη διατομή' στοιχεία. Συνδυάζοντας τα δύο προαναφερθέντα κριτήρια χαρακτηρισμού, μία ράβδος είναι δυνατόν να χαρακτηρισθεί ως:

- 'ενεργό ως προς τη δύναμη' και 'ενεργό ως προς τη διατομή' στοιχείο: Τέτοια στοιχεία συμμετέχουν στη διαδικασία επανασχεδίασης, όπως αυτή παρουσιάζεται στις Ενότητες 2.2 και 2.3.
- 'ενεργό ως προς τη δύναμη' και 'παθητικό ως προς τη διατομή' στοιχείο: Τέτοια στοιχεία συμμετέχουν στη διαδικασία επανασχεδίασης, κατά την οποία αποκτούν εμβαδόν διατομής μικρότερο από $A_{\min}$. Ωστόσο, λόγω της επιβολής του κάτω ορίου $A_{\min}$, τελικά αποδίδεται σε αυτά τα στοιχεία εμβαδόν $A_{\min}$. Αυτή η απόδοση είναι αποδεκτή, δεδομένου ότι μια διατομή αποκτά μεγαλύτερο εμβαδόν από το απαιτούμενο.
- 'παθητικό ως προς τη δύναμη' και 'ενεργό ως προς τη διατομή' στοιχείο: αυτή η περίπτωση είναι ιδιαιτέρως ενδιαφέρουσα και εξετάζεται στην επόμενη παράγραφο.
- 'παθητικό ως προς τη δύναμη' και 'παθητικό ως προς τη διατομή' στοιχείο: τέτοια στοιχεία εξαιρούνται από τη διαδικασία επανασχεδίασης και αποκτούν εμβαδόν $A_{\min}$.

Πιο συγκεκριμένα, τα 'παθητικά ως προς τη δύναμη' και 'ενεργά ως προς τη διατομή' στοιχεία $\mathbf{A}_{pass-act}$ φέρουν τα ακόλουθα χαρακτηριστικά:

C1) Για την τρέχουσα επανάληψη, δηλαδή για την επανάληψη κατά την οποία προκύπτει ο χαρακτηρισμός του στοιχείου, δεν επιτρέπεται η συμμετοχή τους στη διαδικασία επανασχεδίασης, όπως αυτή περιγράφεται στις ενότητες 5.2.2 και 5.2.3. Ειδικότερα, ο αριθμητής της Εξ.(5.17) τείνει προς το μηδέν, οπότε τα εν λόγω στοιχεία κρατούν το εμβαδόν διατομής που απέκτησαν κατά την εκτέλεση της προηγούμενης επανάληψης.

C2) Διαθέτουν εμβαδόν διατομής μεγαλύτερο από το κάτω όριο $A_{\min}$, οπότε εάν τους αποδοθεί το εμβαδόν $A_{\min}$, τότε ο επιβαλλόμενος περιορισμός μετατόπισης θα παραβιασθεί. Ωστόσο, χωρίς βλάβη της γενικότητας, είναι δυνατή η περαιτέρω μείωση της διατομής χρησιμοποιώντας κάποιο σχήμα αναζήτησης γραμμής, όπως είναι η μέθοδος binary search. Η διαδικασία μείωσης της διατομής εφαρμόζεται επαναληπτικά, μέχρι παραβίασης του περιορισμού μετατόπισης. Υπό αυτό το πρίσμα, διαμορφώνεται το ακόλουθο υπο-πρόβλημα βελτιστοποίησης:.

$$\text{Min } \mathbf{A}_{pass-act} \tag{5.28a}$$

$$\text{με } \mathbf{A}_{pass-act} > A_{\min} \tag{5.28b}$$

$$\text{έτσι ώστε } \max|u| = U_{allow} \tag{5.28c}$$

Εάν N_{pass_act} είναι το πλήθος των 'παθητικά ως προς τη δύναμη'/'ενεργητικά ως προ τη διατομή' στοιχείων, τότε ο χώρος λύσεων του ανωτέρω υπο-προβλήματος βελτιστοποίησης είναι το σύνολο $R^{N_{pass\_act}}$. Εν γένει, μια διαδικασία αναζήτησης γραμμής περιγράφεται

μαθηματικά ως $\vec{X}_{i+1} = \vec{X}_i + a\,\vec{d}$, όπου ως $\vec{X}$ δηλώνεται το διάνυσμα σχεδίασης, ως $\vec{d}$ συμβολίζεται η διεύθυνση αναζήτησης, ως a ορίζεται το βήμα αναζήτησης, ενώ i είναι ο αύξων αριθμός της τρέχουσας επανάληψης. Εάν $N_{pass\_act} = 1$, τότε ο χώρος λύσης είναι το σύνολο R^+ των πραγματικών αριθμών, το πρόβλημα αναζήτησης γραμμής είναι βαθμωτό, ενώ η βέλτιστη λύση είναι δυνατόν να εντοπισθεί μέσω μίας αναζήτησης γραμμής κατά μήκος του θετικού ημι-άξονα των πραγματικών αριθμών. Ωστόσο, εάν ισχύει $N_{pass\_act} > 1$, τότε η βέλτιστη λύση ανήκει σε έναν διανυσματικό χώρο και υπάρχουν δύο λύσεις:

1) Χρήση Μεθόδου Μαθηματικού Προγραμματισμού προς επίλυση του προβλήματος, το οποίο περιγράφεται από τις Εξ.(5.28a-5.28c). Το αρχικό πρόβλημα βελτιστοποίησης διαιρείται σε δύο μέρη, το πρώτο εκ των οποίων επιλύεται με την προτεινόμενη διαδικασία βελτιστοποίησης, ενώ το δεύτερο μέρος επιλύεται χρησιμοποιώντας οποιαδήποτε βιβλιογραφική μέθοδο βελτιστοποίησης. Το βασικό πλεονέκτημα του εν λόγω υβριδικού σχήματος βελτιστοποίησης έγκειται στο γεγονός ότι τελικώς εντοπίζεται μία λύση του προβλήματος. Επίσης, το υπολογιστικό κόστος είναι, εν γένει, μικρότερο από εκείνο, το οποίο προκύπτει εάν χρησιμοποιηθεί εξ αρχής κάποια μέθοδος Μαθηματικού Προγραμματισμού για την επίλυση *ολόκληρου* του προβλήματος (αυτή η επίλυση εμπλέκει NEL μεταβλητές σχεδίασης, ενώ η επίλυση του υπο-προβλήματος της Εξ.(5.28) εμπλέκει μόνον $N_{pass\_act} << NEL$ αγνώστους).
2) Χρήση μεθόδου αναζήτησης γραμμής *σταθερής* διεύθυνσης αναζήτησης. Πρακτικά, πρόκειται για την εφαρμογή μίας ομοιόμορφης διακλιμάκωσης επί των 'παθητικά ως προς τη δύναμη'/'ενεργά ως προς τη διατομή' στοιχείων. Αυτή η προσέγγιση αποτελεί έναν συμβιβασμό μεταξύ της χρήσης του διανύσματος σχεδίασης, όπως αυτό προκύπτει από την προτεινόμενη διαδικασία βελτιστοποίησης, χωρίς περαιτέρω επίλυση του υπο-προβλήματος της Εξ.(5.28), και της επίλυσης του υπο-προβλήματος της Εξ.(5.28) με κάποια Μέθοδο Μαθηματικού Προγραμματισμού.

Με βάση τα προαναφερθέντα στα (1) και (2), προκύπτει ότι μία καλή επιλογή θα ήταν η προσαύξηση της διαδικασίας επανασχεδίασης με μία, μικρού υπολογιστικού κόστους, ρουτίνα, έτσι ώστε να λαμβάνεται μια καλύτερη, αλλά μόνον κατά προσέγγιση, βέλτιστη λύση όταν διαγιγνώσκεται η διαμόρφωση του υποπροβλήματος της Εξ.(5.28). Η, δε, αξιοποίηση μίας αναζήτησης κατά σταθερή διεύθυνση σχολιάζεται λεπτομερέστερα στην επόμενη ενότητα.

5.2.6. Αναζήτηση κατά σταθερή διεύθυνση

Σε μία τυπική διαδικασία αναζήτησης, η οποία περιγράφεται απλά ως $\vec{X}_{i+1} = \vec{X}_i + a\,\vec{d}$, το βαθμωτό βήμα αναζήτησης a και η διεύθυνση αναζήτησης $\vec{d}$ υπολογίζονται εκ νέου σε κάθε επανάληψη, μέχρι συγκλίσεως. Εάν η διεύθυνση αναζήτησης $\vec{d}$ διατηρείται σταθερή, τότε ο χώρος λύσης είναι το $R-$σύνολο (1Δ πρόβλημα βελτιστοποίησης). Ισοδύναμα, πρόκειται για μία ομοιόμορφη διακλιμάκωση των αντιστοίχων μεταβλητών σχεδίασης $\vec{X}$. Για το εν λόγω πρόβλημα, ο αντικειμενικός σκοπός είναι η εύρεση εκείνου του βήματος αναζήτησης a, το οποίο συρρικνώνει το διάνυσμα $\mathbf{A}_{pass-act}$ χωρίς να οδηγεί σε παραβίαση του επιβαλλομένου περιορισμού μετατόπισης. Προς αυτήν την κατεύθυνση, είναι δυνατόν να χρησιμοποιηθεί οποιαδήποτε αναζήτηση γραμμής. Στην παρούσα, προτείνεται η ακόλουθη διαδικασία:

Βήμα 1: Ορισμός του κατώτατου ορίου για τις μεταβλητές σχεδίασης ως $A_{pass-act,LowerBound,j} = A_{\min}$, όπου ο δείκτης j είναι ο μετρητής των 'παθητικά ως προς τη δύναμη'/'ενεργά ως προς τη διατομή' στοιχείων.

Βήμα 2: Ορισμός του αρχικού διανύσματος σχεδίασης ως $\mathbf{A}_{pass-act}$.

Βήμα 3: Όσο δεν έχει επιτευχθεί σύγκλιση και δεν έχει ξεπερασθεί το μέγιστο πλήθος των προβλεπομένων επαναλήψεων:

Βήμα 3a: ορισμός $\mathbf{A}_{new,pass-act} = 0.5\left(\mathbf{A}_{pass-act,LowerBound} + \mathbf{A}_{pass-act}\right)$

Βήμα 3b: υπολογισμός του βαθμού κατάστασης του καθολικού μητρώου δυσκαμψίας της κατασκευής (1-norm condition number, έστω $cond\left(\mathbf{K}_{glob}\right)$)

Βήμα 3c: Εάν $cond\left(\mathbf{K}_{glob}\right) \in \left[LB, UB\right]$ τότε

Ανάλυση της κατασκευής με τη (ΜΠΣ)

Εάν $\max|u| > U_{allow}$ τότε $\quad \mathbf{A}_{pass-act,LowerBound} = \mathbf{A}_{new,pass-act}$

Διαφορετικά $\quad \mathbf{A}_{pass-act} = \mathbf{A}_{new,pass-act}$

Βήμα 3d: Αύξηση του μετρητή επαναλήψεων κατά μία επανάληψη

Θεωρείται ότι έχει επιτευχθεί σύγκλιση όταν $\left|\mathbf{A}_{new,pass-act} - \mathbf{A}_{pass-act}\right| \le tol\_1$, όπου tol_1 είναι μια μικρή, θετική ποσότητα, έστω $1E-06$. Το κάτω όριο (LB) και το άνω όριο (UL) για το βαθμό κατάστασης του καθολικού μητρώου δυσκαμψίας της κατασκευής είναι, αντίστοιχα, ένας μικρός και ένας μεγάλος αριθμός, έστω $LB = 1e-3$ και $UB = 1e20$. Ο ορισμός ενός πεδίου επιτρεπομένων τιμών για τον εν λόγω βαθμό κατάστασης εξασφαλίζει τη δυνατότητα αντιστροφής του μητρώου δυσκαμψίας της κατασκευής, συνεπώς εξασφαλίζει τη δυνατότητα εφαρμογής της (ΜΠΣ). Τέλος, όπως άλλωστε σε όλες τις επαναληπτικές διαδικασίες, χρησιμοποιείται, ως ασφαλιστική δικλίδα, και ένας μετρητής πλήθους εκτελεσθέντων επαναλήψεων, για τον ελεγχόμενο τερματισμό της διαδικασίας.

5.2.7. Ειδική περίπτωση επιβολής ενός φορτίου

Μία ειδική περίπτωση επιβολής φορτίου είναι εκείνη στην οποία ο κόμβος εφαρμογής της δύναμης είναι και ο κόμβος με τη μέγιστη μετατόπιση. Ειδικότερα, όταν επιβάλλεται μόνον ένα φορτίο P, τότε από το 2^{o} θεώρημα Castigliano's (Παράρτημα 5.Α), προκύπτει:

$$u = \sum_{i=1}^{NEL}\left(\frac{c_i b_i L_i}{A_i E_i} P\right) \tag{5.29}$$

όπου c_i είναι η σταθμισμένη συνεισφορά του πραγματικού φορτίου P στην αξονική δύναμη της $i-$ράβδου και b_i είναι η σταθμισμένη συνεισφορά του δυνατού φορτίου στη δυνατή αξονική δύναμη, η οποία αναπτύσσεται στη $i-$ράβδο. Εάν ασκηθεί ένα μοναδιαίο φορτίο στο σημείο εφαρμογής του πραγματικού φορτίου P, τότε, λόγω γραμμικότητας, ισχύει:

$$b_i = \left(\frac{c_i}{P}\right) \tag{5.30}$$

Ο συνδυασμός των τελευταίων δύο εξισώσεων δίδει:

$$u = \sum_{i=1}^{NEL}\left(\frac{c_i^2 L_i}{A_i E_i}\right) \tag{5.31}$$

Η Εξ.(5.31) υποδηλοί ότι μία $i-$ράβδος με $c_i \neq 0$ συνεισφέρει μόνον αυξητικά στη μετατόπιση του θεωρούμενου σημείου. Αντιθέτως, όλα τα μέλη με $c_i = 0$ έχουν μηδενική

συνεισφορά. Προφανώς, αυτή η περίπτωση είναι ιδιαιτέρως βολική διότι δεν εμφανίζονται όροι της μορφής $c_i b_i < 0$ στην Εξ.(5.29). Συνεπώς, περιπτώσεις στις οποίες η μέγιστη μετατόπιση εμφανίζεται στο σημείο εφαρμογής του μοναδικού ασκουμένου φορτίου αποτελούν μία ιδιαίτερη (βολική) κλάση προβλημάτων, η οποία ενδεχομένως να μην βοηθά στην αποκάλυψη αδυνάτων σημείων μίας διαδικασίας βελτιστοποίησης, ακριβώς επειδή δεν εμφανίζεται το 'αγκάθι' των μελών με $c_i b_i < 0$. Συνεπώς, μία αξιολόγηση σε ένα πλαίσιο 'ευ αγωνίζεσθαι' θα πρέπει να περιλαμβάνει και παραδείγματα, τα οποία δεν εμπίπτουν στην προαναφερόμενη ειδική κατηγορία προβλημάτων.

5.2.8. Ανάλυση ευαισθησίας

Για μία κατασκευή με δεδομένη τοπολογία και φόρτιση, και υπό την παραδοχή ότι χρησιμοποιείται το ίδιο υλικό σε όλα τα μέλη της κατασκευής, ισχύει (τα σύμβολα είναι εκείνα της Εξ.(5.31)):

$$c_{il} = const \quad L_i = const \quad E_i = const \quad P_l = const \tag{5.32}$$

Οι ποσότητες b_i εξαρτώνται από το σημείο επιβολής του δυνατού φορτίου, ή, ισοδύναμα, από τη θέση του κόμβου για τον οποίο αναζητείται η μετατόπιση. Χωρίς βλάβη της γενικότητας, ισχύει:

$$u = f\left(b_i, A_i\right) \tag{5.33}$$

Από την Εξ.(5.17) προκύπτει ότι η κομβική μετατόπιση u αποτελεί συνεχή συνάρτηση ως προς το εμβαδόν των διατομών και ασυνεχή συνάρτηση ως προς τα σημεία επιβολής του μοναδιαίου φορτίου, δεδομένου ότι αυτά τα σημεία είναι διακριτά και εξαρτώνται από την τοπολογία της κατασκευής. Συνεπώς, για τον εντοπισμό ενός ακροτάτου στο πεδίο των κομβικών μετατοπίσεων, συναρτήσει των συνεχών μεταβλητών A_i, πρέπει να ισχύει:

$$\frac{\partial u}{\partial A_i} = 0 \tag{5.34}$$

Ισοδύναμα, μετά από πράξεις επί της Εξ(5.29), πρέπει να ισχύει:

$$\frac{\partial u}{\partial A_i} = -\left(\frac{b_i L_i}{A_i^2 E_i}\right)\sum_{l=1}^{m} c_{il} P_l = 0 \tag{5.35}$$

Είναι φανερό ότι η Εξ. (5.34) είναι αληθής για κάθε τιμή A_i εάν $b_i = 0$ ή $\sum_{l=1}^{m} c_{il} P_l = 0$. Δηλαδή, όταν η συνεισφορά του μοναδιαίου φορτίου της $i-$ράβδου είναι μηδενική ή όταν η αξονική δύναμη της $i-$ράβδου είναι μηδενική.

5.3. Αριθμητική προσέγγιση

5.3.1. Η προτεινόμενη διαδικασία

Η προτεινόμενη διαδικασία, για την ελαχιστοποίηση του βάρους μίας 2Δ σκελετικής κατασκευής υπό την επιβολή ενός γενικευμένου περιορισμού μετατόπισης έχει ως εξής:

Βήμα 1: Εύρεση της αρχικής σχεδίασης μοναδιαίας δυσκαμψίας (Unit Stiffness Initial Design - U.S.I.D.) για την υπό εξέταση κατασκευή.

Βήμα 2: Ανάλυση της κατασκευής με τη (ΜΠΣ), χρησιμοποιώντας τα πραγματική φορτία.

Βήμα 3: Βάσει των αποτελεσμάτων από το Βήμα 2, εύρεση της μέγιστης κομβικής μετατόπισης $u_{\max,u}$ και εντοπισμός των στοιχείων της κατασκευής για τα οποία ισχύει $|F_i| > tol$ (προσωρινά ενεργά στοιχεία).

Βήμα 4: Ομοιόμορφη διακλιμάκωση των προσωρινά ενεργών στοιχείων με συντελεστή διακλιμάκωσης την ποσότητα $\left(U_{allow} / u_{\max,u}\right)$ και απόδοση της ελάχιστα επιτρεπομένης τιμής διατομής $A_{\min}$ στα υπόλοιπα στοιχεία.

Βήμα 5: Επαναληπτική εφαρμογή των Βημάτων 6-14 μέχρι συγκλίσεως ή μέχρι εξαντλήσεως του προβλεπομένου μεγίστου πλήθους επαναλήψεων.

Βήμα 6: Ανάλυση της κατασκευής με τη (ΜΠΣ) επιβάλλοντας ένα μοναδιαίο φορτίο στο βαθμό ελευθερίας, ο οποίος αντιστοιχεί στη μετατόπιση $u_{\max,u}$.

Βήμα 7: Κατηγοριοποίηση των δομικών μελών, χρησιμοποιώντας το κριτήριο βάσει εμβαδού, σε 'ενεργά ως προς τη δύναμη'/'ενεργά ως προς τη διατομή', 'ενεργά ως προς τη δύναμη'/'παθητικά ως προς τη διατομή', 'παθητικά ως προς τη δύναμη'/'ενεργά ως προς τη διατομή' και 'παθητικά ως προς τη δύναμη'/'παθητικά ως προς τη διατομή' (Ενότητα 5.2.5).

Βήμα 8: Για τα 'ενεργά ως προς τη δύναμη'/'ενεργά ως προς τη διατομή' στοιχεία, εφαρμογή της διαδικασίας επανασχεδίασης της ενότητας 5.2.2, δηλαδή:

Βήμα 8a: Για κάθε ένα από αυτά τα στοιχεία, υπολογισμός της πυκνότητας της συμπληρωματικής ενέργειας παραμόρφωσης w_i χρησιμοποιώντας την Εξ.(5.11).

Βήμα 8b: Για όλα αυτά τα στοιχεία, υπολογισμός της μέσης τιμής $\overline{w}$ μέσω της Εξ.(5.12).

Βήμα 8c: Για κάθε ένα από αυτά τα στοιχεία, επανασχεδίαση βάσει της Εξ.(5.17).

Βήμα 8d: Ανάλυση της κατασκευής με τη (ΜΠΣ) και υπολογισμός της μέγιστης κομβικής μετατόπισης.

Βήμα 8e: Εφαρμογή ομοιόμορφης διακλιμάκωσης χρησιμοποιώντας τις Εξ.(5.21, 5.24).

Βήμα 9: Για τα 'παθητικά ως προς τη δύναμη'/'ενεργά ως προς τη διατομή' στοιχεία, εφαρμογή της διαδικασίας επανασχεδίασης της ενότητας 5.2.3, δηλαδή:

Βήμα 9a: Έλεγχος εάν είναι δυνατή η απόδοση του κατώτερου ορίου $A_{\min}$ σε κάθε ένα από αυτά τα στοιχεία. Εάν ο έλεγχος αποτυγχάνει, τότε μετάβαση στο Βήμα 9b.

Βήμα 9b: Εφαρμογή αναζήτησης τύπου binary search, σε συνδυασμό με ανάλυση της κατασκευής χρησιμοποιώντας τη (ΜΠΣ), προς εντοπισμό του μεγίστου συντελεστού συρρίκνωσης, ο οποίος είναι δυνατόν να εφαρμοσθεί στα 'παθητικά ως προς τη δύναμη'/'ενεργά ως προς τη διατομή' στοιχεία, χωρίς να προκαλείται παραβίαση του επιβαλλομένου περιορισμού μετατόπισης.

Βήμα 10: Για τα 'ενεργά ως προς τη δύναμη'/'παθητικά ως προς τη διατομή' και τα 'παθητικά ως προς τη δύναμη'/'παθητικά ως προς τη διατομή' στοιχεία, απόδοση της ελάχιστης επιτρεπόμενης διατομής $A_{\min}$.

Βήμα 11: Εάν από την εφαρμογή των Βημάτων 9-10 προκύψει μία νέα διατομή $A_{i,new}$ μικρότερη από την $A_{\min}$, τότε $A_{i,new} = A_{\min}$.

Βήμα 14: Επιστροφή στο Βήμα 6, εκτός και εάν έχει επιτευχθεί σύγκλιση και ως προς το βάρος της κατασκευής και ως προς τη μέγιστη μεταβολή διατομής μεταξύ δύο διαδοχικών επαναλήψεων (βλ. επόμενη ενότητα 5.3.2). Εάν ξεπερασθεί το μέγιστο επιτρεπόμενο πλήθος επαναλήψεων, τερματισμός της διαδικασίας με εμφάνιση αντιστοίχου μηνύματος.

Βήμα 15: Παρουσίαση αποτελεσμάτων σε μορφή αναφοράς.

5.3.2. Κριτήρια σύγκλισης

Για τη σύγκλιση της προτεινόμενης διαδικασίας, χρησιμοποιήθηκαν δύο κριτήρια, ως ο Rozvany προτείνει. Ειδικότερα, το πρώτο κριτήριο σύγκλισης αφορά στη μεταβολή του βάρους της κατασκευής μεταξύ δύο διαδοχικών επαναλήψεων, έστω *new* και *old*. Σε αυτήν την περίπτωση, η μαθηματική έκφραση είναι η ακόλουθη (tol_{C1} είναι μία εξ αρχής ορισμένη μικρή, θετική ποσότητα):

$$\frac{\left|W_{new} - W_{old}\right|}{W_{old}} \le tol_{C1} \tag{5.36}$$

Σύμφωνα με το δεύτερο κριτήριο, θεωρείται ότι έχει επιτευχθεί σύγκλιση όταν η μέγιστη μεταβολή στο εμβαδόν διατομής μεταξύ δύο διαδοχικών επαναλήψεων, έστω *new* και *old*, είναι μικρότερη από μία προκαθορισμένη μικρή, θετική ποσότητα, έστω tol_{C2}:

$$\max\left\{\frac{\left|A_{i,new} - A_{i,old}\right|}{A_{i,old}}\right\} \le tol_{C2} \tag{5.37}$$

Εν γένει, εάν χρησιμοποιηθεί μία σχετικά μεγάλη τιμή για τις ποσότητες tol_{C1} και tol_{C2}, τότε η διαδικασία τερματίζεται σχετικά νωρίς, κάτι το οποίο εμποδίζει την εμφάνιση δυσκολιών σύγκλισης. Προς αποφυγή, λοιπόν, διαμόρφωσης ψευδούς εικόνας ως προς την αποτελεσματικότητα της προτεινομένης διαδικασίας, στα παραδείγματα του παρόντος κεφαλαίου θεωρήθηκε ότι $tol_1 = tol_2 = 1E-15$, εκτός και εάν ορίζεται κάτι διαφορετικό.

5.3.3. Αξιολόγηση αποτελεσμάτων

Προς αξιολόγηση της προτεινομένης διαδικασίας, μελετήθηκε ένα εκτεταμένο σύνολο παραδειγμάτων, κάθε ένα εκ των οποίων αντιμετωπίσθηκε ως εξής:

Βήμα Ε1: Ανάκτηση δεδομένων από τη βιβλιογραφία. Εάν ήταν βιβλιογραφικά διαθέσιμο το βέλτιστο διάνυσμα σχεδίασης, τότε εξεταζόταν η εγκυρότητά του μέσα από την ανάλυση της αντίστοιχης κατασκευής με τη (ΜΠΣ) και ελέγχοντας εάν προέκυπταν παραβιάσεις του περιορισμού μετατόπισης.

Βήμα Ε2: Επίλυση του προβλήματος βελτιστοποίησης χρησιμοποιώντας τη ρουτίνα fmincon (διαδικασία SQP) του λογισμικού Matlab, εκκινώντας τη διαδικασία βελτιστοποίησης από 100 διαφορετικά και τυχαίως επιλεγμένα διανύσματα σχεδίασης. Για κάθε επιτυχή εκτέλεση της διαδικασίας βελτιστοποίησης, καταγραφή του πλήθους των επαναλήψεων μέχρι συγκλίσεως, του πλήθους των κλήσεων της αντικειμενικής συνάρτησης (άρα και του αντιστοίχου πλήθους των αναλύσεων με τη ΜΠΣ), του ελαχίστου βάρους της κατασκευής και του βελτίστου διανύσματος σχεδίασης. Το Βήμα Ε2 δεν εκτελείτο για εκείνα τα παραδείγματα για τα οποία ήταν βιβλιογραφικά διαθέσιμες ακριβείς αναλυτικές λύσεις.

Βήμα Ε3: Λύση του προβλήματος βελτιστοποίησης χρησιμοποιώντας την προτεινόμενη διαδικασία, εκκινώντας τη διαδικασία από σχεδίαση μοναδιαίας δυσκαμψίας (Unit Stiffness Design) και καταγραφή, μέχρι συγκλίσεως, του πλήθους των επαναλήψεων, του πλήθους των αναλύσεων με τη (ΜΠΣ), του ελαχίστου βάρους της κατασκευής καθώς και του βελτίστου διανύσματος σχεδίασης. Επιπροσθέτως,

καταγραφή της ιστορίας σύγκλισης ως προς τις ποσότητες της ενότητας 5.3.2 και απεικόνιση σε ημιλογαριθμικό διάγραμμα.

Βήμα Ε4: Επίλυση του προβλήματος βελτιστοποίησης χρησιμοποιώντας την προτεινόμενη διαδικασία βελτιστοποίησης, και εκκινώντας την από 100 διαφορετικά και τυχαίως επιλεγμένα διανύσματα σχεδίασης (διαφορετικά της σχεδίασης Unit Stiffness Design) και καταγραφή του πλήθους των επαναλήψεων μέχρι συγκλίσεως, του πλήθους των αναλύσεων με τη (ΜΠΣ), το ελάχιστο βάρος και το βέλτιστο διάνυσμα σχεδίασης.

Σε αυτό το σημείο, διευκρινίζεται ότι το σύνολο των 100 αναλύσεων, το οποίο αναφέρεται στο Βήμα Ε2, αποσκοπεί στην αύξηση της πιθανότητας εντοπισμού της καθολικά βέλτιστης σχεδίασης, ενώ το σύνολο των 100 αναλύσεων, το οποίο αναφέρεται στο Βήμα Ε4, αποσκοπεί στη διερεύνηση της επίδρασης του αρχικού διανύσματος σχεδίασης στον εντοπισμό της καθολικά βέλτιστης σχεδίασης.

5.4. Παραδείγματα

Για την αξιολόγηση της προτεινομένης μεθοδολογίας βελτιστοποίησης εξετάστηκε ένα εκτενές πλήθος παραδειγμάτων, τόσο βιβλιογραφικών όσο και νέων, τα οποία διατυπώθηκαν ακριβώς για τους σκοπούς της εν λόγω αξιολόγησης. Τα παραδείγματα χωρίστηκαν σε δύο μεγάλες ομάδες. Στην πρώτη ομάδα κατατάχθηκαν τέσσερα διαφορετικά υπερστατικά δικτυώματα, μερικά εξ αυτών με παραλλαγές, και ειδικότερα το δικτύωμα 3-bar (με τρεις παραλλαγές), το δικτύωμα 5-bar, το δικτύωμα 56-bar (με δύο παραλλαγές) και μία τυπική σκελετική προσέγγιση της δοκού MBB (με δύο διαφορετικές πυκνότητες πλέγματος). Συνολικά, η πρώτη ομάδα περιείχε οκτώ δικτυώματα. Στη δεύτερη ομάδα κατατάχθηκαν τρία διαφορετικά ισοστατικά δικτυώματα, μερικά εξ αυτών με παραλλαγές, και ειδικότερα το δικτύωμα 5-bar, η δοκός MBB (με πέντε παραλλαγές, εκάστη εμφανιζόμενη με τρεις διαφορετικές πυκνότητες πλέγματος) και το δικτύωμα 9-bar (έξι παραλλαγές, εκάστη με τέσσερα διαφορετικά σενάρια φόρτισης). Συνολικά, η δεύτερη ομάδα περιείχε 40 περιπτώσεις. Σε αυτό το σημείο, διευκρινίζεται ότι οι πέντε προαναφερθείσες ισοστατικές παραλλαγές της δοκού MMB αφορούν στις πολύ γνωστές σχεδιάσεις κατά Pratt, Howe, Warren, Baltimore και K-truss (Beer and Johnston, 1988). Σε συμφωνία με την προτροπή της ενότητας 5.2.7 για ‘ευ αγωνίζεσθαι’, το δικτύωμα 9-bar δημιουργήθηκε από το πολύ γνωστό δικτύωμα 10-bar και με γνώμονα τη διατύπωση νέων προβλημάτων, ειδικά σχεδιασμένων για την αξιολόγηση της προτεινομένης μεθοδολογίας. Συνολικά, η αξιολόγηση της προτεινομένης μεθοδολογίας εξετάσθηκε μέσα από ένα σύνολο 48 περιπτώσεων

5.4.1. Υπερστατικές σκελετικές κατασκευές

Ο Πίνακας 5.1 παρουσιάζει τις εξετασθείσες υπερστατικές σκελετικές κατασκευές, ενώ οι αντίστοιχες τοπολογίες παρουσιάζονται στα Σχήματα 5.1 έως και 5.4.

Πίνακας 5.1: Εξετασθείσες υπερστατικές σκελετικές κατασκευές

Α/Α	Περιγραφή	Βιβλιογραφική αναφορά	Βιβλιογραφική Λύση
1	δικτύωμα 3-bar (παραλλαγή Α)	Morris, 1982	Αριθμητική
2	δικτύωμα 3-bar (παραλλαγή Β)	Rozvany και Zhou, 1991	Αναλυτική
3	δικτύωμα 5-bar	Patnaik και συν., 1998	Αριθμητική
4	56-bar truss (παραλλαγή Α)	Rozvany και Zhou, 1991	Αναλυτική
5	56-bar truss (παραλλαγή Β)	Rozvany, 1992	Αναλυτική
6	Δοκός MBB	Nha Chu και συν., 1997	Αριθμητική

Οι βιβλιογραφικές αναφορές, οι οποίες αναγράφονται στον Πίνακα 5.1, περιλαμβάνουν περισσότερες λεπτομέρειες σχετικά με τη διατύπωση του εκάστοτε προβλήματος βελτιστοποίησης.

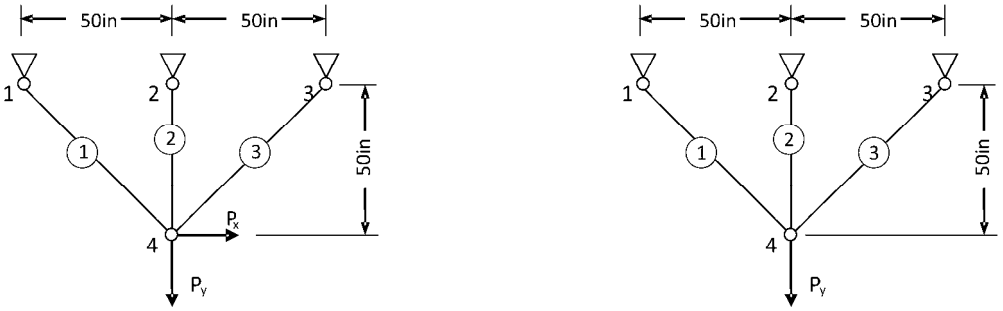

Σχήμα 5.1: Τοπολογία για το δικτύωμα 3-bar (a) παραλλαγή A και (b) παραλλαγή B

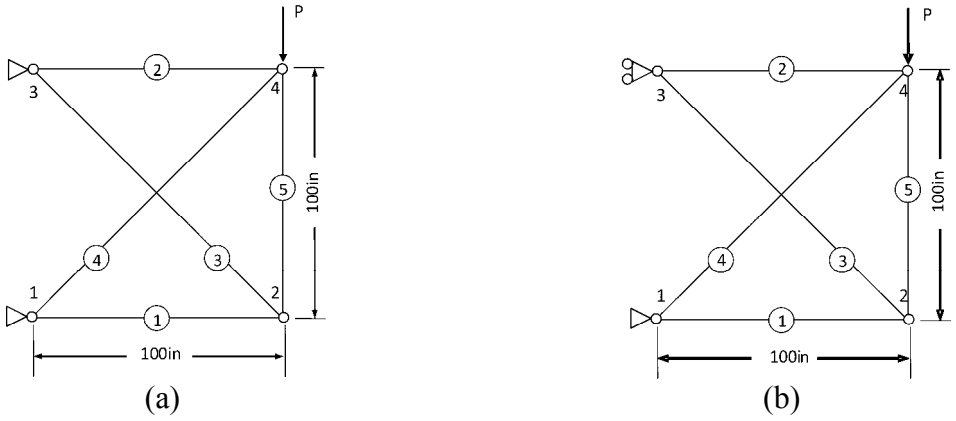

Σχήμα 5.2: Τοπολογία για το δικτύωμα 5-bar: (a) υπερστατική και (b) ισοστατική παραλλαγή

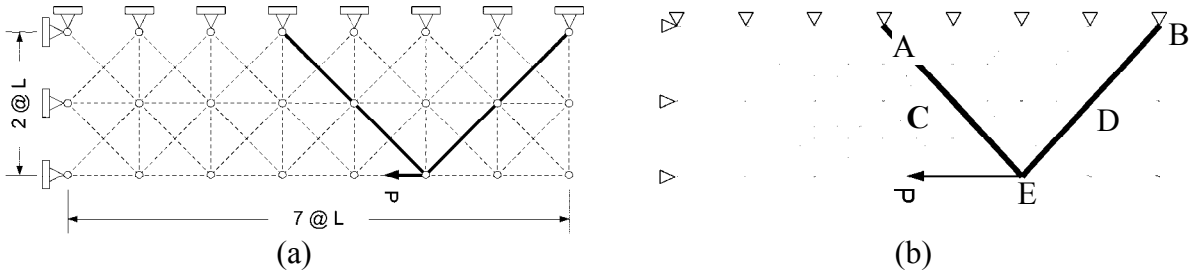

Σχήμα 5.3: Τοπολογία για το δικτύωμα 56-bar: (a) παραλλαγή A και (b) παραλλαγή B (παχιές γραμμές: εναπομείναντα στοιχεία, διακεκομμένες γραμμές: απομακρυθέντα στοιχεία)

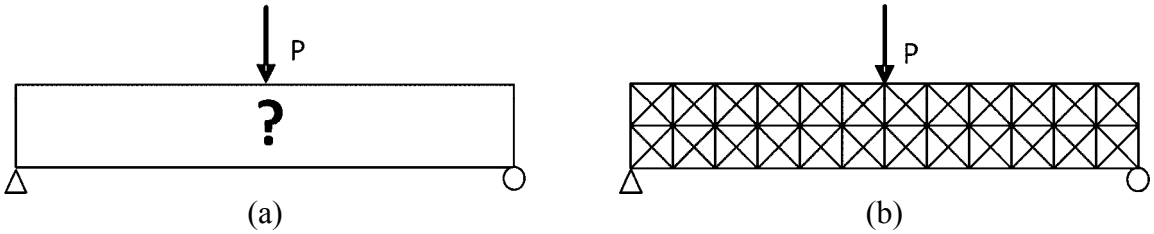

Σχήμα 5.4: Δοκός MBB: (a) πεδίο ορισμού και (b) τυπική υπεστατική διακριτοποίηση

5.4.2. Ισοστατικές σκελετικές κατασκευές

Ο Πίνακας 5.2 παρουσιάζει τις εξετασθείσες ισοστατικές σκελετικές κατασκευές, ενώ οι αντίστοιχες τοπολογίες παρουσιάζονται στα Σχήματα 5.5 έως και 5.8.

Πίνακας 5.2: Εξετασθείσες ισοστατικές σκελετικές κατασκευές

Α/Α	Περιγραφή	Αναφορά / Σύγκριση με	Βιβλιογραφική Λύση
1	δικτύωμα 5-bar	Patnaik και συν., 1995	Αριθμητική
2	Δοκός MBB (Baltimore)	fmincon (SQP) MatLab	Αριθμητική
3	Δοκός MBB (Howe)	fmincon (SQP) MatLab	Αριθμητική
4	Δοκός MBB (K-truss)	fmincon (SQP) MatLab	Αριθμητική
5	Δοκός MBB (Pratt)	fmincon (SQP) MatLab	Αριθμητική
6	Δοκός MBB (Warren)	fmincon (SQP) MatLab	Αριθμητική
7	δικτύωμα 9-bar (σχεδίαση 9a)	fmincon (SQP) MatLab	Αριθμητική
8	δικτύωμα 9-bar (σχεδίαση 9b)	fmincon (SQP) MatLab	Αριθμητική
9	δικτύωμα 9-bar (σχεδίαση 9c)	fmincon (SQP) MatLab	Αριθμητική
10	δικτύωμα 9-bar (σχεδίαση 9d)	fmincon (SQP) MatLab	Αριθμητική
11	δικτύωμα 9-bar (σχεδίαση 9e)	fmincon (SQP) MatLab	Αριθμητική
12	δικτύωμα 9-bar (σχεδίαση 9h)	fmincon (SQP) MatLab	Αριθμητική

Περισσότερες λεπτομέρειες σχετικά με τη διατύπωση των αντιστοίχων προβλημάτων βελτιστοποίησης αναγράφονται στις βιβλιογραφικές αναφορές του Πίνακα 5.2.

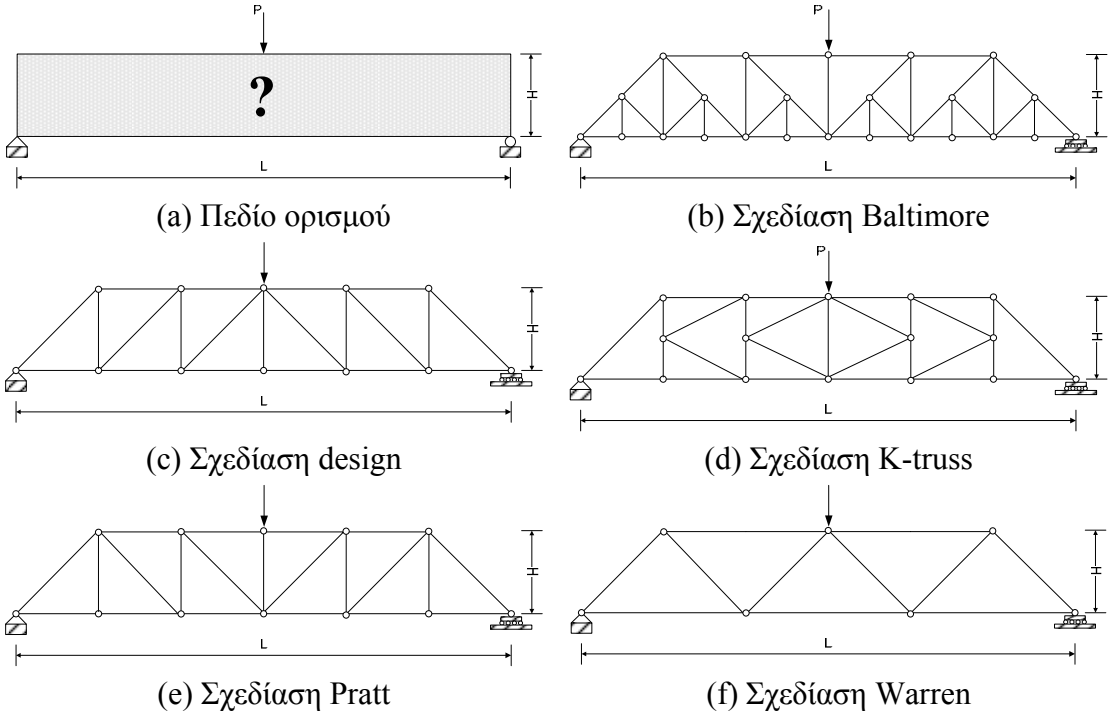

(a) Πεδίο ορισμού (b) Σχεδίαση Baltimore

(c) Σχεδίαση design (d) Σχεδίαση K-truss

(e) Σχεδίαση Pratt (f) Σχεδίαση Warren

Σχήμα 5.5: Πεδίο ορισμού και τυπικές ισοστατικές σχεδιάσεις της δοκού MBB

Το δικτύωμα 9-bar προκύπτει από το δικτύωμα 10-bar truss (Σχήμα 5.8a), όταν, σε μία εκ των δύο θέσεων στήριξης, η άρθρωση αντικατασταθεί με κύλιση και απομακρυνθεί μία ράβδος (Σχήμα 5.8b).

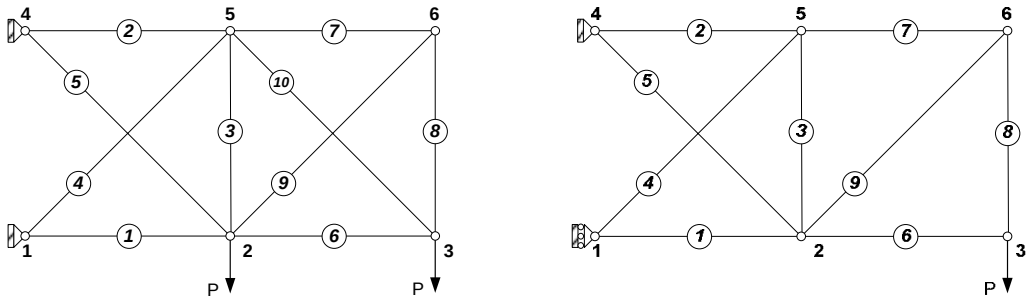

(a) (b)

Σχήμα 5.6: (a) Αρχική διατύπωση και (b) ισοστατική παραλλαγή του δικτυώματος 10-bar

Δέκα ράβδοι, λαμβανόμενες ανά εννέα, δίδουν δέκα διαφορετικούς συνδυασμούς, όπως φαίνεται στον Πίνακα 5.3. Ωστόσο, τέσσερεις από αυτούς τους συνδυασμούς είναι μηχανισμοί (βλ. Πίνακα 5.3, σχεδιάσεις 9f, 9g, 9i και 9j), οι οποίοι, προφανώς, δεν εξετάζονται.

Πίνακας 5.3: Δυνατές τοπολογίας για το δικτύωμα 9-bar (αναφορά: Σχήμα 5.8a)

Design	Remaining elements x_i, $i=1,2,\ldots,9$								
9a	1	2	3	4	5	6	7	8	9
9b	1	2	3	4	5	6	7	8	10
9c	1	2	3	4	5	6	7	9	10
9d	1	2	3	4	5	6	8	9	10
9e	1	2	3	4	5	7	8	9	10
9f	1	2	3	4	6	7	8	9	10
9g	1	2	3	5	6	7	8	9	10
9h	1	2	4	5	6	7	8	9	10
9i	1	3	4	5	6	7	8	9	10
9j	2	3	4	5	6	7	8	9	10

Επίσης, διευκρινίζεται ότι, στο παρόν κεφάλαιο και για το δικτύωμα 9-bar, εξετάσθηκαν τα φορτία, τα οποία περιγράφονται στον Πίνακα 5.4.

Πίνακας 5.4: Φορτία σε [kips] για το δικτύωμα 9-bar

Force component	Load cases			
	#1	#2	#3	#4
F2,y	-100	-100	0	-150
F3,y	-100	0	-100	-150
F5,y	0	0	0	50
F6,y	0	0	0	50

5.5. Αποτελέσματα

5.5.1. Υπερστατικές σκελετικές κατασκευές

Στην παρούσα ενότητα, καταγράφονται τα αποτελέσματα από την μελέτη των κατασκευών, οι οποίες αναφέρονται στους Πίνακες 5.1 και 5.2. Πιο συγκεκριμένα και για την εκάστοτε περίπτωση, παρατίθεται, σε μορφή διαγραμμάτων, η πορεία σύγκλισης και, σε μορφή πινάκων, το βέλτιστο διάνυσμα σχεδίασης, το οποίο προκύπτει από την εφαρμογή της προτεινομένης διαδικασίας, καθώς και το βέλτιστο διάνυσμα σχεδίασης, το οποίο αναφέρεται στη βιβλιογραφία.

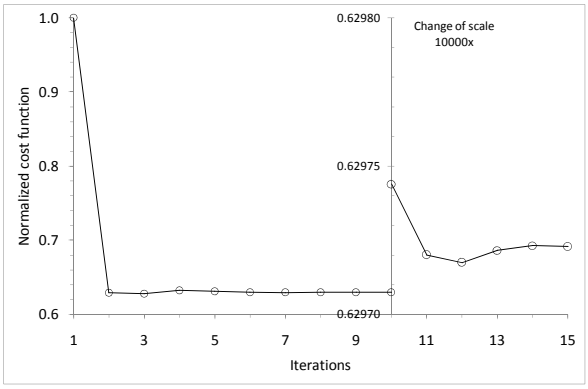

(a)

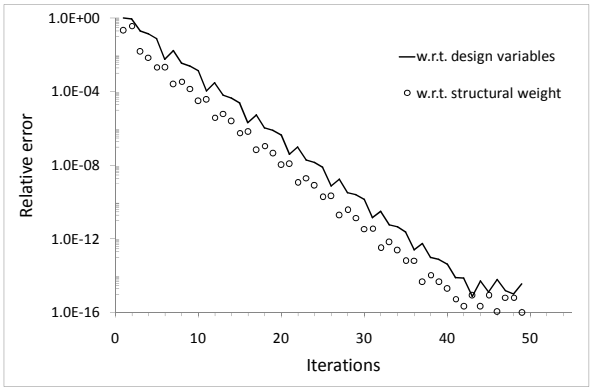

(b)

Σχήμα 5.7: Για το δικτύωμα 3-bar (παραλλαγή Α), πορεία σύγκλισης ως προς (a) την κανονικοποιημένη συνάρτηση κόστους ($tol = 1E-6$) και (b) τα σχετικά σφάλματα ($tol = 1E-16$)

Πίνακας 5.5: Βέλτιστα διανύσματα σχεδίασης για το δικτύωμα 3-bar (παραλλαγή Α)

	Reference	SQP	Present paper			
			Unit Stiffness Design (accuracy:1E-15)	Random Initial Design (accuracy:1E-15)	Convergence accuracy similar to 'Reference'	Convergence accuracy similar to 'SQP'
x_1 [in^2]	15.07	1.50739210E+01	1.50739218E+01	1.80509258E+01	1.52563007E+01	1.50739148E+01
x_2 [in^2]	0.1	1.00000000E-01	1.00000000E-01	3.41640786E+00	1.00000000E-01	1.00000000E-01
x_3 [in^2]	0.9318	9.31786600E-01	9.31786205E-01	3.90879015E+00	7.77238782E-01	9.31793251E-01
U_{4x} [in]	*5.0013E-03*	5.00000014E-03	5.00000001E-03	5.00000000E-03	5.00010978E-03	4.99999999E-03
U_{4y} [in]	*-4.3423E-03*	-4.34112802E-03	-4.34112766E-03	-2.23606798E-03	-4.23037756E-03	-4.34113197E-03
min W [lbs]	113.7	113.67744382	113.67744668	172.36067977	113.87424499	113.67744718

Από τον Πίνακα 5.5, καθίσταται φανερό ότι η προτεινόμενη διαδικασία βελτιστοποίησης καταλήγει στη βιβλιογραφικά βέλτιστη σχεδίαση, η οποία συμπίπτει και με εκείνην που προκύπτει από την εφαρμογή της μεθόδου SQP.

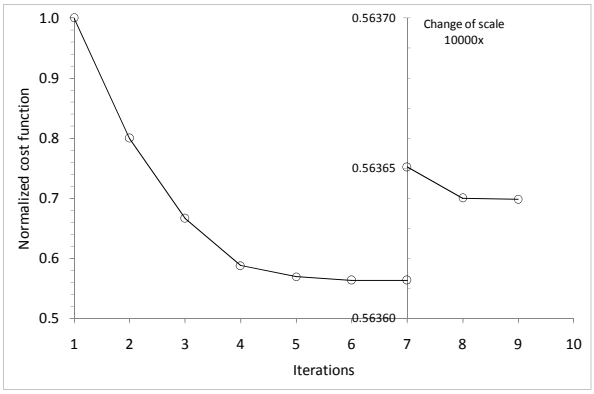

(a)

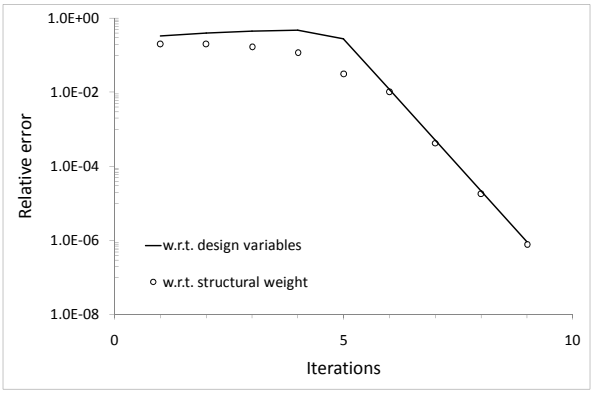

(b)

Σχήμα 5.8: Για το δικτύωμα 3-bar (παραλλαγή Β με ελάχιστα όρια επί των μεταβλητών σχεδίασης), πορεία σύγκλισης ως προς (a) την κανονικοποιημένη συνάρτηση κόστους ($tol = 1E-6$) και (b) τα σχετικά σφάλματα ($tol = 1E-16$)

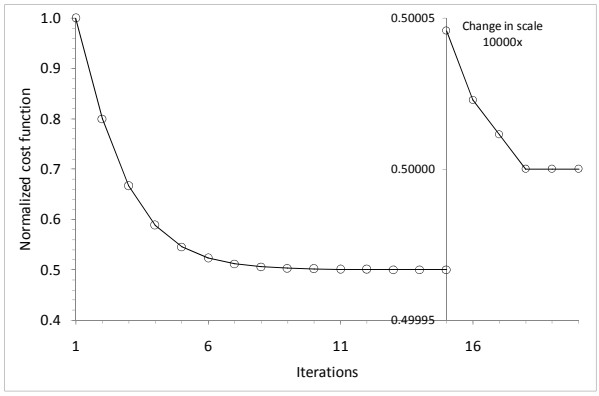

(a)

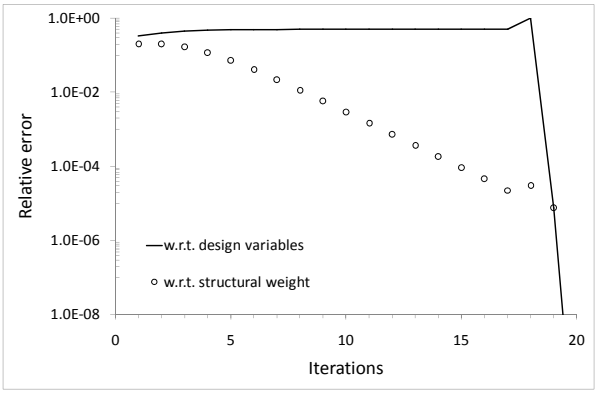

(b)

Σχήμα 5.9: Για το δικτύωμα 3-bar (παραλλαγή B άνευ ελαχίστων ορίων επί των μεταβλητών σχεδίασης), πορεία σύγκλισης ως προς (a) την κανονικοποιημένη συνάρτηση κόστους ($tol = 1E-6$) και (b) τα σχετικά σφάλματα ($tol = 1E-16$)

Πίνακας 5.6: Βέλτιστα διανύσματα σχεδίασης για το δικτύωμα 3-bar (παραλλαγή B)

Normalized variables	Reference		Present paper			
	No lower bound	With lower bound	Unit Stiffness Design (no lower bound)	Random Initial Design (no lower bound)	Unit Stiffness Design (with lower bound)	Random Initial Design (with lower bound)
z_1	0.00	0.06	1.00000000E-13	1.00000000E-13	6.00000000E-02	1.32936075E+00
z_2	1.00	1.00	1.00000000E+00	1.00000000E+00	9.57573593E-01	6.00000000E-02
z_3	0.00	0.06	1.00000000E-13	1.00000000E-13	6.00000000E-02	1.32936076E+00
U_{4x}	0.00	0.00	0.00000000E+00	0.00000000E+00	0.00000000E+00	4.38556657E-09
U_{4y}	-1.00	-1.00	-1.00000000E+00	-1.00000000E+00	-9.999999999998E-01	-9.999999953548E-01
min W	1.0000000	1.1272792	1.0000000000003	1.0000000000003	1.127279221	3.820000019

Από τον Πίνακα 5.6, καθίσταται φανερό ότι η προτεινόμενη διαδικασία βελτιστοποίησης καταλήγει στη βιβλιογραφικά βέλτιστη σχεδίαση, όταν το αρχικό διάνυσμα σχεδίασης αντιστοιχεί σε κατασκευή μοναδιαίας δυσκαμψίας. Σε αντίθετη περίπτωση, είναι δυνατός ο εγκλωβισμός σε κάποιο τοπικό ακρότατο (βλ. τελευταία στήλες 3, 6, 7 του Πίνακα 5.6).

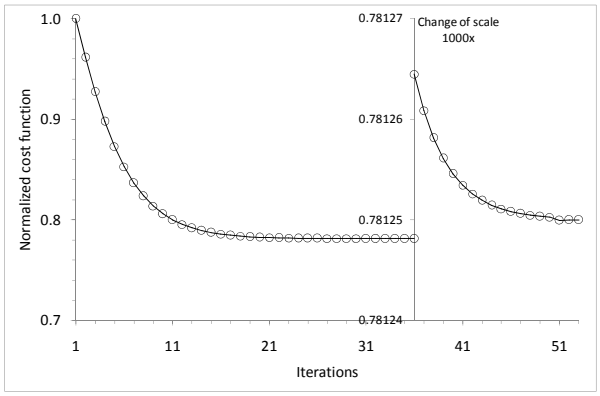

(a)

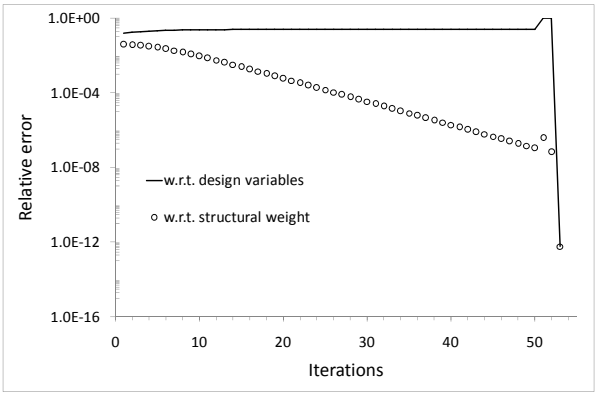

(b)

Σχήμα 5.10: Για το υπερστατικό δικτύωμα 5-bar, πορεία σύγκλισης ως προς (a) την κανονικοποιημένη συνάρτηση κόστους και (b) τα σχετικά σφάλματα

Πίνακας 5.7: Βέλτιστα διανύσματα σχεδίασης για το υπερστατικό δικτύωμα 5-bar

	Reference	SQP	Present paper	
			Unit Stiffness Design (accuracy:1E-12)	Random Initial Design (accuracy:1E-12)
x_1 [in^2]	0.001	9.999999995186E-13	1.000000000000E-12	1.000000000000E-12
x_2 [in^2]	1.475	1.500000008427E+00	1.499999999999E+00	1.499999999999E+00
x_3 [in^2]	0.001	9.999999990372E-13	1.000000000000E-12	1.000000000000E-12
x_4 [in^2]	2.124	2.121320337564E+00	2.121320343559E+00	2.121320343559E+00
x_5 [in^2]	0.001	9.999999998731E-13	1.000000000000E-12	1.000000000000E-12
U_{4x} [in]	*0.677684*	6.666666629209E-01	6.666666666667E-01	6.666666666667E-01
U_{4y} [in]	*-2.008781*	-2.000000000022E+00	-2.000000000000E+00	-2.000000000000E+00
min W [lbs]	44.817	44.9999999995132	45.0000000000155	45.0000000000155

Από τον Πίνακα 5.7, καθίσταται φανερό ότι η προτεινόμενη διαδικασία βελτιστοποίησης καταλήγει στη βιβλιογραφικά βέλτιστη σχεδίαση, η οποία συμπίπτει και με εκείνην που προκύπτει από την εφαρμογή της μεθόδου SQP.

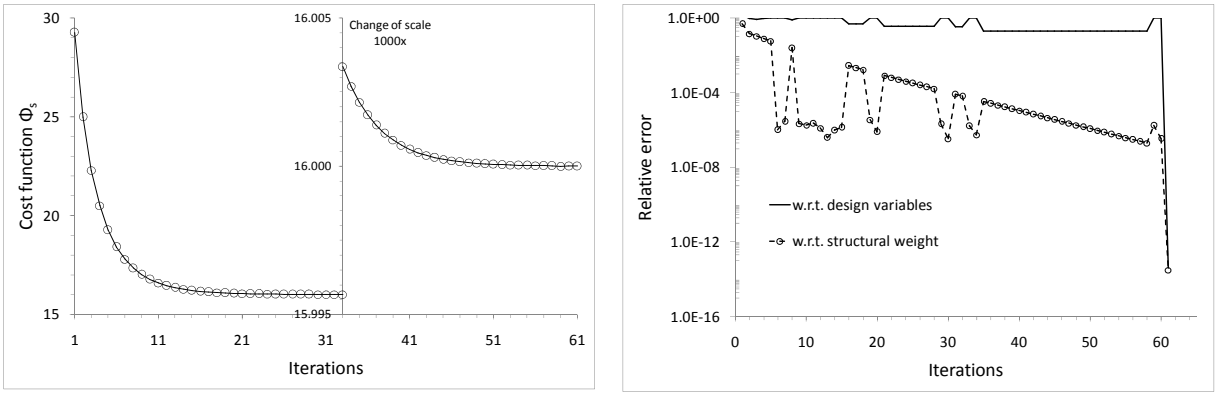

(a) (b)

Σχήμα 5.11: Για το δικτύωμα 56-bar/παραλλαγή Α, πορεία σύγκλισης ως προς (a) την κανονικοποιημένη συνάρτηση κόστους και (b) τα σχετικά σφάλματα

Όπως φαίνεται στο Σχήμα 5.13(b), η πορεία σύγκλισης εμφανίζει ορισμένες απότομες μεταβολές. Η λεπτομερής καταγραφή των αποτελεσμάτων απεκάλυψε ότι οι μεταβολές αυτές παρατηρούνται όταν, στην προτεινόμενη διαδικασία βελτιστοποίησης, ενεργοποιείται η αναζήτησης γραμμής (βλ. Ενότητα 5.3.1/Βήμα9b).

Πίνακας 5.8: Βέλτιστα διανύσματα σχεδίασης για το δικτύωμα 56-bar/παραλλαγή Α

Nondimensional quantities	Reference	SQP	Present paper	
			Unit Stiffness Design (accuracy:1E-12)	Random Initial Design (accuracy:1E-12)
z_1		2.83642084582115E+00	2.82842712474591E+00	2.82842712474591E+00
z_2		2.82931425525085E+00	2.82842712474601E+00	2.82842712474601E+00
z_3		2.82403815657757E+00	2.82842712474600E+00	2.82842712474600E+00
z_4		2.82397042932332E+00	2.82842712474596E+00	2.82842712474596E+00
min Φ_s	16.0000	16.0000684808730	16.0000000000049	16.0000000000049

Από τον Πίνακα 5.8, καθίσταται φανερό ότι, και στην περίπτωση του δικτυώματος 56-bar/παραλλαγή Α, η προτεινόμενη διαδικασία βελτιστοποίησης καταλήγει στη βιβλιογραφικά

βέλτιστη σχεδίαση, η οποία συμπίπτει και με εκείνην που προκύπτει από την εφαρμογή της μεθόδου SQP.

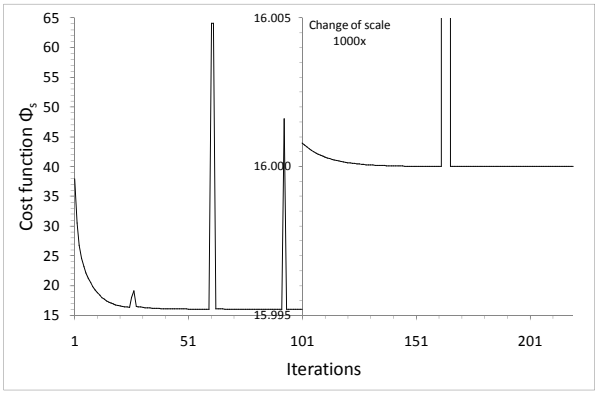

(a)

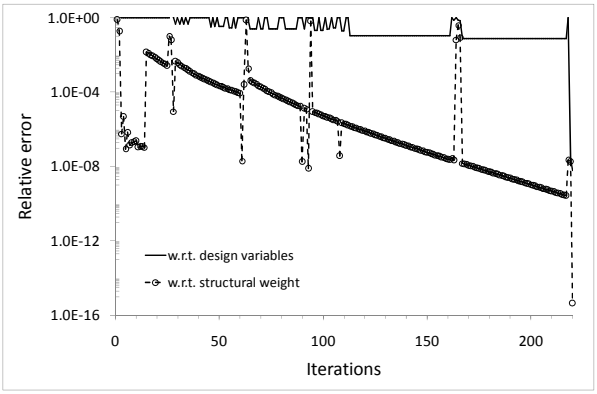

(b)

Σχήμα 5.12: Για το δικτύωμα 56-bar/παραλλαγή Α (συνολικά 276 μέλη), πορεία σύγκλισης ως προς (a) την κανονικοποιημένη συνάρτηση κόστους και (b) τα σχετικά σφάλματα

Όπως στο Σχήμα 5.13(b), έτσι και στο Σχήμα 5.14(b), η πορεία σύγκλισης εμφανίζει ορισμένες απότομες μεταβολές, οι οποίες εμφανίζονται όταν, στην προτεινόμενη διαδικασία βελτιστοποίησης, ενεργοποιείται η αναζήτησης γραμμής (βλ. Ενότητα 5.3.1/Βήμα9b).

Πίνακας 5.9: Βέλτιστα διανύσματα σχεδίασης για το δικτύωμα 56-bar/παραλλαγή Β

Nondimensional quantities	Member	Unit Stiffness Design (accuracy:1E-13)		
		Cross-sectional area	Overlapping	Overlapped cross-sectional area
z_1	(AC)	5.8504246394E-01	(AC) + (AE)	2.8284271247E+00
z_2	(AE)	2.2433846608E+00	(CE) + (AE)	2.8284271247E+00
z_3	(CE)	5.8504246394E-01		
z_4	(BD)	7.7174302143E-01	(BD) + (DE)	2.8284271247E+00
z_5	(DE)	2.0566841033E+00	(BE) + (DE)	2.8284271247E+00
z_6	(BE)	7.7174302143E-01		

Από τον Πίνακα 5.9, καθίσταται φανερό ότι τα εναπομείναντα μέλη εμφανίζουν μεταξύ τους επικάλυψη. Όταν αυτή ληφθεί υπόψη, τότε το βέλτιστο διάνυσμα σχεδίασης του Πίνακα 5.9 (βλ. τελευταία στήλη του Πίνακα 5.9) ταυτίζεται με αυτό του Πίνακα 5.8.

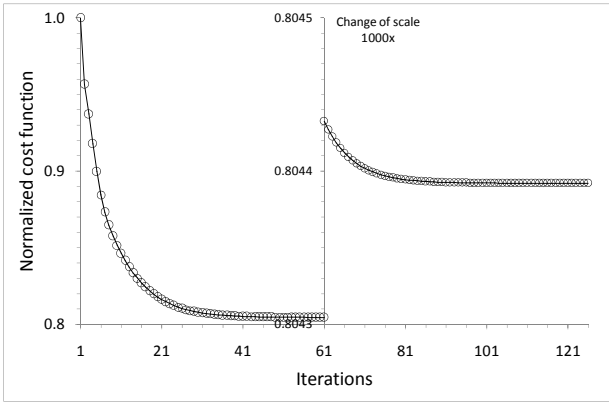

(a)

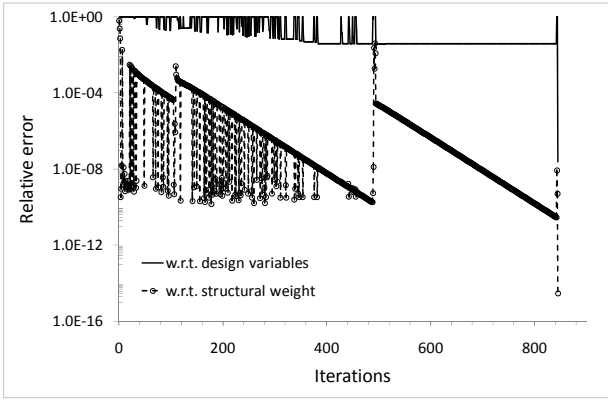

(b)

Σχήμα 5.13: Για τη δοκό MBB, πορεία σύγκλισης ως προς (a) την κανονικοποιημένη συνάρτηση κόστους (πλέγμα 12×2) και (b) τα σχετικά σφάλματα (πλέγμα: 48×8)

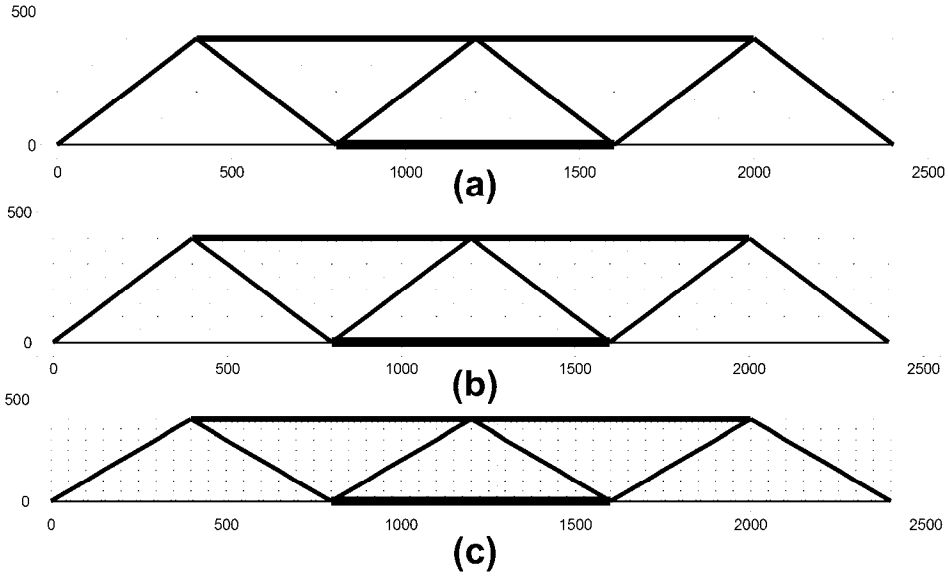

Σχήμα 5.14: Βέλτιστες σχεδιάσεις της δοκού MBB με την προτεινόμενη διαδικασία και για πλέγμα (a) 12×2, (b) 24×4 και (c) 48×8

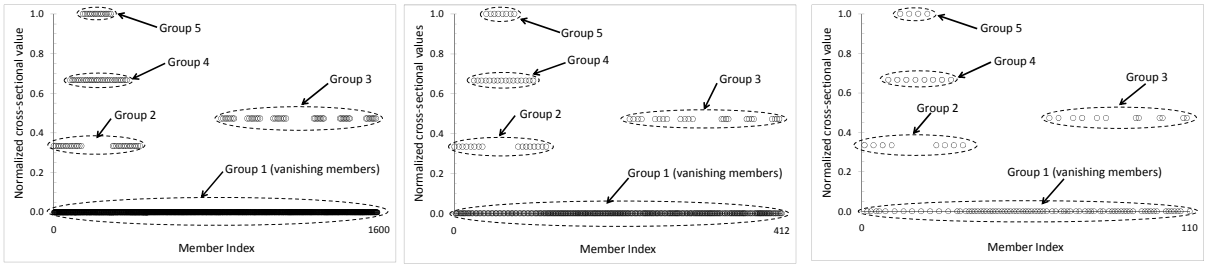

Σχήμα 5.15: Ομαδοποίηση εναπομεινάντων στοιχείων στη βέλτιστη σχεδίαση της δοκού MBB και για πλέγμα (a) 48×8, (b) 24×4 and (c) 12×2

Από το Σχήμα 5.16 προκύπτει ότι η προτεινόμενη διαδικασία συνέκλινε στην ίδια βέλτιστη τοπολογία με αυτήν που καταγράφεται στη βιβλιογραφία. Επίσης, το Σχήμα 5.17 δείχνει ότι, στη βέλτιστη σχεδίαση, παραμένει σημαντικά μικρότερο πλήθος στοιχείων, συγκριτικά με το πλήθος των στοιχείων του αρχικού πλέγματος, τα οποία εμφανίζουν υψηλή κοινοτυπία.

5.5.2. Ισοστατικές σκελετικές κατασκευές

Η βελτιστοποίηση του ισοστατικού δικτύωματος 5-bar αποτυπώνεται στον Πίνακα 5.9.

Πίνακας 5.10: Βέλτιστη σχεδίαση για το ισοστατικό δικτύωμα 5-bar

	Reference	SQP	Present paper	
			Unit Stiffness Design (accuracy:1E-12)	Random Initial Design (accuracy:1E-12)
x_1 [in^2]		1.000000000000E-12	1.000000000000E-12	1.000000000000E-12
x_2 [in^2]		9.715414157277E-01	1.500000000000E+00	1.500000000000E+00
x_3 [in^2]		9.999999999948E-13	1.000000000000E-12	1.000000000000E-12
x_4 [in^2]		2.913778091812E+00	2.121320343560E+00	2.121320343560E+00
x_5 [in^2]		2.867287369717E-07	1.000000000000E-12	1.000000000000E-12
max(abs(U_y)) [in]		2.000000000000E+00	2.000000000000E+00	2.000000000000E+00
min W [lbs]	45.051	45.0000000227642	45.0000000000341	45.0000000000341

Όπως προκύπτει από τον εν λόγω πίνακα, η προτεινόμενη διαδικασία βελτιστοποίησης συνέκλινε στο ίδιο βάρος με αυτό που προκύπτει από την εφαρμογή της μεθοδολογίας SQP. Ωστόσο, με την προτεινόμενη διαδικασία προκύπτει μία καθαρά διμελής κατασκευή, ενώ με τη μεθοδολογία SQP υπάρχει μία διατομής (μέλος x_5) η οποία τείνει να απομακρυνθεί, χωρίς, τελικά, να απομακρύνεται από το βέλτιστο διάνυσμα σχεδίασης.

Η βελτιστοποίηση της ισοστατικής διατύπωσης της δοκού MBB αποτυπώνεται στους Πίνακες 5.9-5.12 και στα Σχήματα 5.18-5.22.

Πίνακας 5.11: Επίδοση ως προς το πλήθος των επαναλήψεων (δοκός MBB)

Variation		DESIGN														
		Baltimore			Howe			K-truss			Pratt			Warren		
		S.Q.P.	R.I.D.	U.S.I.D	S.Q.P.	R.I.D.	U.S.I.D	S.Q.P.	R.I.D.	U.S.I.D	S.Q.P.	R.I.D.	U.S.I.D	S.Q.P.	R.I.D.	U.S.I.D
#1	*mean value*	82	*2 or 3*	2	88	*2 or 3*	2	113	*2 or 3*	2	85	*2 or 3*	2	82	*2 or 3*	2
	st deviation	10	-	-	13	-	-	26	-	-	12	-	-	10	-	-
	(%) CV	11.9	-	-	15.2	-	-	23.0	-	-	14.6	-	-	11.9	-	-
#2	*mean value*	139	*2 or 3*	2	144	*2 or 3*	2	210	*2 or 3*	2	150	*2 or 3*	2	139	*2 or 3*	2
	st deviation	30	-	-	32	-	-	20	-	-	30	-	-	30	-	-
	(%) CV	21.5	-	-	21.9	-	-	9.6	-	-	20.1	-	-	21.5	-	-
#3	*mean value*	202	*2 or 3*	2	210	*2 or 3*	2	253	*2 or 3*	2	206	*2 or 3*	2	202	*2 or 3*	2
	st deviation	21	-	-	17	-	-	17	-	-	20	-	-	21	-	-
	(%) CV	10.3	-	-	8.2	-	-	6.8	-	-	9.7	-	-	10.3	-	-

S.Q.P.: Sequential Quadratic Programming
R.I.D.: Random Initial Design
U.S.I.D.: Unit Stiffness Initial Design

Από τον Πίνακα 5.10 προκύπτει ότι η προτεινόμενη διαδικασία, συγκριτικά με τη μεθοδολογία SQP, απαιτεί σημαντικά μικρότερο πλήθος επαναλήψεων μέχρι συγκλίσεως.

Πίνακας 5.12: Κανονικοποίηση ελαχίστου βάρους ως προς αποτελέσματα SQP (δοκός MBB)

Variation		DESIGN				
		Baltimore	Howe	K-truss	Pratt	Warren
#1	R.I.D.	1.000	1.000	1.000	1.000	1.277
	U.S.I.D.	1.000	1.000	1.000	1.000	1.000
#2	R.I.D.	1.000	1.000	1.130	1.087	1.000
	U.S.I.D.	1.000	1.000	1.000	1.000	1.000
#3	R.I.D.	1.000	1.000	1.050	1.057	1.000
	U.S.I.D.	1.000	1.000	1.000	1.000	1.000

R.I.D.: Random Initial Design
U.S.I.D.: Unit Stiffness Initial Design

Ο Πίνακας 5.11 παρουσιάζει τα αποτελέσματα, στα οποία συγκλίνει η προτεινόμενη διαδικασία, όταν αυτά κανονικοποιηθούν ως προς τα αποτελέσματα, τα οποία προκύπτουν από την εφαρμογή της μεθόδου SQP. Όπως καθίσταται φανερό, η προτεινόμενη διαδικασία συγκλίνει πάντοτε στην καθολικά βέλτιστη σχεδίαση, εάν ως αρχική σχεδίαση χρησιμοποιηθεί εκείνη της μοναδιαίας δυσκαμψίας (Unit Stiffness Initial Design - USID). Αντιθέτως, εάν χρησιμοποιηθεί μία τυχαία σχεδίαση (Random Initial Design - RID) διαφορετικής της (USID) τότε είναι δυνατόν να παρατηρηθεί εγκλωβισμός σε τοπικό ακρότατο.

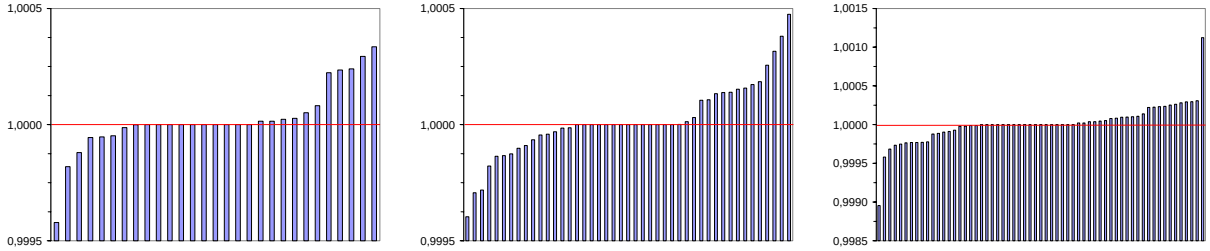

(#1) (#2) (#3)

Σχήμα 5.16: MBB – Σχεδίαση Baltimore

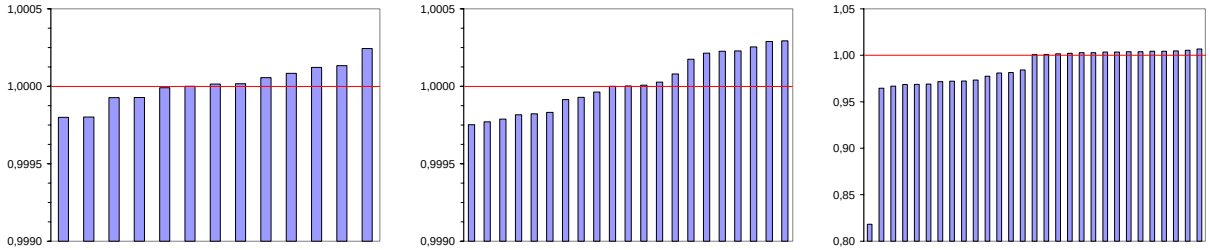

(#1) (#2) (#3)

Σχήμα 5.17: MBB – Σχεδίαση Howe

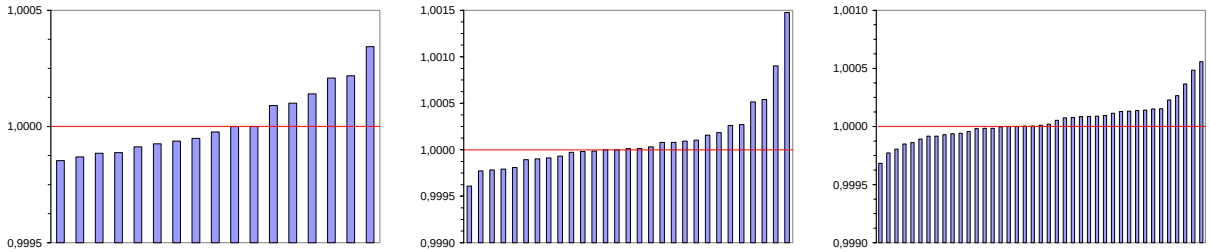

(#1) (#2) (#3)

Σχήμα 5.18: MBB – Σχεδίαση K-truss

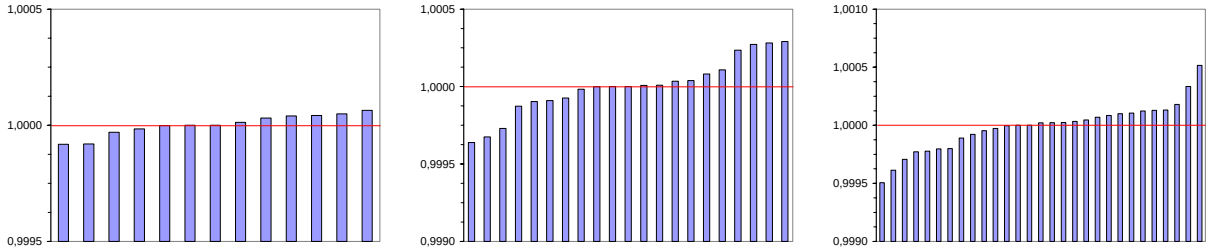

(#1) (#2) (#3)

Σχήμα 5.19: MBB – Σχεδίαση Pratt

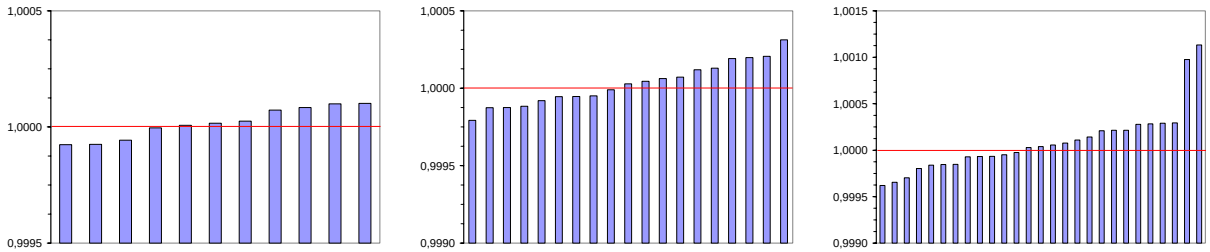

(#1) (#2) (#3)

Σχήμα 5.20: MBB – Σχεδίαση Warren

Τα Σχήματα 5.18-5.22 δείχνουν το λόγο κάθε διατομής ως προς την, με SQP, προκύπτουσα.

Πίνακας 5.13: Κανονικοποίηση ελαχίστου βάρους ως προς τις σχεδιάσεις MBB

Design	Variation #1	Variation #2	Variation #3
Baltimore	1.218	1.294	1.492
Howe	1.211	1.285	1.481
K_truss	1.139	1.069	1.104
Pratt	1.212	1.287	1.482
Warren	1.000	1.110	1.328

Ο Πίνακας 5.12 εμφανίζει μία ενδιαφέρουσα, από κατασκευαστικής απόψεως, πληροφορία. Πιο συγκεκριμένα, τα ελάχιστα βάρη, τα οποία προέκυψαν για κάθε μία σχεδίαση της δοκού MBB και για κάθε ένα από τα τρία διαφορετικά πλέγματα, τα οποία χρησιμοποιήθηκαν, κανονικοποιήθηκαν ως προς το ελάχιστο των ελαχίστων βάρος. Όπως φαίνεται από τον εν λόγω Πίνακα, οι βέλτιστες σχεδιάσεις είναι δυνατόν να διαφέρουν μεταξύ τους από, περίπου, 7% έως και, περίπου, 49%. Συνεπώς, καθίσταται φανερό ότι, ειδικά στις σκελετικές κατασκευές, η πλέον δόκιμη προσέγγιση είναι εκείνη στην οποία, με κάποιον ιεραρχικό τρόπο, θα πρέπει να βελτιστοποιείται και η τοπολογία και το μέγεθος των μελών.

Τα αποτελέσματα από τη διερεύνηση του δικτυώματος 9-bar καταγράφονται στους Πίνακες 5.13 και 5.14.

Πίνακας 5.14: Αποτελέσματα για τη σχεδίαση 9a και για όλες τις φορτίσεις (δοκός MBB)

	Design 9a Load Case 1		Design 9a Load Case 2		Design 9a Load Case 3		Design 9a Load Case 4	
	SQP	Present paper	SQP	Present paper	SQP	Present paper	SQP	Present paper
W_{opti}	8867.234400	8867.234400	1287.228600	1287.228600	6488.691200	6488.691200	9470.672909	9470.672900
x_1	21.045831	21.045835	0.100000	0.100000	18.000021	18.000000	21.750839	21.750841
x_2	51.551611	51.551556	11.236751	11.236753	36.000001	36.000000	53.278522	53.278462
x_3	29.763207	29.763305	7.945585	7.945584	18.000028	18.000000	34.391054	34.391099
x_4	42.091664	42.091670	11.236754	11.236753	25.455901	25.455844	43.501691	43.501682
x_5	0.100000	0.100000	0.100000	0.100000	0.100000	0.100000	0.100000	0.100000
x_6	0.100000	0.100000	0.100000	0.100000	0.100000	0.100000	0.100000	0.100000
x_7	21.045865	21.045835	0.100000	0.100000	17.999898	18.000000	21.750772	21.750841
x_8	21.045884	21.045835	0.100000	0.100000	18.000017	18.000000	26.639117	26.639231
x_9	29.763288	29.763305	0.100000	0.100000	25.455811	25.455844	30.760447	30.760334

Πίνακας 5.15: Αποτελέσματα για όλες τις σχεδιάσεις και για την τρίτη φόρτιση (δοκός MBB)

	9a		9b		9c		9d		9e		9h	
	SQP	Present paper	SQP	Present paper	SQP	Present paper	SQP	Present paper	SQP	Present paper	SQP	Present paper
Weight	6488,70	6488,70	4163,10	4163,10	4164,6	4164,6	4164,6	4164,6	6490,2	6490,2	4164,6	4164,6
x1	18,000	18,000	14,400	14,400	14,400	14,400	14,400	14,400	18,000	18,000	14,400	14,400
x2	36,000	36,000	28,800	28,800	28,800	28,800	28,800	28,800	36,000	36,000	28,800	28,800
x3	18,000	18,000	0,100	0,100	0,100	0,100	0,100	0,100	18,000	18,000	20,365	20,365
x4	25,456	25,456	20,365	20,365	20,365	20,365	20,365	20,365	25,456	25,456	0,100	0,100
x5	0,100	0,100	0,100	0,100	0,100	0,100	0,100	0,100	0,100	0,100	14,400	14,400
x6	0,100	0,100	14,400	14,400	14,400	14,400	14,400	14,400	18,000	18,000	0,100	0,100
x7	18,000	18,000	0,100	0,100	0,100	0,100	0,100	0,100	18,000	18,000	0,100	0,100
x8	18,000	18,000	0,100	0,100	0,100	0,100	0,100	0,100	25,456	25,456	0,100	0,100
x9	25,456	25,456	20,365	20,365	20,365	20,365	20,365	20,365	0,100	0,100	20,365	20,365

Από τους παραπάνω Πίνακες προκύπτει ότι η προτεινόμενη μεθοδολογία βελτιστοποίησης συνέκλινε στα ίδια ελάχιστα βάρη με εκείνα, τα οποία προκύπτουν από την εφαρμογή της μεθοδολογίας SQP. Ειδικότερα, οι όποιες διαφοροποιήσεις εμφανίζονται στα αποτελέσματα, εντοπίζονται μετά από το τέταρτο δεκαδικό ψηφίο.

5.6. Συμπεράσματα

Στο παρόν κεφάλαιο, παρουσιάσθηκε μία νέα μεθοδολογία βελτιστοποίησης, η οποία ανήκει στην κατηγορία των Βελτίστων Κριτηρίων, και αφορά στην περίπτωση ελαχιστοποίησης βάρους σκελετικής κατασκευής υπό την επιβολή ενός γενικευμένου περιορισμού μετατόπισης. Εν συντομία, τα ιδιαίτερα χαρακτηριστικά της μεθοδολογίας είναι:

- Η αναδρομική σχέση για την επανασχεδίαση της κατασκευής είναι εξαιρετικά απλή.
- Δεν απαιτείται ο έμμεσος ή άμεσος υπολογισμός συντελεστών Lagrange.
- Τα διανύσματα σχεδίασης, τα οποία διαμορφώνονται κατά την εξέλιξη της προτεινομένης διαδικασίας, πάντοτε ανήκουν στο αποδεκτό τμήμα του χώρου λύσεων,

συνεπώς ο τερματισμός της διαδικασίας σε οποιαδήποτε επανάληψη δίδει ένα αποδεκτό διάνυσμα σχεδίασης.

- Η συμπεριφορά της αναδρομικής σχέσεως για την επανασχεδίαση της κατασκευής είναι ευσταθής διότι δεν εμπλέκει κάποια παράμετρο σχετικά με το βήμα των μεταβολών, οι οποίες είναι δυνατόν να πραγματοποιηθούν χωρίς να προκύψει πρόβλημα ευστάθειας.

Τα συμπεράσματα, τα οποία προέκυψαν από την ενδελεχή διερεύνηση της εν λόγω μεθοδολογία είναι τα εξής:

- Για τα βιβλιογραφικά παραδείγματα, για τα οποία δεν έχει καταγραφεί αναλυτική λύση, η προτεινόμενη μεθοδολογία, συγκριτικά με τις αντίστοιχες βιβλιογραφικές, κατέληξε στις ίδιες τιμές ελαχίστου βάρους και μετά από, περίπου, το ίδιο πλήθος επαναλήψεων.
- Για τα βιβλιογραφικά παραδείγματα, για τα οποία έχει καταγραφεί αναλυτική λύση, η προτεινόμενη μεθοδολογία, συγκριτικά με τις αντίστοιχες βιβλιογραφικές, κατέληξε στις ίδιες τιμές ελαχίστου βάρους (συμφωνία με αυτές σε τουλάχιστον δώδεκα σημαντικά ψηφία), απαιτώντας λιγότερες επαναλήψεις.
- Για τα νέα παραδείγματα, τα οποία διατυπώθηκαν ειδικά στην παρούσα για λόγους αξιολόγησης, η προτεινόμενη μεθοδολογία, συγκριτικά με την ισχυρότατη μαθηματική μέθοδο SQP (υπορουτίνα fmincon του λογισμικού MatLab), κατέληξε στις ίδιες τιμές ελαχίστου βάρους και σε ελαφρώς διαφορετικά βέλτιστα διανύσματα..
- Σε όλες τις περιπτώσεις, η εκκίνηση της προτεινόμενης διαδικασίας από διάνυσμα σχεδίασης μοναδιαίας δυσκαμψίας (Unit Stiffness Design) κατέληγε στη θεωρούμενη ως καθολικά βέλτιστη σχεδίαση. Αντιθέτως, η εκκίνηση από τυχαίο διάνυσμα σχεδίασης ενίοτε κατέληγε σε εγκλωβισμό σε τοπικό ακρότατο.
- Η κατηγοριοποίηση των μελών μίας σκελετικής κατασκευής, σύμφωνα με τα κριτήτια της Ενότητας 5.3, είναι πιο λεπτομερής, συγκριτικά με την κατηγοριοποίηση της βιβλιογραφίας, και αναδεικνύει την ύπαρξη μίας ομάδος δομικών στοιχείων, τα εδώ αποκαλούμενα ως ‘παθητικά ως προς τη δύναμη’/‘ενεργά ως προς τη διατομή’ στοιχεία, τα οποία επηρεάζουν σημαντικά την πορεία της διαδικασίας βελτιστοποίησης.
- Εν γένει, η πορεία σύγκλισης του βάρους της κατασκευής είναι πολύ ομαλή. Αυξητικές εξάρσεις εμφανίζονται στην καμπύλη σύγκλισης όταν τα προαναφερθέντα ‘παθητικά ως προς τη δύναμη’/‘ενεργά ως προς τη διατομή’ στοιχεία αλλάζουν κατάσταση και ανάγονται σε ‘παθητικά ως προς τη δύναμη’/‘παθητικά ως προς τη διατομή’ στοιχεία.
- Εν γένει, η πορεία σύγκλισης του σχετικού σφάλματος, ως προς το βάρος της κατασκευής, είναι ομαλή και φθίνουσα. Όπως και στην πορεία σύγκλισης του βάρους, αυξητικές εξάρσεις παρατηρούνται στην καμπύλη σύγκλισης όταν τα προαναφερθέντα ‘παθητικά ως προς τη δύναμη’/‘ενεργά ως προς τη διατομή’ στοιχεία αλλάζουν κατάσταση και ανάγονται σε ‘παθητικά ως προς τη δύναμη’/‘παθητικά ως προς τη διατομή’ στοιχεία. Επίσης, μειωτικές εξάρσεις παρατηρούνται στην ίδια καμπύλη όταν ‘παθητικά ως προς τη δύναμη’/‘ενεργά ως προς τη διατομή’ στοιχεία λαμβάνουν την κατώτατη επιτρεπόμενη τιμή διατομής.
- Η πορεία σύγκλισης του σχετικού σφάλματος, ως προς τη μέγιστη μεταβολή των μεταβλητών σχεδίασης μεταξύ δύο διαδοχικών επαναλήψεων, είναι είτε ομαλή και φθίνουσα είτε αρκετά σταθερή και απότομα βυθιζόμενη προς την τιμή σύγκλισης.
- Η επέκταση της προτεινόμενης μεθοδολογίας σε 3Δ σκελετικές κατασκευές είναι τετριμμένη.

Συμπερασματικά, τα αποτελέσματα από τη διερεύνηση της προτεινομένης μεθοδολογίας υποδηλώνουν ότι πρόκειται για ένα απλό και αποτελεσματικό εργαλείο βελτιστοποίησης κατασκευών.

Βιβλιογραφία

Beer FP, Johnston ER Jr (1988) Vector mechanics for engineers: Statics, 5thed., McGraw-Hill.

Belegundu AD, Chandrupatla TR (1999) Optimization concepts and applications in engineering, Prentice Hall.

Bendsøe M. P., Sigmund O., (2001), Topology optimization. Theory, methods and applications, Springer Verlag, Berlin

Berke L Structural optimization of large structural systems by optimality criteria methods NASA TM-105423

Foulkes, J., The Minimum-Weight Design of Structural Frames, Proceedings of the Royal Society of London. Series A, Mathematical and Physical Sciences, Volume 223, Issue 1155, pp. 482-494

Gellatly RA, Berke L (1973) Optimality-criterion-based algorithms. In: Gallagher RH, Zienkiewicz OC (eds) Optimum structural design. Wiley, Chichester, pp 33–49

Goldberg DE (1989) Genetic Algorithms in Search, Optimization and Machine Learning, Kluwer Academic Publishers, Boston, MA.

Heyman, J. 1950: On the absolute minimum weight design of framed structures. Q. J. Mech. Appl. Math. 12, 314–324

Khot NS (1981) Algorithms based on optimality criteria to design minimum weight strucutures. Engineering Optimization, 5:73-90.

Makris P, Provatidis C, (2002), Weight minimisation of displacement-constrained truss structures using a strain energy criterion. Comput Methods Appl Mech Eng 191:2159–2177

Michalewicz Z (1999) Genetic Algorithms+Data Structures=Evolution Programs, Springer.

Michell, A.G.M., (1904) The Limits of Economy of Material in Frame-Structures", Phil. Mag., 8: 589 -- 597.

Morris AJ (1982) Foundations of structural optimization: a unified approach. Wiley.

Nha Chu D, Xie YM, Hira A, Steven GP (1997) On various aspects of evolutionary structural optimization for problems with stiffness constraints. Finite Elements in Analysis and Design; 24: 197-212.

Makris, P.A., Provatidis, C.G., Venetsanos, D.T., (2006) Structural Optimisation of thin-walled tubular trusses using a virtual strain energy density approach, Thin-Walled Structures, Vol.44, pp.235-246

Patnaik SN, Gendy AS, Berke L, Hopkins DA (1998) Modified fully utilized design (MFUD) method for stress and displacement constraints. Int J Numer Methods Eng 41:1171-1194

Patnaik SN, Guptill JD, Berke L (1995) Merits and limitations of optimality criteria method for structural optimization. Int J Numer Methods Eng 38:3087–3120

Provatidis CG, Venetsanos DT, Vossou CG (2004) A comparative study on deterministic and stochastic optimization algorithms applied to truss design. In: Proceedings of 1st International Conference "From Scientific Computing to Computational Engineering", Athens, Greece, 8-10 September.

Provatidis CG, Venetsanos DT, (2003), Performance of the FSD in shape and topology optimization of two-dimensional structures using continuous and truss-like models, In: C. Cinquini, M. Rovati, P. Venini and R. Nascimbene (eds.), Proceedings Fifth World Congress of Structural and Multidisciplinary Optimization, May 19-23, 2003, Lido di Jesolo, Italy, pp. 385-386, Schönenfeld & Ziegler.

Shield R.T., W. Prager, (1970), Optimal structural design for given deflection, J. Appl. Math. Phys, 21, 513-523

Rozvany GIN (1992) Shape and layout optimization of structural systems and optimality criteria methods. Springer Verlag.

Rozvany GIN (1995) What is meaningful in topology design? An engineer's viewpoint. In: Herskovits J (ed), Advances in Structural Optimization, Kluwer, pp 149-188.

Rozvany GIN, Zhou M (1991), The COC algorithm, Part I: cross section optimization or sizing, Comput. Methods Appl. Mech. Eng. 89, 281-308

Rozvany GIN, Zhou M. (1991), The COC algorithm, Part II: topological, geometrical and generalized shape optimization. Comput. Methods Appl. Mech. Eng. 89, 309-336

Schmit LA. (1960), Structural Design by Systematic Synthesis. In: Proceedings of 2nd Conference on Electronic Computation, ASCE, New York, 105-132.

Venkayya VB (1971), Design of optimum structures, Computer and Structures, 1:265-309

Xie, Y.M, Steven, G.P (1997), Evolutionary Structural Optimization, Springer-Verlag, Berlin

Εργασίες

[1] **Venetsanos DT.**, Provatidis CG (2010), "On the layout optimization of 2D skeletal structures under a single displacement constraint", Struct Multidisc Optim, vol.42, pp.125–155.

ΠΑΡΑΡΤΗΜΑ 5.Α: Κομβικές μετατοπίσεις βάσει του 2ου θεωρήματος Castigliano

Σύμφωνα με τη μαθηματική διατύπωση του 2ου θεωρήματος Castigliano, ισχύει:

$$u = \sum_{k=1}^{NEL} \left(\left(\frac{F_k L_k}{A_k E_k} \right) \frac{\partial F}{\partial F_k^*} \right) \Bigg|_{F_k^*=0} \tag{5.A1}$$

Στην Εξ.(5.A1) έχει χρησιμοποιηθεί ο ίδιος συμβολισμός με αυτόν του κυρίου κειμένου, με τη μόνη διαφορά ότι ως F_k^* δηλώνεται το δυνατό φορτίο, όχι απαραιτήτως μοναδιαίου μέτρου. Για ένα ισοστατικό δικτύωμα και υπό την επιβολή των πραγματικών φορτίων P_l, $l = 1,2,...,m$, ισχύει:

$$F_k = c_{k1} P_1 + c_{k2} P_2 + ... + c_{km} P_m + b_k F_a^* \tag{5.A2}$$

$$\left(\frac{\partial F_k}{\partial F_a^*} \right) = b_k \tag{5.A3}$$

$$\left(\frac{F_k L_k}{A_k E_k} \right) \left(\frac{\partial F_k}{\partial F_a^*} \right) = d_{11} P_1 + d_{12} P_2 + ... + d_{1m} P_m + e_k F_a^* \tag{5.A4}$$

Η ανάλυση του δικτυώματος με τη μέθοδο των κόμβων καταλήγει στην περιγραφή κάθε συνιστώσας δύναμης F_k ως συνδυασμό πραγματικών και δυνατών φορτίων. Η ποσότητα c_{il} αποτελεί έναν συντελεστή, εξαρτώμενο αποκλειστικά από την τοπολογία του δικτυώματος και το σημείο εφαρμογής των πραγματικών φορτίων P_l. Ποσοτικά, ο εν λόγω συντελεστής εκφράζει τη συνεισφορά του πραγματικού φορτίου P_l στην αξονική δύναμη, η οποία αναπτύσσεται στην $i-$ράβδο. Συνεπώς, για μία δεδομένη τοπολογία δικτυώματος και ένα δεδομένο σύνολο φορτίων, οι συντελεστές c_{il} είναι σταθεροί. Κατ' αντιστοιχία, η ποσότητα b_k εξαρτάται από την τοπολογία του δικτυώματος και το σημείο εφαρμογής των δυνατών F_k^*, ενώ, ποσοτικά, εκφράζει τη συνεισφορά του δυνατού φορτίου στη δυνατή αξονική δύναμη, η οποία αναπτύσσεται στην $i-$ράβδο. Στην Εξ.(5A.4) έχει χρησιμοποιηθεί μία πιο συνεκτική γραφή, όπου:

$$d_{kl} = \left(\frac{c_{kl} b_k L_k}{A_k E_k} \right) \quad \text{και} \quad e_k = \left(\frac{b_k L_k}{A_k E_k} \right) \tag{5.A5}$$

Ο συνδυασμός των Εξ.(5A.1-5A.5) δίδει:

$$u = \sum_{k=1}^{NEL} \left(\sum_{l=1}^{m} \left(\left(\frac{c_{kl} b_k L_k}{A_k E_k} \right) P_l \right) + \left(\frac{b_k L_k}{A_k E_k} \right) F_k^* \right) \Bigg|_{F_k^*=0} \tag{5.A6}$$

Μετά από πράξεις, προκύπτει:

$$u_j = \sum_{k=1}^{NEL} \left(b_{k,j} \left(\frac{L_k}{A_k E_k} \right) \sum_{l=1}^{m} \left(c_{kl} P_l \right) \right) \tag{5.A7}$$

όπου ο δείκτης j υποδηλώνει το θεωρούμενο βαθμό ελευθερίας. Η Εξ.(5.Α7) περιγράφει τη μετατόπιση u οποιουδήποτε κόμβου σε όρους τοπολογίας, μεγέθους και δυσκαμψίας υπό την επιβολή οποιουδήποτε φορτίου. Στην ειδική περίπτωση επιβολής ενός μόνον φορτίου, δηλαδή όταν $l = 1$, η κομβική μετατόπιση u_j γράφεται ως:

$$u_j = \sum_{k=1}^{NEL} \left(\left(\frac{b_{k,j} c_k L_k}{A_k E_k} P \right) \right) \tag{5.A8}$$

ΚΕΦΑΛΑΙΟ 6
(ΠΕΡΙΛΗΨΗ)

ΒΕΛΤΙΣΤΟΠΟΙΗΣΗ ΣΧΕΔΙΑΣΗΣ
2Δ ΣΥΝΕΧΟΥΣ ΜΕΣΟΥ
ΥΠΟ ΤΗΝ ΕΠΙΒΟΛΗ
ΕΝΟΣ ΓΕΝΙΚΕΥΜΕΝΟΥ ΠΕΡΙΟΡΙΣΜΟΥ ΜΕΤΑΤΟΠΙΣΗΣ

Σε αυτήν την περίληψη κεφαλαίου, παρουσιάζεται η βελτιστοποίηση 2Δ συνεχούς μέσου, όταν επιβάλλεται ένας γενικευμένος περιορισμός μετατόπισης, σύμφωνα με τον αντίστοιχο ορισμού του Κεφαλαίου 5. Αναλυτικότερα, εξετάζεται η βελτιστοποίησης μέσω είτε της πλήρους αποβολής υλικού είτε της μεταβολής του πάχους μίας κατανομής υλικού. Για κάθε μία περίπτωση, προτείνεται μία διαδικασία βελτιστοποίησης, η οποία αξιολογείται μέσα από τέσσερα τυπικά βιβλιογραφικά παραδείγματα (βαθύς πρόβολος, κοντός πρόβολος, δοκός MBB και μία κατασκευή Michell). Τα προκύπτοντα αποτελέσματα υποδηλώνουν ότι η προτεινόμενες διαδικασίες βελτιστοποίησης αποτελούν ένα ικανό εργαλείο για τη διαμόρφωση ανώτερων σχεδιάσεων, συγκριτικά με εκείνες της βιβλιογραφίας.

6.1. Εισαγωγή

Ένα από τα πλέον δημοφιλή προβλήματα στην περιοχή της βελτιστοποίησης 2Δ κατασκευών συνεχούς μέσου είναι εκείνο της αναζήτησης του ελαχίστου βάρους, υπό την επιβολή ενός περιορισμού μετατόπισης. Η εν λόγω δημοτικότητα οφείλεται στο γεγονός ότι οι 2Δ συνεχείς κατασκευές αποτελούν τις πλέον απλές κατασκευές συνεχούς μέσου, συνεπώς αποτελούν το πλέον πρόσφορο έδαφος για έρευνα. Επίσης, οι 2Δ συνεχείς κατασκευές είναι δυνατόν να θεωρηθούν ως ψευδό-3Δ συνεχείς κατασκευές, συνεπώς οποιαδήποτε μεθοδολογία διατυπώνεται για αυτές είναι οιονεί εφαρμόσιμη και στις 3Δ συνεχείς κατασκευές. Για τη, δε, βελτιστοποίησή τους απαιτείται η απομάκρυνση πλεονάζοντος υλικού, δηλαδή υλικού, το οποίο πιο πολύ επιβαρύνει με την παρουσία του στην κατασκευή παρά ωφελεί. Προς τούτο, απαιτείται η διατύπωση κάποιου κριτηρίου, βάσει του οποίου υλικό θα χαρακτηρίζεται ως πλεονάζον, ή ως παραμένον, καθώς και η διαμόρφωση κάποιας διαδικασίας αποβολής του πλεονάζοντος υλικού. Στο παρόν κεφάλαιο εξετάζονται δύο τέτοιες διαδικασίες αποβολής.

Σύμφωνα με την πρώτη διαδικασία αποβολής υλικού (βλ. Ενότητα 6.2), μέσω μίας επαναληπτικής διαδικασίας, αφαιρείται, προοδευτικά και εξ ολοκλήρου, υλικό από μία ισοπαχή κατανομή, αφήνοντας κενά στις θέσεις του αφαιρούμενου υλικού. Στην περίπτωση αυτή, προτείνεται μία διαδικασία βελτιστοποίησης, η οποία προέκυψε από μία υπάρχουσα βιβλιογραφική μεθοδολογία (μεθοδολογία ESO), στην οποία χρησιμοποιήθηκε διαφορετικό ενεργειακό κριτήριο επιλογής υλικού προς αποβολή.

Σύμφωνα με τη δεύτερη διαδικασία αποβολής υλικού (βλ. Ενότητα 6.3), πάλι μέσω μίας επαναληπτικής διαδικασίας, μεταβάλλεται προοδευτικά το πάχος μίας αρχικώς ισοπαχούς κατανομής υλικού, καταλήγοντας σε μία σχεδίαση, εν γένει, ανισοπαχούς κατανομής υλικού. Στην περίπτωση αυτή, προτείνεται μία διαδικασία βελτιστοποίησης, η οποία εμφανίζει δύο σημαντικές ιδιαιτερότητες: αφ' ενός μεν αποτελεί την επέκταση της πρωτότυπης μεθοδολογίας του Κεφαλαίου 5 και στις 2Δ κατασκευές συνεχούς μέσου, αφ' ετέρου δε εμπεριέχει τη χρησιμοποίηση πεπερασμένων στοιχείων με ισοπαραμετρική ενδοστοιχειακή παρεμβολή του πάχους.

Η ενδελεχής μελέτη των προαναφερομένων δύο διαδικασιών αποβολής υλικού μέσω τεσσάρων τυπικών βιβλιογραφικών παραδειγμάτων καταλήγει στο συμπέρασμα ότι οι προτεινόμενες διαδικασίες παρέχουν τη δυνατότητα διαμόρφωσης βελτίστων σχεδιάσεων, οι οποίες είναι ανώτερες είτε από εκείνες της βιβλιογραφίας (βλ. πρώτη διαδικασία αποβολής υλικού) είτε από εκείνες που προκύπτουν χρησιμοποιώντας πεπερασμένα στοιχεία σταθερού πάχους (βλ. δεύτερη διαδικασία αποβολής υλικού)

6.2. Ολική αποβολή υλικού από κατανομή υλικού σταθερού πάχους

6.2.1. Θεωρητικό υπόβαθρο

Η διατύπωση του προβλήματος ελαχιστοποίησης βάρους κατασκευής υπό την επιβολή ενός περιορισμού μετατόπισης είναι η ακόλουθη:

$$min\ W = \sum_{j=1}^{NEL} w_j(t) \tag{6.1}$$

$$\text{έτσι ώστε } \frac{\max|u_i|}{u_{allow}} - 1 \le 0 \tag{6.2}$$

Αυτή η διατύπωση υποδηλοί ότι ένα 2Δ συνεχές χωρίο αντικαθίσταται από ένα σύνολο NEL πεπερασμένων στοιχείων, κάθε ένα από τα οποία έχει πάχος t. Το βάρος του $j-$στοιχείου σημειώνεται ως $w_j(t)$, το συνολικό βάρος της κατασκευής είναι W, η μέγιστη

κομβική μετατόπιση είναι $\max|u_i|$, ενώ η μέγιστη επιτρεπόμενη τιμή της κομβικής μετατόπισης είναι u_{allow}. Για την αναζήτηση της βέλτιστης σχεδίασης, πρέπει να προσδιορισθούν τρεις βασικοί παράγοντες: το κριτήριο αποβολής υλικού (επανασχεδίαση), το κριτήριο τερματισμού της επαναληπτικής διαδικασίας και το κριτήριο βάσει του οποίου θα κριθεί μία σχεδίαση ως βέλτιστη. Οι εν λόγω παράγοντες σχολιάζονται στις επόμενες ενότητες.

6.2.1.1. Κριτήριο αποβολής υλικού

Σύμφωνα με τη μέθοδο Evolutionary Structural Optimization (ESO), η επανασχεδίαση στηρίζεται στην προοδευτική απομάκρυνση πλεονάζοντος υλικού, ή, ακριβέστερα, στην απομάκρυνση πεπερασμένων στοιχείων με χαμηλή ενεργειακή συμμετοχή. Ο χαρακτηρισμός ενός πεπερασμένου στοιχείου του πλέγματος ως πλεονάζοντος στηρίζεται στην απόλυτη τιμή της συμπληρωματικής ενέργειας παραμόρφωσης u_i του στοιχείου αυτού, η οποία προκύπτει από την επιβολή ενός μοναδιαίου φορτίου στον πλέον κρίσιμο βαθμό ελευθερίας:

$$u_i = \{U_{q,i}\}\left[K_{elem,i}\right]\{U_{p,i}\} \tag{6.3}$$

όπου

u_i: συμπληρωματική ενέργεια παραμόρφωσης του $i-$στοιχείου

$\{U_{q,i}\}$: διάνυσμα μετατόπισης του $i-$στοιχείου λόγω επιβολής μοναδιαίου φορτίου

$\left[K_{elem,i}\right]$:μητρώο δυσκαμψίας του $i-$στοιχείου

$\{U_{p,i}\}$: διάνυσμα μετατόπισης του $i-$στοιχείου λόγω επιβολής πραγματικού φορτίου

Όλα τα στοιχεία ταξινομούνται κατά αύξουσα σειρά με κριτήριο τη συμπληρωματική ενέργεια παραμόρφωσης, ενώ ένα προκαθορισμένο ποσοστό των στοιχείων με τις χαμηλότερες τιμές u_i αποβάλλεται. Οι επινοητές της μεθόδου ESO παρατήρησαν ότι, σε περίπτωση κατά την οποία το πλέγμα αποτελείται από ανισομεγέθη στοιχεία, θα πρέπει να χρησιμοποιείται η πυκνότητα της συμπληρωματικής ενέργειας παραμόρφωσης. Επίσης, παρατήρησαν ότι το αποκαλούμενο 'προβλήματα σκακιέρας' (checkerboard problem) αντιμετωπίζεται αποτελεσματικά εάν χρησιμοποιηθεί ο μέσος όρος των κομβικών τιμών των ενεργειών παραμόρφωσης γειτονικών στοιχείων

6.2.1.2. Κριτήριο τερματισμού

Η διαδικασία τερματίζεται όταν η μέγιστη, εμφανιζόμενη στην κατασκευή, μετατόπιση καταστεί μεγαλύτερη από την επιτρεπόμενη τιμή:

$$\frac{\max|u_i|}{u_{allow}} > 1 \tag{6.4}$$

Όταν προκύψει ότι ισχύει η Εξ.(6.4), τότε λαμβάνεται η σχεδίαση της προηγούμενης επανάληψης και εφαρμόζεται στο πάχος αυτής μια ομοιόμορφη διακλιμάκωση, έτσι ώστε να ικανοποιηθεί ισοτικά ο περιορισμός της μετατόπισης

6.2.1.3. Κριτήριο βελτίστου σχήματος

Σε μία νεώτερη έκδοση της μεθόδου ESO, χρησιμοποιείται ένα διαφορετικό κριτήριο για τη διαδικασία βελτιστοποίησης, το οποίο εμπλέκει έναν Δείκτη Επίδοσης (Performance Index

- PI). Ο εν λόγω δείκτης αποτελεί μέσο σύγκρισης μεταξύ της τρέχουσας σχεδίασης και της αρχικής σχεδίασης, η οποία χρησιμοποιείται ως αναφορά:

$$PI = \frac{u_{o,\max}}{u_{cur,\max}} \frac{W_o}{W_{cur}} \tag{6.5}$$

όπου

$u_{o,\max}$: η απόλυτη τιμή της μέγιστης κομβικής μετατόπισης στην αρχική σχεδίαση

$u_{cur,\max}$: η απόλυτη τιμή της μέγιστης κομβικής μετατόπισης στην τρέχουσα σχεδίαση

W_o : το βάρος της κατασκευής στην αρχική σχεδίαση

W_i : το βάρος της κατασκευής στην τρέχουσα σχεδίαση

Με βάση τον ορισμό του Δείκτη Επίδοση (Εξ.6.5), προκύπτει ότι, όταν η τρέχουσα σχεδίαση είναι χειρότερη από την αρχική, χαρακτηρίζεται από τιμή μικρότερη της μονάδος. Συνεπώς, η διαδικασία βελτιστοποίησης έχει νόημα να εκτελείται όσο ο δείκτης PI είναι μεγαλύτερος της μονάδος. Με βάση αυτό το σκεπτικό, ορίζεται το ακόλουθο κριτήριο τερματισμού της επαναληπτικής διαδικασίας:

$$PI < 1 \tag{6.6}$$

6.2.2. Η προτεινόμενη διαδικασία βελτιστοποίησης

Ένα από τα βασικά πλεονεκτήματα διαδικασιών βελτιστοποίησης τύπου ESO είναι η χρήση του ίδιου πλέγματος καθ' όλη τη διάρκεια της βελτιστοποίησης. Αντιθέτως, οι ιδιότητες υλικού των στοιχείων του πλέγματος μεταβάλλονται και, πιο συγκεκριμένα, αποδίδεται μοναδιαία τιμή στο μέτρο ελαστικότητας σε εκείνο το στοιχείο, το οποίο χαρακτηρίζεται ως πλεονάζον και πρέπει να απομακρυνθεί. Με αυτόν τον, αριθμητικής φύσεως, τρόπο εξασφαλίζεται η αμελητέα συμμετοχή των εν λόγω στοιχείων στο καθολικό μητρώο δυσκαμψίας. Ωστόσο, προκειμένου να εξασφαλισθεί η ελάχιστη δυνατή επίδραση των προς απομάκρυνση στοιχείων επί της εξελικτικής πορείας της διαδικασίας βελτιστοποίησης, προτείνεται η χρήση της κανονικοποιημένης πυκνότητας της συμπληρωματικής ενέργειας παραμόρφωσης, στην οποία συμμετέχουν μόνον τα ενεργά στοιχεία:

$$n_j = \frac{u_{VSED,j}}{\left(\frac{1}{NAE}\right)\sum_{j=1}^{NAE} u_{VSED,j}} \tag{6.7}$$

όπου

n_j : η κανονικοποιημένη πυκνότητα συμπληρωματικής ενέργειας παραμόρφωσης του ενεργού $j-$στοιχείου

$u_{VSED,j}$: η πυκνότητα συμπληρωματικής ενέργειας παραμόρφωσης του ενεργού $j-$στοιχείου

NAE : το συνολικό πλήθος των ενεργών στοιχείων

Με βάση όλα τα ανωτέρω, η προτεινόμενη διαδικασία έχει ως εξής:

Φάση #1:

Βήμα 1: Διακριτοποίηση του χώρου σχεδίασης χρησιμοποιώντας ένα λεπτό πλέγμα πεπερασμένων στοιχείων.
Βήμα 2: Ανάλυση της κατασκευής για τα επιβαλλόμενα φορτία.
Βήμα 3: Εάν παραβιάζεται το κριτήριο τερματισμού (Εξ.6.4), τότε ΤΕΡΜΑΤΙΣΜΟΣ.
Βήμα 4: Υπολογισμός του Δείκτη Επίδοσης (PI) για την τρέχουσα σχεδίαση (Εξ.6.5).
Βήμα 5: Εφαρμογή ενός μοναδιαίου φορτίου στον πλέον κρίσιμο βαθμό ελευθερίας.
Βήμα 6: Υπολογισμός της κανονικοποιημένης πυκνότητας της συμπληρωματικής ενέργειας παραμόρφωσης n_j (Εξ.6.7) για όλα τα ενεργά στοιχεία της κατασκευής
Βήμα 7: Ταξινόμηση των ενεργών στοιχείων κατά αύξουσα σειρά των n_j τιμών τους
Βήμα 8: Απομάκρυνση (αποβολή) ενός μικρού και προκαθορισμένου ποσοστού στοιχείων με τις μικρότερες τιμές n_j (πλεονάζον υλικό)
Βήμα 9: Επιστροφή στο Βήμα 3

Φάση #2:

Βήμα 10: Από τα αποτελέσματα της Φάσης #1, εντοπισμός της σχεδίασης με την υψηλότερη τιμή PI (βέλτιστο σχήμα)
Βήμα 11: Για τη σχεδίαση του Βήματος 10, εφαρμογή ομοιόμορφης διακλιμάκωσης της κατασκευής έτσι ώστε να ικανοποιηθεί οριακά ο περιορισμός μετατόπισης

6.2.3. Δείκτες αξιολόγησης

Για την αξιολόγηση της προτεινομένης διαδικασίας, χρησιμοποιήθηκαν οι δείκτες, οι οποίοι παρουσιάζονται στις επόμενες παραγράφους.

6.2.3.1. Πλήθος επαναλήψεων

Καταγράφεται το μέγιστο πλήθος επαναλήψεων, το οποίο απαιτείται μέχρι τερματισμού της διαδικασίας, ή, ισοδύναμα, μέχρι εντοπισμού της βέλτιστης σχεδίασης.

6.2.3.2. Κανονικοποιημένο βάρος κατασκευής ως προς το αρχικό βάρος

Προκειμένου να διαπιστωθεί η μείωση του βάρους της κατασκευής μεταξύ τρέχουσας και αρχικής σχεδίασης, ορίζεται ο ακόλουθος δείκτης:

$$PI\_1 = \left(\frac{W_{cur} - W_{ini}}{W_{ini}} \right) \tag{6.8}$$

όπου

W_{cur} : το βάρος της κατασκευής στην τρέχουσα σχεδίαση και

W_{ini} : το βάρος της κατασκευής στην αρχική σχεδίαση (σχεδίαση αναφοράς)

6.2.3.3. Κανονικοποιημένο βάρος κατασκευής ως προς το βάρος της σχεδίασης OUD

Ως σχεδίαση αναφοράς είναι δυνατόν να χρησιμοποιηθεί η αποκαλούμενη Βέλτιστη Ισοπαχής Σχεδίαση (Optimized Uniform Design - OUD), η οποία προκύπτει από την ομοιόμορφη μεταβολή μίας ισοπαχούς κατανομής υλικού, έτσι ώστε να ικανοποιηθεί ισοτικά ο εκάστοτε επιβαλλόμενος καθολικός περιορισμός τάσης ή μετατόπισης. Συνεπώς, προκειμένου να διαπιστωθεί η μείωση του βάρους της κατασκευής μεταξύ τρέχουσας σχεδίασης και της Σχεδίασης OUD, ορίζεται ο ακόλουθος δείκτης:

$$PI\_2 = \left(\frac{W_{cur} - W_{OUD}}{W_{OUD}} \right) \tag{6.9}$$

όπου

W_{cur}: το βάρος της κατασκευής στην τρέχουσα σχεδίαση και

W_{OUD}: το βάρος της κατασκευής στη Βέλτιστη Ισοπαχή Σχεδίαση (OUD)

6.2.3.4. Συνολικό εμβαδόν επιφανείας

Για πρακτικούς λόγους, είναι χρήσιμη η γνώση της πληρότητας μίας επιφανείας. Χαρακτηριστικό παράδειγμα αποτελεί η δοκός MBB, η οποία χρησιμοποιείται στην άτρακτο των αεροσκαφών Airbus. Για τη βέλτιστη σχεδίαση, απαιτείται μεν η γνώση του τασικού και παραμορφωσιακού πεδίου για λόγους αντοχής και λειτουργικότητας, αλλά απαιτείται και η πληρότητα της επιφανείας του κορμού της δοκού, διότι από αυτά τα κενά (οπές) θα διέλθουν οι καλωδιώσεις και οι σωληνώσεις διαφόρων συστημάτων του αεροσκάφους. Συνεπώς, εκτός της ελαχιστοποίησης του βάρους θα πρέπει να ελεγχθεί και η πρακτική αξία της κατασκευής. Για το λόγο αυτό, είναι δυνατή η χρήση του ακόλουθου λόγου πληρότητας:

$$PI\_3 = \left(\frac{A_{N_{ActElem}}}{A_{NEL}} \right) \tag{6.10}$$

όπου

$A_{N,ActElem}$: η συνολική επιφάνεια των ενεργών πεπερασμένων στοιχείων

A_{NEL}: η συνολική αρχική επιφάνεια του συνεχούς μέσου

Εάν το συνεχές μέσο διακριτοποιηθεί με ισομεγέθη πεπερασμένα στοιχεία, τότε ο ανωτέρω δείκτης είναι δυνατόν να λάβει την ακόλουθη απλοποιημένη μορφή:

$$PI\_3 = \left(\frac{N_{ActElem}}{NEL} \right) \tag{6.11}$$

όπου

$N_{ActElem}$: το πλήθος των ενεργών πεπερασμένων στοιχείων

NEL: το συνολικό πλήθος των πεπερασμένων στοιχείων του πλέγματος

6.2.3.5. Δείκτης (PI)

Χρήση του δείκτη (PI) (Εξ.6.5) ως δείκτη αξιολόγησης, και όχι μόνον ως δείκτη για τον τερματισμό της διαδικασίας:

$$PI\_4 = PI \tag{6.12}$$

6.2.4. Παραδείγματα αξιολόγησης

Για την αξιολόγηση της προτεινομένης διαδικασίας, χρησιμοποιήθηκαν τέσσερα βιβλιογραφικά παραδείγματα και ειδικότερα ο βαθύς πρόβολος (deep cantilever), ο κοντός πρόβολος (short cantilever), η δοκός MBB και μία κατασκευή τύπου Michell (Σχήμα 6.1).

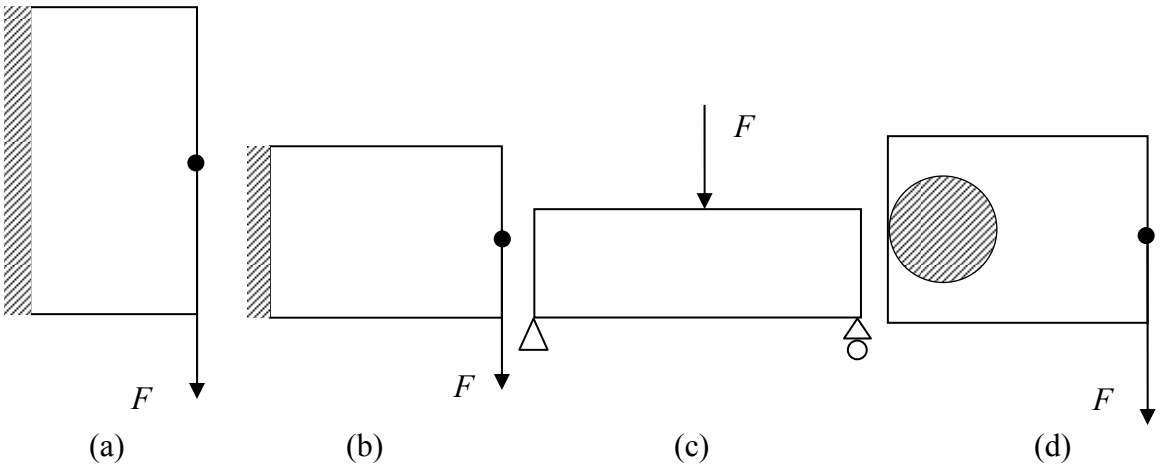

Σχήμα 6.1: Το πεδίο ορισμού των εξετασθέντων παραδειγμάτων (a) βαθύς πρόβολος, (b) κοντός πρόβολος, (c) δοκός MBB και (d) κατασκευή τύπου Michell

6.2.4.1. Παράδειγμα #1: Βαθύς πρόβολος

Ο βαθύς πρόβολος απεικονίζεται στο Σχήμα 6.1a. Οι διαστάσεις $L_x \times L_y$ *(Μήκος x'Υψος)* του, ορθογωνικής μορφής, χώρου σχεδίασης είναι $L_x = 200mm$ και $L_y = 450mm$, ενώ το αρχικό ομοιόμορφο πάχος του προβόλου είναι $t = 1mm$. Ολόκληρη η αριστερή πλευρά της κατασκευής είναι πακτωμένη, ενώ ένα σημειακό φορτίο $F = 200N$ ασκείται στο μέσο της δεξιάς πλευράς. Επιβάλλεται περιορισμός μετατόπισης $1mm$ και κατά την οριζόντια και κατά την κατακόρυφη διεύθυνση. Θεωρείται ότι το υλικό της κατασκευής έχει μέτρο ελαστικότητας $E = 200GPa$, μοναδιαία πυκνότητα και λόγο Poisson $v = 0.3$. Το πεδίο ορισμού διακριτοποιείται με 36×16 4-κομβικά ορθογωνικά πεπερασμένα στοιχεία. Σε κάθε επανάληψη, ο λόγος αποβολής υλικού (Element Elimination Ratio – ERR) ήταν σταθερός και ίσος προς 2%, ενώ εφαρμοζόταν μόνον επί των εναπομεινάντων στοιχείων.

6.2.4.2. Παράδειγμα #2: Κοντός πρόβολος

Ο βαθύς πρόβολος απεικονίζεται στο Σχήμα 6.1b. Οι διαστάσεις $L_x \times L_y$ *(Μήκος x'Υψος)* του, ορθογωνικής μορφής, χώρου σχεδίασης είναι $L_x = 160mm$ και $L_y = 100mm$, ενώ το αρχικό ομοιόμορφο πάχος του προβόλου είναι $t = 1mm$. Οι συνθήκες στήριξης και φόρτισης είναι ίδιες με αυτές του προηγουμένου παραδείγματος, με τη μόνη διαφορά ότι η ασκούμενη δύναμη έχει μέτρο $F = 3kN$. Επιβάλλεται ένας περιορισμός μετατόπισης κατά την οριζόντια και την κατακόρυφη διεύθυνση, ενώ εξετάζονται τρεις διαφορετικές τιμές επιτρεπόμενης μετατόπισης ($u_{allow} = 1mm$, $u_{allow} = 0.50mm$ και $u_{allow} = 0.75mm$). Θεωρείται ότι το υλικό της κατασκευής έχει μέτρο ελαστικότητας $E = 207GPa$, μοναδιαία πυκνότητα και λόγο Poisson $v = 0.3$. Το πεδίο ορισμού διακριτοποιείται με 32×20 4-κομβικά ορθογωνικά πεπερασμένα στοιχεία, ο λόγος αποβολής υλικού (Element Elimination Ratio – ERR), σε κάθε επανάληψη, ήταν σταθερός και ίσος προς 1%, ενώ εφαρμοζόταν μόνον επί των εναπομεινάντων στοιχείων.

6.2.4.3. Παράδειγμα #3: Δοκός MBB

Η δοκός MBB είναι η αμφιέρειστη δοκός του Σχήματος 6.1c. Οι διαστάσεις $L_x \times L_y$ *(Μήκος x'Υψος)* του, ορθογωνικής μορφής, χώρου σχεδίασης είναι $L_x = 2400mm$ και $L_y = 400mm$, ενώ το αρχικό ομοιόμορφο πάχος του προβόλου είναι $t = 1mm$. Ασκείται ένα

συγκεντρωμένο φορτίο $F = 20kN$ στο μέσο της άνω πλευράς της δοκού. Το βέλος κάμψης της κατασκευής προβλέπεται να είναι το πολύ ίσο προς $9.4mm$. Και σε αυτήν την περίπτωση, θεωρείται ότι το υλικό της κατασκευής έχει μέτρο ελαστικότητας $E = 200GPa$, μοναδιαία πυκνότητα και λόγο Poisson $\nu = 0.3$. Το πεδίο ορισμού διακριτοποιείται με 66×11 32×20 4-κομβικά ορθογωνικά πεπερασμένα στοιχεία, ο λόγος αποβολής υλικού (Element Elimination Ratio – ERR), σε κάθε επανάληψη, ήταν σταθερός και ίσος προς 1%, ενώ εφαρμοζόταν μόνον επί των εναπομεινάντων στοιχείων.

6.2.4.4. Παράδειγμα #4: Κατασκευή Michell

Η κατασκευή Michell απεικονίζεται στο Σχήμα 6.1d. Ο χώρος σχεδίασης είναι ορθογωνικής μορφή διαστάσεων $L_x \times L_y$, όπου $L_x = 550mm$ και $L_y = 400mm$, από τον οποίο έχει αφαιρεθεί ένας κύκλος ακτίνας $r = 100mm$. Ο κύκλος εφάπτεται στο μέσο της αριστερής πλευράς του ορθογωνικού χωρίου και είναι πακτωμένος καθ' όλο το μήκος της περιφερείας του. Το αρχικό ομοιόμορφο πάχος της κατασκευής είναι $t = 1mm$. Επιβάλλεται ένα σημειακό φορτίο $F = 50kN$ στο μέσο της δεξιάς πλευράς του ορθογωνικού χωρίου. Επιβάλλεται ένας περιορισμός μετατόπισης ενώ εξετάζονται τρεις διαφορετικές τιμές επιτρεπόμενης μετατόπισης ($u_{allow} = 9mm$, $u_{allow} = 5mm$ και $u_{allow} = 7mm$). Θεωρείται ότι το υλικό της κατασκευής έχει μέτρο ελαστικότητας $E = 205GPa$, μοναδιαία πυκνότητα και λόγο Poisson $\nu = 0.3$. Το πεδίο ορισμού διακριτοποιείται με 33×24 4-κομβικά ορθογωνικά πεπερασμένα στοιχεία, ο λόγος αποβολής υλικού (Element Elimination Ratio – ERR), σε κάθε επανάληψη, ήταν σταθερός και ίσος προς 0.5%, ενώ εφαρμοζόταν μόνον επί των εναπομεινάντων στοιχείων. Διευκρινίζεται ότι λόγω συμμετρίας, απαιτείται η ανάλυση μόνον του άνω μισού της κατασκευής.

6.2.5. Αποτελέσματα

Τα αποτελέσματα των εξετασθέντων παραδειγμάτων καταγράφονται στον Πίνακα 6.1.

Πίνακας 6.1: Δείκτες αξιολόγησης εξετασθέντων παραδειγμάτων

Example	Scenario	ERR (%)	Iterations	PI_1	PI_2	PI_3	PI_4
Deep cantilever	A	2	73	-99.80	-44.23	19.44	1.793
	B	2	52	-99.80	-44.14	19.79	1.790
			-28.77%	***0.00%***	***-0.22%***	***1.79%***	***-0.17%***
Short cantilever	A	1	52	-72.70	-16.37	56.88	1.196
	B	1	42	-73.16	-17.79	55.00	1.216
			-19.23%	***0.63%***	***8.64%***	***-3.30%***	***1.71%***
MBB beam	A	1	82	-99.98	-35.50	39.67	1.550
	B	1	68	-99.98	-35.99	39.95	1.562
			-17.07%	***0.00%***	***1.39%***	***0.70%***	***0.77%***
Michell structure	A	0.5	171	-77.28	-28.40	37.88	1.397
	B	0.5	78	-76.84	-27.02	56.06	1.370
			-54.39%	***-0.57%***	***-4.85%***	***48.00%***	***-1.89%***

Οι όροι 'Scenario A' και 'Scenario B' αντιστοιχούν στην εφαρμογή της τυπικής διαδικασίας ESO και της προτεινόμενης διαδικασίας, αντίστοιχα. Οι στήλες 'Iterations',

PI_1, PI_2, PI_3 και PI_4 αντιστοιχούν στους Δείκτες Αξιολόγησης. Σε κάθε παράδειγμα του Πίνακα 6.1, αντιστοιχούν τρεις γραμμές, εκ των οποίων οι πρώτες δύο περιέχουν τιμές δεικτών αξιολόγησης ενώ η τρίτη αντιστοιχεί στη σύγκριση μεταξύ των 'Scenario A' και 'Scenario B', σύμφωνα με την ακόλουθη έκφραση:

$$Value = \left(\frac{Value_{Scenario\_B} - Value_{Scenario\_A}}{Value_{Scenario\_A}} \right) \tag{6.13}$$

Για κάθε παράδειγμα, η βέλτιστη σχεδίαση απεικονίζεται στο Σχήμα 6.2.

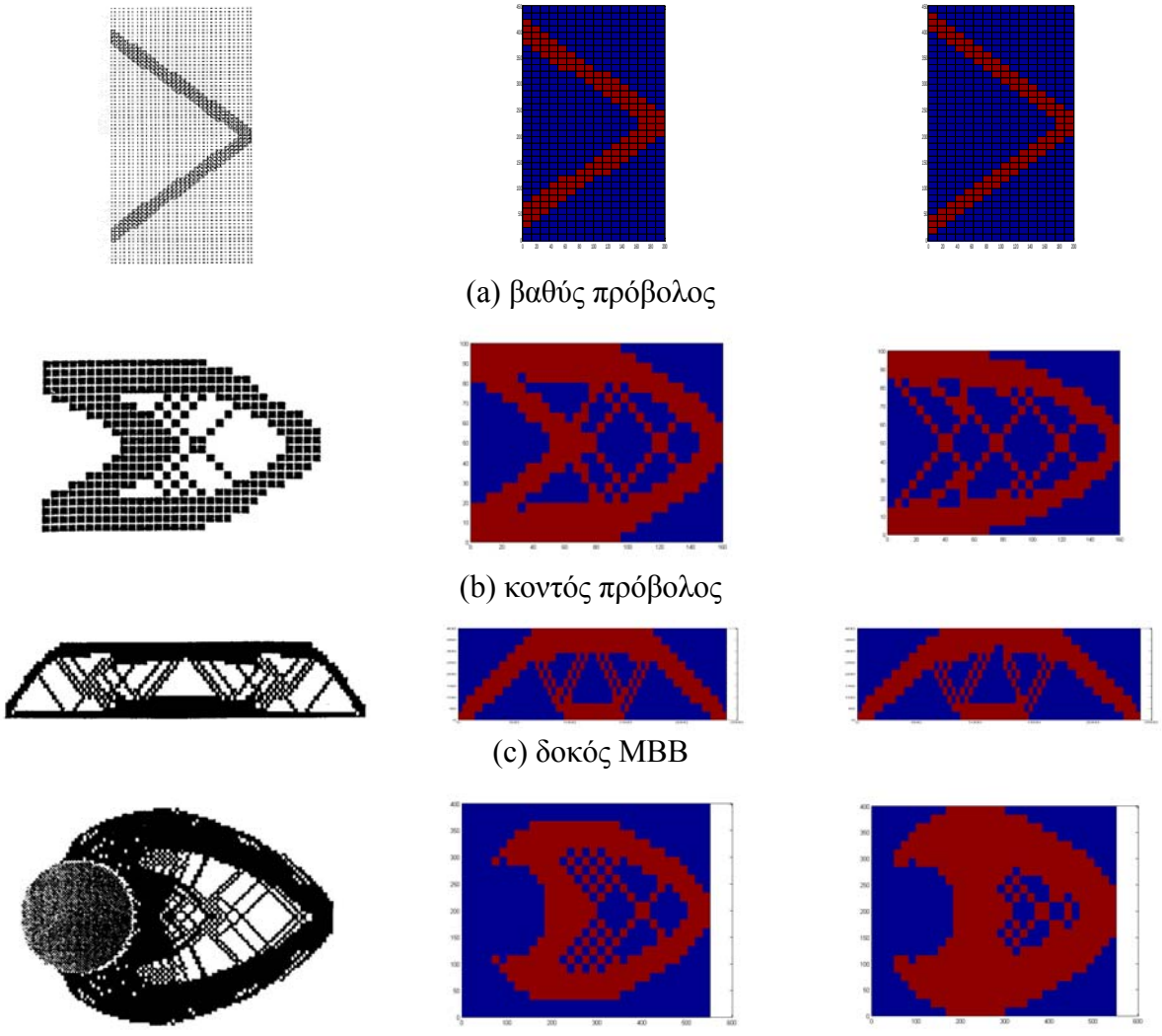

Σχήμα 6.2: Βέλτιστες σχεδιάσεις

6.2.6. Συμπεράσματα

Από τα αποτελέσματα, τα οποία παρουσιάσθηκαν στην Ενότητα 6.2.5, προκύπτει ότι η προτεινόμενη διαδικασία βελτιστοποίησης καταλήγει σε σχεδιάσεις, οι οποίες, συγκριτικά με τις υπάρχουσες βιβλιογραφικές, είναι το πολύ του αυτού βάρους (υπάρχουν περιπτώσεις στις οποίες είναι ελαφρύτερες) και έχουν προκύψει με σαφώς χαμηλότερο (από 17% έως και 54%)

υπολογιστικό κόστος. Συνεπώς, εκτός από τον ρυθμό αποβολής στοιχείων (EER) και την πυκνότητας του πλέγματος, κατεδείχθη ότι το προτεινόμενο ενεργειακό κριτήριο χαρακτηρισμού του υλικού ως πλεονάζοντος αποτελεί έναν βασικό παράγοντα στη διαδικασία βελτιστοποίησης.

6.3. Κατανομή υλικού μεταβλητού πάχους υπό την επιβολή ενός γενικευμένου περιορισμού μετατόπισης

6.3.1. Θεωρητικό υπόβαθρο

Η προτεινόμενη διαδικασία βελτιστοποίησης εμπλέκει δύο θεωρητικά στοιχεία: την βελτιστοποιημένη επανασχεδίαση της κατασκευής υπό την επιβολή ενός γενικευμένου περιορισμού μετατόπισης και το σχηματισμό του μητρώου δυσκαμψίας ενός πεπερασμένου στοιχείου μεταβλητού πάχους. Για λόγους πληρότητας, τα εν λόγω θεωρητικά στοιχεία σχολιάζονται συνοπτικά στις επόμενες παραγράφους. Διευκρινίζεται εκ των προτέρων ότι, ως ενεργό, χαρακτηρίζεται εκείνο το τμήμα της κατασκευής, στο οποίο το πάχος είναι μεγαλύτερο από την κατώτατη τιμή του αντιστοίχου περιορισμού.

6.3.2. Βέλτιστο Κριτήριο για το πρόβλημα βελτιστοποίησης υπό την επιβολή ενός περιορισμού μετατόπισης

Στο Κεφάλαιο 5 παρουσιάσθηκε ένα Βέλτιστο Κριτήριο για την περίπτωση βελτιστοποίησης σκελετικής κατασκευής υπό την επιβολή ενός γενικευμένου περιορισμού μετατόπισης, ενώ διατυπώθηκε και μία μεθοδολογία βελτιστοποίησης, κατάλληλη για την επίλυση του εν λόγω προβλήματος βελτιστοποίησης. Η προέκταση της εφαρμογής της μεθοδολογίας αυτής σε 2Δ συνεχή μέσα είναι δυνατόν να επιτευχθεί εάν στον αναδρομικό τύπο της επανασχεδίασης (Εξ.5.17) το βασικό γεωμετρικό μέγεθος της σκελετικής κατασκευής (εμβαδόν διατομής A_i ράβδου) αντικατασταθεί από το βασικό γεωμετρικό μέγεθος του συνεχούς μέσου (πάχος στοιχείου t_i):

$$t_{i,new} = t_i \left(\frac{w_i}{\overline{w}} \right) \tag{6.14}$$

Επιπροσθέτως, προτείνεται η επιβολή ομοιόμορφης διακλιμάκωσης των μεταβλητών σχεδίασης σε κάθε επανάληψη, εξασφαλίζοντας, με αυτόν τον τρόπο, την ισοτική ικανοποίηση του επιβαλλομένου περιορισμού μετατόπισης.

6.3.3. Μητρώο δυσκαμψίας 4-κομβικού τετραπλευρικού πεπερασμένου στοιχείου μεταβλητού πάχους

Το μητρώο δυσκαμψίας του 4-κομβικού τετραπλευρικού στοιχείου με ενδοστοιχειακή ισοπαραμετρική παρεμβολή πάχους περιγράφεται λεπτομερέστερα στο Παράρτημα 4Β, σύμφωνα με το οποίο ισχύει:

$$\mathbf{K}^e = \int_{-1}^{+1} \int_{-1}^{+1} \sum_{i=1}^{4} \left(N_i t_i \right) \mathbf{B}^T \, \mathrm{E} \, \mathrm{B} \, \det J \, d\xi \, d\eta \tag{6.15}$$

όπου t_i είναι το πάχος του $i-$γωνιακού κόμβου του $e-$στοιχείου, N_i είναι η αντίστοιχη συνάρτηση μορφής, **B** είναι ο 3×8 πίνακας παραμορφώσεων-μετατοπίσεων, **E** είναι το 3×3 μητρώο ελαστικότητας και **J** είναι η Ιακωβιανή, η οποία χρησιμοποιείται για τη μετάβαση από το καθολικό σύστημα $\{x, y\}$ στο τοπικό σύστημα αναφοράς $\{\xi, \eta\}$.

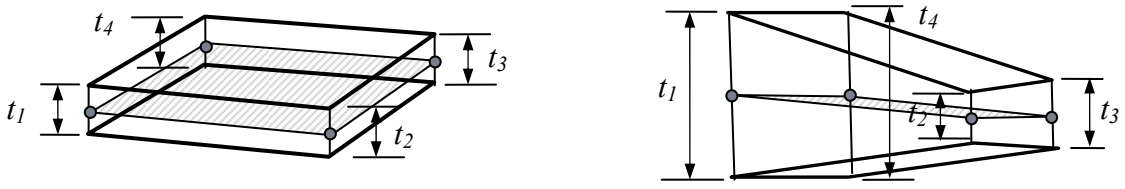

($t_1 = t_2 = t_3 = t_4$) (a)

($t_1 \neq t_2 \neq t_3 \neq t_4$) (b)

Σχήμα 6.3: 4-κομβικό τετραπλευρικό στοιχείο με (a) σταθερό και (b) μεταβλητό πάχος

6.3.4. Προτεινόμενη διαδικασία βελτιστοποίησης

Στο παρόν κεφάλαιο προτείνεται και εξετάζεται η χρήση πεπερασμένων στοιχείων μεταβλητής ενδοστοιχειακής κατανομής πάχους (Προσέγγιση #1). Για λόγους σύγκρισης, αναπτύχθηκε η αντίστοιχη προσέγγιση, όταν χρησιμοποιούνται πεπερασμένα στοιχεία σταθερής ενδοστοιχειακής κατανομής πάχους (Προσέγγιση #2). Και στις δύο περιπτώσεις, πραγματοποιείται σύγκριση με τη Σχεδίαση (OUD) (βλ. Ενότητα 6.2.3.3),

6.3.4.1. Διαδικασίας βελτιστοποίησης χρησιμοποιώντας πεπερασμένα στοιχεία μεταβλητού πάχους (Προσέγγιση #1)

Η προτεινόμενη διαδικασία είναι η ακόλουθη:

Βήμα 1: Προσδιορισμός της σχεδίασης (OUD) και καταγραφή βάρους, πάχους και συμπληρωματικής ενέργειας παραμόρφωσης (τιμές αναφοράς).

Βήμα 2: Εφαρμογή μοναδιαίου φορτίου στον πλέον κρίσιμο βαθμό ελευθερίας.

Βήμα 3: Υπολογισμός της κανονικοποιημένης πυκνότητας της συμπληρωματικής ενέργειας παραμόρφωσης για κάθε ενεργό στοιχείο.

Βήμα 4: Υπολογισμός της κανονικοποιημένης πυκνότητας της συμπληρωματικής ενέργειας παραμόρφωσης σε κάθε κόμβο ενεργών στοιχείων (ενεργοί κόμβοι)

Βήμα 5: Ανανέωση του πάχους των *ενεργών* κόμβων χρησιμοποιώντας την προτεινόμενη αναδρομική σχέση (Εξ. 6.15).

Βήμα 6: Εφαρμογή ομοιόμορφης διακλιμάκωσης πάχους ώστε καμία κομβική μετατόπιση να μην παραβιάζει τον επιβαλλόμενο περιορισμό μετατόπιση.

Βήμα 7: Έλεγχος σύγκλισης. Εάν δεν έχει επιτευχθεί σύγκλιση ούτε έχει ξεπερασθεί το μέγιστο επιτρεπόμενο πλήθος επαναλήψεων, επιστροφή στο Βήμα 2.

Βήμα 8: Εφαρμογή μίας διαδικασίας εξομάλυνσης (π.χ. τεχνικής Kriging) των κομβικών τιμών της κατανομής του πάχους.

Βήμα 9: Εφαρμογή ομοιόμορφης διακλιμάκωσης στην εξομαλυμένη κατανομή υλικού (Βήμα 7), έτσι ώστε να μην παραβιάζεται κανένας περιορισμός μετατόπισης.

Βήμα 10: Υπολογισμός των Δεικτών Αξιολόγησης.

Ο υπολογισμός της κομβικής τιμής της πυκνότητας της συμπληρωματικής ενέργειας παραμόρφωσης προκύπτει παρεμβάλλοντας κατάλληλα τις αντίστοιχες τιμές των στοιχείων, τα οποία συντρέχουν στον εκάστοτε εξεταζόμενο κόμβο. Στην παρούσα, χρησιμοποιήθηκαν τρία σχήματα παρεμβολής, τα οποία περιγράφονται στην ενότητα 6.3.6.

6.3.4.2. Διαδικασίας βελτιστοποίησης χρησιμοποιώντας πεπερασμένα στοιχεία σταθερού πάχους (Προσέγγιση #2)

Η διαδικασία είναι η ακόλουθη:

Βήμα 1: Προσδιορισμός της σχεδίασης (OUD) και καταγραφή βάρους, πάχους και συμπληρωματικής ενέργειας παραμόρφωσης (τιμές αναφοράς).
Βήμα 2: Εφαρμογή μοναδιαίου φορτίου στον πλέον κρίσιμο βαθμό ελευθερίας.
Βήμα 3: Υπολογισμός της κανονικοποιημένης πυκνότητας της συμπληρωματικής ενέργειας παραμόρφωσης για κάθε ενεργό στοιχείο.
Βήμα 4: Ανανέωση του πάχους των *ενεργών* στοιχείων χρησιμοποιώντας την προτεινόμενη αναδρομική σχέση (Εξ. 6.15).
Βήμα 5: Εφαρμογή ομοιόμορφης διακλιμάκωσης πάχους ώστε καμία κομβική μετατόπιση να μην παραβιάζει τον επιβαλλόμενο περιορισμό μετατόπιση.
Βήμα 6: Έλεγχος σύγκλισης. Εάν δεν έχει επιτευχθεί σύγκλιση ούτε έχει ξεπερασθεί το μέγιστο επιτρεπόμενο πλήθος επαναλήψεων, επιστροφή στο Βήμα 2.
Βήμα 7: Εφαρμογή μίας διαδικασίας καθολικής εξομάλυνσης (π.χ. τεχνικής Kriging) της κατανομής πάχους των στοιχείων.
Βήμα 8: Εφαρμογή ομοιόμορφης διακλιμάκωσης στην εξομαλυμένη κατανομή υλικού (Βήμα 7), έτσι ώστε να μην παραβιάζεται κανένας περιορισμός μετατόπισης.
Βήμα 9: Υπολογισμός των Δεικτών Αξιολόγησης.

Στο σημείο αυτό, διευκρινίζεται ότι η κομβική τιμή της πυκνότητας της συμπληρωματικής ενέργειας παραμόρφωσης προκύπτει παρεμβάλλοντας κατάλληλα τις τιμές των πεπερασμένων στοιχείων, τα οποία συντρέχουν στον εκάστοτε εξεταζόμενο κόμβο. Στην επόμενη ενότητα παρουσιάζονται τρία τέτοια σχήματα παρεμβολής

6.3.5. Υπολογισμός κομβικών τιμών συμπληρωματικής ενέργειας παραμόρφωσης

Η κεντρική ιδέα της προτεινομένης διαδικασίας είναι πρώτα να υπολογισθεί η πυκνότητα συμπληρωματικής ενέργειας παραμόρφωσης (ΠΣΕΠ) για κάθε πεπερασμένο στοιχείο του πλέγματος και στη συνέχεια να παρεμβληθούν οι εν λόγω τιμές στους κόμβους του πλέγματος. Συνολικά, προτείνονται τρία σχήματα παρεμβολής (έστω Σχήμα #1, Σχήμα #2 και Σχήμα #3). Για το Σχήμα #1, ως κομβική τιμή χρησιμοποιείται η μέγιστη εκ των τιμών (ΠΣΕΠ) των πεπερασμένων στοιχείων, τα οποία συντρέχουν στον εκάστοτε κόμβο. Για το Σχήμα #2, ως κομβική τιμή χρησιμοποιείται ο μέσος όρος των τιμών (ΠΣΕΠ) των πεπερασμένων στοιχείων, τα οποία συντρέχουν στον εκάστοτε κόμβο, ενώ για το Σχήμα #3 χρησιμοποιείται η ελάχιστη εκ των τιμών (ΠΣΕΠ) των πεπερασμένων στοιχείων, τα οποία συντρέχουν στον εκάστοτε κόμβο. Στην περίπτωση ενός δομημένου πλέγματος με 4-κομβικά τετραπλευρικά ορθογωνικά στοιχεία, είναι προφανές ότι σε κάθε *εσωτερικό* κόμβο του πλέγματος συντρέχουν τέσσερα πεπερασμένα στοιχεία, ενώ σε κάθε κόμβου *επί του συνόρου* συντρέχουν δύο πεπερασμένα στοιχεία. Σε κάθε, δε, γωνιακό κόμβο, η εν λόγω ενεργειακή συνεισφορά οφείλεται σε ένα και μόνον πεπερασμένο στοιχείο.

6.3.6. Αξιολόγηση της προτεινομένης διαδικασίας

Η αξιολόγηση της προτεινομένης διαδικασίας περιελάμβανε δύο στάδια. Το πρώτο στάδιο αφορούσε στη διακρίβωση του πεπερασμένου στοιχείου (4-κομβικό τετραπλευρικό στοιχείο με ισοπαραμετρική ενδοστοιχειακή παρεμβολή πάχους), το οποίο αναπτύχθηκε για τις ανάγκες της παρούσας μελέτης. Το δεύτερο στάδιο αφορούσε στην αξιολόγηση της προτεινομένης διαδικασίας βελτιστοποίησης επί τη βάσει του βελτίστου βάρους κατασκευής, της κατανομής της πυκνότητας της συμπληρωματικής ενέργειας παραμόρφωσης και της πορείας σύγκλισης.

6.3.6.1. Διακρίβωση πεπερασμένου στοιχείου μεταβλητού πάχους

Για τη διακρίβωση του πεπερασμένου στοιχείου, το οποίο προγραμματίστηκε για τις ανάγκες της παρούσας μελέτης, χρησιμοποιήθηκε το στοιχείου SHELL63 του εμπορικού

λογισμικού Ansys (ver.10). Ειδικότερα, εξετάσθηκε ένα 2Δ ορθογωνικό χωρίο σε απλή κάμψη και στη συνέχεια σε ασύμμετρο εφελκυσμό/θλίψη, για διάφορες πυκνότητες πλέγματος λόγου πλευρών 1:1. Το εν λόγω χωρίο αναλύθηκε πρώτα με κώδικα, ο οποίος αναπτύχθηκε στο πλαίσιο της παρούσας Διδακτορικής Διατριβής, και στη συνέχεια με το εμπορικό λογισμικό Ansys (επιλογές για το στοιχείο SHEL63: extra displacement shape functions excluded, membrane element stiffness only). Από τη σύγκριση των λύσεων, προέκυψε σύμπτωση των τιμών των κομβικών μετατοπίσεων μεταξύ των δύο περιπτώσεων.

6.3.6.2. Ορισμός Δεικτών Αξιολόγησης

Για την αξιολόγηση της προτεινομένης διαδικασίας χρησιμοποιήθηκαν οι ακόλουθοι δείκτες:

- Δείκτης Αξιολόγησης EI_1 : αφορά στην κανονικοποίηση του βάρους της κατασκευής πριν από την εφαρμογή της ομοιόμορφης διακλιμάκωσης του πάχους και του βάρους της κατασκευής, το οποίο αντιστοιχεί στη σχεδίαση (OUD):

$$EI_1 = \left(\frac{W_{opti}}{W_{OUD}} \right) \tag{6.16}$$

- Δείκτης Αξιολόγησης EI_2 : αφορά στην κατανομή της πυκνότητας της συμπληρωματικής ενέργειας παραμόρφωσης πριν από την εφαρμογή της ομοιόμορφης διακλιμάκωσης του πάχους και ορίζεται ως ο συντελεστής μεταβλητότητας (Coefficient of Variation – *CV*) της εν λόγω κατανομής στους ενεργούς κόμβους:

$$EI_2 = CV\left(VSED_{active\_nodes} \right) \tag{6.17}$$

- Δείκτης Αξιολόγησης EI_3: αφορά στο μέγεθος των ενεργών μελών της κατασκευής και ορίζεται, αντίστοιχα για τα στοιχεία σταθερού και μεταβλητού πάχους, ως:

$$EI_3 = \left\{ \left(\frac{NN_{active}}{NN} \right), \left(\frac{NEL_{active}}{NEL} \right) \right\} \tag{6.18}$$

όπου NN είναι το πλήθος των κόμβων και NEL είναι το πλήθος των στοιχείων.

Επιπροσθέτως, η πορεία σύγκλισης ως προς το βάρος της κατασκευής, κατεγράφη και απεικονίσθηκε με τη μορφή διαγραμμάτων.

6.3.6.3. Διακρίβωση των εξομαλυμένων βελτιστοποιημένων κατανομών

Προς εξασφάλιση της μη-παραβίασης των επιβαλλομένων περιορισμών εξ αιτίας της διαδικασίας εξομάλυνσης, επιβάλλεται μία τελευταία ανάλυση της κατασκευής με τη (ΜΠΣ), βάσει των αποτελεσμάτων της οποίας θα εφαρμοσθεί μία τελευταία ομοιόμορφη μεταβολή της κατανομής του πάχους. Με αυτόν τον τρόπο, ελαφρώς υπερ-διαστασιολογημένες κατανομές θα συρρικνωθούν και ελαφρώς υπο-διαστασιολογημένες κατανομές θα διογκωθούν. Πρόκειται για μία διαδικασία δύο βημάτων, η οποία, αν και δεν αποτελεί αναγκαία συνθήκη βελτίστου, είναι απολύτως αποδεκτή για πρακτικές εφαρμογές μηχανικού.

6.3.7. Παραδείγματα αξιολόγησης

Τα εξετασθέντα 2Δ παραδείγματα παρουσιάζονται σχηματικά στο Σχήμα 6.4.

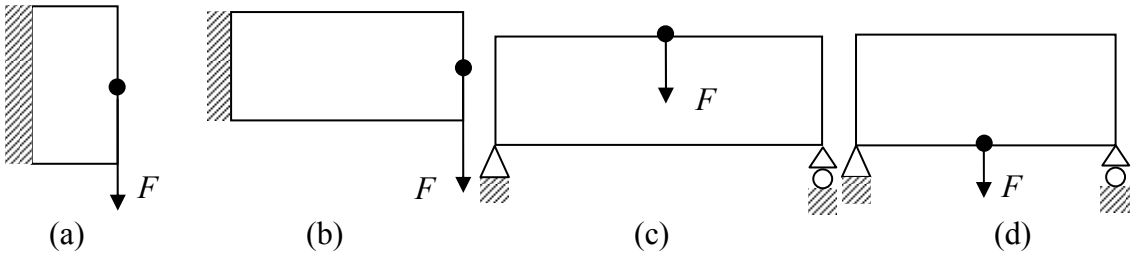

Σχήμα 6.4: Το πεδίο ορισμού των εξετασθέντων παραδειγμάτων (a) βαθύς πρόβολος, (b) κοντός πρόβολος, (c) δοκός MBB και (d) γέφυρα Michell

6.3.7.1. Παράδειγμα #1: Βαθύς πρόβολος

Τα δεδομένα του εν λόγω προβλήματος αναφέρθηκαν στην Ενότητα 6.2.4.1.

6.3.7.2. Παράδειγμα #2: Βραχύς πρόβολος

Τα δεδομένα του εν λόγω προβλήματος αναφέρθηκαν στην Ενότητα 6.2.4.2.

6.3.7.3. Παράδειγμα #3: δοκός MBB

Τα δεδομένα του εν λόγω προβλήματος αναφέρθηκαν στην Ενότητα 6.2.4.3.

6.3.7.4. Παράδειγμα #4: γέφυρα Michell

Η γέφυρα Michell απεικονίζεται στο Σχήμα 6.4d. Πρόκειται για μια αμφιέρειστη δοκό, μήκους $L_x = 2400mm$ και ύψους $L_y = 400mm$. Το αρχικό ομοιόμορφο πάχος της κατασκευής είναι $t = 1mm$. Επιβάλλεται ένα σημειακό φορτίο $F = 50kN$ στο μέσο της εφελκυόμενης ίνας της δοκού κάτω πλευράς του ορθογωνικού χωρίου. Επιβάλλεται ένας περιορισμός μετατόπισης ($u_{allow} = 9.4mm$). Θεωρείται ότι το υλικό της κατασκευής έχει μέτρο ελαστικότητας $E = 200GPa$, μοναδιαία πυκνότητα και λόγο Poisson $v = 0.3$. Το πεδίο ορισμού διακριτοποιείται με 66×11 4-κομβικά ορθογωνικά πεπερασμένα στοιχεία.

6.3.8. Αποτελέσματα

Τα αποτελέσματα των εξετασθέντων παραδειγμάτων καταγράφονται στον Πίνακα 6.2.

Πίνακας 6.2: Δείκτες Αξιολόγησης εξετασθέντων προβλημάτων

		VSED interpolation scheme #1			VSED interpolation scheme #2			VSED interpolation scheme #3		
		EI_1	EI_2	EI_3	EI_1	EI_2	EI_3	EI_1	EI_2	EI_3
Deep cantilever	t=const	0,5061	0,6420	0,9340	0,5061	0,6420	0,9340	0,5061	0,6420	0,9340
	t≠const	0,5180	1,1399	0,9094	0,5025	3,1369	0,9030	0,5044	0,3627	0,9634
	% difference	2,34%		-2,64%	-0,72%		-3,32%	-0,34%		3,15%
Short cantilever	t=const	0,6220	1,5188	0,9906	0,6220	1,5188	0,9906	0,6220	1,5188	0,9906
	t≠const	0,6356	2,9201	0,9740	0,6112	2,5655	0,9870	0,6116	0,0179	1,0000
	% difference	2,20%		-1,68%	-1,73%		-0,36%	-1,67%		0,95%
MBB beam	t=const	0,5343	0,0078	1,0000	0,5343	0,0078	1,0000	0,5343	0,0078	1,0000
	t≠const	0,5603	2,1304	0,9876	0,5094	1,9019	0,9988	0,5099	0,0025	1,0000
	% difference	4,86%		-1,24%	-4,66%		-0,12%	-4,56%		0,00%
Michell structure (bridge)	t=const	0,5343	0,0078	1,0000	0,5343	0,0078	1,0000	0,5343	0,0078	1,0000
	t≠const	0,5603	2,2111	0,9888	0,5093	1,9877	1,0000	0,5098	0,0017	1,0000
	% difference	4,87%		-1,12%	-4,68%		0,00%	-4,58%		0,00%

Από τον Πίνακα 6.2 καθίσταται φανερό ότι, σε όλες τις περιπτώσεις, είναι δυνατόν να προκύψει μία κατανομή υλικού μικρότερου βάρους, εάν χρησιμοποιηθεί η προτεινόμενη διαδικασία βελτιστοποίησης σε συνδυασμό με πεπερασμένα στοιχεία σταθερού πάχους.

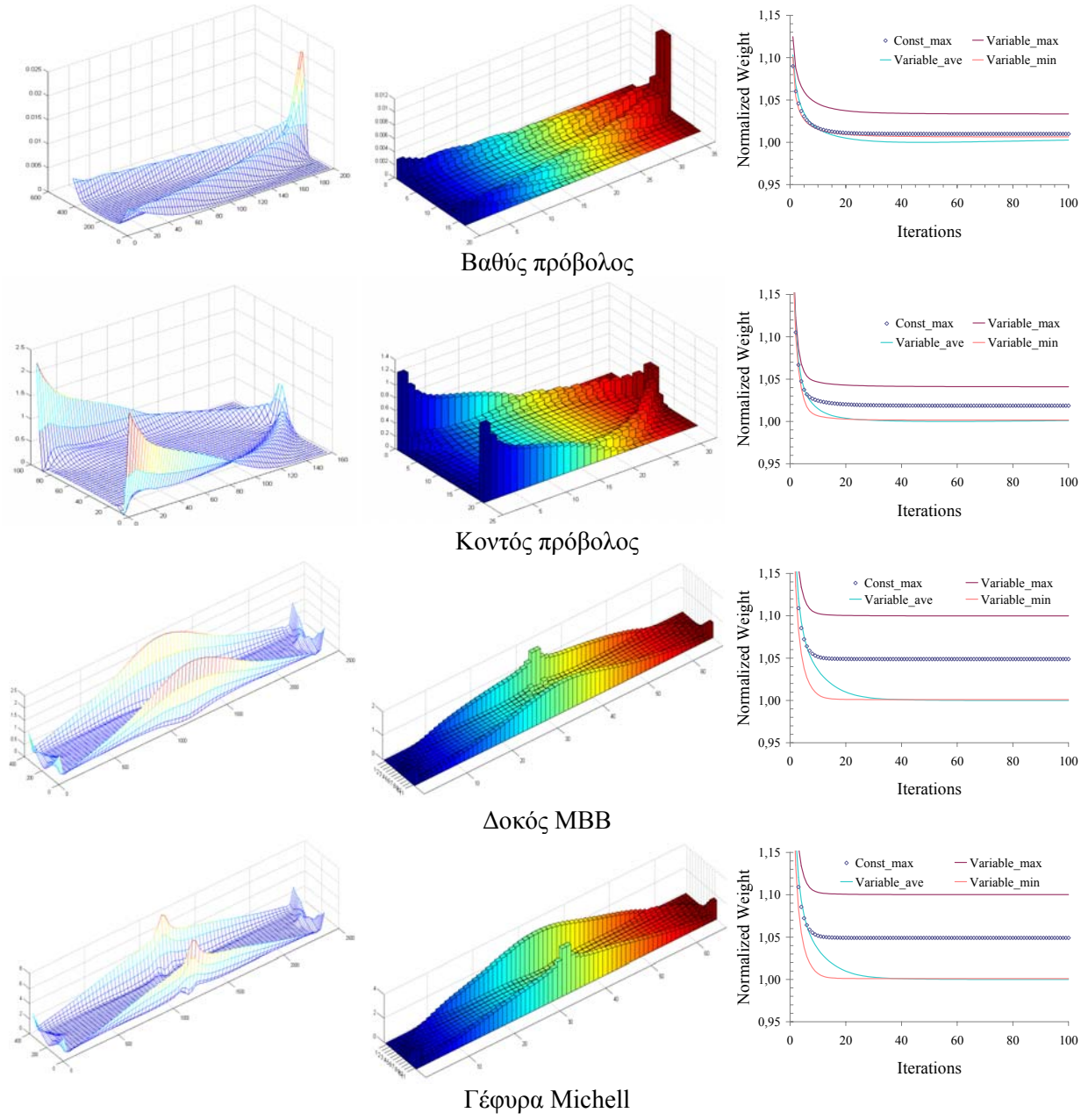

Σχήμα 6.5: Βέλτιστες κατανομές για τα εξετασθέντα παραδείγματα: (a) προσέγγιση #1, (b) προσέγγιση #2 και (c) πορεία σύγκλισης

6.3.9. Συμπεράσματα

Τα αποτελέσματα της προηγούμενης ενότητας, υποδηλώνουν ότι η μεθοδολογία, η οποία παρουσιάσθηκε στο Κεφάλαιο 5 για σκελετικές κατασκευές, είναι δυνατόν να προσαρμοσθεί και για την επίλυση προβλημάτων βελτιστοποίησης 2Δ συνεχούς μέσου υπό την επιβολή ενός γενικευμένου προβλήματος βελτιστοποίησης. Η κεντρική ιδέα αυτής της προσαρμογής ήταν η χρήση της προτεινόμενης αναδρομικής σχέσης επανασχεδίασης σε συνδυασμό με πεπερασμένα στοιχεία, στα οποία το πάχος παρεμβαλλόμενο με τις συναρτήσεις παρεμβολής του στοιχείου (ισοπαραμετρική ενδοστοιχειακή παρεμβολή πάχους). Προέκυψε ότι, με τον προτεινόμενο τρόπο βελτιστοποίησης, είναι δυνατόν να ληφθούν κατανομές, οι οποίες

αντιστοιχούν σε μικρότερο βάρος από εκείνες, οι οποίες λαμβάνονται με πεπερασμένα στοιχεία σταθερού πάχους.

Βιβλιογραφία

Belegundu, A.D., Chandrupatla, T.R. (1999), *Optimization concepts and applications in engineering*, Prentice Hall.

Bendsøe, M.P., Sigmund O. (2003), *Topology Optimization, Theory, Methods and Applications*, Springer-Verlag, Berlin.

Chu Nha, D., Xie, Y.M., Hira, A., Steven, G.P. (1996), "Evolutionary structural optimization for problems with stiffness constraints", Finite Elements in Analysis and Design, Vol. 21, pp.239-251.

Foulkes, J. (1954), "The Minimum-Weight Design of Structural Frames", *Proceedings of the Royal Society of London*, A 223 (1155), pp. 482-494.

Gellatly, R.A., Berke, L. (1973), "Optimality-criterion-based algorithms", In: Gallagher RH, Zienkiewicz OC (eds) *Optimum structural design*, Wiley, Chichester, pp 33–49.

Haftka, R.T., Gurdal, Z., Kamat, M. (1990), *Elements of Structural Optimization*, Kluwer.

Heyman, J. (1950), "On the absolute minimum weight design of framed structures", *Q. J. Mech. Appl. Math*., Vol.12, pp. 314–324.

Makris, P., Provatidis, C. (2002), "Weight minimisation of displacement-constrained truss structures using a strain energy criterion", Computer Methods Appl. Mech. Engrg., Vol. 191, pp. 2159-2177.

Michell, A.G.M. (1904), "The Limits of Economy of Material in Frame-Structures", *Phil. Mag.*, Vol. 8, pp. 589-597.

Morris, A.J. (1982), *Foundations of Structural Optimization: A Unified Approach*, John Wiley & Sons.

Ostola-Starzewski, M. (2001), "Michell trusses in the presence of microscale material randomness: limitation of optimality", *Proceedings of the Royal Society of London*, A 457, pp. 1787-1797.

Patnaik, S.N., Guptill, J.D., Berke, L. (1995), "Merits and limitations of optimality criteria method for structural optimization", *Int J Numer Methods Eng,* Vol.38, pp.3087–3120.

Pham, D.T., Karaboga D. (2000), *Intelligent Optimisation Techniques: Genetic Algorithms, Tabu Search, Simulated Annealing and Neural Netwroks*, Springer-Verlag.

Querin, O.M., Steven, G.P., Xie, Y.M., (2000), "Evolutionary structural optimisation using an additive algorithm", *Fin Elem Anal Design*, Vol. 34, Issues 3-4, pp.291-308.

Rozvany, G.I.N. (2001), "Aims, scope, methods, history and unified terminology of computer-aided topology optimization in structural mechanics", Struct. Multidisc Optim, Vol. 21, pp. 90-108.

Rozvany, G.I.N., (1989), *Structural design via optimality criteria*, Kluwer, Dordrecht.

Rozvany, G.I.N., (1992), *Shape and Layout optimization of structural systems and optimality criteria methods*, Springer-Verlag, Wien-NewYork.

Rozvany, G.I.N., (1997), *Topology optimization in structural mechanics*, CISM, Springer-Verlag.

Rozvany, G.I.N.; Zhou, M. (1991), "The COC algorithm, Part I: cross section optimization or sizing", *Comput. Methods Appl. Mech. Eng*., Vol.89, pp.281-308.

Schmit, L. A., (1960), "Structural Design by Systematic Synthesis", *Proceedings of the 2nd Conference on Electronic Computation, American Society of Civil Engineers*, New York, pp. 105-132.

Shield, R.T., Prager, W. (1970), "Optimal structural design for given deflection", *J. Appl. Math. Phys*, Vol. 21, pp. 513-523.

Venetsanos, D.T. Magoula, E.A.T. and Provatidis, C.G. (2008), "Layout optimization of stressed constrained 2D continua using finite elements of variable thickness", *6th GRACM International Congress on Computational Mechanics,* Thessaloniki, 19-21 June 2008.

Venkayya, V.B. (1971), "Design of optimum structures", *Computer & Structures*, Vol. 1, pp. 265-309.

Xie, Y.M., Steven, G.P. (1997), *Evolutionary Structural Optimization*, Springer-Verlag.

Εργασίες

[1] Provatidis C. G. and **Venetsanos, D. T.**, "The influence of normalizing the virtual strain energy density on the shape optimization of 2D continua", 1st IC-EpsMsO, 6-9 July 2005, Athens, Greece.

[2] **Venetsanos D.** and Provatidis C., "Layout Optimization of Single Displacement Constrained 2D Continua Using Finite Elements of Variable Thickness", 6th International Congress on Computational Mechanics (GRACM), Thessaloniki, 19-21 June 2008.

[3] **Venetsanos, D.T.**, Provatidis, C.G., Minimum weight designs for single displacement constrained 2D continua using variable element-wise thickness, 8th World Congress on Structural and Multidisciplinary Optimization (WCSMO8), LNEC (National Laboratory for Civil Engineering), Lisboa, Portugal, June 1- 5, 2009.

ΚΕΦΑΛΑΙΟ 7
(ΠΕΡΙΛΗΨΗ)

ΠΕΡΙ ΤΗΣ ΕΛΑΧΙΣΤΟΠΟΙΗΣΗΣ ΤΟΥ ΚΑΤΑΣΚΕΥΑΣΤΙΚΟΥ ΚΟΣΤΟΥΣ

Είναι γνωστό ότι, στις κατασκευές, ελάχιστο βάρος δεν σημαίνει απαραίτητα και ελάχιστο κόστος, οπότε η ταυτόχρονη μείωση βάρους και κόστους είναι υψηλής πρακτικής αξίας. Ωστόσο, δεν υπάρχει μία μεθοδολογία γενικής ισχύος, τέτοια ώστε να επιτυγχάνονται ταυτόχρονα οι προαναφερθέντες στόχοι, διότι, ειδικά αναφορικά με το κόστος, είναι επιβεβλημένος ο συνυπολογισμός των ιδιαιτεροτήτων της εκάστοτε κατασκευής. Αντιθέτως, είναι πιο συμφέρουσα και αποδοτική η διαμόρφωση διαδικασιών καθέτου εφαρμογής. Σε αυτό το πλαίσιο, στην παρούσα περίληψη κεφαλαίου, παρουσιάζονται δύο διαδικασίες βελτιστοποίησης, η πρώτη εκ των οποίων είναι κατάλληλη για σκελετικές κατασκευές υπό την επιβολή περιορισμών τάσης, ενώ η δεύτερη είναι κατάλληλη για συγκολλητές δεξαμενές αποθήκευσης πετρελαιοειδών. Αναφορικά με την πρώτη διαδικασία, πρόκειται για μία μετά-τη-βελτιστοποίηση τεχνική, σύμφωνα με την οποία, αρχικά, τα δομικά μέλη της ίδιας ή περίπου της ίδιας διατομής ομαδοποιούνται κατάλληλα και, τελικά, τα δομικά μέλη με κρίσιμη ή περίπου κρίσιμη διατομή διαγράφονται (απομακρύνονται) από την κατασκευή. Τόσο η ομαδοποίηση όσο και η διαγραφή στηρίζονται σε μία στατιστική προσέγγιση. Η προτεινόμενη διαδικασία εφαρμόσθηκε σε τέσσερα βιβλιογραφικά παραδείγματα, ήτοι στον κοντό πρόβολο, στον μακρύ πρόβολο, στη δοκό MBB και στη δοκό σχήματος L. Προέκυψε ότι η προτεινόμενη διαδικασία κατέληξε σε μείωση και του βάρους και του κόστους. Η, δε, επέκταση της εν λόγω διαδικασίας είτε σε 3Δ σκελετικές κατασκευές είτε σε περιπτώσεις επιβολής άλλων περιορισμών είναι τετριμμένη. Η δεύτερη εκ των προτεινομένων διαδικασιών αφορά στην ελαχιστοποίηση του κατασκευαστικού κόστους δεξαμενής αποθήκευσης πετρελαιοειδών, όταν λαμβάνονται υπόψη το χρησιμοποιούμενο υλικό, το κόστος συγκολλήσεων και η φύρα. Η εν λόγω διαδικασία εφαρμόσθηκε για πλήθος σχεδιάσεων τέτοιων δεξαμενών και τα αποτελέσματα από τις εκάστοτε βελτιστοποιήσεις καταγράφηκαν κατάλληλα σε νομογραφήματα. Από τη συνολική διερεύνηση προέκυψε ότι η διαμόρφωση διαδικασιών βελτιστοποίησης καθέτου εφαρμογής, σε αντίθεση με διαδικασίες γενικής ισχύος, είναι δυνατόν να ανταποκρίνονται καλύτερα στην απαίτηση για βελτιστοποίηση της εκάστοτε εξεταζόμενης κατασκευής.

7.1.Εισαγωγή

Είναι γνωστό ότι σε πρακτικές εφαρμογές Μηχανικού, η επιδίωξη για ελάχιστο βάρος δεν καταλήγει πάντοτε στο ελάχιστο κόστος, διότι στο κατασκευαστικό κόστος εμπλέκονται έμμεσα αρκετές παράμετροι, τρεις εκ των οποίων, ίσως οι πλέον σημαντικές, είναι η έλλειψη κοινοτυπίας, το κόστος των συγκολλήσεων και η ποσότητα του μη-αξιοποιηθέντος υλικού (φύρα).

Ο όρος 'κοινοτυπία' αφορά την ομοιότητα μεταξύ των δομικών μελών μίας κατασκευής ως προς τη διατομή τους. Ως παράδειγμα αναφέρεται ένα δικτύωμα, το οποίο αποτελείται από πεπερασμένο πλήθος ράβδων. Θεωρητικά, κάθε ράβδος δύναται να έχει διαφορετική διατομή από τις υπόλοιπες. Αυτό, αν και ενδεχομένως να είναι επιθυμητό από πλευράς μείωσης του βάρους της κατασκευής, δεν αποτελεί καλή επιλογή από πλευράς κατασκευαστικού κόστους διότι πάντοτε είναι φθηνότερη η αγορά μεγάλης ποσότητας δομικών μελών της ίδιας διατομής παρά η αγορά μικροτέρων ποσοτήτων από μέλη διαφορετικής διατομής. Συνεπώς, είναι σημαντική η αύξηση της κοινοτυπίας μίας κατασκευής.

Μία άλλη παράμετρος, η οποία επηρεάζει σημαντικά το κόστος της κατασκευής, άρα και τη σχεδίασή της, είναι κόστος των συγκολλήσεων. Ως παράδειγμα αναφέρεται η γερανογέφυρα με φορέα κλειστής διατομής. Η ελαχιστοποίηση του βάρους του εν λόγω φορέα εμπλέκει και τη χρήση διαμήκων ενισχυτικών. Ωστόσο, αυτά τα ενισχυτικά συγκολλούνται στο εσωτερικό της διατομής, κάτι το οποίο αυξάνει το κατασκευαστικό κόστος, όχι μόνον διότι η ίδια η συγκόλληση κοστίζει αλλά διότι απαιτείται και χρόνος για την κατάλληλη προετοιμασία των προς συγκόλληση τεμαχίων (τοποθέτηση τεμαχίων και οδηγών). Εναλλακτικά, είναι δυνατή η επιλογή ελασμάτων τέτοιου πάχους ώστε να μην απαιτείται η χρήση διαμήκων ενισχυτικών. Με αυτόν τον τρόπο, προσαυξάνεται μεν το βάρος αλλά μειώνεται σημαντικά το μήκος των συγκολλήσεων. Συνολικά, λοιπόν, μειώνεται το κατασκευαστικό κόστος διότι η αγορά του πλεονάζοντος υλικού κοστίζει λιγότερο από όσο θα κόστιζαν οι συγκολλήσεις, οι οποίες πλέον αποφεύγονται. Ως εκ τούτου, είναι δυνατόν να υιοθετηθεί μία εντελώς νέα σχεδιαστική τάση, η οποία καταλήγει σε βαρύτερες αλλά φθηνότερες κατασκευές.

Η φύρα, δηλαδή η ποσότητα του αγορασθέντος αλλά αναξιοποίητου υλικού, αποτελεί μία ακόμα σημαντική παράμετρο στον καθορισμό του κατασκευαστικού κόστους. Προφανώς, το ιδανικό θα ήταν η ύπαρξη μηδενικής φύρας. Προκειμένου να επιτευχθεί αυτός ο στόχος, επιβάλλεται η αξιοποίηση των ιδιαιτεροτήτων και αναγκών, τις οποίες καλείται να ικανοποιήσει η εκάστοτε κατασκευή. Στην ιδανική περίπτωση της μηδενικής φύρας, η κατασκευή αποτελείται από ακέραιο πλήθος δομικών στοιχείων, όπως είναι τα ελάσματα και οι δοκοί, στις εμπορικά διαθέσιμες διαστάσεις τους.

Στις επόμενες ενότητες παρουσιάζεται συνοπτικά η έννοια της κοινοτυπίας, η οποία εξετάζεται μέσα από παραδείγματα σκελετικών κατασκευών. Τέτοιες κατασκευές είναι δυνατόν να χρησιμοποιηθούν ως υποκατάστατα συνεχών μέσων. Επιπροσθέτως, παρουσιάζεται μία διαδικασία ελαχιστοποίησης του κατασκευαστικού κόστους, εφαρμόσιμη στην περίπτωση σχεδίασης δεξαμενών αποθήκευσης πετρελαιοειδών.

7.2. Ελαχιστοποίηση κόστους μέσω της αύξησης της κοινοτυπίας

7.2.1. Θεωρητική προσέγγιση

Η προτεινόμενη διαδικασία για την ελαχιστοποίηση κόστους κατασκευής μέσω της αύξησης της κοινοτυπίας αποτελείται από τέσσερα βήματα. Τα δύο πρώτα βήματα, δηλαδή η αντικατάσταση της κατασκευής από μία σκελετική διάταξη καθώς και η βελτιστοποίηση της διάταξης αυτής, έχουν σχολιασθεί εκτενώς σε προηγούμενα κεφάλαια. Για την πληρότητα του κειμένου, θα επαναδιατυπωθεί το πρόβλημα βελτιστοποίησης. Τα τελευταία δύο βήματα, δηλαδή η ομαδοποίηση των μελών της εν λόγω διάταξης καθώς και η διαγραφή εκείνων των

μελών, τα οποία δεν συνεισφέρουν στην αντοχή της κατασκευής, θα παρουσιασθούν με σχετικά μεγαλύτερη λεπτομέρεια.

Η έννοια της ομαδοποίησης είναι στενά συνυφασμένη με την αρχή της κοινοτυπίας (Papalambros, 1995, Fellini et al, 2003). Σύμφωνα με αυτήν την αρχή, όσο λιγότερα μέλη έχει μία κατασκευή και όσο περισσότερο όμοια είναι αυτά τα μέλη μεταξύ τους, τόσο μειώνεται το κόστος της κατασκευής. Η διαγραφή μελών από μία κατασκευή είναι στενά συνυφασμένη με το γεγονός ότι μέλη με κρίσιμη τιμή διατομής, δηλαδή με διατομή έχουσα τη μικρότερη τιμή από τις διαθέσιμες, θα έπρεπε να απομακρυνθούν από την κατασκευή διότι πρακτικά δεν συνεισφέρουν στη δυσκαμψία της κατασκευής, ενώ ταυτόχρονα αυξάνουν το βάρος της κατασκευής. Συνεπώς, το συνολικό πρόβλημα βελτιστοποίησης υποδιαιρείται σε τρία υπο-προβλήματα, ήτοι την εύρεση της βέλτιστης σχεδίασης της κατασκευής, την ομαδοποίηση των δομικών μελών και τη διαγραφή των μελών εκείνων με κρίσιμη τιμή διατομής. Τα εν λόγω επί μέρους προβλήματα είναι δυνατόν να αντιμετωπισθούν με διάφορους τρόπους. Ένας τρόπος είναι η διαμόρφωση μίας επαναληπτικής διαδικασίας, στην οποία ένας κύκλος περιλαμβάνει την εκτέλεση μίας επανάληψης για κάθε ένα από τα προαναφερθέντα υποπροβλήματα. Ένας άλλος τρόπος είναι η ενεργοποίηση της επίλυσης ενός υποπροβλήματος αφού προηγηθεί η πλήρης επίλυση του προηγομένου υποπροβλήματος, θεωρώντας ότι έχει προαποφασισθεί η σειρά με την οποία τα εν λόγω υποπροβλήματα θα αντιμετωπισθούν. Στην παρούσα υλοποιήθηκε ο δεύτερος εκ των προαναφερομένων τρόπων. Η φυσική σημασία της ομαδοποίησης σχετίζεται τόσο με τις διατομές των δομικών μελών όσο και τις ομάδες αυτών.

Αναφορικά με τις διατομές, έστω ότι σε μία κατασκευή υπάρχουν N δομικά μέλη. Στην πλέον γενική περίπτωση, η βέλτιστη σχεδίαση θα περιλαμβάνει N_c διατομές με κρίσιμη τιμή εμβαδού και $N_{nc} = N - N_c$ διατομές με μη-κρίσιμη τιμή εμβαδού. Αν και δεν είναι απαραίτητο, οι N_{nc} διατομές είναι δυνατόν να διαιρεθούν σε N_g ομάδες, σε κάθε μία εκ των οποίων τα μέλη θα έχουν την ίδια ή περίπου την ίδια διατομή. Σε μία τέτοια περίπτωση και από την οπτική γωνία του κατασκευαστικού κόστους, θα ήταν επιθυμητό όλα τα μέλη μίας ομάδας να αποκτήσουν την ίδια διατομή, κάτι που θα κατέληγε στη χρησιμοποίηση N_g διαφορετικών διατομών και όχι $N > N_g$. Από καθαρά θεωρητική άποψη, κάτι τέτοιο δεν ενδείκνυται διότι ακόμα και μία ελαφρά διαφοροποίηση των διατομών μίας βέλτιστης σχεδίασης προκαλεί την παραβίαση κάποιου εκ των επιβαλλομένων περιορισμών. Ωστόσο, στις πρακτικές εφαρμογές Μηχανικού, κάτι τέτοιο ενδείκνυται διότι είναι δυνατόν να οδηγήσει σε σημαντική μείωση του κατασκευαστικού κόστους, ενώ οι παραβιάσεις των περιορισμών να είναι πολύ μικρές, έως και αμελητέες.

Αναφορικά με τις ομάδες διατομών, έστω ότι τα μέλη μίας κατασκευής έχουν ήδη ομαδοποιηθεί με κριτήριο τη διατομή τους και έστω ότι κάποια μέλη ίδια διατομής είναι συνευθειακά. Σε αυτήν την περίπτωση, είναι δυνατή η μεταξύ τους συνένωση, υπό την έννοια ότι δύο ή περισσότερα συνευθειακά μέλη και της αυτής διατομής, αντικαθίστανται από ένα δομικό μέλος της ίδια διατομής και με μήκος ίσο προς το άθροισμα των μηκών των επί μέρους μελών. Από καθαρά θεωρητικής απόψεως, αυτή η επιλογή πιθανότατα να καταλήξει στο σχηματισμό ενός κακώς ορισμένου μητρώου δυσκαμψίας, διότι η συνένωση μελών πρακτικά εμπεριέχει την απομάκρυνση κόμβων από το πλέγμα, οπότε τα μέλη που συντρέχουν στους προς απομάκρυνση κόμβους ίσως να μην στηρίζονται πλέον επαρκώς. Η αναίρεση ενός τέτοιου προβλήματος είναι εφικτή με ελαφρές σχεδιαστικές τροποποιήσεις. Ωστόσο, από πρακτικής απόψεως, η ομαδοποίηση μελών είναι μία πολύ καλή ιδέα διότι με αυτόν τον τρόπο μειώνεται και το πλήθος των σημείων σύνδεσης, άρα και το κόστος συναρμολόγησης και συντήρησης.

7.2.2. Διατύπωση του προβλήματος

Μία 2Δ σκελετική κατασκευή, η οποία είναι δυνατόν να θεωρηθεί ως δικτύωμα αντικαθιστόν ένα 2Δ συνεχές μέσο, δεν είναι τίποτε άλλο παρά ένα σύνολο ράβδων, το βάρος W των οποίων ισούται με:

$$W = \sum_{i=1}^{n} x_i \rho_i l_i \tag{7.1}$$

Η αξονική τάση της *i*-ράβδου ισούται με:

$$\sigma_i = \left(\frac{^{\text{int}}F_i}{x_i} \right) \tag{7.2}$$

και ο περιορισμός τάσης σχετικά με την *i*-ράβδο εκφράζεται ως εξής:

$$g_i = \left(\frac{\sigma_i}{\sigma_{\max,i}} - 1 \right) \le 0 \tag{7.3}$$

Εάν αναζητείται το ελάχιστο βάρος W της κατασκευής, είναι δυνατόν να διατυπωθεί η ακόλουθη τετραγωνική μορφή του προβλήματος:

$$\min\ W\left(\Delta \underset{\sim}{x}\right) = W\left(\underset{\sim}{x}\right) + \nabla W\left(\underset{\sim}{x}\right)\Delta \underset{\sim}{x} + \left(\frac{1}{2}\right)\Delta \underset{\sim}{x}^T \nabla^2 W\left(\underset{\sim}{x}\right)\Delta \underset{\sim}{x} \tag{7.4}$$

$$\text{subject to } g_i\left(\underset{\sim}{x}\right) + \nabla g_i\left(\underset{\sim}{x}\right)^T \Delta \underset{\sim}{x} \le 0, \quad i = 1,2,...,N \tag{7.5}$$

Εάν θεωρηθεί ότι οι ράβδοι είναι κυκλικής διατομής, τότε το βάρος της κατασκευής εκφράζεται συναρτήσει του τετραγώνου της ακτίνας R_i της εκάστοτε διατομής:

$$W = \sum_{i=1}^{n} \pi R_i^2 \rho_i l_i \tag{7.6}$$

Σε αυτήν, δε, την περίπτωση, η αξονική τάση της *i*-ράβδου εκφράζεται ως:

$$\sigma_i = \left(\frac{^{\text{int}}F_i}{\pi R_i^2} \right) \tag{7.7}$$

Ως προς την ακτίνα R_i της εκάστοτε κυκλικής διατομής, η τετραγωνική μορφή του προβλήματος διατυπώνεται ως εξής:

$$\min\ W\left(\Delta \underset{\sim}{R}\right) = W\left(\underset{\sim}{R}\right) + \nabla W\left(\underset{\sim}{R}\right)\Delta \underset{\sim}{R} + \left(\frac{1}{2}\right)\Delta \underset{\sim}{R}^T \nabla^2 W\left(\underset{\sim}{R}\right)\Delta \underset{\sim}{R} \tag{7.8}$$

$$\text{subject to } g_i\left(\underset{\sim}{R}\right) + \nabla g_i\left(\underset{\sim}{R}\right)^T \Delta \underset{\sim}{R} \le 0, \quad i = 1,2,...,N \tag{7.9}$$

Η τελευταία διατύπωση είναι προτιμητέα έναντι εκείνης των Εξ.(7.4, 7.5), διότι η αντικειμενική συνάρτηση αποτελεί έκφραση τετραγωνικής μορφής ως προς τις μεταβλητές σχεδίασης, συνεπώς ο πίνακας Hessian $\nabla^2 W\left(\underset{\sim}{R}\right)$ είναι ένας καλώς ορισμένος διαγώνιος πίνακας.

7.2.3. Η έννοια της ομαδοποίησης

Η *ομαδοποίηση διατομών* (Σχήμα.7.1) αφορά δομικά μέλη με ίδια ή περίπου ίδια διατομή. Σε αυτήν την περίπτωση, είναι δυνατόν να αποδοθεί η ίδια διατομή σε όλα αυτά τα μέλη, τα οποία και εντάσσονται σε μία ομάδα με κοινή διατομή. Με αυτόν τον τρόπο, το πλήθος των διαφορετικών διατομών, οι οποίες τελικά θα χρησιμοποιηθούν για τη βέλτιστη σχεδίαση, μειώνεται.

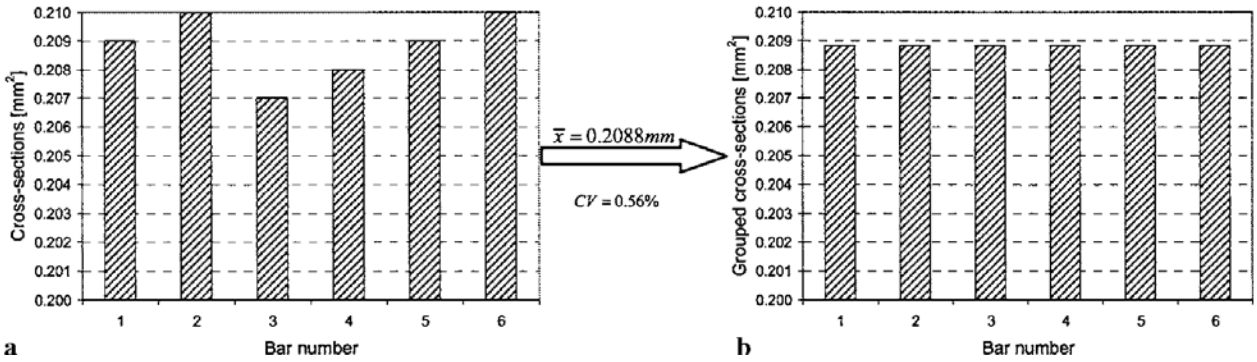

Σχήμα 7.1: Ομαδοποίηση διατομών

Από την άλλη πλευρά, η *ομαδοποίηση μελών* (Σχήμα.7.2) αφορά σε δομικά μέλη τα οποία όχι μόνον διαθέτουν ίδια διατομή αλλά είναι και συνευθειακά. Σε αυτήν την περίπτωση, τα εν λόγω μέλη συνενώνονται και αντικαθίστανται από ένα μέλος, ίδιας διατομής με τα επί μέρους μέλη, το μήκος του οποίου ισούται με το άθροισμα των μηκών των επί μέρους μελών. Με αυτόν τον τρόπο, μειώνεται το πλήθος των μελών μίας ομάδας διατομών.

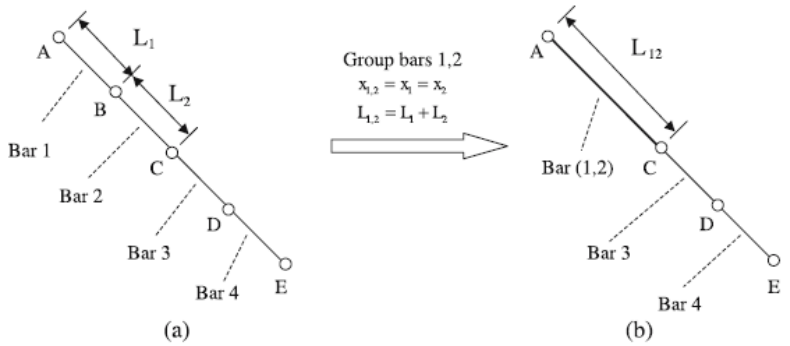

Σχήμα 7.2: Ομαδοποίηση μελών

7.2.4. Διαδικασία ομαδοποίησης διατομών

Η προτεινόμενη ομαδοποίηση διατομών, μετά το πέρας της διαδικασίας βελτιστοποίησης, στηρίζεται στον απλό στατιστικό κανόνα σύμφωνα με τον οποίο μία ομάδα τιμών *xi* είναι δυνατόν να αντικατασταθεί από την μέση τιμή τους $\bar{x}$ εάν η αντίστοιχη τυπική απόκλιση s, ή, ισοδύναμα, η τιμή του συντελεστή μεταβλητότητα CV, είναι αρκούντως μικρή. Ειδικότερα, η προτεινόμενη διαδικασία ομαδοποίησης είναι η ακόλουθη:

Βήμα 1: ταξινόμηση κατά φθίνουσα όλων διατομών $x_i, i = 1,2,...,N$ της βέλτιστης σχεδίασης

Βήμα 2**:** απόδοση της τιμής 1 στον μετρητή των ομάδων διατομών (gn) και του τρέχοντος στοιχείου (ce) $(gn = ce = 1)$

Βήμα 3: απόδοση της τιμής x_1 στην ομάδα $gn = 1$

Βήμα 4: απόδοση στον μετρητή ce του τρέχοντος στοιχείου της τιμής 2

Βήμα 5: απόδοση της τιμής x_{ce} στην ομάδα gn

Βήμα 6: για την ομάδα gn, υπολογισμός της μέσης τιμής $\overline{x}_{gn}$ και της τυπικής απόκλισης s_{gn} (ή του συντελεστού μεταβλητότητας CV_{gn})

Βήμα 7: ΕΑΝ $s_{gn} \le tol$ (ή $CV_{gn} \le tol$) ΤΟΤΕ αύξηση του μετρητή ce κατά 1 και επιστροφή στο Βήμα 5

Βήμα 8: ΕΑΝ $s_{gn} > tol$ (ή $CV_{gn} > tol$) ΤΟΤΕ

Απομάκρυνση του στοιχείου ce από την ομάδα gn

Αύξηση του μετρητή των ομάδων διατομών gn κατά 1

Απόδοση του στοιχείου ce στη νέα ομάδα gn

Αύξηση του μετρητή του τρέχοντος στοιχείου ce κατά 1

Βήμα 9: ΕΑΝ $ce < N$ ΤΟΤΕ επιστροφή στο Βήμα 5 ΔΙΑΦΟΡΕΤΙΚΑ Τερματισμός

Σημειώνεται ότι η ποσότητα tol είναι μία μικρή, θετική ποσότητα και ορίζεται από τον χρήστη. Είναι προφανές ότι σημαντικών διαφορετικές τιμές της ποσότητας tol είναι δυνατόν να καταλήξουν σε σημαντικώς διαφορετικές βέλτιστες σχεδιάσεις. Η ανωτέρω διαδικασία αποτελεί μία συστηματική, στατιστικής φύσεως, ταξινόμηση των διατομών σε ομάδες. Το επόμενο βήμα είναι η απομάκρυνση (διαγραφή) ομάδων διατομών με αμελητέα συνεισφορά στην κατασκευή. Με άλλα λόγια, το επόμενο βήμα είναι η ελαχιστοποίηση του μετρητή gn.

7.2.5. Διαγραφή ομάδων διατομών

Από στατιστικής απόψεως, η διαγραφή ομάδων διατομών έχει την έννοια της συνένωσης, μία διαδικασία η οποία υπακούει σε συγκεκριμένους στατιστικούς κανόνες (Petruccelli, 1999). Από την οπτική γωνία ενός Μηχανικού, η διαγραφή ομάδων διατομών, μετά την εφαρμογή μίας διαδικασίας βελτιστοποίησης, έχει την έννοια της απομάκρυνσης όλων εκείνων των μελών με διατομή ίση ή περίπου ίση με την μικρότερη δυνατή διατομή, διότι αυτά τα μέλη δεν συνεισφέρουν στην αντοχή της κατασκευής. Στην πραγματικότητα, πρόκειται για μέλη τα οποία πολύ πιθανώς να απομακρύνονταν κατά τη διαδικασία της βελτιστοποίησης, ωστόσο διατηρούνται στην κατασκευή για λόγους αριθμητικής ευστάθειας. Η διαγραφή μίας ομάδας διατομών είναι δυνατόν να επιτευχθεί μέσα από μία διαδικασία δύο βημάτων. Στο πρώτο βήμα, κατασκευάζεται ένα ιστόγραμμα με όλες τις διατομές, οι οποίες εμφανίζονται στη βέλτιστη σχεδίαση, προκειμένου να εντοπισθούν πιθανές προς απομάκρυνση ομάδες διατομών. Στο δεύτερο βήμα, ελέγχεται κατά πόσον διακυβεύεται η ευστάθεια της κατασκευής από την απομάκρυνση μίας υποψήφιας ομάδος διατομών. Αυτό ελέγχεται πολύ εύκολα, εκτιμώντας, για το μητρώο δυσκαμψίας της εκάστοτε ελεγχόμενης κατασκευής, το βαθμό κατάστασης, μέσω του οποίου διαπιστώνεται κατά πόσον το εν λόγω μητρώο είναι αντιστρέψιμο ή όχι. Στην παρούσα, χρησιμοποιήθηκε η προσέγγιση των προαναφερθέντων δύο βημάτων.

7.2.6. Περαιτέρω δυνατές επεμβάσεις

Η διαδικασία της διαγραφής διατομών δεν είναι τίποτε άλλο παρά απομάκρυνση υλικού από την κατασκευή, οπότε η ποσότητα του εναπομείναντος στην κατασκευή υλικού μειώνεται. Αυτό σημαίνει ότι το βάρος της κατασκευής μειώνεται, ενώ οι αναπτυσσόμενες τάσεις αυξάνονται, ενδεχομένως παραβιάζοντας ελαφρά τους επιβαλλόμενους περιορισμούς τάσης. Σε εφαρμογές Μηχανικού, αυτή η προσέγγιση είναι αποδεκτή και εάν η προκύπτουσα σκελετική κατασκευή είναι υπερστατική τότε δεν απαιτείται η λήψη κάποιων πρόσθετων μέτρων. Στην περίπτωση διαμόρφωσης ισοστατικού δικτυώματος, η επιπρόσθετη εφαρμογή μίας διαδικασίας βελτιστοποίησης επί του εν λόγω δικτυώματος θα οδηγήσει σε μία νέα διαστασιολόγηση με ταυτόχρονη ικανοποίηση όλων των περιορισμών. Εάν, δε, η προκύπτουσα σκελετική κατασκευή είναι υποστατική (μηχανισμός), τότε απαιτείται πρώτα η προσθήκη δομικών μελών προς διαμόρφωση μίας τουλάχιστον ισοστατικής κατασκευής και στη συνέχεια η επιπρόσθετη εφαρμογή μίας διαδικασίας βελτιστοποίησης, όπως αναφέρθηκε προηγουμένως.

7.2.7. Αριθμητικά παραδείγματα

Στην παρούσα ενότητα, μελετήθηκαν τέσσερα βιβλιογραφικά παραδείγματα, ήτοι ο κοντός πρόβολος, ο μακρύς πρόβολος, η δοκός MMB (Messerschmitt-Bölkow-Blohm) και η δοκός σχήματος L (L-δοκός). Πιο συγκεκριμένα, η διαδικασία, η οποία εφαρμόσθηκε, αποτελείται από τις ακόλουθες φάσεις (κατά σειρά εκτέλεσης):

Φάση 1: Βελτιστοποίηση της κατασκευής με τη μέθοδο SQP (βλ. Ενότητα 8.2.3)
Φάση 2: Ομαδοποίηση των δομικών μελών (βλ. Ενότητα 8.2.4)
Φάση 3: Διαγραφή ‘άχρηστων’ δομικών μελών (βλ. Ενότητα 8.2.5)
Φάση 4: Όπου εφικτόν, εφαρμογή διαδικασίας μετά-ομαδοποίησης (βλ. Ενότητα 8.2.6)

Μετά το πέρας των Φάσεων 1, 3 και 4, καταγράφηκαν και συγκρίθηκαν ο όγκος της κατασκευής και η μέγιστη αξονική τάση. Για λόγους ελέγχου και επιβεβαίωσης των αποτελεσμάτων, οι εκάστοτε προκύπτουσες βέλτιστες σχεδιάσεις αναλύονταν με το εμπορικό λογισμικό ανάλυσης κατασκευών ALGOR (ver.12).

Στις επόμενες ενότητες, παρουσιάζονται τα αποτελέσματα για κάθε ένα από τα εξετασθέντα παραδείγματα. Κάθε παράδειγμα συνοδεύεται από δύο Σχήματα. Το πρώτο Σχήμα διαθέτει τέσσερεις απεικονίσεις, εκ των οποίων η πρώτη (a) δείχνει την προς μελέτη κατασκευής (οι διαστάσεις σε [m]), η δεύτερη (b) δείχνει το πλέγμα (σκελετική προσέγγιση) της κατασκευής, η τρίτη (c) παρουσιάζει το αποτέλεσμα της Φάσεως 1, ενώ η τέταρτη (d) παρουσιάζει το αποτέλεσμα της Φάσεως 4. Το δεύτερο Σχήμα περιλαμβάνει ένα διάγραμμα κατανομής διατομών, για την εκάστοτε κατασκευή και μετά το πέρας της Φάσεως 1, καθώς και έναν Πίνακα με στατιστικά στοιχεία σχετικά με την ομαδοποίηση των διατομών της βελτιστοποιημένης σχεδίασης.

7.2.7.1. Ο κοντός πρόβολος

Ο κοντός πρόβολος, ως μία 2Δ σκελετική κατασκευή, απεικονίζεται στο Σχήμα 8.3a. Η αριστερή πλευρά $(x=0)$ του προβόλου είναι πακτωμένη, ενώ ένα κατακόρυφο φορτίο $F=12N$ ασκείται στη δεξιά πλευρά του και στη θέση $(x,y)=(1,1.5)$. Η μέγιστη επιτρεπόμενη τάση είναι $\sigma_{\max}=30Pa$, ενώ το μέτρο ελαστικότητας είναι $E=1Pa$. Για τον εν λόγω πρόβολο, είναι γνωστό ότι η βέλτιστη σχεδίαση της σκελετικής του διαμόρφωσης προκύπτει όταν χρησιμοποιηθεί πλέγμα με λόγο πλευρών $\lambda=1$ (Provatidis και Venetsanos,

2003). Βάσει αυτής της πληροφορίας, δημιουργήθηκε το πλέγμα του Σχήματος 8.3b, το οποίο αποτελείται από 456 ράβδους.

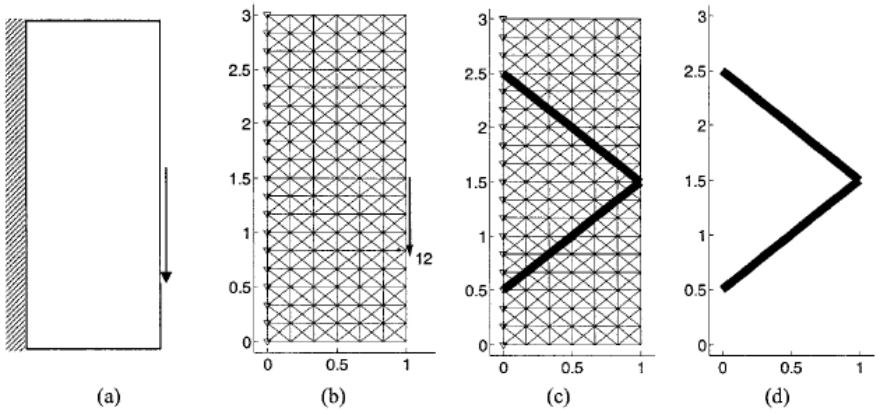

Σχήμα 7.3: Ο κοντός πρόβολος

Το αποτέλεσμα της εφαρμογής της Φάσεως 1 απεικονίζεται στο Σχήμα 7.3c, ενώ το αποτέλεσμα της εφαρμογής της Φάσεως 4 φαίνεται στο Σχήμα 7.3d. Η κατανομή των διατομών μετά τη Φάση 1 παρουσιάζεται στο Σχήμα 7.4a, ενώ αναλυτικότερα στατιστικά στοιχεία σχετικά με τη Φάση 4 παρουσιάζονται στο Σχήμα 7.4b.

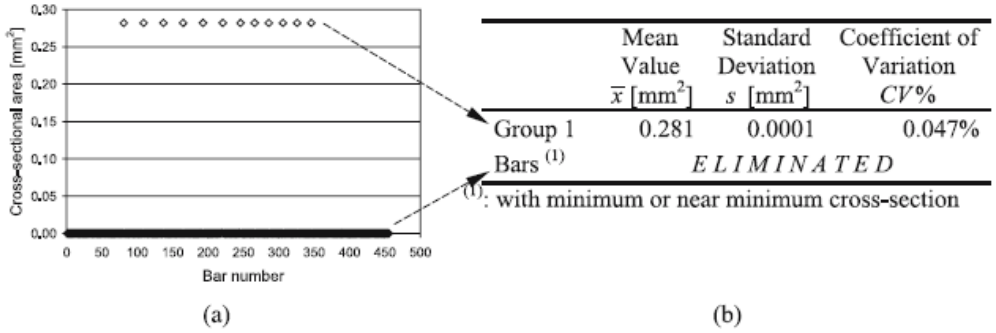

	Mean Value $\overline{x}$ [mm²]	Standard Deviation s [mm²]	Coefficient of Variation CV%
Group 1	0.281	0.0001	0.047%
Bars (1)	*ELIMINATED*		

(1): with minimum or near minimum cross-section

Σχήμα 7.4: Στατιστική ανάλυση δομικών στοιχείων για τον βελτιστοποιημένο κοντό πρόβολο

7.2.7.2. Ο μακρύς πρόβολος

Ο μακρύς πρόβολος απεικονίζεται στο Σχήμα 7.5a. Η αριστερή πλευρά $(x=0)$ του προβόλου είναι πακτωμένη, ενώ ένα κατακόρυφο φορτίο $F=12N$ ασκείται στη δεξια πλευρά του και στη θέση $(x,y)=(16,5)$. Η μέγιστη επιτρεπόμενη αξονική τάση είναι $\sigma_{\max}=30Pa$, ενώ το μέτρο ελαστικότητας είναι $E=1Pa$. Για τον εν λόγω πρόβολο, είναι γνωστό ότι η βέλτιστη σχεδίαση της σκελετικής του διαμόρφωσης προκύπτει όταν χρησιμοποιηθεί πλέγμα με λόγο πλευρών $\lambda=(5/8)$ (Provatidis και Venetsanos, 2003). Βάσει αυτής της πληροφορίας, δημιουργήθηκε το πλέγμα του Σχήματος 7.5b, το οποίο αποτελείται από 420 ράβδους. Το αποτέλεσμα της εφαρμογής της Φάσεως 1 απεικονίζεται στο Σχήμα 7.5c, ενώ το αποτέλεσμα της εφαρμογής της Φάσεως 4 φαίνεται στο Σχήμα 7.5d. Η κατανομή των διατομών μετά τη Φάση 1 παρουσιάζεται στο Σχήμα 7.6a, ενώ αναλυτικότερα στατιστικά στοιχεία σχετικά με τη Φάση 4 παρουσιάζονται στο Σχήμα 7.6b.

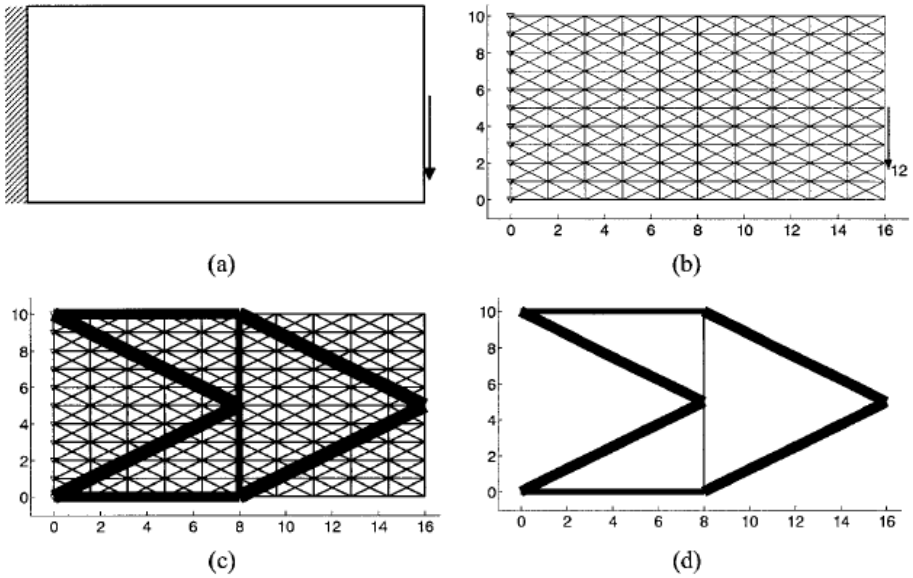

Σχήμα 7.5: Ο μακρύς πρόβολος

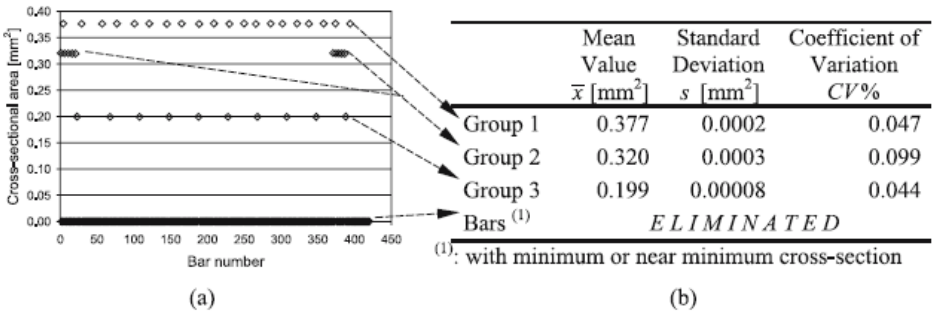

	Mean Value $\overline{x}$ [mm²]	Standard Deviation s [mm²]	Coefficient of Variation CV%
Group 1	0.377	0.0002	0.047
Group 2	0.320	0.0003	0.099
Group 3	0.199	0.00008	0.044
Bars (1)	*ELIMINATED*		

(1): with minimum or near minimum cross-section

Σχήμα 7.6: Στατιστική ανάλυση δομικών στοιχείων για τον βελτιστοποιημένο μακρύ πρόβολο

7.2.7.3. Η δοκός MBB

Η δοκός MBB απεικονίζεται στο Σχήμα 7.7a. Το κάτω αριστερό άκρο $(x, y) = (0,0)$ της δοκού είναι αρθρωμένο, ενώ το κάτω δεξιό άκρο της $(x, y) = (6,0)$ φέρει κύλιση. Ένα κατακόρυφο φορτίο $F = 2N$ ασκείται στο μέσο $(x, y) = (3,1)$ της δοκού. Η μέγιστη επιτρεπόμενη τάση είναι $\sigma_{\max} = 20Pa$, ενώ το μέτρο ελαστικότητας είναι $E = 1Pa$. Για τη δοκό MBB είναι γνωστό ότι η βέλτιστη σχεδίαση της αντίστοιχης σκελετικής διαμόρφωσης επιτυγχάνεται όταν ο λόγος πλευρών είναι ίσος προς $\lambda = 1$ (Provatidis και Venetsanos, 2003). Με βάση αυτήν την πληροφορία, δημιουργήθηκε το πλέγμα του Σχήματος 7.7a, το οποίο περιλαμβάνει 412 ράβδους.

Το αποτέλεσμα της εφαρμογής της Φάσεως 1 της προτεινομένης διαδικασίας απεικονίζεται στο Σχήμα 7.7c και το τελικό αποτέλεσμα της εφαρμογής της Φάσεως 4 παρουσιάζεται στο Σχήμα 7.7d. Η κατανομή των διατομών των ράβδων μετά τη Φάση 1 φαίνεται στο Σχήμα 7.8a, ενώ αναλυτικότερα στατιστικά στοιχεία σχετικά με τη Φάση 4 παρουσιάζονται στο Σχήμα 7.8b.

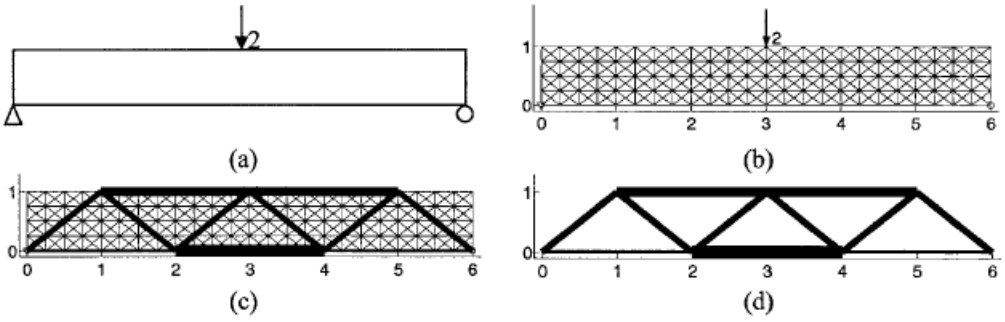

Σχήμα 7.7: Η δοκός MBB

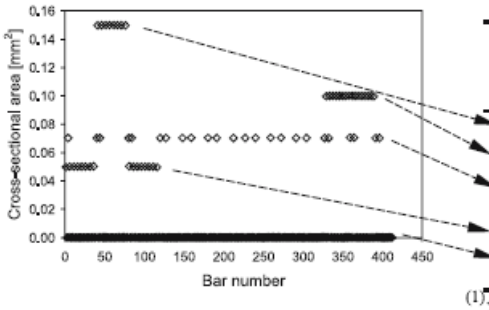

	Mean Value $\bar{x}$ [mm²]	Standard Deviation s [mm²]	Coefficient of Variation CV%
Group 1	0.149	0.00015	0.100
Group 2	0.099	0.00029	0.299
Group 3	0.070	0.00014	0.206
Group 4	0.049	0.00033	0.659
Bars (1)	*ELIMINATED*		

(1): with minimum or near minimum cross-section

(b)

Σχήμα 7.8: Στατιστική ανάλυση δομικών στοιχείων για τη βελτιστοποιημένη δοκό MBB

7.2.7.4. Η δοκός σχήματος L (L-δοκός)

Η δοκός σχήματος L απεικονίζεται στο Σχήμα 7.10a. Όπως φαίνεται, η άνω ακμή $(y=0)$ της δοκού είναι πακτωμένη, ενώ ένα κατακόρυφο φορτίο $F=1N$ ασκείται στη θέση $(x,y)=(1,0.2)$. Η μέγιστη επιτρεπόμενη τάση είναι $\sigma_{\max}=30Pa$, ενώ το μέτρο ελαστικότητας είναι ίσο με $E=1Pa$. Για την L-δοκό είναι γνωστό ότι εάν χρησιμοποιηθεί ενιαίο πλέγμα, δηλαδή εάν ο λόγος πλευρών είναι σταθερός σε όλη την έκταση του πλέγματος, τότε το ελάχιστο βάρος προκύπτει για λόγο πλευρών $\lambda=(1/2)$ (Provatidis και Venetsanos, 2003). Ωστόσο, σε αυτήν την περίπτωση, προκύπτει μία κατανομή διατομών με αρκετά μεγάλη διασπορά, όπως φαίνεται στο Σχήμα 7.9b, κάτι που λειτουργεί εις βάρους της κοινοτυπίας. Συνεπώς, η χρήση μη-ενιαίου πλέγματος (Σχήμα 7.10b). Θεωρώντας λόγους πλευρών $\lambda_1=1$, $\lambda_2=(1/2)$ και $\lambda_3=(1/3)$, ως φαίνεται στο Σχήμα 7.10b, κατασκευάσθηκε ένα πλέγμα με 825 ράβδους. Το αποτέλεσμα της εφαρμογής της Φάσεως 1 της προτεινόμενης διαδικασίας απεικονίζεται στο Σχήμα 7.10c, ενώ το τελικό αποτέλεσμα της Φάσεως 4 φαίνεται, με συνεχείς γραμμές, στο Σχήμα 7.10d. Η κατανομή των διατομών μετά την επιβολή της Φάσεως 1 απεικονίζεται στο Σχήμα 7.11a, ενώ στατιστικά στοιχεία σχετικά με την εν λόγω κατανομή παρουσιάζονται στο Σχήμα 7.11b. Σε αυτό το σημείο διευκρινίζεται ότι ο χρήστης είναι δυνατόν να επέμβει στην τελική κατασκευή, προκειμένου να τοποθετήσει, κατά την κρίση του, επιπρόσθετα δομικά μέλη (διακεκομμένη γραμμή στο Σχήμα 7.10d και μεταξύ των κόμβων *A* και *C*).

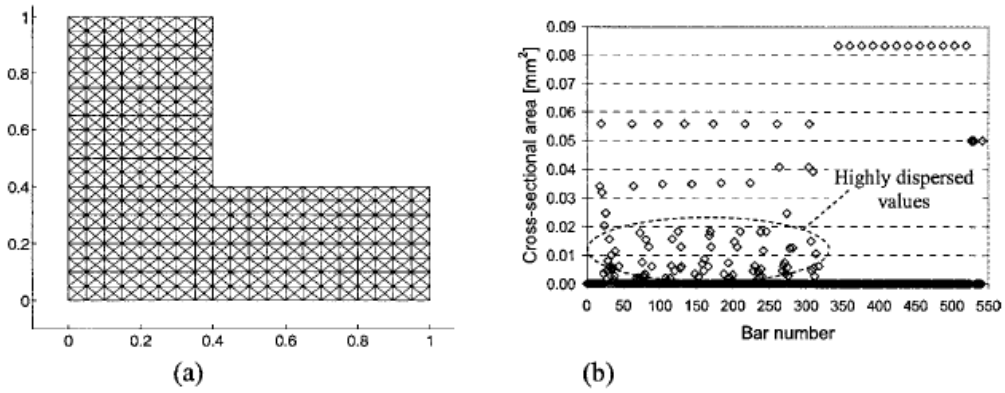

Σχήμα 7.9: Η L-δοκός (λόγος πλευρών πλέγματος: *λ=const*)

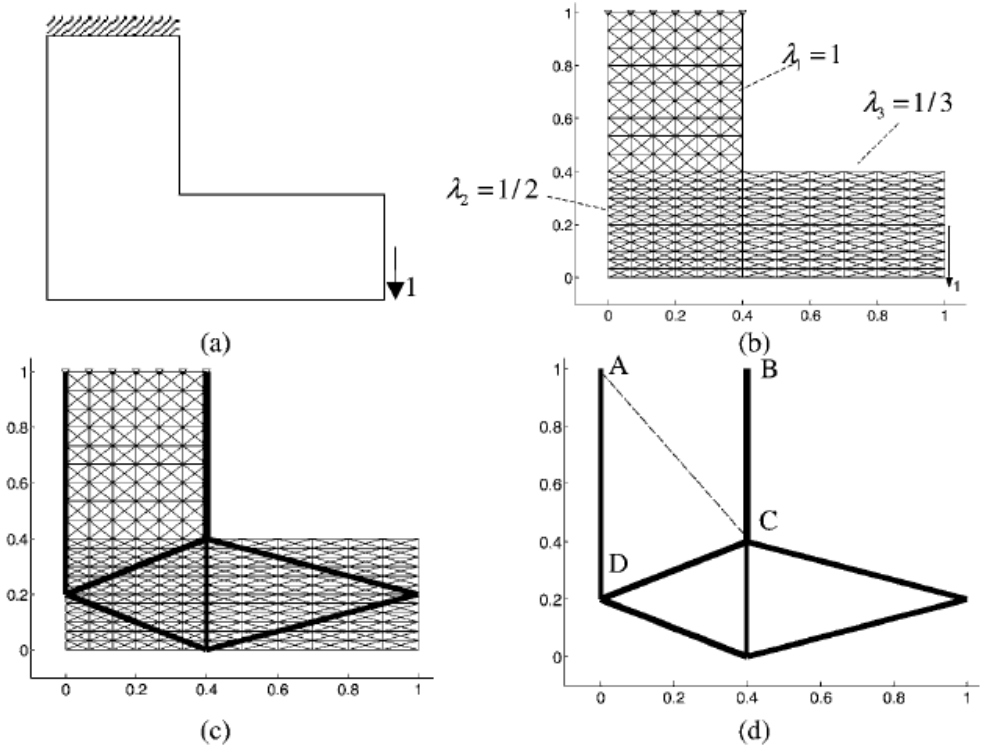

Σχήμα 7.10: Η L-δοκός (λόγος πλευρών πλέγματος: *λ≠ const*)

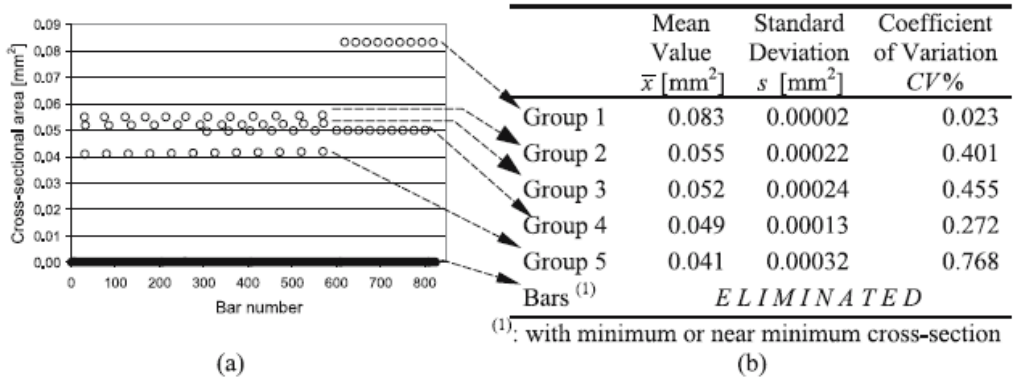

	Mean Value $\overline{x}$ [mm²]	Standard Deviation s [mm²]	Coefficient of Variation CV%
Group 1	0.083	0.00002	0.023
Group 2	0.055	0.00022	0.401
Group 3	0.052	0.00024	0.455
Group 4	0.049	0.00013	0.272
Group 5	0.041	0.00032	0.768
Bars (1)	*ELIMINATED*		

(1): with minimum or near minimum cross-section

Σχήμα 7.11: Στατιστική ανάλυση δομικών στοιχείων για τη βελτιστοποιημένη L-δοκό (λόγος πλευρών πλέγματος: *λ≠const*)

7.2.8. Αξιολόγηση

Η διερεύνηση, η οποία παρατέθηκε ανωτέρω, στηρίζεται στην εφαρμογή της προτεινόμενης διαδικασίας τεσσάρων φάσεων. Για λόγους αξιολόγησης, πραγματοποιήθηκε σύγκριση με τα αποτελέσματα, τα οποία λαμβάνονται όταν χρησιμοποιηθεί μία ισχυρή, βιβλιογραφική διαδικασία βελτιστοποίησης, όπως είναι η μέθοδος SQP (Sequential Quadratic Programming). Προς αυτήν την κατεύθυνση, δημιουργήθηκαν οι Πίνακες 7.1 και 7.2. Πιο συγκεκριμένα, το αποτέλεσμα από το πέρας της Φάσεως 1 σημειώνεται ως [P1], ενώ το αποτέλεσμα από το πέρας της Φάσεως 4 σημειώνεται ως [P4]. Μία σύγκριση μεταξύ των καταστάσεων [P1] και [P4] παρουσιάζεται στον Πίνακα 7.1 με κριτήριο την κατασκευαστική απλότητα, δηλαδή ως προς το πλήθος των ομάδων διατομών και το πλήθος των ράβδων.

Πίνακας 7.1: Σύγκριση ως προς την κατασκευαστική απλότητα (ομάδες διατομών και πλήθος ράβδων)

	Short cantilever			Long cantilever			MBB beam			L-shape beam		
Bars	[P1]	[P4]	[%]	[P1]	[P4]	[%]	[P1]	[P4]	[%]	[P1]	[P4]	[%]
$x_i = x_{\min}$	408	0	−100	322	0	−100	279	0	−100	722	1	−99
$x_i \approx x_{\min}$	36	0	−100	58	0	−100	69	0	−100	43	0	−100
$x_i \neq x_{\min}$	12	2	−84	40	8	−80	64	11	−83	60	7	−88
$x_i \not\approx x_{\min}$												
Total	456	2	−99	420	8	−98	412	11	−97	825	8	−99
Groups	20	1	−95	33	3	−91	41	4	−90	48	6	−87

Ειδικότερα, σε κάθε ένα από τα εξετασθέντα παραδείγματα αντιστοιχεί μία τριάδα στηλών. Οι, σημειούμενες ως [P1] και [P4], στήλες παρουσιάζουν δεδομένα σχετικά με τις καταστάσεις [P1] και [P4], αντίστοιχα. Οι, σημειούμενες με [%], στήλες παρουσιάζουν μια σχετική σύγκριση, σε εκατοστιαία γραφή, μεταξύ των καταστάσεων [P1] και [P4], θεωρώντας ως αναφορά την κατάσταση [P1]. Η γραμμή με την ένδειξη $x_i = x_{\min}$ αναφέρεται σε εκείνες τις ράβδους, των οποίων η διατομή x_i λαμβάνει την κατώτερη δυνατή τιμή $x_{\min}$. Η γραμμή με την ένδειξη $x_i \approx x_{\min}$ αναφέρεται σε εκείνες τις ράβδους, των οποίων η διατομή x_i λαμβάνει τιμή πλησίον της κατώτερης δυνατής τιμής $x_{\min}$. Οι γραμμές με ένδειξη $x_i \neq x_{\min}$ και $x_i \not\approx x_{\min}$ αναφέρονται σε ράβδους, οι διατομές x_i των οποίων δεν είναι ούτε ίσες ούτε περίπου ίσες με την κατώτερη δυνατή τιμή $x_{\min}$. Η γραμμή με την ένδειξη 'Total' αναφέρεται σε πλήθος ράβδων, οι οποίες εμφανίζονται στις καταστάσεις [P1] και [P4], αντίστοιχα. Τέλος, η γραμμή με την ένδειξη 'Groups' αναφέρεται στο πλήθος των διαφορετικών διατομών, οι οποίες εμφανίζονται στη βέλτιστη σχεδίαση. Διευκρινίζεται ότι, για λόγους απλοποίησης στη γραφή, οι % διαφορές στρογγυλοποιούνται στην πλησιέστερη ακέραιη τιμή.

Από τον Πίνακα 7.1, προκύπτει ότι η κατάσταση [P4] υπερτερεί έναντι της κατάστασης [P1]. Πιο συγκεκριμένα, για την περίπτωση του κοντού προβόλου, η κατάσταση [P4] εμπλέκει μόνον δύο δομικά μέλη, τα οποία, μάλιστα, είναι της αυτής διατομής, άρα σχηματίζουν μία ομάδα διατομών. Αντιθέτως, η κατάσταση [P1] περιλαμβάνει 456 δομικά μέλη και 20 διαφορετικές διατομές, άρα 20 ομάδες διατομών. Συνεπώς, η εφαρμογή της προτεινομένης διαδικασίας κατέληξε σε μία μείωση του πλήθους των συμμετεχόντων δομικών στοιχείων της τάξεως του 99% και του πλήθους των εμπλεκομένων διατομών κατά 95%. Λαμβάνοντας υπόψη και τα τέσσερα παραδείγματα, προέκυψε ότι το πλήθος των συμμετεχόντων δομικών στοιχείων μειώθηκε από 97% έως και 99%, ενώ το πλήθος των εμπλεκομένων διατομών μειώθηκε κατά 87% έως και 95%.

Ο Πίνακας 2 παρουσιάζει μία σύγκριση μεταξύ των καταστάσεων [P1] και [P4], με κριτήριο τον όγκο της κατασκευής. Η γραμμή με την ένδειξη $\delta volume(\%)$ δηλώνει διαφορά όγκου μεταξύ των καταστάσεων [P1] και [P2], με αναφορά την κατάσταση [P1].

Πίνακας 7.2: Σύγκριση ως προς τον όγκο της κατασκευής

	Short cantilever	Long cantilever	MBB beam	L-shape beam
Volume [P1]	0.807	21.392	1.505	22.750
Volume [P4]	0.800	21.360	1.503	22.342
δVolume (%)	−0.81	−0.15	−0.13	−1.79

Από τον Πίνακα 2, προκύπτει ότι, συγκριτικά με την κατάσταση [P1], η κατάσταση [P4] συνοδεύεται από μείωση του όγκου της τάξεως από 0.13% έως και 1.79%. Προφανώς, αυτή η μείωση, αν και υπαρκτή, δεν είναι εντυπωσιακή. Ωστόσο, το μεγάλο κέρδος από την αύξηση της κοινοτυπίας δεν είναι τόσο η χρησιμοποίηση μικρότερης ποσότητας υλικού όσο η χρησιμοποίηση αυξημένου πλήθους ομοίων δομικών στοιχείων, κάτι που μειώνει σημαντικά το κατασκευαστικό κόστος. Υπό αυτό το πρίσμα, η σημασία της ομαδοποίησης, ή, ισοδύναμα, η σημασία της αύξησης της κοινοτυπίας σε μία κατασκευή, είναι αυταπόδεικτη.

7.3. Ελαχιστοποίηση κόστους θεωρώντας κόστος συγκόλλησης και φύρα

7.3.1. Γενικά

Η μείωση του κατασκευαστικού κόστους είναι εφικτή εάν, εκτός του κόστους αγοράς της πρώτης ύλης, συνυπολογισθούν το κόστος των συγκολλήσεων και το κόστος της φύρας. Ωστόσο, δεν υπάρχει μία διαδικασία βελτιστοποίησης γενικού χαρακτήρα, τέτοια ώστε να λαμβάνει υπόψη τα προαναφερθέντα κόστη, χωρίς να απαιτείται κάποια διαδικασία υπολογισμών καθέτου εφαρμογής. Με άλλα λόγια, αντί μίας γενικής διαδικασίας, είναι προτιμητέα η ανάπτυξη διαδικασιών βελτιστοποίησης προσανατολισμένων στις ανάγκες των εκάστοτε εξεταζομένων κατασκευών. Σε αυτό το πλαίσιο, επελέγη η ανάπτυξη διαδικασίας βελτιστοποίησης σχεδίασης μεταλλικών δεξαμενών αποθήκευσης πετρελαιοειδών. Για τη σχεδίαση χρησιμοποιήθηκε το πρότυπο API650.

7.3.2. Ορισμός παραμέτρων

Οι πλέον σημαντικές παράμετροι στη σχεδίαση δεξαμενών είναι η χωρητικότητά τους και οι διαστάσεις τους. Διευκρινίζεται ότι ο πλέον συνήθης προσανατολισμός δεξαμενών αποθήκευσης πετρελαιοειδών είναι ο κατακόρυφος (Σχήμα 7.12).

Σχήμα 7.12: Τυπικές δεξαμενές αποθήκευσης πετρελαιοειδών διαφορετικών λόγων ακτίνας προς ύψος

Σε μία δεξαμενή υπάρχουν τρία βασικά τμήματα, ήτοι η οροφή, το πλαϊνό τοίχωμα και ο πυθμένας, ο οποίος είναι επικαλυμμένος με μεταλλικές πλάκες και τοποθετείται επί καταλλήλου θεμελίου. Η οροφή και η θεμελίωση αποτελούν ευθύνη Πολιτικού Μηχανικού,

ενώ το πλαϊνό τοίχωμα και ο πυθμένας αποτελούν αντικείμενο Μηχανολόγου Μηχανικού. Για αυτόν τον λόγο, στην παρούσα εξετάζονται μόνον τα δύο τελευταία. Συνεπώς, από την οπτική του Μηχανολόγου Μηχανικού, η βέλτιστη σχεδίαση μίας δεξαμενής αποτελείται από τρία επί μέρους προβλήματα βελτιστοποίησης:

- Βελτιστοποίηση του πλαϊνού τοιχώματος
- Βελτιστοποίηση των δακτυλιοειδών πλακών (sketch plates) του πυθμένα
- Βελτιστοποίηση των ελασμάτων επίστρωσης του πυθμένα

Κάθε ένα από αυτά τα προβλήματα αναλύεται συνοπτικά στις επόμενες ενότητες.

7.3.3. Βελτιστοποίηση του πλαϊνού τοιχώματος της δεξαμενής

7.3.3.1. *Layout optimization*

Για κατασκευαστικούς λόγους, το πλαϊνό τοίχωμα της δεξαμενής σχηματίζεται από ελάσματα ορθογωνικού σχήματος. Μετά από ειδική κατεργασία (κουρμπάρισμα), κάθε έλασμα αποκτά μία συγκεκριμένη καμπυλότητα. Πολλά τέτοια ελάσματα συνδεδεμένα μεταξύ τους μέσω μετωπικής συγκόλλησης σχηματίζουν μία δακτυλιοειδή κλειστή επιφάνεια, ή, για συντομία, δακτυλίδι (course). Το πλαϊνό τοίχωμα της δεξαμενής σχηματίζεται όταν δακτυλίδια τοποθετούνται το ένα επάνω στο άλλο. Ειδικά για δεξαμενές αποθήκευσης πετρελαιοειδών, απαιτείται η χρήση πιστοποιημένων ελασμάτων, τόσο ως προς τις γεωμετρικές τους διαστάσεις όσο και ως προς τις ιδιότητες του υλικού.

Από κατασκευαστικής απόψεως, η βέλτιστη σχεδίαση του πλαϊνού τοιχώματος επιτυγχάνεται όταν απαιτείται η χρήση ακεραίου πλήθους ελασμάτων, ή, ισοδύναμα, όταν αξιοποιείται όλο το υλικό το οποίο έχει αγορασθεί (μηδενική φύρα). Συνεπώς, μία πρώτη προσέγγιση του προβλήματος της σχεδίασης μίας δεξαμενής θα ήταν η αναζήτηση εκείνης της σχεδίασης δεξαμενής 'μηδενικής φύρας' για την οποία η χωρητικότητά της είναι η πλησιέστερη δυνατή στην χωρητικότητα προδιαγραφής. Η μαθηματική διατύπωση αυτού του προβλήματος βελτιστοποίησης είναι η εξής:

$$\begin{gathered}
\text{Ελαχιστοποίηση } \left(V - V_{specif}\right) \\
\text{με } V = f\left(N_{circ,j}, L_{circ,j}, N_{vert,j}, W_{vert,j}\right),\ \ j = 1,2,3,... \\
\text{και } D_{specif,low} \le D \le D_{specif,high},\ H_{specif,low} \le H \le H_{specif,high}, \\
\left(H/D\right)_{specif,low} \le \left(H/D\right) \le \left(H/D\right)_{specif,high}
\end{gathered} \tag{7.10}$$

όπου

V είναι η χωρητικότητα της βελτιστοποιημένης δεξαμενής,

V_{specif} είναι η χωρητικότητα προδιαγραφής της δεξαμενής,

$L_{circ,j}$ είναι το μήκος των ελασμάτων κατά την περιφερειακή διεύθυνση της δεξαμενής,

$N_{circ,j}$ είναι το πλήθος ελασμάτων μήκους $L_{circ,j}$ κατά την περιφερειακή διεύθυνση της δεξαμενής,

$W_{vert,j}$ είναι το πλάτος των ελασμάτων κατά την κατακόρυφη διεύθυνση της δεξαμενής,

$N_{vert,j}$ είναι το πλήθος ελασμάτων πλάτους $W_{vert,j}$ κατά την κατακόρυφη διεύθυνση της δεξαμενής,

D είναι η διάμετρος της δεξαμενής,

D_{specif} είναι η διάμετρος προδιαγραφής της δεξαμενής,

H είναι η ύψος της δεξαμενής και

H_{specif} είναι το ύψος προδιαγραφής της δεξαμενής.

Η επιβολή περιορισμού σχετικά με τον λόγο ύψους δεξαμενής προς διάμετρο δεξαμενής είναι υποχρεωτική, διαφορετικά είναι δυνατόν να προκύψουν ακραίες σχεδιάσεις μηδενικής πρακτικής αξίας. Δεδομένου, δε, ότι για την εξεταζόμενη περίπτωση δεξαμενής πρέπει χρησιμοποιηθούν πιστοποιημένα ελάσματα, σε συνδυασμό με το γεγονός ότι στην Ελληνική αγορά διατίθενται πιστοποιημένα ελάσματα διαστάσεων $2m \times 6m$ και $2.5m \times 6m$, το πρόβλημα βελτιστοποίησης της Εξ.(7.10) είναι δυνατόν να εκφρασθεί ως εξής (αναφέρεται μόνον η αντικειμενική συνάρτηση μιας και οι περιορισμοί είναι οι ίδιοι):

$$\begin{aligned} &\text{Ελαχιστοποίηση } \left(V - V_{specif}\right) \\ &\text{με } V = f\left(N_{circ}, L_{circ} = 6, N_{vert,1}, W_{vert,1} = 2, N_{vert,2}, W_{vert,2} = 2.5\right) \end{aligned} \tag{7.11}$$

Εκτός από τη χωρητικότητα, η οποία είναι η κυριαρχούσα προδιαγραφή σε μία δεξαμενή, υπάρχουν και άλλες παράμετροι καθοριστικές για την επιλογή της τελικής σχεδίασης, όπως είναι ο χρόνος που απαιτείται για την αμμοβολή και το χρωματισμό του πλαϊνού τοιχώματος της δεξαμενής, καθώς και ο χρόνος για την εκτέλεση των συγκολλήσεων. Συνεπώς, το ανωτέρω πρόβλημα βελτιστοποίησης είναι δυνατόν να επαναδιατυπωθεί με έναν πιο λεπτομερή τρόπο, ως εξής:

$$\begin{aligned} &\text{Ελαχιστοποίησης } \left(V - V_{specif}\right),\ A_{shell},\ L_{weld,circ},\ L_{weld,vert} \\ &\text{με } V = f\left(N_{circ}, L_{circ} = 6, N_{vert,1}, W_{vert,1} = 2, N_{vert,2}, W_{vert,2} = 2.5\right) \end{aligned} \tag{7.12}$$

όπου A_{shell} δηλώνει το εμβαδόν του πλαϊνού τοιχώματος, $L_{weld,circ}$ είναι το μήκος της συγκόλλησης κατά την περιφερειακή διεύθυνση της δεξαμενής και $L_{weld,vert}$ είναι το μήκος της συγκόλλησης κατά την κατακόρυφη διεύθυνση της δεξαμενής. Ωστόσο, ενδέχεται η, προκύπτουσα από την επίλυση του προβλήματος (7.12), σχεδίαση να είναι σημαντικά διαφορετική από την προδιαγραφή. Αυτό σημαίνει ότι η θεωρητικώς βέλτιστη σχεδίαση ενδέχεται να χαρακτηρίζεται από μικρή, έως και αμελητέα, αξία. Για τον λόγο αυτό, είναι προτιμητέα η αναζήτηση της βέλτιστης σχεδίασης σε μία περιοχή ενδιαφέροντος, οπότε το πρόβλημα (7.12) διατυπώνεται ως ακολούθως:

$$\begin{aligned} &\text{Ελαχιστοποίηση } \left(V - \left(V_{specif} \pm \Delta V\right)\right),\ A_{shell},\ L_{weld,circ},\ L_{weld,vert} \\ &\text{Με } V = f\left(N_{circ}, L_{circ} = 6, N_{vert,1}, W_{vert,1} = 2, N_{vert,2}, W_{vert,2} = 2.5\right) \end{aligned} \tag{7.13}$$

όπου ΔV είναι η αποδεκτή απόκλιση της χωρητικότητας της τελικής σχεδίασης από τη χωρητικότητα προδιαγραφής.

7.3.3.2. Βελτιστοποίηση πάχους

Το πλαϊνό τοίχωμα παραλαμβάνει το ίδιον βάρος, το βάρος όλων των, ανηρτημένων σε αυτό, εξαρτημάτων, φορτίο χιονιού, φορτίο ανέμου και φορτία από εργαλεία συντήρησης, τα οποία είναι δυνατόν να τοποθετηθούν στην οροφή της δεξαμενής κατά τη διαδικασία συντήρησης. Επίσης, ανάλογα με την σεισμική δραστηριότητα της περιοχής τοποθέτησης των δεξαμενών, συνυπολογίζονται και φορτία λόγω σεισμού. Όλα αυτά τα φορτία έχουν ως αποτέλεσμα την ανάπτυξη τάσεων στο πλαϊνό τοίχωμα, οι οποίες δεν πρέπει να ξεπερνούν κάποια ανώτατη τιμή, επιβαλλόμενη από κανονισμούς. Συνεπώς, το πρόβλημα βελτιστοποίησης του πάχους του πλαϊνού τοιχώματος είναι δυνατόν να διατυπωθεί ως εξής:

$$\text{Ελαχιστοποίηση } V_{shell} = \sum_{j=1}^{N_c} V_{shell,j} \text{ με } V_{shell,j} = f\left(H, D, t_1, S_d, S_t, E, G, CA\right)$$

$$\text{υπό τον περιορισμό } \tau_{shell,j} \le \tau_{shell,allow} \tag{7.14}$$

όπου

D	είναι η διάμετρος της δεξαμενής,
H	είναι το ύψος της δεξαμενής,
t_1	είναι το πάχος του πρώτου δακτυλιδιού (first course),
S_d	είναι η επιτρεπόμενη τάση για την κατάσταση σχεδίασης (design condition),
S_t	είναι η επιτρεπόμενη τάση για την κατάσταση δοκιμής υπό υδροστατική πίεση (hydrostatic test condition),
E	είναι ο συντελεστής ασφαλείας των συγκολλήσεων,
G	είναι η ειδική πυκνότητα του προς αποθήκευση πετρελαιοειδούς,
CA	είναι το πάχος προστασίας έναντι διάβρωσης και
τ	δηλώνει τάση.

Οι δείκτες j και $allow$ δηλώνουν τον αύξοντα αριθμό του δακτυλιδιού (course) και την επιτρεπόμενη τάση , αντίστοιχα, ενώ ως N_c δηλώνεται το συνολικό πλήθος των δακτυλιδιών της δεξαμενής.

7.3.4. Βελτιστοποίηση των sketch plates

7.3.4.1. Κοπή των sketch plates

Η δακτυλιοειδής ζώνη ελασμάτων (sketch plates), επί της οποίας επικάθεται το πλαϊνό τοίχωμα, διαμορφώνεται από, την μεταξύ τους μετωπική συγκόλληση, κατάλληλα κομμένων ελασμάτων. Τα εν λόγω ελάσματα είναι ορθογωνικής γεωμετρίας και διατίθενται σε τυποποιημένες διαστάσεις, όπως φαίνεται στον Πίνακα 5.3. Διευκρινίζεται ότι, για την περίπτωση των sketch plates, δεν απαιτείται η χρήση πιστοποιημένων ελασμάτων.

Πίνακας 7.3: Ελάσματα εμπορίου για την κοπή των sketch plates

Width [mm]	Available thicknesses [mm]																					
	3	4	5	6	7	8	9	10	11	12	14	15	16	18	20	22	25	30	35	40	45	50
1000	✓	✓	✓	✓	✓	✓	✓	✓	✓	✓	✓	✓	✓	✓	✓	✓	✓	✓	✓	✓	✓	✓
1250	✓	✓	✓	✓	✓	✓	✓	✓	✓	✓	✓	✓	✓	✓	✓	✓	✓	✓	✓	✓	✓	✓
1500	✓	✓	✓	✓	✓	✓	✓	✓	✓	✓	✓	✓	✓	✓	✓	✓	✓	✓	✓	✓	✓	✓
1800		✓	✓	✓	✓	✓	✓	✓	✓	✓	✓	✓	✓	✓	✓	✓	✓	✓	✓	✓	✓	✓
2000		✓	✓	✓	✓	✓	✓	✓	✓	✓	✓	✓	✓	✓	✓	✓	✓	✓	✓	✓	✓	✓
2300		✓	✓	✓	✓	✓	✓	✓	✓	✓	✓	✓	✓	✓	✓	✓	✓	✓	✓	✓	✓	✓
2500		✓	✓	✓	✓	✓	✓	✓	✓	✓	✓	✓	✓	✓	✓	✓	✓	✓	✓	✓	✓	✓

Ωστόσο, τα sketch plates, ως τμήματα δακτυλίου, έχουν τοξοειδή μορφή, άρα η κοπή τέτοιων τμημάτων από ορθογώνια ελάσματα συνοδεύεται από απώλεια υλικού (φύρα). Ανάλογα με τη διάταξη των προς κοπή τμημάτων, μεταβάλλεται και η εν λόγω φύρα, όπως φαίνεται στο Σχήμα 7.13.

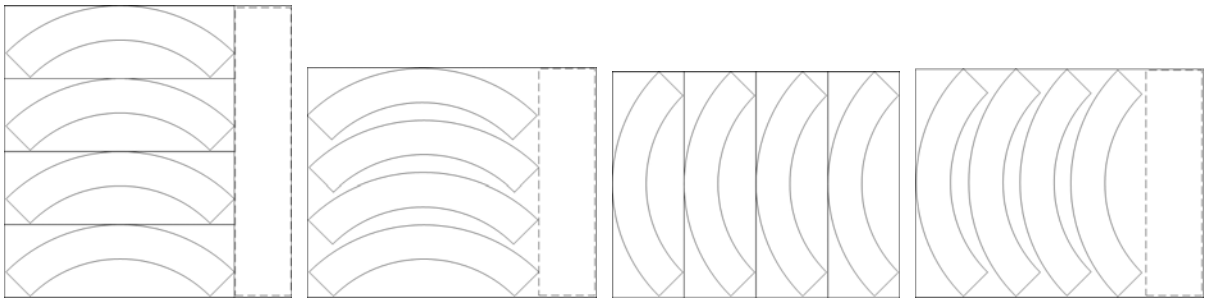

(a) (b) (c) (d)

Σχήμα 7.13: Διαφορετική διάταξη των sketch plates σε έλασμα τυποποιημένων διαστάσεων

Συνεπώς, είναι επόμενο να αναζητείται εκείνη η διάταξη για την οποία η φύρα ελαχιστοποιείται, οπότε το αντίστοιχο πρόβλημα βελτιστοποίησης διατυπώνεται ως εξής:

$$\text{Ελαχιστοποίηση } A_{\text{unexploitable}} \text{ ή } A_{scrap}, \text{ με } N \in \mathrm{N}^{*} \tag{7.15}$$

όπου N είναι το συνολικό πλήθος των sketch plates.Διευκρινίζεται ότι μετά την εύρεση της βέλτιστης σχεδίασης για το πλαϊνό τοίχωμα της δεξαμενής, η διάμετρος της δεξαμενής, άρα η εσωτερική και εξωτερική ακτίνα των sketch plates, είναι σαφώς ορισμένη και η μεταβλητή N καθίσταται η μόνη άγνωστη ποσότητα.

7.3.4.2. Βελτιστοποίηση πάχους

Σύμφωνα με τον κανονισμό API Standard 650, το ελάχιστο πάχος των εν λόγω ελασμάτων (sketch plates) συσχετίζεται άμεσα με τη διάμετρο της δεξαμενής, η οποία εκτιμάται κατά τη βελτιστοποίηση του πλαϊνού τοιχώματος της δεξαμενής (API 650/Section 3.5.3). Συνεπώς, δεν έχει έννοια η επίλυση αντιστοίχου προβλήματος βελτιστοποίησης.

7.3.5. Βελτιστοποίηση των ελασμάτων επίστρωσης του πυθμένα

7.3.5.1. Βέλτιστη επίστρωση πυθμένα

Ο πυθμένας μίας δεξαμενής αποθήκευσης πετρελαιοειδών πρέπει να είναι καλυμμένος με χαλύβδινα ελάσματα πιστοποιημένης ποιότητας και ακρίβειας γεωμετρικών διαστάσεων. Στην Ελληνική αγορά, τέτοιου τύπου ελάσματα είναι διαθέσιμα στις διαστάσεις $2m \times 6m$ και $2.5m \times 6m$. Συνεπώς, το πρόβλημα της κάλυψης του πυθμένα με τέτοια ελάσματα ανάγεται σε πρόβλημα προσαρμογής, στο οποίο ορθογωνικά ελάσματα πρέπει να τοποθετηθούν με τέτοιον τρόπο εντός κύκλου, ώστε το αναξιοποίητο υλικό (φύρα) να ελαχιστοποιηθεί. Το προαναφερθέν πρόβλημα απεικονίζεται στο Σχήμα 7.14, στο οποίο έχει αξιοποιηθεί η συμμετρία της κατασκευής.

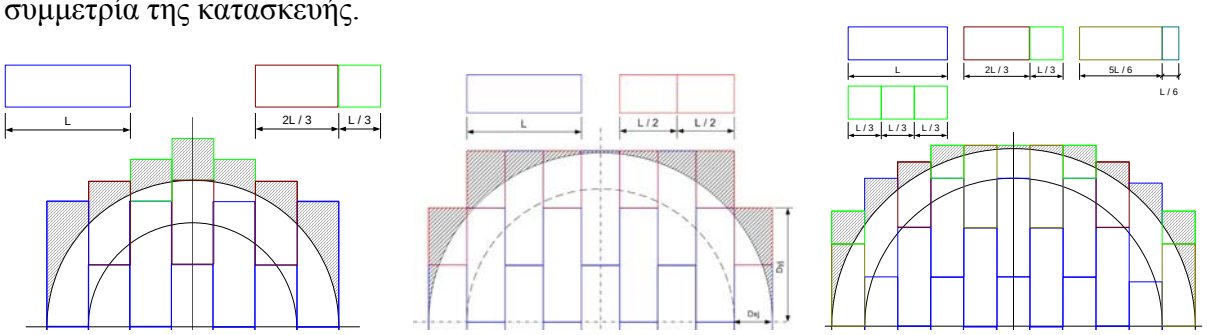

(a) $10m < D < 14m$ (b) $14m < D < 18m$ (c) $18m < D < 22m$

Σχήμα 7.14: Κάλυψη πυθμένα με ελάσματα για δεξαμενές διαφόρων διαμέτρων

Η κεντρική ιδέα είναι η χρήση *περιττού* πλήθους ελασμάτων N_j κατά την οριζόντια διεύθυνση και η προσαρμογή του ελάσματος κατά την εγκάρσια διεύθυνση (κατακόρυφη διεύθυνση στο Σχήμα 7.14), έτσι ώστε να χρησιμοποιείται είτε ένα ολόκληρο έλασμα είτε ένα καλώς ορισμένο τμήμα αυτού. Στο Σχήμα 7.14 απεικονίζεται η περίπτωση δεξαμενής με διάμετρο D μεταξύ των τιμών $D_{\min}$ και $D_{\max}$, όπου ως εσωτερικός κύκλος αντιστοιχεί στη διάμετρο $D_{\min}$ και ο εξωτερικός κύκλος αντιστοιχεί στη διάμετρο $D_{\max}$. Οι υποδιαιρέσεις των ελασμάτων, οι οποίες απαιτούνται για κάθε μία εκ των περιπτώσεων του Σχήματος 7.14, δηλώνονται με διαφορετικό χρώμα ως φαίνεται στο ίδιο Σχήμα. Οι γραμμοσκιασμένες περιοχές αντιστοιχούν σε αναξιοποίητο υλικό (φύρα), έστω S, το εμβαδόν του οποίου υπολογίζεται πολύ εύκολα εάν αφαιρεθεί, από το συνολικό εμβαδόν των ελασμάτων, το εμβαδόν του κυκλικού πυθμένα ακτίνας R. Με βάση το σχήμα 7.14, κατά μήκος της οριζόντιας διεύθυνσης σχηματίζονται N_j στήλες από ελάσματα, κάθε μία εκ των οποίων έχει πλάτος Δx_j και ύψος Δy_j. Η μαθηματική έκφραση υπολογισμού της φύρας δίδεται από την εξίσωση:

$$S = \sum_{j=1}^{N_j} S_j = \sum_{j=1}^{N_j} \left(\Delta x_j \, \Delta y_j - \int_{x_{j-1}}^{x_j} \sqrt{\left(R^2 - x^2 \right)} \, dx \right) \tag{7.16}$$

Συνεπώς, το πρόβλημα βελτιστοποίησης των ελασμάτων πυθμένα ορίζεται ως:

$$\text{Ελαχιστοποίηση του } S \text{ όπου } S_j = f\left(L \le 6, W \in \{2.0, 2.5\} \right) \tag{7.17}$$

όπου L και W δηλώνουν το μήκος και το πλάτος των, πιστοποιημένων και διαθεσίμων στην Ελληνική αγορά, ελασμάτων, με τα οποία καλύπτεται ο πυθμένας της δεξαμενής.

7.3.5.2. Βελτιστοποίηση πάχους

Το πάχος των ελασμάτων του πυθμένα καθορίζεται από κανονισμούς (API 650 / Section 3.4.1), συνεπώς δεν έχει έννοια η επίλυση αντιστοίχου προβλήματος βελτιστοποίησης.

7.3.6. Υπολογισμοί

Ενδεικτικά, αναφέρεται η διαδικασία υπολογισμού της φύρας, η οποία προκύπτει από την κοπή των sketch plates (οριζόντιος προσανατολισμός, Σχήμα7.13a):

Βήμα 0: Χρήση της διαμέτρου D και του ύψους H, τα οποία προκύπτουν από τη βελτιστοποίηση του πλαϊνού τοιχώματος

Βήμα 1: Καθορισμός των ποσοτήτων d_1 και d_2 από κανονισμούς (για κανονισμό API650: $d_1 = 2"$, $d_2 = 24"$)

Βήμα 2: Προσδιορισμός του πάχους t_{c_1} του πρώτου δακτυλιδιού (first course)

Βήμα 3: Προσδιορισμός της εσωτερικής διαμέτρου του sketch plate $R_{in} = 0.5D - d_1$

Βήμα 4: Προσδιορισμός της εξωτερικής διαμέτρου του sketch plate $R_{out} = 0.5D + t_{c_1} + d_2$

Βήμα 5: Για διάφορα $N \ge 2$, $N \in \mathrm{N}^*$

Βήμα 6: Προσδιορισμός της πολικής γωνίας θ κάθε sketch plate

Βήμα 7: Προσδιορισμός του πλάτους του ελάσματος $W_j = 2R_{out}\sin(0.5\theta)$, από το οποίο θα κοπεί το κάθε sketch plate

Βήμα 8: Εύρεση τυποποιημένου πλάτους W_{st} αμέσως μεγαλυτέρου του W_j (Πίνακας 1)

Βήμα 9: Εάν $W_{st} > 2300mm$ Τότε το N απορρίπτεται; $N = N + 1$; επιστροφή στο Βήμα 5

Βήμα 10: Προσδιορισμός του μήκους του ελάσματος $L_j = R_{out} - R_{in}$, από το οποίο θα κοπεί το κάθε sketch plate

Βήμα 11: Προσδιορισμός εμβαδού $A_{pp,j} = W_j L_j$ της περιγεγραμμένης ορθογωνίου πλάκας

Βήμα 12: Προσδιορισμός εμβαδού $A_{sp,j} = \theta_j\left(R_{out}^2 - R_{in}^2\right)$ του sketch plate

Βήμα 13: Προσδιορισμός εμβαδού φύρας $A_{scrap,j} = A_{pp,j} - A_{sp,j}$ ανά sketch plate

Βήμα 14: Προσδιορισμός συνολικού εμβαδού φύρας $A_{scrap,sp} = \sum_{j=1}^{j=N_{sp}} A_{scrap,j}$

Βήμα 15: Προσδιορισμός συνολικού μήκους $h_{tot} = N\,h$

Βήμα 16: Προσδιορισμός του μήκους της συγκόλλησης #1 $L_{w,1} = N\left(R_{out} - R_{in}\right)$ (τα sketch plates συγκολλούνται μεταξύ τους μετωπικά),

Βήμα 17: Προσδιορισμός του μήκους της συγκόλλησης #2 $L_{w,2} = \pi D_{in}$ (τα sketch plates συγκολλούνται με τις πλάκες του πυθμένα),

Βήμα 18: Καταγραφή των μεγεθών N, ΔE_{tot}, $L_{w,1}$, $L_{w,2}$, h_{tot}

Οι δείκτες *pp* και *sp* αντιστοιχούν στους όρους 'prescribing plate' (περιγεγραμμένη ορθογώνια πλάκα) και 'sketch plate'.

7.3.7. Αποτελέσματα

Τα διαγράμματα στο Σχήμα 7.15 απεικονίζουν τη διάμετρο της δεξαμενής συναρτήσει του λόγου (D/H), για διάφορους συνδυασμούς πιστοποιημένων ελασμάτων. Κάθε σημείο σε αυτά τα διαγράμματα αντιστοιχεί σε μία βέλτιστη σχεδίαση. Διευκρινίζεται ότι το εύρος τιμών του λόγου (D/H) καθορίζεται από τον Μηχανικό.

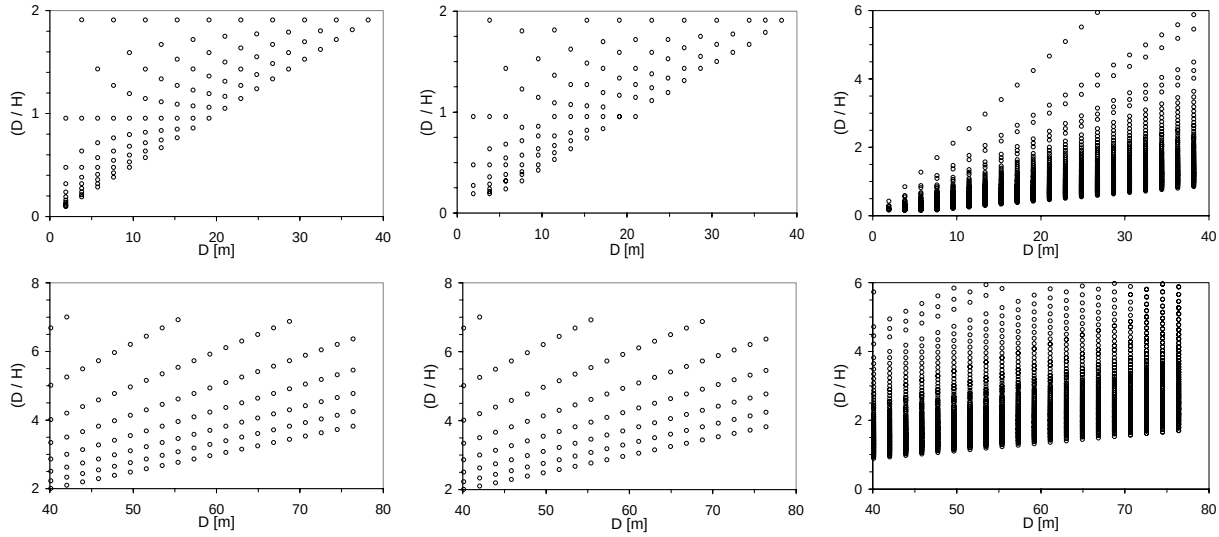

(a) (b) (ψ)

Σχήμα 7.15: Διάμετροι δεξαμενών για βέλτιστες σχεδιάσεις πλαϊνού τοιχώματος χρησιμοποιώντας πιστοποιημένα ελάσματα της Ελληνικής αγοράς: (a) μόνον ελάσματα 2m × 6m, (b) μόνον ελάσματα 2.5m × 6m και (c) ελάσματα 2m × 6m / 2.5m × 6m

Τα διαγράμματα στο Σχήμα 7.16 απεικονίζουν τη χωρητικότητα της δεξαμενής συναρτήσει του λόγου (D/H) για διάφορες περιπτώσεις πιστοποιημένων ελασμάτων.

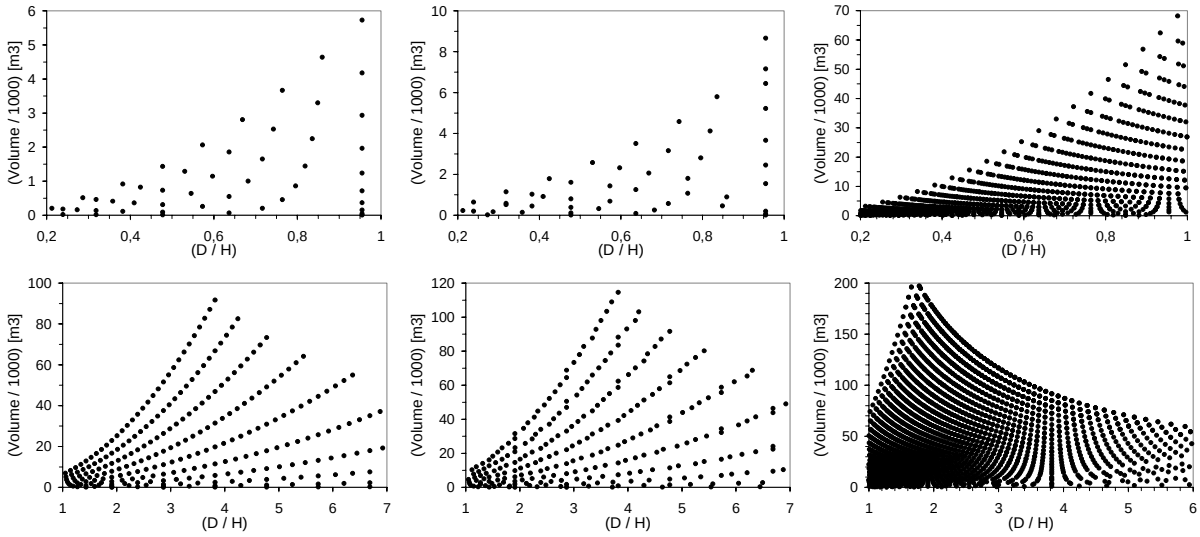

(a) (b) (c)

Σχήμα 7.16: Χωρητικότητα δεξαμενών για βέλτιστες σχεδιάσεις πλαϊνού τοιχώματος χρησιμοποιώντας πιστοποιημένα ελάσματα της Ελληνικής αγοράς: (a) μόνον ελάσματα 2m × 6m, (b) μόνον ελάσματα 2.5m × 6m και (c) ελάσματα 2m × 6m / 2.5m × 6m.

Τα διαγράμματα στο Σχήμα 7.17 απεικονίζουν το εμβαδόν των πλαϊνών τοιχωμάτων της δεξαμενής συναρτήσει του λόγου (D/H). Με τη βοήθεια αυτών των διαγραμμάτων είναι δυνατή η εκτίμηση της, προς αμμοβολή και χρωματισμό, επιφανείας. Πρόκειται για πληροφορία άκρως χρήσιμη για λόγους προγραμματισμού εργασιών.

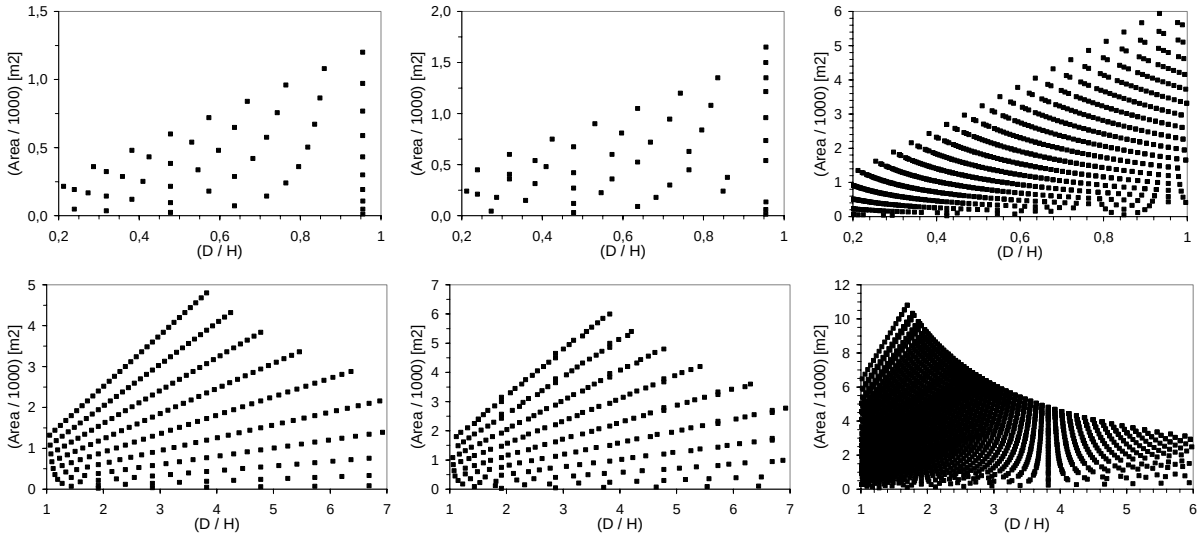

(a) (b) (c)

Σχήμα 7.17: Εμβαδόν πλαϊνών τοιχωμάτων για βέλτιστες σχεδιάσεις χρησιμοποιώντας πιστοποιημένα ελάσματα της Ελληνικής αγοράς: (a) μόνο ελάσματα 2m × 6m, (b) μόνο ελάσματα 2.5m × 6m και (c) ελάσματα 2m × 6m / 2.5m × 6m

Τέλος, τα διαγράμματα στο Σχήμα 7.18 απεικονίζουν το συνολικό μήκος των συγκολλήσεων για την κατασκευή της δεξαμενής. Η συγκεκριμένη πληροφορία είναι καθοριστικής σημασίας όχι μόνον από πλευράς κόστους, το οποίο είναι πολύ υψηλό από μόνο του, αλλά και από πλευράς απαιτούμενου χρόνου διεκπεραίωσης της εργασίας.

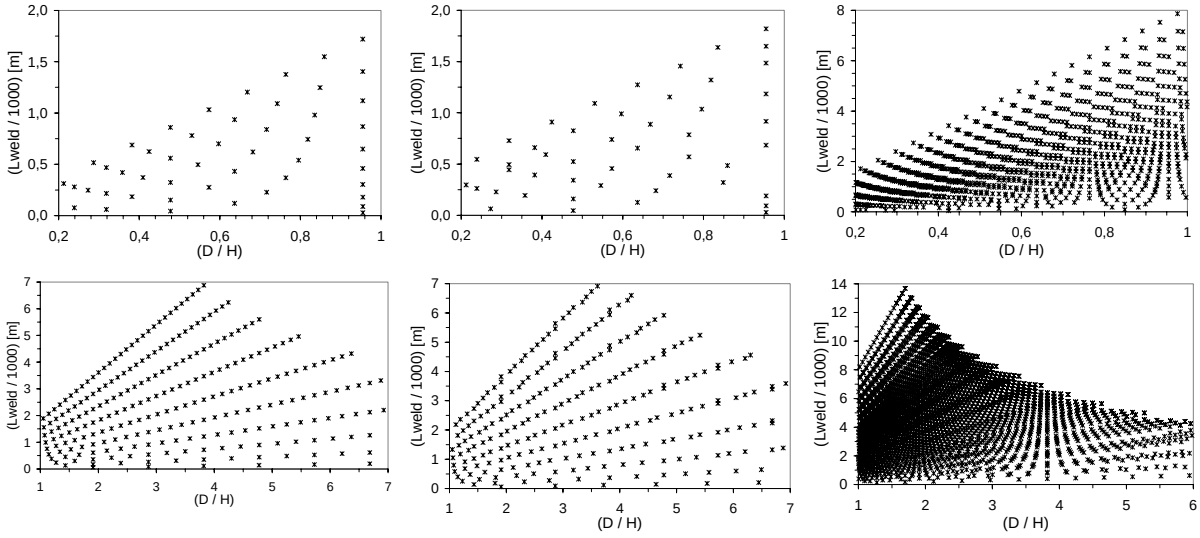

Σχήμα 7.18: Μήκος συγκόλλησης για βέλτιστες σχεδιάσεις χρησιμοποιώντας πιστοποιημένα ελάσματα της Ελληνικής αγοράς: (a) μόνο ελάσματα $2\text{m} \times 6\text{m}$, (b) μόνο ελάσματα $2.5\text{m} \times 6\text{m}$ και (c) ελάσματα $2\text{m} \times 6\text{m}$ / $2.5\text{m} \times 6\text{m}$

Βιβλιογραφία

API 12B, (1995), *Specification for Bolted Tanks for Storage of Production Liquids*, 14th Edition, API.

API 650 (1988), *Welded Steel Tanks for Oil Storage*, 8th Edition, API.

Belegundu AD, Chandrupatla TR (1999) Optimization concepts and applications in engineering. Prentice Hall.

Bendsøe MP (1995) Optimization of Structural Topology, Shape, and Material. Berlin: Springer-Verlag.

Berke L, Khot NS (1987) Structural optimization using optimality criteria, in: Computer Aided Optimal Design: Structural and Mechanical Systems, edited by C.A. Mota Soares, NATO, ASI series, F27B.

BS 2654 (1984), *Specification for manufacture of vertical steel welded storage tanks with butt-welded shells for the petroleum industry*, British Standards Institution, London.

Dawson M.A., Gibson, L.J., (2006), "Optimization of cylindrical shells with compliant cores", Int J Solids Structs, in press.

Duysinx P, Bendsøe MP (1998) Topology optimization of continuum structures with local stress constraints. Int J Num Meth Eng, 43, 1453-1478.

Fellini R, Kokkolaras M, Papalambros P (2003) Efficient Product Portfolio Reduction. Proceedings of the 5th World Congress on Structural and Multidisciplinary Optimization, Lido di Jesolo-Venice, Italy, May 19-23.

Gallagher RH (1973) Fully Stressed Design, In: R. H. Gallagher & O. C. Zienkiewicz (eds.), Optimum Structural Design: Theory and Applications. John Wiley & Sons.

Haftka RT, Gurdal Z, Kamat M (1990) Elements of Structural Optimization. Kluwer.

Hagihara, S., Miyazaki, N. (2003), "Bifurcation Buckling Analysis of Conical Roof Shell Subjected to Dynamic Internal Pressure by the Finite Element Method", J Pressure Vessel Technology, Vol. 125, pp. 78-84.

Kirsch U (1989) Optimal Topologies of Structures. Appl Mech Rev, 42, 238.

Kirsch U (1993) Structural Optimization. Springer-Verlag.

Makris P, Provatidis C (2002) Weight minimisation of displacement-constrained truss structures using a strain energy criterion, Computer Methods Appl. Mech. Engrg., 191, 2159-2177.

Morris AJ (1982) Foundations of Structural Optimization: A Unified Approach. John Wiley & Sons.

Papalambros P (1995) Optimal Design of Mechanical Components and Systems. ASME Journal of Mechanical Design, Special 50th Anniversary Design Issue (B. Ravani, ed.), 117, 55-62.

Patnaik SN, Guptill JD, Berke L (1995) Merits and limitations of optimality criteria method for structural optimization. Int. J. Numer. Meth. Engng, 38, 3087-3120.

Perelmuter, A.V., Fialko, S.Y., Karpilovsky, V.S., Kryksunov, E.Z., "Analysis of the Stressed State of Cylindrical Tanks with Defects of Geometrical Shape", Computer Methods in Mechanics, June 3-6, 2003, Gliwice, Poland.

Petruccelli JD (1999) Applied statistics for engineers and scientists. Prentice Hall.

Pham DT, Karaboga D (2000) Intelligent Optimisation Techniques: Genetic Algorithms, Tabu Search, Simulated Annealing and Neural Networks. Springer.

prEN 1991-4: *Eurocode 1 – Actions on structures, Part 4: Actions of silos and tanks*.

Provatidis CG, Venetsanos DT (2003) Performance of the FSD in Shape and Topology Optimization of Two-Dimensional Structures Using Continuous and Truss-like Models. Proc. of the 5th World Congress on Structural and Multidisciplinary Optimization, Lido di Jesolo-Venice, Italy, May 19-23.

Qing L, Steven GP, Xie YM (2000) Evolutionary structural optimization for stress minimization problems by discrete thickness design. Comp. Struct., 78(6), 769-780.

Rozvany GIN (2001) Aims, scope, methods, history and unified terminology of computer-aided topology optimization in structural mechanics. Struct. Multidisc Optim., 2, 90-108.

Rozvany GIN (2001b) Stress ratio and compliance based methods in topology optimization – a critical review. Struct. Multidisc. Optim., 21, 109-119.

Rozvany GIN, Pomezanski V, Gaspar Z (2005) Some Pivotal Issues in Structural Topology Optimization. Proc. of the 6th World Congress on Structural and Multidisciplinary Optimization, Rio De Janeiro, Brazil, May 30-June3.

Schmit LA (1995) Fully Stressed Design of elastic redundant trusses under alternative loading systems. Australian Journal of Applied Science, 9, 337-348.

Song, J., Park, H., Lee D.Y., Park S. (2002), "Scheduling of Actual Size Refinery Processes Considering Environmental Impacts with Multiobjective Optimization", Ind. Eng. Chem. Res., Vol. 41, pp. 4794-4806.

Suzuki K, Kikuchi N (1991) A Homogenization Method for Shape and Topology Optimization. Computer Methods Appl. Mech. Engrg., 93, 291-318.

Tank version 2.5, ©1994-2003, COADE/Engineering Physics Software, Inc., Houston, Texas, USA.

Xie YM, Steven GP (1997) Evolutionary Structural Optimization. Springer-Verlag.

Yoshida, S. (2001), "Buckling of aboveground oil storage tanks under internal pressure", Steel and Composite Structures, Vol.1.

Young, W. C. (1989), *Roark's Formulas for Stress and Strain*, McGraw Hill.

Εργασίες

[1] **Venetsanos, D.T.**, Mitrakos, D. and Provatidis, C.G., "Layout optimization of 2D skeletal structures using the fully stressed design", 1st International Conference on Information Technology and Quality, 5-6 June 2004, Athens, Greece.

[2] Provatidis, C.G. and **Venetsanos, D.T.**, Cost minimization of 2D continuum structures under stress constraints by increasing commonality in their skeletal equivalents, Forschung im Ingenieurwesen vol.70 (3), pp. 159-169, 2006.

[3] Provatidis, C.G., **Venetsanos, D.T.,** Linardos, M.D., "Cost Minimization Of Welded Steel Tanks For Oil Storage According To API Standards", 2nd International Conference "From Scientific Computing to Computational Engineering", Athens, 5-8 July, 2006.

ΚΕΦΑΛΑΙΟ 8
(ΠΕΡΙΛΗΨΗ)

ΒΕΛΤΙΣΤΟΠΟΙΗΣΗ ΔΙΑΚΡΙΤΩΝ ΚΑΤΑΣΚΕΥΩΝ ΒΑΣΕΙ ΛΕΙΤΟΥΡΓΙΚΗΣ ΑΡΤΙΟΤΗΤΑΣ

Στο παρόν κεφάλαιο, εξετάζεται η βελτιστοποίηση διακριτών κατασκευών βάσει της λειτουργικής τους αρτιότητας. Στην πράξη, πολλές μηχανολογικές κατασκευές αποτελούν συναρμολογήματα από τυποποιημένα δομικά στοιχεία εμπορίου, όπως είναι τα ελάσματα και οι δοκοί. Για τέτοιες κατασκευές, η βέλτιστη σχεδίαση αντιστοιχεί σε εκείνον τον συνδυασμό τυποποιημένων στοιχείων, για τον οποίο το βάρος της κατασκευής είναι ελάχιστο, ενώ, ταυτόχρονα, ικανοποιούνται και όλοι οι, επιβαλλόμενοι από κάποιον κανονισμό, περιορισμοί. Πρακτικά, αυτό σημαίνει την αναζήτηση του βέλτιστου, μεταξύ πολλών υποψηφίων, συνδυασμού. Πρόκειται για ένα πρόβλημα συνδυαστικού τύπου, η επίλυση του οποίου είναι δυνατή χρησιμοποιώντας κάποια, ολικώς ή μερικώς παραγοντική, διαδικασία. Σε αυτό το πλαίσιο, διατυπώθηκαν συνολικά τρεις νέες διαδικασίες βελτιστοποίησης. Η πρώτη διαδικασία αφορά στη βελτιστοποίηση κατασκευής, στην οποία εμπλέκεται μία μεταβλητή σχεδίασης. Η δεύτερη διαδικασία αφορά στη βελτιστοποίηση κατασκευής, η οποία κατασκευάζεται πλήρως από στοιχεία τυποποιημένης διατομής. Η τρίτη διαδικασία αφορά στη βελτιστοποίηση κατασκευής, η οποία κατασκευάζεται πλήρως από ελάσματα τυποποιημένου πάχους. Οι δύο τελευταίες είναι ευρυστικού χαρακτήρα, μερικώς παραγοντικές, διαδικασίεςβελτιστοποίησης. Ως εφαρμογές, εξετάσθηκαν επικαθήμενες γερανογέφυρες απλού και διπλού φορέα φέρουσες ένα φορείο, γεραδοκός συγκολλητής διατομής φέρουσα μία γερανογέφυρα καθώς και ένα υπόστεγο αεροσκαφών. Σε όλες τις περιπτώσεις, επεβλήθησαν τα κατά τον Ευρωκώδικα προβλεπόμενα. Επίσης, πραγματοποιήθηκε σύγκριση με εμπορικό λογισμικό ανάλυσης μεταλλικών κατασκευών, από την οποία προέκυψε η ανωτερότητα της αντίστοιχης (δεύτερης) εκ των προτεινομένων διαδικασιών.

Στην περίληψη του παρόντος κεφαλαίου παρουσιάζονται συνοπτικά οι τρεις προτεινόμενες διαδικασίες.

8.1.Εισαγωγή

Τα προβλήματα βελτιστοποίησης κατασκευών χρησιμοποιώντας τυποποιημένες διατομές, δηλαδή προβλήματα συνδυαστικού τύπου, χαρακτηρίζονται κυρίως από το τεράστιο πλήθος των δυνατών συνδυασμών, οι οποίοι πρέπει να εξετασθούν προκειμένου να βρεθεί εκείνος ο συνδυασμός για τον οποίο το βάρος της κατασκευής είναι ελάχιστο και ταυτόχρονα ικανοποιούνται όλοι οι επιβαλλόμενοι περιορισμοί. Από θεωρητικής απόψεως, ο βέλτιστος συνδυασμός εντοπίζεται εύκολα και με ακρίβεια εάν ελεγχθούν όλοι οι δυνατοί συνδυασμοί και τελικά επιλεγεί ο καλύτερος. Ωστόσο, κάτι τέτοιο συνοδεύεται από πολύ υψηλό, έως και απαγορευτικά υψηλό, υπολογιστικό κόστος. Επιπροσθέτως, σε μία κατασκευή είναι δυνατή η χρήση εν μέρει τυποποιημένων διατομών και εν μέρει μη-τυποποιημένων διατομών, οπότε η διατύπωση του αντιστοίχου προβλήματος βελτιστοποίησης είναι μικτού τύπου. Κάτι τέτοιο προσαυξάνει την δυσκολία του προς επίλυση προβλήματος βελτιστοποίησης διότι κάποιες από τις μεταβλητές σχεδίασης είναι διακριτές, άρα οι πιθανές τιμές τους είναι πεπερασμένες σε πλήθος, ενώ κάποιες άλλες είναι συνεχείς, άρα οι πιθανές τιμές τους είναι άπειρες σε πλήθος. Διαπιστώνεται, λοιπόν, ότι τα συνδυαστικού τύπου προβλήματα βελτιστοποίησης κατασκευών εμφανίζουν ιδιαιτερότητες. Ένας τρόπος αντιμετώπισης τέτοιων προβλημάτων είναι ευρυστικών διαδικασιών. Αυτές, αν και δεν αποδεικνύεται με αυστηρά μαθηματικό τρόπο ότι οδηγούν στην καθολικά βέλτιστη σχεδίασης, αποτελούν έναν πολύ καλό συμβιβασμό μεταξύ αποτελεσματικότητας και αλγοριθμητικής απλότητας.

Στην παρούσα περίληψη κεφαλαίου, αντιμετωπίζονται τρία είδη προβλημάτων βελτιστοποίησης κατασκευών συνδυαστικού τύπου. Τα δύο πρώτα σχετίζονται με τη χρήση τυποποιημένων δοκών θερμής έλασης (χρήση αμιγώς διακριτών μεταβλητών σχεδίασης) και το τρίτο αφορά σε συγκολλητές διατομές, οι οποίες προκύπτουν όταν ελάσματα τυποποιημένων παχών συγκολληθούν μεταξύ τους (χρήση και διακριτών και συνεχών μεταβλητών σχεδίασης). Και στις τρεις περιπτώσεις, αντικειμενικός σκοπός είναι η ελαχιστοποίηση του βάρους της κατασκευής. Για την επίλυση των ανωτέρω προβλημάτων, προτείνονται, αντίστοιχα, τρεις διαδικασίες βελτιστοποίησης, οι οποίες εφαρμόζονται σε αντίστοιχες κατασκευές με πρακτική εφαρμογή.

8.2. Διακριτή βελτιστοποίηση κατασκευών με μία μεταβλητή σχεδίασης

8.2.1. Γενικά

Ο συγκεκριμένος τύπος προβλήματος συναντάται στην πράξη σε κατασκευές, οι οποίες είναι δυνατόν να θεωρηθούν ως μία δοκός τυποποιημένης διατομής, όπως συμβαίνει σε ορισμένες περιπτώσεις γερανογεφυρών, απλού ή διπλού φορέα, και γερανοδοκών. Τέτοια προβλήματα δεν εμφανίζουν ιδιαίτερη δυσκολία στην επίλυσή τους. Μία απλή διαδικασία επίλυσης θα ήταν η δημιουργία λιστών με υποψήφιες διατομές, έτσι ώστε κάθε λίστα να περιλαμβάνει διατομές μίας συγκεκριμένης οικογενείας διατομών, π.χ. HEA, HEB, HEM, κλπ., η επίλυση του προβλήματος βελτιστοποίησης χρησιμοποιώντας κάθε μία λίστα ξεχωριστά, ώστε για κάθε λίστα να προκύψει μία βέλτιστη διατομή, και τελικά η επιλογή της βέλτιστης, μεταξύ των βελτίστων, διατομής. Αναφορικά με την επίλυση του προβλήματος βελτιστοποίησης για κάθε μία λίστα, είναι δυνατή η χρήση οποιασδήποτε διαδικασίας αναζήτησης γραμμής (π.χ. μέθοδος binary search, μέθοδος bisection, μέθοδος dichotomous search, μέθοδος interval halving). Τα κομβικά σημεία σε αυτό το βήμα επίλυσης είναι πρώτον η χρήση *ταξινομημένων* λιστών με τις διαθέσιμες διατομής και δεύτερον η αναζήτηση χρησιμοποιώντας τον *αύξοντα αριθμό*, τον οποίο φέρει κάθε διατομή στην εκάστοτε λίστα. Σε αυτό το πλαίσιο, προτείνεται η διαδικασία βελτιστοποίησης, η οποία παρουσιάζεται στην επόμενη Ενότητα.

8.2.2. Προτεινόμενη διαδικασία βελτιστοποίησης

Έστω LL το μήκος μίας λίστας από δοκούς του ιδίου τύπου διατομής, x_l ο δείκτης της πρώτης διατομής της λίστας, x_u ο δείκτης της τελευταίας διατομής της λίστας και x_m ο δείκτης της διατομής στο μέσο της λίστας. Θεωρείται ότι στην εν λόγω λίστα, οι δοκοί είναι ταξινομημένες κατά αύξουσα σειρά του βάρους τους ανά μονάδα μήκους. Εάν πραγματοποιηθεί μία ανάλυση με τη Μέθοδο των Πεπερασμένων Στοιχείων (ΜΠΣ) χρησιμοποιώντας τη δοκό με δείκτη x_u και διαπιστωθεί ότι παραβιάζεται έστω και ένας περιορισμός, τότε απορρίπτεται όλη η λίστα. Στην αντίθετη περίπτωση, πραγματοποιείται μία ανάλυση με τη (ΜΠΣ) και χρησιμοποιώντας τη διατομή με δείκτη x_l. Εάν διαπιστωθεί ότι ικανοποιούνται όλοι οι περιορισμοί, τότε αυτή θεωρείται η βέλτιστη διατομή. Διαφορετικά εκκινείται μία διαδικασία αναζήτησης, όπως είναι αυτή της διχοτόμησης. Πιο συγκεκριμένα, τίθεται $x_m = \text{int}\{0.5(x_l + x_u)\}$ και πραγματοποιείται μία ανάλυση με τη (ΜΠΣ), χρησιμοποιώντας τη δοκό με δείτκη x_m. Έαν παραβιάζεται έστω και ένας περιορισμός, τότε ο δείκτης x_l τίθεται ίσος με τον δείκτη x_m και εκτελείται μία νέα επανάληψη. Εάν ικανοποιούνται όλοι οι περιορισμοί, τότε ο δείκτης x_u τίθεται ίσος με το δείκτη x_m και εκτελείται μία νέα επανάληψη. Η όλη διαδικασία επαναλαμβάνεται έως ότου οι δείκτες x_u και x_l καταστούν συνεχόμενοι μεταξύ τους, οπότε η τρέχουσα βέλτιστη διατομή θεωρείται ως και η καθολικά βέλτιστη. Στη συνέχεια, η ίδια διαδικασία επαναλαμβάνεται με μία λίστα διατομών άλλου τύπου. Με αυτόν τον τρόπο, τελικά διαμορφώνεται ένας πληθυσμός από βέλτιστες διατομές, η ελαφρύτερη εκ των οποίων αποτελεί τη 'βέλτιστη των βελτίστων' διατομή. Αλγοριθμικά, η προτεινόμενη διαδικασία περιγράφεται ως εξής:

Βήμα 1: Διαχωρισμός των διαθεσίμων δοκών σε κατηγορίες, ανάλογα με τον τύπο της διατομής, και για κάθε κατηγορία δημιουργία μιας ταξινομημένης λίστας κατά αύξουσα σειρά βάρους ανά μονάδα μήκους
Βήμα 2: Για κάθε λίστα, εκτέλεση των Βημάτων 2a και 2b:
Βήμα 2a: Προσδιορισμός του μήκους LL της λίστας
Βήμα 2b: Επιλογή της τελευταίας διατομής της λίστας και ανάλυση της κατασκευής με τη (ΜΠΣ)
ΕΑΝ παραβιάζεται έστω και ένας περιορισμός ΤΟΤΕ
Απόρριψη της λίστας
ΔΙΑΦΟΡΕΤΙΚΑ
Αποδοχή της διατομής ως της τρέχουσας καλύτερης
Επιλογή της πρώτης διατομής της λίστας
Ανάλυση της κατασκευής με τη (ΜΠΣ)
ΕΑΝ παραβιάζεται έστω και ένας περιορισμός ΤΟΤΕ
Απόρριψη της διατομής
Εκκίνηση διαδικασίας αναζήτησης λίστας (π.χ. μέθοδος διχοτόμησης)
ΔΙΑΦΟΡΕΤΙΚΑ
Αποδοχή της διατομής ως της καθολικά

Η προτεινόμενη διαδικασία διακρίνεται για την ευελιξία της, υπό την έννοια ότι, αλλάζοντας μόνον κάποια υπορουτίνα, είναι δυνατή η ενσωμάτωση σε αυτήν διαφόρων και διαφορετικών επιλογών. Ενδεικτικό παράδειγμα αποτελεί η διαδικασία αναζήτησης. Αντί της μεθόδου της διχοτόμησης, είναι δυνατή η χρήση οποιουδήποτε άλλου σχήματος αναζήτησης, απλά αλλάζοντας την αντίστοιχη ρουτίνα. Επίσης, αναφορικά με τον τρόπο ανάλυσης της

κατασκευής, είναι δυνατή η χρήση τόσο κλασσικής μηχανικής όσο και υπολογιστικής μηχανικής (ΜΠΣ), πάλι αλλάζοντας την αντίστοιχη υπορουτίνα. Με αυτόν τον τρόπο επιτυγχάνεται η επιλογή εκείνης της θεωρίας ανάλυσης (π.χ. γραμμική ή μη-γραμμική ανάλυση), η οποία ανταποκρίνεται καλύτερα στο εκάστοτε εξεταζόμενο πρόβλημα. Για παράδειγμα, έστω ότι αναζητείται η βέλτιστη τυποποιημένη διατομή για μία γερανοδοκό. Εάν επιλεχθεί διατομή Κατηγορίας-1, κατά τον Ευρωκώδικα 3, τότε μία γραμμική ανάλυση είναι επαρκής διότι, σύμφωνα πάντα με τον Ευρωκώδικα 3, στις διατομές της εν λόγω κατηγορίας εμφανίζεται πρώτα η διαρροή του υλικού και μετά ο λυγισμός. Ωστόσο, εάν επιλεχθεί διατομή Κατηγορίας-4, πάντα κατά τον Ευρωκώδικα 3, τότε ο λυγισμός εμφανίζεται πριν τη διαρροή του υλικού, οπότε η πλέον ενδεδειγμένη είναι μία μη-γραμμική ανάλυση (snap-through buckling), προκειμένου να εκτιμηθεί με ασφάλεια το κρίσιμο φορτίο λυγισμού.

8.2.3. Εφαρμογή: Βέλτιση επιλογή δοκού θερμής έλασης ως φορέα γερανογέφυρας

8.2.3.1. Βασικά θεωρητικά στοιχεία

Στο Σχήμα 8.1 παρουσιάζεται η εξετασθείσα εφαρμογή. Ειδικότερα, πρόκειται για μία τυπική επικαθήμενη γερανογέφυρα μονού φορέα (Σχήμα 8.1a), φέρουσα ένα τυπικό ανηρτημένο βαρουλκοφορείο με σχέσεις κλάδων 4/2 (Σχήμα 8.1b). Το ιδιαίτερο χαρακτηριστικό των φορείων τύπου /2 είναι ότι εξασφαλίζεται η κατακόρυφη κίνηση του αγκίστρου, εξ αιτίας της οποίας αφ' ενός μεν το ανηρτημένο φορτίο ισοκατανέμενεται μεταξύ των τροχών του ίδιου άξονα και αφ' ετέρου δε οι δυνάμεις στους τροχούς δεν μεταβάλλονται κατά την ανύψωση του φορτίου.

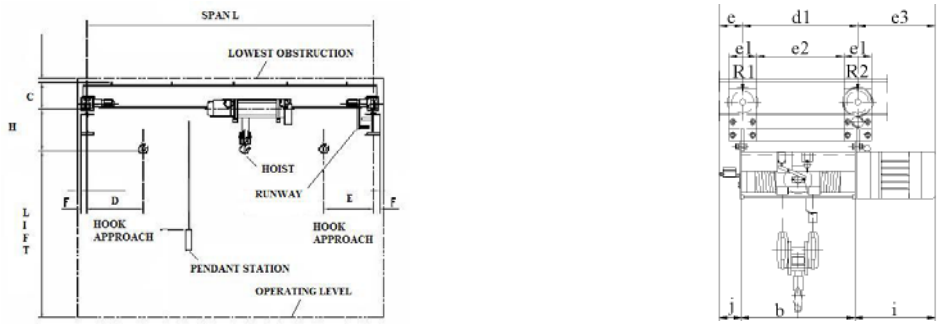

(a) (b)

Σχήμα 8.1: Σκίτσο (a) απλής επικαθήμενης γερανογέφυρας και (b) βαρουλκοφορείου

Σχετικά με τα φορτία, τα οποία αναπτύσσονται στους τροχούς του φορείου, ισχύει:

$$R_{11} = R_{12} = 0.5\left(0.5Q + aW\right) \tag{8.1}$$

$$R_{21} = R_{22} = 0.5\left(0.5Q + \left(1-a\right)W\right) \tag{8.2}$$

όπου

R_{11}, R_{12}: δυνάμεις στους τροχούς του άξονα #1 (Σχήμα 8.1b)

R_{21}, R_{22}: δυνάμεις στους τροχούς του άξονα #2 (Σχήμα 8.1b)

Q: συνολικό ανηρτημένο φορτίο

W: ίδιον βάρος

a: % ποσοστό ιδίου βάρους στον άξονα #1

Από τις Εξ. (8.1, 8.2) προκύπτει ότι η κατανομή φορτίου μεταξύ των τροχών του φορείου είναι σταθερή. Τα χαρακτηριστικά του βαρουλκοφορείου φαίνονται στον Πίνακα 8.1.

Πίνακας 8.1: Στοιχεία βαρουλκοφορείου

W	$575kg$		d_1	$498mm$
a	50%		e_3	$900mm$
Q	$3200kg$		e	$50mm$

Σχετικά με την διατομή του φορέα, εξετάσθηκαν τυποποιημένες διατομές (Σχήμα 8.2), οι οποίες είναι διαθέσιμες στην Ελληνική αγορά.

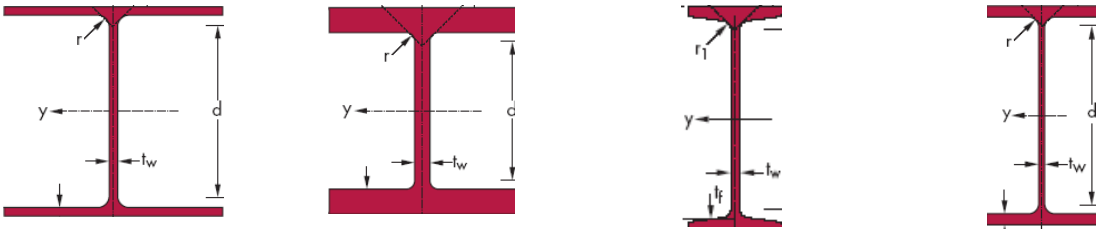

(a) (b) (c) (d)

Σχήμα 8.2: Εξετασθείσες διατομές (a) HEA-IPBL, (b) HEB-IPB, (c) INP και (d) IPE

Όπως αναφέρθηκε προηγουμένως, για την εξεταζόμενη επικαθήμενη γερανογέφυρα απλού φορέα, επελέγη μία ανοικτή, τυποποιημένη διατομή και ένα βαρουλκοφορείο ανηρτημένου τύπου. Ως εκ τούτου, κάθε τροχός του φορείου έρχεται σε επαφή με την άνω επιφάνεια του κάτω πέλματος της διατομής του φορέα (Σχήμα 8.3a) και ασκεί σε αυτήν ένα συγκεντρωμένο φορτίο, το οποίο είναι έκκεντρο ως προς τον κατακόρυφο κεντροβαρικό άξονα του κορμού της διατομής (Σχήμα 8.3b). Επιπροσθέτως, δεν είναι δυνατόν να αναρτηθεί οποιδήποτε φορείο σε οποιαδήποτε δοκό, λόγω γεωμετρικών περιορισμών σχετικά με το πάχος και το πλάτος του πέλματος της εν λόγω διατομής (Σχήμα 8.3b).

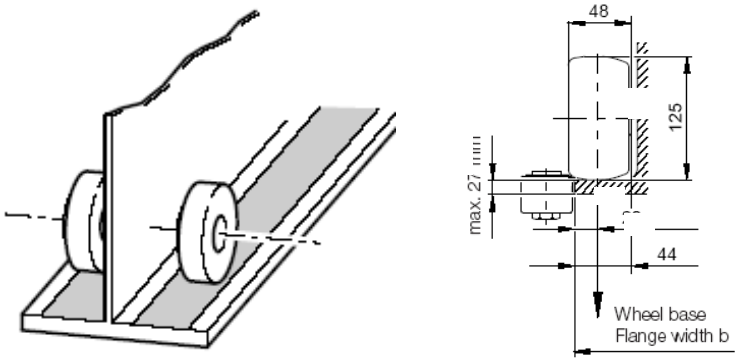

(a) (b)

Σχήμα 8.3: Τροχοί ενός τυπικού ανηρτημένου φορείου

Μία δοκός θερμής έλασης αποτελεί δυνατή λύση αν και μόνον αν παρέχει επαρκή αντίσταση στο επιβαλλόμενο φορτίο. Οι ποσότητες, οι οποίες, κατά κύριο λόγο, καθορίζουν την εν λόγω αντίσταση είναι (α) το μέγιστο βέλος κάμψης, (β) η μέγιστη διατμητιμή τάση, (γ) η μέγιστη ορθή τάση λόγω κάμψης και (β) η μέγιστη τάση από το συνδυασμό των (β) και (γ). Για τον υπολογισμό των (α) – (γ), είναι απαραίτητη η εξέταση τριών διαφορετικών θέσεων του φορείου επί του φορέα (βλ. Σχήμα 8.4):

Θέση #1: μέγιστο βέλος κάμψης, όπου $x_1 = \frac{L}{2} - \frac{a}{2}$ (Σχήμα 8.4a)

Θέση #2: μέγιστη διατμητική τάση, όπου $x_2 = \min\left\{\frac{d_1}{2} + e_3, \frac{d_1}{2} + e\right\}$ (Σχήμα 8.4b)

Θέση #3:μέγιστη καμπτική ροπή, όπου $x_3 = \frac{L}{2} - \frac{a}{4}$ (Σχήμα 8.4c)

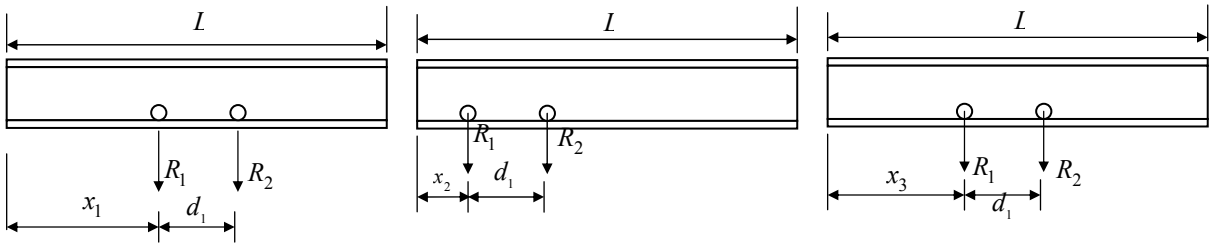

(a) **(b)** **(c)**

Σχήμα 8.4: Θέσεις φορείου για (a) μέγιστο βέλος κάμψης, (b) μέγιστη διάτμηση και (c) μέγιστη κάμψη

8.2.3.2. Αριθμητική προσέγγιση

Η μοντελοποίηση του φορέα απαιτεί την αντικατάσταση της φυσικής οντότητας με κάποιο αριθμητικό ισοδύναμο. Η πλέον απλή επιλογή είναι η χρήση στοιχείων δοκού. Ωστόσο, σε αυτήν την περίπτωση θεωρείται ότι τα φορτία ασκούνται κατά τον κατακόρυφο κεντροβαρικό άξονα του κορμού της διατομής, κάτι το οποίο δεν επιτρέπει τον συνυπολογισμό επιδράσεων ούτε λόγω τοπικής επιβολής φορτίου (Σχήμα 8.3b) ούτε λόγω διατμητικής υστέρησης (Cook, 1995; Σχήμα 8.5a). Μια άλλη δυνατότητα θα ήταν η χρήση στοιχείων 3Δ ελαστικότητας, όπως είναι το οκτακομβικό εξαπλευρικό πεπερασμένο στοιχείο (brick element, Σχήμα 8.5b). Σε αυτήν την περίπτωση, τα αριθμητικά αποτελέσματα είναι αξιόπιστα υπό δύο πολύ βασικές προϋποθέσεις:

α) η διακριτοποίηση του φορέα είναι τέτοια ώστε κατά το πάχος των ελασμάτων της διατομής του φορέα να υπάρχουν τουλάχιστον δύο πεπερασμένα στοιχεία και

β) ο λόγος πλευρών (aspect ratio) των στοιχείων του πλέγματος του φορέα είναι αποδεκτός.

Οι ανωτέρω προϋποθέσεις, σε συνδυασμό με το μήκος του φορέα, το οποίο είναι πολύ μεγάλο σε σχέση με τις διαστάσεις της διατομής του, έχουν ως αποτέλεσμα την απαίτηση για δημιουργία πλέγματος με μεγάλο αριθμό πεπερασμένων στοιχείων, κάτι το οποίο μεταφράζεται σε εξαιρετικά υψηλό υπολογιστικό κόστος. Αυτή δεν είναι μία καλή επιλογή όταν πρόκειται να εφαρμοσθεί μία επαναληπτική διαδικασία, όπως αυτή της βελτιστοποίησης.

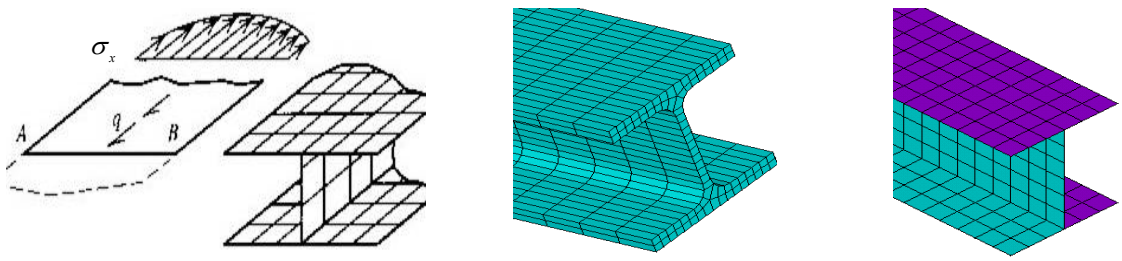

(a) (b) (c)

Σχήμα 8.5: (a) Φαινόμενο διατμητικής υστέρησης, (b) μοντέλο με στοιχεία τύπου brick και (c) μοντέλο με στοιχεία πλακός

Στην παρούσα διερεύνηση χρησιμοποιήθηκαν τυπικά τετρακομβικά στοιχεία πλακός (Σχήμα 8.5c), τα οποία αποτελούν πολύ καλό συμβιβασμό μεταξύ κόστους και αξιοπιστίας.

8.2.3.3. Περιορισμοί

Σε μία κατασκευή, επιβάλλονται περιορισμοί σύμφωνα με κάποιο πρότυπο (π.χ. κανονισμοί DIN, κανονισμοί BS, κανονισμοί ASD - LRFD - AASHTO, κανονισμοί JIS, κλπ). Στον ευρωπαϊκό χώρο, εφαρμόζονται πλέον οι Ευρωκώδικες. Χωρίς βλάβη της γενικότητας, είναι δυνατόν να επιβληθούν οι κατωτέρω περιορισμοί:

$$U_y \le \frac{L}{600} \qquad \sigma_{x,\max} \le \sigma_{x,allow} \qquad \tau_{\max} \le \tau_{allow} \qquad \sigma_{vonMises} \le \sigma_{vm,allow} \tag{8.3}$$

όπου U_y είναι το μέγιστο βέλος κάμψης, ενώ οι δείκτες 'x' και '$allow$' καταδεικνύουν τον διαμήκη άξονα του φορέα και την εκάστοτε επιτρεπόμενη τιμή, αντίστοιχα. Για τον συνδυασμό των εμφανιζομένων τάσεων, είναι δυνατόν να χρησιμοποιηθεί ο περιορισμός:

$$\left(\frac{\sigma_{x,Ed}}{f_y/\gamma_{M_o}}\right)^2 + \left(\frac{\sigma_{z,Ed}}{f_y/\gamma_{M_o}}\right)^2 - \left(\frac{\sigma_{x,Ed}}{f_y/\gamma_{M_o}}\right)\left(\frac{\sigma_{z,Ed}}{f_y/\gamma_{M_o}}\right) + 3\left(\frac{\tau_{Ed}}{f_y/\gamma_{M_o}}\right)^2 \le 1 \tag{8.4}$$

όπου

$\sigma_{x,Ed}$: τιμή σχεδίασης της ορθής, και κατά τον διαμήκη άξονα, τάσης

$\sigma_{z,Ed}$: τιμή σχεδίασης της ορθής, και κατά τον εγκάρσιο άξονα, τάσης

τ_{Ed}: τιμή σχεδίασης της διατμητικής τάσης

f_y: τάση διαρροής υλικού

γ_{M_o}: μερικός συντελεστής ασφαλείας $\left(\gamma_{M_o} = 1.1\right)$

Στην πλέον γενική περίπτωση, υπάρχουν ακόμα δύο περιορισμοί, οι οποίοι αφορούν στο λυγισμό και στο διατμητικό λυγισμό εξ αιτίας της επιβολής των φορτίων. Ωστόσο, οι εξετασθείσες διατομές ανήκουν στην, κατά τον Ευρωκώδικα 3, Κατηγορία-1 διατομών, στις οποίες η διαρροή του υλικού εμφανίζεται πριν από το λυγισμό, ενώ αυτές παρέχουν επαρκή αντίσταση έναντι διατμητικού λυγισμού (Falke, 1996).

8.2.3.4. Διαδικασία βελτιστοποίησης

Η διαδικασία βελτιστοποίησης της Ενότητας 8.2.2 ουσιαστικά αποτελεί μία αναζήτηση γραμμής σε λίστες. Πρόκειται για ένα πρόβλημα αριθμητικής ανάλυσης, το οποίο έχει διευρευνηθεί διεξοδικά στη διεθνή βιβλιογραφία. Η ιδιαιτερότητα στην περίπτωση των κατασκευών είναι ότι δεν χρησιμοποιείται μία μόνον λίστα αλλά περισσότερες, κάθε μία εκ των οποίων αντιστοιχεί και σε μία διαφορετική οικογένεια τυποποιημένων διατομών. Συνεπώς, εκτός της επίλυσης του αντιστοίχου προβλήματος βελτιστοποίησης, θα ήταν ιδιαιτέρως χρήσιμη η κατασκευή διαγραμμάτων (νομογραφημάτων), βάσει των οποίων είναι δυνατή η, με γραφικό τρόπο, επιλογή της βέλτιστης διατομής. Προς αυτήν την κατεύθυνση, η διαδικασία που ακολουθεί διακρίνεται σε δύο φάσεις: στην πρώτη φάση επιλύεται το πρόβλημα βελτιστοποίησης και ταυτόχρονα καταγράφονται οι μέγιστες τιμές των μεγεθών ενδιαφέροντος (Εξ. 8.3, 8.4), ενώ στη δεύτερη φάση οι εν λόγω μέγιστες τιμές αποτυπώνονται σε διαγράμματα, έτοιμα προς χρήση για πρακτικούς σκοπούς. Οι

χρησιμοποιηθείσες τυποποιημένες διατομές φαίνονται στον Πίνακα 8.2, ενώ η γεωμετρία τους ελήφθη από τη βιβλιογραφία (Stahl im Hochbau, 1967).

Πίνακας 8.2: Χρησιμοποιηθείσες διατομές

Κατηγορία	Μέγεθος					
HEA-IPBL	200	220	240	260	280	300
HEB-IPB	200	220	240	260	280	300
INP	280	300	320	340	360	400
IPE	330	360	400	450	500	550

Ειδικότερα, η εφαρμοσθείσα διαδικασία είναι η ακόλουθη:

Φάση Α: Επίλυση προβλήματος βελτιστοποίησης
Για κάθε κατηγορία τυποποιημένων δοκών (HEA-IPBL, HEB-IPB, INP, IPE)
Για κάθε εξετασθέν άνοιγμα φορέα (από $5m$ μέχρι $30m$ με βήμα $1m$)

Βήμα 1: Μοντελοποίηση του φορέα με στοιχεία πλακός

Βήμα 2: Επίλυση του προβλήματος βελτιστοποίησης χρησιμοποιώντας τη διαδικασίας της Ενότητας 8.2.2 και για τις εξής περιπτώσεις φόρτισης:

i) *Φορείο στη θέση #1 (βλ. Σχήμα 8.4a)*

ii) *Φορείο στη θέση #2 (βλ. Σχήμα 8.4b)*

iii) *Φορείο στη θέση #3 (βλ. Σχήμα 8.4c)*

Step 3: Για την προκύπτουσα από το Βήμα 2 βέλτιστη σχεδίαση, εφαρμογή εκ νέου των Βημάτων 2i, 2ii και 2iii και καταγραφή του μεγίστου βέλους κάμψης, της μέγιστης διατμητικής τάσης, της μέγιστης καμπτικής τάσης και της μέγιστης ισοδύναμης κατά von Mises τάσης.

Φάση Β: Αποτύπωση των αποτελεσμάτων της Φάσης #1 σε διαγράμματα
Για κάθε εξετασθείσα κατηγορία διατομών
Για όλα τα εξετασθέντα ανοίγματα φορέα, δημιουργία των εξής διαγραμμάτων:

- Διάγραμμα #1: μέγιστο βέλος κάμψης σε [mm] συναρτήσει ανοίγματος φορέα σε [m] (Σχήμα 8.6a)
- Διάγραμμα #2: μέγιστη διατμητική τάση σε [MPa] συναρτήσει ανοίγματος φορέα σε [m] (Σχήμα 8.6b)
- Διάγραμμα #3: μέγιστη καμπτική τάση σε [MPa] συναρτήσει ανοίγματος φορέα σε [m] (Σχήμα 8.6c)
- Διάγραμμα #4: μέγιστη von Mises τάση σε [MPa] συναρτήσει ανοίγματος φορέα σε [m] (Σχήμα 8.6d)

Ειδικά για το Διάγραμμα #1, έχει σχεδιασθεί μία επιπρόσθετη γραμμή, η οποία αντιστοιχεί στον επιβαλλόμενο περιορισμό μετατόπισης (Εξ.8.3). Διευκρινίζεται ότι τα προαναφερθέντα διαγράμματα αφορούν σε μία ποιότητα χάλυβα, ενώ για διαφορετική ποιότητα θα πρέπει να εκτελεσθούν εκ νέου οι Φάσεις Α και Β. Επίσης, διευκρινίζεται ότι το ίδιον βάρος των φορέων έχει ληψθεί υπόψη ως ομοιόμορφα κατανεμημένο φορτίο κατά μήκος του φορέα.

8.2.3.5. Αποτελέσματα - Διαγράμματα (νομογραφήματα)

Προκειμένου να ελεγχθεί η αποτελεσματικότητα της προτεινομένης διαδικασίας, ελύθησαν τα ίδια προβλήματα βελτιστοποίησης, με το ίδιο πεδίο ορισμού και τους ίδιους περιορισμούς, χρησιμοποιώντας την τεχνική της σαρωτικής αναζήτησης (exhaustive search), κατά την οποία επιλύεται το εκάστοτε πρόβλημα για κάθε ένα από τα διανύσματα σχεδίασης

του πεδίου ορισμού. Προέκυψε ότι, σε όλες τις περιπτώσεις, η προτεινόμενη διαδικασία βελτιστοποίησης συνέκλινε στην καθολικά βέλτιστη διατομή. Επίσης, με βάση τη διαδικασία της Ενότητας 8.2.3.4 και τα στοιχεία του Πίνακα 8.2, συνολικά προκύπτουν 16 νομογραφήματα. Στο Σχήμα 8.6 απεικονίζεται, ενδεικτικά, μία τετράδα τέτοιων διαγραμμάτων αφορούσα την οικογένεια διατομών HEA-IPBL.

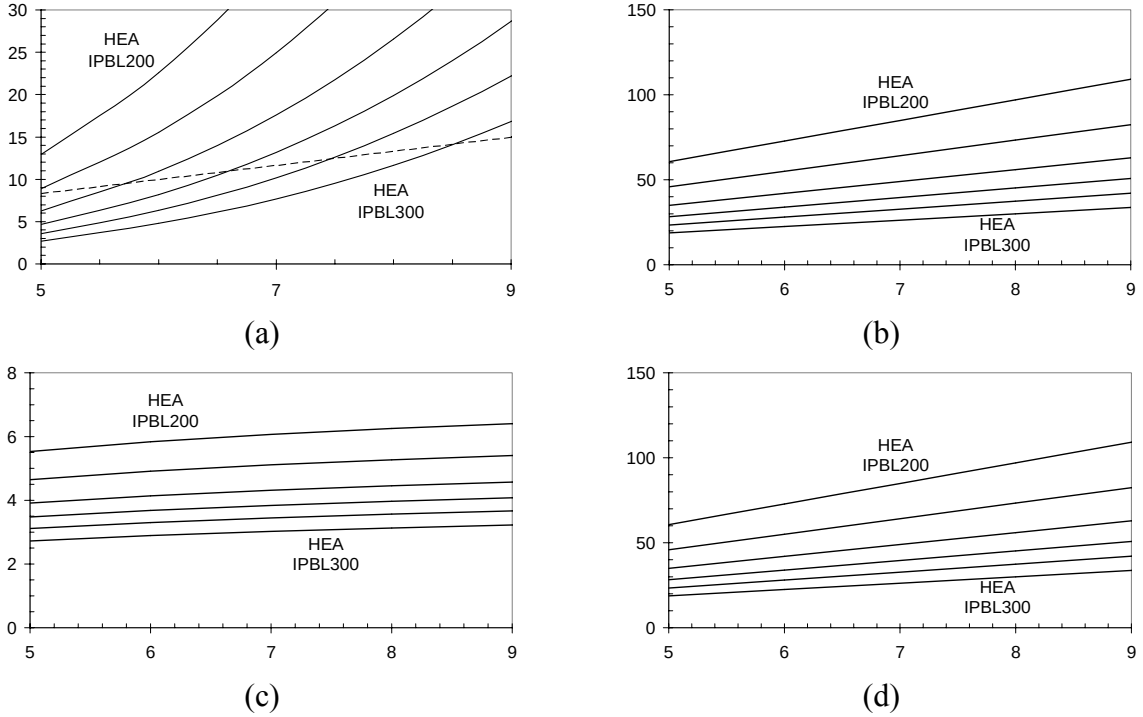

Σχήμα 8.6: Νομογραφήματα συναρτήσει του ανοίγματος φορέα (a) μεγίστου βέλους κάμψης, (b) μεγίστης διατμητικής τάσεως, (c) μεγίστης ορθής τάσεως και (δ) τάσης vonMises

Τα εν λόγω διαγράμματα, είναι δυνατόν να χρησιμοποιηθούν με δύο τρόπους:

Τρόπος (Α): για δεδομένη οικογένεια διατομών, εύρεση της απόκρισης μίας συγκεκριμένης διατομής

Βήμα 1: από τον x-άξονα και για δεδομένο άνοιγμα, φέρεται κάθετη γραμμή, έστω (VL)

Βήμα 2: από το σημείο τομής της γραμμής (VL) και ενός εκ των καμπυλών του διαγράμματος, φέρεται οριζόντια γραμμή, έστω (HL), προς τον y-άξονα

Βήμα 3: ανάγνωση της τιμής του σημείου τομής της γραμμής (HL) και του y-άξονα

Τρόπος (Β): για δεδομένη οικογένεια διατομών, εύρεση εκείνης της διατομής, η απόκριση της οποίας είναι πλησιέστερα, από την ασφαλή πλευρά, σε μία δεδομένη τιμή

Step 1: από τον x-άξονα και για δεδομένο άνοιγμα, φέρεται κάθετη γραμμή, έστω (VL)

Step 2: από τον y-άξονα και για δεδομένη τιμή του μεγέθους ενδιαφέροντος (επιλέγεται και το κατάλληλο διάγραμμα), φέρεται οριζόντια γραμμή, έστω (HL)

Step 3: εντοπισμός του σημείου τομής των ευθειών (VL) και (HL)

Step 4: επιλογή της πρώτης εκ των καμπυλών του διαγράμματος, οι οποίες κείτονται κάτω από το σημείο τομής του Βήματος 3, και η, αντιστοιχούσα στην εν λόγω καμπύλη, διατομή αποτελεί τη βέλτιστη επιλογή

Με την ανωτέρω ανάλυση παρουσιάστηκε ένας γρήγορος γραφικός τρόπος επιλογής της βέλτιστης τυποποιημένης διατομής, στην περίπτωση αναζήτησης ελαχίστου βάρους κατασκευής, όταν εμπλέκεται μία διακριτή μεταβλητή σχεδίασης. Στις δύο επόμενες ενότητες παρουσιάζεται η γενίκευση της προσέγγισης αυτής, δηλαδή όταν εμπλέκονται πολλές μεταβλητές σχεδίασης, και μάλιστα κάποιες από αυτές δεν είναι διακριτής φύσεως.

8.3. Διακριτή βελτιστοποίηση κατασκευών με πολλές μεταβλητές σχεδίασης

8.3.1. Γενικά

Το πλήθος των περιπτώσεων στι οποίες οι κατασκευές είναι δυνατόν να μοντελοποιηθούν ως δοκοί είναι αρκετά περιορισμένο. Πιο τυπική είναι η περίπτωση κατά την οποία μία μηχανολογική κατασκευή αποτελεί ένα συναρμολόγημα από ομάδες δομικών στοιχείων, εκ των οποίων κάθε ομάδα περιέχει διαφορετικό πλήθος δομικών μελών αλλά αφορά σε μία συγκεκριμένη διατομή. Σε μία τέτοια περίπτωση, εάν αναζητείται το ελάχιστο βάρος της κατασκευής, τότε η διαδικασία βελτιστοποίησης της Ενότητας 8.2.2 δεν είναι κατάλληλη, διότι αυτή δύναται να διαχειρισθεί μόνο μία ομάδα δομικών μελών. Συνεπώς, απαιτείται μία άλλη προσέγγιση. Προς αυτήν την κατεύθυνση, η διαδικασία της Ενότητας 8.2.2 επεκτείνεται καταλλήλως, έτσι ώστε να είναι δυνατή η διαχείριση ενός μεγάλου πλήθος ομάδων δομικών μελών. Θεωρητικά, αυτό το πλήθος είναι άπειρο, ωστόσο, για πρακτικούς λόγους, δηλαδή για λόγους υπολογιστικού κόστους, το εν λόγω πλήθος περιορίζεται σε λίγες δεκάδες. Η προαναφερθείσα γενίκευση είναι δυνατόν να διατυπωθεί ως ένα γενικό πρόβλημα βελτιστοποίησης στο οποίο αναζητείται εκείνο το διάνυσμα σχεδίασης $\mathbf{X}$ για το οποίο η βαθμωτή ποσότητα $f(\mathbf{X})$ ελαχιστοποιείται υπό την προϋπόθεση ότι οι επιβαλλόμενοι ισοτικοί $h_j(\mathbf{X}) = 0$ και/ή ανισοτικοί περιορισμοί $g_j(\mathbf{X}) \le 0$ δεν παραβιάζονται:

$$\min f(\mathbf{X}) \tag{8.5}$$

$$h_j(\mathbf{X}) = 0, \quad j = 1,2,...,m \tag{8.6}$$

$$g_j(\mathbf{X}) \le 0, \quad j = m+1, m+2, ..., p \tag{8.7}$$

όπου

$$\mathbf{X} = \begin{bmatrix} x_1 & x_2 & ... & x_n \end{bmatrix}^T \tag{8.8}$$

Στην Εξ.(8.8), ως x_i συμβολίζεται η διατομή ενός συνόλου δοκιμών στοιχείων, το πεδίο ορισμού των οποίων είναι:

$$x_i \in \begin{bmatrix} A_1 & A_2 & ... & A_n \end{bmatrix}^T \tag{8.9}$$

όπου ο δείκτης i αφορά σε ένα σύνολο δοκιμών στοιχείων και $A_k, k = 1,...,n$ είναι οι εμπορικώς διαθέσιμες τυποποιημένες διατομές.

8.3.2. Προτεινόμενη ευρυστική διαδικασία βελτιστοποίησης

Έστω ότι μία κατασκευή έχει N ομάδες διατομών και ότι κάθε ομάδα περιλαμβάνει M διαφορετικές τυποποιημένες διατομές. Μια πλήρως παραγοντική (full-factorial) διαδικασία απαιτεί την εξέταση N^M συνδυασμών, κάτι το οποίο ενδεχομένως να είναι απαγορευτικό. Αντιθέτως, η προτεινόμενη διαδικασία χρησιμοποιεί μεν N ομάδες διατομών με M μέλη η καθεμιά, αλλά με τέτοιον τρόπο ώστε να πραγματοποιείται μια προοδευτική ολίσθηση προς το, φαινομενικά, βέλτιστο διάνυσμα σχεδίασης. Ειδικότερα, η διαδικασία έχει ως εξής:

Βήμα 1: Ορίζονται οι πίνακες (λίστες), οι οποίοι περιέχουν τις τυποποιημένες διατομές και αποτελούν το πεδίο ορισμού κάθε μεταβλητής σχεδίασης. Αρχικά, αποδίδεται μία πολύ μεγάλη τιμή στο βέλτιστο βάρος της κατασκευής. Διευκρινίζεται ότι οι εν λόγω λίστες πρέπει να είναι ταξινομημένες.

Βήμα 2: Ορίζεται το αρχικό διάνυσμα σχεδίασης (είτε δηλώνεται από τον χρήστη είτε επιλέγεται τυχαία)

Βήμα 3: Ορίζεται το εύρος αναζήτησης (search width) σχετικά με τους πίνακες του Βήματος 1. Το διάνυσμα σχεδίασης, σε συνδυασμό με το εύρος αναζήτησης, ορίζει έναν υποπίνακα, ο οποίος θα διευρενηθεί σαρωτικά. Σε περίπτωση κατά την οποία είτε το άνω είτε το κάτω όριο του εν λόγω υποπίνακα βρεθεί εκτός του πεδίο ορισμού του προβλήματος, τότε το συγκεκριμένο όριο τίθεται ίσο με το αντίστοιχο άνω ή κάτω όριο του πεδίου ορισμού, έτσι ώστε ο υποπίνακας να αποτελεί πάντοτε υποσύνολο του πεδίου ορισμού.

Βήμα 4: Για κάθε μεταβλητή σχεδίασης, λαμβάνεται μία τιμή από τον υποπίνακα του Βήματος 3. Με αυτόν τον τρόπο σχηματίζεται ένα νέο διάνυσμα σχεδίασης.

Βήμα 5: Αναλύεται η κατασκευή, χρησιμοποιώντας είτε ιδιωτικό (in-house) κώδικα είτε κάποιο εμπορικό λογισμικό.

Βήμα 6: Αξιολογούνται τα αποτελέσματα του Βήματος 5. Εάν ικανοποιούνται όλοι οι περιορισμοί και το βάρος της κατασκευής είναι μικρότερο από το τρέχον ελάχιστο βάρος, τότε το νέο διάνυσμα σχεδίασης θεωρείται ως το τρέχον βέλτιστο διάνυσμα.

Βήμα 7: Εάν προκύψει νέο βέλτιστο διάνυσμα σχεδίασης από το Βήμα 6, τότε αυτό το διάνυσμα καθίσταται ως αρχικό διάνυσμα για τον επόμενο κύκλο αναζήτησης.

Βήμα 8: Εάν δεν προκύψει νέο βέλτιστο διάνυσμα σχεδίασης από το Βήμα 6, τότε ως αρχικό διάνυσμα για τον επόμενο κύκλο αναζήτησης χρησιμοποιούνται οι διατομές του διανύσματος σχεδίασης του προηγουμένου κύκλου αναζήτησης, 'μετατοπισμένες' στη λίστα του Βήματος 1 κατά ένα προκαθορισμένο βήμα.

Βήμα 9: Η διαδικασία τερματίζεται όταν όλες οι μεταβλητές σχεδίασης αποκτούν τη μέγιστη δυνατή διατομή, όπως αυτή προκύπτει από τις λίστες του Βήματος 1.

Στην προαναφερθείσα επαναληπτική διαδικασία, είναι δυνατή η ενσωμάτωση τεσσάρων κανόνων, οι οποίοι βελτιώνουν σημαντικά την ικανότητα αναζήτησης. Αυτοί οι κανόνες είναι οι ακόλουθοι:

Κανόνας #1: Εάν η ανάλυση της κατασκευής για ένα διάνυσμα σχεδίασης, του οποίου οι μεταβλητές σχεδίασης φέρουν τις μέγιστες δυνατές τιμές (άνω όριο πεδίου ορισμού), οδηγεί σε παραβίαση έστω και ενός εκ των περιορισμών, τότε δεν υπάρχουν δυνατές σχεδιάσεις στον ορισθέντα χώρο σχεδίασης, συνεπώς δεν συντρέχει λόγος εκκίνησης της διαδικασίας βελτιστοποίησης.

Κανόνας #2: Εάν η ανάλυση της κατασκευής για ένα διάνυσμα σχεδίασης, του οποίου οι μεταβλητές σχεδίασης φέρουν τις ελάχιστες δυνατές τιμές (κάτω όριο πεδίου ορισμού), οδηγεί σε ικανοποίηση όλων των περιορισμών, τότε το εν λόγω διάνυσμα σχεδίασης είναι και το βέλτιστο στον ορισθέντα χώρο σχεδίασης. Και σε αυτήν την περίπτωση, δεν συντρέχει λόγος εκκίνησης της διαδικασίας βελτιστοποίησης.

Κανόνας #3: Διάνυσμα σχεδίασης $\mathbf{X}$, στο οποίο όλες οι μεταβλητές σχεδίασης, μία-προς-μία, είναι μεγαλύτερες από τις αντίστοιχες του τρέχοντος βελτίστου διανύσματος σχεδίασης, αντιστοιχεί σε βαρύτερη κατασκευή. Σε αυτήν την περίπτωση δεν συντρέχει λόγος ανάλυσης της κατασκευής για το διάνυσμα σχεδίασης $\mathbf{X}$.

Κανόνας #4: Έστω ότι ένα διάνυσμα σχεδίασης παραβιάζει έστω και έναν περιορισμό. Το διάνυσμα αυτό ονομάζεται $\mathbf{X}_{viol}$. Κάθε διάνυσμα σχεδίασης, στο οποίο όλες οι μεταβλητές σχεδίασης έχουν μία-προς-μία μικρότερη τιμή από τις μεταβλητές σχεδίασης του $\mathbf{X}_{viol}$ θα παραβιάζει και αυτό τουλάχιστον έναν περιορισμό, συνεπώς δεν συντρέχει λόγος ανάλυσης της κατασκευής. Το

διάνυσμα $\mathbf{X}_{viol}$ ενημερώνεται κάθε φορά που κάποιο διάνυσμα, με όλες τις μεταβλητές σχεδίασής του μία-προς-μία μεγαλύτερη από τις αντίστοιχες του τρέχοντος $\mathbf{X}_{viol}$, προκαλεί την παραβίαση έστω και ενός περιορισμού.

8.3.3. Εφαρμογή: Ελαχιστοποίηση βάρους υποστέγου αεροσκαφών

Η προδιαγραφή του προς εξέταση υποστέγου αεροσκαφών αφορά στη στάθμευση δύο αεροσκαφών τύπου Boeing 737-700. Σύμφωνα με την επίσημη ιστοσελίδα της κατασκευάστριας εταιρίας, ο συγκεκριμένος τύπος αεροσκάφους έχει μήκος $33.6m$, εκπέτασμα $35.8m$ και μέγιστο ύψος $12.5m$. Βάσει αυτών των μεγεθών, θεωρήθηκε ότι το υπόστεγο θα είχε μήκος $80m$, πλάτος $44m$ και εσωτερικό ύψος $16m$, το μέγιστο ύψος στην είσοδο του υποστέγου θα ήταν $9.55m$, ενώ αυτό θα έφερε και μια γερανογέφυρα $5t$.

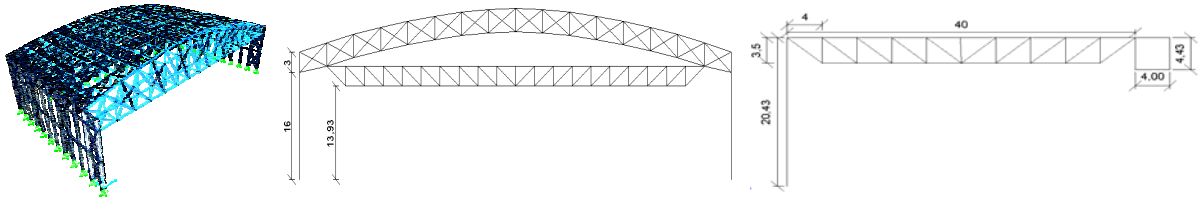

(a) (b) (c)

Σχήμα 8.7: Το υπόστεγο αεροσκαφών (a) 3D όψη της κατασκευής, (b) τμήμα του υποστέγου και (c) γερανογέφυρα.

Τα εξωτερικώς επιβαλλομένα φορτία (ιδίου βάρους, φορτίου ανέμου, φορτίου χιονιού καθώς και όλων των συνδυασμών αυτών) καθώς και οι περιορισμοί αντοχής και λειτουργικότητας ήταν σύμφωνα με τον Ευρωκώδικα 1 και τον Ευρωκώδικα 3, αντίστοιχα.

8.3.3.1. Στοιχεία για το υπόστεγο

Συνολικά, τα δομικά στοιχεία της μεταλλικής κατασκευής του υποστέγου συγκεντρώθηκαν σε 16 ομάδες (groups), όπως φαίνεται στον Πίνακα 8.1.

Πίνακας 8.3: Ομάδες δομικών στοιχείων του εξεταζομένου υποστέγου

Group1	**Group5**	**Group9**	**Group13**
HEA200	HEA360	TUBO-D193.7X4.5	HEM180
HEB200	HEA400	TUBO-D219.1X5	HEM200
	HEA450	TUBO-D244.5X5.4	HEM220
Group2	**Group6**	**Group10**	**Group14**
TUBO-D323.9X5.9	TUBO-D193.7X4.5	HEA120	TUBO-D139.7X4
TUBO-D323.9X5.9	TUBO-D219.1X5	HEB140	TUBO-D152.4X4
	TUBO-D244.5X5.4	HEA160	TUBO-D168.3X4
Group3	**Group7**	**Group11**	**Group15**
TUBO-D298.5X5.9	HEA180	HEA240	HEA140
TUBO-D323.9X5.9	HEA200	HEA260	HEA160
	HEB220	HEB280	HEA180
Group4	**Group8**	**Group12**	**Group16**
HEB800	HEA140	TUBO-D193.7X4.5	HEB200
HEB1000	HEA160	TUBO-D219.1X5	HEB220
	HEA180	TUBO-D244.5X5.4	HEB240

Το υπόστεγο βελτιστοποιήθηκε δύο φορές, μία χρησιμοποιώντας την, ενσωματωμένη στο εμπορικό λογισμικό SAP2000, δυνατότητα βελτιστοποίησης και μία με την προτεινόμενη διαδικασία. Τα αποτελέσματα από αυτές τις δύο βελτιστοποιήσεις, δηλαδή το βέλτιστο διάνυσμα σχεδίασης και το βάρος της κατασκευής, παρουσιάζονται στον Πίνακα 8.4.

Πίνακας 8.4: Βέλτιστες σχεδιάσεις για το εξεταζόμενο υπόστεγο

Ομάδα δομικών στοιχείων	Βελτιστοποίησης με εμπορικό λογισμικό	Βελτιστοποίηση με την προτεινόμενη διαδικασία
Group #1	HEB220	HEA200
Group #2	TUBO-D323,9X5,9	TUBO-D323,9X5,9
Group #3	TUBO-D355,6X6,3	TUBO-D298,5X5,9
Group #4	HEB800	HEB800
Group #5	HEB400	HEA400
Group #6	TUBO-D219,1X5	TUBO-D219,1X5
Group #7	HEB220	HEA180
Group #8	HEB200	HEA160
Group #9	TUBO-D244,5x5,4	TUBO-D193,7X4,5
Group #10	HEA160	HEB140
Group #11	HEB280	HEA240
Group #12	TUBO-D273x5,6	TUBO-D219,1X5
Group #13	HEM200	HEM180
Group #14	TUBO-D168,3x4	TUBO-D152,4X4
Group #15	HEA180	HEA140
Group #16	HEB240	HEB220
Συνολικό βάρος κατασκευής [t]	***62.7***	***55.0***

Από τους δύο ανωτέρω πίνακες, προκύπτει ότι η προτεινόμενη διαδικασία καταλήγει σε μία σχεδίαση ελαφρύτερη κατά 12.3% συγκριτικά με εκείνην, η οποία προέκυψε χρησιμοποιώντας το εμπορικό λογισμικό. Ειδικά για τη λειτουργικότητα, ισχύει:

- Κατά τον άξονα x, οι μέγιστες μετατοπίσεις είναι $\left(L = 19m\right)$:

$$u_{x,\min} = \left|-51.046mm\right| < L/300 = 63mm \text{ και } u_{x,\max} = 56.105 < L/300 = 63mm \qquad (8.10)$$

- Κατά τον άξονα y, οι μέγιστες μετατοπίσεις είναι $\left(L = 80m\right)$:

$$u_{y,\min} = \left|-143.851mm\right| < L/300 = 267mm \text{ και } u_{y,\min} = 81.621 < L/300 = 267mm \qquad (8.11)$$

- Κατά τον άξονα z, οι μέγιστες μετατοπίσεις είναι $\left(L = 44m\right)$:

$$u_{z,\max} = 211.325 < L/200 = 220mm \qquad (8.12)$$

Από τους ανωτέρω ελέγχους, προκύπτει ότι η βέλτιστη σχεδίαση, όπως αυτή προκύπτει από την εφαρμογή της προτεινομένης διαδικασίας, ικανοποιεί όλους τους, σχετικούς με τη λειτουργικότητα της κατασκευής, περιορισμούς. Συγκριτικά, δε, με τις μετατοπίσεις, οι οποίες αντιστοιχούν στο βέλτιστο διάνυσμα σχεδίασης, όπως αυτό προέκυψε από τη χρήση

του εμπορικού λογισμικού, σημαντική διαφορά υπάρχει μόνο στην κατακόρυφη μετατόπιση, όπως φαίνεται και στον Πίνακα 8.5.

Πίνακας 8.5: Σύγκριση βελτίστων σχεδιάσεων με κριτήριο τις μετατοπίσεις

Διεύθυνση		Μετατόπιση [mm]	
		Βελτιστοποίηση με εμπορικό λογισμικό	Βελτιστοποίηση με την προτεινόμενη διαδικασία
Οριζόνια	κατά τον άξονα x	57	56,105
		-51	-51,046
	κατά τον άξονα y	143	143,851
		-81	-81,621
Κάθετη	κατά τον άξονα z	145	211,325

8.3.3.2. Στοιχεία για τη γερανογέφυρα

Σχετικά με την ανηρτημένη γερανογέφυρα, αυτή ήταν μορφής δικτυώματος, ύψους $3m$ και ανοίγματος $70m$

Τα αναπτυσσόμενα κατακόρυφα φορτία στις γερανοδοκούς οφείλονται στο ανηρτημένο φορτίο, στο ίδιον βάρος της γερανογέφυρας και στο ίδιον βάρος του βαρουλκοφορείου. Για τις ανάγκες της παρούσης, θεωρήθηκε ανηρτημένο φορτίο $5t$ και ίδια βάρη $15.2t$, ενώ υπολογίστηκαν οι αντιδράσεις, για το χειρότερο σενάριο φόρτισης, στις δύο θέσεις στήριξης της γερανογέφυρας ίσες $87kN$ και $53kN$, αντίστοιχα.

Οι οριζόντιες δυνάμεις, οι οποίες αναπτύσσονται στη γερανοδοκό, θεωρείται ότι οφείλονται στην επιτάχυνση/επιβράδυνση της γερανογέφυρας. Σύμφωνα με τον Ευρωκώδικα, θεωρείται ότι οι οριζόντιες δυνάμεις δρουν ταυτόχρονα με τις κατακόρυφες δυνάμεις. Για τις ανάγκες της παρούσης, οι οριζόντιες δυνάμεις θεωρήθηκαν ίσες με το 15% των κατακορύφων δυνάμεων, ήτοι $10kN$.

Ο χώρος σχεδίασης για την ανηρτημένη γερανογέφυρα περιγράφεται στον Πίνακα 8.6, στον οποίο οι, προκύπτουσες με την προτεινόμενη διαδικασία, διατομές σημειώνονται με έντονα γράμματα.

Πίνακας 8.6: Χώρος σχεδίασης για την ανηρτημένη γερανογέφυρα

Group 1	**Group 2**	**Group 3**	**Group 4**	**Group 5**
2L150X100X14/25/	2L150X100X14/25/	L90X8	L65X6	L65X6
2L150X100X14/30/	***2L150X100X14/30/***	L90X10	***L65X7***	***L65X7***
2L150X100X14/40/	2L150X100X14/40/	***L90X12***	L70X10	L70X10

Σημειώνεται ότι, τόσο το εμπορικό λογισμικό όσο και η προτεινόμενη διαδικασία βελτιστοποίησης, κατέληξαν στο ίδιο βέλτιστο διάνυσμα σχεδίασης για τη γερανογέφυρα. Αυτό σημαίνει ότι είναι εφικτή μία μείωση στο βάρος της γερανογέφυρας εάν μεταβληθεί η τοπολογία ή το σχήμα της γερανογέφυρας, και όχι το μέγεθος της διατομής των δομικών της στοιχείων.

8.3.3.3. Ανάλυση υπολογιστικού κόστους

Για την αξιολόγηση του υπολογιστικού κόστους της προτεινομένης διαδικασίας βελτιστοποίησης, εκτιμήθηκε ο υπολογιστικός χρόνος (CPU time) κάθε μίας από τις εμπλεκόμενες λειτουργίες (Σχήμα 8.8).

R1: άνοιγμα αρχείων
R2: ανάγνωση δεδομένων από αρχεία SAP
R3: νέο διάνυσμα σχεδίασης (NDV)
R4: αποθήκευση του (NDV)
R5: άνοιγμα βοηθητικών αρχείων
R6: δημιουργία νέου αρχείου SAP
R7: κλήση λογισμικού SAP
R8: έλεγχος περιορισμών
R9: διαγραφή παλαιών αρχείων SAP, νέο βέλτιστο διάνυσμα σχεδίασης

(a)

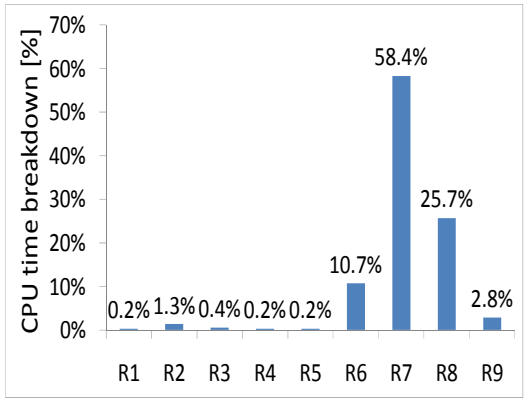

(b)

Σχήμα 8.8: Ανάλυση συνολικού υπολογιστικού χρόνου (a) λειτουργίες και (b) ποσοστό επί του συνολικού υπολογιστικού χρόνου

Οι κύριες λειτουργίες κατά την εκτέλεση της προτεινόμενης διαδικασίας παρουσιάζονται στο Σχήμα 8.8a. Από το Σχήμα 8.8b προκύπτει ότι τέσσερεις λειτουργίες, από τις εννέα συνολικά, καταναλώνουν το μεγαλύτερο μέρος του υπολογιστικού χρόνου. Η πλέον χρονοβόρος λειτουργία, με ποσοστό 58.4% επί του συνολικού υπολογιστικού χρόνου, αφορά στην κλήση του εμπορικού λογισμικού και στην εκτέλεση μίας ανάλυσης της κατασκευής. Ένα μεγάλο μέρος αυτού του κόστους αποτελεί κυριολεκτικά σπατάλη χρόνου διότι αφορά στην έναρξη και στον τερματισμό του εμπορικού λογισμικού, κάθε φορά που πρέπει να εξετασθεί ένα διάνυσμα σχεδίασης. Το υπολογιστικό κόστος θα μειωνόταν σίγουρα εάν θα ήταν εφικτή η διατήρηση του εμπορικού λογισμικού σε κατάσταση λειτουργίας και η χρήση του όποτε αυτό απαιτείτο.

Δύο άλλες, επίσης χρονοβόρες, λειτουργίες σχετίζονται με τη δημιουργία, διαχείριση και διαγραφή αρχείων τύπου txt, τα οποία χρησιμοποιούνται για την επικοινωνία μεταξύ του εμπορικού κώδικα και του ιδιωτικού (in-house) κώδικα που αναπτύχθηκε στο περιβάλλον MatLab. Η χρήση αρχείων txt δεν αποτελεί την καλύτερη επιλογή, σε αντίθεση με τη χρήση μίας βάσης δεδομένων. Ωστόσο, στο πλαίσιο της παρούσης, ο κύριος σκοπός ήταν η διερεύνηση της δυνατότητας ενσωμάτωσης ενός εμπορικού λογισμικού για την ανάλυση κατασκευής σε μία διαδικασία βελτιστοποίησης. Η επικοινωνία μεταξύ ιδιωτικού κώδικα και εμπορικού λογισμικού μέσω αρχείων βάσης δεδομένων θα μπορούσε να αποτελέσει μία μελλοντική βελτίωση.

Τέλος, σημειώνεται ότι για το εξετασθέν υπόστεγο αεροσκαφών και για τον χρησιμοποιηθέντα χώρο σχεδίασης, το συνολικό πλήθος συνδυασμών ήταν $8,503,056$. Με την προτεινόμενη ευρυστική διαδικασία βελτιστοποίησης, εξετάσθηκαν λιγότερο από 0.01% αυτών των συνδυασμών, μέχρι να εντοπισθεί η βέλτιστη σχεδίαση, το βάρος της οποίας είναι μικρότερο κατά 12.3% συγκριτικά με εκείνο που προέκυψε χρησιμοποιώντας το εμπορικό λογισμικό.

8.4. Μικτού τύπου βελτιστοποίηση κατασκευών με πολλές μεταβλητές σχεδίασης

8.4.1. Γενικά

Έστω ότι μία κατασκευή, π.χ. ο φορέας μίας γερανογέφυρας, αποτελείται από εμπορικώς διαθέσιμα ελάσματα, τα οποία διατίθενται σε συγκεκριμένες διαστάσεις. Αν και με διαδικασίες κοπής και συγκόλλησης είναι, θεωρητικά, δυνατή η δημιουργία οποιασδήποτε επιφανείας, ωστόσο το πάχος των ελασμάτων είναι τυποποιημένο και διακριτό. Εάν, λοιπόν,

αναζητείται το ελάχιστο βάρος ενός φορέα, τότε στο εν λόγω πρόβλημα βελτιστοποίησης εμπλέκονται και διακριτές μεταβλητές, το πάχος των ελασμάτων εν προκειμένω, και συνεχείς μεταβλητές, το πλάτος και το μήκος των ελασμάτων εν προκειμένω. Τέτοιου είδους προβλήματα, στα οποία εμπλέκονται μεταβλητές σχεδίασης διαφορετικού τύπου, ονομάζονται προβλήματα βελτιστοποίησης μικτού τύπου. Ωστόσο, για πρακτικούς λόγους, είναι δυνατόν οι συνεχείς μεταβλητές να λαμβάνουν μόνον ακέραιες τιμές. Στην περίπτωση των ελασμάτων, για λόγους κατεργασίας και κατασκευαστικού κόστους, οι διαστάσεις, μήκος και πλάτος, των τεμαχίων στα οποία θα κοπούν τα ελάσματα, στρογγυλοποιούνται με μία προκαθορισμένη ακρίβεια. Συνεπώς, οι συνεχείς μεταβλητές σχεδίασης, αν και αρχικώς ορίζονται στο χώρο των πραγματικών αριθμών, τελικά λαμβάνουν τιμές από το χώρο των ακεραίων αριθμών, οι οποίες είναι διακριτές μεν αλλά άπειρες στο πλήθος. Υπό αυτήν την έννοια, οι εν λόγω μεταβλητές είναι δυνατόν να ορισθούν ως ψευδο-διακριτές. Βάσει αυτού του ορισμού, η διαδικασία της Ενότητας 8.3.2 αναδιατυπώνεται, ως φαίνεται στην επόμενη Ενότητα.

8.4.2. Προτεινόμενη ευριστική διαδικασία βελτιστοποίησης

Έστω ότι σε μία κατασκευή ορίζονται N μεταβλητές σχεδίασης, εκ των οποίων οι N_D είναι διακριτής φύσεως και οι N_{qD} είναι ψευδο-διακριτής φύσεως. Ως 'ψευδοδιακριτές' ορίζονται εκείνες οι μεταβλητές, οι οποίες, αν και στην πραγματικότητα είναι συνεχείς, λαμβάνουν μόνον ακέραιες τιμές. Έστω ότι σε κάθε μία από τις N_D μταβλητές αποδίδεται μία διακριτή τιμή $M_i, i = 1,...,D$ και σε κάθε μία από τις N_{qD} είναι αποδίδεται μία ακέραια τιμή $M_i, i = 1,...,D$. Μια πλήρως παραγοντική (full-factorial) προσέγγιση απαιτεί την εξέταση ενός τεραστίου πλήθους συνδυασμών. Αντιθέτως, η προτεινόμενη διαδικασία στηρίζεται σε μία μερικώς παραγοντική (partial-factorial) διαδικασία αναζήτησης, η οποία είναι διαδραστική υπό την έννοια ότι ο χρήστης έχει τη δυνατότητα να επέμβει και να επηρεάσει την πορεία της βελτιστοποίησης αξιοποιώντας την κρίση και την εμπειρία του. Η προτεινόμενη ευριστική διαδικασία έχει ως εξής:

Βήμα 1: Σχηματισμός των λιστών, οι οποίες αποτελούν το πεδίο ορισμού κάθε μίας μεταβλητής. Αυτές οι λίστες είναι ταξινομημένες κατά αύξουσα.

Βήμα 2: Ορισμός ενός αρχικού διανύσματος σχεδίασης (επιλογή του χρήστη ή τυχαία δημιουργία).

Βήμα 3: Για κάθε μία μεταβλητή σχεδίασης, ορισμός του άνω ορίου, του κάτω ορίου και του βήματος αναζήτησης του υποπεδίου που πρόκειται να διερευνηθεί. Η διερεύνηση θα είναι σαρωτική και εμπεριέχει τους λογικούς κανόνες της Ενότητας 8.3.2, προκειμένου να περιορισθεί το υπολογιστικό κόστος.

Βήμα 4: Έναρξη ενός κύκλου αναζήτησης. Εάν σχηματίζονται δυνατά διανύσματα σχεδίασης, τότε αποθηκεύεται εκείνο, το οποίο αντιστοιχεί στο ελάχιστο βάρος. Διαφορετικά, ο χρήστης θα πρέπει να μεταβάλλει τα όρια ή/και το βήμα αναζήτησης του υποχώρου, στον οποίο πραγματοποιείται η αναζήτηση, και το Βήμα 4 εκτελείται εκ νέου έως ότου προκύψει ένα δυνατό διάνυσμα σχεδίασης.

Βήμα 5: Βάσει του διανύσματος σχεδίασης, το οποίο προκύπτει από το Βήμα 4, πραγματοποίηση μίας σαρωτικής αναζήτησης γύρω από το εν λόγω διάνυσμα και για ένα προκαθορισμένο εύρος.

Βήμα 6: Επανάληψη του Βήματος 5μέχρι συγκλίσεως του βάρους της κατασκευής.

Σε αυτό το σημείο διευκρινίζεται ότι, μετά το πέρας ενός κύκλου αναζήτησης, ο χρήστης είναι δυνατόν να μεταβάλλει ή ακόμα και να 'παγώσει' όρια και βήματα αναζήτησης,

προκειμένου να ενσωματώσει την προσωπική του κρίση και εμπειρία στην πορεία της βελτιστοποίησης. Αν και δεν αποδεικνύεται ότι η ανωτέρω διαδικασία καταλήγει πάντοτε στο καθολικά βέλτιστο διάνυσμα σχεδίασης, ο χρήστης έχει τη δυνατότητα να εκκινήσει τη διαδικασία βελτιστοποίησης από διαφορετικά αρχικά διανύσματα σχεδίασης και να πειραματισθεί με διάφορες επιλογές. Με τον τρόπο αυτό, είναι δυνατόν να αποκτήσει μία αίσθηση σχετικά με το πόσο βέλτιστη είναι τελικά η προκύπτουσα σχεδίαση. Σε αυτήν την διερεύνηση, σημαντικό αρωγό αποτελεί η χρήση των κανόνων της Ενότητας 8.3.2, διότι αυτοί δεν επιτρέπουν την εκτέλεση μίας ανάλυσης όταν διαγιγνώσκεται ότι το τρέχον διάνυσμα σχεδίασης θα οδηγήσει σε παραβίαση τουλάχιστον ενός εκ των επιβεβλημένων περιορισμών.

8.4.3. Εφαρμογή: Βελτιστοποίηση γερανογέφυρας διπλού φορέα κλειστής διατομής

8.4.3.1. Γενικά

Η εξετασθείσα εφαρμογή αφορά στην ελαχιστοποίηση του βάρους επικαθήμενης γερανογέφυρας διπλού φορέα κλειστής συγκολλητής διατομής (Σχήμα 8.9).

(a) (b) (c) (d)

Σχήμα 8.9: Τυπικές μορφές γερανογέφυρας διπλού φορέα: (a) τύπου πυλώνα, (b) επικαθήμενη, (c) ανηρτημένη και (d) τύπου tri-girder.

Για τη διαμόρφωση της διατομής του φορέα θεωρήθηκε ότι θα χρησιμοποιηθούν τυποποιημένα ελάσματα, διαθέσιμα στην Ελληνική αγορά. Το εν λόγω πρόβλημα είναι μικτού τύπου διότι εμπλέκονται διακριτές και συνεχείς μεταβλητές. Ειδικότερα, δεδομένου ότι τα διαθέσιμα ελάσματα διαθέτουν τυποποιημένα πάχη, έπεται ότι τα πάχη των κορμών και των πελμάτων είναι δυνατόν να λάβουν μόνον συγκεκριμένες και διακριτές τιμές, άρα αποτελούν διακριτές μεταβλητές σχεδίασης. Από την άλλη πλευρά, το ύψος των κορμών, το πλάτος των πελμάτων αλλά και η εσωτερική απόσταση μεταξύ των κορμών, είναι δυνατόν να λάβουν οποιαδήποτε θετική πραγματική τιμή. Συνεπώς, αυτά τα μεγέθη αποτελούν συνεχείς μεταβλητές σχεδίασης. Ωστόσο, για κατασκευαστικούς λόγους και λόγους κόστους, τα εν λόγω μεγέθη στρογγυλοποιούνται και λαμβάνουν μόνον θετικές, ακέραιες τιμές, άρα είναι ψευδο-διακριτής φύσεως (βλ. Ενότητα 8.4.2). Συνολικά, βελτιστοποιήθηκαν 75 περιπτώσεις, όπως αυτές προκύπτουν από το συνδυασμό των παραμέτρων του Πίνακα 8.7.

Πίνακας 8.7: Παράμετροι και τιμές αυτών

Index	Variable	Value	Units
1	***C***rane ***B***ridge ***S***pan	$CBS \in \{10,15,20,25,30\}$	[m]
2	***T***otal ***H***oisting ***M***ass	$THM \in \{10,15,20,25,30\}$	[t]
3	***T***rolley ***W***heel ***B***ase	$TWB \in \{1000,1250,1500\}$	[mm]

Διευκρινίζεται ότι όλα τα σενάρια φόρτισης υπολογίσθηκαν κατά τον Ευρωκώδικα 1, ενώ όλοι οι περιορισμοί (Πίνακας 8.8) επεβλήθησαν-σύμφωνα με Ευρωκώδικα 3.

Πίνακας 8.8: Περιορισμοί κατά Ευρωκώδικα 3

Οριακή Κατάσταση Αστοχίας	
Αξονική δύναμη	$\frac{N_{Ed}}{A_{eff}\, f_y / \gamma_{M_o}} \le 1.0$
Καμπτική ροπή	$\frac{M_{Ed}}{W_{eff}\, f_y / \gamma_{M1}} \le 1.0$
Εγκάρσια δύναμη	$\frac{F_{Ed}}{f_y\, L_{eff}\, t_w / \gamma_{M_1}} \le 1.0$
Διάτμηση	$\frac{V_{Ed}}{\chi_V\, d\, t_w f_y / \sqrt{3}\gamma_{M_1}} \le 1.0$
Διαξονική κάμψη και αξονική φόρτιση	$\frac{N_{Ed}}{f_y\, A_{eff} / \gamma_{M_o}} + \frac{M_{y,Ed} + N_{Ed}\, e_{y,N}}{f_y\, W_{eff,y} / \gamma_{M_o}} + \frac{M_{z,Ed} + N_{Ed}\, e_{z,N}}{f_y\, W_{eff,z} / \gamma_{M_o}} \le 1.0$
Συνδυασμός καμπτικής ροπής και διατμητικής δύναμης	$\frac{M_{Ed}}{W_{eff}\,(1-\rho) f_y / \gamma_{M_1}} \le 1.0 \;\; \rho = \left(2 V_{Ed} / V_{pl,Rd} - 1\right)^2$ $V_{pl,Rd} = \frac{A_V f_y}{\sqrt{3}\gamma_{M_o}}$
Συνδυασμός καμπτικής τάσης και αξονικής φόρτισης	$n_1 + \left(1 - \frac{M_{f,Rd}}{M_{pl,Rd}}\right)\left(2 n_3 - 1\right)^2 \le 1.0$
Συνδυασμός καμπτικής τάσης, εγκάρσιας και αξονικής φόρτισης	$n_2 + 0.8 n_1 \le 1.4$
Λυγισμός	$\frac{N_{Ed}}{\chi\, A_{eff}\, f_y / \gamma_{M_1}} \le 1.0$
Οριακή Κατάσταση Λειτουργικότητας	
Κατακόρυφο βέλος κάμψης	$w_z \le \min\left\{0.25, \frac{L}{600}\right\}$
Οριζόντιο βέλος κάμψης	$w_y \le \min\left\{0.25, \frac{L}{600}\right\}$
Ταλάντωση κάτω πέλματος	$\frac{L}{i} < 250$
Κόπωση συγκόλλησης	
Συγκόλληση - Συνισταμένη τάση	$\sigma_{Ed} < \frac{f_u}{\sqrt{3}\beta_w \gamma_{M_w}} \quad \sigma_{Ed} = \left[(\sigma_w + \sigma_{w,Ed})^2 + 3\left(\tau_1^2 + \tau_2^2\right)\right]^{1/2}$
Κόπωση λόγω ορθών τάσεων	$\gamma_{F_f}\, \Delta\sigma_{E_2} < \frac{\Delta\sigma_c}{\gamma_{M_f}}$
Κόπωση λόγω διατμητικών τάσεων	$\gamma_{Ff}\, \Delta\tau_{E_2} \le \frac{\Delta\tau_c}{\gamma_{M_f}}$
Κόπωση λόγω αλληλεπίδρασης ορθών και διατμητικών τάσεων	$\left[\frac{\gamma_{F_f} \Delta\sigma_{E_2}}{\Delta\sigma_c / \gamma_{M_f}}\right]^3 + \left[\frac{\gamma_{F_f} \Delta\tau_{E_2}}{\Delta\tau_c / \gamma_{M_f}}\right]^5 \le 1$

8.4.3.2. Αποτελέσματα - Διαγράμματα

Για την αξιολόγηση της προτεινομένης διαδικασίας, πραγματοποιήθηκε σύγκριση με τη μέθοδο της σαρωτικής αναζήτησης (exhaustive search) του πεδίου ορισμού. Σε όλες τις περιπτώσεις, προέκυψε ότι η προτεινόμενη διαδικασία βελτιστοποίησης συνέκλινε στο καθολικά βέλτιστο διάνυσμα σχεδίασης.

Με βάση, δε, τα βέλτιστα διανύσματα σχεδίασης από τις 75 εξετασθείσες περιπτώσεις, κατασκευάσθηκαν διαγράμματα προκειμένου να αποκαλυφθεί κάποια συσχέτιση μεταξύ των μεταβλητών σχεδίασης. Ειδικότερα, ορίσθηκαν τρεις ομάδες κανονικοποιημένων δεικτών. Η πρώτη ομάδα περιλαμβάνει τους ακόλουθους δείκτες:

$$\left(t_1/t_2\right)_i \quad \left(t_2/t_3\right)_i \quad \left(t_2/b\right)_i \quad \left(b/h_w\right)_i \quad \left(t_4/h_w\right)_i \quad \left(t_3/h_w\right)_i \tag{8.13}$$

όπου b_1, t_1 είναι το πλάτος και το πάχος του κάτω πέλματος, b_2, t_2 είναι το πλάτος και το πάχος του άνω πέλματος, ενώ h_w, t_3, t_4 είναι το ύψος και τα πάχη των κορμών, αντίστοιχα. Ο δείκτης $i \in [1,2,...,75]$ αντιστοιχεί στον αύξοντα αριθμό της εξετασθείσης γερανογέφυρας. Η δεύτερη ομάδα δεικτών περιλαμβάνει τις ακόλουθες ποσότητες:

$$\left(\frac{A_1}{A_4}\right)_i \quad \left(\frac{A_2}{A_4}\right)_i \quad \left(\frac{A_2}{A_3}\right)_i \quad \left(\frac{A_2}{A_{tot}}\right)_i \quad \left(\frac{A_3}{A_{tot}}\right)_i \quad \left(\frac{A_4}{A_{tot}}\right)_i \tag{8.14}$$

όπου A είναι το εμβαδόν διατομής και οι δείκτες $1,2,3,4,tot$ υποδηλώνουν το κάτω πέλμα, το άνω πέλμα, τον αριστερό κορμό, το δεξιό κορμό και τη συνολική διατομή, αντίστοιχα, μίας κλειστής διατομής φορέα. Ο δείκτης i χρησιμοποιείται όπως και στην Εξ.(8.13). Διευκρινίζεται ότι οι δείκτες της Εξ.(8.13) και της Εξ.(8.14) αποσκοπούν στην αποκάλυψη συσχέτισης σε όρους διαστάσεων και σε όρους εμβαδού διατομής, αντίστοιχα. Η τρίτη ομάδα δεικτών περιλαμβάνει τις ακόλουθες ποσότητες:

$$\begin{array}{ccc} \left(\dfrac{\left(I_{yy,uf}/I_{yy,w}\right)_i}{\left(I_{yy,uf}/I_{yy,w}\right)_{\max}}\right) & \left(\dfrac{\left(I_{yy,lf}/I_{yy,w}\right)_i}{\left(I_{yy,lf}/I_{yy,w}\right)_{\max}}\right) & \left(\dfrac{\left(I_{yy,uf}/I_{yy,lf}\right)_i}{\left(I_{yy,uf}/I_{yy,lf}\right)_{\max}}\right) \\ \left(\dfrac{\left(I_{yy,uf}/I_{yy,tot}\right)_i}{\left(I_{yy,uf}/I_{yy,tot}\right)_{\max}}\right) & \left(\dfrac{\left(I_{yy,lf}/I_{yy,tot}\right)_i}{\left(I_{yy,lf}/I_{yy,tot}\right)_{\max}}\right) & \left(\dfrac{\left(I_{yy,w}/I_{yy,tot}\right)_i}{\left(I_{yy,w}/I_{yy,tot}\right)_{\max}}\right) \end{array} \tag{8.15}$$

όπου ως I δηλώνεται η ροπή αδρανείας της διατομής, οι δείκτες uf, lf, w δηλώνουν το άνω πέλμα, το κάτω πέλμα και τους κορμούς, αντίστοιχα, ενώ ο δείκτης y δηλώνει τον οριζόντιο άξονα της διατομής.

Οι δείκτες των Εξ.(8.13, 8.14, 8.15) απεικονίσθηκαν σε ραβδοδιαγράμματα (Σχήμα 8.10), στα οποία εφαρμόσθηκε πολυωνυμική διαδικασία αναδρομής. Όπως φαίνεται, υπάρχει υψηλή συσχέτιση μεταξύ των αποτελεσμάτων, κάτι που υποδηλώνει ότι οι ορισθέντες κανονικοποιημένοι δείκτες υπακούουν σε πολυωνυμικούς νόμους μικρού έως και μεσαίου βαθμού πολυωνύμου. Επίσης, από αυτά τα διαγράμματα, προκύπτουν χρήσιμες παρατηρήσεις για τη σχεδίαση κλειστών διατομών γερανογεφυρών διπλού φορέα. Χαρακτηριστικά, αναφέρεται ότι η συνεισφορά των κορμών στη ροπή αδρανείας ως προς τον οριζόντιο άξονα είναι μεγαλύτερη από αυτή των πελμάτων (Σχήμα 8.8c), ενώ, μεταξύ των δύο πελμάτων, το άνω πέλμα είναι εκείνο το οποίο συνεισφέρει πολύ περισσότερο στη ροπή αδρανείας ως προς τον οριζόντιο άξονα (Σχήμα 8.8c).

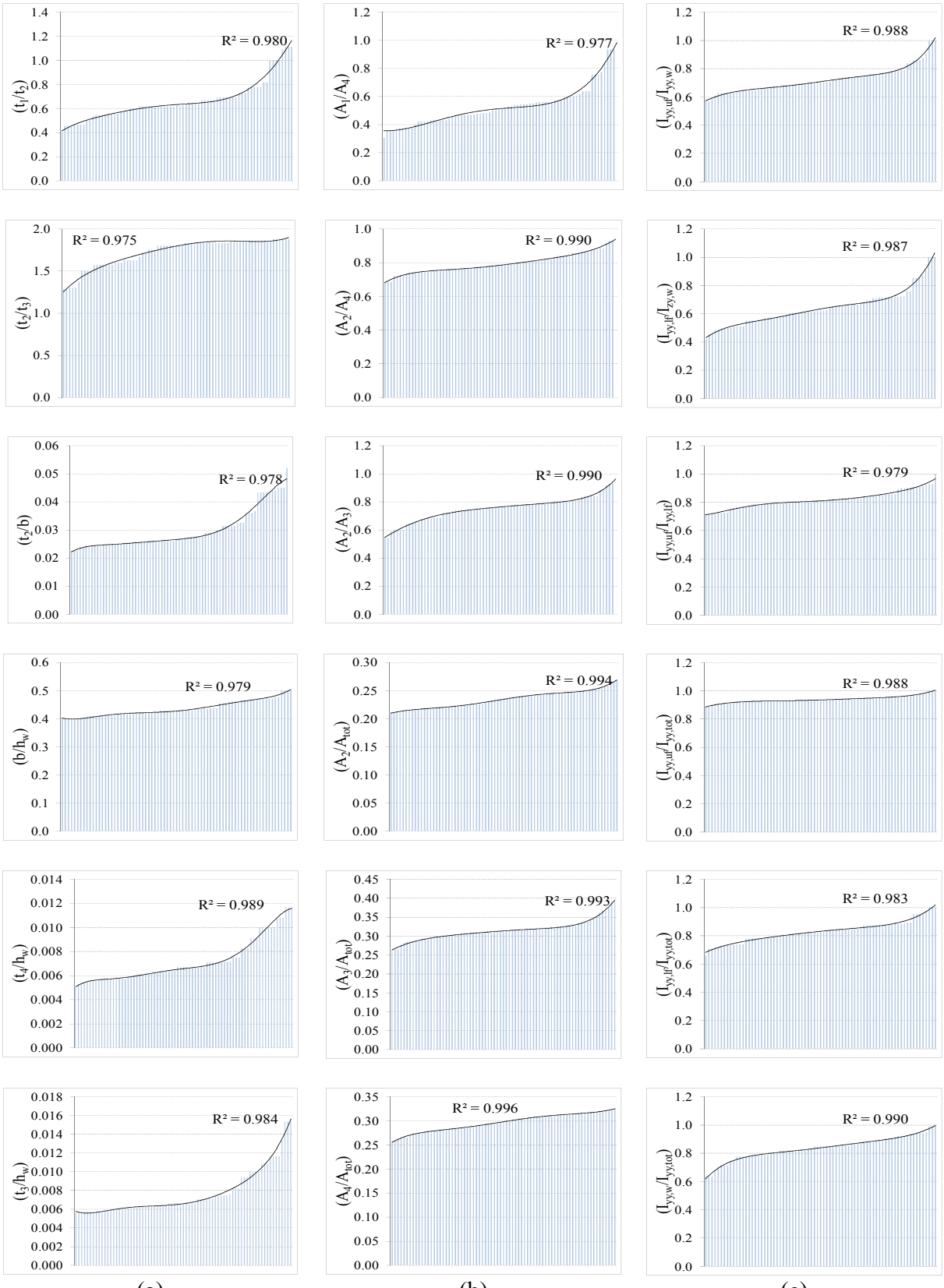

Σχήμα 8.10: Διαγράμματα κανονικοποιημένων δεικτών ως προς (a) τις γεωμετρικές διαστάσεις, (b) το εμβαδόν και (c)τις ροπές αδρανείας των βελτίστων διατομών

Βιβλιογραφία

Ambrose J (1997), Simplified design of steel structures, Wiley.

Bremicker, M., Papalambros, PY., Loh, H.T., (1990), "Solution of mixed-discrete structural optimization problems with a new sequential linearization algorithm", Computers & Structures, Vol. 37(4), pp.451-461.

Demo, D.A., (1976), "Analysis of Fatigue of Welded Crane Runway Girders", J. of Struct Div, Vol.102(5), pp. 919-933.

Draft prEN 1991-3, EUROCODE 1 - Actions on structures Part 3: Actions induced by cranes and machinery

EC-3 PrENV 1993-6 Crane Supporting Structures (N760e), CEN/TC250/SC3, 1998.

Erbatur, F., Hasançebi, O., Tütüncü, I., Kiliç, H., (2000), "Optimal design of planar and space structures with Genetic Algorithms", Computers & Structures, Vol. 75, pp. 209-224.

Falke J (1996), Ingenieurhochbau: Tragwerke aus Stahl nach Eurocode 3 (DIN V ENV 1993-1-1), DIN, Werner Verlag.

Grierson, D.E., Lee, W.H., (1984), "Optimal Synthesis of Steel Frameworks Using Standard Sections", Mechanics Based Design of Structures and Machines, Vol. 12(3), pp.335-370.

Guerlement, G., Targowski, R., Gutkowski, W., Zawidzka, J., Zawidzki, J., (2001), "Discrete minimum weight design of steel structures using EC3 code", Struct Multidisc Optim, Vol. 22, pp. 322–327.

Hernández, S, Fontán, A.N., Perezzán, J.C., Loscos, P., (2005), "Design optimization of steel portal frames", Advances in Engineering Software, Vol. 36, pp.626–633.

Hua, H. (1983), "Optimization for structures of discrete-size elements", Computers & Structures,Vol. 17(3), pp. 327-333.

Köppe, U. (1981), "Nutzlastkollektive von kranen", Hebezeuge und Fördermittel, vol. 21(2), pp.36–39.

Lagaros, N.D., Papadrakakis, M., (2007) "Robust seismic design optimization of steel structures", Struct Multidisc Optim, Vol. 33, pp.457–469.

Pasternak, H., Rozmarynowski, B., Wen, Y.-K. (1996), "Crane load modeling", Structural Safety, vol. 17, pp. 205–224.

prEN 1991-3, EUROCODE 1 - Actions on structures Part 3: Actions induced by cranes and machinery

prEN 1993-1-1, Eurocode 3: Design of steel structures - Part 1-1: General rules and rules for buildings

prEN 1993-1-5, 2004: Part 1-5: Plated structural elements, CEN.

prENV 1993-6, Crane Supporting Structures (N760e), CEN/TC250/SC3, 1998.

Salmon, CG, Johnson JE (1997), Steel structures: design and behavior (4th ed.), Prentice Hall.

Schmit, L., Fleury, C. (1980), "Discrete-continuous variable structural synthesis using dual methods", AIAA J, Vol. 18, pp. 1515–1524.

Stahl im Hochbau (1967), Verlag Stahleisen MBH.

Tsompanakis, Y., Papadrakakis, M., (2204), "Large-scale reliability-based structural optimization", Struct Multidisc Optim, Vol. 26, pp.429–440.

Vinnakota RS (2005), Steel structures: behavior and LRFD, McGraw-Hill.

Weaver, WM (1979), Crane handbook: Design data and engineering information used in the manufacture and application of overhead and gantry cranes (4th ed.), Whiting Corp.

Wu, S.J., Chow, P.T., (1995), "Steady-state genetic algorithms for discrete optimization of trusses", Computers & Structures, Vol. 56(6), pp.919-991.

Εργασίες

[1] Provatidis C.G., Tzanakakis E.D., and **Venetsanos D.T.**, "Optimum selection of doubly symmetric rolled beams for single-girder overhead travelling cranes using finite element plate models", 1st IC-EpsMsO, 6-9 July 2005, Athens, Greece.

[2] **Venetsanos D.T.**, Provatidis C.G., Magoula E-A.T., "Optimal design of a welded open cross-section crane runway beam in accordance with EC1 and EC3", 2nd International Conference on Experiments/Process/System Modelling/Simulation & Optimization Athens, 4-7 July, 2007.

[3] **Venetsanos D.T.**, Provatidis C.G., Skarmeas S.G., "Optimal Design Of A Box Cross Section Of A Double Girder Crane In Accordance With EC1 AND EC3", 2nd International Conference on Experiments/Process/System Modelling/Simulation & Optimization, Athens, 4-7 July, 2007.

[4] **Venetsanos D.**, Magoula E. and Provatidis C., "Performance-based optimization of the welded box of a single girder overhead travelling crane according to EC3 and EC1, 8th. World Congress on Computational Mechanics (WCCM8), 5th. European Congress on Computational Methods in Applied Sciences and Engineering (ECCOMAS 2008), June 30–July 4, 2008, Venice, Italy.

[5] **Venetsanos D.** and Provatidis C., "Performance-based optimization of a welded open cross section runway beam according to EC3 and EC1", 8th. World Congress on Computational Mechanics (WCCM8), 5th.

European Congress on Computational Methods in Applied Sciences and Engineering (ECCOMAS 2008), June 30–July 4, 2008, Venice, Italy.

[6] Kapogiannis A.K., **Venetsanos D.T.** and Provatidis C.G., Weight minimization of a steel hangar using a new heuristic optimization procedure and according to the Eurocode standards, 3rd International Conference "From Scientific Computing to Computational Engineering", Athens, 8-11 July, 2009.

ΚΕΦΑΛΑΙΟ 9
(ΠΕΡΙΛΗΨΗ)

ΣΥΜΠΕΡΑΣΜΑΤΑ

ΚΑΙ

ΠΕΡΑΙΤΕΡΩ ΕΡΕΥΝΑ

Σε αυτήν την περίληψη κεφαλαίου παρουσιάζεται εν συντομία η συνεισφορά της παρούσας Διδακτορικής Διατριβής καθώς θέματα για περαιτέρω έρευνα.

9.1. Συνεισφορά Διδακτορικής Διατριβής

Εν συντομία, η συνεισφορά της παρούσης Διδακτορικής Διατριβής είναι δυνατόν να συνοψισθεί στα κατωτέρω:

- Διατύπωση νέων κανονικοποιημένων δεικτών για την αξιολόγηση μίας μεθόδου βελτιστοποίησης.
- Ανάπτυξη μίας νέας υβριδικής μεθόδου για την επίλυση προβλημάτων ελαχιστοποίησης του βάρους μίας κατασκευής υπό την επιβολή οποιουδήποτε πλήθους περιορισμών μετατόπισης ή/και τάσης. Η εν λόγω μέθοδος εφαρμόσθηκε για τη βελτιστοποίηση σκελετικών κατασκευών, ενώ η εφαρμογή της μεθόδου και σε κατασκευές συνεχούς μέσου είναι τετριμμένη.
- Διατύπωση ενός νέου Βελτίστου Κριτηρίου για την επίλυση του προβλήματος ελαχιστοποίησης του βάρους μίας κατασκευής συνεχούς μέσου υπό την επιβολή ενός περιορισμού ανάπαλσης.
- Ανάπτυξη μίας νέας διαδικασίας βελτιστοποίησης, για την επίλυση του προβλήματος ελαχιστοποίησης του βάρους μίας 2Δ κατασκευής συνεχούς μέσου υπό την επιβολή περιορισμών τάσης, εισάγοντας ισοπαραμετρική ενδοστοιχειακή παρεμβολή πάχους και χρησιμοποιώντας τους κόμβους του πλέγματος ως σημεία ελέγχου σμίλευσης της επιφανείας της κατασκευής.
- Διερεύνηση και σύγκριση των βιβλιογραφικών μεθόδων ESO και FSD στην επίλυση του προβλήματος ελαχιστοποίησης του βάρους 2Δ πλακών υπό την επιβολή περιορισμού τάσης.
- Ανάπτυξη μίας νέας διαδικασίας βελτιστοποίησης για την επίλυση του προβλήματος ελαχιστοποίησης του βάρους μίας 3Δ κατασκευής συνεχούς μέσου υπό την επιβολή περιορισμού τάσης.
- Διατύπωση ενός νέου Βελτίστου Κριτηρίου για την επίλυση του προβλήματος ελαχιστοποίησης του βάρους 2Δ και 3Δ σκελετικών κατασκευών υπό την γενικευμένη επιβολή ενός περιορισμού τάσης.
- Ανάπτυξη μίας νέας διαδικασίας βελτιστοποίησης για την επίλυση του προβλήματος ελαχιστοποίησης του βάρους 2Δ και 3Δ σκελετικών κατασκευών υπό την γενικευμένη επιβολή ενός περιορισμού τάσης.
- Διατύπωση ενός νέου Βελτίστου Κριτηρίου για την επίλυση του προβλήματος ελαχιστοποίησης του βάρους 2Δ και 3Δ σκελετικών κατασκευών υπό την γενικευμένη επιβολή ενός περιορισμού μετατόπισης.
- Ανάπτυξη μίας νέας διαδικασίας βελτιστοποίησης για την επίλυση του προβλήματος ελαχιστοποίησης του βάρους 2Δ και 3Δ σκελετικών κατασκευών υπό την γενικευμένη επιβολή ενός περιορισμού μετατόπισης.
- Ανάπτυξη μίας παραλλαγής της μεθόδου ESO για την επίλυση του προβλήματος ελαχιστοποίησης του βάρους 2Δ συνεχών μέσων υπό την επιβολή ενός περιορισμού μετατόπισης.
- Ανάπτυξη μίας νέας διαδικασίας βελτιστοποίησης για την επίλυση του προβλήματος ελαχιστοποίησης του βάρους μίας 2Δ κατασκευής συνεχούς μέσου υπό τη γενικευμένη επιβολή ενός περιορισμού μετατόπισης, εισάγοντας ισοπαραμετρική ενδοστοιχειακή παρεμβολή πάχους και χρησιμοποιώντας τους κόμβους του πλέγματος ως σημεία ελέγχου σμίλευσης της επιφανείας της κατασκευής.
- Ανάπτυξη μίας νέας διαδικασίας βελτιστοποίησης για την επίλυση του προβλήματος ελαχιστοποίησης του κόστους μίας σκελετικής κατασκευής, επιδιώκοντας την ομαδοποίηση των ενεργών δομικών στοιχείων και την αύξηση της κοινοτυπίας τους.
- Ανάπτυξη μίας νέας διαδικασίας βελτιστοποίησης για την επίλυση του προβλήματος ελαχιστοποίησης του κατασκευαστικού κόστους δεξαμενών αποθήκευσης

πετρελαιοειδών, χρησιμοποιώντας εμπορικά διαθέσιμα ελάσματα, λαμβάνοντας υπόψη το κόστος των συγκολλήσεων και επιδιώκοντας την ελαχιστοποίηση της φύρας.

- Ανάπτυξη μίας νέας διαδικασίας βελτιστοποίησης για την επίλυση του προβλήματος ελαχιστοποίησης του βάρους κατασκευών, οι οποίες είναι δυνατόν να θεωρηθούν ως απλές δοκοί, όπως συμβαίνει στην περίπτωση γερανογέφυρας απλού φορέα.
- Ανάπτυξη μίας νέας ευρυστικής διαδικασίας βελτιστοποίησης για την επίλυση του προβλήματος ελαχιστοποίησης του βάρους κατασκευών, οι οποίες αποτελούνται από τυποποιημένα ραβδόμορφα ή δοκιδόμορφα στοιχεία.
- Ανάπτυξη μίας νέας ευρυστικής διαδικασίας βελτιστοποίησης μικτού τύπου για την επίλυση του προβλήματος ελαχιστοποίησης του βάρους κατασκευών, οι οποίες αποτελούνται από πλακόμορφα στοιχεία. Στην περίπτωση αυτή, το πάχος των πλακών είναι τυποποιημένο (διακριτό πρόβλημα βελτιστοποίησης) αλλά οι άλλες δύο γεωμετρικής διαστάσεις είναι δυνατόν να θεωρηθούν ως συνεχείς μεταβλητές (πρόβλημα βελτιστοποίησης συνεχών μεταβλητών).
- Επίλυση του προβλήματος ελαχιστοποίησης του βάρους μίας σειράς κατασκευών με πρακτική εφαρμογή, επιβάλλοντας όλους τους, προβλεπόμενους από κανονισμούς και πρότυπα, περιορισμούς και χρησιμοποιώντας ανάλυση ευαισθησίας ή/και εμπορικό κώδικα.

9.2. Περαιτέρω έρευνα

Σχετικά με ιδέες για περαιτέρω έρευνα, ένα άμεσο βήμα είναι η εφαρμογή της προτεινομένης διαδικασίας βελτιστοποίησης υπό την γενικευμένη επιβολή ενός περιορισμού μετατόπισης σε 3Δ κατασκευές συνεχούς μέσου. Το επόμενο βήμα θα ήταν η εφαρμογή του προτεινομένου Βελτίστου Κριτηρίου για την επίλυση του προβλήματος ελαχιστοποίησης του βάρους υπό την γενικευμένη επιβολή ενός περιορισμού τάσης, σε διάφορες 2Δ και 3Δ κατασκευές. Στη συνέχεια θα ήταν δυνατή η σύζευξη των προτεινομένων, στην παρούσα Διδακτορική Διατριβή, Βελτίστων Κριτηρίων προς επίλυση προβλημάτων ελαχιστοποίησης βάρους κατασκευών υπό τη γενικευμένη επιβολή ενός περιορισμού μετατόπισης και υπό τη γενικευμένη επιβολή ενός περιορισμού τάσης. Επίσης, ενδιαφέρον θα παρουσίαζε η διερεύνηση της επιβολής άλλων ειδών περιορισμών, όπως είναι οι περιορισμοί σχετικά με τις ιδιοσυχνότητες, πάντοτε υπό τη μορφή προβλήματος βελτιστοποίησης υπό τη γενικευμένη επιβολή ενός περιορισμού. Προφανώς, ένας υψηλός στόχος θα ήταν η αντιμετώπιση του προβλήματος βελτιστοποίησης υπό τη γενικευμένη επιβολή ενός περιορισμού μετατόπισης, ενός περιορισμού τάσης, ενός περιορισμού ιδιοσυχνότητας και ενός περιορισμού ευστάθειας. Ένα ακόμα πεδίο ερεύνης θα αποτελούσε η χρήση ιδεών και τεχνικών από το χώρο του CAD (Computer Aided Design) για τη σμίλευση του σχήματος ενός συνεχούς μέσου, κατά την οποία οι κόμβοι θα χρησιμοποιούνταν ως σημεία ελέγχου μίας καλώς και σαφώς ορισμένης επιφανείας, ενώ για την παρεμβολή του πάχους θα χρησιμοποιούνται διαφορετικά σχήματα ισοπαραμετρικής παρεμβολής. Τέλος, ένας εντελώς διαφορετικός δρόμος έρευνας θα ήταν η ενσωμάτωση ιδεών, όπως των προαναφερθέντων, σε άλλες υπολογιστικές μεθόδους, όπως είναι η Μέθοδος των Συνοριακών Στοιχείων (Boundary Element Method) και η Μέθοδος Άνευ Πλέγματος (Meshless Method), και σε άλλα υλικά, όπως είναι τα σύνθετα υλικά.

Αυτή η σελίδα είναι σκοπίμως κενή

ΠΑΡΑΡΤΗΜΑ Α

ΔΗΜΟΣΙΕΥΣΕΙΣ

ΚΑΙ

ΑΝΑΚΟΙΝΩΣΕΙΣ

Σε αυτό το Παράρτημα παρατίθενται οι δημοσιεύσεις και οι ανακοινώσεις, οι οποίες προέκυψαν από τμήμα υλικού της παρούσης Διδακτορικής Διατριβής. Συνολικά, αναφέρονται δύο δημοσιεύσεις σε έγκριτα επιστημονικά περιοδικά και 25 ανακοινώσεις σε διεθνή συνέδρια και παγκόσμιες συνόδους, με κρίση επί εκτεταμένης περίληψης.

Δημοσιεύσεις, σε έγκριτα επιστημονικά περιοδικά, τμήματος υλικού της Διδακτορικής Διατριβής (Δ.Δ.)

(αναφέρεται και το κεφάλαιο της Δ.Δ. στο οποίο γίνεται σχετική μνεία)

Κεφάλαιο 5

[1] **Venetsanos D.T.**, Provatidis C.G. (2010), "On the layout optimization of 2D skeletal structures under a single displacement constraint", Struct Multidisc Optim, vol.42, pp.125–155.

Κεφάλαιο 7

[2] Provatidis, C.G. and **Venetsanos, D.T.** (2006), "Cost minimization of 2D continuum structures under stress constraints by increasing commonality in their skeletal equivalents", Forsch Ingenieurwes, vol.70, pp.159–169.

Ανακοινώσεις, σε διεθνή συνέδρια και παγκόσμιες συνόδους με κρίση επί εκτεταμένης περίληψης, τμήματος υλικού της Διδακτορικής Διατριβής (Δ.Δ.)

(αναφέρεται και το κεφάλαιο της Δ.Δ. στο οποίο γίνεται σχετική μνεία)

Κεφάλαιο 2

[1] Provatidis, C.G., Vossou C.G., **Venetsanos D.T.**, "Verification of popular deterministic and stochastic optimization methods using benchmark mathematical functions", In: D.Tsahalis (ed.), CD Proc. *1st International Conference "From Specific Computing to Computational Engineering", 8-10 September, 2004, Athens, Greece.*

[2] Provatidis C.G., **Venetsanos D.T.**, Vossou C.G., "A comparative study on deterministic and stochastic optimization algorithms applied to truss design", In: D.Tsahalis (ed.), CD Proc. *1st International Conference "From Specific Computing to Computational Engineering", 8-10 September, 2004, Athens, Greece.*

[3] Provatidis C.G., **Venetsanos D.T.**, Markos P.A., "Investigation Of Hybrid Optimization Schemes With A Deterministic Search Direction And A Stochastic Step Size", *2nd International Conference "From Scientific Computing to Computational Engineering", 5-8 July, 2006, Athens, Greece.*

[4] Papageorgiou A.A., **Venetsanos D.T.**, Provatidis C.G., "Investigating The Influence Of Typical Genetic Algorithm Parameters On The Optimization Of Benchmark Mathematical Functions", *2nd International Conference "From Scientific Computing to Computational Engineering", 5-8 July, 2006, Athens, Greece.*

Κεφάλαιο 4

[5] Provatidis, C.G. and **Venetsanos, D.T.**, "Performance of the FSD in shape and topology optimization of two-dimensional structures using continuous and truss-like models", In: C. Cinquini, M. Rovati, P. Venini and R. Nascimbene (eds.), Proceedings *Fifth World Congress of Structural and Multidisciplinary Optimization, May 19-23, 2003, Lido di Jesolo, Italy, pp. 385-386, Schönenfeld & Ziegler (ISBN 88-88412-18-2).*

[6] **Venetsanos D.T.** and Provatidis C.G., "Fully stressed 2D continua formed by applying the stress-ratio technique to finite elements of variable thickness", *1st IC-EpsMsO, 6-9 July 2005, Athens, Greece.*

[7] Provatidis C.G., **Venetsanos D.T.**, Kesimoglou N.C., "Layout Optimization Of A Stress-Constrained Plate Under Out-Of-Plane Loading", *2nd International Conference "From Scientific Computing to Computational Engineering", Athens, 5-8 July, 2006.*

[8] Provatidis C.G., **Venetsanos D.T.**, Champilos S.D. "Weight Minimization Of 3D Continuum Structures Under Stress Constraints", *2nd International Conference "From Scientific Computing to Computational Engineering", Athens, 5-8 July, 2006.*

[9] **Venetsanos D.**, Magoula E. and Provatidis C. "Layout Optimization of Stressed Constrained 2D Continua Using Finite Elements of Variable Thickness", *6th International Congress on Computational Mechanics (GRACM), Thessaloniki, 19-21 June 2008.*

Κεφάλαιο 6

[10] Provatidis C. G. and **Venetsanos, D. T.**, "The influence of normalizing the virtual strain energy density on the shape optimization of 2D continua", *1st IC-EpsMsO, 6-9 July 2005, Athens, Greece.*

[11] **Venetsanos D.** and Provatidis C., "Layout Optimization of Single Displacement Constrained 2D Continua Using Finite Elements of Variable Thickness", *6th International Congress on Computational Mechanics (GRACM), Thessaloniki, 19-21 June 2008.*

[12] **Venetsanos, D.T.**, Provatidis, C.G., Minimum weight designs for single displacement constrained 2D continua using variable element-wise thickness, *8th World Congress on Structural and Multidisciplinary Optimization (WCSMO8), LNEC (National Laboratory for Civil Engineering), Lisboa, Portugal, June 1- 5, 2009.*

Κεφάλαιο 7

[13] **Venetsanos, D.T.**, Mitrakos, D. and Provatidis, C.G., "Layout optimization of 2D skeletal structures using the fully stressed design", *1st International Conference on Information Technology and Quality, 5-6 June 2004, Athens, Greece.*

[14] Provatidis, C.G., **Venetsanos, D.T.,** Linardos, M.D., "Cost Minimization Of Welded Steel Tanks For Oil Storage According To API Standards", *2nd International Conference "From Scientific Computing to Computational Engineering", Athens, 5-8 July, 2006.*

Κεφάλαιο 8

[15] Provatidis C.G., Tzanakakis E.D., and **Venetsanos D.T.**, "Optimum selection of doubly symmetric rolled beams for single-girder overhead travelling cranes using finite element plate models", *1st IC-EpsMsO, 6-9 July 2005, Athens, Greece.*

[16] **Venetsanos D.T.**, Provatidis C.G., Magoula E-A.T., "Optimal design of a welded open cross-section crane runway beam in accordance with EC1 and EC3", *2nd International Conference on Experiments/Process/System Modelling/Simulation & Optimization Athens, 4-7 July, 2007.*

[17] **Venetsanos D.T.**, Provatidis C.G., Skarmeas S.G., "Optimal Design Of A Box Cross Section Of A Double Girder Crane In Accordance With EC1 AND EC3", *2nd International Conference on Experiments/Process/System Modelling/Simulation & Optimization, Athens, 4-7 July, 2007*.

[18] **Venetsanos D.**, Magoula E. and Provatidis C., "Performance-based optimization of the welded box of a single girder overhead travelling crane according to EC3 and EC1, *8th. World Congress on Computational Mechanics (WCCM8), 5th. European Congress on Computational Methods in Applied Sciences and Engineering (ECCOMAS 2008), June 30–July 4, 2008, Venice, Italy.*

[19] **Venetsanos D.** and Provatidis C., "Performance-based optimization of a welded open cross section runway beam according to EC3 and EC1", *8th. World Congress on Computational Mechanics (WCCM8), 5th. European Congress on Computational Methods in Applied Sciences and Engineering (ECCOMAS 2008), June 30–July 4, 2008, Venice, Italy.*

[20] Kapogiannis A.K., **Venetsanos D.T.** and Provatidis C.G., Weight minimization of a steel hangar using a new heuristic optimization procedure and according to the Eurocode standards, *3rd International Conference "From Scientific Computing to Computational Engineering", Athens, 8-11 July, 2009.*

Appendix I ***(αναφέρεται στο αγγλικό κείμενο της Διδακτορικής Διατριβής)***

[21] Provatidis, C., **Venetsanos**, D. and Spentzas, C., "Parametric investigation of car suspension design", Proceedings MVM XIII, *International Scientific Meeting Motor Vehicle & Engines, 4-6 October 2004, Kragujevac, Serbia*.

[22] **Venetsanos**, D.T., Alysandratos, Th. and Provatidis, C.G., "Investigation of symmetric reinforcement of metal plates under tension using the finite element analysis", *1st International Conference on Information Technology and Quality, 5-6 June 2004, Athens, Greece.*

[23] Provatidis, C.G., **Venetsanos**, D.T., Kyriazi, E.A., "Optimum Design Of Single-Sided And Double-Sided Bolted Reinforcement Of A Plate Under Axial Loading According To Eurocode-3", *2nd International Conference "From Scientific Computing to Computational Engineering", Athens, 5-8 July, 2006.*

[24] Provatidis, C.G., **Venetsanos**, D.T., Moissiadou, S.K., "Optimum Design Of Racking Systems According To The Eurocode Standards", *2nd International Conference "From Scientific Computing to Computational Engineering", Athens, 5-8 July, 2006.*

[25] Spatharis, E.F., **Venetsanos**, D.T. and Provatidis, C.G., Layout optimization of a dual-axis solar tracker according to the Eurocode standards, *3rd International Conference "From Scientific Computing to Computational Engineering", Athens, 8-11 July, 2009.*

Αυτή η σελίδα είναι σκοπίμως κενή

Αυτή η σελίδα είναι σκοπίμως κενή

Αυτή η σελίδα είναι σκοπίμως κενή